UNDERWATER PHYSIOLOGY VII

THE SEVENTH SYMPOSIUM ON UNDERWATER PHYSIOLOGY
GOVERNING BOARD

ARTHUR J. BACHRACH, Chairman
Naval Medical Research Institute (NMRI), USA

KENNETH N. ACKLES
Canadian Defence Liaison Staff, USA

ALFRED A. BOVE
Temple University of Health Science Center, USA

BERNARD BROUSSOLLE
Centre d'Etudes et de Recherches Biophysiologiques Appliquees a la Marine, France

JAMES M. CLARK
University of Pennsylvania Medical Center, USA

DAVID H. ELLIOTT
Shell U.K. Ltd., England

CARL MAGNUS HESSER
Karolinska Institutet, Sweden

SUZANNE KRONHEIM*
Office of Naval Research, USA

LEONARD M. LIBBER
Office of Naval Research, USA

JAMES W. MILLER
National Oceanic and Atmospheric Administration, USA

HERBERT A. SALTZMAN
Duke University Medical Center, USA

Affiliations as of July 1980.
*In Memoriam

UNDERWATER PHYSIOLOGY VII

PROCEEDINGS OF THE SEVENTH SYMPOSIUM
ON UNDERWATER PHYSIOLOGY

Sponsored by

The University of Pennsylvania

The Undersea Medical Society, Inc.

The U.S. Office of Naval Research

The U.S. National Oceanic and Atmospheric Administration

Edited by Arthur J. Bachrach and Mary Margaret Matzen
Naval Medical Research Institute

Assistant Editors Doris N. Auer and Sally T. McAllister

CONTENTS

PART I

OXYGEN TOXICITY

PART II

CARDIORESPIRATORY RESPONSES TO EXERCISE
CARDIORESPIRATORY EFFECTS

PART III

HIGH PRESSURE NERVOUS SYNDROME
PSYCHOMOTOR PERFORMANCE AND HIGH PRESSURE NERVOUS
SYNDROME

PART IV

OXYGEN SUFFICIENCY AND UTILIZATION WITHIN THE CELL

PART V

METABOLISM AND THERMAL PHYSIOLOGY

PART VI

MOLECULAR AND CELLULAR EFFECTS OF HYDROSTATIC PRESSURE

PART VII

INERT GAS EXCHANGE AND DECOMPRESSION

PART VIII

HEALTH HAZARDS

The first eight papers and the discussion thereof were presented at the European Undersea Biomedical Society Meetings in conjunction with the Seventh Symposium on Underwater Physiology

LIST OF AUTHORS AND CONTRIBUTORS*

K. G. M. M. Alberti, Royal Victoria Infirmary, Newcastle-upon-Tyne, England

S. R. Alcock, University of Aberdeen, Aberdeen, Scotland

D. A. Allen, University of Maryland, College Park, Maryland

H. Arita, Tokai University School of Medicine, Bohseidai, Isehara, Japan

M. L. J. Ashford, Marischal College, University of Aberdeen, Aberdeen, Scotland

S. E. Austen, Oxford University, Oxford, England

A. Axelsson, University of Washington School of Medicine, Seattle, Washington

J. A. Baker, Clinical Research Centre, Harrow, Middlesex, England

E. W. Banister, Simon Fraser University, Burnaby, British Columbia, Canada

L. Barthélémy, Laboratoire de Physiologie, Faculte de Medecine de Brest, Brest, France

D. J. P. Bassett, University of Pennsylvania School of Medicine, Philadelphia, Pennsylvania

R. W. Beaver, Institute of Marine Biomedical Research, University of North Carolina at Wilmington, Wilmington, North Carolina

A. Belaud, Laboratoire de Physiologie, Faculte de Medecine de Brest, Brest, France

P. B. Bennett, F. G. Hall Environmental Laboratory, Duke University Medical Center, Durham, North Carolina

K. R. Bondi, Naval Submarine Medical Research Laboratory, Groton, Connecticut

L. Booth, Houlder Diving Research Facility, London, England

---

*Affiliations as of July 1980.

A. A. Bove, Health Science Center, Temple University, Philadelphia, Pennsylvania

M. E. Bradley, Naval Medical Research Institute, Bethesda, Maryland

J. I. Brady, Naval Medical Research Institute, Bethesda, Maryland

P. Branden, Beth Israel Medical Center and Mount Sinai School of Medicine of the City University of New York, New York, New York

L. Braswell, Harvard Medical School, Massachusetts General Hospital, Boston, Massachusetts

R. W. Brauer, Institute of Marine Biomedical Research, University of North Carolina at Wilmington, Wilmington, North Carolina

D. Brickley-Parsons, The George Washington University, Washington, D.C.

B. Broussolle, Centre d'Etudes et de Recherches Biophysiologiques Appliquees a la Marine, Toulon, France

G. L. Brown, Marine Biomedical Institute, Department of Internal Medicine and Shriners Burn Center, The University of Texas Medical Branch, Galveston, Texas

F. Brue, Centre d'Etudes et de Recherches Biophysiologiques Appliquees a la Marine, Toulon, France

I. P. Buckingham, Defence and Civil Institute of Environmental Medicine, Downsview, Ontario, Canada

S. Burgstahler, School of Medicine, University of Minnesota-Duluth, Duluth, Minnesota

S. R. Burns, F. G. Hall Environmental Laboratory, Duke University Medical Center, Durham, North Carolina

B. D. Butler, University of Texas Medical Branch, Galveston, Texas, and Medical School, University of Dundee, Dundee, Scotland

I. Calder, The London Hospital, London, England

E. M. Camporesi, F. G. Hall Environmental Laboratory, Duke University Medical Center, Durham, North Carolina

R. F. Carlyle, Admiralty Marine Technology Establishment (Physiological Laboratory), Alverstoke, Gosport, Hants, England

C. Chastel, Laboratoire de Virologie, Faculte de Medecine, Brest, France

A. Chaumont, Centre d'Etudes et de Recherches Biophysiologiques Appliquees a la Marine, Toulon, France

M-J. Chiang, Pulmonary Toxicology Laboratory, V.A. Hospital, and the Calvin and Flavia Oak Asthma Research Center; University of Miami School of Medicine, Miami, Florida

C. Chryssanthou, Beth Israel Medical Center and Mount Sinai School of Medicine of the City University of New York, New York, New York

M. Cimsit, Tibbi Ekologive Hidro-Klimatologi Kürsüsü, Gapa Klinikleri, Topkapi, Istanbul, Turkey

J. M. Clark, Institute for Environmental Medicine, University of Pennsylvania Medical Center, Philadelphia, Pennsylvania

J. R. Clarke, Naval Medical Research Institute, Bethesda, Maryland

J. R. Claybaugh, University of Hawaii, Honolulu, Hawaii

R. Coggin, F.G. Hall Laboratory, Duke University Medical Center, Durham, North Carolina

R. R. Colwell, University of Maryland, College Park, Maryland

M. L. Conn, Simon Fraser University, Burnaby, British Columbia, Canada

J. Corriol, Laboratorie de Physiologie, Faculte de Medecine, Marseille, France

M. Cross, Houlder Diving Research Facility, London, England

O. P. Daily, Naval Medical Research Institute, Bethesda, Maryland

S. Daniels, Oxford University, Oxford, England

J. M. Davies, Oxford University, Oxford, England

R. C. Dirks, University of Kansas, Lawrence, Kansas

D. E. Dodd, University of Kansas, Lawrence, Kansas

L. R. Dodd, School of Medicine, University of California, Davis, California

T. J. Doubt, State University of New York at Buffalo, Buffalo, New York

J. Doucet, SDR, Direction de Recherches d'Etudes Techniques, Paris, France

J. C. Duflot, G.I.S. Physiologie Hyperbare-C.N.R.S., Marseille, France

J. Durand, Faculte de Medecine, Universite Paris XI, C.C.M.L., Le Plessis-Robinson, France

K. C. Eastaugh, Oxford University, Oxford, England

B. C. Eatock, Defence and Civil Institute of Environmental Medicine, Downsview, Ontario, Canada

P. O. Edel, 515 Chalmette St., Harvey, Louisiana

G. Egstrom, Performance Physiology Laboratory, University of California at Los Angeles, Los Angeles, California

D. H. Elliott, Shell U.K. Ltd., London, England

L. Fagni, Universite d'Aix-Marseille I, ERA CNRS 272, Marseille, France

L. Fagraeus, Duke University Medical Center, Durham, North Carolina

M. D. Faiman, University of Kansas, Lawrence, Kansas

L. Fairbanks, School of Medicine, University of Minnesota-Duluth, Duluth, Minnesota

L. E. Farhi, School of Medicine and Dentistry, State University of New York at Buffalo, Buffalo, New York

J. C. Farmer, Jr., F. G. Hall Environmental Laboratory, Duke University Medical Center, Durham, North Carolina

A. B. Fisher, University of Pennsylvania School of Medicine, Philadelphia, Pennsylvania

M. A. Fisher, School of Medicine, University of Florida, Gainesville, Florida

V. Flook, Marischal College, University of Aberdeen, Aberdeen, Scotland

B. Fowler, York University, Downsview, Ontario, Canada

L. Frank, Pulmonary Toxicology Laboratory, V.A. Hospital, and the Calvin and Flavia Oak Asthma Research Center; Pulmonary Division, University of Miami School of Medicine, Miami, Florida

D. Frierson, Jr., Institute for Marine Biomedical Research, University of North Carolina at Wilmington, Wilmington, North Carolina

H. D. Fust, Institut fur Flugmedizin, Deutsche Forschungs-und Versuchsanstalt fur Luft-und Raumfahrtimedizin, Bonn-Bad Godesberg, West Germany

H-J. Galla, Stanford University, Stanford, California

M. C. Gardette-Chauffour, G.I.S. Physiologie Hyperbare-C.N.R.S., Marseille, France

M. P. Garrard, Admiralty Marine Technology Establishment (Physiological Laboratory), Alverstoke, Gosport, Hants, England

J. Gething, The Associated Octel Company Ltd., London, England

H. W. Gillen, Institute of Marine Biomedical Research, University of North Carolina at Wilmington, Wilmington, North Carolina

J. D. Gillmore, Naval Medical Research Institute, Bethesda, Maryland

P. Giry, Centre d'Etudes et de Recherches Biophysiologiques Appliquees a la Marine, Toulon, France

J. M. Goldinger, State University of New York at Buffalo, Buffalo, New York

S. M. Gošović, Naval Medical Institute, Split, Yugoslavia

S. Granger, York University, Downsview, Ontario, Canada

R. M. Gray, Institute of Naval Medicine, Alverstoke, Gosport, Hants, England

S. D. Gray, School of Medicine, University of California, Davis, California

A. R. Green, Radcliffe Infirmary, Oxford, England

C. Grimaud, G.I.S. Physiologie Hyperbare-C.N.R.S., Marseille, France

M. Haddaway, The London Hospital, London, England

A. C. Hall, Marischal College, University of Aberdeen, Aberdeen, Scotland

J. M. Hallenbeck, Naval Medical Research Institute, Bethesda, Maryland

M. J. Halsey, Clinical Research Centre, Harrow, Middlesex, England

R. de G. Hanson, Institute of Naval Medicine, Alverstoke, Gosport, Hants, England

A. A. Harper, Marischal College, University of Aberdeen, Aberdeen, Scotland

K. Haya, University of Kansas, Lawrence, Kansas

P. A. Hayes, Admiralty Marine Technology Establishment (Physiological Laboratory), Alverstoke, Gosport, Hants, England

F. G. Hempel, F.G. Hall Environmental Laboratory, Duke University Medical Center, Durham, North Carolina

C. M. Hesser, Karolinska Institutet, Stockholm, Sweden

B. A. Hills, University of Texas Medical Branch, Galveston, Texas, and Medical School, University of Dundee, Dundee, Scotland

P. M. Hogan, State University of New York at Buffalo, Buffalo, New York

L. D. Homer, Naval Medical Research Institute, Bethesda, Maryland

S. K. Hong, State University of New York at Buffalo, Buffalo, New York

T. F. Huang, College of Medicine, National Taiwan University, Taipei, Taiwan, Republic of China

M. Hugon, Universite d'Aix-Marseille I, ERS CNRS 272, Marseille, France

R. Hyacinthe, Centre d'Etudes et de Recherches Biophysiologiques Appliquees a la Marine, Toulon, France

G. Imbert, G.I.S. Physiologie Hyperbare-C.N.R.S., Marseille, France

M. J. Jaeger, School of Medicine, University of Florida, Gainesville, Florida

Y. Jammes, G.I.S. Physiologie Hyperbare-C.N.R.S., Marseille, France

P. Joanny, Laboratorie de Physiologie, Faculte et Medecine, Marseille, France

F. F. Jöbsis, Duke University Medical Center, Durham, North Carolina

S. W. Joseph, Naval Medical Research Institute, Bethesda, Maryland

B. S. Kang, State University of New York at Buffalo, Buffalo, New York

P. G. Kaufmann, F.G. Hall Environmental Laboratory, Duke University Medical Center, Durham, North Carolina

J. J. Kendig, Stanford University School of Medicine, Stanford, California

D. Kerem, Faculty of Medicine, Technion-Israel Institute of Technology, Haifa, Israel

K. E. Kisman, Defence and Civil Institute of Environmental Medicine, Downsview, Ontario, Canada

D. D. Koblin, San Francisco Medical Center, San Francisco, California

T. D. Kunkle, University of Hawaii, Honolulu, Hawaii

D. I. Kurss, Hyperbaric Research Laboratory, State University of New York at Buffalo, Buffalo, New York

S. Lahiri, University of Pennsylvania, Philadelphia, Pennsylvania

J. Le Chuiton, Commission d'Etudes Pratiques d'Intervention Sous la Mer, Toulon, France

C. Lemaire, Centre d'Etudes Hyperbare, COMEX, Marseille, France

R. Levy, Naval Medical Research Institute, Bethesda, Maryland

B. D. Lia, School of Medicine, University of California, Davis, California

Y. C. Lin, School of Medicine, University of Hawaii, Honolulu, Hawaii

F. Lind, Karolinska Institutet, Stockholm, Sweden

R. G. Lister, Oxford University, Oxford, England

H. J. Little, Oxford University, Oxford, England

C. E. G. Lundgren, State University of New York at Buffalo, Buffalo, New York

A. G. Macdonald, Marischal College, Aberdeen University, Aberdeen, Scotland

J. W. Macdonald, Catalina Marine Science Center, University of Southern California, Avalon, California

J. T. Mader, Marine Biomedical Institute and Shriners Burn Center, The University of Texas Medical Branch, Galveston, Texas

W. M. Mansfield, Jr., Institute of Marine Biomedical Research, University of North Carolina at Wilmington, Wilmington, North Carolina

R. E. Marquis, School of Medicine and Dentistry, University of Rochester, Rochester, New York

A. Marroni, Industrial Medicine Department, Saipem, Milan, Italy

D. Massaro, Pulmonary Toxicology Laboratory, V.A. Hospital, and the Calvin and Flavia Oak Asthma Research Center; University of Miami School of Medicine, Miami, Florida

G. Masurel, Centre d'Etudes et de Recherches Techniques Sous-Marines, Toulon, France

M. M. Mathias, Colorado State University, Fort Collins, Colorado

M. Matsuda, Japan Marine Science and Technology Center, Yokosuka, Japan

N. Matsui, Nagoya University, Nagoya, Japan

R. D. McCall, Institute for Marine Biomedical Research, University of North Carolina at Wilmington, Wilmington, North Carolina

H. McElroy, Naval Medical Research Institute, Bethesda, Maryland

A. E. McKee, Naval Medical Research Institute, Bethesda, Maryland

R. S. McKenzie, Admiralty Marine Technology Establishment (Physiological Laboratory), Alverstoke, Gosport, Hants, England

D. McPherson, University of Washington School of Medicine, Seattle, Washington

S. Meisel, Technion-Israel Institute of Technology, Haifa, Israel

D. B. Millar, Naval Medical Research Institute, Bethesda, Maryland

J. M. Miller, University of Washington School of Medicine, Seattle, Washington

J. N. Miller, F. G. Hall Environmental Laboratory, Duke University Medical Center, Durham, North Carolina

K. W. Miller, Harvard Medical School, Massachusetts General Hospital, Boston, Massachusetts

M. Monti, Commission d'Etudes Pratiques d'Intervention Sous la Mer, Toulon, France

R. E. Moon, F.G. Hall Environmental Laboratory, Duke University Medical Center, Durham, North Carolina

R. A. Morin, State University of New York at Buffalo, Buffalo, New York

J. B. Morrison, Simon Fraser University, Burnaby, British Columbia, Canada

A. F. Mott, Clinical Research Centre, Harrow, Middlesex, England

R. Myers, Maryland Institute for Emergency Medical Services, University of Maryland, Baltimore, Maryland

H. Nakayama, Japan Marine Science and Technology Center, Yokosuka, Japan

R. Naquet, Laboratorie de Physiologie Nerveuse-C.N.R.S., Gif-Sur-Yvette, France

N. Naraki, G.I.S. Physiologie Hyperbare-C.N.R.S., Marseille, France

H. F. Nicodemus, Naval Medical Research Institute, Bethesda, Maryland

R. Y. Nishi, Defence and Civil Institute of Environmental Medicine, Downsview, Ontario, Canada

R. J. Nolan, University of Kansas, Lawrence, Kansas

T. Obrénovitch, Centre d'Etudes et de Recherches Biophysiologiques Appliquees a la Marine, Toulon, France

Y. Ohta, Tokai University School of Medicine, Bohseidai, Isehara, Japan

C. V. Paganelli, State University of New York at Buffalo, Buffalo, New York

J. Parc, Commission d'Etudes Pratiques d'Intervention Sous la Mer, (President Capt. Salmon Legagneur), Toulon, France

W. M. Park, The Robert Jones and Agnes Hunt Orthopaedic Hospital, Oswestry, Salop, England

Y. S. Park, Yonsei University, Seoul, Korea

J. L. Parmentier, F.G. Hall Environmental Laboratory, Duke University Medical Center, Durham, North Carolina

A. J. Påsche, Norwegian Underwater Institute, Bergen, Norway

W. D. M. Paton, Oxford University, Oxford, England

C. T. Peng, College of Medicine, National Taiwan University, Taipei, Taiwan, Republic of China

A. J. R. Péqueux, University of Liege, Laboratory of Animal Physiology, Liege, Belgium

A. A. Pilmanis, Catalina Marine Science Center, University of Southern California, Avalon, California

J. Pooley, Royal Victoria Infirmary, Newcastle-upon-Tyne, England

W. Potter, University of Washington School of Medicine, Seattle, Washington

M. R. Powell, Institut fur Flugmedizin, Deutsche Forschungs-und Versuchsanstalt fur Luft-und Raumfahrtimedizin, Bonn-Bad Godesberg, West Germany

R. S. Pozos, School of Medicine, University of Minnesota-Duluth, Duluth, Minnesota

M. W. Radomski, Defence and Civil Institute of Environmental Medicine, Downsview, Ontario, Canada

A. I. Radović, Institute of Aviation Medicine, Zemun, Yugoslavia

J. Raynaud, Faculte de Medecine, Universite Paris XI C.C.M.L., Le Plessis-Robinson, France

K. D. Reimann, Sandberg 3, 2203 Gettorf, West Germany

E. M. Renkin, School of Medicine, University of California, Davis, California

F. Bowser Riley, Oxford University, Oxford, England

J. Roby, F.G. Hall Environmental Laboratory, Duke University Medical Center, Durham, North Carolina

L. Rodriguez, Beth Israel Medical Center and Mount Sinai School of Medicine of the City University of New York, New York, New York

J. C. Rostain, G.I.S. Physiologie Hyperbare-C.N.R.S., Marseille, France

A. Saliou, Laboratoire de Physiologie, Faculte de Medecine de Brest, Brest, France

H. A. Saltzman, F.G. Hall Environmental Laboratory, Duke University Medical Center, Durham, North Carolina

J. V. Salzano, F.G. Hall Environmental Laboratory, Duke University Medical Center, Durham, North Carolina

J. F. Sauter, Harvard Medical School, Massachusetts General Hospital, Boston, Massachusetts

C. L. Schatte, Colorado State University, Fort Collins, Colorado

R. J. Seidler, Oregon State University, Corvallis, Oregon

K. Seki, Japan Marine Science and Technology Center, Yokosuka, Japan

S. G. Shaw, Oxford University, Oxford, England

K. Shiraki, University of Occupational and Environmental Health, Kitakyushu, Japan

B. B. Shrivastav, F.G. Hall Environmental Laboratory, Duke University Medical Center, Durham, North Carolina

A. K. Singh, Simon Fraser University, Burnaby, British Columbia, Canada

E. B. Smith, Oxford University, Oxford, England

R. M. Smith, University of Hawaii at Manoa, Honolulu, Hawaii

C. C. Spicer, Clinical Research Centre, Harrow, Middlesex, England

M. J. Stock, St. George's Hospital Medical School, London, England

B. W. Stolp, F.G. Hall Environmental Laboratory, Duke University Medical Center, Durham, North Carolina

Y. Talmon, Technion-Israel Institute of Technology, Haifa, Israel

S. Tamaya, Tokai University School of Medicine, Bosheidai, Isehara, Japan

S. R. Thom, School of Medicine and Dentistry, University of Rochester, Rochester, New York

J. R. Trudell, Stanford University, Stanford, California

H. D. Van Liew, State University of New York at Buffalo, Buffalo, New York

P. Varéne, U.E.R. de Biologie et de Physiopathologie des Facteurs d'Ambiance, Universite de Bordeaux 11, Bordeaux, France

J. M. Waechter, University of Kansas, Lawrence, Kansas

D. N. Walder, Royal Victoria Infirmary, Newcastle-upon-Tyne, England

P. Wankowicz, Harvard Medical School, Massachusetts General Hospital, Boston, Massachusetts

K. T. Wann, Marischal College, University of Aberdeen, Aberdeen, Scotland

B. Wardley-Smith, Clinical Research Centre, Harrow, Middlesex, England

L. P. Watson, Naval Medical Research Institute, Bethesda, Maryland

W. J. Watson, Defence and Civil Institute of Environmental Medicine, Downsview, Ontario, Canada

C. R. Weatherley, The Robert Jones and Agnes Hunt Orthopaedic Hospital, Oswestry, Salop, England

P. K. Weathersby, Naval Medical Research Institute, Bethesda, Maryland

P. Webb, Webb Associates, Yellow Springs, Ohio

S. Wilcock, University of Aberdeen, Aberdeen, Scotland

M. M. Winsborough, Admiralty Marine Technology Establishment (Physiological Laboratory), Alverstoke, Gosport, Hants, England

L. E. Wittmers, Jr., School of Medicine, University of Minnesota-Duluth, Duluth, Minnesota

R. T. Wloch, Clinical Research Centre, Harrow, Middlesex, England

C. M. Yeung, University of Hawaii, Honolulu, Hawaii

D. E. Yount, University of Hawaii, Honolulu, Hawaii

D. Zannini, Institute of Occupational Medicine, University of Genoa, Genoa, Italy

J. A. Zempel, University of Kansas, Lawrence, Kansas

PREFACE

Underwater Physiology VII represents the seventh in a continuing series of Symposia initiated 27 years ago by the University of Pennsylvania and the Office of Naval Research. This volume was sponsored by the University of Pennsylvania, the Undersea Medical Society, Inc., the U.S. Office of Naval Research, and the U.S. National Oceanic and Atmospheric Administration. At the request of the sponsors, the Undersea Medical Society assumed the responsibility for planning and publication of the Seventh Symposium, with the assistance of the Underwater Symposium Governing Board.

FOREWORD

The current volume in the series of Underwater Physiology Symposia over the years since the first in 1955 represents a microcosm not only of the development of underwater physiology over the past 25 years but the development of a science as well. As any science develops, the beginnings are in precise observation in which determining the presence and magnitude of an event form an early stage, followed by hypothesis testing and theory development in which various explanations of causes and correlations of events are explored. As the science matures it is inevitable that the event carefully described needs further analysis in terms of basic mechanisms. This, indeed, has happened in underwater physiology.

To take as an example a field in which I have a personal interest—the high pressure nervous syndrome (HPNS)—I believe we see a representation of such a progression, going from reports in the 1960's of observed tremor in chamber dives, through quantification of HPNS symptoms such as tremor, to a growing emphasis on molecular and cellular effects of high pressure and membrane activity—basic mechanism approaches strongly represented in the current Symposium. The development is reflected in many areas and represents, I believe, a trend in maturing that will provide invaluable information in the near future for fuller comprehension of the niceties of underwater physiology and for support of diving operations. The papers on health hazards incorporated into this volume from the section of the Symposium sponsored by the European Undersea Biomedical Society represent an important orchestration of the talents of the basic science of physiology and the application of these talents to an operation world.

For the Governing Board, I would like to express sincere gratitude to the participants in the Symposium, to C. J. Lambertsen for his direction of the excellent symposia that led to the current one, to Dr. C. W. Shilling for his warm support and preparation of the excellent Subject Index for this volume, to Barbara Nichols and John Rice for their fine management of the meetings, and to members of the government of Greece and the Greek scientific community for their superb hospitality.

Arthur J. Bachrach
Chairman, Seventh Symposium on
Underwater Physiology

ACKNOWLEDGMENTS

Part I

OXYGEN TOXICITY

CURRENT CONCEPTS OF OXYGEN TOXICITY

J. M. Clark

Soon after Priestley isolated oxygen, he suspected its toxic potential (1). Near the end of the nineteenth century, the universal nature of oxygen poisoning was firmly established by the imaginative and comprehensive studies of Paul Bert (2). J. Lorrain Smith (3) described the gross pathological manifestations of pulmonary oxygen poisoning. Early reviews by Bean (4) and Stadie, Riggs, and Haugaard (5) summarized the results obtained over the next 50 years. Concurrent series of experiments by Dickens (6) at the National Institute for Medical Research in London and Stadie, Riggs, and Haugaard (7,8) at the University of Pennsylvania demonstrated multiple biochemical manifestations of oxygen poisoning. At about the same time, stimulated by operational requirements arising from underwater use of oxygen for military purposes in World War II, Donald (9) in the Royal Navy and Behnke et al. (10) in the United States Navy studied the signs and symptoms of central nervous system oxygen poisoning in man. Soon after World War II, Lambertsen, at the Institute for Environmental Medicine, initiated a broad program of basic and applied studies of hyperoxic effects that has continued without interruption until the present (11,12). As interest in the problems of oxygen toxicity has expanded over the past several years, these early workers have been joined by many additional investigators in laboratories throughout the United States and in other countries.

Although this review emphasizes recent contributions to the understanding of hyperoxia, awareness of the foundations of this research area is required to place the newer findings into proper perspective. In many cases recent experimental evidence has confirmed the insights of previous investigators. Much remains to be learned, and progress will occur most rapidly if interrelationships between the early foundations and recent work in several different laboratories are fully appreciated.

3

At the outset it is important to restate (12,13) that oxygen is a universal poison: at sufficient pressure and exposure duration, hyperoxia will ultimately have toxic effects on every organ, tissue, and individual cell throughout the body. Despite its toxic properties, hyperoxia has many operational and therapeutic applications which make exploitation and expansion of its usefulness both desirable and practical. Achieving this goal requires understanding and extension of cellular antioxidant defense mechanisms that have evolved over centuries of adaptation to the earth's atmospheric oxygen tension (14). Because these mechanisms are universal and vital, their functional roles are among the most basic of all biological processes.

BIOCHEMICAL MANIFESTATIONS OF NEUROLOGIC OXYGEN POISONING

Numerous biochemical effects of hyperoxia have been demonstrated in vitro and proposed as mechanisms for the development of neurologic oxygen poisoning in intact animals and man. The proposed mechanisms include: inactivation of critical enzymes by oxidation of essential sulfhydryl groups (15); formation of active free radicals (16); inhibition of pyridine nucleotide reduction (17); and lipid peroxide formation (18).

Some of these effects, such as sulfhydryl oxidation (19) and inhibition of pyridine nucleotide reduction (17), have also been shown in vivo, yet the precise biochemical events that lead first to convulsions and ultimately to neural damage and death have not been explained. A major problem with most of the previous in vitro work is that known effects of oxygen toxicity occurred only after longer exposures to higher levels of hyperoxia than those required to cause convulsions in intact animals (20). However, the development of new experimental methods affords hope that former discrepancies between in vivo and in vitro results can be reduced, if not eliminated, and promises to provide new data for critical reappraisal of current proposed mechanisms of neurologic oxygen poisoning.

Metabolic Effects on Susceptibility to Oxygen Poisoning

In recent work with rat brain slices, Kovachich (21) found that an increased rate of glucose metabolism in brain tissue is accompanied by a parallel increase in susceptibility to oxygen poisoning (Fig. 1). These concurrent effects are produced by a variety of conditions including an increased potassium concentration in the incubation medium, addition of the depolarizing agent veratridine to the medium, uncoupling oxidative phosphorylation by addition of dinitrophenol (DNP), and omission of calcium ions from the medium. Each of these conditions increases the respiratory rate of brain tissues, thereby making it more sensitive to oxygen toxicity. The fact that all four conditions do not act by the same mechanism lends support to the conclusion that metabolic stimulation is the common link that augments susceptibility to oxygen poisoning (21).
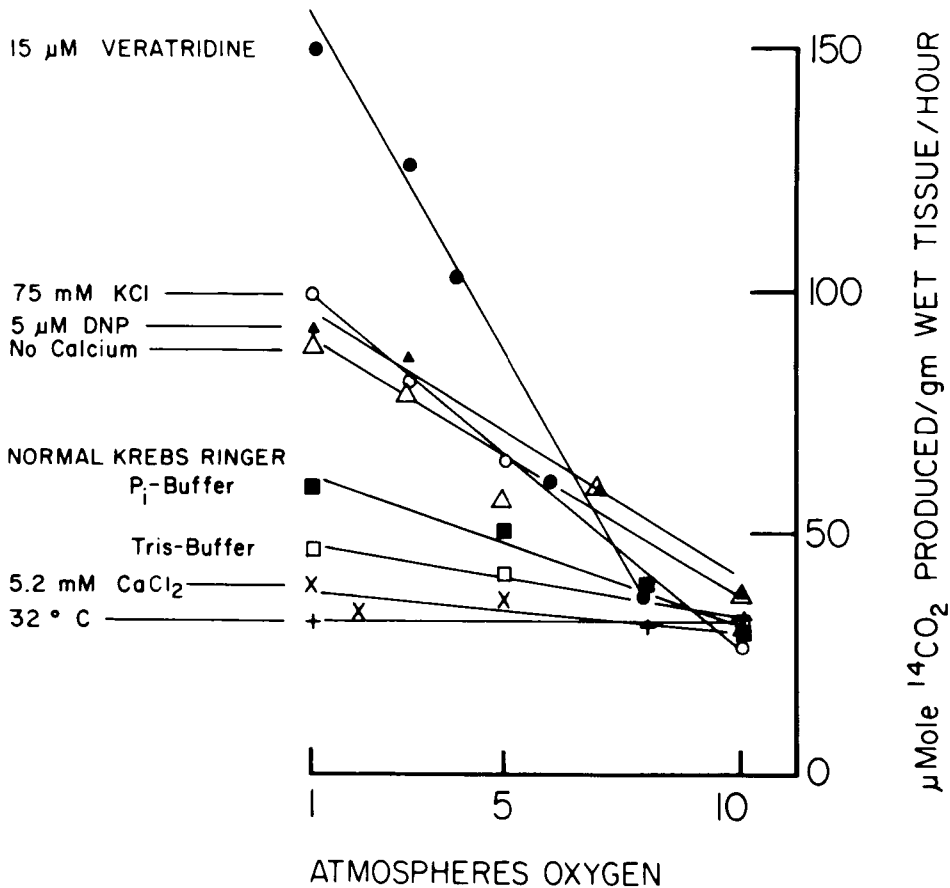
Fig. 1. Effects of increased glucose metabolism on susceptibility of rat brain cortical slices to oxygen poisoning in vitro. Each point represents the mean of 5 to 7 experiments. All slices were incubated for 1h at 37°C in Krebs-Ringer phosphate medium with the indicated changes, except for one group maintained at 32°C. The data show that an increased rate of $^{14}CO_2$ production at 1 ATA of O_2 is correlated with enhanced susceptibility to oxygen poisoning. [From Kovachich (21)]

Two possible mechanisms have been suggested for the effect of increased metabolic rate on sensitivity to oxygen toxicity (22). One is that enhanced free radical formation generated by increased electron transport may, in the presence of hyperoxia, promote the formation of highly reactive molecular species. Another more speculative possibility is that increased metabolic activity may alter the configurations of cellular membranes to make them more vulnerable to oxidizing free radicals.

A similar link between susceptibility to oxygen poisoning and metabolic rate was established in intact animals many years ago. Poikilotherms, which are normally relatively resistant to oxygen toxicity, become less resistant when they are warmed (23). Alterations in metabolic rate produced by hibernation

and hypothermia (24), anesthesia (25), and changes in thyroid activity (26) are accompanied by parallel shifts in sensitivity to hyperoxic exposure. It is also possible that the enhanced susceptibility to oxygen convulsions observed in exercising men (27) may be attributed to increased neural activity.

Comparison of Oxygen Pressure-Exposure Duration Relationships In Vivo and In Vitro

The relationship between oxygen pressure and exposure duration for many toxic manifestations of oxygen poisoning is a rectangular hyperbola (28). Pooling data from several laboratories, Dickens (20) was one of the first investigators to show this relationship for neurological symptoms in intact animals and man. Using in vitro measurements from three different laboratories, Dickens showed a similar pressure-duration relationship for 50% depression of oxygen uptake in rat brain slices. However, comparison of the linear forms of these relationships on log-log coordinates revealed that they had different slopes and that more severe oxygen pressure-exposure duration combinations were required for in vitro depression of glucose metabolism than for neurologic symptoms in vivo (Fig. 2).

Dickens' early in vitro work was obtained with brain slices incubated in normal Krebs-Ringer phosphate medium. It is now known that such media maintains brain tissue in a resting state with an oxygen uptake about half that measured in the intact brain (22). When the metabolic rate of brain slices in vitro is stimulated to approach or equal that found in vivo, the pressure-duration relationship for hyperoxic inhibition of tissue respiration approximates the in vivo relationship more closely, both with respect to susceptibility and the slope of the curve (Fig. 2). Although differences in experimental conditions and methods invalidate direct comparisons of these curves, it appears that discrepancies between in vivo and in vitro results can be reduced or eliminated by more accurate in vitro simulations of in vivo states.

Biochemical Effects of Oxygen Poisoning in Vivo

Chance et al. (17) were the first to measure in vivo biochemical effects of hyperoxic exposure before the onset of convulsions. Using a fluorometric technique, these investigators observed the oxidation of pyridine nucleotides in the brain, liver, and kidney of anesthetized rats breathing oxygen at high pressure. Mayevsky et al. (29) later used a similar method in conjunction with chronically implanted light guides (30) to perform surface fluorometry of the brain cortex in awake rats exposed to oxygen with simultaneous electroencephalographic recording. Compared to the time course of events observed at 6 ATA with oxygen alone, the occurrence of pyridine nucleotide oxidation was hastened by addition of 1.5% CO_2 to the gas mixture and delayed by pretreatment with succinate. In all three conditions, pyridine nucleotide oxidation was correlated with and preceded seizure activity.
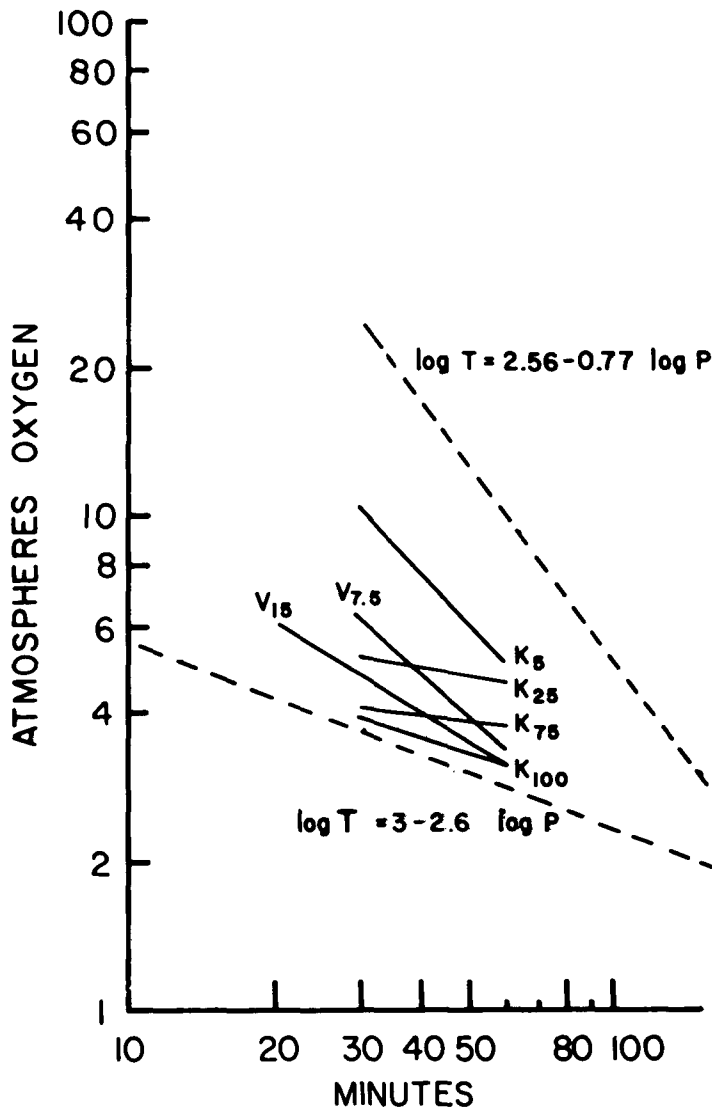
Fig. 2. Oxygen pressure-exposure duration relationships for in vivo and in vitro manifestations of oxygen poisoning. The *dashed line on the left* (log T = 3-2.6 log P) represents the oxygen pressure-exposure duration relationships for neurologic symptoms in intact animals and man. The *dashed line on the right* (log T = 2.56-0.77 log P) represents the corresponding relationship for 50% depression of oxygen uptake in rat brain slices incubated in normal Krebs-Ringer phosphate medium. The *solid lines* represent pressure-duration relationships for 25% decrements in $^{14}CO_2$ production in rat brain slices incubated in media with increased potassium concentration (K_{mM}) or with added veratridine ($V_{\mu M}$). As metabolic activity of the brain slices is progressively stimulated, the in vitro sensitivity to oxygen poisoning approaches that found in vivo. *Dashed lines* are from data summaries by Dickens (20). *Solid lines* are from data of Kovachich and Haugaard (22). Adapted by Kovachich and Haugaard (22) from a concept first used by Dickens (20).

Current Status of the Gamma-Aminobutyric Acid Hypothesis

Prominent alterations in the metabolism of gamma-aminobutyric acid (GABA) during exposure to hyperoxia have been established beyond reasonable doubt. Supporting evidence has been summarized by Wood (31):

1) In animals exposed to convulsive oxygen pressures, the decrement in brain GABA concentration starts before the onset of convulsions, is correlated with severity of convulsion, and is reversible upon return to normoxia (32).

2) Rate of decrease in GABA level is correlated with susceptibility to oxygen seizures in different animal species (33), with exposures of the same species to different oxygen pressures (34), and with exposures to different inspired CO_2 concentrations at the same oxygen pressure (34).

3) The oxygen pressure threshold for decreasing brain GABA level is about 3 ATA, which is also near the lower limit for induction of oxygen seizures (34).

4) Intraperitoneal administration of GABA before hyperoxic exposure delays or prevents convulsions (35).

Nevertheless, a direct cause and effect relationship between decrement in brain GABA concentration and induction of oxygen seizures has not been established. Changes in GABA levels are not always correlated with appropriate changes in convulsion times. Disulfiram delays the onset of seizures while allowing the decrease in GABA content to occur (36,37). Although either amino-oxyacetic or hydrazino-propionic acid interfere with GABA metabolism and elevate brain GABA levels, these agents hasten the onset of convulsions and increase their frequency and severity (36).

It is possible that hyperoxic effects on brain GABA metabolism may parallel the development of oxygen seizures without a direct causal relationship (22). Radomski and Watson (38) have suggested that these effects may be related to hyperoxic alterations in ionic gradients. There is evidence that oxygen toxicity inactivates membrane transport systems in the brain cortical slices of guinea pigs (39) and in the isolated toad bladder (40). Similar membrane effects in fat cell and red blood cell suspensions are described elsewhere in this volume (41). Membrane transport inactivation in brain cells could lead to extracellular accumulations of potassium and glutamate, a GABA precursor (22). Both effects could increase neuronal excitability because potassium is a depolarizing agent and glutamate is thought to be an excitatory neurotransmitter (22). Banister and Singh (42) have proposed central roles for ammonia and glutamate in a complex chain of events that ultimately precipitates convulsions. Although none of these potential mechanisms precludes brain GABA reduction as a contributing factor, it now appears unlikely that it is the dominant mechanism for the production of hyperoxic seizures.

Correlation of Convulsion Incidence and Inactivation of Cerebral Cortical NaK-ATPase in Rats Exposed to O_2 at 4 ATA

Kovachich et al. (43) recently found that the activity of membrane-bound NaK-ATPase in the cerebral cortex of rats exposed to O_2 at 4 ATA is signifi-

cantly depressed at least 90 min before the onset of seizures. As stated above, inactivation of membrane transport systems could increase neuronal excitability and, ultimately, precipitate convulsions. Furthermore, there is preliminary evidence that modification of susceptibility to hyperoxic seizures is accompanied by parallel shifts in rate of inactivation of cortical NaK-ATPase (Fig. 3). Elevation of the inspired Pco_2 to 60 Torr in rats exposed to O_2 at 4 ATA greatly hastens the onset of convulsions and is accompanied by an earlier onset and increased magnitude of NaK-ATPase inactivation. Prior adaptation to the same PI_{CO_2} level for 5 days delays the onset of convulsions in rats exposed to hyperoxia with superimposed hypercapnia and also ameliorates the associated depression of NaK-ATPase activity (Fig. 3). These results can be largely or completely explained by cerebral vasodilation with gross increase of brain oxygen pressure in acute hypercapnia (44) and by partial reversal of this response following an adaptation to chronic hypercapnia (45).

CELLULAR MANIFESTATIONS OF PULMONARY OXYGEN POISONING

Early studies of pulmonary oxygen poisoning emphasized description of the pathologic changes found in the lungs of animals fatally exposed to hyperoxia (4). Later it became clear that these changes could be grouped into acute exudative and subacute proliferative categories on the basis of their nature and sequence of appearance (13). It is now known that many of the anatomical alterations associated with oxygen poisoning, particularly those in the proliferative category, are adaptive responses that delay or compensate for the progressive deterioration of pulmonary function caused by oxygen toxicity.

The anatomical adaptations are accompanied by biochemical defense mechanisms that appear to play an even greater role in the prevention or amelioration of oxidant damage to the lung. Identification of these biochemical adaptations and their association with increased oxygen tolerance have been areas of significant recent progress (46). In fact, it now appears that more is known about antioxidant defenses than about the specific forms of oxidant damage by which they are activated.

Hyperoxic Effects on Specific Lung Cell Types

Anatomical effects. Stereologic and morphologic studies of pulmonary oxygen poisoning in rats (47) and monkeys (48) have demonstrated a characteristic progression of toxic effects in different cell types. In the rat, the first indication of cellular damage is occasional early destruction of capillary endothelia cells after 48 h of exposure to oxygen at 1 ATA. At 72 h, endothelial cells are extensively destroyed and completely absent in some places. At the same time alveolar epithelial cells show hyperplasia, but are little changed morphologically.

A similar sequence of cellular morphologic changes occurs in the monkey over a much longer time course (Fig. 4) (48). At 2 days of exposure capillary
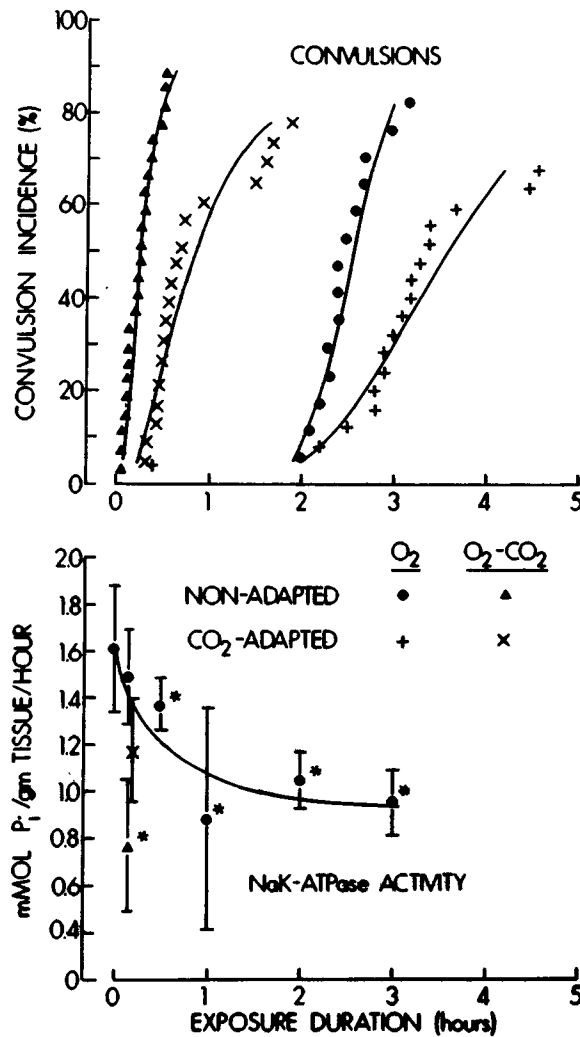
Fig. 3.   Correlation of convulsion incidence and inactivation of cerebral cortical NaK-ATPase in rats exposed to O_2 and O_2-CO_2 at 4 ATA. Normal and CO_2-adapted rats were exposed at 4 ATA to 100% O_2 and O_2-CO_2 (P'_{CO_2} 60 Torr). Symbols for each of the four groups are shown on the graph. Each data point on the *upper half* represents the convulsion time of one rat. The curves are probability-log transformations of the data. Data points on the *lower half* are averages of NaK-ATPase activity in cortical slices removed from 4 to 6 rats after exposure to the conditions indicated by the symbol for durations shown on the graph. The *brackets* represent one standard deviation, and the *asterisk* indicates a statistically significant difference from control measurements in unexposed rats on the same day. The control point on the graph is an overall average of the individual controls. The curve was drawn by eye through the data for rats exposed to 100% O_2. The three points shown on the *lower half* for 10-min exposures to the indicated conditions have the same relative order as the corresponding convulsion incidence curves shown above. Data shown in the *bottom* of the figure are after Kovachich et al. (43) and curves in the *top half* are after Clark (45).
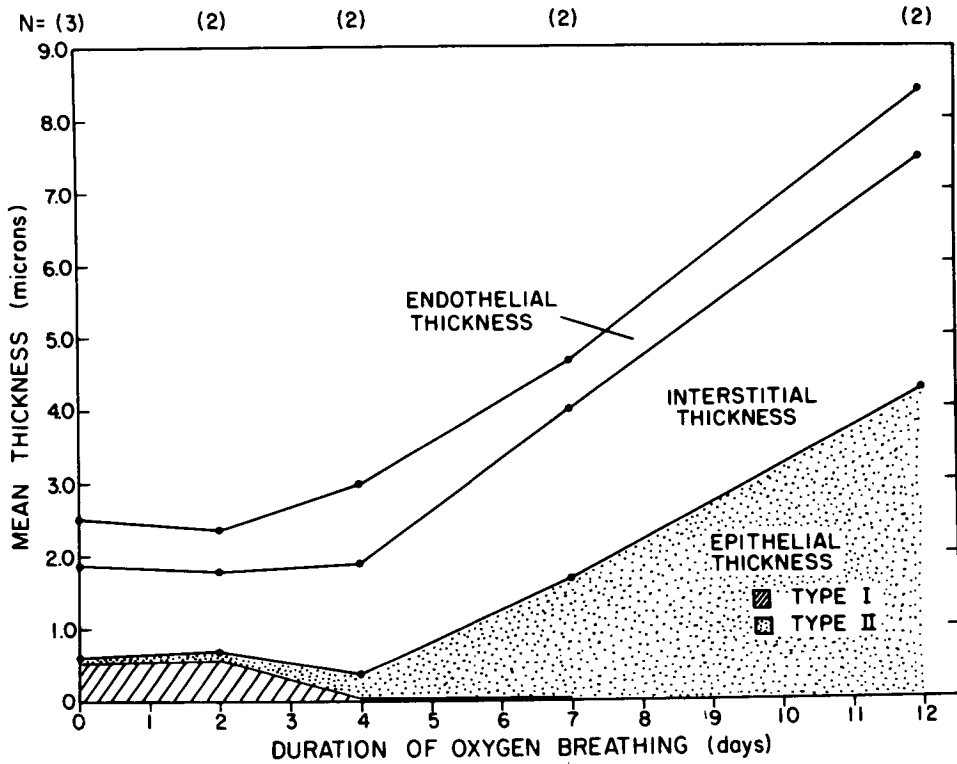
Fig. 4.   Effect of pulmonary oxygen poisoning on the alveolar-capillary tissue barrier in the monkey. Points on the graph represent average morphometric measurements obtained in monkeys exposed to 0.98-0.99 ATA of O_2 for 2, 4, 7, and 12 days. The stippled areas indicate the relative proportions of Types I and II alveolar epithelial cells (membranous and granular pneumocytes, respectively). *N* indicates the number of monkeys included in each average. Estimated resistance to diffusion was roughly proportional to the total thickness of the alveolar-capillary tissue barrier. [After Kapanci et al. (48)]

endothelial cells are slightly swollen and show cytoplasmic changes. At 4 days of exposure the most striking effect is almost total destruction of alveolar epithelial Type I cells. At 7 and 12 days of exposure there is massive hyperplasia of epithelial Type II cells to more than 20 times the control volume. Concurrent progressive endothelial damage is manifested initially by increased swelling and later by destruction of endothelial cells with loss of endothelial volume.

Biochemical effects. Recent biochemical studies are consistent with an early effect of oxygen toxicity on pulmonary capillary endothelial cells. It is known that mammalian lungs remove serotonin from the pulmonary circulation, and the capillary endothelial cell has been identified as the site of uptake (49). It is also likely that endothelial cell uptake of serotonin is a carrier-mediated, active-transport process (49). In view of these observations, it is interesting that serotonin clearance in lungs removed from rats exposed to 1 ATA O_2 for 4, 12, 18, and 48 h is depressed by 5, 12, 20, and 35%, respectively

(50). Serotonin clearance is decreased by 30% in lungs from rats exposed to 4 ATA O_2 for 1 h, and the reversibility of this change is shown by the finding of only a 10% decrement following a 3-h recovery period in room air (51).

Mechanisms of Pulmonary Oxygen Poisoning

During exposure to convulsive oxygen pressures, toxic effects on lung enzymes and metabolism are accompanied by additional pathological changes induced by indirect mechanisms acting through hypophyseal-adrenocortical and sympatho-adrenomedullary pathways (13). However, this should not be interpreted as an indication that direct toxic effects of oxygen do not play a primary and prominent role. After differential catheterization of the two main bronchi, much more severe pathology is produced in the hyperoxic lung (13) by prolonged exposure of one lung to hyperoxia while the other remains normoxic. Extrapulmonary manifestations of oxygen poisoning in dogs exposed to oxygen at 2.0 to 2.5 ATA can be essentially eliminated by surgical production of a sufficiently large intrapulmonary shunt (52). Although such animals have a prolonged survival time, they ultimately die of pulmonary oxygen poisoning.

Mechanisms of direct oxidant damage. With general acceptance that hyperoxia has direct toxic effects on the lung, increased attention has been directed in recent years to determination of how these effects occur. Generation of toxic free radicals as an initial event was first proposed by Gerschman (16). It is now known that superoxide anions are produced normally during cellular metabolism, and their rate of generation in at least some reactions appears to be augmented by increased Po_2 (53). Other toxic species that may also be produced include hydrogen peroxide, hydroperoxy and hydroxyl radicals, and singlet oxygen (53). Damage to cellular membranes may occur by lipid peroxidation (18), and enzymes may be inactivated by oxidation of essential sulfhydryl groups (15). Progressive lipid peroxidation and enzyme inactivation can be propagated by chain reactions that involve alternate formation of lipid peroxides and lipid free radicals.

Antioxidant Defense Mechanisms in the Lung

Superoxide dismutase. Discovery of the enzyme superoxide dismutase (54) and partial definition during the past decade of its biological role in removal of superoxide radicals made a major contribution to understanding cellular mechanisms of antioxidant defense. Recently, Fridovich (55) summarized multiple lines of evidence that indicate superoxide dismutase is an important cellular defense against oxygen toxicity. Increased lung concentrations of superoxide dismutase also have been associated with several conditions that augment pulmonary oxygen tolerance, to be described in the next paragraph.

Enhanced pulmonary oxygen tolerance by prior hyperoxic exposure. Survival time of rats exposed to oxygen at 1 ATA can be increased from 3 to 4 days to several weeks by prior adaptation to slightly lower levels of hyperoxia (13). This increased tolerance is associated with a significant increase in total

superoxide dismutase activity (56). Furthermore, both the rate of increase in oxygen tolerance during adaptation and its rate of decrement following the adaptive period are correlated with parallel changes in pulmonary superoxide dismutase activity (56). Adaptation of the rat lung to hyperoxia is accompanied by mitochondrial changes in alveolar Type II cells (57) with no ultrastructural alterations in alveolar Type I or endothelial cells (58). Although proliferation and hypertrophy of alveolar Type II cells occurred in rats exposed to 0.85 ATA O_2 for 5 days, their total change in mass did not appear sufficient to account for associated increments in lung contents of superoxide dismutase, glucose-6-phosphate dehydrogenase, and catalase without intracellular induction of enzyme activity (59,60). This discrepancy has been partly explained by the demonstration that alveolar Type II cells isolated from hyperoxia-adapted rats have a significant increment in mitochondrial superoxide dismutase activity per unit mass (61). Activities of cytosolic superoxide dismutase, glucose-6-phosphate dehydrogenase, and catalase were not significantly changed.

Age differences in antioxidant defenses. The well established resistance of immature animals to pulmonary oxygen poisoning (13) is also associated with differences in antioxidant defenses between neonatal and adult animals (62). During exposure to 0.95–1.0 ATA O_2, survival times of adult rats, mice, and rabbits ranged from about 3 to 5 days, while almost all the neonates of the same species were still alive when the exposure was ended at 7 days. In animals exposed to hyperoxia for only 1 day, whole lung enzyme activities of superoxide dismutase, catalase, and glutathione peroxidase were significantly increased in the neonates, but not in adults. Neonatal guinea pigs and hamsters did not show a lung antioxidant enzyme response to hyperoxia, and their susceptibility to pulmonary oxygen poisoning was also identical to that of adults.

Effects of bacterial endotoxin on antioxidant defenses. Inadvertent administration of bacterial endotoxin to adult rats before hyperoxic exposure led to the interesting observation that pulmonary oxygen tolerance is greatly increased in these animals (63). The protection afforded by small doses of endotoxin was later linked to marked stimulation of activities of lung antioxidant enzymes such as superoxide dismutase, catalase, and glutathione peroxidase (63,64). Pleural fluid accumulation and histological changes associated with pulmonary oxygen poisoning were greatly decreased in endotoxin-treated rats (64). A more detailed description of endotoxin effects on oxygen tolerance and antioxidant defense systems is given elsewhere in this volume (65).

Activation of the pentose shunt. The pentose pathway for glucose oxidation is an important antioxidant defense system because it provides reduced nicotinamide adenine dinucleotide phosphate that in turn replenishes the supply of reduced glutathione and may also be used in the synthesis and repair of damaged cell components (66). Total lung content of glucose-6-phosphate-dehydrogenase, the rate-limiting enzyme of the pentose pathway, is increased in rats adapted to hyperoxia (59,67). A significant increase in pentose cycle activity has also been demonstrated in isolated perfused rat lungs ventilated with O_2 at 5 ATA (68).

Oxidant-antioxidant interactions in the lung. As stated, it is likely that superoxide anions and other toxic species are produced in the lung even at a

normal inspired Po_2 and that their rates of formation are increased during exposure to hyperoxia. Thus, the interaction between rate of generation of toxic species and the overall capacity of lung antioxidant defenses to remove them or to repair the damage caused by them determines the rate of development of overt manifestations of oxygen poisoning. Some of the probable oxidant-antioxidant interactions are shown in Fig. 5. The number and complexity of these interactions provide many potential sites and mechanisms for influencing both the nature and the severity of toxic effects.

OXYGEN TOLERANCE IN MAN

Over the range of oxygen pressures that are now used most extensively in diving operations, decompression, and in many therapeutic applications, pulmonary oxygen poisoning is the most limiting effect of oxygen toxicity.
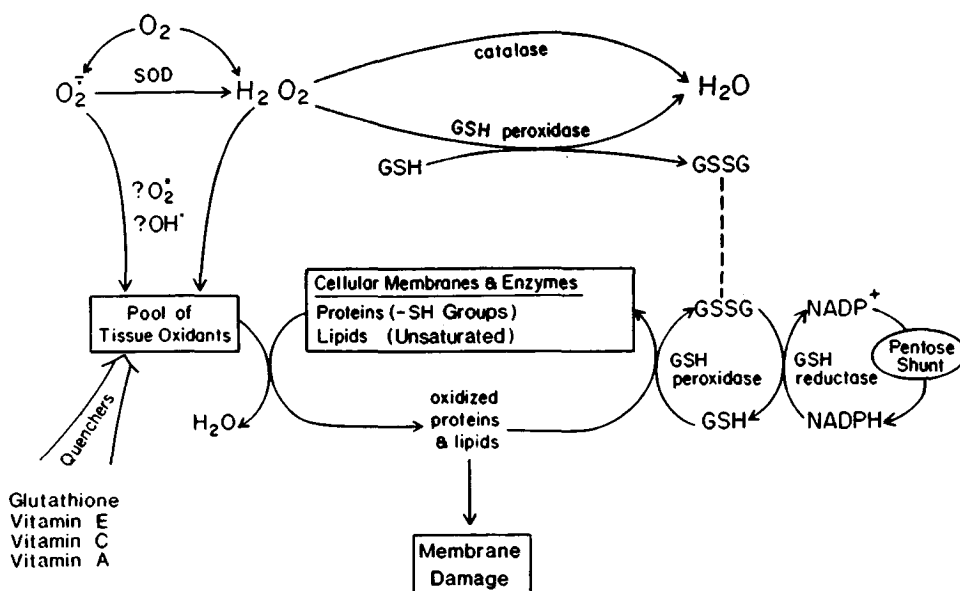
Fig. 5. Oxidant-antioxidant interactions in the lung. Represented are possible metabolic events induced by elevation of inspired Po_2. The sequence is initiated by enhanced generation of superoxide anion, H_2O_2, and possibly other active species such as singlet oxygen and hydroxyl radicals to form a pool of tissue oxidants. These oxidants may damage cell membranes and intracellular enyzmes by oxidizing tissue proteins and lipids. The tissue oxidant pool is diminished and free-radical chain reactions are stopped by interactions of quenchers with active species and oxidized tissue components. Superoxide anions can be removed specifically by superoxide dismutase (SOD). Damaged tissues may also be repaired by reduction of oxidized components by glutathione (GSH) to form oxidized glutathione (GSSG). Regeneration of GSH from GSSG may be accomplished by interaction with reduced nicotinamide adenine dinucleotide phosphate (NADPH), which is, in turn, restored by action of the pentose shunt pathway of glucose metabolism. Extent of lung damage may be determined by the net result of opposing radical-producing and radical-quenching actions with concurrent interactions between tissue-damaging and tissue-repairing processes. [After Fisher et al. (53)]

Awareness of this fact more than 10 years ago stimulated the initial development of pulmonary oxygen tolerance curves for man (13,69) and the related derivation of a system for calculating the pulmonary toxic dose for any exposure to hyperoxia (70,71). Although the unit pulmonary toxic dose (UPTD) concept is now used widely to provide guidelines for safe hyperoxic exposure in commercial and military diving operations, calculated UPTD totals do not always correlate with observed changes in vital capacity (72,73). Therefore, it is appropriate to review here the current status of the UPTD system, its uses, and its limitations.

Vital Capacity Decrement as an Index of Pulmonary Oxygen Poisoning

During the series of exposures that provided the experimental basis for pulmonary oxygen tolerance curves (74–76), many pulmonary function measures were evaluated as indices of oxygen poisoning in normal men who breathed oxygen continuously at 2 ATA (Table I). At a time when there were obvious subjective and objective manifestations of pulmonary oxygen poisoning, the measures in Table I*A* were significantly altered, while those in Table I*B* were not. Decrease in vital capacity was selected as the best available means to monitor the development of pulmonary oxygen poisoning in groups of men. Vital capacity could be measured quickly and reproducibly in trained subjects and it decreased progressively throughout the oxygen exposure in association with increasing severity of symptoms (Fig. 6). Furthermore, the fact that it had been measured in several previous studies of oxygen poisoning at lower pressures provided valuable data for description of pulmonary oxygen tolerance in man over a wide range of oxygen pressures. Although other measures of pulmonary function were also changed significantly (Table I*A*), none fulfilled all of the above criteria as well as decrease in vital capacity.

TABLE I

Indices of Pulmonary Oxygen Poisoning In Man	
Vital Capacity	A
Inspiratory Capacity	
Expiratory Reserve Volume	
Functional Residual Capacity	
Inspiratory Flow Rate	
Lung Compliance	
Carbon Monoxide Diffusing Capacity	
Respiratory Rate	
Residual Volume	B
Expiratory Flow Rate	
Airway Resistance	
Alveolar-Arterial Oxygen Difference	

A. Statistically significant change. *B*. Not significantly changed.
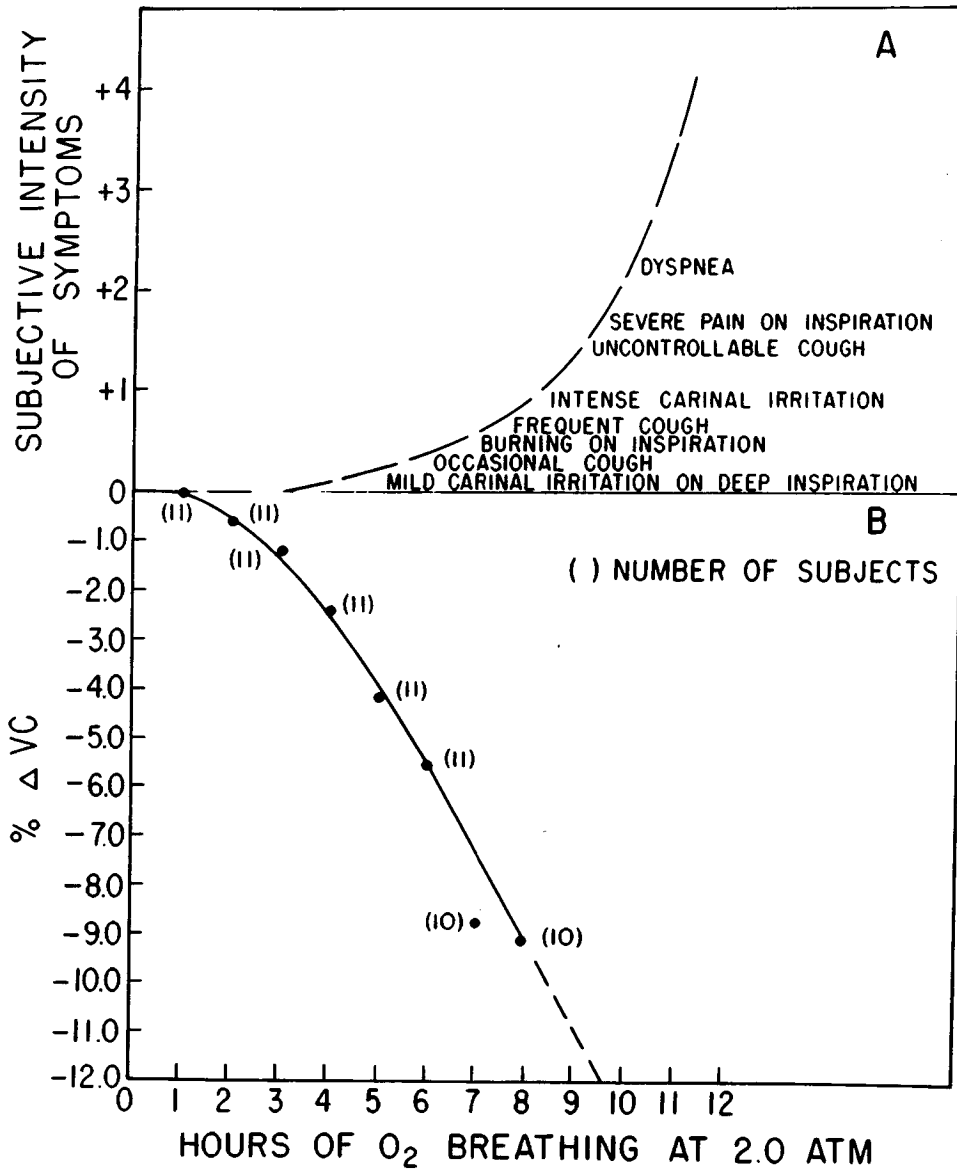
Fig. 6.   Rate of decrease in vital capacity and increasing severity of symptoms during continuous oxygen breathing at 2 ATA. *A*. Hypothetical curve showing rate of development of symptoms during oxygen breathing at 2 ATA was obtained from combined subjective observations of all subjects. *B*. Points plotted on graph are average values of vital capacity measurements in 11 men. Curve drawn through the points is a linear transformation of a regression line fitted to the same data on probability-log coordinates. Durations of oxygen breathing that caused average vital capacity decrements of 4% and 10% are shown. [After Clark and Lambertsen (74)]

Applications and Limitations of the UPTD System

The UPTD system is a method devised at the Institute for Environmental Medicine for expressing any pulmonary toxic dose of oxygen in terms of an equivalent duration of exposure to 1 ATA O_2 (70,71). The system incorporates the known acceleration of oxygen poisoning as inspired oxygen pressure is raised above 0.5 ATA. It was developed to incorporate all available data into a best possible estimate of the rate of development of pulmonary oxygen poisoning over a wide range of oxygen pressures. Although the cause of the oxygen-induced decrement in vital capacity is not known, the pattern of change is mathematically precise and empirically useful for predictive purposes (Fig. 6).

In its present stage of development the UPTD system still has limitations recognized by its originators (70,71). Since it is based on vital capacity changes in 50% of the subjects, measurements in any individual may show smaller or larger decrements (Fig. 7). Even more critical in practical applica-
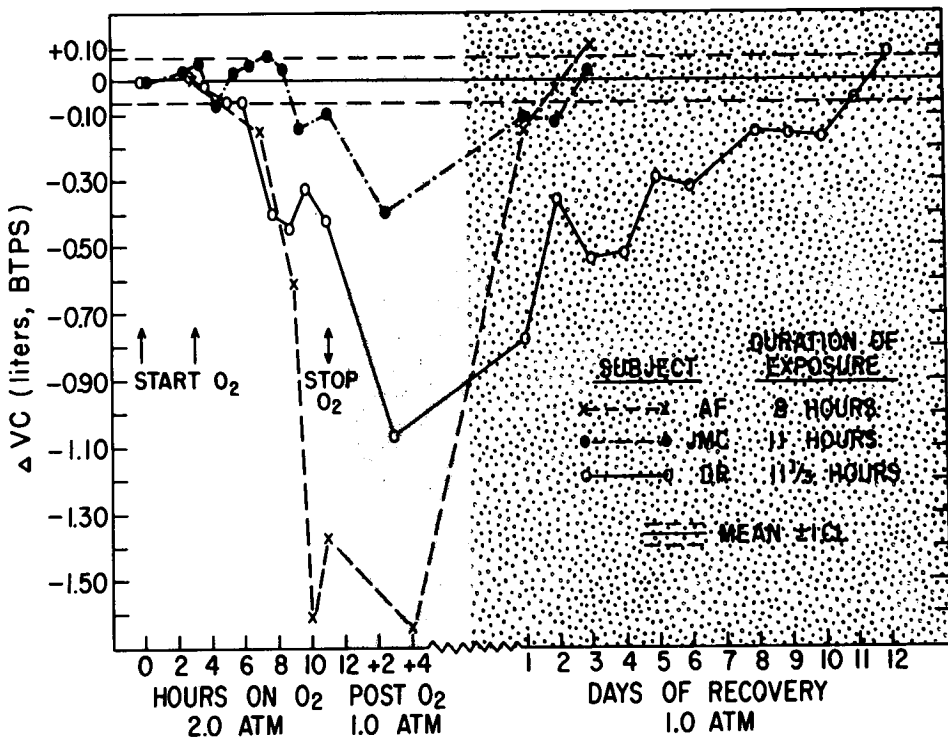
Fig. 7. Individual variation in rates of development of, and recovery from, pulmonary oxygen poisoning. The *solid horizontal line* indicates the control value of vital capacity for each subject, and the *dashed lines* are 95% confidence limits for the subject with the widest limits. The start of oxygen breathing is adjusted on the graph to allow all three exposures to end at the same time. Note that rate of recovery is not necessarily proportional to magnitude of decrement in vital capacity. [From Clark and Lambertsen (74)]

tions of the UPTD concept is the lack of adequate information describing rate of recovery from various degrees of pulmonary intoxication. Awareness of this information gap and recognition of the fact that some individuals recover more slowly than others (Fig. 7) prompted an intentionally conservative approach in which it is assumed that the pulmonary toxic dose is cumulative with no recovery between hyperoxic exposures (70,71). Although this certainly leads to overestimation of toxic dose, it is preferable to dangerous overexposure of an individual on the basis of a UPTD calculation that incorporates an unrealistically rapid recovery rate. This is especially true in the absence of information concerning long-term effects of repeated, low-grade toxicity.

Oxygen Tolerance in Other Organs

Although pulmonary oxygen tolerance must be defined more completely for optimal use of hyperoxia without harmful sequelae, even less is known about rates of development of oxygen poisoning in other organs. Onset times for neurologic symptoms have been studied in man at oxygen pressures up to 7 ATA (77), but little is known about hyperoxic effects on auditory, vestibular, psychomotor, and cognitive functions (12). Measurements of subtle visual responses are needed to complement previous observations of gross decrement in visual acuity during prolonged hyperoxic exposure (10,78). Manifestations of oxygen poisoning should be sought after in organs that are exposed to nearly arterial levels of hyperoxia, such as the carotid body, choroid plexus, and renal glomerulus (12). Other organ sites, such as the retina, renal tubules, and hepatic parenchyma should prove to be relatively susceptible to oxygen toxicity by virtue of their metabolic constitution and rich supply of active transport systems (12).

EXTENSION OF OXYGEN TOLERANCE

Extension of oxygen tolerance by any effective means would provide a more practical and safer alternative to remaining just within inherent tolerance limitations for maximal application of hyperoxygenation. There have been many attempts to delay the progression of oxygen poisoning by pharmacologic agents (13). All of these agents have toxic side effects or other characteristics that restrict their usefulness in man. A major limitation is the universal scope of oxygen toxicity that requires an agent to be effective in each body organ and tissue (12).

Tetraethylthiuram disulfide (disulfiram) is an excellent example of a drug whose administration delays the progression of some manifestations of oxygen poisoning while apparently enhancing that of others. Early studies showed that pretreatment with disulfiram greatly delays the onset of convulsions and lung damage in animals exposed to hyperbaric oxygenation (79,80). Because large doses of the drug could be tolerated with virtually no side effects, it appeared to be particularly promising for use in man. However, in rats breathing oxygen

at 1 ATA (81) or 2 ATA (82), administration of disulfiram decreased survival time significantly. The finding that a metabolite of disulfiram inhibits superoxide dismutase provides a possible mechanisms for this effect (82).

Programmed Intermittency of Hyperoxic Exposure

In contrast to the current lack of effective drug therapy for extension of oxygen tolerance, periodic brief interruption of hyperoxic exposure is a proven means of delaying progression of intoxication at oxygen pressures ranging from 1.0 to 5.5 ATA (13). The theoretical basis for the gain in oxygen tolerance afforded by intermittent hyperoxia and the operational significance of this principle were both described in the First Underwater Physiology Symposium (27). The only attempt so far to optimize schedules for intermittent exposure to a single oxygen pressure was carried out by Hall (83) at the Institute for Environmental Medicine. As an example of the optimization procedures, mortality curves for guinea pigs exposed to oxygen at 3 ATA continuously and with various intermittency programs are shown in Fig. 8. Brief periods of hyperoxia (3 ATA Po_2 for 10 min) were alternated with brief periods of normoxia (0.21 ATA Po_2 for 5, 10, or 20 min). Results show progressive extension of oxygen tolerance with increasing duration of the normoxic interval
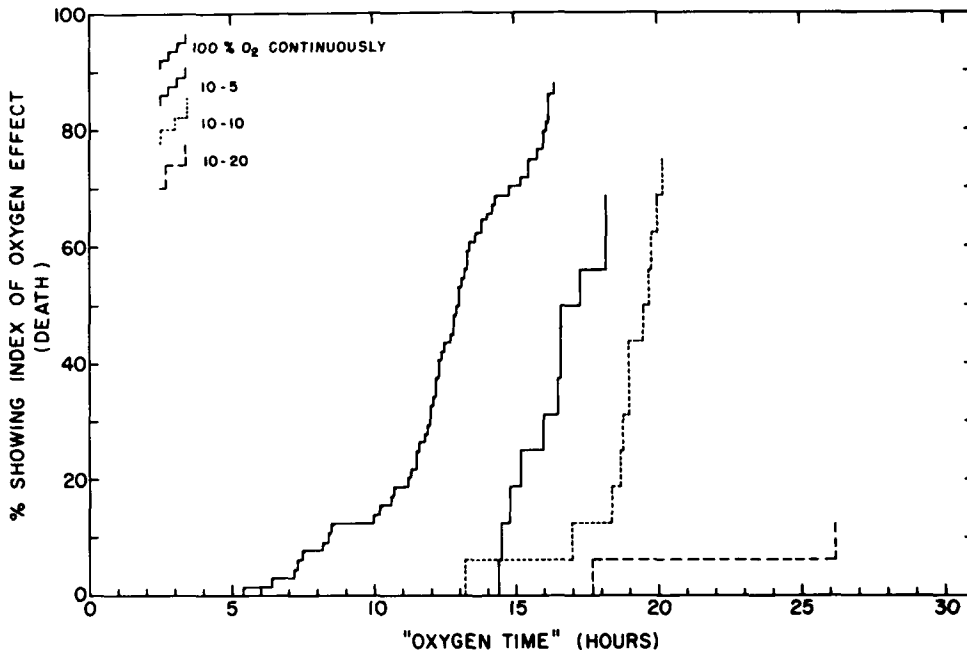
Fig. 8. Survival time in guinea pigs during continuous and intermittent oxygen breathing at 3 ATA. "Oxygen time" on the *abscissa* does not include intervals of normoxic exposure (7% O_2 in N_2 at 3 ATA). [From Hall (83)]

while holding the hyperoxic interval constant. The concept of intermittent hyperoxic exposure was quickly incorporated into the oxygen treatment tables that are now widely used by the U.S. Navy (84) as well as in support of other military and commercial diving operations throughout the world (85).

Recent experimental evidence shows conclusively that pulmonary oxygen tolerance in man can also be extended by programmed intermittency (Fig. 9). At an ambient pressure of 2 ATA, insertion of a 5-min normoxic interval after every 20 min of oxygen breathing greatly delays the occurrence of symptoms and progressive decrement in vital capacity relative to that found during continuous oxygen breathing (86). Once vital capacity begins to fall, however, its rate of decrease is similar to that for continuous exposure (Fig. 9).

Extension of oxygen tolerance by intermittent exposure has been evaluated in man only for the lung at a single oxygen pressure. Even at this pressure, it is unlikely that an optimal sequence of hyperoxic and normoxic intervals has been determined. Since both the rates of progression and resolution of
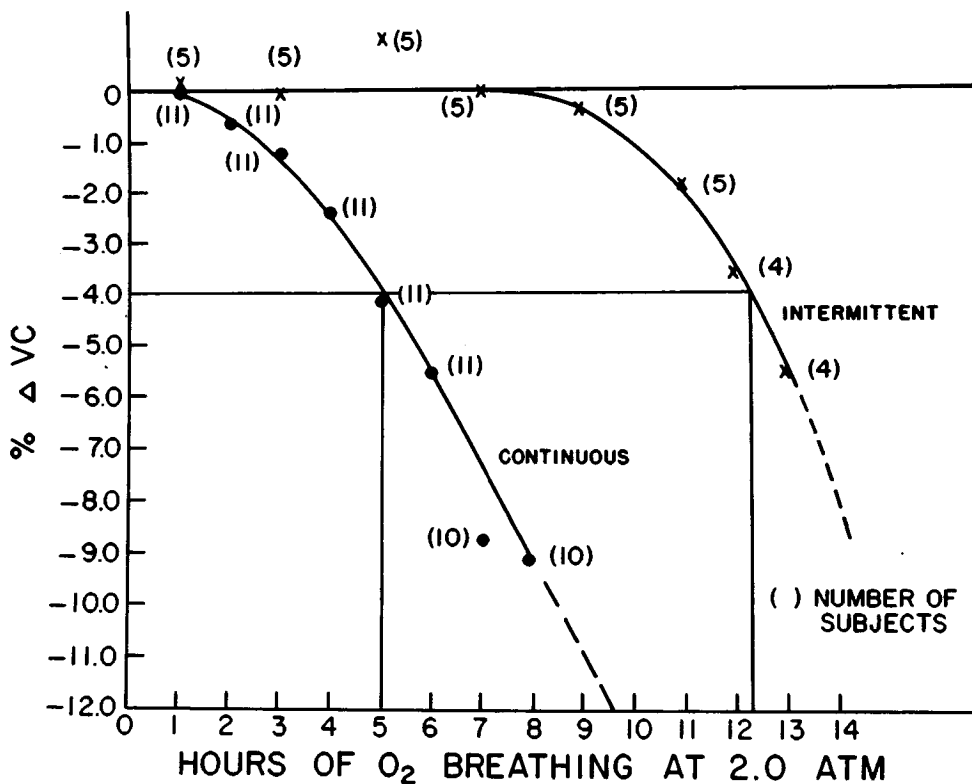
Fig. 9.   Extension of pulmonary oxygen tolerance at 2 ATA in man. The curve showing rate of decrease in vital capacity during continuous oxygen breathing is the same curve shown in Fig. 6 (74). The curve for intermittent oxygen exposure is from the data of Hendricks et al. (86), and the indicated duration of oxygen breathing represents a summation of all of the intermittent, 20-min oxygen intervals.

toxic effects can be expected to vary in different organs, optimal application of programmed intermittency over a range of useful oxygen pressures will require studies in many organs and at many levels of hyperoxia (12). This task could be accomplished most efficiently by the performance of related experiments in several different laboratories. It can be anticipated that programmed intermittency will prove to be the most effective and practical means of extending oxygen tolerance in many, if not all, of the numerous applications of hyperoxic exposure.

References

1. Priestley J. The discovery of oxygen (1775). Alembic Club Reprints No. 7. Chicago: Univ Chicago Press, 1906.
2. Bert P. Barometric pressure; researches in experimental physiology, translated by M.A. Hitchcock and F.A. Hitchcock. Columbus: College Book Co, 1943.
3. Smith JL. The pathological effects due to increased oxygen tension in the air breathed. J Physiol (London) 1899;24:19-35.
4. Bean JW. Effects of oxygen at high pressure. Physiol Rev 1945;25:1-147.
5. Stadie WC, Riggs BC, Haugaard N. Oxygen poisoning. Amer J Med Sci 1944;207:84-114.
6. Dickens F. The toxic effects of oxygen on brain metabolism and on tissue enzymes. Biochem J 1946;40:145-186.
7. Stadie WC, Riggs BC, Haugaard N. Oxygen poisoning. III. The effect of high oxygen pressures upon the metabolism of brain. J Biol Chem 1945;160:191-208.
8. Stadie WC, Riggs BC, Haugaard N. Oxygen poisoning. IV. The effect of high oxygen pressures upon the metabolism of liver, kidney, lung and muscle tissue. J Biol Chem 1945;160:209-216.
9. Donald KW. Oxygen poisoning in man. I and II. Brit Med J 1947;1:667-672, 712-717.
10. Behnke AR, Forbes HS, Motley EP. Circulatory and visual effects of oxygen at 3 atmospheres pressure. Amer J Physiol 1935;114:436-442.
11. Lambertsen CJ, Kough RH, Cooper, DY, Emmel GL, Loeschcke HH, Schmidt CF. Oxygen toxicity. Effects in man of oxygen inhalation at 1 and 3.5 atmospheres upon blood gas transport, cerebral circulation and cerebral metabolism. J Appl Physiol 1953;5:471-486.
12. Lambertsen CJ. Effects of hyperoxia on organs and their tissues. In: Robin ED, ed. Extrapulmonary manifestations of respiratory disease. Vol. 8 of Lenfant C, ed. Lung biology in health and disease. New York: Marcel Dekker, 1978: 239-303.
13. Clark JM, Lambertsen CJ. Pulmonary oxygen toxicity. A review. Pharmacol Rev 1971;23:37-133.
14. Gilbert DL. Atmosphere and evolution. In: Dickens F, Neil E, eds. Oxygen in the animal organism. New York: Macmillan, 1964:641-654.
15. Haugaard N. Cellular mechanisms of oxygen toxicity. Physiol Rev 1968;48:311-373.
16. Gerschman R. Biological effects of oxygen. In: Dickens F, Neil E, eds. Oxygen in the animal organism. New York: Macmillan, 1964: 475-494.
17. Chance B, Jamieson D, Williamson JR. Control of the oxidation reduction state of reduced pyridine nucleotides in vivo. In: Brown IW Jr, Cox BG, eds. Hyperbaric medicine. Proceedings of the third international conference on hyperbaric medicine. Washington: NAS-NRC Publ. 1404, 1966:15-41.
18. Kovachich GB, Mishra OP. Lipid peroxidation in rat brain cortical slices. J Neurochem (in press).
19. Jamieson D, Ladner K, van den Brenk, HAS. Pulmonary damage due to high pressure oxygen breathing in rats. 4. Quantitative analysis of sulfhydryl and disulphide groups in rat lungs. Aust J Exp Biol Med Sci 1963;41:491-497.
20. Dickens F. The toxic effect of oxygen on nervous tissue. In: Elliott KAC, Page IH, Quastel JH, eds. Neurochemistry. Springfield: Thomas, 1962:851-869.
21. Kovachich GB. Depression of $^{14}CO_2$ production from [U-^{14}C] glucose in brain slices under high-pressure oxygen: relationship between metabolic rate and tissue sensitivity to oxygen. J Neurochem 1980;34:459-462.

22. Kovachich GB, Haugaard N. Biochemical aspects of oxygen toxicity in the metazoa. In: Gilbert DL, ed. Oxygen and living processes: an interdisciplinary approach. New York: Springer-Verlag (in press).

23. Faulkner JM, Binger CAL. Oxygen poisoning in cold blooded animals. J Exp Med 1927;45:865-871.

24. Popovic V, Gerschman R, Gilbert DL. Effects of high oxygen pressure on ground squirrels in hypothermia and hibernation. Am J Physiol 1964;206:49-50.

25. Bean JW, Zee D. Metabolism and the protection by anesthesia against toxicity of O_2 at high pressure. J Appl Physiol 1965;20:525-530.

26. Grossman MS, Penrod KE. The thyroid and high oxygen poisoning in rats. Am J Physiol 1949;156:182-184.

27. Lambertsen CJ. Respiratory and circulatory actions of high oxygen pressure. In: Goff LG, ed. Proceedings of the underwater physiology symposium. Washington: NAS-NRC Publ. 377;1955:25-38.

28. Clark, JM. The toxicity of oxygen. Am Rev Resp Dis 1974;10:40-50.

29. Mayevsky A, Jamieson D, Chance B. Oxygen poisoning in the unaesthetized brain: correlation of the oxidation-reduction state of pyridine nucleotide with electrical activity. Brain Res 1974;76:481-491.

30. Mayevsky A, Chance B. A new long-term method for the measurement of NADH fluorescence in intact rat brain with chronically implanted cannula. In: Bicher HI, Bruley DF, eds. Oxygen transport to tissue. New York: Plenum, 1973:239-244.

31. Wood JD. Oxygen toxicity in neuronal elements. In: Lambertsen CJ, ed. Underwater physiology. Proceedings of the fourth symposium on underwater physiology. New York: Academic Press, 1971:9-17.

32. Wood JD, Watson WJ. Gamma-aminobutyric acid levels in the brain of rats exposed to oxygen at high pressures. Can J Biochem Physiol 1963;41:1907-1913.

33. Wood JD, Watson WJ, Ducker AJ. Oxygen poisoning in various mammalian species and the possible role of gamma-aminobutyric acid metabolism. J. Neurochem 1967;14:1067-1074.

34. Wood JD, Watson WJ, Murray GW. Correlation between decreases in brain gamma-aminobutyric acid levels and susceptibility to convulsions induced by hyperbaric oxygen. J Neurochem 1969;16:281-287.

35. Wood JD, Watson WJ, Clydesdale FM. Gamma-aminobutyric acid and oxygen poisoning. J Neurochem 1963;10:625-633.

36. Alderman J, Culwer BW, Shellenberger MK. An examination of the role of gamma-aminobutyric acid in hyperbaric oxygen induced convulsions in the rat. I. Effects of increased gamma-aminobutyric acid and protective agents. J Pharmacol Exp Ther 1974;190:334-340.

37. Faiman MD, Nolan RJ, Baxter CF, Dodd DE. Brain gamma-aminobutyric acid, glutamic acid decarboxylase, glutamate, and ammonia in mice during hyperbaric oxygenation. J Neurochem 1977;28:861-865.

38. Radomski MW, Watson WJ. Effect of lithium on acute oxygen toxicity and associated changes in brain gamma-aminobutyric acid. Aerosp Med 1973;44:387-392.

39. Kaplan SA, Stein SN. Effects of oxygen at high pressure on the transport of potassium, sodium and glutamate in guinea pig brain cortex. Am J Physiol 1957;190:157-162.

40. Allen JE, Goodman DEP, Besarab A, Rasmussen H. Studies on biochemical basis of oxygen toxicity. Biochim Biophys Acta 1973;320:708-728.

41. Pooley J, Walder DN. Changes in cell volume following hyperbaric exposure: a manifestation of oxygen toxicity. In: Bachrach AJ, Matzen MM, eds. Underwater physiology VII. Proceedings of the seventh symposium on underwater physiology. Bethesda, MD: Undersea Medical Society, 1981:45-53.

42. Banister EW, Singh AK. The central role of ammonia in OHP induced convulsions. In: Bachrach AJ, Matzen MM, eds. Underwater physiology VII. Proceedings of the seventh symposium on underwater physiology. Bethesda, MD: Undersea Medical Society, 1981:37-44.

43. Kovachich GB, Mishra OP, Clark JM. Depression of cortical NaK-ATPase activity in rats exposed to hyperbaric oxygen. Brain Res (in press).

44. Lambertsen, CJ, Ewing JH, Kough RH, Gould R, Stroud MW III. Oxygen toxicity. Arterial and internal jugular blood gas composition in man during inhalation of air, 100% O_2 and 2% CO_2 in O_2 at 3.5 atmospheres ambient pressure. J Appl Physiol 1955;8:255-263.

45. Clark JM. Effects of acute and chronic hypercapnia on oxygen tolerance in rats. J Appl Physiol: Respirat Environ Exercise Physiol (in press).

46. Forman HJ, Fisher AB. Anti-oxidant defenses. In: Gilbert DL, ed. Oxygen and living processes: an interdisciplinary approach. New York: Springer-Verlag (in press).

47. Kistler GS, Caldwell PRB, Weibel ER. Development of fine structural damage to alveolar and capillary lining cells in oxygen-poisoned rat lungs. J Cell Biol 1967;32:605-628.

48. Kapanci Y, Weibel ER, Kaplan HP, Robinson FR. Pathogenesis and reversibility of the pulmonary lesions of oxygen toxicity in monkeys. II. Ultrastructural and morphometric studies. Lab Invest 1969;20:101-118.

49. Fisher AB, Block EJ, Pietra GG. Environmental influences on uptake of serotonin and other amines. Environ Health Perspect 1980;35:191-198.

50. Block ER, Fisher AB. Depression of serotonin clearance by rat lungs during oxygen exposure. J Appl Physiol: Respirat Environ Exercise Physiol 1977;42:33-38.

51. Block ER, Fisher AB. Effect of hyperbaric oxygen exposure on pulmonary clearance of 5-hydroxytryptamine. J Appl Physiol: Respirat Environ Exercise Physiol 1977;43:254-257.

52. Winter PM, Gupta RK, Michalsky AH, Lanphier EH. Modification of hyperbaric oxygen toxicity by experimental venous admixture. J Appl Physiol 1967;23:954-963.

53. Fisher AB, Bassett DJP, Forman HJ. Oxygen toxicity of the lung: biochemical aspects. In: Fishman AP, Renkin EM, eds. Pulmonary edema. Bethesda, MD: ¡American Physiological Society, 1979:207-216.

54. McCord JM, Fridovich I. Superoxide dismutase, an enzymic function for erythrocuprein. J Biol Chem 1969;244:6049-6055.

55. Fridovich I. The biology of oxygen radicals. Science 1978;201:875-880.

56. Crapo JD, Tierney DF. Superoxide dismutase and pulmonary oxygen toxicity. Am J Physiol 1974;226:1401-1407.

57. Rosenbaum RM, Wittner M, Lenger M. Mitochondrial and other ultrastructural changes in great alveolar cells of oxygen-adapted and poisoned rats. Lab Invest 1969;20:516-528.

58. Yamamoto E, Wittner M, Rosenbaum RM. Resistance and susceptibility to oxygen toxicity by cell types of the gas-blood barrier of the rat lung. Am J Pathol 1970;59:409-436.

59. Crapo JD, Sjostrom K, Drew RT. Tolerance and cross-tolerance using No$_2$ and O$_2$. I. Toxicology and biochemistry. J Appl Physiol: Respirat Environ Exercise Physiol 1978;44:364-369.

60. Crapo JD, Marsh-Salin J, Ingram P, Pratt PC. Tolerance and cross-tolerance using No$_2$ and O$_2$. II. Pulmonary morphology and morphometry. J Appl Physiol: Respirat Environ Exercise Physiol 1978;44:370-379.

61. Forman HJ, Berman H, Furia L, Fisher A. Increased mitochondrial superoxide dismutase in lung type II epithelial cells from oxygen-exposed rats. Fed Proc 1979;38:1436.

62. Frank L, Bucher JR, Roberts RJ. Oxygen toxicity in neonatal and adult animals of various species. J Appl Physiol: Respirat Environ Exercise Physiol 1978;45:699-704.

63. Frank L, Yam J, Roberts RJ. The role of endotoxin in protection of adult rats from oxygen-induced lung toxicity. J Clin Invest 1978;61:269-275.

64. Frank L, Roberts RJ. Endotoxin protection against oxygen-induced acute and chronic lung injury. J Appl Physiol: Respirat Environ Exercise Physiol 1979;47:577-581.

65. Frank L, Chiang MJ, Massaro D. Protection from pulmonary oxygen toxicity by treatment with low doses of bacterial endotoxin. In: Bachrach AJ, Matzen MM, eds. Underwater physiology VII. Proceedings of the seventh symposium on underwater physiology. Bethesda, MD: Undersea Medical Society, 1981:65-74.

66. Tierney DF, Ayers L, Kasuyama RS. Altered sensitivity to oxygen toxicity. Am Rev Resp Dis 1977; 115:59-65.

67. Tierney D, Ayers L, Herzog S, Yang J. Pentose pathway and production of reduced nicotinamide adenine dinucleotide phosphate. Am Rev Resp Dis 1973;108:1348-1351.

68. Bassett DJP, Fisher AB. Glucose metabolism in rat lung during exposure to hyperbaric O$_2$. J Appl Physiol: Respirat Environ Exercise Physiol 1979;45:943-949.

69. Clark JM, Lambertsen CJ. Pulmonary oxygen tolerance and the rate of development of pulmonary oxygen toxicity in man at two atmospheres inspired oxygen tension. In: Lambertsen CJ, ed. Underwater physiology. Proceedings of the third symposium on underwater physiology. Baltimore: Williams & Wilkins, 1967; 439-451.

70 Bardin H, Lambertsen CJ. A quantitative method for calculating pulmonary toxicity. Use of the "Unit Pulmonary Toxicity Dose" (UPTD). Institute for Environmental Medicine Report, 1970.

71. Wright WB. Use of the University of Pennsylvania Institute for Environmental Medicine procedure for calculation of pulmonary oxygen toxicity. Experimental Diving Unit Report 2-72, 1972.

72. Lemaire C. Determination du taux d'hyperoxie acceptable pour les plongees au long cours par la mesure de la capacite vitale. Med Sub Hyp 1975;12:82-86.

73. Gardette B, Lemaire C. Variations de la capacite vitale en fonction de la quantite d'oxygene inhalee au cours des decompressions. Revue de Medecine Subaquatique et Hyperbare 1977;61:66-69.

74. Clark JM, Lambertsen CJ. Rate of development of pulmonary O_2 toxicity in man during O_2 breathing at 2.0 atm abs. J Appl Physiol 1971;30:739-752.

75. Fisher AB, Hyde RW, Puy RJM, Clark JM, Lambertsen CJ. Effect of oxygen at 2 atmospheres on the pulmonary mechanics of normal man. J Appl Physiol 1968;24:529-536.

76. Puy RJM, Hyde RW, Fisher AB, Clark JM, Dickson J, Lambertsen CJ. Alterations in the pulmonary capillary bed during early O_2 toxicity in man. J Appl Physiol 1968;24:537-543.

77. Haldane JBS. Human life and death at high pressures. Nature 1941;148:458-460.

78. Nichols CW, Lambertsen CJ, Clark JM. Transient unilateral loss of vision associated with oxygen at high pressure. Arch Ophthalmol 1969;81:548-552.

79. Faiman MD, Mehl RG, Oehme FW. Protection with disulfiram from central and pulmonary oxygen toxicity. Biochem Pharmacol 1971;20:3059-3067.

80. Faiman MD, Nolan RJ, Oehme FW. Effect of disulfiram on oxygen toxicity in beagle dogs. Aerosp Med 1974;45:29-32.

81. Deneke SM, Bernstein SP, Fanburg BL. Enhancement by disulfiram (antabuse) of toxic effects of 95-97% O_2 on the rat lung. J Pharmacol Exp Ther 1979;208:377-380.

82. Forman HJ, York JL, Fisher AB. Mechanism for the potentiation of oxygen toxicity by disulfiram. J Pharmacol Exp Ther 1980;212:452-455.

83. Hall DA. The influence of the systematic fluctation of P_{O_2} upon the nature and rate of the development of oxygen toxicity in guinea pigs. University of Pennsylvania: Graduate School of Arts and Sciences, 1967. (M.S. Thesis).

84. U.S. Navy diving manual. Washington: Navy Department, 1979. (NAVSEA 0994-LP-001-9010). Distributed by Best Bookbinders, Carson, CA.

85. Lambertsen CJ, ed. Decompression sickness and its therapy. Allentown, PA: Air Products and Chemicals, 1979.

86. Hendricks PL, Hall DA, Hunter WH Jr, Haley PJ. Extension of pulmonary O_2 tolerance in man at 2 ATA by intermittent O_2 exposure. J Appl Physiol: Respirat Environ Exercise Physiol 1977;42:593-599.

MECHANISM(S) OF CENTRAL OXYGEN TOXICITY: A RE-EVALUATION

M. D. Faiman, R. J. Nolan, D. E. Dodd, J. M. Waechter, R. C. Dirks, K. Haya, and J. A. Zempel

The deleterious effect of oxygen has been recognized for almost a century. However, the mechanism(s) by which high oxygen pressure (OHP) produces convulsions or other toxic manifestations remains unresolved. Although several theories have been suggested to explain the cause of central oxygen toxicity, no single hypothesis has received universal acceptance.

It has been suggested by several investigators that acute oxygen toxicity may be due to the effects of molecular oxygen on a few particularly sensitive and critical enzymes (1). The specific mechanisms of oxygen toxicity proposed involved reversible oxidation of sulfhydryl groups either on the enzymes per se or on nonprotein cofactors involved in enzymatic activity. Oxidation of sulfhydryls bound to lysosomal or mitochondrial membranes also has been cited as the cause of oxygen toxicity. The concept that OHP causes oxidation of thiol groups seems supported by several lines of evidence. First, sulfhydryl dehydrogenases have been shown to be inactivated by hyperbaric oxygen in vivo (1). Secondly, in vivo OHP studies with lung (2–5) and liver (5) have shown a decrease in sulfhydryl and an increase in disulfide content. Finally, many thiol and disulfide compounds delay the onset of oxygen-induced convulsions (7).

The formation of free radicals also has been suggested to play an important role in the initiation of central oxygen toxicity. The formation of free radicals by OHP was originally proposed by Gerschman and associates (6) who found a high degree of correlation between drugs protecting against oxygen toxicity and drugs protecting against x-irradiation. Furthermore, when oxygen and x-irradiation were combined a synergistic action was observed (8). Superoxide anion, a free radical, has been studied extensively with respect to oxygen toxicity. The superoxide anion is formed by the one-electron election re-

duction of oxygen; therefore it is a logical component in oxygen toxicity mechanisms. Support for the role of the superoxide anion in OHP toxicity comes from the finding that superoxide dismutase (SOD) catalyzes the dismutation of the superoxide anion and that SOD is ubiquitous in all oxygen metabolizing cells (9).

Hydrogen peroxide and lipid peroxides are intimately associated with free radical mechanisms. Zirkle et al. (10) observed an increase in brain lipid peroxides by OHP and proposed that lipid peroxidation may be responsible for cellular membrane disruption and/or enzyme inhibition. Becker and Galvin (11) found an increase in cerebral lipid peroxides but were unable to find any correlation between lipid peroxidation and the susceptibility to oxygen-induced convulsions. Since reduced glutathione (GSH) has been associated with lipid peroxide inactivation through enzymatic mechanisms (12), any observed changes in glutathione content by OHP have been attributed to lipid peroxide formation (13).

Gamma-aminobutyric acid (GABA) is a putative inhibitory neurotransmitter and has been implicated in oxygen convulsions. In studies by Wood and coworkers (14), OHP was found to decrease brain GABA with the magnitude of decrease in GABA correlated with seizure susceptibility. Furthermore, GABA administered i.p. protected animals against oxygen convulsions. The protective effect of GABA has been explained by Wood and Peesker (15) by relating the excitable state of the brain to the level of glutamic acid decarboxylase (GAD) activity and GABA content.

The apparent reliance of the brain on an uninterrupted supply of energy, and the in vitro observations that OHP inhibits numerous enzymes involved in brain energy metabolism, has led many investigators to propose that oxygen-induced seizures may be due to a disturbance in brain energy metabolism. Sanders et al. (16) found that brain adenosine triphosphate (ATP) fell before the onset of seizures. Succinate prevented the fall in ATP and delayed the appearance of the seizure. Based on these observations, Sanders et al. (16) concluded that OHP-induced seizures were the result of a fall in brain energy reserves.

High oxygen pressure has been found to cause oxidation of reduced pyridine nucleotides in isolated mitochondria and in tissues of the brain, kidney, and liver (17). As a result of these rapid oxidations, these changes in pyridine nucleotides were believed to play a role in oxygen-induced seizures. More recently, Mayevsky et al. (18) using surface fluorometry observed an association between pyridine nucleotide oxidation and electrical activity in brain cortex of unanesthetized oxygen-poisoned rats.

In light of the several hypotheses attempting to explain the toxic effects of OHP on the central nervous system, detailed studies were carried out to re-evaluate these earlier concepts. In these investigations, we exposed mice to OHP for various time periods, determined changes in biochemical parameters, and correlated these changes with seizure susceptibility.

METHODS

Animals

In all experiments male Swiss-Webster albino mice (HA/ICR, Madison, WI) weighing 25–38 g were used. Animals were quartered under a 12–h light-dark cycle with food and water available ad libitum.

Oxygen Exposures

The possible effects of circadian rhythms were minimized by conducting all oxygen exposures in the morning. Animals were subjected to euthanasia while still under pressure in a modified hyperbaric chamber. The hyperbaric chamber was constructed from a Plexiglas cylinder having a capacity of 25 L. The chamber floor was fitted with a platform containing a trap door that opened over a container of liquid nitrogen. The trap door could be opened at any time by activating an external mechanism. The temperature in the chamber was maintained at 25°C ± 1°. At the end of the 13-min flush and compression period, mice were exposed to 6 ATA of 100% O_2 for the various time periods under study. During all exposures, oxygen was metered through the chamber at a rate of 4 L/min to prevent the accumulation of carbon dioxide, nitrogen, or water vapor.

Oxygen Studies

Mice exposed to oxygen but which exhibited no convulsions or other signs of oxygen toxicity were referred to as preconvulsed animals. In these studies two mice were placed inside the hyperbaric chamber, the chamber was then pressurized to 6 ATA. Mice were exposed to the 6 ATA 100% O_2 pressure for either 0, 4, 8, 12, and 16 min depending upon the particular study. These time intervals corresponded to 0, 25, 50, 75, and 100% of the CT_{50}, where the CT_{50} is the time taken for 50% of the mice to convulse.

Other stages of oxygen toxicity investigated were a hyperactive state, characterized by rapid running around the chamber by the mice; a convulsive state; and a postconvulsive stage.

Tissue Analysis

After the animals were subjected to euthanasia, they were removed from the chamber, decapitated, the brain removed, and the cortex excised. For tissue analysis, $NADP^+$, NADPH, NAD^+, and NADH were determined by enzymatic cycling methods of Burch et al. (19); ATP and phosphocreatine (PC) by the methods of Lowry et al. (20); GABA by the method of Collins (21); GAD and gamma aminobuytric acid-transminase (GABA-T) by the method of Van Gelder (22); and glutamate by the method of Folkergrová et al. (23). Oxi-

dized glutathione (GSSG) was determined by the method of Halprin and Ohka-
wara (24). Reduced glutathione was calculated by substraction of GSSG from
the total GSH and GSSG. Nonprotein sulfhydryl (total thiol) was determined
by the method of Owens and Belcher (25). Lipid peroxidation was determined
by the thiobarbituric acid method of Jerret et al. (26) modified by adding
0.003 M of EDTA to the homogenizing solution and by the diene conjugation
method of Recknagel and Ghoshal (27).

RESULTS

Exposure of mice to 6 ATA 100% O_2 had no effect on cerebral ATP or
PC before convulsions, at seizure onset, or 10 s postconvulsions (Fig. 1). The
effect of OHP on cortical pyridine nucleotides is shown in Figs. 2 and 3. As
soon as the mice were exposed to the high oxygen pressure, the NAPD$^+$/
NADPH ratio began to increase (Fig. 2). For example, after the 3-min flush
period, the NADP$^+$/NADPH ratio increased by approximately 8%; by the time
the hyperbaric chamber reached 6 ATA, the ratio had increased to 25%. This
increase remained constant throughout the exposure period, including the var-
ious stages of oxygen toxicity. Cortical NADP$^+$ was increased maximally by
the time the oxygen pressure in the chamber reached 6 ATA, while the maxi-
mal decrease in NADPH occurred after 16 min of oxygen exposure. In a sepa-
rate series of experiments, the effect of OHP on cortical NAD$^+$ and NADH
was investigated (Fig. 3). Statistically significant decreases of approximately
20% in cortical NADH were found in mice exposed to 6 ATA of 100% O_2 for
0 and 16 min during hyperactivity, seizure onset, and postconvulsion. Cerebral
NAD$^+$ did not appear to differ significantly from corresponding controls.
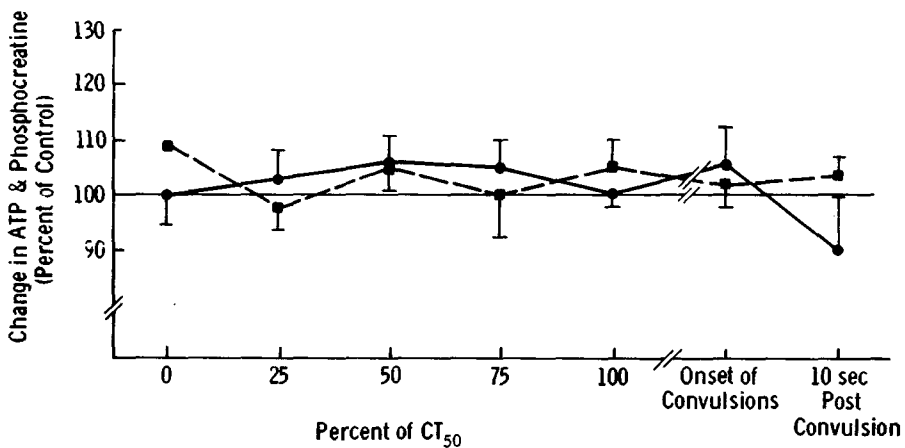
Fig. 1.   Mice were exposed to 6 ATA 100% O_2 for 0, 4, 8, 12, and 16 min, which corresponds to 0, 25,
50, 75, and 100% of the CT_{50}, or until they exhibited convulsions. The CT_{50} was 16 min. ATP (●) and
phosphocreatine (■) was determined (see Methods). Each value is the mean ± SE for 6 mice. The solid line
represents the control values, which were 2.06 ± 0.03 for ATP and 3.24 ± 0.06 mM/kg for phosphocreatine.
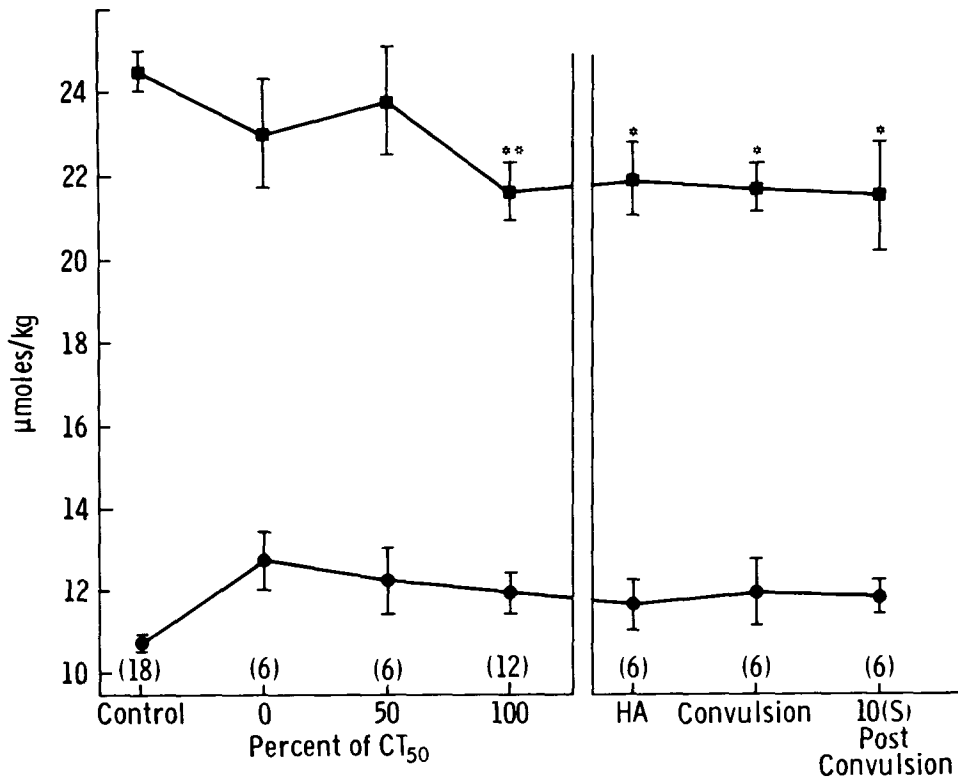
Fig. 2. Mice were exposed to 6 ATA 100% O_2 for 0, 8, and 16 min, or until they exhibited hyperactivity or convulsions. The exposure periods reflect the 0, 50, and 100% of the CT_{50}. $NADP^+$ (●) and NADPH (■) were determined (see Methods). Each point is the mean ± SE. Numbers of mice in parenthesis. *$P < 0.05$; **$P < 0.01$.

The effect of OHP on cerebral oxidized and reduced glutathione also was studied. Exposure of mice to 100% O_2 until animals became hyperactive had no effect on cortical glutathione (Table I). Furthermore, no effect on oxidized or reduced glutathione, or nonprotein sulfhydryl was found in mice made vitamin E deficient for 10 weeks (Table II).

Lipid peroxidation in cerebral cortex by OHP also was investigated by exposing mice to 6 ATA 100% O_2 for either 16 min or seizure onset. No OHP-induced lipid peroxidation in oxygen-exposed mice was found (Table III).

It also has been proposed that OHP decreases brain GABA and changes in both GABA and GAD contribute to the susceptibility of mice to oxygen convulsions. Although OHP decreased cortical GABA and GAD, no relationship was apparent between the susceptibility of mice to oxygen convulsions and decreases in either GABA or GAD (Table IV).
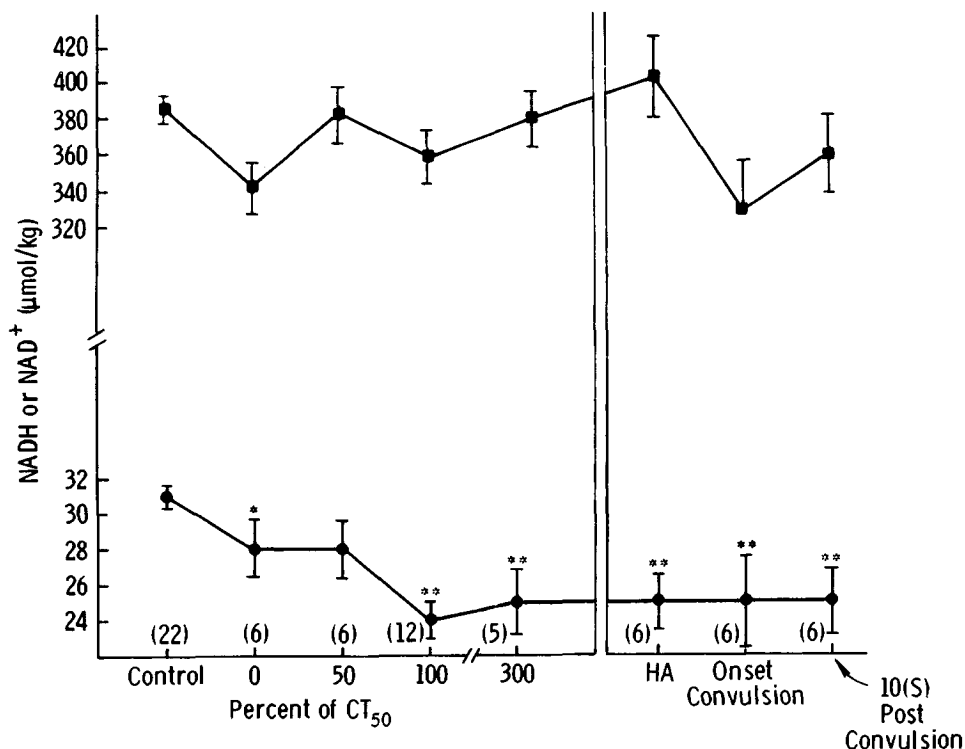
Fig. 3. Mice were exposed to 6 ATA 100% O_2 for 0, 8, 16, 48, or until they exhibited hyperactivity or convulsions. The exposure periods reflect the 0, 50, 100, and 300% of the CT_{50}. NAD^+ (■) and NADH (●) were determined (see Methods). Each point is the mean ± SE. Number of mice in parenthesis. *$P < 0.05$; **$P < 0.01$.

DISCUSSION

Although the toxic effects of OHP have been known for almost 100 years, the mechanism by which oxygen causes its toxic manifestations is both unknown and speculative. Furthermore, the question whether the mechanism(s) for oxygen toxicity in different organs (CNS, lung, eye, etc.) is similar is controversial.

As a result of the initial findings of Sanders et al. (16), it was expected that oxygen would cause a decrease in cerebral high energy phosphates before the onset of seizures. However, no decrease was observed (Fig. 1). The possibility exists that a fall in high energy phosphates was not detected because a) oxygen caused a precipitous decrease in these substances just before the seizure, and b) by excluding mice exhibiting symptoms of toxicity, those animals in which cerebral ATP and PC were reduced were selectively eliminated. However, this does not appear to be the case as evidenced by the findings that neither ATP or PC decreased in mice sacrificed at the onset of seizures, or

TABLE I

Cortical GSSG, Nonprotein Sulfhydryl (NPSH), and Total Glutathione
(GSH + GSSG) During Exposure to 6 ATA O$_2$

Treatment	GSSG	NPSH	Total Glutathione
Control	0.150 ± 0.010	2.64 ± 0.11	2.48 ± 0.07
Hyperactivity	0.158 ± 0.007	2.55 ± 0.08	2.46 ± 0.08

Mice were exposed to 6 ATA 100% O$_2$ until they exhibited hyperactivity. Each value is the mean ± SE of six mice.

10 s after seizures. These results therefore suggest that oxygen-induced convulsions are not due to a single fall in cerebral high energy reserves. This conclusion appears consistent with the findings of Teng and Harris (28) and Chance et al. (29).

In the studies investigating the effect of OHP on pyridine nucleotides, OHP increased the cortical NADP$^+$/NADPH ratio at all stages of oxygen toxicity. The increased NADP$^+$/NADPH ratio was generally associated with significant decreases in NADPH (Fig. 2). Cortical NADP$^+$ was higher than controls in all oxygen treatments. High pressure oxygen also increased the NAD$^+$/NADH ratio at all stages of oxygen toxicity with an increase in the ratio generally caused by a decreased NADH (Fig. 3). The in situ fluorometry studies by Chance et al. (29) and Mayevsky et al. (18) suggest that OHP-induced changes in reduced pyridine nucleotides (NADPH and NADH) may contribute to biochemical alterations of sufficient magnitude to produce convulsions. Mayevsky et al. (18) identified three stages of pyridine nucleotide oxidation in rats exposed to 6 ATA 100% O$_2$: a) an oxidized stage caused by OHP before seizures, b) an oxidation stage concurrent with convulsions, and c) an oxidation wave following convulsions (spreading depression). The results from the present study (Figs. 2,3), however, do not appear to support the association of pyridine nucleotide oxidation with oxygen convulsions. For example, marked changes in cerebral NADPH and NADH were not found before seizure onset. Furthermore, mice exposed to 1, 3.5, and 6 ATA O$_2$ for 16 min had similar changes in reduced pyridine nucleotides. Yet the CT$_{50}$ values of mice exposed to 1, 3.5, and 6 ATA O$_2$ has been found in our laboratory to be 960, 102, and 16 min, respectively.

Previous investigators have considered the role of sulfhydryl oxidation in oxygen toxicity. However, these studies have been concerned primarily with the lung (2,4). Nishiki et al. (5) found that in the isolated perfused lung, oxygen caused an increased release of GSSG when rats were vitamin E deficient; no effect of oxygen on GSSG release was found in normally fed animals. It is generally assumed that toxic oxidants such as peroxides formed by OHP (5,10,26) may be inactivated through enzymatic mechanisms with reduced GSH (12). Maintenance of glutathione in the reduced state requires both NADPH and glutathione reductase with the availability of NADPH associated

TABLE II

Cortical GSSG, Nonprotein Sulfhydryl (NPSH), and Total Glutathione (GSH + GSSG) during exposure to 6 ATA O$_2$

Treatment	GSSG (μM/g wet weight)		NPSH (μM/g wet weight)		Total Glutathione (μM/g wet weight)	
	Vit. E Def.	Vit. E Def./Starved	Vit. E Def.	Vit. E Def./Starved	Vit. E Def.	Vit. E Def./Starved
Control	0.167 ± 0.015	0.143 ± 0.011	2.81 ± 0.05	2.79 ± 0.06	2.86 ± 0.08	2.56 ± 0.15
Oxygen	0.161 ± 0.009	0.172 ± 0.012	2.74 ± 0.06	2.92 ± 0.06	2.73 ± 0.16	3.03 ± 0.11
Hyperactivity	0.161 ± 0.008	0.156 ± 0.005	2.69 ± 0.04	2.71 ± 0.02	2.69 ± 0.16	2.82 ± 0.13

Mice were exposed to 6 ATA 100% O$_2$ for 16 min or until hyperactive. Each value is the average of 5 mice ± SE. Starved mice were fasted for 38-42 h before oxygen exposure.

TABLE III

Effect of 6 ATA O_2 on Mouse Brain Lipid
Peroxidation

DIENE CONJ. TBA	Brain Region	
	Cortex	Midbrain
Control	0.84 ± 0.15	0.74 ± 0.30
	16.11 ± 0.24	7.62 ± 0.41
Oxygen (16 min)	0.83 ± 0.15	0.78 ± 0.25
	14.79 ± 0.25	7.00 ± 0.41
Oxygen (Convulsed)	1.0 ± 0.23	0.80 ± 0.60
	15.51 ± 0.20	6.16 ± 0.44

Diene Conjugation: Absorbance/gram wet weight. *Thiobarbituric Acid (TBA):* nMoles Malonaldehyde/gram wet weight.
Male Mice Exposed to 6 ATA 100% O_2 for 16 min, or until onset of convulsions. Each value is the average of 6 mice ± SE.

with the hexose monophosphate shunt. It has been shown that the hexose monophosphate shunt serves a major role in the guinea pig brain for maintenance of reduced glutathione (30), and the $NADP^+$/NADPH ratio has been observed to play a regulatory function on hexose monophosphate dehydrogenases. It has been suggested that removal of endogenously formed peroxides by GSH may preserve neuronal integrity (12). In our studies, however, no change in GSH

TABLE IV

Effect of 6 ATA O_2 on Cerebral GABA

Exposure Time	GABA (μmol/g)	Glu (μmol/g)	GAD (μmol/g/h)	GABA-T (μmol/g/h)
Control	4.32 ± 0.8	15.59 ± 0.33	22.5 ± 1.8	70.6 ± 3.3
0 min (% of Control)	3.33 ± 0.16† (77)	14.03 ± 0.56* (90)	21.6 ± 1.3 (96)	62.6 ± 3.4 (89)
16 min (% of Control)	3.32 ± 0.13† (77)	13.92 ± 0.21* (89)	19.3 ± 1.2 (86)	67.2 ± 2.6 (95)
Convulsed (% of Control)	3.30 ± 0.14† (76)	13.24 ± 0.30† (85)	21.7 ± 0.9 (96)	61.4 ± 2.2 (87)

Male mice were exposed to 6 ATA 100% O_2 for 0(0% of CT_{50}), 16 min (100% of CT_{50}), or until seizure onset. Animals were sacrificed without chamber decompression and cerebral cortex removed. Each value is the mean ± SE of 6 mice. *Significant ($P<0.05$) from control; †Significant ($P<0.01$) from control.

or GSSG was evident in brains of mice exposed to OHP for various stages of oxygen toxicity, or in mice made vitamin E deficient by dietary manipulation, even though NADPH was decreased. Thus, although lung GSH has been found to be decreased by OHP, brain appears to be more resistant.

Under OHP conditions, oxygen itself may initiate formation of radicals such as superoxide anion (9) or hydrogen peroxide (26,31). Superoxide anion also has been implicated in pulmonary oxygen toxicity (13,32). An indirect measure of free-radical formation is lipid peroxidation. In our studies, however, no increase in lipid peroxidation in cerebral cortex was found in mice exposed to OHP, which is in contrast to the proposed formation of lipid peroxides in lung (5).

Although Wood and coworkers (14) have provided considerable evidence for a central role of GABA in oxygen-induced convulsions, the exact involvement of GABA is still not clear. Furthermore, although oxygen decreases brain GABA, the mechanism by which this occurs remains speculative. Exposure of mice to 6 ATA 100% O_2 decreased brain GABA by approximately 25% (Table IV) as soon as the 6-ATA pressure was reached, and it remained at this lower level throughout the oxygen exposure period including the onset of seizures. Cerebral GAD also decreased, but this decrease was found only at the 16-min exposure period (Table IV). Our studies do not seem to support a role for GABA in oxygen convulsions. For example, similar decreases in GABA were found at 0- and 16-min exposures (0 and 100% of the CT_{50}), yet no evidence of CNS toxicity was apparent at the 0-min exposure. Even though it has been suggested that both GABA and GAD need to be considered in explaining the onset of oxygen convulsions (15), the RE_{GABA} term calculated in our studies at seizure onset is considerably higher (97.5%) than the 65% critical value proposed by Wood and Peesker (15). Furthermore, pretreatment with gabaculine, a GABA-T inhibitor that markedly increased brain GABA, had no effect on seizure susceptibility (33). In addition, treatment with disulfiram, a CNS oxygen protectant (7) did not prevent the decrease in brain GABA, yet protected against oxygen convulsions (34). Finally, the relationship between GABA synthesis and metabolism is extremely complex, and a mathematical derivation indicated that the percentage change in GABA is dependent on the percentage change in GAD, the K_m for GABA-T, the V_{max} for GAD and GABA-T, and the concentration of brain GABA.

In conclusion, oxygen-induced convulsions do not appear to be correlated with changes in ATP and PC, or pyridine nucleotide oxidation. Furthermore, cerebral GSH/GSSG is not altered in oxygen-exposed mice, and lipid peroxidation does not occur. In addition, brain GABA levels per se do not appear to influence the susceptibility of mice to oxygen convulsions. Thus, it appears that new theories are needed to explain the mechanism(s) of central oxygen toxicity. Furthermore, free-radical formation and subsequent lipid peroxidation as well as increased thiol oxidation have been found in lung and have been suggested as possible mechanisms in pulmonary oxygen toxicity; therefore, the mechanism by which oxygen induces central and pulmonary toxicity may indeed be different.

Acknowledgments

References

1. Haugaard N. Cellular mechanisms of oxygen toxicity. Physiol Rev 1968;48:311-373.
2. Jamieson D, Ladner K, van den Brenk HAS. Pulmonary damage due to high pressure oxygen breathing in rats. IV. Quantitative analysis of sulphydryl and disulphide groups in rat lungs. Aust J Exp Biol Med Sci 1963;41:491-498.
3. Harris JW, van den Brenk HAS. Comparative effects of hyperbaric oxygen and pentylenetetrazol on lung weight and non-protein sulfhydryl content of experimental animals. Biochem Pharmacol 1968;17:1181-1188.
4. Willis RJ, Kratzing CC. Changes in levels of tissue nucleotides and glutathione after hyperbaric oxygen treatment. Aust J Exp Biol Med Sci 1972;50:725-729.
5. Nishiki K, Jamieson D, Oshino N, Chance B. Oxygen toxicity in the perfused rat liver and lung under hyperbaric conditions. Biochem J 1976;160:343-355.
6. Gerschman R, Gilbert DL, Caccamise D. Effects of various substances on survival times of mice exposed to different high oxygen tensions. Am J Physiol 1958;192:563-571.
7. Faiman MD, Mehl RG, Oehme FW. Protection with disulfiram from central and pulmonary oxygen toxicity. Biochem Pharmacol 1971;20:3059-3067.
8. Gerschman R. Biological effects of oxygen. In: Oxygen in the animal organism. MacMillan Co. 1964:475-492.
9. McCord JM. Keele BB Jr, Fridovich I. An enzyme based theory of obligate anaerobiosis: the physiological function of superoxide dismutase. Proc Natl Acad Sci 1971;68:1024-1027.
10. Zirkle LG Jr, Mengel CE, Horton BD, Duffy EJ. Studies of oxygen toxicity in central nervous system. Aerospace Med 1965;36:1027-1032.
11. Becker NH, Galvin JF. Effect of oxygen-rich atmospheres on cerebral lipid peroxides. Aerospace Med 1962;33:985-987.
12. Christophersen BO. Formation of monohydroxy-polyenic fatty acids from lipid peroxides by a glutathione peroxidase. Biochem Biophys Acta 1968;164:35-46.
13. Kimball RE, Reddy K, Peirce TH, Schwartz LW, Mustafa MG, Cross CE. Oxygen toxicity: augmentation of antioxidant defense mechanisms in rat lung. Am J Physiol 1976;230:1425-1431.
14. Wood JD. The role of γ-aminobutyric acid in the mechanism of seizures. Prog Neurobiol 1975;5:77-95.
15. Wood JD, Peesker SJ. The anticonvulsant action of GABA-elevating agents: A re-evaluation. J Neurochem 1975;25:277-282.
16. Sanders AP, Hall IH, Cavanaugh PJ, Woodhall B. Effects of hyperbaric oxygen on metabolism. I. ATP concentration in rat brain, liver and kidney. Proc Soc Exp Biol Med 1966;121:32-34.
17. Chance B, Jamieson D, Coles H. Energy-linked pyridine nucleotide reduction: inhibitory effects of hyperbaric oxygen in vitro and in vivo. Nature 1965;206:257-263.
18. Mayevsky A, Jamieson D, Chance B. Oxygen poisoning in the unanesthetized brain: correlation of the oxidation-reduction state of pyridine nucleotides with electrical activity. Brain Res 1974;76:481-491.
19. Burch HB, Bradley ME, Lowry OH. The measurement of triphosphopyridine nucleotide and reduced triphosphopyridine nucleotide and the role of hemoglobin in producing erroneous triphosphopyridine nucleotide values. J Biol Chem 1967;242:4546-4554.
20. Lowry OH, Passonneau JV, Hasselberger FX, Schulz DW. Effect of ischemia on known substrates and cofactors of the glycolytic pathway in brain. J Biol Chem 1964;239:18-30.
21. Collins GGS. GABA-2 oxoglutarate transaminase, glutamate decarboxylase, and the half-life of GABA in different areas of rat brain. Biochem Pharmacol 1972;21:2849-2859.
22. Van Gelder NM. Glutamate dehydrogenase, glutamic acid decarboxylase and GABA amino transferase in epileptic mouse cortex. Can J Physiol Pharmacol 1974;52:952-959.

23. Folbergrová J, Passonneau JV, Lowry OH, Schulz DW. Glycogen, ammonia and related metabolites in the brain during seizures evoked by methionine sulphoximine. J Neurochem 1969;16:191-203.

24. Halprin KM, Ohkawara. The measurement of glutathione in human epidermis using glutathione reductase. J Invest Derm 1967;48:149-152.

25. Owens CWI, Belcher RV. A colorimetric micro-method for the determination of glutathione. Biochem J 1965;94:705-711.

26. Jerrett SA, Jefferson D, Mengel CE. Seizures, H_2O_2 formation and lipid peroxides in brain during exposure to oxygen under high pressure. Aerosp Med 1973;44:40-44.

27. Recknagel RO, Ghoshal AK. Quantitative estimation of peroxidative degeneration of rat liver microsomal and mitochondrial lipids after carbon tetrachloride poisoning. Exp Mol Path 1966;5:413-426.

28. Teng SS, Harris JW. Effect of hyperbaric oxygen on cellular dehydrogenases and sulphydryls. Exp Cell Res 1970;60:451-453.

29. Chance B, Jamieson D, Williamson JR. Control of the oxidation-reduction state of pyridine nucleotides in vivo and in vitro by hyperbaric oxygen. In: Proceedings of Third International Conference on Hyperbaric Medicine. Washington DC: National Academy of Sciences, National Research Council, 1966:15-41.

30. Hotta SS, Seventko JM, Jr. The hexomonophosphate shunt and glutathione reduction in guinea pig brain tissue: changes caused by chlorpromazine, amytal, and malonate. Archs Biochem Biophys 1968;123:104-108.

31. Boveris A, Chance B. The mitrochondrial generation of hydrogen peroxide: general properties and effects of hyperbaric oxygen. Biochem J 1973;134:707-716.

32. Crapo JD, Tierney DF. Superoxide dismutase and pulmonary oxygen toxicity. Am J Physiol 1974;226:1401-1407.

33. Faiman MD, Katsuji J, Zempel JA. GABA metabolism in O_2-induced convulsions. Brain Res Bull 1980; (in press).

34. Faiman MD, Nolan RJ, Baxter CF, Dodd DE. Brain γ-aminobutyric acid, glutamic acid decarboxylase, glutamate and ammonia in mice during hyperbaric oxygenation. J Neurochem 1977;28:861-865.

THE CENTRAL ROLE OF AMMONIA IN OHP-INDUCED CONVULSIONS

E. W. Banister and A. K. Singh

Ammonia is formed extensively in many tissues during the course of normal metabolism and its rate of formation is considerably increased during abnormal states.

Ammonia is released to blood from muscle in particularly large amounts during exercise (1) and by both tetany and convulsions (2). In muscle ammonia formation is accompanied by a decrease in the level of total adenine mononucleotides (3). Ammonia production from both nerve tissue and brain slices by electrical stimulation is well documented (4,5).

Lowenstein (6) has observed that the amount of ammonia formed by brain slices during electrical stimulation greatly exceeds the amount that could be formed by deamination of adenine nucleotides alone, and that an additional probable source is deamination of amino acids via aspartate or glutamate.

Iversen and Simmonds (7) have reported the normal rate of synthesis of norepinephrine stores in rat brain stem and mesencephalon to be 0.109 $\mu g \cdot g^{-1} hr^{-1}$, which is elevated to 0.152 $\mu g \cdot g^{-1} hr^{-1}$ after electroconvulsive shock treatment.

Schildkraut et al. (8) have also observed an increased turnover of brain catecholamines mediated by lithium ions and oxygen exposure. They proposed an enhanced intraneuronal discharge and deamination of catecholamines to account for this observation. This implication of brain catecholamines as a definite source of brain ammonia during periods of intense oxidative activity is important.

The experiments reported here investigated:

1) The time course of change in the concentration of gamma-aminobutyric acid (GABA), ammonia, glutamate, glutamine, adrenaline, and norepinephrine in oxygen toxicity; and

2) Catecholamines as a potential source of ammonia during exposures to high oxygen pressure (OHP).

METHODS AND MATERIALS

Animal Groups

Time course of brain and blood metabolites during hyperoxia. Groups of rats (*n* = 5) were allocated to control and oxygen exposure up to the production of convulsive activity. Blood and brain samples were taken for analysis of GABA (brain only) ammonia, adrenaline and noradrenaline, glutamate and glutamine.

Catecholamines as a potential ammonia source during oxygen exposure. Groups of rats (*n* = 5) were exposed to high pressure oxygen after drug treatment with 6-hydroxy dopamine, hexamethonium, α-methyl-p-tyrosine, or with adrenalectomy, respectively, to alter the concentration of catecholamines in the blood or brain. Ammonia, glutamate, glutamine; GABA (brain only), adrenaline and noradrenaline concentrations were measured in blood and brain tissues of both control and oxygen-convulsed animals (9).

Chamber Operations

A small chamber of about 100 L was used for hyperbaric oxygenation of animals. All animals were exposed singly for the stated time and experimental condition. Oxygen was flushed through the pressure chamber after the animal was placed in it at a rate of 5 L/min and pressurized up to 72.5 psig. The pressurization was completed over a period of 6 min and thereafter gas flow was maintained at 5 L/min to minimize carbon dioxide accumulation. After specific time intervals or after convulsions, the rats were decompressed with stops of 4 min at 40 psig and 1 min at 30 psig, followed by 3 min of continuous, slow decompression to ambient pressure.

Under these experimental conditions, 10 min elapsed between the beginning of decompression and collection of blood and brain tissue. Thus a rat exposed for 10 min lived a further 10 min before being killed. Because in this experiment interest was in the collection of blood as well as brain, a liquid-nitrogen freezing technique was not used.

Collection of Blood and Brain Samples

Blood and brain samples were taken and analyzed as described previously (4). Briefly, the abdomen of each animal was opened under light ether anesthesia and blood was taken from the bifurcation of the abdominal aorta. The animal was decapitated and the brain was removed intact. The time interval between the development of anesthesia and the removal and freezing of brain

tissues was never more than 2 min. Up to the time of decapitation the animal was respiring; from this point to the point of rapid freezing of the intact brain was less than 1 min.

Blood samples were centrifuged and the serum separated. Part of the serum was processed immediately for estimation of ammonia and amino acids and the remainder was frozen with glutathione at $-20°C$ for later estimation of catecholamines.

Brain samples were frozen rapidly in liquid nitrogen. These samples were later analyzed for ammonia, amino acids, and catecholamines.

Biochemical Analysis

Catecholamines. Serums were centrifuged with S-adenosyl-L-(methyl-^{3}H) methionine and catechol-o-methyltransferase for 1 h. After incubation, the metanephrines were separated by thin-layer chromatography extracted by toluene, and the radioactivity was determined in each fraction (10).

Brain Catecholamines. Brain samples were homogenized with cold 0.2 N perchloric acid (1:4, v/w) and centrifuged. The pH of the supernatant was adjusted to 7.5 and 0.1 mL was used for estimating adrenaline and noradrenaline as described by Passon and Peuler (10).

Blood and Brain Ammonia and Amino Acids

Blood. Serum was separated from the blood by centrifugation after allowing clotting; an equal amount of citrate buffer was added and the solution was kept at room temperature for 30 min. Protein was precipitated with 80% ethanol and free amino acids were extracted twice. Alcohol was removed from the final extract by evaporation on a water bath at 50°C and amino acids in $0.5 \rightarrow 0.1$ mL of the residue were analyzed by the procedure of Benson, Gordon, and Patterson (11).

Brain. After exsanguination, the brain was quickly removed, weighed, and kept cold. It was homogenized in 5 mL phosphate buffer (pH 7.5). The homogenate was centrifuged for 15 min (2000 g) and the supernatant removed. It was deproteinized and amino acids extracted twice with 80% ethanol. Alcohol was removed from the final extract by evaporation on a water bath at 50°C. Amino acids in $0.05 \rightarrow 0.1$ mL of the final residue were analyzed as previously described for blood.

RESULTS

Table I shows the time course of change in concentration of brain tissue concentration of GABA, ammonia, glutamate, glutamine, adrenaline, and noradrenaline during high pressure oxygen exposure. It is apparent in normal animals that there is relatively little change in the major fraction of brain catecholamines (only adrenaline changes significantly). Nevertheless, a significant increase occurs in brain ammonia, and GABA is significantly depleted. We

TABLE I

Brain GABA, Ammonia, Glutamate, Glutamine, Adrenaline, and Noradrenaline in
Normal Rats Exposed to OHP for Different Time Intervals

	Control	10 min	15 min	20 min	25 min	30 min	Convulsions
GABA (μmol/g)	1.15 ±0.12	1.36 ±0.35	1.04 ±0.16	0.93 ±0.05	0.89 ±0.05	0.59* ±0.06	0.75* ±0.10
NH$_3$ (μg/g)	5.25 ±0.72	5.47 ±0.54	5.70 ±0.50	9.30* ±0.80	10.99* ±0.87	13.18* ±0.54	17.7* ±1.1
GLU (μmol/g)	9.42 ±0.63	8.80 ±0.60	5.70* ±0.90	4.56* ±0.51	4.36* ±0.8	5.36* ±0.62	5.18* ±0.49
GLU. NH$_2$ ASP. NH$_2$ (μmol/g)	0.97 ±0.16	1.74* ±0.23	2.04* ±0.21	2.83* ±0.20	2.56* ±0.45	2.91* ±0.52	2.88* ±0.73
A (ng/g)	2.2 ±0.4	0.32* ±0.03	0.36* ±0.03	1.64* ±0.09	1.75 ±0.13	1.97 ±0.38	1.35* ±0.17
NA (ng/g)	128.9 ±3.6	79.1* ±10.3	83.0* ±18.5	98.3* ±5.6	105.9* ±12.2	130.6 ±4.0	124.6 ±19.1

*$P < 0.05$ when compared with control; $n = 5$; mean ± SD.

have previously observed (12) that adrenaline, noradrenaline, and ammonia concentrations all increase significantly in the blood until convulsions occur during hyperoxia.

Table II shows the effect of various procedures that interfere with catecholamine concentration in the brain and blood.

The effect of 6-OH dopamine is to produce a chemical sympathectomy by replacing noradrenaline in the vesicles of the nerve endings. Adrenalectomy effectively removes the circulating catecholamines produced from the adrenal medulla. Hexamethonium acts on the acetylcholine receptor site at the pre/post synapse to interfere with catecholamine release in the postganglionic fiber. Tyrosine hydroxylase, an essential enzyme in the synthesis of catecholamine in the brain, is inhibited by α-methyl-p-tyrosine.

Adrenalectomy and hexamethonium both reduced circulating catecholamines in rats and, despite a large variability, brain adrenaline and noradrenaline seemed to accumulate more in these animals than in groups treated with other drugs. The point of convulsion in adrenalectomized and hexamethonium-treated animals was considerably delayed, although the final concentration of all the metabolites studied did not vary significantly in these groups from the others. The catecholamine concentration of the brain in the preoxygen exposure condition was significantly reduced by 6-OH dopamine; concomitantly, brain ammonia was significantly elevated and GABA significantly depleted. Convulsive latency during oxygen exposure under these conditions was consid-

TABLE II

Time to Convulsion and Brain GABA, Ammonia, Glutamate, Glutamine, Adrenaline, and Noradrenaline Levels in Normal and 6-Hydroxy Dopamine-, Hexamethonium-, α-Methyl-p-Tyrosine-Treated and Adrenalectomized Rats Before and After Convulsions

	NORMAL		6-OHDA		HEXAMETHONIUM		α-Methyl-p-Tyrosine		SHAM-OP		ADRENALECTOMY	
	C	CON	C	CON	C	CON	C	CON	C	CON	C	CON
GABA (μmol/g)	1.52 ±0.11	0.78* ±0.07	0.87 ±0.13	0.70* ±0.15	1.33 ±0.26	0.75*† ±0.07	1.20 ±0.10	0.77*† ±0.10	1.29 ±0.19	0.66*† ±0.05	1.20 ±0.26	0.65*† ±0.12
NH₃ (μg/g)	5.25 ±0.72	17.8* ±0.90	8.24* ±0.67	19.9*† ±0.90	5.5 ±1.1	18.56*† ±1.11	4.74 ±0.73	17.35*† ±2.39	4.81 ±0.32	17.1*† ±2.5	3.6* ±0.4	16.9*† ±2.7
GLU (μmol/g)	9.42 ±0.63	5.18 ±0.48	6.70 ±0.87	4.14* ±0.87	9.04 ±0.89	4.08*† ±0.98	8.48 ±1.77	4.3*† ±2.3	8.37 ±0.83	4.10*† ±0.90	7.20 ±0.80	4.40*† ±0.60
GLU. NH₂ ASP. NH₂ (μmol/g)	0.97 ±0.17	2.88* ±0.73	0.20 ±0.22	3.22*† ±0.55	0.99 ±0.19	2.72*† ±0.73	0.66* ±0.11	2.1*† ±0.70	0.99 ±0.08	3.13*† ±0.68	1.38 ±0.39	3.02*† ±0.63
A (ng/g)	2.22 ±0.40	1.35 ±0.17	0.51* ±0.07	0.47* ±0.10	2.54 ±0.37	1.46 ±0.46	1.28 ±0.45	1.21 ±0.16	1.92 ±0.23	1.13 ±0.10	2.05 ±0.25	2.54 ±0.37
NA (ng/g)	128.9 ±3.6	124.6 ±19.3	64.8*† ±6.4	91.4 ±18.6	141.4 ±31.9	172.6 ±60.2	78.8*† ±11.4	54.2*† ±14.5	133.4 ±12.0	124.0 ±9.2	130.8 ±15.9	121.3 ±9.5
CONVULSION LATENCY (min)		43.0 ±7.0		20.6* ±6.1		98.0* ±9.0		43.0 ±8.0		76.4* ±3.0		102.8* ±5.0

*P < 0.05 when compared with normal control; †P < 0.05 when compared with corresponding drugged control; n = 5; mean ± SD.

erably abbreviated. In the control state, before oxygen exposure α-methyl-p-tyrosine caused a significant depletion in brain catecholamines, OHP treatment produced a further significant depletion, but convulsion latency remained unaltered from that of the undrugged control animal. The general effect of producing a depletion of catecholamines in the brain or blood by enhancing their release, and hence catabolism, rather than by preventing their release (i.e., adrenalectomy or hexamethonium treatment) is to increase brain and blood ammonia, decrease brain GABA, increase glutamine/asparagine, and decrease glutamate.

DISCUSSION

The catecholamines have long been implicated in toxicity resulting from oxygen at high pressure (13). Perhaps the facility with which catecholamines and, more generally, ATP and some amino acids become deaminated and form toxic ammonia finally determines the convulsive state. Glutamic acid seems to lie at the center of a mosaic of events leading to the induction of convulsions. Quastel (14) designated glutamate, glutamine, and GABA as the glutamate system, one function of which is to exercise a buffer action for ammonia that converts the dicarboxcyclic amino acid glutamate to its amide glutamine. It is the preferential use of glutamate in this action rather than in its role as a percursor for GABA that may precipitate convulsive activity when ammonia production is excessive. Gamma-aminobutyric acid is a CNS depressant and a putative inhibitory neurotransmitter in the peripheral nervous system. There is evidence (15,16) for the buffering of infused ammonia directly by a CO_2 fixation system that would spare glutamic acid in its buffering capacity within the glutamate system. Whether the demands made on any CO_2 fixation system for the direct buffering of ammonia are sufficient when ammonia production becomes excessive remains uncertain. Certainly, direct buffering of brain ammonia would spare the conversion of a α-ketoglutarate by transamination and preserve the integrity of the Krebs cycle to support adenosine triphosphate (ATP) production. Collaborative evidence for CO_2 fixation and information on the adequacy of the pathway when ammonia production increases has recently been presented by Weyne et al. (17). During hypercapnia these authors observed that brain glutamine and GABA increased and glutamine and aspartic acids decreased. Hypercapnia also stimulated ammonia formation but brain ammonia did not increase in the first hour of hypercapnia because CO_2 fixation and amidation sufficed to buffer it. Glutamate concentrations naturally would first have to increase to initiate the buffer action, and early in the hypercapnic period one might assume that an enhanced GABA formation would also occur, as was indeed observed. When ammonia production became too great to be buffered by a balancing CO_2 fixation, then glutamic and aspartic acid concentrations declined. Thus, limitations in the capacity of the CO_2 fixation systems provide an explanation for the preceding observations.

Figure 1 illustrates the multi demands placed upon glutamate concentrations during hyperoxia: as a potential deviator of α-ketoglutarate from the Krebs cycle; as a component of the γ-glutamyl cycle (18) producing glutathione for amino acid transport and free radical scavenging; and as a precursor in the formation of GABA, a neuronal depressant. The figure also emphasizes the complex hierarchy of events leading to convulsive action within which ammonia and glutamate occupy central roles.

In the experiments described here convulsive activity has been delayed wherever experimental manipulation of the animals has been able to attenuate the production of ammonia from either oxidative deamination of brain or the circulating catecholamines. Figure 1 depicts the possible inter-relationship of the events described and attempts to rationalize biochemical events attendant upon the phenomenon of convulsive activity in hyperoxia.
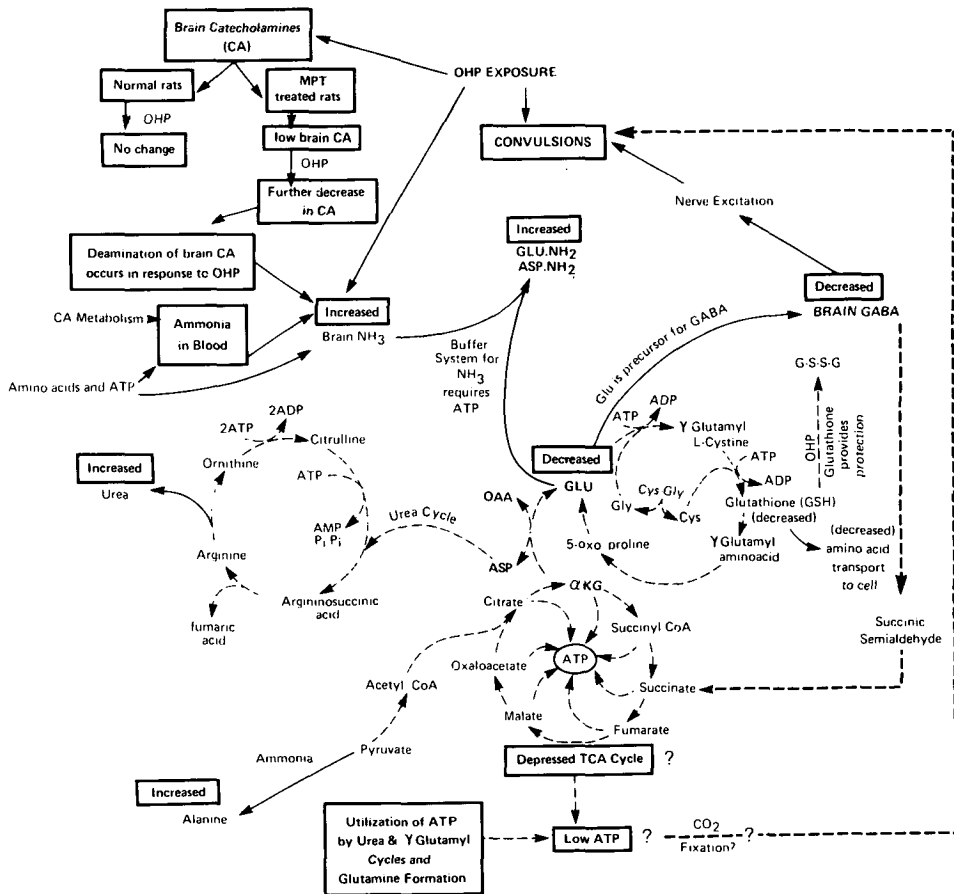
Fig. 1.   Contributing effects of catecholamine deamination and ammonia acting upon glutamic acid (GLU) to produce convulsive activity in hyperoxic states.

References

1. Parnas JK, Mozolowski W, Lewinski W. Uber der ammniakgehalt und die ammniakbildung im blute in der zusammenham des blutammoniaks met der muskelarbilt. Biochem Z 1927;188:15-23.
2. Schwartz AE, Lawrence W, Roberts KE. Elevation of peripheral blood ammonia following muscular exercise. Proc Soc Exp Biol Med 1958;98:548-550.
3. Khairallah PA, Mommaerts WFHM. Nucleotide metabolism in cardiac activity. I: Initial methods and initial observations. Circ Res 1953;1:8-11.
4. Weil-Malherbe W. Ammonia metabolism in the brain. In: Elliot KAC, Page H, Quastel JH, eds. Neurochemistry. Springfield: Charles C Thomas, 1962:323.
5. Vrba R. On the participation of ammonia in cerebral metabolism and function. Rev Czechoslovak Med 1957;3:1-26.
6. Lowenstein JM. Ammonia production in muscle and other tissues: the purine nucleotide cycle. Physiol Rev 1972;52:382-414.
7. Iversen LL, Simmonds MA. In: Hooper G, ed. Metabolism of amines in the brain. New York: MacMillan, 1969:53.
8. Schildkraut JJ, Schanberg SM, Kopin IJ. The effects of lithium ion on H³-norepinephrine metabolism in brain. Life Sci 1966;5:1479.
9. Banister EW, Bhakthan NMG, Singh AK. Lithium protection against oxygen toxicity in rats: ammonia and amino acid metabolism. J Physiol (London) 1976;260:587-596.
10. Passon PG, Peuler JD. A simplified radiometric assay of plasma norepinephrine and epinephrine. Anal Biochem 1973;51:618-631.
11. Benson JB, Gordon MJ, Patterson JA. Accelerated chromatographic analysis of amino acids in physiological solutions containing glutamine and aspargine. Anal Biochem 1967;10:228-240.
12. Banister EW, Singh AK. The time course of brain and blood catecholamines, catechol-o-methyltransferase and amino acids in rats convulsed by oxygen at high pressure. Can J Physiol Pharmacol 1979;57:390-395.
13. Bean JW. Hormonal aspects of oxygen toxicity. In: Lambertsen CJ, ed. Underwater physiology symposium. Nat Acad Sci-Nat Res Council 1955;377:12-24.
14. Quastel JH. Amino acids and the brain. Biochem Soc Trans 1974;2:766-780.
15. Berl S, Takagaki G, Clarke DE, Welsch H. Metabolic compartments in vivo: ammonia and glutamic acid metabolism in brain and liver. J Biol Chem 1962;237:2562-2569.
16. Berl S, Takagaki G, Clarke DE, Waelsh H. Carbon dioxide fixation in the brain. J Biol Chem 1962;237:2570-2573.
17. Weyne J, Leuven FV, Kazemi H, Leusen I. Selected brain amino acids and ammonium during chronic hypercapnia in conscious rats. J Appl Physiol: Respirat Environ Exercise Physiol 1978;44:333-339.
18. Meister A. On the enzymology of amino acid transport. Science 1973;180:33.

CHANGES IN CELL VOLUME FOLLOWING HYPERBARIC EXPOSURE: A MANIFESTATION OF OXYGEN TOXICITY

J. Pooley and D. N. Walder

We have previously observed and reported a decrease in blood flow through rabbit femoral bone marrow during long, simulated air dives (1). As no corresponding circulatory change was found to occur in skeletal muscle, we have looked for an explanation by considering the anatomy of the marrow in a long bone.

Bone marrow is a fatty tissue traversed by blood vessels and confined within the rigid boundary of the bone cortex. We postulated that an increase in marrow fat cell volume might occur during hyperbaric exposure and that this, by increasing resistance to intramedullary blood flow, could account for the decrease observed at pressure.

To test this hypothesis, we studied the effect of exposure to compressed air and other gas mixtures on fat cell volume.

MATERIALS AND METHODS

Preparation of Fat Cell Suspensions

Suspensions of isolated fat cells were prepared from rat epididymal fat pad by a modification of the original Rodbell method (2) described by Smith (3).

The complete fat pad was removed from one epididymis of an adult white rat and blocks of tissue weighing 300–600 mg were excised. Each block of tissue was placed in a plastic vial containing 3 mL of Krebs-Ringer bicarbonate buffer, and 5 mg of collagenase (collagenase type II, Sigma (London) Chemical Co., Ltd.) was added. The vials were then incubated in an agitated water bath at 37°C for 1 h. After incubation, solid material was removed with forceps and the liberated fat cells separated from the stromal and vascular cells by centrifugation at 400 × g for 1 min. The fat cells, which floated in the surface layers of the medium, were removed by pipette and resuspended in Krebs-Ringer bicarbonate buffer.

Exposure of the Fat Cells to Compressed Air and Other Gas Mixtures

In each of the described experiments cells obtained from the same epididymal fat pad were used to provide both control and test suspensions.

The control suspensions were maintained at a temperature of 37°C and exposed to air at atmospheric pressure. The test suspensions were placed in a thermostatically controlled compression chamber (Bethlehem Chamber Corporation) set at 37°C. A series of experiments were performed in which fat cell suspensions were exposed to the following gas environments:

1) Air at 6 ATA
2) Trimix: Normal P_{O_2} and P_{N_2} with helium to 6 ATA
3) Oxygen/nitrogen mixture: Normal P_{O_2} with N_2 to 6 ATA
4) 100% O_2 at 1 ATA

After a period of 3 h the test suspensions were removed from the compression chamber. Decompressions were performed at an approximate rate of 1 atm/min.

Assessment of Fat Cell Volume

After removal of the test suspensions from the compression chamber, we obtained the volume distribution curve of the cells in the test suspensions and compared it with that of the control suspension using the following technique.

A Coulter Counter Model ZF (orifice 200 μ; attenuation 4; aperture 512) was connected to a Coulter Channelizer C-1000 (Window width 100; base channel threshold 5; edit switch on; stop at full-scale deflection 400), in turn connected to an XY pen recorder. The control suspension was diluted in isoton and introduced into the Coulter Counter. The cells were thus electronically counted and sized and the result displayed as a volume distribution curve on the channelizer oscilloscope screen. Each curve represented a total of 16,000 to 20,000 cells. These data were then plotted on the XY recorder. Next, the volume distribution curve of the test suspension was obtained and plotted on the same record. In this way any change in cell volume occurring as a result of hyperbaric exposure was determined.

Investigation of Observed Cell Volume Changes Occurring as a Result of Hyperbaric Exposure

An increase in fat cell volume was demonstrated after exposure to both compressed air at 6 ATA and 100% O_2 at 1 ATA. The mechanism of this change was studied by

Investigating the effect of adding albumin to the suspended medium. The experiments described previously were repeated with suspensions of fat cells in a medium of Krebs-Ringer bicarbonate buffer to which bovine albumin had been added to concentrations of 2% w/v and 4% w/v.

Light microscopy. After hyperbaric exposure, microscopic examination of both stained and unstained preparations of the fat cell suspensions was carried out by direct microscopy, dark ground and phase contrast techniques.

Red cell studies. For the purposes of comparison a study of red cells was begun. Freshly drawn human venous blood samples 2.0 mL volume were placed in heparinized containers, maintained at 37°C, and exposed to compressed air at pressures ranging from 3 to 8 ATA for periods of 2–3 h duration. At the end of this time, the volume distribution curve of the red cells was determined using a technique similar to that described above and compared with a control sample from the same donor kept at atmospheric pressure. The effect of the introduction of lithium ions into the venous blood sample before exposure was investigated on an empirical basis by substituting lithium heparin for sodium heparin as the anticoagulant.

RESULTS

The Effect on Cell Volume of Exposing Fat Cell Suspension to Compressed Air and Other Gas Mixtures

Compressed air at 6 ATA. Figure 1 illustrates the results of an experiment in which a fat cell suspension was exposed to compressed air at 6 ATA for 3 h. The volume distribution curve of the test suspension lies to the right of the control suspension indicating that an overall increase in cell volume occurred.

Trimix: Normal Po_2 *and* Pn_2 *with helium to 6 ATA.* Figure 2 shows the effect of exposure to trimix for 3 h. The volume distribution curve of the test suspension overlies that of the control, an indication that no change in fat cell volume occurred.
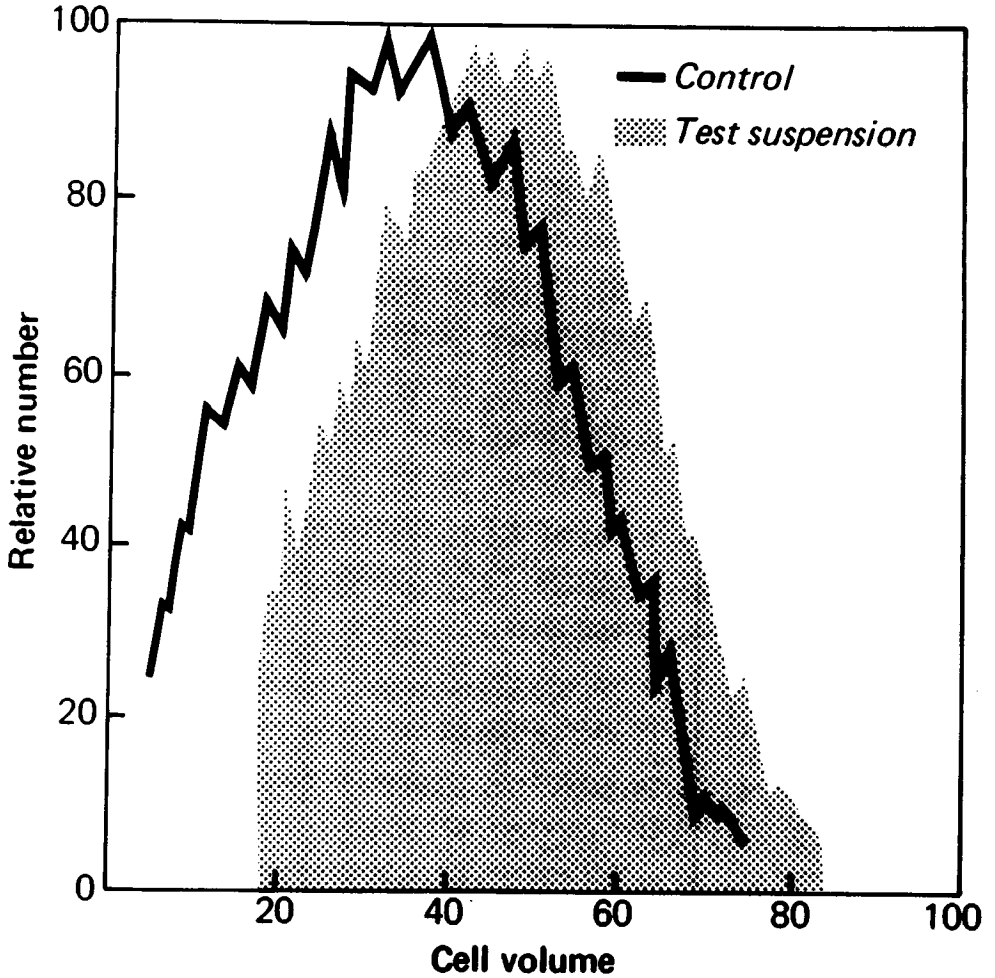
Fig. 1.   The effect on fat cell volume of exposure to compressed air at 6 ATA.

Oxygen/nitrogen mixture: Normal PO₂ *with* N₂ *to 6 ATA*. The results of these experiments were the same as those for trimix, an indication that no change in fat cell volume occurred.

100% O₂ at 1 ATA. Figure 3 illustrates the results of these experiments. The volume distribution curve of the test suspension lies to the right of that of the control, an indication of overall increase in fat cell volume as a result of this exposure.
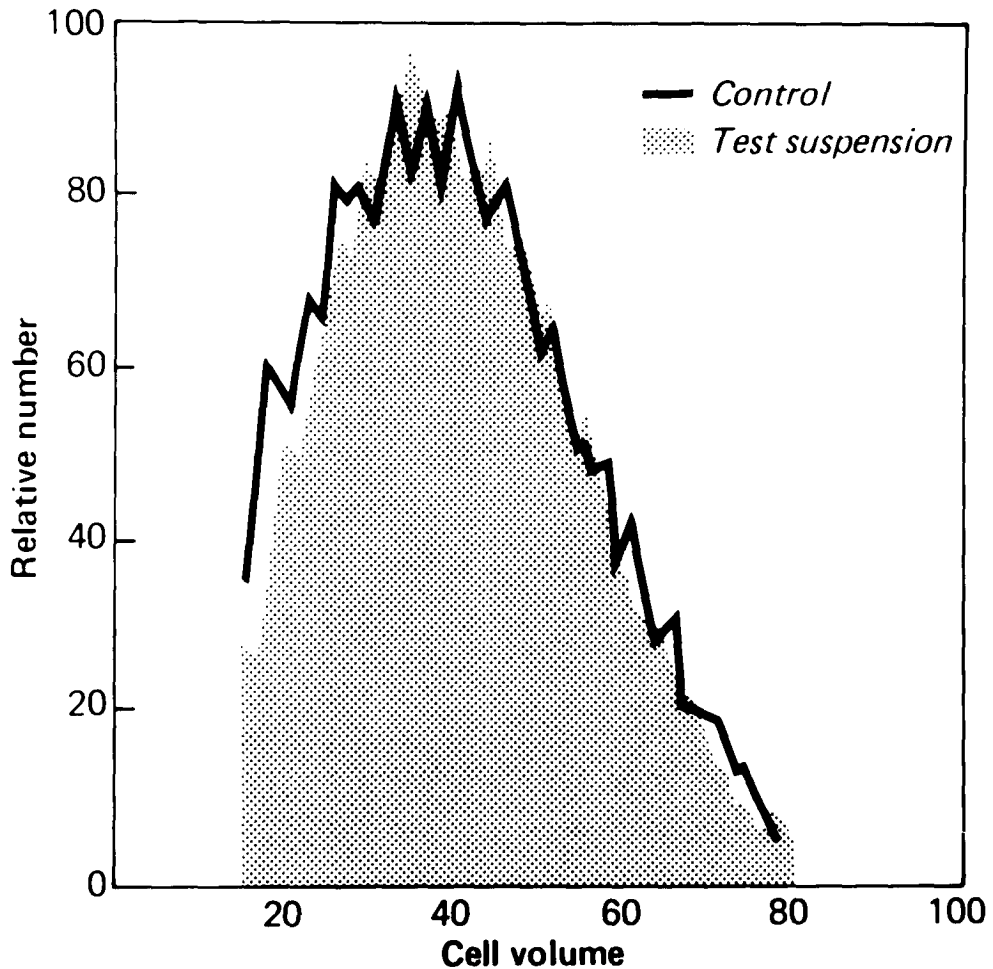
Fig. 2. The effect on fat cell volume of exposure to trimix (normal P_{O_2} and P_{N_2}) with helium to 6 ATA.

The Effect of Adding Albumin to the Suspending Medium

2% Albumin. Fat cells suspended in Krebs-Ringer bicarbonate buffer to which albumin 2% w/v had been added demonstrated no volume change after exposure to either compressed air at 6 ATA or 100% O_2 at 1 ATA.

4% Albumin. The volume distribution curves of fat cell suspensions in Krebs-Ringer bicarbonate buffer containing albumin 4% w/v were shifted to the left by exposure to both compressed air at 6 ATA and 100% O_2 at 1 ATA, indicating that an overall decrease in cell volume had occurred. No change in the volume of the fat cells in this medium occurred on exposure to either trimix or oxygen/nitrogen mixture.
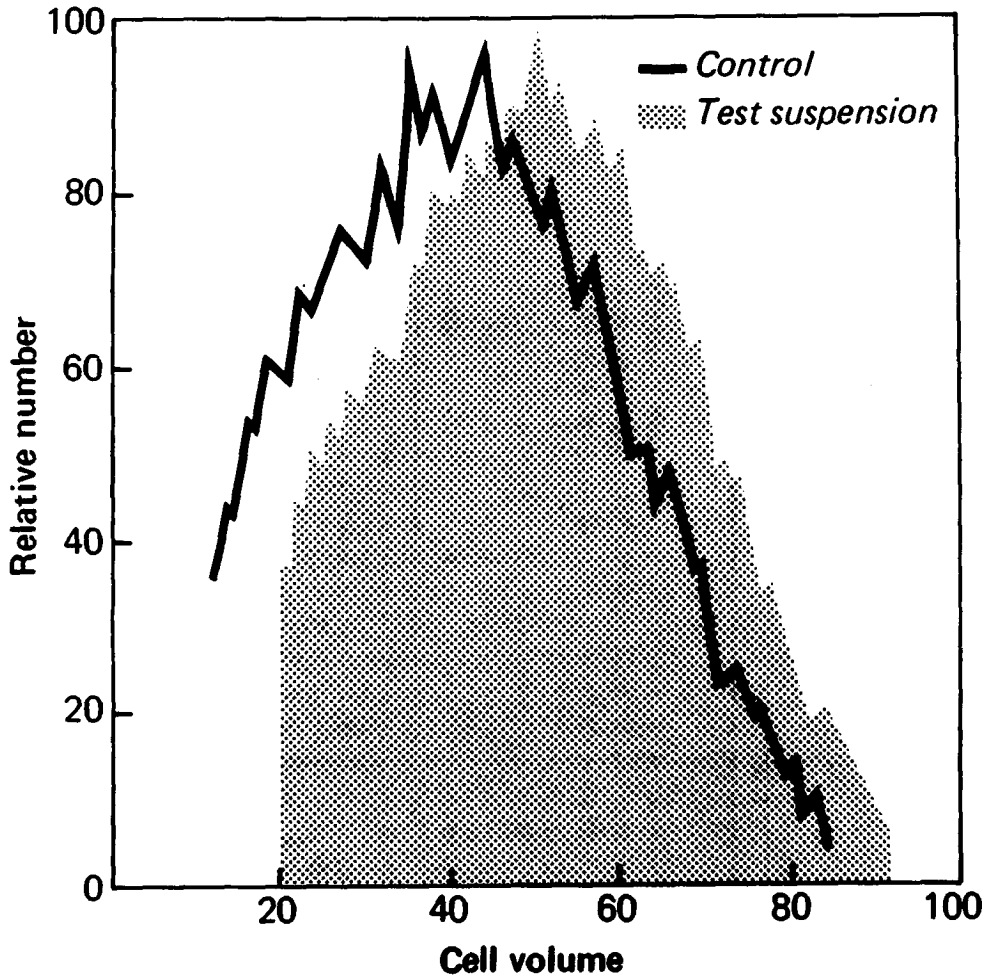
Fig. 3.   The effect on fat cell volume of exposure to 100% O_2.

Light Microscopy

Repeated examinations using the microscope techniques outlined above revealed no obvious morphological change in the fat cells after exposure to any of the gas mixtures. On no occasion were intracellular gas inclusions seen.

Red Cell Studies

The volume distribution curves of red cells exposed to compressed air at pressures between 5 and 8 ATA for 2 to 3 h were found to lie to the right of control samples. This increase in volume could be prevented or reversed by the introduction of lithium ions into the blood sample before exposure.

DISCUSSION

These experiments have demonstrated changes in the volume of fat cells resulting from exposure to both compressed air at 6 ATA and 100% O_2 at 1 ATA in vitro.

There are individual and tissue variations in the volume of fat cells as well as a wide distribution in the diameters of individual fat cells from the same tissue (2, 3) (50–100 μ dia. in rat epididymis [Rodbell, 1964]). This limits the accuracy of direct measurement in assessing mean cell size and complicates the interpretation of results obtained from the tissues of different individuals. We have circumvented these problems in our experiments by employing an objective technique to measure the volumes of a relatively large number of cells (16,000 to 20,000 in each sample) and by using cells derived from the same source to provide both test and control samples. The results are presented as a comparison between samples of cells from the same tissue to demonstrate simply the presence or absence and direction of a volume change. Calculations of absolute volume are not included because we recognize that the magnitude of volume changes occurring in unsupported cells in suspension in vitro at best may only approximate any corresponding changes occurring in vivo.

The increase in fat cell volume occurring after exposure to compressed air appeared to result from the increased partial pressure of oxygen: similar hyperbaric exposures to helium and nitrogen gas mixtures in which the Po_2 remained normal resulted in no such volume increase. This conclusion was confirmed by the occurrence of similar volume increases in fat cell suspensions exposed to 100% O_2 at atmospheric pressure. Because the maintenance of a constant volume is a basic function of mammalian cells, we consider these volume changes to be a manifestation of oxygen toxicity.

The pathological mechanism of these cell volume increases and therefore a possible site for the toxic action of oxygen in this model may be arrived at by considering the results of the experiments in which albumin was added to the suspending medium.

The addition of albumin did not change the findings of the experiments in which fat cells were exposed to gas mixtures with a normal Po_2, the volume distribution curves in both control and test suspensions were identical. However, the presence of extracellular albumin did change the findings of the experiments in which cells were exposed to an increased Po_2.

The addition of 2% albumin prevented the increase in cell volume previously demonstrated to occur on exposure to an increased Po_2, and the addition of 4% albumin resulted in a decrease in fat cell volume on such exposures. These findings can be explained by considering the process of cell volume regulation.

Robinson (4) has reviewed experimental work into the nature of the pathological swelling of cells and concluded that the mechanism by which cells maintain a constant volume is by active extrusion of sodium ions to maintain an osmotic gradient across the cell membrane, counterbalancing the colloid os-

motic pressure of the intracellular proteins. The increase in fat cell volume resulting from exposure to a high Po_2 can, therefore, be explained by postulating a toxic action of oxygen acting on the sodium pump. The reversal of the cell volume change by the presence of intracellular albumin is explained as follows. If the toxic action of oxygen results in paralysis of the sodium pump, cells will swell under the influence of the colloid osmotic pressure of their intracellular proteins. The movement of fluid into cells in these circumstances would be expected to be prevented and finally reversed by the introduction of increasing concentrations of extracellular protein. This was found to be the case in these experiments.

In our microscope studies, in which no attempt at direct measurement was made, no other morphological changes were seen in the fat cells as a result of hyperbaric exposure. The absence of the intracellular gas inclusions described by Gersh et al. (5) in fat cells after in vivo experiments was particularly noted, as expansion of such inclusions could have provided a mechanism for our observed increases in cell volume.

The results of our preliminary investigations on the effect of hyperbaric exposure on red cells are mentioned because an increase in cell volume was induced by experimental conditions similar to those of the fat cell experiments except that the air pressure required was higher (5–8 ATA), which suggests that a similar mechanism was responsible. Furthermore, the prevention or reversal of this effect by the presence of lithium ions provides a link with the action of oxygen toxicity on the central nervous system. Radomski and Watson (6) clearly demonstrated that lithium inhibited hyperbaric oxygen-induced convulsions in rats and suggested that this ion influenced ionic gradients that resulted from deranged membrane transport systems earlier demonstrated to occur in vitro by Kaplan and Stein (7).

The aim of our experiments was to test the hypothesis that the decrease in blood flow through femoral bone marrow of rabbits observed during long exposures to compressed air was due to an increase in marrow fat cell volume. This increase, occurring within the rigid confines of the bone cortex would, therefore, increase the resistance to marrow blood flow.

The increase in fat cell volume observed in vitro, if it occurs in vivo, would support this hypothesis and implicate the toxic action of oxygen as a factor in the pathogenesis of dysbaric osteonecrosis. This possibility would help to explain the relationship between the occurrence of dysbaric osteonecrosis with both increasing depth and increasing time spent at pressure; it would help to account for the fact that despite continually improving decompression procedures the observed incidence of dysbaric osteonecrosis in British commericial divers continues to grow steadily.

Confirmation of the possible role of oxygen toxicity in dysbaric osteonecrosis is being sought because our preliminary work with lithium would then suggest the possibility of prophylaxis against this disease. This possibility becomes important when one considers that treatment remains unsatisfactory and prevention, by manipulating the working environment, may not be technically feasible.

References

1. Pooley J, Walder DN. Studies of bone marrow blood flow in rabbits during simulated dives. Proc 5th EUBS Meeting (Bergen), in press.
2. Rodbell M. Metabolism of isolated fat cells. J Biol Chem 1964;239:375-380.
3. Smith U. Effect of cell size on lipid synthesis by human adipose tissue in vitro. J Lipid Res 1971;12:65-70.
4. Robinson JR. Colloid osmotic pressure as a cause of pathological swelling of cells. In: Trump BF, Arstila AU, eds. Pathobiology of cell membranes, Vol 1. New York: Academic Press 1975:173-192.
5. Gersh I, Hawkinson GE, Rathbum EN. Tissue and vascular bubbles after decompression from high pressure atmospheres—correlation of specific gravity with morphological changes. J Cell Comp Physiol 1944;24(2):35-70.
6. Radomski MW, Watson WJ. Effect of lithium on acute oxygen toxicity and associated changes in brain gamma—aminobutyric acid. Aerosp Med 1973;44(4):387-392.
7. Kaplan SA, Stein SN. Sodium potassium and glutamate content of guinea pig brain following exposure to oxygen at high pressure. Am J Physiol 1957;190(1):166-168.

LUNG ATP TURNOVER DURING OXIDANT STRESS

A. B. Fisher and D. J. P. Bassett

Current evidence suggests that tissue damage during exposure to oxygen at elevated partial pressures results from the increased production of oxygen-derived free radicals which then interact with cellular components (1,2,3). In vitro studies have demonstrated that lipids containing unsaturated fatty acids and proteins containing essential sulfhydryl groups are particularly sensitive to oxidative damage (4). Manifestations of these biochemical derangements in vivo may include inactivation of key enzymes of intermediary metabolism or peroxidation of membranes of cells or organelles. On the other hand, the early alterations in lung metabolism that precede damage to metabolic systems are not well understood. The question can be formulated as to whether inhibition of intermediary metabolism or membrane derangement is the initial toxic event in the series of reactions that lead to cell damage and eventuate in pulmonary edema.

In this study, we investigated the early effects of hyperoxic exposure on the energy status of the lung. We chose the isolated perfused lung preparation for study to evaluate the direct effects of oxygen uncomplicated by neurohumoral or other systemic factors. To provide a relatively large oxidative stress in a relatively short time, we exposed lungs to oxygen at 5 ATA in a hyperbaric chamber. Energy status of the lung was evaluated by calculating the rate of adenosine triphosphate (ATP) synthesis and by measuring lung tissue adenine nucleotide content. Parallel studies were carried out with isolated lungs perfused with paraquat, an agent that exerts its toxic action on the lung by mechanisms that may share common features with oxygen toxicity (5,6). The results presented in this manuscript represent a compilation of previously published data (7–11) with the exception that data for lung adenine nucleotide content during perfusion with paraquat were not previously published. A small adjustment was made in the method for calculating ATP turnover so that present results differ slightly from those previously presented (8).

55

METHODS

Lungs for perfusion were isolated from specific pathogen-free Sprague-Dawley male rats weighing 250–300 g and anesthetized with pentobarbital. Without interruption of ventilation or perfusion, lungs were placed in the apparatus for perfusion under ambient or hyperbaric conditions. Lungs were continously ventilated and perfused in a recirculating system with artificial medium consisting of Krebs-Ringer bicarbonate buffer (pH 7.4) containing added ^{14}C-glucose and bovine serum albumin. Perfusate pH and the pressures required for perfusion and ventilation were continously monitored. Temperature of the perfused lung preparation was maintained at 37°C. Aliquots of perfusate were obtained at intervals for subsequent analysis. Expired gas from the lung was collected in CO_2 traps for measurement of $^{14}CO_2$ produced in the gas phase. The circuit for perfusion of lungs in the hyperbaric chamber is shown schematically in Fig. 1. A modified circuit was used for perfusion at ambient pressure (9).
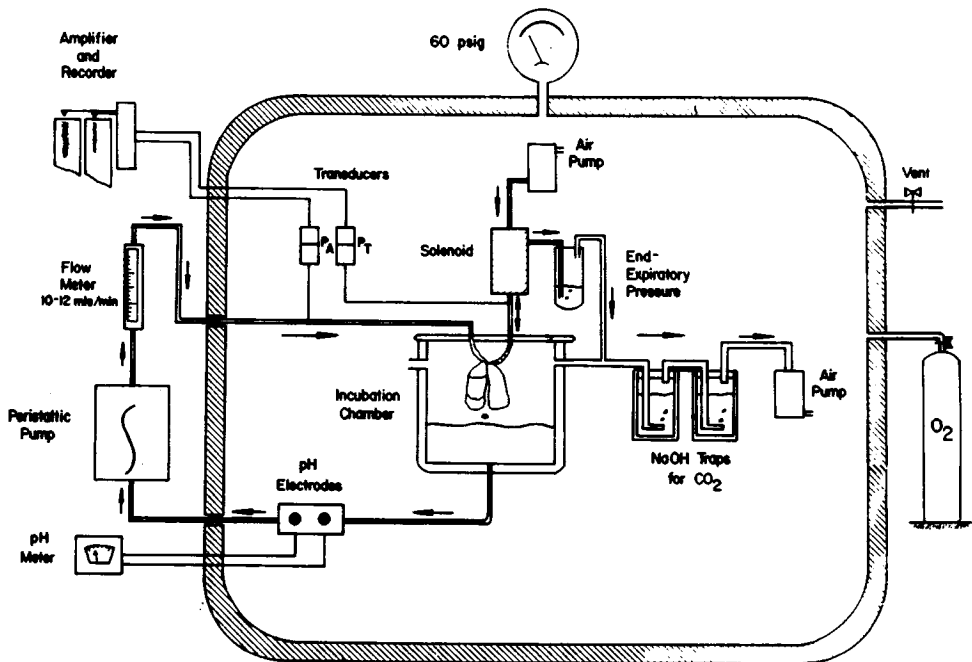
Fig. 1.   Apparatus for perfusion of isolated rat lungs in the hyperbaric chamber. The walls of the hyperbaric chamber are indicated by the *diagonal hatching*. Lungs are continuously ventilated by the solenoid respirator and perfused by the peristaltic pump. The pressure (PT) required for ventilation at constant tidal volume (2 mL) and the pressure (PA) for perfusion at constant flow rate (10-12 mL/min) are monitored with transducers. An end-expiratory pressure of 2-3 cm H_2O is maintained. Perfusate pH is monitored with electrodes. $^{14}CO_2$ liberated from metabolism of ^{14}C-glucose is collected in NaOH. The temperature inside the chamber was maintained at 37°C by a heating plate. A slightly modified apparatus was used to perfuse lungs at ambient pressures of 1 ATA (1). (Reprinted from (8) by permission of the American Physiological Society)

Lungs were generally ventilated with air (0.2 ATA O_2) at ambient pressure. Additional control experiments for tissue ATP content were performed with 0.2 ATA O_2 at 5 ATA total pressure. Experimental perfusions were carried out by ventilating with 100% O_2 at 1 or 5 ATA total pressure. The effect of paraquat was studied by adding buffered 1.5 mM paraquat dichloride to the perfusate; this concentration previously had been shown to produce approximately maximal change in the rate of lung glycolysis (7). The metabolic capacity of the perfused lung preparation was evaluated in parallel experiments with metabolic inhibitors. To demonstrate the metabolic response to complete mitochondrial inhibition, we ventilated the lungs with carbon monoxide. To uncouple mitochondrial oxidative phosphorylation and demonstrate the metabolic response to a rapid rate of energy dissipation, we perfused the lungs with dinitrophenol (DNP, 0.8 mM). Under all experimental conditions the ventilating gas contained 0.05 ATA CO_2 in addition to other components.

The metabolic parameters measured during perfusion were lactate production, pyruvate production, glucose utilization, and CO_2 production from C^{14} labelled glucose. Lactate and pyruvate content of the perfusate were measured by enzyme assay. Glucose utilization was calculated from the rate of ^3H_2O production from [5-^{3}H]-glucose (10,12). Production of $^{14}CO_2$ was measured from glucose labelled with ^{14}C either uniformly or in the 1 or 6 position; using this data, we calculated the fraction of CO_2 produced via the pentose shunt and the fraction of CO_2 produced via mitochondrial (including pyruvate dehydrogenase and Krebs cycle) pathways. It should be noted that three lung perfusion experiments yielded three measurements of lactate and pyruvate production but only one value for mitochondrial and pentose shunt CO_2 production. Results for the pentose shunt measurements are presented elsewhere (8).

The rates of ATP synthesis were calculated from the rates of lactate, pyruvate, and mitochondrial CO_2 production. Lactate and pyruvate production values were corrected for the small component (approximately 10%) that was derived from nonglucose sources. We assumed that production of each mole of lactate or pyruvate generated 1 mol of ATP by the cytoplasmic glycolytic pathway. The production of each mole of mitochondrial CO_2 was assumed to generate 1/3 mol of ATP by the glycolytic pathway and 6 mol of ATP by mitochondrial oxidation to CO_2. This analysis, of course, assumes normal coupling in the respiratory chain. In the presence of dinitrophenol or other uncoupling agent, the calculation yields "potential ATP production" because the energy liberated during the mitchondrial oxidation may be dissipated rather than channelled into ATP synthesis.

Tissue adenine nucleotide content was measured in lungs that were rapidly frozen at the temperature of liquid nitrogen after 1 h of perfusion. The measurement of perfusion at ambient pressure was accomplished by clamping lung tissue with precooled aluminum tongs. At hyperbaric pressures, rapid freezing was accomplished by spraying fine jets of liquid nitrogen onto the surface of the lung as shown in Fig. 2; this procedure succeeded in freezing the pleural surface of the lung to a depth of several millimetres. The frozen lungs were extracted with cold ethanolic perchloric acid, and ATP and ADP were measured in the neutralized extracts by enzymatic assay.
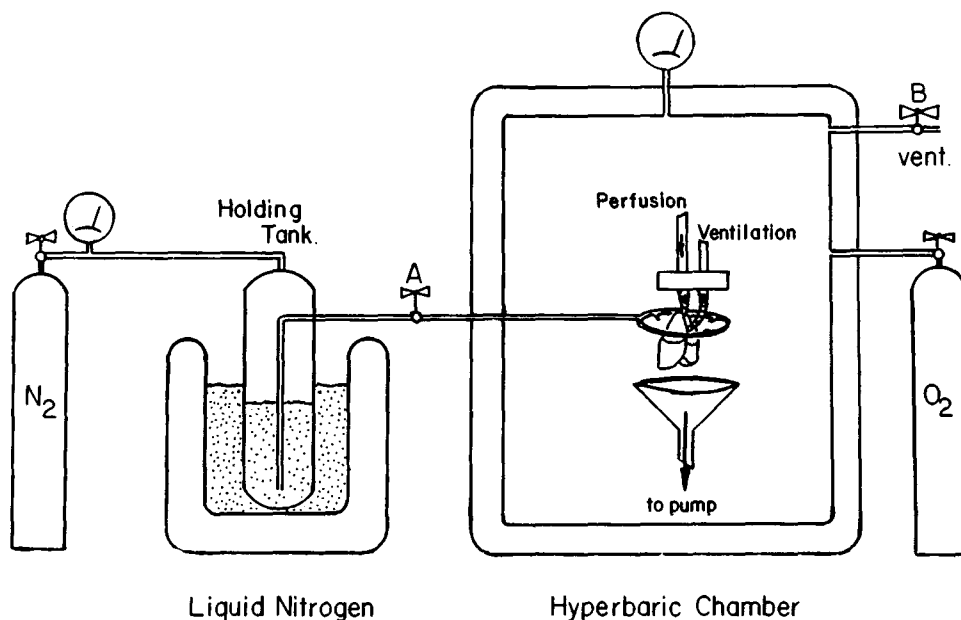
Fig. 2. Method for rapid freezing of the perfused rat lung by liquid N_2 inside the hyperbaric chamber. Liquid N_2 from the holding tank was sprayed onto the pleural surface from jets in the circular ring surrounding the lung.

In an additional small series of experiments, rats were exposed to oxygen at 4 ATA for 1 h. Lungs were then removed from rats, perfused in the isolated lung circuit for 30 min, freeze clamped, and analyzed for tissue adenine nucleotide content.

RESULTS

Metabolic Characteristics of the Isolated Perfused Lung

Isolated rat lungs were perfused in the recirculating system at ambient pressure for 2 or more hours with no evidence of gross alveolar edema. The ventilation pressure at peak inspiration was approximately 5–7 cm H_2O and mean perfusion pressure was approximately 13–15 cm H_2O; these values did not vary appreciably during the course of perfusion. The rates of production of lactate, pyruvate, and CO_2 and utilization of glucose were linear for the duration of perfusion after an initial 10- to 20-min equilibration period. The dry-to-wet weight ratio for lungs at the end of perfusion was in the range 0.16–0.18.

The rate of ATP synthesis by the isolated rat lung under control conditions was 360 μmol/h/g dry weight (approximately 60 μmol/h/g wet lung). Eighty-five percent of ATP synthesis occurred via the mitochondrial pathways

while 15% was cytoplasmic. These results, of course, reflect only ATP synthesis from glucose precursor and do not include a possible contribution from use of endogenous substrates for energy generation. During ventilation with CO, mitochondrial ATP synthesis was reduced by 86%, whereas cytoplasmic ATP production increased by 138%; the net result was a 54% decrease in total ATP synthesis (Fig. 3). The residual mitochondrial activity during CO ventilation may reflect in part a minor component at the early stages of perfusion before complete metabolic inhibition was achieved. During perfusion with 0.8 mM DNP, the "potential ATP synthesis" via mitochondrial pathways increased
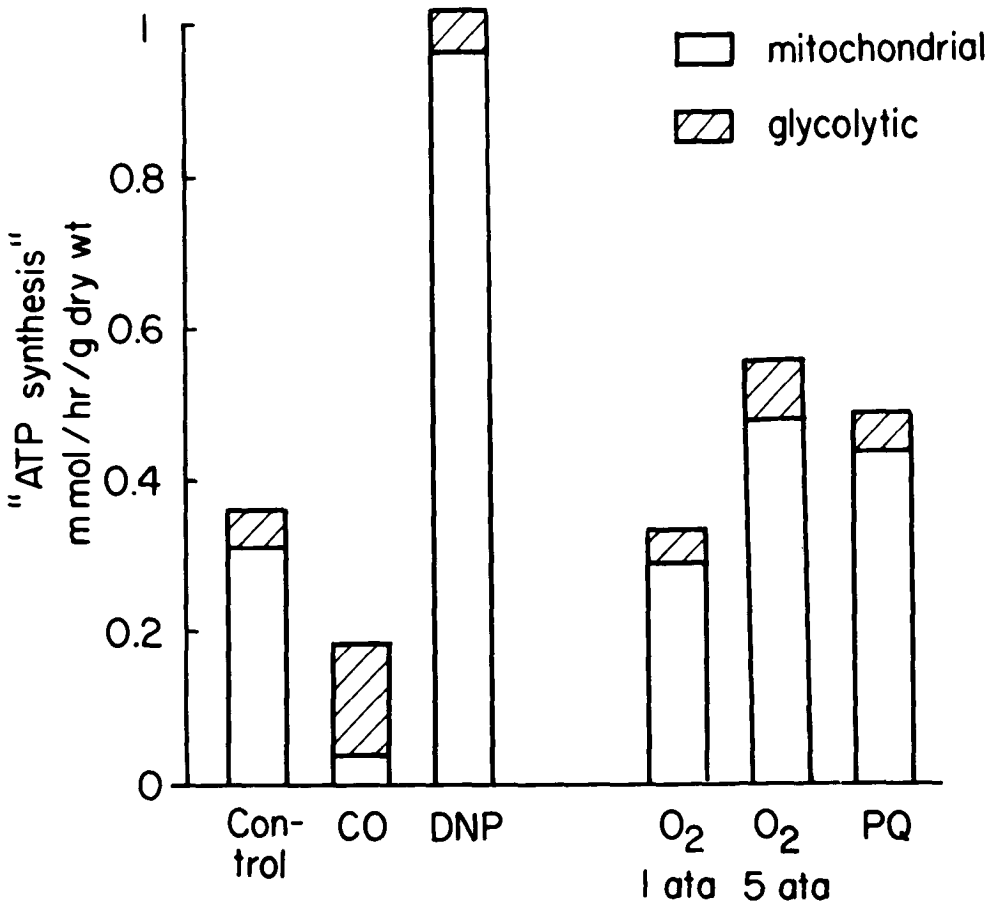
Fig. 3.   Calculated rate of ATP synthesis from glycolytic and mitochondrial pathways by isolated, perfused rat lung under varying metabolic states and oxidative stresses. Glycolytic ATP synthesis was calculated from rates of lactate and pyruvate production, and mitochondrial ATP synthesis was calculated from mitochondrial oxidation of glucose to CO_2 (see text). Control and PQ lungs were ventilated with 5% CO_2 in air, CO lungs with 5% CO_2 in CO, and other lungs with O_2 containing 0.05 ATA CO_2. Results represent *mean values for 21 perfusions* with O_2 at 1 ATA, 12 perfusions with CO, and 9 perfusions for each of the other conditions. CO = ventilation with carbon monoxide (0.95 ATA); DNP = perfusion with 0.8 mM 2,4-dinitrophenol; PQ = perfusion with 1.5 mM paraquat.

216% compared with control while cytoplasmic ATP production increased 75%; total ATP production increased 195% (Fig. 3). These results with CO and DNP reflect the potential range of response of the isolated perfused lung to metabolic challenge and indicate that the ATP synthesis by the mitochondrial pathways may range from 40–970 μmol/h/g dry weight.

Measurement of adenine nucleotide content of the perfused lung indicated that nucleotides were present chiefly in the form of ATP (Table I). The lactate-to-pyruvate ratio (L/P) of the perfusate was characteristic of previous results with this isolated perfused organ. During ventilation with CO, there was a marked decrease in tissue ATP and ATP/ADP and an increase in perfusate L/P. During perfusion with DNP, there was a modest decrease in tissue ATP and ATP/ADP while L/P was essentially unchanged.

Effect of Hyperoxia on Metabolism of Isolated Perfused Lung

Lungs ventilated with O_2 at 1 ATA showed no significant differences from control lungs either in rate of ATP synthesis or tissue content of adenine nucleotides (Fig. 3 and Table I). With exposure of lung to O_2 at 5 ATA, there was an increase in the rate of ATP generation via both the cytoplasmic and mitochondrial components, resulting in a 63% increase in total ATP production (Fig. 3). These results were associated with the increased rate of ATP synthe-

TABLE I

Lactate/Pyruvate Production Ratio and Adenine Nucleotide Content of Isolated Rat Lungs After 1 Hour of Perfusion with Inhibitors or Oxidants

Condition	ATP μmol/g dry wt.	% of Control	ATP/ADP	L/P
Control (0.2 ATA O_2)	10.4 ± 0.1 (8)		7.9 ± 0.2 (8)	10.9 ± 0.6 (9)
CO, 0.95 ATA	4.9 ± 0.2 (4)	47	2.7 ± 0.7 (4)	52.9 ± 4.9 (12)
DNP, 0.8 mM*	9.3 ± 0.2 (3)	89	5.0 ± 0.1 (3)	12.7 ± 0.8 (9)
O_2, 0.95 ATA	10.4 ± 0.2 (17)	100	7.9 ± 0.3 (17)	9.3 ± 0.3 (27)
O_2, 5 ATA†	7.2 ± 0.3 (5)	69	4.4 ± 0.2 (5)	8.2 ± 0.8 (9)
HBO pre-exposure*‡	9.8 ± 0.4 (4)	94	8.0 ± 0.5 (4)	—
PQ, 1.5 mM	8.1 ± 0.2 (4)	78	5.1 ± 0.1 (4)	11.8 ± 0.4 (9)

Results are mean ± SE for the number of experiments in parenthesis.   L/P = lactate/pyruvate. *Ventilating gas was 5% CO_2 in O_2.   †Lungs perfused in hyperbaric chamber.   ‡Rats pre-exposed to O_2 at 4 ATA for 1 h prior to perfusion study.

sis. Significant decreases in the tissue ATP content, tissue ATP/ADP, and per-fusate L/P were associated with the increased rate of ATP synthesis. These results suggest an increased rate of ATP utilization with indication that the tis-sue was "seeking" a new steady state of tissue energy charge. The perfusion system for study of lungs under hyperbaric oxygen was modified from that used for lung perfusion under ambient conditions. Therefore we perfused lungs with the modified apparatus during ventilation of lungs with 0.2 ATA O_2 for comparison with the hyperbaric oxygen results. These experiments indicated that approximately half of the increase in ATP synthesis and half of the de-crease in tissue adenine nucleotide content with O_2 at 5 ATA could be ascribed to hyperoxia while the additional change reflected some undefined influence of the modified perfusion system.

Lungs removed from rats that had been pre-exposed to O_2 at 4 ATA for 1 h were evaluated for tissue adenine nucleotide content after 30 min of perfu-sion under control conditions. The ATP and ATP/ADP in these lungs were similar to values for lungs from normal (unexposed) rats. These results suggest that altered lung adenine nucleotides may be rapidly restored to control levels upon removal of the hyperbaric stress, although difference in exposure condi-tions between the two types of experiments preclude any definitive conclusions.

Effect of Paraquat on Lung Metabolism

Lungs perfused with paraquat (1.5 mM) showed an increased rate of mi-tochondrial ATP generation resulting in a 39% increase in total ATP synthesis. Tissue ATP content and ATP/ADP were decreased by 22% and 35%, respec-tively. There was no change in the L/P. These results suggest an increased rate of ATP utilization in the presence of paraquat similar to that found with expo-sure to hyperbaric oxygen.

DISCUSSION

This study used the isolated perfused lung preparation to investigate the early metabolic changes that accompany exposure to hyperoxia or paraquat. The use of this preparation has the advantage that neurohumoral, circulatory, and other possible mediators of indirect organ toxicity can be eliminated. The disadvantage of the isolated lung preparation is its relatively limited life span until tissue edema develops. For that reason, we chose a relatively high oxy-gen presure for study and limited the observations to the initial hour of perfu-sion. Data previously presented for the second hour of exposure to hyperbaric oxygen are available in the literature for comparison (8), although the presence of interstitial lung edema complicates their interpretation.

Based on results with the isolated lung preparation, the early manifesta-tions of hyperoxic stress include oxidation of tissue pyridine nucleotides (mani-fested by the decreased perfusate L/P) and increased rate of NDPH turnover (as indicated by stimulated activity of the pentose shunt pathway of glucose

metabolism) (8). The rate of tissue ATP utilization is either unchanged or slightly increased. The stimulation of the pentose shunt pathway indicates an increased demand for cytoplasmic reducing equivalents, possibly in response to an increased rate of glutathione oxidation (3) or an increased rate of lipid peroxidation. The findings are consistent with the concept that hyperoxia results in an increased "load" of toxic oxygen-derived radicals that are detoxified by cytoplasmic reductants (1,3).

The results suggest that ATP utilization is increased during these early stages of oxygen exposure, although the degree of stimulation was very modest in comparison with the maximal capacity of the system. Possible mechanisms for stimulation of ATP utilization include uncoupling of oxidative phosphorylation or increased ATPase activity, perhaps related to altered membrane properties. The important point of the data would appear to be that mitochondrial pathways were definitely not inhibited during these initial stages of oxidative stress. On the other hand, the results do not exclude some mitochondrial damage that might become evident only when lung mitochondria are required to operate at maximal capacity or that might develop during later stages of oxygen exposure. Evidence for this might be the relatively modest increase in ATP synthesis despite the significant decrease in tissue ATP/ADP. Our published data further suggest that during the second hour of oxygen exposure of lungs at 5 ATA, mitochondria did not respond normally to the additional stress of interstitial edema (8). Sanders and co-workers have shown that mitochondria from lungs of rats exposed to 2 ATA O_2 for 12 h do not maintain maximal rates of oxygen consumption (13). Thus, energy generation may remain intact during the initial stages of hyperoxia exposure, but mitochondria may participate in the damage that becomes manifest as oxygen poisoning proceeds. The data presented suggest that mitochondrial changes produced during the earliest stages of oxygen exposure are rapidly reversible.

Paraquat produced alterations of NADPH and ATP turnover that were similar to those produced by hyperbaric oxygen. These metabolic consequences also can be interpreted as an increased use of cytoplasmic reducing equivalents and slightly increased ATP turnover. Despite the similarity in effect, though, it is important to note that the target cells for paraquat and oxygen damage may differ and, therefore, different metabolic effects at the cellular level may be masked by study of the whole organ response.

SUMMARY

Isolated rat lungs perfused in a hyperbaric chamber at 5 ATA and ventilated with oxygen showed slightly increased rates of ATP synthesis from the metabolism of glucose and decreased tissue ATP content. There was no difference in lung adenine nucleotide balance between ventilation with O_2 at 1 ATA and control (0.2 ATA O_2). Perfusion with paraquat (1.5 mM) caused changes similar to those observed with hyperbaric oxygen. The results suggest that the early stages of oxidant stress are associated with an increased rate of ATP utilization and that oxidative metabolism is not depressed.

Acknowledgments

References

1. Fridovich I. The biology of oxygen radicals. Science 1979; 201:875-880.
2. Gerschman R. Biological effects of oxygen. In: Dickens F, Neil E, eds. Oxygen in the animal organism. New York: MacMillan, 1964:475-494.
3. Nishiki K, Jamison D, Oshino N, Chance B. Oxygen toxicity in the perfused rat liver and lung under hyperbaric conditions. Biochem J 1976:160:343-355.
4. Haugaard N. Cellular mechanisms of oxygen toxicity. Physiol Rev 1968;48:311-373.
5. Bus JS, Aust SD, Gibson JE. Superoxide and singlet oxygen—catalyzed lipid peroxidation as a possible mechanism for paraquat (methyl viologen) toxicity. Biochem Biophys Res Comm 1974;58:749-755.
6. Fisher HK, Clements JA, Wright RR. Enhancement of oxygen toxicity by the herbicide paraquat. Am Rev Resp Dis 1973;107:246-252.
7. Bassett DJP, Fisher AB. Alterations of glucose metabolism during perfusion of rat lung with paraquat. Am J Physiol 1978;234:E653-E659.
8. Bassett DJP, Fisher AB. Glucose metabolism in rat lung during exposure to hyperbaric O_2. J Appl Physiol 1979;46:943-949.
9. Bassett DJP, Fisher AB. Pentose cycle activity of the isolated perfused rat lung. Am J Physiol 1976; 231:1527-1532.
10. Bassett DJP, Fisher AB. Stimulation of rat metabolism with 2, 4-dinitrophenol and phenazine methosulfate. Am J Physiol 1976;231:898-902.
11. Fisher AB. Energy status of the rat lung after exposure to elevated PO_2. J Appl Physiol 1978;45:56-59.
12. Bassett DJP, Fisher AB. Metabolic response to carbon monoxide by isolated rat lungs. Am J Physiol 1976;230:658-663.
13. Sanders AP, Gelein RS, Currie WD. The effect of hyperbaric oxygenation on the metabolism of the lung. In: Lambertsen CJ, ed. Proceedings of the fifth symposium on underwater physiology. Bethesda, MD; Federation of American Societies for Experimental Biology, 1976:483-492.

PROTECTION FROM PULMONARY OXYGEN TOXICITY BY TREATMENT WITH LOW DOSES OF BACTERIAL ENDOTOXIN

L. Frank, M-J. Chiang, and D. Massaro

Although the toxic consequences to the lung of prolonged exposure to elevated concentrations of oxygen are well documented, many clinical situations necessitate very rigorous and long-term hyperoxic treatment. To date, unfortunately, there are still no specific pharmacological agents available clinically to help prevent the lung-damaging effects associated with high-concentration oxygen therapy.

Exposure of various animal species to 95-100% O_2 at 1 atm results in severe lung damage and substantial mortality within several days of continuous exposure (1,2). Adult rats typically succumb to pulmonary oxygen toxicity within 60-72 h of exposure to 95-100% O_2. It has recently been discovered that purified bacterial lipopolysaccharides (endotoxins) from a variety of gram-negative organisms given to rats immediately before and during exposure to >95% O_2 provide a marked degree of protection against oxygen-induced lung damage and lethality (survival rate at 72 h = 265/275 [98%] for endotoxin-treated vs. 66/201 [33%] for untreated rats). Since these initial findings (3,4) we have been concerned with several major questions:

1) Will endotoxin administration *after* the onset of exposure to >95% O_2 at 1 atm provide protection?

2) Will endotoxin provide protection against the more chronic effects of oxygen toxicity?

3) What is the mechanism by which endotoxin confers protection?

The studies reported here were performed to address these experimental questions.

METHODS AND MATERIALS

Adult male Sprague-Dawley albino rats (225-275 g) free of overt pulmonary disease were used for these studies. The animals were maintained on standard laboratory feed and water ad libitum in the Animal Care Facility of the Miami V.A. Hospital. Exposures to >95% O_2 (or 21% O_2) were conducted as previously reported (3, 4) with careful monitoring of oxygen concentrations (96-98%), carbon dioxide concentrations (<0.5%), temperature (23-26°C), and humidity (60-80%).

Endotoxin (*Salmonella typhimurium* lipopolysaccharide, Sigma Chem. Co., St. Louis, MO) was dissolved in phosphate-buffered saline (PBS) pH 7.4, and administered intraperitoneally according to the injection schedules described in the legends for the figures and tables included in this report. Control animals in oxygen received equivalent injections of PBS (approx. 0.5 cc/100 g body wt). At the end of the exposure periods, animals were subjected to euthanasia by pentobarbital anesthesia, i.p., and exsanguination. The animals' lungs were prepared for histological study by intratracheal fixation with 10% buffered formalin at a constant 20-cm H_2O pressure. For the biochemical analyses, fresh lung tissue was perfused with cold isotonic phosphate buffer (0.1 M potassium phosphate, 0.15 M potassium chloride, pH 7.4) and then homogenized in cold 0.005 M potassium phosphate buffer, pH 7.8 (10:1, volume: lung wt) as described previously (3,4). Assays for superoxide dismutase (5), catalase (6), glutathione peroxidase (7), protein (8), and DNA (9) were by standard methods.

Statistical analysis was by Student's group *t* test or by Fisher's exact nonparametric test; significance level of $P < 0.05$ for rejection of the null hypothesis (10).

RESULTS AND DISCUSSION

Effect of Endotoxin Treatment After Onset of Oxygen Exposure

Figure 1 shows the results of studies to determine if endotoxin administered at various times *after* the onset of hyperoxic exposure would have a protective effect. A single dose of endotoxin given to rats at zero time (just before the start of >95% O_2 exposure) or at 12 or 24 h after the start of hyperoxic exposure resulted in nearly 100% survival at the end of 72 h (Fig. 1). A single dose of endotoxin administered after 36 h of hyperoxia resulted in a 75% survival rate. All of these treatment groups had statistically significant increases in survival compared to the 33% survival rate of the rats simultaneously exposed to oxygen but not given endotoxin ($P < 0.05$). Endotoxin given after 48 h in hyperoxia did not affect survival (35% survival rate) (Fig. 1) (11).
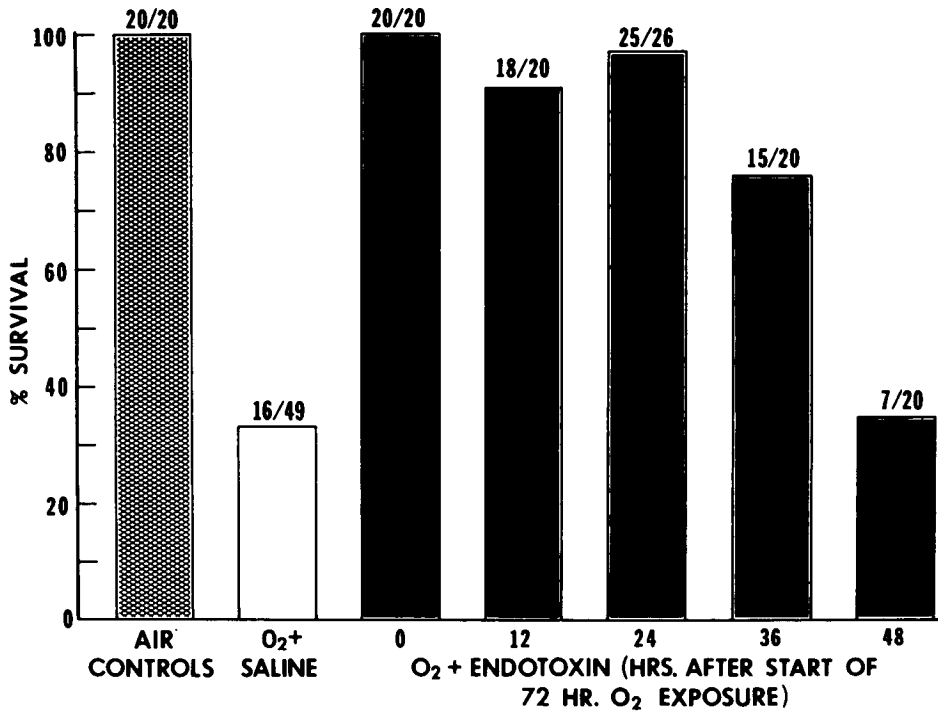
Fig. 1. Effect of delayed endotoxin treatment on survival of adult rats exposed to hyperoxia (96-98% O_2, 72 h). Animals were treated with a single 500 μg/kg dose of endotoxin i.p., either at zero time (just before being placed in hyperoxia) or at 12, 24, 36, or 48 h after the onset of oxygen exposure. Air controls and oxygen-control group received equivolume PBS at zero time. Survival rates for air-control group and endotoxin groups 0, 12, 24, 36 h were all significantly greater than oxygen-control group (oxygen + saline) survival rate, $P <$ 0.05. (Portions reproduced by permission Journal of Clinical Investigation [11])

To our knowledge, all other agents reported to offer a degree of protection from experimental oxygen toxicity, including alpha-naphthylthiourea (12), oleic acid (13), and pre-exposure to 85% O_2 prior to 100% O_2 exposure (14, 15), require a pre-exposure period of several days to achieve any protective action. Endotoxin's effect is therefore unique, both because its protective action occurs even when administered after the onset of oxygen challenge and because it does not produce identifiable lung damage itself, as each of the other protective agents definitely do (12–16).

Effect of Endotoxin Treatment on Chronic Oxygen-Induced Lung Changes

Figure 2 shows the results from a series of experiments designed to determine if the protective effect of endotoxin treatment against the acute manifestations of oxygen toxicity (pulmonary edema, pulmonary hemorrhage, and le-

RESULTS OF 7-DAY EXPOSURE TO >95% O₂
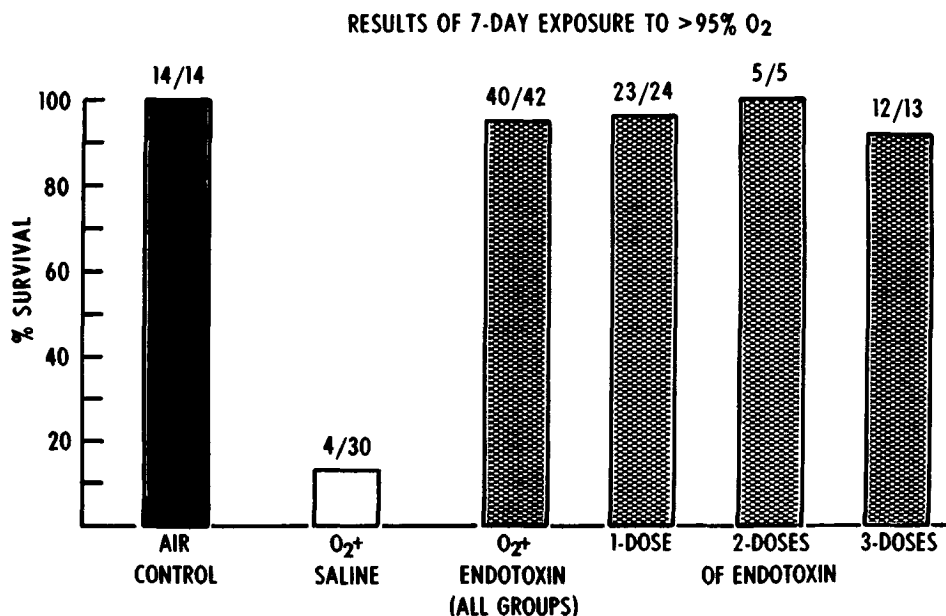
Fig. 2.   Results of 7-day exposure to >95% O₂. Percent survival of adult rats given i.p. injections of endotoxin (oxygen + endotoxin [all groups]) or saline (oxygen + saline) and exposed to >95% O₂ for 7 continuous days. Endotoxin-treated subgroups received either one dose (500 μg/kg) at start of oxygen exposure, or two doses (at start and at 24 h), or three doses (at start and at 24 and 48 h of exposure). Survival values of all groups compared to the oxygen + saline group were $P < 0.05$ (Fisher's test).

thality) would be sustained over a longer period of hyperoxic challenge and to determine if treatment would also offer some degree of protection from the more chronic changes seen in the lungs of animals that do manage to survive prolonged >95% O₂ exposure. The survival values for animals receiving one 500 μg/kg dose (96%), two doses (100%), or three doses (92%) of endotoxin during the 7-day oxygen-challenge period were all significantly greater than for the untreated (saline + oxygen) rats (13%) $(P < 0.05)$.

After the surviving animals from these experiments were maintained in room air for a 6-week recovery period, special stains for evidence of fibrotic lung changes revealed a much reduced deposition of collagen and reticular fibers in the oxygen-exposed endotoxin-treated rats compared to the increased fibrosis demonstrable in the untreated oxygen-exposed survivors (17). Analysis for lung hydroxyproline content gave supportive biochemical evidence for a significant reduction in chronic lung changes (fibrosis) in the endotoxin-treated animals.

Role of Lung Antioxidant Enzymes in Protection by Endotoxin Treatment

Of the possible mechanisms to explain endotoxin's protective action in the hyperoxic setting, we have focused our attention to date on the effect of endo-

toxin treatment on the responses of the lung antioxidant enzyme system to high oxygen exposure. Previously, we have shown that unlike oxygen-tolerant immature animals, adult animals (including rats) typically show an inability to respond to high oxygen exposure with adaptive increases in their lung superoxide dismutase (SOD), catalase (CAT), and glutathione peroxidase (GP) activities, and these mature animals succumb readily to pulmonary oxygen toxicity (18,19). A large number of recent studies from many laboratories have established the important role these endogenous antioxidant defense systems play in providing potential protection from severe lung damage due to hyperoxidant stresses (14,20–22). In our early endotoxin study, we presented suggestive evidence that the improved tolerance to hyperoxia conferred by endotoxin is associated with increases in the protective antioxidant enzyme levels in the lungs of the treated animals (3).

We tested the importance of this stimulation of lung antioxidant enzyme activity by endotoxin treatment in recent studies, comparing the time course of appearance of these lung enzyme changes to the development of pulmonary edema in our treated and untreated oxygen-exposed animals. The results of these studies are summarized in Tables I and II (reproduced from ref. 11). We reasoned that if these enzymes were, in fact, important in protecting the lung against the development of severe pulmonary edema, increased enzyme levels should be detectable in endotoxin-treated oxygen-exposed rats before the usual time of development of severe lung edema in oxygen-exposed rats not given endotoxin. We found that, indeed, these enzymes (SOD, CAT, GP) increased in activity in the lungs of oxygen-exposed endotoxin-treated rats by 36 h of

TABLE I

Time-Course Study: Lung Fluid Accumulation in Adult Rats Exposed to Hyperoxia*

	Pleural Fluid (mL)			
	36 h	48 h	60 h	72 h
Air-Control	0.13 ± 0.03	0.17 ± 0.05	0.15 ± 0.04†	0.17 ± 0.04†
O_2-Saline	0.14 ± 0.03	0.47 ± 0.57	6.53 ± 3.05	8.65 ± 1.64
O_2-Endotoxin	0.09 ± 0.05	0.15 ± 0.07	0.41 ± 0.62†	0.51 ± 0.53†

	Lung Dry Weight/Wet Weight			
	36 h	48 h	60 h	72 h
Air-Control	0.200 ± 0.006	0.200 ± 0.006†	0.199 ± 0.006†	0.200 ± 0.007†
O_2-Saline	0.201 ± 0.004	0.175 ± 0.008	0.162 ± 0.005	0.175 ± 0.006
O_2-Endotoxin	0.198 ± 0.006	0.186 ± 0.006	0.185 ± 0.004†	0.185 ± 0.004†

*Adult rats exposed to 96–98% O_2 for 36, 48, 60, or 72 h. Treated animals received a single 500 µg/kg dose of endotoxin i.p. at 24 h after the onset of O_2 exposure. Air controls received either endotoxin or equivolume phosphate-buffered saline. Results expressed as mean value ± SEM for two experiments (n = 8 animals per treatment group).   †Significant difference from O_2-saline (untreated) group, $P < 0.05$. (Reproduced by permission Journal of Clinical Investigation [11])

TABLE II

Time-Course Study: Lung Antioxidant Enzyme Activity in Adult Rats Exposed to
Hyperoxia*

	36-h Exposure		
Treatment	SOD (units/lung)	CAT (I.U./lung)	GLUT. PEROX. (μM NADPH oxid/min/lung)
Air-Control	691 ± 104	7540 ± 1828	42.6 ± 3.2
O$_2$-Saline	655 ± 139	6566 ± 2455	42.6 ± 8.7
O$_2$-Endotoxin	786 ± 93 (+14%)	8104 ± 1057 (+7%)	51.0 ± 7.0 (+20%)
	60-h Exposure		
	SOD (units/lung)	CAT (I.U./lung)	GLUT. PEROX. (μM NADPH oxid/min/lung)
Air-Control	631 ± 63	6190 ± 976	36.9 ± 6.6
O$_2$-Saline	596 ± 41	7630 ± 1332†	43.2 ± 8.4
O$_2$-Endotoxin	958 ± 96† (+52%)	9490 ± 1890† (+53%)	66.3 ± 6.0† (+80%)

*Adult rats exposed to 96-98% O$_2$ for 36 or 60 h. Treated animals received a single 500 μg/kg dose of endotoxin i.p. at 24 h after the onset of O$_2$ exposure. Air-controls received either endotoxin or equivolume phosphate-buffered saline. Results expressed as mean ± SEM for two experiments (n = 8 animals per treatment group). Values in parentheses are percent increase in enzyme activity compared to air-control values. †Significant difference from air-control enzyme value $P < 0.05$. (Reproduced by permission Journal of Clinical Investigation [11])

exposure time, 12 h before the onset of detectable increases in lung water in the rats that were exposed to hyperoxia but not given endotoxin (Tables I and II). The enzyme levels continued to increase while lung water remained constant in the endotoxin-treated animals during the rest of the 72-h oxygen-exposure period. In contrast, untreated animals showed no such increases in lung antioxidant enzyme activity, and progressive edema formation occurred.

Tables III and IV (reproduced from ref. 11) show the results from two additional types of experiments to explore further the role of these enzymes in the protection against oxygen toxicity conferred by endotoxin. First, we treated rats with diethyldithiocarbamate (DDC), which is known to inhibit SOD activity (23,24). As seen in Table III, DDC treatment blocked the rise in SOD activity in endotoxin-treated rats exposed to hyperoxia and also completely nullified the protective action of endotoxin (11). Next, we treated mice with endotoxin and found that endotoxin treatment in mice exposed to >95% O$_2$ at 1 atm did not result in any increase in pulmonary antioxidant enzyme activity (SOD, CAT, or GP) and also had no protective effect against pulmonary oxygen damage or against the lethal effect of hyperoxia (Table IV) (11).

Finally, we further explored the biochemical basis by which endotoxin confers tolerance to hyperoxia by measuring its effect on lung DNA, RNA, and the ratio of RNA to DNA (Fig. 3). In rats breathing room air, endotoxin

TABLE III

Survival, Pulmonary Edema, and Lung Antioxidant Enzyme Activity in Adult Mice Exposed to Hyperoxia*

Treatment	Survival† (%)	Body Wt (g)	Lung Wt (g)	Lung Wt/ Body Wt (%)	Lung Dry Wt/ Wet Wt
Air-Control	24/24 (100%)	27.74	0.147	0.532	0.221
O₂-Saline	29/41 (71%)	21.97‡	0.322	1.470‡	0.145‡
O₂-Endotoxin	29/40 (73%)	21.54‡	0.376	1.729‡	0.132‡

Treatment	Survival† (%)	SOD (units/lung)	CAT (I.U./lung)	GLUT. PEROX. (μM NADPH oxid/min/lung)
Air-Control	24/24 (100%)	109 ± 6	1922 ± 387	5.67 ± 0.67
O₂-Saline	29/41 (71%)	97 ± 9	1393 ± 410	5.15 ± 1.16
O₂-Endotoxin	29/40 (73%)	96 ± 11	1435 ± 380	5.92 ± 0.74

*Adult mice exposed to 96–98% O_2 for 96 h. Treated animals received 500 μg/kg of endotoxin i.p. at zero time (just before being placed in hyperoxia) and at 24 and 48 h after the onset of O_2 exposure. Air-controls received endotoxin or equivolume phosphate-buffered saline. Results are mean values ± SD for a single experiment with n = 4 animals per treatment group. †Survival at 120 h: O_2-Saline = 1/29 (3%) and O_2-Endotoxin = 2/29 (6%). ‡Significant difference compared to air-control value P < 0.05. (Portions reproduced by permission Journal of Clinical Investigation [11])

TABLE IV

Survival, Lung Fluid Accumulation, and Lung Antioxidant Enzyme Activities in Adult Rats Exposed to Hyperoxia: Effects of Endotoxin Treatment ± DDC*

Treatment	Survival (%)	Pleural Fluid (mL)	Lung Dry Wt/Wet Wt
Air-Saline	15/15 (100%)	0.20 ± 0.02	0.194 ± 0.002
Air-Endotoxin + DDC	17/17 (100%)	0.13 ± 0.06	0.195 ± 0.004
O₂-Endotoxin	17/17 (100%)	0.15 ± 0.07	0.179 ± 0.007
O₂-Endotoxin + DDC	14/35 (40%)†	4.68 ± 2.49†	0.161 ± 0.003†

Treatment	SOD (units/mg DNA)	CAT (I.U./mg DNA)	GLUT. PEROX. (μM NADPH oxid/min/ mg DNA)
Air-Saline	53.5 ± 8.3	504 ± 65	5.21 ± 56
Air-Endotoxin + DDC	53.1 ± 5.7	564 ± 89	5.26 ± 0.69
O₂-Endotoxin	76.3 ± 10.8†	860 ± 124†	7.73 ± 0.83†
O₂-Endotoxin + DDC	51.7 ± 5.2	765 ± 76†	6.79 ± 0.46†

*Adult rats exposed to 96–98% O_2 for 48 h. Animals received a single 500 μg/kg dose of endotoxin i.p. at zero time (just before being placed in O_2) ± DDC (diethyldithiocarbamate), 100 mg/kg i.p. at zero time and at 24 h after the onset of O_2 exposure. Results expressed as mean values ± SEM for two experiments (n = 8 animals per treatment group). †Significant difference from all other treatment groups P < 0.05. (Portions reproduced by permission Journal of Clinical Investigation [11])

resulted in an increase within 24 h in total lung DNA and RNA without any
change in the RNA/DNA ratio; these findings persist for at least 72 h. In rats
exposed to >95% O_2 at 1 atm but not given endotoxin, there was a smaller
rise in total lung DNA and RNA but no change in the RNA/DNA ratio except
at 72 h of exposure time in the few rats who survived without endotoxin treat-
ment. In contrast, in oxygen-exposed rats given endotoxin, a significant rise in
the ratio of RNA to DNA occurred by 48 h of oxygen exposure (Fig. 3); these
RNA/DNA changes suggest an "activation" of the lung to increased cell divi-
sion plus biosynthetic activity (see 25). These preliminary findings also suggest
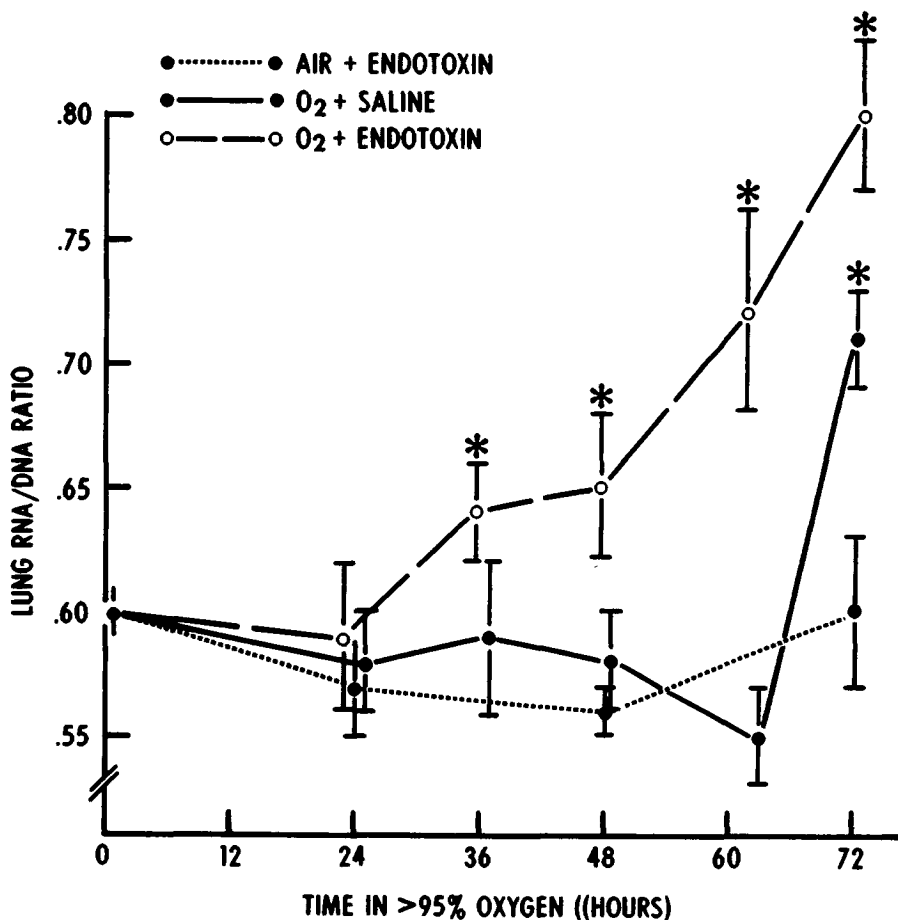
Fig. 3. Lung RNA/DNA ratios for adult rats at intervals during 72-h exposure to air or >95% O_2. Air
+ endotoxin group received a single 500 μg/kg dose of endotoxin at start of room air exposure, oxygen +
saline group received equivolume saline injection, and oxygen + endotoxin group received single 500 μg/kg
dose of endotoxin at start of exposure to >95% O_2. Results expressed as mean ± SEM bars (n = 3-6 animals
per group per time point). * = $P < 0.05$ compared to air control animal value at zero time (DNA ratio of 0.60
± 0.01).

that endotoxin treatment may reverse the usual inhibitory effect that prolonged hyperoxic exposure has on both DNA and protein synthetic mechanisms (1, 26,27).

CONCLUSIONS

We conclude that a) endotoxin confers protection against acute experimental oxygen toxicity even when given in a single dose (500 μg/kg or ~1/50th LD_{50} dose) as late as 36 h *after* the onset of oxygen exposure; b) the antioxidant enzymes of the lung (SOD, CAT, and GP) play an important role in the protective effect produced by endotoxin; and, c) endotoxin treatment may protect against the delayed (fibrotic) changes that follow acute oxygen-induced pulmonary damage. We suggest that endotoxin acts as a mitogen in the lung (increased DNA) and that it "activates" lung cells to respond to metabolic perturbation as evidenced by a rise in the ratio of RNA to DNA in the endotoxin-treated oxygen-exposed animals (compared to the treated, but unperturbed rats breathing room air). We think it may be this activation that facilitates a rapid increase in synthesis of antioxidant enzymes in response to hyperoxic free radical stress in the endotoxin-treated oxygen-challenged animal.

Studies to define further the mechanism for the marked protective action of endotoxin against pulmonary oxygen toxicity may, one hopes, lead to the development of still other agents with similar protective actions but perhaps less toxic potential than endotoxin itself, agents that may be of some future clinical use in helping to circumvent the lung injury associated with prolonged treatment with life-giving oxygen.

Acknowledgment

References

1. Clark JM, Lambertsen CJ. Pulmonary oxygen toxicity: a review. Pharmacol Rev 1971;23:37-133.
2. Shanklin DR. On the pulmonary toxicity of oxygen. I. Relationship of oxygen content to the effect of oxygen on the lung. Lab Invest 1969;21:439-448.
3. Frank L, Yam J, Roberts RJ. The role of endotoxin in protection of adult rats from oxygen-induced toxicity. J Clin Invest 1978;61:269-275.
4. Frank L, Roberts RJ. Oxygen toxicity: protection of the lung by bacterial lipopolysaccharide (endotoxin). Tox Appl Pharm 1978;50:371-380.
5. McCord JM, Fridovich I. Superoxide dismutase: an enzymic function for erythrocuprein (hemocuprein). J Biol Chem 1969;244:6049-6055.

6. Holmes RS, Masters CJ. Epigenetic interconversion of the multiple forms of mouse liver catalase. FEBS Letters 1970;11:45-48.

7. Paglia DE, Valentine WN. Studies on the quantitative and qualitative characterization of erythrocyte glutathione peroxidase. J Lab Clin Med 1967;70:158-169.

8. Schaterle GR, Pollack RL. A simplified method for the quantitative assay of small amounts of protein in biological material. Anal Biochem 1973;51:654-655.

9. Richards GM. Modifications of the diphenylamine reaction giving increased sensitivity and simplicity in the estimation of DNA. Anal Biochem 1974;57:369-376.

10. Steel RG, Torrie JH. Principles and procedures of statistics. New York:McGraw, 1960.

11. Frank L, Summerville JS, Massaro D. Protection from oxygen toxicity with endotoxin. Role of the endogenous antioxidant enzymes of the lung. J Clin Invest (in press).

12. Huber GL, Finder E, LaForce M. Prevention of oxygen toxicity in the lung. Chest 1972;62:365.

13. Smith G, Winter PM, Wheelis RF. Increased normobaric oxygen tolerance of rabbits following oleic acid-induced lung damage. J Appl Physiol 1973;35:394-400.

14. Crapo, JD, Tierney DF. Superoxide dismutase and pulmonary oxygen toxicity. Am J Physiol 1974;226:1401-1407.

15. Tierney DF, Ayers L, Kasuyama RS. Altered sensitivity to oxygen toxicity. Am Rev Respir Dis 1977;115:59-65.

16. Crapo JD, Peters-Golden M, Marsh-Salin J, Shelburne JS. Pathologic changes in the lungs of oxygen-adapted rats. Lab Invest 1978;39:640-653.

17. Frank L, Roberts RJ. Endotoxin protection against oxygen-induced acute and chronic lung injury. J Appl Physiol: Respirat Environ Exercise Physiol 1979;47:577-581.

18. Yam J, Frank L, Roberts RJ. Oxygen toxicity: comparison of lung biochemical response in neonatal and adult rats. Ped Res 1978;12:115-119.

19. Frank L, Bucher JR, Roberts RJ. Oxygen toxicity in neonatal and adult animals of various species. J Appl Physiol: Respir Environ Exercise Physiol 1978;45:699-704.

20. Gregory EM, Fridovich I. Oxygen toxicity and the superoxide dismutase. J Bacteriol 1973;114:1193-1197.

21. Robinson LA, Wolfe WG, Salin ML. Alterations in cellular enzymes and tissue metabolism in the oxygen toxic primate lung. J Surg Res 1978;24:359-365.

22. Chow CK, Tappel AL. Activities of pentose shunt and glycolytic enzymes in lungs of ozone-exposed rats. Arch Environ Health 1973;26:205-208.

23. Heikkila RE, Cabbat FS, Cohen G. In vivo inhibition of superoxide dismutase in mice by diethyldithio-carbamate. J. Biol Chem 1976;251:2182-2185.

24. Frank L, Wood DL, Roberts RJ. Effect of diethyldithiocarbamate on oxygen toxicity and lung enzyme activity in immature and adult rats. Biochem Pharmacol 1978;27:251-254.

25. Chiang M-J, Frank L, Massaro GD, Massaro D. Studies on the biochemical basis of endotoxin (E) protection against O_2 toxicity. Clin Res 1980;28:423A.

26. Northway WH Jr, Petriceks R, Shahinian L. Quantitative aspects of oxygen toxicity in the newborn: inhibition of lung DNA synthesis in the mouse. Pediatrics 1972;50:67-72.

27. Gacad G, Massaro D. Hyperoxia. Influence on lung mechanics and protein synthesis. J Clin Invest 1973;52:559-565.

DEVELOPMENT OF ALTERATIONS IN PULMONARY DIFFUSING CAPACITY AFTER DEEP SATURATION DIVE WITH HIGH OXYGEN LEVEL DURING DECOMPRESSION

R. Hyacinthe, P. Giry, and B. Broussolle

Hyperoxic mixtures are used extensively in operational diving for different purposes:

(a) for safety during the stay at bottom (risk of life-support system failure);

(b) to shorten decompression time by increasing the alveolar tissue pressure gradient of inert gas; and

(c) for increasing tissular Po_2 during therapeutic hyperoxias.

The use of these mixtures is a cause of concern because hyperoxia lasts for days or weeks during deep diving and saturation diving and it is necessary to adapt the Po_2 value to the duration of exposure to avoid the pulmonary toxic effects of oxygen.

Clark and Lambertsen (1) designed the Unit Pulmonary Oxygen Toxicity Dose (UPTD) system to predict oxygen toxicity as function of Pi_{O_2} and exposure duration. During their experiments at low pressure, the index for estimation of pulmonary oxygen toxicity was a decrease in forced vital capacity (FVC). It is generally agreed that a Po_2 below 0.5 ATA does not produce any impairment of pulmonary function.

In hyperbaric conditions the assessment of damage by the calculation of UPTD and the decrement of FVC is not satisfactory when Po_2 is below 1 ATA and when oxygen is combined with other gases (2). Other indexes than FVC have been used for evaluating the effects of oxygen toxicity on lungs. Winsborough (3) measured the pulmonary tissue volume; Caldwell (4), Puy et al. (5), and Prefaut et al. (6) preferred an index of direct impairment of the lung

membrane: the measurement of the pulmonary diffusing capacity for carbon monoxide (DL_{CO}).

We present here the results of a survey of 14 divers; six divers participated in an operational dive to 501 m (*Janus IV*) and eight divers participated in a dry chamber dive to 46 ATA. Both dives used hyperoxic decompression, with a 6-week follow up of $DL_{CO}/\dot{V}E$ modifications.

METHOD AND MATERIALS

Determination of Pulmonary Diffusing Capacity for Carbon Monoxide

The pulmonary diffusing capacity for CO corresponds to the lung transfer coefficient for CO (DL_{CO}):

$$\dot{V}_{CO} = DL_{CO} (\bar{P}A_{CO} - \bar{P}C_{CO})$$

with $\dot{V}_{CO}$ = uptake of CO, in mL STPD · mn^{-1}

$\bar{P}A_{CO}$ = the mean alveolar CO partial pressure, in Torr.

$\bar{P}C_{CO}$ = the mean CO partial pressure in the pulmonary capillary, in Torr.

$\bar{P}C_{CO}$ is considered as negligible because of hemoglobin affinity for CO, so

$$DL_{CO} = \frac{\dot{V}_{CO}}{\bar{P}A_{CO}} \text{ in mL · mn}^{-1} \cdot \text{Torr}^{-1}.$$

The DL_{CO} determination was carried out according to the "steady state" method with the end-tidal P_{CO} used as the mean alveolar P_{CO}. To reduce the DL_{CO} variation due to the ventilation fluctuations, we report DL_{CO} to the litre of ventilation (BTPS):

$$DL_{CO}/\dot{V}E, \text{ in mL STPD · } L_{BTPS}^{-1} \cdot \text{Torr}^{-1}.$$

The apparatus employed was the Godart Diffusion test which includes the following components:

1) A spirometer system for recording of the respiratory volume. The system consists of a wet spirometer and a recorder with paper speed of 60 mm · min^{-1};

2) A "bag in box" system with 150-L latex bags and a valve system for the separation of the inspiratory and expiratory gases;

3) A CO analyzer with a zero to 0.05% CO range; and

4) An end-tidal sampling device according to Rahn for continuous sampling of end-tidal gas, which is considered to represent the alveolar gas.

For the measurement, a mixture of about 0.045% CO in ambient air was prepared and stored in a latex bag. The subject, seated and at rest, was connected to the apparatus via a mouthpiece and initially breathed ambient air.

The alveolar and mean expiratory concentrations of CO were then determined. The subject inspired from the inspiratory bag and expired into the expiratory bag. When a steady state was achieved, the CO concentrations of alveolar, mixed expiratory, and inspiratory gases were determined. These measured values were corrected for the initial alveolar and mean expiratory CO concentrations in air.

The determination required 2 min. With this apparatus and technique, the normal values of $DL_{CO}/\dot{V}E$ obtained from a population of 167 healthy men with an average age of 33 ± 8 years were:

$$\overline{D}L_{CO} \quad \dot{V} \pm SD = 2.7 \pm 1.1 \; mL \cdot L^{-1} \cdot Torr^{-1} \; (ref. \; 7).$$

In our group the $DL_{CO}/\dot{V}E$ control values had a mean ± SE of 2.98 ± 0.72 mL·L^{-1}·Torr^{-1}, with a range between 1.83 and 4.43 mL·L^{-1}·Torr^{-1}. The intervariation of $DL_{CO}/\dot{V}E$ between the divers resulted mainly from the breathing pattern. When the breathing pattern of a diver was steady, the reproducibility of $DL_{CO}/\dot{V}E$ was sufficiently good. Table I shows the $DL_{CO}/\dot{V}E$ and ventilatory measurement values before a saturation dive using 5 divers.

Parameters of the Saturation Dives

Janus IV. Dive profile: a) compression with ternary mixture He-O$_2$-N$_2$ and steps in 30 h, 30 min to 44 ATA; b) 5 days at 44 ATA with Po$_2$ = 400 mb, Pn$_2$ = 1.6 ATA; c) 10 h of work on a platform at 47 ATA with Po$_2$ = 450 mb; d) 20 min at 501 m with Po$_2$ = 450 mb; and e) decompression in 7 days, 17 h, 30 min. The Po$_2$ profile during the decompression consisted of a series

TABLE I

Control Values for $DL_{CO}/\dot{V}E$ and Ventilatory Measurements in
5 Navy Divers

Subjects	SEV	VIA	MOR	BUL	MAR
	(n = 5)	(n = 5)	(n = 4)	(n = 4)	(n = 3)
$DL_{CO}/\dot{V}E$ mL·L^{-1}·Torr^{-1}	2.25 ± 0.14	3.42 ± 0.10	3.49 ± 0.47	4.18 ± 0.19	4.08 ± 0.38
V_T L$_{BTPS}$	1.25 ± 0.39	1.26 ± 0.37	1.31 ± 0.36	1.93 ± 0.28	1.80 ± 0.16
f cycle·mn^{-1}	7.41 ± 3.8	4.75 ± 0.82	5.52 ± 1.50	3.94 ± 0.11	3.78 ± 0.56
$\dot{V}E$ L$_{BTPS}$·mn^{-1}	11.2 ± 1.06	5.72 ± 0.83	6.55 ± 0.64	7.63 ± 1.29	6.75 ± 0.39

Five Navy Divers were followed more than 1 year. Values are mean ± SE. Note the small SE of $DL_{CO}/\dot{V}E$ as compared to the statistical dispersion of other parameters.

of 5 decrements from 800 mb to 400 mb with fractional O_2 concentrations of 0.02 until 23 ATA; 0.03 until 13.4 ATA; 0.06 until 6–8 ATA; 0.12 until 3.3 ATA, and 0.24 ATA until surface.

Simulated dive to 450 m. Dive profile: a) compression with ternary mixture He-O_2-N_2 and steps in 39 h, 15 min to 46 ATA; b) 48 h at 46 ATA with Po_2 = 400 mb, Pn_2 = 2.2 ATA; and c) decompression in 10 days, 20 h with a stop of 6 h, 30 min at 32.4 ATA. The Po_2 profile consisted of a decrement of Po_2 from 700 to 500 mb in 48 h until 32.4 ATA, where Po_2 was established at 600 mb during the step. Between 32.4 and 5.2 ATA Po_2 was at 500 mb for 6 days. Between 5.2 and 2.5 ATA, Po_2 was at 600 mb for 15 h.

The Po_2 profiles during decompression for both saturation dives are shown in Fig. 1.

Subjects

Fourteen professional civilian and military divers were studied. All subjects had been exposed to more than one deep saturation dive before the experiment. The mean age of the divers was 29.8 years, ranging from 24 to 37 years; the mean weight was 73.5 kg, ranging from 57 to 89 kg.

In *Janus IV* two divers worked at 47 ATA and two others went down to 501 m. During the decompression, one diver who had worked at 47 ATA and
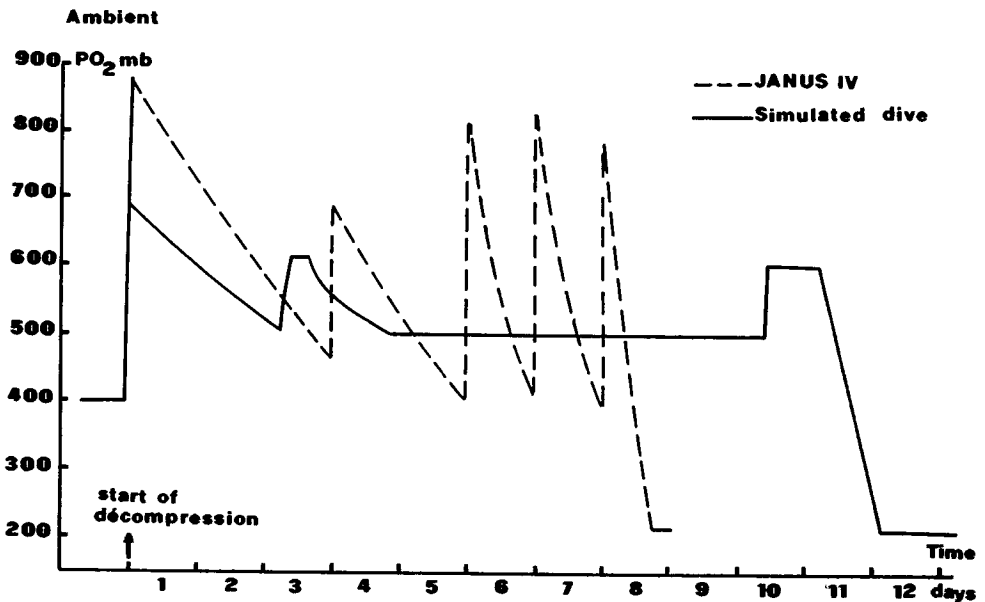
Fig. 1. Ambient Po_2 vs. time during decompression for *Janus IV* and the simulated dive.   *For Janus IV,* decompression was done at constant Fo_2. When Po_2 was less than 400 mb, oxygen was injected to reach 800 mb, and the f_{o_2} remained constant until Po_2 lessened to 400 mb.   *For the simulated dive,* hyperoxic peaks at the beginning and end of decompression are for therapeutic purposes.

another one presented shoulder and knee aches. They breathed oxygen-enriched mixtures with $Po_2 = 1.6$ ATA four times for 25 min each day. In the last meters of the decompression, all divers breathed pure O_2 for two 25-min periods. In the simulated dive during decompression, 5 subjects complained of knee pains and breathed an oxygen-enriched mixture with a Po_2 range of 1.7–1.0 ATA for a 25-min period, 2–6 times a day for 1–5 days.

The *Janus IV* divers had been exposed to an average of 2000 UPTD. In the simulated dive the subjects were exposed to an average of 1500 UPTD.

Sequence of Measurements

The $DL_{CO}/\dot{V}E$ control values were obtained during the week before the dive. The postdive measurements were obtained 1–16 h after surfacing. The follow-up measurements were made 5–9 days, 2 weeks, and 5–6 weeks after the dive.

The paired t test was used for determining whether the difference between various measurements was statistically significant. The level of significance was $P < 0.05$.

RESULTS

The individual $DL_{CO}/\dot{V}E$ values are represented in Fig. 2. The $DL_{CO}/\dot{V}E$ before and after the dive with paired t test is given in Table II.

The postdive measurements showed that $DL_{CO}/\dot{V}E$ decreased significantly. The mean value $\pm$ SE of $DL_{CO}/\dot{V}E$ was: 2.60 ± 0.17 mL $\cdot$ L^{-1} $\cdot$ Torr^{-1} ($P < 0.001$); the mean decreased in $DL_{CO}/\dot{V}E$ compared to control values was -12.3% with a range varying from $+1.2$ to -25.1%.

The first follow-up measurement 5 and 9 days postdive on 12 subjects showed that $DL_{CO}/\dot{V}E$ was decreased more than just after the dive (mean $DL_{CO}/\dot{V}E \pm$ SE $= 2.50 \pm 0.23$ mL $\cdot$ L^{-1} $\cdot$ Torr^{-1} [$P < 0.01$]), with a mean decrease of 16.2% and a range between $+10.7$ and -34.5%. Compared to control values, two divers had $DL_{CO}/\dot{V}E$ values that were normal or higher; two other divers had a $DL_{CO}/\dot{V}E$ decrement similar to that just after the dive; and eight divers had a decrease in $DL_{CO}/\dot{V}E$ greater than that just after the dive.

The follow-up measurement made on 4 subjects 16 days after the *Janus IV* dive showed that 2 divers still had a decreased $DL_{CO}/\dot{V}E$ with a decrement of about 20% and that the other two divers had normal $DL_{CO}/\dot{V}E$ values (Fig. 2). Of the five divers seen 5 or 6 weeks after the dive, four had $DL_{CO}/\dot{V}E$ values close to control values but one had a higher $DL_{CO}/\dot{V}E$ than before the dive.

The 6 divers of *Janus IV* who had been exposed to 2000 UPTD had main $DL_{CO}/\dot{V}E$ decreases of -8.2% and -10.5%, respectively, just after the dive and 5 days later ($P < 0.05$). The 8 divers of the simulated dive exposed to 1500 UPTD had main $DL_{CO}/\dot{V}E$ decreases of -15.9% and -17.4% respec-
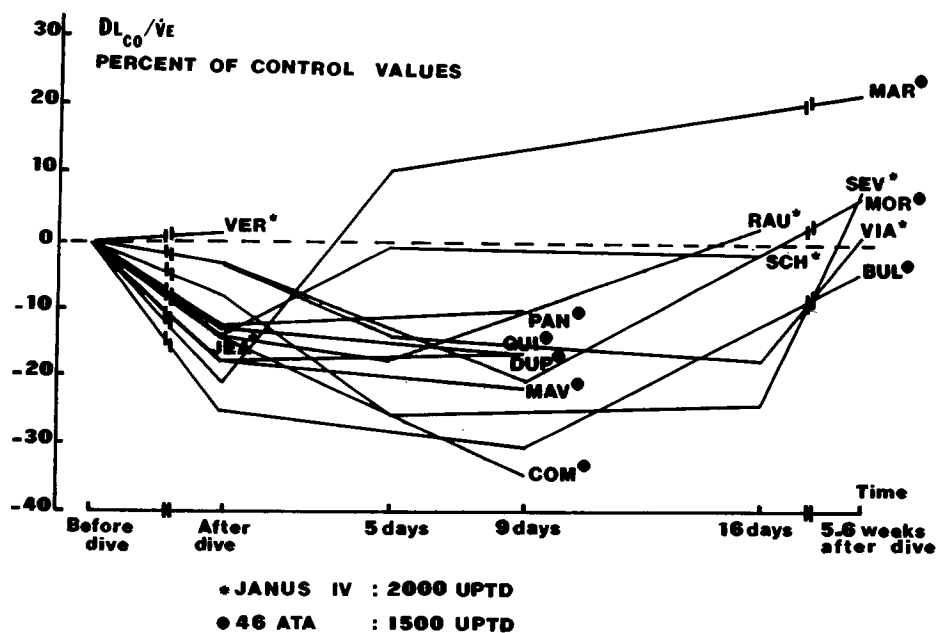
Fig. 2. Individual follow up of $DL_{CO}/\dot{V}E$ values for the 14 divers studied.   Results expressed in percentage of individual control values.

TABLE II

Follow-up of the Ratio $DL_{CO}/\dot{V}E$ in 14 Divers after *Janus IV* and Simulated Dive

	<24 Hours After Dive	1 Week ± 2 Days After Dive	2 Weeks After Dive	5–6 Weeks After Dive
	(n = 14)	(n = 12)	(n = 4)	(n = 5)
Control Values	2.98 ± 0.20	2.985 ± 0.23	2.71 ± 0.4	3.45 ± 0.35
Postdive Follow-up Values	2.60 ± 0.17	2.50 ± 0.23	2.43 ± 0.4	3.65 ± 0.35
P (Paired t test)	<0.001	<0.001	N.S	N.S

All of the individual divers could not be seen exactly at the same time after the dives, therefore the control values are the ones of the same divers as in the postdive follow-up values. Values are the mean ± SE. Student's paired t test was used for statistical comparison.

tively, just after the dive and 9 days later ($P < 0.01$). The differences between the main $DL_{CO}/\dot{V}E$ values for the two different dives were not significant.

DISCUSSION

The primary purpose of this study was twofold: to determine whether the partial pressure of oxygen used during the decompression from deep saturation dives can be toxic to the lungs and to follow the completeness of recovery from pulmonary O_2 toxicity, if it exists.

If we refer to Lambertsen's system, in *Janus IV* there was 2000 UPTD and in the simulated dive 15,000 UTPD.

During the simulated dive we also measured decreases in FVC. The observed decreases of FVC were less than the predicted ones (Fig. 3). However, decreases in $DL_{CO}/\dot{V}E$ were greater than both predicted and measured decreases in FVC, and lasted in 2 subjects less than 1 week, as FVC—in all the remaining 11 subjects, more than 1 week and sometimes more than 2 weeks, while recovery in FVC was obtained in 1 week.

The $DL_{CO}/\dot{V}E$ seems a more powerful index of pulmonary stress than FVC because minute lesions were detected over a longer time. It is generally agreed that the first step of oxygen toxicity is the appearance of an edematous lung. Edema will increase the alveolar-capillary barrier thickness and induce a decreased transfer rate of gases through the lungs.

Caldwell (4) observed in 3 subjects exposed to 1 atm of pure oxygen for 30–74 h a decreased DL_{CO} of -19% just after exposure. Puy et al. (5) ob-
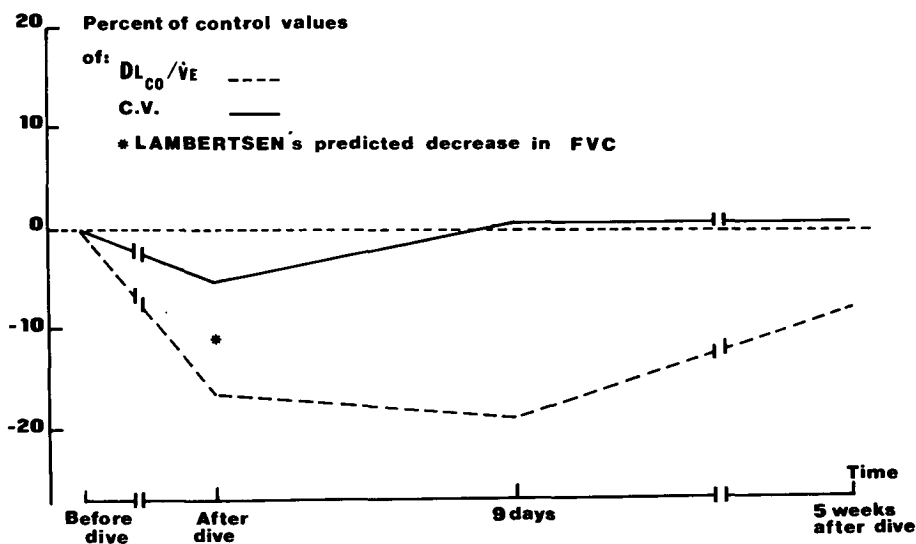
Fig. 3. Follow up of respiratory ($DL_{CO}/\dot{V}E$ and FVC) in the 8 divers participating in the 450-m saturation dive. Values are expressed in percentage of individual control values.   FVC is forced vital capacity.

served a mean decrease in DL_{CO} of 9% immediately after a 6–11 h O_2 exposure; 12–20 h after termination of OHP exposure, they observed a DL_{CO} decrease of -16%. Prefaut et al. (6) observed a DL_{CO} decrease of -20.1% compared to control values 48 h after a saturation dive with 600 mb of PO_2 during 7 days of decompression.

In our experiment, hyperoxia lasted a long time (8 days in *Janus IV* and 11 days in the simulated dive); there was a possibility that the edema would become chronic; and what we detected during the 2 weeks postdive was the fibrinous organization of the chronic edema and healing.

In our experiments, however, there was no correspondence between the UPTD and the $DL_{CO}/\dot{V}E$ of the two different dives. In the simulated dive the decompression time was longer and 5 to 8 divers presented symptoms of decompression sickness. It is possible that decompression also induces pulmonary edema.

After decompression, increased lung water content was reported by Chryssanthou (7). Experimental gaseous embolism reported by Hlastala et al. (8) demonstrated that even if normal pulmonary circulation was resumed within 30 min after gas embolism, lung water content was still increased. After microembolization for 2 h, Ohkuda et al. (9) showed that edema was still present even after 2 h of recuperation.

In our dives decompression and bubble embolization lasted for 8 and 11 days, therefore it is possible that at least part of the lung edema may have been due to decompression. This would explain why even when FVC decrease was less than the one predicted by the UPTD system, DL_{CO} decrease was greater than FVC drop. Our results show that FVC is a gross measurement and that DL_{CO} detects minute variations in alveolar-capillary membrane. But, while there was for all but one subject a diminution of the diffusing capacity, the impairment of the diffusing capacity was slight and was completely reversible in 3 weeks.

It seems that the measurement $DL_{CO}/\dot{V}E$ should be preferred for estimation of global decompression—hyperoxic damage to the lungs and the follow-up of lung healing after deep diving.

Acknowledgment

References

1. Clark JM, Lambertsen CJ. Pulmonary oxygen toxicity: a review. Pharmacol Rev 1971;23:37-133.
2. Lemaire C. Détermination du taux d'hyperoxie acceptable pour les plongées au long cours par la mesure de la capacité vitale. Bull MEDSUBHYP 1976;12:82-87.
3. Winsborough MM, McKenzie. Pulmonary oxygen toxicity and the preoedematous lung: In third congress of the European Undersea Biomedical Society. Med Aeronaut Spat Med Subaquat Hyp 1977;16(63):254-256.

4. Caldwell PRB, Lee WL Jr, Schildkrant HS, Archibald ER. Changes in lung volume diffusing capacity and blood gases in men breathing oxygen. J Appl Physiol 1966;21:1477-1483.

5. Puy RJM, Hyde RW, Fischer AB, Clark JM, Dickson J, Lambertsen CJ. Alterations in the pulmonary capillary bed during early O_2 toxicity in man. J Appl Physiol 1968;24(4):537-543.

6. Prefaut CH, Prosperi D, Chardon G. Note préliminaire sur la détermination de la ductance globale du CO en condition hyperbare. BULL MEDSUBHYP 1973;10:35-39.

7. Chryssanthou CM, Springer M, Lipschitz S. Blood-brain and blood-lung barrier alteration by dysbaric exposure. Undersea Biomed Res 1977;4:117-129.

8. Hlastala MP, Robertson HT, Ross BK. Gas exchange abnormalities produced by venous gas emboli. Resp Physiol 1979;36(1):1-18.

9. Ohkuda K, Nakahara K, Straub NC. Changes in lung fluid protein balance in sheep after microembolism. Physiologist 1976,19:315.

PART I. DISCUSSION: OXYGEN TOXICITY

A. B. Fisher, *Rapporteur*

The major discussion in this session centered around four papers. After the presentation of the Pooley-Walder paper regarding changes in cell volume after hyperbaric exposure, discussion was directed primarily towards clarification of the experimental preparation. It was pointed out that the cytoplasm of the fat cell, exclusive of intracellular fat, is approximately 6% of cell volume. The observed experimental changes resulted in approximate doubling of this cytoplasmic envelope. Dr. Pooley explained that the experiments evaluated relative rather than absolute changes in water content of cells. The possibility that the isolation procedure resulted in an increase in the base-line water content of cells could not be excluded and that in vivo changes in cell volume may be less than those observed in the in vitro experiments. Dr. Pooley speculated that the shrinkage of cells in the presence of albumin was due to loss of water, but could also represent loss of fat due to stimulation of lipolysis by the albumin. The investigators did not evaluate the effect of ouabain on their preparation. A comment from the audience pointed out that the brain, like the bone marrow, is enclosed in a bony casing.

In the discussion after Dr. Fisher's presentation on lung ATP turnover during oxidant stress, Dr. Fisher explained that exposure of the lung to hyperbaric oxygen produced no changes in the physiological function of the lung as indicated by the pressures required for ventilation and perfusion at constant flow rates. However, during a second hour of exposure to hyperbaric oxygen (data were not presented in this preparation), ventilation and perfusion pressures increased and dry-to-wet weight-rate ratios decreased, which indicated the development of lung edema. A comment from the audience pointed out that the changes in metabolism observed with a perfused lung were similar to those previously observed for the retina.

The Frank et al. paper engendered considerable interest and speculation on the possible mechanism for protection against hyperoxia by endotoxin. One questioner asked whether the mechanism for pulmonary edema produced by endotoxin and hyperoxia were different. Dr. Frank responded that the pulmonary edema produced by endotoxin is dose- and species-dependent, and that the dose used in these studies does not produce pulmonary edema. Another questioner commented on the recent observation of induction of indoleamine 2, 3-dioxygenase in mouse lungs by endotoxin. Dr. Frank pointed out that similar results can be obtained with experimental pulmonary viral infections and questioned whether the increased enzyme was actually in white blood cells recruited to the lungs rather than in the lung cells themselves. In response to further questions, Dr. Frank said that he did not know whether cellular margination could prevent lung edema and had not evaluated whether endotoxin affects the bactericidal or phagocytic properties of lung macrophages.

During the discussion after the presentation of the Hyacinthe-Broussolle paper, Dr. James Clark compared the vital capacity and diffusing capacity as indices of pulmonary oxygen toxicity. He pointed out that both are affected by exposure of human subjects to 2 ATA oxygen, but that measurement of vital capacity has the advantage of being essentially "on-line" and technically easier to perform. He believes that measurement of diffusing capacity may be helpful in the future in providing information on recovery from pulmonary oxygen poisoning.

Another questioner asked whether changes in hemoglobin concentration could have affected the measured values for diffusing capacity. Dr. Hyacinthe stated that the hematocrit decreased only 2% in the divers, whereas the diffusing capacity decreased 15%. Therefore, it is unlikely that changes in hemoglobin concentration significantly affected the results. Dr. Hyacinthe further stated that the P_{50} for O_2-hemoglobin was changed during the dive, but that it recovered quickly during decompression. The diffusing capacity, however, took considerably longer to recover, which suggests that changes in P_{50} did not affect the measured results.

The session chairman, Dr. Saltzman, commented on the marked shift in focus of the present underwater physiology symposium with its greater emphasis on metabolic studies. He implied that this was a reasonable direction for research in this area and closed the session.

COMPARATIVE EFFECTS OF VARIOUS PROTECTIVE AGENTS UPON ACUTE CEREBRAL HYPERBARIC OXYGEN TOXICITY IN MICE: PARTICULAR INTEREST OF SOME BENZODIAZEPINES

F. Brue, P. Joanny, A. Chaumont, J. Corriol, and B. Broussolle

Despite the high reactivity of the free radicals resulting from oxygen reduction upon numerous biological compounds, it is well known that acute central nervous system intoxication is restricted to high pressure oxygen (HPO); in this experimental situation, cellular defense mechanisms (1) may be overwhelmed and thus lose their own natural ability to counteract the development of the intoxication. Furthermore, some HPO-induced biological reactions have been shown to behave themselves as toxic aggravating factors.

Pharmacological strategy required at this stage must strengthen natural defense mechanisms or counteract cell-harmful secondary HPO-induced reactions, or both. In the past, many protective agents have been described, but most workers used very different experimental methods, which rendered clearly irrelevant any serious comparison between experimental data. An effort has been made by the authors of this work to use both well-defined and reproducible experimental conditions.

On the other hand, it must be emphasized that in the literature numerous protective agents have intrinsic toxic properties or serious undesirable behavioral side effects (or both), which rendered them clearly unsuitable in man. Therefore, this work has been extended to the study of new pharmacological compounds with particular emphasis on both their lack of toxicity and their very weak, undesirable side effects.

According to these criteria, we have recently found that beyond the well-known anticonvulsants, i.e., diazepam and clonazepam (2), some antianxiety

drugs from the benzodiazepine class afford in mice a powerful protection. These drugs are currently available for prescription in man.

METHODS

Subjects were 25–30 g CD-1 Charles River (France) mice. This species exhibits a high sensitivity towards HPO; it can be used in large numbers in many series of experiments; and its brain size is convenient for use of the rapid freezing method under HPO, which allows concurrently neurochemical approaches (3).

In each series, 20–25 animals were used. Under each HPO exposure, 8 animals were housed in a cage with individual cells. Controls and treated animals were in placed in alternate cells to neutralize any group effect. Protective agents were given i.p. 20 or 30 min before OHP, according to reference works or preliminary tests (0.1 mL/10 g weight). Control animals received the same volume of solvent vehicle for each compound.

The hyperbaric chamber was flushed with pure O_2 during the 5 min before compression. Carbon dioxide was trapped into soda lime scattered on the cage floor under a grid. The O_2 pressure was 6 ATA, thus the various intoxication symptoms were succeeding rapidly enough to maintain the protective drug level for an unchanged brain during HPO exposure. The compression rate was 1 atm·min^{-1}. All delays in the occurrence of various symptoms were taken from the beginning of compression.

Before the compression and during the first minutes after reaching 6 ATA, the activity of the mice was observed; it roughly reflected the possible unsuitable behavioral side effect of the tested drug. This locomotor activity was expressed according to the following different levels as compared with controls: + + + no difference; + + slightly decreased activity; + weak activity; 0, immobility.

Intoxication criteria observed for each animal were: first preconvulsive symptoms (PC), which were often important agitation, tremor, or very brief clonic jerk; first generalized clonic fit (C); first generalized clonicotonic seizure (T); first gasps (G), and death (L).

Statistical Treatment of Results

1) Occurrence times for each symptom appear as lognormally distributed. Thus the curves of cumulated percentages, as functions of time, are in agreement with a lognormal law, which we used to calculate and draw the curves on a Hewlett-Packard 9810-A computer and a 9862-A plotter.

2) For each phenomenon, probit analysis was applied to the time logarithms. This method allowed us to determine and compare the means of logarithm populations according to the Student's t test. We also computed the median (T_{50}) of the times for each symptom, assuming that all animals would have convulsed in the absence of gasps or death. The T_{50} ratios between

treated and control animals can be taken as an index of efficiency for each protector.

When the *t* test could not be used, statistical significance was established according to F, chi 2, or Kolmogorov-Smirnov tests. Also see Brue et al. (4).

RESULTS

Metabolic agents. There was a significant protection from 4 mM/kg of succinate and 12 mM/kg of glutathione (5), but glucose (5 g/kg) plus insulin (1.5 IU/kg) had a weak effect (6). That protection could partly be due to a hyperosmolar effect (7).

Antioxidants and redox-system intermediates. The satisfactory protection induced by 40 mg/kg of 2,5-di-ter-pentyl-hydroquinone (8) could be at least partially explained by its vehicle, i.e., propylene glycol. We did not study the effects of disulfiram. This agent, devoid of efficacy at a 120 mg/kg dose (8) would protect at doses of 200–400 mg/kg, unfortunately very close to the DL 50 (9). Menadione (vit K3) plus Na bisulfite (each at 0.2 mM/kg), showed good protective effects according to Horne (10). Centrophenoxine (Lucidril, 1 mM/kg) delayed significantly the convulsion occurrence.

Cations. Li chloride (11) effectively protected against convulsions, but at a subtoxic dose of 600 mg/kg; further, Mg lactate (2 mM/kg) or Ca chloride (2.5 mM/kg) exhibited clearly a higher protection than Li did, but unfortunately both metals were shown to have a marked toxicity; Ca^{++} protective effect was further increased in the presence of gamma-hydroxybutyrate (0.62 mM/kg) or serotonin.

Vasoactive drugs, betareceptor blockers, and serotonin. Hydergine (14 mg/kg) and Papaverine (6 mg/kg) significantly delayed the onset of convulsions (12). These findings are in keeping with a cerebral protection which may be secondary to a peripheric extra-cerebral predominant vasodilatation (13), 0.025 mM/kg of serotonin, which does not cross the blood-brain barrier, appears as a very effective protector; in addition, propranolol (10 mg/kg) was also clearly effective against OHP toxicity and was devoid of undesirable behavioral side effects.

Phenothiazines and ureides. The two phenothiazines, i.e., chlorpromazine (5 mg/kg) and laevopromazine (5 mg/kg), caused a low protection, as did the two anticonvulsant ureides, i.e., diphenylhydantoin (50 mg/kg) and phenobarbitone (5 mg/kg). (Also see Calcet et al. [14])

Drugs acting on GABA metabolism. The weak protective action afforded by GABA itself (15) required a high concentration of this amino-acid (20 mM/kg); further GABA transaminase inhibitors (AOAA, n-dipropyl-acetic acid)

also showed little beneficial action. We did not study the effects of L-cycloser-ine, which has been reported to afford a powerful protection and significantly increase the GABA cerebral level (16).

Drugs acting on central monoaminergic systems. Pargyline (75 mg/kg), a powerful monoamine oxydase inhibitor, significantly delayed the occurrence of all examined symptoms, in contrast with alpha-methyl-*p*-tyrosine (200 mg/kg, an inhibitor of tyrosine hydroxylase), which promoted very little, but signifi-cantly, the occurrence of convulsions.

Among drugs believed to act specifically upon dopaminergic system, gamma-hydroxybutyrate (1.25 mM/kg), an inhibitory agent of *Substantia nigra* neu-rons, exerted a good protection, as its precursors did, i.e., gammabutyrolac-tone and 1,4-butanediol (17). Haloperidol (10 mg/kg, a blocker of dopami-nergic receptors) given 2 h before HPO delayed all HPO-induced symptoms, but surprisingly enough, apomorphine chlorhydrate (5 mg/kg, an activator of dopaminergic receptors) appeared weakly active in preventing convulsions. L-Dopa was practically devoid of any effect.

Benzodiazepine class. Antiepileptic drugs diazepam (Valium, 1 mg/kg) and clonazepam (Rivotril, 0.1 mg/kg) were found to protect the mice very markedly against the clonicotonic convulsions and pulmonary edema (2). In addition, at the therapeutic low doses used, spontaneous motor activity seemed well preserved.

We have very recently studied some other benzodiazepines mainly used in the clinic in regard to their potent antianxiety properties, as chlordiazepoxide (Librium, 5–10 mg/kg); lorazepam (Temesta, 0.5 mg/kg); oxazepam (Seresta, 1–2 mg/kg); clobazam (Urbanyl, 5 mg/kg); di-K-Chlorazepate (Tranxène, 5 mg/kg); and prazepam (Lysanxia, 2 mg/kg). All these drugs afforded a very potent and homogenous protection against HPO-induced convulsions, and pul-monary toxicity was also significantly delayed (Table I and Fig. 1).

DISCUSSION

It must be underlined that the protective index obtained in the present work appeared a very satisfactory one, according to the following factors: first, the high level of oxygen pressure used herein, and second, the low doses of protectors chosen because of their small, undesirable behavioral side effects.

On the other hand, it should be stressed that in regard to the rapid occur-rence of the neurological symptoms in control animals, the beginning of the compression was chosen as the true origin of symptom time course; this type of representation leads to a significant decrease of protection index.

Whatsoever, after a careful screening among numerous and chemically different drugs, it appears that various pharmacological agents, such as pro-pranolol, gamma-hydroxybutyrate, and, more particularly, the benzodiaze-pines, possess impressive protective effects against acute HPO toxicity. Keep-

TABLE I

Numerical Results of the Protective Effects of i.p.-Injected Benzodiazepines on
6 ATA O_2 Toxicity in Mice

Treatment, locomotor activity preservation		PC	C	CT	G	L
Diazepam 1 mg/kg ++	Med – ratio A w S	21/11 ***	39/14 *** 2/20	70/25 *** 12/20	44/30 ***	92/66 ***
Chlordiazepo- xide, 5 mg/kg +++	M.R. A w S	21/10 ***	31/16 *** 4/24	61/30 *** 12/24	48/33 ***	78/59 ***
Clobazam 5 mg/kg ++	M.R. A w S	19/10 ***	30/10 ***	160/23 *** 22/26	42/30 ***	80/54 ***
Lorazepam 0.5 mg/kg +	M.R. A w S	22/10 ***	59/11 *** 8/28	298/25 *** 26/28	45/30 ***	97/63 ***
Oxazepam 2 mg/kg ++	M.R. A w S	13/9 **	38/11 ***	** 17/18	41/28 ***	92/56 ***
di K-Chloraze- pate, 5 mg/kg +++	M.R. A w S	27/11 ***	66/14 *** 13/21	*** 20/21	43/30 ***	109/66 ***
Prazepam 2 mg/kg +++	M.R. A w S	14/10 **	41/11 *** 7/20	178/21 *** 17/20	44/29 ***	94/58 ***

Symptoms are preconvulsive signs (PC); clonic (C) and clonicotonic (T) fits; gasps (G); and death (L). M.R.: ratio of medians (T_{50}) of symptom occurrence times (min) in treated and control animals. For seizures, medians were computed assuming that all mice would have convulsed in absence of gasps and death. A w S: number of animals without symptoms, compared to the total observed animal number. Spontaneous locomotor activity in treated mice before toxic fits was compared with controls: no difference, + + +; slightly decreased activity, + +; weak activity, +; and immobility, 0. t test or chi^2 test: ** $2P < 0.01$; *** $2P < 0.001$.
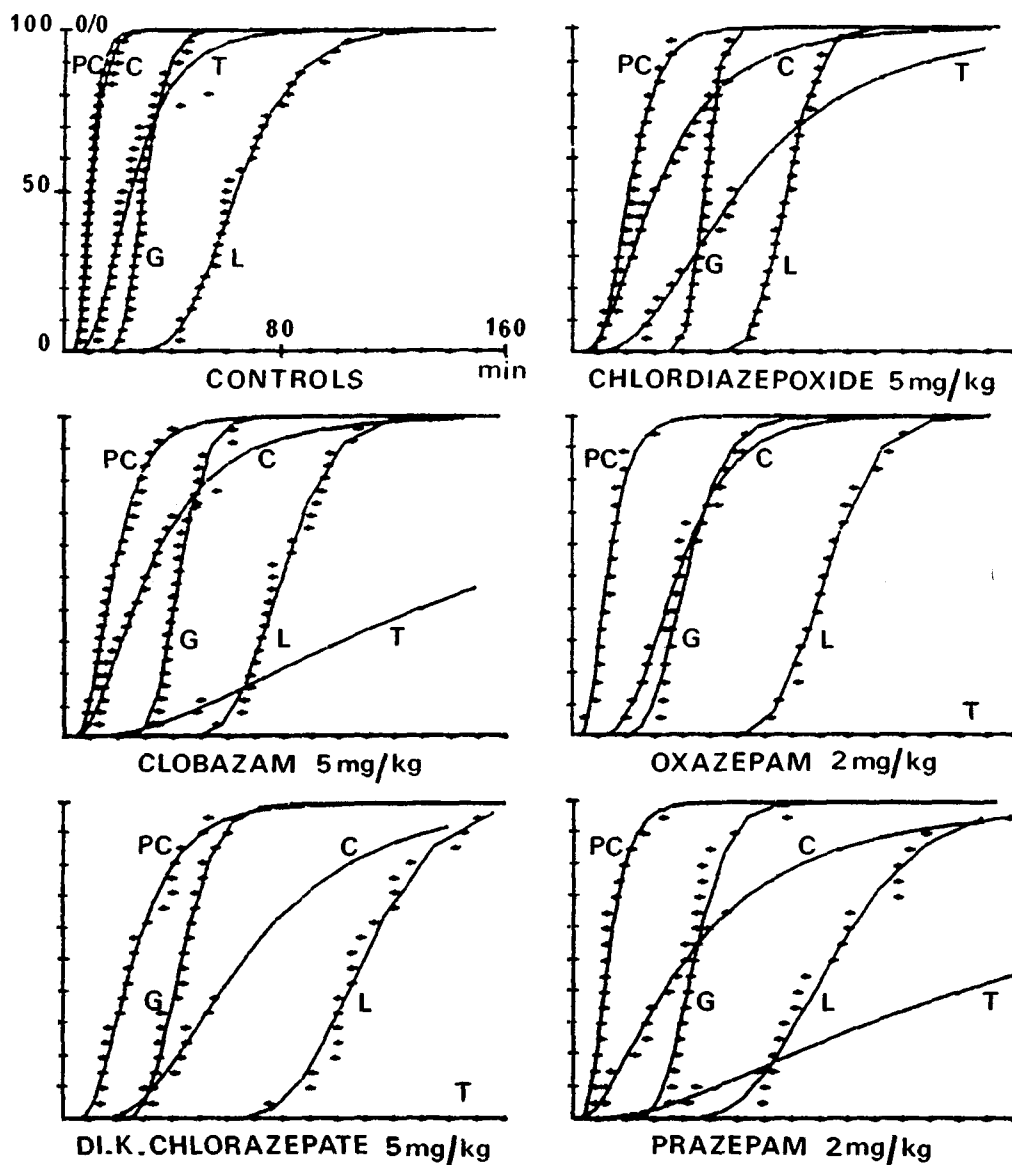
Fig. 1. Protective effects of some benzodiazepines against acute 6 ATA O_2 toxicity in mice. Injection i.p. 30 min before compression; vehicle tween 80 1%, 0.1 mL/10 g weight. Cumulative relative frequencies are plotted as functions of time for each symptom: PC, preconvulsive signs; C, clonic fits, and T, clonicotonic fits; G, gasping; L, death. Curves are drawn according to a lognormal distribution law.

ing in mind that caution is certainly still needed in extrapolating from these preliminary findings, we hope that this work gives a proposal to the use of these pharmacological agents in man submitted to HPO. Indeed, it must be remembered that the benzodiazepine receptor in human brain corresponds to that of rat brain in affinity, stereospecificity, and regional distribution (18).

The antianxiety drugs of the benzodiazepine class, compared to other drugs previously reported in the literature, clearly possess two major advantages: first, very weak undesirable behavioral side effects in both animals and man (the prazepam dose required to abolish the mouse straightening reflex is 1000-fold higher than the found protective dose against oxygen-induced convulsions); and second, the antianxiety effects of these drugs obviously can be useful in patients submitted to HPO in clinics.

Considering the extreme chemical heterogeneity among the protective agents studied herein, as well as in the literature, the intimate mechanism of HPO-induced toxicity remains largely to be solved. Nevertheless, the overall potency towards HPO-induced convulsions exhibited by benzodiazepines raises the problem of the possible involvement in acute oxygen toxicity of the GABAergic synapses, often considered as the primary site of action of benzodiazepines. Such a GABAergic pathway connects the neostriatum with the *Substantia nigra,* mediating postsynaptic inhibition of nigral dopamine neurones. In mice, the fact that diazepam and clonazepam clearly delayed the occurrence of OHP-induced decline of endogenous dopamine as well as the OHP-induced convulsive fits, supports the view that dopamine could be similarly involved in the triggering of OHP seizures (19).

The strionigrostriate loop represents a dopaminergic mechanism by which the striatum regulates its own needs in dopamine; via pallidum and thalamus, it acts on the motor and premotor cortices and plays a major role in the control of motor and psychomotor activity (20). Moreover, bilateral destruction of the recently described dopaminergic mesocortical pathway induces a locomotor hyperactivity in the rat (21). This symptom is precisely a major preconvulsive sign observed under HPO.

Whatever the role of the central dopaminergic system in triggering acute HPO toxicity, other factors, the discussion of which is beyond the scope of this paper, are very likely involved. As a working hypothesis, it seems likely that several protective agents should simultaneously be used to improve further the protection against the different symptoms of the intoxication.

In summary, the antianxiety drugs of the benzodiazepine class have been found to provide a satisfactory and safe protection against acute HPO toxicity.

References

1. Brue F, Joanny P, Morcellet JL, Corriol JH. Metabolic defence mechanisms at the cellular level against oxygen toxicity. Bull Eur Physiopathol Respir 1978;14:152-153.
2. Joanny P, Brue F, Calcet-Veys J, Blanquet F, Corriol J. Toxixité aiguë de l'oxygène hyperbare chez la souris: effets protecteurs du diazepam et du clonazepam. Med Aéronaut Spat Med Subaquat Hyp 1976;15:188-189.
3. Obrenovitch T, Brue F. Congélation de petits animaux isolés en ambiance hyperbare: étude théorique et réalisation pratique. Med Aéronaut Spat Med Subaquat Hyperb 1976;15:271-274.
4. Brue F, Servantie B, De Chabot A, Allemand R. Les critères de l'intoxication aiguë par l'oxygène hyperbare chez la souris. Méthodologie appliquée à la recherche d'agents protecteurs. Med Aéronaut Spat Med Subaquat Hyp 1976;15:206-208.
5. Sanders AP, Currie WD, Woodhall B. Protection of brain metabolism with glutathione, glutamate, GABA and succinate. Proc Soc Exp Biol Med 1967;125:716-721.
6. Brue F. La toxicité de l'oxygène hyperbare; physiopathologie, cytotoxicité, protection. Activation du cycle des pentoses et autodéfense cellulaire. Ann Anesthésiol Fr 1967;8, spécial (1):339-380.
7. De Feudis FV. Dehydration of the brain by intraperitoneal injections of hyperosmotic solutions of gamma aminobutyric acid and DL-alpha-alanine. Experientia 1971;27:1284-1285.
8. Jamieson D, Van Den Brenk HAS. The effects of antioxidants on high pressure oxygen toxicity. Biochem Pharmacol 1964;13:159-164.
9. Faiman MD, Mehl RG, Oehme FW. Protection with disulfiram from central and pulmonary oxygen toxicity. Biochem Pharmacol 1971;20:3059-3067.
10. Horne T. Chemical protection against the toxic action of hyperbaric oxygen. In: Brown IW, Cox BG, eds. Proc 3rd intern Conference on Hyperbaric Medicine. Washington: Nat Acad Sci-Nat Res Council, 1966:113-118.
11. Radomski MW, Rowe J, Watson WJ. Prevention by lithium of acute hyperbaric oxygen toxicity and associated changes in brain gamma-aminobutyric acid levels. In: Lambertsen CJ, ed, Underwater physiology V. Bethesda, MD: Federation of American Societies for Experimental Biology, 1976:517-526.
12. Joanny P, Brue F, Corriol J, Jacquin M, Fredenucci P. Effet de la Papverine, de l'Hydergine, de la Vincamine et de la Carbamazepine sur la toxicité aiguë de l'oxygène hyperbare chez la souris. Med Aéronaut Spat Med Subaquat Hyp 1979;18:84-87.
13. Laborit H. Broussolle B, Perrimond-Trouchet R. Action protectrice de la 5-hydroxytryptamine sur les accidents convulsifs de l'oxygène sous pression chez les souris. CR Soc Biol (Paris) 1957;151:930-933.
14. Calcet J, Joanny P, Corriol J, Dimov S. The protection against the cerebral and pulmonary effects of hyperbaric oxygen by pharmacological agents and lithium salts in mice. Resuscitation 1973;2:37-50.
15. Wood JD, Stacey NE, Watson WJ. Pulmonary and central nervous system damage in rats exposed to hyperbaric oxygen and protection therefrom by gamma-aminobutyric acid. Can J Physiol Pharmacol 1965;43:405-410.
16. Radomski MW, Watson WJ. L-Cycloserine : un puissant antagoniste des convulsions induites par l'oxygène. Med Aéronaut Spat Med Subaquat Hyp 1978;17:364-366.
17. Brue F, Guillemenot R, Berl D, Monget D, Grignon J. Mécanisme et prévention des crises convulsives hyperoxiques. III: Approche pharmacologique. In: Larcan A, ed. Problèmes de réanimation, 8ème série, tome 2. Paris: SPEI, 1975:289-317.
18. Braestrup C. Albrechtsen R, Squires RF. High densities of benzodiazepine receptors in human cortical areas. Nature 1977;269:702-704.
19. Brue F, Joanny P, Dumas C, Chaumont A. Protection agents against hyperbaric oxygen toxicity: effects on the central dopaminergie system. Bull Eur Physiopathol Respir 1978;14:153-154.
20. Poirier LJ. Le système striopallidal et ses meécanismes accessoires au regard de la physiopathologie extrapyramidale. Presse Med 1970;78:1395-1401.
21. Tassin JP, Stinus H et al. Relations between the locomotor hyperactivity induced by A10 lesions and the destruction of the fronto-cortical dopaminergic innervation in the cat. Brain Res 1978;141:267-282.

EFFECT OF EXCESSIVE OXYGEN UPON THE CAPABILITY OF THE LUNGS TO FILTER GAS EMBOLI

B. D. Butler and B. A. Hills

The pulmonary circulation, situated between the heart and systemic beds, has a secondary role as a physiological filter for venous emboli. The effectiveness of this filter has been well established (1), while the ability to trap venous microbubbles as small as 22 μm under normal conditions is evident (2). However, impairment of this filtering ability by overloading the vessels with continuous gas infusions (3,4,5), or by the use of vasodilators (2) has been reported. Another condition that could impair the filtering ability of the lungs involves pulmonary oxygen toxicity.

Prolonged ventilation of high concentrations of oxygen may lead to a progressive sequellae of pulmonary pathological events, which may include edema, atelectasis, airway inflammation, and pulmonary hypertension. The extent of pathology and progression to acute pulmonary damage is dependent upon both the partial pressure of oxygen breathed and the duration of the exposure. Numerous investigators have examined the various hemodynamic, biochemical, and cardiopulmonary changes associated with pulmonary oxygen toxicity as discussed in the review by Clark and Lambertsen (6). The use of oxygen for the treatment of various infectious diseases and traumatic illnesses, including decompression sickness, is widespread. However, recognition of the limits and hazards is essential.

This study was conducted to examine the effects that pathologic changes caused by excessive oxygen exposures can have upon the ability of the pulmonary circulation to serve as a physiological filter for venous micro air emboli. Transcutaneous ultrasonic Doppler probes were used at various arterial sites to monitor any microbubbles injected into the right ventricles of dogs that failed

to be filtered by the pulmonary circulation. An evaluation of these monitoring techniques was reported (2).

MATERIALS AND METHODS

Eight dogs of either sex (20–23 kg) were mildly sedated, not to a level of surgical anesthesia, with sodium pentobarbital (Nembutal, 15 mg/kg i.p.).

Once the animals were sedated they were placed in an experimental pressure chamber, which was then flushed with 100% oxygen for approximately 30 min, until the oxygen percentage exceeded 95%. At this time the pressure was increased with 100% O_2 to 2 ATA. The animals remained at this depth for 17 h. Chamber gas was routinely monitored using a medical gas analyzer (Perkin Elmer 1100) for fluctuations in the carbon dioxide and oxygen levels. Proper flushing with 100% O_2 oxygen was implemented as required.

Following the 17-h exposure to 100% oxygen at 2 ATA, the animals were returned to ambient pressure and anesthetized with sodium pentobarbital (30 mg/kg i.p.). The animals were intubated and the endotracheal tubes connected to a 60-L Douglas bag inflated with 100% O_2 such that the animals remained breathing oxygen throughout the experiment. The animals were allowed to respire spontaneously.

The right femoral artery was cut down for placement of a catheter for monitoring blood pressure from the thoracic aorta; a Swan-Ganz thermodilution catheter was placed in the pulmonary artery via a cut-down in the right femoral vein. We obtained cardiac ouput using the thermodilution technique (Electrodyne CO-100). Once inserted, all of the catheters were allowed to back fill with blood and were then slowly flushed with degassed heparinized saline (3 μ/mL sodium heparin) so that any inadvertent introduction of bubbles was avoided. Needle electrodes were placed in standard lead positions I or II for electrocardiographic recordings. A chest-band strain-gauge was placed around the animal's thorax for monitoring respiration. End-tidal carbon dioxide was measured by mass spectrometry (Perkin Elmer Medical Gas Analyzer 1100). We determined blood gas and pH values from mixed venous and aortic blood samples using standard blood gas analysis methods (Radiometer).

Arterial Doppler monitoring was implemented by transcutaneous placement of 9 MHz probes over the left femoral or popliteal arteries and the right carotid artery. The transceived signal from the Doppler recorder (Sonicaid BV100) was filtered and amplified for recording. The right carotid artery often required dissection for proper placement of the probe. The Doppler probes were held in position with bar clamps, which were suspended independently of the surgical cradle, thus preventing artifacts from gross body movements. Once the surgical procedures were completed, we took control measurements for 30–45 min, allowing for stabilization.

Following the control periods the air emboli were introduced into the right ventricles as either microbubbles (14 μm to 61 μm in diameter) or as gas boluses. Techniques for producing calibrated microbubbles are presented else-

where (2). Gas volumes and bubble diameters are presented in Table I. Infusion rates were controlled by an infusion pump at either 0.97 mL/min or 1.23 mL/min. When the experiments were complete, the animals were subjected to euthanasia with an overdose of sodium pentobarbital and an immediate autopsy was performed. Lung sections were removed for standard histological sectioning.

RESULTS

In four out of eight animals embolized in this study, Doppler signals from arterial bubbles were recorded (See Table I). Microbubble sizes ranged from 14 μm to 61 μm while gas volumes ranged from 0.04 to 3.25 mL for microbubbles and 10 mL for bolus infusions. Relevant changes in physiological parameters are presented in Table II. Mean arterial pressures decreased from 147.8 to 107.3 mmHg or by 27.44% from control. Control values are from postoxygenation, pre-embolization conditions. Pulse pressure and heart rate changes were relatively minor, −9.25% and +1.05% respectively; cardiac index and stroke volume decreased significantly, −48.21% and −52.43% respectively. Mean pulmonary artery pressure showed a significant decrease to 24.56% from control while mean pulmonary wedge pressures dropped to a value of 2.63% from control. Total pulmonary vascular resistance increased by 19.15% from control, while breathing frequencies increased by 31.58%.

The physiological changes for the four animals in which no arterial Doppler signals were recorded showed no significant changes from control values. (See Table III)

TABLE I

Arterial Doppler Detection of Intravenously Infused Microbubbles Following Oxygen Exposure (17 h, 100% O₂ at 2 ATA)

Dog Number	Weight (kg)	Sex (M/F)	Bubble Diameter* (μm)	Arterial Doppler Detection	Total Gas Volume Injected Prior to Detection (cc)	Injection Rate (mL/min)
1	22	M	14	+	4.04 Microbubbles 10 Air Bolus	1.23
2	21.5	F	20	+	0.5	1.23
3	21	F	31	−	0.2	0.97
4	20	F	52	−	3.25 Microbubbles 5 Air Bolus	0.97
5	21	M	39	−	1.4	0.97
6	23	F	27	+	1.2	0.97
7	23	M	30	−	0.9	1.23
8	23	M	61	+	0.3	0.97

*Mean diameter.

TABLE II

Physiological Data Following Microbubble Embolization after Oxygen Exposure
(17 h, 100% at 2 ATA) for Animals in which Arterial Bubbles Were
Detected by Doppler

	Control	Post Embolization	Change From Control (%)	P Value*
$\bar{P}a$	147.8 ± 8.66	107.3 ± 16.92	−27.44	>0.05
PP	44.65 ± 8.74	40.52 ± 12.30	−9.25	0.4
HR	191 ± 27.88	193 ± 17.99	+1.05	<0.9
CI	4.19 ± 0.21	2.17 ± 0.17	−48.21	<0.001
SV/m^2	23.63 ± 5.10	11.24 ± 1.39	−52.43	<0.1
$\bar{P}pa$	15.84 ± 0.59	11.95 ± 0.80	−24.56	<0.05
Ppw	4.94 ± 0.82	4.81 ± 0.74	−2.63	<0.9
TPVR	234 ± 18.83	279.46 ± 13.14	+19.15	<0.1
f	19 ± 6.28	25 ± 5.87	+31.58	<0.025

Values are means ± SE. $\bar{P}a$, mean arterial pressure (Torr); PP, pulse pressure (Torr); HR, heart rate (beats/min); CI, cardiac Index ($1/min/m^2$); SV/m^2, stroke volume ($mL/beat/m^2$); $\bar{P}pa$, mean pulmonary artery pressure (Torr); Ppw, mean pulmonary wedge pressure (Torr); TPVR, total pulmonary vascular resistance (dynes · s · cm^{-5}); f, respiration rate (breaths/min).   *P values for paired t test.

TABLE III

Physiological Data Following Microbubble Embolization After Oxygen Exposure
(17 h, 100% at 2 ATA) for Animals in Which Arterial Bubbles Were not
Detected by Doppler

	Control	Post Embolization	Change From Control (%)	P Value*
$\bar{P}a$	129.2 ± 11.56	120.5 ± 4.43	−6.67	0.5
PP	43.86 ± 6.65	42.19 ± 4.02	−3.81	>0.5
HR	181 ± 16.61	193 ± 11.52	+6.63	>0.1
CI	3.80 ± 0.46	3.71 ± 0.40	−2.37	<0.9
SV/m^2	22.21 ± 4.76	19.90 ± 3.64	−10.40	>0.2
$\bar{P}pa$	15.14 ± 1.22	14.11 ± 0.78	−6.80	>0.4
$\bar{P}pw$	5.06 ± 0.77	4.67 ± 0.33	−7.71	>0.5
TPVR	268.71 ± 18.74	263.89 ± 30.96	−1.79	<0.9
f	26 ± 0.88	31 ± 3.0	+19.23	<0.2

Values are means ± SE. $\bar{P}pa$, mean arterial pressure (Torr); PP, pulse pressure (Torr); HR, heart rate (beats/min); CI, cardiac index ($1/min/m^2$); SV/m^2, stroke volume ($mL/beat/m^2$); $\bar{P}pa$, mean pulmonary artery pressure (Torr); Ppw, mean pulmonary wedge pressure (Torr); TPVR, total pulmonary vascular resistance (dynes · s · cm^{-5}).   *P values for paired t test.

DISCUSSION

The objectives of this study were to examine the effects that excessive exposures to oxygen have on the filtration capability of the pulmonary circulation of dogs. The results indicate that pulmonary oxygen toxicity impairs the filtering action provided by the lung vasculature. The effect, however, is rather inconsistent (Table I) and does not appear to depend exclusively on the size of the bubble. Likewise, the release phenomenon is not necessarily a primary effect of the oxygen but may arise from the pathological changes induced by the oxygen.

The spillover of venous air bubbles into systemic arteries was apparent in four out of eight animals embolized (Table I). However, the physiological changes (Table II) tended to be less severe when compared to other situations where microbubbles entered the arteries (2). Pathological examination of the lungs, both gross and microscopic, revealed areas of marked edema, congestion, and occasional hemorrhaging (Table IV). Pulmonary hemodynamic changes are often observed with pulmonary oxygen toxicity (6), including hypertension (7), increased vascular wall permeability with edema formation (8), capillary endothelial damage (9), and alveolar wall fragmentation (10). These changes are consistent in previous studies and provide evidence for deriving mechanisms to explain the transpulmonary passage of venous microbubbles.

Considerable attention has been given to the existence of arterio-venous shunt vessels in the lungs to explain the venous to arterial transfer of emboli (3, 11). On examining the various factors which might impair venous filtration (e.g., volume overload, vasodilators, or pulmonary oxygen toxicity), consideration must be given to events that might provide triggering mechanisms for opening shunt vessels.

Niden and Aviado (12) suggested that pulmonary perfusion pressures must be elevated before shunt vessels could open and allow venous particles to spill over into the arteries. Reflex control of arterio-venous shunt vessels was suggested by Rahn et al. (13) while other studies (12) determined that the concentration of oxygen in the breathing gas mixture can alter filtration provided by the pulmonary vasculature. Many of these factors are present in conditions of pulmonary oxygen toxicity (6).

Alternative mechanisms to explain these findings may involve physical processes acting on the bubble permitting deformation and transfer through normal pulmonary vessels. The delay in the appearance of arterial bubbles following venous embolization (10-90 min) is similar to the times recorded when other factors are used to compromise the lung as a physiological filter (2). This indicates that the mechanism could be more complex than simple filtration and may involve other factors such as edema, humoral agents, or the intervention of a physical agent such as a surfactant, the level of which is known to be changed by oxygen poisoning (14), especially during the recovery period (15).

Increases in the concentrations of surfactant molecules in the pulmonary blood would result in a reduction in surface tension and would tend to reduce

TABLE IV

Pulmonary Pathophysiology

Animal Number	Weight (kg)	Tracheal Exudate	Rales	Hemorrhage	Atelectasis	Edema Interstitial	Edema Alveolar	Capillary Congestion
1	22	+	+	NA	NA	NA	NA	NA
2	21	-	+	+	+ (Patchy)	+	+ (Moderate)	+ (Profuse)
3	21	-	+	+	+ (Minor)	+ (Minor)	+ (Minor)	-
4	20	+	-	+ (Periphery)	+ (Profuse)	+ (Profuse)	-	+ +
5	21	+	+	+	-	+ (Minor)	+ (Minor)	+
6	23	+	+	-	Patchy	+ (Moderate)	+ (Moderate)	-
7*	23	+	+	+	Patchy	+	+	+ +
8	23	-	-	-	Patchy	+	-	+

*Animal manifested motor difficulties following oxygen exposure.   NA means not available.

the forces preventing the forward movement of an air embolus through a pulmonary vessel. Thus, transpulmonary passage of venous bubbles may be predicted. Other potential sources of molecules with surface-active properties available at close proximities to pulmonary emboli include various blood-borne substances and interstitial molecules.

Whether or not the transpulmonary route for venous bubbles in dogs exposed to excessive amounts of oxygen is by way of shunt vessels or normal channel, is debatable. However, the sequence of pathological events resulting from pulmonary oxygen toxicity do appear to render the filtration capability of the pulmonary circulation less effective. There exists, as well, a wide variation among animals as to the amount of insult tolerated by the pulmonary vasculature before arterial spillover of microbubbles occurs. Although the oxygen exposure in this series was excessive, the pathology observed was consistent with previous experimental and clinical findings following a variety of different exposures. Thus, it is perhaps the extent and particular events surrounding the pathology in pulmonary oxygen toxicity that cause the impairment of venous filtration by the lungs. Conclusions drawn from these studies indicate that excessive oxygen exposures can impair the filtration of venous micro air emboli by the pulmonary circulation.

In the diving situation, it would therefore appear most desirable to be able to monitor the diver for the onset of pulmonary oxygen toxicity to help ensure that the many otherwise "silent" venous bubbles produced during decompression do not become arterial emboli with the risk of promoting neurologic decompression sickness. Thus, if a diver had a simple case of limb bends, it would seem unwise to give him a treatment table with excessive oxygen if he were already showing indications of pulmonary oxygen poisoning arising from his initial decompression.

Acknowledgment

References

1. Heinemann HO, Fishman AP. Non-respiratory functions of mammalian lung. Physiol Rev 1969;49:1-47.
2. Butler BD, Hills BA. The lung as a filter for microbubbles. J Appl Physiol 1979;47:537-543.
3. Mandlebaum I, King H. Pulmonary air embolism. Surg Forum 1963:14:236-238.
4. Oyama T, Spencer NP. Cardiopulmonary effects of intravenous gas embolism, with special reference to fate of intravascular gas bubbles. Japn Circ J 1971;35:1541-1549.
5. Spencer MP, Oyama T. Pulmonary capacity for dissipation of venous gas emboli. Aerosp Med 1971;42:822-827.
6. Clark JM, Lambertsen CJ. Pulmonary oxygen toxicity; a review. Pharmacol Rev 1971;23:37-133.
7. Wood CD, Perkins GF. Factors influencing hypertension and pulmonary edema produced by hyperbaric O₂. Aerosp Med 1970;41:869-872.

8. Bean JW. Effects of oxygen at high pressure. Physiol Rev 1945;25:1-147.

9. Yhap EO, Zeller JA, Levin PM, Solis RT. The effects of high inspired oxygen tension and its relationship to oxygen toxicity. Presented at the Society of University Surgery, New Haven, Conn., Feb. 1971.

10. Cedergren B, Gyllensten L, Wersall J. Pulmonary damage caused by oxygen poisoning; an electron microscopic study in mice. Acta Paediatr Scand 1959;48:477-494.

11. Prinzmetal M, Ornitz E.M, Simken B, Bergman HL. Anteriovenous anastomoses in liver, spleen, and lungs. Am J Physiol 1948;152:48-52.

12. Niden AH, Aviado DM. Effects of pulmonary embolism on the pulmonary circulation with special reference to arterio-venous shunts in the lung. Cir Res 1956;4:67-73.

13. Rahn H, Stroud RC, Tobin CE. Visualization of arterio-venous shunts by cinefluorography in the lungs of normal dogs. Proc Soc Exp Biol Med 1952;80:239-241.

14. Broussolle B, Burnet H, Ricci R, Boutier R, Plouvier S, Hyacinthe R, Baret A, and Barranx A. Effects of a normobaric hyperoxia on pulmonary surfactant in the rat. In: Lambertsen CJ, ed. Underwater physiology V. Proceedings of the fifth symposium on underwater physiology. Bethesda, MD: Federation of American Societies for Experimental Biology, 1976:505-515.

15. Adamson IY, Bowden DH. The type II cell as progenitor of alveolar epithelial regenerations. A cytodynamic study on mice after exposure to oxygen. Lab Invest 1974;30:35-41.

SEM OBSERVATIONS OF OXYGEN TOXICITY IN GUINEA PIGS EXPOSED TO CONTINUOUS 100, 85, AND 75% O_2 AT 1 ATM

A. E. McKee, M. E. Bradley, L. P. Watson, and J. I. Brady

Ongoing research at the Naval Medical Research Institute is directed at defining the nature of pulmonary oxygen toxicity together with the factors that modify it. As part of this study, we are working to relate certain lung functions tests (pressure-volume curves and respiration frequency) to the pathologic findings so that we will have quantifiable indices of the severity of the poisoning. We presently are studying the effects or benefits (or both) of continuous oxygen breathing as the first phase in evaluation of various intermittent oxygen-air schedules. This report describes the results of some of the functional tests performed to date and the scanning electron microscopic observations of pulmonary oxygen toxicity in guinea pigs exposed to continuous 100, 85, and 75% oxygen-breathing or air at 1 atm. A comparison of the development and severity of pulmonary lesions is discussed.

MATERIALS AND METHODS

Young guinea pigs weighing 150–300 g were exposed to air or hyperoxic gas mixtures in sealed Plexiglas chambers. Excess moisture was removed by condensation, and carbon dioxide was removed by soda lime. Chamber gas was analyzed several times daily for oxygen and carbon dioxide. Oxygen was maintained within ± 1–2% of the desired concentration by a 6 L/min flow through the chamber. Carbon dioxide was less than 0.1–0.2%. Temperature remained within 1 to 2°C of laboratory conditions. During the exposures, the animals were provided with water and food ad libitum.

Groups of 24 to 48 animals were exposed to air or to 100, 85, or 75% oxygen. In the course of the exposures, one predesignated subgroup of animals was periodically removed individually from the exposure chamber and placed in a box designed to attentuate light and sound. This box was flooded with a gas identical to that of the exposure chamber. The guinea pig was then placed inside a body plethysmograph which sealed around the animal's neck with a foam neoprene neck seal. Flow in and out of the plethysmograph was measured with a pneumotachograph and recorded on an oscillograph. This permitted us to measure respiratory rate, inspiratory/expiratory time ratios, and inspiratory/expiratory midflow ratios. Measurements were obtained pre-exposure and at 8- to 12-h intervals thereafter until the end of the experiment. All animals were given daily exposures in this apparatus the week preceding the experiment to habituate them to the procedure.

At predetermined times during the exposures, two to three animals were anesthetized by intraperitoneal injections of Nembutal. One or two animals were immediately prepared for histopathological examinations (light microscopy, scanning electron microscopy [SEM], transmission electron microscopy [TEM]) by intratracheal infusion of Karnovsky's fixative (8% paraformaldehyde and 50% glutaraldehyde) buffered with sodium cacodylate at a pH of 7.2.

Samples for light microscopic examination were dehydrated, embedded in paraffin, cut into 6 μ-thick sections, and stained with hematoxylin and eosin. Transmission electron microscopy samples were diced into small cubes, washed in 0.1 M sodium cacodylate buffer, postfixed for 1 h in sodium cacodylate-buffered 1% osmium tetroxide, dehydrated, and embedded in Epon. Thin sections were cut with a diamond knife on a Porter-Blum MT-2 ultramicrotome and stained with uranyl acetate and lead citrate. Samples to be viewed by SEM were dehydrated in ethanol, critical-point dried using liquid CO_2, and sputter-coated with approximately 20 nm of palladium-gold. All samples prepared for electron microscopy were viewed in a JEOL-100CX electron microscope with an ASID-4D attachment.

The other anesthetized animal(s) were then given 1 cc of intraperitoneal succinylcholine, and quasistatic air pressure-volume curves of the respiratory system (lung and chest wall) were obtained. The lungs were inflated and deflated through a tracheal cannula connected to an automatic syringe-infusion system. Tracheal pressure was detected by a differential pressure transducer. A potentiometer was adapted to the infusion pump, and the output from this and from the pressure transducer after suitable amplification activated the Y and X axes, respectively, of an X-Y recorder.

Air P-V curves were plotted automatically as the lungs were filled and emptied at 30 s/cycle from a transmural pressure of 0–25 cm H_2O and back. As a limit to reduce losses from lung alveolar rupture, 25 cm H_2O was taken. Four to five air P-V curves were routinely run over a 10- to 12-min period. Stability and reproducibility were generally obtained by the third cycle.

RESULTS

Guinea pigs exposed to 100% oxygen continuously showed a precipitous fall in respiratory frequency during the first 24 h of the exposure (Fig. 1a). Over the next 36 h of exposure there was a lesser decrease in frequency, so that a 60 h postexposure frequency was 51% of the pre-exposure value. Over the next 40 h of exposure there was a gradual rise in frequency, so that at 100 h the frequency was 66% of the pre-exposure value. Inspiratory-expiratory time and flow ratios did not change in the course of the exposure. There was essentially no change in compliance up to 60 h. Thereafter, there was a progressive decrease in the elasticity of the respiratory system. Figure 1b shows the expiratory curves obtained with the fourth cycle of inflation-deflation, which demonstrates this progressive decrease in compliance. After 68 h of 100% oxygen exposure, there was a 25% reduction in respiratory system compliance. In animals breathing 85 and 75% oxygen, similar decreases in compliance were noted at 95 and 190 h, respectively. The first noticeable change in the pressure-volume curves was noted at 36 h. With the first inflation, the inspiratory curve showed large opening pressures and had a serrated appearance (Fig. 2a). As the exposure increased in duration (68 h), this phenomenon became more pronounced (Fig. 2b).

Gross lesions of mild hyperemia and pin-point hemorrhage on the surface of the lung were observed after exposure to 100% oxygen for 36 and 48 h.
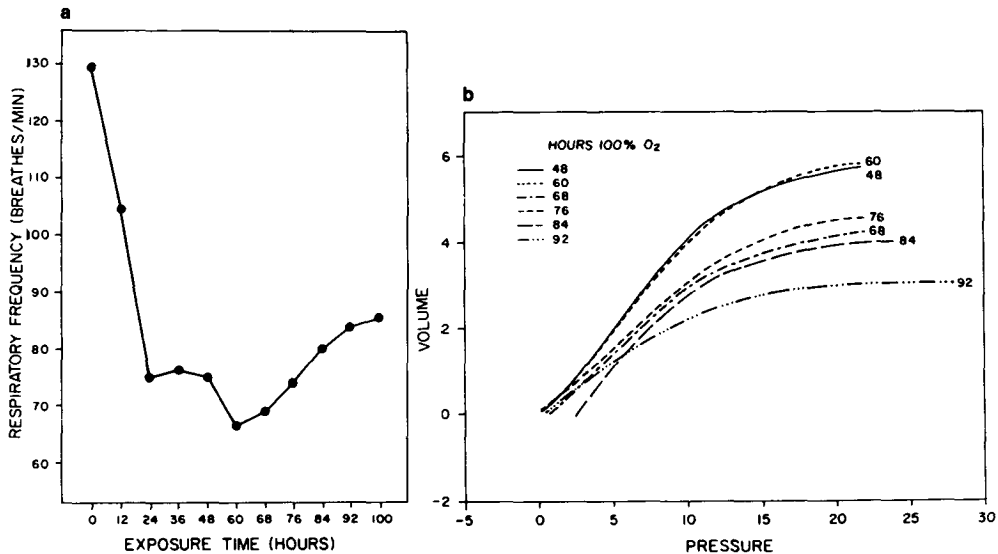
Fig. 1a. Respiratory frequency of guinea pigs exposed to 100% O_2 vs. time. Each point is an average of 12 animals.

Fig. 1b. Fourth cycle expiratory pressure-volume curves of animals exposed to 100% oxygen for 48, 60, 68, 76, 84, and 92 h.
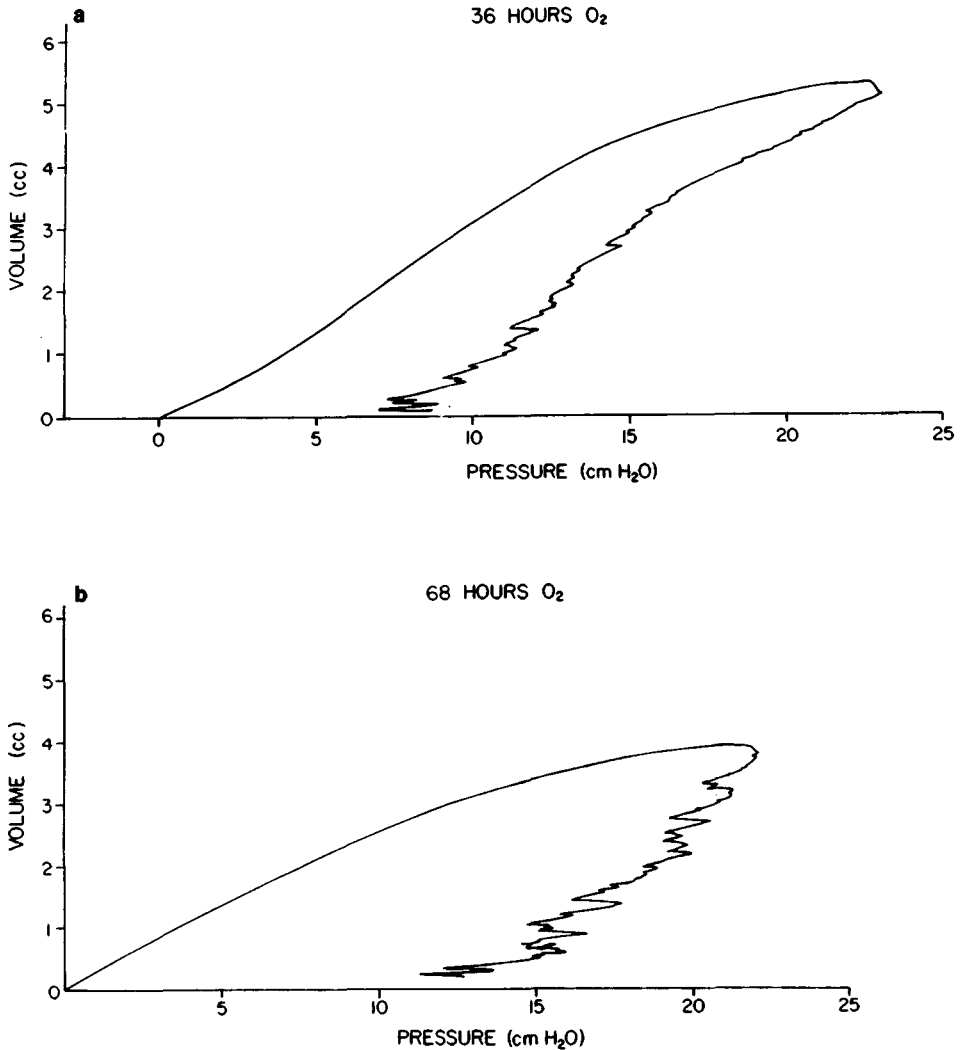
Fig. 2.   Pressure-volume curves of animals exposed to 100% O_2 for (a) 36 h and (b) 68 h.

There were also foci of atelectasis. By SEM examination, the lungs of control animals appeared normal (Fig. 3a) (1,2). Animals exposed to 100% for 36 h showed only minimal lung changes as compared to the 48-h exposure group, which presented evidence of generalized thickening of the alveolar septa and prominent congestion of alveolar vessels (Fig. 3b). Ultrastructural lesions observed by TEM after 36 h were alveolar interstitial edema (swelling) and subendothelial edema of alveolar capillaries (Fig. 4a). After 48 h, marked capillary endothelial cell edema and endothelial cell necrosis were present. The capillary lumen often contained numerous thrombocytes (Fig. 4b). Lesions ob-
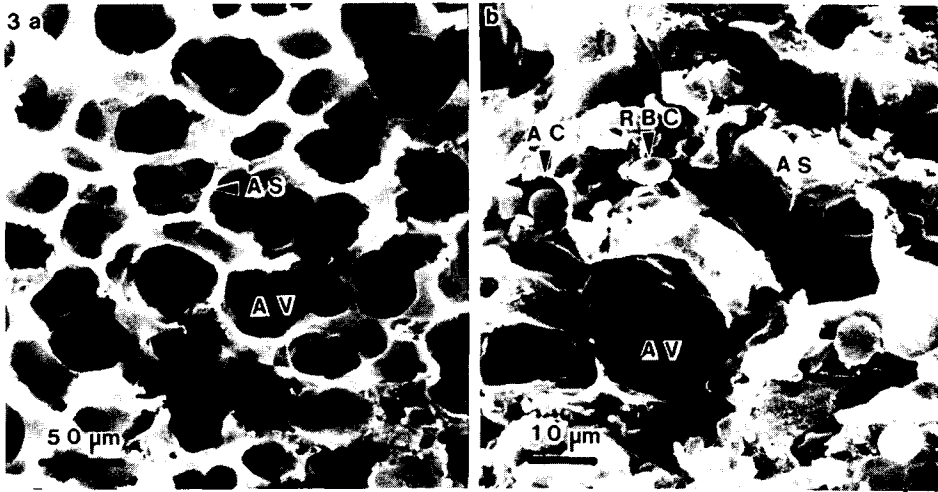
Fig. 3a. Normal "control" lung. AV, alveolus; AS, alveolar septum.

Fig. 3b. Alveolar septa thickening and capillary congestion after 100% O_2 exposure for 48 h. AC, alveolar capillary; RBC, red blood cell.
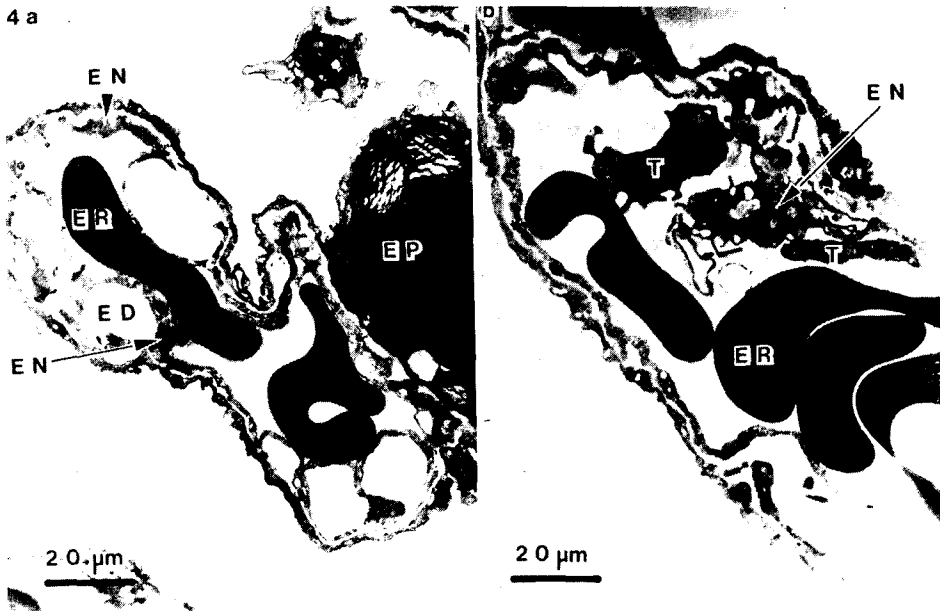
Fig. 4a. Alveolar capillary showing disruption of the endothelial cell (EN) by subendothelial edema (ED) after 36 h of 100% O_2 exposure. ER, erythrocyte; EP, granular pneumocyte (Type II).

Fig. 4b. Capillary endothelial cell damage after 48 h of 100% O_2 exposure. Notice thrombocytes (T) associated with lesion.

served by both SEM and TEM after 60 h of exposure to 100% oxygen included interstitial edema, intra-alveolar hemorrhage, and advanced destruction of capillary endothelial cells. Separation of endothelial cell junctions and mitochondrial swelling and loss of cristae were frequent changes noted. SEM examination of respiratory bronchioles after 60–68 h showed marked proliferation of nonciliated cells. The opening to many of the terminal bronchioles appeared reduced because of marked proliferation of epithelial cells (Fig. 5a). Also, it was noted that after 60-68 h focal areas of atelectasis became prominent and widely disseminated (Fig. 5b). After 70 h of 100% oxygen exposure, the pathologic changes were characterized by generalized accumulation of a plasma-like exudate in the alveolar spaces. This exudate contained abundant amounts of fibrin, leukocytes, macrophages, and some erythrocytes (Fig. 6). Also, active proliferation of Type II granular pneumocytes was observed (Fig. 6 insert). In the normal lung these Type II pneumocytes are associated with the secretion of surface-active phospholipids. As a comparison of the effects of varied oxygen concentrations, the first evidence of interstitial edema and congestion in the 85 and 75% exposure groups was at 84 and 100 h, respectively. These changes were observed at 48 h in the 100% oxygen group. Morphological changes characterized by infiltrating inflammatory cell exudate, which appeared at 70 h in the 100% oxygen group, did not appear until 92 and 116 h in the 85 and 75% exposure groups, respectively.

DISCUSSION

We hypothesize that the decrease in respiratory frequency during the first 60 h of exposure may reflect a progressive increase in airway resistance. Am-
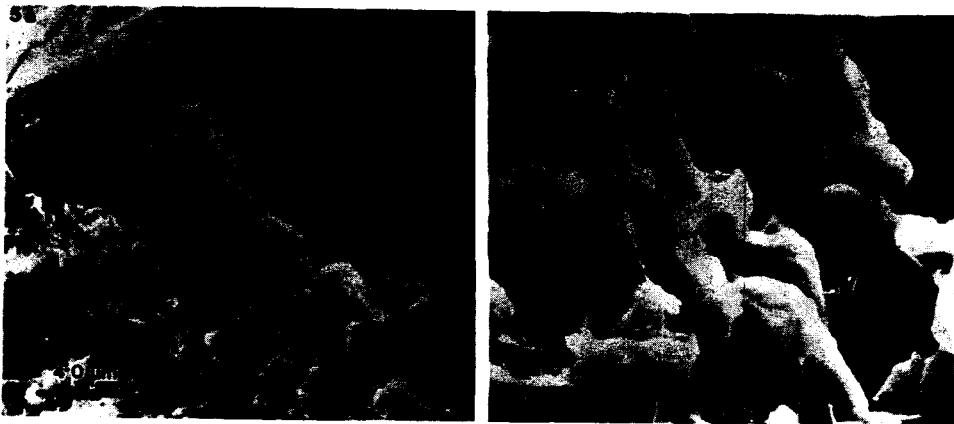
Fig. 5a. Luminal surface of respiratory bronchiole showing proliferation of epithelial cells. BA, bronchiole airway; EC, epithelial cell.

Fig. 5b. Focal area of lung demonstrating atelectasis. AS, alveolar septum; AV, alveolus.
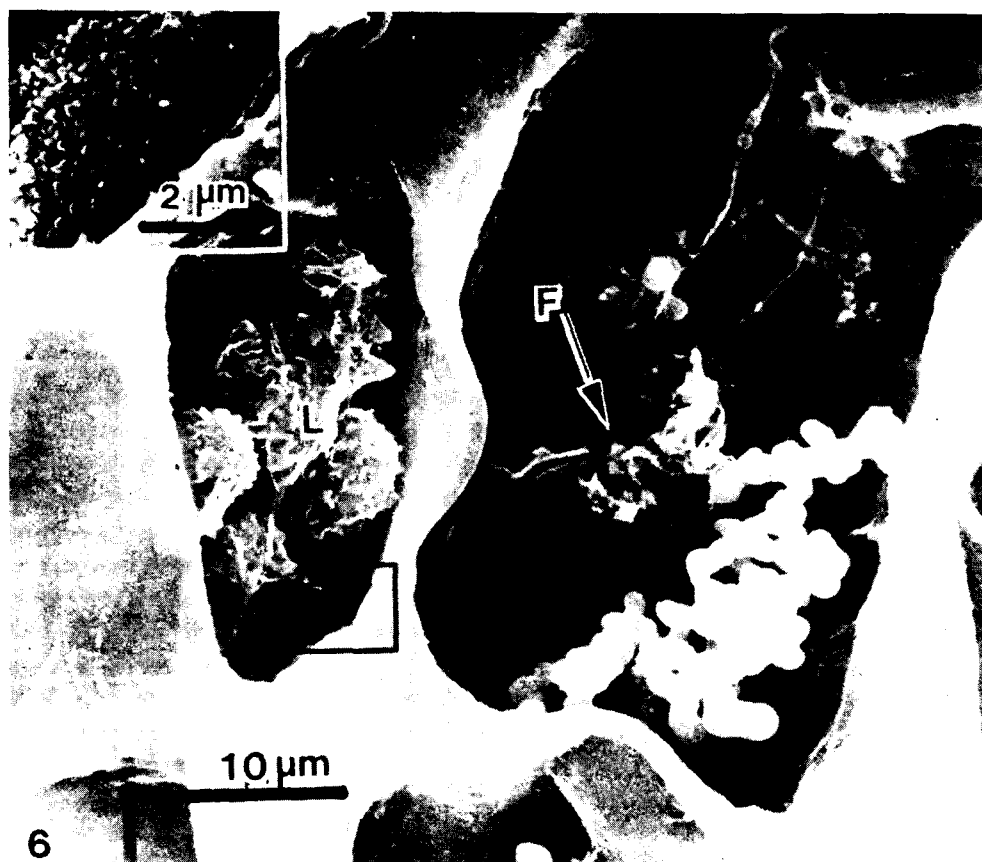
Fig. 6. Alveolar fibrocellular exudate after 100% O_2 exposure for 70 h.

dur (3) has shown that guinea pigs exposed to sulfur dioxide have marked increases in airway resistance, which are accompanied by large falls in frequency, although compliance is affected very little. Bronchoconstriction is thought to be partly responsible for the increased resistance together with plugging and partial closure of airways. Widely disseminated changes, as seen in Fig. 5, could produce such an effect. Otis (4) has shown that when flow resistance is increased, a low-frequency pattern is most economical from the standpoint of minimizing the mechanical work of breathing. Conversely, when elastic work is increased, an increased frequency pattern is optimal. Thus, the gradual rise in frequency between 60 and 100 h may reflect the progressive fall in compliance that we observed during this period.

We are unable to confirm the observations of Barrow et al. (5) that with the progression of pulmonary oxygen poisoning there was an associated increase in *inspiratory-expiratory midflow ratios*. Species differences may account for this, as they used rabbits in their study while we chose to use guinea pigs.

We consider the large opening pressures and serrated appearance of the initial inflation pressure-volume curves to be the result of opening previously closed or atelectatic air spaces, or both. The pressure-volume curves obtained in the course of this study suggest that large decreases in compliance are not present in the early to mid phases of pulmonary oxygen toxicity. However, during the later phases of poisoning, there is a substantial increase in elastic recoil, which reflects increases in both tissue and surface retractive forces (6). The increased tissue-retractive forces appear to result from interstitial edema and hemorrhage; the increased surface forces reflect a reduction in or degradation of surfactant. Additionally, our work suggests that rather modest reductions in oxygen concentration can substantially increase the time required to produce a modest drop in compliance.

The pathologic alterations we have observed in the lungs as a result of the 100, 85, and 75% oxygen exposure are similar to those described by other investigators (7–12). However, the degree of early alveolar endothelial cell damage and the SEM appearance of proliferative nonciliated epithelial cells of the respiratory bronchioles, which results in narrowing of the air ways, were striking observations.

At this point in our work, we strongly believe that the development and severity of oxygen toxicity lesions are greatly influenced by the concentration of oxygen and the duration of exposure.

Acknowledgments

REFERENCES

1. Nowell, JA, Tyler WS. Scanning electron microscopy of the surface morphology of mammalian lungs. Am Rev Respir Dis 1971;103:313-328.
2. McLaughlin RF Jr, Tyler WS, Canada RO. Subgross pulmonary anatomy of the rabbit, rat, and guinea pig, with additional notes on the human lung. Am Rev Respir Dis 1966;94:380-387.
3. Amdur MO. The respiratory response of guinea pigs to sulfasic acid mist. AMA Arch Indust Health 1958;81:407-414.
4. Otis AB. The work of breathing. In: Fenn WO, Rahn H, eds. Handbook of physiology, Sec. 3, Respiration. Washington, DC: Am Physiol Soc 1964;1:463-476.
5. Barrow RE, Hills BA, Sutton TE. A new index for monitoring oxygen poisoning in the lung. Undersea Biomed Res 1979; Suppl 66(1):38, Abstr. 50.
6. Beckman DL, Weiss HS. Hyperoxia compared to surfactant washout on pulmonary compliance in rats. J Appl Physiol 1969;26(6):700-709.

7. Cedergren B, Gyllensten L, Wersall J. Pulmonary damage caused by oxygen poisoning: an electron-microscopic study in mice. Acta Paediatr Scand 1959;48:477-494.

8. Kistler GS, Caldwell PRB, Weibel ER. Development of fine structural damage to alveolar and capillary lining cells in oxygen-poisoned rat lungs. J Cell Biol 1967;33:605-628.

9. Kapanci Y, Weibel ER, Kaplan HP, Robinson FR. Pathogenesis and reversibility of the pulmonary lesions of oxygen toxicity in monkeys. II. Ultrastructural and morphometric studies. Lab Invest 1969; 20(1):101-118.

10. Adamson IYR, Bowden DH, Wyatt JP. Oxygen poisoning in mice; ultrastructural and surfactant studies during exposure and recovery. Arch Pathol 1970;90:463-472.

11. Clark JM, Lambersten CJ. Pulmonary oxygen toxicity: a review. Pharmacol Rev 1971;23(2):37-133.

12. Ross BK, Akers TK. Scanning electron microscopy of normoxic and hyperoxic hyperbaric exposed lungs. Undersea Biomed Res 1976;3(3):283-299.

THE INFLUENCE OF INERT GAS CONCENTRATION ON PULMONARY OXYGEN TOXICITY

M. R. Powell and H. D. Fust

The use of oxygen to reduce the time for bringing a diver to surface is one of the most universal similarities of decompression procedures. Regrettably, the relatively high chemical reactivity of this gas gives it unwanted "side effects." These are managed in current hyperbaric practice by limitations of pressure and exposure duration. At the present time, drugs to ameliorate the toxicity have not been suitable for human use in subsea work.

Pulmonary oxygen toxicity in men is generally calculated by the method proposed by Wright (1), and the result is expressed in "Unit Pulmonary Oxygen Toxicity Doses," or UPTD for short.

Basically, one UPTD is equal to one bar of oxygen breathed for one minute. As it is known that the effects of pulmonary oxygen toxicity appear more rapidly and in a disproportionate manner with increased oxygen pressure, the calculation method is proportionately weighted.

The end-points for a specific number of toxicity doses was expressed as a reduction in the vital capacity of human subjects in addition to such subjective feelings as nausea and substernal burning, two of the most commonly occurring initial events. While the algorithm has appeared to be a useful one, in our opinion it suffers from its inability to account for air pauses commonly made in the final stages of decompression, relative humidity, and gas temperature; also we question its initial premise (2) that inert gas diluents play a negligible role in the development of pulmonary oxygen toxicity.

In diving procedures developed over the past several years at the Institut für Flugmedizin (3), oxygen is employed during the decompression phase with a time-weighted average of 1.9 bars. This results in reductions of decompression times of often more than 50% over other published tables (4) with no subjective symptoms of pulmonary oxygen toxicity. Furthermore, since the to-

113

tal decompression time is shortened, the total number of UPTD's is kept comparatively low (Table I). By means of the employment of oxygen-enriched gas mixtures, the inert gas is quickly eliminated without the need of the long "oxygen-breathing tail" normally found in conventional decompression methods.

In terms of the normally employed UPTD calculation method, this means that most of the oxygen breathing in our procedure is done with diluted oxygen. For a 150-m 30-min dive, only about 20% of the toxicity doses are acquired under 100% oxygen. We therefore wish to determine if there exists a constant effect of the presence of a diluent gas or relative humidity on chronic pulmonary oxygen toxicity, or both.

The observation that oxygen at higher than normal pressure has a deleterious effect upon lung tissue dates back to Lavoissier. Two effects are generally noted. The first, acute oxygen toxicity, is dependent upon the exposure time but seldom occurs when oxygen tension is less than 2.5 bars. Here, a neurological component is prominent with convulsions occurring. It was Paul Bert who, in 1878, first showed that the toxic substance responsible for this central nervous system (CNS) effect was the oxygen in compressed air. The second effect, so-called chronic pulmonary oxygen toxicity, was first described by J. Lorraine-Smith in 1899 and is noted after a long exposure when the oxygen pressure is greater than 0.5 bar. It is primarily directed toward the pulmonary tissue with death the ultimate outcome.

TABLE I

Total Decompression Time and Unit Pulmonary Toxicity Dose (UPTD) for Various Tables

Depth (m)	Bottom Time (min)	UPTD	Decompression Time (min)	Institution
90	30	360	123	DFVLR*
90	30	340	158	US Navy (5)
90	60	720	245	DFVLR
100	30	420	146	DFVLR
100	30	340	181	US Navy (5)
100	60	850	302	DFVLR
125	30	550	211	DFVLR
125	45	1050	399	DFVLR
150	30	820	314	DFVLR
150	30	780	727	Duke U. (6)
150	30	580	581	V.M.-Sub Sea Inter (6)
150	30	800	790	Int. Underwater Con (6)
150	60	0	1600	R. Navy (6)
153	30	350	500	Bühlmann (6)
180	30	990	389	DFVLR
200	30	1130	454	DFVLR

*Deutsche-Forschungs-und Versuchsanstalt für Luft-und Raumfahrt.

The literature contains conflicting evidence concerning the effect of added amounts of inert gas on each of these two types of oxygen toxicity. Added amounts of inert gas appear to exert little influence on CNS oxygen toxicity, which has a very rapid onset, although Burns (7) did report increased latency to convulsions when helium was added to the oxygen as did Almquist et al. (8) with oxygen-nitrogen mixtures.

There does exist some experimental evidence in the literature that increased amounts of inert gas will influence the course of chronic pulmonary oxygen toxicity. Lambertsen (9) reported the beneficial effects of interruption of oxygen breathing by the substitution of compressed air. The early investigations of Penrod (10) indicated that the extent of pulmonary damage in guinea pigs was reduced by the presence of inert gas. He postulated that, to a great extent, the chronic toxic effects of oxygen were the result of a locally high oxygen tension in the lungs. Norman and coworkers (11) found that pulmonary damage in rats and mice was reduced when breathing a given oxygen tension with added nitrogen. Protection was not found when systemic oxygen levels were reduced by the addition of carbon monoxide to the oxygen, although anemia and pulmonary denervation were found to be protective by Moss et al. (12). Belizi and Powell (13) reported a reduction of pulmonary toxicity in rats when either helium or nitrogen was added to oxygen. No protection of added nitrogen was noted by Rokitka and Rahn (14) in a treadmill study with mice.

It was the purpose of this study to determine with mice if commonly measured pulmonary and blood gas parameters are changed when equal oxygen toxicity doses are administered, that is, at a constant time and oxygen partial pressure; the oxygen is administered either in pure form or diluted with inert gas. Additionally, the effect of high and low humidity in the breathing mixture was also studied.

MATERIALS AND METHODS

An initial investigation was started to observe the gross effects of pure vs. diluted oxygen by means of survival times. For these studies, adult female mice (NMRI strain) with an average weight of 38.6 $\pm$ 1.5 g were used as subjects. Gender and age had to be controlled as it influences oxygen toxicity (15). The mice were divided into groups of 15 each and exposed in a hyperbaric chamber fitted with observation port; decompression was thus not needed to determine the number of survivors.

Premixed gas was supplied to the chamber from cylinders. Residual air was flushed out quickly so that the end result would be either 100% O_2 (at 1.75 bars) or 50% O_2 (1.75 bars)/ 50% N_2 (1.75 bars). The chamber was constantly purged with either of these two mixtures, and at the chamber pressure, flow was approximately 2 L/min. Carbon dioxide level was determined with Dräger gas analysis tubes; the chamber equivalent Pco_2 was 4.2 $\pm$ 1.5 mbars. For the experiments with elevated humidity, the gas was bubbled through airstones in water; for the low humidity cases, the floor of the chamber was covered with silica gel granules. Relative humidity was determined electronically.

The high humidity series ranged from 90 to 95%; the low humidity series was between 10 and 15%. All experiments were conducted at temperatures between 21 and 23°C.

To investigate the sequence of events in the preterminal period, blood-gas measurements and gross lung morphological studies were performed. Mice, in groups of 15, were placed in a hyperbaric chamber and exposed for periods of 14 to 27 h to a Pco$_2$ of 1.75 bars. After exposure at high humidity with and without nitrogen, the subjects were removed and allowed to come to equilibrium with room air for a minimum of 30 min. They were then lightly anesthetized with Nembutal, and blood was collected in a heparinized syringe from a small incision made in the posterior aorta. Repetitive measurements were then immediately made of PaO$_2$ using an Eschweiler blood-gas analyzer. The lungs were also excised and the degree of edema estimated from the lung/body weight ratio. Gross morphology was also noted and graded with a system similar to that of Norman et al. (11), that is, 0 = normal, 1 = minimal congestion, 2 = small areas of atelectasis, 3 = predominant collapse in one or both lungs, 4 = complete collapse in both lungs, "hepatization."

RESULTS

Figure 1 shows the results of survival time in oxygen and nitrogen-diluted oxygen when the relative humidity is low. A difference in the two curves is easily seen between the 0 and 50% nitrogen cases.
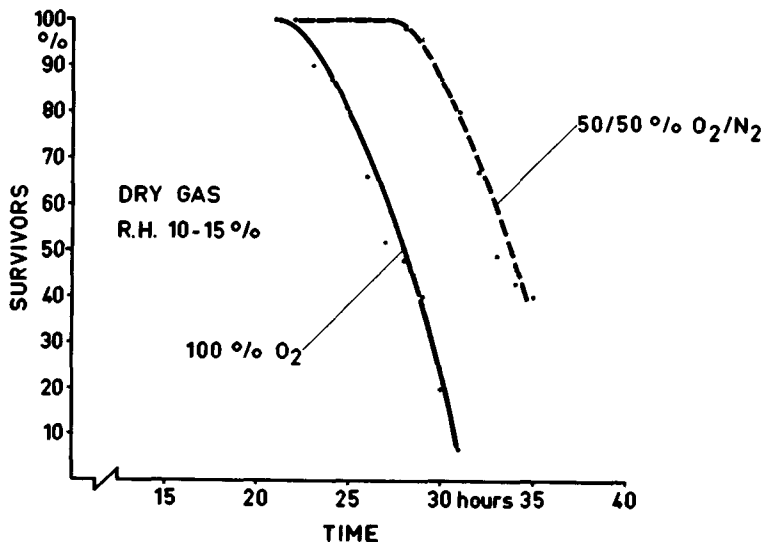
Fig. 1.   Survival time of mice at an oxygen pressure of 1.75 bars. The *left-hand* curve is pure oxygen; that on the *right* shows survival time when nitrogen (at 1.75 bars) has been added.

Figure 2 shows pure and inert-gas-diluted oxygen, but this time with a high relative humidity. In all of the variations, a minimum of three trials was made, each with 15 mice. The points represent the sum of these trials; a total of 285 mice were used. Figure 2 further shows the results of varying also the type of inert gas (argon, helium, or nitrogen). All experiments, made at 3.5 bars (90-95% relative humidity), produced survival curves that are statistically equivalent.

A Wilcoxon Rank Sum Test performed on the results shows that the statistical difference between the two curves in Fig. 1 is meaningful at the $P = 0.01$ level while that between the N_2/O_2 and O_2 curves in Fig. 2 is at the $P = 0.05$ level.

Figure 3 gives the results of the blood-gas and lung morphology studies. It is clear that detectable pathological changes are occurring in that portion of the "survival curve" indicating no fatalities. This continuous change is most evident in the degree of edema (lung/body weight) and the gross morphology.

Though not quantitated, there was also a marked decrease in activity, an increased amount of plural fluid, and greater dyspnea in the mice in the pure oxygen for a given exposure period as compared to the 50/50 mixture.

The "survival curve" indicates a shift to the right of about 6 h for the 50% diluted oxygen. This shift is likewise reflected in a proportionally slower rate of development of edema and gross pathology (lung/body weight and morphological index) and delayed decrease of arterial oxygen tension.
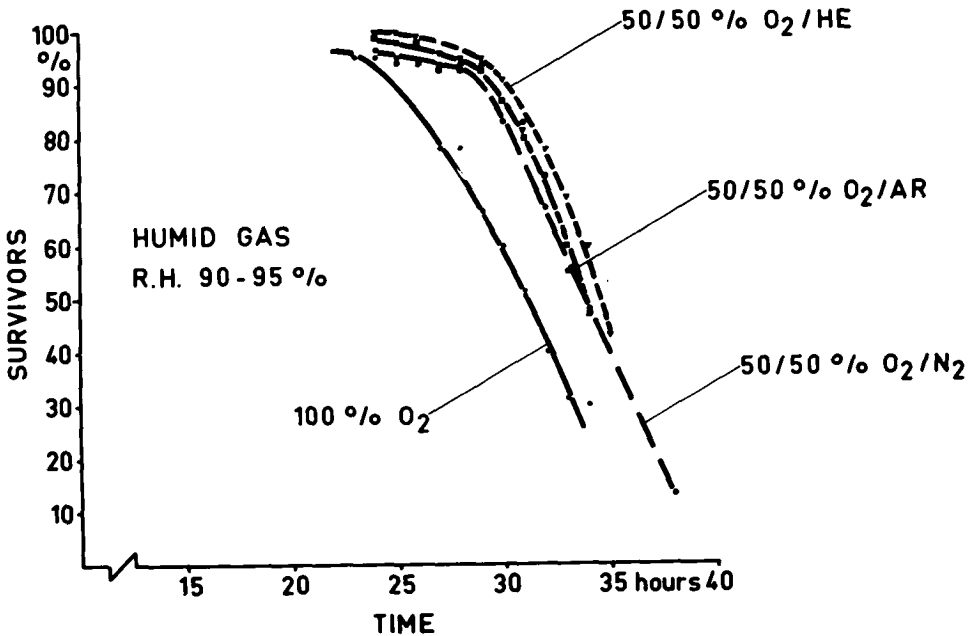
Fig. 2. Survival time of mice at an oxygen pressure of 1.75 bars. The *left-most* curve is pure oxygen while the three on the *right* show survival times when various gas diluents (at 1.75 bars) have been added.
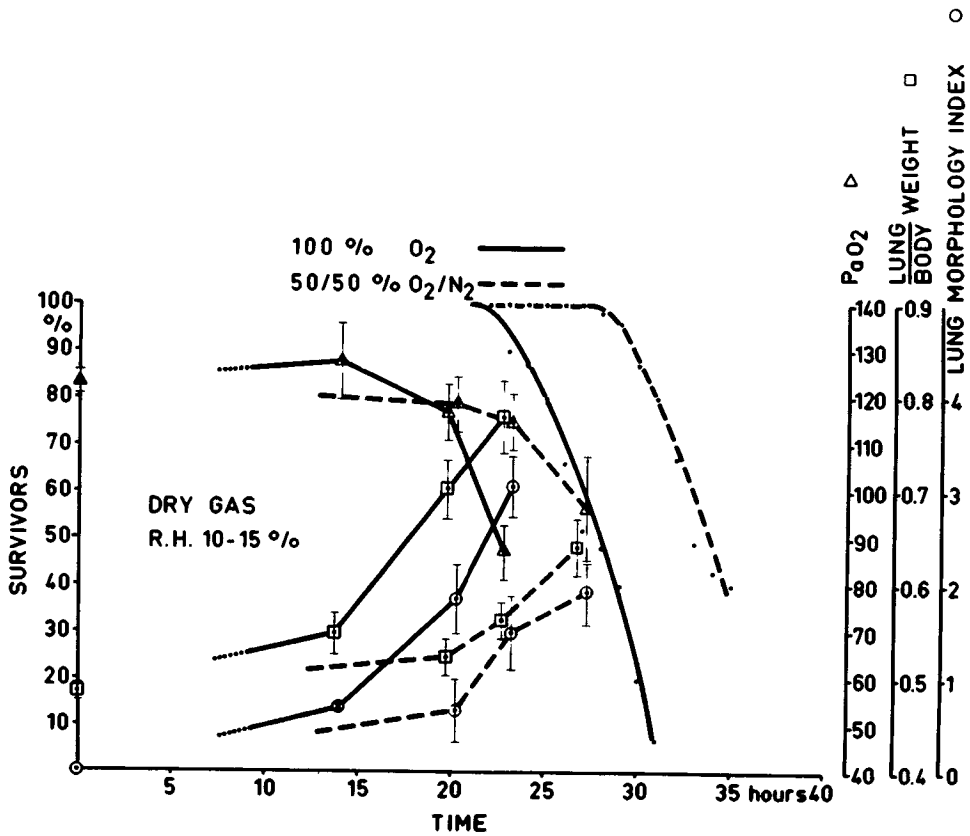
Fig. 3. Percent survival (*dots*), arterial oxygen tension (*triangles*), lung/body weight ratio (*squares*, × 100), and lung morphology index (*circles*) as a function of time for mice in oxygen (1.75 bars) and an oxygen/nitrogen mixture (1.75/1.75 bars). *Bars* indicate the standard error of the mean.

DISCUSSION

Arterial oxygen tension was not found to be a sensitive indicator of oxygen damage. Similar results were found by Clark and Lambertsen (16) concerning Pa_{O_2} in men during oxygen breathing. They interpreted their results, however, as not necessarily indicating a significant role for pulmonary edema in the early phase of human pulmonary oxygen toxicity.

The rate of decrease in arterial oxygen tension and the increase in arterial carbon dioxide and lung/body weight at 1 bar has been studied earlier in mice by Schäfer and Citoler (17) and in rats by Välimäki (18). Both groups found a continuous degeneration in these variables as a function of time in oxygen. The rate of degeneration was not constant, however, being more rapid near the end of the subject's survival time. Our findings show that dilution of the

breathing oxygen by gases delays this degeneration. The ultimate outcome, death, appears to be the result of respiratory acidosis (18,19).

The physiological role of the diluent gas is difficult to define at this time. The prolongation of the survival time does appear to be a function of the concentration of the oxygen (partial pressure, of course, of oxygen being held a constant); it is, for example, as much as twice as long for compressed air at 5 bars compared to pure oxygen at 1 bar in mice (13). The difference in survival time in wet and dry 100% O_2 cannot, however, be ascribed to dilution by water vapor as the reduction of oxygen concentration is insignificant at room temperature, being only 2%.

Capillary endothelial cells appear to be the initial site for chronic pulmonary oxygen poisoning, but it is not yet resolved if systemic effects play a major or minor role. Atelectasis in the absence of an inert gas diluent does not appear to be a deciding factor, and, indeed, in inert-free hypobaric environments, adverse effects of chronic pulmonary oxygen toxicity are not observed. The absence of a chemical reactivity of our diluents at body temperature should rule out effects through covalent bonds, although adsorption (for example, on enzymes) remains possible.

Whether the effect reported here is similar in mechanism to the protection gained through short air-breathing intervals is unclear. It would certainly seem that they possess points of correspondence, and that the protection is effected in the lung itself as contrasted to a generalized systemic effect involving neural hormonal components.

CONCLUSION

The results found thus far in mice do not allow one to make adjustments in UPTD calculations for manned diving. They do indicate, however, that in a mammalian system, simple calculations of exposure time and oxygen partial pressure are not always sufficient to describe correctly the degree of chronic pulmonary oxygen toxicity. They, furthermore, agree with the results and findings of our manned dive experiments, which also indicate a beneficial effect for moisture and inert gas.

While the exact cause of death from pulmonary oxygen toxicity has not been proved, it is clearly evident that the physiological changes leading to death are either mitigated or forestalled by the inert gas fraction.

References

1. Wright WB. Use of the University of Pennsylvania, Institute for Environmental Medicine procedure for calculation of cumulative pulmonary oxygen toxicity. Washington, DC: Experimental Diving Unit, 1972. (EDU-2-72).
2. Clark SM, Lambertsen CJ. Pulmonary oxygen toxicity: a review. Pharmacol Rev 1971;23:37-133.
3. Cabarrou P, Müller KG, Fust HD, Krekeler H, Finkelsey U. Development and testing of heliox dives in excess of 100 meters. In: Shilling CW, Beckett MW, eds. Underwater physiology VI. Proceedings of

the sixth symposium on underwater physiology. Bethesda, MD: Federation of American Societies for Experimental Biology, 1978:383-388.

4. Krekeler H, Cabarrou P, Fust HD. Untersuchung zur Verträglichkeit der Sauerstoffatmung im Bereich von 2,2 bis 2,8 bar abs. Bonn-Bad Godesberg (West Germany): Institut für Flugmedizin, DFVLR, 1978. (DFVLR-FB-78-10)

5. U.S. Navy Diving Manual. Navy Dept., Washington, DC (Navships 0994-001-9010), 1973.

6. Hamilton RW Jr. Development of decompression procedures for depths in excess of 400 feet. Bethesda, MD: Undersea Medical Society, 1975. (WS: 2-28-76)

7. Burns JD. Concentration-dependent attenuation of hyperbaric oxygen toxicity. Aerosp Med 1972; 43:989-992.

8. Almquist H, Arborelius M Jr, Barr PO, Jansson B, Kaijser L. Oxygen toxicity in nitrogen mixtures. Acta Physiol Scand 1969;75:64-68.

9. Lambertsen CJ. Respiratory and circulatory actions of high oxygen pressure. In: Goff LC, ed. Proceedings of the first symposium on underwater physiology. Washington, DC: Nat. Acad. Sci.-Nat. Res. Council, 1955:25-28.

10. Penrod KE. Effect of intermittent nitrogen exposures on tolerance to oxygen at high pressures. Am J Physiol 1956;186:149-151.

11. Norman JN, MacIntyre J, Ross RR, Smith G. Etiological studies of pulmonary oxygen poisoning. Am J Physiol 1971;220:492-498.

12. Moss G, Dworing P, Stein AA. The centrineurogenic etiology of the respiratory stress syndrome. J Thorac Cardiovasc Surg 1976;71:614-616.

13. Belizi PJ, Powell MR. The amelioration of chronic pulmonary oxygen toxicity by inert gas dilution. 48th Annual Meeting, Las Vegas: Aerospace Medical Association, 1977.

14. Rokitka MA, Rahn H. Effects of O_2 and N_2-O_2 pressures on the physical performance of deer mice. Aviat Space Environ Med 1977;48:323-326.

15. Benny S, Fitch JW, Schatte CL. Influence of sex and age on the susceptibility of mice to oxygen poisoning. Aviat Space Environ Med 1977;48:37-39.

16. Clark JM, Lambertsen CJ. Rate of development of pulmonary O_2 toxicity in man during O_2 breathing at 2.0 ATA. J Appl Physiol 1971;30:739-752.

17. Schäfer G, Citoler P. Blood gas tension and development of lung damage in mice exposed to oxygen at 1 ATA. Aviat Space Environ Med 1978;49:476-479.

18. Välimäki M. Arterial and tissue gas tensions in rats during development of pulmonary oxygen poisoning. Aviat Space Environ Med 1975;46:883-886.

19. Matalon S, Farhi LE. Respiratory acidosis in conscious sheep breathing 100% O_2 at 1 ATA. Physiologist 1979;22:82.

BRAIN GABA AND CYCLIC GMP AS INDICES OF METABOLIC LESIONS IN CNS OXYGEN TOXICITY

M. W. Radomski and W. J. Watson

Alterations in various neurotransmitters in the central nervous system (CNS) (gamma-aminobutyric acid, norepinephrine, dopamine, serotonin) have been found in animals exposed to hyperbaric oxygen (HBO) (1–4). Of the various neurotransmitters studied, only changes in gamma-aminobutyric acid (GABA) metabolism have been related to the numerous variables observed in oxygen toxicity, such as species differences, carbon dioxide sensitivity, pressure, and the protective action of drugs on GABA metabolism (1). Certain agents that protect against HBO, however, do not protect the GABA system, disulfiram being one example (5).

Recent advances in neurophysiology have demonstrated interrelationships between GABAergic, monoaminergic, and cholinergic pathways (6). It is unlikely, therefore, that the various neurotransmitters act independently in the CNS but must interact at functional and neurochemical levels to modulate behavior in a balanced manner. Thus, alteration of one or more neurotransmitters by HBO could produce an imbalance in excitation-inhibition that would be manifested in a seizure. One possibility is the relationship between GABA and cyclic GMP (cGMP). Cyclic GMP, which mediates the action of acetylcholine, is involved in excitatory responses in the cerebellum and is consistently elevated by seizures produced by chemical agents, physical stimuli, or electroshock (7). GABAergic mechanisms affect the cGMP content of the cerebellar cortex, and an inverse relationship between GABA and cGMP has been reported in various seizure states (8). In fact, it has been suggested that cGMP may act as an index of GABA receptor function in the cerebellum (9).

Although a large number of drugs suppress HBO seizures, metabolic disturbances may continue to occur in the CNS (10). Thus, in the evaluation of various drugs against oxygen seizures, it is important to measure, in addition

to motor activity, some biochemical marker in the brain (11). Because GABA
is an important inhibitory transmitter in the brain and may account, along with
glycine, for about 50% of all synapses in the brain, and because various
groups have confirmed the effects of HBO on GABA (1), we have used
changes in GABA metabolism as biochemical indices of drug efficacy against
oxygen seizures (1,11,12).

In this study we re-examined several classes of drugs (acid-base, hypogly-
cemics, antioxidants, disulfiram, pargyline, and succinate) known to affect ox-
ygen seizures using changes in GABA levels as a biochemical index. The ef-
fect of HBO on the relationship between GABA and cGMP was also assessed
as well as the effect of diazepam on these changes. Diazepam is known to
affect cGMP and GABA changes caused by certain chemical convulsants (8).

METHODS

Male Wistar rats (190–220 g) fasted overnight were used. For the determi-
nation of drug potency against seizures, the animals were exposed to 6.0 ATA
for 60 min and time to generalized seizures was recorded (12). We calculated
the 50% convulsion time (CT_{50}) for each treatment using logarithmic probabil-
ity paper; the drug effectiveness was expressed as the Convulsion Reduction
Factor (CRF; ratio of the CT_{50} in the drug group to the CT_{50} of the control
group).

All of the drugs were injected intraperitoneally (1 mL/100 g body
weight), except where indicated otherwise, 15 min before HBO exposure.
Control animals received the solvent. The doses used are shown in Table I.

In the experiments involving measurement of brain GABA and cGMP,
animals were exposed to HBO for only 20 min, rapidly decompressed, decapi-
tated, and the heads frozen in liquid nitrogen. Only animals that had not con-
vulsed were used. Whole brains were extracted and assayed for GABA (12),
and cGMP with the New England Nuclear RIA kit. Changes in GABA were
also expressed as the ratio of the change in GABA in treated animals to the
change in control animals (ΔGABA-t/ΔGABA-c). The ΔGABA-t was calcu-
lated by the difference between the GABA level in the nonexposed-nondrug-
treated group and that in the exposed treated group.

RESULTS

Table I shows the effects of the various drugs tested in this study on the
CRF and GABA ratio (Δtreated/Δcontrol). A value of CRF greater than 1 indi-
cates protection against convulsions. A GABA ratio of less than 1 indicates a
drop in brain GABA in the treated group less than that seen in the control
exposed group, that is, protection of the GABA system.

Of the three hypoglycemics tested, only tolbutamide protected against ox-
ygen convulsions (CRF, 1.93) and the oxygen-induced decrease in GABA
(GABA ratio, 0.45). Acetohexamide was without effect and phenformin poten-

TABLE I

Effects of Various Agents on Oxygen Convulsions and Oxygen-Induced Changes in
Brain GABA

Drug	Dose	CRF	GABA Ratio* $\Delta t/\Delta c$
Tolbutamide	250 mg/kg	1.93	0.45
Acetohexamide	250	1.15	1.28
Phenformin	100	0.68	1.07
Diamox	250	0.39	1.76
Tris	1.20 g/kg	1.44	0.22
NaHCO$_3$ (oral)	1.50 g/kg	1.47	0.44
Na succinate	10 mmol/kg	1.23	0.67
Glutathione	10	2.19	0.39
Cysteine + succinate	4 + 10	1.53	0.43
Cysteine + glutamate	4 + 10	1.42	0.50
Pargyline	80 mg/kg	1.29	0.71
Disulfiram	400 mg/kg	1.57	1.21
Diazepam	8 μmol/kg	1.88	1.31

*$\Delta t/\Delta c$: Ratio of change in GABA levels in treated animals exposed to OHP to change in control animals exposed to OHP.

tiated convulsions (CRF, 0.68). In both of these cases, decreases in GABA occurred similar to control groups.

Alkalosis (Tris and NaHCO$_3$) significantly delayed the onset of convulsions and the decrease in GABA, whereas acidosis with Diamox accelerated the development of convulsions. Diamox also potentiated a greater decrease in brain GABA than in controls (GABA ratio, 1.76).

With the exception of disulfiram all of the remaining agents in Table I increased the CRF concomitant with a decrease in the GABA ratio. Disulfiram increased the CRF without any effect on the oxygen-induced decrease in GABA.

The two doses of diazepam used in this study (4 and 8 μmol/kg) significantly delayed the onset of oxygen-induced convulsions (Fig. 1). Although HBO did not alter cGMP levels in the brain (Table II, 1 vs. 3), the ratio of cGMP/GABA was increased by HBO primarily due to a decrease in GABA. Diazepam in animals maintained at normal oxygen partial pressures (2) did not alter GABA but lowered cGMP, resulting in a net decrease in the cGMP/GABA ratio. The HBO-induced decrease in GABA was not altered by diazepam (4), but cGMP levels remained lower in diazepam-treated (4) than in saline-treated (3) groups. The ratio of cGMP/GABA in the HBO diazepam group (4) was lower than the HBO control group (3).
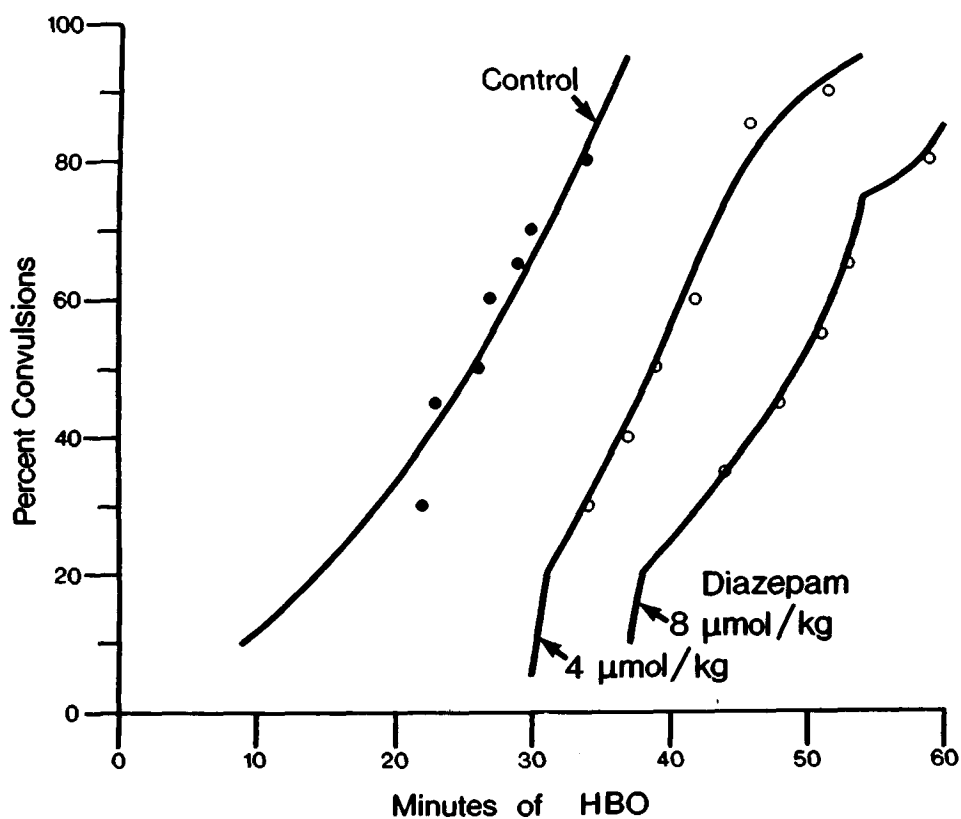
Fig. 1. Effect of 6 ATA O$_2$ on the development of convulsions in control and diazepam-treated rats.

TABLE II

Effect of HBO and Diazepam (8 μmol/kg) on Whole Brain Levels of GABA and cGMP*

Drug	ATA O$_2$	GABA μmol/g	cGMP pmol/g	cGMP/GABA
1 Control	0.2	1.76 ± 0.03	9.82 ± 0.34	5.58 ± 0.21
2 Diazepam	0.2	1.76 ± 0.02	8.10 ± 0.78	4.60 ± 0.45
3 Control	6.0	1.50 ± 0.03	9.48 ± 0.44	6.34 ± 0.30
4 Diazepam	6.0	1.42 ± 0.02	6.74 ± 0.65	4.80 ± 0.46

*Values shown are the means ± SEM. Significant differences: GABA: 1 vs. 3, $P < 0.001$; 2 vs. 4, $P < 0.001$. cGMP: 1 vs. 2, $P < 0.05$; 3 vs. 4, $P < 0.01$. cGMP/GABA: 1 vs. 3, $P < 0.05$; 3 vs. 4, $P < 0.02$.

DISCUSSION

The three hypoglycemics used in this study were selected on the basis of their differential effects on brain GABA. In mice at normal PO_2's, tolbutamide increases brain GABA, phenformin has no effect, and acetohexamide decreases it (13). The doses of the three hypoglycemics used in this study are also effective in reducing blood sugar in animals (13). Brain GABA's in non-exposed rats in this study were not altered by any of the three hypoglycemics with the time-dose protocol used. The qualitatively variable effect of these three hypoglycemics on the inhibition of oxygen convulsions, however, corresponded with their ability to maintain GABA levels; tolbutamide, of the three agents tested, inhibited both the development of convulsions and the decrease in GABA. Although glucose is a GABA precursor (14), the effect of tolbutamide on the GABA content of the brain does not appear to be mediated through its reduction of blood glucose since GABA decreased in animals treated with phenformin and actohexamide. The mechanism by which tolbutamide maintains GABA levels in HBO-exposed animals is unclear.

Alkalotic agents have been shown previously to inhibit oxygen convulsions (15) but their action has not been related to brain GABA. This study shows that Tris and sodium bicarbonate inhibited the development of convulsions concomitantly with an inhibition of the oxygen-induced decrease GABA. Diamox, which significantly shortened the latency of oxygen convulsions, also induced a precipitous decrease in brain GABA. Caspers et al. (16) have reported a similar effect of diamox on CNS oxygen poisoning and found an increase in arterial PCO_2 and a decrease of arterial pH resulting in an increase in cortical blood flow and tissue PO_2. Wood et al. (1) found that elevated respiratory CO_2 levels potentiate convulsions and decreases in brain GABA.

With the exception of disulfiram and diazepam, the anticonvulsant activity of the other drugs tested in this study (succinate, glutathione, cysteine + succinate, cysteine + glutamate, pargyline) (17,18) was associated with an inhibition of the decrease in GABA as evidenced by GABA ratios of less than 1. Schatz and Lal (18) also have reported a correlation between susceptibility to oxygen convulsions and brain levels of GABA in pargyline-treated mice.

Although disulfiram and diazepam inhibited the development of convulsions, they had no effect on the decrease in GABA. If changes in brain GABA are accepted as a metabolic derangement caused by HBO poisoning, then the use of disulfiram and diazepam would be contraindicated. Anesthetics are also effective against HBO toxicity but they increase residual brain damage (10). Thus, metabolic disturbances may continue in diazepam- and disulfiram-treated animals in the absence of convulsions, resulting possibly in permanent damage to the CNS.

The changes in cGMP suggest some possibilities by which diazepam may act to suppress the development of HBO convulsions. Although various chemical and physical stimuli elevate cGMP and induce seizures (7), this does not appear to be the case with respect to HBO because cGMP levels in the whole brain were not altered. This was surprising because convulsant agents, such as
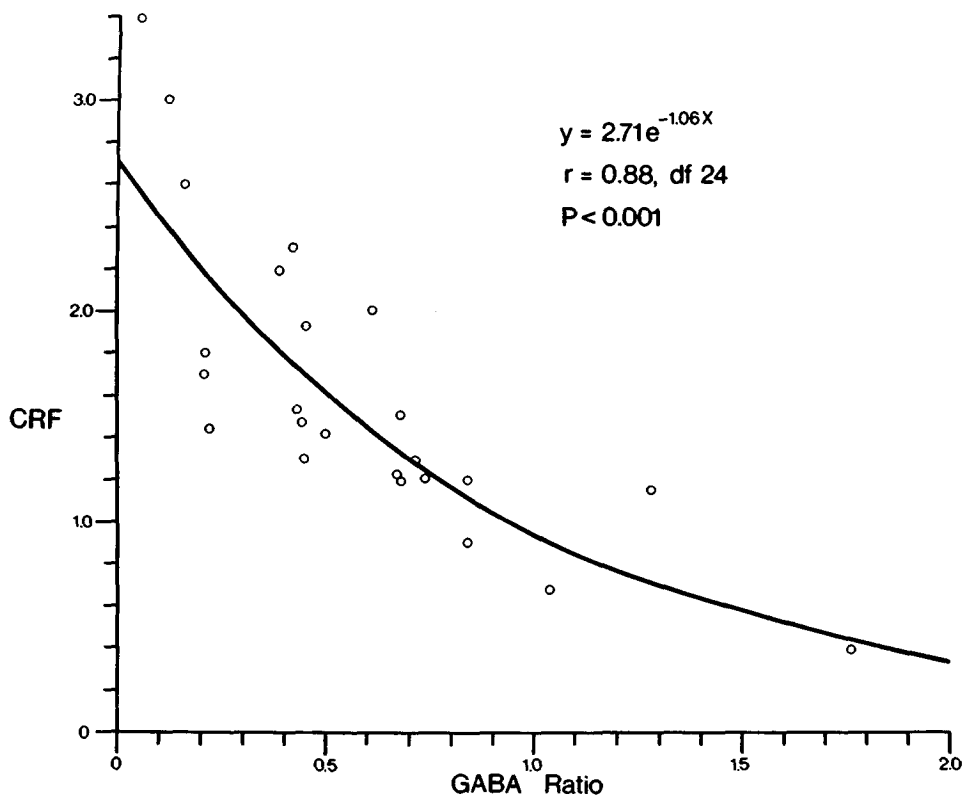
Fig. 2. Relationship between the protective action of drugs on the development of convulsions (CRF—convulsion reduction factor) and on the rate of decrease in brain GABA (GABA ratio-change in brain GABA in drug-treated animals vs. change in brain GABA in solvent-treated animals). A value of CRF and GABA ratio of 1 indicates no effect of the drug.

isoniazid, reduce brain GABA and elevate cGMP levels (7). Furthermore, drugs that either block the synthesis of, or are GABA antagonists, increase the cGMP content in the cerebellar cortex (7,8). Our analyses were carried out, however, on frozen whole brain, whereas the cerebellum is the area of highest concentration of cGMP in the brain (7), and freezing is known to lower cGMP. Because our analyses were carried out on frozen whole brain, any HBO-induced changes in cGMP may have been masked. It is also possible that HBO may act on areas of the brain in which GABAergic neurons are not related to cGMP. Further work on specific brain regions is required to resolve this question.

Diazepam, although without effect on brain GABA levels, lowered the cGMP content in nonexposed and HBO-exposed animals. If neurotransmission is a result of a balance between inhibition and excitation and cGMP reflects the level of excitation (9), then diazepam may act indirectly by reducing cGMP levels and restoring the inhibition-excitation balance previously upset by

the decrease in GABA. If the ratio of cGMP/GABA is examined (Table II), it is seen that HBO elevates this ratio above that seen in control animals, and diazepam lowers this ratio to normal or below normal by decreasing cGMP. Thus some agents may act on nonGABAergic pathways and indirectly inhibit seizures by restoring the balance of inhibition/excitation. Metabolic disturbances, however, may still be occurring in the GABA system and perhaps in other sytstems such as ammonia metabolism (19).

This study provides further evidence for the fact that agents which modify the oxygen-induced decrease in brain GABA also protect to varying degrees against oxygen seizures. With the exception of disulfiram and diazepam, the CRF varied inversely as the GABA ratio in an exponential fashion (Fig. 2). The CRF and the GABA ratios are plotted in Fig. 2 for the drugs examined in this study and for drugs examined by us in previous reports (lithium [3,12]; propylene glycol, Tween 80, S-(2-aminoethyl) isothiourea, β-mercaptoethylamine, 2-methyl-2-thiopseudorea sulfate [11]; magnesium, manganese and zinc [12]). A highly significant hyperbolic relationship ($r = 0.88$, $P<0.001$) was found between protection against seizures (CRF) and the drug-modified HBO-decrease in GABA (GABA ratio). It is interesting that CNS oxygen toxicity also exhibits a similar hyperbolic relationship in humans (20), small organisms (21), and mice (22). This provides further circumstantial evidence for the involvement of GABA, albeit not as a primary mechanism, in the etiology of CNS oxygen toxicity.

References

1. Wood JD. Oxygen toxicity. In: Bennett PB, Elliott DH, eds. Physiology and medicine of diving and compressed air work. London: Baillière, Tindall, and Cassell, 1969:114-143.
2. Faiman MD, Mehl RG, Myers MB. Brain norepinephrine and serotonin in central oxygen toxicity. Life Sci 1971;10:21-34.
3. Radomski MW, Rowe J, Watson WJ. Prevention by lithium of acute hyperbaric oxygen toxicity and associated changes in brain GABA levels. In: Lambersten CJ, ed. Underwater physiology V. Proceedings of the fifth symposium on underwater physiology. Bethesda, MD: Federation of American Societies for Experimental Biology, 1976:517-526.
4. Blenkarn CD, Schanberg SM, Saltzman HA. Cerebral amines and acute hyperbaric oxygen toxicity. J Pharmacol Exp Ther 1969;166:346-353.
5. Faiman MD, Mehl RG, Oehme FW. Protection with disulfiram from central and pulmonary oxygen toxicity. Biochem Pharmacol 1971;20:3059-3067.
6. Pradhan SN, Bose S. Interactions among central neurotransmitters. In: Lipton MA, DiMascio A, Killam KF, eds. Psychopharmacology. New York: Raven Press, 1978:271-281.
7. Ferrendelli JA. Distribution and regulation of cyclic GMP in the central nervous system. In: George WJ, Ignarro LJ, eds. Advances in cyclic nucleotide research. New York: Raven Press, 1978;9:453-464.
8. Costa E, Guidotti A, Mao CC. A GABA hypothesis for the action of benzodiazepines. In: Roberts E, Chase TN, Tower DB, eds. GABA in nervous system function. New York: Raven Press, 1976:413-426.
9. Costa E. Some new vistas on neuronal communication mechanisms: Impact on the neuropharmacology of GABA transmission. In: Garattini S, Pujol JF, Samanin R, eds. Interactions between putative neurotransmitters in the brain. New York: Raven Press, 1978:75-78.
10. Van den Brenk HAS, Jamieson D. Brain damage and paralysis in animals exposed to high pressure oxygen. Biochem Pharmacol 1964;13:165-182.

11. Radomski MW, Watson WJ, McBurney LJ. Effect of natural antioxidants and radioprotectants on acute oxygen toxicity and brain GABA in rats. In: Trapp WG, Bannister WE, Davison AJ, Trapp PA, eds. Fifth international hyperbaric congress proceedings. Burnaby: Simon Fraser, 1974:142-149.

12. Radomski MW, Watson WJ. Effect of lithium on acute oxygen toxicity and associated changes in brain GABA. Aerosp Med 1973;44:387-392.

13. Saad SF. Effect of some oral hypoglycaemics on the gamma-aminobutyric acid content in the cerebral hemispheres of adult male mice. Eur J Pharmacol 1970;13:30-34.

14. Craviota RO, Massieu G, Izquierdo JJ. Free amino acids in rat brain during insulin shock. Proc Soc Exp Biol Med 1951;78:856-858.

15. Nahas GG. Control of acidosis in hyperbaric oxygenation. In: Hyperbaric oxygenation. Ann NY Acad Sci 1965;117:774-786.

16. Caspers H, Speckmann EJ, Simmich W, Zoll WR. Effects of carbonic anhydrase inhibition on oxygen poisoning of the central nervous system. Res Exp Med 1974;163:125-136.

17. Currie WD, Gelein RM, Sanders AP. Effects of hyperbaric oxygenation on metabolism. V. Comparison of protective agents at 5 atmospheres 100% oxygen. Proc Soc Exp Biol Med 1969;132:660-662.

18. Schatz RA, Lal H. Elevation of brain GABA by pargyline: a possible mechanism for protection against oxygen toxicity. J Neurochem 1971;18:2553-2555.

19. Banister EW, Bhakthan NMG, Singh AK. Lithium protection against oxygen toxicity in rats: ammonia and amino acid metabolism. J Physiol (Lond) 1976;260:587-596.

20. Clark JM, Lambertsen CJ. Rate of development of pulmonary oxygen toxicity in man during oxygen breathing at 2.0 ATA. J Appl Physiol 1971;30:739-752.

21. Williams CM, Beacher HK. Sensitivity of drosophila to poisoning by oxygen. Am J Physiol 1943;140:566-573.

22. Helvey WM. A problem of man and milieu: prolonged exposure to pure oxygen. Fed Proc 1963;22:1057-1059.

PULMONARY PROSTAGLANDIN METABOLISM DURING NORMOBARIC HYPEROXIA

C. L. Schatte and M. M. Mathias

We have evaluated the effect of several dietary constituents on the incidence and time course of pulmonary oxygen toxicity. The most striking alteration of relative susceptibility to pulmonary toxicity was produced by varying dietary fat content (Table I). Since two antioxidant enzymes known to increase their activity as part of the cellular response to oxidant gases (1,2) were unaltered by the diets, we looked for some other factor that could have caused the differential response to hyperoxia. The ratio of polyunsaturated fatty acids (PUFA) to saturated fatty acids, P/S ratio, was held constant as fat content was increased in this experiment. We therefore wondered if the differential content of the PUFA, linoleic acid, a precursor of prostaglandins (PG) and thromboxanes (Tx), might account for the differences in mortality.

TABLE I

Mean ± SD Pulmonary Activities (e.u./100 mg fresh tissue) of Pulmonary Antioxidant Enzymes in Rats Fed Diets Containing Various Amounts of Fat Calories and Mortality After 72 h Exposure to Normobaric Hyperoxia

Fat Content*	GSH-Px†	G6PDH‡	Mortality
Lab chow, 5%	0.28	0.33	1/11
Semi-synthetic, 5%	0.40	0.27	3/10
Semi-synthetic, 9%	0.63	0.32	5/11
Semi-synthetic, 21%	0.47	0.31	10/11
Semi-synthetic, 36%	0.56	0.29	9/10

*Percent by weight. P/S ratio was 0.7 for all diets.   †Glutathione peroxidase.   ‡Glucose-6-phosphate dehydrogenase.

We have subsequently performed experiments to investigate the effects of dietary fat content on pulmonary PG synthesis and any changes in PG metabolism which might occur during hyperoxic exposure. Our intention is to develop a dietary regimen optimum for toleration of a potentially toxic oxygen exposure.

METHODS AND RESULTS

Effect of PUFA on Lung PG Profiles

We demonstrated that endogenous levels of PGE_1, PGE_2, $PGF_{2\alpha}$, and PGI_2 can be altered in rat lung by varying P/S ratio of the dietary fat. Table II shows an upward trend of PG concentrations as P/S ratio rises. However, marked differences occurred only with the diet containing the highest PUFA level. All experiments reported in this paper utilized a semi-synthetic diet which approximates that of the average American male. It contained, by weight, 21% fat, 19% balanced protein, 50% carbohydrate, 2.5% fiber, and nutritionally adequate amounts of vitamins and minerals. In all experiments, weanling male Sprague-Dawley rats (CDF-1 strain, Charles River Co.) were fed the diets for 2–4 weeks before the experimental procedures. Prostaglandin analyses were done by radioimmunoassay as previously described (3).

Four observations are pertinent. First, the increase in PG concentrations with increasing P/S ratio was probably due to increasing amounts of linoleic acid. By weight, beef tallow contains about 2.5%, soybean oil about 50%, and safflower oil about 75% linoleate. Second, the relative magnitude of the concentrations of PG may have biological significance. $PGF_{2\alpha}$, a pulmonary vasoconstrictor (4), and PGE_1, a vasodilator (4), are in about equal concentration. It is interesting to speculate whether or not vascular resistance might be influenced by a specific balance between the two. If so, an imbalance in the con-

TABLE II

Endogenous Prostaglandin Concentrations (ng/g fresh tissue) in Rat Lung as a Function of P/S Ratio

Fat type*	P/S ratio	$PGF_{2\alpha}$	PGE_2	PGE_1	TxB_2†	6-keto-$PGF_{1\alpha}$‡
Fat-free	0.00	21.3	3.4	22.7	9.2	215
Beef tallow	0.05	26.9	6.8	28.3	9.3	253
Beef tallow/ soybean oil	0.55	26.3	4.8	29.6	11.9	359
Soybean oil	5.50	40.9	5.0	39.5	18.8	332
Safflower oil	10.32	91.1§	13.6§	69.8§	26.2§	798§

*Twenty per cent of diet, by weight.   †Spontaneous degradation product of TxA_2.   ‡Spontaneous degradation product of PGI_2.   §Significant ($P < 0.05$ or better) effect of dietary fat.

centrations or activities of the two substances could play a role in the vascular stasis and congestion that characterizes the toxic stage of hyperoxia. Third, TxA_2 is a potent vasoconstrictor and platelet aggregator that has been implicated in pulmonary hypertension (5). While its concentration is relatively low, it increased with increasing dietary fat content. It is possible that the correlation between fat content and mortality may have been associated with pulmonary hypertension. Fourth, PGI_2 is one of the most potent vasodilators and inhibitors of platelet aggregation yet discovered (6). Its concentration in the lung was 10 times that of the other PG. The implications for oxygen poisoning of this high concentration are uncertain but bear further scrutiny.

Effect of Hyperoxia and Aspirin on Lung PG Profiles

Prostaglandin concentrations might reasonably be expected to be altered by hyperoxia, and possibly play a role in the pulmonary response to it, because oxygen is required for PG synthesis. Consistent with this, PG synthesis in vitro by kidney slices was significantly enhanced by hyperoxygenation of the medium (7).

If PG profiles do change during hyperoxia, it might be possible to alter the lungs' response to hyperoxia by inhibiting their synthesis. Aspirin, which inhibits the rate-controlling synthetase enzyme, has been reported to exacerbate the toxic central nervous system effects attendant upon hyperbaric oxygen exposure (8). But indomethacin, another synthetase inhibitor, did not alter mortality rates of rats during normobaric hyperoxia (9).

We fed rats the semi-synthetic diet containing either 21% beef tallow or safflower oil for 3 weeks and then exposed them to normobaric hyperoxia for up to 60 h (3). Half the animals in each diet group were injected intraperitoneally with aspirin during each day of the oxygen exposure, at a dose determined during preliminary experiments to provide 50% inhibition of PG synthesis. Animals were sacrificed at 0, 24, 48, and 60 h and the lungs analyzed for PGE_1, PGE_2, and $PGF_{2\alpha}$.

Figure 1 shows the results for $PGF_{2\alpha}$, which are representative of the pattern seen for the other PG. The safflower oil diet stimulated PG synthesis to levels about 10 times those in the tallow-fed rats. Aspirin depressed synthesis of all the PG before oxygen exposure in both diet groups. But hyperoxia powerfully stimulated synthesis even in the presence of aspirin. While diet had no effect on mortality at 60 h, aspirin-injected rats had an 80% death rate vs. 50% for saline controls at that time.

The fact that the safflower oil diet markedly altered PG synthesis but did not alter mortality suggests that concentration changes of at least the PG measured here do not appear to play a role in the toxic response. We now believe that TxA_2 and PGI_2, for which we did not have assays at the time of this experiment, may have been responsible for the effects observed rather than the PGE and PGF series measured. Aspirin clearly can enhance the toxicity although it is not certain that its effect on PG synthesis is the mechanism.
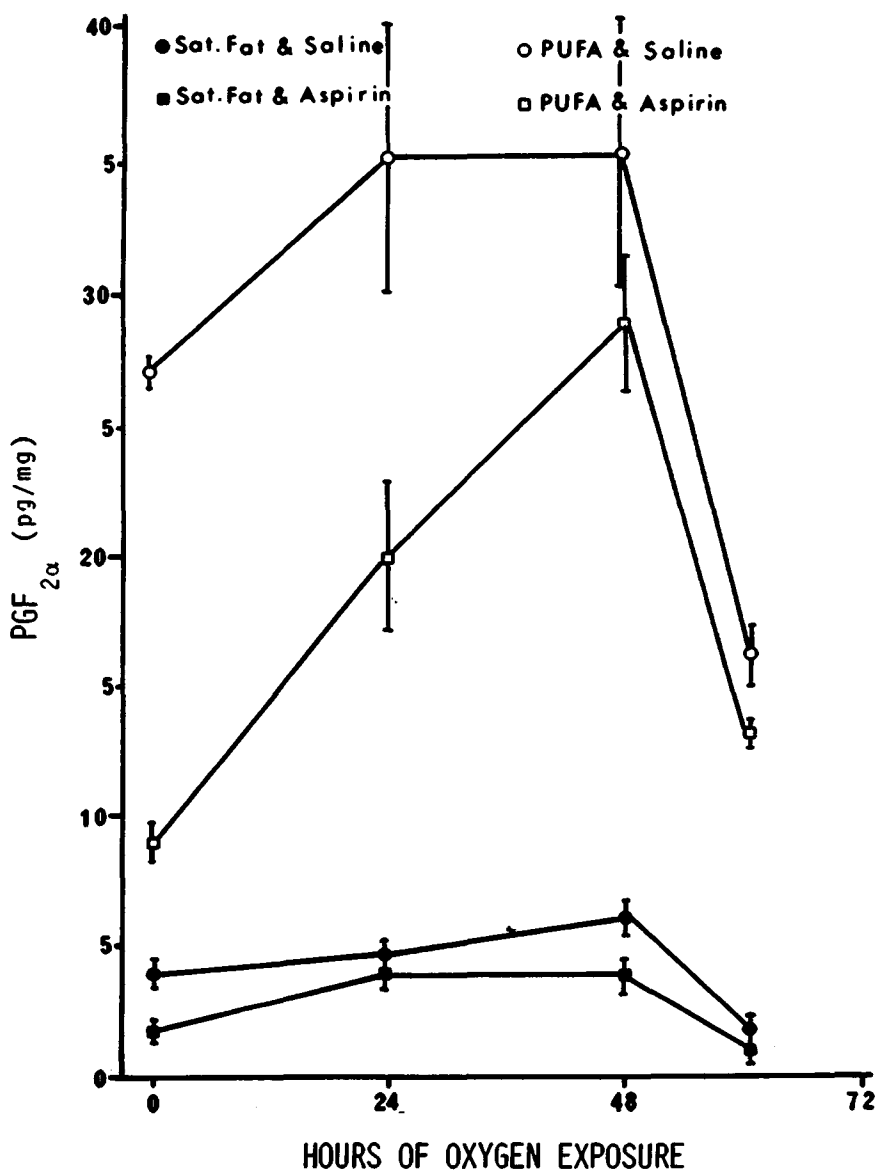
Fig. 1.   Mean ± SE PGF$_{2\alpha}$ concentration in rat lung during normobaric hyperoxia.

Effect of Oxygen on PG Synthesis and Degradation

We next wished to ascertain whether or not hyperoxia altered the activity of PG synthetic or degradative enzymes in rats. We had assumed that hyperoxia increased PG concentrations by providing substrate, O_2. However, Parkes and Eling (10) reported that oxygen exposure did not alter the activity of PG synthetase but did decrease that of PG dehydrogenase in guinea pigs. They

suggested that degradation of circulating PG by the lungs might be impaired during prolonged oxygen exposure. Studies using isolated-perfused lung preparations have shown that clearance of infused PG is indeed reduced in lungs exposed to hyperoxia (11,12). If degradation were impaired, PG levels might increase without a change in rate of synthesis.

Rats were fed the semi-synthetic diet with a P/S ratio of 0.7, then exposed to air or oxygen at atmospheric pressure for 0, 6, 24, or 48 h. Lung concentrations of PGE_2, $PGF_{2\alpha}$, TxB_2, 6-keto-$PGF_{1\alpha}$, and 13,14-dihydro-15-keto $PGF_{2\alpha}$ (m$PGF_{2\alpha}$) the metabolite of $PGF_{2\alpha}$ were assayed. Plasma levels of m$PGF_{2\alpha}$ were also measured as an indicator of clearance of $PGF_{2\alpha}$ from the blood by the lungs. This metabolite assay was the only one available at the time of the experiment. It was assumed that it would be representative of the clearance of other PG from the blood. In addition, the activities of PG synthetase and the PG dehydrogenase/reductase (PGDH/R) complex were measured in pulmonary tissue as previously described (13).

Figure 2 shows that synthetase activity was not altered by oxygen exposure (13), suggesting that synthetic capacity was not altered. PGDH/R activity decreased substantially between 24 and 48 h of oxygen exposure (Fig. 3). In Table III, it may be seen that circulating levels of m$PGF_{2\alpha}$ declined progressively during hyperoxia and were significantly different from both zero time
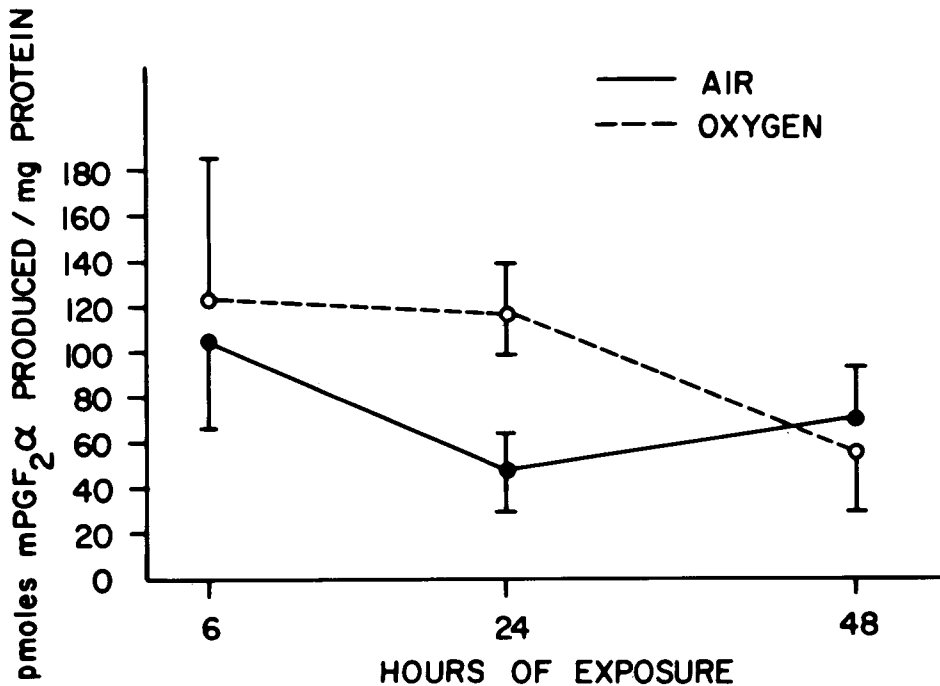
Fig. 2. Mean ± SD pulmonary prostaglandin synthetase activity during normobaric hyperoxia.
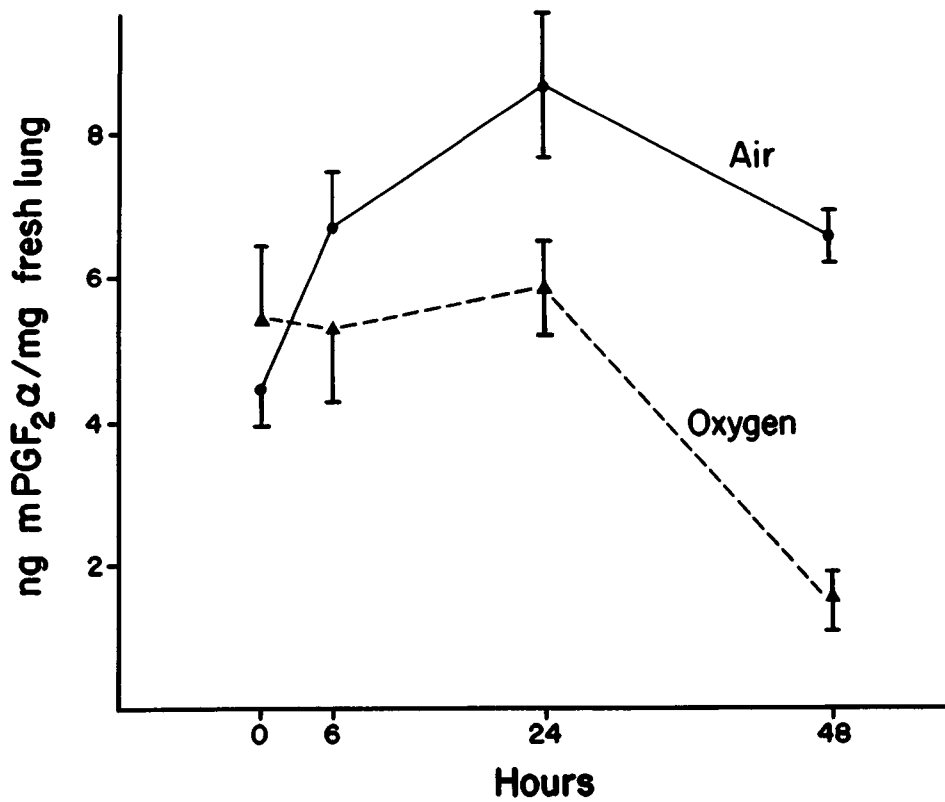
Fig. 3.   Mean ± SD pulmonary prostaglandin dehydrogenase/reductase activity during normobaric hyperoxia.

TABLE III

Plasma mPGF$_{2\alpha}$ (ng/ml) and Pulmonary Prostaglandin (ng/g fresh tissue)
Concentrations of Rats Exposed to Normobaric Hyperoxia

Hyperoxia (h)	Plasma		Lung			
	mPGF$_{2\alpha}$	PGE$_2$	PGF$_{2\alpha}$	mPGF$_{2\alpha}$	TxB$_2$*	6-keto-PGF$_1$†
0	14.5	5.4	40.6	14.5	6.7	74.8
6	9.8	7.5	29.7	17.6	9.1	113.6
24	10.1	11.7	48.1	30.7	10.1	133.0
48	6.8†	12.3‡	42.9	27.9	12.5†	110.0

*Spontaneous degradation product of TxA$_2$.   †Spontaneous degradation product of PGI$_2$.   ‡Significant ($P < 0.05$ or better) effect of time.

and air-exposed controls at 48 h. Thus, our in vivo results are supportive of the previous findings in isolated lungs with regard to PG clearance during hyperoxia.

Concentrations of PGE_2 and TxA_2 increased with oxygen exposure but were not significantly different from air-exposed controls. The other measured PG did not change during the exposures. The absence of systematic changes in endogenous PG concentration and the decline in circulating metabolite during hyperoxia confirm our previous results (13). These results suggest that pulmonary PG synthesis during oxygen exposure is not markedly enhanced when the rats are fed a mixed fat diet. They also suggest that an apparent change in PG degradation does not significantly change endogenous pulmonary PG concentrations.

DISCUSSION

PG Degradation and Oxygen Toxicity

We cannot yet say whether or not the decline in activity of PGDH/R and levels of circulating $mPGF_{2\alpha}$ are causally-related to the development of pulmonary toxicity. But they coincide chronologically with the appearance of visible symptoms of that toxicity. Our rat model tolerates hyperoxia well for 24 h; no change in the activity of antioxidant enzymes (14) or histopathology is evident at that time. Between 24 and 48 h, one or more biochemical events occur to produce visible symptoms of dyspnea, pulmonary hemorrhage, and intrapleural edema at 48 h. Mortality is close to 100% by 72 h. The declining activity of PGDH/R and an impaired ability to remove circulating PG could be one of the critical biochemical events.

Possible Mechanisms of PG

Although PG involvement in pulmonary oxygen poisoning is not yet proved, there are at least two ways in which they might play a role. All of the PG are vasoactive and at least PGI_2 and TxA_2 influence platelet aggregatibility (15). It is possible that alterations in the vasoactivity of one or more PG during hyperoxia contribute to the vascular congestion and edema which characterize toxicity.

A second possibility hinges on the fact that the integrity of the pulmonary capillary endothelium is compromised. The vasodilator PGI_2 is probably synthesized by these cells (16). And it is endothelial cells that seem most susceptible to hyperoxia, undergoing death and necrosis before the onset of edema (17). If PGI_2 synthesis were impaired as a result, changes in pulmonary vascular pressure might contribute to the edema. Alternatively, it may be an aberration of PG production that initiates endothelial cell necrosis since PG are involved in membrane transport and intracellular functions (18).

Clinical Implications of PG in Pulmonary Oxygen Poisoning

If PG prove to play a part in the etiology of oxygen toxicity, manipulation of their concentrations and activity by the use of diet and drugs might allow reduction of the occurrence and severity of symptoms. Several drugs with demonstrated efficacy in altering PG synthesis are already used clinically to treat platelet hyper-aggregatibility (19). Our results thus far suggest that PG synthesis might also be altered by manipulation of dietary fat content. Further definition of any role these important and ubiquitous substances might have in preliminary toxicity includes the promise of usable clinical treatments to reduce the detrimental effects of normobaric hyperoxia.

Acknowledgment

References

1. Kimball RE, Reddy K, Peirce TH, Schwartz LW, Mustafa MG, Cross CE. Oxygen toxicity: augmentation of antioxidant defense mechanisms in rat lung. Am J Physiol 1976;230:1425-1431.
2. Chow CK, Tappel AL. Activities of pentose shunt and glycolytic enzymes in lungs of ozone-exposed rats. Arch Environ Health 1973;26:205-208.
3. Meydani SM, Mathias MM, Schatte CL. Dietary fat type and ambient oxygen tension influence pulmonary prostaglandin synthetic potential. Prostaglandin Med 1978;1:241-249.
4. Kadowitz PJ, Spannhake FW, Levin JL, Hyman AL. Differential actions of the prostaglandins on the pulmonary vascular bed. In: Samuelsson B, Ramwell PW, Paoletti R, eds. Adv Prostaglandin Thromboxane Res. New York: Academic Press 1980;7:731-743.
5. Frolich JC, Ogletree M, Peskor BA, Brigham KL. Pulmonary hypertension correlated to pulmonary thromboxane synthesis. Adv Prostaglandin Thromboxane Res. New York: Academic Press 1980;7:745-750.
6. Moncada S, Vane JR. The role of prostacyclin in vascular tissue. Fed Proc 1979;38:6-71.
7. Zenser TV, Levitt MJ, Davis BB. Effect of oxygen and solute on PGE and PGF production by rat kidney slices. Prostaglandin 1977;13:145-151.
8. Serrill S, Jefferson D, Quick J, Mengel CE. Effect of acetylsalicylic acid and ascorbic acid on oxygen toxicity. Aerosp Med 1971;42:436-438.
9. Yam J, Roberts RJ. Pharmacological alteration of oxygen-induced lung toxicity. Tox Appl Pharmacol 1979;47:367-375.
10. Parkes DG, Eling TE. The influence of environmental agents on PG biosynthesis and metabolism in the lung. Biochem J 1975;146:549-556.
11. Chaudhari A, Sivarajah K, Warnock R, Feling TF, Anderson MW. Inhibition of pulmonary prostaglandin metabolism by exposure of animals to oxygen or nitrogen dioxide. Biochem J 1979;184:51-57.
12. Klein LS, Fisher AB, Soltoff S, Coburn RF. Effect of O_2 exposure on pulmonary metabolism of prostaglandin E_2. Ann Rev Res Dis 1978;118:622-625.
13. Vader CR, Mathias MM, Schatte CL. Pulmonary prostaglandin metabolism during normobaric hyperoxia. Prostaglandin Med (in press).
14. Schatte CL. Dietary selenium and vitamin E as a possible prophylactic to pulmonary oxygen poisoning. In: Smith GB, ed. Proceedings of the sixth international congress on hyperbaric medicine. Aberdeen: Aberdeen University Press, 1979:84-91.

15. Gorman RR. Modulation of human platelet function by prostacyclin and thromboxane A_2. Fed Proc 1979;38:83-88.
16. MacIntyre DE, Pearson JD, Gordon JL. Localization and stimulation of prostaglandin production in vascular cells. Nature 1978;271:549-551.
17. Kistler GS, Caldwell PRB, Weibel ER. Development of fine structural damage to alveolar and capillary lining cells in oxygen-poisoned rat lungs. J Cell Biol 1967;33:605-628.
18. Kuehl FA. Prostaglandins, cyclic nucleotides and cell function. Prostaglandin 1974;5:325-340.
19. Busch JW, Stanford N. Majesus PW. Inhibition of platelet prostaglandin synthetase by oral aspirin. J Clin Invest 1978;61:314-321.

Part II

CARDIORESPIRATORY RESPONSES TO EXERCISE
CARDIOVASCULAR EFFECTS

CURRENT CONCEPTS OF DYSPNEA AND VENTILATORY LIMITATIONS TO EXERCISE AT DEPTH

L. Fagraeus

The range of undersea regions in which man can use his unique mental and physical abilities has expanded significantly in recent years. The capability divers now have to explore depths beyond the continental shelves makes sub-surface areas available that can best be measured in terms of continents.

However, by penetrating into the deeper regions of the underwater environment man is exposed to a combination of physiological stresses that has no equal in the history of human exercise. Despite the various stress factors it has now become possible for divers to carry out useful work in the open sea at pressures equivalent to 1600 fsw (49.5 ATA) or greater. Furthermore, controlled exercise studies have been carried out in hyperbaric chambers at even higher pressures, the current maximum being 2132 fsw (65.6 ATA), and depths of 2500 to 3000 fsw (76.7–91.9 ATA) seem within reach. An analysis of data shows, however, that the progression from moderate to deep diving has significantly accentuated some respiratory problems, especially dyspnea. This review will present new data relating to dyspnea, which is associated with ventilatory limitations during exercise at raised ambient pressures.

SIGNS AND SYMPTOMS OF DYSPNEA

Dyspnea cannot be measured objectively as can vital capacity or arterial blood gases. It is a subjective feeling and, like pain, can only be identified and graded by the individual suffering from it. As a basis for discussion, a short description of clinical manifestations of dyspnea is presented.

Dyspnea is defined as a feeling of breathlessness, shortness of breath, or an awareness of difficulty in breathing. At normal ambient pressure it is often one of the cardinal symptoms of cardiorespiratory disease. People are not usually aware of their breathing, unless their attention is directed to it, except under circumstances in which the ventilatory drive has increased considerably, such as exercise, or when a given level of ventilation requires an increased effort. The severity of dyspnea is normally assessed by determining the minimum level of activity that is associated with the subjective feeling. In this context one should recognize that a person who exercises (or dives) regularly becomes accustomed to the respiratory effort required for this particular activity and therefore no longer characterizes such an experience as dyspnea; a less-active or less-experienced person may suffer from dyspnea in the same situation.

As can be seen from Table I, a diver performing exercise at a raised ambient pressure and gas density is exposed to a number of factors conducive to dyspnea. For instance, it is easy to understand how a lone diver in the darkness of the deep experiences an increased awareness of his breathing, probably related to a generally increased awareness brought about by the hostile environment. In addition, many of the other factors listed in Table I become important during hyperbaric exercise. Increased respiratory work by the addition of resistance (e.g., a breathing apparatus, increased gas density, or both) will cause an increased awareness of breathing, because the respiratory muscles must perform more work to achieve a given ventilation. Furthermore, if the mechanical advantage of the respiratory muscles is reduced (e.g., after significant changes in functional residual capacity), dyspnea also may be experienced. The key factor appears to be whether or not the level of ventilation or associated effort is recognized as being appropriate to the activity. However, the mechanism by which an inappropriateness is recognized has not been es-

TABLE I

Factors Conducive to Dyspnea at Depth

A. *Increased awareness of breathing*
B. *Increased respiratory work*
    1. Hyperventilation
       a. Exercise
       b. Hypercapnia
       c. Hypoxia
       d. Metabolic acidosis
    2. Altered physical properties
       a. Increased lung tissue resistance
       b. Increased airway resistance
C. *Abnormality of respiratory muscles*
    1. Muscular diseases
    2. Change in mechanical efficiency
       a. Marked inspiratory position
       b. Marked expiratory position
    3. Change in neuromuscular coordination

tablished. It has been suggested that a misalignment between intrafusal and extrafusal fibers in the respiratory muscles are responsible for the reflex response and that dyspnea is recognized when there is an altered length-tension relationship in the respiratory muscles. When the muscles of breathing are required to perform an inappropriate amount of work, these receptors send impulses to the higher centers through pathways that have not yet been defined. For further discussion see Comroe (1) and Cherniack et al. (2).

MECHANICS OF BREATHING

It is generally agreed that maximal exercise ventilation (V_{Emax}) as well as maximal voluntary ventilation (MVV) are reduced during exposure to increased air pressures and gas densities (3–6). V_{Emax} has been reported to be consistently smaller than MVV, at least up to 6.0 ATA (4), although some investigators have found that V_{Emax} may be close to or equal to MVV at pressures exceeding 4 ATA (3,6,7). One of the important causes of hypoventilation is the excessive work of breathing associated with increased gas density and airway resistance. At high flow rates, the extra effort to overcome this resistance causes dynamic airway compression during expiration and flow becomes effort-independent (5–7). Although expiratory changes and limitations have been relatively well described, little is known about the changes occurring in inspiratory flow and work of breathing at raised ambient pressure.

In a recent investigation, Hesser et al. (8) studied the mechanisms that limit maximal respiratory performance at 1.0, 3.0, and 6.0 ATA air. Transpulmonary pressures, gas flows, and volumes were measured during forced vital capacity and MVV maneuvers, as well as during maximal exercise. It was found that V_{Emax} was significantly lower than MVV at all pressures; V_{Emax} ranged from 0.77 to 0.82% of MVV. Two main factors were responsible for the fact that MVV was about 20% larger than V_{Emax} both at normal and raised pressures. First, MVV was accomplished at significantly higher lung volumes than V_{Emax}, (ref. 8, Fig. 2) allowing higher expiratory flows (ref. 8, Fig. 1). Second, inspiratory peak and mean flows were about 25% higher during MVV than during V_{Emax} at all pressures.

The expiratory transpulmonary pressures during MVV were three to five times greater than those found in maximal exercise both at normal and raised pressures, although peak flows did not differ over comparable lung volumes (ref. 8, Fig. 1). These results show that much greater expiratory effort than necessary can be generated during MVV than during V_{Emax}, both at normal and raised air pressures (ref. 8, Fig. 3). The expiratory effort during V_{Emax} on the other hand, seems limited by a proprioceptive mechanism, the nature of which is unknown, but it results in a significantly reduced work of breathing (ref. 8, Fig. 3). The observed difference in breathing effort between MVV and V_{Emax} was dissipated into useless work of breathing, but, theoretically, under different circumstances, could have been used to overcome an added expiratory resistance, e.g., a breathing apparatus.

During inspiration in maximal exercise, it was found that the transpulmonary pressures were much greater than during expiration, even though inspired and expired air flows were only slightly different (ref. 8, Fig. 1). This finding can be explained, to a large extent, by the opposite effect that the elastic recoil pressure of the lung has on the relationship between transpulmonary and driving pressures during inspiration and expiration; this finding also accounts for the inspiratory work being higher than the expiratory work during maximal exercise (ref. 8, Fig. 3). On the other hand, inspiratory efforts during V_{Emax} were significantly lower than during MVV at any given pressure, a fact ascribed to a reduction of the maximal achievable power output of the inspiratory muscles toward the end of the maximal exercise periods and a consequent reduction of the force obtainable at a given flow. It was concluded that at increased air pressures, V_{Emax} becomes inadequate, as a result not only of expiratory flow limitation caused by dynamic airway compression, but also because of inspiratory force limitation caused by depletion of the energy stores in the inspiratory muscles.

CENTRAL RESPIRATORY RESPONSE

Because of pulmonary ventilation and respiratory responses to exercise as well as carbon dioxide decrease during acute exposure to hyperbaric air, the question has been raised whether the neural structures involved in the control of breathing might be depressed. This issue was addressed in 1978 by Linnarsson and Hesser (9), who compared responses of ventilation and central inspiratory activity (CIA) to progressive hypercapnia at 1.3 ATA breathing 100% O_2 and at 6 ATA breathing air (with the same PI_{O_2} as 1.3 ATA O_2). Central inspiratory activity was assessed noninvasively by the inspiratory occlusion pressure technique ($P_{.01}$). Linnarsson and Hesser (9) found that the decreased ventilatory response to carbon dioxide in hyperbaric air was met by a concurrent increase of CIA (Fig. 1); this finding has been observed during exercise ventilation in hyperbaric air (10) and during carbon dioxide rebreathing in helium-oxygen mixtures (11). These investigators (9) concluded that the raised gas density increased flow resistance in the airways and caused a reflex stimulation of the respiratory centers, which led to the increased CIA in hyperbaric air. No explanation was given as to adequate stimulus, receptor location, or neural pathways for the mechanism leading to the increased CIA. Because the relative hypoventilation at raised air pressure often leads to significant hypercapnia (5–7,12,13), it is clear that the observed increase in CIA is inadequate with respect to metabolic requirements, a fact that may contribute to the feeling of dyspnea.

STATIC LUNG LOADING

A factor of importance for the work of breathing in the submerged diver is the static lung loading, i.e., the difference between the hydrostatic pressure surrounding the chest and the pressure at the mouth. To study this factor Thal-
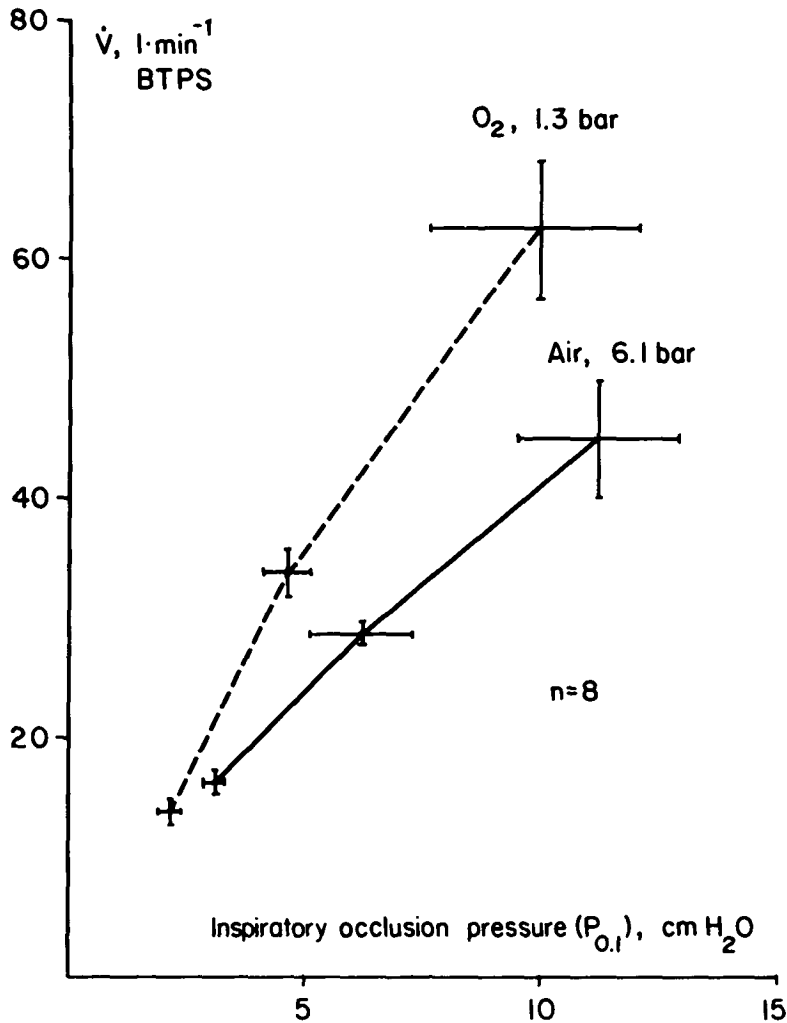
Fig. 1. Pulmonary ventilation (V) as a function of inspiratory occlusion pressure ($P_{0.1}$) during progressive hypercapnia in 8 subjects rebreathing O_2 at 1.3 bar (*broken line*) and air at 6.1 bar (*solid line*). Values are means ± SE of data obtained at end-tidal P_{CO_2} (from *left to right*) 40 Torr, 50 Torr, and 60 Torr. Modified after (9).

mann et al. (14) exposed 3 divers to static lung loading in the range + 20 cm H_2O − 20 cm H_2O (14). The subjects were breathing air during submerged exercise in the prone position at pressures ranging from 1.45 to 6.76 ATA. Both submaximal and maximal exercise studies were performed and the data were compared with that of dry controls at 1.45 ATA. During submaximal exercise it was found that frequently the intensity of dyspnea increased at negative static lung load at higher pressures and at higher work rates, but the dyspnea did not affect the ability of any subject to complete a given work load. During maximal exercise, however, negative static loads produced severe

work-limiting dyspnea in two subjects, but not in the third. A load of $+10$ cm H_2O produced less dyspnea, and all subjects could perform their maximal work tasks at 6.76 ATA. These results are interesting because they indicate that assisted inspiration will improve working capacity under pressure by decreasing the inspiratory work of breathing and by alleviating dyspnea.

DYSPNEA AT GREAT DEPTHS

The studies discussed so far have presented data on the effects of hyperbaric air at pressures up to 10 ATA. When going to higher pressures (deeper depths), helium-oxygen or helium-nitrogen-oxygen mixtures are used to avoid nitrogen narcosis and extremely high gas densities. At 18.6 ATA, Dressendorfer et al.[15] reported that all 4 subjects could perform maximal exercise to exhaustion without a decrease in oxygen uptake. Inspired gases were heliox mixtures with relative gas densities of 2.8 and 3.8, corresponding to air pressures of 3–4 ATA. Their good exercise performance is not surprising at these moderately raised gas densities, and the pressure effects seem to have been minimal at this pressure. Elsewhere in this Proceedings, Ohta et al. [16] have reported results from maximal exercise studies at 31 ATA. Dyspnea apparently was not a problem in the Ohta et al. [16] study either, because no ventilatory limitation to maximal exercise performance was reported, but the maximal tolerable work load and oxygen uptake under pressure were significantly lowered.

At greater pressures, however, Dwyer et al. [17] at 43.4 ATA, and Spaur et al. [18] at 49.5 ATA reported that their divers working under water rapidly became exhausted at moderate levels of oxygen uptake and experienced severe dyspnea. Gas densities in these studies were approximately 7–8 g/liter. The perceived effort expended to breathe was at the extreme limit for each man. In the study by Dwyer et al., the divers complained that the inability to inhale sufficient gas each breath to relieve the sensation of dyspnea was a prominent symptom associated with the cessation of exercise. In addition, Dwyer et al. found only a moderate carbon dioxide retention (max 49.7 mm Hg) at the end of exercise. Spaur et al. did not find any carbon dioxide retention or hypoxia, nor any significant changes in metabolism and cardiovascular parameters. The results of these two studies (17,18) deviate importantly from those obtained during air breathing with corresponding gas densities in that the divers at 43.4 and 49.5 ATA became exhausted and dyspneic at moderate levels of oxygen uptake, and at the point of exhaustion only limited signs of carbon dioxide retention and metabolic changes were observed.

Salzano et al. [19] reported data from 47 and 66 ATA, at which pressures the subjects experienced sudden severe inspiratory dyspnea not only during submaximal exercise, but also during rest or light physical activity such as talking, eating, drinking, and even sleeping. No hypoxia and only mild hypercapnia were observed. Thalmann et al. [20] recently reported similar results: at 1800 fsw (56 ATA) the submerged divers experienced a profound dyspnea that limited the exercise performance to about 30 to 40% of what they could perform on the surface. The dyspnea was reduced somewhat by applying a slight

positive pressure at the mouth. On the other hand, raising the inspired oxygen tension had no effect on this dyspnea, which also affected the divers during mastication, speech, and minimal exercise.

DISCUSSION

Exercise at raised ambient pressure is associated with a decreased ventilatory response leading to carbon dioxide retention and dyspnea. The severity of the dyspnea symptoms will depend on the level of physical activity, the amount of internal and external breathing resistance imposed by raised gas density, and the use of imperfect breathing apparatus (5). If the exercise level is high or the combined respiratory resistance is significantly increased, or both, the ensuing feeling of dyspnea could become extremely unpleasant. For instance, in 1963 Lanphier (21) described this feeling as "a period of terror that has no equal in my experience." Although flow limitation during expiration undoubtedly is an important factor to explain the decreased ventilatory response during exercise at depth, the bulk of evidence from recent studies indicates that, subjectively as well as objectively, failure of inspiratory power constitutes a major problem. An analog often used to describe the situation can be found in the observations of severely asthmatic or emphysematous patients. Clinically, these patients are limited by expiratory flow, but they all perceive inspiration as exhausting.

When a diver's exercise ventilation becomes limited by effort-independent expiratory flow, there are two basic ways by which he can increase his total ventilation: he can allow more time for expiration by shortening the inspiratory phase, or he can breathe at higher lung volumes where maximum effort-independent flow is greater. The changes in inspiratory dynamics require greater inspiratory work, which, theoretically, could be offset by some kind of respiratory assistance. This concept is supported by the results from the studies by Thalmann et al. (11,20), which showed that a slightly positive static lung load improved work performance and alleviated the subjective feeling of dyspnea. The observed increase in central inspiratory activity at given ventilations at depth might further contribute to the feeling of dyspnea (9–11).

Dyspnea is a subjective phenomenon and cannot be measured objectively. However, the parallel between objective observations during the inspiratory phase of the ventilatory cycle and the subjective experience of divers who report that the hyperbaric dyspnea feels like an inability to inhale sufficient gas per breath is impressive and provoking. The dyspnea during maximal exercise in hyperbaric air has been associated with significant carbon dioxide retention and metabolic acidosis (7,13,14), while the dyspnea at greater pressures limited exercise at light submaximal levels with no or only moderate changes in blood gases (17,18). In addition, at pressures exceeding 50 ATA dyspnea was felt even during rest or minimal physical activity. Thus, it seems that with increasing pressure the dyspnea changes character—from being appropriate for the situation in hyperbaric air to being inappropriate at great pressures. One

could postulate that the inappropriate dyspnea at great pressure is caused by different mechanism(s) than that in hyperbaric air. One such possible mechanism might be the HPNS and its effect on the neural structures involved in breathing at great pressures. A mismatch between afferent and efferent impulse flows, or a lack of coordination between muscle groups involved in breathing, could conceivably cause significant changes in the perception of effort. Further research in this area is needed, because it is becoming increasingly clear from current investigations that previous extrapolations and predictions based on results from high gas-density studies at lower pressures (7,22) are inadequate and must be interpreted with caution. An objective relationship between dyspnea and a physiologic test would be extremely valuable in either screening those divers who may be especially susceptible to hyperbaric dyspnea, or in predicting when a diver under pressure is coming close to his ventilatory limit or dyspnea barrier.

Thalmann et al. (14) drew attention to another important aspect of exercise-induced dyspnea, i.e., its consequences. As has been mentioned earlier, the respiratory distress associated with hyperventilation during heavy or maximal exercise is unpleasant and potentially dangerous under dry hyperbaric conditions. To a submerged diver with ventilation further hampered by a breathing apparatus, sudden choking dyspnea would be life-threatening. Without clarification as to the causal mechanism for the dyspnea, Thalmann et al. (14) emphasized the combination of education, training, and experience as a practical way to deal with this problem. However, another and more physiological approach might be the use of different work profiles. Many forms of underwater work are inherently intermittent in nature; therefore a certain amount of work probably could be performed in short bursts instead of in a steady-state fashion. At the present time there are no studies of intermittent work in the hyperbaric literature, a fact that should receive greater attention from hyperbaric physiologists.

CONCLUSION

Evidence from recent studies indicates that the dyspnea and exercise-limiting ventilatory impairment under hyperbaric pressure are closely related to inspiratory work and power failure, although the major restriction to flow occurs during expiration. Results further show that inspiratory assistance is helpful by decreasing the inspiratory work of breathing, alleviating dyspnea, and increasing exercise capacity.

References

1. Comroe JH. Physiology of respiration. Chicago: Year Book Medical Publishers, Inc., 1966:211–213.
2. Cherniack RM, Cherniack L, Naimark A. Respiration in health and disease. Philadelphia: W.B. Saunders Company, 1972:180–182.
3. Anthonisen NR, Utz G, Kryger MH, Urbanetti JS. Exercise tolerance at 4 and 6 ATA. Undersea Biomed Res 1976;3:95–102.

4. Fagraeus L, Linnarsson D. Maximal voluntary and exercise ventilation at high ambient air pressures. Swedish J Defense Med 1973;9:275–278.

5. Lanphier EH. Pulmonary function. In: Bennett PB, Elliott DH, eds. The physiology and medicine of diving and compressed air work. London: Bailliere Tindall, 1975:102–154.

6. Miller JN, Wangensteen OD, Lanphier EH. Respiratory limitations to work at depth. In: Fructus X, ed. Proceedings 3rd international conference on hyperbaric and underwater physiology. Paris: Doin, 1972:118–123.

7. Wood LDH, Bryan AC. Exercise ventilatory mechanics at increased ambient pressure. J Appl Physiol: Respirat Environ Exercise Physiol 1978;44:231–237.

8. Hesser CM, Linnarsson D, Fagraeus L. Pulmonary mechanics and work of breathing at maximal ventilatory performance and raised air pressure. J Appl Physiol (in press).

9. Linnarsson D, Hesser CM. Dissociated ventilatory and central respiratory responses to CO_2 at raised N_2 pressure. J Appl Physiol: Respirat Environ Exercise Physiol 1978;45:756–761.

10. Hesser CM, Lind F. Effects of exercise and hyperbaric air on ventilation and central inspiratory activity. In: Bachrach AJ, Matzen MM, eds. Underwater physiology VII. Proceedings of the seventh symposium on underwater physiology. Bethesda, MD: Undersea Medical Society, 1981:173–180.

11. Camporesi EM, Salzano J, Fortune JB, Feezor MD, Saltzman HA. CO_2 response in He at 5.5 ATA: V_E and $P_{0.1}$ comparison (Abstract) Fed Proc 1976;35:368.

12. Fagraeus L, Hesser CM, Linnarsson D. Cardiorespiratory responses to graded exercise at increased ambient air pressure. Acta Physiol Scand 1974;91:259–274.

13. Fagraeus L. Maximal work performance at raised air and helium-oxygen pressures. Acta Physiol Scand 1974;91:545–556.

14. Thalmann ED, Sponholtz, Lundgren CEG. Effects of immersion and static lung loading on submerged exercise at depth. Undersea Biomed Res 1979;3:259–290.

15. Dressendorfer RH, Hong SK, Morlock JF, Pegg J, Respicio B, Smith RM, Yelverton C. Hana Kai II: a 17-day dry saturation dive at 18.6 ATA. V. Maximal oxygen uptake. Undersea Biomed Res 1977;4:283–296.

16. Ohta Y, Arita H, Nakayama H, Tamaya S, Lundgren C, Lin YC, Smith RM, Morin R, Farhi LE, Matsuda M. Cardiopulmonary functions and maximal aerobic power during a 14-day saturation dive at 31 ATA (SEADRAGON IV). In: Bachrach AJ, Matzen MM, eds. Underwater physiology VII. Proceedings of the seventh symposium on underwater physiology. Bethesda, MD: Undersea Medical Society, 1981:209–221.

17. Dwyer J, Saltzman HA, O'Bryan R. Maximal physical work capacity of man at 43.4 ATA. Undersea Biomed Res 1977;4:359–372.

18. Spaur WH, Raymond LW, Knott MM, Crothers JC, Braithwaite WR, Thalmann ED, Uddin DF. Dyspnea in divers at 49.5 ATA: Mechanical, not chemical in origin. Undersea Biomed Res 1977;2:183–198.

19. Salzano JV, Stolp BW, Moon RE, Camporesi EM. Exercise at 47 and 66 ATA. In: Bachrach AJ, Matzen MM, eds. Underwater physiology VII. Proceedings of the seventh symposium on underwater physiology. Bethesda, MD: Undersea Medical Society, 1981:181–196.

20. Thalman ED, Piantadosi CA, Spaur WH. U.S. Navy 1800 fsw dive. Pressure 1980;9:1.

21. Lanphier EH. Influence of increased ambient pressure upon alveolar ventilation. In: Lambertsen CJ, Greenbaum LJ, Jr, eds. Proceedings of the second symposium on underwater physiology. Washington DC: National Academy of Sciences—National Research Council, 1963:124–131.

22. Lambertsen CJ. Collaborative investigation of the limits of human tolerance to pressurization with helium, neon, and nitrogen. Simulation of density equivalent to helium-oxygen respiration at depths of 2000, 3000, 4000, and 5000 feet of sea water. In: Lambertsen CJ, ed. Proceedings of the fifth symposium on underwater physiology. Bethesda, MD: Federation of American Societies for Experimental Biology, 1976:35–48.

EXERCISE METABOLISM IN HUMANS ON ACUTE EXPOSURE TO 5.8 BARS NORMOXIC OXYHELIUM

R. de G. Hanson, R. M. Gray, M. M. Winsborough,
R. S. McKenzie, and K. G. M. M. Alberti

The main object of putting a man under pressure is to enable him to carry out a task as efficiently as possible. To enable the diver to do this it is important to investigate the effect that the breathing gases have on his capacity for physical work. Because diving to depths below 50 m requires the use of helium-oxygen mixtures, we believed there was a need to investigate the effect of helium on exercise metabolism.

Helium is generally regarded as a completely inert gas. However, it was noted by Chouteau (1) that goats exposed to 49.8 bars breathing a normoxic mixture 159 mmHg (0.21 bar) showed behavioral disturbances and progressive paralysis, but they immediately returned to normal when the Po_2 was raised to 191 mmHg (0.25 bar). Attempts were made to delineate the limits of oxyhelium mixtures by taking goats to 71, 81, 91, and 101 bars. The final pressure was not tolerated and at the others there were normoxic crises, which were all reversed by raising the Po_2. It was postulated that these findings might be due to disturbances in the alveolar/capillary exchange of oxygen. More recent work by Guillerm (2) using goats as subjects showed that the arterial Po_2 pH and Pco_2 remained unchanged at 81 and 101 bars. It must be that the sheep in that study (2) were at rest and restrained with an extra corporeal shunt and a pump, while Chouteau's goats were free ranging.

There may be an explanation for cellular hypoxia with normal arterial Po_2 in the findings of Kiesow (3) and Hyacinthe et al. (4). Kiesow, working with a small pressure cell and a red cell suspension, showed a shift to the left in the oxygen/hemoglobin dissociation curve with increasing pressure; Hyacinthe et al. (4) found a similar effect in blood taken from divers during a dive to 31 bars. Unfortunately, the blood taken from the divers had to be de-

compressed, a process that can take about 90 min, so that the change seen may have been only a shadow of the full effect of pressure. To study this effect, it is necessary not only to measure the oxygen dissociation curve under pressure, but also to measure at the same time such variables as pH, P_{CO_2}, and 2, 3-diphosphoglycerate. Methods for doing this are currently being studied in Britain, France, and the USA; they involve the modification of a dissociation curve analyzer as developed by Hahn et al. (5) at the Radcliffe Infirmary, Oxford.

The experiments reported here compared the effect of three environments on exercise metabolism: air at 1 bar and normoxic oxyhelium at 1.3 bars and 5.8 bars, the former pressure was the minimum for chamber integrity and the latter gave an equivalent density to air at 1 bar.

METHODS

The subjects were six adult males, aged between 24 and 35 years, all with previous experience of compression chamber work and familiar with the bicycle ergonometer and other equipment used.

After an overnight fast (12–14 h), a cannula was inserted into an antecubital vein: after 5 min the first resting sample was taken; 5 min later the second was taken. After compression a further sample was taken; the subjects exercised on the bicycle ergonometer at a work load equivalent to 60% of their predetermined V_{O_2} maximum (see Table I). Blood was taken at 5-min intervals and 2 mL was transferred to chilled perchloric acid (5% v/v) for later analysis of lactate, pyruvate, 3-hydroxybutyrate, acetoacetate, glucose, glycerol, and alanine. The remaining blood was transferred to plain glass tubes and centrifuged after decompression; the plasma was stored at $-20°C$ for later analysis of insulin and nonesterified fatty acids (NEFA). For assaying the blood metabolites in these experiments, we used the method described by Price et al. (6) for determining the acetoacetate concentration and the method described by Lloyd et al. (7) for determining the other metabolites. Insulin was determined by modification of the double antibody radioimmunoassay of Soeldner and Slone (8). NEFA were measured by a radiocobalt method based on that of Ho and Meng (9). During exercise the pulse rate was monitored by means of a Hewlett-Packard telemetering system, which had been found on previous occasions to operate well in compression chambers to a depth of 300 m in oxyhelium.

We measured ventilatory volume using a dry gasometer and carried out continuous analysis of expired oxygen and carbon dioxide using a quadrupole respiratory mass spectrometer (Twentieth Century Electronics Q806 Residual Gas Analyzer). The sampling was done with a probe placed in the mouthpiece for the first 3 min and then moved to a mixing box to obtain a mixed expired air sample. Oxygen consumption and carbon dioxide production was found by calculating the difference between the concentrations in the chamber atmosphere and expired gas. Calibrations were carried out before and after each ex-

TABLE I

$\dot{V}O_2$ and Work Loads of Subjects

Subject	Weight (kg)	Age (yr)	$\dot{V}O_2$ max L/min (STPD)	60% $\dot{V}O_2$ max L/min (STPD)	Work load (W)
HA	67	28	3.15	1.89	163
HB	73	24	3.20	1.92	165
HC	71	32	2.85	1.71	147
HD	73	35	3.40	2.04	177
HE	80	26	3.78	2.27	196
HF	75	36	3.24	1.94	168

perimental run. We found at the end of the experiments that the calibrations used for the 1.3-bar experiments were nonlinear and these respiratory results were excluded from the experiment. This did not occur with the 5.8-bar exposures when the percentage of oxygen in the chamber and in the calibration gases was low.

The exercise period lasted for 20 min at the end of which the subjects stopped pedalling, but remained seated on the ergonometer while samples were taken at 5, 10, and 15 min after the exercise. At this stage it was necessary to terminate the experiments at depth because of the problem of decompression. For the other experimental runs the subjects continued to rest while further measurements were made at 30 and 60 min after exercise. The results were analyzed using a paired t test.

The original experimental plan was to expose 6 subjects to each of the 3 atmospheres in a random order; the subjects were to have a week between each run to obviate any training effect. The decompression schedule chosen after consultation with both medical and diving experts was the U.S. Navy "partial pressure decompression table" for 190 ft of helium for 2 min, though the exposure was only to the equivalent of 184 ft of helium for 50 min. The dive profile is shown in Fig. 1. We believed this profile should provide a safe decompression. However, after four exposures on this schedule the subjects reported fleeting joint pains on surfacing and one of the investigators developed a large urticarial rash and edema over the left shoulder. These signs and symptoms were indicative of mild decompression sickness, so it seemed unethical to expose any further subjects to the risk.

RESULTS

The results are summarized in Tables II and III. The general pattern of response of the blood metabolites to the exercise was the same at each pressure. The lactate and pyruvate levels both rose with exercise; the lactate then stabilized and fell rapidly at the end of exercise while the pyruvate level
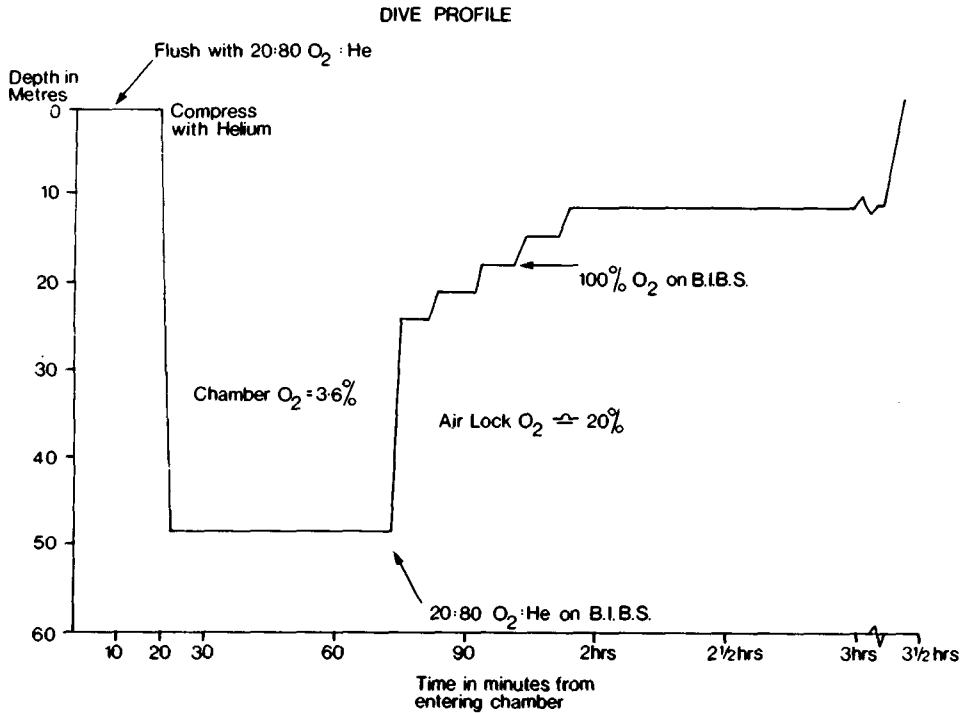
DIVE PROFILE

Fig. 1. Dive profile for simulated dive, 48 m = 5.8 bars.

reached a peak after the end of exercise and fell more slowly. Alanine concentration rose with exercise as did glycerol; the level of ketone bodies fell while the NEFA level showed a slight fall with a postexercise rise. However, there were some differences between the 5.8-bar exposures and the other two. The statistically significant changes occurred in the blood lactate level, which was higher at 5.8 bars both during and after exercise, as was the lactate/pyruvate ratio (Figs. 2 and 3). The glycerol, however, was lower at 5.8 bars during and after exercise and was significant at 35 min. The NEFA level was higher during the exercise period at 5.8 bars and the postexercise rise was not so marked; in fact, after exercise the levels were lower than at the surface and were significant at 35 min.

Perhaps the most interesting finding was the failure of plasma insulin levels to show the characteristic drop with exercise; the difference in levels was statistically significant at the end of exercise. Despite this failure to fall, plasma insulin concentration still showed a postexercise rise to the same level as that with air exposures. The relationships of NEFA, glycerol, and insulin can be seen in Fig. 4.

The main difference between the 1.3-bar oxyhelium exposure and air exposure was seen in the different lactate/pyruvate ratios, which were significantly higher in the oxyhelium environment at both 30 and 60 min after the

TABLE II
Blood Metabolites and Insulin Data

Metabolites (mM)	Pressure (bar)	Baseline	Post Compression	Time (in min) from Start of Exercise									
				5	10	15	20 (stop)	25	30	35	50	80
Glucose	1.0	5.2±0.1	5.2±0.3	5.2±0.1	5.0±0.2	5.0±0.1	5.0±0.2	5.5±0.2	5.3±0.25	5.2±0.2	5.2±0.2	5.00±0.1
	1.3	5.1±0.2	5.3±0.3	5.8±0.5	4.8±0.3	4.8±0.3	5.2±0.3	5.1±0.4	5.2±0.31	5.1±0.3	4.6±0.3	4.98±0.3
	5.8	5.5±0.2		5.6±0.2	5.7±1.0	5.7±0.5	3.6±0.2	5.6±0.6	5.5±0.65	5.1±0.5		
Insulin (µU/mL)	1.0	3.8±0.2	4.5±0.9	4.5±0.6	3.4±0.4	2.8±0.3	2.6±0.3	7.4±0.6	5.4±0.8	4.7±0.6	4.4±0.5	4.2±0.5
	1.3	5.0±0.5		4.5±0.6	3.4±0.4	2.8±0.3	3.3±0.7	7.9±1.8	7.7±1.8	3.9±1.1		4.7±0.7
	5.8	5.2±0.8		4.2±0.8	5.3±0.6	4.8±0.6	4.7±0.6	7.0±1.3	8.2±1.6	7.5±1.2		
Lactate	1.0	0.73±0.04		3.10±0.35	4.62±0.96	4.32±0.89	4.36±0.81	3.69±0.71	3.02±0.66	2.35±0.54	1.40±0.25	0.94±0.10
	1.3	0.89±0.09	0.88±0.12	3.75±0.68	4.81±1.03	4.62±1.04	5.05±1.13	4.04±0.88	3.16±0.68	2.59±0.58	1.82±0.29	1.30±0.21
	5.8	1.13±0.14	1.01±0.10	2.24±0.12	4.86±0.71	6.55±0.91	6.30±0.85	5.11±0.90	4.90±1.04	3.56±0.42		
Pyruvate	1.0	0.08±0.00		0.13±0.01	0.20±0.03	0.20±0.03	0.20±0.03	0.24±0.04	0.21±0.04	0.17±0.03	0.12±0.02	0.09±0.01
	1.3	0.08±0.00	0.07±0.02	0.16±0.02	0.20±0.02	0.21±0.03	0.21±0.03	0.22±0.04	0.22±0.03	0.17±0.04	0.13±0.02	0.09±0.01
	5.8	0.09±0.01	0.07±0.01	0.12±0.01	0.18±0.02	0.23±0.02	0.23±0.02	0.25±0.04	0.30±0.05	0.22±0.02		
L/P	1.0	10.1±0.04		24.1±1.4	22.7±1.8	2.13±1.4	21.9±1.3	14.9±1.0	14.2±0.9	13.1±0.6	11.3±0.2	10.7±0.5
	1.3	11.5±0.5	13.1±0.7	23.2±1.7	23.4±2.6	21.8±2.1	22.4±2.4	16.3±1.5	14.8±1.9	14.6±1.1	14.3±0.9	13.7±0.5
	5.8	12.4±0.6	13.2±0.7	19.3±0.6	26.3±1.3	27.9±0.4	27.1±1.4	20.6±0.5	16.0±0.7	16.0±0.8		
Alanine	1.0	0.30±0.01		0.34±0.02	0.38±0.01	0.38±0.02	0.40±0.01	0.37±0.01	0.37±0.02	0.35±0.03	0.30±0.03	0.30±0.01
	1.3	0.32±0.03	0.33±0.05	0.35±0.03	0.34±0.04	0.37±0.03	0.39±0.04	0.35±0.04	0.36±0.04	0.33±0.02	0.30±0.01	0.30±0.01
	5.8	0.36±0.03	0.35±0.04	0.38±0.03	0.41±0.04	0.43±0.04	0.45±0.04	0.43±0.06	0.47±0.10	0.43±0.04		
A/P	1.0	4.1±0.1		2.6±0.2	2.1±0.2	2.0±0.2	2.2±0.2	1.7±0.2	2.0±0.2	2.2±0.2	2.9±0.3	3.7±0.3
	1.3	4.1±0.2	4.9±0.3	2.5±0.3	1.8±0.2	1.9±0.3	2.0±0.3	1.7±0.3	2.0±0.3	2.2±0.4	2.6±0.4	3.5±0.6
	5.8	4.0±0.1	4.6±0.3	3.2±0.2	2.3±0.3	1.9±0.3	2.0±0.2	1.8±0.2	1.6±0.3	2.0±0.2		
Glycerol	1.0	0.06±0.01		0.06±0.01	0.08±0.01	0.10±0.02	0.11±0.03	0.16±0.03	0.14±0.03	0.13±0.02	0.08±0.01	0.09±0.01
	1.3	0.09±0.01	0.10±0.02	0.15±0.02	0.11±0.01	0.13±0.02	0.14±0.02	0.15±0.02	0.15±0.02	0.13±0.02	0.11±0.02	0.10±0.01
	5.8	0.05±0.01	0.06±0.03	0.08±0.03	0.09±0.02	0.08±0.01	0.09±0.01	0.10±0.02	0.10±0.03	0.08±0.01		
NEFA	1.0	0.72±0.08		0.62±0.09	0.61±0.08	0.64±0.09	0.61±0.12	0.99±0.21	1.05±0.25	1.04±0.23	0.87±0.15	0.73±0.12
	1.3	0.76±0.13	0.81±0.22	0.82±0.15	0.67±0.10	0.66±0.13	0.66±0.13	0.90±0.21	0.99±0.19	0.86±0.22	0.68±0.20	0.86±0.22
	5.8	0.84±0.09		0.80±0.08	0.91±0.16	0.72±0.10	0.71±0.07	0.93±0.11	0.97±0.12	0.73±0.06		
Ketones	1.0	0.07±0.01		0.05±0.01	0.05±0.01	0.04±0.10	0.05±0.01	0.07±0.01	0.10±0.03	0.13±0.04	0.14±0.05	0.10±0.02
	1.3	0.12±0.05	0.13±0.07	0.15±0.06	0.10±0.04	0.08±0.03	0.07±0.03	0.10±0.02	0.12±0.02	0.14±0.02	0.15±0.04	0.17±0.04
	5.8	0.07±0.02	0.06±0.02	0.07±0.02	0.05±0.02	0.05±0.01	0.05±0.00	0.06±0.01	0.07±0.02	0.06±0.02		

Values are for 6 subjects in air at 1 bar and normoxic oxyhelium at 1.3 bars and for 4 of the 6 subjects in normoxic oxyhelium at 5.8 bars (mean ± SE). *P < 0.05; **P < 0.01. +, 1 v 1.3 bars; o, 1 v 5.8 bars; x, 1.3 v 5.8 bars. L/P is Lactate/Pyruvate ratio; A/P is Alanine/Pyruvate ratio; NEFA is Non-esterified fatty acids. (The 5 + 15-min concentrations of insulin + NEFA are the mean of 3 specimens.)

TABLE III

Physiological Variables of Subjects under Experimental Conditions

Variable	Pressure (bar)	Baseline	Post Compression	Time (in min) from Start of Exercise								
				5	10	15	20 (stop)	25	30	35	50	80
V_{O_2} (L/min)	1.0			1.78 ± 0.13	1.91 ± 0.10	1.97 ± 0.10	2.10 ± 0.14	0.47 ± 0.13	0.29 ± 0.02	0.24 ± 0.02	0.23 ± 0.02	0.22 ± 0.02
	5.8			1.92 ± 0.13	2.36 ± 0.10 *o	2.38 ± 0.15	2.52 ± 0.13	–	0.30 ± 0.02	0.29 ± 0.02	–	–
RQ	1.0			1.09 ± 0.03	1.02 ± 0.01	1.00 ± 0.01	0.99 ± 0.01	–	0.89 ± 0.03	0.88 ± 0.02	0.86 ± 0.03	0.86 ± 0.02
	5.8			0.98 ± 0.02	0.94 ± 0.02	0.98 ± 0.02	0.94 ± 0.01 *o	–	0.86 ± 0.06	0.76 ± 0.06	–	–
Pulse Rate (beats/min)	1.0	72 3		148 ± 8	156 ± 8	160 ± 6	164 ± 6	106 ± 6	101 ± 4	97 ± 3	89 ± 4	80 ± 2
	1.3	76 2	76 4	150 ± 6	157 ± 6	163 ± 7	167 ± 7	115 ± 7	105 ± 5	102 ± 6	89 ± 4	79 ± 4
	5.8	73 2	74 5	147 ± 8	164 ± 6	168 ± 5	170 ± 4	118 ± 2	104 ± 3	100 ± 3	–	–

Values are for 6 subjects in air at 1 bar and normoxic oxyhelium at 1.3 bars and for 4 of the 6 subjects in normoxic oxyhelium at 5.8 bars. $*P < 0.05$.
+, 1 v 1.3 bars; o, 1 v 5.8 bars; ×, 1.3 v 5.8 bars.

Fig. 2.   Mean lactate levels. *$P < 0.05$ compared with air.
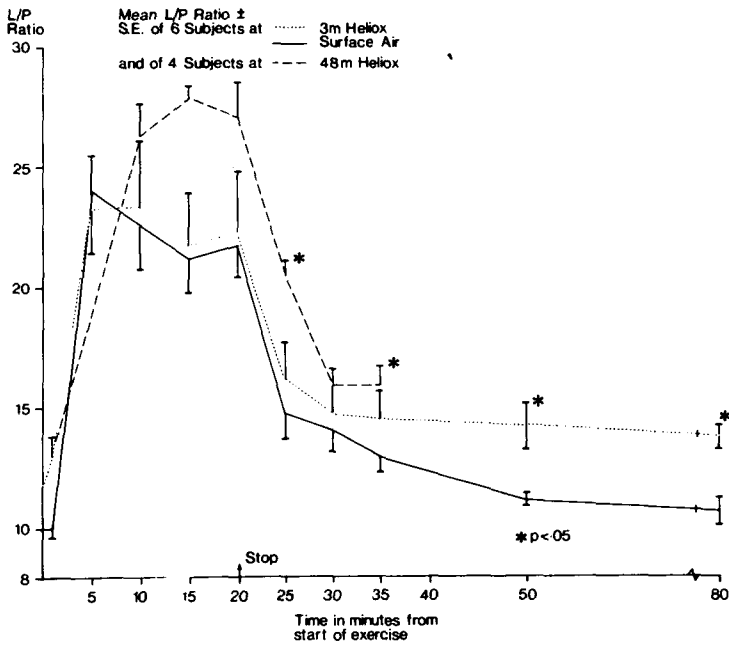
Fig. 3.   Mean L/P ratios. *$P < 0.05$ compared with air.
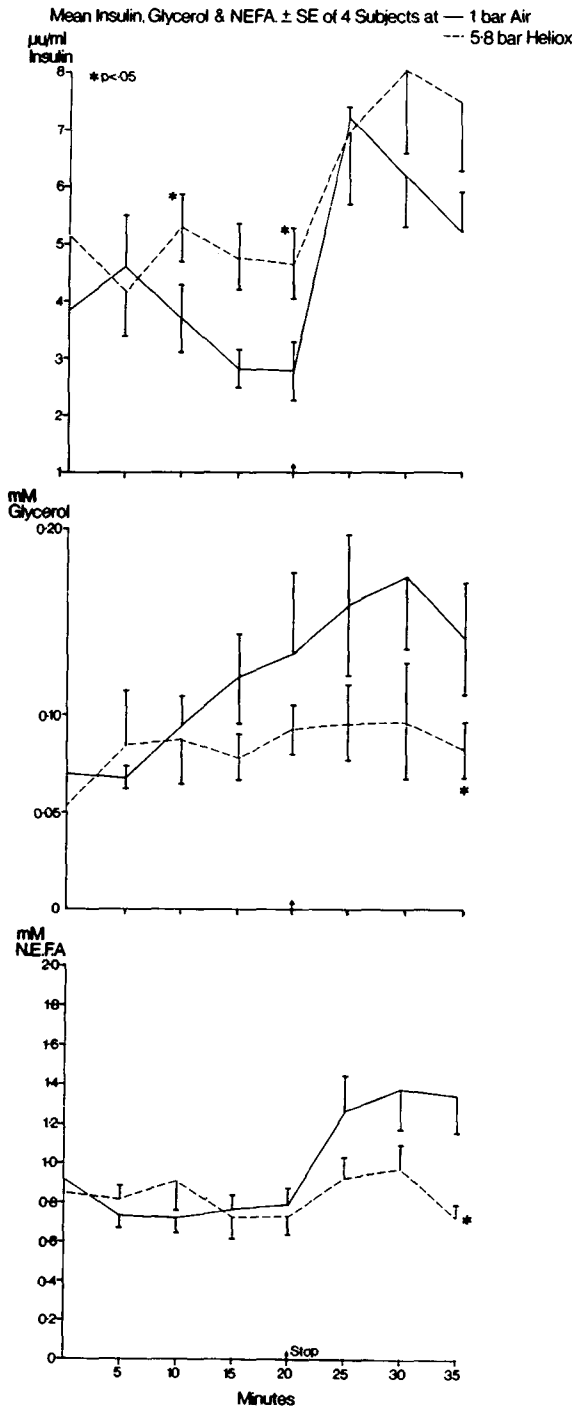
Fig. 4.   Mean insulin, glycerol and NEFA levels.

end of exercise (Fig. 3). The heart rate rose with exercise but there was no significant difference between the environments. The V_{O_2} was not significantly raised in the 5.8-bar environment compared to air at 1 bar, except at the 10-min point during the exercise period (Table III).

DISCUSSION

It must be remembered that while subjects are exposed to pressure their tissues are equilibrating with the new environment. Nitrogen elimination studies (10) have shown that the nitrogen content in the expired air falls by about 98% in the first 3 or 4 min when subjects breathe an oxyhelium mixture. This initial rapid elimination of nitrogen has also been noted by other investigators (11). We believed that any discrepancy in the respiratory measurements caused by dilution with nitrogen would be slight.

Only a few studies have been carried out in normoxic hyperbaric environments; these studies used normoxic hyperbaric nitrogen mixtures (12,13). In both studies there was an increase in the work of breathing because of the increased density of the gas mixture, but no biochemical measurements were made. Exercise studies have also been made during saturation dives in oxyhelium, when equilibration with the environment has been reached (14,15). These investigations were carried out with a slightly hyperoxic mixture (P_{O_2}, 0.3 bar), but with a far greater partial pressure of helium. The measurements taken were, once again, of a physiological rather than biochemical nature and showed a higher O_2 consumption and slightly lower heart rate under pressure when compared to surface controls. This bradycardia associated with hyperbaric environments (16–18) was not seen in our series of studies. This is not surprising as the major cause of the bradycardia is thought to be an increase in the P_{O_2} (18).

The findings of our exercise studies on the surface are what might be expected in response to the level of exercise studied. There are, however, interesting differences between the findings in air and those at 1.3 bars and 5.8 bars in the oxyhelium environments. The difference at 1.3 bars was the higher lactate/pyruvate (L/P) ratio at 50 and 80 min; however, the base-line L/P ratio for the 1.3-bar exposures was higher, and if this is taken into consideration the significance disappears. The differences at 5.8 bars were more numerous. There was the increase in O_2 consumption at the start of exercise, which was maintained during this period, together with a slight but statistically significant decrease in the respiratory quotient (RQ) after 20 min (shown in Table III); these changes could point to the use of a higher proportion of fatty acids or ketone bodies. However, the glycerol levels were lower during the exercise period, a finding that points to a lack of increase in lipolysis. This pattern was followed by NEFA, which is unaccompanied by a drop in glycerol, and could indicate an increase in usage that might account for the drop in RQ. One must remember that the RQ was still 0.94, which is approximately the level one would expect in untrained subjects breathing normobaric air (19). In addition,

RQ values during exercise can be distorted because of the blowing off of CO_2 while contracting an oxygen debt (20).

The failure of insulin to show the expected drop at 48 m is surprising. The drop is thought to be mediated by catecholamines acting on the α-receptors of the β-cells (21,22). One would think that the catecholamine level would be higher during this exposure compared to the surface area since it was probably more stressful. The higher level of insulin may have had an effect on lipolysis and account for the lower levels of glycerol and NEFA. It is now recognized that insulin inhibits lipolysis and ketogenesis at much lower levels than those required to stimulate glucose transport (23). The glucose/insulin ratio is lower at 5.8 bars during the exercise period, reflecting the higher insulin levels. The glucose levels themselves are higher at pressure, but this difference is not statistically significant and could indicate the presence of insulin resistance in this environment. However, the interrelationships of metabolic substrates and hormones are not simple, and the slight increase in $\dot{V}O_2$ and lowering of the RQ may prove to be compatible with the raised insulin levels and lower levels of glycerol and NEFA. Certainly this is an area that would reward further study.

References

1. Chouteau J. Respiratory gas exchange in animals during exposure to extreme ambient pressures. In: Lambertsen CJ, ed. Underwater physiology. Proceedings of the fourth symposium on underwater physiology. New York: Academic Press. 1971;385–399.
2. Guillerm R, Hee J, Masurel G, Pane J. Arterial blood PO_2, PCO_2, pH in awake animals under chronic hyperbaric situations. Medecine Aeronautique et Spatiale, Medecine Subaquatique et Hyperbare 1978;65:93–96.
3. Kiesow LA. Hyperbaric inert gases and the hemoglobin-oxygen equilibrium in red blood cells. Undersea Biomed Res 1974;1:29–45.
4. Hyacinthe R, Broussolle B, Baret A, Fructus X. Etudes des phosphates organiques erythrocytaires et de l'affinite de l'hemoglobine pour l'oxygene en ambiance hyperbare et mélange helium oxygen légerment hyperoxique. Le Poumon et le Coeur 1975;31:191–195.
5. Hahn CEW, Föex P, Raynor CM. A development of the oxyhemoglobin dissociation curve analyser. J Appl Physiol 1976;41:259–267.
6. Price CP, Lloyd B, Alberti KGMM. A kinetic spectrophotometric assay for rapid determination of acetoacetate in blood. Clin Chem 1977;23:1893–1897.
7. Lloyd B, Burrin J, Smythe P, Alberti KGMM. Enzymic fluorometric continuous-flow assays for blood glucose lactate, pyruvate, alanine, glycerol, and 3-hydroxybutyrate. Clin Chem 1978;24:1724–1729.
8. Soeldner JS, Slone D. Critical variables in the radioimmunoassay of serum insulin using the double antibody technique. Diabetes 1965;14:771–779.
9. Ho RJ, Meng HC. A simple and ultra sensitive method for determination of free fatty acid by radiochemical assay. Anal Biochem 1969;31:426–436.
10. Barnard EEP, Hanson R de G, Reid BJ, Williams J. Studies in nitrogen elimination. Försvarsmedicin 1973;9:496–502.
11. Vorosmarti J, Barnard EEP, Williams J, Hanson R de G. Nitrogen elimination during steady-state hyperbaric exposures. Undersea Biomed Res 1978;5:243–253.
12. Cook JC. Work capacity in hyperbaric environments without hyperoxia. Aerosp Med 1970;41:1133–1135.
13. Anthonisen NR, Utz G, Kryger MH, Urbanetti JS. Exercise tolerance at 4 and 6 ATA. Undersea Biomed Res 1976;3:95–102.
14. Bradley ME, Anthonisen NR, Vorosmarti J, Linaweaver PG. Respiratory and cardiac response to exercise in subjects breathing helium-oxygen mixtures at pressures from sea level to 192 bar. In: Lambert-

sen CJ, ed. Underwater physiology. Proceedings of the fourth symposium on underwater physiology. New York: Academic Press, 1971:325–339.

15. Salzano J, Overfield EM, Rausch DC et al. Arterial blood gases, heart rate, and gas exchange during rest and exercise in man saturated at a simulated seawater depth of 1000 ft. In: Lambertsen CJ, ed. *Underwater physiology. Proceedings of the fourth symposium on underwater physiology.* New York: Academic Press, 1971:347–357

16. Albano G. Principles and observations on the physiology of the scuba diver. Arlington, VA: Office of Naval Research, 1970.

17. Linnarsson D, Karlsson J, Fagraeus L, Saltin B. Muscle metabolites and oxygen deficit with exercise in hypoxia and hyperoxia. J Appl Physiol 1974;36:399–401.

18. Fagraeus L, Linnarsson D. Heart rate in hyperbaric environments after autonomic blockade. Försvarsmedicin 1973;9:260–269.

19. Astrand PO, Rodahl K. Testbook of work physiology. New York and London: McGraw-Hill, 1970.

20. Ganog WF. Review of medical physiology. Los Altos, CA: Lange, 1977.

21. Leclerq-Meyer V, Malaisse WJ. Participation of catecholamines in inhibition of insulin-secretion and stimulation of glucagon release during exercise and stress. Diabete Metab 1975;1:119—122.

22. Porte D. A receptor mechanism for the inhibition of insulin release by epinephrine in man. J Clin Invest 1967;46:86–94.

23. Schade DS, Eaton RP. Dose response to insulin in man: differential effects on glucose and ketone body regulation. J Clin Endocrinol Metab 1977;44:1038–1052.

COMPARISON OF METABOLIC RESPONSES AND GROWTH HORMONE RELEASE DURING SUBMAXIMAL EXERCISE IN MAN BREATHING HELIOX OR AIR AT NORMAL BAROMETRIC PRESSURE

J. Raynaud, P. Varène, and J. Durand

At least five physiological functions of mammals are sensitive to the quality of the neutral gas present in the surrounding atmosphere; they are thermal, respiratory, cardiovascular, nervous, and metabolic functions (1). Reports in the literature about metabolic alterations induced by helium-oxygen (heliox) breathing in diving are conflicting because it is difficult to delineate the role played by hyperbaria, helium, or the increase in environmental thermal conductivity.

To avoid the effects that thermoregulation might have in the assessment of the effects of helium and other rare gases on the cellular metabolism, investigators studied tissue slices of mammals or microorganisms, plants, and the like (2–6). The results of these studies varied, but favor the finding that helium and the other rare gases had a depressing effect on the cellular metabolism.

In mammal research, Leon et al. (7) and later Rhoades et al. (8) attributed the overall metabolic effect observed on rats to thermoregulatory reactions. On the contrary, Clarkson et al. (9) and Schatte et al. (10) measured a decrease of oxygen consumption associated with an increase of the respiratory quotient in rats living in a normobaric heliox environment. According to Jordan et al. (11), " . . . there is reason to question the simple explanation that metabolic effects on replacing nitrogen in air with helium are due to thermal conductivity alone."

In human research, the large number of diving experiments in a heliox atmosphere have shown that the metabolic effects of helium breathing are

probably very little, if any. The respiratory exchanges generally are not modified when thermal comfort is satisfied (12). Nevertheless, the data obtained in diving conditions vary, and small variations can be overlooked. No modifications of metabolic function have been observed in normobaric conditions by Bowers et al. (13) nor in hypobaric ones by Glatte et al. (14) or Zeft et al. (15) using heliox atmospheres. Finally, the only feature observed in heliox-breathing man is the increase of blood concentration of growth hormone reported by Raymond et al. (16).

To verify the increase of blood concentration of growth hormone reported by Raymond et al. (16) and to overcome the difficulties involved in diving environmental conditions, we studied our subjects comparatively at normal barometric pressure while they breathed either room air or a normoxic heliox mixture.

METHODS AND MATERIALS

Seven male students ranging in age from 19 to 24 years were the subjects of this investigation. Their physical characteristics are given in Table I. None gave a history of previous cardiac or respiratory disease, and physical examination and chest radiograph were within the normal limit in each instance. No subject was participating regularly in athletic activities, although three subjects practiced diving as a hobby during the summer. The experiments were carried out in the morning. The temperature in the laboratory varied between 19 and 23°C. The subjects had a slight breakfast without fat on the day of the experiment; the diet on the day of the experiment was as usual, not controlled. Venous blood was taken from a catheter inserted into an antecubital vein. An infusion of physiological saline without heparin at 1 mL·min^{-1} was maintained to avoid clotting.

The control blood samples were taken immediately after catheterization during room air experiments or after breathing heliox for 30 min. Afterwards, the subject rested comfortably for 1 h. Two additional control samples were drawn at the 30th and 60th min of this control period. At the end of the con-

TABLE I

Anthropometric Characteristics of the Subjects

Subjects	Age (yr)	Height (m)	Weight (kg)	Max HR min^{-1}	Vo$_2$ max l·min^{-1}
C	21	1.75	60	193	2.8
G	22	1.87	70	192	3.1
T	24	1.67	65	191	3.0
D	19	1.80	60	194	2.7
B	19	1.83	63	195	2.75
G	19	1.72	64	194	2.1
G	19	1.80	83	194	2.4

trol period, the subject mounted a bicycle ergometer (type, Fleish). Exercise was performed at a constant speed (60 rpm) for 1 h. The subject was studied for 20 min during recovery. Two intensities of work were explored: 30 and 50 watts per m^2 of body surface area.

Oxygen consumption ($\dot{V}O_2$) was calculated by the open-circuit method: the expired gas was collected in a Douglas bag and analyzed for CO_2 (Infra Red analyzer, Cosma type 80) and O_2 (Paramagnetic analyzer, Servomex, type OA 250). The calibrations were made with pure gas mixtures of either N_2, O_2, and CO_2 in room air experiments, or He, O_2, and CO_2 in heliox experiments (Air Liquide, N_2:N_{48}; O_2:N_{48}; CO_2:N_{45}; He:N_{60}). The gases were delivered by a Wösthoff volumetric pump. The responses of the analyzers were slightly modified by helium. The relationships of O_2 or CO_2 fraction vs. mV remained linear in the range considered. However, the slope was slightly steeper but passing through zero in the case of CO_2; whereas the slope remained parallel but shifted upward in the case of O_2. Bag volume was measured with a Tissot spirometer. Resting $\dot{V}O_2$ was determined three times during 5 min-sampling periods. The bag collections were for 1-min periods during the first 10 min of exercise and for 2- or 5-min periods during the remainder of the work. Initial O_2 deficit was computed by adding the sequential differences between steady state $\dot{V}O_2$ ($\dot{V}O_2$ st.st.ex) and the actual values of $\dot{V}O_2$ measured every minute during the transient phase. The mean value of $\dot{V}O_2$ measured from the 25th min of exercise to the 35th min was taken as the steady state $\dot{V}O_2$ value in the calculation of deficit and estimation of $\dot{V}O_2$ max. Electrocardiographic recordings were continuous.

Blood samples (6 mL) were drawn during exercise at minutes 3, 10, 20, 40, 60, and during recovery at minutes 3, 8, and 20. Every blood sample was divided into two ice-cold tubes, one of them containing FNa. The tubes were centrifuged immediately at 4°C. Fluorided plasma samples were deproteinized with 20% perchloric acid. Boehringer test kits were used to measure lactate enzymatically. Non-fluorided plasma samples were stored at -20°C for further analysis of plasma free fatty acid concentration ([FFA]) and growth hormone. Total plasma [FFA] was determined by the method of Dole modified by Lauwerys (17). Duplicate determinations of the concentration of the metabolites and hormone were carried out from each plasma sample.

Plasma growth hormone concentration ([IRHGH]) was analyzed by Hunter and Greenwood's radioimmunologic technique modified by Donnadieu et al. (18). Standard curves were determined with duplicate measurements of concentrations of standard hormone from 0.25 to 40 ng·mL^{-1} for every experiment. The results were expressed using the ratio Bound hormone/Total hormone (B/T). The B/T values were plotted vs. logarithm of the concentrations of the standard hormone, a program intended to compute precision, sensitivity, and actual value of every sample, and to point out the aberrant values. Precision was defined as the standard deviation, s, calculated from: s $\sqrt{(\Sigma d^2/2n)}$ where d is the difference between 2 duplicate values of B/T and n, the number of pairs. Sensitivity was defined as the concentration of standard hormone corresponding to the value of B/T equal to $2s$ at zero standard. In the 23 standard

curves determined in this study, s was equal to $\pm$ 0.011 and the sensitivity threshold was equal to 0.50 ng·mL^{-1}. The time course of [IRHGH] is described in terms of maximal concentration, mean concentration during exercise ($\overline{C}_{IRHGH}$), delay of rise, and half life. The $\overline{C}_{IRHGH}$, was computed as the area limited by the curve of concentration as a function of time (measured by planimetry) divided by 60 min. The delay was determined as follows: the absolute values of concentration were expressed in percentage of the peak concentration value; the sequential relative values obtained in this way were statistically compared; and, finally, the value of the delay was located within the interval between two sequential values statistically different at the level of $P < 0.05$ (Cochran test). The half life is the time for [IRHGH] to decrease to half the maximal value of concentration; it was determined by plotting sequential decreasing values on semi-logarithmic paper.

We estimated the maximal oxygen consumption ($\dot{V}O_{2max}$) using the indirect method of Maritz (19); the same relationship—maximal heart rate vs. age was used—the subject breathed either air or heliox.

RESULTS

The means are given plus or minus 1 standard error. The results are summarized in Table II and illustrated in Figs. 1, 2, and 3. We compared the means using a test for paired data and small samples.

Energetic and cardiac data. Two parameters were not modified by heliox breathing at rest as well as at exercise: $\dot{V}O_2$ and heart rate. In contrast, $\dot{V}_{BTPS}$, initial O_2 deficit, and respiratory quotient (RQ) were modified during heliox breathing, but the level of statistical significance was never reached. Compared to room air breathing, the following were observed in heliox protocols: $\dot{V}_{BTPS}$ tended to be more elevated, mainly at the highest intensity of exercise, and RQ tended to be lowered. Initial O_2 deficit, which is an index of anaerobic metabolism, was more important in Exercise II, but the difference was nonsignificant.

Blood metabolites. Plasma lactate concentration ([LA]) followed a similar course in subjects breathing room air or heliox: that is, [LA] increased within the first 20 min of exercise, then reached a plateau, and decreased as soon as exercise stopped. The comparison of the curves of Fig. 1 demonstrates that the [LA] curve in heliox experiments is always situated above that in room air at the two work loads, but the upward shifting averages half one mmol·L^{-1} only. When the maximal values obtained at the two work loads were combined in the statistical analysis, the mean difference between heliox and air protocols was +0.63 mmol·L^{-1}, $P< 0.05$. The curves of [FFA] are not so smoothly defined as those of [LA]. However, the time courses of [FFA] tend to indicate that the release of FFA was earlier and faster in heliox protocols, but the differences were not significant because of the small number of subjects and because of the measurement technique, which is not as precise as that of LA.

Growth hormone. There was no difference in air or heliox [IRHGH] resting values even when all of the control data of Exercise I and II were com-

TABLE II

Energetic and Metabolic Data Obtained at Rest (R) and at the Steady State (Ex) of Exercise I (30 watts·m^{-2}) and Exercise II (50 watts·m^{-2})

		Exercise I		Exercise II	
		Air	Heliox	Air	Heliox
V̇o$_2$ L·min^{-1}	R	0.272	0.265	0.325	0.240
		0.013	0.010	0.018	0.014
	Ex	1.250	1.275	1.700	1.730
		0.033	0.051	0.040	0.063
V̇$_{BTPS}$ L·min^{-1}	R	8.990	9.130	10.150	9.750
		0.51	0.65	0.46	0.71
	Ex	34.840	35.640	39.250	46.400
		2.310	2.420	1.80	2.70
R	R	0.89	0.86	0.90	0.89
		0.02	0.03	0.02	0.03
	Ex	0.95	0.89	0.89	0.88
		0.02	0.02	0.02	0.02
Fc min^{-1}	R	80	78	76	75
		3	3	2	3
	Ex	133	134	157	162
		6	6	9	7
O$_2$-Deficit STPD	Ex	0.990	1.070	2.560	3.340
		0.063	0.150	0.800	0.710
[LA] max mmoL·L^{-1}	R	1.00	1.30	1.20	1.15
		0.32	0.25	0.20	0.25
	Ex	2.70	3.20	4.30	4.75
		0.40	0.31	0.35	0.28
[FFA] max m eq·L^{-1}	R	0.890	1.200	0.885	1.160
		0.100	0.050	0.090	0.050
	Ex	1.400	2.200	2.010	2.530
		0.170	0.180	0.160	0.190

Values are the means ± 1 SE. The average of the maximal values of lactate and free fatty acids are slightly superior to those observed in Figs. 1 and 2 because the maximal values are not exactly synchronous from one experiment to another.

bined: air: 3.77 ± 0.60 ng·mL^{-1}; heliox: 4.92 ± 0.80. The time course of [IRHGH] showed some common characteristics during air and heliox breathing exercises in that maximal values varied widely among the subjects and a very sharp fall occurred either precisely at the cessation of exercise or a few minutes later. In spite of these similarities, the time sequence of [IRHGH] differed during heliox breathing protocols mainly at the highest work load when compared to room air protocols. In air experiments, concentration of [IRHGH] was maintained at resting level for 20 min (delay between 20 and 40 min) after the
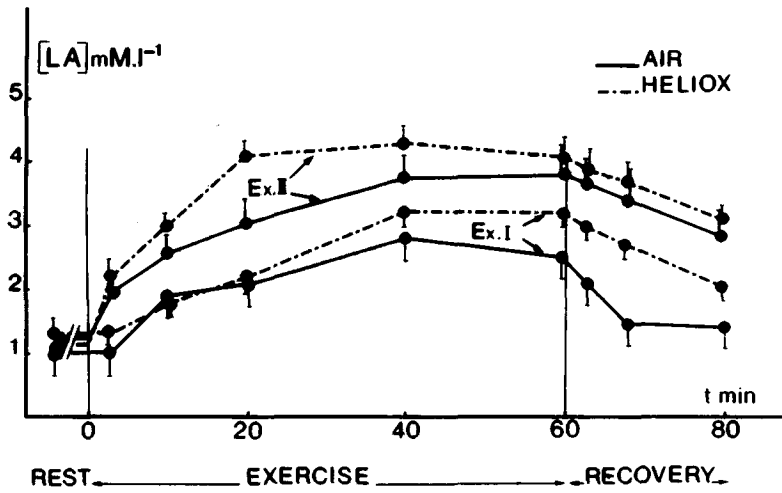
Fig. 1. Time course of plasma lactate concentration during Exercise I (30 W·m^{-2}) and II (50 W·m^{-2}).   The *vertical bars* represent 1 SE.
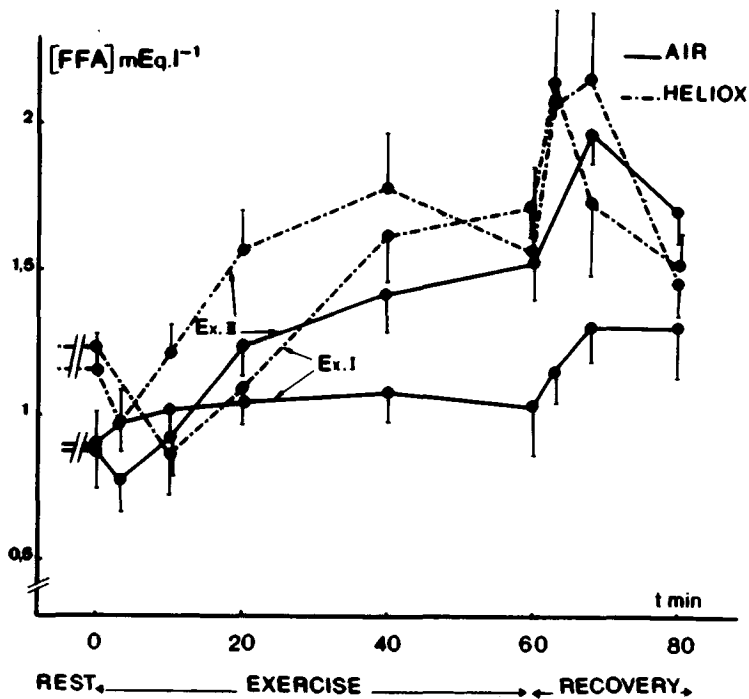
Fig. 2. Time course of plasma free fatty acids concentration during Exercise I (30 W·m^{-2}) and II (50 W·m^{-2}).   The *vertical bars* represent 1 SE.
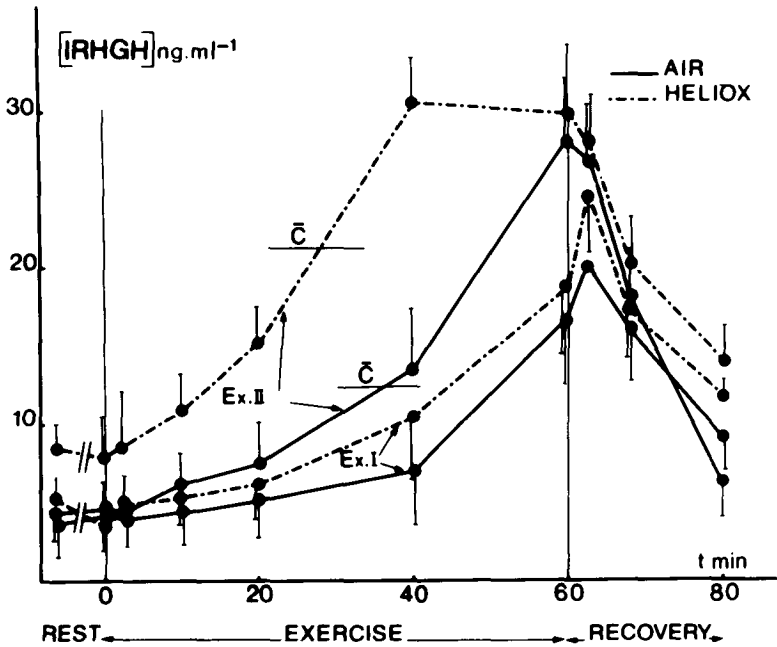
Fig. 3.   Time course of plasma immunoreactive growth hormone during Exercise I (30 W·m⁻²) and II (50 W·m⁻²). $\bar{C}$ indicates the value of the mean concentration calculated over the corresponding 60-min exercise period; $\bar{C}$ was computed for Exercise II only.

beginning of exercise and the maximal value was reached at the end of exercise (Exercise II: 28.2 ± 4.2 ng·mL⁻¹).

During recovery, [IRHGH] decreases with a half-life of 12 ± 4 min. When the same subjects are studied during heliox breathing, the main difference is that [IRHGH] increases more sharply (delay between 10 and 20 min). The maximal value (30.6 ± 2.8 ng·mL⁻¹ is reached at the 40th min, then reaches a plateau until the end of exercise, but it is of the same order of magnitude as that reached in air. The half-life is slightly longer than that calculated in air experiments (22 ± 5 min). The alteration of the time sequence at the beginning of exercise in heliox breathing is confirmed by the comparison of the values of $\bar{C}_{IRHGH}$: air: 12.4 ng·mL⁻¹; heliox; 21.6. In heliox breathing at the lowest intensity of muscular exercise modifications are less marked.

DISCUSSION

This study showed that breathing heliox under barometric pressure at rest and during exercise induced some metabolic alterations. However, the main result was that these modifications were very limited and would not have been significant if their development as a function of time had not been considered.

Confusing findings regarding $\dot{V}o_2$ and heart rate appear in the literature. Our results showed no change in $\dot{V}o_2$ either at rest or during exercise, which is in agreement with Bowers et al.(14), who showed no decrease in heart rate, but contrast with the findings of Raymond et al. (20).

Ventilatory rate has been shown to be increased when helium is the main contributor of the ventilated gas. Brès et al. (21) reported that this relative hyperventilation probably was caused by the physical characteristics of helium and was confirmed by the decrease in Pa_{CO_2}.

From a metabolic point of view, there emerges a set of responses consistent with an enhancement of the anaerobic metabolism at the onset of exercise: higher production of lactic acid and larger O_2 deficit. Morever, the time sequence of [IRHGH] during exercises in heliox breathing mimicked that described in hypoxic conditions (22): it was shown that shorter delay in [IRHGH] rise, accompanied by a more abrupt rate of increase, is a constant response to hypoxia observed either in adaptation to high altitude or during the breathing of a low-pressure O_2 gas mixture. Higher [FFA] release also occurred in these hypoxic conditions. Such a response pattern has just been described in the protocols of the present study, particularly at the highest work load. Although the differences reported were not significant, the fact that they combined to give a consisent picture with higher levels of hypoxia occurring during heliox breathing makes the conclusions more reliable.

Two main questions remain: What mechanisms could be advanced that would impede or delay O_2 utilization by the tissues, and What mechanisms could modify time course of [IRHGH] in hypoxia? Guenard et al. (23) clearly demonstrated that the (A-a) O_2 difference was enlarged during heliox breathing, consequently inducing relative hypoxic conditions. As helium seems to act at membrane level, the impediment to O_2 utilization could be enhanced at tissular level because of a defect in O_2 diffusion to the cells. This last assumption is highly hypothetical. The second question concerns more specifically [IRHGH] response to hypoxia. As the alteration of a blood substance concentration is the result of the imbalance between production and catabolism, a hypoxic agent could act either by triggering the secretion or by diminishing the clearance of the hormone. The role of [LA] as a direct stimulating agent is now dubious (24). According to the second alternative, one should assume that hepatic blood flow or hepatic function is modified by helium. As far as we know, there is no experimental argument for such an hypothesis in the literature.

From a general point of view, this study points out the importance of closely describing the time course of [IRHGH] during the transient phase and following the time sequence over a long duration. Comparisons of results without considering all of the experimental conditions, particularly duration of the observation, can lead to discrepant conclusions. In our study, if exercise duration had been reduced to 20 min, for instance, our conclusions would agree with those of Raymond et al. (16); that is, hormone release was enhanced by heliox breathing, whereas this was no longer true 40 min later because at the end of exercise the maximal values reached during heliox and room-air breathing were very similar.

References

1. Varène P, Valiron M. Effets biologiques des gaz inertes. Bull Eur Physiopathol Respir 1980;16:79–109.
2. South FE, Cook SF. Effect of helium on the respiration and glycolysis of mouse liver slices. J Gen Physiol 1951;36:513–528.
3. Maio DA, Neville JR. Effects of chemically inert gases on oxygen consumption in living tissues. Aerosp Med 1967;38:1049–1056.
4. Schreiner HR, Gregoire RC, Lawrie JA. New biological effect of the gases of the helium group. Science 1962;136:653–654.
5. Schreiner HR. General biological effects of the helium xenon series of elements. Fed Proc 1968;27:872–878.
6. Jenkin HM, Yang TK, Nielsen TW, Bitter RA. The effect of hyperbaric exposure of 20 atmospheres-absolute (He-O$_2$) on sphingoglycolipids of rat tissues. Proc Soc Exp Biol Med 1975;148:870–874.
7. Leon HA, Cook SF. A mechanism by which helium increases metabolism in small mammals. Am J Physiol 1960;199:243–245.
8. Rhoades RA, Wright RA, Hiatt EP, Weiss HS. Metabolic and thermal responses of the rat to a helium oxygen environment. Am J Physiol 1967;233:1009–1014.
9. Clarkson DP, Schatte CL, Jordan JP. Thermal neutral temperature of rats in helium oxygen, argon oxygen, and air. Am J Physiol 1972;222:1494–1498.
10. Schatte CL, Jordan JP, Philips RW, Clarkson DP, Simmons JB. Non-thermal metabolic response of rats to He-O$_2$, N$_2$-O$_2$, and Ar-O$_2$ at 1 atmosphere. Am J Physiol 1973;225:553–558.
11. Jordan JP, Simmons JB, Lassiter DV, Deshpande Y, Dierschke DJ. Metabolic effects of nitrogen and neon as diluent environmental gases. In: Proceedings of the First International Conference on "Depressed Metabolism." Musacchia XJ, Saunder JF, eds. New York: Elsevier, 1969, pp. 67–113.
12. Timbal J, Vieillefond H, Guénard H, Varène P. Metabolism and heat losses of resting man in a hyperbaric helium atmosphere. J Appl Physiol 1974;36:444–448.
13. Bowers RW, Fox EL. Metabolic and thermal responses of man in various He-O$_2$ and air environments. J Appl Physiol 1967;23:561–565.
14. Glatte H, Bartek MJ, Uldeval F, Brown HE, Gianneta CL, Roberts JA. Study on man during a 56 day exposure to an oxygen helium atmosphere at 258 mmHg total pressure: renal and endocrin response. Aerosp Med 1966;37:279–280.
15. Zeft HJ, Behar VS, Quigley DG, Uldeval F, Shaw EG, Welch BE. Observation on man in an oxygen helium environment at 380 mmHg total pressure. Aerosp Med 1966;37:449–461.
16. Raymond LW, Sode J, Langworthy HC, Blosser J, Johnsonbaugh RE. Increase in plasma growth hormone concentration: a new effect of helium breathing. Undersea Biomed. Res 1974;1:91–98.
17. Lauwerys RR. Colorimetric determination of free fatty acids. Ann Biochem 1969;32:331–332.
18. Donnadieu M, Schimpff RM, Sevaux D, Girard F. Utilisation du charbon dextran lors du dosage radio-immunologique de l'hormone de croissance. Pathol Biol 1968;16:865–867.
19. Maritz JS, Morrisson JF, Peter J, Strydom NB, Wyndham CH. Practical method of estimating an individual's maximum oxygen uptake. Ergonomics 1970;4:97–122.
20. Raymond LW, Weiskopf RB, Halsey HJ, Goldfien A, Eger EI, Severinghaus JW. Possible mechanism of the antiarrhytmic effect of helium in anesthetized dogs. Science 1972;176:1250–1252.
21. Brès M, Hatzfeld C. Three gas diffusion. Experimental and theoretical study. Pfluegers Arch Gesamte Physiol 1977;371:227–233.
22. Raynaud J, Drouet L, Coudert J, Durand J. Time course of plasma growth hormone during exercise in man at altitude. In: Brendel W, Zink RA, eds. High altitude physiology and medicine. Vol. 1: Physiology of adapatation. New York: Springer-Verlag, 1980.
23. Guénard H, Chaussain M, Lebeau C. Respiratory gas exchange under normobaric helium-oxygen breathing at rest and during muscular exercise. Bull Eur Physiopathol Respir 1978;14:417–429.
24. Klimeš I, Vigaš M, Jurčovičova J, Németh S. Lack of effect of acid-base alterations on growth hormone secretion in man. Endocrinol Exp (Bratislava) 1977;11:155–162.

EFFECTS OF EXERCISE AND HYPERBARIC AIR ON VENTILATION AND CENTRAL INSPIRATORY ACTIVITY

C. M. Hesser and F. Lind

Several studies in the past have shown that the respiratory responses to carbon dioxide and muscular exercise may become depressed by acute exposure to raised air pressure (1–4). To what extent these effects might be due to increased breathing resistance secondary to the increased density of the respired gas, or to a depressant (narcotic) effect of the raised nitrogen pressure on the respiratory centers has been a matter of debate. In a recent report from this laboratory (5) it was shown that hypercapnic hyperventilation induced by carbon dioxide rebreathing is reduced by high nitrogen pressure despite a concurrent increase of the central inspiratory activity (CIA). The present experiment investigated whether the relationship between pulmonary ventilation and CIA is changed by hyperbaric air and nitrogen during the hyperpnea of exercise.

METHODS AND MATERIALS

Eight healthy male volunteers were studied. Their age, height, weight, vital capacity, and maximal oxygen uptake are listed in Table I. All subjects were nonsmokers; seven subjects were in regular physical training and five were active sport divers.

Each subject performed two tests with incremental-load exercise on an electrically braked cycle ergometer (Elema-Schönander) placed inside a dry compression chamber. In a first test (control) the subject inhaled oxygen at an ambient pressure of 1.3 atmospheres absolute (ATA); in the other he inhaled air at 6 ATA (P_{O_2} = 1.3 ATA, P_{N_2} = 4.7 ATA). The respired gases were humidified and administered from large Douglas bags via a mouthpiece, a low

TABLE I

Anthropometric and Functional Data of Subjects

Subject	Age (yr)	Height (cm)	Weight (kg)	Vital Capacity (L BTPS)	$\dot{V}O_{2max}$* (mL·kg⁻¹·minL⁻¹
PB	28	178	78	6.1	55
HC	26	181	75	5.7	60
KC	33	178	71	5.3	54
LJ	34	190	82	5.9	61
BL	29	177	67	4.5	46
FL	24	184	77	6.1	58
DL	34	172	61	4.1	57
BM	29	184	75	5.0	48

*Aerobic work capacity, determined from nomogram of Åstrand (6).

dead-space (10 mL) respiratory valve, and large-caliber tubes. The resistive pressures offered by the inspiratory and expiratory conduits at a flow rate of 1 L·s⁻¹ amounted to (respectively) 1.4 and 1.0 cm H_2O at 1.3 ATA, and 3.4 and 2.3 cm H_2O at 6 ATA.

The tests started with a 4-6 min rest period with the subject seated on the cycle ergometer, followed by a 2-min period of loadless pedalling (zero watts [W]) at a cycling speed of approximately 60 rpm. The load was then increased successively to 200 W in steps of 10 W at the end of each minute. Ventilation ($\dot{V}$) and tidal volume were recorded continuously on-line on a breath-by-breath basis (7), using signals from a Venturi-type flowmeter (8) inserted in the inspiratory line. Central inspiratory activity was assessed by measuring the mouth pressure ($P_{0.1}$) generated during the first 0.1 s of an occluded inspiration (9) at intervals of 25–35 s. For this purpose a pneumatic valve, interposed on the inspiratory side of the breathing valve, was closed during an expiration and opened 0.2 s after the onset of the ensuing occluded inspiration (cf. ref. 5). For determination of the lung volume at which ventilation was carried out, the subjects were requested to make maximal inspirations at approximately 2-min intervals during the exercise runs. Heart rate and P_{CO_2} of the expired gas were recorded continuously as described elsewhere (5,10). All signals were displayed on a multichannel strip-chart recorder and stored on magnetic tape for subsequent detailed analysis of the variables under study.

Where relevant, regression analysis was carried out for first- and second-order polynomials by the method of least squares. A statistical F test was applied to examine whether the regressions showed a significant departure from linearity (11). The statistical significance of differences between data obtained in the control and hyperbaric air conditions was determined by Student's t test for paired observations, and the significance level was set at $P \leq 0.05$.

RESULTS

In the control experiments at 1.3 ATA breathing oxygen, all subjects completed the incremental work test without difficulty or any signs of respiratory distress. At 6 ATA breathing air, most of the subjects were aware of the increased breathing resistance and two of the eight subjects experienced mild-to-moderate dizziness at the highest work loads. However, none of the subjects noticed dyspnea or chest pain at any load.

In all subjects and in both the control and the hyperbaric air condition the exercise responses obtained by plotting $\dot{V}$ or $P_{0.1}$ against work load were curvilinear, the $\dot{V}$ and $P_{0.1}$ responses increased more rapidly as the load increased. However, as shown in Fig. 1, the rate of increase of $P_{0.1}$ was greater than that of $\dot{V}$ in both conditions. The $\dot{V}$ values at 6 ATA were similar to the control values up to 100 W, but were significantly lower at loads exceeding 100 W (Fig. 1A). In contrast, the $P_{0.1}$ values at any given load were about 70% higher at 6 ATA than in the control condition (Fig. 1B). Thus, the ventilation per unit occlusion pressure ($\dot{V}/P_{0.1}$) was considerably lower in the hyperbaric than in the control experiments and decreased with increasing load in both conditions (Fig. 2A). There was a wide variation between subjects in the relation of $\dot{V}$ to $P_{0.1}$ as illustrated in Fig. 2B, which shows calculated individual regression lines for this relationship at 6 ATA. In six out of eight subjects the regression of $\dot{V}$ on $P_{0.1}$ was described significantly better ($P < 0.01$) by a second-order than by a first-order equation. At 1.3 ATA this also applied in five of the subjects.
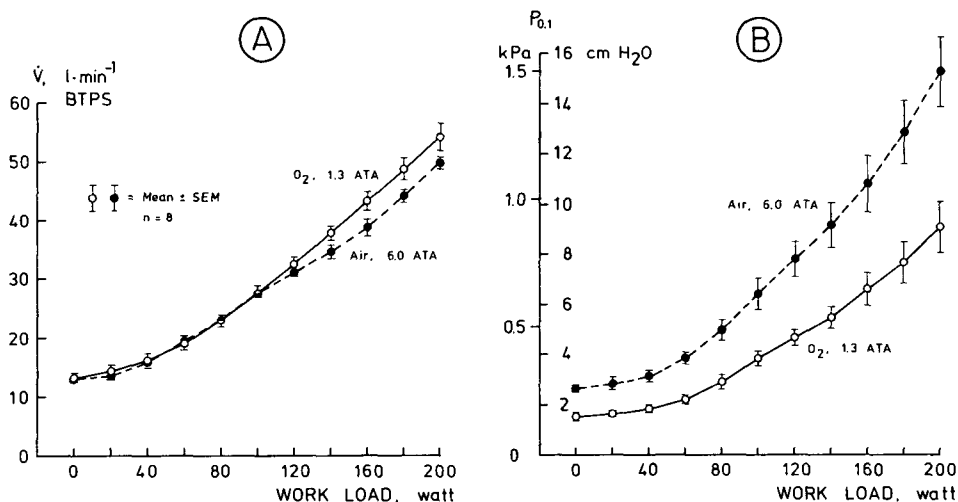
Fig. 1. Relationships of pulmonary ventilation (A) and inspiratory occlusion pressure $P_{0.1}$ (B) to work load during incremental-load exercise in subjects breathing oxygen at 1.3 ATA; control, *open circles*, and air at 6 ATA, *filled circles*.
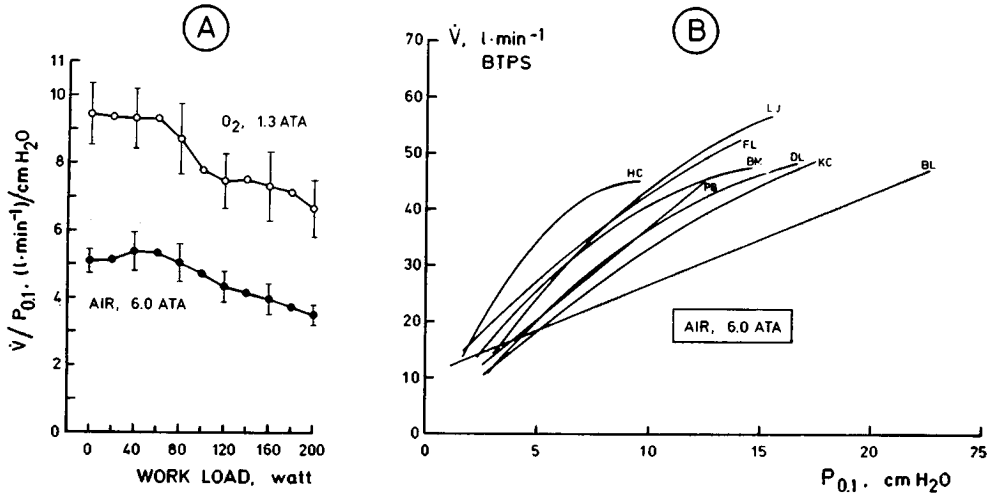
Fig. 2. From the same experiments as in Fig. 1. A: Relationship between ventilation per unit occlusion pressure ($\dot{V}/P_{0.1}$) and work load; symbols the same as in Fig. 1. B: The regression of $\dot{V}$ on $P_{0.1}$ for each subject at 6 ATA air, obtained by the method of least squares.

As shown in Fig. 3, tidal and mid-expiratory volumes increased in both conditions as the work load increased, while the end-expiratory reserve volume (hereafter referred to as the expiratory reserve volume, ERV) decreased slightly. In general, the tidal volumes at 6 ATA were 0.2–0.3 L larger than at 1.3 ATA, whereas the respiratory rates were 1–4 breaths · min⁻¹ lower at 6 ATA than in the control condition. End-tidal Pco_2 rose with the load: in the control experiments from a mean value of 38 to 51 Torr, and in the 6 ATA experiments from a mean value of 38 to 59 Torr when the load was increased from zero to 200 W. Corresponding values for arterial Pco_2, estimated from observed values of end-tidal Pco_2 and tidal volume (12), were 37 and 46 Torr at 1.3 ATA, and 37 and 53 Torr at 6 ATA. Heart rate rose progressively with increasing load, in the control experiments from an average of 73 beats · min⁻¹ at zero W, to 143 beats · min⁻¹ at 200 W. At any given load, the heart rate at 6 ATA was 4–6 beats · min⁻¹ lower than in the control condition (P 0.05).

DISCUSSION

Provided that $P_{0.1}$ represents a true index of CIA both during normal and hyperbaric conditions, our observation of higher $P_{0.1}$ values at 6 ATA air than at 1.3 ATA O_2 (Fig. 1B) would indicate that the CIA during muscular exercise is enhanced by acute exposure to raised air and nitrogen pressures. If so, the unchanged or reduced exercise ventilation observed at raised air pressure (Fig. 1A) occurred in spite of an increased neural input to the inspiratory mus-
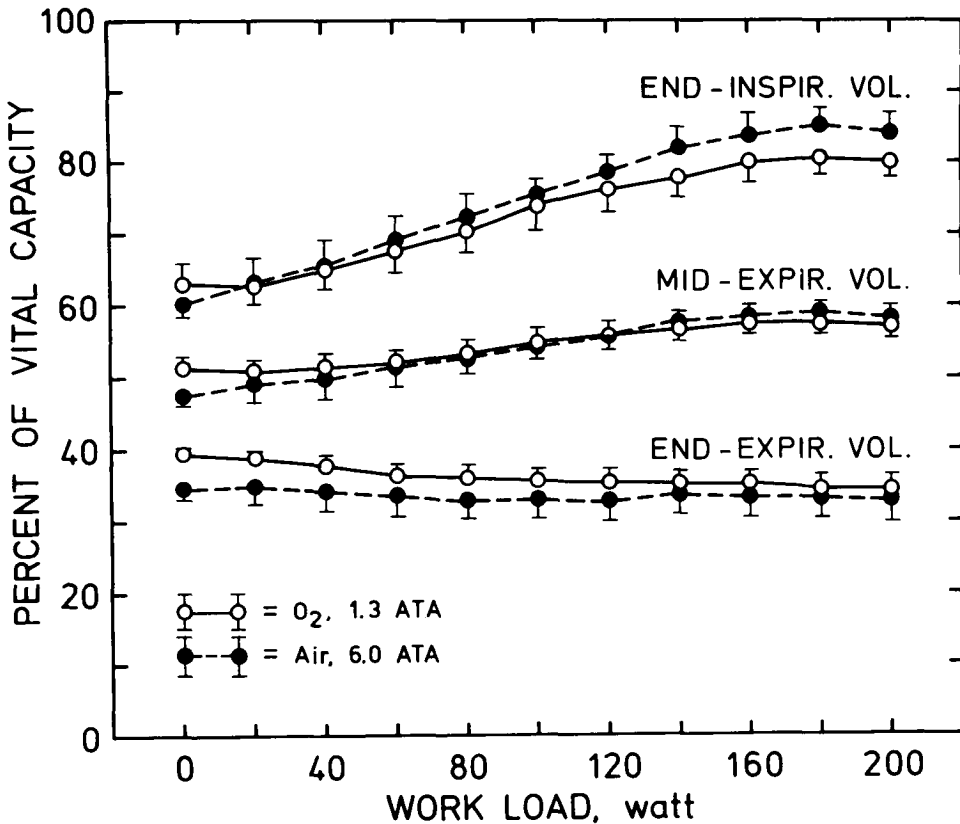
Fig. 3. Relationships of end-expiratory, mid-expiratory, and end-expiratory lung volumes to work load. Tidal volume is difference between end-inspiratory and end-expiratory volumes. Legends are the same as in Fig. 1. Vital capacity = 5.32 ± 0.27 L BTPS.

cles. However, as discussed in detail in a previous report (5), the $P_{0.1}$–CIA relationship found at normal atmospheric pressure (9,13–15) may for various reasons become altered at raised pressures. First, because of the difference in compressibility of the breathing medium, $P_{0.1}$ at a given neural input to the inspiratory muscles should be somewhat higher at raised than at normal atmospheric pressures. In the present 6-ATA experiments the calculated increases of $P_{0.1}$ due to such effects amounted to approximately 0.1 and 0.8 cm H_2O at zero and 200 W, respectively. Thus, only a small fraction of the differences in $P_{0.1}$ between 1.3 and 6 ATA can be attributed to the difference in gas compressibility. Second, changes in the breathing pattern at raised pressures may alter the functional residual capacity (FRC), which will affect the $P_{0.1}$–CIA relationship (9). It is likely that the higher $P_{0.1}$ values in the hyperbaric air as compared to the control condition were only to a minor degree caused by such FRC-dependent changes in $P_{0.1}$. This would be expected because at any given

load, ERV and probably FRC differed but slightly in the two conditions (Fig. 3). Therefore the relation between $P_{0.1}$ and CIA probably was about the same in the two series of experiments. The higher $P_{0.1}$ at 6 ATA indicates that the CIA was increased. It follows then that the highly increased PN_2 in the 6-ATA experiments caused no narcotic nor depressant effect on the respiratory centers or other neural structures involved in the control of respiration during muscular exercise. One may also conclude that the reduced ventilatory response to exercise at 6 ATA at loads higher than 100 W (Fig. 1A) was mainly caused by the increased gas density and consequent increase of breathing resistance.

The above reasoning suggests that the causes and mechanisms responsible for the higher $P_{0.1}$ at 6 ATA than at 1.3 ATA must be sought among factors other than pharmacological effects of the high nitrogen pressure or differences in FRC and gas compressibility. The raised oxygen pressure can be ruled out as a causative factor because the same high Po_2 was present in the control condition. That the high pressure per se was the cause is unlikely; much higher pressures usually must be applied to evoke EEG changes and other signs of CNS affection. End-tidal and estimated arterial Pco_2 were higher at 6 ATA than at 1.3 ATA at loads exceeding 100 W, which may explain part of the difference in $P_{0.1}$ in the high-load range. The difference in $P_{0.1}$ in the low-load range, on the other hand, cannot be ascribed to any carbon dioxide effect, because both end-tidal and arterial Pco_2 were of similar magnitudes in the two conditions at loads lower than 100 W. The predominant factor responsible for the augmented $P_{0.1}$ response at 6 ATA probably was the enhanced airway resistance caused by the raised gas density. This is supported by the observation that at normal pressure the $P_{0.1}$ response to carbon dioxide rebreathing is increased in conscious man by added inspiratory resistance (13,16,17). The present data then support the belief (5) that a) acute exposure to raised air and nitrogen pressures causes an increase of the CIA when pulmonary ventilation is unchanged or reduced, and b) increased airway resistance induced by the raised gas density is the major factor responsible not only for the reduction of ventilation but also for the increase of CIA by causing a reflex stimulation of the respiratory centers. As shown by our present experiments, this occurs also during exercise conditions.

In agreement with previous studies (9,16), this study found that the relationship between $\dot{V}$ and $P_{0.1}$ varied markedly from subject to subject (Fig. 2B). In the majority of subjects $P_{0.1}$ increased at a faster rate than $\dot{V}$. That $P_{0.1}$ increased faster than $\dot{V}$ at loads higher than 40 W both at 1.3 and 6 ATA, is shown by the fact that at these loads the $\dot{V}/P_{0.1}$ ratio decreased significantly in both conditions as the load increased (Fig. 2A). A likely explanation for these findings and for the fact that $\dot{V}/P_{0.1}$ was less at 6 ATA than in the control condition (Fig. 2A) would be as follows. In the single individual $P_{0.1}$ is a relative measure of the neuromuscular component of the inspiratory drive (9), part of which is used to generate the pressure required to overcome the inspiratory nonelastic resistance of the lungs. This resistance, expressed as cm $H_2O/L \cdot s^{-1}$), is known to increase with rate of flow and gas density (18,19). Hence, in

conditions with progressive hyperventilation, $P_{O.1}$ should increase at a faster rate than $\dot{V}$ and, at a given ventilation, should be larger the higher the gas density. Because $P_{O.1}$ gives only information about the rate of inspiratory discharge, the relation of $\dot{V}$ to $P_{O.1}$ will depend to a great extent on the relative amounts of time spent in inspiration and expiration (9).

That the heart rate at any particular load was 4–6 beats $\cdot$ min^{-1} lower at 6 ATA air than at 2.3 ATA O_2 confirms and extends observations previously reported from this laboratory (2,20,21) that part of the relative bradycardia occurring in man during acute exposure to raised air pressure is caused by non-oxygen-dependent factors. Evidence has been presented that this non-oxygen-dependent slowing of the heart is caused by a reduction of the beta-adrenergic stimulation (20) and that changes in alveolar (arterial) P_{CO_2} in the range 30–50 Torr have no significant effect on heart rate in man either at normal or at raised air pressure (21).

In conclusion, the present study shows that the ventilatory response to incremental-load leg exercise in the range of zero to 200 W remains unchanged or is reduced by acute exposure to raised air and nitrogen pressures in spite of a concurrent increase of the CIA response. Increased airway resistance consequent to the raised gas density is considered the predominant factor responsible for both the reduction in ventilatory response and for the enhancement in CIA response.

Acknowledgment

References

1. Fagraeus L, Hesser CM. Ventilatory response to CO_2 in hyperbaric environments. Acta Physiol Scand 1970;80:19A–20A.
2. Fagraeus L, Hesser CM, Linnarsson D. Cardiorespiratory responses to graded exercise at increased ambient air pressure. Acta Physiol Scand 1974;91:259–274.
3. Lanphier EH. Pulmonary function. In: Bennett PB, Elliott DH, eds. The physiology and medicine of diving and compressed air work. 2nd ed. London: Baillière Tindall, 1975:102–154.
4. Wood, LDH, Bryan AC. Exercise ventilatory mechanics at increased ambient pressure. J Appl Physiol: Respirat Environ Exercise Physiol 1978;44:231–237.
5. Linnarsson D, Hesser CM. Dissociated ventilatory and central respiratory responses to CO_2 at raised N_2 pressure. J Appl Physiol: Respirat Environ Exercise Physiol 1978;45:756–761.
6. Åstrand I. Aerobic work capacity in men and women with special reference to age. Acta Physiol Scand 1960;40:Suppl 169:1–92.
7. Åström T, Wigertz O. A digital computer for automatic breath-by-breath calculation of respiratory functions. Stockholm; Karolinska Institutet, 1966 (Report Lab Aviat Naval Med).
8. Wigertz O. A low-resistance flow meter for wide-range ventilatory measurement. Respir Physiol 1969;7:263–270.
9. Whitelaw WA, Derenne J-P, Milic-Emili J. Occlusion pressure as a measure of respiratory center output in conscious man. Respir Physiol 1975;23:181–199.

10. Lindborg B, Wigertz O, Ödman T. A beat-to-beat heart-rate meter with linear analog output for muscular exercise studies. Stockholm: Karolinska Institutet, 1969 (Report Lab Aviat Naval Med).
11. Snedecor GW, Cochran WG. Statistical methods. 6th ed. Ames, IA: Iowa State Univ Press, 1967:447–471.
12. Jones NL, Robertson DG, Kane JW. Difference between end-tidal and arterial P_{CO_2} in exercise. J Appl Physiol: Respirat Environ Exercise Physiol 1979;47:954–960.
13. Altose MD, Kelsen SG, Stanley NN, Levinson RS, Cherniack NS, Fishman AP. Effects of hypercapnia on mouth pressure during airway occlusion in conscious man. J Appl Physiol 1976;40:338–344.
14. Altose MD, Kelsen SG, Stanley NN, Cherniack NS, Fishman AP. Effects of hypercapnia and flow-resistive loading on tracheal pressure during airway occlusion. J Appl Physiol 1976;40:345–351.
15. Evanich MJ, Lopata M, Lourenco RV. Phrenic nerve activity and occlusion pressure changes during CO_2 rebreathing in cats. J Appl Physiol 1976;41:536–543.
16. Kryger MH, Yacoub O, Anthonisen NR. Effect of inspiratory resistance on occlusion pressure in hypoxia and hypercapnia. Respir Physiol 1975;24:241–248.
17. Altose MD, Kelsen SG, Cherniack NS. Respiratory responses to changes in airflow resistance in conscious man. Respir Physiol 1979;36:249–260.
18. Marshall R, Lanphier EH, DuBois AB. Resistance to breathing in normal subjects during simulated dives. J Appl Physiol 1956;9:5–10.
19. Maio DA, Farhi LE. Effect of gas density on mechanics of breathing. J Appl Physiol 1967;23:687–693.
20. Fagraeus L, Linnarsson D. Heart rate in hyperbaric environment after autonomic blockade. Swed J Defence Med 1973;9:260–264.
21. Hesser CM, Fagraeus L, Linnarsson D. Respiratory gases and hyperbaric bradycardia. Proceedings of the 3rd annual scientific meeting of the European Undersea Biomedical Society. Méd Aéronautique Spatiale Subaquatique et Hyperbare 1978;17:110–113.

EXERCISE AT 47 AND 66 ATA

J. V. Salzano, B. W. Stolp, R. E. Moon, and E. M. Camporesi

The debilitating effects of HPNS and the respiratory problems associated with breathing a gas considerably more dense than air would appear to be the main determinants of the amount of work that can be performed at great pressures in the sea. It is possible to attenuate or ameliorate HPNS by using nitrogen to counterbalance the effects of rapid changes in pressure or of pressure per se, or both. However, the addition of nitrogen to heliox necessarily increases the density of the breathing gas. The net effect, therefore, might be a lessening or absence of HPNS accompanied by a gas-density-dependent reduction in ventilation with concomitant reduction in gas exchange and work capacity.

Recently, we conducted studies on divers exposed to simulated depths up to 650 msw (65.6 ATA) with varying amounts of nitrogen in the inspired gas. The responses of the divers at rest and during exercise constitute the basis of this report.

METHODS

Atlantis I (April 1979) and *II* (March 1980) are part of an ongoing series of dives at the F.G. Hall Laboratory of Duke University (1). One purpose of these dives is to assess the respiratory and exercise responses to inspired gas density, hydrostatic pressure, and narcosis. Both dives employed identical rapid compression to 46.7 ATA (460 msw) and an inspired Po_2 of 0.5 ATA; they differed at this pressure only in the chamber gas and experimental inspired gas composition as listed in Table I. The *Atlantis I* chamber atmosphere was 5% trimix (5% nitrogen, 1.1% oxygen, balance helium); the *Atlantis II* atmosphere was 10% trimix. Metabolic and ventilation measurements were

made on each of three volunteers during *Atlantis I* in the morning and after-
noon of one of Days 3, 4, and 5 at 46.7 ATA. This enabled isobaric compari-
sons to be made between a 10.1 g · L^{-1} inspired gas (5% trimix) in the morn-
ing, and a 7.9 g · L^{-1} inspired gas (heliox) in the afternoon. Experiments
were similarly conducted on three subjects during *Atlantis II*, two of whom
had participated in *Atlantis I*. Characteristics of all experimental subjects are
listed in Table II.

In *Atlantis II*, morning measurements using a 12.3 g · L^{-1} inspiratory gas
(10% trimix) were compared to afternoon measurements using a 10.1 g · L^{-1}
gas (5% trimix). After completion of the 46.7 ATA studies during *Atlantis II*,
subjects were further compressed to 65.6 ATA where a limited exercise proto-
col was carried out on each of the three subjects using 8% trimix (16.1 g
L^{-1}).

A complete experimental protocol was rehearsed at 1 ATA for both dives
during the morning and afternoon. Each subject was studied during several of
these sessions in the month preceding each dive. During these protocols in-
spired gas was room air except the afternoon sessions of *Atlantis I* controls
when 0.5 ATA O_2 in N_2 was used. During each experimental session, the sub-
ject performed a 15-s MVV maneuver by freely choosing a breathing rate and

TABLE I

Control and Experimental Breathing Gases During *Atlantis I* and *Atlantis II* Dives

Inspired gas	Pressure (ATA)	Depth (msw)	PI_{O_2} (ATA)	PI_{N_2} (ATA)	PI_{He} (ATA)	Density (g·L^{-1})	*Atlantis* Dive No.
Air	1	0	0.21	0.79	—	1.1	—
O_2-N_2	1	0	0.50	0.50	—	1.2	—
Heliox	46.7	460	0.48	—	46.3	7.9	I
5% Trimix	46.7	460	0.50	2.34	43.9	10.1	I, II
10% Trimix	46.7	460	0.50	4.67	41.6	12.3	II
8% Trimix	65.6	650	0.67	5.37	59.6	16.1	II

TABLE II

Subjects in *Atlantis I* and *Atlantis II* Dives

Subject	Age (yr)	Height (cm)	Weight (kg)	VC (L BTPS)	MVV_{15} (L · min^{-1} BTPS)	$\dot{V}O_{2max}$ (L · min^{-1} STPD)	*Atlantis* Dive No.
WB	25	183	71	6.23	253	3.10	I,II
SP	24	185	87	7.36	244	3.14	II
DS	40	175	79	4.87	195	3.60	I,II
LW	27	173	77	5.20	230	2.95	I

tidal volume during hyperventilation that he believed would produce the largest ventilation (MVV$_{15}$). This procedure was repeated 2–3 times with 3-min rest periods between trials. Four levels of 6-min exercises were then performed on a Monark bicycle ergometer, modified to provide continuous analog recordings of work load and pedal rate (60 $\pm$ 2 rpm). Work rates were performed at 1 ATA up to a level at which oxygen uptake rate was maximal ($\dot{V}o_{2max}$). During *Atlantis II* the heaviest exercises resulted in rates of oxygen uptake ranging from 77% of $\dot{V}o_{2max}$ (*Subject DS*) to 91% (*Subjects WB* and *SP*). Rest periods of 20 min were provided between exercises, and sessions were separated by lunch and a rest period of 2–3 h.

Electrocardiographic recordings were continuous during each exercise protocol. To monitor arterial blood pressure and obtain samples for arterial blood gas (ABG) analysis, we performed percutaneous catheterization of the radial artery on each subject under pressure and on 1 day during 1-ATA control sessions. Arterial blood samples were collected during the 6th min of each exercise period. We analyzed the samples for Po$_2$, Pco$_2$, and pH using a modified blood gas analyzer (Instrumentation Laboratory Micro-13) calibrated with special gases. The electrode was calibrated and used inside the chamber.

Changes in anteroposterior (AP) and laterolateral (LL) chest and abdominal dimensions were monitored using four paired magnetometer coils (N. Petersen, Harvard University). Signals were recorded on an FM tape recorder (Vetter Model A) for future analysis. Calibration was performed before each exercise session.

Humidified gas was supplied from a 200-L Douglas bag through two heated pneumotachographs (Fleisch #4) connected in parallel with wide-bore tubing to the inspiratory port of the respiratory valve (Koegel valve). The volume of gas in the bag was maintained at approximately 100 L through visual observation by a technician in control of a high pressure valve outside the chamber. Expired gas was collected for 1-min periods in Douglas bags connected to the expiratory side of the breathing valve via large-bore tubing and large stopcocks with 45° angles. The respiratory circuit resistance was minimized during both dives such that peak mouthpiece pressure swings during the highest work-rate ventilations were no greater than $\pm$ 5 cm water.

The inspiratory and expiratory bags had a vent system for collection of gas samples outside the chamber. After bleeding sufficiently to clear the dead space of the sample lines, duplicate 100-mL samples of gas were collected in wet, acidified, glass syringes during *Atlantis I*. The O$_2$ and CO$_2$ content of the samples was analyzed by gas chromatography technique (modified Quintron Model S gas chromatograph). The larger samples required for improved oxygen analysis during *Atlantis II* (using Applied Electronics Model S-3A fuel cell oxygen analyzer) necessitated modifications of the gas-sampling manifold outside the chamber. For this dive, the inspired and expired gases were sampled in pre-evacuated 500-mL steel cylinders that were flushed three times before a final fill to chamber pressure.

After samples of gas were withdrawn for analysis, we measured the remaining gas volumes in the bags by exhausting the gas to a constant negative

bag pressure (-8 cm H_2O) through a calibrated dry gasometer (Parkinson-Cowan). An analog electrical signal proportional to volume was recorded on paper and appropriate corrections were applied for volume removed during sampling. Constant temperature (31°C) and depth were maintained and recorded by the chamber personnel during each experimental session.

During both dives subjects were instructed to report any respiratory discomfort during exercise by raising from one to three fingers depending on their subjective feelings of distress (1, mild discomfort; 2, moderate, but not work-limiting; 3, severe, possibly work-limiting).

Error Analysis

For each subject, all measurements obtained under pressure were compared to the relevant measurements at the surface. To assess the significance of any differences, we performed a worst-case error analysis for each type of measurement. The limited number of subjects precluded the use of traditional statistical analysis.

Seven gravimetrically produced primary calibration gases for CO_2 and O_2 were obtained and verified; they yielded an uncertainty in their assigned concentrations of 10 ppm for O_2 and 7 ppm for CO_2. All calibration gases, including those used in the ABG analysis, were related to these primary standards.

Total worst-case errors for rate of oxygen uptake ($\dot{V}O_2$), which comprised errors in gas analysis, ventilation, depth, and temperature, were 4.2–6.8% at rest and less than 3.5% at levels of ventilation greater than 80 L $\cdot$ min^{-1}. The errors in carbon dioxide elimination rate ($\dot{V}CO_2$) measurement were also of this order.

Individual physiological variability could not be accurately assessed except at the surface, where each subject exercised several times. Minute ventilation ($\dot{V}E$), $\dot{V}O_2$, and $\dot{V}CO_2$ and heart rate varied very little (coefficient of variation, 5%) at the surface after a training plateau was achieved. In addition, comparison of the $\dot{V}E$ and $\dot{V}CO_2$ of each subject breathing 5% trimix in *Atlantis I* and *II* revealed only small differences. We believe, therefore, that changes in any measurement larger than the worst-case-error estimate may be ascribed to the effect of the independent variables (e.g., gas density, hydrostatic pressure, and the narcotic effect of the breathing mixture).

RESULTS

Dyspnea

There appeared to be two types of respiratory symptoms at 46.7 ATA in both deep dives: rest-related and exercise related. At rest major complaints included increased awareness of breathing, difficulty in coordinating swallowing

and breathing, and inability to breathe through the nose. The subjects also complained of sudden momentary airway obstruction during rapid inspiration, which was immediately relieved by slowing their inspiration. These complaints were not reported during metabolic studies on the ergometer or during maximum voluntary ventilation (MVV) measures.

During exercise in *Atlantis I*, however, all subjects experienced some degree of dyspnea while breathing both gases. In every case the symptoms were described by the subjects as sensations associated with inspiratory insufficiency. Some of the comments were "inability to catch up on my breathing," "a tremendous increase in inspiratory resistance of the breathing valve," and "a complete lack of any inspiratory gas." One subject indicated he was able to tolerate the discomfort at the highest work rate but felt he could not have continued longer than the prescribed 6 min. Two subjects were unable to complete exercises at 720 and 810 kp $\cdot$ m $\cdot$ min^{-1}, respectively. One subject experienced dyspnea only during the highest work rate in both the trimix and heliox (Fig. 1).

In *Atlantis II* exercise-related dyspnea occurred much less frequently, despite higher gas density and heavier work loads (Fig. 1). The commercial diver (*Subject SP*) reported no dyspnea, even at his highest work loads. Only one subject experienced work-limiting dyspnea (*Subject WB* at 1080 kp $\cdot$ m $\cdot$ min^{-1}). *Subjects WB* and *DS* described the sensation of dyspnea differently. *Subject WB* reported a transient inability to catch up on his breathing whenever he had to swallow or cough. After catching up, however, he usually felt less discomfort. *Subject DS* described the sensation as "trying to breathe through a straw." Unlike that in *Atlantis I*, the dyspnea was not overtly inspiratory, but when questioned closely *Subjects WB* and *DS* reported that perhaps inspiration was harder than expiration.

To investigate the effect of the breathing circuit on dyspnea during *Atlantis II*, *Subjects DS* and *WB* removed the mouthpiece before stopping an exercise in which dyspnea occurred; they then continued exercising for a full minute. Each subject reported only momentary relief followed by recrudescence of the symptoms. We therefore concluded that dyspnea was not related to the breathing circuit.

Considering all exercise periods from *Atlantis I* and *II* it was impossible to relate dyspnea solely to work rate, $\dot{V}E$, MVV, $\dot{V}E$/MVV, vital capacity (VC), gas density, arterial blood gases, pH, or the subject's age. Multiple linear regression analysis was used to attempt to predict the dyspnea index from these variables. No single variable or linear combination of the above variables could predict dyspnea reliably, nor could any empirically derived nonlinear function.

During *Atlantis II*, *Subjects DS* and *WB* experienced easily audible wheezing during all exercise levels higher than 360 kp $\cdot$ m $\cdot$ min^{-1}. This wheezing usually began about a minute after starting exercise and persisted for 3–4 min after the end of the exercise period. It was inspiratory and expiratory in nature and was not related to dyspnea. No wheezing was reported during MVV maneuvers. Neither subject had a prior history of wheezing. *Subject SP*
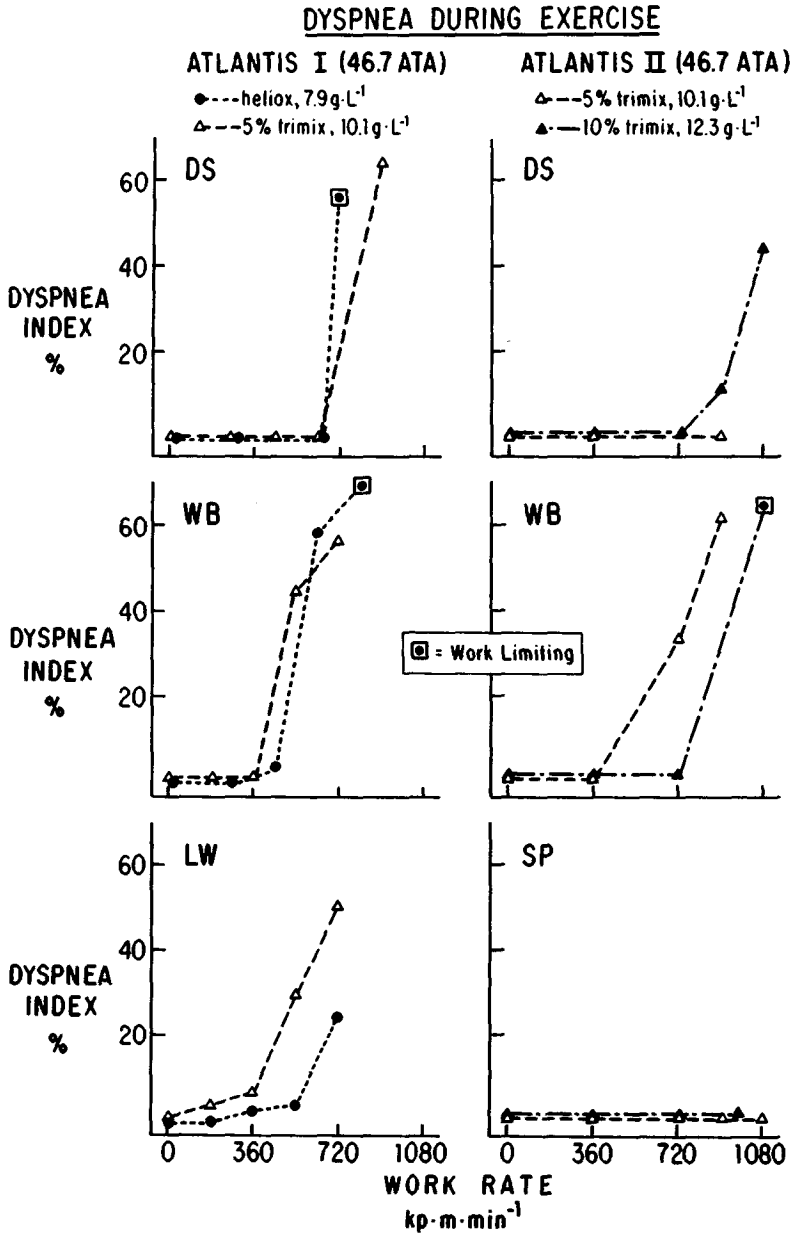
Fig. 1.   Dyspnea index elicited from individual subjects during *Atlantis I* and *II* at various levels of exercise. The index in percent was obtained from the number of fingers raised (1–3) and the duration of each finger rating, as follows: Dyspnea Index (%) $= 100 \cdot \left[1 - \dfrac{3m - s}{18} \right]$, where m, number of minutes worked; s, sum (over in m minutes) of rating X duration. The index is scaled such that a subject working for 6 min without dyspnea would have a zero index; a subject working for 6 min with "3-finger" dyspnea each minute would score 100.

did not wheeze at any time during the dive. Wheezing did not occur during *Atlantis I.*

Exercise at 46.7 ATA

Surface control for each subject was defined in both dives to be the average of the morning and afternoon values measured at the surface on the day an arterial catheter was inserted. Data analysis revealed that there was no consistent difference in any variable between breathing air or 50% O_2 in N_2, nor between morning and afternoon.

Ventilation ($\dot{V}E$) at rest and up to moderate exercise was higher at depth than during 1-ATA control, but at higher work rates was equal to or less than 1-ATA control (Fig. 2). In most cases (3 of 4 subjects) the increased ventilation was achieved with increased VT. No systematic relationship between increasing gas density and ventilation could be established.

Heart rate response to exercise was not altered at 46.7 ATA when compared to surface control.

For technical reasons, $\dot{V}O_2$ was obtained only during *Atlantis II;* there was a borderline (5–10%) increase above control during all work rates. The calculated increase was greatest for the highest exercise levels (Fig. 3).

EXERCISE VENTILATION
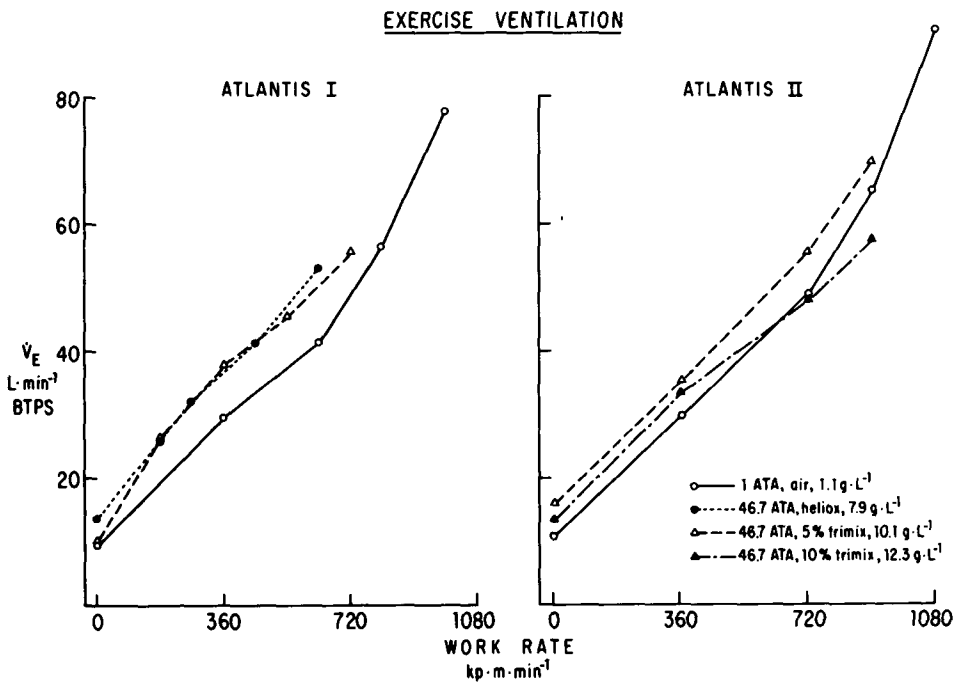
Fig. 2.   Ventilatory response to graded 6-min exercise at 1 ATA and during the deep dives at 46.7 ATA (mean of 3 subjects).

OXYGEN UPTAKE
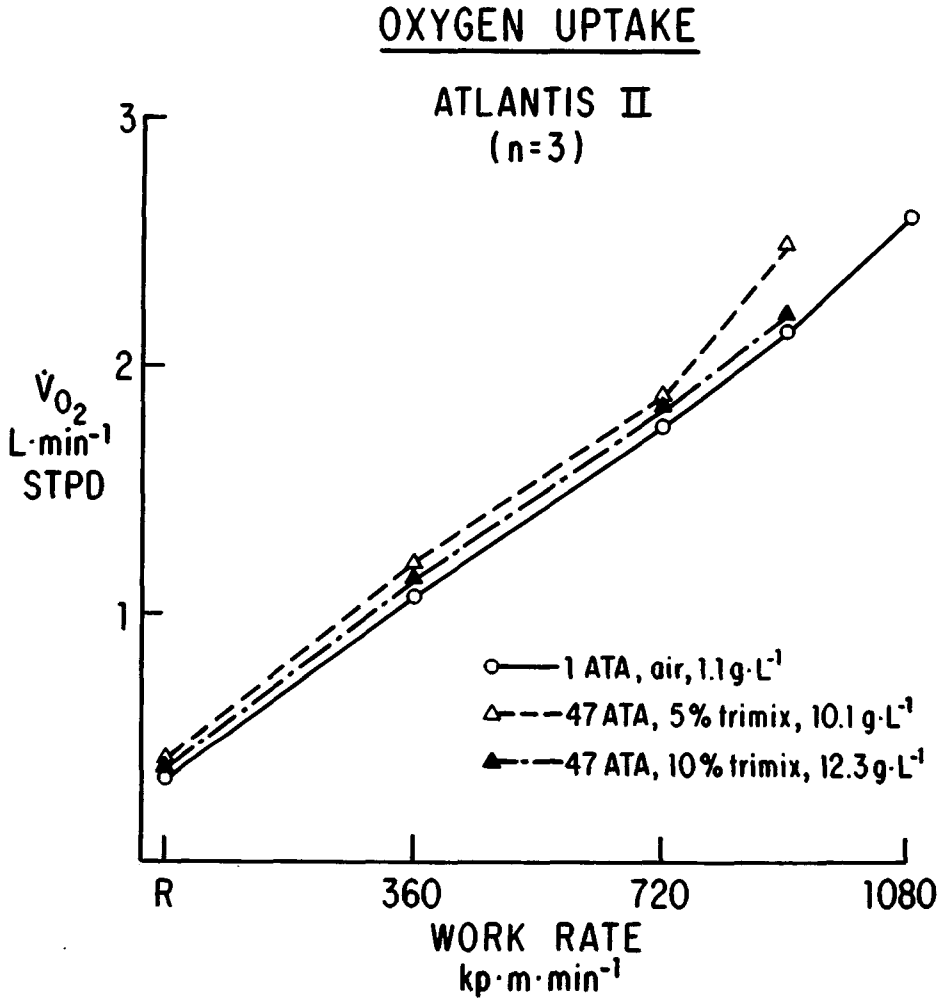
ATLANTIS II
(n=3)

Fig. 3.   Oxygen consumption (mean of 3 subjects) during the 6th min of exercise at 1 ATA during *Atlantis II* at 46.7 ATA.

Measurements during *Atlantis I* and *II* indicated a small increase in $\dot{V}_{CO_2}$ at gas densities of 7.9 and 10.1 g $\cdot$ L^{-1}, both at rest and during moderate exercise. This increase was abolished or even reversed at high work rates when the heaviest gas mixture (12.3 g$\cdot$ L^{-1}) was used. These changes are illustrated in Fig. 4.

Arterial blood gas analysis indicated sufficient variability of Pa_{CO_2} among the various subjects to warrant presentation of each individual response in Fig. 5. Of note is the fact that Pa_{CO_2} was elevated above control at rest; in some subjects there was a further elevation induced by exercise. Significant

CARBON DIOXIDE PRODUCTION RATE
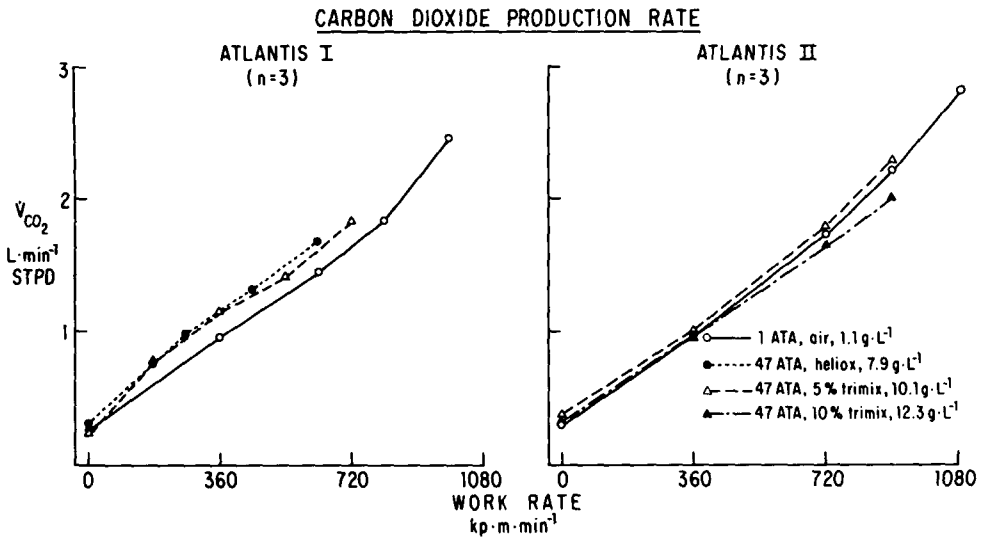
Fig. 4. Carbon dioxide elimination rate (mean of 3 subjects) during the 6th min of exercise at 1 and 46.7 ATA during the deep dives.

exercise-induced hypercapnea occurred only in *Atlantis II* except for *Subject DS*, the oldest subject, who manifested it in both dives. Arterial pH decreased with exercise-induced increase of Pa_{CO_2}. In *Subject DS*, for which a wide enough range of values permitted a reasonable regression, the change in $[H+]$ per unit change in Pa_{CO_2} was 1.4 nM · mmHg^{-1} during *Atlantis I* and 1.0 nM · mmHg^{-1} during *Atlantis II*.

The lowest recorded pH_a (7.22) was obtained in this subject with a corresponding highest recorded Pa_{CO_2} of 65 mmHg, while exercising at 1080 kp · m · min^{-1} for 6 min in 10% trimix.

The lowest recorded Pa_{CO_2} was 175 mmHg. Most values were between 250 and 300 mmHg.

V_D (dead space) was calculated from the following formula both at 1 and 46.7 ATA:

$$V_D = V_T \cdot \left[\frac{Pa_{CO_2} - P_{E_{CO_2}}}{Pa_{CO_2}} \right] \tag{1}$$

where V_T is tidal volume and $P_{E_{CO_2}}$ is mixed expired partial pressure of carbon dioxide.

Mean values for *Atlantis I* and *II* of V_D and alveolar ventilation ($\dot{V}_A$) indicate an unexpected increase in V_D and a proportional reduction of $\dot{V}_A$ at pressure (Fig. 6).

ARTERIAL pCO_2

ATLANTIS I

○── 1 ATA, air/50% O_2, 1.1 g·L^{-1}
●···· 46.7 ATA, heliox, 7.9 g·L^{-1}
△── 46.7 ATA, 5% trimix, 10.1 g·L^{-1}

ATLANTIS II

○── 1 ATA, air, 1.1 g·L^{-1}
△── 46.7 ATA, 5% trimix, 10.1 g·L^{-1}
▲─·─ 46.7 ATA, 10% trimix, 12.3 g·L^{-1}
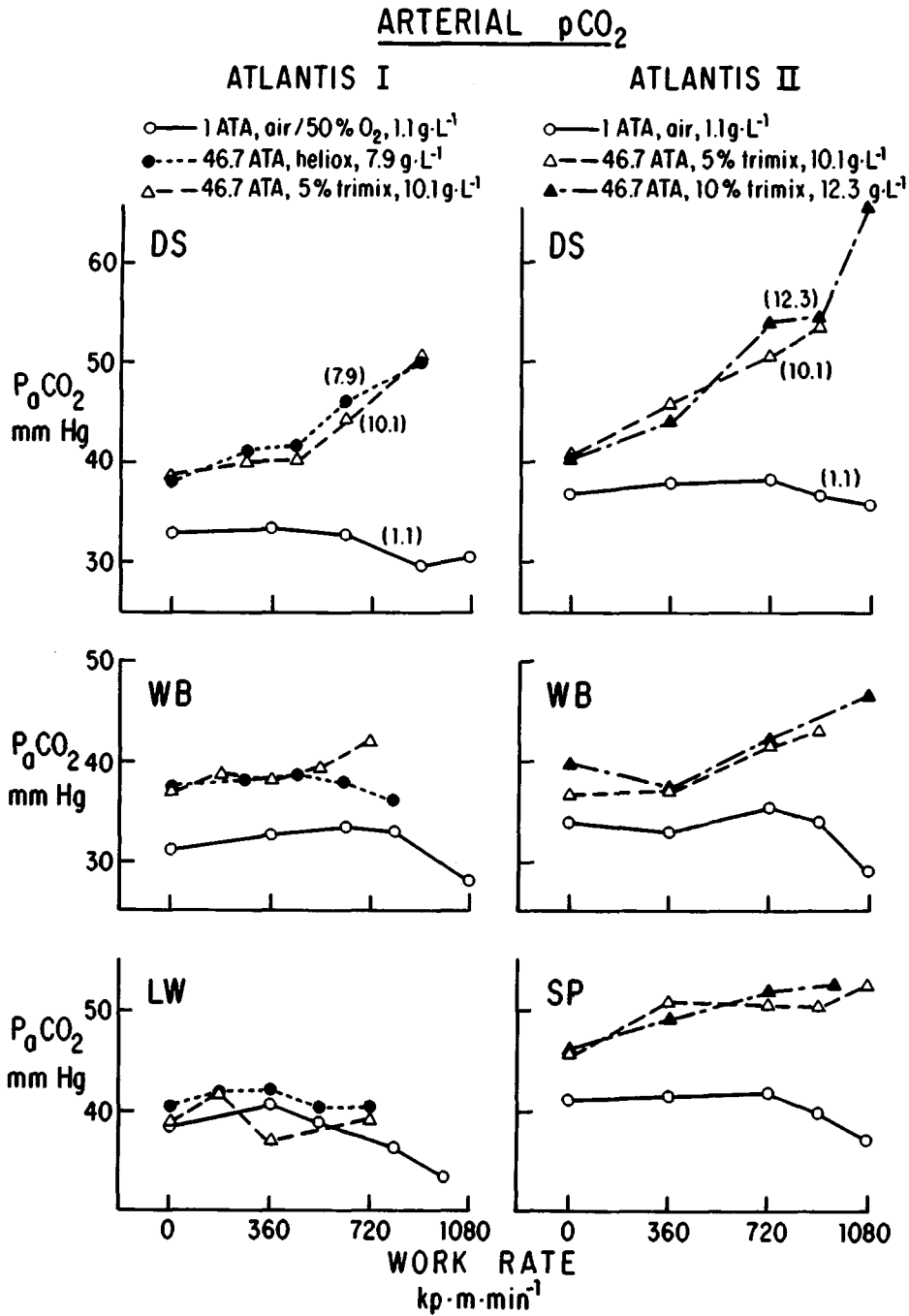
Fig. 5. Pa_{O_2} at rest and during the 6th min of exercise at 1 and 46.7 ATA for *Atlantis* I and II for the individual subjects. Variability among subjects is evident.

ALVEOLAR VENTILATION AND DEAD SPACE
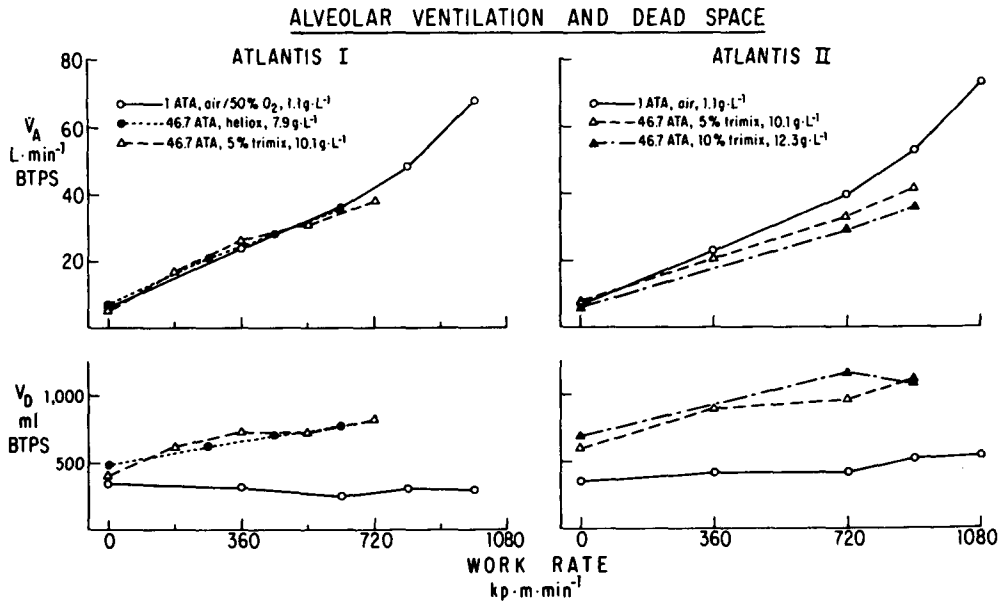
Fig. 6.   Alveolar ventilation (VA) and dead space (VD) at rest and during the 6th min of exercise at 1 and 46.7 ATA (mean of 3 subjects).

Exercise at 65.6 ATA

After completion of the 3 days of respiratory studies at 46.7 ATA during *Atlantis II*, it was decided that their splendid performance warranted further studies during a deeper stage at 65.6 ATA. On arrival at the maximum depth the two younger divers felt no subjective change in their general well-being. *Subject DS*, on the other hand, was more distressed for several hours, with shortness of breath while eating and climbing into bed. Two subjects (*WB* and *SP*) completed an exercise protocol at 65.6 ATA, with multiple 15-s MVV maneuvers and 6-min periods of exercise up to 720 kp $\cdot$ m $\cdot$ min^{-1} without dyspnea. *Subject DS* was not asked to exercise at a rate higher than 180 kp $\cdot$ m $\cdot$ min^{-1} despite finishing this work load without experiencing dyspnea. $\dot{V}E$ at rest and during exercise at 65.6 ATA was increased substantially above surface control in all cases. Heart rate at rest and during exercise was unaltered from 1 ATA control. $\dot{V}CO_2$ and $\dot{V}O_2$ were decreased at 720 kp $\cdot$ m $\cdot$ min^{-1} (Fig. 7).

EXERCISE RESPONSES AT 65.6 ATA

●——— 1 ATA, air, 1.1 g·L⁻¹
●---- 65.6 ATA, 8 % trimix, 16.1 g·L⁻¹
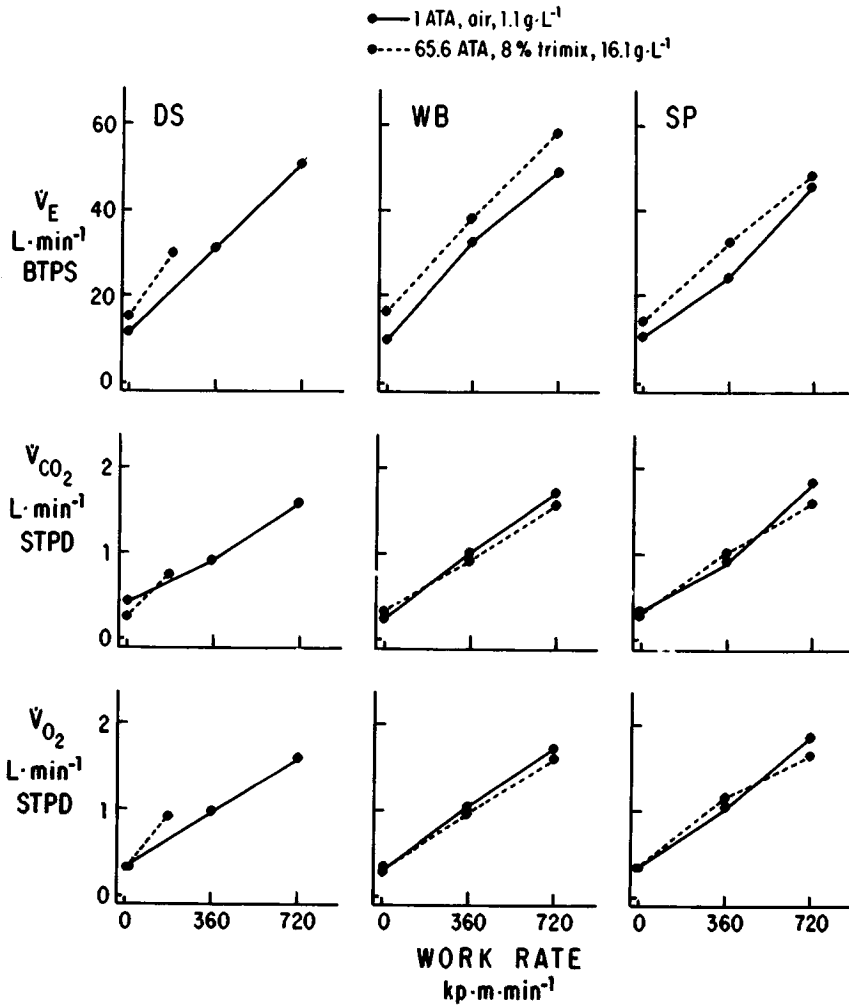
Fig. 7. Ventilation (VE), VCO$_2$ and VO$_2$ at various work rates at 65.6 ATA during *Atlantis II*. The three individual responses are represented.

DISCUSSION

Exercise-induced dyspnea was substantially less during *Atlantis II* than during *Atlantis I*. No function of mechanical or chemical variables could be derived that could predict dyspnea. In addition, analysis of magnetometer data revealed no systematic change in FRC within each exercise period or in relation to onset of dyspnea. There are several possibilities that might explain the difference in incidence of dyspnea between *Atlantis I* and *II*. First, of necessity any method of measuring dyspnea is subjective. Two of the *Atlantis II* subjects participated in *Atlantis I*, and they may have been less likely to report dyspnea because of familiarity. Second, our method of quantitation (Fig. 1) may not accurately represent the degree of dyspnea. In spite of these methodologic difficulties, we believe that the subjects experienced less respiratory difficulty in *Atlantis II* because they were able to complete exercise at higher work rates with only one premature termination because of dyspnea. If indeed this difference is real, it may be due to some other variable of the breathing gas such as the amelioration of HPNS by the nitrogen in the mixture. Evidence for this is that exercise limitation occurred more frequently in heliox than in 5% trimix during *Atlantis I*. An alternative explanation is that the dyspnea is related to differing rates of respiratory heat loss for the different gases at 46.7 ATA.

Variation in breathing gas density from 1.1 to 16.1 $g \cdot L^{-1}$ did not appear to alter the metabolic measurements of physical performance to a great degree; the results were only minor changes in $\dot{V}O_2$ and $\dot{V}CO_2$ up to the levels of exercise studied. However, there was considerable variability in arterial PCO_2, with *Subject DS* exhibiting marked hypercapnea at his heaviest work rate in both *Atlantis I* and *II*. Moreover, VD calculated from Eq. 1 was unexpectedly increased over control in all subjects both at rest and during exercise. Using this calculated VD, we partitioned $\dot{V}E$ into alveolar (effective) ventilation ($\dot{V}A$) and dead space (wasted) ventilation (VD). Alveolar ventilation decreased with increasing work load and density (Fig. 6) but with variation among subjects. It is also noteworthy that VD increased markedly with increasing tidal volume under pressure but not at the surface.

Dead space calculated from Eq. 1 may include a) anatomic dead space; b) ventilation/perfusion ($\dot{V}/\dot{Q}$) mismatching; c) intra-alveolar diffusion limitation because of high density; and d) defect in carbon dioxide transport between erythrocyte and alveolus. It is unlikely that increases in anatomic dead space caused by, for example, increased lung volume under pressure, could explain the large elevation in VD. Ventilation/perfusion measurements have not been performed under these dive conditions, however, SF_6 breathing at 1 ATA (2) and exercise in chronic obstructive lung disease (3) do not apparently worsen $\dot{V}/\dot{Q}$ distribution.

Evidence against the hypotheses described in c) and d) is the fact that VD increases markedly with VT at depth. If alveolar diffusion impairment were the operative cause, larger tidal volumes, and therefore slower rates of breathing, might be expected to improve gas mixing, thereby decreasing dead space (4,5). In addition, VD should not vary with VT if CO_2 transport impairment of

the type described in d) is the explanation. Ventilation/perfusion mismatch is therefore a better explanation for this variation of V_D with V_T.

On the other hand, hypotheses in both c) and d) are compatible with our data as follows. Both would postpone the attainment of steady-state gas exchange within an exercise run. Indeed, we could interpret the depressed $\dot{V}_{CO_2}$ at high work rates at 46.7 ATA and the similar depression of both $\dot{V}_{CO_2}$ and $\dot{V}_{O_2}$ at 65.6 ATA by such an explanation. The alveolar diffusion limitation hypothesis in c) would predict a defect in carbon dioxide transport at a lower density than would be required to affect oxygen transport because of the different molecular weights of the two gases. Perhaps this applies at 46.7 ATA; at 65.6 ATA the density might be high enough to affect diffusion of both oxygen and carbon dioxide, which would explain the depression of $\dot{V}_{O_2}$ and $\dot{V}_{CO_2}$ at high work rates at that depth. One example of a carbon dioxide transport defect, hypothesis in d), is a reduced carbonic anhydrase activity in the erythrocyte at pressure as reported by Carlyle et al. (6). This type of defect would cause a gradual increase in P_{CO_2} of blood as it passed from the alveolar capillary bed to the radial artery. The blood P_{CO_2} would similarly continue to rise in the collection syringe until H_2CO_3 dissociated to equilibrium. The V_D calculated from Eq. 1 therefore would be artifactually increased in addition to any real increase in $\dot{V}/\dot{Q}$ mismatching induced by the defect. If in fact the subjects are in steady state, the hypotheses in c) and d) would still predict an increase in measured dead space.

We cannot delineate more clearly the cause of the decrement in $\dot{V}_A$, or indeed what proportion of the decrement may be artifactual. It is possible, however, that in some individuals there is a gas density at which adequate gas exchange cannot be maintained while performing work. This possibility is suggested by extrapolation of the curves for *Subject WB* in Fig. 8 to higher density at work rates of 720 kp $\cdot$ m $\cdot$ min^{-1} or greater. This variation in individuals may represent a new form of respiratory limitation during deep diving.

CONCLUSIONS

It is possible for subjects to perform work at useful levels at 46.7 ATA. Our data indicate that subjects can perform useful work (720 kp $\cdot$ m $\cdot$ min^{-1}) at 65.6 ATA. Dyspnea experienced when 5% trimix was used as the background gas was largely ameliorated in 10% trimix, but at the cost of less efficient gas exchange. Subjects trained and experienced in commercial diving had the least respiratory difficulty at under pressure. There appears to be a density-related decrement in $\dot{V}_A$ under pressure, a phenomenon that requires further investigation.

ALVEOLAR VENTILATION vs. GAS DENSITY
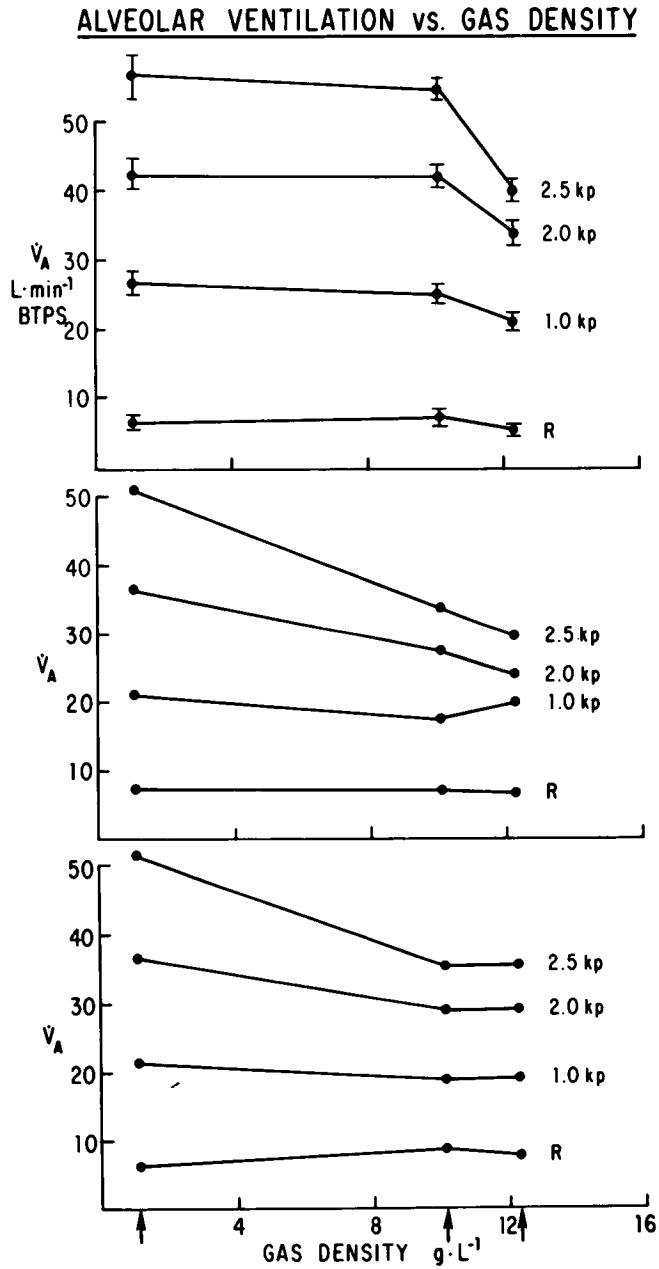
Fig. 8. Alveolar ventilation (VA) during the 6th min of exercise at the indicated work rates vs. inspired gas density from *Atlantis II*. Air at 1 ATA represents 1.1 g · L⁻¹. *Top panel*, WB; *middle panel*, DS; *bottom panel*, SP.

Acknowledgments

References

1. Bennett PB, Coggin R, Roby J, Miller JN. Prevention of HPNS in man by rapid compression with trimix to 2132 ft (650 m). In: Bachrach AJ, Matzen MM, eds. Underwater physiology VII. Bethesda, MD: Undersea Medical Society, 1981:345–355.
2. Gledhill N, Froese AB, Buick FJ, Bryan AC. V_A/Q inhomogeneity and Aa_{DO_2} in man during exercise: effect of SF_6 breathing. J Appl Physiol 1978;45:512–515.
3. Wagner PD, Dantzker R, Dueck JL, Clausen JL, West JB. Ventilation-perfusion inequality in chronic obstructive pulmonary disease. J Clin Invest 1977;59:203–216.
4. Engel LA, Menkes H, Wood LDH, Utz G, Joubert J, Macklem PT. Gas mixing during breath holding studied by intrapulmonary gas sampling. J Appl Physiol 1973;35:9–17.
5. Knelson JH, Howatt WF, DeMuth GR. Effect of respiratory pattern on alveolar gas exchange. J Appl Physiol 1970;29:328–331.
6. Carlyle RF, Nichols G, Rowles PM. Abnormal red cells in blood of men subjected to simulated dives. Lancet 1979;i:1114–1116.

CARBON DIOXIDE RETENTION WITH UNDERWATER WORK IN THE OPEN OCEAN

J. W. Macdonald and A. A. Pilmanis

Elevation of carbon dioxide (CO_2) in the arterial blood can result in a variety of manifestations ranging from headaches to unconsciousness. Underwater, CO_2 retention can lead to work limitations and potentially life-threatening conditions. Increased CO_2 levels also have been implicated in increased susceptibility to oxygen toxicity, nitrogen narcosis, and decompression sickness (1). Most investigators agree that elevations in the partial pressure of alveolar CO_2 (PA_{CO_2}) do occur with hyperbaric work (1–7). Furthermore, the PA_{CO_2} tends to rise with increasing pressure and increasing workloads (1,2,5,8–10). However, the simulated diving conditions of these studies varied greatly and specific correlations and tolerance limits to PA_{CO_2} with pressure and work load have not been identified. In addition, these data have been obtained almost exclusively from studies using hyperbaric chambers and immersion tanks to simulate diving conditions. Although some of the environmental and life-support variables such as immersion, thermal stress, and equipment restraint can be successfully simulated in the laboratory, the complete diving situation can only be studied in the sea.

The overall goal of this study was to determine the PA_{CO_2} levels in experienced scuba divers during working open-ocean dives. Methods developed in this laboratory over the past decade allow for the acquisition of such data. In a previous study (11) using this methodology, preliminary data were obtained that show considerable inter- and intra-subject PA_{CO_2} variations during ocean work. No consistent relationship between CO_2 retention and pressure or work load could be shown. However, the method was validated and CO_2 retention was found. The current study was directed toward defining the PA_{CO_2} levels during underwater ocean work requiring energy expenditures up to maximal

oxygen consumption ($\dot{V}O_{2max}$) at 10, 20, and 30 msw. The ventilatory frequency (f), tidal volume (V_T), and minute ventilation ($V_{E_{BTPS}}$) were measured and related to the PA_{CO_2} changes. The question was asked whether or not the CO_2 retention in diving could become symptomatic or a work-limiting factor at these depths. And, if this were possible, at what depth and at what work loads would it happen? In addition, because arm work is of equal importance to leg work in the undersea environment and, because the physiology of arm and leg work differ (12), the above objectives were applied to both modes.

Low ventilatory response to CO_2 appears to be characteristic of diver populations (13–18). Morrison et al. (19–21) have identified divers with a history of underwater loss of consciousness as "CO_2 retainers." Thus, testing the subjects for CO_2 sensitivity was also included in this study.

METHODS

All land and underwater experiments were conducted at the Catalina Marine Science Center (CMSC). The combination of mild and predictable weather and sea-state conditions, and the proximal physical accessibility to clear ocean waters of any depth made these open-sea experiments possible.

Ten male subjects with an average of 6.2 ± 2.9 years of diving experience were selected for this study. All subjects were nonsmokers and averaged over 100 dives a year during their time as participants in this study. The subjects used their own wet suits, masks, and weight belts. Standard equipment provided to the subjects included Jet Fins (Scubapro), a Fenzy buoyancy compensator, twin 72 ft³ compressed air tanks, and modified Conshelf regulator (U.S. Divers).

The Underwater Data Recorder (22) was used to record the f, the heart rate (HR), the volume of inspired air ($V_{I_{ATPS}}$), water temperature, ambient pressure, and event marks. The f was sensed by a thermistor in the regulator mouthpiece. The $V_{I_{ATPS}}$ was measured by a tank pressure transducer connected to the high pressure side of the regulator's first stage. This transducer was calibrated with the assumption that the air was saturated with water vapor upon compression and acted as an ideal gas upon expansion back to 1 ATA. With this assumption and the fraction of O_2 and CO_2 from the expired gas samples, the $\dot{V}O_{2STPD}$, $\dot{V}CO_{2STPD}$, V_T, PA_{CO_2}, $V_{E_{STPD}}$, and respiratory quotient (RQ) were calculated (23). The following equations were adapted for gas analysis under pressure:

$$V_{E_{BTPS}} = \frac{(V_{E_{STPD}}) \, (310) \, (760 + (75.6) \, (msw)}{(P_{bar} - 47) \, (273)}$$

$$V_D = \frac{(0.150 \text{ L physiological dead space})}{(0.5 \text{ L})} (V_T)$$
$$+ \, (0.102 \text{ L regulator dead space})$$

$$V_{A_{BTPS}} = (V_{E_{BTPS}}) - (V_D) \, (f)$$

$$PA_{CO_2} = (PI_{CO_2}) + \frac{\dot{V}CO_{2\,STPD}}{\dot{V}A_{BTPS}}(P_{bar} - 47)$$

$$+ (PI_{CO_2})\left(\frac{1}{RQ} - 1\right)\frac{\dot{V}CO_{2\,STPD}}{\dot{V}A_{BTPS}}$$

The Underwater Gas Sampler (11) was used to collect mixed expired gas samples during the underwater exercise. Exhaled gas passed from the exhaust port of the regulator through a 3-cm diameter hose to a 1.5 L baffled mixing chamber, then through a manifold with five 100-mL evacuated steel collecting cylinders, and finally through a hose to a nonreturn valve at the regulator for venting. Compressed air was the only breathing gas used for the underwater exercise. The intermediate pressure of the regulator was 140 psi. The inhalation differential pressure varied from 3.3 to 4.0 cm H$_2$O. The exhalation differential pressure ranged from 1.0 to 1.8 cm H$_2$O. All regulator pressures were measured at 1 ATA before each drive.

During experimental sessions the subjects performed incremental work loads until $\dot{V}O_{2max}$ was obtained. This point was identified when increasing workloads did not elicit a higher $\dot{V}O_2$. In a series of chamber experiments this method was validated for one subject by determining serum lactate concentrations in venous whole blood samples taken 5–15 min after maximal exercise. The subject was found to have 70–80 mg/dL of blood lactate, which is within the accepted range for determination of maximal aerobic work capacity (24). On land both the arm and leg exercises were performed on a Monark bicycle ergometer at 60 rpm. A constant room temperature of 22°C with a humidity between 35 and 60% was maintained. The subjects were exercised for 10 continuous min; they performed at a submaximal work load during the first 6 min. During the 6th min, the expired gas was collected in a 100-L latex bag, the HR was recorded, and the f was counted. The work load was increased to a higher submaximal level at 6 min and samples of expired gas, HR, and f were taken during the 8th min. The work load was increased at 8 min to a predicted maximal level (25), which the subject performed for the last 2 min of the test. All measurements along with the expired gas collection were carried out during the 10th min. On a subsequent day the subject repeated the exercise with a different predicted maximal workload. If the two predicted maximal workloads elicited a $\dot{V}O_2$ within 50 mL of each other the average of the $\dot{V}O_2$ was identified as the $\dot{V}O_{2max}$. The expired gas volume was measured in a water-balanced spirometer. Two 50-mL aliquots of the expired gas were taken with syringes sealed with a three-way stopcock and lubricated with 5% lactic acid. These samples were analyzed for CO$_2$ and O$_2$ content on a Quintron Model R gas chromatograph.

Underwater exercise was carried out with incremental work loads done in the same manner as the land exercise. Exercise was performed at 10, 20, and 30 msw; mean underwater temperatures were 16.2, 15.0, and 13.5°C, respectively. Leg exercise was performed with a leg ergometer which contains a spring-loaded resistance shield (26). The faster the subject swims the more the

spring is compressed creating a greater work load. Degrees of spring compression were calibrated in kilogram increments. Arm exercise was done on a bicycle ergometer converted for underwater use. The ergometer consisted of a bicycle crank that turned a wheel retarded by a friction belt. Attached to the friction belt was a container for kilogram weights. Addition of weights increased the work load. An underwater strobe light set for 40 flashes per minute was used as a metronome for the arm exercise. During the 6th, 8th, and 10th min of incremental exercise the evacuated cylinders were used for collecting expired gas samples. These samples were analyzed by gas chromatograph for CO_2 and O_2 content.

Four gas samples were collected for each work load. The means of the respiratory measurements calculated from these samples were used to represent the work load. Means and standard deviations were compiled for the respiratory measure of all subjects at: a) the lowest $\dot{V}O_2$ attained, b) the point at which the PA_{CO_2} reached its greatest value, and c) at $\dot{V}O_{2max}$ for each depth. Test of significance was performed with the t statistic for two means at the 95% ($P < 0.05$) confidence level between underwater and land exercise data. A linear regression was computed for $\dot{V}O_2$ with f, $\dot{V}E_{BTPS}$, VT and PA_{CO_2} for land and 30-msw values.

The ventilatory response to elevated CO_2 concentrations was determined for seven subjects at 1 ATA. The subject inhaled concentrations ranging from 2 to 8% CO_2, with 50% O_2 and N_2 making up the balance of the breathing gas. End-tidal CO_2 was measured by a Beckman medical gas analyzer model LB-1. The fraction of end-tidal CO_2, along with the dry ambient barometric pressure, was multiplied to calculate the partial pressure of end-tidal CO_2 (PET_{CO_2}). The minute volume of expired gas was measured in a water-balanced spirometer and corrected to BTPS. The CO_2 sensitivity was determined as the slope of change in $\dot{V}E_{BTPS}$ over change in PET_{CO_2} ($\Delta\dot{V}E/\Delta PET_{CO_2}$) by a linear relation with the equation $\dot{V}E = S (PET_{CO_2} - B)$, where S equals slope and B equals horizontal intercept of PET_{CO_2} axis (27).

RESULTS

The physical characteristics of the subjects are compiled in Table I. Ten subjects participated in the leg exercise and 5 of these 10 were involved in the arm exercise. The mean slopes of $\Delta\dot{V}E/\Delta PET_{CO_2}$ are presented for the arm and leg experiment in Table I. The subject most sensitive to CO_2 showed a slope of 2.10 $\Delta\dot{V}E/\Delta PET_{CO_2}$ and a PA_{CO_2} high of 54.13 mmHg at 30-msw leg exercise. Under the same circumstances the subject least sensitive to CO_2 had a slope of 0.35 $\Delta\dot{V}E/\Delta PET_{CO_2}$ and a PA_{CO_2} high of 65.17 mmHg.

Figure 1 compares the central tendency of VT, f, $\dot{V}E_{BTPS}$, and PA_{CO_2} with $\dot{V}O_2$ for land and 30-msw exercise. At a $\dot{V}O_2$ of 2.0 L·min^{-1} and greater, exercise at 30 msw resulted in hypoventilation and CO_2 retention as compared to land exercise. Table II presents $\dot{V}O_2$, f, $\dot{V}E_{BTPS}$, and PA_{CO_2} values at $\dot{V}O_{2max}$. On land the $\dot{V}O_{2max}$ for arm exercise was 68% of the $\dot{V}O_{2max}$ for land leg exercise.

TABLE I

Physical Characteristics of Subjects and Ventilatory Response to Hypercapnia

	Height (cm) Mean ± SD	Weight (kg)	Age (yr)	Slope ($\Delta\dot{V}_E/\Delta GP_{ET_{CO_2}}$)
Leg Exercise (n = 10)	175.4 ± 5.9	70.8 ± 8.0	26.6 ± 4.4	1.28 ± 0.64
Arm Exercise (n = 5)	176.0 ± 5.2	68.4 ± 4.8	25.8 ± 5.3	1.21 ± 0.48

TABLE II

Respiratory Responses at $\dot{V}_{O_{2max}}$

		$V_{E_{BTPS}}$ (L·min^{-1})	f (b·min^{-1})	V_T (L)	$P_{A_{CO_2}}$ (mmHg)	V_{O_2} (L·min^{-1})
LEG EXERCISE						
Land	mean	122.46	39.90	3.09	37.25	3.54
	SD	± 37.72	± 9.94	± 0.45	± 6.75	± 0.64
	n	10	10	10	10	10
10 msw	mean	67.65*	26.60	2.62*	45.04	2.95*
	SD	± 24.54	± 7.37	± 0.79	± 6.40	± 0.79
	n	10	10	10	10	10
20 msw	mean	53.05*	25.00	2.24*	47.94	2.39*
	SD	± 11.76	± 5.78	± 0.59	± 6.21	0.56
	n	8	8	8	8	8
30 msw	mean	45.19*	23.22	2.03*	48.49*	2.35*
	SD	± 7.59	± 5.49	± 0.41	± 5.54	± 0.36
	n	9	9	9	9	9
ARM EXERCISE						
Land	mean	91.57	37.80	2.73	33.39	2.40
	SD	± 30.50	11.65	± 0.43	± 4.69	± 0.37
	n	5	5	5	5	5
10 msw	mean	54.91	24.50	2.54*	44.52*	2.49*
	SD	± 16.90	± 9.98	± 0.99	± 6.52	± 0.97
	n	4	4	4	4	4
20 msw	mean	55.45	20.00	2.82*	41.26*	2.48*
	SD	± 26.29	± 5.94	± 1.20	± 4.32	± 0.97
	n	4	4	4	4	4
30 msw	mean	40.16*	19.75	2.15*	43.40*	2.02*
	SD	± 3.80	± 2.75	0.43	± 4.73	± 0.17
	n	4	4	4	4	4

*t-significant difference (P<0.05) from land values.
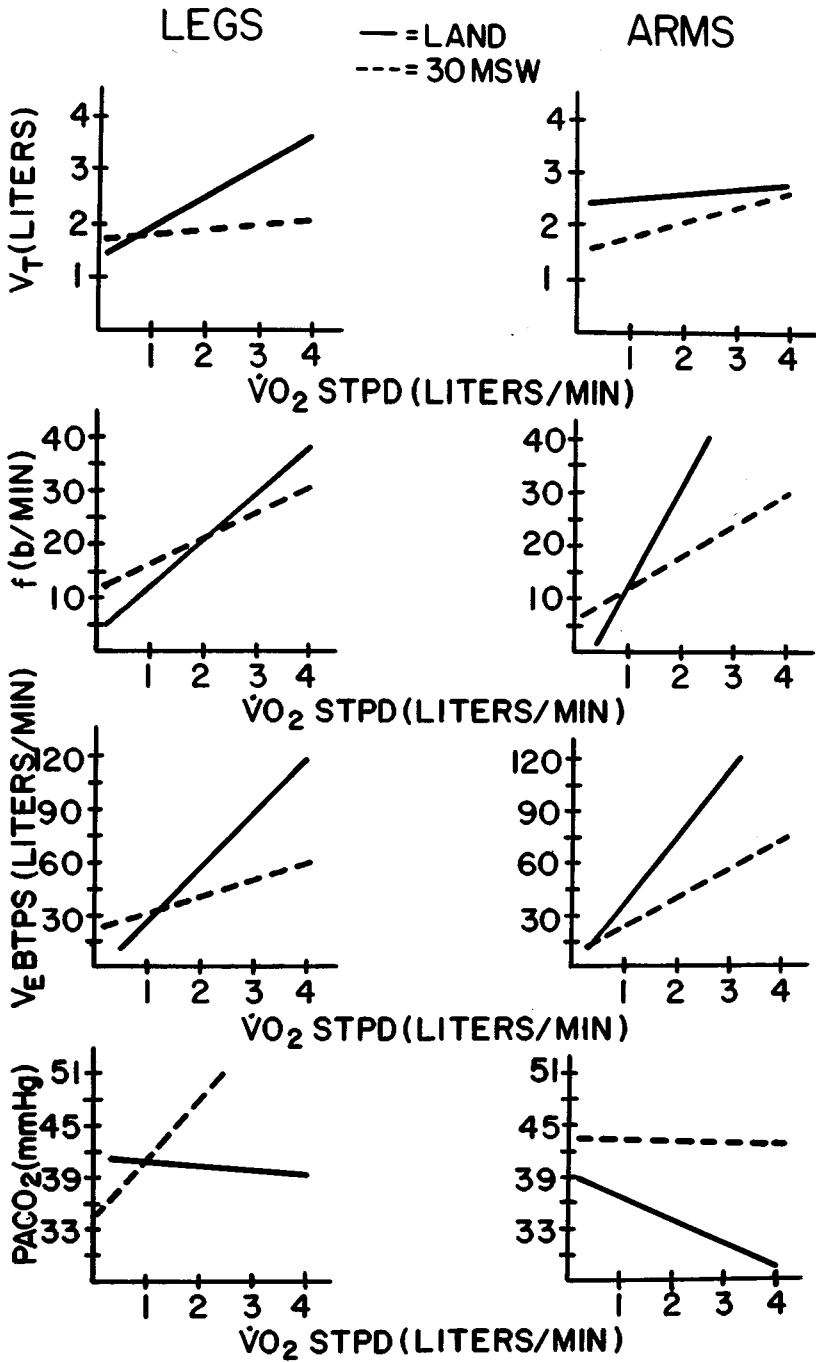
Fig. 1. Correlation between V_T, $V_{E_{BTPS}}$, f, and $P_{A_{CO_2}}$ with $\dot{V}_{O_2}$ for arm and leg exercise on land at 30 msw.

Figure 2 graphically represents PA_{CO_2} in mmHg at three different percentages of $\dot{V}O_{2max}$ for land leg exercise. Similarly, Fig. 3 graphically shows arm exercise data. The maximal PA_{CO_2} for underwater leg exercise occurred at between 54 and 62% $\dot{V}O_{2max}$ of land leg exercise. For underwater arm exercise, the maximal PA_{CO_2} occurred at between 44 and 66% of land arm $\dot{V}O_{2max}$. There were no significant differences between $\dot{V}O_2$ levels at the point where peak PA_{CO_2} values occurred. The mean maximal PA_{CO_2} values reached with underwater leg exercise were 52.86 mmHg ± 6.70 at 10 msw; 57.00 mmHg ± 7.45 at 20 msw; and 55.29 mmHg ± 7.49 at 30 msw. With arm exercise the corresponding values were 46.64 mmHg ± 6.60; 51.53 mmHg ± 9.30; and 50.11 mmHg ± 3.91, at 10, 20, and 30 msw. For land leg exercise the mean PA_{CO_2} value was 52.38 mmHg ± 9.96; land arm exercise was 38.40 mmHg ± 2.99.
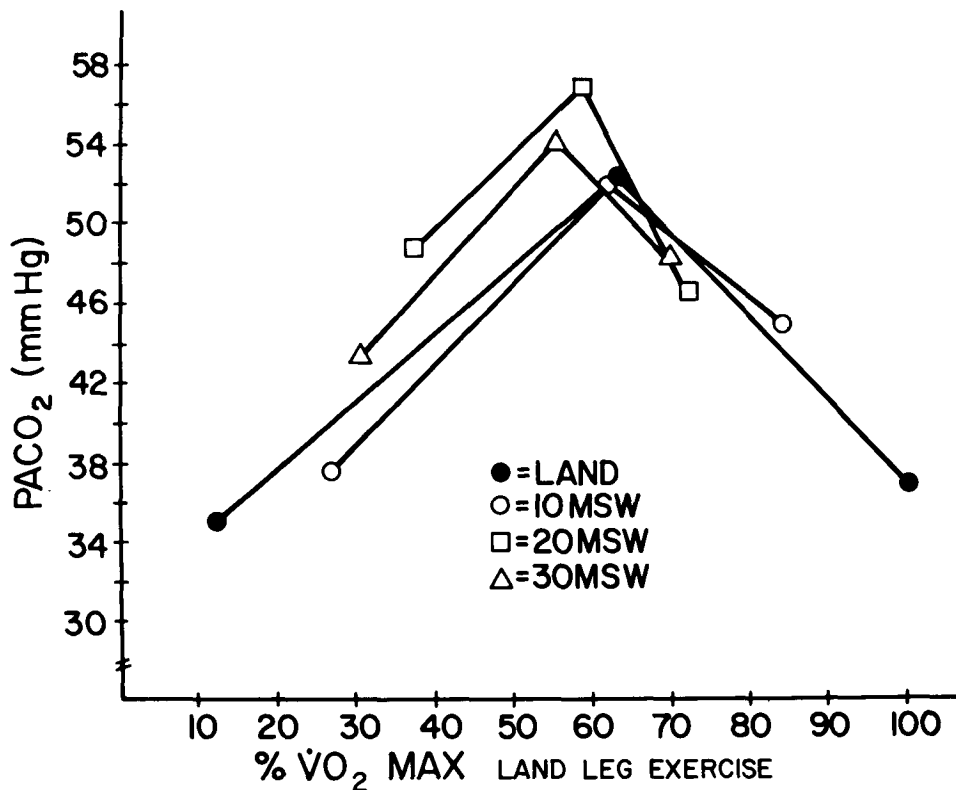
Fig. 2. PA_{CO_2} values represented at three percentages of maximal $\dot{V}O_2$ land leg exercise: at the lowest $\dot{V}O_2$ attained, at the highest PA_{CO_2} attained, at $\dot{V}O_{2max}$ for each depth.
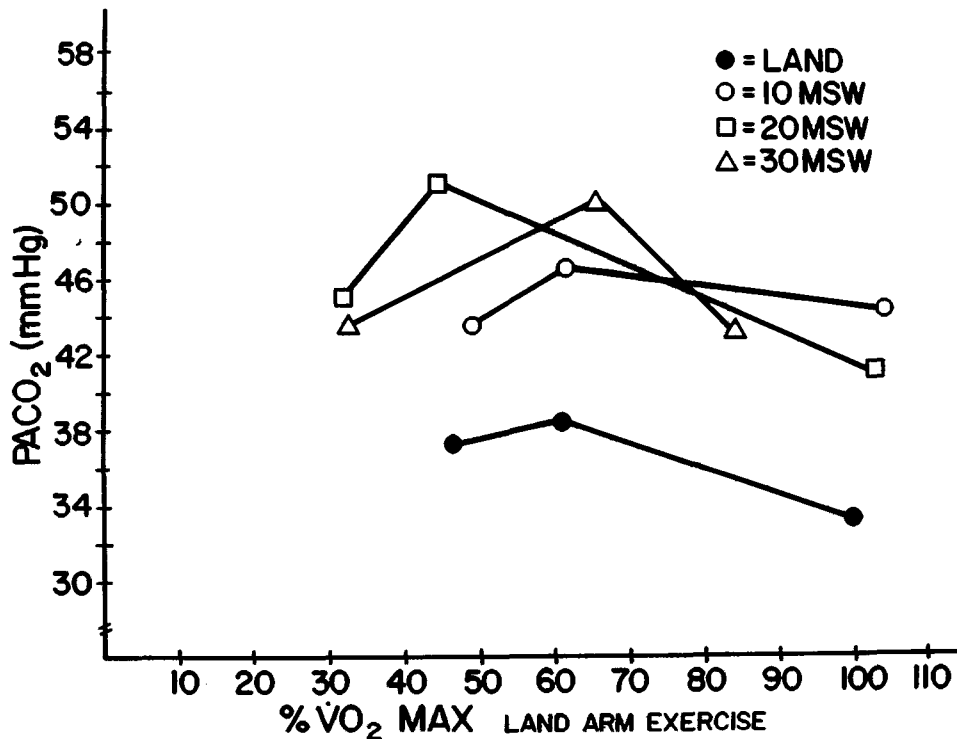
Fig. 3. PA_{CO_2} values represented at three percentages of maximal Vo_2 land arm exercise: at the lowest Vo_2 attained, at the highest PA_{CO_2} attained, and at the Vo_{2max} for each depth.

DISCUSSION

The subjects of this study demonstrated a very low ventilatory response to hypercapnia (Table I). Their CO_2 insensitivity correlated well with their CO_2 retention during underwater exercise. The only criteria for our subject selection was diving experience and availability. Previous studies in which experienced divers showed low ventilatory response to CO_2 build-up also showed CO_2 retention during underwater work (14,15,17,21). It is yet to be determined whether this condition is a learned response in divers or the result of a selection process. In any event, the condition would appear to be counterproductive to diver safety.

It is generally accepted that the PA_{CO_2} values over 50 mmHg in normal people reflect symptomatic CO_2 toxicity and increased susceptibility to oxygen toxicity, nitrogen narcosis, and probably decompression sickness (1,16,28). In our study individual maximal PA_{CO_2} values for underwater exercise did on occasion exceed 60 mmHg. In comparison, other investigators have reported peak values to 70 mmHg and higher. No significant CO_2 toxicity problem was

observed at these high CO_2 levels in our subjects, which is probably explained by the brief exposure at these levels and the relative insensitivity to CO_2 of our diver population. However, we noted that there was a high incidence of head-aches associated with these peak CO_2 levels of underwater exercise, and no-ticeable subjective dyspnea was also occasionally reported.

Our data show that PA_{CO_2} levels are lower at $\dot{V}O_{2max}$ than at submaximal levels. We believe that at submaximal exercise the ventilatory drive had not been stimulated sufficiently to maintain normal PA_{CO_2} levels (see ref. 7). At approximately 60% of the $\dot{V}O_{2max}$ and greater, the ventilatory drive was suffi-cient to increase ventilation and reduce PA_{CO_2}. With increasing depth this effort tends to diminish, probably because of a progressive ventilatory decrement. Thus, it is suggested that with underwater exercise to 30 msw, CO_2 accumula-tion still can be controlled by ventilatory compensation and although CO_2 re-tention does occur during steady-state aerobic exercise, it does not become a work-limiting factor. However, it is apparent from the literature that in the depth range below 30 msw the respiratory system may not keep up with the CO_2 elimination requirements of increasing work loads (1,5,15,29).

There is general agreement in the literature that with exercise in a hyper-baric environment hypoventilation leads to hypercapnia (1,2,5,6,13,14,21,30–32). A lower than normal $\dot{V}E$ appears to be the direct result of inadequate rise of f and VT with exercise. Our ventilatory results (reduced f and VT underwater) agree with those of Fagraeus and Bennett (6). There was a significant hypo-ventilation during underwater exercise at all three depths for leg exercise and at 30 msw for arms (Table II). Temperature may also have had an effect on the observed hypoventilation; as depth increased the water temperature de-creased. This decrease in water temperature deters ventilation and hinders oxy-gen uptake. (32).

There may be a number of interrelated explanations for the hypoventila-tion and CO_2 retention associated with underwater exercise. The higher than normal gas density can reduce ventilation by inhibition of alveolar CO_2 diffu-sion and by increasing the work of respiration (2,3,29). The higher PO_2 at depth contributes to decreased ventilation through a decrease in sensitivity of the central chemoreceptors (33). Body immersion causes a shift of blood vol-ume centrally, which, in turn, may increase airway resistance and reduce ven-tilation. It also causes ventilation/perfusion inequality, which can hinder CO_2 elimination (1). A condition breathing pattern, "skip breathing," associated with most sport divers may also be a major factor (1,18). The low individual sensitivity of our subjects has been discussed and such sensitivity has been ob-served in other groups of divers (17).

The restrictive effects on ventilation by diving equipment, especially the wet suit and buoyancy compensator, have been suggested previously (1,6) and may have been of special importance in the "real" diving situation of this study. The diving experience of our subjects and their familiarity with the un-derwater conditions of the ocean test sites would seem to preclude the influ-ence of underwater anxiety as a major contributing factor. If this was a signifi-cant factor, it was not apparent in the ventilation data.

It was pointed out in the METHODS section that the regulator inspiratory and expiratory resistances were closely monitored. Great effort was directed toward keeping this variable in ventilation at a minimum. By adjusting the regulator, we learned that increases in inhalation resistance (7.0 cm H_2O or greater) resulted in subjective discomfort in ventilation with underwater exercise. Although the intent was to eliminate this resistance factor as a variable on ventilation, it nevertheless contributed to hypoventilation (29).

CONCLUSIONS

Arm and leg aerobic exercise to depths of 30 msw in the open ocean resulted in hypoventilation and CO_2 retention. The subjects of this study demonstrated a low ventilatory response to elevated CO_2 levels. The CO_2 retention was not a work-limiting factor nor was CO_2 toxicity demonstrated. The factors thought to influence CO_2 retention with underwater work in the open ocean included a) increased gas density, b) low subject CO_2 sensitivity, c) body immersion, d) conditioned breathing patterns, e) increased Po_2 effect on central chemoreceptors, f) diving equipment restraints, and g) scuba regulator breathing resistance.

Acknowledgments

References

1. Lanphier EH. Pulmonary function. In: Bennett PB, Elliott DH, eds. The physiology and medicine of diving and compressed air work. Baltimore: Williams & Wilkins Co, 1975:102–154.
2. Jarrett AS. Alveolar carbon dioxide tension at increased ambient pressure. J Appl Physiol 1966;21:158–162.
3. Wood LDH, Bryan AC, Bau SK, Weng TR, Levison H. Effect of increased gas density on pulmonary gas exchange in man. J Appl Physiol 1976;41(2):206–210.
4. Linnarsson D, Karlsson J, Fagraeus L, Saltin B. Muscle metabolites and oxygen deficit with exercise in hyperoxia and hypoxia. J Appl Physiol 1974;36(4):399–402.
5. Salzano JD, Rausch C, Saltzman HA. Cardiorespiratory responses to exercise at a simulated seawater depth of 1000 feet. J Appl Physiol 1970;28(1):34–41.
6. Fagraeus L, Bennett PB. Cardiorespiratory function during arm exercise in water at 500 and 600 feet. In: Shilling CW, Beckett MW, eds. Underwater physiology VI. Proceedings of the sixth symposium of underwater physiology. Bethesda, MD: Federation of American Societies for Experimental Biology, 1978:157–165.
7. Kurenkov HI. Human work performance in hyperbaric environment. In: Hesser CM, Linnasson D, eds. Försvärsmedicin. Proceedings of the first annual scientific meeting of the European Undersea Biomedical Society. Stockholm: Swed J Defense Med 1973;9(3):332–336.

8. Fagraeus L. Maximal work performance at raised air and helium-oxygen pressures. Acta Physiol Scand 1974;91:545–556.

9. Spaur WH, Raymond LW, Knott MM, Crothers JC, Braithwaite WR, Thalmann ED, Uddin DF. Dyspnea in divers at 49.5 ATA: mechanical, not chemical in origin. Undersea Biomed Res 1977;4(2):183–198.

10. Thalmann ED, Sponholtz D, Lundgren CEG. Effects of immersion and static lung loading on submerged exercise at depth. Undersea Biomed Res 1979;6(3):259–290.

11. Dwyer J. Measurement of oxygen consumption in scuba divers working in open water. Ergonomics 1977;20(4):377–388.

12. Vokac Z, Bell H, Bautz-Holter E, Rodahl K. Oxygen uptake/heart rate relationship in leg and arm exercise, sitting and standing. J Appl Physiol 1975;39:54–59.

13. Goff LG, Frasetto R, Specht H. Oxygen requirements in underwater swimming. J Appl Physiol 1956;9:219–221.

14. Lally DA, Zechman FW, Tracy RA. Ventilatory responses to exercises in divers and non-divers. Respir Physiol 1974;20:117–129.

15. Lanphier EH. Influence of increased ambient pressure upon alveolar ventilation. In: Lambersten CJ, Greenbaum LS, eds. Underwater physiology. Proceedings of the second symposium on underwater physiology. Washington DC: National Academy of Sciences-National Research Council, 1963:124–133.

16. Schaefer KE. Carbon dioxide effects under conditions of raised environmental pressure. In: Bennett PB, Elliott DH, eds. The physiology and medicine of diving and compressed air work. Baltimore: Williams & Wilkins Co., 1975:185–206.

17. Sherman D, Eilender E, Shefer A, Kerem D. Ventilatory and occlusion-pressure responses to hypercapnia in divers and non-divers. Undersea Biomed Res 1980;7(1):61–74.

18. Kerem D, Melamed Y, Moran A. Alveolar Pco$_2$ during rest and exercise in divers and non-divers breathing O$_2$ at 1 ATA. Undersea Biomed Res 1980;7(1):17–26.

19. Morrison JB, Florio JT, Butts WS. Loss of consciousness underwater: 1. Some physiological observations following a naval diving incident. Alverstoke, UK: Roy Nav Physiol Lab. 1974, Rep. 1–74:18.

20. Morrison JB, Florio JT, Butts WS. Loss of consciousness underwater: 2. some physiological observations following a civilian diving incident. Alverstoke, UK: Roy Nav Physiol Lab. 1974; Rep. 2–74:15.

21. Morrison JB, Florio JT, Butts WS. The effect of insensitivity to CO$_2$ on the respiratory responses to exercise at 4 ATA. Alverstoke, UK: Roy Nav Physiol Lab. 1976; Rep. 2–76:21.

22. Pilmanis A, Radar R, Henriksen J, Meehan J. Instrumentation for underwater data acquisition. In: Neukomm PA, ed. Biotelemetry II. Proceedings of the second international symposium on biotelemetry, Davos, Basel: S Karger, 1974:64–66.

23. Otis AB. Quantitative relationships in steady state gas exchange. In: Fenn WO, Rahn H, eds. Handbook of physiology, Section 3: Respiration. Washington DC: American Physiological Society, 1964:681–698.

24. Diamant B, Karlsson J, Saltin B. Muscle tissue lactate after maximal exercise in man. Acta Physiol Scand 1968;72:383–384.

25. Åstrand PO, Ryhming I. A nomogram for calculation of aerobic capacity (physical fitness) from pulse rate during submaximal work. J Appl Physiol 1954;7:218–221.

26. Pilmanis A, Henriksen J, Dwyer J. An underwater ergometer for diver work performance studies in the ocean. Ergonomics 1977; 20(1):51–55.

27. Irsigler G. Carbon dioxide response lines in young adults: the limits of normal response. Am Rev Respir Dis 1976;114:529–536.

28. Slonim NB, Bender NK. Responses to carbon dioxide—containing atmospheres. In: Slonim NB, ed. Environmental physiology. St. Louis: C.V. Mosby, 1974:437–476.

29. Uhl RR, Van Dyke C, Cook RB, Horst RA, Merz JM. Effects of externally imposed mechanical resistance on breathing dense gas at exercise: mechanics of breathing. Aerosp Med 1972;43(8):836–841.

30. Russell CJ, McNeil A, Evonuk E. Some cardiorespiratory and metabolic responses of scuba divers to increased pressure and cold. Aerosp Med 1972;43:998–1000.

31. Winsborough M. Changes in lung function during diving. Br J Dis Chest 1977;71(1):69.

32. Pirnay F, Deroanne R, Petit JM. Influence of water temperature on thermal circulatory and respiratory responses to muscular work. Eur J Appl Physiol 1977;37:129–136.

33. Wang SC, Ngai SH. General organization of central respiratory mechanisms. In: Fenn WO, Rahn H, eds. Handbook of physiology, Section 3: Respiration. Washington DC: American Physiological Society, 1964:487–506.

CARDIOPULMONARY FUNCTIONS AND MAXIMAL AEROBIC POWER DURING A 14-DAY SATURATION DIVE AT 31 ATA (SEADRAGON IV)

Y. Ohta, H. Arita, H. Nakayama, S. Tamaya, C. E. G. Lundgren,
Y. C. Lin, R. M. Smith, R. Morin, L. E. Farhi, and M. Matsuda

A simulated saturation dive to an equivalent depth of 300 m was performed at the Japan Marine Science and Technology Center in Yokosuka, Japan, from July to September of 1979. This dive provided us with the opportunity to study changes in cardiopulmonary and neurophysiological function, and energy and body fluid balance during a 14-day stay in an oxygen-helium environment.

We addressed ourselves to the following aspects of cardiopulmonary functions: changes in residual volume, adaptive response in ventilatory functions, CO_2 sensitivity in a hyperbaric helium environment, and limitations on maximum exercise performance at depth. Only the results from measurements on cardiopulmonary functions are reported in this paper.

METHODS AND MATERIALS

Subjects

The physiological measurements were conducted on 4 experienced, well-trained divers in excellent physical condition, all of whom had participated in at least two of the previous saturation dives to depths of more than 100 m.

Vital statistics of the subjects (mean $\pm$ SE) are as follows: age (yr): 30 $\pm$ 2; height (cm): 171.2 $\pm$ 3.1; weight (kg): 64.5 $\pm$ 4.2; body surface area

(m^2): 1.77 ± 0.08. Two of the subjects were smokers but did not smoke during the study.

Dive Profile and Environmental Parameters

The dive profile consisted of 5 consecutive periods: 4 days of predive observation while subjects were breathing ambient air inside the chamber; 3 days of compression at a rate of 10 m/h (during which there were two 14-h stops at 100 and 200 m); 14 days at the bottom (31 ATA); 12 days of stepwise decompression at 4 different rates depending on depth; and 4 days of postdive observation inside the chamber while subjects were breathing ambient air.

Environmental parameters recorded throughout the dive are shown in Fig. 1. The composition of the atmosphere in the chamber was maintained at 0.4 ATA O_2, 0.79 ATA N_2, and the remainder helium throughout the dive. Carbon dioxide in the chamber never exceeded 0.004 ATA. Ambient temperature at the bottom was maintained at 31°C (range: 30.4°–31.2°) and relative humidity was kept at around 60%.
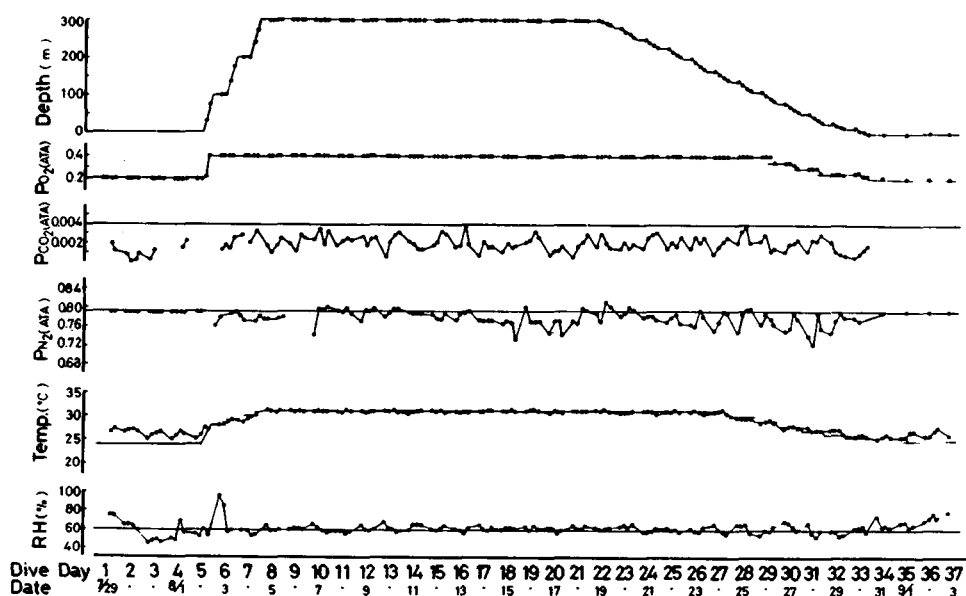
Fig. 1. Dive profile and environmental parameters in a 300-m saturation dive.   RH = relative humidity.

Measurements

Lung volumes and flow rates were determined by conventional spirometry and recordings of maximal expiratory flow-volume curves through the use of a low-resistance bell spirometer (Pulmorecorder, ANIMA Corp., Japan), fitted with an electrical potentiometer and a differentiator for flow recordings. Free frequency measurement of maximal voluntary ventilation (MVV) were obtained by electronic integration over a 15-s period. We made spirometric measurements, excluding those for MVV, in duplicate or triplicate on each subject to obtain a set of values from which means could be calculated. Residual volume (RV) was measured by a rebreathing technique (1).

The maximal expiratory pressure (PE_{max}) at total lung capacity (TLC) level and the maximal inspiratory pressure (PI_{max}) at RV level were measured by means of an aneroid manometer calibrated against a mercury manometer outside the chamber. We tested the CO_2 sensitivity of the respiratory regulation by measuring $P_{0.1}$ (2) and ventilatory response to CO_2 (3), using a microcomputerized system. End-tidal CO_2 concentrations were monitored by a mass spectrometer (Perkin Elmer, MGA 1100, USA).

Maximal and submaximal work performance at 31 ATA were determined on an electrically braked bicycle ergometer and evaluated in relation to cardiopulmonary functions. Ventilation ($\dot{V}E$), O_2 consumption ($\dot{V}O_2$), and CO_2 elimination ($\dot{V}CO_2$) were measured using the standard Douglas bag method, and gas analysis by a gas chromotograph (Quintron Model R, USA) the flow resistance of the breathing system was <1.25 cm H_2O/L/s at a flow of 5 L/s and gas density of 8 g/L.

With respect to circulatory functions, we recorded thoracic impedance (Z_0), dZ/dt, ventricular ejection time, heart sounds and ECG at various depths with the Minnesota Impedance Cardiograph (Model 400, Instrumentation for Medicine, Inc., USA) Cardiac stroke volume was computed by the method of Kubicek (4).

RESULTS[1]

Ventilatory Changes

No systematic differences between the results in smokers and nonsmokers were evident. Table I summarizes consecutive changes of lung volumes, tidal volume, air trapping index (ATI), and maximal voluntary ventilation observed in this dive. Vital capacity (VC) increased slightly but significantly at depth and remained elevated during the decompression and postdive observation period.

The expiratory reserve volume (ERV) was increased during compression, at bottom, during decompression, and postdive. However, the increase in ERV

[1]Unless otherwise stated results are given as mean ± SE.

TABLE I

Ventilatory Functions During a 300 m (31 ATA) Saturation Dive

| Dive Day | | 2 | 6 | 7 | 10 | 13 | 17 | 21 | 25 | 29 | 34 |
Depth (m)		0	100	200	300	300	300	300	215	100	0
VC	$\bar{X}$	5.33	5.40	5.46*	5.45*	5.43*	5.48*	5.49*	5.46*	5.56*	5.49*
(L, BTPS)	SE	0.26	0.23	0.24	0.23	0.24	0.24	0.25	0.27	0.26	0.26
IRV	$\bar{X}$	2.70	2.45	2.39*	2.20*	2.08*	2.32*	2.30*	2.45*	2.61	2.67
(L, BTPS)	SE	0.17	0.23	0.17	0.17	0.18	0.15	0.21	0.22	0.20	0.18
ERV	$\bar{X}$	1.83	2.19*	2.21*	2.36*	2.30*	2.26*	2.22*	2.17*	2.04*	2.03*
(L, BTPS)	SE	0.11	0.18	0.20	0.13	0.12	0.13	0.11	0.17	0.09	0.10
V_T	$\bar{X}$	0.80	0.76	0.86	0.89	1.05*	0.90	0.97	0.84	0.91*	0.79
(L, BTPS)	SE	0.07	0.05	0.12	0.05	0.04	0.07	0.03	0.07	0.05	0.05
$FEV_{1.0}/FVC$	$\bar{X}$	84.3	73.0*	63.5*	64.8*	63.3*	65.0*	64.8*	68.3*	72.5*	83.8
(%)	SE	3.2	4.2	4.7	4.0	3.9	4.6	3.7	4.0	4.2	4.4
ATI	$\bar{X}$	2.7	2.6	2.2	2.3	1.8	4.3	2.7	3.9	3.7	4.2
(%)	SE	0.5	0.4	0.4	0.4	1.0	1.0	0.3	0.9	0.5	0.5
MVV	$\bar{X}$	178.5	132.0*	110.3*	98.0*	94.8*	100.0*	100.8*	105.0*	129.3*	179.5
(L/min, BTPS)	SE	15.8	17.2	14.2	14.1	16.5	8.5	12.8	7.2	12.7	20.6

Values are means ($\bar{X}$) and standard errors (SE) of duplicate measurements obtained in four subjects, respectively.   * Significantly different from control values of *Dive Day 2* (1 ATA) at $P<0.05$ and better (paired t test).   VC, vital capacity; IRV, inspiratory reserve volume; ERV, expiratory reserve volume; V_T, tidal volume; FEV, forced expiratory volume; ATI, air trapping index; MVV, maximum voluntary ventilation.

reached its maximum during the early part of the bottom depth and then decreased gradually. Although VC increased slightly at depth, the increase in ERV far exceeded the increase in VC and the RV remained unchanged.

Tidal volume (VT) remained essentially unchanged throughout the dive except for values on *Dive Days 13* and *29*. The minute ventilation (V̇E), however, showed significant decreases at high pressure: 12.74 ± 0.37 L/min predive; 10.24 ± 0.43 at 31 ATA ($P<0.001$); 10.68 ± 0.50 at 100 m during decompression ($P<0.001$); and 11.38 ± 0.40 postdive ($P<0.005$). These decreases reflect that the respiratory rate decreased at depth.

The results of respiratory tests that are known to be sensitive to gas density such as forced expiratory volume ($FEV_{1.0}/FVC$), MVV, and maximal expiratory flow rates (MEFR) (Fig. 2) showed a well-known tendency to decrease as depth increased. However, the ATI, which was derived from the difference between VC and forced vital capacity (FVC) and expressed in percent of VC, was within normal limits throughout the dive.

The peak flow (Table I and Fig. 2) showed a tendency to recover during the stay at the bottom. Thus, on *Dive Day 21* (31 ATA) it was significantly higher ($P<0.05$) than on *Dive Day 10* (31 ATA). No such changes were apparent in MVV and $FEV_{1.0}$.
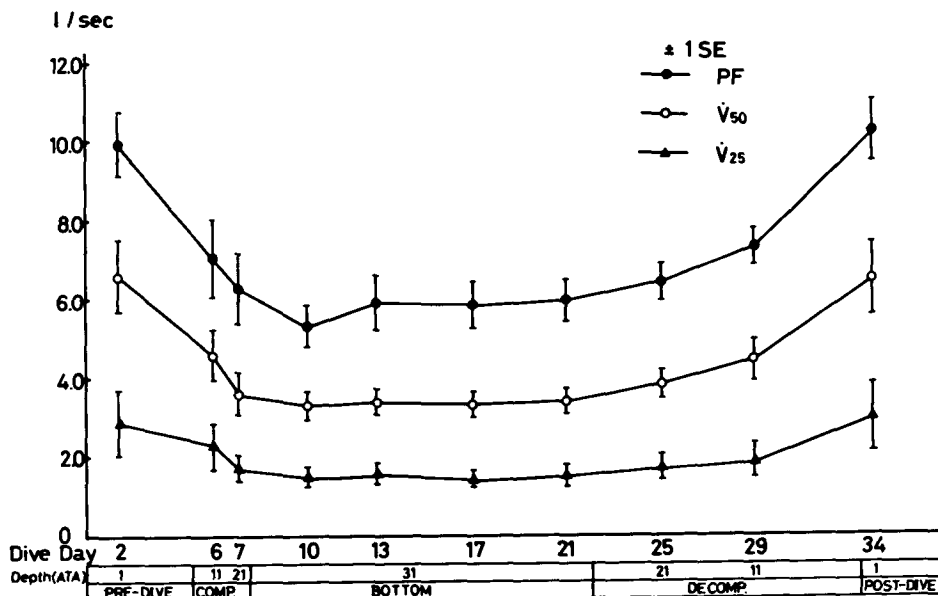
Fig. 2.   Changes in peak flow (PF), flow at 50% (V̇$_{50}$) and at 25% (V̇$_{25}$) of vital capacity. Bars indicate ± SE. PF and V̇$_{50}$ during compression, at the bottom, and during decompression significantly differ from those predive at $P<0.025$ and better (paired t test).

The ventilatory response to CO_2 at 300 m was significantly depressed to 82.7% ± 7.3% of the response at 1 ATA ($P<0.02$) at a PA_{CO_2} of 50 Torr and to 79.1% ± 6.5% ($P<0.05$) at a PA_{CO_2} of 60 Torr (Fig. 3). Although $P_{0.1}$ at 31 ATA was slightly higher than at 1.0 ATA at each level of PA_{CO_2}, there were considerable variations among the subjects, and mean value at 300 m did not significantly differ from that at 1.0 ATA (Fig. 3).

Maximal inspiratory pressures increased gradually but significantly, except on *Dive Day 13*, from a control level of 84.0 ± 5.0 Torr towards a maximum value of 136.0 ± 9.0 Torr on *Dive Day 17*, and then started decreasing towards the postdive value, which was not significantly different from predive. Maximal expiratory pressures, however, remained essentially unchanged (control 151.3 ± 7.0 Torr) except for a significant increase on *Dive Day 17* ($P<0.01$) and a significant decrease to 115.3 ± 8.3 Torr postdive ($P<0.05$).

Circulatory Changes

Table II summarizes the changes in circulatory functions at rest throughout the dive. Heart rate decreased during compression from 63 ± 2 beats/min predive to 58 ± 2 beats/min at 200 m ($P<0.025$). However, it returned to
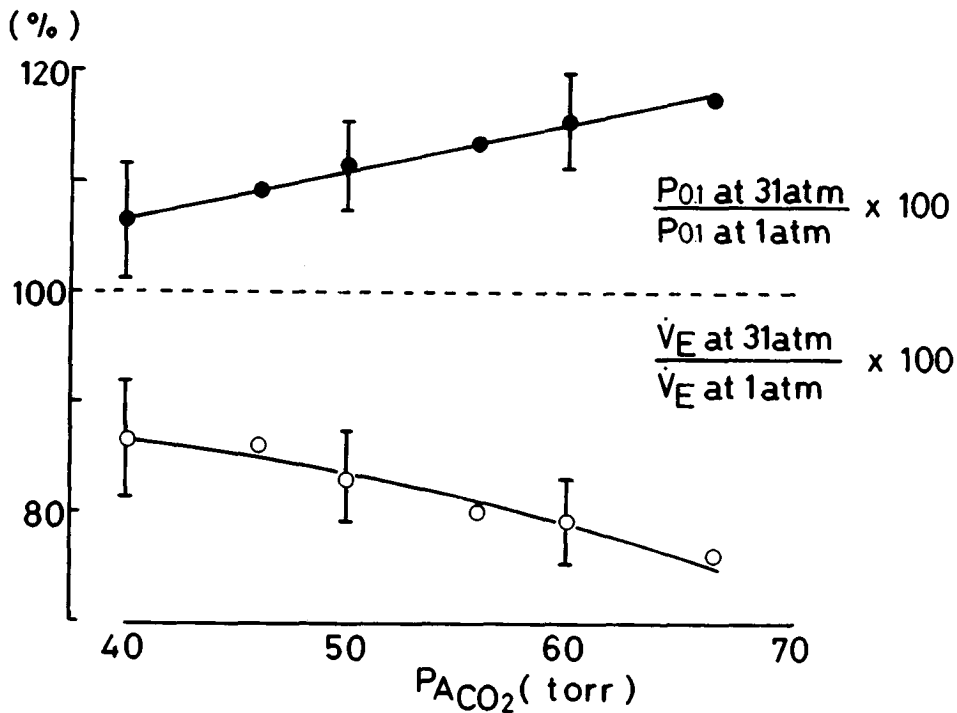
Fig. 3. $P_{0.1}$ and ventilatory responses to CO_2 at various PA_{CO_2} values at 31 ATA expressed as percent of those at 1.0 ATA.

TABLE II

Circulatory Functions at Rest During a 300 m (31 ATA) Saturation Dive

Dive Day		2	6	7	10	13	17	21	25	29	34
Depth (m)		0	100	200	300	300	300	300	215	100	0
HR (beats/min)	$\bar{X}$	63	58	58*	71	69	73	72	78	72	92*
	SE	2	4	2	6	5	8	6	7	3	4
SI (mL/beat/m²)	$\bar{X}$	46.4	56.6	50.1	44.1	50.7	54.1	53.8	50.6	49.1	40.2*
	SE	4.4	12.3	12.9	8.0	6.6	16.3	7.4	8.6	3.4	5.0
CI (L/min/m²)	$\bar{X}$	2.92	3.15	2.87	3.02	3.44	3.64	3.76*	3.84	3.52	3.69
	SE	0.21	0.43	0.66	0.41	0.31	0.72	0.34	0.52	0.33	0.51
Z_0/L (ohm/cm)	$\bar{X}$	0.92	0.86	0.91	0.93	0.90	0.81*	0.86*	0.85	0.85	0.89
	SE	0.05	0.06	0.05	0.04	0.05	0.06	0.05	0.07	0.03	0.03

Values are means ($\bar{X}$) and standard errors (SE) of duplicate measurements obtained in four subjects, respectively.   * Significantly different from control values of *Dive Day 2* (1 ATA) at $P<0.05$ and better (paired t test).   HR, heart rate; SI, stroke index; CI, cardiac index; Z_0/L, specific thoracic impedance; m², body surface area.

values not significantly different from those at the predive stay at the bottom. A slight increase was observed postdive ($P<0.025$). There were no significant changes in blood pressure throughout the dive.

The impedance cardiography produced stroke and cardiac indices which remained unchanged at depth, while specific thoracic impedance (Z_0/L) showed slight decreases on *Dive Days 17* and *21* ($P<0.025$).

Maximal and Submaximal Work Performance

Data obtained at maximal tolerable work loads during the predive, bottom, and postdive periods are shown in Table III.

Both the maximal tolerable work load and minute ventilation during the work at 31 ATA decreased significantly at $P<0.01$, and the postdive values did not significantly differ from the predive control values. The decrease in maximal O_2 uptake ($P<0.05$) and in CO_2 elimination ($P<0.005$) at the bottom continued postdive ($P<0.01$ for O_2, and $P<0.025$ for CO_2). The gas exchange ratio slightly decreased at the bottom ($P<0.025$) because of a more marked change in $\dot{V}CO_2$ than in $\dot{V}O_2$.

TABLE III

Circulatory and Respiratory Variables During Maximal
Exercise in a 300 m (31 ATA) Saturation Dive

		Predive (1 ATA)	Bottom (31 ATA)	Postdive (1 ATA)
$\dot{W}$	$\bar{X}$	240	205*	230
(watt)	SE	12	10	19
$\dot{V}E$	$\bar{X}$	132.8	73.6*	122.6
(L/min, BTPS)	SE	7.5	3.1	6.3
$\dot{V}O_2$	$\bar{X}$	3.11	2.71*	2.89*
(L/min, STPD)	SE	0.18	0.19	0.16
$\dot{V}CO_2$	$\bar{X}$	3.59	2.70*	3.32*
(L/min/STPD)	SE	0.10	0.07	0.16
R	$\bar{X}$	1.16	1.00*	1.15
	SE	0.04	0.05	0.01
HR	$\bar{X}$	179	162*	182
(beats/min)	SE	4	2	6
CI	$\bar{X}$	10.23	11.96	9.12
(L/min/m²)	SE	1.07	1.82	0.67

Values are means ($\bar{X}$) and standard errors (SE) for four subjects. *Significantly different from predive control values at $P<0.05$ and better (paired t test) W, maximal work rate; $\dot{V}E$, minute ventilation; $\dot{V}O_2$, oxygen consumption; $\dot{V}CO_2$, carbon dioxide elimination; R, respiratory exchange ratio; HR, heart rate; CI, cardiac index; m², body surface area.

A decrease in heart rate at maximal exercise at 31 ATA was significant at $P<0.01$, while the cardiac index remained unchanged.

Ventilatory equivalent ($\dot{V}E/\dot{V}O_2$) decreased from 43.48 $\pm$ 4.72 at 1.0 ATA to 27.53 $\pm$ 2.23 at 31 ATA ($P<0.025$), while $\dot{V}E/MVV$ and O_2 pulse ($\dot{V}O_2/HR$) remained unchanged. The ventilatory equivalent increased as work load increased at 1.0 ATA, whereas at 31 ATA it decreased as work load increased.

If we compare changes in cardiorespiratory functions at the same work load at 1.0 ATA as the maximal tolerable work load of each subject at 31 ATA, the work load for a given $\dot{V}O_2$ and ventilatory equivalent at 31 ATA was much less than those at 1.0 ATA, while O_2 pulse was consistently larger at the bottom than at 1.0 ATA.

DISCUSSION

This dive to a depth of 300 m has a distinctive feature in the prolonged stay at the bottom for 14 days, which allowed us to observe consecutive changes in ventilatory functions at the bottom. There was a tendency for recovery of the forced expiratory flow during the stay at 31 ATA. An even more marked recovery was noted by Schaefer et al. (5), who also observed that the higher the compression rate the larger the depression in MEFR and VC. Schaefer et al. (5) suggested that the coincident decrease and recovery of these two variables reflected airway collapse during rapid compression, causing air trapping and than a reopening of airways during the subsequent saturation period. To the extent that airway closure occurred in our subjects, it was at least not pronounced enough to reduce VC measurably because VC was already increased at 21 ATA, i.e., before reaching the maximum depth of 31 ATA. It is conceivable that secondary changes in pulmonary function (6) including vagal stimulation resulting in different bronchial tone (5) do exist during extended exposures to depth. The compression rate employed in this study was one quarter of that used by the above-mentioned authors and the ''recovery mechanism'' may have exerted its effect during compression. The unchanged ATI at depth reflects increases in FVC's proportional to the VC increases.

We can probably discount training as an explanation for the recovery of flow capacity at depth in this study since the postdive values of peak flow, $FEV_{1.0}/FVC$ and MVV did not differ from the predive values.

Flow limitation by dynamic airway compression (7,8) is generally accepted as the mechanism behind the decreases in MEFR and MVV at depth (9–11) because increase in nonelastic resistance due to increased gas density (12) causes the upstream movement of equal pressure points. Wood and Bryan (10) conceptualized the relationships between density, viscosity, and flow, which were supported by observations at depth. The power function $\dot{V}E_{max} = A$ (Density)^B has been suggested to best relate peak flows to gas density (10,13). However, compared to an exponent (B) of, for instance, -0.45 for maximum expiratory flow above 25% of VC obtained in the earlier men-

tioned work (10), those found in this study were consistently numerically less negative, i.e., -0.336 for peak flow, -0.388 for $\dot{V}_{50}$, and -0.327 for $\dot{V}_{25}$, respectively. The exponent for MVV was -0.368. This means that the impairment in ability to achieve high gas flows was less than what had been observed during acute pressure exposures. It is possible that the lesser density dependence of maximal ventilatory flow in our subjects was an expression of adaptation achieved in connection with the relative slow compression and the long sojourn at high pressure. The possibility of such an adaptation, still to be explained, gains support from observations of Peterson and Wright (13) who also found that density exponents measured after ½ to 2½ days at depth were relatively close to zero. Of particular significance are the findings in serial measurements in earlier investigations indicating, as was the case with our peak flow results, that there is a gradual enhancement in flow capacity at depth (5,14).

The increase in ERV presumably reflected a simple change in end-expiratory position because ERV increased far more than VC and RV remained stable at depth. Other adaptational phenomena in ventilatory functions at depth may be explained in terms of increased VC and ERV (15). Campbell (16) has suggested that an increase in airway resistance commonly induces increases in RV or FRC. According to McIlroy et al. (17), sudden increases in respiratory load and nonelastic resistance result in either an increase in tidal volume together with a decrease in respiratory frequency or an increase in ERV, or both. Our results showed both a decrease in respiratory frequency and an increase in ERV, which might lead to an increase in passive elastic recoil pressure and to a decrease in airway resistance as discussed by Smith et al. (15). These changes may be said to be adaptive, reducing the work of breathing dense gas (15,18). The mechanisms behind these changes are yet to be explained.

Whereas ventilatory response to CO_2 at 31 ATA was significantly depressed, $P_{0.1}$ at 300 m did not differ from that at 1.0 ATA. Gas physics imply that, if an amount of central inspiratory activity (CIA) produced the same volume expansion of the lungs under 31 ATA as at 1.0 ATA, $P_{0.1}$ should be 31 times greater at 31 ATA than at 1.0 ATA. Linnarsson and Hesser (19) observed that $P_{0.1}$ during air rebreathing at 6.1 bar was slightly greater than during oxygen rebreathing at 1.3 bar. This increase may be explained by either gas compressibility or by gas density as discussed in their paper, but was much smaller than that predicted according to the laws of gas physics.

We may interpret our results of recording $P_{0.1}$ in two ways: the absence of an increased $P_{0.1}$ at depth may have reflected a decrease in CIA, or there was a change in the relation between CIA and inspiratory muscle shortening. Should the latter have occurred, the stable $P_{0.1}$ may have reflected a tendency for a stable relation between CIA and inspiratory muscle tension rather than between CIA and inspiratory muscle shortening.

The mechanism behind the increased PI_{max} at depth is obscure. Training is an unlikely explanation because postdive the value was not different from predive. The possibility must be considered that the different compressibility of

the gas in the lungs at 31 ATA and 1 ATA provided for differences in chest volume and therefore in length and power exerted by the inspiratory muscles. Extrapolating from the data of Rahn et al. (20), who actually measured the effects of compression and expansion of lung gas on PI_{max} and PE_{max}, it becomes evident that testing PI_{max} at 31 ATA and RV (in which case RV is not going to change appreciably) will only yield about 10 Torr more pressure than at 1 ATA, where RV will expand by 10–15%. If the volume pressure relationships determined in a larger number of subjects by Ringqvist (21) are applied, even less of a volume dependence of PI_{max} in the volume range near RV is evident.

Hyperbaric bradycardia, which appears to be at least partly a direct hydrostatic pressure effect on the sinal node, has been observed in many dives under different conditions (6,15,22–25). As seen in Table II, circulatory function in the present dive essentially remained unchanged with some minor exceptions.

During compression there was initially a small but significant decrease in the heart rate, which then during the stay at 31 ATA became relatively variable and not different from the predive heart rate.

It may be speculated that the slight decrease in specific thoracic impedance measured on *Dive Days 17* and *21* indicated a relative increase in intrathoracic blood volume. The concomitant increase in CI and a tendency to lowered ERV also lend some support to the notion of an increased intrathoracic blood volume. However, we realize that quantitative comparisons of results based on impedance measurements on different days are uncertain because of possible differences in electrode placement.

Our findings of decreases in heart rate and ventilatory equivalent and increase in oxygen consumption for a given work rate at depth are consistent with previous reports (5,6,19,25–27). The $\dot{V}O_{2max}$ at 31 ATA decreased significantly compared to that at 1.0 ATA (Table III) but the maximal tolerable work load also decreased at 31 ATA, resulting in a stable $\dot{V}O_2$ for a given work load. The present observations cannot answer the question of whether or not limitations in oxygen transport or utilization, or both, determined the lowered maximal tolerable work load, nor can they answer whether or not a primarily lowered working capacity was reflected in the reduced $\dot{V}O_{2max}$ at 31 ATA. The reduction in $\dot{V}E/\dot{V}O_2$ at maximal work from 42.7 at 1.0 ATA to 27.2 at 31 ATA, which is consistent with other observations (5,6,26), seems to suggest a limitation in ventilation. However, this becomes a less likely explanation for the $\dot{V}O_{2max}$ depression in light of the $\dot{V}E/MVV$ quotients which averaged 0.76 ± 0.09 at 31 ATA. It would appear that a limitation in ventilatory flow capacity is not a likely explanation for the depressed $\dot{V}O_{2max}$ at 31 ATA. Indeed, there are other studies indicating that the restriction in ventilatory capacity would only begin to reduce a physical performance at 500 m (28) or relative gas densities of 6.0 to 7.8 (9,29).

The cardiac index during maximal exertion at 31 ATA in the present study remained unchanged compared to the control situation at 1 ATA. It therefore seems reasonable to conclude that the depression of $\dot{V}O_{2max}$ at depth

was not caused by a failure of cardiac output to adapt to the metabolic demands. The reason why the maximal tolerable work load at 31 ATA was depressed still remains to be answered.

Acknowledgment

References

1. Rahn H, Fenn WO, Otis AB. Daily variations of vital capacity, residual air, and expiratory reserve including a study of the residual air method. J Appl Physiol 1949;1:725–736.
2. Whitelaw WA, Derenne J-P, Milic-Emili J. Occlusion pressure as a measure of respiratory center output in conscious man. Respir Physiol 1975;23:181–199.
3. Read DJC. A clinical method for assessing the ventilatory response to carbon dioxide. Aust Ann Med 1958;16:20–32.
4. Kubicek WG, Kottke FJ, Ramos MU, et al. Non-invasive blood flow monitoring. The Minnesota impedance cardiograph-theory and applications. Biomed Eng 1974;9:410–416.
5. Schaefer KE, Carey CR, Dougherty JH Jr. Pulmonary function and respiratory gas exchange during saturation-excursion diving to pressures equivalent to 1000 feet of sea water. In: Lambertsen CJ, ed. Underwater physiology. Proceedings of the fourth symposium on underwater physiology. New York: Academic Press, 1971:357–370.
6. Winsborough MM, Vorosmarti J Jr, McKenzie RS. Some cardiopulmonary responses to exercise in man at an increased ambient pressure of oxygen-helium. In: Shilling CW, Beckett MW, eds. Underwater physiology VI. Proceedings of the sixth symposium on underwater physiology. Bethesda, MD: Federation of American Societies for Experimental Biology, 1978:145–155.
7. Mead J, Turner JM, Macklem PT, Little JB. Significance of the relationships between lung recoil and maximum expiratory flow. J Appl Physiol 1967;22:95–108.
8. Pride NB, Permutt S, Riley RL, Bromberger-Barnea B. Determinations of maximum expiratory flow from the lungs. J Appl Physiol 1967;23:646–662.
9. Miller JN, Wangensteen OD, Lanphier EH. Ventilation limitations on exertion at depth. In: Lambertsen CJ, ed. Underwater physiology. Proceedings of the fourth symposium on underwater physiology. New York: Academic Press, 1971:317–323.
10. Wood LDH, Bryan AC. Effect of increased ambient pressure on flow-volume curve of the lung. J Appl Physiol 1969;27:4–8.
11. Anthonisen NR, Bradley ME, Vorosmarti J Jr, Linaweaver PG. Mechanics of breathing with helium-oxygen and neon-oxygen mixtures in deep saturation diving. In: Lambertsen CJ, ed. Underwater physiology. Proceedings of the fourth symposium on underwater physiology. New York: Academic Press, 1971: 339–345.

12. Maio DA, Farhi LE. Effect of gas density on mechanics of breathing. J Appl Physiol 1967;23:687–693.
13. Peterson RE, Wright WB. Pulmonary mechanical functions in man breathing dense gas mixtures at high ambient pressures-predictive studies III. In: Lambertsen CJ, ed. Underwater physiology V. Proceedings of the fifth symposium on underwater physiology. Bethesda, MD: Federation of American Societies for Experimental Biology, 1976:67–77.
14. Dougherty JH Jr, Schaefer KE. Pulmonary functions during saturation-excursion dives breathing air. Aerosp Med 1968;39:289–292.
15. Smith RM, Hong SK, Dressendorfer RH, Dwyer HJ, Hayashi E, Yelverton C. Hana Kai II: a 17-day dry saturation dive at 18.6 ATA. IV. Cardiopulmonary functions. Undersea Biomed Res 1977;4:267–281.
16. Campbell EJM. Respiration. Ann Rev Physiol 1968;30:105–132.
17. McIlroy MB, Eldridge FL, Thomas JP, Christie RV. The effect of added elastic and non-elastic resistances on the pattern of breathing in normal subjects. Clin Sci 1956;15:337–344.
18. Bradley ME, Anthonisen NR, Vorosmarti J Jr, Linaweaver PG. Respiratory and cardiac responses to exercise in subjects breathing helium-oxygen mixtures at pressures from sea level to 19.2 atmospheres. In: Lambertsen CJ, ed. Underwater physiology. Proceedings of the fourth symposium on underwater physiology. New York: Academic Press, 1971:325–337.
19. Linnarsson D, Hesser CM. Dissociated ventilatory and central respiratory responses to CO_2 at raised N_2 pressure. J Appl Physiol 1978;45:756–761.
20. Rahn H, Otis AB, Chadwick LE, Fenn WO. The pressure-volume diagram of the thorax and lung. Am J Physiol 1946;146:161–178.
21. Ringqvist T. The ventilatory capacity in healthy subjects. Scand J Clin Lab Invest 1966;18(88).
22. Örnhagen HCh, Hogan PM. Hydrostatic pressure and mammalian cardiac-pacemaker function. Undersea Biomed Res 1977;4:347–358.
23. Matsuda M, Nakayama H, Kurata FK, et al. Physiology of man during a 10-day dry heliox saturation dive (SEATOPIA) to 7 ATA. I. Cardiovascular and thermoregulatory functions. Undersea Biomed Res 1975;2:101–118.
24. Hong SK, Smith RM, Webb P, Matsuda M. Hana Kai II: a 17-day dry saturation dive at 18.6 ATA. I. Objectives, design, and scope. Undersea Biomed Res 1977;4:211–220.
25. Dressendorfer RH, Hong SK, Morlock JF, et al. Hana Kai II: a 17-day dry saturation dive at 18.6 ATA. V. Maximal oxygen uptake. Undersea Biomed Res 1977;4:283–296.
26. Salzano J, Overfield EM, Rausch DC, et al. Arterial blood gases, heart rate, and gas exchange during rest and exercise in men saturated at a simulated seawater depth of 1000 feet. In: Lambertsen CJ, ed. Underwater physiology. Proceedings of the fourth symposium on underwater physiology. New York: Academic Press, 1971:347–356.
27. Lundgren CEG, Örnhagen HCh. Heart rate and respiratory frequency in hydrostatically compressed liquid-breathing mice. Undersea Biomed Res 1976;3:303–320.
28. Broussolle B, Chouteau J, Hyacinthe R, et al. Respiratory function during a simulated saturation dive to 51 ATA (500 meters) with a helium-oxygen mixture. In: Lambertsen CJ, ed. Underwater physiology V. Proceedings of the fifth symposium on underwater physiology. Bethesda, MD: Federation of American Societies for Experimental Biology, 1976:79–89.
29. Linnarsson D, Fagraeus L. Maximal work performance in hyperbaric air. In: Lambertsen CJ, ed. Underwater physiology V. Proceedings of the fifth symposium on underwater physiology. Bethesda, MD: Federation of American Societies for Experimental Biology, 1976:55–60.

PART II. DISCUSSION: CARDIORESPIRATORY RESPONSES TO EXERCISE

A. A. Bove, *Rapporteur*

There were two general areas of interest discussed in this session. In the first area, involving metabolic responses to exercise in helium environments, the papers by R. DeG. Hanson et al., and Raynaud et al., showed differences between air and oxyhelium at relatively low pressures. The statistical validity of the studies because of the small number of subjects was discussed. However, some discussants believed that the results were valid, and because these studies cannot be done on large populations, the data are nonetheless useful.

The interrelation between glucose, insulin, and growth hormone responses in exercise was considered. Because the Hansen et al., and Raynaud et al., papers were done in similar environments, it seemed reasonable to hypothesize some overall endocrine response. The discussion ended on this theme with the hope of the audience that the data presented can be used better to understand the changes in the endocrine interactions that occur in response to exercise and the diving environment. A question was raised concerning the validity of venous blood sampling from the arm in studies of leg exercise. Bove pointed out in further discussion that the whole-body metabolic response to exercise has been studied for many years using similar methods, and most exercise physiologists would accept these data as valid. Sampling venous blood from the exercising leg veins would give an inaccurate picture of the whole-body response to exercise because of the concentrated metabolites in blood sampled immediately downstream of the exercising muscle.

The second area of general interest in this session was that of the respiratory response to exercise in diving environments. After the paper of Hesser and Lind was presented, there was some discussion of the differences between air and oxyhelium on studies of central inspiratory pressure. The data showed a decreased carbon dioxide sensitivity in hyperbaric air, but no data are yet available for oxyhelium. After the paper of Salzano et al. on the *Atlantis I* and *II* dives at Duke University and the paper by Ohta et al., on the SEADRAGON dives, a discussion arose concerning the mechanisms of the dyspnea found with deep hyperbaric exposures. Lambertsen pointed out the multifactorial nature of dyspnea and the fact that careful studies must be done in the future to evaluate the contribution of each of these factors. Other discussants agreed with this need. Hills pointed out that dead space changes may be calculation artifacts and the apparent dead space changes found at 650 m may be caused by abnormal gas mixing in the upper airways. Other discussants also believed that abnormal gas mixing, or central core flow in the large airways, may be a factor in dyspnea on inspiration.

A comment was made that factors inducing dyspnea should be associated with abnormal arterial blood P_{O_2}, P_{CO_2}, or pH and these measurements were not abnormal in the subject with dyspnea at 650 m. It was also pointed out that the dyspnea of exercise is usually not associated with abnormal arterial blood gas measures.

Diaphragm fatigue was mentioned and the possibility of respiratory muscle training before deep exposures was suggested by several discussants. The exercise response of the subjects in several studies was questioned relative to the state of conditioning of the subjects. Because the degree of aerobic conditioning will alter the results of exercise studies, the state of conditioning of experimental subjects should be evaluated before starting the experiment.

223

The study by MacDonald and Pilmanis in open ocean was mentioned by Elliott as a significant contribution because it included all the environmental factors found in an operational dive. Other discussants also believed that physiologic studies in the open ocean were valuable in spite of the difficulty in controlling the environment.

INERTANCE AS A FACTOR IN UNEVEN VENTILATION IN DIVING

J. R. Clarke, M. A. Fisher, and M. J. Jaeger

A great deal has been written about the effect of dense gas on breathing resistance (1;2). Little is known, however, about the consequences of elevated inertance in diving, in spite of the fact that inertance (L) increases with pressure at a much faster rate than resistance.

A working definition of inertance is the pressure required to accelerate a gas divided by the acceleration (L = Paccel/V̇); analogous to the definition of resistance (R = Pflow/V̇). At 1-ATA, accelerative pressure is a small fraction of resistive pressure, and is negligible from a diver's standpoint (3). However, for some pulmonary function tests to be properly interpreted, inertial effects must be considered (4,5). We have examined the theoretical effects of inertance in dense atmospheres and found that inertance influences a wide variety of pulmonary function tests and exerts broad effects on ventilation as well.

METHODS

Although gas inertance can be measured readily (3), the inertial effects of a dense gas cannot be experimentally isolated from its effects on resistance. A theoretical treatment is therefore required. The historical and successful two-compartment model of the lung (6) has been used in our work, with the addition of inertance (or its electrical equivalent, inductance) to a common upper airway and to each of two lower or branch airways (Fig. 1). Normal values for resistance (R), inertance (L), and compliance (C) at 1 ATA were taken from the literature. Inertance was assumed to increase directly as gas density (a 99% helium, 1% oxygen gas mixture at 1500 fsw ([46 ATA]) would yield a respiratory inertance of about 0.1 cm $H_2O \cdot litre^{-1} \cdot s^2$). The ratio of upper airway
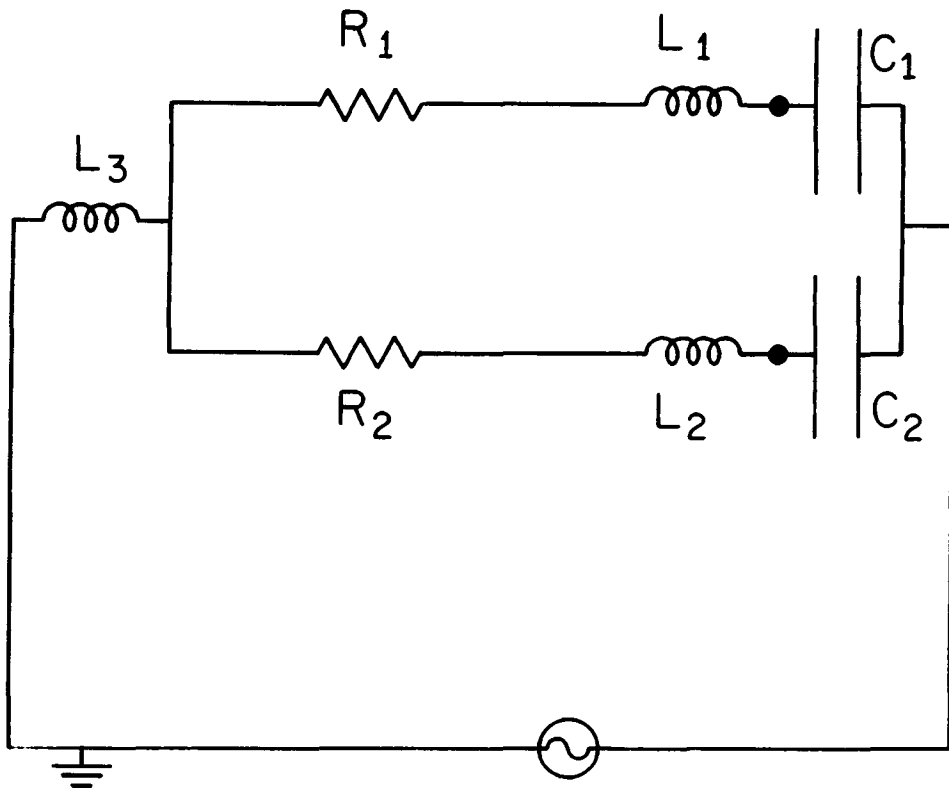
Fig. 1. The model. Two parallel branches with resistance (R), inertance (L), and compliance (C) elements are in series with a third inertance. The pressure (voltage) appearing at the nodes between the inertances and compliances represents alveolar pressure. The peak-to-peak driving voltage remains constant, whereas R, L, and C vary.

to lower airway (bronchial) inertance was maintained at 2 to 1 as suggested by Mead (3). From the branch and total impedance equations were obtained alveolar pressure, branch and total flows, and compartment volumes. Phase angles between branch flows and between mean alveolar pressure and total flow, as well as ratios of compartmental tidal volumes, were determined for various conditions of branch resistance, lung compliance, respiratory frequency, and inertance. Effective resistance (Re) was defined as the real portion of the complex impedance, or the ratio of driving pressure to the in-phase flow.

RESULTS

Ventilation increases at relatively low frequencies whenever inertance is elevated, and only at much higher frequencies is ventilation depressed (Table I). This dual effect occurs whether compartmental ventilation is equal

TABLE I

Effect of Inertance (L) on Compartmental Ventilation ($\dot{V}_E$)
and Effectiveness Resistance (Re)

F	R_1:R_2	L	$\dot{V}_E$	Re
40	1:1	0	1.84	0.5
40	"	0.1	3.16	0.5
40	"	0.2	4.74	0.5
40	1:10	0	1.15	1.20
40	"	0.1	1.58	1.12
40	"	0.2	2.22	1.04
90	1:1	0	1.46	0.50
90	"	0.1	1.04	0.50
90	"	0.2	0.46	0.50
90	1:10	0	0.83	0.98
90	"	0.1	0.86	0.91
90	"	0.2	0.40	0.95
240	1:1	0	0.74	0.50
240	"	0.1	0.11	0.50
240	"	0.2	0.05	0.50
240	1:10	0	0.41	0.92
240	"	0.1	0.10	1.15
240	"	0.2	0.05	1.67

Values are provided for three respiratory frequencies (BPM) and for both even
and uneven compartmental resistances.

or not. When compartment resistances are unequal, the effect of inertance on
total ventilation is somewhat reduced. However, under these conditions inert-
ance affects the frequency dependence of resistance, again in a dual fashion.

The phase difference between mean alveolar pressure and flow at the
mouth increases from 0° to 1.5° when inertance is zero and the ratio of branch
resistances increases from 1 to 10. Lung compliance was assumed to be 0.2
litre · cm H_2O^{-1}. However, with L equal to 0.1 cm H_2O · $litre^{-1}$ · s^2, phase
increases from −4.2° to −0.1°. As inertance increases, phase difference be-
comes increasingly negative.

The ratio of ventilation in compartments 1 and 2 is portrayed in Fig. 2 as
a function of respiratory frequency (Fr, in breaths per minute, BPM). The
dashed line represents an inertance of zero, and the *solid line* represents inert-
ance equal to 0.24 cm H_2O · $litre^{-1}$ · s^2. Compliances are equal to 0.2 litre ·
cm H_2O^{-1}, and resistances equal 1 and 10 cm H_2O · $litre^{-1}$ · s. The point
where the *solid* and *dashed lines* meet near 60 BPM is the crossing-frequency
(Fx) and marks the point at which inertance begins to suppress uneven ventila-
tion. The point at which unevenness is maximized (about 40 BPM in this in-
stance) will be referred to as Fm and is higher than the resonant frequency for
the system.

The effect of inertance on unevenness is more pronounced when resis-
tances rather than compliances are unequal (Fig. 3). With the resistance ratio
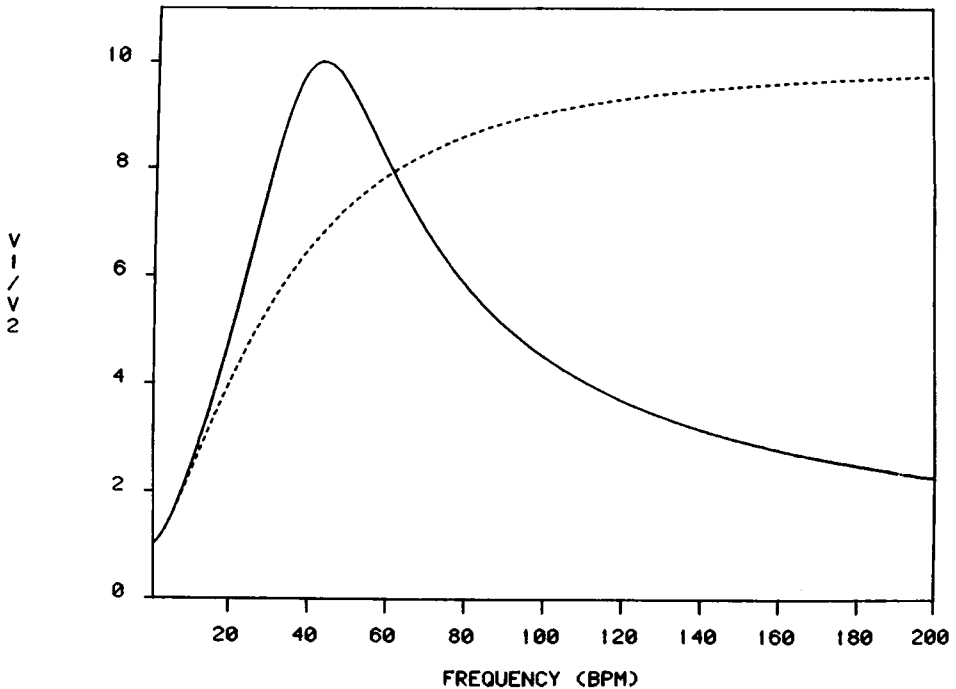
Fig. 2. Frequency dependence of the compartmental volume ratio (tidal volume, V_1/V_2). The curves are for the case with $R_1 = 1$, $R_2 = 10$ cm $H_2O \cdot litre^{-1} \cdot s$, C_1 and $C_2 = 0.2$ litres $\cdot$ cm H_2O^{-1}. L was set equal to 0.24 cm $H_2O \cdot litre^{-1} \cdot s^2$ (*solid line*) or zero (*dashed line*). The frequency at which the two lines intersect is termed crossing-frequency (Fx), and the frequency of maximum unevenness (the peak in the *solid line*) is termed Fm in the text.

fixed at 1:10 the results of a modeled dive to 20 ATA on air are displayed in Fig. 4. As the dive progressed, V_1/V_2 peaks narrowed and moved to lower frequencies.

DISCUSSION

The model reveals that under pressure both ventilation and measurements of pulmonary function may be influenced by inertance. Resistance measurements, for example, are influenced by both uneven ventilation and inertance as evidenced by the present model and by the work of Fredberg and Mead (7). The latter authors reported increases in resistance at frequencies above 1–2 Hz in normal individuals. Our model concurs, but further indicates that at relatively low frequencies inertance depresses effective resistance. The high frequencies of "panting" plethysmographic and forced oscillation techniques for measuring resistance (8,9) make these methods particularly susceptible to inertial effects.
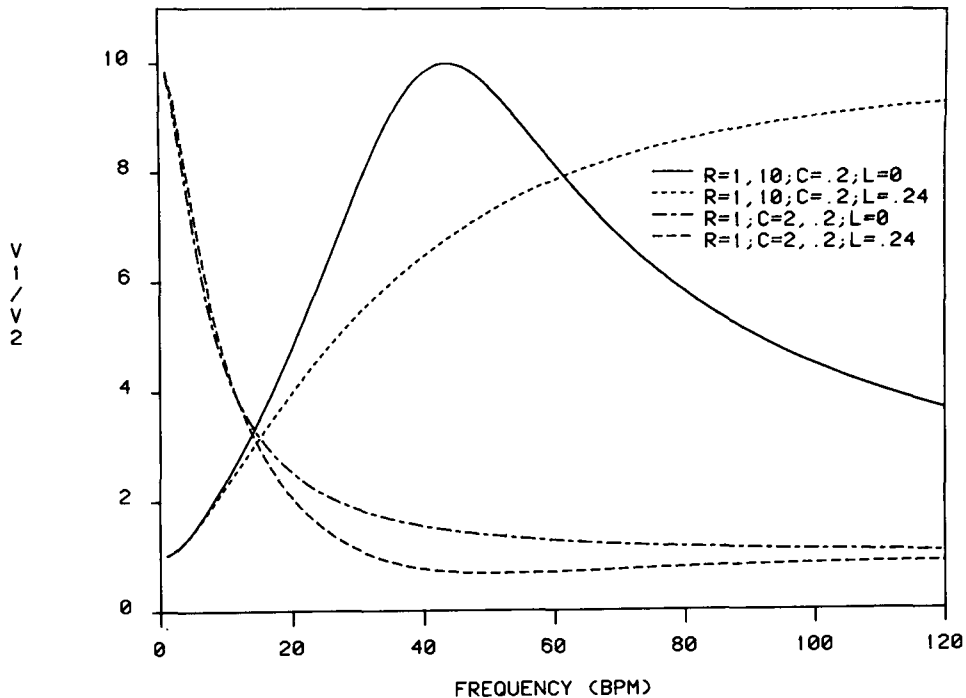
Fig. 3. Comparison of uneven resistances to uneven compliances. Uneven ventilation both with and without elevated inertance is presented.

The phase difference between mean alveolar pressure and flow at the mouth is also affected by gas density. Banerjee et al. (10) found the phase difference to be a sensitive indicator of uneven ventilation and, in theory, to increase directly with unevenness at 1 ATA. Under pressure the phase still becomes more positive as unevenness increases, but the absolute value may decrease because of an initial negative value. Due attention to the sign of the phase difference is therefore crucial when one uses this test during dense gas inhalation.

Dynamic compliance measurements are heavily influenced by inertance at frequencies above 30 BPM (4,5), even during supposedly even ventilation. The effects of unevenness and inertance observed in our model should add to the intricacies involved in correcting and interpreting dynamic compliance data under pressure: the assumptions about inertial effects made by other authors are likely to be too simplistic for hyperbaric studies. It should be stressed that during dense gas breathing the interplay between resistance and inertance adds a complexity to all but static pulmonary function measurements, a complexity which cannot be experimentally resolved.
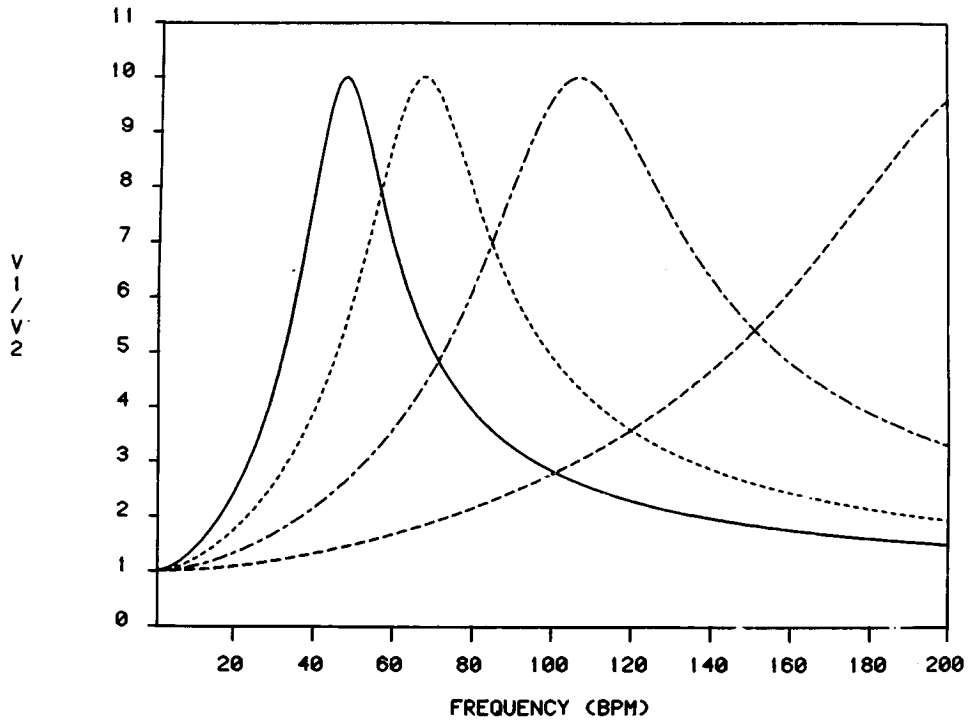
Fig. 4. A simulated dive to 20 ATA on air. At 1 ATA initial values were R = 0.1 and 1; C = 0.1 for each compartment, and L = 0.01 in the respective units. L increased directly with pressure, and R increased as the square root of pressure. The peaks represent conditions at (from *right to left*) 1, 4, 10, and 20 ATA.

Physiology

Winsborough et al. (11) succinctly summarized the known effects of diving on respiration: there is a "considerable loss in overall mechanical efficiency and physiological reserve of the gas transport system." Depending on equipment, gas density, and respiratory frequency, inertance may or may not hamper respiration.

The inertance of external equipment creates an impedance that may, surprisingly, either depress or augment alveolar ventilation. From Table I, we see that as long as Fr remains relatively low, inertance helps offset some of the resistive influence of equipment. Above Fm, however, both resistance and inertance combine to depress ventilation. This effect occurs regardless of ventilation distribution, but is more pronounced when compartment resistances are equal.

Inertance in a common pathway has no influence on unevenness, but compartmental inertance may either improve or degrade evenness. The dy-

namic character of gas exchange during a dive can be appreciated from Table II. For the Table we have assumed that inertance can separately alter CO_2 and O_2 tensions through its effect on total ventilation and evenness of ventilation, respectively. Unevenness may affect Pa_{O_2} by changing ventilation-perfusion ratios and their distribution (12). The situation portrayed in Table II would be further complicated during an actual hyperbaric exposure, because Fm and Fx both decrease whenever depth and inertance increase.

Divers tend to slow their respiration at depth, minimizing the work of breathing caused by resistive and inertial forces. This probably keeps Fr below Fm. If respiratory frequency did not change or if for some reason it increased, then a diver could find himself in the worst possible situation with Pa_{CO_2} elevated and Pa_{O_2} depressed (Case 2; Table II). The rapidity with which gas exchange would deteriorate with a change in either inertance or frequency is demonstrated by the increasing sharpness of the peaks in Fig. 4. Here, both L and R are assumed to increase with depth, L as a direct function of density, and R as the square root of density (2).

Unevenness

The model assumes uneven resistances and therefore uneven ventilation even without inertial influences. In at least one study (13) divers ventilated less evenly than young nondivers. Smokers, whether they are divers or not, likewise have unevenly distributed venilation (10). At 1 ATA even normal nonsmokers exhibit some degree of unevenness.

Uneven ventilation is also normal in animals, or at least anesthetized animals—anesthetized dog (14); rat (15); excised hamster lung (16). Anesthetics may aggravate unevenness by stimulating the release of histamine (17), which in turn causes unevenly distributed bronchoconstriction (18).

TABLE II

Frequency Dependence of Inertial Effects on Ventilation and Unevenness

CASE	$\dot{V}_E$	V_1/V_2	Pa_{CO_2}	Pa_{O_2}
Fr<Fm<Fx	↑	↑	⋮↧	⋮↧
Fm<Fr<Fx	↓	↑	↥⋮	⋮↧
Fm<Fx<Fr	↓	↓	↥⋮	↥⋮

For a given combination of R, L, and C, the final effect depends on where respiratory frequency (Fr) lies in relation to FM (frequency of maximum unevenness) and Fx (crossing frequency). A hypothesized relationship to gas exchange is indicated by *stippled arrows*.

As seen in Fig. 3, the effect of L on unevenness is greatest when resistances are unequal rather than when compliances are unequal. Evidence exists supporting either R or C as the controlling factor in uneven ventilation. We have used for our model the resistance ratio of 1:10, which Forkert et al. (5) found to fit their data for asymptomatic young males (both smokers and non-smokers were included in their study). Because the maximum unevenness occurring under pressure is a direct function of the unevenness at 1 ATA, pre-dive evaluation of uneven ventilation seems pertinent.

CONCLUSIONS

Inertia should be considered as a respiratory variable whenever respiratory frequency or gas density is elevated. The phenomena that might arise from various combinations of R, L, and C are numerous and are dependent upon the variation of R, L, and C with depth and equipment. Effects are dependent upon respiratory frequency and pattern, the degree and cause of uneven ventilation, and the relative contribution of common and parallel pathways to the total respiratory impedance. If inertance is not considered in measurements of resistance, dynamic compliance, and phase differences of pressure and flow, large errors in interpretation may result. Inertance, furthermore, has the potential for altering ventilation and gas exchange, but the effect is complex even in this simple model.

The testing of uneven ventilation in divers should gain new significance in light of this analysis. Especially important are those tests most sensitive to unequal resistance at 1 ATA, notably frequency dependence of resistance and phase difference of pressure and flow.

Acknowledgments

References

1. Otis AB, Bembower WC. Effect of gas density on resistance to respiratory flow in man. J Appl Physiol 1949;2:300–306.
2. Wood LDH, Engel LA, Griffin P, Despas P, Macklem PT. Effect of gas physical properties and flow on lower pulmonary resistance. J Appl Physiol 1976;41:234–244.
3. Mead J. Measurement of inertia of the lungs at increased ambient pressure. J Appl Physiol 1956;9:208–212.
4. Dosman J, Bode F, Urbanetti J, Antic R, Martin R, Macklem PT. Role of inertia in the measurement of dynamic compliance. J Appl Physiol 1975;38:64–69.

5. Forkert L, Wood LDH, Cherniack RM. Effect of gas density on dynamic pulmonary compliance. J Appl Physiol 1975;6:906–910.

6. Otis AB, McKerrow CB, Bartlett RA, Mead J. McIlroy MB, Selverstone NJ, Radford EP. Mechanical factors in distribution of pulmonary ventilation. J Appl Physiol 1956;8:427–443.

7. Fredberg JJ, Mead J. Impedance of intra-thoracic airway models during low-frequency periodic flow. J Appl Physiol 1979;47:347–351.

8. DuBois AB, Botelho SY, Bedell GN, Marshall R, Comroe JH Jr. A rapid plethysmographic method for measuring thoracic gas volume: a comparison with a nitrogen washout method for measuring functional residual capacity in normal subjects. J Clin Sci 1956;35:322–335.

9. DuBois AB, Brody AW, Lewis DH, Burgess BF. Oscillation mechanics of lungs and chest in man. J Appl Physiol 1956;8:587–599.

10. Banerjee M. Evans JN, Jaeger MJ. Uneven ventilation in smokers. Respir Physiol 1976;27:277–291.

11. Winsborough MM, Vorosmarti J Jr, McKenzie RS. Some pulmonary responses to exercise in man at an increased ambient pressure of oxygen-helium. In: Shilling CW, Beckett MW, eds. Underwater physiology VI. Proceedings of the sixth symposium on underwater physiology. Bethesda, MD: Federation of American Societies for Experimental Biology, 1978:145–165.

12. Neufeld GR, Williams JJ, Klineberg PL, Marshall BE. Inert gas a-A differences: a direct reflection of V/Q distribution. J Appl Physiol 1978;44:277–283.

13. Lenfant C. Measurement of factors impairing gas exchange in man with hyperbaric pressure. J Appl Physiol 1964;19:189–194.

14. D'Angelo E. Effect of papain-induced emphysema on the distribution of pleural surface pressure. Respir Physiol 1976;27:1–20.

15. Boyd RL, Fisher MJ, Jaeger MJ. Noninvasive lung function tests in rats with progressive papain-induced emphysema. Respir Physiol (in press).

16. Niewoehner DE, Kleinerman J. Effects of experimental emphysema and bronchiolitis on lung mechanics and morphometry. J Appl Physiol 1973;35:25–31.

17. Goodman LS, Gilman A. The pharmacological basis of therapeutics. New York: Macmillan, 1975.

18. Drazen JM, Schneider MW, Venugopalan CS. Modulation of central and peripheral airway contractile activity of histamine in vitro by H2 receptor activation. Physiologist 1978;21:31.

THE ARRHYTHMOGENIC POTENCY OF HYDROSTATIC PRESSURE ON CARDIAC CONDUCTION

T. J. Doubt and P. M. Hogan

Exposure of humans to hyperbaric environments often produces alterations in cardiac rate and rhythm (1,2). Elucidation of the mechanisms responsible for these arrhythmias is complicated by the multiplicity of contributing factors; the most notable of these include hydrostatic pressure per se, neurogenic responses, breathing gas composition, and oxygen tension.

Evidence has accumulated indicating that hydrostatic pressure alone is capable of disrupting normal cardiac electrical behavior. For example, elevated hydrostatic pressure slows pacemaker activity, i.e., hyperbaric bradycardia, in intact animals (3) and isolated sinus node preparations (4). In the latter study it was also demonstrated that hydrostatic pressure can cause intermittent sinoatrial exit block (see I of Table I). Exit blocks developed upon compression to 60–150 ATA, and were manifest by a failure of some sinus impulses to propagate into the surrounding atrial myocardium.

Subsequent investigations from our laboratory have been directed toward delineating the mechanisms underlying the pressure effects on the electrogenic process in heart cells. During the course of these experiments various arrhythmias were encountered that are explicable on the basis of what is now known about the effects of hydrostatic pressure on normal membrane events during the cardiac cycle. The present report describes the occurrence of arrhythmias in several types of cardiac tissue, details the predisposing factors associated with the arrhythmias, and discusses the probable cellular mechanisms responsible for the development of the aberrant rhythms.

In all experiments, the cardiac tissue was hydrostatically compressed in a special tissue bath that isolated the bath contents from the helium gas used to pressurize the chamber (5,6). The Po_2 of the Tyrode solution was kept con-

TABLE I

Arrhythmias Encountered During Hydrostatic Compression

	Tissue	Pressure (ATA)	Temp. (°C)	Rate (pulses·min⁻¹)	Arrhythmia
I	Sinus Node*	60–150	23–32	-	Bradycardia, Exit Block
II	Atria† (2 of 8)	100–150	30	150–200	3:2 Block, 2:1 Block
III	Purkinje	100	37	60	Coupled Extrasystoles
IV	Purkinje (4 of 11)	150	27	90	2:1 Block, Oscillatory Conduction
V	Purkinje (4 of 8)	150	37	240	2:1 Block, Oscillatory Conduction

Numbers below tissue indicate frequency of recorded arrhythmias in each series. In I and III arrhythmias were observed but not routinely recorded in every experiment.   *See reference (4).   †See reference (5).

stant at 0.98 ATA, and the temperature remained with ± 0.05°C of the selected set-point. Further, the tissues were paced at constant rates using stimulus pulses of just threshold value.

Two previous reports (5,6) have documented the basic effects of hydrostatic pressure on cardiac conduction. Briefly, elevations in pressure up to 150 ATA significantly decrease conduction velocity. Part of the decrease in velocity can be attributed to a decrease in membrane excitability. In addition, slowing of conduction is associated with a reduction in the maximum upstroke velocity ($\dot{V}$max) of the action potential over the range of resting potentials from which a response can be initiated, and indicates depressed membrane responsiveness. The refractory period for successful impulse propagation is increased at pressure, an effect due to both a decreased responsiveness and to a significant increase in action potential duration (APD).

Table I presents the overt arrhythmias encountered throughout this study. Pressure-induced increases in conduction time were not classified as an overt arrhythmia as long as conduction occurred in a regular 1:1 pattern. Further, the arrhythmias were not present prior to compression and could be abolished by decompression to 1 ATA. Hydrostatic pressure alone (see III in Table I) produced documented evidence of an arrhythmia in at least one case. Figure 1 shows the action potential traces recorded from this Purkinje preparation at 1 and 100 ATA. In this example, coupled extrasystoles appeared at 100 ATA. The extrasystolic pattern could be eliminated by a slight increase in stimulation frequency. The most plausible explanation for this pressure-induced arrhythmia is reentry of the excitatory impulse due to unidirectional block and slowed conduction in the return pathway.

It is evident from Table I that the arrhythmogenic potency of hydrostatic pressure is enhanced when combined with other stresses known to depress
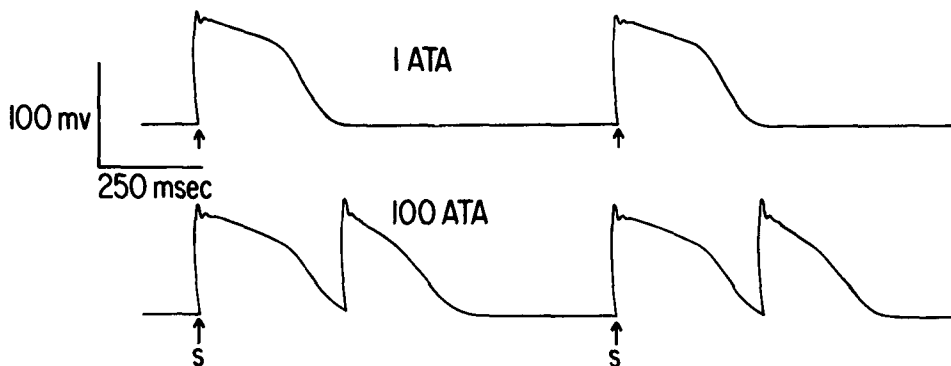
Fig. 1. Action potential traces from a cardiac Purkinje cell at 1 and 100 ATA. Normal responses, marked by *arrows*, were evoked by stimulus pulses at a rate of 60 min^{-1}. Coupled extrasystoles appeared upon compression to 100 ATA.

conduction. The combination of increased stimulating frequency and elevated pressure produced arrhythmias in two of eight rabbit atria (II in Table I). Abnormal atrial conduction first appeared as a 3:2 block at 100 ATA when the pacing frequency was increased to 200 pulses · min^{-1}. Increasing the pressure demonstrated the additive nature of the rate/pressure stress. At 150 ATA the 3:2 block was evident at a slower frequency (150 pulses · min^{-1}). Increasing the frequency to 200 pulses · min^{-1} increased the conduction deficit, resulting in a 2:1 block.

Rapid stimulation of ventricular Purkinje fibers at 150 ATA also produced aberrant rhythms in four of eight preparations (V in Table I). In two preparations a 2:1 conduction block developed when the stimulus frequency was increased to 240 pulses · min^{-1}. Figure 2 illustrates this type of block in one preparation. In this example, at 150 ATA the APD was markedly longer than the stimulus cycle length (250 ms). The pressure-induced lengthening of the action potential reflects an increase in the refractory period of the tissue. Thus, the next stimulus pulse was delivered during the absolute refractory period and was unable to evoke a propagated response. The resultant dropped beat enabled the tissue to recover sufficiently to respond to the next stimulus pulse. As a result, excitation occurred during every other pulse, establishing the 2:1 conduction pattern.

A similar type of rate-pressure related arrhythmia developed in two other Purkinje preparations. At 150 ATA an oscillation in impulse conduction time appeared at a rate of 240 pulses · min^{-1}. As shown in Fig. 3, pressure increased APD such that every other stimulus pulse (shown by the longer arrows in the figure) occurred during the terminal repolarization limb of the preceding action potential. The resultant response, evoked during the relative refractory period, was initiated from a more depolarized level of membrane potential. As
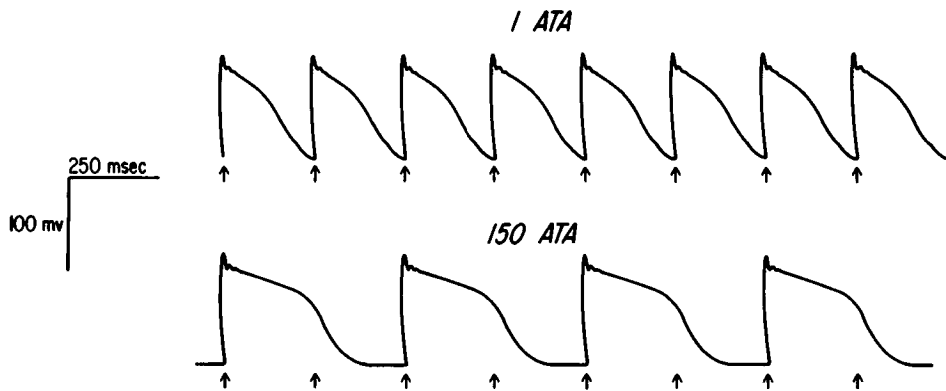
Fig. 2. Action potential traces from one Purkinje preparation at 1 and 150 ATA. Stimulus pulses, marked by *arrows*, were delivered at a rate of 240 min⁻¹. At 150 ATA, a 2:1 block occurred.
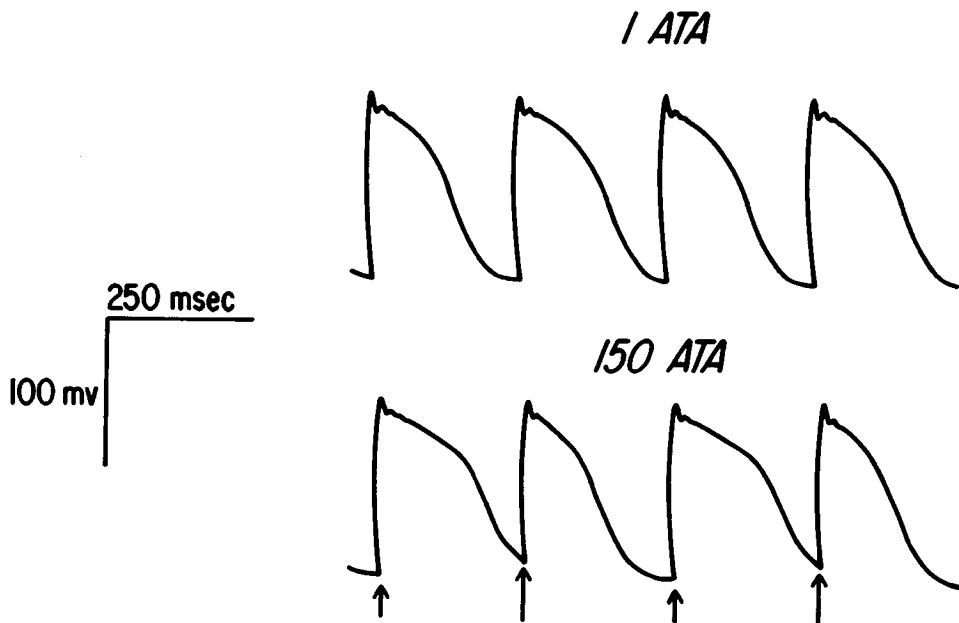
Fig. 3. Purkinje action potentials recorded at 1 and 150 ATA. Stimuli, denoted by *arrows*, were delivered at a frequency of 240 min⁻¹. At 150 ATA every other evoked response, shown by *longer arrows*, was initiated from the repolarization limb of the preceding action potential, and resulted in slower propagation.

a consequence, this action potential had a reduced $\dot{V}_{max}$ and propagated more slowly than the preceding response. The APD of the slowly conducted response was shortened, allowing repolarization to be completed before the occurrence of the next stimulus. The next response, therefore, originated from a more fully polarized membrane and propagated more effectively. Thus, an oscillatory conduction pattern was established because of the alteration in APD.

The interaction of low temperature and high pressure also increased the likelihood of arrhythmia development. Cooling Purkinje fibers at 150 ATA resulted in the occurrence of aberrant conduction in 4 of 11 experiments (see IV in Table I). In two instances a 2:1 conduction block developed that was a function of the APD. At 150 ATA reducing the temperature to 27°C lengthened the action potential beyond the basic stimulus cycle length (667 ms). Thus, the recovery of an initiated action potential was incomplete at the time the next pulse was delivered to the tissue. Consequently, conducted responses were blocked during application of alternate stimulus pulses, establishing the 2:1 conduction pattern. Warming the tissue to 30°C shortened the action potential duration sufficiently to permit 1:1 conduction.

In the other two examples of pressure-temperature stress an oscillation occurred in the conduction time between the stimulating and recording sites. There was no appreciable variation in APD, which suggests that membrane excitability and responsiveness were alternately diminished at 27°C/150 ATA. Warming the tissue to 30°C abolished the arrhythmia.

The present findings offer insight into the arrhythmogenic potency of elevated hydrostatic pressure. High pressure reduces the safety margin for cardiac conduction by depressing excitability, decreasing membrane responsiveness, and prolonging the refractory period. These pressure-induced perturbations may be of sufficient degree, under certain circumstances, to lead to the development of overt arrhythmias.

Decreases in temperature or increases in frequency have a combined effect with pressure to further lower the safety margin for conduction. This fact is evident in the present report, where arrhythmias were encountered at 100–150 ATA when either the temperature was lowered to 27°C or when the stimulus frequency exceeded 150 pulses·min^{-1}.

It should be pointed out that the pressure, temperature, and rate perturbations used in these studies were applied to isolated, healthy, and carefully maintained tissues. Thus, relatively large perturbations were required to produce arrhythmias in isolated segments of normal myocardium. On the other hand, it is a recognized fact that abnormal cardiac rhythms in intact hearts can be produced by a lesser magnitude of stress. This is due, in part, to the added complexities of maintaining a normal rhythm in functional hearts (i.e., coronary perfusion, O_2 consumption, autonomic innervation, etc.). Consequently, it is not surprising that arrhythmias reported in human divers (1,2) have occurred at lower pressures, temperatures, or heart rates.

The results obtained in the present experiments may have direct application to diving man. Typically, depth, workload, and hypothermia are three of the primary safety concerns during an open-water dive. Our in vitro experi-

ments may simulate the conditions of a diver working in cold water. Our findings suggest that a diver exposed to these conditions may have an increased probability of developing an aberrant cardiac rhythm. Undoubtedly, the occurrence and severity of any arrhythmia will also be dependent on other factors affecting cardiac conduction. Awareness of such risk factors could enhance the overall safety of manned exploration of the sea.

Acknowledgments

References

1. Argeles, HJ, Feezor MD, Saltzman HA. Human vectorcardiographic responses at increased pressures to 1000 fsw. Undersea Biomed Res 1977;4:A30.
2. Wilson JM, Kligfield PD, Adams GM, Harvey C, Schaefer KE. Human ECG changes during prolonged hyperbaric exposures breathing N_2-O_2 mixtures. J Appl Physiol: Respirat Environ Exercise Physiol 1977;42:614.
3. Lundgren CEG, Örnhagen HC. Heart rate and respiratory frequency in hydrostatically compressed liquid-breathing mice. Undersea Biomed Res 1976;3:303.
4. Örnhagen HC, Hogan PM. Hydrostatic pressure and mammalian cardiac pacemaker function. Undersea Biomed Res 1977;4:347.
5. Doubt TJ, Hogan PM. Effects of hydrostatic pressure on conduction and excitability in rabbit atria. J Appl Physiol: Respirat Environ Exercise Physiol 1978;45:24.
6. Doubt TJ, Hogan PM. Acting potential correlates of pressure-induced changes in cardiac conduction. J Appl Physiol: Respirat Environ Exercise Physiol 1979;47:1169.

EFFECTS OF ALCOHOL ON THE CARDIOVASCULAR ADJUSTMENTS OF THE DIVING REFLEX IN MAN

L. E. Wittmers, Jr., L. Fairbanks, S. Burgstahler, and R. S. Pozos

The *diving reflex* was first described in nonhuman species by Bert (1). Following a submersion of the animal the components of this reflex are: a) breath holding (apnea); b) decreased heart rate (bradycardia); c) changes in blood pressure; and d) alterations in tissue blood flow distribution (2). The redistribution of blood flow in the organism results in a priority blood supply to the heart and brain with a minimum blood supply to muscle, gastrointestinal tract, kidneys, and skin. Those tissues that can do without an oxygen supply for some period of time or are able to utilize anaerobic pathways are deprived of blood flow and those that cannot do without an oxygen supply are supplied with at least a minimum amount. For this reason the diving reflex is often referred to as the *oxygen conserving reflex* (3). Many animals that employ diving as a mechanism for food supply or protection exist in a cold water environment so that the peripheral vasoconstriction acts to increase the thickness of the insulating tissue layer to minimize heat loss.

The diving or oxygen conserving reflex has been demonstrated in nondiving species including man (4). In man this reflex is not as well developed and its magnitude depends on a large number of physiological and environmental conditions that include a) lung volume at which apnea occurs (5,6); b) water temperature (7); c) magnitude of immersion (8); and d) emotional state (3).

The functional significance of the diving reflex in man has been implicated in a near-drowning situation and in the sudden-drowning syndrome. In the case of drowning it has been suggested that the diving reflex may result in arrhythmias leading to myocardial infarction (3). This is a possible explanation of the sudden-death syndrome in drowning. These victims are submerged for only a short period of time yet cannot be resuscitated. On the other hand, indi-

viduals immersed for long periods of time in cold water can be resuscitated successfully—a near drowning situation (9,10). In these cases, investigators have suggested that the diving reflex acts as a protective mechanism converting the organism into a heart-brain circulatory system preserving life for a considerable period of time. The possibility of this physiological state suggests that victims without apparent vital signs recovered from cold water must be treated vigorously in an attempt to recover what "spark" of life may remain.

Investigators found that the diving reflex in man could be elicited by simply submerging the face in water (11,12). This finding provides the investigator a very simple method of eliciting a complex cardiovascular reflex and studying these cardiovascular alterations under conditions of physiological and environmental change.

The combination of cold + water + alcohol or cold + alcohol in man is not an uncommon situation (13). For this reason we embarked on an experimental design that employed the diving reflex at different lung volumes to study the effect of both cold stress and a combination of cold + alcohol stress on cardiovascular adjustments in man.

MATERIAL AND METHODS

The subjects for these experiments were healthy male and female volunteers, ranging in age from 20 to 38 years. The electrocardiographic data were continuously monitored by a single-lead telemetry system and the heart rate was calculated from a 5-beat span. When heart rates were very slow, the R-R interval was employed to determine rate. Blood pressures (systolic and diastolic) were measured with a semiautomatic pneumatic cuff and microphone system similar to that described by Winn et al. (14). The diving reflex was elicited by submerging the subject's face (up to, but not covering the ears) in cold water (4°C ± 2°). Lung volumes were obtained with a simple spirometer (Collins Co., Braintree, Mass.). Blood alcohol levels were measured by analyzing alveolar gas (Cal Detect Co., Richmond, Calif.). All subjects were exposed to test protocol at least once before the actual experiment to familiarize them with the equipment and the experimental design.

All subjects fasted for 12 h before the experimental period. For each breath-holding period the subject was fitted with a nose clip and seated comfortably with his head bent forward over a pan that was either empty (breath holding in air) or filled with water (breath holding in water). The subject took a breath to either vital capacity or some intermediate lung volume (50–70% vital capacity), and either held that lung volume (as long as possible) in air or with face submerged in water. At the end of breath holding the subject exhaled into a spirometer. Subjects drank the alcoholic beverage of their choice at a comfortable rate until a blood alcohol level of 0.1 g% was achieved. At that point the breath-holding maneuvers at both lung volumes in air and water were repeated.

RESULTS AND DISCUSSION

General physical characteristics, vital capacities, and heart rates for the experimental population are presented in Table I. Figure 1 contains an example of blood pressure and electrocardiographic recordings of a diving reflex response in one subject (RP). During the blood pressure recording, the cuff was inflated to a pressure of 50–75 mmHg above the expected systolic level and allowed to deflate at a rate of approximately 8 mmHg/s. When the Korotkoff sounds are detected by the microphone, the cuff pressure is recorded as a vertical deflection. Therefore, in each group of vertical lines the first line represents systolic and the last line the diastolic blood pressure. The heart rate tracing is an ECG signal with rate indicated by the distance between the QRS peaks. Note: the heart rates were not taken from this recording but from an auxillary recorder running at normal ECG speed. *Subject RP* showed a decrease in heart rate and a rise in blood pressure during face immersion. This subject is included in the experimental population as *Subject 8* (see Table I).

We designed the experiments to study the effects of alcohol on the diving reflex. In light of previous work, these experiments indicated that breath holding alone may cause considerable changes in heart rate and blood pressure and alterations in these measures may be affected by lung volume at the time of the apnea. Heart rate response in air apnea at vital capacity is minimal whereas in water there is an initial increase in heart rate followed by a fall representing a 30% decrease from control levels. At vital capacity these changes are not altered by alcohol ingestion. Water apnea results in an initial rapid rise (0–25 s) in blood pressure of approximately 15 mmHg followed by a slow continual rise throughout the period of apnea. Mean blood pressure changes in these experiments were similar in profile both for control and after

TABLE I

Physical Characteristics of Subject Population

Subject (No.)	Sex	Age (yr)	VC* (litres)	VC % N†	HR‡ (beats/min)
1	M	22	4.2	84	79
2	F	22	3.5	109	72
3	M	24	3.9	85	57
4	M	29	3.7	93	60
5	M	20	5.7	103	73
6	M	23	5.4	110	68
7	M	30	5.3	103	59
8	M	36	5.2	107	71
9	M	38	5.8	110	56

*VC, vital capacity;   †VC % N, VC of subject divided by predicted normal value × 100;   ‡HR, heart rate (control-resting value).
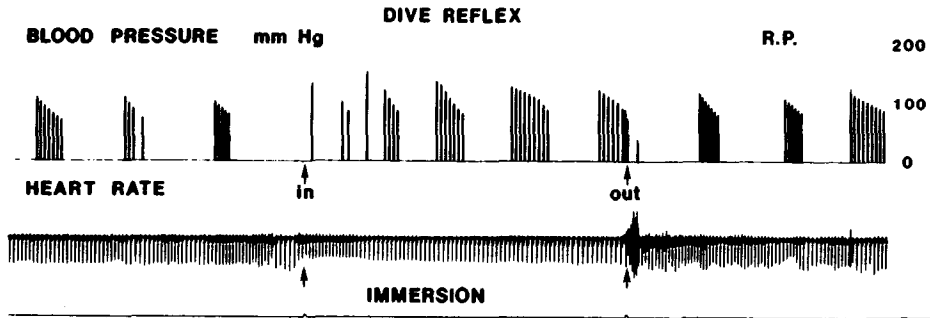
Fig. 1. Examples of ECG and blood pressure recordings on a subject before, during, and after face immersion in cold water, without alcohol consumption. Note, time of immersion is 64 s.

alcohol consumption; however, after alcohol consumption the mean blood pressures were approximately 10 mmHg lower than in the control studies. Air apnea is associated with a slow continuous rise in blood pressure.

Results obtained at the intermediate lung volume differ in these respects: a) the initial increase in heart rate seen in water immersion did not appear; b) further blood pressure changes in the control experiments showed a delayed rise in both air and water apnea; c) after alcohol ingestion there was no increase in blood pressure after water immersion (see Fig. 2).

In the group of nine subjects presented here, there was a wide variety of heart rate responses to breath holding in air and water at any given lung volume. Figures 3 and 4 illustrate the heart rate response in *Subjects 2* and *3* (see Table I) to four experimental situations. The data on the heart rate responses are presented in each panel as both air and water apnea. Note that in the data of *Subject 3* there is no difference between the heart rate responses in air and water at vital capacity before alcohol consumption. After consumption of alcohol the absolute level of heart rate is increased in both air and water and there is a slower decrease in heart rate with air apnea when compared to water apnea. At the intermediate lung volume the decrease in heart rate before alcohol consumption is less in air than in water and the difference is magnified after alcohol consumption.

Subject 2 (see Table I and Fig. 4) is included to illustrate a different response in heart rate at vital capacity with a minimal change after alcohol consumption. At intermediate lung volume there is a larger difference in heart rate during the control breath holding with a magnification of this difference after alcohol consumption. The individual variability is such that a much larger group of subjects must be studied to determine if there are certain patterns associated with some other physiological, anatomical, or environmental conditions.

Preliminary data presented here indicates that alcohol may alter cardiovascular response of the diving reflex but observation of this effect depends on the lung volume at which the reflex is elicited. In addition, there is a large
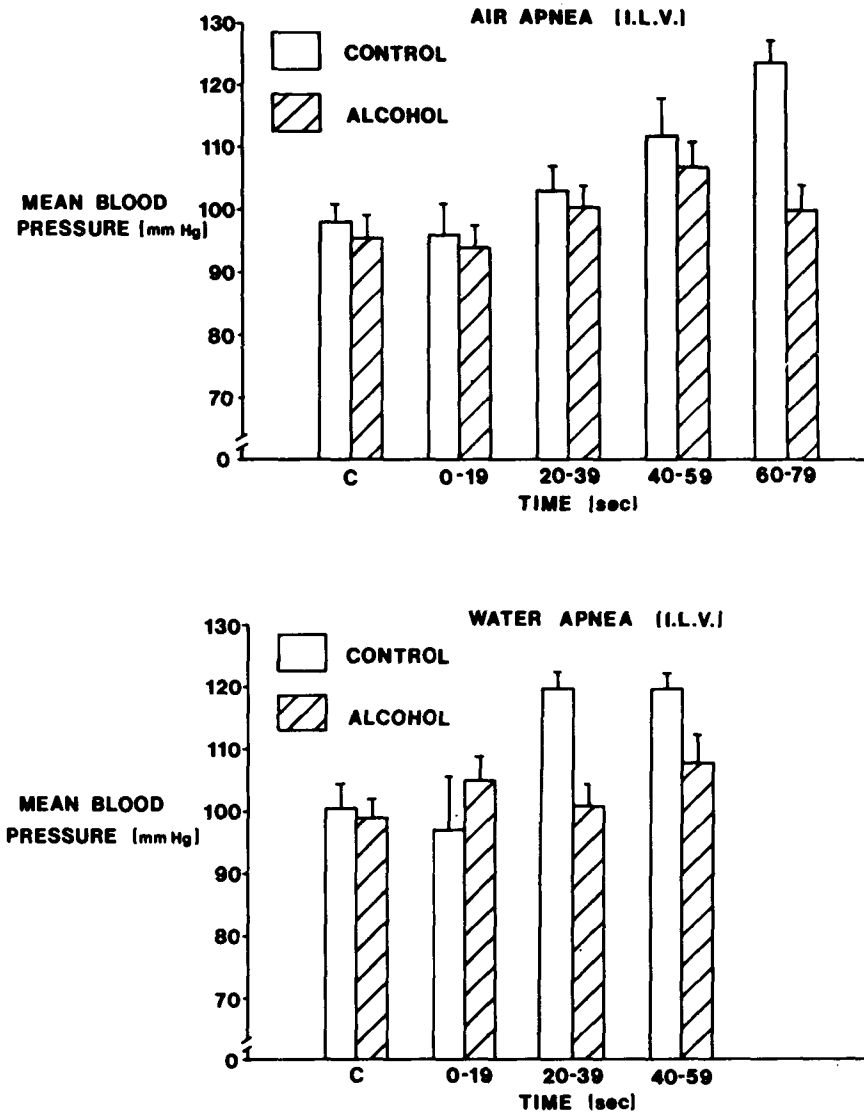
Fig. 2. Mean blood pressure changes at intermediate lung volume (ILV) for air and water apnea before and after alcohol consumption. *Bars* represent mean values of the 9 subjects. *Vertical lines* represent + 1 SEM.
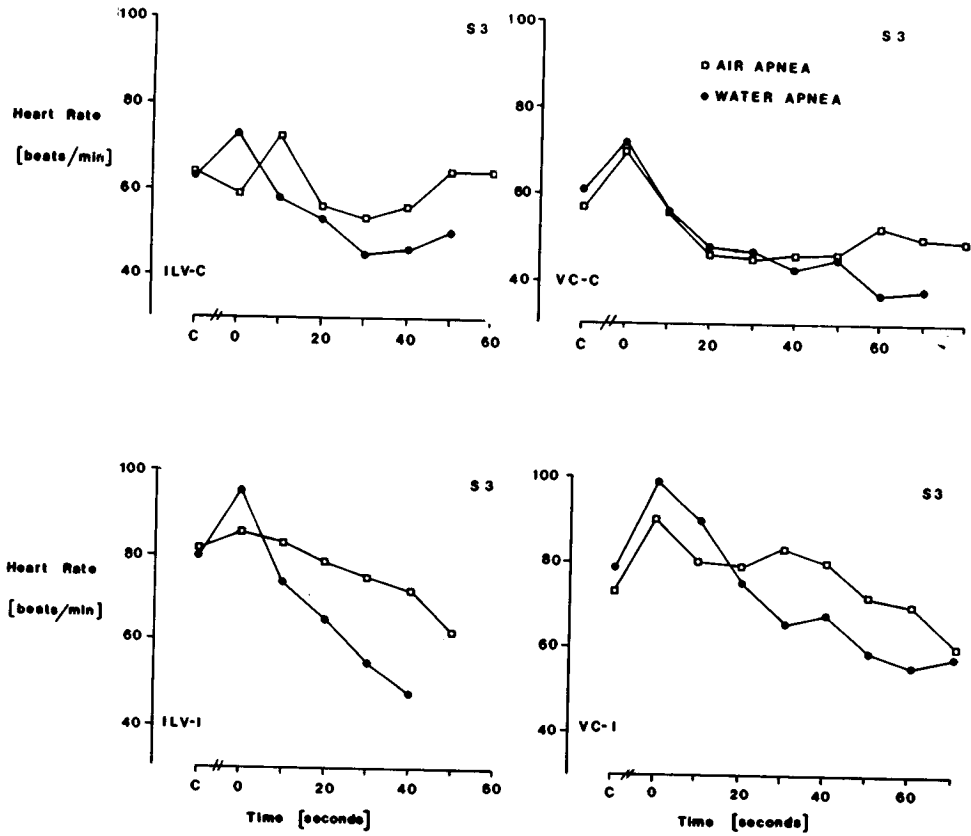
Fig. 3.   Heart rate responses of *Subject 3* (see Table I) to air and immersion apnea under four experimental conditions. ILV-C is at intermediate lung volume before alcohol consumption; ILV-1 is at intermediate lung volume after alcohol consumption. VC-C is at vital capacity before alcohol consumption and VC-1 is at vital capacity after alcohol consumption.
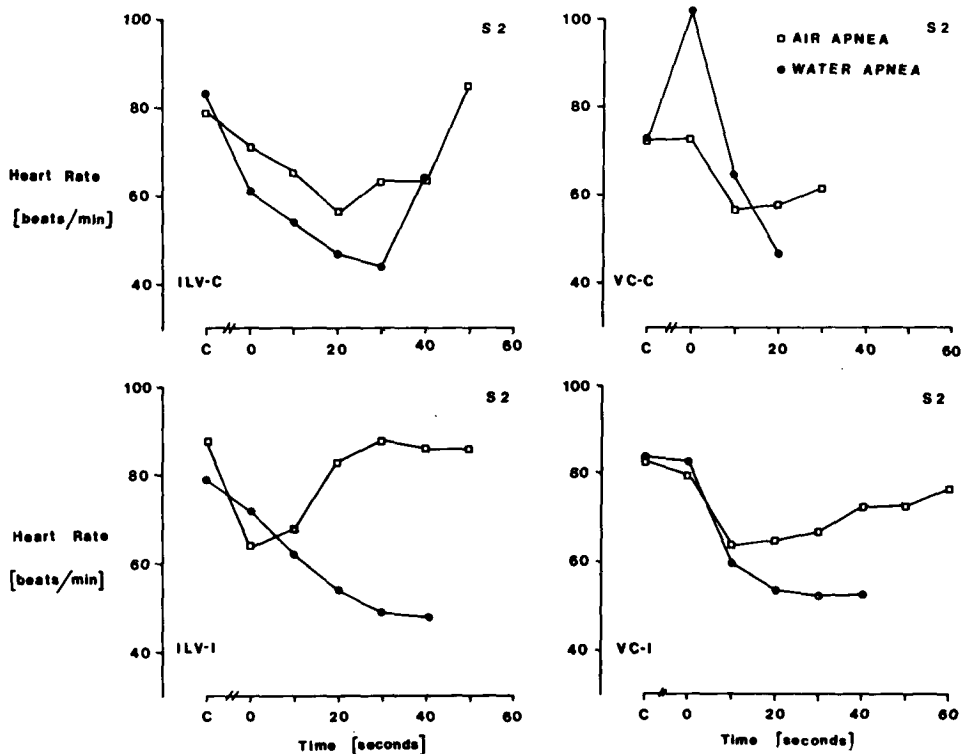
Fig. 4. Heart rate responses of *Subject 2* (see Table I) to air and immersion apnea under four experimental conditions. ILV-C is at intermediate lung volume before alcohol consumption; ILV-1 is at intermediate lung volume after alcohol consumption. VC-C is at vital capacity before alcohol consumption and VC-1 is at vital capacity after alcohol consumption.

variability in the diving reflex in man and much more information must be collected on this reflex before proper interpretation can be made.

Acknowledgment

References

1. Bert P. Leçon sur la physiologie comparée de la respiration. Paris: Baillère, 1870:526-553.
2. Irving L. Comparative anatomy and physiology of gas transport mechanisms. In: Handbook of physiology. Respiration, Vol. 1. Washington, DC: American Physiology Society, 1964:177-202.
3. Wolf S. The bradycardia of the dive reflex—a possible mechanism of sudden death. Trans Am Clin Climat Assoc 1964;76:192-200.

4. Anderson HT. Physiological adaptations in diving vertebrates. Physiol Rev 1966;46:212–243.
5. Hong SK, Moore TO, Seto G, Park HK, Hiatt WR, Bernauer EM. Lung volumes and apneic bradycardia in divers. J Appl Physiol 1970;29:172–176.
6. Openshaw PHM, Woodroof GMF. Effects of lung volume on diving responses in man. J Appl Physiol 1978;45:783–785.
7. Corriol J, Rohner JJ. Rol de la temperature de l'eau dans la bradycardie d'immersion de la face. Arch Sci Physiol 1968;22:265–274.
8. Campbell LB, Gooden BA, Horowitz JP. Cardiovascular responses to partial and total immersion in man. J Physiol 1969; 202:239–250.
9. Gooden BA. Drowning and the dive reflex in man. Med J Aust 1972;2:583–587.
10. Nemiroff MJ, Saltz GR, Weg JC. Survival after coldwater near-drowning: the protective effect of the diving reflex. Am Rev Respir Dis 1977;115:145.
11. Elsner R, Franklin DL, Van Citters RL, Kenny DW. Cardiovascular defense against asphyxia. Science 1966;153:941–949.
12. Brick I. Circulatory responses to immersing the face in water. J Appl Physiol 1966;21:33–36.
13. Pozos RS. Urban hypothermia of elderly, children, alcoholics, and handicapped. Panel discussion, International Hypothermia Conference and Workshop, Univ. of Rhode Island, Narragansett, RI, Jan. 23–27, 1980.
14. Winn R, Hildebrandt JR, Hildebrandt J. Semiautomatic blood pressure monitor utilizing an electronic sphygmomanometer. J Appl Physiol 1977;43:379–381.

PULMONARY FUNCTION IN DIVERS

M. Cimsit and V. Flook

Divers make up an increasingly important subgroup in the population seen by some medical practitioners, and there is now a need for evaluation of the "normal" values of important physiological measurements for the diving population. The ventilatory system more than any other is subject to continuous stress during diving, and therefore might be expected to show changes related to the diving history of the individual. At medical examination the diver is judged to be fit according to the standards set for the nondiving population, and there is growing evidence that these standards are not appropriate. In 1977 Crosby et al. (1) published data showing that the average forced expiratory volume in one second (FEV_1) for divers is 17% above predicted and the forced vital capacity (FVC) is 20% above predicted when compared with the Kory (2) prediction nomogram. The Crosby et al. (1) study did not include information that would allow examination of the results with reference to the individual's diving history. This report presents work designed to fill that gap.

METHODS

A total of 280 divers took part in this study, 227 commercial divers and 53 Royal Navy divers. CIRIA forms and the MRC questionnaire on respiratory symptoms were used to obtain information about the diver's medical, diving, and smoking histories. The weight, height, and age of each diver was recorded.

Measurements were made of vital capacity (VC), forced vital capacity (FVC), and forced expiratory volume in one second (FEV_1) using a Vitalograph. All measurements were made with the subject standing. The procedure was identical for all subjects: three deep breaths preceded the measurement of

VC, of which three recordings were made. This was followed by three recordings of FVC. Of the VC and FVC recordings made, those that lay within 200 mL of the maximum value were used in the calculation of an average value.

The Kamburoff nomogram (3) was used to find predicted values of FEV_1 and FVC for each diver. This nomogram was chosen for two reasons: it gives the closest agreement with more recent population studies, and it gives the highest predicted values compared with other nomograms in common use. For example, the Kory nomogram (2) gives predicted values 8–10% below the Kamburoff (3). Thus, use of the Kamburoff nomogram (3) would minimize apparent effects of diving.

From the basic measurements, five respiratory measurements were evaluated for each diver: FEV_1/FVC, $VC - FVC$, and three relating measured values (subscript a) to predicted values (subscript p) FEV_{1a}/FEV_{1p}, FVC_a/FVC_p, $(FEV_1/FVC)_a/(FEV_1/FVC)_p$.

RESULTS

The average values for 280 divers for FEV_1 were significantly higher than predicted by 4.2%. Forced vital capacity was significantly higher than predicted by 8.6% and FEV_1/FVC was 3% below predicted. All values were $P<0.001$. The average FEV_1/FVC was 81.5% and the mean $VC - FVC$ was 82 mL. The average age was 27.7 years and the average height 1.78 m.

Preliminary statistical analysis showed no significant difference between Royal Navy divers and commercial divers nor between smokers and nonsmokers; therefore, subsequent statistical analyses were carried out using all 280 divers as a single population.

Tables I and II show summaries of the results grouped according to the length of time that the subject had been diving (Table I) and according to the maximum depth to which the subject had dived (Table II).

The factors that may influence respiratory measurements can be listed as the age of the subject, height of the subject, number of years for which the

TABLE I

Summary of Results Grouped According to Length of Time Subject Had Been Diving

Duration (yr)	No. of Divers	Age Mean	$FEV_1/FVC\%$	$VC - FVC$	FVC_a/FVC_p	FEV_{1a}/FEV_{1p}	$\left[\dfrac{FEV_1}{FVC}\right]_a / \left[\dfrac{FEV_1}{FVC}\right]_p$
0.5	16	25.9	76.4	− 0.07	1.02	1.03	0.90
0.5–1	23	25.2	81.0	− 0.07	1.04	0.98	0.91
1–2	29	25.3	84.6	− 0.11	1.08	1.06	0.99
2–3	30	23.9	82.1	− 0.12	1.06	1.009	0.95
3–5	57	26.0	80.3	− 0.16	1.09	1.04	0.96
5–10	67	27.6	81.0	− 0.06	1.13	1.05	0.97
10–15	40	32.5	80.8	− 0.04	1.07	1.06	0.94
15+	17	38.7	79.3	0.01	1.06	1.02	0.97

TABLE II

Summary of Results Grouped According to Maximum Depth to Which
Subject Had Dived

Depth (m)	No. of Divers	$FEV_1/FVC\%$	$VC - FVC$	FVC_a/FVC_p	FEV_{1a}/FEV_{1p}	$\left[\dfrac{FEV_1}{FVC}\right]a/\left[\dfrac{FEV_1}{FVC}\right]p$
50	47	81.7	− 0.123	1.077	1.034	0.959
50–100	93	82.2	− 0.085	1.063	1.019	0.971
100–150	77	81.1	− 0.077	1.079	1.040	0.962
150+	63	80.8	− 0.080	1.086	1.081	0.960

subject has been diving, maximum depth to which the subject has dived, and whether or not the subject has done saturation diving. Of the five respiratory measurements under consideration, those that relate measured values to predicted values should be independent of age and height if the prediction nomogram is appropriate to the diving population.

Single regression analyses were carried out relating each respiratory measurement to age, length of time as a diver, and maximum diving depth. Student's t values were calculated for each correlation coefficient and the significance of the correlation coefficient evaluated, there being 278 degrees of freedom. Unpaired comparisons of means were used to compare divers who had experience of saturation diving with those who had not.

FEV_1/FVC

The correlation of this measurement with age was significant $(P < 0.001)$

$$FEV_1/FVC = 88.93 - 0.264 \times age \qquad (1)$$

The correlation with number of years as a diver was also significant $(P < 0.01)$

$$FEV_1/FVC = 82.78 - 0.196 \times years. \qquad (2)$$

FEV_{1a}/FEV_{1p}

This measurement increased significantly with increased maximum diving depth $(P < 0.01)$

$$FEV_{1a}/FEV_{1p} = 0.988 + 0.0004 \times depth \qquad (3)$$

where depth is in metres.

The mean value for divers who had saturation experience was 1.07 and was significantly higher (with $P < 0.01$) than the value of 1.023 found in divers without saturation experience.

FVC$_a$/FVC$_p$

This measurement increased significantly with increasing age ($P < 0.001$)

$$FVC_a/FVC_p = 0.928 + 0.005 \times age \qquad (4)$$

and with depth as shown in Fig. 1

$$FVC_a/FVC_p = 1.044 + 0.0003 \times depth \; P < 0.01. \qquad (5)$$

The mean value for divers with saturation experience was 1.10 and was significantly higher than the value 1.07 for those without saturation experience ($P < 0.02$).

(FEV$_1$/FVC)$_a$/(FEV$_1$/FVC)$_p$

No significant correlations were found and there was no difference between the average values for divers with or without saturation experience.

VC − FVC

This measurement increased with diver age ($P < 0.02$)

$$VC - FVC = -0.237 + 0.005 \times age \qquad (6)$$

and with number of years as a diver ($P < 0.001$)

$$VC - FVC = -0.126 + 0.006 \times years. \qquad (7)$$
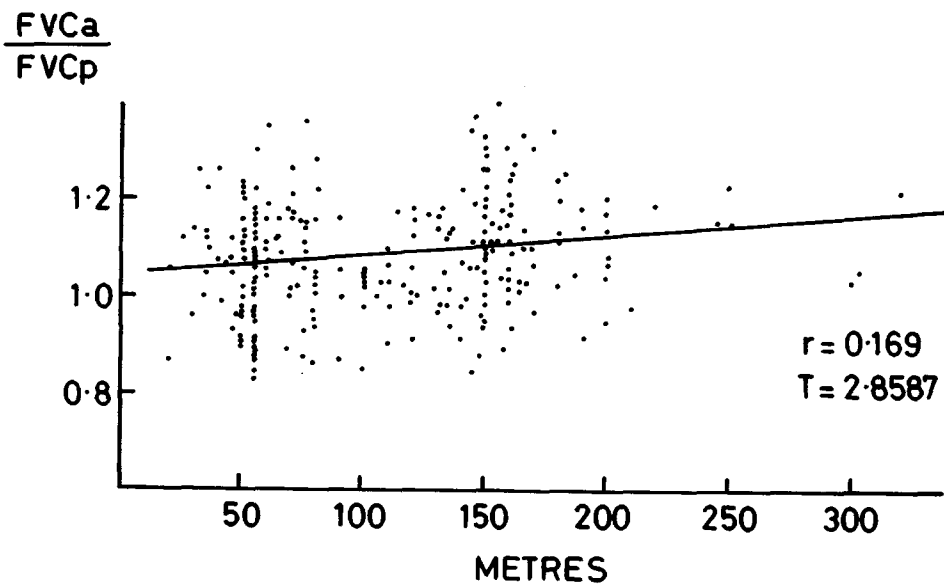
Fig. 1.   Forced vital capacity of the diver as a ratio of predicted forced vital capacity against the maximum depth at which the diver had worked.

In an attempt to evaluate the relative magnitude of the regressions, we carried out multiple regression analyses. This was necessary because, for example, the correlation of a respiratory measurement with age is not independent of the correlation of the same measurement with number of years as a diver. As seen from Table I, subjects with more diving experience are on average older than those with less diving experience. Likewise, those with saturation diving experience had dived to greater depths than those without and there was also evidence in the results that those who had been divers for longer had dived deeper.

Table III ranks the factors that could influence the respiratory measurements according to the standardized regression coefficient found from the multiple regression analyses. Column 1 represents the biggest standardized coefficient and column 5 the smallest. From this it can be seen that with the exception of VC − FVC, the coefficient for depth or saturation is bigger than that for number of years as a diver. The coefficients for age and height are larger for the measurements that do not involve nomogram predictions.

DISCUSSION

From the multiple regression analysis, it is seen that FEV_1/FVC, FEV_{1a}/FEV_{1p}, FVC_a/FVC_p, and $(FEV_1/FVC)_a/(FEV_1/FVC)_p$ correlate stronger with depth and/or saturation experience than with the number of years as a diver. The single regression analysis and statistical comparison of means show that the changes are significant for FEV_{1a}/FEV_{1p} and FVC_a/FVC_p. In addition to the strong correlation of VC − FVC with height, there is a strong correlation with number of years diving, and this is a statistically significant correlation.

Correlation with age and height are, as expected, more important for FEV_1/FVC and VC − FVC. The correlations of the other three respiratory measurements with age and height, though less important than correlations with diving experience, indicate that the nomogram is not entirely satisfactory for use for divers.

TABLE III

Relative Magnitude of the Standardized Coefficients From a Multiple Regression Analysis of the Respiratory Measurements with the Possible Influencing Factors*

Respiratory Measurement	1	2	3	4	5
FEV_1/FVC	height	age	saturation	depth	years
FEV_{1a}/FEV_{1p}	saturation	height	age	depth	years
FVC_a/FVC_p	depth	saturation	age	years	height
$(FEV_1/FVC)_a/(FEV_1/FVC)_p$	depth	saturation	age	height	years
VC − FVC	height	years	age	saturation	depth

*See text.

FEV₁ and FVC

Figure 2 shows lines describing the relationship of actual to predicted FEV₁ and FVC to age. The horizontal line at FEV₁ and FVC = 1.0 represents the predicted values from the nomogram normalized to 1.0. From this it is seen that the nomogram correctly predicts rate of change of FEV₁ with age, but underestimates FEV₁ at all ages above 20 years by 4.2%. In this study there were 11 subjects age 20 or less, and they had an average diving experience of 3 years. The nomogram underestimated FVC by 2.8% in the 20-year-old diver and by a further 5% for every 10 years. Thus, the nomogram could be used for divers if these corrections were made and if the population seen in this study is considered a representative sample of the diving population in terms of age and number of years as a diver.

The strongest correlations for FEV₁ and FVC are, however, with maximum depth of diving and saturation experience. The regression equations presented earlier show that the nomogram underestimates FEV₁ by 0.8% for divers whose maximum depth is 50 m and by a further 2% for every 50-m increase in depth. FVC is underestimated by almost 6% in divers with a maximum depth of 50 m and by a further 1.5% for every 50-m increase in maximum depth. The Kamburoff nomogram (3) can therefore be used if the predicted values derived from it are corrected appropriately for the diving history of the individual.
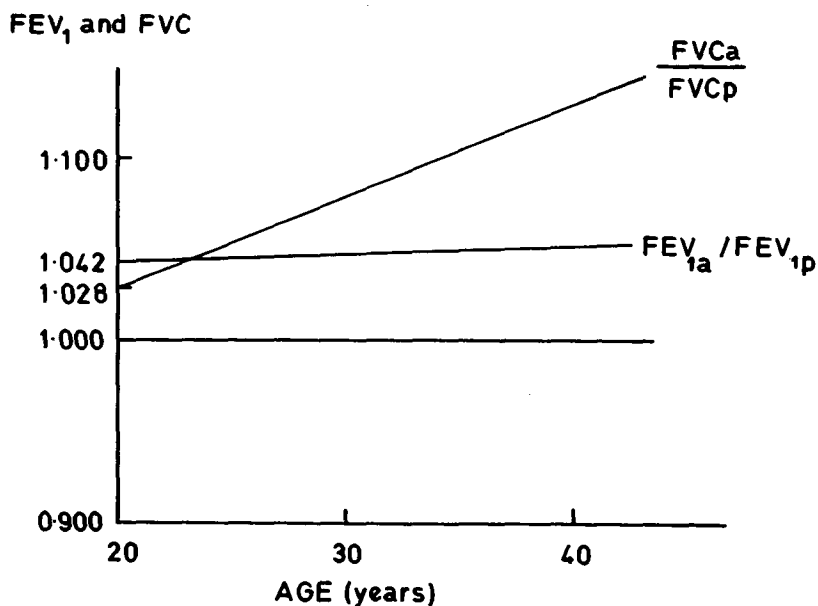
Fig. 2. Forced vital capacity and forced expiratory volume in 1 s as ratios of predicted volume compared with normalized predicted volumes.

VC − FVC

The strongest correlation with diving history and VC − FVC is with the number of years as a diver, and it is interesting that this measurement should in this way differ from the others. VC − FVC was evaluated because it is a simple measurement that could give early warning of small airway disease. Air trapping behind closed airways happens during maximum expiratory effort and may happen in the early stages of lung elastic tissue degeneration and will be enhanced by any degree of airway narrowing. As the trapping will not occur during a measurement of vital capacity, it should be detected as a volume difference between VC and FVC. This is not the most sensitive test for air trapping but it is worth using in a large population study.

The results show that the difference between VC and FVC increases steadily with years of diving experience and with age but not significantly with diving depth. This would suggest that probably we have seen only the normal changes that occur in the aging lung and not changes attributable to diving.

CONCLUSIONS

The Kamburoff nomograms (3) can be used for predicting values for FEV_1 and FVC if corrections are made to the values either according to the number of years for which the individual has been a diver or, and this would be the preferred technique, according to the maximum depth to which the individual dives. The Kory nomogram (2) would require bigger corrections. Predictions from other nomograms would have to be corrected with reference to the Kamburoff nomogram.

Inasfar as the measurement VC − FVC is an indication of lung tissue degeneration, the changes seen in this study can be explained by the normal aging process and may not be a result of diving. Only a small proportion of divers taking part in this study had dived beyond 200 m; it may be that those who dive to greater depths will show greater changes as the years go by.

References

1. Crosby WA, Clarke MB, Cox RAF, et al. Physical characteristics and ventilatory function of 404 commercial divers working in the North Sea. Br J Ind Med 1977;34:19–25.
2. Kory RC, Callahan R, Boren HG, et al. The Veterans Administration–Army Cooperative Study of Pulmonary Function. I. Clinical spirometry in normal men. Am J Med 1961;30:243.
3. Kamburoff PL, Woitowitz HJ, Woitowitz RH. Prediction of spirometric indices. Respir News Bull 1973;17:9–13.

FREQUENCY AND REGULATION OF HEART RATE DURING OPEN-SEA SATURATION DIVING

S. M. Gosŏvić and A. I. Radović

From the time of the GENESIS program until the present, many saturation dives have been simulated in hyperbaric chambers, and famous projects like CONSHELF, Man-in-the-Sea, and SEALAB have been carried out from an underwater habitat in the open sea. Offshore, commercial divers have spent thousands of hours in saturation diving. From 1967 to 1970 U.S. Navy divers alone completed over 200 saturation and subsaturation dives to depths of 850 ft (259 m) which in itself shows the importance and expansion of this diving method (1–3).

During this period, only a few open-sea saturation dives included continuous monitoring of various physiological data.

In the course of our study, cardiorespiratóry data, standard hematological and biochemical analyses, as well as measures of urinary excretion of corticosteroids and catecholamines were taken. In this report we present the results from collected data regarding heart rate frequency and instantaneous pulse rate during rest and dynamic exercise on an ergocycle as well as during sleep.

MATERIALS AND METHODS

Saturation diving was performed from a rescue vessel equipped with a deep diving system consisting of a three-compartment DDC, diving bell, and handling system. Heart rate and instantaneous pulse rate recordings were made during compression, 80-h saturation at 100 m with excursion to 120 m, 104 h of decompression, and at normobaric conditions before and after saturation diving.
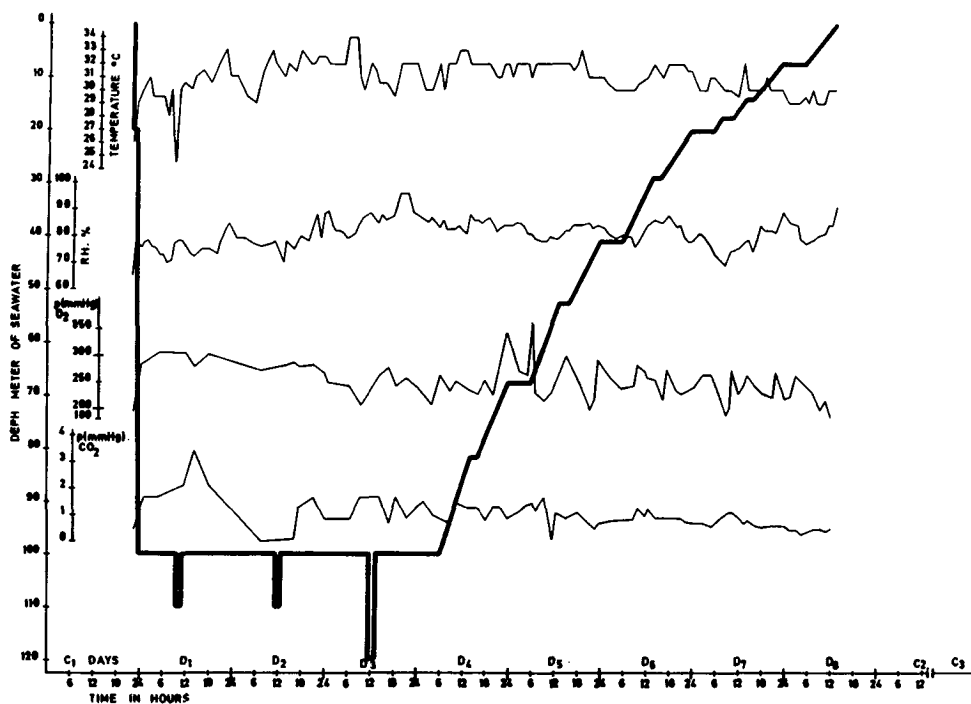
Fig. 1. Diving profile and habitat environmental data.

Subjects

Four healthy, male, experienced divers aged 26–27 years were the subjects of this research. This was their first open-sea saturation dive. They were chosen from among a group of divers with similar experience. During the subject selection process, special emphasis was placed on a subject's psychosomatic state, diving experience, and motivation.

Procedures

This investigation included predive (C1) and postdive control periods (C2), 80-h bottom time at 100 m with excursions to 120 m (D1, D2, D3), and decompression lasting 104 h (D4–D8). During the control period and saturation, heart rate frequency and instantaneous heart rate were registered on an 8-channel Beckman Dynograph RN biomedical recorder. The electrocardiogram and instantaneous pulse rate were recorded from 8:30 to 10:30 a.m. and from 5:00 to 7:30 p.m. Recordings in the morning were made with divers in a sitting position. Recordings in the afternoon were made during a 5-min exercise on an ergocyle with a load of 147 watts, followed by a 7-min recovery period. During decompression, we did not record physiological measurements during
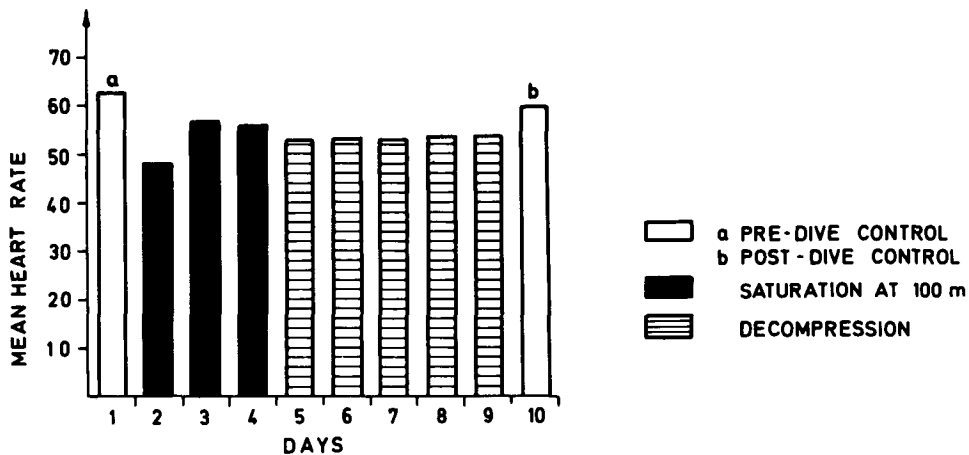
Fig. 2.   Average frequency of heart rate in divers who had bradycardia.

exercise; recordings were made during rest periods only. Every night during sleep, from 10 p.m. to 6 a.m. the following morning, ECG and instantaneous pulse rate were continously recorded alternately for each diver.

Obtained data were processed by standard statistical procedures. An average pulse rate for each diver and for each period was calculated from the ECG traces. Histographic analyses of the instantaneous heart rate were made by application of a modified form of the Parin-Baeviski method (4). The average frequency of heart rate during sleep was calculated from recordings taken during the first 10 min of each hour. An average histographic curve of instantaneous heart rate that covered a complete 8-h observation (control) period was established.

During bottom time and decompression, the average habitat temperature was 30.98 ± °C; humidity varied between 65 and 95%, with an average value of 81.01 ± 5.04%. Oxygen partial pressure varied between 183 and 363 mmHg, with an average value of 248.5 ± 30.9 mmHg. Average P_{CO_2} was 0.964 ± 0.536 mmHg.

RESULTS

Average heart rate frequency and the histographic curve of instantaneous pulse rate will be described according to these stages: in normal and hyperbaric conditions, during rest and exercise, and throughout sleep.

Average Heart Rate During the Rest Period

Under hyperbaric conditions bradycardia appeared during rest in three of the four divers. An average decrease in heart rate varied from 24.53% the first day under 100 m pressure to 9.9% the second day after decompression had
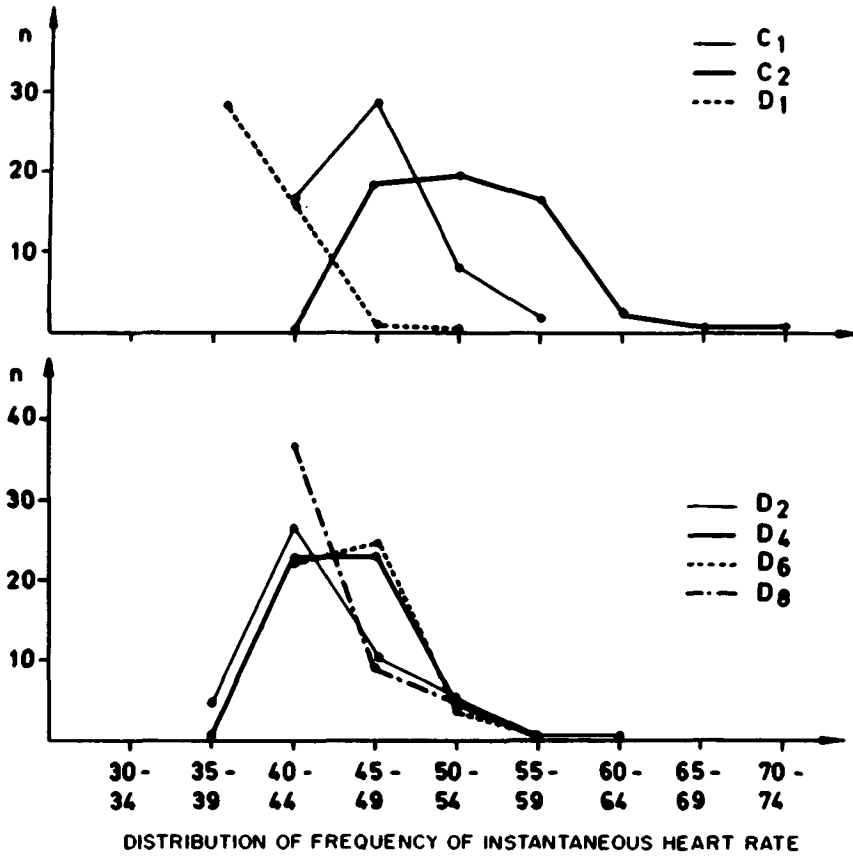
Fig. 3.   Instantaneous heart rate of *Diver PM* under control conditions (C1, C2) and under pressure (D1–D8).

TABLE I

Diver Heart Rate Frequency During Rest Periods

Diver	Day/Phase									
	2	4	5	6	7	8	9	10	11	12
	K1	D1	D2	D3	D4	D5	D6	D7	D8	K2
MM	60.8	64.2	73.0	86.8	65.6	61.8	65.8	69.0	63.8	56.4
ŠD	67.8	50.0	67.2	59.6	57.4	59.6	62.6	60.0	59.0	54.6
RD	67.8	49.4	53.6	59.4	58.0	51.6	51.4	52.4	58.2	69.6
PM	55.2	44.7	51.0	49.2	50.4	50.0	50.0	50.4	46.0	56.2
Mean $n-4$	62.9	52.1	61.2	63.7	56.3	55.7	57.4	57.9	56.7	59.2
Mean $n-3$	63.6	48.0	57.3	56.1	53.3	57.1	54.7	54.3	54.4	60.1

begun. The average decrease in the pulse rate of these divers was 15.41% at maximum pressure and 14.47% throughout the entire stay under pressure.

This phenomenon was not observed in *Diver MM*. At bottom time his pulse rate increased when compared to control conditions: 6.5% on the first day, 17.8% on the second day, and 30.9% on the third day. Hyperbaric bradycardia is even more evident in the histographic curves of the instantaneous pulse rate of *Diver PM* and on the average histographic curve for the divers who had experienced bradycardia. It should be added that the peaks of the histographic curves of instantaneous pulse rate of divers who had bradycardia varied between 35–39 and 54–59 beats/min under hyperbaric conditions, as compared to normal conditions when peaks were between 45–49 and 60–64 beats/min.

Heart Rate Frequency During Exercise

Variation of heart rate frequency during exercise at normal pressure and in a hyperbaric environment is shown in Table II.

Table II with Fig. 5 indicate that the heart rate during exercise under hyperbaric conditions is markedly slower when compared to the pulse rate during the same exercise at normal pressure.

The average decrease in the heart rate of divers who experienced bradycardia during exercise was 17.5% when compared to exercise in a normal environment. Histographic curve peaks ranged between 130 and 134 beats/min under control conditions, under hyperbaric conditions they were between 100 and 104 beats at 100 m, and they markedly shifted the histographic curve to the left.

Heart Rate Frequency During Sleep

It was observed that all aquanauts, even *Diver MM*, who had not experienced hyperbaric bradycardia during rest, showed a further decrease in heart

TABLE II

Heart Rate During Exercise

Diver	Exercise at 147 watts			
	K1 (0 m)	D1 (100 m)	D3 (100 m)	K2 (0 m)
MM	138	123	132	117
PM	119	98.7	99.3	131
ŠD	118	104.7	106	131
RD	135	109		120
Mean $n-4$	127.5	108.8	112.4	124.7
Mean $n-3$	124	101.7	102.6	127
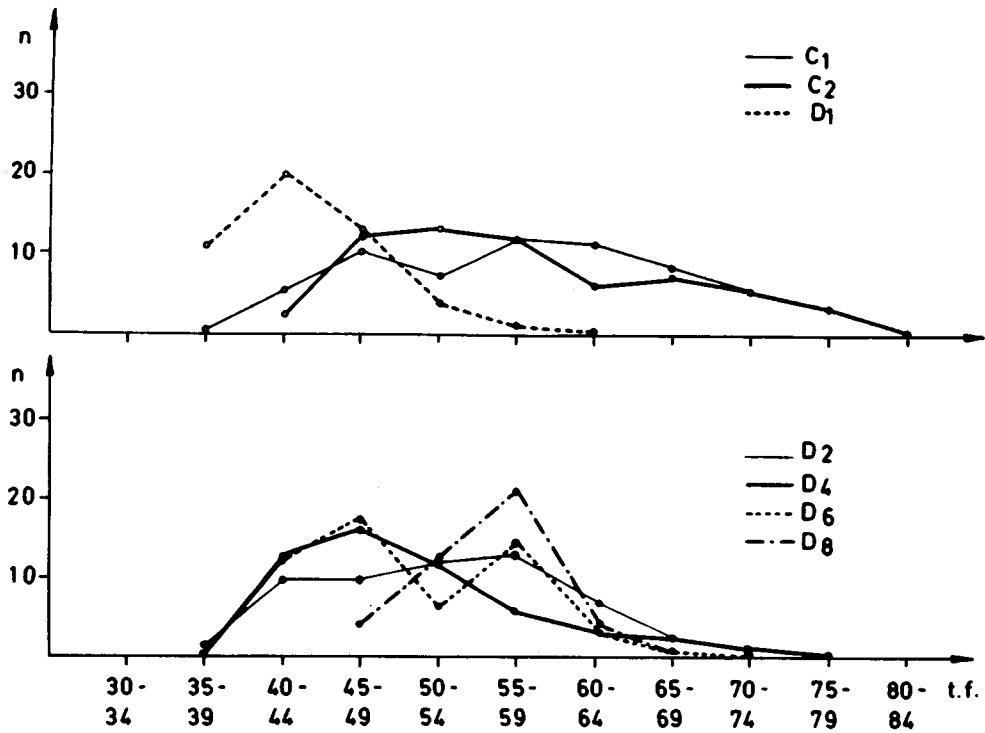
DISTRIBUTION OF FREQUENCY OF INSTANTANEOUS HEART RATE

Fig. 4.   Average instantaneous heart rate of divers who experienced bradycardia.

rate (on the average) during sleep, when compared to the pulse rate recorded the previous morning.

A typical relationship between heart rate frequency under normal conditions before (C1) and after saturation (C2) and under hyperbaric conditions during the day and sleep are shown on cardiotachographic traces of *Diver PM*.

DISCUSSION

It has often been demonstrated and proved that rate frequency decreases in a hyperbaric environment (5). This hyperbaric bradycardia has been present when subjects breathe air, and particularly oxygen, in a hyperbaric environment (5,6). Moreover, moderate bradycardia temporarily persists during the period after which oxygen is switched off and the divers return to normal pressure (6,7). Bradycardia also appears during breath-holding, both underwater and when just the face is submerged. Relative bradycardia is also present
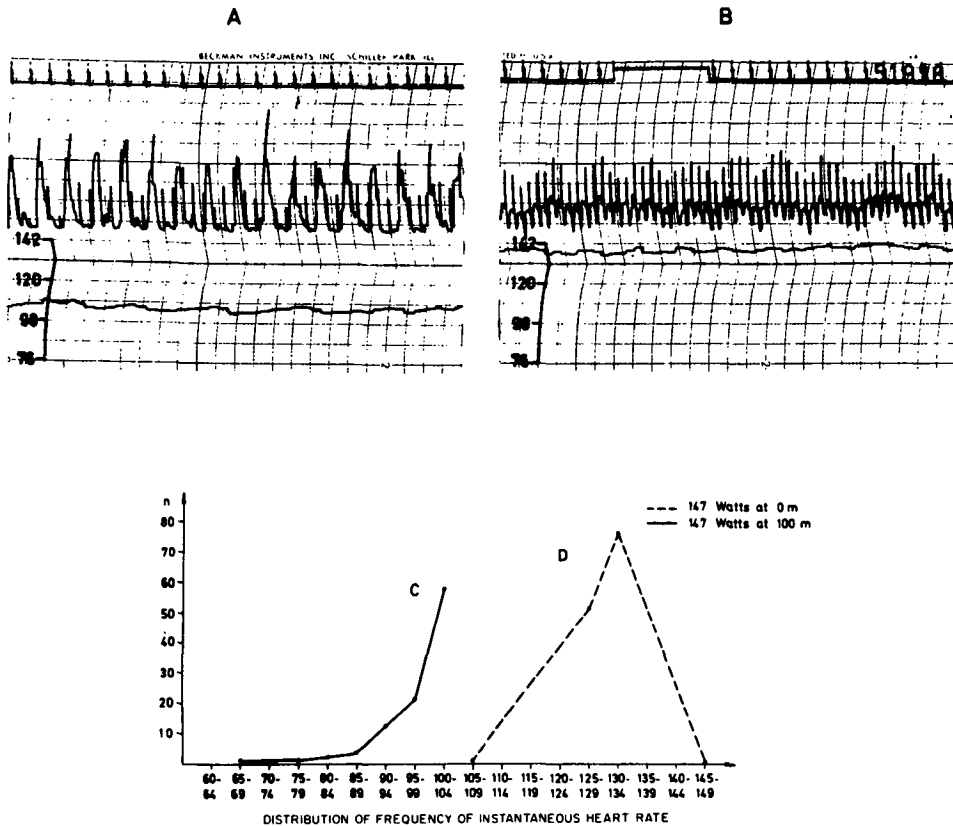
Fig. 5. ECG and cardiotachogram of *Diver PM* during exercise at (B) and 100 m (A) and histographic
curves of instantaneous heart rate obtained from above cardiotachogram trace (D,C).

when the subject performs exercise and breath-holding simultaneously, e.g.,
apnea when the subject walks on a treadmill (8,9).

Hyperbaric bradycardia is an inconsistent finding during exposure in a he-
lium atmosphere. In cases when it does appear, it is not equally manifested in
all the exposed subjects (10–18).

Pronounced bradycardia in three of the four divers, as described in our
study, has been established by Bradley et al. at 19.2 atm (10). Similar results
have been obtained by Bennett at 1000 ft (11), Smith et al. at 580 ft (18),
and, in particular, Nakayama et al. during saturation at 7 ATA (16). As in our
investigation, Bennett, Smith, and Nakayama et al. have established that bra-
dycardia is more pronounced at the beginning of stay at maximum pressure,
thereafter heart rate successively increases, but remains slower than in pre- and
postdive control periods (11,18,16).

Lemaire et al. (15) have not found hyperbaric bradycardia in aquanauts
exposed to 500 m nor have Egava et al. (13) in experimental saturation diving
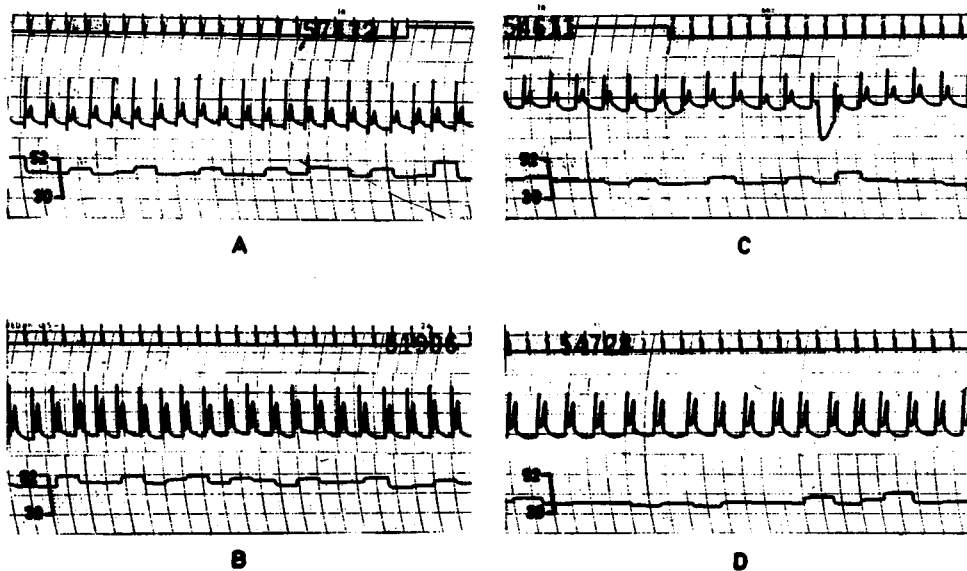
Fig. 6. Typical cardiographic traces before dive (A), after dive (B), and under hyperbaric conditions during daytime (C) and sleep (D).

at 25 and 45 atm. Moreover, Lemaire et al. (15) recorded a certain increase in heart rate under the above described hyperbaric condition.

The finding similar to that presented in this study, i.e., a markedly slower pulse rate during exercise in a hyperbaric environment when compared to the same exercise under normobaric conditions, has also been reported by Bradley et al. (10), Hamilton (14), and Lemaire et al. (15).

Although bradycardia has been established in many human hyperbaric exposures, the underlying mechanism and its significance remain unknown. The generally prevailing opinion is that many factors contribute to this phenomenon, which is probably due to cold, pressure and increased gas density, effect of hyperoxia, and lack of activity within the limited and overcrowded space (17,18). Hesser (19) and Smith (17) have demonstrated that moderate hyperoxia and cold, respectively, have little effect on hyperbaric bradycardia.

Histographic analyses of the instantaneous heart rate of three out of four divers show that the curves pronouncedly shift to the left toward the direction of bradycardia. This finding supports the opinion of the vagal origin of hyperbaric bradycardia. This vagal influence is more pronounced during the first 24 h of exposure under pressure; in the course of further exposure, the vagal influence progressively weakens. Such a trend supports the opinion that this phenomenon would probably disappear if a diver were exposed for a sufficiently prolonged period of time (11,16).

Further slowing of the pulse rate during sleep demonstrated that the human organism, even under unnatural hyperbaric conditions, retains a regular circadian rhytmn. ,

Results shown in this paper, as well as those reported by other investigators, indicate that the human organism, even during exercise under hyperbaric conditions, reacts with tachycardia. Moreover, in this condition, there exists a quantitative difference, because the increase in heart rate at the same level of physical effort is significantly lower. Histographic analysis of the instantaneous pulse rate curve also demonstrated that under hyperbaric conditions there exists a difference in the manner of regulating heart rate frequency. During exercise under normal conditions, histographic curves present entirely within the sympathicotonic area. On the contrary, under hyperbaric conditions, these curves are irregular, showing the most realization in the area of relative tachycardia, while a certain amount of realization is present within the normal sphere of influence of the vegetative system. These curves indicate that under hyperbaric conditions, certain factors regarding the regulation of heart rate frequency are attenuated or missing. For the present, these factors remain unknown. This supposition also supports the fact that the form of most of the histographic curves composed from traces of instantaneous pulse rate during rest under hyperbaric conditions is similar to the curve composed during exercise.

Acknowledgment

References

1. Manzzon UF. Fiziologičeskoe sostojanie ĕkipaža "Silab-2". In: Podvodnaja laboratorija "Silab-2" (Man's extension into the sea). Leningrad: Sudostroenie, 1968:96-106.
2. Bradley ME, Vorosmarti J Jr. Hyperbaric arthralgia during helium-oxygen diving from 100 to 850 fsw. Undersea Biomed Res 1974;2:151-167.
3. Delauze HG, Bender C. Technologie de la plongée. In: La plongée profond. Paris: ed. Technique, 1971:147-184.
4. Parin VV, Baevski RM, Volkov JN, Gazenko OG. In: Kosmičeskaja Kardiologija. Leningrad: Medicina, 1967:64-84.
5. Bean JW. Effects of oxygen at increased pressure. Physiol Rev 1945;25:2-169.
6. Gošović SM, Radović AI. Some cardiorespiratory effects of oxygen toxicity. In: Shilling CW, Beckett MW, eds. Underwater physiology. Proceedings of the sixth symposium on underwater physiology. Bethesda, MD: Federation of American Societies for Experimental Biology, 1978:205-214.
7. Donald KW. Oxygen poisoning in man, Part I. Br Med J 1947;24:712-717.
8. Paulev PE, Hansen HG. Cardiac response to apnea and water immersion during exercise in man. J Appl Physiol 1972;33:193-198.
9. Gošović SM, Marisavljević T, Stor J. Utjecaj ambijentalnih uvjeta na trajange i dinamiku pulsa inspiratorne apneje—Influence of environmental conditions upon the duration and pulse rate dynamics during inspiratory breath-holding (English summary). In: Pomorska medicina. Beograd: Mornarički glasnik, 1975:477-488.
10. Bradley ME, Anthonisen NR, Linaweaver PG. Respiratory and cardiac response to exercise in subjects breathing helium-oxygen mixture at pressure from sea level to 19.2 atmospheres. In: Lambertsen CJ, ed. Underwater physiology. Proceedings of the fourth symposium on underwater physiology. New York: Academic Press, 1971:325-357.
11. Bennett PB. Some physiological measurements during human saturation diving to 1500 ft. In: Third international conference of hyperbaric and underwater physiology. Paris: Doin, 1969:35-43.

12. Bühlmann AA, Mathis E, Overrath G, Bennett PB, Elliott DH, Gray SP. Saturation exposures at 31 ATA in an oxygen-helium atmosphere with excursions to 36 ATA. Aerosp Med 1970;4:394-402.

13. Egava N, Gelend R, Hammond RE, Lambertsen CJ. Cardiac, electrical, and mechanical function. In: Lambertsen CJ, ed. Work capability and physiological effects in He-O$_2$ excursions to pressures of 400-800-1200 and 1600 fsw—Predictive studies IV. Philadelphia: Institute for Environmental Medicine, University of Pennsylvania, 1978:E13-1-E13-57.

14. Hamilton RW Jr. Physiological responses at rest and exercise during saturation at 20 atmospheres of He O$_2$. In: Lambertsen CJ, ed. Underwater physiology. Proceedings of the third symposium on underwater physiology. Baltimore: Williams & Wilkins Co, 1967:361-374.

15. Lemaire C, Rostain JC, Bergonzi M. Frequences cardiaques au repos et pendant le travaill musculair au cours d'une saturation a 500 metres (50,68 ATA) in hyperoxie moderée (Sagitair II). Bull MEDSUBHYP 1973;9:7-13.

16. Nakayama H, Matsuda M, Itoh A, et al. Physiological functions during 10-day heliox saturation dive to 7 ATA. In: Shilling CW, Beckett MW, eds. Underwater physiology. Proceedings of the sixth symposium on underwater physiology. Bethesda: Federation of American Societies for Experimental Biology, 1978:99-105.

17. Smith RM. Cardiovascular functions during saturation diving. In: Hong SK, ed. Man in the sea. Bethesda, MD: Undersea Medical Society, 1975:112-123.

18. Smith RM, Hong SK, Dressendorfer RH, Dwyer HJ, Hayashi E, Velverton C. Hana Kai II: a 17-day dry saturation dive at 18.6 ATA. IV. Cardiopulmonary functions. Undersea Biomed Res 1977;3:276-282.

19. Hesser CM, Fagraeus L, Linnarsson D. Cardiorespiratory responses to exercise in hyperbaric environment. Proc Int Union Physiol Sci 1959;7:191.

INFLUENCE OF THE INSPIRATORY EFFORT AND SWALLOWING ON THE CARDIOVASCULAR RESPONSE TO SIMULATED DIVING AND BREATH-HOLDING

T. F. Huang and C. T. Peng

The characteristic cardiovascular responses to diving are well known (1–7). It has been reported that reflex bradycardia during diving is reduced by swallowing and by an inspiratory effort against a closed glottis (8). Apparently swallowing or inspiratory efforts can modify diving bradycardia, but their effect on the reflex vasoconstriction remains to be clarified.

Our previous study (9) showed that bradycardia appeared during face immersion and breath-holding, but not during the Valsalva maneuver, while vasoconstriction occurred in response to each of them. The present study attempted to analyze the modification of the cardiovascular response to face immersion and breath-holding by an intervention of the inspiratory effort or swallowing.

METHODS AND MATERIALS

Twenty-one healthy male subjects, aged 22–27 years, volunteered for the experiments. The experimental procedures were similar to those of our previous study (9). Briefly, a subject was seated leaning forward and holding his breath for 30 s during either normal inspiration or expiration. After a rest period of 3–5 min with normal respiration, he was asked to hold his breath again during which time an inspiratory effort was made against a closed glottis (i.e., Müller maneuver) or swallowing. After another rest period, he immersed his face for 30 s in a basin of water at room temperature (23–28°C). Finally, he

repeated face immersion during which either swallowing or the inspiratory effort was performed. During these processes, a photoelectric plethysmographic transducer (Grass PTTI–6) was placed on the tip of the index finger. A pneumatic cuff connected to a Statham P23 DA pressure transducer was placed around the chest. The finger plethysmogram (PGM), the respiratory exertion, and ECG lead 2 were monitored on a Grass model-7 polygraph. Heart rate was counted from the ECG tracings. The data were analyzed with the paired t test.

RESULTS

The response of heart rate and the finger plethysmogram to face immersion and breath-holding are presented in Table I. During face immersion for 30 s, bradycardia developed in 19 of 20 subjects. Heart rate decreased from 77.7 ± 3.5 beats/min (bpm) (mean ± SE) to 64.3 ± 2.9 bpm ($P < 0.001$, $n = 20$). Infrequently did we observe remarkable sinus arrhythmia or atrial and ventricular premature contractions. When an inspiratory effort was performed during face immersion, bradycardia was attenuated in 6 cases, but heart rate still decreased from 76.2 ± 2.6 bpm to 70.7 ± 2.8 bpm ($P < 0.001$, $n = 20$). When swallowing was performed during face immersion, bradycardia did not develop in 9 cases. The heart rate was 75.8 ± 2.8 bpm during the control period and 72.0 ± 3.0 bpm (NS, $n = 20$) during face immersion intervened by swallowing. However, vasoconstriction of the finger tip

TABLE I

Modification of Heart Rate and Finger Plethysmogram (PGM) in
Response to Face Immersion and Breath-Holding by the Inspiratory
Effort or by Swallowing

Number of Subjects	Procedure	Heart Rate (bpm)			Finger PGM (mm)		
		Before	During	After	Before	During	After
20	Face Immersion	77.7 ±3.5	64.3‡ ±2.9	75.7 ±2.6	12.9 ±1.2	9.1† ±0.9	16.0* ±7.2
	+ Inspiratory Effort	76.2 ±2.6	70.7‡ ±2.8	74.4 ±2.7	11.8 ±1.1	7.9‡ ±0.9	14.3* ±1.6
	+ Swallowing	75.8 ±2.8	72.0 ±3.0	73.8 ±2.4	12.5 ±1.2	9.3‡ ±1.0	15.9* ±1.9
21	Breath-holding	78.8 ±2.8	74.2† ±3.2	79.0 ±2.8	13.8 ±1.6	10.0‡ ±1.1	15.0‡ ±1.9
	+ Inspiratory Effort	79.2 ±3.3	80.0 ±3.1	79.0 ±3.2	12.3 ±1.1	8.9‡ ±0.9	14.9† ±1.6
	+ Swallowing	76.7 ±2.8	79.0 +2.9	76.2 ±2.8	14.2 ±1.2	9.4‡ ±0.8	16.0* ±1.8

Values are mean ± SE.   *$P < 0.05$ †$P < 0.01$ ‡$P < 0.001$ vs. control.

during immersion was not affected by these interventions. After immersion, heart rate recovered rapidly and remarkable vasodilation of the finger tip appeared in a few seconds.

During breath-holding for 30 s, heart rate decreased from 78.8 ± 2.8 bpm to 74.2 ± 3.2 bpm ($P < 0.01$, $n = 21$). When a inspiratory effort was made against closed airways or swallowing was made during breath-holding, heart rate did not slow down, while the vasoconstricting response of the finger tip was not affected by these interventions (Table I). Figure 1 shows a typical response in which bradycardia during breath-holding or face immersion was attenuated by either the inspiratory effort or swallowing, while the vasoconstricting response was affected very little.
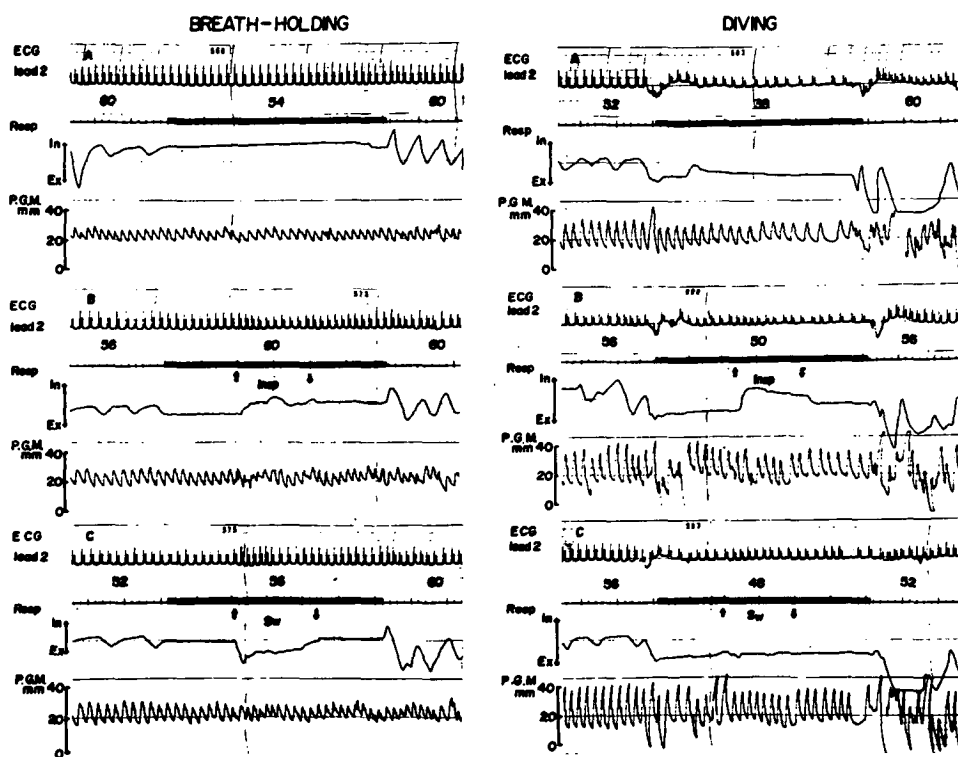
Fig. 1. Influence of swallowing and the inspiratory effort on the cardiovascular responses to breath-holding and diving in a healthy young subject. Tracings from the *top* in each panel: ECG, time mark (superimposed by signal), respiration, and finger plethysmogram (PGM). Numerical figures under *top tracing* are heart rate in bpm. *Arrows* under signal indicate swallowing or an inspiratory effort.

Breath-holding: A) Heart rate decreased from 60 to 54 bpm during breath-holding; B) Decrease in heart rate during breath-holding was eliminated by an inspiratory effort (*between arrows*); C) Bradycardic response during breath-holding was eliminated by an intervention of swallowing (*between arrows*).   Finger plethysmogram during breath-holding was not affected by either swallowing or inspiratory effort.

Diving: A) Heart rate decreased from 52 to 38 bpm during diving; B) Bradycardia during diving was attenuated by the inspiratory effort (*between arrows*); C) Bradycardia during diving was attenuated by swallowing (*between arrows*).   Finger plethysmogram during diving was barely affected by an intervention of either swallowing or inspiratory efforts.

DISCUSSION

Characteristic cardiovascular adjustment to diving has been well established. The reflex bradycardia associated with diving appears to depend upon different mechanisms in various species of animals. Respiratory-related cardiovascular reflexes are involved in both the initiation of and recovery from the cardiovascular response to diving (10). It has been generally accepted that submersion of the nares initiates the diving reflex and produces apnea and bradycardia (5); in addition, stimulation of the chemoreceptors by gradual development of hyperpnea and hypoxia reinforces the fully developed response (11). Other types of receptors such as those in beaks of ducks (5), proprioceptors in thorax (12), and cold receptors of skin (13,14) may initiate the reflex.

Other findings conclude: the principal determinant of the bradycardic response appears to be with a cessation of respiration (15). Apparently diving bradycardia can be modified by respiration or swallowing. Bradycardia during face immersion was reduced when an inspiratory effort against a closed glottis was performed (8). Swallowing is known to evoke transient tachycardia and can reduce diving bradycardia. Swallowing also can activate respiratory neurons without causing an accompanying distortion of the lungs and can reduce reflex bradycardia. However, a report that denervation of the lung eliminated the inspiratory modification of the reflex bradycardia indicates that the intrapulmonary receptor plays an important role in the reflex: the bradycardia evoked by baro- and chemoreceptor reflexes is mediated by the vagus and modulated by the respiratory cycle (16). The respiratory modulation of reflex bradycardia can be attributed to two mechanisms: one, an inhibitory effect on the reflexes arising from the activity of inspiratory neurons in the central nervous system (17,18); and two, a further inhibitory effect arising from the excitation of intrapulmonary receptors (16). The postulation was made that both central and peripheral inhibitory mechanisms operate together. However, it seems possible that cortical influence can modulate the bradycardic response to diving, because in an alarming or panicky condition diving bradycardia may disappear (7).

The present study shows that swallowing or inspiratory effort reduced diving bradycardia, but not the finger vasoconstricting response. The intervention of swallowing or an inspiratory effort during breath-holding eliminated bradycardia. Further, the vasoconstricting response to breath-holding was not eliminated by swallowing or by an inspiratory effort. Our previous study (9) showed that the Valsalva maneuver could induce a remarkable vasoconstriction, but did not reduce heart rate. The response to the Valsalva maneuver can be attributed to an increase in intrathoracic pressure resulting in a decrease of cardiac output. On the other hand, the Müller maneuver decreased the intrathoracic pressure. Nevertheless, both maneuvers evoked a vasoconstricting response, although they exerted an opposite effect on the intrathoracic pressure.

The possible occurrence of arrhythmia during diving or breath-holding (2,19,20) has been reported. The present study observed that an intervention with swallowing or inspiratory efforts during diving or breath-holding modified

the bradycardic response, but it did not evoke severe arrhythmia in healthy subjects. Further, swallowing or inspiratory efforts could attenuate the reflex bradycardia, but not the vasoconstricting response to diving in human subjects. In contrast, elimination of bradycardia by atropine in rats attenuated the vasoconstricting response during diving (9).

References

1. Scholander PF. Physiological adaptation to diving in animals and in man. Harvey Lecture 1961;57:93-110.
2. Scholander PF, Hammel H-T, LeMessurier H, Hemmingen E, Garey W. Circulatory adjustment in pearl divers. J Appl Physiol 1962;17:180-190.
3. Irving L. Bradycardia in human divers. J. Appl Physiol 1963;18:489-491.
4. Andersen HT. Physiological adaption in diving vertebrates. Physiol Rev 1966;46:212-243.
5. Andersen HT. The reflex nature of the physiological adjustment to diving and their afferent pathway. Acta Physiol Scand 1963;58:263-273.
6. Elsner R. Cardiovascular adjustment in diving. In: Andersen HT, ed. The biology of marine mammals. New York: Academic Press, 1969:117-145.
7. Younce LR. The integration of the cardiovascular response in diving. Am Heart J. 1970;79:1-4.
8. Gandevia SC, McClosky DI, Potter EK. Reflex bradycardia occurring in response to diving, nasopharyngeal stimulation and swallowing. J Physiol 1978;276:383-394.
9. Huang TF, Yu YC, Peng YI. Cardiovascular response to the simulated diving in man and rat. Proc Nat Sci Counc 1978;2:135-139.
10. Bamford OS, Jones DR. Respiratory and cardiovascular interactions in ducks: the effect of lung denervation on the initiation of and recovery from the cardiovascular responses to submergence. J Physiol 1976;259:575-596.
11. Angell-James JE, Daly MdeB. The interaction of reflexes elicited by stimulation of carotid body chemoreceptor and receptors in the nasal mucosa affecting respiration and pulse intervals in the dog. J Physiol 1973;229:133-149.
12. Cohn JE, Krog J, Shannon R. Cardiopulmonary response to head immersion in domestic geese. J Appl Physiol 1968;25:36-41.
13. Paulev PE. CArdiac rhythm during breath-holding and water immersion in man. Acta Physiol Scand 1968;73:139-150.
14. Song SE, Lee WK, Chang YA, Hong SK. Mechanism of apneic bradycardia in man. J Appl Physiol 1969;27:323-327.
15. Asmussen E, Kristiansson NG. The diving bradycardia in exercising man. Acta Physiol Scand 1968;73:527-535.
16. Gandevia SC, McClosky DI, Potter EK. Inhibition of baroreceptor and chemoreceptor reflexes on heart rate by afferent from the lungs. J Physiol 1978;276:369-381.
17. Davidson NS, Golder S, McClosky DI. Respiratory modulation of baroreceptor and chemoreceptor reflexes affecting heart and vagal efferent nerve activity. J Physiol 1976;259:523-530.
18. Koepchen HP, Wagner PH, Lux HD. Über die Zusammenhänge zwischen zentralen Erregbarkeit reflektorischen Tonus and Atemrhythmus bei der nervösen Steuerung der Herzfrequenz. Pflügers Arch ges Physiol 1961;273:443-465.
19. Lamb LE, Dermkisian G, Sarnoff CA. Significant cardiac arrhythmias induced by common respiratory maneuvers. Am J Cardiol 1958;2:563-571.
20. Olsen CR, Fanestil DD, Scholander PF. Some effects on breath holding and apneic underwater diving on cardiac rhythm in man. J Appl Physiol 1962;17:461-466.

VENTILATION, PATTERN OF BREATHING, AND ACTIVITY OF RESPIRATORY MUSCLES IN AWAKE CATS DURING OXYGEN-HELIUM SIMULATED DIVES (1000 msw)

G. Imbert, Y. Jammes, N. Naraki, J. C. Duflot, and C. Grimaud

Ventilatory function is limited during diving as a consequence of the compression of the breathing mixture and the subsequent increase in its absolute density (1,2,3). This limitation is thought to be due to the dynamic compression of the airways, which counters the expiratory flow rate (4). This has been shown to occur in man in hyperbaric atmospheres even during quiet breathing and even when helium is used as the diluent gas: it depends upon the development of turbulent flow in the airways. Under these conditions, the resistance is mainly dependent on gas density. Thus, the effects of breathing oxygen-helium at high pressures can be predicted in man from studies of respiration of heavier mixtures at moderate pressures. Using oxygen-neon as a respiratory mixture, such predictive studies demonstrated that it would be possible for man breathing oxygen-helium to maintain a level of pulmonary ventilation sufficient to perform moderate work at depths greater than 1000 msw, if there were no other source of limitation other than pulmonary resistance (5).

On the other hand, experiments on animals at extreme pressures can also be used for predicting the efficiency of the ventilatory system to sustain breathing at depths greater than those actually reached by human beings (6-8). It is worth noting that when authors have described the behavior of animals during simulated dives around 1000 msw, they generally have reported ventilatory distress. However, no quantitative finding was reported dealing with pulmonary ventilation, pattern of breathing, activity of respiratory muscles, nor output of the respiratory centers in such conditions. The present work was undertaken to study in awake cats how the respiratory muscles could sustain

breathing at pressures up to 100 atmospheres of oxygen-helium (1000 msw) and to describe the resulting pattern of ventilation. Some preliminary results were published in a short note (9).

MATERIALS AND METHODS

Preparation of Animals

The subjects were nine cats that weighed 2.7–5.3 kg and were 10–30 months old. Myographic potentials were recorded through platinum bipolar electrodes (1.0–1.2 mm in diameter) soldered to a stainless steel, Teflon-coated wire (0.2 mm in diameter) and inserted in respiratory muscles. Surgery was performed under total anesthesia and aseptic conditions 10 to 15 days before diving. The electrodes were implanted in the cupolae of the diaphragm, the external obliquus (abdominal muscle) and in 2 cats in the intercostal muscles (3rd and 10th spaces). All wires were threaded under the skin and soldered to a connector, which was secured to the skull with dental acrylic. This preparation proved to be efficient for 4 to 6 weeks; therefore the animals could be used for repetitive dives.

Measurement and Treatment of Respiratory Data

During the recovery period, the animals were trained to stay in a whole body volume displacement plethysmograph, with the head protruding through a rubber seal. The box (volume about 15 L) was connected to a Krogh's spirometer (volume: 200 mL) coupled with an angular displacement sensor (Penny and Giles, Ltd, APT 25). This system made it possible to record the spirogram and to measure the following variables: tidal volume (V_T), inspiratory time (T_I), and ventilatory period (T_{TOT}). Its response had been verified at depths to 1000 msw using a ventilatory pump able to work against high pressures. The mechanical characteristics of the system have been previously reported (9). No change was found in the response between sea level and the maximal depth (1000 msw) within the range of normal respiratory frequencies of a cat (20–90 min^{-1}) (9).

The plethysmograph containing the animal was fitted into a hyperbaric chamber (volume: 165 L), as shown in Fig. 1. Ventilation and EMG potentials were simultaneously recorded on a multichannel polygraph (Beckman, Dynograph R), displayed on an oscilloscope (Tektronix 5111), and stored on an FM magnetic recorder (Schlumberger, MP 5522).

Diving Techniques

Environmental conditions are given in Table I.
The hyperbaric chamber was connected to an external atmosphere scrub-
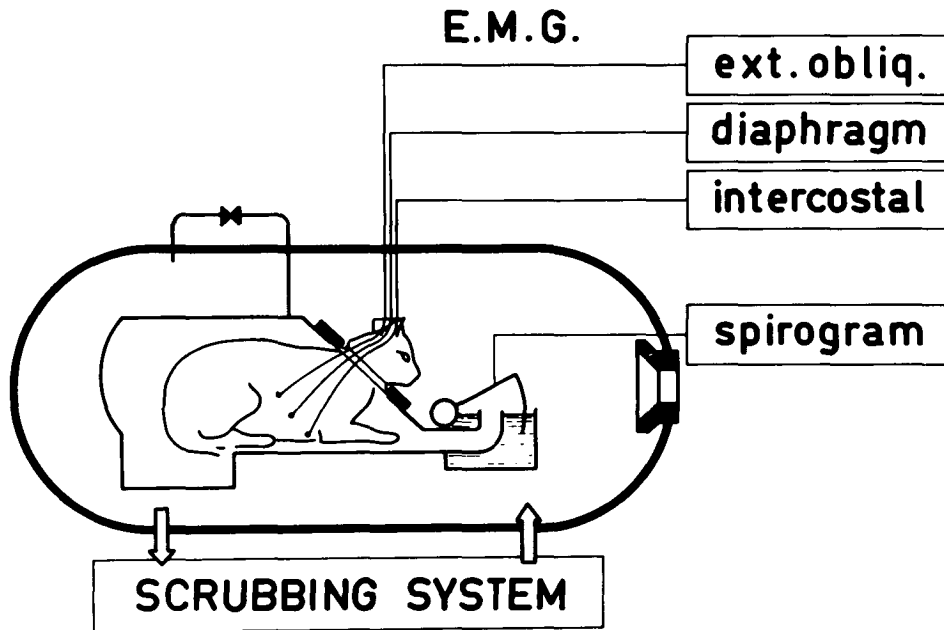
Fig. 1. The plethysmograph system for the high pressure chamber is shown. The unanesthetized cat, breathing chamber gas, is contained 3 to 4 days in the plethysmographic box, the head protruding through a rubber seal. The equilibration circuitry is open during compression and decompression; accurate measurements are possible only during stops. The box is connected to a Krogh's spirometer. EMG potentials are recorded through the chamber wall. An external scrubbing system is connected to the chamber.

bing system, which allowed the removal of carbon dioxide, excessive water vapor, hydrocarbon pollutants, and dusts on a series of filters containing soda lime, silica gel, and activated charcoal (10). The regeneration circuitry worked at the same pressure as the chamber (7,11), and the flow rate through this system was 0.25 $m^3 \cdot min^{-1}$ estimated in the ambient temperature and pressure conditions. The oxygen partial pressure, the temperature, and the relative humidity in the hyperbaric atmosphere were automatically monitored. We measured the oxygen content using a galvanometric cell (Sedam) placed directly inside the chamber; we used a paramagnetic analyzer (Servomex OA 184) to measure the fractional oxygen concentration (Fo_2) in the expanded gas. As shown in Table I, the experiments were performed in normoxic conditions.

The carbon dioxide content of the atmosphere was estimated using an infrared spectrometric analyzer (Maihak Unor II), which measured the fractional carbon dioxide concentration (Fco_2) in the expanded gas. The partial pressure of carbon dioxide was always below 3 mb. The nitrogen content of the atmosphere was not monitored and the values given in Table I were estimated from the air content of the chamber at the onset of compression. The ambient temperature given in Table I was that of the gas surrounding the plethysmographic box and was breathed by the animal. The temperature inside the box was gen-

TABLE I

Experimental Conditions

Depth (msw)	10	300	600	900	1000
Number of Subjects	8	6	9	7	2
Compression Time (h)	0.05	2	5-9	12-19	17
Bottom Time (h)	12-18	0.5-4	1.5-2.0	2-18	2
Decompression Time (h)	1.5	26.5	38.5	44.5	45.5
Environmental Conditions					
PI_{O_2} (bar)	0.23 ± 0.01	0.23 ± 0.01	0.23 ± 0.01	0.24 ± 0.02	0.22 ± 0.01
PI_{CO_2} (bar)	$< 10^{-3}$	$< 10^{-3}$	$< 10^{-3}$	$< 2.10^{-3}$	$< 2.10^{-3}$
Ambient Temperature (°C)	27.8 ± 0.5	29.7 ± 0.3	30.3 ± 0.3	31.6 ± 0.4	32.7 ± 0.2
Relative Humidity (%)	30 ± 4	17 ± 3	16 ± 3	27 ± 2	36 ± 2
Atmosphere Composition					
FI_{O_2}	0.112	0.007	0.004	0.003	0.002
FI_{N_2}	0.385	0.026	0.013	0.009	0.008
FI_{He}	0.503	0.967	0.983	0.989	0.990
Compressibility Factor (Z)	1.000	1.014	1.028	1.041	1.046
Gas Concentration (mole·L⁻¹)	0.082	1.21	2.35	3.45	3.80
Specific Gravity (g·L⁻¹ATPD)	1.34	5.85	10.4	14.8	16.1
Dynamic Viscosity (μPL)	20.0	20.0	20.1	20.2	20.2

Durations of compressions, stops and decompressions, and environmental conditions during stops. This table gives the composition of the inspired gas with the fractional concentrations of oxygen (FI_{O_2}), nitrogen (FI_{N_2}), and helium (FI_{He}). Values are given $\pm$ 1 SE.

erally 1 to 1.5°C higher than the inspired gas temperature. These values were thought to approximate the thermal comfort of cats in hyperbaric oxygen-helium environments.

Estimations of the molar concentration of the breathing mixture and of its specific gravity in ATPD conditions (ambient temperature, pressure, dry) are given in Table I. They were corrected for the deviation to the Boyle-Mariotte law, taking into account the compressibility factor Z of helium. The values of Z and of the dynamic viscosity μ were computed according to the thermodynamic tables for helium (12).

The compression was achieved by injecting pure helium into the chamber; the compression rates were progressively decreased with depth:
3 msw/min⁻¹ from surface to 180 msw; 2 msw/min⁻¹ from 180 to 600 msw; 1 msw/min⁻¹ from 600 to 1000 msw.

Stops were performed at 300, 600, 900, and 1000 msw, which allowed physiological measurements in steady conditions (Table I). The maximal depths reached were 600 msw for 2 animals, 900 msw for 5 animals, and 1000 msw for 2 animals. The total duration of decompression from 1000 msw to surface was 45 h, following an exponential curve that was computed by taking into account the body weight of the cats.

Eight animals survived the decompression to surface (among them, the two animals exposed to 1000 msw). This allowed postdive ventilatory and electromyographic controls.

RESULTS

Changes in Ventilation and Pattern of Breathing

In all of the cats an important hyperventilation was observed during the compression. This was associated with lengthening periods of excitement and motor activity; this effect was enhanced by high rates of compression. Hence, high pressures and high rates of compression increased the muscular and the respiratory activities. Between 800 and 1000 msw, the minute volume of ventilation ($\dot{V}$I) could reach more than 4 times the control value measured at rest in the reference conditions (10 msw). This was achieved by increasing the tidal volume (VT) and the respiratory rate (f). No respiratory distress was clearly exhibited up to 1000 msw, although transient panting (f) up to 90 c·min^{-1} was observed in some animals.

During the stops, the animals continued to hyperventilate but breathed more regularly. The respiratory rates tended to return to values close to control conditions. During these periods of steady states, the pattern of breathing was analyzed in terms of four variables that are independent with respect to the control of breathing: f, VT, TI/T$_{TOT}$ (ratio between the duration of the inspiration and the duration of the total cycle), and VT/TI (mean inspiratory flow rate). $\dot{V}$I can be expressed from these variables (13) by two equations:

$$\text{either } \dot{V}I = f \cdot VT$$

$$\text{or } \dot{V}I = \frac{VT}{TI} \cdot \frac{TI}{T_{TOT}}$$

Table II shows values of ventilatory variables measured in 8 animals at rest in control conditions at 10 msw and 2 to 10 min after the introduction of the animal into the chamber. This table gives the relative changes measured during stops at 300, 600, and 900 msw in 2 cats compressed up to 1000 msw. The measurements refer to a resting state. Twenty successive breaths were taken into account for each animal in each situation. Significant changes between different depths were assessed by Student's t test (2 $P < 0.05$). From 300 msw, significant increases in $\dot{V}$I, VT, and VT/TI occurred. On the other hand, no significant change could be observed in either f or TI/T$_{TOT}$ at rest up to 1000 msw, despite marked increases in minute volume of ventilation and respiratory resistance.

Changes in the Activities of Respiratory Muscles

Inspiratory activities of the diaphragm. As shown in Fig. 2, the activity of the diaphragm recorded at rest in the control conditions was characterized during the inspiratory time (TI) by a ramp-shaped activity due to a progressive recruitment of motor units (the peak activity was recorded at the end of the inspiration); and by a progressive extinction of the activity during the first part of the expiration time.

TABLE II
Relative Changes in Ventilation and Pattern of Breathing at Rest

	Control Values (± SE)		Mean Percent Changes in Ventilatory Variables			
Depth	(msw)	10	300	600	900	1000
n		8	6	6	6	2
f	(min^{-1})	24.3 ± 3.0	+ 19.5	− 11.5	+ 23.3	+ 32.0
V_T	(mL BTPS)	37.2 ± 5.3	+ 32.2	+ 63.1	+ 16.2	+ 28.5
T_I/T_{TOT}		0.40 ± 0.02	+ 10.5	+ 3.0	+ 3.3	− 1.5
V_T/T_I	(mL BTPS·s^{-1})	37.8 ± 3.1	+ 42.3	+ 48.5	+ 67.5	+ 56.0
$\dot{V}_I$	(L BTPS min^{-1})	0.91 ± 0.07	± 58.7	± 70.7	± 99.3	± 72.5
Body Weight	(kg)	4.15 ± 0.38				

Relative changes in respiratory rate (f), tidal volume (V_T), ratio between the duration of the inspiration and the duration of the total cycle (T_I/T_{TOT}), and mean inspiratory flow (V_T/T_I) in the resting awake cat, during stops at 300, 600, 900, and 1000 msw. Values were measured at 10 msw.

The succession of these two phases gives a losengic shape to the normal pattern of the diaphragmatic discharge.

In diving conditions, an important rise in the activity of the diaphragm was observed. The increase in the recruitment of the motor units appeared from 300 msw onward and was associated with the increase in the mean inspiratory flow rate. On the other hand, the disappearance of the postinspiratory activity under high pressures gave a triangular shape to the diaphragmatic discharge. The normal pattern was recovered when the animal returned to sea level.

During panting, the pattern of diaphragmatic activity was characterized by a sudden rectangular discharge, which could be observed either in control or diving conditions.

Expiratory activities in different muscles. During the compressions and from 300 msw onward, a phasic abdominal activity was observed during the expiration. This discharge started abruptly at the onset of the inspiratory time (Fig. 2). This active expiration occurred for all cycles and continued when the compression was stopped. It disappeared during decompression at about 200 msw.

In one animal, transient expiratory activities were observed at rest at very high pressures (800 msw) in internal intercostal muscles (10th space). This was associated with an expiratory activity in the diaphragm (see Fig. 3). Such "paradoxical" expiratory diaphragmatic discharges were equally observed at high pressure in other cats either during hyperventilation or quiet breathing.
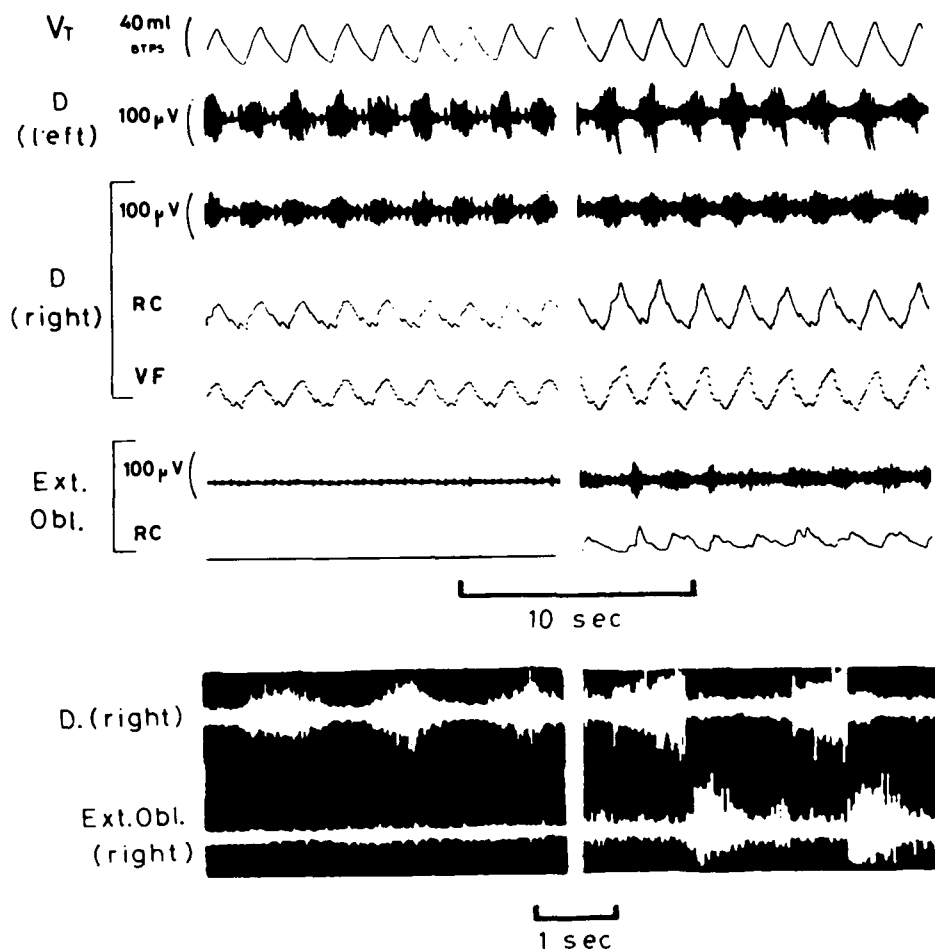
Fig. 2. Shown are the spirogram (VT) and electromyograms of respiratory muscles in the awake cat at rest, both in the control conditions (*left*) and during an He-O₂ simulated dive at 900 msw (*right*). *The upper part* of the figure shows the EMG recorded on an oscillograph from the D (*left*) and the D (*right*) cupolae of the diaphragm and from the external obliquus (*Ext. Obl.*). RC and VF refer to averaged signals, using an RC integrator or a frequency-to-voltage converter, respectively. The peak activity of the diaphragm is related to the mean inspiratory flow rate (*i.e.*, to the tidal volume when the inspiratory time is constant). *The lower part* of the figure shows the direct EMGs as simultaneously displayed on an oscilloscope. Under high pressures (*right*) the activities of muscles facilitate the expiration: the abdominal muscles exert a phasic expiratory activity and the postinspiratory discharge of the diaphragm (which normally acts as an expiratory brake) is greatly reduced.

DISCUSSION

To verify whether the changes in the activity of respiratory muscles essentially resulted from the increase in the airways resistance, we performed a control experiment at sea level. The cat wore an oronasal mask connected to a two-way valve, which allowed the addition of a resistive load either to the in-

D (left)

30 ml

V_T BTPS

D (right)

I.C.
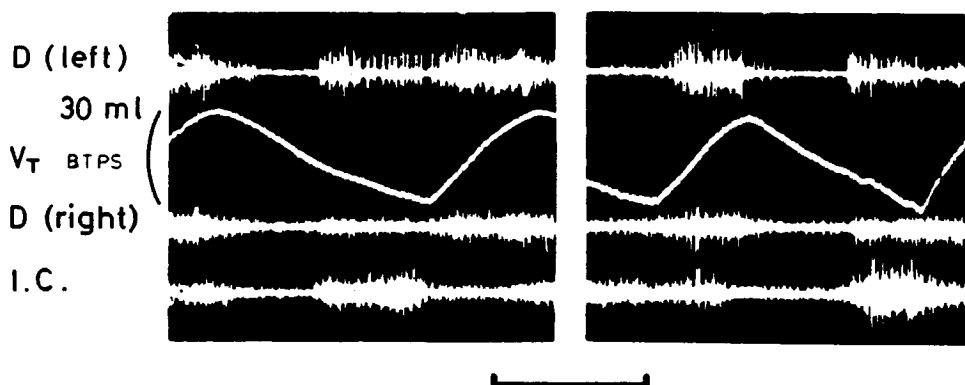
Fig. 3. The diaphragmatic activity during expiration at rest under high pressure (simulated depth: 800 msw) is shown. The "paradoxical" activities are present in the D (*left*) and the D (*right*) cupolae of the diaphragm. They are associated with a phasic activity in an internal intercostal muscle of the 10th space (*I.C.*). The horizontal bar represents 1 s.

spiratory or the expiratory lines. When the resistive load was added to the inspiratory side, the activity of the diaphragm increased during the inspiration, without change in the postinspiratory activity. On the other hand, when the resistive load was added to the expiratory side, the postinspiratory activity of the diaphragm was greatly reduced (see Table III). However, the expiratory discharge of the diaphragm did not entirely disappear and no phasic activity

TABLE III

Effects of External Added Respiratory Resistances

Variable (s)	Control Values	R_E	R_I
T_I	0.93 ± 0.03	0.83 ± 0.01 ($2P < 0.001$)	1.07 ± 0.03 ($2P < 0.001$)
PIDA	0.37 ± 0.03	0.25 ± 0.03 ($2P < 0.001$)	0.35 ± 0.02 (NS)

Effects at sea level of added expiratory (R_E) or inspiratory (R_I) resistive loads on the duration of inspiration (T_I), and on the post-inspiratory diaphragmatic activity (PIDA) in the awake cat.   In this control experiment, $R_E = R_I = 240$ cm H_2O (i.e., about 10 times the normal value of pulmonary resistance in cats). Diaphragmatic EMG was recorded from electrodes inserted in the right cupola, and T_I was measured using an open body plethysmograph. Ten successive breaths were taken into account in each situation. Results are given ± 1 SE.

was observed in abdominal muscles. Thus, some discrepancies did exist between data obtained during the dive and data obtained at 1 atm with external resistive loads. In fact, adding resistive loads did not change the mechanical properties of the lung, and thus did not change the activity of pulmonary receptors and proprioceptors in the thoracic wall, as an increase in intrapulmonary resistance could do.

During the inspiration, the increase in the airways resistance acts as a resistive load able to counter the shortening of thoracic expiratory muscles (i.e., the internal intercostal ones). In anesthetized cats, it has been found (14) that changes in respiratory loads increased the afferent discharge of intercostal neuromuscular spindles. An intercostal-phrenic reflex has been described (15) from proprioceptive afferents of both external and intercostal muscles. The simultaneous expiratory activities of internal intercostal muscles and of the diaphragm, observed at very high pressure in an awake animal, could result from that intercostal-phrenic reflex. These findings show the possible physiological importance of that reflex mechanism during loaded expiration in extreme environmental conditions. That phenomenon could also be compared to the expiratory discharge of the diaphragm observed in man during voluntary forced expiration (16).

Changes in the pattern of breathing did not seem to depend on increased airway resistance. As shown by the steadiness of the TI/T_{TOT} ratio, the reflex control of the ventilatory timing from broncho-pulmonary afferents (17,18) appeared to be unaltered despite the increase in gas density.

On the other hand, increases in VT and VT/TI in resting conditions are principally observed at sea level, when chemoreceptors are simulated either by hypoxemia (19) or by hypercapnia (20). An increase in energy expenditure associated with an impairment of pulmonary gas exchange, as postulated by some investigators (21), possibly could explain an increase in the output of the respiratory center at rest.

In conclusion, the most evident change in the pattern of breathing observed in awake resting cats at simulated depths up to 1000 msw was an increase in the mean inspiratory flow rate, which seems to translate an enhancement of the respiratory center output. Time-dependent ventilatory variables (i.e., f and TI/T_{TOT}) did not vary, despite the marked increase of gas density. This was associated with important variations of the activity of respiratory muscles. The variations prevailed in the expiratory time and acted in facilitating the expiration. Thus, in the awake animal at high pressures of oxygen-helium, active expiration has occurred even during quiet breathing; but no symptoms of respiratory distress were observed up to 1000 msw at rest.

Acknowledgments

References

1. Maio DA, Farhi LE. Effects of gas density on mechanics of breathing. J Appl Physiol 1967;23:687-693.
2. Wood LDH, Bryan AC Effect of increased ambient pressure on flow-volume curve of the lung. J Appl Physiol 1969;27:4-8.
3. Lanphier, EH. Pulmonary function. In: Bennett PB, Elliott DH, eds. The physiology and medicine of diving and compressed air work, 2nd ed. London: Baillière Tindall, 1975:102-154.
4. Mead J, Turner JM, Macklem PT, Little JB. Significance of the relationship between lung recoil and maximum expiratory flow. J Appl Physiol 1967;22:95-108.
5. Peterson RE, Wright WB. Pulmonary mechanical functions in man breathing dense gas mixtures at high ambient pressures—Predictive studies III. In: Lambertsen CJ, ed. Underwater physiology. Proceedings of the fifth symposium on underwater physiology. Bethesda, MD: Federation of American Societies for Experimental Biology, 1976:67-77.
6. McInnis JB, Dickson JG, Lambertsen CJ. Exposure of mice to a helium-oxygen atmosphere at pressures up to 122 atmospheres (4000 fsw). J Appl Physiol 1967;22:694-698.
7. Chouteau J. Respiratory gas exchange in animals during exposure to extreme ambient pressure. In: Lambertsen CJ, ed. Underwater physiology. Proceedings of the fourth symposium on underwater physiology. New York: Academic Press, 1971:385-397.
8. Parc J, Michaud A, Le Chuiton J, Michel A, Barthelemy L, Balouet G. Very deep diving experiments on miniature pigs. In: Lambertsen CJ, ed. Underwater physiology. Proceedings of the fifth symposium on underwater physiology. Bethesda, MD: Federation of American Societies for Experimental Biology, 1976:251-261.
9. Imbert G, Jammes Y. Plethysmographie volumétrique en hyperbarie. J Physiol (Paris) 1979;75:204.
10. Imbert G, Installation de plongé fictive pour le petit mammifère. Marseille: GIS de Physiologie Hyperbare, Rapport au CNEXO 76-1514, 1979.
11. Chouteau J, Bianco V, Oriol P, et al. Expérimentation animale et humaine de vie prolongée sous pression en atmosphère oxygène-hélium. Technologie et résultats biologiques. Ann Anesthesiol Fr (Suppl) 1967;8:238-280.
12. Drut R. Caractéristiques thermodynamiques de l'hélium. Formules et tables. Saclay: Centre d'Etudes Nucléaires, Rapport CEA-R-3791, 1969.
13. Milic-Emili J, Grunstein MM. Drive and timing components of ventilation. Chest (Suppl) 1976;70:131-133.
14. Corda M, Eklund G, von Euler C. External intercostal and phrenic alpha motor responses to changes in respiratory load. Acta Physiol Scand 1965;63:391-400.
15. Decima E, von Euler C. Excitability of phrenic motoneurons to afferent input from lower intercoastal nerves in the spinal cat. Acta Physiol Scand 1969:75:580-591.
16. Agostoni E, Torri G. Diaphragm contraction as a limit to maximum expiration. J Appl Physiol 1962;17:427-428.
17. Clark FJ, von Euler C. On the regulation of depth and rate of breathing. J Physiol (Lond) 1972;222:267-295.
18. Winning AJ, Widdicombe JG. The effect of lung reflexes on the pattern of breathing in cats. Respir Physiol 1976;27:253-266.
19. Jammes Y, Fornaris M, Guillot C, Grimaud C. Pattern of the ventilatory response to transient hypoxia in man: differences from transient hypercapnia test. Arch Int Physiol Biochim 1979;87:229-243.
20. Grunstein MM, Younes M, Milic-Emili J. Control of tidal volume and respiratory frequency in anesthetized cats: J Appl Physiol 1973;35:463-476.
21. Chouteau J, Imbert G. La limitation hypoxique de la plongée profonde de longue duré. Maroc Med 1971;51:229-236.

PHYSIOLOGICAL RESPONSES TO IMMERSION AT 31 ATA (SEADRAGON IV)

M. Matsuda, S. K. Hong, H. Nakayama, H. Arita, Y. C. Lin,
J. R. Claybaugh, R. M. Smith and C. E. G. Lundgren

During the last two decades many simulated, dry saturation diving experiments have been carried out as an attempt to identify both psychological and physiological problems that might affect a diver's performance at high pressures. Consequently, remarkable progress has been made in the field of diving physiology and medicine. However, it is important to recognize that actual diving involves not only the exposure to high pressure but also the act of immersion in water. It is well known that immersion even in thermoneutral water (34–35°C) at 1 ATA induces profound cardiorespiratory and renal effects (1–4) that could compromise physiological performance. Since the exposure to a high pressure also induces certain cardiorespiratory and renal changes (5,6), it is important to understand the effects of immersion at high pressures. However, little attention has been given to this problem in the past.

The present investigation was undertaken to study the effects of a head-out immersion in thermoneutral water at 31 ATA on selected thermoregulatory, cardiorespiratory, and renal functions. The dive (code-named SEADRAGON IV) was sponsored by and carried out at the Japan Marine Science and Technology Center (JAMSTEC) during July-September, 1979, as a U.S.-Japan Cooperative Diving Research project.

METHODS

The physical characteristics of four subjects as well as the dive profile and environmental parameters are described in a paper by Nakayama et al. (7) included in these proceedings.

Three immersion experiments were carried out in fresh water: 1 ATA predive (July 27-28), 31 ATA (7th and 11th days) and 1 ATA postdive (September 4–5). Two subjects were run each day: one starting at 0900 h and the other at 1400 h. The starting time for a given subject was the same in all three series. The immersion was carried out in the wet chamber (6.2 m high, 3.6 m wide) connected to the main hyperbaric complex.

Each experiment consisted of three periods: 1 h preimmersion, 2 h immersion, and 1 h postimmersion. Before the start of the experiment, electrical tapes (Nihon Koden Co., Ltd., Japan) for the impedance cardiography were placed around the neck, chest, and abdomen (8). A rectal thermistor probe (Yellow Springs Instrument Co.) was then inserted 15 cm into the rectum. At zero time, the subject emptied his urinary bladder and started the preimmersion period while seated by the wet pot. Both the rectal and skin temperatures were measured at 10 sites every 15 min (see ref.9). An impedance cardiogram was taken at 20 and 40 min, while the minute ventilation ($\dot{V}E$), O_2 consumption ($\dot{V}O_2$), and CO_2 output ($\dot{V}CO_2$) were determined at 25–30 min. The vital capacity and its subdivisions were determined at 50 min. At 55 min, a venous blood sample was obtained, followed by a urine collection at 60 min. The subject then entered the wet pot and immersed himself to the neck in a sitting position for 2 h during which the various measurements described above were repeated each hour, except for the skin temperature and venous blood sampling. At the end of 1 h immersion, the subject came out of the wet pot briefly to urinate and then reimmersed immediately. At the end of 2 h immersion, the subject came out of the wet pot and urinated immediately; a venous blood sample was then obtained. During the 1-h postimmersion period, all measurements were repeated except for the venous blood sampling.

The water temperature was regulated at 34.1 ± 0.1°C for predive 1-ATA experiments, but was regulated at 35.0 ± 0.1°C for 31 ATA and postdive 1 ATA because of technical problems.

The changes in transthoracic impedance (Z_0) and dZ/dt with each heart beat were measured, as described by Smith et al. (5). The respiratory minute volume was determined by the usual Douglas bag-method. The expired gas, as well as the inspired gas, were analyzed for O_2 and CO_2 by a gas chromatograph (Quintron Model R). The vital capacity and its subdivisions were determined by a 13-L Collins spirometer.

Immediately after the withdrawal of venous blood samples (10 mL each), a portion of each sample was drawn into capillary tubes for determination of hematocrit inside the chamber. The rest of the samples were centrifuged to separate the plasma. The plasma samples were then locked out along with urine samples and frozen for later analysis.

All plasma and urine samples were analyzed for osmolality (Fiske Model 230D); creatinine, urea, Na, and K were analyzed using a Technicon Auto Analyzer (Model AAII); and protein was analyzed by the Lowry et al. method (10). All urine samples were radioimmunoassayed for antidiuretic hormone (ADH) (11), aldosterone (Radioassay Systems), and prostaglandin E_2 (PGE_2) (12). In addition, all plasma samples were assayed for aldosterone using the method referred to above.

RESULTS

Body Temperature and Oxygen Consumption

Both rectal and mean skin temperatures and oxygen consumption measured before, during, and after 2 h immersion are summarized in Table I. Overall, the rectal temperature showed no significant changes throughout the experiment. Because the skin temperature was not measured during immersion, only pre- and postimmersion data are shown in this table. The only significant change was noted at postimmersion 30 min at 1 ATA predive. Likewise, the oxygen consumption remained unchanged; the only significant change was seen during postimmersion at 1 ATA postdive. These results indicate that the water temperature of 34–35°C used in the present experiment is thermoneutral at both 1 and 31 ATA.

TABLE I

Body Temperature and Oxygen Consumption Before, During, and After Immersion

Time (min)	Rect. Temp(°C)			Mean Skin Temp (°C)			O₂ Consump. (mL/min STPD)		
	1 ATA Predive	31 ATA	1 ATA Postdive	1 ATA Predive	31 ATA	1 ATA Postdive	1 ATA Predive	31 ATA	1 ATA Postdive
Preimmersion									
30	36.92 ±0.9	37.08 ±0.10	36.92 ±0.14	34.48 ±0.21	33.64 ±0.22	33.29 ±0.26	272 ±29	353 ±16	288 ±9
60	36.80 ±0.09	36.98 ±0.13	36.70 ±0.12	34.67 ±0.03	33.68 ±0.16	33.17 ±0.20	—	—	—
Immersion									
30	36.68 ±0.10	36.98 ±0.11	36.70 ±0.17	—	—	—	281 ±47	309 ±48	272 ±21
60	36.53 ±0.14	37.07 ±0.07	36.71 ±0.14	—	—	—	—	—	—
90	36.58 ±0.14	37.07 ±0.10	36.82 ±0.13	—	—	—	263 ±9	257 ±30	268 ±10
120	36.47 ±0.20	37.14 ±0.21	36.83 ±0.14	—	—	—	—	—	—
Postimmersion									
30	36.34 ±0.20	37.16 ±0.13	37.00 ±0.15	32.67* ±0.54	33.75 ±0.08	32.95 ±0.22	293 ±8	298 ±21	238* ±14
60	36.09 ±0.24	37.10 ±0.20	36.70 ±0.15	33.82 ±0.25	33.63 ±0.17	32.66 ±0.23	—	—	—

Each value represents the mean ($\pm$ SE) of 4 subjects. $*P<0.05$ compared to preimmersion values (60 min values for body temperature data; paired t test).

Cardiorespiratory Changes

The average specific thoracic impedance (Z_0/L) at the total lung capacity, calculated stroke volume, and heart rate before, during, and after immersion are shown in Fig. 1. The thoracic impedance decreased (by more than 20%) reversibly during immersion. Perhaps this reduction in impedance observed during immersion can be attributed to both an increase in thoracic blood volume and a decrease in lung gas volume (see below). The average stroke volume increased reversibly during immersion, with the magnitude of increase greatest at 1 ATA predive and smallest at 1 ATA postdive (65 ± 9 mL at 1 ATA predive vs. 31 ± 5 mL at 1 ATA postdive, $P<0.025$). Caution should be used in interpreting these data, because the baseline impedance was lowest at 1 ATA predive and highest at 1 ATA postdive and this strongly affects the stroke volume calculation. The heart rate was generally higher during preimmersion as compared to immersion and postimmersion periods. Perhaps this is because the subjects were somewhat apprehensive and restless preceding immersion. However, there was no significant difference in the heart rate between the two pressures. Consequently, the patterns of changes in the cardiac output were practically the same as those in the stroke volume.

Various systolic time intervals were calculated from ECG and impedance cardiograms, and the average values are shown in Table II. The left ventricular ejection time (T) increased significantly during immersion in all experiments, which is most likely due to the increase in the cardiac interval. The pre-ejection period (PEP) tended to decrease during immersion. Because PEP is sensitive to the preload of the heart, no conclusion can be drawn regarding PEP changes during immersion that increased the stroke volume (Fig. 1). However, it is important to note the overall PEP/T ratios were highest at 1 ATA predive and decreased progressively at 31 ATA and 1 ATA postdive. This ratio is known to correlate inversely with the ejection fraction (13). Thus, such a progressive decrease in this ratio (reflecting an increased ejection fraction) concurrent with a lowered stroke volume at 31 ATA and 1 ATA postdive is most likely a result of a smaller ventricular volume. The Q-Z interval (between the Q wave on ECG and the lowest dZ/dt point on the impedance cardiogram) has been shown to be inversely related to the maximal velocity of myocardial contraction (14). This interval remained unchanged during immersion, indicating that the increase in stroke volume observed during immersion is not due to the increased contractility. The O wave on the impedance cardiogram was exaggerated during immersion in all experiments. Overall, there was a highly significant positive correlation between the stroke volume and the amplitude of O wave ($r = 0.80$, $P<0.01$). The latter finding is consistent with the notion that the O wave reflects the rapid filling phase of the ventricles and its amplitude can be used as an indicator of preload of the heart (15,16).

As described in a companion paper by Ohta et al. (17), the expiratory reserve volume (ERV) increased while the inspiratory capacity (IC) decreased by approximately 300 mL during exposure to 31 ATA as compared to 1 ATA. Despite these differences in the static lung volumes during preimmersion be-
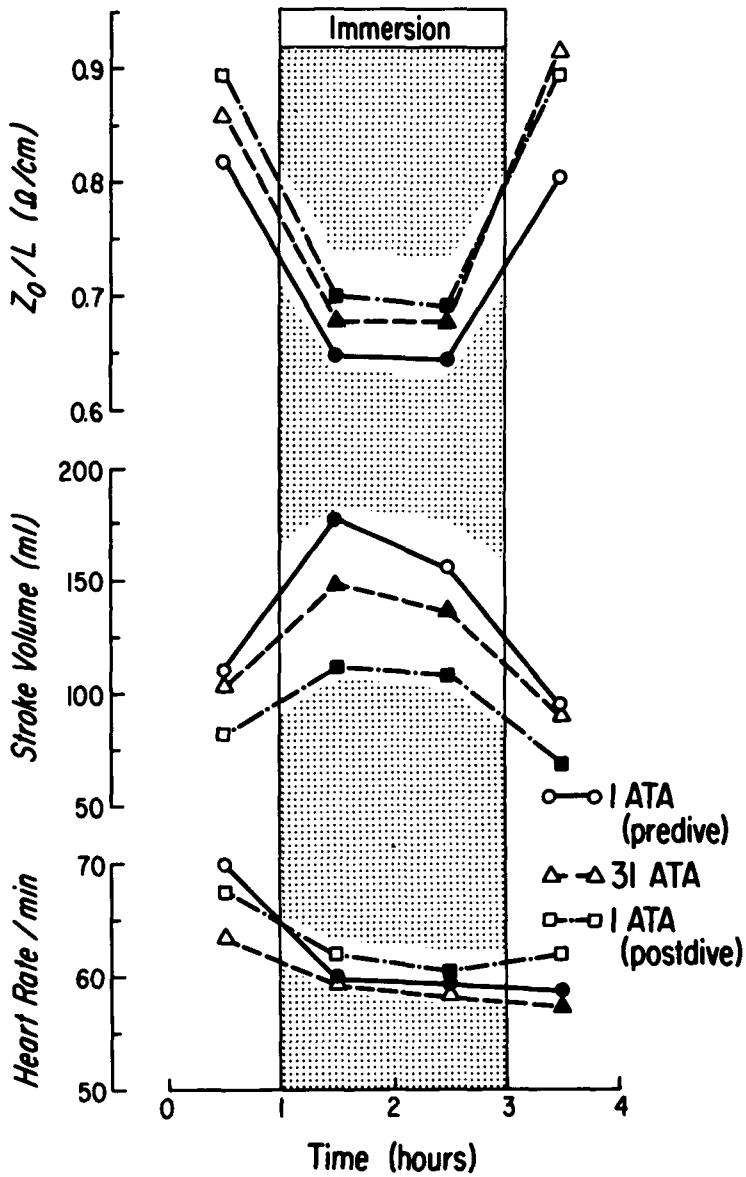
Fig. 1.   Specific thoracic impedance (Z_0/L), stroke volume, and heart rate before, during, and after immersion. Each point represents the mean of 4 subjects. Solid symbols indicate significant differences ($P<0.05$) from the corresponding preimmersion value. Z_0 and L represent the impedance and the longitudinal distance between the two electrodes (placed on upper and lower parts of thorax), respectively.

TABLE II

Systolic Time Intervals Before, During, and After 2-h Immersion

Measurements	1 ATA Predive	31 ATA	1 ATA Postdive
Cardiac interval (s)			
Preimmersion	0.87±0.04	0.95±0.03	0.88±0.04
Immersion 1 h	1.03±0.06	1.00±0.02	0.98±0.04
Immersion 2 h	1.04±0.06	1.03±0.02	1.00±0.03
Postimmersion	1.05±0.06	1.05±0.03	0.98±0.04
Left Ventr. Eject. Time (T) (s)			
Preimmersion	0.27±0.01	0.30±0.01	0.29±0.01
Immersion 1 h	0.34±0.01*	0.32±0.01*	0.32±0.01*
Immersion 2 h	0.34±0.01*	0.32±0.01*	0.32±0.01*
Postimmersion	0.29±0.01	0.28±0.01	0.29±0.01
Pre-Ejection Period (PEP) (s)			
Preimmersion	0.14±0.02	0.10±0.01	0.09±0.02
Immersion 1	0.11±0.02	0.09±0.01	0.08±0.01
Immersion 2	0.11±0.02	0.09±0.01	0.08±0.01
Postimmersion	0.15±0.02	0.11±0.01	0.10±0.02
PEP/T			
Preimmersion	0.54±0.08	0.35±0.04†	0.30±0.05†
Immersion 1	0.33±0.06*	0.30±0.03*	0.24±0.02*
Immersion 2	0.34±0.05*	0.30±0.02*	0.26±0.02*
Postimmersion	0.52±0.07	0.38±0.05†	0.35±0.03†
Q-Z Interval (s)‡			
Preimmersion	0.18±0.02	0.15±0.02	0.14±0.02
Immersion 1 h	0.17±0.02	0.14±0.04	0.14±0.04
Immersion 2 h	0.17±0.02	0.14±0.02	0.14±0.02
Postimmersion	0.19±0.02	0.16±0.02	0.15±0.02

Each value represents the mean (±SE) of 4 subjects.   *$P<0.05$ compared to corresponding preimmersion value (paired t test);   † $P<0.05$ compared to corresponding 1 ATA predive value (paired t test);   ‡ Interval between Q wave (ECG) and the lowest dZ/dt (impedance cardiogram).

tween the two pressures, immersion induced significant reductions in ERV (approx. 1100 mL) and increases in IC (approx. 800 mL) at both pressures. Therefore, a reduction of the vital capacity (approx. 300 mL) was noted during immersion at both pressures. These findings indicate that the mechanical effect of immersion on the static lung volumes is not altered by pressure.

Renal Responses

The average urine flow (V), urine osmolality (U_{osm}), and urinary excretion of total osmotic substances ($U_{osm}V$) before, during, and after immersion are shown in Fig. 2. The urine flow during preimmersion was about 1 mL/min in all experiments. Although the urine flow increased continuously during 2 h immersion, the magnitude of increase was greatest at 1 ATA predive and smallest at 1 ATA postdive. In fact, the increase in urine flow during immersion at
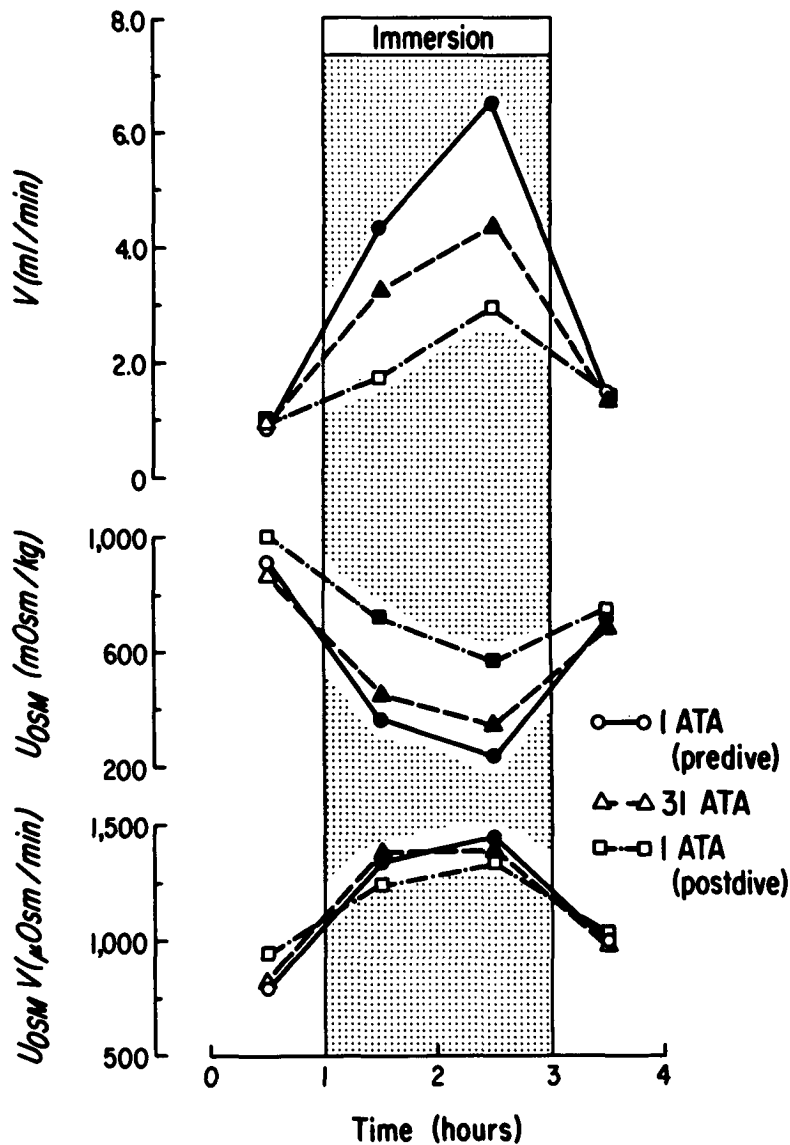
Fig. 2. Urine flow (V), urine osmolality (U_{osm}), and urinary excretion of total osmotic substances ($U_{osm}V$) before, during, and after immersion. Each point represents the mean of 4 subjects. Solid symbols indicate significant differences ($P<0.05$) from the corresponding preimmersion value.

1 ATA postdive was not even statistically significant ($P>0.05$). In general, the urine osmolality changed inversely with the urine flow. It should be noted that the urine actually became hypotonic (258 ± 51 mOsm/kg) only during the second hour of immersion at 1 ATA predive. Despite the inverse relationship between the urine flow and osmolality during immersion, the urinary excretion of total osmotic substances increased similarly during immersion ($P<0.05$ at 1 ATA predive and 31 ATA; $P>0.05$ at 1 ATA postdive). Increases in the excretion of Na^+ and K^+ (and attendant anions) and urea fully accounted for the above increase in the excretion of total osmotic substances during immersion.

As stated under METHODS, two venous blood samples were obtained from each subject, one immediately before immersion and the other at the end of immersion. The changes in plasma chemistry (K, urea, creatinine, and total proteins) as a result of increased urine flow during immersion were insignificant in all cases. Small but significant increases ($P<0.05$ by paired t test) in plasma osmolality (ΔP_{osm} = 2.7 mOsm/kg) and Na (ΔP_{Na} = 0.8 mEq/L) and hematocrit (Δhct = 2.1%) were noted only at 1 ATA predive, where the greatest increase in urine flow was observed.

To assess the renal hemodynamics and the tubular handling of various osmotic substances during immersion, we calculated plasma clearances for the preimmersion period (using the plasma data of the first blood sample) and the second hour of the immersion period (using the plasma data of the second blood sample). As shown in Fig. 3, at 1 ATA predive the average endogenous creatinine clearance (C_{cr}) tended to increase during immersion, but this increase was not significant. At both 31 ATA and 1 ATA postdive, C_{cr} tended to decrease during immersion, but again the reduction was not significant. The fractional excretion of filtered water (V/C_{cr}) increased significantly during immersion in all experiments; this increase indicates the inhibition of tubular reabsorption of filtered water. In this regard, it is interesting to note that the increase in V/C_{cr} was least at 1 ATA postdive. On the other hand, the fractional excretion of filtered osmotic substances (C_{osm}/C_{cr}) increased significantly to the same extent during immersion in all experiments; this increase indicates the inhibition of the tubular reabsorption of filtered osmotic substances. Overall, the relative increase in V/Cr during immersion was greater than that of C_{osm}/C_{cr}, and thus the normalized free water clearance (CH_2O/C_{osm}) increased in all instances. These results are consistent with the current view that a head-out immersion induces both a water diuresis and natriuresis (4). However, the results also suggest that the water diuresis component was considerably attenuated at 1 ATA postdive, while the natriuresis component was not altered during the course of the present dive.

The urinary excretion of ADH, aldosterone, and PGE_2 before, during, and after immersion is summarized in Table III. There were large individual variations, and no significant changes were observed during immersion. However, there was an overall negative correlation between the urine flow and the rate of ADH excretion (r = 0.36, $P<0.05$), which indicates that the difference in the degree of immersion-induced increase in urine flow observed in three experiments is at least in part due to the difference in the degree of ADH inhibi-
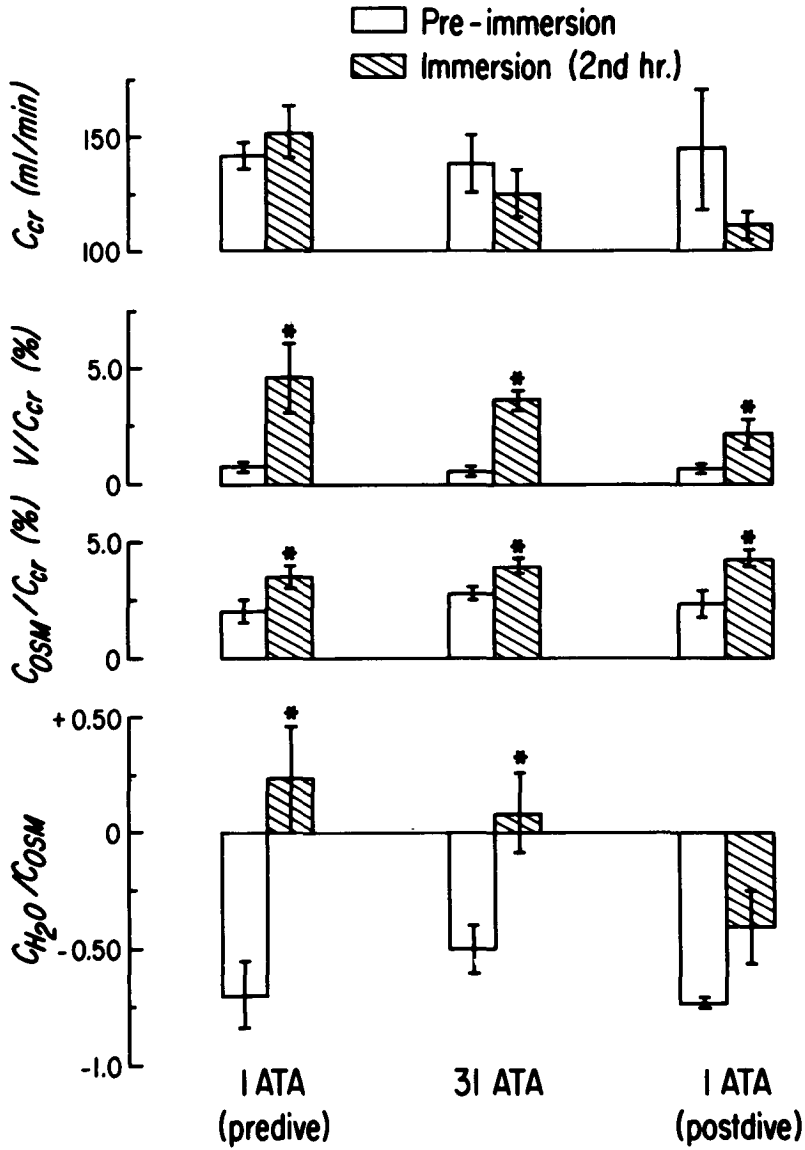
Fig. 3. Endogenous creatinine clearance (C_{cr}), fractional excretions of water (V/C_{cr}) and total osmotic substances (C_{osm}/C_{cr}), and normalized free water clearance (CH_2O/C_{osm}) during preimmersion and immersion (2nd h). Each bar represents the mean ($\pm$ SE) of 4 subjects.   *$P < 0.05$ as compared to the corresponding preimmersion value.

tion. The average rate of excretion of aldosterone increased during immersion in all experiments. This was due to one subject who showed a marked increase in the aldosterone excretion during immersion for totally unknown reasons. Therefore, the plasma level of aldosterone was additionally determined. It decreased from the preimmersion level of 4.48 ± 0.87 to 3.40 ± 0.67 ng% at the end of immersion at 1 ATA predive, and from 2.98 ± 0.27 to 2.15 ± 0.58 ng% at 31 ATA ($P<0.05$ by paired t test for the combined data set). However, the plasma aldosterone level showed no difference between before and after immersion at 1 ATA postdive. These findings indicate that the increase in fractional excretion of osmotic substances during immersion at 1 ATA predive and 31 ATA are at least in part due to the reduction in aldosterone release as indicated by the decrease in plasma aldosterone level. On the other hand, the similar phenomenon observed during immersion at 1 ATA postdive cannot be correlated with either plasma level or urinary excretion of aldosterone.

The urinary excretion of PGE_2 increased during immersion at both 1 ATA predive and 31 ATA. Although these changes were only marginally significant ($0.05<P<0.10$ at both pressures by paired t test), these findings are consistent with the opinion that the immersion diuresis is at least in part due to the increase in the release of PGE_2 (4), which is known to antagonize the hydrosmotic effect of ADH (18). However, there was no difference in the PGE_2 excretion between the two pressures either before or during immersion.

TABLE III

Urinary Excretion of Antidiuretic Hormone (ADH), Aldosterone, and Prostaglandin E_2 (PGE_2) Before, During, and After Immersion

	ADH (µU/min)			Aldosterone (ng/min)			PGE_2 (pg/min)		
	1 ATA Predive	31 ATA	1 ATA Postdive	1 ATA Predive	31 ATA	1 ATA Postdive	1 ATA Predive	31 ATA	1 ATA Postdive
Preimmersion	70.1 ±10.2	55.3 ±9.7	94.9 ±26.6	2.74 ±0.62	4.99 ±2.20	3.86 ±1.16	762 ±195	470 ±141	—
Immersion 0–1 h	61.9 ±19.9	46.3 ±16.7	66.5 ±18.1	7.39 ±4.83	9.47 ±5.84	6.16 ±0.74	—	—	—
1–2 h	68.7 ±25.8	49.0 ±10.2	62.2 ±12.6	9.72 ±8.67	4.86 ±2.94	9.71 ±4.08	1,664 ±534	1,096 ±362	—
Postimmersion	60.0 ±4.7	48.1 ±10.2	54.0 ±12.0	3.15 ±1.75	5.24 ±3.20	5.12 ±2.75	—	—	—

Each value represents the mean (±SE) of 4 subjects.   None of the immersion and postimmersion values were significantly different from the respective preimmersion value.

DISCUSSION

In the present study, the temperature of water was set at 34–35°C at both 1 and 31 ATA. Both the body temperature and oxygen consumption data (Table I) as well as the subjective sensations clearly support a view that the water was thermoneutral at both pressures. In other words, the thermoneutral temperature of water does not change with pressure. Moreover, the mechanical effect of immersion on the static lung volumes was identical at both pressures. Although qualitatively similar changes in cardiac and renal functions were observed during immersion, there were significant, quantitative differences in the response among three experiments carried out at 1 ATA predive, 31 ATA, and 1 ATA postdive. These differences were particularly noteworthy for the magnitude of increase in stroke volume (and cardiac output) and for that of diuresis.

The stroke volume increased significantly during immersion in agreement with the results reported in the literature (3,16). However, the magnitude of this increase in stroke volume during immersion was 65 ± 9 mL at 1 ATA predive as compared to 41 ± 8 mL at 31 ATA and 31 ± 5 mL at 1 ATA postdive. In other words, there was a progressive reduction in the magnitude of immersion-induced increase in stroke volume as the dive progressed. Although we cannot completely rule out other factors, it appears that the duration of stay inside the chamber is primarily responsible for the above phenomenon. The immersion experiments were carried out on *Dive Days 13* (for *Subjects A and B*) and *17* (for *Subjects C and D*) for the 31 ATA series, and on *Dive Days 37* and *39* for the 1 ATA postdive series. Before the start of the present dive, the subjects were physically very active and were engaged in regular, daily physical exercise regimens. However, once they entered the hyperbaric chamber on *Dive Day 1*, they were fully occupied with the performance of physiological and psychomotor tests, which were not physically demanding except for the measurements of maximal tolerable work load and maximal aerobic power. As described in a paper by Ohta et al. (17), the latter measurements were made only once on each subject at 1 ATA predive, 31 ATA, and 1 ATA postdive, and each measurement took only 10–15 min. In other words, under the present experimental design, all subjects suffered from the lack of adequate physical exercise during the dive and thus there is a possibility that the subjects were progressively deconditioned. In fact, the average resting heart rate increased from 58 ± 1 beats/min at 1 ATA predive to 68 ± 1 ($P<0.001$) at 1 ATA postdive while the maximal aerobic power decreased from 3.11 ± 0.18 L O_2/min to 2.89 ± 0.16 ($P<0.05$) (17). These observations are consistent with the view that the subjects were indeed being deconditioned during the long dive period.

Based on these considerations, it is tempting to postulate that the progressive reduction in the magnitude of immersion-induced increase in stroke volume as the dive progressed is a result of deconditioning. Physical deconditioning is known to be accompanied by decrease in plasma volume, maximal aerobic power, and tilt tolerance (a greater tachycardia and smaller stroke vol-

ume) (19). Although it is beyond the scope of this communication to discuss the mechanisms underlying the above phenomenon, it appears that the immersion-induced enhancement of diastolic filling is primarily affected by deconditioning. There is no evidence to indicate that the basic cardiac contractility was altered during the course of the dive (Table II).

The immersion diuresis and natriuresis are primarily attributed to the increase in the intrathoracic blood volume (resulting from the increased venous return), which inhibits the release of both ADH and aldosterone through stimulation of the left atrial volume receptors (4,16). As discussed above, the magnitude of immersion-induced increase in stroke volume decreased progressively with the dive time. This decrease indicates that there must have been a corresponding, progressive reduction in the degree of stimulation of volume receptors during immersion as the dive progressed. Therefore, it is not surprising that the magnitude of immersion diuresis was greatest at 1 ATA predive and decreased at 31 ATA and 1 ATA postdive, in that order (Fig. 2). Although the glomerular filtration rate tended to decrease at 1 ATA postdive, there was a significant overall negative correlation between the urine flow and the urinary ADH excretion, an indication that the degree of ADH inhibition during immersion is a determinant of urine flow.

In contrast to the predicted behavior of the above diuretic response to immersion, the natriuretic response (as represented by the excretion of total osmotic substance) was quantitatively similar at 1 ATA predive and 31 ATA (Fig. 2). At 1 ATA postdive, the natriuretic response was somewhat less than in other experiments. The latter may be explained by the tendency for lower glomerular filtration rate at 1 ATA postdive, because the fractional excretion of Na^+ was the same in all experiments (Fig. 3). As predicted, the immersion-induced natriuresis was accompanied by a reduction in plasma aldosterone level at 1 ATA predive and 31 ATA, but not at 1 ATA postdive. These findings indicate a) that the threshold (as expressed by the degree of increase in intrathoracic blood pooling) for the inhibition of renin-angiotensin-aldosterone system during immersion may be different from that for the inhibition of ADH, and b) that there is another natriuretic factor either activated or released during immersion under certain experimental conditions. The possibility for the latter factor has also been pointed out by Neuman et al. (20).

In summary, the present study revealed a possible consequence of deconditioning of subjects during a prolonged dive. The results indicate certain alterations in the cardiovascular and endocrine mechanisms that are involved in the maintenance of body fluid volume regulation.

References

1. Agostoni E, Gurtner G, Torri G, Rahn H. Respiratory mechanics during submersion and negative pressure breathing. J Appl Physiol 1966;21:251–258.
2. Hong SK, Cerretelli P, Cruz JC, Rahn H. Mechanics of respiration during submersion in water. J Appl Physiol 1969;27:535–538.
3. Arborelius M Jr, Balldin UI, Lilja B, Lundgren CEG. Hemodynamic changes in man during immersion with the head above water. Aerosp Med 1972;43:592–598.
4. Epstein M. Renal effects of head-out water immersion in man: implications for an understanding of volume homeostasis. Physiol Rev 1978;58:529–581.
5. Smith RM, Hong SK, Dressendorfer RH, Dwyer HJ, Hayashi E, Yelverton C. Hana Kai II: a 17-day dry saturation dive at 18.6 ATA. IV. Cardiopulmonary functions. Undersea Biomed Res 1977;4:267–281.
6. Hong SK. Body fluid balance during saturation diving. In: Hong SK, ed. International symposium on man in the sea. Bethesda, MD: Undersea Medical Society, 1975:127–140.
7. Nakayama H, Hong SK, Claybaugh JR, Matsui N, Park YS, Ohta Y, Shiraki K, Matsuda M. Energy and body fluid balance during a 14-day dry saturation dive at 31 ATA (SEADRAGON IV). In: Bachrach AJ, Matzen MM, eds. Underwater physiology VII. Proceedings of the seventh symposium on underwater physiology. Bethesda, MD: Undersea Medical Society, 1981:541–554.
8. Kubicek WG, Kottke EJ, Ramos MU, Patterson RP, Witsoe DA, Labree JW, Remole W, Layman TE, Schoenin H, Garamela JT. Non-invasive blood flow monitoring. The Minnesota impedance cardiograph-theory and application. Biomed Eng 1974;9:410–416.
9. Consolazio CF, Johnson RE, Pecora LJ. Physiological measurements of metabolic function in man. New York: McGraw-Hill Book Co., 1963.
10. Lowry OH, Rosebrough NO, Farr AL, Randall RJ. Protein measurement with the Folin phenol reagent. J Biol Chem 1951;193:265–275.
11. Hong SK, Claybaugh JR, Frattali V, Johnson R, Kurata F, Matsuda M, McDonough AA, Paganelli CV, Smith RM, Webb P. Hana Kai II: a 17-day dry saturation dive at 18.6 ATA. III. Body fluid balance. Undersea Biomed Res 1977;4:247–266.
12. Walker BR, Attallah AA, Lee JB, Hong SK, Mookerjee BK, Share L, Krasney JA. Antidiuresis and inhibition of PGE$_2$ excretion by hyperoxia in the conscious dog. Undersea Biomed Res 1980;7:113–126.
13. Garrard CD, Weissler AM, Dodge HT. The relationship of alterations in systolic time intervals to ejection fraction in patients with cardiac disease. Circulation 1970;42:455–462.
14. Matsuda Y, Yamada S, Kurogane H, Sato H, Maeda K, Fukuzaki H. Assessment of left ventricular performance in man with impedance cardiography. Japn Circ J 1978;42:945–954.
15. Lababidi AD, Ehmke A, Durnin RE, Leaverton PE, Laurer RM. The first derivative thoracic impedance cardiogram. Circulation 1970;41:651–658.
16. Matsuda M, Nakayama H, Arita H, Morlock JF, Claybaugh J, Smith RM, Hong SK. Physiological responses to head-out immersion in water at 11 ATA. Undersea Biomed Res 1978;5:37–52.
17. Ohta Y, Arita H, Nakayama H, Tamaya S, Lundgren C, Lin YC, Smith RM, Morin R, Farhi LE, Matsuda M. Cardiopulmonary functions and maximal aerobic power during a 14-day saturation dive at 31 ATA (SEADRAGON IV). In: Bachrach AJ, Matzen MM, eds., Underwater physiology VII. Proceedings of the seventh symposium on underwater physiology. Bethesda, MD: Undersea Medical Society, 1981:209–221.

18. Anderson RJ, Berl T, McDonald KM, Schrier RW. Evidence for an in vivo antagonism between vasopressin and prostaglandin in the mammalian kidney. J Clin Invest 1975;56:420–426.
19. Chobanian AV, Lille RD, Tercyah A, Blevins P. The metabolic and hemodynamic effects of prolonged bed rest in normal subjects. Circulation 1974;49:551–559.
20. Neuman TS, Goad RF, Hall D, Smith RM, Claybaugh JR, Hong SK. Urinary excretion of water and electrolytes during open-sea saturation diving to 850 fsw. Undersea Biomed Res 1979; 6:291–302.

EFFECT OF WATER TEMPERATURE AND VITAL CAPACITY IN HEAD-OUT IMMERSION

D. I. Kurss, C. E. G. Lundgren, and A. J. Påsche

Immersion may reduce vital capacity (VC). The mechanism has traditionally been ascribed to hydrostatic effects, in particular to intrathoracic blood pooling (1). However, during lung volume measurements in immersed subjects we noticed a tendency for VC to recover during exercise. A reduction in intrathoracic blood pooling secondary to warming and vasodilation in peripheral tissues was a possible mechanism that we considered for explaining this observed increase in VC.

As a way to illuminate this hypothesis we tested the influence of different water temperatures on VC in the immersed condition. Various maneuvers were subsequently performed to manipulate the blood distribution in connection with immersion.

METHODS

Between three and nine subjects were studied in different experiments. An upright sitting position was assumed throughout all procedures. Subjects wore swim trunks during head-out immersion and a bathrobe when nonimmersed. Air temperature ranged between 18° and 23°C and water temperature was 20°, 35°, or 40°C, controlled within ±0.25°C. A series of measurements was also made in subjects wearing a 5-mm neoprene wet suit while immersed in 10°C water. In some experiments inflatable tourniquets were placed as proximally as possible on upper arms and thighs. Vital capacity was recorded repetitively at 2.5-min intervals. When tourniquets were used the desired pressure was achieved within a few seconds. A pressure of 250 Torr used for arterial stasis and 60 and 90 Torr (compensating for differences in depth of

immersion) was applied on arms and legs, respectively, for venous stasis. The Valsalva maneuver was performed at 80–90% of VC and was immediately followed by a rapid full inspiration and VC measurement.

RESULTS

The results of VC measurements in nine subjects are shown as normalized mean values ±SE in Fig. 1. Immediately upon immersion there was a fall in VC to approximately 94% of the preimmersion value, with no significant difference between any two water temperatures. However, within 2.5 min and for the remainder of the immersion period, the VC was clearly affected by water temperature. The mean values of all measurements in the latter period are shown for each temperature in Fig. 1. As a measure of conservatism in the interpretation of data, mean values of measurements spanning 12.5 min were used for the immersion period. There was no significant difference between pre- and postimmersion VC. The mean VC in 35°C water was 94.6% ± 0.2% of preimmersion control values ($P<0.005$). In 20°C water the VC went down from the preimmersion level to a mean value of 91.1% ± 0.5% ($P<0.005$). This differed significantly from the 35°C level ($P<0.025$) as well as from the 40°C level ($P<0.005$). It may be noted that there was a gradual fall in VC in
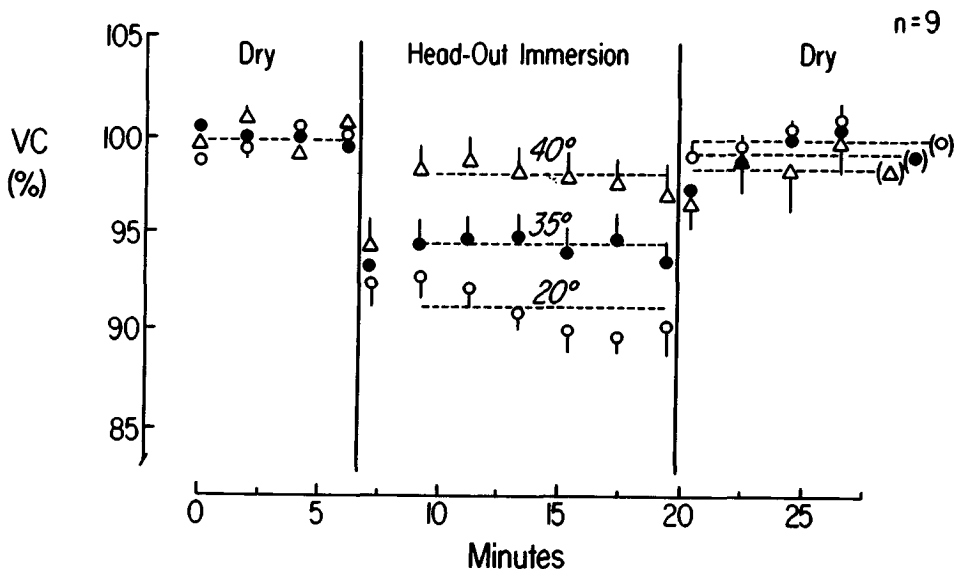
Fig.1. Vital capacity (VC) in the sitting position during nonimmersion (dry) and head-out immersion in water of 20°, 35°, and 40°C. Results were normalized to means of preimmersion values and means ±SE are given for 9 subjects. *Dashed lines* indicate mean values for measurements obtained during related time span.

20°C water from 92.7% ± 1.5% to 90.5% ± 1.6% ($P<0.01$). Remarkably, the 40°C VC value at 98.0% ± 0.2% was not significantly different from the preimmersion result, and it was higher than the 35°C value ($P<0.025$). While all subjects were comfortable in thermoneutral condition, i.e., 35°C water (cf. ref. 2), some felt overly warm in 40°C water and all felt cold and shivered in 20°C water. In three subjects immersed in 10°C water and wearing wet suits there were no subjective feelings of cold and no shivering. Yet, their mean VC went as low as 88.9% ± 1.4%, which was close to their VC (89.3% ± 0.5%) when wearing swim trunks in 20°C water.

As shown in Fig. 2, the application of arterial stasis to the extremities before immersion in 20°C water largely prevented the decline in VC otherwise seen. The mean VC in 4 measurements was only reduced to 98.0% ± 0.5% ($P<0.025$). However, upon release of the arterial stasis there was a rapid reduction in VC to 87.3% ± 0.5% of the preceding level ($P<0.005$). After this, venous stasis was applied and the VC values climbed to a mean of 91.6% ± 1.3%, which was higher than during the preceding period ($P<0.01$) and lower than during the preimmersion control period ($P<0.01$). Following the release of the venous stasis the VC fell significantly ($P<0.01$), assuming a value of 86.5% ± 1.1% of preimmersion control ($P<0.005$). Doing a Valsalva maneuver allowed the subjects to increase their mean VC to 92.5% ± 2.8% from the preceding 86.5% level ($P<0.01$). Returning to the nonimmersed situation the mean VC increased but, at 96.8% ± 1.1%, did not quite attain the preimmersion level ($P<0.05$).
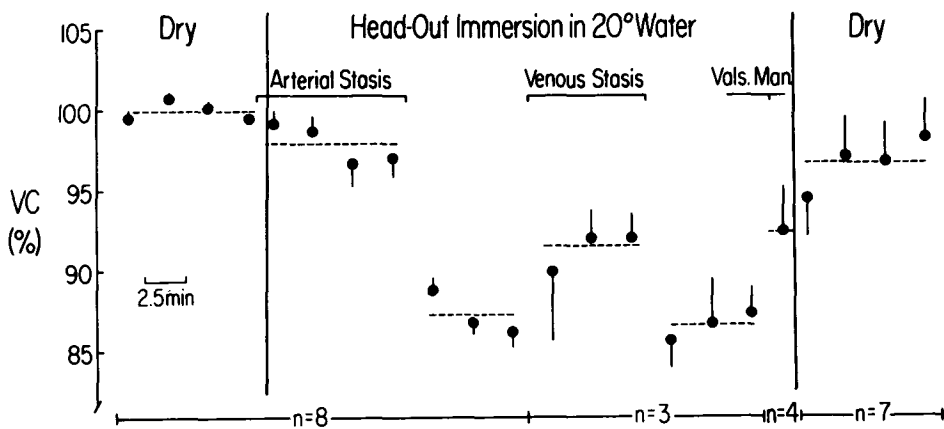
Fig. 2. Vital capacity (VC) in the sitting position during nonimmersion (dry) and head-out immersion in 20°C water. The effects of periods of arterial and venous occlusions by tourniquets on arms and legs and the Valsalva maneuver are shown. Values are means ±SE from 3 to 8 experiments (see *abscissa*) in 3 or 4 subjects. *Dashed lines* indicate mean values for measurements obtained during related time span.

DISCUSSION

The immediate 6–7% reduction in VC upon immersion was unaffected by widely differing water temperatures (20°, 35°, and 40°C). The lowering of the lungs' capacity to hold air was presumably caused by a sudden redistribution of blood from the peripheral into thoracic vessels. This notion gains some support by the fact that arterial stasis on the extremities prevented this first drop in VC in 20°C water. The slight reduction (2%) in VC despite the use of the arterial stasis may be ascribed to blood movement not prevented by the tourniquets. The VC in water of neutral temperature (35°C) remained at the initial immersion level. The mean reduction of 5.4% is in good agreement with 14 other studies yielding an average VC reduction of 6.1% (cf. ref. 2). It may therefore be concluded that, after the initial redistribution of blood due to hydrostatic immersion effects, there were no further major adjustments in blood distribution in the 35°C water. However, such adjustments apparently occurred in both the cool and warm water. After the initial 7.5% drop in VC in 20°C water, there was a further reduction by 2.2% during the immersion period. The nature of this slower change is still open to speculation. In addition to the hydrostatic effect on VC evident in 35°C water, there was probably an element of cold vasoconstriction in 20°C water accounting for part of the large, and increasing, drop in VC. The possibility cannot be excluded, however, that some of the VC reduction toward the end of the exposure to 20% water was caused by lessening of neuromuscular performance.

The crucial role of blood redistribution for the observed effects is further borne out by the gains in VC achieved by the application of venous stasis and the Valsalva maneuver (4.3% and 6.0%, respectively). The effect of the venous stasis is to allow blood to accumulate distal to the tourniquets. The increased intrathoracic pressure generated by the Valsalva maneuver forces blood out of the chest cavity (cf. ref. 3). After the initial drop in VC by 5.7% upon immersion in 40°C water the VC rapidly recovered almost to the preimmersion level. In all likelihood this reflected, after the initial increase in intrathoracic blood volume, a redistribution of blood from the chest cavity to peripheral vessels that were subject to thermoregulatory vasodilation.

Remarkably, when the subjects were protected by a wet suit and comfortable in 10°C water, the loss in VC was the same (11.1%) and equally as rapid as it was (10.7%) when they were naked and shivering in 20°C water. It is therefore reasonable to conclude that both that part of the intrathoracic blood redistribution which depends on peripheral cold vasoconstriction and that caused by hydrostatic effects of the immersion were of the same magnitude in the two conditions.

It follows from the present observations that when lung volumes are measured during immersion, and possibly in nonimmersion, the thermal situation of the subject should be considered. In addition, to the extent that intrathoracic blood pooling has secondary effects on cardiorespiratory function, for example, causing air trapping, changes in compliance (2,4) and cardiac output (5), these effects may also be modified by changes in thermal stress. One

should also note that warm water immersion, presumably through peripheral vasodilation, almost completely counteracted the hydrostatic effect evidenced throughout the neutral temperature immersions. This indicates that in high temperatures the external hydrostatic load during immersion may be overcome by intravascular hydrostatic forces. A new piece of evidence is presented demonstrating that physiologically significant cooling may occur in the suited, immersed subject in the absence of subjective sensations and shivering (cf. ref. 6).

Acknowledgment

References

1. Dahlbäck GO, Jönsson E, Linér MH. Influence of hydrostatic compression of the chest and intrathoracic blood pooling on static lung mechanics during head out immersion. Undersea Biomed Res 1978;5:71–85.
2. Dahlbäck GO. Lung mechanics during immersion in water with special reference to pulmonary air trapping. Thesis. Institute of Physiology and Biophysics. Sweden: University of Lund, 1978.
3. Fowler RC Guillet M, Rahn H. Lung volume changes with positive and negative pulmonary pressures. In: AF Technical Report 6528. 1951; 522–528.
4. Sterk W. Respiratory mechanics of diver and diving apparatus. Thesis. University of Utrecht. Utrecht: Drukkery Elinkwijk, 1971.
5. Arborelius M Jr, Baldin UI, Lilja B, Lundgren CEG. Hemodynamic changes in man during immersion with the head above water. Aerosp Med. 1972;43:592–598.
6. Webb, P. Body temperature monitoring. In: Monitoring vital signs in the diver. The Sixteenth Undersea Medical Society Workshop, 17–18 March 1978. Lundgren CEG, ed. Bethesda, MD: Undersea Medical Society Inc, 1978.

Part III

HIGH PRESSURE NERVOUS SYNDROME
PSYCHOMOTOR PERFORMANCE AND HIGH
PRESSURE NERVOUS SYNDROME

A VIEW OF SOME FUNDAMENTS OF THE HIGH PRESSURE NERVOUS SYNDROME

J. M. Hallenbeck

I have been asked to deliver an outsider's view of the high pressure nervous syndrome (HPNS) and the initial, overwhelming impression gained is that the scope of the subject is vast. The object of study extends from the electron at one extreme to human behavior at the other. The observations, approaches, and problems in this field are interrelated with the biophysics, biochemistry, pharmacology, and electrophysiology of membranes and, more specifically, the molecular basis of anesthesia. Such interrelationships have attracted a multidisciplinary corps of investigators whose varied backgrounds and approaches have catalyzed intellectual ferment on the one hand, but have created some problems of communication and conceptualization on the other. Some of the more arcane concepts in underwater physiology form the current mechanistic explanations for the perturbation of membrane function by pressure. Even the instruments employed in these studies have a sort of "Star Wars" quality for ordinary mortals. I could, for instance, pass close by a differential scanning calorimeter in broad daylight and fail to identify it.

The scope and diversity of this field exclude any possibility of presenting an exhaustive account of the accomplishments of every investigator working in it. Instead, I will sketch the essential elements of HPNS in humans, state the general problem, and then describe some fundamental principles which should aid in understanding the papers that follow in this session.

DEFINITION OF THE PROBLEM

As humans are exposed to ambient pressures equivalent to 500 feet of sea water (fsw) and deeper, a disturbance of neurologic function becomes manifest, which has been termed the high pressure nervous syndrome (HPNS) (1).

The signs and symptoms of the syndrome are manifold (2,3). A prominent feature is tremor, which has been variously observed to be resting, postural, and intentional, with a frequency ranging from about 1–10 cycles per second or Hertz (Hz). Also comprising the syndrome are fasciculations, myoclonic jerks, incoordination, nausea, lightheadedness, dysequilibrium, disorientation, shortened attention span, brief bouts of somnolence (microsleep), sleep disturbances, ease of fatigue, and decrements in performance. In animals, further compression can lead to seizures and death. Electroencephalographic changes are integral to the syndrome. In general, a reduction occurs in total EEG activity, which is most pronounced in the alpha frequency band and is associated with a relative or absolute increase in theta frequency-band activity. An interesting and potentially important aspect of the syndrome is that the depth of onset is a fairly stable attribute of an individual and susceptibility to development of HPNS varies widely among individuals. These circumstances suggest that selection of relatively HPNS-resistant personnel might prove feasible. Another characteristic of the syndrome is that its depth of onset tends to vary inversely with compression rate.

It is readily apparent that full-blown HPNS constitutes a formidable barrier to man's efforts to perform useful work at great depths. In order to expand the area of sea-bed on the continental slope accessible to the working diver, measures that will attenuate or eliminate HPNS must be devised and applied. This, then, is the practical challenge of HPNS. But additionally, research in this area may be expected to provide insights with far-reaching implications for the function of excitable membranes.

The papers in this session address the lipid-protein structure and physical chemistry of membranes, neurophysiology, neurochemistry, neuropharmacology, anesthesia, prevention of HPNS by "trimix," and the neuroanatomic substrate for HPNS. A brief discussion of some principles and concepts that underlie such specialized studies might enhance understanding and provide a background context within which the work can be interrelated.

THE MEMBRANE ASSEMBLY

A fundamental assumption shared by the majority of investigators is that HPNS arises from the effects of pressure on excitable membranes. A clear picture of the molecular make-up of the membrane assembly might help in understanding these hypothetical pressure effects. Phospholipids form the structural matrix of cell membranes (4,5). The phospholipids are amphipathic with both a hydrophilic region ("polar head group") and a hydrophobic region. Since the two regions of the molecule have incompatible solubilities, they tend to spontaneously organize into a minimum-energy configuration, the bilayer, in an aqueous medium. In this double-layer configuration the hydrophobic tails are in apposition and the hypdrophilic heads are exposed to the aqueous me-

dium on both sides of the membrane. Cholesterol, another membrane lipid, is interspersed with the phospholipid in a similar orientation.

Protein associated with the membrane falls into two general classes (6,7). *Integral* membrane proteins are amphipathic and span the phospholipid bilayer with their hydrophobic molecular regions embedded in the bilayer and their hydrophilic regions protruding into aqueous medium on each side. *Peripheral* membrane proteins are not inserted into the bilayer but tend to be on the cytoplasmic (inner) side of the membrane bound to integral protein. Membrane proteins of all cells are of five types: pumps, channels, receptors, enzymes, and structural proteins. The proteins may be viewed as resembling icebergs floating in a sea of lipid. Carbohydrates, attached to either protein or lipid, are invariably on the exterior surface of the membrane and seem to function as receptors. The membrane components are by no means static. Each apposed monolayer is fluid in two dimensions, and phospholipid molecules can rotate a million times a second within the monolayer. Integral proteins can also diffuse laterally within the membrane. However, flip-flops of the phospholipids from one monolayer to the other (motions in the third dimension) are distinctly uncommon and are estimated to occur only about once a month. Proteins do not flip-flop. These attributes of the membrane constituents preserve a definite sidedness and asymmetry in the membrane that is vital to proper function despite the frenetic molecular motion.

THERMOTROPIC TRANSITION OF MEMBRANE LIPIDS

An interesting and important characteristic of biomembranes is their ability to undergo a reversible thermotropic transition from a crystalline gel state at low temperatures to a liquid crystalline state at high temperatures (8,9). As the temperature rises above values in the transition range, the hydrocarbon fatty acid chains "melt" and acquire considerably more mobility and fluidity. However, the glycerol "backbone" and polar groups of the phospholipids retain a fairly regular order preserving some crystalline structure. The phase-transition therefore does not involve a change of state from solid crystal to a liquid (e.g., olive oil), but rather a shift from a crystalline gel to a liquid crystal. Anesthetics decrease the phase-transition temperature in purified phospholipid model membranes (10), and hyperbaric pressure antagonizes the decrease in phase-transition temperature induced by anesthetics (11). The physical state of the lipid milieu immediately surrounding pump and channel proteins may affect their mobility or stability and thereby influence transmembrane cation flux. One can easily visualize the crude analogy of a channel protein as an iceberg floating freely in slush corresponding to the milieu provided by the "melted" liquid crystalline state of the lipid and, on the other hand, the same iceberg relatively fixed in ice, corresponding to the milieu provided by the crystalline gel state of the lipid.

MEMBRANE POTENTIAL AND THE SODIUM PUMP

The major manifestations of HPNS are thought to arise from the effects of pressure on excitable membranes. The ability to maintain steady-state ion gradients and conduct electric currents confers upon a membrane the property of excitability. Nerve cells maintain an intracellular transmembrane potential of approximately −75 mV with respect to the extracellular fluid. This transmembrane potential is primarily due to metabolically maintained steady-state gradients for potassium (K^+) and sodium (Na^+) ion concentration, to the intracellular presence of impermeable anions, and to the very low permeability of Na^+ relative to K^+ at the resting membrane potential (12). In order to maintain the −75 mV intracellular potential, metabolic work must be performed by a specific pump protein, the $Na^+ - K^+$ ATPase. This integral membrane protein is composed of two alpha and two beta subunits with a combined molecular weight of about 275,000 daltons (13,14). There are roughly 100–200 Na^+ pumps/μm^2 of neuronal membrane, and each pump measures about 6×8 nm. If the membrane were scaled up to become a corridor in a building and each pump represented as a 1-m wide door, the next door would be 160 m down the hall. Operating at the maximum rate, each pump can transport across the membrane some 200 Na^+ ions and 130 K^+ ions/s. A typical neuron has perhaps a million sodium pumps with a capacity to move about 200 million Na^+ ions/s (14). This extraordinary pumping process requires the coupling of ATP hydrolysis to rapid cyclic configurational changes in the subunits that make up the integral membrane protein, $Na^+ - K^+$ ATPase. The membrane effects of pressure could be imagined to influence the freedom to vibrate of the subunits and, thereby, to alter the pump's function. Indeed, several workers have documented that the $Na^+ - K^+$ ATPase is sensitive to pressure, although further work is necessary to fully define this relationship (15–17).

CHANNEL PROTEINS

Conduction of ionic current is an essential property of excitable membranes. An explosive increase in sodium conductance generates the nerve action potential, and a subsequent increase in potassium conductance is involved in membrane repolarization. Transmembrane movement of cations occurs through pores in specific channel proteins (18–20). Such channel proteins have two fundamental properties: a) selective permeability, and b) excitability. A portion of the channel protein with a relatively fixed conformation acts as a selectivity filter and is responsible for allowing only ions of appropriate charge and physical dimensions to traverse its pore. Excitability is conferred by a different portion of the channel protein. This portion contains an electric field sensor coupled to mobile subunits that can react to membrane depolarization with rapid configurational change. Thus, this subassembly of the channel protein serves as a gating mechanism and links channel permeability to membrane potential.

Although the details of its molecular structure remain indistinct, the sodium channel is the most thoroughly studied of the channel proteins. Its molecular weight is between 230,000 and 300,000 daltons, which is in the same weight range as the sodium pump. The channel pore is about 0.3×0.5 nm at its narrowest point, the region of the selectivity filter. In this region, ionized carboxyl groups form part of the channel wall and negatively charged oxygen atoms protrude into the channel creating a permeability barrier that restricts the entrance of many ions but allows relatively free access to sodium ions. The selectivity filter is located on the external side of the membrane near the channel entrance. The gating mechanism is thought to be situated internally within the channel. Because the cell membrane is very thin (about 6 nm across), the resting membrane potential difference of 70–75 mV gives rise to a large intramembrane electric field, on the order of 100 kV/cm. Just as magnetic dipoles tend to align themselves with the lines of force in a magnetic field, the electric field sensors of the channel protein, acting as dipoles, tend to align themselves with the membrane electric field. As the strength of the membrane electric field changes during depolarization, the gates are driven from a closed conformation to an open conformation. After about 1 ms, and despite the continued state of membrane depolarization, the gates again close in a process termed inactivation. During the 1 ms that a channel gate is in the open conformation, about 100 Na^+ ions will pass through it in single file and contribute to the action potential. Since there are about 50 Na^+ channels/μm^2 of axonal membrane, the relevant spatial relations may be visualized by scaling up the dimensions and representing the membrane as the wall of a building corridor, just as was done with sodium pump proteins. If the sodium channel protein were represented as a 1-m wide door in a corridor, the next door would be 280 m down the hall, so the membrane is penetrated by sodium channels that are quite fine and widely spaced.

The selectivity filter and gating mechanism are two parts of the sodium channel protein that could be sensitive to perturbation by pressure. The dimensions of the pore in the filter region have a very close tolerance for optimal function, and small changes caused by membrane effects of pressure could have a pronounced effect on channel permeability to various ions. As mentioned, the configurational change of protein subunits in response to changes in the strength of the intramembrane electric field constitutes the gating mechanism of the channel. Such opening and closing of the gates normally occurs in a fraction of a millisecond, and pressure-induced rigidification of membrane could influence the mobility of the protein subunits and thereby influence the kinetics of gating. A fanciful possibility is that pressure-induced distortion of the spatial relations of subunits vis-à-vis one another could lead to gating incompetance similar to valvular incompetance in the heart.

The Voltage Clamp

Faced with measuring the time course of ion conductance during an action potential, a situation in which a changing ion conductance changes mem-

brane potential while a changing membrane potential changes ion conductance, all but the most clever investigators would be daunted. However, an ingenious technique has been devised to follow transmembrane ion flux under these conditions. The technique is the voltage clamp (22).

This technique employs two fine silver wires inserted longitudinally into an axon; one measures voltage and the other delivers current. The membrane may be forced from its resting potential to some new desired "clamped" potential by setting a variable voltage source to the new desired potential. This voltage is fed into one grid of a special differential amplifier while the other grid is exposed to the resting membrane potential. In one instant, a difference of potential appears between the two inputs to the amplifier, which instantaneously passes a current in such a direction as to drive the inside of the nerve fiber to the new desired potential. This is a process of negative feedback. Fluctuations in the direction and magnitude of the "clamp current" from the feedback differential amplifier hold the membrane potential at the new desired level, despite fluctuations in transmembrane ionic current, and maintain equal inputs of potential to the two grids of the feedback differential amplifier. The clamp current compensates for ionic currents flowing across the membrane at the new desired potential and mirrors them exactly. That is, the clamp current when measured is exactly equal and opposite to the net current carried by ions flowing across the membrane. This technique has allowed a number of workers to study the effect of pressure on transmembrane currents (21,23) and has identified a pressure-responsive inward (depolarizing) current that may contribute to pressure-generated repetitive impulse activity in axons (24). Such repetitive impulse activity could be a factor in the neuronal hyperexcitability of HPNS.

Synaptic Transmission

In general, transmission of information from one nerve cell to another in the human central nervous system occurs electrochemically via chemical synapses (12). Several of the papers in this session deal directly with synaptic transmission; a discussion of some fundamental principles may place the papers in context and give them perspective. It would be easy to assume as a first approximation that synaptic transmission is essentially a unidimensional process in which release of a chemical neurotransmitter couples electrical activity in one cell to electrical activity in another. On closer inspection, however, the process is multivariate and complex (14,25,26). Most of the following principles were derived from study of the neuromuscular junction of the frog.

The initial event at a synapse is depolarization of the presynaptic terminal. This leads to a specific increase in local membrane conductance for calcium ions and a consequent influx of calcium into the cell. The voltage-dependent opening of gates in calcium channels could conceivably be susceptible to perturbation by pressure in a manner analogous to that postulated for voltage-gated sodium channels. The rise in intracellular calcium triggers fusion of

neurotransmitter-containing synaptic vesicles to the presynaptic membrane. This fusion is followed by a release of the vesicle contents into the synaptic cleft, a process termed *exocytosis*. The membrane effects of pressure on this process are not clear at present. The chemical neurotransmitter is released in integral multiples of a basic multimolecular unit termed the *quantum*. Each quantum includes between 1000 and 10,000 molecules of neurotransmitter. As the magnitude in millivolts of the presynaptic membrane depolarization increases, there is a logarithmic increase in the amount of neurotransmitter released. A normal action potential generally leads to the simultaneous release of 200–300 quanta of neurotransmitter. The neurotransmitter diffuses across the synaptic cleft in 50–100 μs and, in the case of acetylcholine at the frog neuromuscular junction, two molecules of neurotransmitter bind to a specific receptor on the subsynaptic membrane. Such binding lowers the energy state of the open conformation of the chemically gated channel protein and thereby increases the probability that the channel will open. Each quantum of acetylcholine is estimated to open between 1000 and 2000 channels. The channels in the subsynaptic membrane remain open for about 1 ms and during that time roughly 40,000–50,000 univalent ions pass through each channel and the subsynaptic membrane is depolarized toward zero. As the subsynaptic membrane is depolarized below threshold, voltage-gated channels in it open and propagation of an action potential begins in the postsynaptic cell. After about 1 ms in a process causing closure of the chemically gated channel, acetylcholine diffuses off the receptor and is hydrolyzed by acetylcholinesterase. This disposal mechanism insures that the effect on receptors of each quantum of acetylcholine is rapid and independent. The hydrolyzed neurotransmitter is reabsorbed by the presynaptic terminal, synthesized into acetylcholine by enzymes supplied through an axonal transport system and stored in vesicles. Again, any influence of pressure on transmitter recycling processes is currently imponderable.

At excitatory synapses, chemically gated channels increase their conductance of Na^+ and K^+ in response to receptor-binding of neurotransmitter. At inhibitory synapses, the channels increase their conductance of K^+ and Cl^- in response to transmitter-binding. It is important to note that the same neurotransmitter (e.g., acetylcholine, serotonin or GABA) may be excitatory at one synaptic site in the nervous system and inhibitory at another.

Consideration of the intricacy and multiplicity of the steps involved in synaptic transmission as well as the fact that a single neurotransmitter may have diametrically opposite effects at different sites in the nervous system suggests a principle. Attempts to define mechanisms by which pressure affects excitable tissue will necessarily include studies that measure a single, elemental process such as one step in synaptic transmission. Such studies must characterize any disturbance that occurs in the process as a result of pressure. At the other extreme, sensitive whole-animal models are required to probe the effect of experimental manipulation of the single process on the development of HPNS. As you might expect, simple in-vitro models in which elemental processes are observed and complex whole-animal models in which HPNS can be accurately measured have already been coupled in a number of laboratories.

RELATIONSHIP BETWEEN PRESSURE AND ANESTHESIA

The relationship between pressure and anesthesia is both fascinating and provocative. Study of this relationship may reveal molecular mechanisms underlying anesthesia on the one hand and may guide efforts to protect divers from HPNS on the other. Speculation concerning molecular mechanisms of anesthesia has derived in large measure from correlations between physical properties of anesthetic agents and anesthetic potency (27). Perhaps the best-known correlation is between potency and solubility of anesthetic in olive oil, as described by Meyer and Overton in 1901. Correlations between potency and lipid solubility have led to the conclusion that anesthetics act by entering hydrophobic membrane regions such as hydrocarbon chains of the bimolecular lipid leaflet or hydrophobic residues of integral membrane proteins. Because the anesthetic concentration required to block synaptic transmission is one-third to one-tenth that required to block axonal conduction, the membrane surrounding the synapse is probably the site principally affected by general anesthetics (28).

Efforts to glimpse the nature of a phenomenon by its correlation with another phenomenon can cause befuddlement, as is well known by investigators in this area (28). For example, erythrocytes are regarded as a useful model of the membrane action of anesthetics for reasons that include a strong correlation between a) the anesthetic concentration reducing by 50% the hemolysis that occurs in a hypotonic solution, and b) the anesthetic concentration required to block a nerve (29). Anesthetic agents therefore protect against hemolysis and perhaps such protection could serve as an index of anesthetic effect. However, hydrostatic pressure acts in some respects opposite to anesthetic agents in that it is known to cause a hyperexcitable state (2) and to reverse the effect of anesthesia (30). On this basis, pressure might be expected to promote hemolysis of erythrocytes in a hypotonic solution and to antagonize the protective effect of anesthetics. At this point the correlation between anesthesia and hemolysis runs afoul because pressures up to 130 atm do not potentiate hemolysis and do not remove the protection against hypotonic hemolysis conferred by general anesthetics (31). Apparently, anesthesia and protection from hypotonic hemolysis, while related, are not essentially the same.

Studies of the erythrocyte membrane have, however, yielded the very important finding that at concentrations of anesthetic agents causing general anesthesia, a 0.02% bulk volume of the anesthetic occupies the membrane causing it to swell by that volume and leading to an even further membrane expansion. This additional expansion exceeds the van der Waals' volume of the absorbed anesthetic by more than tenfold so that the total membrane expansion is about 0.4%, an effect that possibly stems from changes in the conformation of integral membrane proteins (29,32). Lever et al. (33) have calculated that the pressure which reverses general anesthesia causes about 0.4% compression of membrane volume. A unifying theory has been adduced to explain the interactions of anesthetics and pressure. It has been termed the *critical volume hypothesis* and represents an extension of work by Mullins (34). It states that

anesthesia occurs when the volume of a hydrophobic region is caused to expand beyond a critical amount by the absorption of molecules of an inert substance. If the volume of this hydrophobic region can be restored by changes of temperature or pressure, then the anesthesia will be removed (35). The principal frailty of this hypothesis has been that it leads to easily testable predictions, the bane of any theory, and it has become inconsistent with several experimental observations.

A more recent modification of the critical volume theory, the *multi-site expansion hypothesis*, suggests that general anesthesia results from expansion of any of several hydrophobic sites, each with somewhat different physical properties (36). This hypothesis accommodates the previously discrepant data but was, in fact, formulated to do so. These theories are regarded as compatible with theories of anesthetic action which specify thermodynamic effects on membrane lipids that cause an increase in membrane fluidity. Such theories include the *phase-transition hypothesis*, the *lateral-phase separation hypothesis*, and the *fluidized-lipid hypothesis* (27,37). Compatibility among these theories rests on the observation that increases in membrane fluidity are associated with membrane expansion (38). It should be emphasized, however, that consequences of increased membrane fluidity other than expansion could be determinant (27,37).

Although the molecular details of anesthetic action remain elusive, an anesthetic agent can be pictured as a substance that enters hydrophobic membrane sites and electrically stabilizes neuronal membranes in the vicinity of synapses (28,29). Such stabilization is achieved by interfering with generation of the action potential without appreciably affecting resting potential and may involve a decrease in the permeability of channel proteins to cations (29,32). Indeed, cation restriction by the selectivity filter of a channel protein is partially based on steric hinderance and requires a precise pore size (19). Anesthetic-induced membrane expansion could easily be imagined to impede cation conductivity at this point.

High ambient pressure increases membrane excitability (24) by mechanisms that remain to be defined. Compression of a hydrophobic membrane site (36) or inhibition of a multimeric enzyme in which subunits must undergo rapid configurational change such as $Na^+ - K^+$ ATPase (39) are among the possibilities.

In any case, whether by direct mutual antagonism or by exertion of distinctly different membrane actions that tend to neutralize each other, pressure reverses the effects of anesthesia (30) and anesthesia protects against the effects of pressure (40). This relationship provides the rationale for adding nitrogen to a heliox breathing medium for deep diving. Bennett and colleagues have recently concluded a dive to a simulated depth of 650 m with $He-N_2-O_2$, or trimix, as the breathing medium and HPNS was virtually eliminated. This dive is a major achievement and a detailed account will be presented in this session.

COMPARISON OF HPNS AND METABOLIC ENCEPHALOPATHY

In the context of the present discussion, a constellation of symptoms and signs that included fatigue, drowsiness, inability to concentrate, short attention span, sleep disturbances, muscular fascicular twitching, tremor, dysequilibrium, myoclonic jerks, seizures, and EEG slowing with increased theta activity, would be equated with HPNS. These symptoms and signs could certainly indicate HPNS (41,42). They could also indicate uremic encephalopathy, hepatic encephalopathy, water intoxication, hypernatremia, acidosis, alkalosis, nonketotic hyperosmolar encephalopathy, hypoxic-hypercarbic encephalopathy, and the like. In short, this constellation of signs and symptoms is compatible with a number of metabolic encephalopathies (43,44). This is not to imply that the secret of HPNS may be found in the serum creatinine or blood ammonia level but rather that pressure, like a number of metabolic derangements, acts as a pervasive stimulus for neuraxis dysfunction and produces a clinical picture that closely resembles the metabolic encephalopathies. Although the entire neuraxis is diffusely exposed to the deranging stimulus in these disorders, dysfunction in one or more neuroanatomic regions characteristically predominates and the manifestations of the disease process vary accordingly.

There is an arresting parallel between "type I" and "type II" HPNS convulsions as delineated by Brauer and colleagues (45) and the seizure patterns observed in a study of the mechanisms underlying uremic encephalopathy in the cat (46). Myoclonic seizures arising from paroxysmal activity in the nucleus reticularis gigantocellularis and nucleus reticularis caudalis were induced by a slow intravenous infusion of urea, and the neurophysiologic and behavioral manifestations closely resembled type I HPNS convulsions. Hyperosmolar dehydration from infusion of 50% sucrose or 15% sodium chloride produced a distinctly different set of responses. Tonic-clonic seizures were associated with paroxysmal activity in forebrain structures and the net effect can be compared with type II HPNS convulsions.

GENERAL CONCLUSIONS

In summary, the research domain of HPNS has a vast sweep and touches many disciplines. It has drawn together many highly talented investigators, but their diversity and subspecialization has introduced the potential for communication problems. Information exchange would profit if the reported research in this field expressly stated background principles and discussed the findings in terms understandable to the broadest audience possible. The models and techniques exist and are generally being exploited to answer the major questions in the field and the prospect for continued rapid progress is excellent. I think investigators in this field are to be admired and congratulated.

Acknowledgments

References

1. Brauer RW. Seeking man's depth level. Ocean Ind 1968;3:28–33.
2. Hunter WL Jr, Bennett PB. The causes, mechanisms and prevention of the high pressure nervous syndrome. Undersea Biomed Res 1974;1:1–28.
3. High Pressure Nervous Syndrome. In: National Plan for the Safety and Health of Divers in their Quest for Subsea Energy, Part 12. Bethesda, MD: Undersea Medical Society, 1975.
4. Lodish HF, Rothman JE. The assembly of cell membranes. Sci Am 1979;240:48–63.
5. Singer SJ. Architecture and topography of biologic membranes. In: Weissmann G, Claiborne R, eds. Cell membranes. Biochemistry, cell biology and pathology. New York: HP Publishing Co. Inc., 1975:35–44.
6. Rothman JE, Lenard J. Membrane asymmetry. The nature of membrane asymmetry provides clues to the puzzle of how membranes are assembled. Science 1977;195:743–753.
7. Wickner W. The assembly of proteins into biological membranes: the membrane trigger hypothesis. Ann Rev Biochem 1979;48:23–45.
8. Melchior DL, Steim JM. Thermotropic transitions in biomembranes. Ann Rev Biophys Bioeng 1976;5:205–238.
9. Chapman D. Lipid dynamics in cell membranes. In: Weissmann G, Claiborne R, eds. Cell membranes. Biochemistry, cell biology and pathology. New York: HP Publishing Co. Inc., 1975:13–22.
10. Hill MW. Interaction of lipid vesicles with anesthetics. Ann NY Acad Sci 1978;308:101–110.
11. Kamaya H, Ueda I, Moore PS, et al. Antagonism between high pressure and anesthetics in the thermal phase-transition of dipalmitoyl phosphatidylcholine bilayers. Proc Natl Acad Sci 1975;72:201–210.
12. Schmidt RF, ed. Fundamentals of neurophysiology. New York: Springer-Verlag;1978.
13. Sweadner KJ, Goldin SM. Active transport of sodium and potassium ions. Mechanism, function and regulation. N Engl J Med 1980;302:777–783.
14. Stevens CF. The neuron. In: Flanagan D, ed. The brain. Scientific American Inc. San Francisco: WH Freeman Co., 1979:15–25.
15. Goldinger JM, Kang BS, Choo YE, Paganelli CV, Hong SK. The effect of hydrostatic pressure on ion transport and metabolism in human erythrocytes. J Appl Physiol (in press).
16. Hemrick SK, Gottlieb SF. Effect of increased pressures of oxygen, nitrogen, and helium on activity of a Na-K-Mg ATPase of beef brain. Aviat Space Environ Med 1977;48:40–43.
17. Sanders AP, Currie WD. $Na^+ - K^+$ ATPase and Mg^{++} ATPase in the genesis of HPNS. Undersea Biomed Res (in press).
18. Hille B. Gating in sodium channels of nerve. Ann Rev Physiol 1976;38:139–152.
19. Ulbricht W. Ionic channels and gating currents in excitable membranes. Ann Rev Biophys Bioeng 1977;6:7–31.
20. Keynes RD. Ion channels in the nerve-cell membrane. Sci Am 1979;240:126–135.
21. Henderson JV, Gilbert DL. Slowing of ionic currents in the voltage-clamped squid axon by helium pressure. Nature (London) 1975;258:351–352.
22. Hodgkin AL, Huxley AF, Katz B. Measurement of current-voltage relations in the membrane of the giant axon of Loligo. J. Physiol 1952;116:424–448.
23. Parmentier JL, Shrivastav BB, Bennett PB, Wilson KM. Effect of interaction of volatile anesthetics and high hydrostatic pressure on central neurons. Undersea Biomed Res 1979;6:75–91.

24. Kendig JJ, Schneider TM, Cohen EN. Pressure, temperature and repetitive impulse generation in crustaceon axons. J Appl Physiol 1978;45:742–746.
25. Kuffler SW, Nicholls JG. From neuron to brain. Sunderland, Mass: Sinauer Associates Inc., 1976.
26. Neumann E, Bernhardt J. Physical chemistry of excitable biomembranes. Ann Rev Biochem 1977;46:117–141.
27. Wardley-Smith B, Halsey MJ. Recent molecular theories of general anesthesia. Br J Anaesth 1979;51:619–626.
28. Halsey MJ. Mechanisms of general anesthesia. In: Eger EI, ed. Anesthetic uptake and action. Baltimore: Williams & Wilkins Co., 1974:45–76.
29. Seeman P. The membrane actions of anesthetics and tranquilizers. Pharmacol Rev 1972:24:583–655.
30. Johnson FH, Flagler EA. Hydrostatic pressure reversal of narcosis in tadpoles. Science 1951;112:91–92.
31. Brewster E, Collins S, Funnell GR, Smith EB. The effect of high pressure on the hemolysis of red blood cells. Undersea Biomed Res 1976;3:151–155.
32. Seeman P. The actions of nervous system drugs on cell membranes. In: Weissmann G, Claiborne R, eds. Cell membranes. Biochemistry, cell biology and pathology. New York: HP Publishing Co. Inc., 1975:239–247.
33. Lever MJ, Miller KW, Paton WDM, Smith EB. Pressure reversal of anesthesia. Nature (London) 1971;231:368–371.
34. Mullins LJ. Some physical mechanisms in narcosis. Chem Rev 1954;54:289–323.
35. Miller KW, Paton WDM, Smith RA, Smith EB. The pressure reversal of anesthesia and the critical volume hypothesis. Mol Pharmacol 1973;9:131–143.
36. Halsey MJ, Wardley-Smith B, Green CJ. Pressure reversal of general anaesthesia—a multi-site expansion hypothesis. Br J Anaesth 1978;50:1091–1097.
37. Koblin DD, Eger EI. Theories of narcosis. N Engl J Med 1979;301:1222–1224.
38. Trudell JR, Payan DG, Chin JH, Cohen EN. The antagonistic effect of an inhalational anesthetic and high pressure on the phase diagram of mixed dipalmitoyl-dimyristoyl-phosphatidylcholine bilayers. Proc Natl Acad Sci 1975;72:210–213.
39. Penniston JT. High hydrostatic pressure and enzymic activity: inhibition of multimeric enzymes by dissociation. Arch Biochem Biophys 1971;142:322–332.
40. Brauer RW, Goldman SM, Beaver RW, Sheehan ME. N_2, H_2, and N_2O antagonism of high pressure neurological syndrome in mice. Undersea Biomed Res 1974;1:59–72.
41. Brauer RW. The high pressure nervous syndrome: animals. In: Bennett PB, Elliott DH, eds. The physiology and medicine of diving and compressed air work. London: Baillière Tindall, 1975:231–247.
42. Bennett PB. The high pressure nervous syndrome: man. In: Bennett PB, Elliott DH, eds. The physiology and medicine of diving and compressed air work. London: Baillière Tindall, 1975:248–263.
43. Metabolic brain diseases causing coma. In: Plum F, Posner JB. Diagnosis of stupor and coma. Philadelphia: FA Davis Co., 1966:106–187.
44. Brain dysfunction in metabolic disorders. Plum F, ed. Assoc Res Nerv Mental Disease. New York: Raven Press, 1974:53.
45. Brauer RW, Mansfield WM Jr, Beaver RW, Gillen HW. HPNS as a composite entity: consequences of an analysis of the convulsion stage. In: Bachrach AJ, Matzen MM. Underwater physiology VII. Proceedings of the seventh symposium on underwater physiology. Bethesda, MD: Undersea Medical Society, 1981:391–399.
46. Zuckermann EC, Glaser GH. Urea-induced myoclonic seizures: an experimental study of site of action and mechanism. Arch Neurol 1972;27:14–28.

EFFECTS OF GENERAL ANESTHETICS ON POSTSYNAPTIC RESPONSES

H. J. Little, S. E. Austen, and W. D. M. Paton

For many years it has been known that physiological interactions occur between high pressure and general anesthetics in vivo, in that helium or hydrostatic pressure reverses general anesthesia in vivo and general anesthetics postpone the high pressure neurological syndrome (HPNS) to higher pressures (1). The neurophysiological basis of these interactions, however, has not yet been elucidated. There is evidence that all anesthetics act by a single mechanism, such as the excellent correlation between anesthetic potency in vivo and lipid solubility and the demonstration that pressure reverses the anesthesia due to all the different types of general anesthetic agents. But, evidence has also been presented that different mechanisms of action are involved (2). It is possible that the membrane site(s) at which pressure reverses anesthesia and at which it produces the HPNS are different (3), but the fact remains that the general anesthetics are the most effective agents found so far which are active in postponing the HPNS; for example, they are considerably better than the classic anticonvulsant agents. Evidence is therefore needed concerning the neurophysiological changes that underlie the actions of general anesthetics.

Determination of the neuronal basis of anesthesia is complicated by the problem of distinguishing between the nonspecific actions, which are due to the presence of the drug in the membrane, and the more specific ones, which involve binding to protein components of the cell membrane and are dependent on the structures rather than the physico-chemical properties of the drugs. It is therefore important to compare the effects of various types of anesthetic agents.

There is evidence that the basis of the actions of general anesthetics lies in their effects on synaptic transmission (4). However, no single action of an-

esthetics on synaptic transmission has yet been identified that correlates well with their effects in vivo.

During the last few years we have been conducting a detailed analysis of the effects of general anesthetics and pressure on isolated tissue systems to compare their effects on the different components of neuronal transmission with their effects in vivo.

The first part of the project explored the effects of pressure and anesthetics on transmitter output (5,6). The guinea pig ileum was used as a model preparation, and the spontaneous and electrically stimulated release of acetylcholine was measured. Helium pressure alone caused a small (20%) but statistically significant increase in acetylcholine output. There were some radical differences between the actions of anesthetics: certain gaseous agents—nitrous oxide, argon, nitrogen, sulphur hexafluoride, and carbon tetrafluoride—increased the acetylcholine output while urethane, octanol, and phenobarbitone decreased it. In addition, it was found that whether the anesthetics increased or decreased the transmitter release the changes were not reversed by high pressures of helium (130 atm). From these results it was concluded that the effects of anesthetic action on transmitter release, as judged from their actions on this peripheral tissue, would not provide a common element that could form the basis for their in vivo actions.

This suggested that an important site for anesthetic action might be the postsynaptic membrane responses. There is considerable evidence that low concentrations of anesthetics do affect these postsynaptic responses, but little direct comparison of their effects on the responses of mammalian tissues to different agonists has been made. Postsynaptic responses also have been reported to be more sensitive to pressure than other neuronal functions (7).

Changes in the permeability of the neuronal membrane to various ions are fundamental processes underlying the stages of synaptic transmission and of axonal conduction. These changes are characteristic of excitable tissues and must be distinguished from the passive permeability properties of nonexcitable cell membranes and from active transport. Nonspecific effects of general anesthetics on membrane lipids or on proteins within the lipid can be envisaged, which might prevent the changes in the conformation of membrane proteins that occur during synaptic transmission.

We are currently investigating the effects of anesthetics and pressure on the actions of agonists that cause different conductance changes within the postsynaptic membrane. Our purpose is to determine whether in our conditions there is any selectivity of action by anesthetics and pressure on these ion permeability changes, such as Barker found with certain anesthetics on invertebrate ganglion cells (8). Two preparations are being used for these studies: the guinea pig ileum, which provides a direct comparison with the studies on transmitter release, and the rat superior cervical ganglion. The responses on the ileum to acetylcholine, which increases sodium, potassium, and possibly chloride conductances (9), and to substance P, which is thought to decrease potassium conductance (10), have been studied. Most of the work on the effects of anesthetics on synaptic transmission has involved cholinergic synapses and little is known of their effects on peptidergic transmission.

METHOD AND MATERIALS

We compared both the effects of several different anesthetics on the responses of the ileum to substance P, acetylcholine, potassium chloride, and electrical stimulation and their effects on desensitization to these agonists.

The ileum preparation was set up as described previously (11). Solid or liquid anesthetics were added to the Krebs' solution after control dose-response curves had been established and the doses repeated after a 1-h equilibration with the anesthetic.

The steroid anesthetic alphaxalone was added as the commercial solution Althesin, which has the following composition: alphaxalone 0.9% wt/vol, alphadolone acetate 0.3% wt/vol, Cremophor EL 20% wt/vol, NaCl 0.25% wt/vol. The concentration in the RESULTS section refers to the concentration of alphaxalone only. The corresponding concentration of Cremophor EL alone was used in the control experiments.

Results were obtained from six different preparations of ileum. The responses to repeated dose-response curves on control preparations in the absence of anesthetic were reproducible throughout.

Desensitization was investigated in two ways: First, by the addition of repeated doses of concentrations of each agonist, which produced a nearly maximal response, and then repetition of these doses in the presence of anesthetic; and second, by comparing the desensitization to subsequent doses after exposure to a very high dose of agonist for 5 min in the presence and absence of anesthetic.

Preliminary work has been carried out on the ganglion preparation. Apparatus has been designed and built in which the surface potential changes in the ganglion caused by the addition of agonist drugs can be recorded. The effects of helium pressure on the responses to different agonists are currently being compared.

RESULTS

Dose-Response Curves

The responses of the ileum to acetylcholine, substance P, potassium chloride, and electrical stimulation were depressed by the following anesthetics: octanol, urethane, pentobarbitone, ethanol, ketamine, and Althesin; phenobarbitone had less effect. The effective concentrations are given in Table I.

For the purposes of this paper we have chosen to express the results rather simply as the percentage reduction of response by the anesthetics when the tissue is exposed to a concentration of agonist that produces 50% of the maximum responses under control conditions (Table I).

Illustrative graphs of the dose-response curves are shown in Figs. 1–3, which reveal the complexity of the effects of the anesthetic. The reduction of the response at the control ED_{50} dose is achieved by a lateral shift in the log

TABLE I
Dose Concentrations and Percentage of Response Decrease

Anesthetic	Agonist	Decrease in Response at Control ED_{50} Concentration (%)
Ketamine	ACh	66
0.8 mM	Substance P	74
	KCl	72
	Voltage	72
Ethanol	ACh	90
400 mM	Substance P	90
	KCl	58
	Voltage	90
Urethane	ACh	79
100 mM	Substance P	57
	KCl	74
	Voltage	90
Octanol	ACh	70
0.25 mM	Substance P	74
	KCl	86
	Voltage	70
Althesin	ACh	85
0.5 mM	Substance P	84
	KCl	88
	Voltage	70
Pentobarbitone	ACh	20
0.2 mM	Substance P	30
	KCl	24
	Voltage	22
Phenobarbitone	ACh	−3
0.4 mM	Substance P	−4
	KCl	8
	Voltage	40
Cremophor EL	ACh	40
	Substance P	25
	KCl	16
	Voltage	−8

Ach, acetylcholine; KCl, potassium chloride.

dose-response curve (seen in Figs. 1 and 2) and also by a change of slope and gross change in maximum (as seen for potassium chloride in Fig. 3).

These two types of behavior (and combinations of them) present an analytical problem because usually they would imply rather different mechanisms of action. The uncertainty is how far one should allow for the presence of "spare" receptors. For the time being we have simply used the percentage changes shown in Table I, on the basis that the control ED_{50} probably represents an intensity of agonist action not too far from the physiological so that
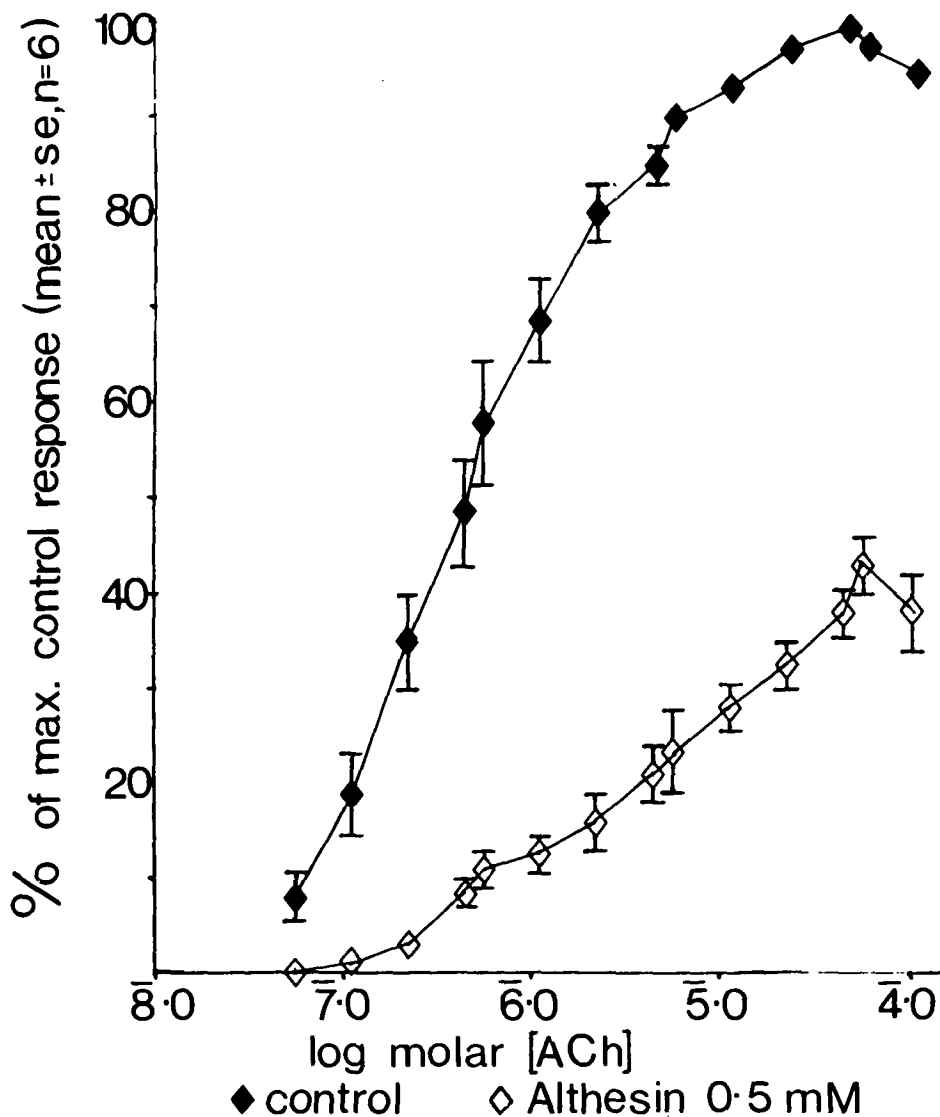
Fig. 1. Depressive effects of Althesin on the responses of the ileum to acetylcholine.

the proportionate reduction in this should give a reasonably fair estimate of the practical impairment of synaptic function. The reduction of the maximum response could be used as a measure, but the magnitude of this response with the tissue stretched to the limits of its capacity is not easy to be confident about as it incorporates a considerable (although variable) degree of desensitization—itself a phenomenon that can be brought about in various ways and one we found to be affected by the anesthetic agents.
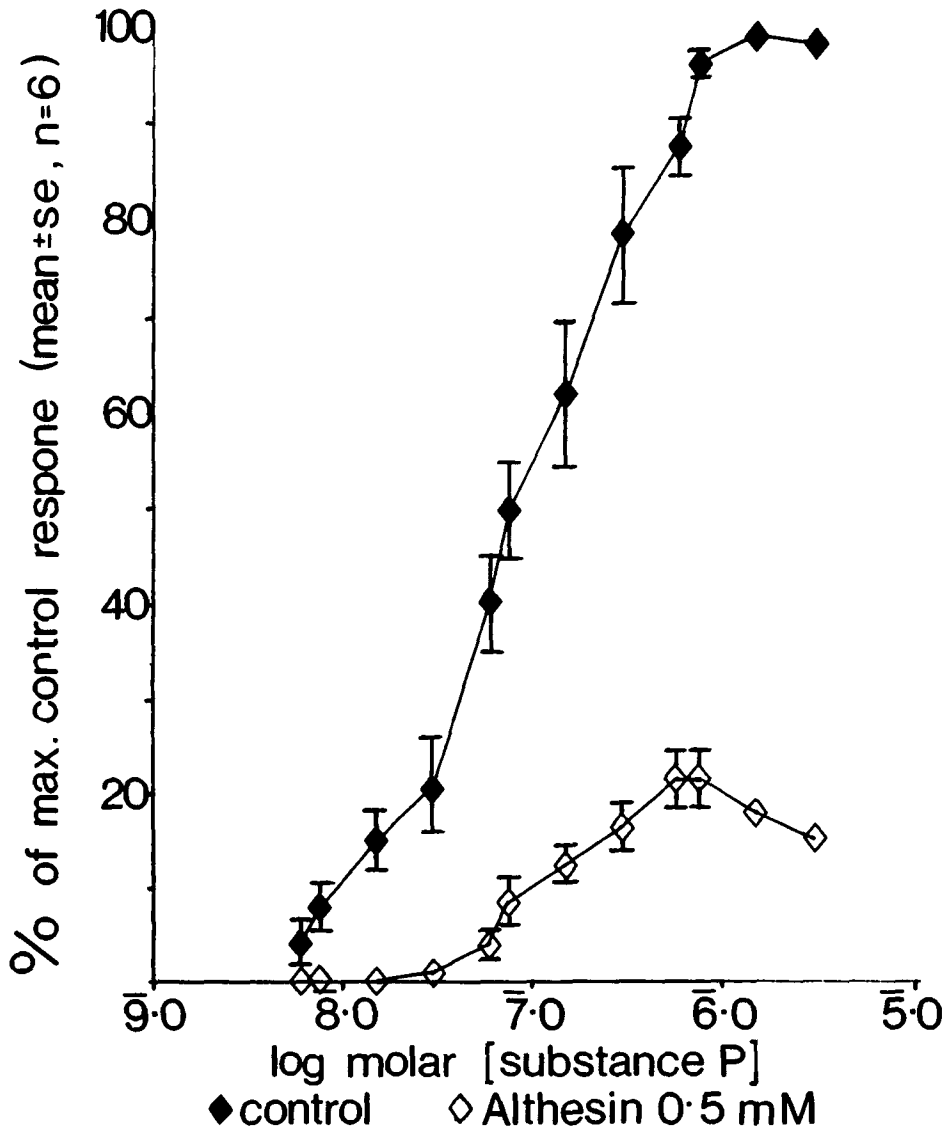
Fig. 2.   Depressive effects of Althesin on responses of ileum to substance P.

The degree of depression of the responses to each agonist was very similar for each agonist at the control ED_{50} doses, and with the exception of phenobarbitone there did not appear to be any clear pattern of selective interference with the responses to any particular agonist.

The maximum responses obtained to substance P were consistently decreased more than those to acetylcholine. This was seen with all the anes-
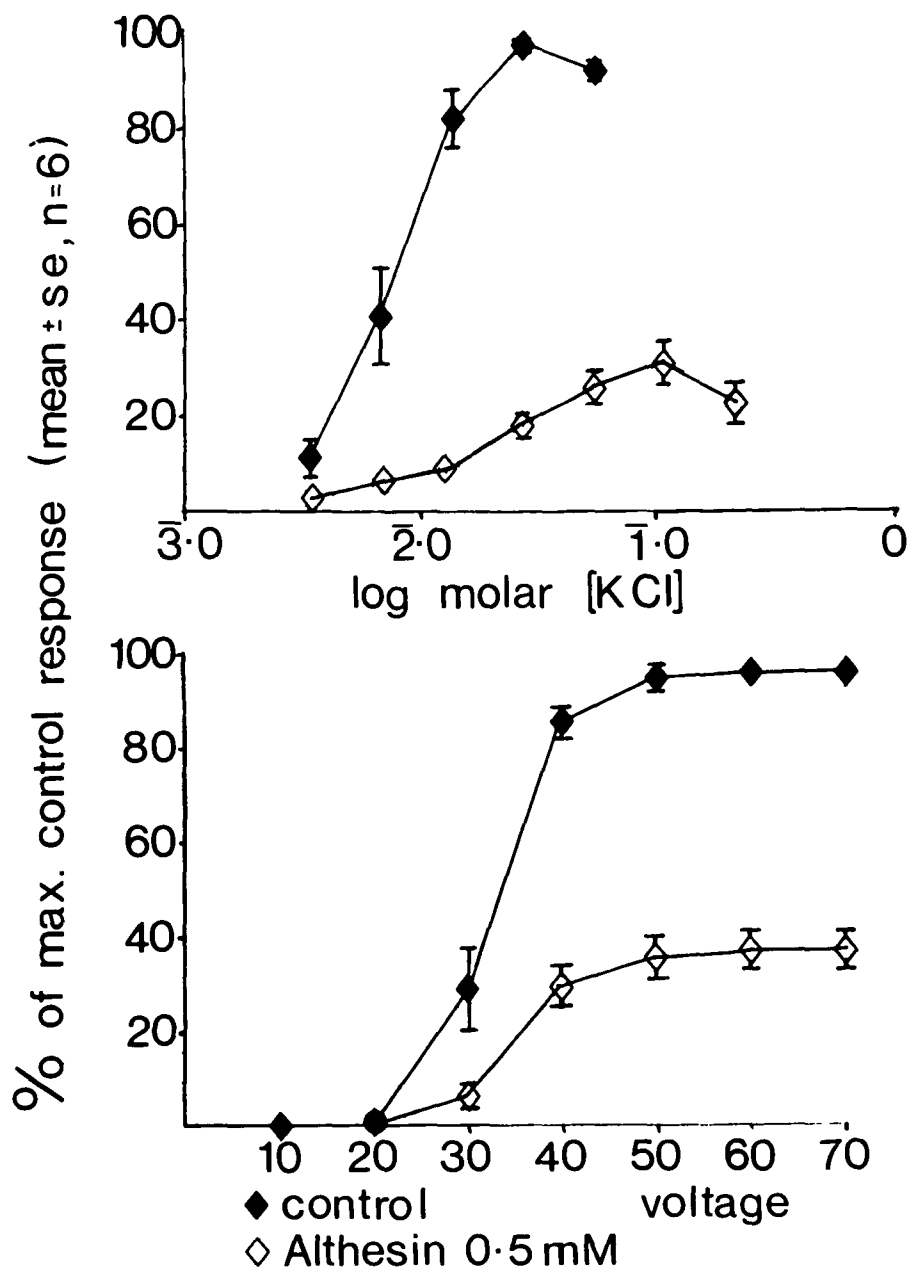
Fig. 3. Depressive effects of Althesin on the responses of the ileum to potassium chloride (KCl) (*upper curves*) and to electrical stimulation (voltage) (*lower curves*).

thetics except ethanol. It is of interest to relate this decrease to the effects of the anesthetics on desensitization to these agonists.

Phenobarbitone, which differs from pentobarbitone in having a more sedative and anticonvulsant action in vivo than being a general anesthetic, had less effect on the responses than did the equimolar concentration of pentobarbitone (0.4 mM). With acetylcholine and substance P the dose-response curves in the presence of the anesthetic crossed the control ones. This effect was small but significant and could be important because investigators working at different levels of response might see diametrically opposite results. The greater depression of the response to electrical stimulation than that seen with acetylcholine is most likely due to the decrease in acetylcholine release found previously with this concentration (6).

For each individual tissue the absolute heights of the maximum responses to each agonist were of the same amplitude. Therefore, the effects of the anesthetics were not likely to be caused by the differences in the amplitude of the maximum responses.

Cremophor El alone, in the same final concentration as used in the Althesin solution, caused decreases in the responses but these were less than those seen with Althesin.

Studies in Desensitization

It has been suggested (12) that an increase in receptor desensitization may contribute to general anesthesia. To determine how far this effect contributed to the present results, we determined the effects of the anesthetics on the development and recovery from desensitization. This work is still in progress but preliminary results are presented.

The doses of substance P were given at 3-min intervals during the dose-response curves, because preliminary tests showed that no desensitization is seen when this time schedule is used. To investigate whether the greater effects of the anesthetics on substance P compared with those to acetylcholine were due to greater desensitization, we tested the effects of the anesthetics on the repeated administration (at 3-min intervals) of a concentration of substance P, which produced a submaximal response. No significant desensitization was seen in the presence of urethane, octanol, or pentobarbitone.

When this concentration of substance P is added at the shorter interval of 1 min, a small amount of desensitization is seen on control preparations. When this time schedule was used a clear effect of certain anesthetics was seen. In the absence of anesthetic, the decrease in response amplitude to 10 doses was 12% for substance P, 59% for urethane (100 mM), and 100% for octanol (0.5 mM), but the decrease was only 10% for pentobarbitone (0.4 mM). No significant changes were seen when doses of potassium chloride were given at 1-min intervals, either with or without these anesthetics. The time intervals between the successive doses were sufficient to exclude nonspecific desensitization.

Using the second method for studying desensitization, we obtained evi-

dence that ketamine and Althesin also increased desensitization to substance P, but had less effect on acetylcholine.

DISCUSSION

These results show that all the general anesthetics tested depressed the postsynaptic responses to all the agonists used, but phenobarbitone was almost ineffective in this respect at the concentrations used.

The response of the ileum to acetylcholine involves increases in permeability to sodium and potassium ions. The responses to substance P by the ganglion cells of the myenteric plexus have been suggested to be due to a decrease in potassium conductance (10). The same effect has been shown to occur with substance P at many other sites, e.g., motoneurones (13), and it is likely that it has the same effect on smooth muscle. Hyoscine does not affect its action on the ileum so this is not due to release of acetycholine from the myenteric plexus. Potassium chloride causes some depolarization of the ganglion cells leading to acetylcholine release, but at the concentrations used most of the response is due to a direct deplorization of the smooth muscle (14).

These results provide a direct comparison of the effects of the anesthetics on the actions of different types of agonist and show, in contrast to results on invertebrate tissues, that there appears to be no selectivity for those responses involving sodium conductance changes.

The changes seen in the dose-response curves involve several factors: a decrease in slope, with a resulting decrease in the maximum response obtained, and a lateral shift, which may suggest a change in receptor affinity. Until these factors can be differentiated, it is premature to compare the effects of the types of anesthetic agents. It is possible that selectivity for particular conductance changes is masked by other changes.

When the effects of anesthetics on the extent of desensitization to different agonists are compared, it is important to remember that the number of spare receptors for a particular agonist may affect the extent to which desensitization to the agonist is seen when tissue responses are measured. Greater desensitization to substance P than to acetylcholine is seen in control preparations, and our results suggest that this is increased by urethane, octanol, ketamine, and Althesin but not by pentobarbitone. Ethanol, in contrast to the other agents, had a considerable effect in increasing acetylcholine desensitization.

These changes in desensitization may explain part of the changes obtained in the shape of the dose-response curves seen after addition of the anesthetic agents. The depression of the maximum was greater for substance P than for acetylcholine for all the anesthetics except ethanol, but when the depressions of the responses at the ED_{50} level are compared there were no consistent differences between the effects on responses to different agonists. Increases in desensitization would be expected to affect maximal responses but have less effect at lower concentrations.

It has been shown that part of the desensitization developing in this tissue

is not specific to particular agonists (15) and may involve changes beyond the receptor, such as hyperpolarization. Experiments are in progress to check how far the effects of the anesthetics on desensitization involve changes specific to each agonist.

Acceleration of the development of desensitization at the nicotinic receptor has been shown for several general anesthetic agents (16), and binding studies have shown that anesthetics can increase the high affinity binding (12, 17,18), which has been suggested to be the desensitized form of the receptor.

After phenobarbitone the only changes found were small decreases in the maximum responses obtained with each agonist. This may reflect the different effects seen in vivo with pentobarbitone and phenobarbitone mentioned in the RESULTS section. The concentration of phenobarbitone (0.4 mM) used is close to that found in body fluids at sedative doses in vivo and was found to affect the release of acetylcholine from the ileum (6).

The main conclusions to be drawn from the results thus far are that they are compatible with the theory that an action common for all general anesthetics is a depression of postsynaptic responses, and that there does not appear to be any selectivity for different types of conductance changes. Further, there are two important points to be made from the studies on desensitization; first, that increases in desensitization may contribute to the effects of general anesthetics on postsynaptic responses, especially with agonists other than acetylcholine; and second, that the effects on desensitization show some selectivity, which may contribute to the characteristic differences between different anesthetics superimposed upon their general similarity of action.

Present work is being directed toward a further analysis of the different components of the actions of anesthetics. The ganglion preparation is being used to extend the work on postsynaptic responses to include the effects of helium pressure and its interaction with the effects of anesthetics described in this paper.

References

1. Lever MJ, Miller KW, Paton WDM, Smith EB. Pressure reversal of anesthesia. Nature 1971;231:368–371.
2. Halsey MJ, Wardley-Smith B, Green CJ. Pressure reversal of general anesthesia—a multisite hypothesis. Br J. Anaesth 1978;50:1091–1097.
3. Miller KW. Inert gas narcosis; the high pressure neurological syndrome and the critical volume hypothesis. Science 1974;185:867–869.
4. Larrabee MG, Posternak JM. Selective action of anesthetics on synapses and axons in mammalian sympathetic ganglia. J Neurophysiol 1952;15:91–114.
5. Little HJ, Paton WDM. The effects of high pressure helium and nitrogen on the release of acetylcholine from the guinea pig ileum. Br J. Pharmacol 1979;67:221–228.
6. Halliday DJX, Little HJ, Paton WDM. The effects of inert gases and other general anesthetics on the release of acetylcholine from the guinea pig ileum. Br J Pharmacol, 1979;67:229–237.
7. Henderson JV, Lowenhaupt MT, Gilbert DL. Helium pressure alteration of function in squid giant synapse. Undersea Biomed Res 1977;4:19–26.
8. Barker JL. Selective depression of post-synaptic excitation by general anesthetics. In: Fink BR, ed. Molecular mechanisms of anesthesia. Progress in anesthesiology, Vol. 1. New York: Raven Press, 1975:135–154.

9. Bolton TB. Action of acetycholine on the longitudinal muscle of guinea pig ileum: the role of an electrogenic sodium pump. Philos Trans R Soc Lond B Biol Sci 1973;265:107–114.

10. Katayama Y, North RA. Does substance P mediate slow synaptic excitation within the myenteric plexus. Nature 1978;274:387–388.

11. Paton WDM. Cholinergic transmission and acetylcholine output. Can J Biochem Physiol 1963;41:2637–2653.

12. Young AP, Sigman DS. Allosteric facilitation of in vitro desensitization of the acetylcholine receptor by volatile anesthetics. In: Fink BR, ed. Molecular mechanisms of anesthesia. Progress in anesthesia, Vol. 2. New York: Raven Press, 1980:209–228.

13. Krnjevic K. Effects of substance P on central neurones in cat. In: von Euler C, Pernow B, eds. Substance P. New York: Raven Press, 1977:217–230.

14. Paton WDM, Aboo Zar. A denervated preparation of the longitudinal muscle of the guinea pig ileum. J Physiol 1965;179:85–86P.

15. Paton WDM. A theory of drug action based on the rate of drug-receptor combination. Proc R Soc Lond B Biol Sci 1961;154:21–69.

16. Magazanik LG, Vyskocil F. Desensitization at the motor end plate. In: Rang HP, ed. Drug receptors, 1973:105–120.

17. Sauter JF, Braswell LM, Miller KW. Action of anesthetics and high pressure at the acetylcholine receptor. In: Fink BR, ed. Molecular mechanisms of anesthesia. Progress in anesthesia, Vol. 2., New York: Raven Press, 1980:199–207.

18. Katz B, Thesleff S. A study of the desensitization produced by acetylcholine at the motor endplate. J Physiol 1957;138:63–80.

PHARMACOLOGICAL INVESTIGATION OF THE HIGH PRESSURE NEUROLOGICAL SYNDROME: BRAIN MONOAMINE CONCENTRATIONS

S. Daniels, A. R. Green, D. D. Koblin, R. G. Lister, H. J. Little,
W. D. M. Paton, F. Bowser Riley, S. G. Shaw, and E. B. Smith

The high pressure neurological syndrome (HPNS) was first described in man by Bennett (1) and in a variety of other animals by Brauer (2,3) after compression with helium at pressures up to 140 bars. The application of pressure with helium, which has been shown to act essentially only as a pressure-transmitting agent (4), causes the following behavioral signs in mice: tremors at approximately 30–50 bars, convulsions at 70–100 bars, and death at 110–140 bars. At lower pressures, in humans the initial stages of the syndrome are manifested as tremors, nausea, dizziness, and deficiencies in psychomotor performance tests (5).

Although the signs and symptoms of HPNS are well established, there is little evidence on which to formulate a clear understanding of the physiological mechanisms underlying HPNS. General anesthetics have long been known to ameliorate the condition, postponing the onset of signs to higher pressures (6). Conversely, reserpine, the monoamine-depleting alkaloid, has been shown to reduce the onset pressures (7) in a manner suggesting that HPNS may consist of two components: the first, a dependence on the rate of compression, and the second, the absolute magnitude of the pressure (7). Reserpine was observed to act only on the first of these, reducing the thresholds at slow compression rates compared to those observed at fast compression rates. It was also reported that the reserpine effect at slow compression rates was partially reversed by the administration of a monoamine precursor (L-tryptophan) and a monoamine oxidase inhibitor (tranylcypromine). Although not excluding the involvement of other systems, this work (7) suggests an important role for the monoamine

group of neurotransmitters in the compression-rate-dependent component of HPNS.

We were therefore interested in investigating further the effects of high pressure on central nervous system (CNS) monoamines in an attempt to determine whether any correlation exists between the observed manifestations of HPNS and the whole brain levels of dopamine (DA), noradrenaline (NA), 5-hydroxytryptoamine (5-HT), and its metabolic product 5-hydroxyindoleacetic acid (5-HIAA). We extended this approach by employing pharmacological agents, which selectively perturb the individual levels of the monoamines, in an attempt further to elucidate the role of these central transmitters in the mechanism of HPNS. In addition, we examined the protective role of general anesthetics to establish whether this effect may also involve the same group of transmitters.

METHODS

Animals and Drug Administration

Male Mice (CD-1 strain) (Charles River), weighing 25–30 g, were used in all experiments. Drugs were administered intraperitoneally; they were obtained from the following sources: α-methyl p-tyrosine methyl ester HCl, p-chlorophenylalanine methyl ester HCl, reserpine (Sigma, Poole); FLA-63 (Bis (4-methyl-1-homopiperazinylthiocarbonyl) disulphite (Astra, Sodertalje, Sweden). All doses quoted refer to the salt where appropriate.

For α-methyl p-tyrosine (αMPT) animals were injected with 200 mg/kg 8 and 16 h before exposure to high pressure. Controls received saline at these times. A dose of 200 mg/kg p-chlorophenylalanine (PCPA) was given at 42, 48, and 24 h before exposure to high pressure, with controls receiving saline in place of the drug. We dissolved FLA 63 (50 mg/kg) in a small volume of acetic acid and adjusted the pH to 7 with sodium hydroxide. The drug was injected 1 h before pressurization, with controls receiving the vehicle. Reserpine (10 mg/kg) was dissolved in a vehicle similar to FLA-63 and given 24 h before pressure administration. The control animals were fasted because it was observed that after reserpine administration the animals did not eat; they then were injected with the vehicle. It is known that overnight fasting has some effects on 5-HIAA concentrations (8).

Protocol for Administration of High Pressure

The experiments were performed in a 1.61-L hyperbaric chamber in which single mice were restrained in a mesh cage. We controlled the temperature by means of an external water jacket to maintain the rectal temperature of animals (monitored using a thermistor) between 36.5 and 38°C. This required chamber temperatures between 33 and 35°C. A fan was used to mix the gases,

assisting in the removal of carbon dioxide and effluent gases by soda lime and activated charcoal. Before compression, the chamber was flushed with oxygen so that all experiments began with a Po_2 of 1 bar. Exposure to elevated Po_2 has been reported to reduce brain concentrations of NA and 5-HIAA, although at a Po_2 of 1 bar these changes were reported to be less than 2% (9).

With one exception, the compression rate was 1 bar·min^{-1}, with helium. The rapid compressions were at a rate of 15 bar·min^{-1}. When nitrogen was added the first 30 bars of the compression were with pure nitrogen and were followed by a 30-min hold at 30 bars. The remaining compression was with helium. Decompression was carried out within 1 min, and the maximum time between the initiating of decompression and removal of the brain was 5 min. Changes in content of whole brain monoamine during this period were expected to be minimal (10,11).

Four behavioral end-points were employed. Mild tremors were characterized by intermittent twitching of the neck and back muscles during which the mouse often adopted a hunched posture. Coarse tremors were defined by a shivering of the whole body during which the animal found coordinated movement difficult. Convulsions were characterized as seizures of sufficient severity to prevent the animal from righting itself. They were often followed by a brief period of respiratory failure. Death was defined by a complete absence of movement for a 1-min period. A minimum of six animals were used for each treatment group.

Brain Monoamine Analysis

Excised brains were kept at $-20°C$ until analysis. The brains were homogenized in acidified butanol (12), centrifuged, and divided into two fractions. We used one fraction for analysis of 5-HT and 5-HIAA using the fluorometric method of Curzon and Green (13), and the other fraction for analysis of DA and NA using the fluorometric assay of Chang (12).

The original assay gave NA concentrations that were somewhat lower than equivalent literature values for the control animals; therefore, a means for improving the assay was sought. It was eventually determined that for mouse brain homogenate the necessary oxidation conditions for the conversion of the catecholamines to fluorescent indoles differed from those used for rat brain homogenate. When the oxidation procedures were optimized for mouse brain, the homogenate catecholamine concentrations obtained for control mice were in agreement with other published values.

RESULTS

The aim of the investigation was to determine whether or not the levels of centrally occurring monoamines could be correlated with the application of pressure and the subsequent appearance of the behavioral signs of HPNS. However, the experimental procedure could also be interpreted as a stressful

procedure; therefore, we performed a series of control experiments to assess the role of stresses arising from restraint of the animals in the pressure vessel and from the drug administration procedure. Periods of restraint of 20 min and 2.5 h, similar to those involved in fast- and slow-compression experiments, respectively, had no marked effects on the levels of DA, NA, or 5-HT. However, an indication of increased 5-HIAA levels was observed, which is consistent with other reports of increased 5-HT turnover, after stress induced by immobilization (Table I) (e.g., refs. 14,15). No consistent differences were seen in any of the amine levels after injection of drug vehicle solutions.

The effects of pressure when compared to the controls produced no significant changes in the levels of the brain amines. There was no difference between the amine levels after either fast (15 bar·min^{-1}) or slow (1 bar·min^{-1}) compressions, although a significant reduction in the onset pressures of HPNS was produced by the rapid compressions. It was noted, however, that 5-HIAA levels were increased by compression more than by restraint alone. Throughout the remainder of the study of the slow-compression procedure was adopted to study the effects of these agents: the monoamine-depleting alkaloid, reserpine; a tryptophanhydroxylase inhibitor, PCPA; a tyrosine hydroxylase inhibitor, α-MPT; and a dopamine β-hydroxylase inhibitor, FLA-63.

After reserpine pretreatment the brain monoamine levels were markedly reduced relative to the comparable (vehicle-injected) controls. This reduction is well documented (e.g., 16). The application of pressure to the reserpine-pretreated animals was found partially to restore the DA and 5-HT levels, whereas the NA level apparently was further reduced (although here the data

TABLE I

Whole Brain Monoamine Concentrations and HPNS Onset
Pressures for Mice

	Control $n = 12$	Restraint $n = 12$	Slow Compression $n = 6$	Rapid Compression $n = 6$
HPNS Signs Onset Pressure/Bar				
Fine Tremors	—	—	74 ± 6	*
Coarse Tremors	—	—	93 ± 5	*
Convulsion	—	—	102 ± 4	72 ± 5
Death	—	—	128 ± 6	139 ± 11
Amine concentrations (mg/kg)†				
5-HT	0.68 ± 0.03	0.67 ± 0.03	0.62 ± 0.02	0.58 ± 0.02
5-HIAA	0.45 ± 0.02	0.58 ± 0.03	0.70 ± 0.05	0.74 ± 0.05
DA	1.12 ± 0.07	1.23 ± 0.05	1.10 ± 0.07	1.09 ± 0.07
NA‡	0.20 ± 0.01	0.18 ± 0.02	0.20 ± 0.02	0.15 ± 0.03

* Could not be measured because of high pressure.   † Error as standard error of mean.   ‡ An improved assay has provided absolute levels of NA concentrations in closer agreement with literature values (0.40 ± 0.04).

were more limited). Reserpine pretreatment considerably lowered the onset pressures of the characteristic signs of HPNS (Table II).

Pretreatment with PCPA decreased brain 5-HT and 5-HIAA, while, as expected, the DA and NA levels were not significantly affected. No significant changes in the levels of brain amines were seen after pressurization although 5-HIAA levels appeared to increase. Administration of PCPA did not affect the development of HPNS (Table II).

Animals treated with αMPT exhibited a significant decrease in brain NA levels and a small decrease in DA, whereas the 5-HT and 5-HIAA were unaffected. No further change in these concentrations was caused by pressure although the 5-HIAA level markedly increased. The onset pressures for HPNS remained unaffected (Table II).

Pretreatment with FLA-63 produced a marked decrease in brain NA concentrations, a small rise in brain DA, and no change in the levels of 5-HT or 5-HIAA. After pressure treatment there was a marked increase of the 5-HIAA level, with some restoration of NA and DA levels toward the control values and no changes in 5-HT. Pretreatment with FLA-63 resulted in a lowering of the onset pressures of the characteristic signs of HPNS (Table II).

TABLE II

Relative Monoamine Concentrations and HPNS Onset Pressures for
Mice Treated with Pharmacological Agents. All Amine Concentrations
are Relative to the Untreated Control of Table I

	Reserpine $n = 6$	αMPT $n = 10$	PCPA $n = 6$	FLA-63 $n = 9$	Nitrogen $n = 16$
HPNS Signs Slow Compression Onset Pressure/Bar					
Fine Tremors	40 ± 5	62 ± 5	66 ± 3	50 ± 5	*
Coarse Tremors	42 ± 3	88 ± 4	82 ± 3	65 ± 5	*
Convulsions	47 ± 4	101 ± 3	95 ± 5	74 ± 2	123 ± 3
Death	65 ± 3	124 ± 3	122 ± 6	88 ± 7	181 ± 6
Amine Concentrations (Relative)					
5-HT	0.40	0.99	0.59	0.97	0.91
5-HIAA	1.29	0.84	0.42	0.89	1.19
DA	0.29	0.70	0.97	1.17	1.11
NA	[0.40]†	0.40	0.80	0.35	1.21
Amine Concentrations (relative) After High Pressure					
5-HT	0.57	0.92	0.69	0.95	0.66
5-HIAA	1.91	1.60	0.82	1.44	1.56
DA	0.64	0.83	1.37	1.09	0.43
NA	[0.2]†	[0.55]†	0.95	0.60	0.74

*Could not be measured because of high pressure.   † Errors within ± 10%; three determinations only.

To investigate the affects of a general anesthetic combined with pressure on amine levels, we employed partial pressures of nitrogen in the ranges 30–40 bars; because the signs of HPNS have been shown to occur under such conditions as well as at significantly higher onset pressures (6). The effect of the partial pressure of nitrogen was to increase significantly the levels of NA and 5-HIAA. The simultaneous application of pressure (to death) caused a substantial fall in all the amine concentrations, with a concomitant increase in 5-HIAA (Table II). Further experiments were performed in which the animals were, after the administration of nitrogen, taken only to 120 bars before decompression. This pressure is comparable to the normal lethal pressure for mice compressed with helium and also to that required to fully restore activity after a normal anesthetic dose of nitrogen. The relative amine levels observed were DA, 0.67; NA, 0.97; 5-HT, 1.07. Levels of 5-HIAA were similar to those in the previous experiment. Interestingly, at this pressure the NA concentrations have been restored to the control value and the DA levels are intermediate between values obtained with nitrogen alone and values with nitrogen-plus-pressure to lethality.

DISCUSSION

The assay of whole brain amines in animals exposed to high pressures raises a number of problems peculiar to this type of experiment. The prompt recovery of the intact brain, required by the assays, is hampered by the problem of tissue damage arising from the necessarily rapid decompression. Nevertheless, our results suggest that despite this trauma assays can be performed on animals recovered from high pressure. Our analyses reproduce many of the drug-induced effects on brain amines that have been reported in the literature for experiments at normal pressure (16–19). To this extent the assays for amines in animals not exposed to pressure are entirely consistent with previous work (e.g., 9,20). The difficulty of recovering intact brains from the animals exposed to high pressures indicates caution in interpreting these results, and we have chosen only to emphasize the most striking features of our measurements. There is, however, no direct evidence to suggest that the high pressure results are in any way less reliable.

Apart from the increase in 5-HIAA levels, no significant effects on brain monoamine levels were detected after helium compressions using either fast or slow rates. This concurs with the suggestion based on the work with reserpine that the compression-rate-dependent component of HPNS is not mediated exclusively by monoamines (7). The observed increases in 5-HIAA are entirely consistent with other studies in which the effects of stressful procedures have been investigated (14,15).

It has not been possible after pharmacological intervention to clearly associate the effects of pressure with any particular amine. Although 5-HIAA is consistently raised, suggesting perhaps some involvement of 5-HT, the experiments with PCPA, which decreases 5-HT, showed no modification of the on-

set pressures of the signs of HPNS. In common with reserpine, FLA-63, which did reduce the threshold pressures of the behavioral signs, does reduce NA. However, αMPT, which also reduces NA, does not affect the development of HPNS. It is possible that the increased level of DA after treatment with FLA-63 may play a part in mediating the effect of this drug on HPNS. In this connection it is interesting that in reserpine-treated animals the subsequent application of pressure increases by 30% the reduced DA level; however, any direct comparison must be made with caution as the mode of action of reserpine for monoamine storage differs from that of the synthesis inhibitors.

The greater effects on the HPNS of reserpine and of FLA-63, compared to those of αMPT and PCPA, parallel the effects of these agents on electroshock and pentylenetetrazol-induced convulsions (e.g., 19). Therefore, there may be some common factor in the production of convulsions by these techniques and by pressure. Taken with the present results this may indicate that more than one transmitter is involved.

Of the pharmacological agents tested, only reserpine and FLA-63 significantly affected the development of the behavioral signs of HPNS. General anesthetics (such as high-pressure nitrogen) are known to have the opposite effect and confer some measure of protection from the HPNS. Under conditions of 30 bars of nitrogen, the amine levels were increased. At lethal pressures of helium in the presence of an anesthetic dose of nitrogen, the amine levels were depressed, which appears to be contrary to the finding that at lethal pressures, generated by the application of helium alone, no changes in amine levels were observed. Nevertheless, when the application of pressure was restricted to 120 atm in the presence of nitrogen there was some restoration of the amine levels to control values.

We suggest that the changes in amine levels after application of pressure alone are either small or restricted to specific regions of the CNS, whereas, in the presence of nitrogen, which enables considerably higher pressures to be attained, the changes become sufficiently large to be detectable by a whole brain assay. This supposition could be further tested by exploring more fully the effects of the interaction between nitrogen and pressure on the monoamine levels.

The ability of nitrogen to suppress the signs of the HNPS may be used to test whether any such changes in amine levels occur as a direct consequence of the application of pressure and not as a result of the behavioral manifestations of this syndrome.

From the results of the experiments in which the levels of individual transmitters were selectively modified, we cannot associate the signs of HPNS with any single monoamine. This, taken in conjunction with the results obtained with nitrogen, suggests the possibility that the effects may arise in a more complicated way from the balance of the catecholamines within the brain as well as from their interactions with other neurotransmitters. This may be resolved by an investigation of amine levels in discrete areas of the CNS, which will avoid the difficulties imposed by whole brain measurements in which the information from many distinct functional systems is pooled.

Acknowledgment

References

1. Bennett PB. The aetiology of compressed air intoxication and inert gas narcosis. Oxford: Pergamon Press, 1966.
2. Brauer RW, Way RO, Perry RA. Narcotic effects of helium and hydrogen in mice and hyperexcitability phenomena at simulated depths of 1500 to 4000 feet of sea water. In: Fink BR, ed. Toxicity of anesthetics. Baltimore: Williams & Wilkins, 1968:241-258.
3. Brauer RW, Beaver RW, Hogue CD, Ford B, Goldman SM, Venters RP. Intra- and interspecies variability of vertebrate high pressure neurological syndrome. J Appl Physiol 1974;37:844-851.
4. Miller KW, Paton WDM, Street WB, Smith EB. Animals at very high pressures of helium and neon. Science 1967;157:97-98.
5. Hunter WL, Bennett PB. The causes, mechanisms, and prevention of the high pressure nervous syndrome. Undersea Biomed Res 1974;1:1-28.
6. Lever MJ, Miller KW, Paton WDM, Street WB, Smith EB. Effects of hydrostatic pressure on mammals. In: Lambertsen CJ, ed. Underwater physiology. Proceedings of the fourth symposium on underwater physiology. New York & London: Academic Press, 1971:101-108.
7. Brauer RW, Beaver RW, Sheehan ME. Role of monoamine neurotransmitters in the compression-rate dependence of HPNS convulsions. In: Shilling CW, Beckett MW, eds. Underwater physiology VI. Proceedings of the sixth symposium on underwater physiology. Bethesda, MD: Federation of the American Societies for Experimental Biology, 1978:49-60.
8. Curzon G, Knott PJ. Fatty acids and the disposition of tryptophan. Ciba Foundation Series, 22, 217-229. Aromatic amino acids in the brain. Amsterdam: Elsevier/North Holland.
9. Faiman MD, Heble AR. The effect of hyperbaric oxygenation on cerebral amines. Life Sci 1966;5:2225-2234.
10. Joyce D. Changes in the 5-hydroxytryptamine content of rat, rabbit, and human brain after death. Br J Pharmacol 1962;18:370-380.
11. Blank CO, Sasa S, Isernham R, Meyerson LR, Wassil D, Wong P, Modak AT, Stavinoha WB. Levels of norepinephrine and dopamine in mouse brain regions following microwave inactivation—rapid postmortem degradation of striatal dopamine in decapitated animals. J Neurochem 1979;33:213-219.
12. Chang CC. A sensitive method for spectrophotofluorometric assay of catecholamines. Int J Neuropharmacol 1964;3:643-649.
13. Curzon G, Green AR. Rapid method for the determination of 5-hydroxytryptamine and 5-hydroxyindoleacetic acid in small regions of rat brain. Br J Pharmacol 1970;39:653-655.
14. Corrodi H, Fuxe K, Hokfelt T. The effect of immobilization stress on the activity of central monoamine neurons. Life Sci 1968;7:107-112.
15. Curzon G, Green AR. Effects of immobilization on rat liver tryptophan pyrrolase and brain 5-hydroxytryptamine metabolism. Br J Pharmacol 1969;37:689-697.
16. Glowinski J, Iversen LL, Axelrod J. Regional studies of catecholamines. IV. Effects of drugs on the disposition and metabolism of H³norepineperine and H³dopamine. J. Pharmacol Exp Ther 1966;153:30-42.
17. Svenson TH. Increased dopamine concentrations in the striatum of the mouse brain by FLA-63. J Pharm Pharmacol 1973;25:73-75.
18. Green AR, Grahame-Smith DG. The role of brain dopamine in the hyperactivity syndrome produced by increased 5-hydroxytryptamine synthesis in rats. Neuropharmacology 1974;13:949-959.
19. Kilian M, Frey H-H. Central monoamines and convulsive thresholds in mice and rats. Neuropharmacology 1973;12:681-692.
20. Fennessy MR, Lee JR. The effects of benzodiazepenes on brain amines of the mouse. Arch Int Pharmacodyn 1972;197:37-44.

PREVENTION OF HPNS: THE POSSIBLE USE OF STRUCTURAL ISOMERS OF ANESTHETICS

B. Wardley-Smith and M. J. Halsey

Mammals exposed to increased ambient pressures exhibit first uncoordinated tremors around 50 atmospheres absolute (ATA) then convulsions, respiratory distress, and finally death as the total pressure is raised to 100–150 ATA. These changes are encompassed in the high pressure neurological syndrome (HPNS) (1). These physiological perturbations of high pressure are now the major limiting factors in diving to sea depths greater than 300 m (30 ATA). Low concentrations of a variety of anesthetic substances have been demonstrated to ameliorate some of the adverse effects of high pressure in amphibians (2,3). Nevertheless, only a limited range of gaseous anesthetics have been studied in animals (4) and the underlying mechanisms of action are unknown. There have been a number of human studies at pressures up to 60 ATA (5); currently the deepest chamber dive (in March, 1980 at Duke University) has been to a depth of 650 m. This depth was reached by using a breathing mixture containing 10% nitrogen (trimix) and no signs of HPNS were reported at this depth (P.B. Bennett, personal communication). However, the deepest ocean dive has only been to a depth of 460 m (X. Fructus, personal communication).

Although low doses of some anesthetics are successful in reducing HPNS, there are obvious risks associated with the potential occurrence of either anesthesia or euphoria. Our recent experiments to investigate the interaction of pressure and anesthetics in rats have led us to postulate that the molecular receptors for anesthesia and HPNS may be separate (6). One aspect of the data on which this hypothesis is based is that although all the anesthetics were antagonized by pressure, there were considerable differences in their ability to provide protection against HPNS. For example, Althesin and ketamine were both effective in preventing HPNS even in subanesthetic doses, whereas me-

thohexitone actually potentiated the tremors and convulsions seen in HPNS in the rat.

Although some anesthetics have no effect on HPNS, (e.g., thiopentone), no compound unrelated to an anesthetic has yet been found to have any significant effect in preventing it (7). It thus seemed possible that a nonanesthetic compound with a close structural relationship to an anesthetic might prove useful in the treatment of HPNS. The steroid anesthetic alphaxalone (the main component of Althesin) has several nonanesthetic isomers with only small structural changes: because alphaxalone is effective in preventing HPNS these compounds seemed appropriate to study for antiHPNS activity.

METHODS

Adult, male Sprague-Dawley rats, weighing 250–300 g, were used in all experiments; the lateral tail vein was cannulated to permit infusion of drugs at pressure from a pump that was externally controlled. Temperature was measured via a colonic thermistor and was maintained at 37 ± 0.5°C.

We used tremor as a means of assessing the severity of HPNS because it has been shown to have a reproducible onset pressure (8) and any improvement subsequent to drug administration easily can be detected. The method we have developed for measuring tremor is described in detail elsewhere (9). Our original method consisted of a small strain gauge (Endevco Pixie type 8120) taped directly onto a rat enclosed in a rodent "hammock" (10). However, this involved moderate restraint of the rat, which we felt was undesirable. Subsequently, we have used the strain gauge incorporated into a small cage in which the rat is restrained only by taping its tail. Both systems gave an excellent signal indicating onset of tremor, but the signal from the cage allowed detailed analysis of tremor frequency, and more recent experiments have used this technique only. After preparation under halothane anesthesia, the restrained rat was placed in the pressure chamber and allowed to wake up. Once a suitable control reading had been obtained, 0.4 ATA O_2 was added and compression with helium at 3 ATA/min was commenced. The signal from the strain gauge was continuously recorded on magnetic tape and observed on an oscilloscope.

We compared the effects of Althesin (9 mg/mL alphaxalone + 3 mg/mL alphadalone acetate dissolved in Cremophor EL); Δ16-alphaxalone (50 mg/mL sonicated in Cremophor EL); 3 β-hydroxy-alphaxalone (10 mg/mL sonicated in Cremophor EL) and Cremophor EL alone as a control. Once tremor had become moderate to severe, each compound was infused for up to 3 min. In addition to continuous recording of the signal, we constantly watched the animals to detect any observed change in tremor. After each infusion, all animals were carefully observed to ensure that time-adaptation to pressure did not eliminate tremor (11).

Each experiment was terminated by adding an overdose of nitrous oxide. This was also done if tremor became uncontrollable and severe, or if convulsions began to occur.

RESULTS

Both methods of monitoring tremor gave a good end-point for detecting the onset of tremor and, conversely, reliably detected any improvement in HPNS, as shown by tremor being attenuated or abolished. Control experiments, which consisted of infusing Cremophor EL alone to rats with tremor, showed that this had no effect on either the duration or severity of tremor. Results of the administration of Althesin to a rat with tremor are shown in Fig. 1. Tremor is completely abolished after 45 s infusion: this corresponds to 1.4 mg total steroid. However, anesthesia rapidly follows the abolition of tremor. Previous experiments with Althesin (12) have shown that tremor can be greatly reduced with 50% of the anesthetic dose, but at this dosage the rat is moderately sedated.

Results for the isomers of alphaxalone, Δ16-alphaxalone, and 3β-hydroxy-alphaxalone are shown in Figs. 2 and 3. Delta 16-alphaxalone reduced the severity of HPNS as assessed by both observed and measured tremor after 90 s infusion, which corresponded to an infusion of 11.8 mg steroid. The high dose required, compared to that of Althesin, is probably due to

Althesin ON   60 s   OFF
77.5 ATA

74.2 ATA   after 90s   81.7 ATA
                  Althesin
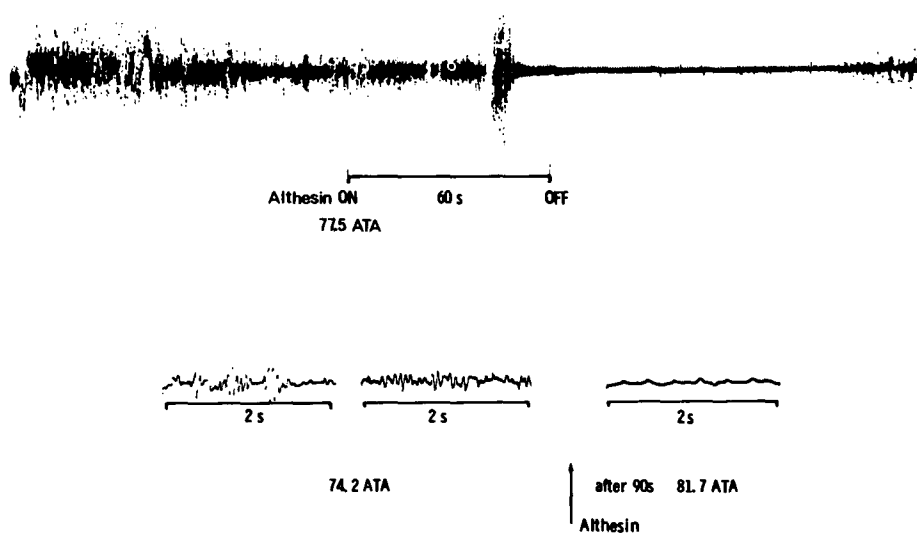
Fig. 1. Recordings from a rat at pressure before and after administration of Althesin. Tremor was monitored using the strain gauge, recorded on magnetic tape, and subsequently written out on a Devices chart recorder. The *upper trace* shows the overall effect of an intravenous infusion of 1.4-mg Althesin on pressure-induced tremor. The trace runs from left to right, and the irregular pattern of tremor changes to that of respiration after 45 s Althesin. Tremor starts to return at the far right of the trace. The *lower traces* show the characteristics of tremor at a faster recording speed, before and after addition of Althesin. Episodes of tremor are easily recognized by their smooth, even frequency.

its relative insolubility in Cremophor EL, and to ensure a fully saturated solution we prepared it as a suspension. Also prepared as a suspension, 3β-hydroxy-alphaxalone was effective at a lower dose, and tremor was markedly reduced after 1.6 mg steroid.

Neither isomer had any anesthetic effect. Once tremor had returned, usually about 3 min after the initial drug infusion, a second dose was given; Δ16-alphaxalone was still effective, but 3β-hydroxy-alphaxalone had much less effect on tremor during second or subsequent doses, which suggests that its metabolized form partially blocked the HPNS receptor.

Although the isomers of alphaxalone improved HPNS as shown by a reduction of tremor, both observed and recorded, they were not totally effective as shown in the lower traces in Figs. 2 and 3. It can be seen that although the severity is greatly reduced, the basic frequency of the tremor is still present. This appears as a higher frequency signal superimposed on the respiratory signal. We found that the frequency of the tremor was consistent between different animals, varying from 11–14 Hz. The threshold for tremor onset was 56.1 ± 1.9 (ATA ± SEM).

ON   **3 min**   **OFF**

95 ATA

90.2 ATA   **93.5 ATA**   **after 90 s**   **102 ATA**
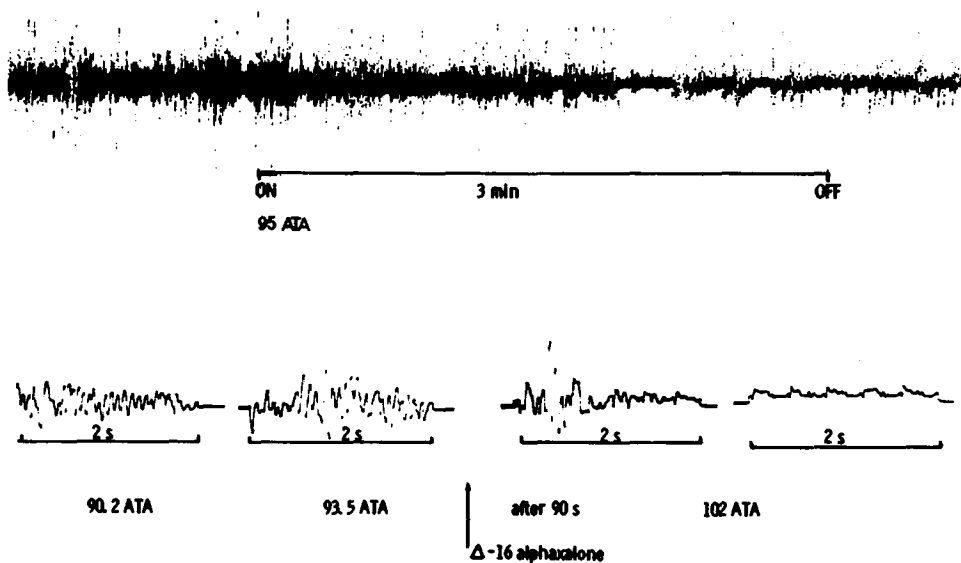
Δ-16 alphaxalone

Fig. 2.   Recordings from a rat at pressure before and after treatment with Δ 16-alphaxalone. Recording methods as in Fig. 1. The *upper trace* shows the effect of 3-min infusion of 11.8 mg Δ 16-alphaxalone suspended in Cremophor EL. Although tremor is not abolished it is considerably reduced in severity, and periods of almost normal respiration can be seen on the right of the trace.   The *lower traces* are sections chosen to show the characteristics of tremor at a faster recording speed. Frequency of the tremor (14 Hz) is clearly seen at this recording speed.
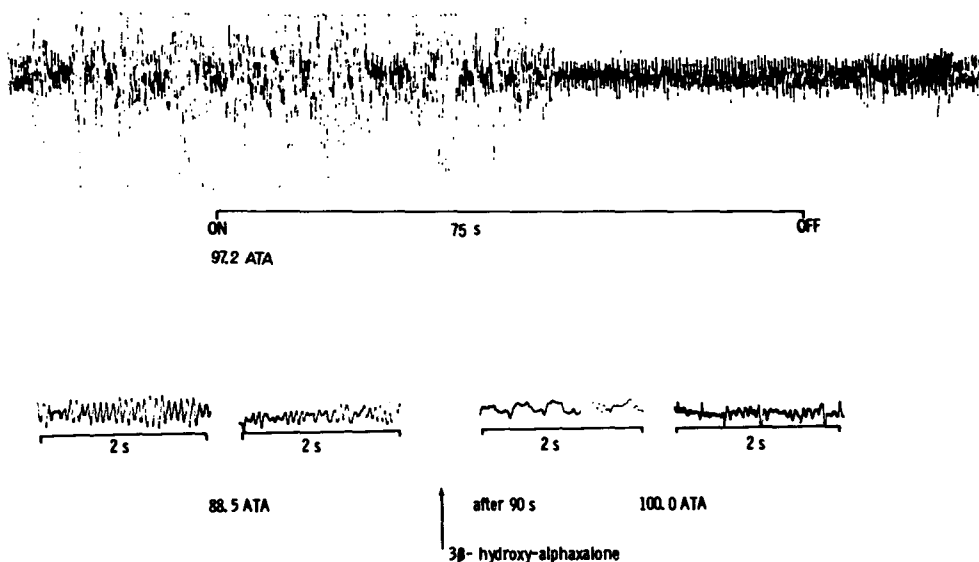
Fig. 3.   Recordings from a rat at pressure before and after-treatment with 3β-hydroxy-alphaxalone. Methods of recording are as in Fig. 1. The *upper trace* shows the effect of 1.6-mg 3β -hydroxy-alphaxalone suspended in Cremophor EL. The irregular pattern associated with tremor is replaced by respiratory movement; however, the lower sections recorded at a faster speed show that the basic tremor frequency is still present, but the amplitude, and thus the severity of tremor, is greatly reduced.

DISCUSSION

The use of structural isomers of anesthetics is an approach that may make it possible to distinguish between separate molecular receptors for anesthesia and HPNS, and thus to enable a drug to be found that is safe and effective in treating HPNS. Isomers of an anesthetic already shown to be effective in preventing tremor could have considerable potential as a pharmacological approach. Our results so far are encouraging, but a number of further questions remain. It has been suggested that the isomers of alphaxalone are nonanesthetic simply because they do not reach the molecular receptor for anesthesia. The fact that we found the isomers only partially effective in preventing tremor could be due to an insufficient concentration at the molecular level, but the existence of any effect on HPNS demonstrates at least a partial concentration of the drug being available to the receptor. It is possible that isomers of the newer water soluble steroids would be more successful, because a much greater reservoir of the drug should be available to the molecular receptor, and we are currently investigating other anesthetics with inactive isomers to test this idea further. However, preliminary experiments with the new water soluble steroid anesthetic Minaxalone have shown it to be much less effective than

Althesin in preventing HPNS, which suggests that the ability to protect against HPNS is not common to all steroid anesthetics.

Attempts to find a drug not related to anesthetics to treat HPNS have so far not been successful. A study in which we screened anticonvulsant drugs for antiHPNS activity in mice showed that only those compounds which were anesthetic at higher concentrations, such as diazepam and primidone, were of any value. Nonanesthetic anticonvulsants such as phenytoin were completely inactive against HPNS in our preparation (7). These data do not eliminate the possibility that some anticonvulsants may be partially effective in ameliorating HPNS. However, the lack of dramatic effect is evidence against the hypothesis of a direct link between HPNS and other neurological syndromes that also lead to convulsions and motor incoordination in man. Further evidence against this idea has been provided by our preliminary experiments with low doses of naloxone, which is known to prevent drug-related convulsions in mice (13). However, we have so far failed to demonstrate any protective effects of the antagonist on pressure-induced tremors.

All these data provide further support for the concept of some interaction between anesthesia and HPNS receptors. Nevertheless, it seems certain that the receptors are not identical in view of the considerable variation between different anesthetics in their ability to prevent HPNS in rats (14).

This idea of linked receptors is not inconsistent with other experiments in intact animals which have demonstrated that the area of the brain affected by anesthetics and pressure is the same (15), i.e., in the somatosensory pathway leading to the cerebral cortex. These experiments looked at the reduction of the evoked somatosensory cortical response by urethane followed by its recovery on increasing ambient pressure. These data also suggest that the effects of pressure, both alone and on anesthesia, are not due to a general excitation, such as might be mediated by catecholamine release.

It is of potential importance to understand more about the precise receptors for anesthesia and HPNS, because the separate sites would allow the possibility of a drug entirely effective in treating HPNS without undesirable anesthetic "side effects." We hope the study of inactive isomers of anesthetics shown to be of value in ameliorating HPNS will continue to provide promising results.

Acknowledgement

References

1. Hunter WL, Bennett PB. The causes, mechanisms, and prevention of the high pressure nervous syndrome. Undersea Biomed Res 1974;1;1–28.
2. Miller, KW. Inert gas narcosis and animals under high pressure. In: Symposia of the Society for Experimental Biology XXVI; the effects of pressure on organisms. Cambridge: University Press, 1972;363–378.

3. Halsey MJ, Wardley-Smith B. Pressure reversal of narcosis produced by anesthetics, narcotics, and tranquilizers. Nature (Lond) 1975;257:811–813.
4. Brauer RW, Goldman SM, Beaver RW, Sheenan ME. H_2, N_2, and N_2O antagonism of high-pressure neurological syndrome in mice. Undersea Biomed Res 1974;1:59–72.
5. Lambertsen, CJ. ed. Underwater physiology V. Proceedings of the fifth symposium on underwater physiology. Bethesda, MD: Federation of American Societies for Experimental Biology, 1976.
6. Halsey MJ, Wardley-Smith B, Green CJ. Pressure reversal of general anesthesia—a multi-site expansion hypothesis. Br J Anesth 1978;50;1091–1097.
7. Wardley-Smith B, Halsey MJ. Pressure reversal of narcosis: possible separate molecular sites for anesthetics and pressure. In: Fink BR, ed. Progress in anesthesiology, Vol. 2. New York: Raven Press, 1980:489–493.
8. Brauer RW, Beaver RW, Hogue, CD, Ford B, Goldman SM, Venters RT. Intra- and interspecies variability of vertebrate high pressure neurological syndrome. J Appl Physiol 1974;37:844–851.
9. Baker JA, Halsey MJ, Wardley-Smith B, Wloch RT. Assessment of HPNS: a new method of measuring tremor in an animal model. In: Bachrach AJ, Matzen MM, eds. Underwater physiology VII. Proceedings of the seventh symposium on underwater physiology. Bethesda, MD: Undersea Medical Society, 1981:415–420.
10. Danscher G. An instrument for immobilization of small experimental animals. Z Versuchstierkd 1972;14S:69–71.
11. Brauer RW, Beaver RW, Mansfield WM, O'Connor F, White LW. Rate factors in development of the high-pressure neurological syndrome. J Appl Physiol 1975;38:220–227.
12. Bailey CP, Green CJ, Halsey MJ, Wardley-Smith B. High pressure and intravenous steroid anesthesia. J Appl Physiol 1977;43:183–188.
13. Blum K, Futterman S, Wallace JE, Schwestner HA. Naloxone-induced inhibition of ethanol dependence in mice. Nature 1977;265:49–51.
14. Green CJ, Halsey MJ, Wardley-Smith B. Possible protection against some of the physiological effects of high pressure. J Physiol 1977;267:49P.
15. Angel A, Halsey MJ, Wardley-Smith B. Reversal of the effect of urethane on the evoked somatosensory cortical response by high ambient pressure. J Physiol 1979;289:61–62P.

PREVENTION OF HPNS IN MAN BY RAPID COMPRESSION WITH TRIMIX TO 2132 FT (650 m)

P. B. Bennett, R. Coggin, J. Roby, and J. N. Miller

In 1965 men were first compressed to 600 ft for 4 h and 800 ft for 2 h at a rate of 91 ft/min to produce the first report of signs and symptoms (initially attributed to the helium but later to the pressure itself) of the high pressure nervous syndrome (HPNS) (1–3). It is now well recognized that rapid compression to pressures greater than 16 ATA (500 ft) induces HPNS with dizziness, nausea, vomiting, postural and intention tremors, fatigue and somnolence, myoclonic jerking, stomach cramping, increased slow wave and decreased fast wave activities of the EEG, decrements in intellectual and psychomotor performance, poor sleep with nightmares, and in animals convulsions (4–7). The faster the rate of compression and the deeper the depth, the more severe are the signs and symptoms, so that human exposures between 46 ATA (1500 ft) and 60.5 ATA (2001 ft), even with operationally unrealistic 3- to 10-day compression times, have often resulted in incapacitating HPNS (8,9).

Various strategies therefore have been utilized to ameliorate the signs and symptoms of HPNS (10), including selection of less sensitive divers, slow exponential compression with stages for adaptation, use of excursions from a shallow saturation exposure, adaptation with time at depth, and the use of narcotics to antagonize the effects of HPNS.

This paper will describe the use over the past decade at the F.G. Hall Laboratory of the narcotic effects of increased pressures of nitrogen in mixtures of helium-nitrogen-oxygen, called "trimix," to ameliorate or prevent the debilitating effects of the syndrome. This work culminated in March 1980 in the first rapid compression of 3 divers to 650 m (2132 ft) without causing the classic incapacitating signs and symptoms of HPNS.

USE OF TRIMIX

In 1961 Zaltsman (11) in Russia, reported a so-called "antagonism" of the narcotic effect of nitrogen by helium (more correctly pressure) and studied the use of air-helium mixtures with a maximum nitrogen partial pressure of 4.5 ATA during dives to 527 ft. Under these conditions heavy work between 221–580 kg/m/min was possible with little or no sign of HPNS and no thermal balance or voice distortion problems. Zaltsman, in fact, was replicating in humans a study by Johnson and Flagler (12), which had shown that on addition of ethyl alcohol tadpoles would fall unconscious to the bottom of a tank of water, but application of some 150 atm hydrostatic pressure nullified the effects of the alcohol and the tadpoles behaved normally.

In 1967 Bennett et al. (13) noted that inert gases adsorped to an egg phospholipid monolayer. Although gases such as argon and nitrogen caused a decrease in surface tension implying a spreading of the area of the monolayer, helium and neon caused the opposite: an increase in surface tension that infers a constriction in the area of the monolayer. Lever et al. (14) in 1971 also reported a similar antagonism of narcosis (righting reflex) and anesthesia by increased pressures of helium in mice.

Thus, in 1973 a series of human investigations were initiated at the F.G. Hall Laboratory at Duke Medical Center to utilize this phenomenon in the reverse way—that is to use the addition of nitrogen to helium-oxygen to ameliorate or prevent the HPNS.

Four divers in 1973 therefore were compressed in 20 min to 720 ft with 25% N_2, 0.5 ATA O_2, and the remainder helium. The same men were exposed also to 1000 ft in 33 min with 18% N_2 (i.e., 5.6 ATA N_2 in both cases) in heliox and also to the same depths with helium-oxygen only and again to compressed air at 200 ft (with the same 5.6 ATA N_2). This allowed comparison of what was called "trimix" (i.e., $He/N_2/O_2$) to helium-oxygen and also to see if nitrogen narcosis was present (15). A battery of neurophysiological and performance tests were given. The trimix suppressed the nausea, dizziness, intention and postural tremors noted with helium-oxygen alone. Psychomotor performance markedly improved with the nitrogen present, but some decrement in intellectual performance remained. The electroencephalogram (EEG) showed little effects with either mixture. Subjectively, two of the subjects were HPNS-sensitive and preferred trimix, whereas the other two reported that nitrogen narcosis reduced their efficiency.

A model therefore was developed to compute the correct percentage of nitrogen to be added to the helium (16) to prevent either HPNS or nitrogen narcosis. Based on the Gibbs adsorption equation, the model required the following assumptions:

1) Anesthetic molecules act at nonspecific sites in a membrane with the same oil-water partition coefficient as olive oil.

2) The gases obey Henry's Law at all pressures.

3) Helium compresses membranes, whereas nitrogen and oxygen expand them.

4) The condition for elimination of HPNS and narcosis is that the membrane volume should remain constant at the pressure desired.

The model predicted 10% N_2 as the correct nitrogen percentage.

Further studies were made with 5 divers from Oceaneering International Inc., and Duke University, who were compressed to 1000 ft, as previously, in 33 min. However, the compression profile was modified to provide an increasingly slower descent starting at 60 ft/min and between 700 ft and 1000 ft slowing to 20 ft/min with three brief stages of 1 to 2 min. The trimix contained 3.2 ATA N_2 (10%), 0.5 ATA O_2, and the remainder helium. Compression started by adding 75% He/25% N_2 on air to 320 ft and helium from 320 ft to 1000 ft, oxygen was made up as required (17).

During the 2 h at depth, measurements were made of postural tremor, EEG, psychomotor and intellectual performance, and subjective impressions. One diver worked underwater for 40 min wearing closed-circuit breathing apparatus in water temperature of 56°F (14°C).

The performance tests showed little or no signs of decrement from either narcosis or HPNS. No tremor or EEG changes were noted and there was no nausea, dizziness, or fatigue. Some euphoria was reported by the wet diver.

To verify whether or not rapid compression with trimix to pressures greater than 31 ATA (1000 ft) would be equally successful, further studies were made by F.G. Hall Laboratory investigators at the R.N. Physiological Laboratory in England again using Oceaneering International divers. Compression was made to 40.6 ATA (1312 ft) by 2 men breathing 6% N_2, 0.5 ATA O_2, and the rest helium. The lower nitrogen mixture was chosen initially to reduce the potential risks of the higher density adversely affecting ventilation or producing undue narcosis. Dizziness, lightheadedness, nausea, tremors, and marked fatigue occurred, which indicated little or no protection from HPNS.

A week after the successful 6-day decompression with 0.6 ATA O_2, a further dive involved the same nitrogen percentage but a slower compression rate of 2½ h instead of 1 h 40 min to 1312 ft. During a 30-min stage at this depth, the divers were fit and well. However, during further compression from 1312 ft at 3 ft/min the dive was aborted at 47 ATA (1521 ft) because of the presence of undue HPNS with marked tremors, fatigue, nausea, and dizziness.

THE ATLANTIS DIVE SERIES

In 1978–79 two new pressure chambers with a depth capability of 3600 ft were added to the six existing chambers at the F. G. Hall Laboratory. A series of deep trimix dives named *Atlantis* was planned, to be accomplished over 3 to 5 years. The first dive to 460 m was in April 1979; culmination of the series was to be in 5 years to 650 m.

The two primary objectives of this series were first, to establish the relationship between a given nitrogen percentage and the rate of compression required to prevent HPNS. Second, to determine the effects of inspired gas density, hydrostatic pressure, and narcosis on various respiratory and circulatory

measurements. This included the inspiratory dyspnea reported in various deep diving studies, which involved measurements of arterial blood gases during rest and exercise.

Approximately two dives per year were planned, with only one variable changing per dive from two nitrogen percentages, 5% or 10%, and three basically exponential rates of compression with stages totalling 6, 12, or 24 h, and using so far as possible the same subjects. It was intended that this would determine as inferred from the earlier 10% nitrogen studies of Bennett et al. (17) with a 33-min compression to 1000 ft and the French CORAZ series (18,19) with 4.5% and 9% N_2 and 4-h compressions, whether a slower rate of compression required less nitrogen or euphoria would result. For the 4-h compression Rostain found 4.5% N_2 best for ameliorating HPNS without causing euphoria compared to the 10% N_2 recommended by Bennett for the faster compression.

Atlantis I

Atlantis I began on April 19, 1979 when 3 volunteers, who were not specially selected, were compressed with 5% N_2 in He/O_2 in 12 h 20 min to 460 m (1509 ft) (Fig. 1), where they spent 4 days as subjects for a series of per-
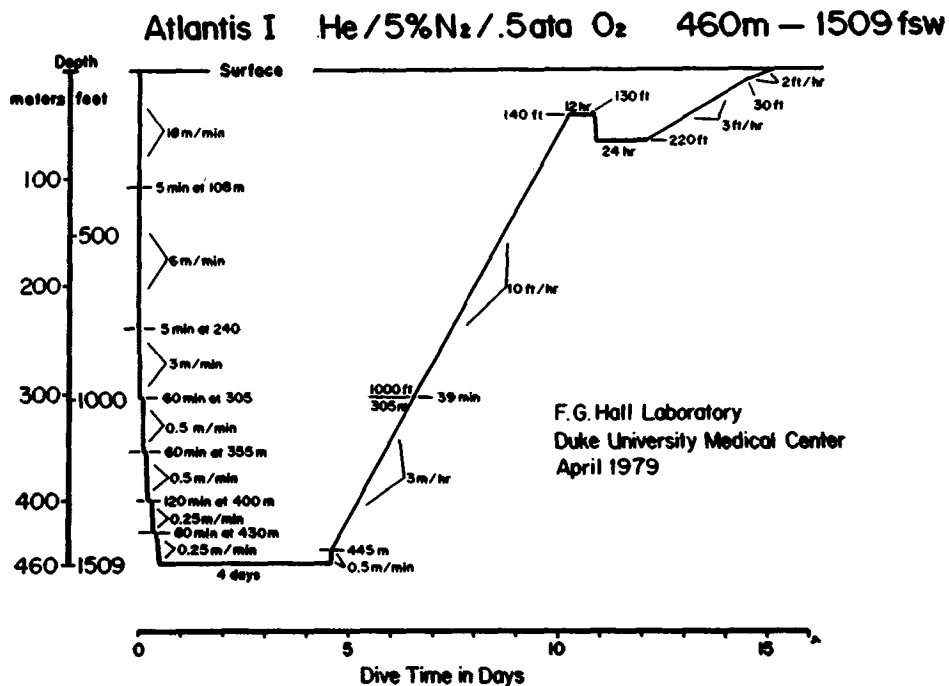

Fig. 1. Profile, *Atlantis I*.

formance, neurophysiological, and pulmonary tests. A significant difference from earlier trimix dives was that compression was with trimix throughout, rather than starting with air and continuing with helium. This resulted from the important work of Rostain and coworkers (20) with the Papio papio monkey, which showed that the best method for preventing HPNS in a trimix dive (N_2 = 6.5%) to 1000 m (3282 ft) was injection of nitrogen 7 times during compression every 100 m from 300 m, rather than just at the start or end.

Measurements of subjective mood at 460 m showed increased tendencies toward behaviors that were withdrawn, depressed, tense, excited, drowsy, lethargic, clumsy, and incompetent, but which improved by Day 2 for most moods except lethargy and tenseness, which were present throughout the time at maximum depth.

Sleep quality was poor, with vivid dreams and nightmares during the time at maximum depth.

During the latter stages of compression, and immediately on arrival, the divers experienced HPNS with various degrees of nausea, fatigue, and somnolence. One subject vomited during compression. Because of the synergistic effects of compression rate and pressure (Fig. 2), intellectual performance tests throughout Day 1 indicated a decrement almost twice that of the second and subsequent days, when the residual effects probably were due to hydrostatic pressure alone. Return to normal values occurred during decompression by 31 ATA (1000 ft).
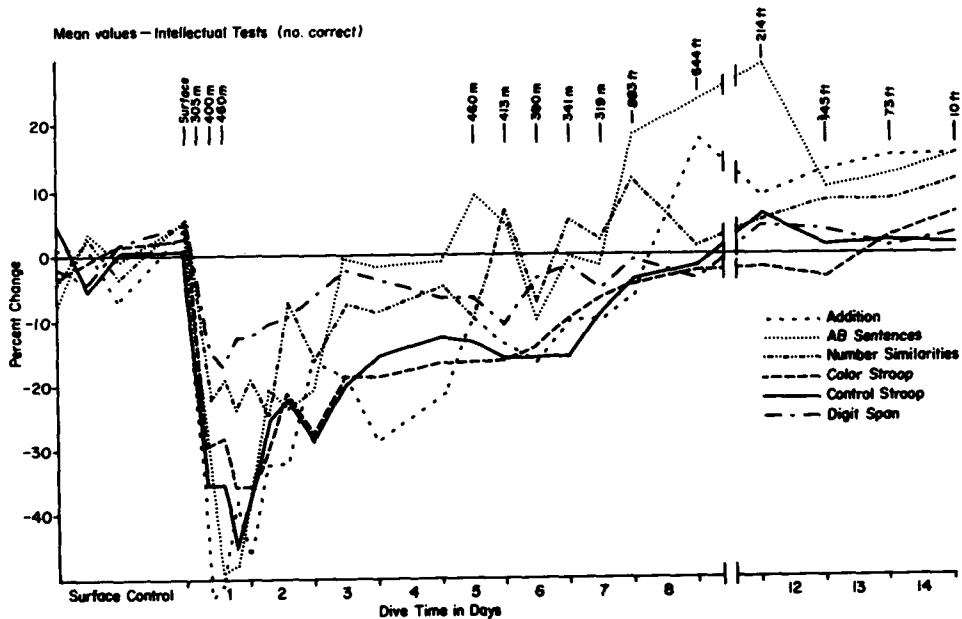

Fig. 2.   Intellectual performance, *Atlantis I*.

Postural tremor was absent but intention tremor was marked, which caused difficulty with arterial cannulation although this was completed satisfactorily in all three subjects. The psychomotor tests were less adversely affected than the intellectual tests but showed a similar biphasic depression of ability especially in the Bennett Hand-Tool Test (Fig. 3).

The EEG showed an increase in all frequencies on *Day 1* with delta and theta activity reaching peak increases over predive controls of +85% and +60%, respectively, and alpha and beta frequencies to +10 and +30%. By *Day 2* the alpha and beta frequencies had fallen to between −10 and −30% below normal but the delta and theta remained +20% above normal.

Although the divers were able to function very well after *Day 2* of this especially fast compression rate, clearly signs and symptoms of HPNS were present. This result seemed mainly due to the divers working more slowly than previously, as all tests were completed satisfactorily, including the very complex pulmonary function measurements, arterial catheterization, and blood gas sampling and analysis. Work-limiting dyspnea was present during moderate exercise but the arterial blood gases were within normal limits. Indeed, the dyspnea seemed worse when the subjects breathed helium-oxygen alone rather than trimix, which suggests it may be another part of HPNS mediated centrally.

Decompression was designed for just over 7 days but at 0.5 ATA O_2 rather than the previous 0.6 ATA O_2. Bends occurred at 140 ft and after aug-
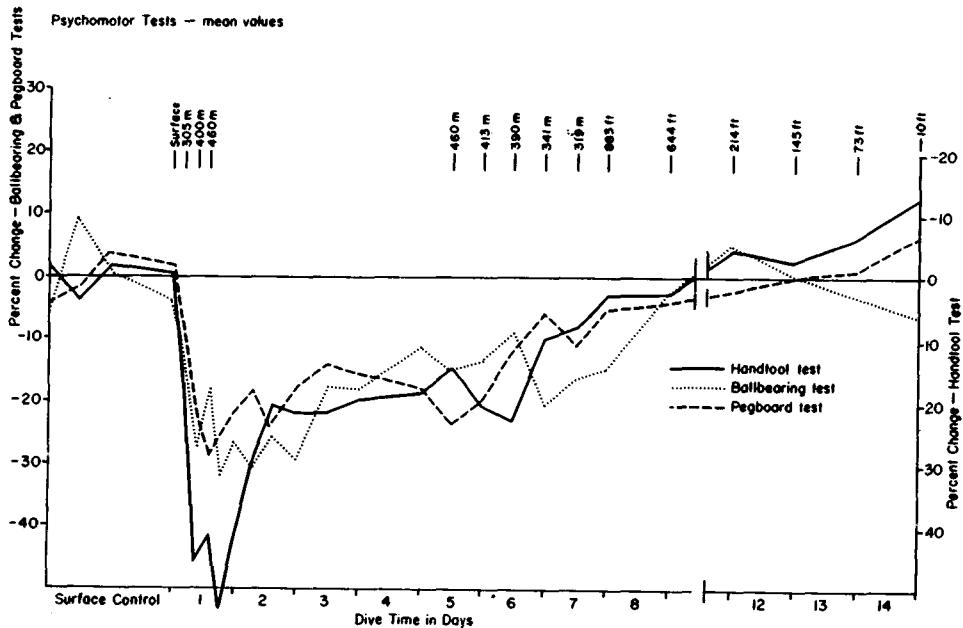

Fig. 3.   Psychomotor tests, *Atlantis I*.

mented oxygen breathing, recompression was made to 220 ft with a 24-h hold at this depth before continuing decompression at 0.6 ATA O_2 at 3 ft/h to the surface.

The French (COMEX) made a similar dive to 450 m (1476 ft) in 1979 with 4.8 N_2, but with a slower exponential compression with stages of 40 h. Tremors and myoclonic jerking were suppressed but the EEG theta and delta increase and decrease of alpha remained.

As with the Duke dive, the presence of nitrogen seemed to differentiate between compression and hydrostatic pressure effects and the divers' performance was much improved by the second day to only some 10% below controls, which is better than in previous oxygen-helium dives to this depth. Thus, although the *Atlantis I* 12-h-20 min compression rate was too fast with 5% N_2 trimix, the French 40-h compression was more satisfactory. Therefore, in *Atlantis II*, 10% N_2 trimix was chosen with the same rate of compression to examine whether or not at this faster rate the higher nitrogen would be optimal as with the earlier Duke 1000-ft studies.

Atlantis II

The profile for *Atlantis II* to 460 m (1509 ft) was the same as for *Atlantis I* except for the 10% nitrogen (Fig. 4). Two of the divers were the same and one was new. The results were remarkable with the divers arriving at 460 m in fine condition with no problems at all. The questionnaires reported "slight dif-
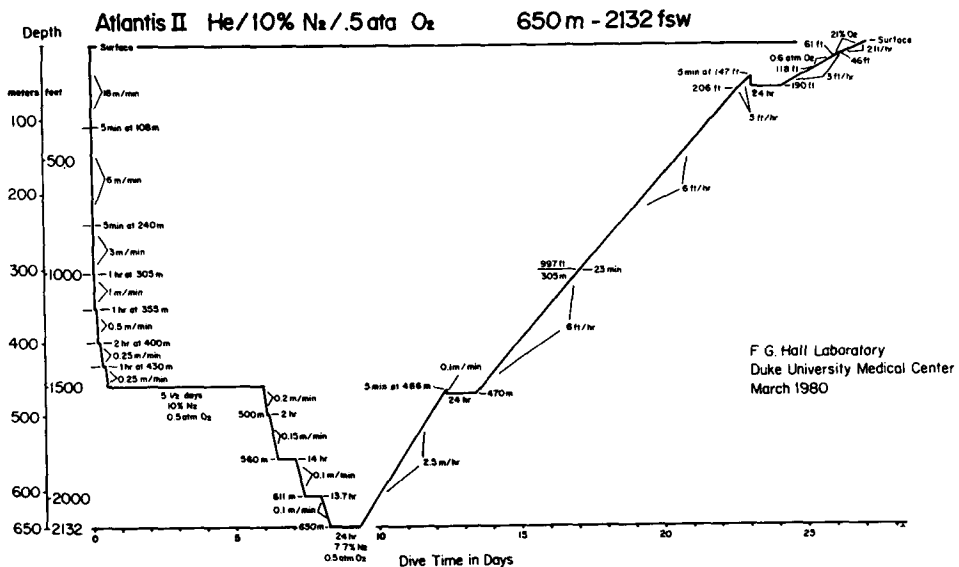
Fig. 4.   Profile, *Atlantis II*.

ficulty with breathing'' and very minor dizziness and lightheadedness in two subjects during compression around 1000 ft. At 460 m all subjects were by their own admission feeling considerably better than during *Atlantis I* (5% N_2). The nitrogen had clearly suppressed not only the postural tremor but also intention tremor, nausea, vomiting, dizziness, and lightheadedness—especially below 400 m. It is interesting, therefore, that the performance results for the two dives at 460 m were much the same (Figs. 2,3,5,6). The subjects ate and slept well with no nightmares and suffered no loss of body weight, which had occurred in many deep U.S. Navy dives with heliox.

The respiratory/exercise tests were carried out in their entirety over three days with arterial blood analysis. Work up to 180 watts was completed and inspiratory dyspnea was less evident than in *Atlantis I*.

The continuing excellent condition of the divers on *Day 5* raised the possibility of extending the depth of the dive. After a thorough examination of the logistic, scientific, ethical, and medical implications, approval was sought and
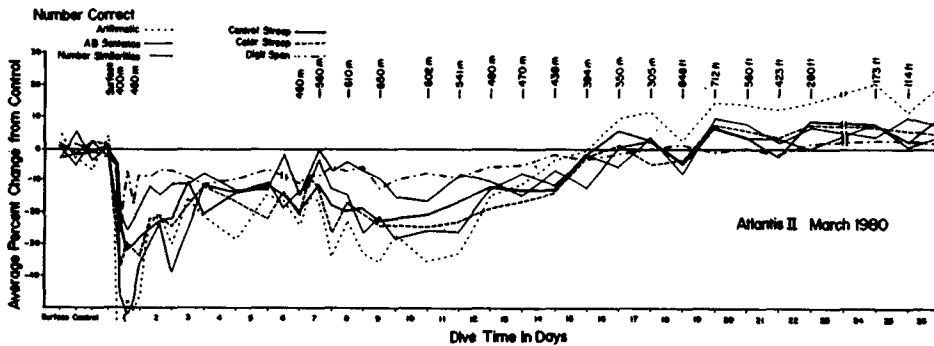
Fig. 5.   Intellectual tests, *Atlantis II*.
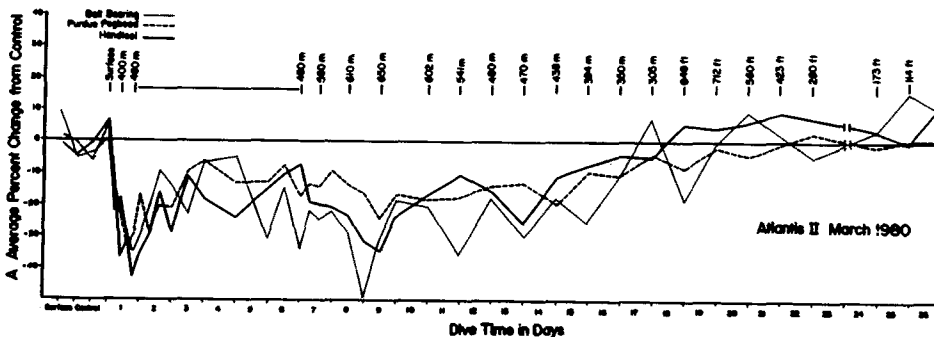
Fig. 6.   Psychomotor tests, *Atlantis II*.

given by the Duke Human Investigation Committee to proceed in stages to 650 m (2132 ft).

Compression was therefore initiated but with helium only so that the nitrogen percentage slowly fell to 7.7% N_2 at 650 m. This was a precaution against potential density or undue narcosis problems in this first dive to this depth. However, one subject did breathe 10% N_2 in He/O_2 for 15 min at 650 m through an AGA mask and reported no problems.

Interviewed on arrival at 650 m all subjects claimed to be "feeling real good." Slight intention tremor was present in two subjects, DS and WB; DS appeared fatigued due to persistent dyspnea. Subject SP, the only commercial diver, was in remarkably good condition with no problems. Subject WB stated that he became used to the extra work of breathing and that gas density was not function-limiting. Surprised by the lack of HPNS except for mild intention tremors and brief mild nausea while approaching 650 m, he reported feeling as well as, if not better than, at 460 m. In fact, the performance tests were better than those on reaching 460 m but slightly worse than before leaving 460 m (Figs. 5 and 6). Subject WB also claimed that it should certainly be possible to go deeper and faster. Subject SP noted a "real change in gas density" and had more feelings of dyspnea when relaxing, eating, or sleeping than when exercising at up to 120 watts. Conversely, Subject DS stated that approaching and at 650 m the dyspnea he experienced was function-limiting. Chewing gum, eating, talking, anything which interrupted regular ventilation, produced an alarming inspiratory dyspnea. However, he attempted 30 watts' work with no difficulty.

Normal meals were eaten. Two of the subjects noted the alarming violence of coughing and sneezing caused by the gas density.

During the 24-h stay at 650 m the subjects among them clearly demonstrated that it is possible to lead a normal existence without nausea, dizziness, vomiting, somnolence, undue tremors, or myoclonic jerking, and to carry out complicated tasks requiring fine manual dexterity, such as venipunctures, and do moderately heavy work on a bicycle ergometer without undue distress (see Salzano et al. 21).

The slight intention tremor and possibly much of the dyspnea and inspiratory dyspnea that affected Subject DS may be due to HPNS manifestations as a consequence of the 7.7% N_2 and may not appear at the recommended level of 10%.

It should be remembered, too, the rapid 2½-day compression to 650 m and the 24-h stay there were after an extensive and arduous scientific program of 6 days at 460 m.

As early as 600 m to 550 m during decompression when the nitrogen was allowed to fall towards only 5% at 460 m, HPNS started to appear, with bizarre dreams, myoclonic jerking, and to a lesser degree, intention tremor, until about 180 m.

At 466 m one of the subjects reported persistent knee pain, which resolved after only a 2.5-m recompression, but a 4-m recompression was instituted with a 24-h hold and oxygen treatment gas. Additional decompression

problems were experienced at 147 ft in two of the divers including the individual with the previous incident. After recompression and oxygen treatment the divers emerged 28 days after entering the chamber and were passed as fit with no weight loss or gain.

Thus, this dive confirmed the value of 10% trimix to ameliorate or prevent most of the HPNS in very deep diving. The experiments will continue over the next few years to further identify and clarify the value of trimix and to provide better understanding of the limitations of inspiratory dyspnea in susceptible individuals.

Acknowledgments

References

1. Bennett PB. Psychometric impairment in men breathing oxygen-helium at increased pressures. Medical Research Council. R.N. Personnel Research Committee Report UPS. 251. London, 1965.
2. Bennett PB, Dossett AN. Undesirable effects of oxygen-helium breathing at great depths. Medical Research Council. R.N. Personnel Research Committee Report UPS. 260. London, 1967.
3. Bennett PB. Performance impairment in deep diving due to nitrogen, helium, neon, and oxygen. In: Lambertsen CJ, ed. Underwater physiology. Proceedings of the third symposium on underwater physiology. Baltimore: Williams & Wilkins, 1973:327–340.
4. Bachrach AJ, Bennett PB. Tremor in diving. Aerosp Med 1973:44:613–623.
5. Hunter WL, Bennett PB. The causes, mechanisms, and prevention of the high pressure nervous syndrome. Undersea Biomed Res 1974;1:1–28.
6. Bennett PB. High pressure nervous syndrome: man. In: Bennett PB, Elliott DH, eds. The physiology and medicine of diving and compressed air work. London: Bailliére Tindall, 1975:248–284.
7. Bennett PB, Bachrach AJ, Brauer R, Rostain JC. High pressure nervous syndrome. Report No. 12, National plan for the safety and health of divers in their quest for subsea energy. Bethesda, MD: Undersea Medical Society, 1976.
8. Fructus X, Rostain JC. HPNS: A clinical study of 30 cases. In: Shilling CW, Beckett MW, eds. Underwater physiology VI. Proceedings of the sixth symposium on underwater physiology. Bethesda, MD: Federation of the American Societies for Experimental Biology, 1978:3–8.
9. Rostain JC, Naquet R. Human neurophysiological data obtained from two simulated heliox dives to a depth of 610 m. In: Shilling CW, Beckett MW, eds. Underwater physiology VI. Proceedings of the sixth symposium on underwater physiology. Bethesda, MD: Federation of the American Societies for Experimental Biology, 1978:9–19.
10. Bennett PB. A strategy for deep diving. In: Halsey MJ, Settle W, Smith EG, eds. Proceedings, workshop "The strategy for future diving to depths greater than 1000 ft." Bethesda, MD: Undersea Medical Society, 1975:71–76.
11. Zaltsman GL. Physiological principles of a sojurn of a human in conditions of raised pressure of the gaseous medium. 1961. English Trans. Foreign Tech Div, Wright Patterson AFB, Ohio, 1967. AD655360.
12. Johnson FH, Flager EA. Hydrostatic pressure reversal of narcosis in tadpoles. Science 1950;112:91–92.
13. Bennett PB, Papahadjopoulos D, Bangham AD. The effect of raised pressure of inert gases on phospholipid membranes. Life Sci 1967;6:2527–2533.
14. Lever MJ, Miller KW, Paton WDM, Street WB, Smith EG. Pressure reversal of anesthesia. Nature 1971;231:368–371.

15. Bennett PB, Blenkarn GD, Roby J, Youngblood D. Suppression of the high pressure nervous syndrome in human deep dives by He-N_2-O_2. Undersea Biomed Res 1974;1:221–237.
16. Simon S. Katz Y, Bennett PB. Calculation of the percentage of a narcotic gas to permit abolition of the high pressure nervous syndrome. Undersea Biomed Res 1975;2:299–303.
17. Bennett PB, Roby J, Simon S, Youngblood D. Optimal use of nitrogen to suppress the high pressure nervous syndrome. Aviat Space Environ Med 1975;46:37–40.
18. Rostain JC. Le tremblement au cours de decompression rapides: Influence de l'azote dans le melange respiratoire. Med Aeronaut Spat Med Subaquat Hyp 1976;15:267–270.
19. Charpy JP, Murphy E, Lemaire C. Performance psychometriques apres compressions rapides a 300 m. Med Aeronaut Spat Med Subaquat Hyp 1976;15:192–195.
20. Rostain JC, Dumas JC, Gardette B, Imbert JP, Lemaire C, Naquet R. Compression au melange helium-azote-oxygen de singes Papio papio a 1000 m. Med Aeronaut Spat Med Subaquat Hyp 1977;17:266–270.
21. Salzano JV, Stolp BW, Moon RE, Camporesi EM. Exercise at 47 and 66 ATA. In: Bachrach AJ, Matzen MM, eds. Underwater physiology VII. Proceedings of the seventh symposium on underwater physiology. Bethesda, MD: Undersea Medical Society 1981:181:196.

THE EFFECT OF HIGH PRESSURE ON COOPERATIVE LIPID-PROTEIN INTERACTIONS

H-J. Galla and J. R. Trudell

The discovery that high pressure antagonizes the effects of anesthesia (1) led directly to the suggestion that anesthetic agents might antagonize some of the effects of high pressure. The finding that nitrogen was an anesthetic agent at high pressures led to the suggestion by Bennett that small amounts of nitrogen added to helium-oxygen diving mixtures might afford some protection against high pressure nervous syndrome (HPNS). This suggestion was tested in model phospholipid systems (2), laboratory animals (3), and in a number of human diving experiments that led to a safe dive to record depths, recently accomplished at the Hall laboratories at Duke University. We have carried out a long series of experiments designed to elucidate the molecular basis for the antagonism of high pressure and anesthetic agents. Because of recent renewed interest in this antagonism, we will review some of our earlier results on pure phospholipid model systems and then describe a new model system in which a protein-lipid interaction in a phospholipid bilayer exhibits appropriate pressure-anesthetic antagonism.

REVIEW OF EARLY WORK

In our early work with pure phospholipid bilayer model systems, we showed that the application of high pressure decreased fluidity of the fatty acid chains in membranes as measured by electron paramagnetic resonance (EPR) (4). We first showed that inhalation anesthetics reversed this pressure-induced ordering of the phospholipid bilayer. We then studied the effect of applying 102 atmospheres of helium, hydrogen, nitrogen, argon, or xenon, as well as 51 atmospheres of nitrous oxide (5). The initial application of pressure to these

357

systems decreased the fluidity or increased the order of the phospholipid bilayers; however, as the gases slowly diffused into and dissolved in the bilayer suspension the fluidity increased in direct proportion to the Bunsen solubility coefficient for each gas. Therefore, in this model system, all of the high pressure gases were behaving as pure anesthetics and were exhibiting a linear pressure antagonism at pressures as high as 102 atmospheres. As expected, helium did not dissolve well in phospholipid bilayers and, therefore, after the initial decrease in fluidity in the bilayer, little additional change was produced on standing. This led to the expectation that appropriate mixtures of any of the gases with helium should result in an antagonism such that after equilibrium of gas solubility has been achieved there would be no net change in membrane fluidity as compared to the control. In a test of this hypothesis (6) we applied a series of binary mixtures of helium with nitrogen, xenon, or nitrous oxide to suspensions of phosphatidylcholine-cholesterol vesicles to determine those mixtures of lipid soluble gases that would exactly antagonize the membrane rigidifying effect of 100-atmosphere compression. We found that binary mixtures of helium with 88% nitrogen, 3.8% xenon, or 2.8% nitrous oxide resulted in zero net change in the fluidity of the bilayers at 100 atmospheres pressure after equilibrium had been accomplished. An important result of this study was a nonlinear graph of percent of narcotic gas needed to produce a zero net effect in the bilayer system as a function of pressure. This suggested that the ratios of gases in trimix would have to be varied as a function of total pressure.

THE NEW MODEL SYSTEM

It is clearly inappropriate to apply directly to diving mixtures for humans any quantitative values derived from pure egg phosphatidylcholine-cholesterol vesicles. However, insofar as there are many good correlations between effects in phospholipid model systems and corresponding effects in the central nervous system, this kind of information may be useful in planning future experimentation. In an attempt to make the results of our model system studies more relevant to human physiology, we have developed a new model system in which we have incorporated a strongly interacting protein into a phospholipid vesicle system. In this way, we are able to directly observe pressure-anesthestic antagonism on protein-phospholipid interactions in a bilayer. Our previous work had shown that the effect of high pressure on a phospholipid bilayer system containing lateral phase separations was as much as 100 times greater (7) than in a heterogeneous phospholipid bilayer system. Therefore, in selecting our phospholipid-protein model system we used a protein that would induce lateral phase separations in a phospholipid bilayer. The polypeptide antibiotic polymyxin was previously shown by Sixl and Galla (8) to induce a lateral phase separation in phosphatidic acid bilayers. We propose that the positively-charged polymyxin binds to the negative headgroups of the phosphatidic acid and forms a protein-lipid cluster in the plane of the bilayer. The fatty acid chains

of the phospholipids in this cluster remain in a bilayer, exhibit cooperative interactions, but have a phase transition temperature approximately 20°C lower.

A model of the proposed structure for the binding of polymyxin to a phosphatidic acid bilayer is shown in Fig. 1. The central domain (T_2) of each cluster contains polymyxin bound to phosphatidic acid by hydrophobic as well as electrostatic interactions. Under certain conditions a second domain (T_3) is also observed by spectroscopy. This second domain is suggested to consist of an annular ring of polymyxin bound to phosphatidic acid bilayers by only hydrophobic interactions. The cluster containing these two protein-phospholipid domains is surrounded by a phosphatidic acid bilayer (T_1) in which the fatty acid chains exhibit a slightly lower phase transition temperature and cooperativity than those of pure phosphatidic acid.

This model system has many advantages for studying the interactions of proteins with phospholipid bilayers. Polymyxin is known to bind to bilayers by two separate molecular interactions. The positively-charged main part of the polypeptide binds directly to the negative head-groups of phosphatidic acid molecules on the bilayer surface. In addition, polymyxin has a fatty acid side chain that intercollates into the bilayer and serves to further bind the antibiotic by the sort of hydrophobic interactions that exist between phospholipids. Therefore this protein may be used to study both electrostatic and hydrophobic interactions and is also seen to show some properties characteristic of both extrinsic and intrinsic proteins.

RESULTS

Figure 2 shows the results of a study of the application of 100 atmospheres to the polymyxin-phosphatidic acid bilayer system (9). One can see that the application of pressure increases the phase transition temperature of the fatty acid region shown in Fig. 2 as the change from temperature a to b. The
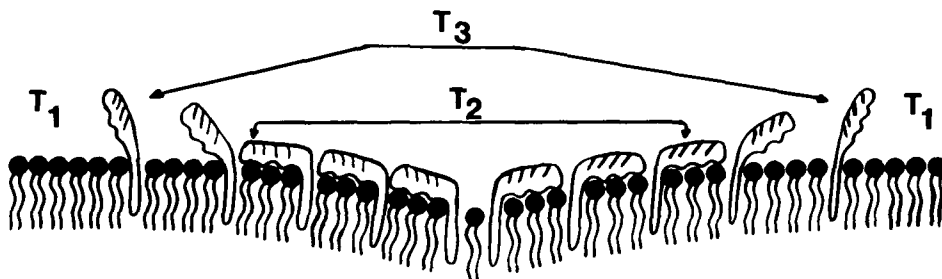

Fig. 1.   Model proposed for the phosphatidic acid-polymyxin cluster: an inner domain of polymyxin bound to a phosphatidic acid layer by both electrostatic and hydrophobic interactions (T_2) is surrounded by an annular ring (T_3) that exhibits only hydrophobic interaction, which is in turn surrounded by a free phosphatidic acid domain (T_1). (Reproduced from ref. 9 with permission.)
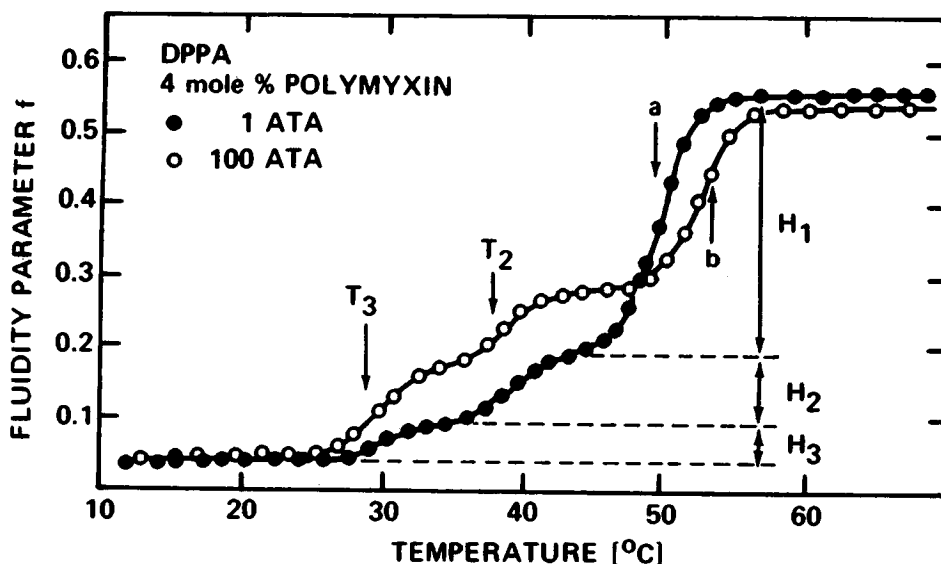
Fig. 2. Phase transition curves of dipalmitoylphosphatidic acid membranes (DPPA) containing 4 mol% polymyxin at 1 and 100 atmospheres of helium pressure. T_1, T_2, and T_3 identify the temperatures of each phase transition step; H_1, H_2, and H_3 are the amplitudes of the fluidity change corresponding to each domain. The difference (ΔT_1) between arrows a and b, that is, the shift of the phase transition temperature (T_1) of the phosphatidic acid domain, with pressure is about 3°C. (Reproduced from ref. 9 with permission.)

protein-phospholipid cluster appears to be noncompressible in that the phase transition temperatures of both the inner domain (T_2) and its annular ring (T_3) are constant up to 100 atmospheres of pressure. This means that the volume and the molecular packing of the phospholipids in the two domains are not altered by pressure. The molecular structure of the phosphatidic acid-polymyxin cluster that best fits our results includes an expanded bilayer surface, the area of which is dominated by the projected area of extrinsic polymyxin bound to negatively-charged head-groups.

One also sees in Fig. 2 that 100 atmospheres of pressure causes a significant redistribution of the amount of phosphatidic acid that exists in the three domains designated by H_1, H_2, and H_3. This suggests that the molecular events that lead to the apparent change in the surface area of the three domains are such that under high pressure, the small amount of polymyxin that was randomly dispersed throughout the pure phosphatidic acid domain surrounding the protein-lipid clusters is forced to join the clusters. This redistribution would occur if the total volume of the system is decreased when the independent polymyxin molecules join one of the clusters on the bilayer surface. We believe that this redistribution of proteins in a phospholipid matrix may have important implications for understanding of the effects of high pressure on functional components of cells. It is known that the spatial orientation of proteins in membranes is very important to the direct functioning of the proteins and that, in many cases, the forces that control this orientation are weak and delicately balanced. This study provides evidence that pressure could cause a redistribu-

tion of important elements in membranes important for nerve function or meta-bolic processes.

The striking results of the application of 100 atmospheres of pressure to the polymyxin-phosphatidic acid bilayers (10) suggested that we should study the effect of high pressure on pure phosphatidic acid bilayers better to under-stand the factors that might determine protein-phospholipid cooperativity. The influence of the negatively-charged head-group on phosphatidic acid may be very important to cellular membrane functions in that many membranes con-tain as much as 15% negatively-charged phospholipids. Our subsequent study showed that, in fact, negatively-charged phospholipid bilayers have very un-usual properties with respect to application of high pressure and pressure-anesthetic antagonism.
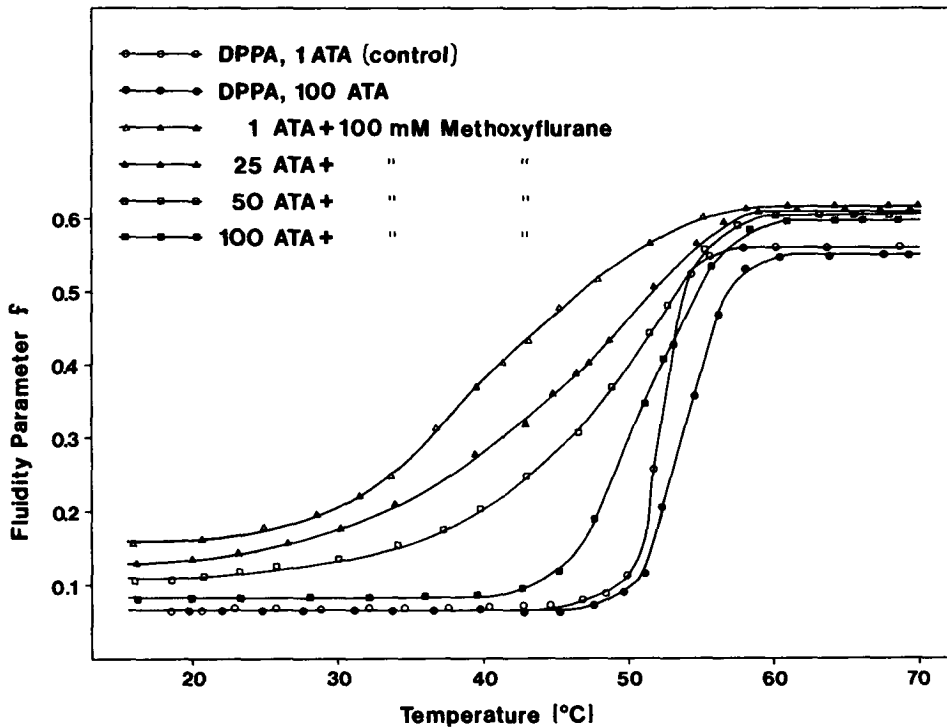
Fig. 3. Pressure-dependent phase transition curves of dipalmitoylphosphatidic acid bilayers (DPPA) in the presence and absence of the inhalation anesthetic methoxyflurane (100 mmol/mol lipid). Note the asymmetric change in the phase transition temperature with increasing helium pressure. (Reproduced from ref. 10 with permission.)

An earlier study (7) showed that in the case of a bilayer formed from uncharged dipalmitoylphosphatidylcholine, a phase transition curve like that of the unmodified control bilayer was obtained when an amount of pressure suf-ficient to raise the phase transition temperature by 2° was applied to a sus-pension containing sufficient inhalation anesthetic to cause an equivalent depression of the phase transition temperature. This linear and symmetric

pressure-inhalation anesthetic antagonism was observed over a wide range of pressure and anesthetic concentrations. For example, 60 mmol of methoxy-flurane/mole dipalmitoylphosphatidylcholine depressed the phase transition temperature by 3.5°C, and application of 100 atmospheres of helium pressure increased the transition temperature by 2.5°. Simultaneous application of anesthetic agent and pressure resulted in a spectrum much like that of the control.

In contrast, the phase transition temperature of a bilayer composed of di-palmitoylphosphatidic acid is depressed 10°C by 100 mmol methoxyflurane/mole lipid. Whereas, 100 atmospheres of helium pressure applied to pure phosphatidic acid bilayers increases the phase transition temperature only 1.5°C. Surprisingly, application of 100 atmospheres helium pressure to bilayers of dipalmitoylphosphatidic acid containing 100 mmol methoxyflurane/mole lipid almost completely antagonized the effect of the anesthetic (10). In Fig. 3 the very large effect of the inhalation anesthetic and the asymmetric pressure-anesthetic antagonism are shown.

The results described from these recent studies show that large effects of pressure may be expected to occur in biological membranes. In addition, these effects will depend on the composition of phospholipids found in the bilayer and will vary according to the structure of each individual protein that participates in the biologically important events. We hope that these studies will add to the understanding of the molecular basis by which gas mixtures and drugs may be used to antagonize the effect of high pressure on biological systems.

Acknowledgments

References

1. Johnson FH, Flagler EA. Hydrostatic pressure reversal of narcosis in tadpoles. Science 1950;112:91–92.
2. Bennett PB, Papajadjopoulos D, Bangham AD. The effect of raised pressures of inert gases on phospholipid model membranes. Life Sci 1967;6:2527–2533.
3. Cromer JA, Bennett PB, Hunter WL Jr, Zinn D. Effect of helium/nitrogen/oxygen mixture on HPNS convulsion threshold in euthermic rats. Undersea Biomed Res 1979;6:367–377.
4. Trudell JR, Hubbell WL, Cohen EN. Pressure reversal of inhalation anesthetic-induced disorder in spin-labeled phospholipid vesicles. Biochim Biophys Acta 1973;291:328–334.
5. Chin JA, Trudell JR, Cohen EN. The compression-ordering and solubility-disordering effects of high pressure gases on phospholipid bilayers. Life Sci 1976;18:489–498.
6. Mastrangelo CJ, Trudell JR, Cohen EN. Antagonism of membrane compression effects by high pressure gas mixtures in a phospholipid bilayer system. Life Sci 1978;22:239–299.
7. Trudell JR, Payan DG, Chin JH, Cohen EN. The antagonistic effect of an inhalation anesthetic and high pressure on the phase diagram of mixed dipalmitoyl-dimyristoylphosphatidylcholine bilayers. Proc Nat Acad Sci 1975;72:210–213.
8. Sixl F, Galla H-J. Cooperative lipid protein interaction–effect of pH and ionic strength on polymyxin binding to phosphatidic acid membranes. Biochim Biophys Acta 1979;557:320–330.
9. Galla H-J, Trudell JR. Pressure-induced changes in the molecular organization of a lipid-peptide complex: polymyxin binding to phosphatidic acid membranes. Biochim Biophys Acta (in press).
10. Galla H-J, Trudell JR. Asymmetric antagonistic effects of an inhalation anesthetic and high pressure on the phase transition of dipalmitoylphosphatidic acid bilayers. Biochim Biophys Acta 1980;559:336–340.

CURRENTS IN A VOLTAGE CLAMPED VERTEBRATE NEURON AT HYPERBARIC PRESSURE

J. J. Kendig

In previous studies on both vertebrate and invertebrate axons, we have identified and characterized a phenomenon that may be related to the high pressure nervous syndrome (HPNS) (1). Some axons, when exposed to high pressure, generate repetitive impulses in response to a single stimulus. As pressure increases, the train of repetitive impulses becomes longer; eventually these axons begin to generate impulses spontaneously in the absence of a stimulus. Repetitive impulse generation could well be the foundation for the increased central nervous system excitability associated with HPNS (2). As occurs with HPNS, pressure-induced repetitive impulse generation is inhibited by anesthetic agents (3). The phenomenon can be observed at moderate pressures well within the range associated with HPNS, i.e., from 20 to 100 atmospheres absolute (ATA). In the studies previously reported extracellular recording techniques were employed; analysis of the basic mechanism was therefore necessarily limited.

In our present studies we have employed a voltage clamped preparation, in which membrane ionic currents can be directly monitored. With this technique the voltage or potential across the membrane of a single nerve cell is held or clamped at a defined level. The potential can be rapidly switched to a new level at which voltage-sensitive membrane channels open to permit the passage of selected ions. The current required to hold the membrane potential at the new level is the image of the ionic current flowing through the channels. Previous studies using the voltage clamp technique have documented some effects of pressure on molluscan ganglion cell bodies and squid giant axon, (4–6 and personal communication with B.B. Shrivastov, 1980). This paper presents the first reported effects of hyperbaric pressure on ion channels in a vertebrate neuron.

363
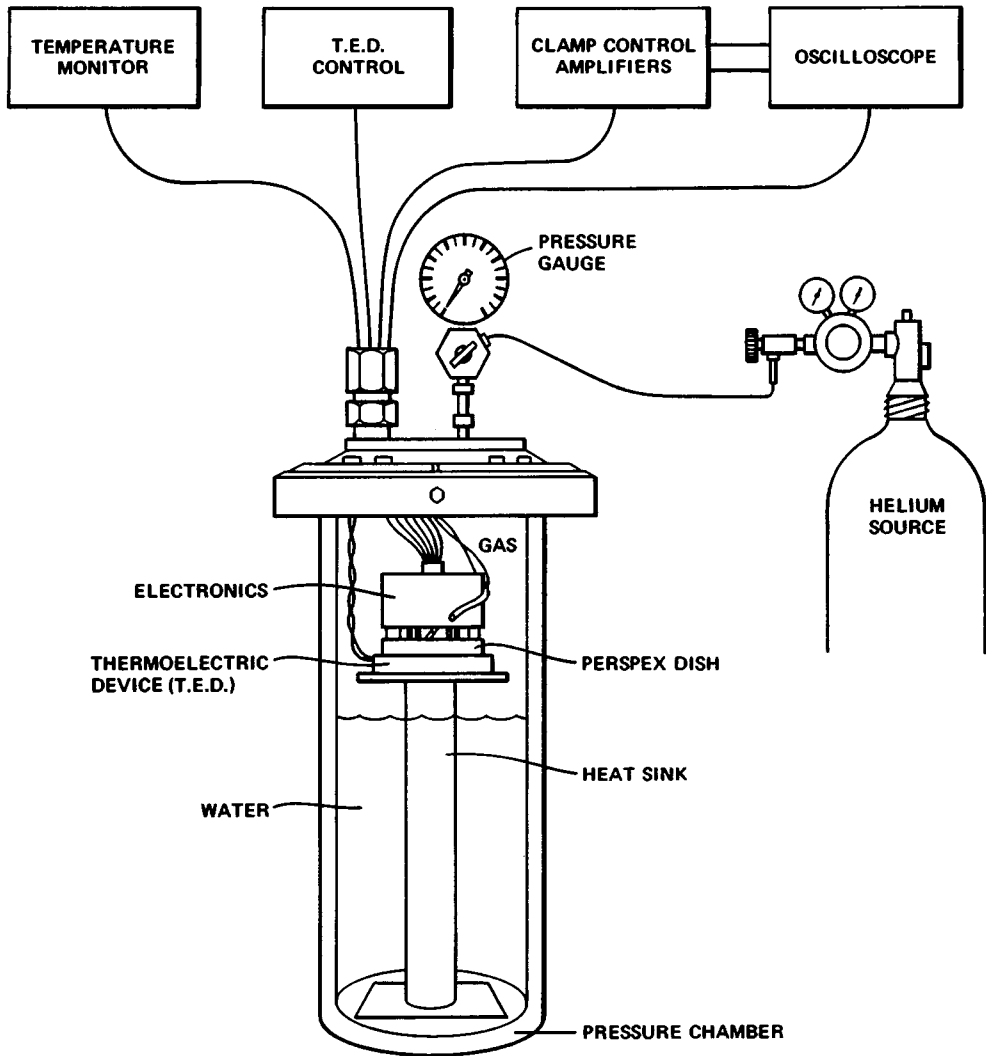
Fig. 1.   Arrangement of the voltage clamp apparatus in the hyperbaric pressure chamber. The axon encompassing a nodal region is mounted on a perspex dish and interfaced with the first stage clamp electronics through agar salt bridges inserted into pools in the perspex dish. The salt bridges are in contact with the Ag/AgCl electrodes. Temperature is controlled by a thermoelectric device (T.E.D.) beneath the perspex dish and monitored by thermistors in the pool of Ringer's solution containing the nodal region and in the gas phase above the solution. Pressure is applied to the preparation by admitting helium from a commercial high-pressure cylinder at a slow compression rate designed to minimize temperature increases at the node.

METHODS

The node of Ranvier of amphibian (*Rana catesbiana*) sciatic nerve axon was arranged for voltage clamping by a technique similar to that previously described (7,8). The node with its adjacent internodes was dissected in standard frog Ringer's solution (NaCl 114 mM, KCl 2.4 mM, CaCl$_2$ 2 mM, HEPES buffer 10 mM, pH adjusted to 7.4) and mounted in a vaseline gap voltage clamp chamber of the Dodge and Frankenhaeuser type. The solution in contact with the cut internodes was 120 mM KCl buffered with 20 mM HEPES, pH adjusted to 7.4. The electronics of the clamp system are substantially similar to those we have used in previous studies at normobaric pressures (9). Modifications have been made in the configuration of the electrodes in contact with the solution and in the dimensions and position of the first amplifier stage, to allow for positioning in the cylindrical 1.8-L pressure chamber (Fig. 1). The modification included a reduction in lengths of the KCl-agar bridges which constitute the interface between the sintered Ag/AgCl electrodes and the solutions in contact with the axon, and provision of a permanent contact between the KCl-agar bridge and the electrode surface, so that bridge and electrode are a single unit. TheAg/AgCl electrodes are welded to gold pins, which are inserted into sockets in the amplifier head at the beginning of each experiment. It proved possible to compress the wiring of the first stage into the required dimensions by strict attention to separation of critical leads to avoid unwanted capacitive interaction.

Of special circumstances in the hyperbaric environment that might produce artifacts, temperature changes resulting from compression heating are probably the most important. This is of particular significance in these experiments, because the rate constants that govern ion channel configuration changes have large temperature coefficients, with Q_{10} in the range 1.8 to 3(10). In our previous experiments on intact nerves at hyperbaric pressure, temperature currents were made immediately on temperature stabilization following compression, and also in some instances after up to 30 min at a given pressure, to assure that the recorded pressure effects were stable rather than transient. In some of the experiments measurements were made with either tetraethylammonium chloride (TEA) (7.5 mM) in the Ringer's solution or with choline chloride substituted for sodium chloride in the Ringer's solution to block potassium or sodium channels respectively; thus, the sodium and potassium currents were separated pharmacologically for measurement of the time constants. The following measurements were made at 1 ATA and at stages of 10, 20, 35, 70, and 100 ATA. In experiments with sodium currents intact, holding potential was adjusted to set the level of sodium channel inactivation (h) equal to approximately 0.6. This usually corresponded to a holding potential of about − 80 mV. Holding potential was arbitrarily set to − 80 mV in experiments with sodium currents blocked. Sodium and potassium channel function was assessed by imposing depolarizing test pulses of variable magnitude and duration, and monitoring the transient inward and steady state outward currents carried by sodium and potassium ions, respectively. In TEA-treated nodes, the curve relating the time constant of sodium activation (τ_m) to voltage was plot-

ted by measuring the time from the onset of the test pulse to $1/e$, the distance between the base line and the peak of the sodium current at voltages between -80 and -5 mV. The time constant of inactivation (τ_h) was measured over the same voltage range by measuring the time required for the sodium current to decay to $1/e$ of its final value during the 20-ms test pulse. The potassium activation time constant, τ_n, was similarly measured in choline-substituted Ringer's solution over the voltage range between -80 and $+25$ mV.

It has proved possible to obtain measurements on decompression on some but not all nodes. Decompression measurements to check the reversibility of problems were minimized by immersing the biological preparation deep below the surface of a large volume of aqueous medium, in which the heat of compression is minimal. The requirements of vaseline gap voltage clamp recording make this strategy impossible, because the node necessarily is at or near the surface of a relatively small volume of solution, and thus is exposed to the much larger heat of compression of the gas phase. In the voltage clamp experiments, temperature of the solution around the node was controlled by a Peltier thermoelectric device beneath the clamp chamber. The solution temperature was maintained at approximately 10°C, a standard temperature for this preparation and one that permits good resolution of ion channel time constants. Temperature of the node pool solution was monitored by a thermistor in the pool containing the node. There was also a thermistor in the gas phase above the node. Measurements were made following compression when both thermistors recorded temperatures within 0.25°C of the 1-ATA control reading, to assure that the temperature at the node itself had not changed. Temperature within the brass block enclosing the first stage electronics was monitored by a separate thermistor and maintained with 0.5°C of control temperatures.

After temperature stabilization in the pressure chamber, compression was carried out by admitting helium from a commercial cylinder pressurized to 4000 psi, at a rate slow enough to limit transient gas phase temperature increases to ~5°C. Forty-five minutes to one hour was required to raise the pressure from 1 to 100 ATA. In our previous studies on nerves, helium and hydrostatic pressure were found to exert identical effects (11). It is assumed that this applies in the present study; the electrical constraints of the node voltage clamp do not permit the identity of helium and hydrostatic pressure to be tested on this preparation. Photographic records of ion pressure effects were made whenever possible. All pressure effects reported in the present study were reversible on decompression. Most of the nodes are viable over the time course required for a complete experiment, i.e., approximately 1.5-2 h after the establishment of the voltage clamp. Loss of the nodal membrane is usually sudden and accompanied by a sudden large increase in the leakage conductance (g_L).

RESULTS

The present report concerns itself primarily with those findings that may be related to HPNS.

Change in Baseline Current Level

On compression, there was a consistent, pressure-related shift in the current required to maintain the transmembrane holding potential at its present level. The direction of the shift corresponded to the generation of an inward current. Its magnitude varied considerably among preparations, ranging from barely detectible to 4 nA at 100 ATA. The current was stable at periods up to 20 min at any given pressure. The current level was restored to control value on decompression.

The current corresponded to depolarization of the membrane; nodes held in the current-clamped rather than voltage-clamped mode showed a pressure-related depolarization on compression. Current-clamped nodes depolarized to the point of block of action potential generation did not completely regain the control resting potential on decompression; however, there was a return toward control values. In the early stages of compression-related depolarization, there was a decrease in threshold for action potential initiation.

Experiments to identify the basis for the inward current are in progress, but the results are as yet too preliminary to permit positive conclusions to be stated. It does not appear, however, that exposure to high pressure is associated with any consistant increase in the leakage conductance, g_L. This finding, if confirmed, suggests that increases in membrane resting permeability are not involved in the generation of the current.

Increase in Membrane Time Constants

The time constants associated with sodium channel activation (τ_m) and inactivation (τ_h) showed a marked increase at pressure (Fig. 2), as did the time constant for potassium activation (τ_n) (Fig. 3). The increase in τ_h was particularly marked. At test potentials that evoke the maximum sodium current, complete inactivation does not develop during a long (17 ms) depolarization at high pressure. At corresponding potentials, pressure considerably diminishes the amplitude of the potassium current. The combination of the effects on membrane time constants would produce a broad action potential in a conducting nerve. We have documented this effect in our earlier extracellular studies on compound nerves at high pressure (11). It would also be expected that a prolonged depolarization would follow each action potential in individual nerves, or that any after-hyperpolarization from potassium conductance would be considerably reduced, or both. The possible relationship of these changes to HPNS symptoms will be discussed.

DISCUSSION

Is the inward current responsible for the repetitive activity observed in other axons? A depolarizing shift in membrane potential, with accompanying inward current, will produce repetitive activity in axons capable of generating trains of impulses in response to a prolonged stimulus. A similar depolarizing

$\mathcal{T}_h$
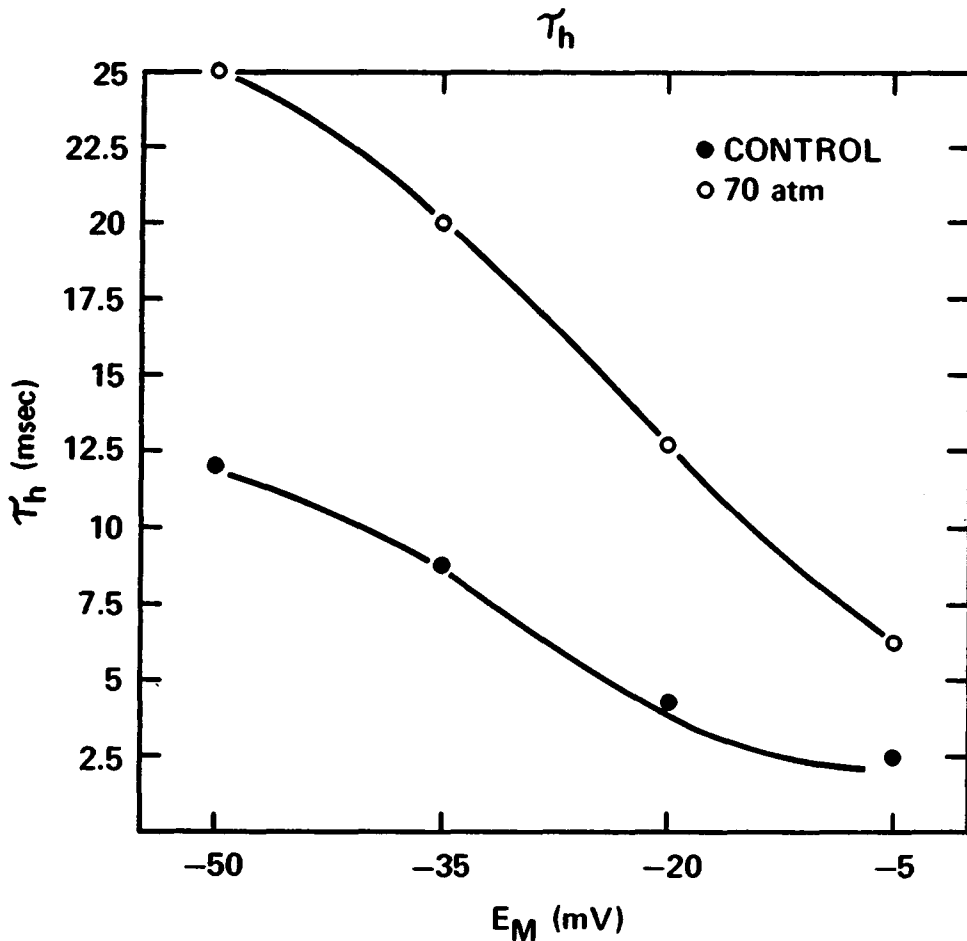
Fig. 2. Increase in time constant of sodium channel inactivation (τ_h) at hyperbaric pressure. Temperature 10°C, pressures 1 ATA (control) and 70 ATA. τ_h is markedly prolonged at all voltages more depolarized than the resting potential.

current would have produced repetitive activity in the axons used in our previous studies (12). It is proposed that a pressure-responsive membrane depolarization is the basis for the pressure-generated repetitive impulse activity. The evidence linking these phenomena to the HPNS is indirect but plausible; repetitive impulse generation has been linked to some drug-induced convulsive phenomena and could well be responsible for the seizure activity associated with HPNS. The lower threshold for action potential generation observed at moderate pressures would also contribute to a pressure-induced increase in excitability, which might well be involved in HPNS. At present the basis for the depolarizing effect of pressure is undefined, as is its sensitivity to pharmacologic intervention.
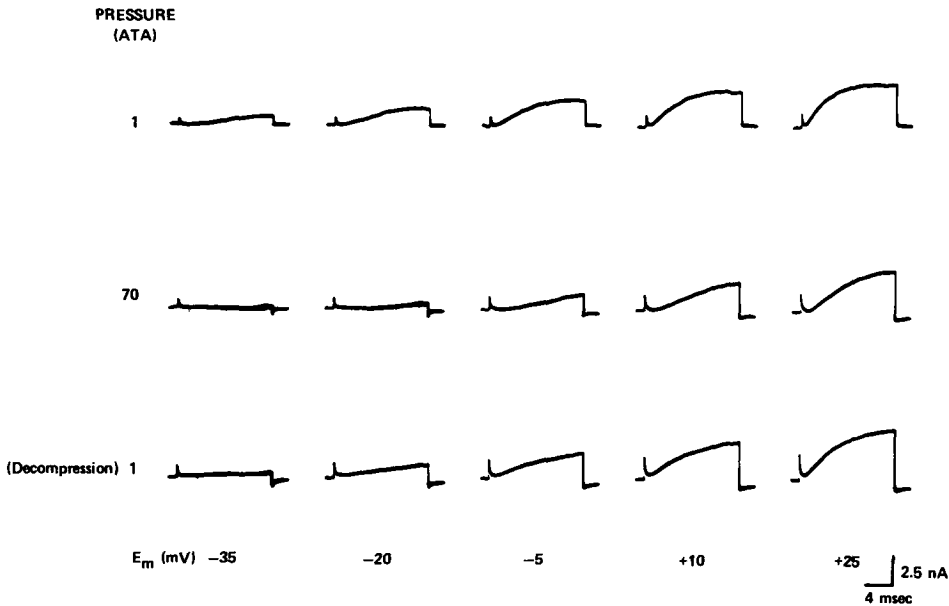
PRESSURE
(ATA)

Fig. 3. Potassium currents at 1 ATA, 70 ATA, and on decompression to 1 ATA. Temperature 10.5°C. There is a reversible increase in the time constant of potassium channel activation (τ_n) at high pressure; the magnitude of the current is smaller at any given membrane voltage.

The prolongation of τ_h and τ_n would enhance the tendency of an axon to fire repetitively by reducing the extent to which it accommodates to a constant stimulus. The relative depolarization induced by a decrease in sodium channel inactivation and in potassium channel activation would contribute to axon instability. It is proposed that the two phenomena, membrane depolarization and membrane time constant prolongation, are related to the increased nervous system irritability that characterizes some of the symptoms of HPNS.

Acknowledgments

References

1. Kendig JJ, Schneider TM, Cohen EN. Pressure, temperature, and repetitive impulse generation in crustacean axons. J Appl Physiol 1978;45:742–746.

2. Noebels JL, Prince DA. Presynaptic origin of penicillin after-discharges at mammalian nerve terminals. Brain Res 1977;138:59–74.

3. Kendig JJ, Schneider TM, Cohen EN. Anesthetics inhibit pressure-induced repetitive impulse generation. J Appl Physiol 1978;45:747–750.

4. Henderson JV, Gilbert DL. Slowing of ionic currents in the voltage-clamped squid axon by helium pressure. Nature 1975;258:351–352.

5. Parmentier JL, Shrivastav BB, Bennett PB, Wilson KW. Effects of interaction of volatile anesthetics and high hydrostatic pressure on central neurons. Undersea Biomed Res 1979;6:75–91.

6. Wann KT, Macdonald AG, Harper AA. The effects of high hydrostatic pressure on the electrical characteristics of *Helix* neurons. Comp Biochem Physiol 1979;64A:149–159.

7. Hille B. The permeability of the sodium channel to organic cations in myelinated nerve. J Gen Physiol 1971;58:599–619.

8. Courtney KR, Kendig JJ, Cohen EN. The rates of interaction of local anesthetics with sodium channels in nerve. J Pharmacol Exp Ther 1978;207:594–604.

9. Kendig JJ, Courtney KR, Cohen EN. Anesthetics: molecular correlates of voltage- and frequency-dependent sodium channel block in nerve. J Pharmacol Exp Ther 1979;210:446–452.

10. Frankenhaeuser B, Moore LE. The effect of temperature on the sodium and potassium permeability changes in myelinated nerve fibers of *Xenopus laevis*. J Physiol (Lond) 1963;169:431–437.

11. Kendig JJ, Trudell JR, Cohen EN. Effects of pressure and anesthetics on conduction and synaptic transmission. J Pharmacol Exp Ther 1975;195:216–224.

12. Tomita T, Wright EB. A study of the crustacean axon repetitive response: the effect of membrane potential and resistance. J Cell Comp Physiol 1965;65:195–210.

DIFFERENTIAL EFFECTS OF PRESSURE ON THE MAMMALIAN CENTRAL NERVOUS SYSTEM

P. G. Kaufmann, P. B. Bennett, and J. C. Farmer, Jr.

Perhaps the most striking influence of high pressures on biological processes is expressed in alterations of function of excitable tissues, such as changes in muscle tension (1), or the excitability and conduction velocity in nerve fibers (2). In the intact animal, the underlying biophysical and biochemical alterations affect the basic elements of the nervous system—membranes, synapses and so forth—and translate into a chain of events that manifest themselves in symptoms called the high pressure neurological syndrome (HPNS) (3). In animals, this process has been observed to culminate in generalized seizures when pressures are sufficiently high.

Anatomically, the brain is known to be organized into regions subserving specific functions. Even though extensive reciprocal connections exist between regions serving different as well as similar functions, epileptic seizures are thought frequently to occur as a result of sudden pathological changes in a limited region, or focus, in the central nervous system (CNS), often in the cerebral cortex. A generalized seizure occurs when the abnormal activity spreads beyond the spatial limits of such a focus through various interconnecting pathways and invades large regions of the CNS. Focal origins have also been considered in the case of seizures resulting from elevated hydrostatic pressure. The aim of this paper is to examine the results of several experiments in the mammalian nervous system that illustrate the diversity of anatomical structures affected by high pressure, and to place in perspective the relative contribution of each in the total syndrome.

METHODS

All surgery was performed under pentobarbital anesthesia, except for the sectioning of spinal nerves L_2–L_6 in animals previously rendered painless by spinal transection at levels T_7–T_{13}. Animals were generally allowed to recover 3 days. Cerebellectomized rats recovered for 2 weeks.

Electroencephalograms (EEG) and cortical field potentials were obtained by means of 1-mm stainless steel screw electrodes inserted into the skull. Recording from and stimulation of deep structures took place through 0.25-mm stainless steel wires insulated to within 0.5-mm of the tip and implanted according to stereotactic coordinates. All animals were awake during compression.

Compression was carried out in a 208-L pressure vessel equipped with electrical penetrations, viewing ports, CO_2 scrubber, temperature sensors, gas lines, external heating, and facilities for sampling the chamber atmosphere. Oxygen was supplied by adding 0.3 bar of the gas to the existing chamber air. Compression continued at 1 bar/min to a maximum pressure of 120 bars, interrupted for 3–5 min at 10-bar intervals to gather data.

The Influence of Cerebellar Inhibition

Electroencephalographic recordings show that the typical spike-and-wave pattern of pressure-induced seizures can be recorded simultaneously from every structure so far examined: the cortex, hippocampus, red nucleus, cerebellum, reticular formation, and vestibular nuclei (4–6). We found the evidence of cerebellar participation particularly interesting because a number of authors have suggested that cerebellar inhibition is involved in terminating or modulating a variety of seizures (7,8). For example, cerebellar ablation aggravates cobalt (9) as well as hyperoxic seizures (10). Cerebellar dysfunction is also believed to contribute toward the vestibular symptoms of HPNS (11,12).

If high pressures were to totally eliminate such inhibitory cerebellar output, then cerebellar ablation should be without further effect on the threshold or severity of hyperbaric seizures. We therefore surgically ablated the cerebellum in six albino rats and tube-fed them for 2 weeks, so that most of their preoperative weight was recovered by the day of compression. When we compared these cerebellectomized animals with normal rats, we did find modest changes in the convulsion threshold pressure: normal animals seized at 99 bars, while cerebellectomized rats seized at 89 bars. However, the latter group sustained about twice the number of multiple seizures. The fact that HPNS convulsions were aggravated by cerebellar removal suggests that pressure does not completely abolish cerebellar inhibitory tone. Indeed, the relatively modest change in seizure threshold, although statistically significant ($P < 0.05$), and the similarity of other HPNS symptoms in both groups suggests that the fundamental processes resulting in HPNS proceed in substantially unaltered fashion despite extensive cerebellar lesions. On the other hand, one cannot conclude that loss of cerebellar inhibition does not contribute to the vestibular or paroxysmal symptoms of HPNS. It simply is not the only or even the most impor-

tant factor. Because pressure uniformly acts on the entire nervous system, normal neuronal functions are simultaneously disrupted throughout the CNS, until excitability reaches a critical level and generalized seizures ensue. Restoration of a normal cerebellum alone would not result in suppression of HPNS.

The Spinal Cord as a Minimal Convulsive Aggregate

Most studies on tissues in vitro require relatively high pressures (above 200 bars) to affect variables such as action potential amplitude and conduction velocity, or membrane resistance and capacitance. The question then arises as to the size of the neuronal pool necessary to bring about a maximal response, or seizures, at the lower pressures (100 bars) that are usually effective in intact mammals. One way this question can be addressed is to examine the progression of HPNS in limbs served by the distal portion of a transected spinal cord; thus, all influences from the higher centers are eliminated.

Long ago, Ebbecke (13) reported that high pressure continued to evoke spontaneous contractions in the hindlimbs of spinalized frogs, but this finding could not be verified in liquid-breathing spinal mice (14). We performed the experiment in rats breathing a helium-oxygen mixture. Twenty Wistar rats were implanted with EEG electrodes over the frontal cortex and allowed to recover. In 16 rats the spinal cord was transected at levels T_7—T_{13}; and 4 rats served as unoperated controls. After 3 days, spinal reflexes had recovered sufficiently so that clearly defined withdrawal responses were seen after one pinched the hind feet. In three of the spinalized animals, we sectioned spinal nerves L_2–L_6 after exciting the intervertebral foramina, thus totally denervating one hind limb on the day of compression. Compression took place with the animal suspended in a whole-body sling and all limbs hanging free. Needle electrodes for recording electromyographic (EMG) activity were placed in both hind limbs and one fore limb.

Symptoms of HPNS (tremors and myoclonic jerks) in the fore limbs of spinalized animals were indistinguishable from those seen in intact animals, becoming progressively more intense with increasing pressure. This pattern was also observed caudal to the lesion, but at a much lower intensity.

In all animals, increased EMG activity was usually evident at about 30 bars; mild fasciculations were observable at 50–75 bars, progressing to tremors and myoclonic jerks, and seizures occurred between 75 and 110 bars (Fig. 1A,B). On the other hand, limbs in which spinal nerves had been sectioned, remained flaccid throughout compression and showed no EMG activity (Fig. 1C). Activity profiles constructed by computing the area encompassed by EMG records at 10-bar intervals revealed fluctuations of intensity with increasing pressure, which suggests that the effects of pressure do not progress linearly throughout a given exposure. No evidence was seen that the threshold for pressure effects at the spinal level is different from that in the intact CNS or that there is a rostro-caudal progression along the neuraxis. The tonic-clonic convulsions of the anterior trunk and limbs, usually accompanied by spike-wave complexes in the cortical EEG, sometimes preceded and sometimes fol-
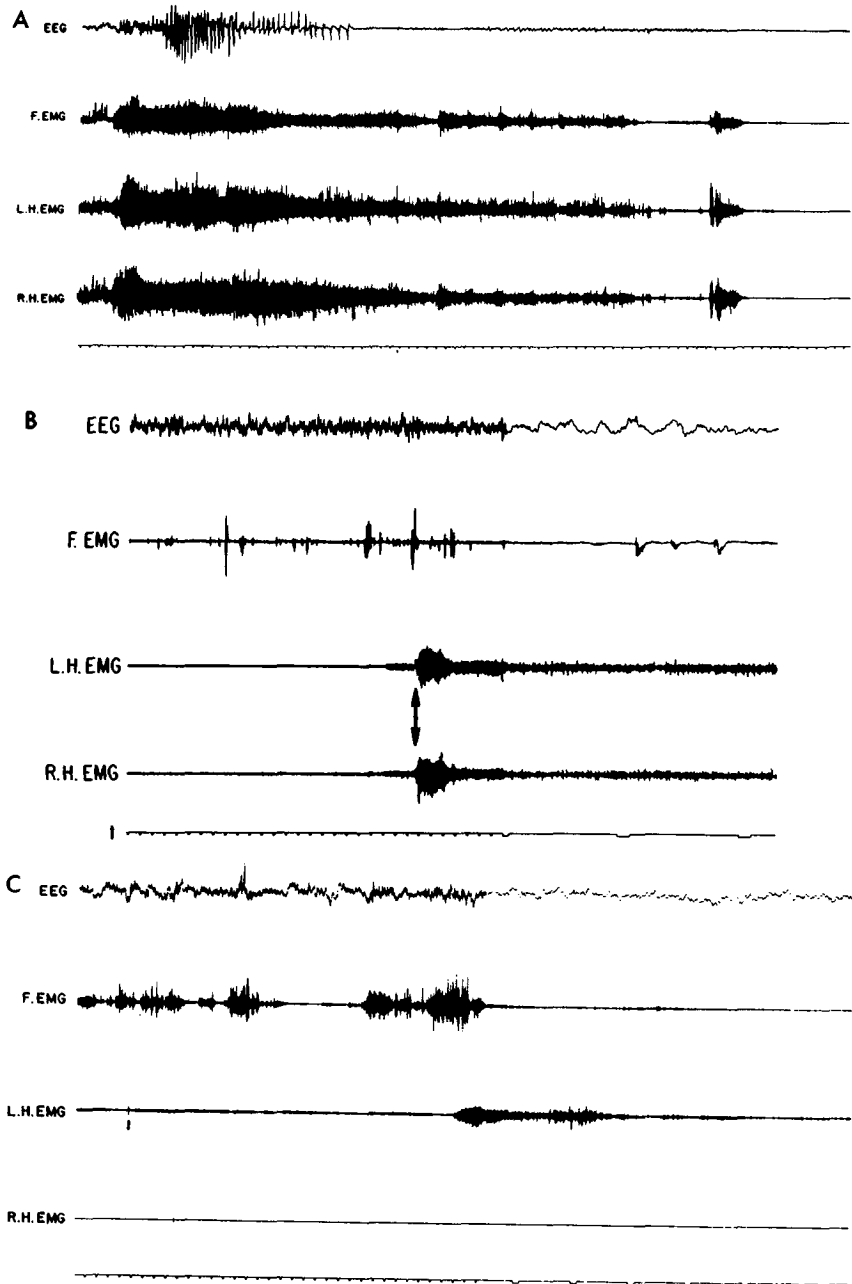
Fig. 1. Frontal cortex electroencephalograms (EEG) and electromyograms from one fore limb (F.EMG) and two hind limbs (L.H.EMG; R.H.EMG) of three different rats; t, timing marks, 1 s. A: at 118 bars, a tonic-clonic seizure was accompanied by spiking in the EEG and a sudden increase in amplitude of EMG's recorded from all limbs. B: a spinal seizure below transaction at T_{10} resulted in a similar, sudden burst of activity in hind limb EMG's (arrow) at 76 bars. Hind limbs were suddenly flexed, with all digits active and many fasciculations visible below the skin surface. The EEG remained normal, and no seizure was evident rostral to the transection. C: when spinal nerves L_2–L_6 were cut on the right side, R.H. EMG remained flat throughout compression and during the burst of L.H. EMG activity which accompanied a spinal seizure at 90 bars..

lowed spinal discharges (8 instances each). This contrasts with the simultaneous appearance of paroxysmal discharges at various sites in the brain. It is evident that the neuronal pool of the spinal cord is sufficiently large to independently sustain massive, synchronized discharges. The lowest level of transection in this group of animals was at T_{13}. Because the spinal cord in the adult rat terminates between segments L_4 and L_5 (15), only four or five segments of cord are sufficient to sustain hyperbaric seizures. The nerve-muscle system, on the other hand, has a much higher threshold and, lacking the circuitry for regenerative activity, does not show pressure-evoked discharges or contractions until 300–400 bars (16). These results are consistent with the premise that pressure affects a variety of neuronal aggregates. The expression, or the form of the dysfunction, however, depends on the local neuronal organization and on the modality served by the system in question.

Hyperbaric Pressure and Serial Processing in the CNS

We chose for this study the geniculo-striate pathway. Stainless steel electrodes were implanted in the optic chiasm (OC), lateral geniculate nucleus (LGN) of the thalamus, and the surface of the striate cortex (SCX) in 30 guinea pigs. The position of each electrode was functionally localized by recording its characteristic response to photic stimulation. After several days of recovery, short-latency evoked potentials (EP) were recorded in the LGN ($<$ 10 ms) and SCX ($<$ 50 ms) in response to weak electrical stimuli (10–100 μA, 0.02–0.05 ms duration) applied to the OC at 2-s intervals. Amplified, 32 response sequences were summed by means of a signal-averaging computer. Responses at pressures up to 100 bars He-O_2 in 10-bar increments were compared with responses at surface, at a variety of stimulus intensities. Interpretation of the presynaptic and postsynaptic components of the evoked potentials was based on published criteria (17,18). In the LGN, repetitive stimulation at high frequencies led to a reduction in amplitude of the postsynaptic component and complete synaptic block at about 150/s. In the visual cortex, electrical stimulation of the optic nerve yielded a series of surface-positive primary responses superimposed on a slower positive potential, followed by a longer surface-negative wave (Fig. 2). These deflections are numbered 2–6 in Fig. 3B, after the nomenclature of Chang and Kaada (19). The first wave is a very small wiggle at a latency of about 0.6 ms preceding wave 2 and is not numbered. Waves 2–6 have latent periods of 1.2, 2.3, 3.7, 5.0, and 6.1 ms, which correspond well with latencies in cats and monkeys (18). The first two waves followed optic nerve stimuli up to 100/s, the third was partially blocked, and all later deflections disappeared at stimulus rates of 40/s. After injecting a lethal dose of barbiturate, waves 1–3 survived long after the remaining cortical response vanished. We therefore concur with the interpretation that the first two surface-positive components are due to activity ascending in the optic radiation fibers, the third is mixed in character, and subsequent waves arise largely from intracortical postsynaptic activity (20). Deflections arising after wave 6 are not usually recorded, but become enhanced following strychninization of the cortex (19).
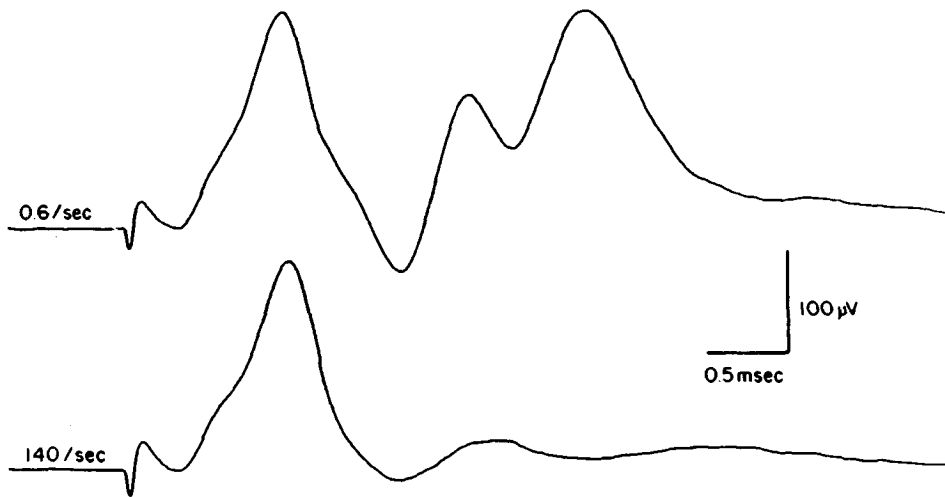
Fig. 2. Typical evoked responses recorded from the LGN following optic nerve stimulation at 0.6/s and 140/s. In the upper trace, the two later peaks correspond to postsynaptic responses to inputs from two fiber groups with different conduction velocities. Synaptic block occurs at the higher stimulus rate, and only the compound action potential of the optic tract remains.

Field potentials recorded through macroelectrodes are composed of polarizing as well as depolarizing postsynaptic potentials distributed on soma, dendrites, and axons, as well as action potentials. The arrival of impulses over pathways with different conduction velocities further complicates the time course of the currents from these various sources, and interpretation of primary evoked responses must necessarily be restricted.

Exposure to pressure resulted in virtually no changes in the latency of either the presynaptic or postsynaptic components of field potentials recorded from the geniculate (Fig. 3A). Variations in latency correlated nearly perfectly with small excursions ($\pm$ 1.0°C) of body temperature during the experiments. Changes in amplitude were also usually correlated with temperature fluctuations, but occasionally increased pressure resulted in a small reduction of the postsynaptic component (r) not related to temperature changes. This can be interpreted as an enhancement of transmitter release from presynaptic terminals and results in partial synaptic block as seen during moderately high rates of stimulation. However, because experiments were generally performed using submaximal stimulus intensities, we should have seen an amplitude fascilitation before synaptic block appeared. It is therefore more likely that the decrease, with pressure, of postsynaptic evoked potential amplitude is due to a suppression of transmitter release at excitatory synapses in the LGN, as has also been shown in the rat diaphragm (21), the crustacean neuromuscular junction (22), and the squid stellate ganglion (23).

Although pressure caused only small changes in the field potentials recorded from the LGN, its influence on cortical electrical activity was dramatic.

Latency changes were very similar to those seen at the geniculate and corre-
lated with temperature. The amplitudes of the postsynaptic cortical response,
however, increased as early as 30 bars, and the large surface-negative wave
attained values of up to 300% with increasing pressure, until a seizure ensued.
In Fig. 3B, this occurred soon after the recording at 60 bars. After a period of
post-ictal depression, the process of amplitude augmentation was again re-
peated if pressure continued to increase. By varying the stimulus intensity and
duration, it was possible to compare response thresholds at surface and at 50
bars pressure. Again, the effects of pressure on field potentials recorded from
the lateral geniculate were modest. At the cortex, however, amplitude changes
were a nonlinear function of the stimulus intensity, becoming greater for
strong than for weak stimuli and suggesting a change in excitability of the cor-
tical elements.

Even a cursory examination of the cortical EP (Fig. 3B) reveals that in
addition to an augmentation of the cortical EP amplitude, the number of spikes
visible on the large surface-negative wave has increased substantially. Because
we found no evidence of repetitive firing in the lateral geniculate, these spikes
must arise from repetitive firing of intracortical axons. Repetitive impulse gen-
eration already has been demonstrated in crayfish claw nerves under pressure
(24). In cortical penicillin epileptogenic foci, repetitive spike generation might
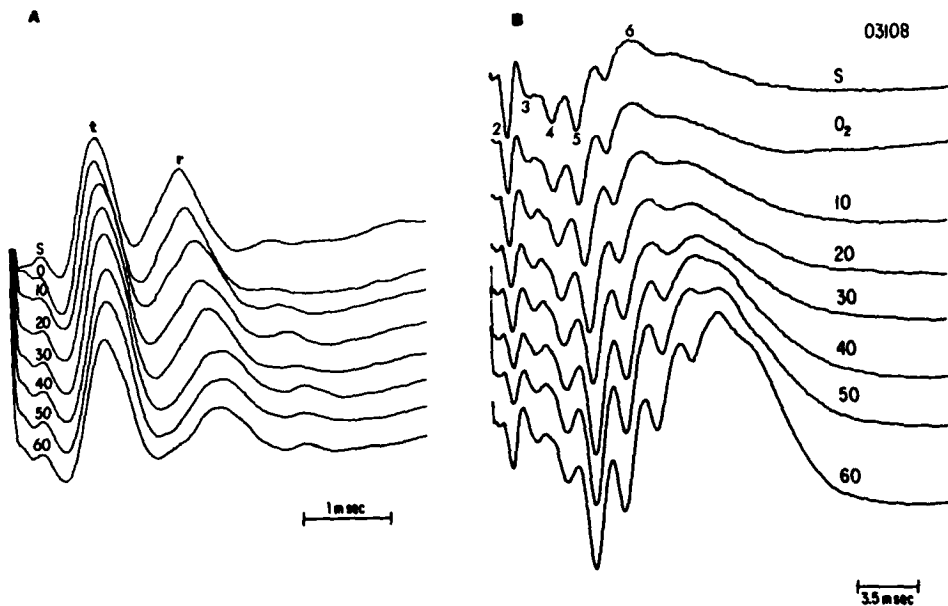
Fig. 3. A: Increasing pressure from surface(s) to 60 bars results in a reduction of the postsynaptic, radia-
tion response (r) in the LGN, but no change in the input through optic tract (t) fibers. B: In the striate
cortex, amplitudes of waves 5 and 6, representing activity in intracortical elements, become substantially
augmented. Especially prominent is the emergence of repetitive spikes following wave 5. Latency changes
are due to small fluctuations in body temperature. Constant current optic nerve stimuli at surface were 0.02
ms duration, 70 μA, and 50 μA after raising oxygen content to 40% (O_2) and all subsequent traces.   Each
trace represents an average of 32 consecutive responses. Negativity upwards.

be mediated by intracortical increases in extracellular K$^+$ (25). Decreases in extracellular Ca^{2+} have also been noted during seizures (26). Because alterations in calcium channels have been shown to occur at as little as 69 bars (27), changes in the extracellular ionic environment may play a substantial role in generation of afterdischarges at high hydrostatic pressures.

Also of great interest in regard to the facilitation we observe under pressure is the fact that local application of strychnine on the cortical surface results in a tremendous enhancement of the later components of the field potential (19). Similar augmentation is also seen after medial thalamic (28) and reticular (29) stimulation and after natural arousal (18). However, strychininization appears to be unique in producing the additional surface-negative spikes that are the most prominent feature of hyperbaric EP facilitation. Strychnine greatly enhances the amplitude of *wave 5*, which is also the component most affected in our studies. Strychnine is well known to block inhibitory processes in the CNS (30,31,32); therefore, we infer that one of the most significant effects of pressure in the mammalian CNS is a reduction of inhibitory synaptic transmission.

The question remains as to why a similar augmentation is not seen at the thalamic level. The difference cannot be attributed to a lack of inhibitory synapses, because inhibitory postsynaptic potentials can be recorded in the LGN (33). It is highly unlikely that pressure has opposite effects on identical structures at two different locations. Rather, the dissimilar effects may be due to characteristics of the local neuronal circuitry, such as regional distribution of specific neurotransmitter; cell types; and the quantity or arrangement of recurrent excitatory and inhibitory collaterals.

It is evident that hydrostatic pressure exerts diverse effects on different portions of the mammalian CNS. It is likely that synaptic processes, such as the time course of transmitter release at presynaptic terminals, their action at the subsynaptic membrane, and their inactivation or re-uptake play a prominent role.

Acknowledgments

References

1. Cattell M, Edwards DJ. Conditions modifying the influence of hydrostatic pressure on striated muscle, with special reference to the role of viscosity changes. J Cell Comp Physiol 1932;1:11–36.
2. Grundfest H. Effects of hydrostatic pressures on the excitability, the recovery, and the potential sequence of frog nerve. Cold Spring Harbor Symp Quant Biol 1936;4:179–187.
3. Brauer RW. Seeking man's depth level. Ocean Industry 1968;3:28–33.
4. Cromer JA, Hunter WL Jr, Kaufmann PG. Effect of compression rate on HPNS convulsion threshold in the euthermic rat. Undersea Biomed Res 1977;4:403–408.
5. Kaufmann PG, Bennett PB, Farmer JC Jr. Cerebellar and cerebral electroencephalogram during the high pressure nervous syndrome (HPNS) in rats. Undersea Biomed Res 1977;4:391–402.

6. Kaufmann PG, Finley CC, Bennett PB, Farmer JC Jr. Spinal cord seizures elicited by higher pressures of helium. Electroencephalogr Clin Neurophysiol 1979;47:31–40.

7. Cooke PM, Snider RS. Some cerebellar influences on electrically induced cerebral seizures. Epilepsia 1955;4:19–28.

8. Cooper IS, Amin I, Gilman S, Waltz JM. The effect of stimulation of cerebellar cortex on epilepsy in man. In: Cooper IS, Kirkland M, Snider RS, eds. The cerebellum, epilepsy, and behavior. New York: Plenum Press, 1974:119–171.

9. Dow RS, Fernandez-Guardiola A, Manni E. The influence of the cerebellum on experimental epilepsy. Electroencephalogr Clin Neurophysiol 1962;14:383–398.

10. Rucci FS, Giretti ML, LaRocca M. Cerebellum and hyperbaric oxygen. Electroencephalogr Clin Neurophysiol 1968;25:359–371.

11. Farmer JC Jr, Thomas WG, Smith RW, Bennett PB. Vestibular function during HPNS. Undersea Biomed Res 1974;1:A11.

12. Gauthier GM. Alterations of the human vestibulo-ocular reflex in a simulated dive at 62 ATA. Undersea Biomed Res 1976;3:103–112.

13. Ebbecke U. Über das Verhalten des Zentralnervensystems (Rückenmarkfrosch) unter der Einwirkung hoher Drucke. Pfluegers Arch Gesamte Physiol 1936;237:785–789.

14. Kylstra JA, Nantz R, Crowe J, Wagner W, Saltzman HA. Hydraulic compression of mice to 166 atmospheres. Science 1967;158:793–794.

15. Greene EC. Anatomy of the rat. Philadelphia: American Philosophical Society, 1935.

16. Cattell M. The physiological effects of pressure. Biol Rev 1936;11:441–476.

17. Bishop PO, McLeod JG. Nature of potentials associated with synaptic transmission in the lateral geniculate of the cat. J Neurophysiol 1954;17:387–414.

18. Creutzfeldt OD, Kuhnt U. Electrophysiology and topographical distribution of visual evoked potentials in animals. In: Jung R, ed. Handbook of sensory physiology. Vol. VII/3. Central processing of visual information, Part B. New York: Springer Verlag, 1973:595–646.

19. Chang HT, Kaada B. An analysis of primary response of visual cortex to optic nerve stimulation in cats. J Neurophysiol 1950;13:305–318.

20. Widen L, Ajmone-Marsan C. Unitary analysis of the response elicited in the visual cortex of cat. Arch Ital Biol 1960;98:248–274.

21. Kendig JJ, Cohen EN. Neuromuscular function at hyperbaric pressures: pressure-anesthetic interations. Am J Physiol 1976;230:1244–1249.

22. Campenot RB. The effects of high hydrostatic pressure on transmission at the crustacean neuromuscular junction. Comp Biochem Physiol 1975;52B:133–140.

23. Henderson JV. Squid giant synapse at high pressure. Fed Proc 1976;35:237.

24. Kendig JJ, Schneider TM, Cohen EN. Repetitive impulses in nerves: a possible basis for HPNS. Undersea Biomed Res 1978;5(Suppl):49.

25. Gutnick MJ, Prince DA. Thalamocortical relay neurons: antidromic invasion of spikes from a cortical epileptogenic focus. Science 1972;176:424–426.

26. Heineman U, Lux HD, Gutnick MJ. Extracellular free calcium and potassium during paroxysmal activity in the cerebral cortex of the cat. Exp Brain Res 1977;27:237–243.

27. Otter T, Salmon ED. Hydrostatic pressure reversibly blocks membrane control of ciliary motility in Paramecium. Science 1979;206:358–360.

28. Landau WM, Bishop GH, Clare MH. The interactions of several varieties of evoked response in visual and association cortex of the cat. Electroencphalogr Clin Neurophysiol 1961;13:43–53.

29. Creutzfeldt OD, Watanake S, Lux HD. Relations between EEG-phenomena and potentials of single cortical cells. I. Evoked responses after thalamic and epicortical stimulation. Electroencephalogr Clin Neurophysiol 1966;20:1–18.

30. Bradley K, Easton DM, Eccles JC. An investigation of primary or direct inhibition. J. Physiol (Lond) 1953;122:474–488.

31. Curtis DR. Pharmacological investigations upon inhibition of spinal neurons. J Physiol (Lond) 1959;145:175–192.

32. Stephanic C, Jasper H. Strychnine reversal of inhibitory potentials in pyramidal tract neurons. Int J Neuropharmacol 1965;4:125–138.

33. Fuster JM, Creutzfeldt OD, Straschill M. Intracellular recording of neuronal activity in the visual system. Z Vgl Physiol 1965;49:605–622.

SOMATIC EVOKED POTENTIALS AND REFLEXES IN MONKEY DURING SATURATION DIVES IN DRY CHAMBER

M. Hugon, L. Fagni, J. C. Rostain, and K. Seki

Both man and monkey when placed under high pressure produced by helium develop difficulties referred to as the high pressure nervous syndrome (HPNS) (1–4). Frequency components of the electroencephalogram (EEG), primarily from anterior areas, undergo distinctive slowing; theta rhythm begins to develop. High-frequency tremor is seen in active muscles (8–13 Hz). Such changes appear at and above 20 to 30 ATA. Above 60 ATA and depending on the compression profile, ictal-like EEG signs, spasms, and clonies develop in the monkey, and, finally, may result in epileptic seizures.

To further extend this description, we have studied the effects of high pressure on cortical somatic evoked potentials (SEP), spinal reflexes, and nerve-muscle "direct" responses. Changes in latency and amplitude of SEP in reflexes and SEP recovery cycles are evidence of neurophysiological defects. Pressure per se and rate of compression are believed to be environmental causes for such defects. The effects of nitrogen will be discussed.

MATERIAL AND METHODS

Material

Six monkeys were studied in He-O_2 or He-O_2-N_2 at the "Centre Expérimental Hyperbare" (CEH-COMEX) under the direction of B. Gardette and J. C. Rostain. Table I shows the main characteristics of "RESO" dives (*R Dives*). The animals weighed 6–8 kg. Gas, humidity, and temperature were

TABLE I

Characteristics of RESO Dives (R Dives)

Dives	Initial Rate of Compression	Final Rate of Compression	Saturation pressure	Total Duration for Saturation Pressure	Duration of Interspersed Stages	Duration at Saturation Stage	PI_{O_2} at Saturation	PI_{N_2} at Saturation
	m/h	m/h	msw	h	h/msw	h	bars	bars
	1	2	3	4	5	6	7	8
R-I	800	240	600	2	0.25 × 100	6	0.4	4.8
R-II	1200	180	600	2	0.25 × 100	6	0.4	4.8
R-III	1200	180	700	2	0.25 × 100	2	0.4	4.8
R-IV	360	60	600	9	0.66 × 100	7	0.4	0.8
R-V	120	15	800	32	0.66 × 100	6	0.4	0.8
R-VI	120	15	800	32	0.66 × 100	6	0.4	4.5

Profiles for monkey R-Dives:

1, Mean rate of compression onto 200 msw; 2, mean rate of compression during the last 50 msw; 3, saturation pressure; 4, total duration for access to saturation pressure (stages included); 5, duration of (interspersed) stages and their pressure (× 100 means every 100 msw); 6, duration at saturation stage; 7, partial pressure of oxygen at saturation pressure; 8, partial pressure of nitrogen at saturation pressure.

monitored and maintained at about 50% and 31 to 33°C, respectively. Food, water, and general care were provided by specific devices.

Methods

Chronically implanted gross electrodes were used for a) stimulation of tibialis posterior and sural nerves; b) electromyographic recording of soleus and tibialis anterior muscles; c) recording of SEP and EEG in motor-sensory areas, contralateral and ipsilateral to nerve stimulation; d) recording current EEG in frontal, temporal, and occipital areas; and finally, e) electro-oculographic and electromyographic recording of the splenius. To control the state of alertness of the animals, we continuously monitored EEG signals.

Direct motor responses (M) and monosynaptic reflex (Hoffmann responses [H]) in the soleus were elicited by electrical pulses of 1 ms of duration delivered every 5 s. Each of these pulses also evokes SEP. The latencies, durations, shapes, and amplitudes of M, H responses, and SEP were studied in relation to the intensity of the stimulus. Polysynaptic reflex in tibialis anterior and SEP, both induced by sural nerve stimulation, were studied in a similar way. Recovery cycle of excitability was studied for the H reflex and the earliest wave of the SEP, through the double-stimulus technique (5). Mean values (and standard duration for reflexes and latencies) were calculated from 10 or 20 readings in each experimental subset; each subset consisted of a specific combination of breathing mixture, stimulus intensity, and interstimulus delay at different pressures (including pre- and postexperimental surface readings). All results were obtained from awake animals.

This paper is a preliminary presentation of the main data.

RESULTS

Motor Responses

Single stimulation responses. Latencies and durations of M and H responses were seen not to change under pressure, which confirms earlier published data (6). Comparison of stimulus and amplitudes of M responses failed to disclose any variation in the excitability of the myelinated motor fibers during either He-O_2 or He-O_2-N_2 exposures. We believe this conclusion is also true for large sensory fibers. Under pressure, H responses are only slightly facilitated, if at all, and polysynaptic reflexes, as a rule, are facilitated. Startle-like responses may develop under pressure, after sciatic nerve stimulus (and auditory stimulus), with or without nitrogen.

Double stimulation responses. In Papiola experiments (*P Dives*) we found that recovery cycles develop weaker and shorter phases of early inhibition (6). Similar recovery curves have developed in *R-V* and *R-VI* dives, which can be

called "slow compression dives" (Table I). The use of nitrogen correlates with general depression of the recovery. In contrast, early inhibition in fast compression *R Dives* is total at 700 msw (Fig. 1, *middle*), as in normal pressure (Fig. 1, *upper*), but it is shorter. Subsequently, a strong and durable rebound of excitability (100–300 ms) develops, which subsides without any late phase of depression. Such normal late inhibition can be seen Fig. 1, *upper* and *lower* curves, before and near the end of the dive, respectively. Such modifications of the H recovery curves develop with or without the addition of nitrogen. However, fine tremor is reduced or absent in nitrogen dives.

Somatic Evoked Potentials (SEP)

Single stimulus responses. See Fig. 2*A,B*. Tibial posterior nerve stimulation evoked central SEP (contralateral and partly ipsilateral). Large sural SEP were also recorded at the same place, mainly because of the lack of selectivity of our gross electrodes. Taking advantage of this, we had the possibility to study both proprioceptive and exteroceptive SEP at the same point. The SEP shape varied somewhat with the animal, because of variations in local morphology of the cortex. Yet positive (P) and negative (N) waves can be consistently recognized on every recording: P15 (simple or double), N30, N60, P80–100, according to the mean latency measured at the wave maxima (milliseconds). Early waves (P15 and N30, N60) are present under pressure, with some changes in latencies and amplitudes. Above 40 to 50 ATA, the amplitudes of the waves increased dramatically (see Fig. 2*A* and *B*), apparently as precursor, and, more clearly, as a consequence of seizures. P15 can increase by twofold or threefold compared to that at 1 ATA, and the facilitation of N30 can be larger than the P15 facilitation. Later waves demonstrate inconstant variations. After return from pressure, initial values are found again, more or less (Fig. 2*A* and *B, lower traces*). Facilitation of early waves in sciatic SEP were not due to some increase of the initial incoming volley because the tibial posterior nerve stimulus always was adjusted to the M response threshold. This criterion was satisfied to provide constant recruitment of motor fibers in the hope of inducing similarly constant sensory fiber recruitment in the same tibial nerve. Sural SEP were set just at their maximal value for any readings. The early wave facilitation in the *R-VI Dive* is larger than in *R-V;* this may be due to the use of nitrogen. Interestingly, in this experiment there was no increase of sural SEP in contrast to the large facilitation of the proprioceptive SEP.

Surprisingly, there was no variation under pressure in the latencies (Fig. 3*C*) for fast dives. The SEP curve latencies in the *R-VI Dive* demonstrate some increase in latency, as seen in the *P Dives* (personal data from ref. 6).

Double stimulus responses. (See Fig. 3*A*) The amplitude of the P15 wave elicited after the first wave depends on the interstimulus delay (i.e., two equal stimuli given at the same place on the tibial nerve). The curves in Fig. 3*A* show a) a standard P15 recovery curve at 1 ATA, resulting from pooled data from three monkeys in normal pressure (*triangles*); b) a similar recovery curve
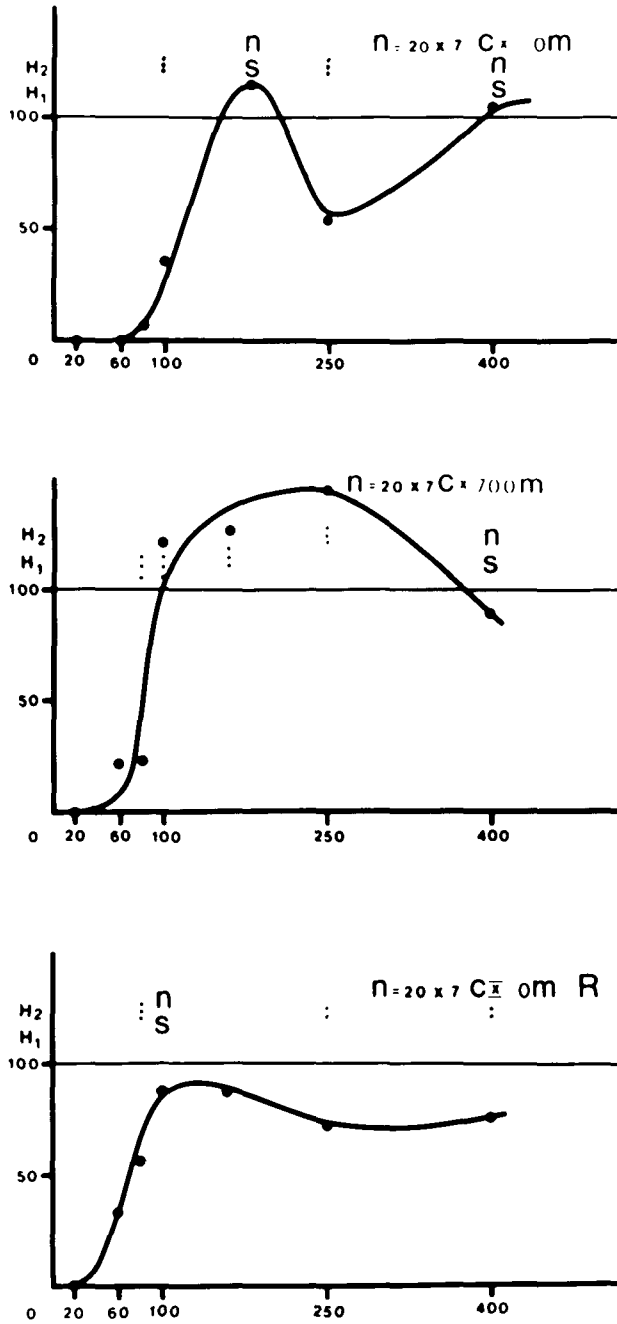
Fig. 1.   Modifications of the Hoffmann (H) recovery curve under high pressure.   A H₂ reflex is inhibited, then facilitated, and then inhibited after a preceding H₁ reflex, depending on the interstimulus delay (in abscissa: milliseconds). Data are for one monkey.   *Upper graph,* recovery cycle in normal air;   *middle graph,* recovery cycle at 700 msw (seawater equivalent; dry chamber);   *lower graph,* recovery cycle, shortly after return *at 0 msw.*   *Each point:* 20 values, stars: signification (0.01 and 0.001); NS, not significant. The "late depression" gives way to a strong facilitation under pressure. Details in the text.
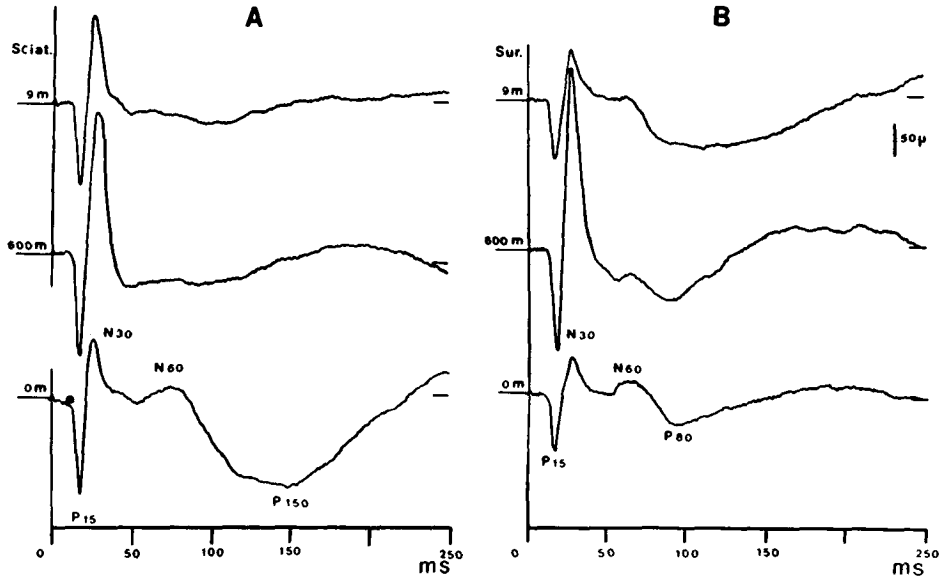
Fig. 2. Somatic evoked potentials are facilitated after fast compression.   *A*, SEP after tibial posterior nerve stimulation (one shock; 1-ms duration at threshold for alpha motor response in soleus);   *B*, SEP after sural nerve stimulation (nonpainful, but maximal for SEP in each situation).   *Upper traces,* SEP at 9 msw (air × 400 mb O_2);   *middle traces,* SEP at 600 msw (seawater equivalent, dry chamber; He-O_2-N_2: 4.8 bars);   *lower traces,* SEP after return to 0 msw (air).   Each trace is the average of 20 responses. Positive downward. Data are for one awake monkey. Fast compression (600 msw in 2 h). Fast compression resulted in strong SEP facilitation.

for *R-V Dive* at 81 ATA, He-O_2, 32 h to reach saturation level (*squares*); c) recovery curve for *R-VI Dive,* the same as *R-V,* but 4.5 bars of nitrogen were added (*filled circles*); d) recovery curve for *R-VI* animal after a 6-h sojourn at 81 ATA (*open circles*).

The *R-VI Dive* curves demonstrate that nitrogen use and sojourn at constant pressure both improve the recovery curve.

DISCUSSION

Briefly, compression and then constant pressure resulted in modifications of latency and amplitude of SEP, and in recovery cycles. Fast compression elicited at constant latency SEP facilitation, a distinctive defect in SEP recovery curve, and late facilitation in the H recovery curve. Slow compression tended to give increases in SEP latencies, depressed SEP recovery curves, and depressed H recovery curves. Nitrogen reduced tremor, facilitated SEP, improved SEP recovery, and depressed the H recovery curve after slow procedures.

Defects in H recovery curves after compression are provisionally explained in this way: Under normal pressure, H discharge elicits early then late Renshaw cell (RC) activity in the spinal cord (7). The late RC activity and the
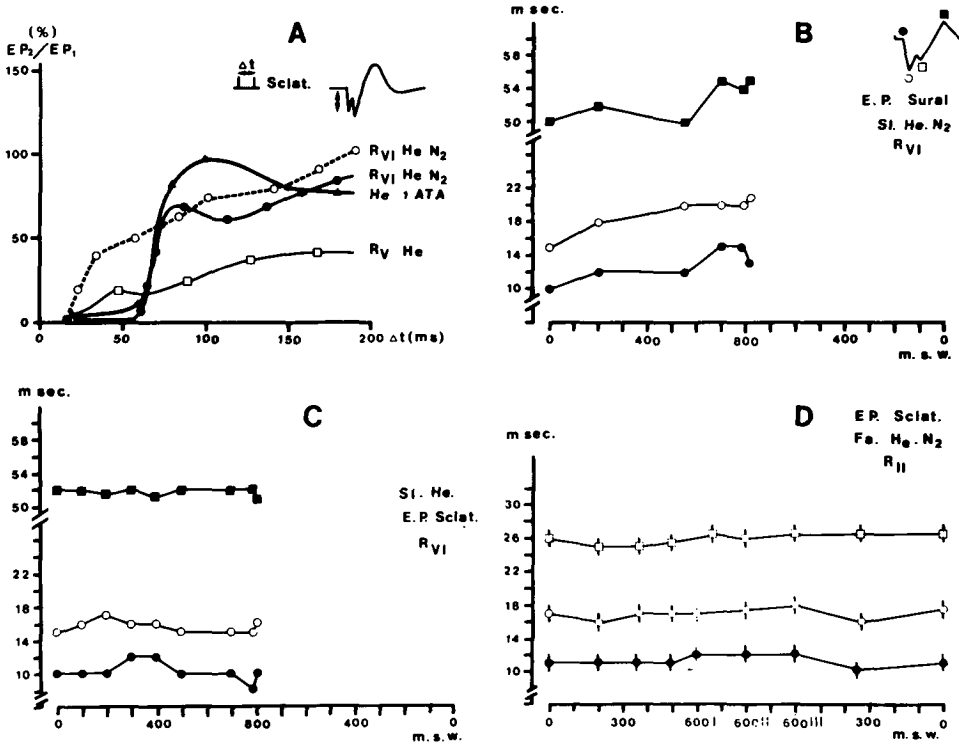
Fig. 3. Somatic evoked potentials under pressure: recovery cycles and latencies.   Triangles, recovery cycle for P15 wave at ground level (He = 1 ATA);   squares, id. at 81 ATA (He-O₂ mixture; R-V Dive);   filled circles, id. arriving at 81 ATA with HE-O₂-N₂ mixture, R-VI Dive;   empty circles, the same after 6 h at 81 ATA.   Slow compression depressed the recovery cycle; nitrogen improved it. Sojourn at constant pressure can induce improvement (acclimatization).

late inhibition in recovery cycle develop in parallel. Atropine, when administered intravenously suppresses the late RC activity (7). When administered to the monkey, atropine (3 mg/kg, i.v.) also suppresses the late depression of H reflexes in the recovery cycle (8). Atropine is known as a muscarinic receptor blocker. We conclude that late inhibition in H recovery is due to a late RC activity that depends upon acetylcholine release and fixation of muscarinic receptors. Acetylcholine release and its nicotinic efficiency at neuromuscular junctions appear to be normal, because there is no distinctive impairment of the gross M responses under pressure (9,10). Early inhibition in the H recovery cycle is thought to be due to a cholinergic nicotinic effect of the recurrent terminals from the same motoneurons (9). This inhibition appears to be normal at 700 msw (Fig. 1, middle), another indication of normal acetylcholine release after a fast dive. Finally, the absence of late inhibition would be due to a defect in the postsynaptic efficiency of acetylcholine on muscarinic sites rather than a defect in acetylcholine production. Such a conclusion suggests some spatial modification of the receptor under the helium compression strain; this

modification corresponds to that in some models for drug effects (11,12). Helium per se could also play a role in such "compression block." These interpretations are not exclusive of others that are related to some membrane structure changes (13) or to some modifications of the cellular events after the receptor activation (14).

Comparing the effects of "fast" and "slow" compression, we must consider different mechanisms to explain depressed recovery cycles in slow compression dives (6,9). The absence of the so-called antimuscarinic compression block after slow compression could be due to some cellular or multicellular regulatory processes. Mandell (15) proposed a number of cellular regulatory responses after a sustained administration of drugs. Slow compression could allow sufficient time for late compensatory responses to develop.

Obviously, compensation for modifications in muscarinic receptors does not preclude parallel development of pressure changes at other sites. It is worth noting that nicotinic receptors can also be modified by helium pressure, which alters the sensitivity of this receptor to drugs at neuromuscular junctions (16). A nicotinic receptor alteration could result in reduction of the early inhibition in the H recovery curve after slow compression under high pressure (6,9).

At the cortical level, scopolamine and atropine, both muscarinic blockers, give a strong facilitation of SEP (ref. 18 and personal data). Similarly, fast compression results in SEP facilitation. This similarity is an indication of a central antimuscarinic effect of compression. Cholinergic corticopetal activating pathways are known (18). Impairment of their activity results in EEG slowing and synchronizing effects. Synchronization can be a facilitating factor for P15 and N30 SEP waves, which are premises of seizures (19). The facilitation of the N30 wave is reminiscent of the "spike wave" depicted by Chauvel et al. (19) in alumina cream epilepsy, an experimental model for reflex epilepsy. The development under pressure of startle-like responses to brisk input could also be explained as some "transcortical" response, a sign of preseizure state due to fast compression, such as that to anti-muscarinic drugs (20).

At its onset, the latency of the P15 wave mainly depends upon the delays along the ascending lemniscal pathway, provided that the sensory input is large enough. This applies in our experiments and constitutes evidence of an absence of changes in conduction velocity along central fibers and of an increase in transmission delays. These conclusions are in harmony with the interpretations of the constancy of the M and H reflex response latencies under pressure (9) and with previous observations on the constancy of the latencies of evoked potentials (21). Increases in latencies after slow compression require opposite conclusions perhaps in relation to delayed cellular response to helium pressure, as suggested previously.

The present comparison between "fast" and "slow" compression effects is by no means a new one (4). On clinical grounds slow compression is believed to be safer, as suggested by Chouteau for *P Dives*. Similar conclusions are drawn from human dives (4). Nevertheless, it is clear that slow compression, if it reaches high pressure, is far from innocuous. As an anti-pressure-

strain procedure the use of nitrogen is of equivocal benefits: tremor is reduced and SEP recovery cycle is improved, but H recovery cycles still display tremendous changes after H_2-O_2-N_2 fast dives; in addition, the SEP shows large increases and the spontaneous EEG displays anomalies (4). One questions whether nitrogen corrects for pressure alterations at the sites of the alterations without causing deleterious side effects at different cellular sites.

Acknowledgment

References

1. Brauer RW, Dimov S, Fructus X, Gosset A, Naquet R. Syndrome neurologique et électrologique des hautes pressions. Rev Neurol 1969;121:264–265.
2. Bennett PB, Towse EJ. The high pressure nervous syndrome during a simulated oxygen-helium dive to 1500 feet. Electroencephalogr Clin Neurophysiol 1971;31:383–393.
3. Brauer RW. The high pressure nervous syndrome: animals. In: Bennett PB, Elliott DH, eds. The physiology and medicine of diving and compressed air work. Baillière Tindall, 1975:231–247.
4. Rostain JC. Le syndrome nerveux des hautes pressions chez l'Homme et le Singe Papio papio. Thèse Sciences, Université d'Aix-Marseille I, 1980:195 + XXVII.
5. Roll JP, Bonnet M, Hugon M. Comparative study of proprioceptive reflexes in man and baboon (P.papio). Proc 3rd Conf. exper. Med. Surg. Primates, Lyon, Med. Primatology. 1972:305–314.
6. Bonnet M, Chouteau J, Hugon M, Imbert G, Roll JP. Activités motrices réflexe et spontanée chez le Singe sous Heliox (99 ATA). In: Hesser CM, Linnarsson D, eds. Swedish Journal Defence Medicine. First annual scientific meeting of the European Undersea Biomedical Society, 1973;9:314–317.
7. Curtis DR, Ryall RW. The synaptic excitation of Renshaw cells. Exp Brain Res 1966;2:81–96.
8. Hugon M, Fagni L, Rostain JC. Observations de physiologie hyperbare chez les Primates. In: Dussardier M, ed. J Physiol (Paris). Compte rendu de la réunion de Lyon de l'Association des Physiologistes. Masson, Paris. 1980. A paraître.
9. Roll JP, Lacour M, Hugon M, Bonnet M. Spinal reflex activity in man under hyperbaric heliox conditions (31 and 62 ATA). In: Shilling CW, Beckett MW, eds. Underwater physiology VI. Proceedings of the sixth symposium on underwater physiology. Bethesda, MD: Federation of American Societies for Experimental Biology 1978:21–28.
10. Hugon M, Seki K. Preliminary report on an experimental human dive at 31 ATA, heliox. SEA-DRAGON IV. 1980, 16p.
11. Akers TK, Carlson LC. The changes in smooth muscle receptor coupling of acetylcholine and norepinéphrine at high pressure. In: Lambertsen CJ, ed. Underwater physiology V. Proceedings of the fifth symposium on underwater physiology. Bethesda, MD: Federation of American Societies for Experimental Biology, 1976:587–593.
12. Athey, GR, Akers TK. Analysis of frog neuromuscular function at hyperbaric pressures. Undersea Biomed Res 1978;5:199–208.
13. Finch ED, Kiesow LA. Pressure, anesthetics, and membrane structure: a spin-probe study. Undersea Biomed Res 1979;6:41–45.
14. Fish E, Shankaran R, Hsia JC. High pressure neurological syndrome: antagonistic effects of helium pressure and anesthetics on the dopamine sensitive cyclic AMP response. Undersea Biomed Res 1979;6:189–196.
15. Mandell AJ. Seven neurons of psychopharmacology: adaptative regulation in biogenic amine neurons. In: Haber B, Aprison MH, eds. Neuropharmacology and behavior. New York: Plenum Press, 1978:175–190.

16. Friess SL, Durant RC, Hudak WV, Boyer RD. Effects of moderate pressure He-O$_2$ saturation and response modifiers on neuromuscular function. Undersea Biomed Res 1975; 2:35–41.
17. Marczynski TJ. Invited discussion: post-reinforcement synchronization and the cholinergic system. Fed Proc 1969;28:132–134.
18. Karczmar AG, Dun JD. Cholinergic synapses: physiological, pharmacological, and behavioral considerations. In: Lipton MA, Di Mascio A, Killam KF, eds. Psychopharmacology: a generation of progress. New York: Raven Press, 1978:293–305.
19. Chauvel P, Louvel J, Lamarche M. Transcortical reflexes and focal motor epilepsy. Electroencephalogr Clin Neurophysiol 1978;45:309–318.
20. Tan U, Senyuva F, Marangoz C. Electrocorticographic effects of topically applied scopolamine. Epilepsia 1978;19:223–232.
21. Bennett PB. The effects of high pressures of inert gases on auditory evoked potentials in cat cortex and reticular formation. Electroencephalogr Clin Neurophysiol 1964;17:388–397.

THE HPNS AS A COMPOSITE ENTITY—
CONSEQUENCES OF AN ANALYSIS OF THE
CONVULSION STAGE

R. W. Brauer, W. M. Mansfield, Jr., R. W. Beaver, and H. W. Gillen

The term high pressure neurological syndrome (HPNS) was introduced to designate a clinical entity associated with the exposure of man and of experimental animals to high pressures in helium-oxygen atmospheres; it is characterized by a regular progression of symptoms of increasing severity, culminating, in the animal experiments, in convulsions. While as a clinical designation this term retains its usefulness, evidence is growing to suggest that in fact the clinical progression is the result of complex events and very likely comprises more than one entity.

As early as 1974, we called attention to the fact that the effect of inert gas anesthetics on the coarse tremor stage of the HPNS is less pronounced than on the convulsion stage (1). Since then, both with respect to the two components of the convulsion stage and with respect to several other components of the HPNS complex, evidence has accumulated to show substantial, and at times, qualitative, differences in the manner in which they severally are affected by various drugs, or by changes in compression rate (2,3). Evidence from radioautographic (4) (to be discussed later in this paper) and neurosurgical (ref. 5 and Table 1) experiments is providing support for the view that very substantial differences exist between the neuroanatomical substratum involved in the different components of the HPNS.

ALTERNATIVE APPROACHES

Such a situation may be thought of as arising in two basically different ways: it may reflect a single chain of development characterized by a progres-

TABLE I

HPNS Seizures in Spinal CD-1 Mice

Pressure—atm	Event Proximal to Transsection	Event Distal to Transsection
40		Activation, evidence of motor activity—90%

76.4	Type I seizure threshold pressure seemingly not affected by transsection	Seizure Activity:
		at 3d: motor 10%
		          EMG 15%
		at 15d: motor 0%
		          EMG 10%
		NB—all caudal seizures associated with seizures cephalad to transsect, either simultaneously or (in 20%) with 1 to 2″ delay.

108	Mean type II seizure threshold pressure, seemingly unaffected by transsection	Seizure Activity:
		at 3d: motor 30%
		          EMG 85%
		at 15d: motor 0%
		          EMG 70%
		All seizures of cephalad segments in caudal ones, with 1 to 2″ delay. Seizures confined to distal cord region only after 1st type II anterior segment seizure, and then only in 15d postoperative group.

sion of events certain among which stand out enough to provide the clinical evidence for successive stages of HPNS development, and links between them which provide the basis for modifying the course of development; alternatively, the syndrome may be truly composite in the sense that it results from the co-mingling and superposition of discrete chains of events, each leading to a distinct end point at which changes leading to that component stage have attained a critical degree of severity.

Although we are far from definitively adopting either of these alternatives—a matter which has an obvious bearing on a number of practical problems, as well as on the choice of approach to an analysis of these events in biophysical terms—it seems that some progress has been made toward an answer in relation to the convulsion stage of the HPNS in the CD-1 mouse.

Clinically, this consists of two types of events, crudely characterizable as clonic and tonic seizures, or, in our terms, as type I and type II HPNS seizures (2). These differ not only as discrete motor events, but also in terms of differences in electrophysiologic manifestations (2) in terms of the invariable association of severe transient bradycardia with type II HPNS seizures but not with type I (6). In terms of mortality, these events are never observed with type I, but occur in more than one fifth of all type II seizures (2) (Table II).

The four severe stages of the HPNS—coarse tremors, two types of seizures, and high pressure death—can be distinguished further by differences in

TABLE II

Differences Between Type I and Type II HPNS Seizures
in CD-1 Mice

Criteria	Type I Seizure	Type II Seizure
Clinical	Clonic burst	Tonic/clonic sequence
EEG	Little change	4 to 5 spike and wave; post-ical silence
Heart Rate	No change; no atropine effect	80–90% decrease; atropine blocked partially
Compression Rate	Very − k = 11	None − k = 0 or negative
Phenobarbital	Protects	Protects, but to a much greater degree than·in type I
Diphenylhydantoin	Sensitizes	Markedly protects
Trimethadione	Sensitizes early, protects slightly late	Protects early, no effect late
Reserpine	Sensitizes, especially at low compression rate	Little effect
Ontogenetic	Mature, more resistant than newborn	Little change from birth to maturity
Spinal Animal	No seizures below transsection	Seizures also in isolated part of spinal cord
Mortality	None	29%

the changes undergone by threshold pressures that elicit each stage in response to a variety of experimental manipulations: thus, the drug diphenylhydantoin markedly lowers the threshold for coarse tremors, slightly lowers it for type I seizures (2,7), substantially raises it for type II seizures, and seems to have little effect on high pressure death (2,7). More detailed data, available for the two seizure stages, show differences in response to changes in compression rate (2) and in the pattern of change with maturation of baby CD-1 mice (8).

All of these observations support the view stated previously that the HPNS and specifically its convulsion stage, is a complex entity and that its clinical appearance may be varied substantially by changing compression conditions. Two examples involve changes in the pressure interval separating type I and type II seizures: in the CD-1 mouse, type II seizure thresholds vary little with compresssion rates, while type I seizure threshold pressures decrease markedly with increase in compression rate. As a result, the two seizure thresholds coincide when compression rates fall below 10 atm/h, and give rise to a compound seizure having some of the characteristics of each (2) (Fig. 1). At the same time, this fusion probably defines the maximum pressure practically attainable in the mouse by manipulation of the compression profile (9).
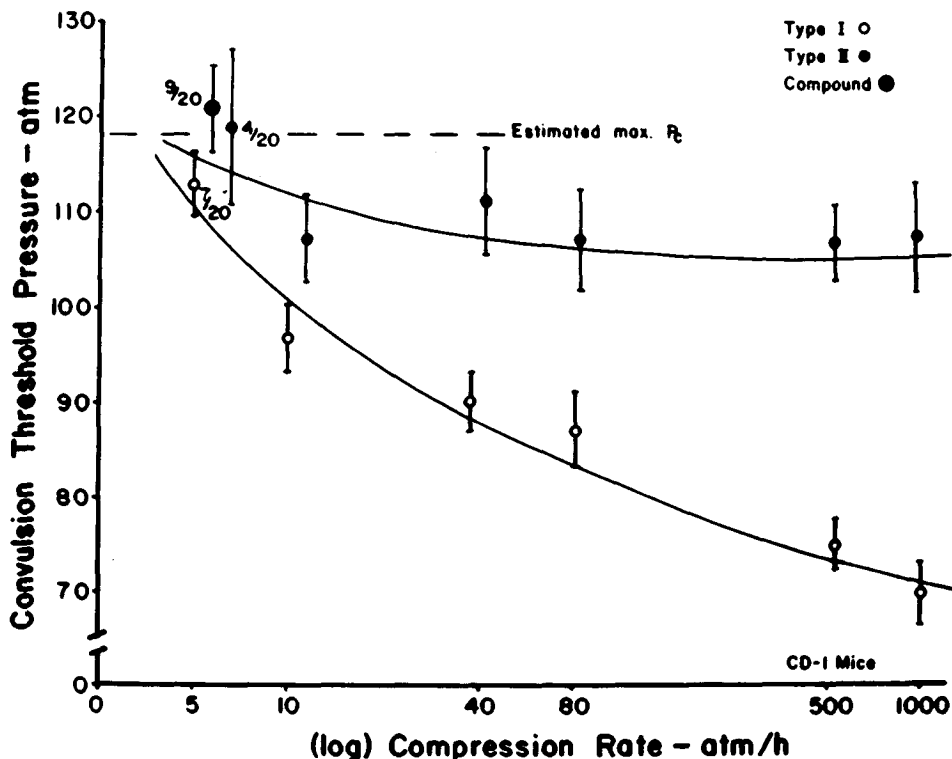
Fig. 1. Change in convulsion thresholds of CD-1 mice as a function of compression rate, illustrating convergence of two types at low compression rates, emergence of compound type seizures in the region of coincidence of type I and type II convulsion thresholds, and relation of this zone to the maximum type I convulsion threshold pressure, Pc (max), as defined by interrupted compression experiments (9).

Again, the typical HPNS seizure in the adult Sprague-Dawley rat clinically resembles the compound seizure of the mouse on extremely slow compression. If, however, the pattern is observed during maturation of the baby rat, two seizures like those in the mouse are observed early, but because of different progression of the two types with age, the thresholds coincide by about the 20th day of age, giving rise to the compound seizure, which persists to adulthood (10).

Although observations such as these illustrate and support the view that the HPNS is a composite entity made up of more than one component, they do not by themselves allow one to distinguish between the "monophyletic" and the "polyphyletic" options, they do not help one to decide whether one is looking at a single chain of events, the linkages between which are being modified, or at multiple, more-or-less concurrent chains of events, each culminating at its own critical point. It seems to us that the very different patterns of change of the two seizure thresholds during maturation (8,10), the lack of correlation of individual susceptibilities (to be discussed; cf. ref. 11) and the differences in genetic determinacy (12) all are rather more compatible with the

multichain concept than with a single chain; but, clearly, either concept could be made to jibe with the data presented so far.

A stronger argument in favor of the mutichain hypothesis of HPNS development, we believe derives from examination of the neuroanatomic representation of the HPNS seizure events in terms of mapping sites of enhanced glucose metabolism on the basis of radioautographic pictures (4) (Fig. 2). Such mapping reveals that both type I and type II seizures develop as qualitative
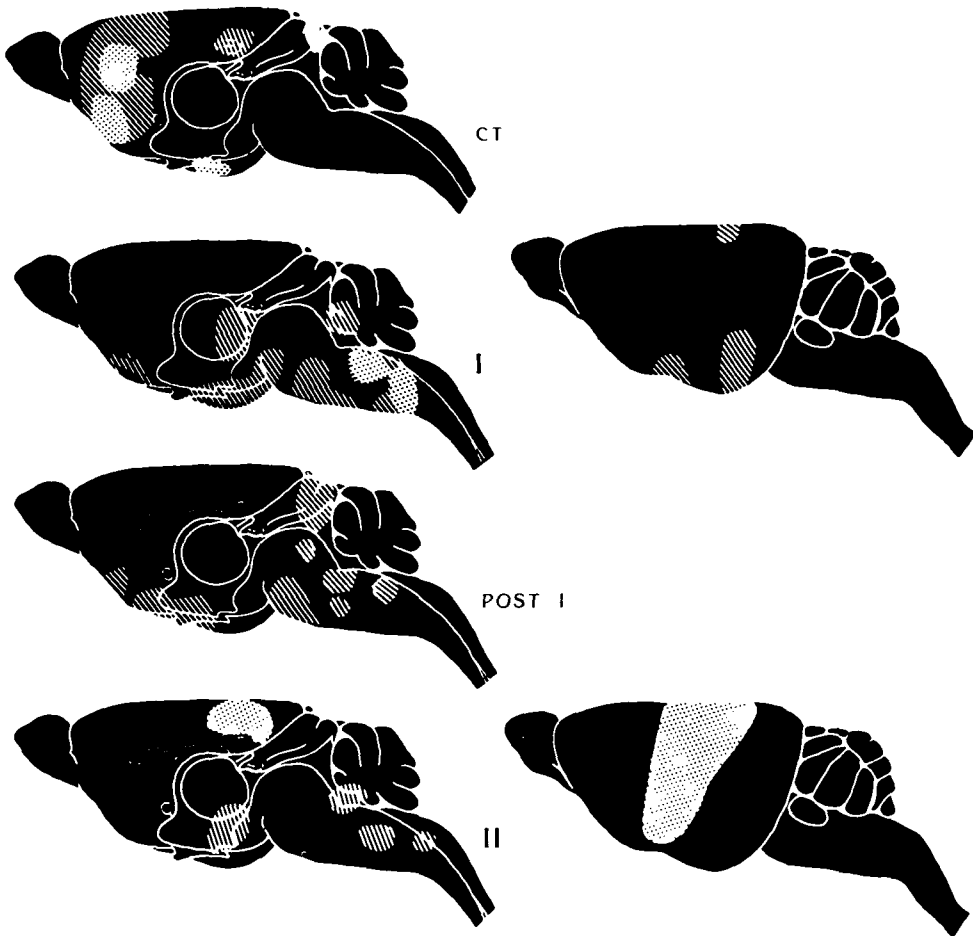

Fig. 2.   Summary of radioautographic data for distribution of 5 deoxy-6C^{14} before, during, and after type I HPNS seizures, and during type II HPNS seizures in CD-1 mice. *First column,* mid-sagittal sections, schematic; *second column,* brain surface schematic. Three degrees of severity are shown:

changes in distribution of uptake sites upon altogether different backgrounds characterizing the coarse tremor stages both before and after the type I seizure. Furthermore, the regions of enhanced glucose utilization in type I seizure are confined largely to the ventral thalamic regions, posterior hypothalamus, and pontine and medullary reticular formations. The regions involved in the type II seizure include a sharply defined band in the parietal cortex, amygdala, and central thalamic regions, specifically excluding virtually all components characteristic of the type I seizure.

It seems to us that this morphologic evidence strongly indicates that the two seizure events are discrete entities and cannot be viewed as arising out of one another. Such a view would be compatible with the hypothesis that the two events reflect different neurophysiological changes. However, in the absence of convincing data linking any clearly defined neurophysiological changes at the cellular level to any HPNS-like manifestation, further analysis of this problem must remain speculative for the time being.

The concept of a composite nature for the HPNS has some important practical implications. For instance, it bears on the problem of ranking of personnel with respect to suspectibility to the HPNS. From what has already been said, it might be expected that individual degrees of susceptibility to the two types of HPNS seizures might vary independently of one another. That is indeed found to be true: regardless of rate of compression, only about 15% of the total variability in type II convulsion threshold pressures is associated with variation in type I convulsion threshold pressures (11). Thus, a ranking of subjects for type II susceptibility on the basis of data for type I convulsion thresholds for the same individuals is little better than a chance guess. Even worse, because of the near lack of correlation, selection of type I-resistant individuals also selects those for which the interval between the onset of the two types of seizures is smallest; this is another instance of unfavorably affecting the clinical progression of the HPNS by procedures designed to ameliorate one of its manifestations (Fig. 3).

As though this constraint were not enough, correlation data comparing results of two successive compressions reveal that while predictions for type I convulsion threshold pressures from the results of a preceding compression are excellent ($r^2 \geq 0.8$) if the second test is performed at the same compression rate, the degree of correlation vanishes once again when comparison involves dives performed at different compression rates ($r^2 \leq 0.15$) (11). Thus, the mechanisms responsible for delaying convulsion onset in slowly compressed mice (13) vary from one individual to the next independently of the factors determining convulsion susceptibility at high compression rates. Because these mechanisms appear to become activated quite early during compression (9), their further exploration from the point of view of individual variability (and perhaps its genetic basis) should provide valuable insight into the nature of the cause and effect chains leading to HPNS seizures.
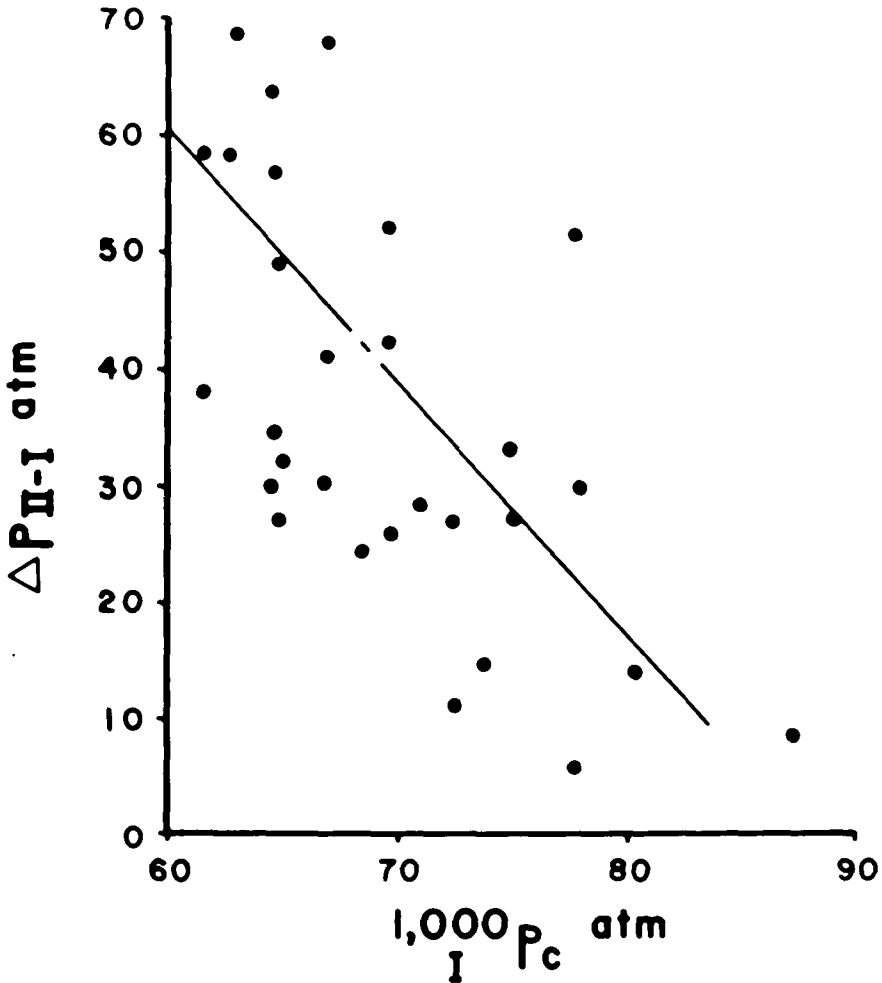
Fig. 3.   Interval between individual threshold pressures for type I and type II HPNS convulsions in CD-1 mice at a compression rate of 1000 atm/h, as a function of the convulsion threshold pressure for type I HPNS seizures in the same individuals. Regression line, least square computation. Correlation: $r^2 = 0.28$.

CONCLUSIONS

A final point that may be worth making is that we fully realize that the analyses presented so far all bear on rodents, and mostly on one strain of mouse. Nevertheless, we are convinced that the substance of what we have said will apply to primates, and, we believe, ultimately to man: HPNS sequences have been described for 12 mammalian models, 7 of which show the

characteristic 2-seizure pattern described previously, while 4 conform to the rat model (cf.14). Variance of HPNS convulsion thresholds in primates is rather larger than in mice (14); replication of ranking, and indeed replication of absolute convulsion threshold pressures, follows the same pattern (15). Differences between susceptibility of tremor and of convulsion threshold pressures to the effect of changes in compression rate have been demonstrated in the monkey as in the mouse (1). Involvement of different parts of the neuraxis in different stages seems quite compatible with reported electromyographic and electroencephalographic data: we suggested that in the squirrel monkey, the cortical electrical manifestations of HPNS seizures are a relatively late reflection of more significant and earlier sub-cortical seizure-like events (16). The first HPNS seizure in the squirrel monkey has been fairly well characterized. Comparison of the data with those for the two types of mouse seizures, and the compound rat HPNS seizure shows that the primate event is unlike mouse type II seizure, but intermediate in many respects between the mouse type I and the rat compound seizures, perhaps rather closer to the former (Table III). Indeed, tonic HPNS seizures have been recorded at pressures substantially above the threshold pressure for the clonic first seizure. Nonetheless, only neuroanatomic data will ultimately allow a more decisive determination of the real nature of this seizure.

In summary, we feel that recognition of the composite nature of the HPNS will allow us to trace backward the chain of events leading to now

TABLE III

Comparison of Characteristics of HPNS Convulsions in Mouse,
Rat, and Squirrel Monkey

Characteristic	CD-1 Mouse		SD Rat Compound Seizure	Squirrel Monkey First Seizure
	Type I	Type II		
Clinical Type	Clonic	Tonic/Clonic	Clonic/Tonic	Clonic
EEG	No Recognizable Change	Spike and Wave	Spike and Wave	Spike and Wave or Grand Mal
Heart Rate Changes	None	Transient Bradycardia (90%)	Transient Bradycardia (40%)	None
Compression-Rate Effect (cf.ref.4)	12	4	8–10	17–20
Repetition of Seizures at Threshold Pressures	Yes	No	No	Yes
5-Deoxyglucose Radioautography	Subcortical (cf. Fig. 2)	Cortical (cf. Fig. 2)	Cortical and Subcortical	?
Isolated Spinal Cord Seizure Activity	None	Yes	Yes	?

well-characterized specific critical manifestations of the HPNS, and thus help to build the much-needed bridge to biophysical studies of whatever will prove to be the simplest organization of neurons within which HPNS-like events can still occur.

Acknowledgment

References

1. Brauer RW, Goldman SM, Beaver RW, Sheehan ME. N_2, H_2, and N_2O antagonism of high pressure neurological syndrome in mice. Undersea Biomed Res 1974;1:59–72.
2. Brauer RW, Mansfield WM, Beaver RW. Lahser S, Venters R. Stages in the development of the HPNS in the mouse. J Appl Physiol: Respir Environ Exercise Physiol 1974;46:128–135.
3. Smith RA, Miller KW. Amelioration of the high pressure neurologic syndrome by anesthetic gases. Undersea Biomed Res 1978;5(Suppl):48.
4. Brauer RW, Beaver RW, Lahser S, Venters R. Comparative physiology of the high pressure neurologic syndrome—compression rate effects. J Appl Physiol: Respir Environ Exercise Physiol 1979;43(2):128–135.
5. Brauer RW, Gillen HW, Beaver RW. HPNS convulsions in the spinal mouse. Undersea Biomed Res 1978;5(Suppl):34.
6. Beaver RW, Brauer RW, Fuquay J. Changes in the heart rate associated with high pressure convulsions in rodents. J Appl Physiol: Respir Environ Exercise Physiol 1979;47:834–845.
7. Rowland JP. Studies in high pressure pharmacology, Thesis Part II. Oxford: School of Natural Sciences, 1976.
8. Mansfield WM, Brauer RW, Gillen HW, Nash K. Changes in CNS responses to high pressure during maturation of newborn mice. J Appl Physiol: Respir Environ Exercise Physiol 1980;49:390–397.
9. Brauer RW, Beaver RW, Lahser S, Mansfield WM, Sheehan ME. Time, rate, and temperature factors in the onset of high pressure convulsions. J Appl Physiol: Respir Environ Exercise Physiol 1977;43(2):173–182.
10. Mansfield WM, Nash KL, Gillen HW, Brauer RW. Age dependence of EEG activity in rats exposed to high pressure heliox. Fed Proc 1976;35:368.
11. Brauer RW, Beaver RW, Gillen HW. Physiological basis of variability in response to environmental stress—correlation of individual susceptibilities to different components of the high pressure neurologic syndrome. J Appl Physiol: Respir Environ Exercise Physiol (in press).
12. McCall RD, Frierson D Jr. A genetic analysis of susceptibility to HPNS Type I seizure in mice. In: Bachrach AJ, Matzen MM. Underwater physiology VII. Proceedings of the seventh symposium on underwater physiology. Bethesda, MD: Undersea Medical Society, 1981:421–433.
13. Brauer, RW, Beaver RW, Sheehan ME. The role of monamine neurotransmitters in the compression rate dependence of HPNS convulsions. In: Shilling CW, Beckett MW, eds. Underwater physiology VI. Proceedings of the sixth symposium on underwater physiology. Bethesda, MD: Federation of American Societies for Experimental Biology, 1978:49–59.
14. Brauer RW, Beaver RW, Hogue CD, Ford B, Goldman SM, Venters RT. Intra and inter-species variability of vertebrate high pressure neurological syndrome. J Appl Physiol 1974;37(6):844–851.
15. Brauer RW, Way RO, Jordan MR, Parrish DE, Beaver RW, Goldman SM. Neurologic effects of repeated exposures to high pressure heliox atmospheres. Undersea Biomed Res 1974;1(3):239–250.
16. Brauer, RW, Way RO, Jordan MR, Parrish DE. Experimental studies on the high pressure hyper-excitability syndrome in various mammalian species. In: Lambertsen CJ, ed. Underwater physiology. Proceedings of the fourth symposium on underwater physiology. New York: Academic Press, 1971:487–500.

PART III. DISCUSSION: HIGH PRESSURE NERVOUS SYNDROME

D. B. Millar, *Rapporteur*

A present consensus of opinion is that many of the neurological and behavioral deficits that manifest themselves in the high pressure neurological syndrome (HPNS) can somehow be attributed to pressure effects on the structure and function of neural membranes. On both a fundamental and applied level this concept has been experimentally challenged by appropriate models and sophisticated experimental regimes. The difficulty that arises in employing this simple but appealing concept is amply illustrated in the studies presented in the session on the HPNS.

Significantly, the relationship between this concept and HPNS symptoms becomes less tangible as the level of organization in the observed model increases. However, on the fundamental level, a simple lipid bilayer with appropriately included protein or peptides can serve as a useful beginning. Thus, with a poly-mixin-phosphatidic acid membrane, one aspect of pressure-induced lipid phase changes is the shift of membrane fluidity and reorganization of lipid-protein domains. For integral membrane proteins and membrane bound proteins such lipid domain alterations would be expected to have significant alterations in neurochemical and enzymatic function. While models and concepts such as these are of critical importance in assessing basic physico-chemical phenomena that may underlie the HPNS, more biologically complex systems are required to study electrophysiological phenomena similar to that demonstrated in the more organized excitable tissues.

Thus, in the voltage clamped bullfrog's node of Ranvier, there is a pressure-related shift in the trans-membrane maintenance potential. If an increase in Na^+ ion permeability is responsible, then the speculation that the Na^+ ion channel dimensions could be altered by pressure-induced fatty acid alkyl group compression might be relevant here. Since a lowered action potential threshold was observed in this preparation, a pressure-induced increase in neural excitability might also be involved in the HPNS symptoms. However, the biochemical and physical complexity of the neurologic domains involved in the HPNS is amply shown in the differing effects of anesthetics on release of the neurotransmitter, acetylcholine, from guinea pig ileum. A variety of gaseous anesthetics increased neurotransmitter output, but octanol, methane, and phenobartitones decreased it. Regardless of the effect, pressure had no effect upon the direction of the response. At the same time, the well recognized amelioration of HPNS by certain anesthetics and narcotic gases appears to offer a novel means to study HPNS and anesthetic receptors: that of structural isomers of anesthetics which themselves have no anesthetic properties but which do suppress certain HPNS symptoms, e.g, tremor.

The concept of experimentally and distinguishable baric and anesthetic receptors is consistent with the observation that while anesthetics have different ameliorative properties against the HPNS (some even lower the convulsion pressure threshold value so that one can have an anesthetized rat exhibiting tremors), all anesthetics so far studied are antagonized by pressure. It appears, therefore, that even using the simplest perspective, a complex linkage exists between anesthetic and baric receptors but that this aspect of HPNS research is potentially resolvable by the approach discussed previously and possibly by the use of pharmacological convulsants. The pharmacological sensitivity of the HPNS receptor(s) is further highlighted by the action of the tranquilizer, reserpine, which reduces the threshold pressure of HPNS symptoms in male CD

mice. The idea that reserpine reduction of brain monoamine levels is involved in the onset of HPNS is clearly not isotropic since selective monoamine metabolic inhibition did not display a clear-cut picture of HPNS pressure threshold modification. Paradoxically, some of the monoamine metabolic inhibitors can potentiate the action of reserpine.

Further complicating this view of the HPNS monoamine connection is the observation that 30–40 atm of N_2 does not result in significant alteration in the brain levels of the monoamines studied while at the same time increasing HPNS symptom onset pressure. Thus, there appears to be evidence implicating monoamine metabolism in the HPNS, but a precise description is as yet impossible. Aside from the underlying phenomena that are manifest as the HPNS, the problem of precisely identifying and quantifying the HPNS symptoms is one of considerable importance. In this context, somatic evoked potentials in Papio papio monkeys are facilitated at depth and are responsive to the rate of compression. In terms of locating major HPNS modifying or control centers, it is worthwhile noting that cerebellectomized rats seize at lower pressures and sustain more seizures than control animals. But, because other HPNS symptoms between the two groups are similar, other neural centers clearly are of major importance in HPNS etiology. This is further illustrated by the observation that the hind limbs of spinalized frogs displayed pressure-induced tremors and myoclonic jerks, while totally denervated limbs were unresponsive to the same pressure levels. The latter point indicates the peripheral neuromusculature system to be more refractory to pressure than the CNS.

Difference in pressure response of elements of the guinea pig visual pathway taken together with the above observations suggest that the response of neural elements to high pressure may depend upon the functional organization of neural circuitry. Additionally, the size of the expressing neuronal pool may be important. In terms of HPNS expression, HPNS-associated convulsions can be characterized by a variety of clinical, pharmacological, animal strain, and other criteria into two different kinds: type I (clonic) and type II (tonic) seizures. The presence of these seizures can be well correlated with discrete functional areas in the brains of CD-1 mice by means of [^{14}C]deoxyglucose injection immediately following seizure. Analysis of the data indicates that type I seizure appears to involve deinhibition of CNS activity marked anatomically from structures in the brain stem to ventral and lateral structures in the diencephalon. Though considerable work remains to be done in this area, it offers a method to electrophysiologically dissect the HPNS. Although the philosophy generated by observing the HPNS from the properties of a lipid bilayer under pressure is not apparent in most of the work summarized here, it is gratifying to reflect that the proper amount of nitrogen gas added to trimix (helium-nitrogen-oxygen) to offset the effects of helium pressure was calculated from experiments dealing with the effects of nitrogen on lipid monolayers. The *Atlantis* dives generated a plethora of data on human performance as a function of compression rate, pressure, and nitrogen gas level in the trimix. The flexibility of the *Atlantis* dive regime is very high. Indeed, the apparent symptoms of the HPNS can be reversibly "titrated" with nitrogen under this experimental setup. Further, the physiological effects (other than HPNS) on humans of breathing trimix of various compositions can be readily studied.

In spite of the complexity of some of the results arising from current studies of the HPNS both in model systems and primates and the difficulty in linking specific molecular events and fundamental thermodynamic arguments to HPNS manifestation, there is a strong impression that large strides in both the practical as well as analytical sense are about to be made in this field.

A THEORY OF INERT GAS NARCOSIS EFFECTS ON PERFORMANCE

B. Fowler and S. Granger

One theoretical approach to the explanation and prediction of narcotic performance deficits in humans on complex tasks is the hierarchical organization hypothesis (1–3) although the usefulness of this approach has been questioned (4). Another approach is the information processing or black box model (4,5). It is the purpose of this paper to review various studies in the light of this latter model, report the results of a study designed to add to this picture, and then propose an explanation for the underlying cause of narcotic performance deficits. For this purpose it will be assumed that both nitrous oxide (N_2O) and hyperbaric nitrogen exert identical narcotic effects (6,7).

Analysis of performance in terms of the information processing model can be sophisticated, e.g., Atkinson and Shiffrin (8) and Welford (9), but for present purposes a simplified model will be used (Fig. 1). In terms of Fig. 1, the aim is to discover how and where the flow of information is disrupted by narcosis. With reference to perceptual processing, it has been reported that sensory thresholds to touch, pain, warmth, vision, and hearing are raised by narcosis (10), but only one study, concerned with pain threshold, had used the methodologically sound technique of signal detection theory to separate sensory sensitivity from response bias (11). Because this study found shifts in β as well as d', the possibility cannot be dismissed that changes in β may have influenced the results obtained by Burns et al. (10). Changes in visual size judgment but not visual acuity have been reported (12), the latter finding has been confirmed by Biersner (13), who also found unimpaired visual functioning on a number of tests. Banks et al. (14) investigated the effects of narcosis on two size-recognition tasks. On these tasks narcosis increased reaction time by a constant amount regardless of stimulus size. If one uses the logic of the Additive Factor Method (15), this result implies, in disagreement with Stein-
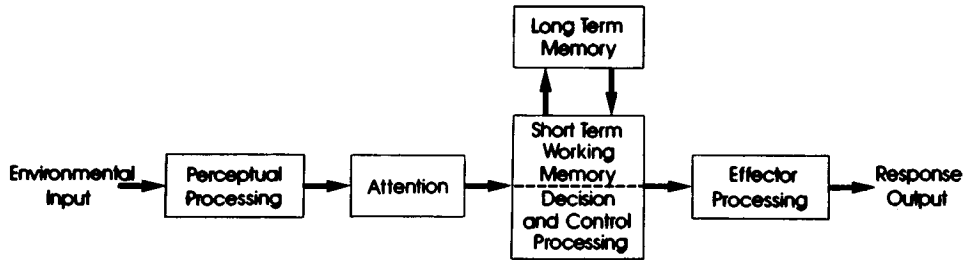
Fig. 1. A simplified model of the human sensory-motor system. *Arrows* indicate direction of flow of information. For details of the functions of each box refer to Atkinson and Shiffrin (8) and Welford (9).

berg et al. (12), that visual size processing is not degraded by narcosis. Accuracy of visual word recognition is also unaffected by narcosis. Without exception, perfect performance in word naming has been obtained in various memory studies in which words have been presented visually and the word was said aloud by the subject as a perceptual control (16,17). Furthermore, Fowler et al. (7) have concluded, in disagreement with Adolfson and Fluur (18), that auditory word recognition is unaffected by narcosis. In sum, the weight of recent evidence favors the view that the accuracy of complex perceptual processes is unaffected by narcosis.

In Fig. 1, an aspect of control and decision processing is reflected by choice reaction time. Berry et al. (5), in their second experiment, found that narcosis added a constant to reaction time when plotted as a function of $\log_2 n$ where n = number of choices. On the basis of the Additive Factor Method this implies that the decision mechanism relating perception to response is unaffected by narcosis. Parallel results have been obtained by Fowler et al. (manuscript in preparation) for movement time. In a reciprocal tapping task, which combines elements of decision and control processing with effector processing, the major effect of narcosis was to slow movement time by a constant when task difficulty was plotted as a function of $\log_2 \left(\dfrac{A}{W} + 0.5 \right)$, where A = target amplitude and W = effective target width. But it is not always true that narcosis adds a constant when time is the dependent variable. Whitaker and Findley (19), using a task where reaction time to a previously learned set of digit pairs was measured, found that narcosis interacted with digit set size to increase the slope of the function. This result is consistent with the finding in numerous studies that narcosis disrupts memory. These studies have been summarized by Fowler et al. (7), who have argued that input to long-term memory (LTM) is the source of this deficit and short-term memory (STM), memory organization and retrieval from LTM, are not involved.

The foregoing indicates that response slowing caused by narcosis is a common finding but, with the exception of LTM, there is little evidence of a breakdown in the accuracy with which each function processes information. Yet there is no evidence concerning attention, despite its importance in complex performance. Here, "attention" refers to mechanisms controlling the selection of information (20). Consequently, an experiment was undertaken to examine the effects of narcosis on attention and perception; performance was assessed by two measures, time and accuracy, so that a comparison of the two could be made. The task was the detection of a target embedded in a list of words presented monaurally with the amount of perceptual interference manipulated by varying the synchronicity of a second list of words presented to the opposite ear. In addition, the influence of attention and perception on the memory deficits seen with narcosis was probed by use of the paradigm described previously, but recall and recognition memory were assessed.

METHODS AND MATERIALS

The subjects were 9 males and 3 females, volunteers from the staff of the Defence and Civil Institute of Environmental Medicine where the experiment was carried out. They had all experienced the symptoms of narcosis and before the experiment proper were given practice versions of the tasks until their performance was relatively stable.

Air was used as a control and narcosis was induced with a 35% N_2O-65% O_2 mixture; both gases were administered via a nonrebreathing oral-nasal mask.

All word lists were presented with a Revox stereophonic tape recorder (Model B-77) via Sony stereophonic headphones (Model DR-3A). Detection monaural lists consisted of 15 one-syllable words recorded in a male voice at 2 words/s. Words used were drawn from Thorndike and Lorge (21) with a frequency of occurrence greater than 5 per million, and each list contained one animal target word randomly assigned to a serial position between 3 and 13. Detection synchronous lists were constructed in the same manner by additionally recording a second list of 15 words containing no animals on another tape track for stereophonic reproduction such that the onset of each word pair was synchronized. Detection asynchronous lists were constructed as described above except the onset of the words was staggered so that a minimum degree of overlap existed between words on each channel. Maximum difference in onset of word pairs and maximum degree of overlap was ≤ 80 ms, the bulk of differences being ≤ 60 ms. Recall monaural, synchronous and asynchronous word lists for the memory task were constructed in the same manner as the detection lists except two-syllable words were used, which recorded at 1.5 words/s.

A memory recognition answer sheet corresponding to each recall list was prepared by typing 15 sets of 3 words in a column on a sheet of paper. One word in each triplet was drawn from the recall list so that every word in the

list was represented on the recognition sheet. The remaining two words were fillers, different from all recall words but selected in the same manner. Recall words were randomized with respect to position within a triplet and order between triplets so their serial position was not the same as the recall list. We measured word detection reaction time using a Sony stereophonic tape recorder (Model TC 270) running at 19 cm/s and recording on one track the word to be detected at the time of presentation to the subject; the subject's response was recorded on the second track, a square wave produced by a tone generator (Mirtone Model TE–22) triggered by a hand-held response button. The two tracks were later played into separate channels of a pen recorder (Harvard Model 45) running at 2.5 cm/s; the distance between onset of the target word and onset of the square wave was measured and converted to the nearest 0.01 s using an appropriate conversion factor.

A repeated-measures design was used, one-half of the subjects was tested in a detection session first then a recall session; the other half was tested in the reverse order. Within each session the subjects breathed both air and N_2O; the order of administration of the gases was also counterbalanced across subjects. In a detection session the subject received six of each kind of list (monaural, synchronous, and asynchronous) in each part; in a recall session the subject received three of each kind in each part. Lists, kinds of lists, and the ear to which presentation was made were counterbalanced across subjects and gas mixtures.

Each subject was tested individually, the two sessions were at least 1 week apart. With either order of breathing the gases, a 20-min acclimatization period elapsed after changing gases before testing commenced. During the time the narcotic mixture was breathed, the subjects were required to clear their ears approximately every 60 s to equilibrate middle ear pressure (7). In a detection session the subjects pressed the reaction-time button as soon as they heard an animal word in their left (right) ear and named the animal aloud at the conclusion of the list, but they were required to continue monitoring the list in case they decided their initial response was in error. They were informed of the nature of the list just before its presentation and, if necessary, were to ignore any words played to the opposite ear. In a recall session they were to remember as many words as possible played to their left (right) ear, ignoring if necessary any words in the opposite ear, and, after hearing each recall list four times in succession, they were to write down as many words. as possible in any order on a blank sheet of paper. After at least 1 min, and longer if the subject needed more time, they were provided with the appropriate recognition answer sheet and with the recall answer sheet still in view, circled one word in each triplet, guessing if necessary.

RESULTS

For all dependent variables it was found from plotting the data that presentation order of gas mixtures did not alter the pattern of results, therefore

this variable was ignored in subsequent analyses. All analyses of variance mentioned below refer to a repeated measures on all factors design.

Detection

Figure 2 shows the mean number of animal target words correctly detected in each condition. Analysis of variance indicated listening condition was significant (F = 14.6; df = 2,22; $P < 0.001$), but the other factors were not. The relatively small standard errors in the monaural condition can be ascribed to a ceiling effect due to almost perfect performance, a matched pairs t test on this condition alone confirmed the lack of difference between breathing mixtures ($t = 1.17$, df = 11). An analysis of simple main effects on listening condition indicated that both synchronous and asynchronous were different from monaural ($P < 0.001$ respectively) but not from each other. Thus, narcosis did not affect number of words detected but listening condition did.
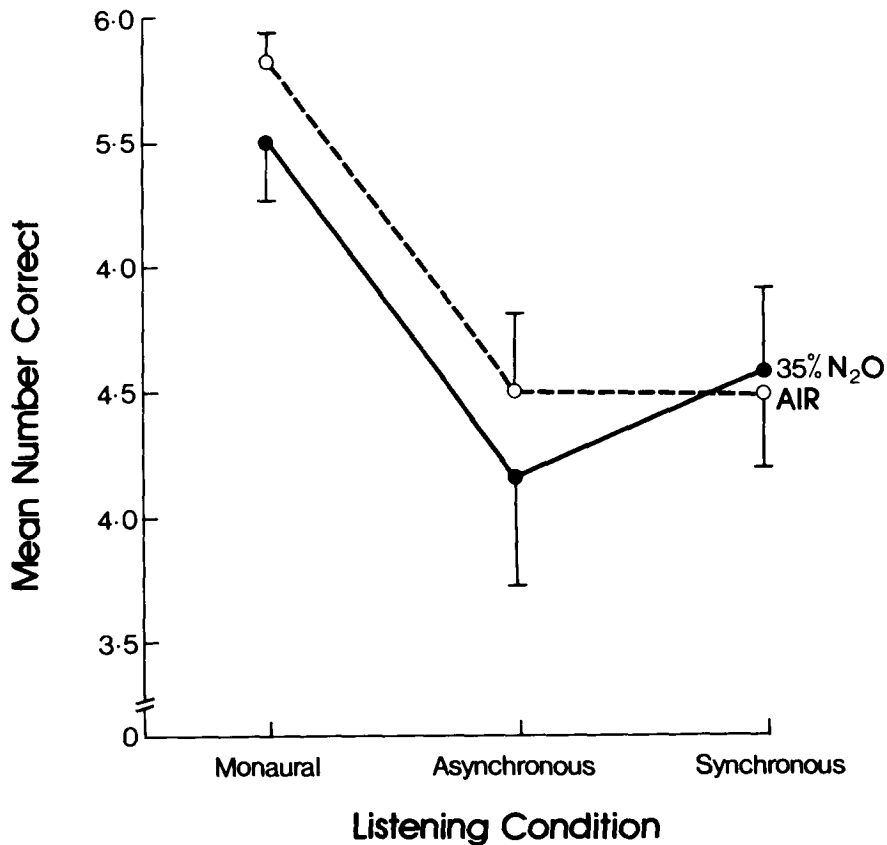

Fig. 2.   Mean number of target words correctly detected (out of 6) as a function of breathing mixture and listening condition. *Bars* are SEMs.

Figure 3 shows mean reaction times to target words correctly verbalized. These data are based on 11 subjects. An analysis of variance indicated breathing mixture was significant (F = 8.1; df = 1,10; $P < 0.025$) but the other factors were not, which led to the conclusion that reaction time was slowed by narcosis but was unaffected by listening condition.

Detection errors are shown in Table I. In general, rates were low and therefore difficult to interpret, but there is little indication of a narcotic effect although synchronous and asynchronous conditions increased rate somewhat. The pattern follows the one found for correct detections.

Recall and Recognition

Figure 4 shows the mean percentage of words correctly recalled and recognized. An analysis of variance on these data indicated the three main effects of listening condition (F = 8.9; df = 2,22; $P < 0.01$), breathing mixture
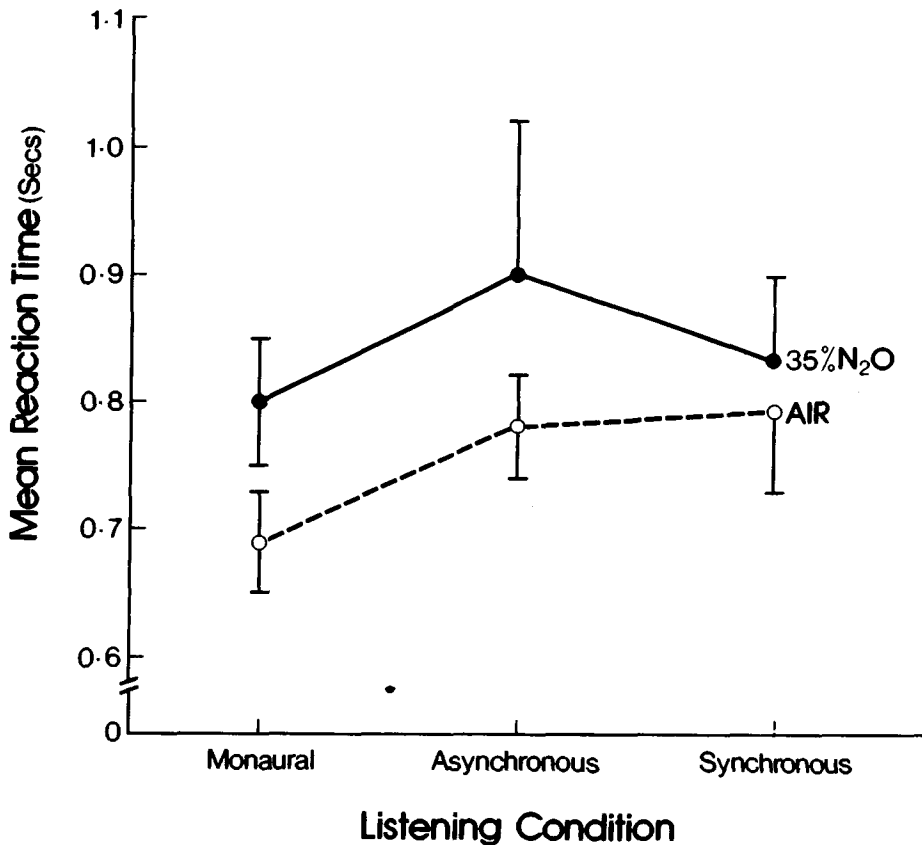
Fig. 3. Mean reaction time to words correctly detected as a function of breathing mixture and listening condition. *Bars* are SEMs.

TABLE I

Detection Errors, Defined as Wrong Word Verbalized and Expressed as
a Percentage of Total Possible Errors Assuming One Error per List, for
Each Listening Condition and Breathing Mixture

Breathing Mixture	Listening Condition		
	Monaural	Asynchronous	Synchronous
Air	3%	10%	7%
35% N₂O	5%	11%	7%

($F = 30.2$; df $= 1,11$; $P < 0.001$), and memory condition (recall/recognition)
$F = 656.9$; df $= 1,11$; $P < 0.001$) were all significant, but the other factors
were not. An analysis of simple main effects on listening condition established
that both synchronous and asynchronous were different from monaural ($P <$
0.005 respectively), but not different from each other. These results show that
fewer words were recalled or recognized in synchronous or asynchronous com-
pared to monaural, recognition memory was superior to recall memory, nar-
cosis affected both recall and recognition memory equally, and listening condi-
tion did not influence narcotic memory deficits.

Recall errors were classified into the categories used by Fowler et al. (7)
with an additional category of intrusions from words played to the opposite
ear; these results are shown in Table II. Synchronous and asynchronous condi-
tions have been averaged since no systematic differences were evident. The
bulk of errors are acoustic, other categories being rare. There is no evidence
of difference caused by listening condition or narcosis except for intrusions
from the opposite list, where a trend for increased errors under narcosis is evi-
dent but statistical significance could not be established clearly.

DISCUSSION

The results of this experiment provide confirmatory evidence for the con-
clusions reached in our literature review. In word detection, the decreased per-
formance in the presence of words in the opposite ear is probably due to dis-
traction, not perceptual masking, because it occurred irrespective of word
synchronicity. More importantly, it is noteworthy that N₂O had no effect on
accuracy of word detection for any listening condition, a result paralleled in
the error data, and thus there is no evidence of narcotic deficits in auditory
perception or attention. The results for detection reaction time are different,
narcosis caused a slowing which was proportionately the same for all listening
conditions so there is no evidence that perception or attention was implicated
in this slowing. There is some indication that reaction time was slower when a
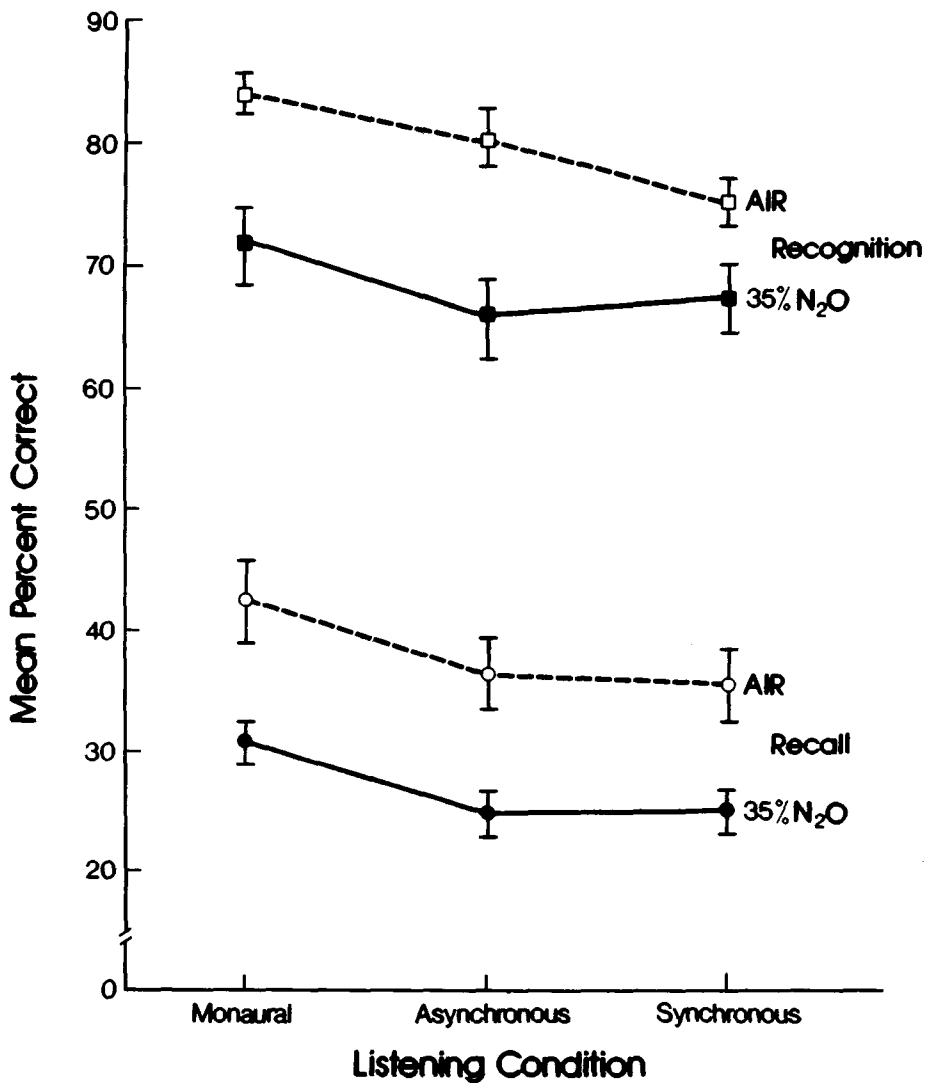
Fig. 4. Mean percentage of words correctly recalled and recognized as a function of breathing mixture and listening condition. *Bars* are SEMs.

distracting list was present, but this effect did not approach statistical significance. The results for memory performance are consistent with previous data in two respects. The usual narcotic memory deficit was apparent and there was no evidence this was due to retrieval difficulties because the difference in words remembered between recall and recognition was proportionately the same with air or N$_2$O. The use of a sensitive method to probe for any evidence of retrieval difficulties, i.e., forced choice recognition, reinforces the conclusions reached on the basis of other methods (7,16,17). In addition to the above

TABLE II

Total Number of Recall Errors in Various Categories in Monaural and
Dichotic (Average of Asynchronous and Synchronous) Listening Conditions
for Each Breathing Mixture

Categories	Listening Condition			
	Monaural		Dichotic	
	Air	35% N_2O	Air	35% N_2O
Acoustic	15	18	16	15.5
Semantic	1	0	1.5	1.5
Compound	0	1	0.5	1.0
Intrusions	4	1	5.5	4.5
Words Twice	0	4	1	2
Unclassified	10	4	14	9.5
Intrusions from Opposite Ear	NA	NA	5.5	12.5

findings, the lack of an interaction between the narcotic memory deficit and listening condition provides no hint that perception influenced the deficit, although it must be acknowledged that the perceptual manipulations were very basic and were probably not representative of the kinds of perceptual processing that have been hypothesized to influence memory (22). Finally, narcosis had no effect on any category of memory error, with the possible exception of intrusions from the opposite list. These results are in agreement with those reported by Fowler et al. (7) and the confimation of this finding contradicts Adam's (1) claim that acoustic memory errors increase under narcosis, a prediction derived from the hierarchical organization hypothesis.

A simple model can explain the pattern of narcotic effects revealed by the literature review and examined further in the experiment reported herein. It is proposed that the basic deficit caused by narcosis is a slowing in the rate of transmission of information through the sensory-motor system outlined in Fig. 1 and that the manner in which each function processes information, with the major exception of LTM, is unaffected by narcosis. This conclusion comes from various studies that show timing is slowed, but this slowing cannot be attributed to a deficit in a specific function. The memory deficit seen with narcosis, a failure to input information into LTM, is regarded as a direct result of this slowing. If time to access LTM increases, this could disrupt sensitive mechanisms that rely on timing to lay down a permanent memory trace (23). Because specific functions are not regarded as malfunctioning under narcosis, the decrease in accuracy seen on some tasks is assumed to be due to a failure on the part of the subjects to adjust their speed-accuracy operating characteristic (15) appropriately while narcotic. Two points should be kept in mind when considering this model. The first point is that the model is directed toward pre-

dicting the effects of narcosis on complex performance, and the disruption of some specific functions, e.g., pain perception (11), is not precluded but may be considered of minor importance in the performance of most tasks. The second point is that the model is limited to dose ranges in which experienced subjects are still functional (approximately 10 ATA hyperbaric air or 40% N_2O) but in which performance decrements are serious.

It is perhaps useful to give an outline of how the model explains performance decrements in mental arithmetic, a complex task that is popular as a measure of narcosis and one in which both time to complete the task and number of errors typically increase (24). Hitch (25) has proposed that mental arithmetic is performed by breaking down the problem into a series of simple stages that involve the retrieval of arithmetical transformations from LTM and their processing in STM. An important source of errors is the forgetting of interim computations stored in STM, but not always utilized immediately. The greater the time lag between storage and use of these interim computations, the greater the probability that forgetting will occur. It is a straightforward prediction that time to complete the task will increase under narcosis; further, it would also be predicted that the increase in time would be related to the number of stages into which the problem is broken, because an operation involving each stage will add its own time increment to the total. Errors come about in two ways that are interrelated. First, the subject generally is not willing to slow down sufficiently to maintain constant accuracy and this leads to guessing, which will increase the error rate. Second, the increased time required to carry out operations, such as accessing LTM for an arithmetical transformation, means that interim calculations stored in STM are more likely to be forgotten, and this secondary deficit increases guess rate and, consequently error rate.

Acknowledgments

References

1. Adam A. Effects of general anesthetics on memory functions in man. J Comp Physiol Psychol 1973;83:294–305.
2. Kiessling RJ, Maag CH. Performance impairment as a function of nitrogen narcosis. J Appl Psychol 1962;46:91–95.
3. Steinberg H. Selective effects of an anesthetic drug on cognitive behaviour. Q J Exp Psychol 1954;6:170–180.
4. Fowler B. Some comments on "A behavioral approach to nitrogen narcosis." Psychol Bull 1972;3:234–240.
5. Berry C, Gelder MG, Summerfield A. Experimental analysis of drug effects on human performance using information theory concepts. Br J Psychol 1965;56:255–265.

6. Biersner RJ, Hall DA, Neuman TS, Linaweaver PG. Learning rate equivalency of two narcotic gases. *J Appl Psychol* 1977;62:747–750.

7. Fowler B, White PL, Wright GR, Ackles KN. Narcotic effects of nitrous oxide and compressed air on memory and perception. *Undersea Biomed Res* 1980;7:35–46.

8. Atkinson RC, Shiffrin RM. The control of short-term memory. *Sci Am* 1971;225:82–90.

9. Welford AT. Fundamentals of skill. London: Methuen, 1968.

10. Burns BD, Robson JG, Welt PJL. The effects of nitrous oxide upon sensory thresholds. *Can Anaesth Soc J* 1960;7:411–422.

11. Chapman CR, Murphy TM, Butler SH. Analgesic strength of 33 percent nitrous oxide: A signal detection theory analysis. *Science* 1973;179:1246–1248.

12. Steinberg H, Legge D, Summerfield A. Drug induced changes in visual perception. In: Rothlin E, ed. Neuro-psychopharmacology. Vol. 2. London:Elsevier, 1961:392–396.

13. Biersner RJ. Selective performance effects of nitrous oxide. *Hum Factors* 1972;14:187–194.

14. Banks WW, Berghage TE, Heaney DM. Visual recognition thresholds in a compressed air environment. *Aviat Space Environ Med* 1979;50:1003–1006.

15. Pachella RG. The interpretation of reaction time in information-processing research. In: Kantowitz BH, ed. Human information processing: tutorials in performance and cognition. New York: Lawrence Erlbaum, 1974:41–82.

16. Fowler B. Effect of hyperbaric air on short-term and long-term memory. *Aerosp Med* 1973;44:107–1022.

17. Fowler B, Ackles KN. Effect of hyperbaric air on long-term memory organization and recall. *Aviat Space Environ Med* 1975;46:655–659.

18. Adolfson J, Fluur E. Hearing discrimination in hyperbaric air. *Aerosp Med* 1967;38:174–175.

19. Whitaker LA, Findley MS. Nitrogen narcosis measured by dual task performance. *J Appl Psychol* 1977;62:735–746.

20. Posner MI, Boies SJ. Components of attention. *Psychol Rev* 1971;78:391–408.

21. Thorndike EL, Lorge I. The teacher's word book of 30,000 words. New York: Columbia University Press, 1944.

22. Cermak LS, Craik FIM. Levels of processing in human memory. New Jersey: Lawrence Erlbaum, 1979.

23. Pribram KH. Languages of the brain. Chap 8. Englewood Cliffs NJ: Prentice-Hall, 1971.

24. Ackles KN, Fowler B. Cortical evoked response and inert gas narcosis in man. *Aerosp Med* 1971;42:1181–1184.

25. Hitch GJ. The role of short-term working memory in mental arithmetic. *Cognitive Psychol* 1978;10:302–323.

ASSESSMENT OF THE HIGH PRESSURE NEUROLOGICAL SYNDROME (HPNS): A NEW METHOD OF MEASURING TREMOR IN AN ANIMAL MODEL

J. A. Baker, M. J. Halsey, B. Wardley-Smith, and R. T. Wloch

One of the signs of the high pressure nervous syndrome (HPNS) seen in both man and mammal is the onset of tremor. The tremor threshold pressure varies between species (for example, in man it is about 30 ATA, in rats about 50 ATA), but it is a reproducible end point (1) and a useful variable for the assessment of the severity of HPNS. The main advantage in using tremor to monitor the progress of HPNS is that it can be measured by a noninvasive technique. This is of particular importance when using an animal model because if the animal is reasonably free of apparatus, a more realistic situation is likely to be obtained. This paper is concerned with the method we have developed to measure tremor in the rat: detailed results of the pharmacological experiments using this new technique are presented elsewhere in these proceedings (2).

In man, there are several satisfactory methods for measuring tremor, both simple and complex, but they all require a degree of co-operation. Previous workers have used three main approaches for monitoring tremor in animals: a) simple behavioral observation of the animal, b) electrical recording from implanted electrodes, and c) noninvasive techniques.

Behavioral observation of the animal is essential in any experiment. Nevertheless an assessment of tremor onset pressure by this method requires that one individual makes all the observations; also it is difficult to quantify tremor and to assess small changes by observation alone.

Invasive techniques in animals such as electromyography (EMG) (3) can provide a reliable signal, which can be quantified and analyzed for both ampli-

tude and frequency information. However, the necessity for a moderately restrained animal and the discomfort of implanted electrodes make this technique more suitable for use in anesthetized animals.

Two noninvasive methods for assessing tremor in animals have been reported: magnetic induction and mechanical transducers. The magnetic-induction device consisted of a magnet taped to the leg of a small animal, which was then placed in a cage over a coil. Movement of the limb together with the magnet would cause a change on the local magnetic field that would be picked up by the coil and thus generate an electromotive force (4). This apparatus is useful in determining factors such as tremor frequency, duration, percent of tremor time, or other motor activity produced by a single limb of a freely moving animal. As the authors (4) point out, however, it is not suitable for amplitude data because both the orientation and distance of the magnet with respect to the coil will affect the size of the signal. This method was used subsequently to measure tremor in the guinea pig (5) although the amplitude variations had been overlooked.

The mechanical transducer (6) consisted of an animal cage suspended by steel springs with its base in contact with the stylus tip of a phonograph cartridge. This equipment is useful for measuring general activity but may require adjustment for each animal. However, the frequency response of the phonograph cartridge (30 Hz–14 kHz) precludes any measurement of tremor frequency.

METHODS

Before finalizing our present design for tremor measurement, we tried several different methods. The first method involved a modified abdominal respiration monitor (7). It consists of a simple pressure transducer: a small plastic cylinder, closed at one end and rubber diaphragm on the other end. A small flexible tube leads from the cylinder to a variable parallel plate capacitor. As the rubber diaphragm is moved the pressure variation changes the value of the capacitor. The capacitor forms part of an oscillator circuit, the demodulated output of which is proportional to the diaphragm movement. The transducer was taped either directly onto an anesthetized rat or beneath a small rat cage. This system gave an excellent signal, but it proved difficult to remove all the artifacts because the environmental pressure constantly changed.

Subsequently, we developed a device that we hope will be more versatile. In our experiments we have used rats, but the principle of the system is suitable for any size of animal. It consists of a small silicon strain gauge (Endevco Pixie Type 8120) mounted beneath a small rat cage. The mounting assembly is made of four nylon pillars attached to the corners of a perspex base (0.3 m × 0.15 m). A metal frame is mounted on top of the four pillars. Three nylon straps are slung across the metal frame, at equidistant points along the length. The strain gauge itself (12 mm × 2 mm) is bonded to a strip of 22-gauge beryllium copper sheet to reduce fragility, and the assembly is sewn underneath the central nylon strap.

A small rat cage is placed onto the three nylon straps. Initial experiments with extruded aluminum mesh produced a cage that exhibited unacceptable mechanical resonance. We now have made a cage consisting of netting stretched over wire hoops attached to a flexible rubber base (see Fig. 1). The cage has removable perspex windows at each end, with a hole cut in the rear window to locate the tail. Several turns of Elastoplast prevent the tail from being pulled through the hole. This preparation allows the rat, with cannulation of the tail vein where necessary, to be maintained in a fairly constant position without causing fear or discomfort. With this arrangement we have found only a low level of resonance, the frequency of which is considerably above that where tremor occurs.

Figure 2 illustrates the simple electronic circuit. The F.E.T. (fixed-effect transistor) provides a constant current through the strain gauge and the resultant potential difference developed across it is capacitively coupled to the operational amplifier (Type 741). The ratio of R_1 to R_3 provides the required gain and the capacitor C_2 provides high frequency roll-off. This reduces electrical noise as picked up from fluorescent lights (100 Hz) and neighboring equipment (50 Hz). As the animal moves or develops tremor the stress on the strain
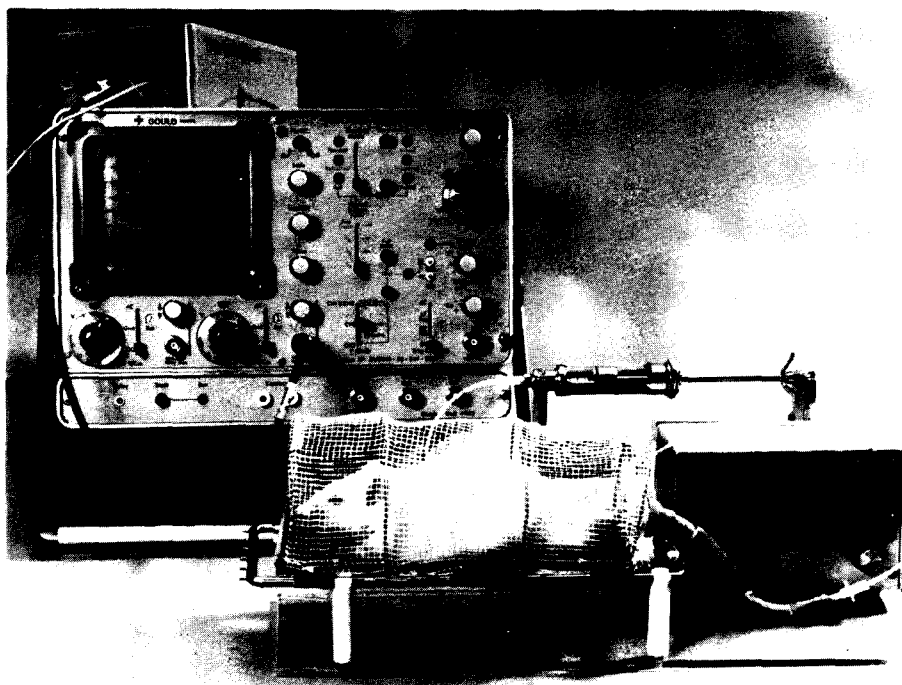

Fig. 1. *Shown are the rat cage and associated apparatus. Strain gauge is mounted centrally beneath the rat cage, sewn to a nylon strap.*
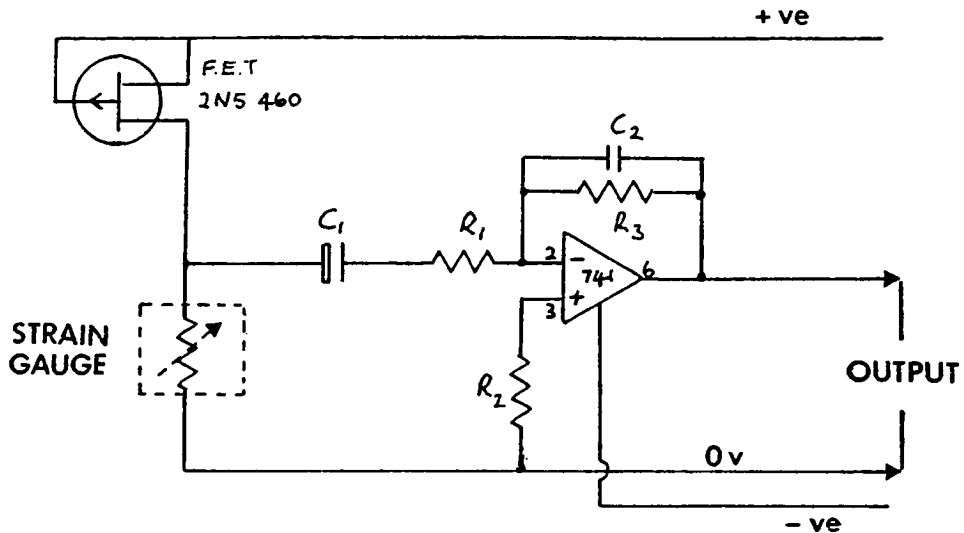
Fig. 2.   Circuit diagram of the strain gauge device.

gauge is altered. This change produces a potential difference, which is amplified and appears at the output. This output may be fed directly to either an oscilloscope or a pen recorder.

RESULTS AND DISCUSSION

We have successfully used the cage and strain gauge in both awake and anesthetized rats inside a pressure chamber (8). In addition to recording tremor, the system responds to voluntary movement, respiration and the ballistrocardiograph (BCG). However, the BCG is seen only in anesthetized rats, because it is obscured by the larger signal associated with voluntary movements. We have found that the actual tremor signal has a regular smooth frequency, which does not change throughout the experiment. This signal is quite different in character from the constantly changing frequency spectrum associated with voluntary movement of the rat, and is easily distinguished from it. An example of the onset of tremor recorded from a rat at pressure anesthetized with methohexitone is shown in Fig. 3.

As the pressure is increased, the onset of tremor can be seen as short bursts of tremor, lasting for up to 500 ms and occurring every few seconds. These initial spells of tremor establish the frequency of tremor for the individual rat, and we have found it to remain constant (usually between 11–14 Hz). We have not seen any significant differences in frequency between awake or anesthetized rats, or between different anesthetics. As tremor gets worse the episodes occur more often and have a longer duration, until finally tremor is almost continuous.

61.3 ATA   2 s
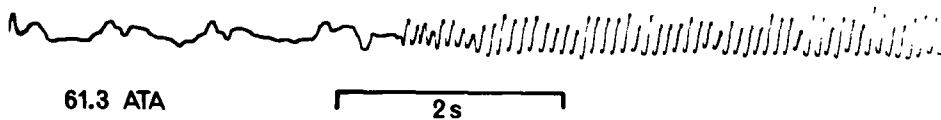
Fig. 3.   Recording from the strain gauge device showing onset of tremor. The rat was anesthetized with methohexitone; the large oscillations on the left of the trace are respiration, with the ballistocardiogram superimposed. Onset of tremor is clearly seen on the right of the trace and has a frequency of 11 Hz.

Once tremor is well established, we have used this method to detect any improvement in HPNS by infusing drugs into the precannulated tail vein of the rat. Improvement in tremor is seen initially as a reduction in amplitude, followed by abolition of the basic tremor frequency. More detailed discussions of our results obtained using this technique can be found elsewhere in these proceedings (2).

CONCLUSION

Tremor in small animals is an important variable used in the study of HPNS, but its measurement is very difficult to quantitate. Problems include a) distinguishing tremor from gross movement (including small convulsions), postural changes, small movements such as "washing," respiration and BCG, and the natural resonance of the restraining cage; b) quantitative analysis in terms of both amplitude and frequency; c) the necessity for a noninvasive technique that requires no manual adjustment during the course of a high pressure experiment; d) limitations as to the bulk of the detector; e) independence of other environmental variables such as pressure, temperature, and lighting conditions. The simple strain gauge device that we have developed appears to overcome the majority of these constraints. We now have been using this device continuously for several months and have found it to be consistent and reliable for measuring tremor in small rodents.

References

1. Brauer, RW, Beaver RW, Hogue CD, Ford B, Goldman SM, Venters RT. Intra- and interspecies variability of vertebrate high-pressure neurological syndrome. J Appl Physiol 1974;37:844–851.
2. Wardley-Smith B, Halsey MJ. Prevention of HPNS: the possible use of structural isomers of anaesthetics. In: Bachrach AJ, Matzen MM, eds. Underwater physiology VII. Proceedings of the seventh symposium on underwater physiology. Bethesda, MD: Undersea Medical Society, 1981:337–343.
3. de Luca CJ. Physiology and mathematics of myoelectric signals. IEEE Transactions on Biomedical Engineering BME: 1979;26:313–325.
4. Dill, RH, Dorman HL, Nickey WM. A simple method for recording tremors in small animals. J Appl Physiol 24:598–599.
5. Ackerman MJ, Gruenau SP. System for the passive measurement and analysis of high pressure nervous syndrome tremor in animals. Undersea Biomed Res 1978;5:301–307.

6. Walker E, Mackie CS, Macdonald AG. New observations on pressure-induced motor disturbances in a small mammal. Undersea Biomed Res 1977;4:1–8.
7. Wright BM. An abdominal respiration detector. J Physiol 1977;27:11–12P.
8. Wardley-Smith B, Halsey MJ, Green CJ. Differentiation of the molecular sites for anesthesia and pressure. Br J Anaesth 1979;51:991–992P.

A GENETIC ANALYSIS OF SUSCEPTIBILITY TO THE HPNS TYPE I SEIZURE IN MICE

R. D. McCall and D. Frierson, Jr.

The high pressure nervous syndrome (HPNS) constitutes a serious threat to the health of humans exposed to the high hydrostatic pressures encountered in deep-diving operations. Thus, a serious concern of those entrusted with the safety of divers is that the divers do not reach the hypothesized culmination point of the high pressure neurologic syndrome manifested as the HPNS convulsion.

Susceptibility to HPNS symptoms both in terms of threshold pressure and severity of manifestations are known to vary widely among humans (1) and experimental animals (2). This suggests the possibility of devising experimental studies to provide estimates of the degree to which heritable factors, and the physiological systems they determine, condition the expression of susceptibility to the HPNS. The only suitable biological model for such experimentation is the mouse because a) many inbred strains of mice each of which is genetically uniform are available, b) individual animals are small, and c) as a species mice are usually fecund and have short generation times. Comparative data are available to indicate that HPNS manifestations are surprisingly uniform in a number of mammalian species, including the mouse *Mus musculus* (3); therefore a genetic analysis using mice might reasonably be expected to have relevance to humans.

The strategy underlying the present paper is first to identify as a test parameter a single readily quantifiable characteristic of the HPNS, then to select two inbred mouse strains maximally separated in this characteristic, and from these to generate a series of matings to produce first and second generation hybrids. The resulting test parameter distributions will be compared with distributions theoretically developed from the same pedigree data for a number of models of genetic determinacy so as to select by means of a maximum likeli-

421

hood procedure a preferred (in the sense of most likely) model of the inheritance mode of the strain difference in the test parameter.

The availability of recombinant inbred (RI) mouse strains, the progenitors of which are the two strains originally used, permits the testing of specific predictions generated by the model and thus further refinement of it. In addition, the data derived from the RI strains hold promise for identifying genetic linkage relations possibly leading to identification of the relative positions of the genetic loci in the mouse genome, which, in turn, may lead to critical definition of their physiological and biochemical actions.

METHODS AND MATERIALS

Compression Conditions

The mice used in this study were exposed to compression in a heliox atmosphere under general conditions described in previous work (4) until the HPNS type I convulsion was observed. Key compression parameters were: $P_{O_2} = 0.50 \pm 0.05$ atm; $P_{CO_2} < 0.02$ atm throughout; and chamber temperature $= 34.5 \pm 0.5°C$ except for fast compressions, details for which are given below. A constant mean compression rate of 100 atm/h^{-1} applied in stepwise increments of 2 atm was used in some experiments. That compression profile represents a compromise among reproducibility, resolution, and convenience. In other experiments, the mice were compressed continuously at a rate of 1000 atm h^{-1}. To minimize the effect on the animals of a 4°C adiabatic temperature excursion resulting from the rapid compression rate, those experiments were begun at a chamber temperature at 31°C. Both male and female mice were used in all experiments but, as no significant difference in type I seizure threshold with respect to sex was found, the results for the two sexes were combined in all subsequent analyses.

Mice and Breeding Program

Mice were maintained in the Institute's colony in plastic cages at a temperature of $24 \pm 2°C$ on a 12-h light—12-h dark cycle. Their diet was Charles River mouse chow and water provided ad libitum up to the time of the experiments. Mated pairs were housed separately. When by gross observation the female was judged pregnant, the male was removed. Offspring were separated by sex at weaning and maintained as sibling groups with no more than four sibs to a cage. The experiments were performed on mice 30–58 days old. No systematic effect of age was detected (cf. 5).

Type I HPNS seizure threshold pressures were determined for the following experimental populations at the 100 atm h^{-1} compression rate: inbred strains C57BL/6J ($n = 40$) and DBA/2J ($n = 40$); the two reciprocal F_1 hybrids between the parental strains ($n = 44$); the four backcrosses to C57BL,

which include each of the reciprocal F_1's and either C57BL or F_1 as mother (n = 40); the four backcrosses to DBA (n = 40); the F_2 hybrids (n = 120); 18 BXD recombinant inbred strains derived from C57BL/6J and DBA/2J progenitors (n = 20 for each strain); and the reciprocal F_1 hybrids between 10 BXD strains and the DBA progenitor (n = 8 for each strain). Type I seizure threshold pressures were also determined at a compression rate of 1000 atm h⁻¹ for 8 animals from each of the following experimental populations: strains C57BL/6J and DBA/2J; 14 BXD RI strains; and the reciprocal F_1 hybrids between 10 BXD strains and DBA. There were no significant differences between any of the reciprocal crosses and they were therefore collapsed in the presentation of results.

Maximum Likelihood Modeling

The 100 atm h⁻¹ type I seizure threshold data for the C57BL/6J and DBA/2J strains, their F_1 hybrid, and both backcrosses were utilized in estimating the likelihoods of a variety of models of genetic determinacy by the maximum likelihood procedure of Elston and Stewart (6). A general description of the version of the procedure used in the present study follows: Let $N(\mu,\sigma^2)$ represent a normal distribution with mean μ and variance σ^2 and assume in each model that the C57BL/6J distribution is $N(\mu_1,\sigma^2)$, the DBA/2J distribution is $N(\mu_3,\sigma^2)$. and the F_1 distribution is $N(\mu_2,\sigma^2)$. The theoretical backcross distributions vary from model to model, but in each instance are assumed to be mixtures of normal distributions. For all the models the values of μ_1,μ_2, μ_3, and σ^2 are regarded as unknown parameters to be estimated. First maximum likelihood estimates of the unknown parameters are generated in each model using a computer program that includes a subprogram developed for this purpose by Kaplan and Elston (7). The natural logarithms of the models' likelihoods maximized with respect to the various parameters are then obtained. The functions describing the expected distributions for each of the 11 models tested in the manner are summarized in Table I. The model code presented in the first column of Table I is the same as that used by Stewart and Elston (8).

RESULTS

Genetic Analysis

F_1, F_2, and backcrosses. The distributions of type I seizure threshold pressures in the parental strains, their F_1 and F_2 hybrids, and both backcrosses are shown in Fig. 1. Summary statistics of the distributions are given in Table II. The mean threshold value for C57BL/6J is significantly higher than that of DBA/2J (t = 18.1, P < 0.0001). The mean value of the F_1 hybrids is signifi-

TABLE I

Inheritance Modes of Susceptibility to HPNS Type I Seizure: Models Used in a
Maximum Likelihood Study

Model Code	Model Description*	Theoretical Distribution of Backcross to C57BL/6J[1]
A-1	Single locus	$\frac{1}{2}N(\mu_1,\sigma^2) + \frac{1}{2}N(\mu_2,\sigma^2)$
A-2	Two unlinked additive loci	$\frac{1}{4}N(\mu_1,\sigma^2) + \frac{1}{2}N\{(\mu_1 + \mu_2)/2,\sigma^2\}$ $+ \frac{1}{4}N(\mu_2,\sigma^2)$
A-LC	Many equal additive unlinked loci, $\sigma_\infty^2 = \sigma^2 + C \cdot (\mu_1 - \mu_3)^2, C > 0$	$N\{(\mu_1 + \mu_2)/2, \sigma_\infty^2\}$
A-LO	Same as A-LC except $C = 0$	$N\{(\mu_1 + \mu_2)/2, \sigma_\infty^2\}$
B-AO	Two linked loci with additivity restriction ($\mu_{12} + \mu_{21} = \mu_1 + \mu_2$), r = recombination fraction, μ_{12} and μ_{21} means of recombinant genotypes	$\frac{1}{2}(1-r)N(\mu_1,\sigma^2) + \frac{1}{2}rN(\mu_{12},\sigma^2)$ $+ \frac{1}{2}rN(\mu_{21},\sigma^2) +$ $\frac{1}{2}(1-r)N(\mu_2,\sigma^2)$
B-OS	Same as B-AO except replace additivity restriction with symmetry restriction, $(\mu_{12}-\mu_{21})/(\mu_1-\mu_2) = (\mu_{32}-\mu_{23})/(\mu_3-\mu_2)$, μ_{23} and μ_{32} are means of recombinant genotypes for backcrosses to DBA/2J	Same as in B-AO
B-OO	Same as B-OS except no symmetry restriction is imposed	Same as in B-AO
C-OO	One major locus with a large number of equal additive minor loci	$\frac{1}{2}N(\mu_{12},\sigma^2) + \frac{1}{2}N(\mu_{21},\sigma^2)$
C-OC	Same as C-OO except σ_∞^2 is as in model A-LC	$\frac{1}{2}N(\mu_{12},\sigma_\infty^2) + \frac{1}{2}N(\mu_{21},\sigma_\infty^2)$
C-AO	Same as C-OO except that the additivity restriction of B-AO is imposed	Same as in C-OO
C-AC	Same as C-OC except that the additivity restriction of B-AO is imposed	Same as in C-OC

*$N(\mu, \sigma^2)$ is a normal probability distribution with mean μ and variance σ^2; μ_1, μ_2, and μ_3 are means of P_c for C57BL/6J, F_1, and DBA/2J respectively; C is a constant the value of which determines the additional variance in the backcrosses due to the magnitude of the difference between parental means; r = recombination fraction, $0 \leq r \leq 0.5$. Backcross to DBA/2J may be obtained by replacing the subscript 1 by 3.
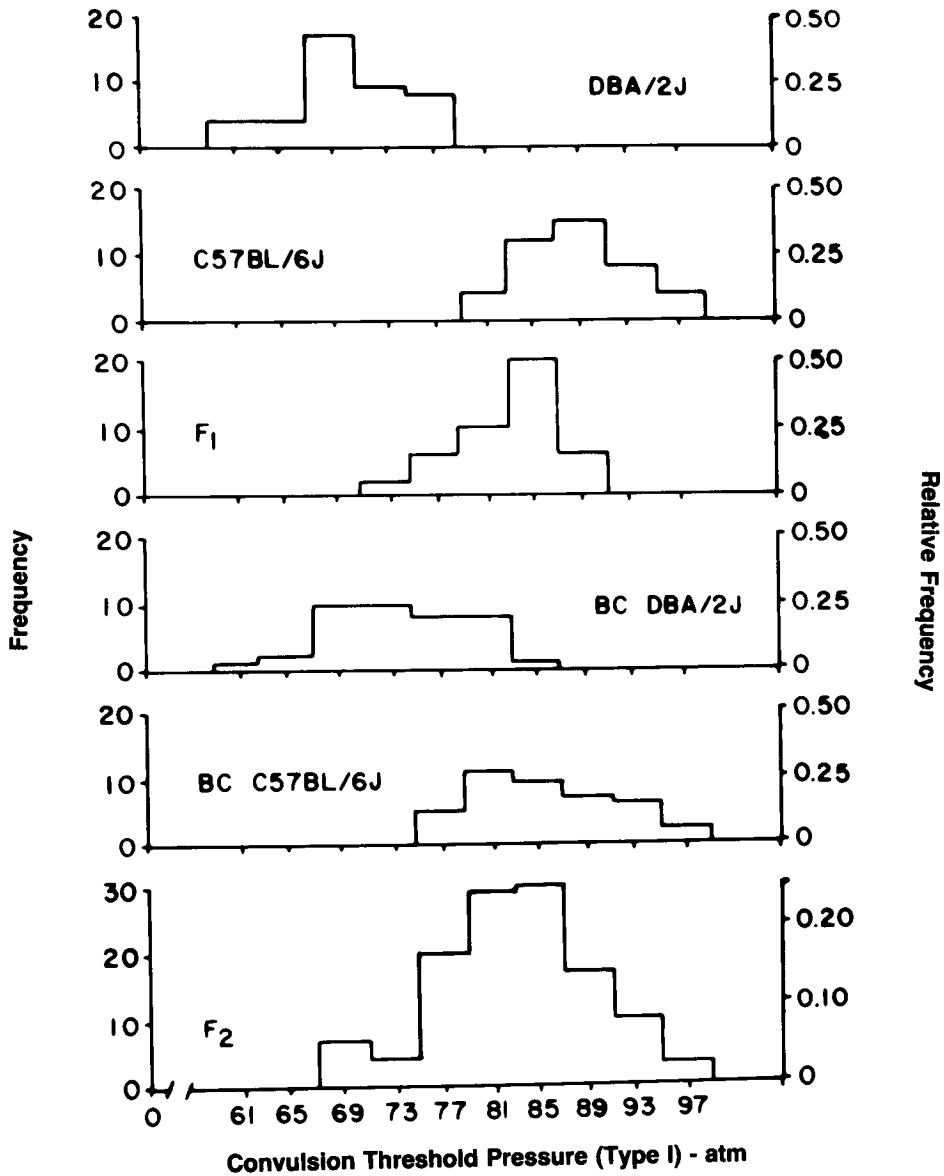
Fig. 1. Frequency distributions of HPNS type I seizure threshold pressures in DBA/2J, C57BL/6J, F_1 hybrids, backcross to DBA/2J, backcross to C57BL/6J, and F_2 hybrids.

TABLE II

Genetic Analysis of the HPNS Type I Seizure Strain Difference: $^{100}_1 P_c$ Distributions of C57BL/6J, DBA/2J and Their First and Second Generation Hybrids

Strain	No. Animals	Mean ± SD	Variance
C57BL/6J	40	88.8 ± 4.5	20.3
DBA/2J	40	70.0 ± 4.8	23.0
F$_1$	44	83.0 ± 4.2	17.6
BC C57BL/6J	40	85.4 ± 5.8	33.6
BC DBA/2J	40	73.8 ± 5.6	31.4
F$_2$	120	82.9 ± 6.6	43.6

cantly higher than DBA's ($t = 13.2$, $P < 0.0001$) and lower than C57BL's ($t = 6.1$, $P < 0.0001$) although closer to the latter, which indicates a degree of dominance.

Tests of the hypothesis of homogeneity of variances among the distributions show the following: among C57BL, DBA, F$_1$, BC C57BL, BC DBA, and F$_2$, at least one of the variances of the distributions is different (Bartlett's $B_c = 16.4$, $P = 0.006$). Inspection of the distributions of variances in Table II indicates that the segregating generations BC C57BL, BC DBA, and F$_2$ are different from (variances are larger than) the genetically homogeneous generations C57BL, DBA, and F$_1$. This result is supported by the finding that the variances of C57BL, DBA, and F$_1$ are homogeneous ($B_c = 0.7$, $P = 0.695$) as are those of BC C57BL, BC DBA, and F$_2$ ($B_c = 2.4$, $P = 0.308$). These results establish that the difference between the parental strains is genetic in origin. Furthermore, the distribution pattern among the six generations suggests the possibility that a single locus, or perhaps a small number of loci, might be associated with most of the difference. This suggestion was subjected to a mathematically rigorous test designed to differentiate the involvement of simple inheritance patterns from more complex "multifactorial" patterns.

Maximum likelihood modeling. The results of the maximum likelihood modeling procedure for eleven different inheritance modes are presented in Table III. Listed in the second column of Table III is the difference in the log$_e$ likelihood for each model from that of the most likely model C-OC. Our interpretations are based upon the approximate criteria for significance of Stewart and Elston (8) in which a log$_e$ likelihood difference between two models of less than 1.0 is considered "not significant," between 1.0 and 2.0 is "suggestive but not conclusive," and greater than 2.0 is "probably significant." On this basis considering their associated log$_e$ likelihoods, we exclude as candidates for the "preferred" model all except the major locus models C-OC and C-OO and possibly B-OO (two linked loci). We tend to exclude B-OO as well since all nonzero arbitrary initial estimates of the additional parameter r quickly converged, by iteration, to 0.5, the value of r at which linkage cannot be distinguished from the case in which the loci are located on different chromosomes. This result implies that the relatively high likelihood of B-OO may

TABLE III

Steps Toward Selection of a Preferred Genetic Model for Susceptibility to HPNS Type I Seizure in Two Strains of Mice

Model Code[†]	Reduced Log_e Likelihood[‡]	Most Likely Estimates of Parameters Characterizing Each Model ($\pm$ SE)[§]									
		μ_1	μ_2	μ_3	σ^2	μ_{12}	μ_{21}	μ_{32}	μ_{23}	r	C
C-OC	0.000	88.7 $\pm$1.0	83.0 $\pm$1.0	70.2 $\pm$1.0	20.3 $\pm$3.5	85.4 $\pm$2.5	85.4 $\pm$2.5	73.8 $\pm$5.3	73.8 $\pm$5.3	1.0	0.033 $\pm$.018
C-OO	0.640	89.1 $\pm$1.0	82.5 $\pm$1.1	70.4 $\pm$1.0	21.4 $\pm$3.9	87.5 $\pm$1.4	83.3 $\pm$1.3	70.0 $\pm$1.5	77.7 $\pm$1.6	1.0	0.0
B-OO	1.020	88.6 $\pm$0.9	82.1 $\pm$0.8	70.2 $\pm$0.9	18.4 $\pm$3.0	91.0 $\pm$2.6	81.5 $\pm$1.9	71.0 $\pm$3.1	75.4 $\pm$3.0	0.5	0.0
B-OS	1.886	89.3 $\pm$0.9	82.1 $\pm$0.9	70.3 $\pm$1.0	20.2 $\pm$3.3	85.6 $\pm$3.5	82.8 $\pm$2.3	70.9 $\pm$3.4	75.5 $\pm$3.3	0.5	0.0
C-AO	1.990	88.8 $\pm$0.8	82.1 $\pm$0.8	69.2 $\pm$0.8	19.1 $\pm$3.1	89.4 $\pm$1.1	81.5 $\pm$1.0	71.7 $\pm$1.0	79.7 $\pm$1.2	1.0	0.0
C-AC	2.328	89.0 *	82.2 *	69.1 *	20.6 *	88.8 *	82.4 *	71.9 *	79.5 *	1.0	0.0
C-LC	3.021	88.8 $\pm$0.9	82.0 $\pm$0.8	69.2 $\pm$0.9	21.0 $\pm$3.7	85.4 $\pm$0.5	85.4 $\pm$0.5	75.6 $\pm$0.6	75.6 $\pm$0.6	1.0	0.032 $\pm$.018
B-AO	3.500	89.1 $\pm$0.8	81.6 $\pm$0.8	69.7 $\pm$0.9	20.9 $\pm$4.0	85.3 $\pm$0.5	85.3 $\pm$0.5	75.6 $\pm$0.6	75.6 $\pm$0.6	.44 $\pm$0.6	0.0
A-2	3.516	89.0 $\pm$0.8	81.6 $\pm$0.8	69.6 $\pm$0.8	21.4 $\pm$3.0	—	—	—	—	—	—
A-1	4.705	89.0 $\pm$0.8	81.4 $\pm$0.7	70.4 $\pm$0.7	19.0 $\pm$2.6	—	—	—	—	—	—
A-LO	4.774	88.8 $\pm$1.0	81.7 $\pm$0.9	68.8 $\pm$1.0	17.7 $\pm$3.2	85.3 $\pm$0.6	85.3 $\pm$0.6	75.3 $\pm$0.6	75.3 $\pm$0.6	1.0	0.0

[†]See Table I for significance of code.   [‡]Log_e is likelihood of C-OC $= -444/820$; values in the column are $\log_e$ likelihood differences from C-OC.   [§]For definition of symbols designating parameters, see Table I.   *Indicates no standard error computed.

be due to unequal effects of the genes or some mode of genic interaction other than unexceptional additivity, or both, because in the latter case B-OO would be equivalent to model A-2 (2 equal, unlinked, additive loci), which is associated with a much lower likelihood. In general, imposition of the additivity restriction (models C-AO, C-AC, and B-AO) resulted in lowering the likelihoods. Models C-OC and C-OO have the highest likelihoods but, as they differ by only 0.64 $\log_e$ units, are probably indistinguishable by this method.

The major locus specified by the preferred models can be shown to be associated with about 64% of the difference in mean type I seizure thresholds between the parental strains. The remainder of the mean difference is associated with an unspecified number of interacting "polygenes." Further breeding tests, the results of which will be presented, are required to confirm the models. However, the discriminative power of this modeling procedure is apparent from consideration of the likelihood ratio between the most likely and

least likely models, which equals $e^{4.8}$ (i.e., the C-OC model is about 120 times more likely to be an adequate "explanation" of the data than model A-LO).

Test of preferred model assumptions using BXD RI strains. The results of a test of the preferred models using 18 BXD RI strains are presented in Fig. 2. Mean type I convulsion thresholds of the BXD strains determined at a compression rate of 100 atm h^{-1} fall into two major groups. Although the right side of Fig. 2 indicates that the strain distributions at the lower end of the "C57BL-like" range overlap extensively with those at the upper end of the "DBA-like" range, the separation of mean values between the two groups attains high statistical significance ($t = 26.8$, $P<0.0001$).

Strain designation	$^{*100}P_{c\ (atm)}$
C57BL/6J	88.8 ± 4.8
BXD-29	89.4 ± 4.2
BXD-2	88.8 ± 2.3
BXD-18	88.5 ± 3.1
BXD-21	88.5 ± 3.1
BXD-28	84.4 ± 2.2
BXD-14	82.8 ± 3.7
BXD-23	81.7 ± 3.7
BXD-15	81.3 ± 3.2
BXD-12	76.9 ± 2.6
BXD-25	76.5 ± 3.6
BXD-11	74.4 ± 4.3
BXD-27	74.3 ± 3.5
BXD-30	72.9 ± 2.7
BXD-16	72.9 ± 3.9
BXD-24	72.7 ± 3.2
VB	72.2 ± 5.0
BXD-5	71.3 ± 3.4
FD	69.8 ± 3.5
DBA/2J	70.0 ± 4.5

*HPNS Type I seizure threshold pressure (atm) at 100 atm hr.$^{-1}$
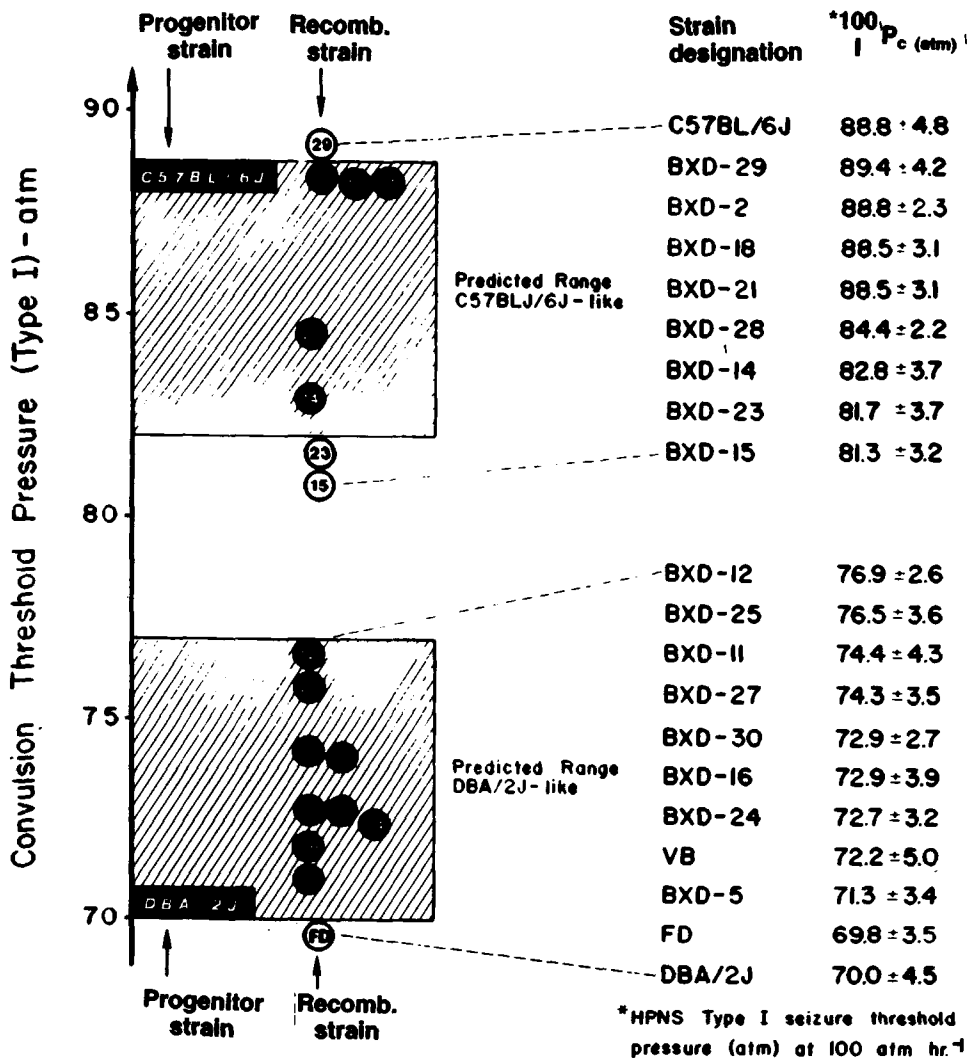
Fig. 2. Grouping of HPNS type I seizure threshold pressures in various mouse strains of the C57BL/6J-DBA/2J system.

The similarity of the experimental distribution of strain mean type I convulsion threshold values to that predicted (shown by the shaded areas representing the 36% of the C57BL-DB mean difference not "accounted for" by the major locus added to the DBA mean and subtracted from the C57BL mean) is consistent with the model assumptions that a) genes of minor effect that raise the type I convulsion threshold are all concentrated in the C57BL/6J strain and all those that lower the threshold are in the DBA/2J strain, and b) the minor threshold-modifying genes segregate independently of the major locus. In addition, the 0.8:1.0 ratio of C57BL-like to DBA-like BXD strains is acceptably close to the 1:1 ratio expected for the strains that were developed without knowledge of their response to high pressure and therefore represent a random sample with respect to HPNS type I seizure phenotype. These results indicate that because segregation of the minor modifying genes causes a substantial degree of blurring of phenotypic classes, "classical" genetic crosses made to confirm the preponderant contribution of a single locus to the type I convulsion threshold strain difference are likely to be less efficient than the tests utilizing the BXD RI strains.

Linkage relations of the $^{1}_{?}^{00}P_c$ *major locus.* Results of a preliminary analysis of the BXD strain distribution pattern, kindly provided by Dr. B. Taylor, suggest that, a) a major locus associated with the mean difference in HPNS type I seizure susceptibility between the C57BL/6J and the DBA/2J mouse strains exists, and b) the locus is linked to the histocompatibility-2 (H-2) locus on chromosome 17. The suggestion of linkage, though strong, remains to be confirmed by further test. Confirmation of linkage will, however, provide conclusive evidence of a major locus by defining for it a relative position in the mouse genome. It will also clearly differentiate the inheritance of the HPNS type I seizure difference from that for the audiogenic seizure the principal locus for which has been mapped onto chromosome 4.

Compression rate effect. Figure 3A shows the effects of rapid compression (1000 atm h^{-1}) on type I threshold in 14 selected BXD strains. Thresholds are lowered for all DBA-like strains and the range of mean values is essentially unchanged from that at the 100 atm h^{-1} compression rate. Among the C57BL-like strains, two patterns of response are present. Five of the strains show a much-compressed range of mean threshold variation featuring small-to-large declines which, however, maintain a C57BL-like distinction from the fast-compressed DBA-like strains. The remaining three strains—C57BL-like at the slower compression rate—change their character and become DBA-like under fast compression.

Among F$_1$ hybrids of selected BXD strains and DBA/2J at the slower rate, the character of the parent strain with the higher threshold is maintained, as shown in Fig. 3B. These results are consistent with assumption a) of the C-models mentioned in indicating a degree of dominance for the genes of minor effect on the type I threshold difference. Under fast compression, the F$_1$'s resemble the BXD parent strain mean at the fast rate, a situation manifest in the essential symmetry of the left and right sides of Fig. 3B.
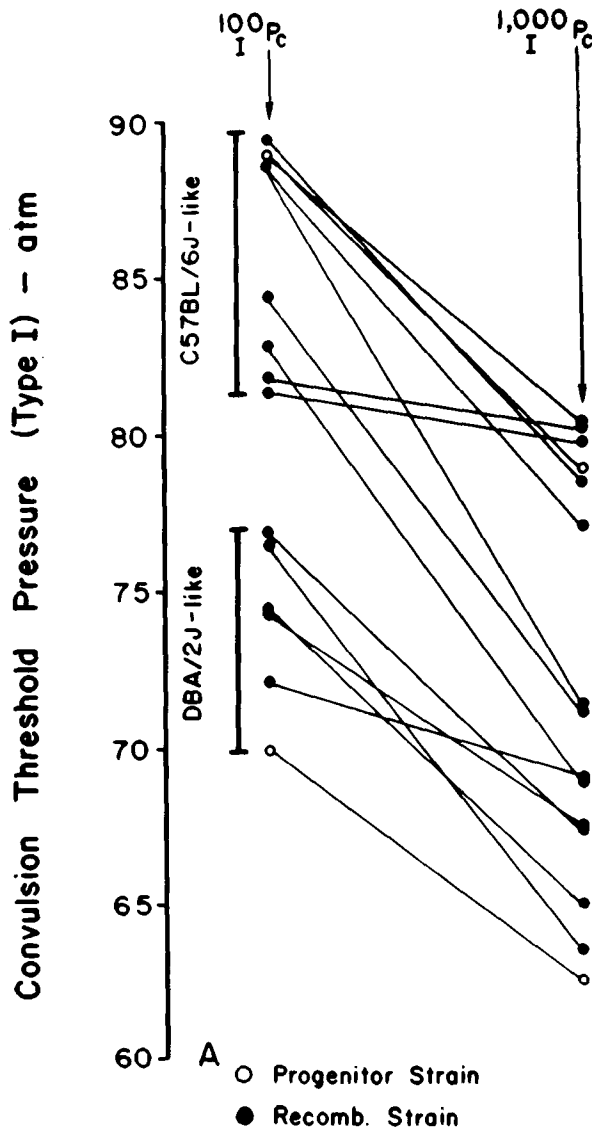
Fig. 3A.   Compression rate effect on HPNS type I seizure threshold pressures in various mouse strains of the C57BL/6J-DBA/2J system.

DISCUSSION

The results reported strongly suggest that the C57BL/6J and DBA/2J mouse strains differ at a single autosomal locus with large effect on suscepti-bility to the HPNS type I seizure modified by an unknown number of genes each with minor effect and segregating partially or wholly independently of the major locus. This conclusion is supported by four lines of evidence: a) the
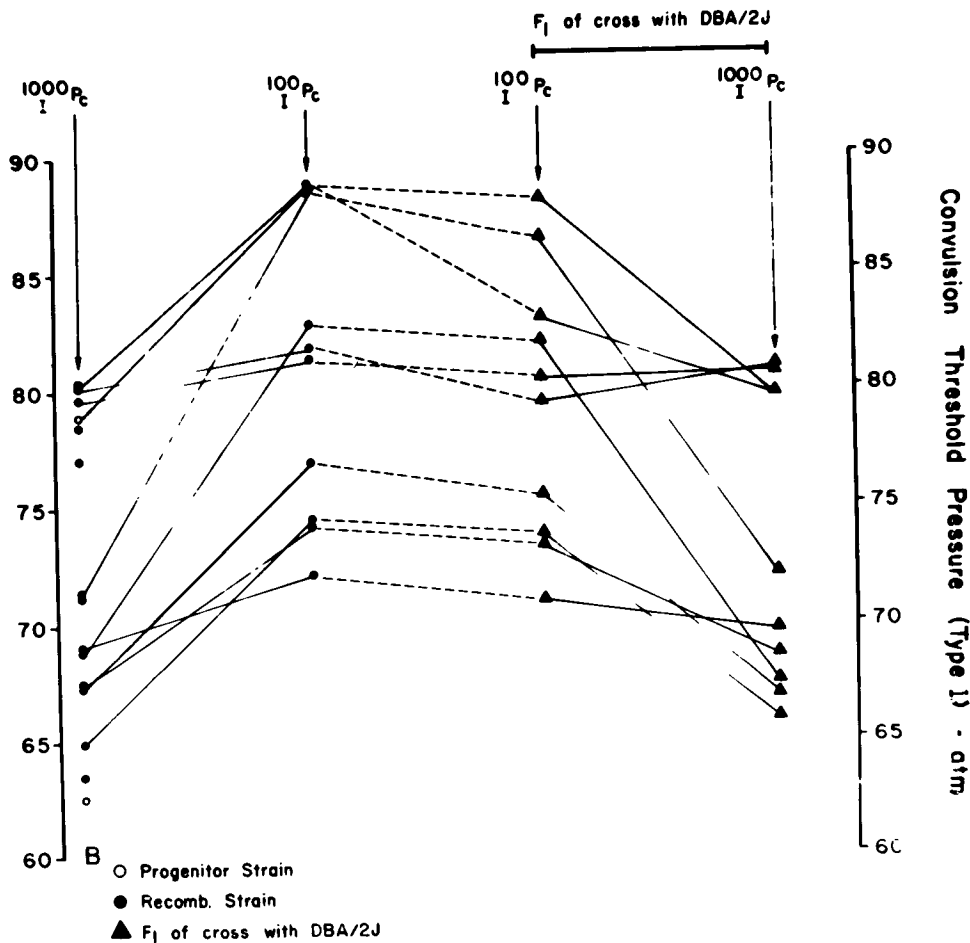
Fig. 3B. Compression rate effect on HPNS type I seizure threshold pressures in strains selected from A and their F_1 hybrids with DBA/2J.

nature of the distributions of type I threshold in the C57BL/6J and DBA/2J parental strains, their F_1 and F_2 hybrids, and the backcross generations; b) consistency of the data from five of the above generations with genetic models of a major locus inheritance mode derived from application of maximum likelihood procedures; c) a test of the models using 18 BXD recombinant inbred strains; and d) a suggestion of genetic linkage based upon analysis of BXD RI strain distribution pattern. A genetic analytical approach can thus be seen to be a powerful addition to the armamentarium of undersea medicine.

Another indication of the great utility of the genetic analytical approach is the relative ease and speed with which other heritable factors complicating explanation may be detected when experimental conditions are changed. For instance, the change in type I seizure threshold character from C57BL-like to DBA-like observed in three of the BXD lines is apparently associated with

compression-rate-sensitive physiological events. Retention of this character change at fast compression in F_1 hybrids of the three strains and DBA suggests a degree of dominance in a genetic system different from the major locus system implicated for the type I seizure difference at the slower compression rate.

Retention of the C57BL-like character of the other five C57BL-like BXD strains under fast compression may reflect the response of a rate-independent physiological event largely unaffected by the effects of other rate-dependent events, also under genetic control, which obtrude at slower compression rates. That is, the thresholds of these strains at fast compression may represent their intrinsic susceptibilities to the type I convulsion. The notion of intrinsic convulsion susceptibility, first suggested by Brauer et al. (9), has since been shown to be consistent with the behavior of the outbred CD-1 mouse strain under a variety of experimental conditions (10).

The absence of a character change among the DBA-like strains exposed to fast compression serves to emphasize the apparent complexity of the type I seizure phenomena. Preliminary results suggest, however, that the major locus inheritence mode may also be the characteristic pattern for the type I seizure difference at compression rates much slower than 100 atm h^{-1}.

The results of this study represent attainment of the following goals: a) finding a test parameter among the HPNS phenomena appropriate for genetic analysis; b) identifying large differences in the test parameter between standardized strains of a suitable animal model; c) maximizing information about the heritable nature of the parameter in a manageably small study by use of a powerful mathematical modeling procedure; d) testing and refinement of models so derived by use of inbred strains representing replicable recombinant genotypes the progenitors of which were the original test strains; and e) estimating the linkage relations of the principal heritable factor involved with others the positions of which in the mouse genome are known with precision.

The advent of genetic analysis of HPNS symptomology is at once a mark of the vigor of undersea medicine and of the widely ramifying nature of its concerns. The approaches made to find answers to the central concerns of this symposium, namely, how is it that the central nervous system perceives and responds to high pressure and how may the response be modified to increase safe working depths for divers, seem certain to have more general applicability to investigation of the biology of the responses of animals to other forms of environmental stress.

Acknowledgment

References

1. Bennett PB. Performance impairment in deep diving due to nitrogen, helium, neon, oxygen. In: Lambertsen CJ, ed. Underwater physiology. Proceedings of the third symposium on underwater physiology. Baltimore: Williams & Wilkins Co., 1967:327–340.

2. Brauer RW, Beaver RW, Lahser S, McCall RD, Venters RT. Comparative physiology of the high pressure neurological syndrome—compression rate effects. J Appl Physiol: Respir Environ Exercise Physiol 1979;46:128–135.

3. Brauer RW, Beaver RW, Hogue CD, Ford B, Goldman SM, Venters RT. Intra-and interspecies variability of vertebrate high pressure neurological syndrome. J Appl Physiol 1974;37:844–851.

4. Brauer RW, Beaver RW, Lahser S, Mansfield WM, Sheehan ME. Time, rate, and temperature factors in the onset of high pressure convulsions. J Appl Physiol: Respir Environ Exercise Physiol 1977;43:173–182.

5. Mansfield WM, Brauer RW, Gillen HW, Nash K. Changes in CNS response to high pressure during maturation of newborn mice. J Appl Physiol: Respir Environ Exercise Physiol 1980;49:390–397.

6. Elston RC, Stewart J. The analysis of quantitative traits for simple genetic models from parental, F_1, and backcross data. Genetics 1973;73:695–711.

7. Kaplan EB, Elston RC. A subroutine package for maximum likelihood estimation (MAXLIK). University of North Carolina Institute of Statistics Mimeo Series, No. 823, 1972.

8. Stewart J, Elston RC. Biometrical genetics with one or two loci: the inheritance of physiological characters in mice. Genetics 1973;73:675–694.

9. Brauer RW, Beaver RW, Sheehan ME. The role of monoamine neurotransmitters in the compression rate dependence of HPNS convulsions. In: Shilling CW, Beckett MW, eds. Underwater physiology VI. Proceedings of the sixth symposium on underwater physiology. Bethesda, MD: Federation of American Societies for Experimental Biology, 1978:49–59.

10. Brauer RW, Beaver RW, Gillen HW. Physiological basis of variability in response to environmental stress—correlation of individual susceptibility to different components of the high pressure neurological syndrome. J Appl Physiol: Respir Environ Exercise Physiol (in press).

CRITERIA ANALYSIS OF SELECTION FOR DEEP DIVING: EEG AND PERFORMANCE

J. C. Rostain, C. Lemaire, M. C. Gardette-Chauffour, J. Doucet, and R. Naquet

The numerous saturation dives made by man in a helium-oxygen atmosphere have shown that an interindividual sensitivity to the hyperbaric environment exists and that in like conditions the HPNS could differ in quality and intensity from one subject to another (1–5). Therefore it seemed important to us to determine the degree of sensitivity of the deep sea diver to certain HPNS symptoms in hyperbaric conditions for dives of 300 m and more.

Symptoms of HPNS have been noticed in certain divers during bounce dives at 180 m. The symptoms generally occur with a latency of 30–60 min after arrival at the bottom.

We sought to learn whether or not the divers who showed certain HPNS symptoms at 180 m in tests of EEG or performance were the same subjects in whom one finds the most marked disturbances during dives to greater depths (dives to 450 m).

METHODS

Two types of tests were chosen to determine individual sensitivity to the hyperbaric conditions: electroencephalographic recording (EEG) at rest and during intellectual work and psychometric tests.

During the first experimental series the various tests were carried out at the surface in atmospheric air during dives to 180 m. After examination of results obtained during this series and the classification of the subjects, we repeated the tests during a dive to 450 m to try to validate this classification.

Electroencephalographic Tests

The EEG activities were registered by "anestho"-type electrodes for the test dives to 180 m and by "hook"-type electrodes for the dive to 450 m. The hook-type electrodes were fixed for the duration of the dive in the fronto-polar, central, middle temporal, and occipital regions. The EEG activities were measured simultaneously in all subjects making the dives. The EEG recordings awake-at-rest and during intellectual work then were analyzed and treated statistically by computer PDP LAB 11/10 methods described elsewhere (4–6).

Psychometric Tests

Manual dexterity. Each subject was given a board measuring 54 × 12 cm, drilled with 100 holes 1 cm in diameter, which were arranged in four columns. At each end of the plank there was a receptacle containing 50 brass cylinders, 4.4 cm long and 0.9 cm in diameter.

At a given signal, the subject was required to take pegs from the left-hand receptacle with his right hand and fit them as quickly as possible into the holes, starting at the extreme right of the plank. He would then work from the opposite end with his left hand.

The observer noted the time taken to place 50 pegs with each hand and calculated the average number of pegs fitted per minute.

Visual choice reaction time. Whenever a red or green light was flashed, the subject was required to react by pressing a button on the side corresponding to the side of the light.

A series lasted 2 min and was preceded by about 30 s practice. Each series consisted of 31 red or green signals, which appeared in a random order with random intervals between them. The subject would use a single finger, poised midway between the two buttons. Performance was assessed by the median time in 0.1 s for 31 correct responses.

Number ordination. Rey's test entailed putting into numerical order figures listed out of order in groups of seven. The experiment lasted 10 min and the subject was asked to note how far he had progressed with the task at the end of each minute (the time was supplied by the tester). Performance was measured by the average number of figures correctly put in order per minute.

Double signal barring. In the Zazzo test the subject was asked to select and bar 250 signs of 2 types from the 1000 signs of 8 types given (squares of 3 mm on a side, with a bar 3 mm long located outside the square either at an angle or in the middle of one of the sides). The page contained 40 rows of 25 signs, and the operator noted the time required by the subject to finish the page.

Diving Methods at 180 m

The 9 dives to 180 m consisted of a compression in 15 min (at 12 m/min). The stay at 180 m lasted 105 min; the mixture was helium-oxygen with 1.14 bars of O_2.

In this experimental series 24 subjects participated (18 COMEX commercial divers and 6 French Navy divers). They were classified in three groups according to the degree of their EEG modifications.

A representative of each of the three established groups made a dive to 180 m in the same conditions as the preceding dives, but with a respiratory mixture of He-N_2-O_2 (10% N_2) to control the influence of nitrogen or the EEG modifications determined by the different groups.

Diving Methods at 450 m

To verify whether or not the EEG classification established at 180 m could be found at a great depth, we selected 8 divers from the three groups to make a dive to 450 m. The diving conditions were:

1) Confinement at 10 m in an He-N_2-O_2 atmosphere (He = 0.8 bar; N_2 = 0.8 bar; O_2 = 0.4 bar; duration, 48 h).

2) Compression of 10 m to 450 m in 38 h with a resting stage of 150 min every 100 m and the addition of N_2 to the mixture before each stage, reaching a level of 2.2 bars N_2 at 450 m (4.8%) (PI_{O_2} = 0.4 bar; T = 32°C ± 1°C; H_2O = 40–60%). This compression is an extrapolation to man of the compression method used in the *Papio papio* baboon (7,8).

3) Stay at 450 m was 50 h (PI_{O_2} = 0.4 bar).

4) Decompression was 10 days (PI_{O_2} = 0.6 bar).

RESULTS

Electroencephalographic Modifications

Test dives to 180 m. The EEG tests carried out during the test dives in He-O_2 showed that the 24 subjects could be divided into 3 groups according to the increase in the power of the theta frequency activities on the anterior derivation of the scalp (frontopolar-central) at 180 m:

Group 0 (6 subjects): EEG not or slightly modified (less than 20% increase in theta activity);

Group 1 (15 subjects): EEG significantly modified (between 20 and 100% increase in theta activity);

Group 2 (3 subjects): EEG very modified (theta activity increase beyond 100%).

Eight subjects were selected to make the dive to 450 m: three from *Group* 0, three from *Group* 1, two from *Group* 2. Among these 8 subjects, a diver selected from each group made a dive to 180 m in He-N_2-O_2 before the dive to 450 m, to examine the eventual influence of nitrogen on the established classification. During these dives to 180 m in He-N_2-O_2, the EEG modifications are analogous to those of the He-O_2 dives in 2 out of 3 subjects (*Subject A* [BA] *Group* 0 and *Subject B* [CM] *Group* 2). A third subject (*Subject M* [PG]

Group 1) showed greater EEG modifications with this mixture than with the He-O$_2$ mixture: increase in theta activity beyond 200% on the anterior region and reaching 950% on the central region (Fig. 1).

Dives to 450 m

The dive to 450 m induced EEG modifications that appeared in certain subjects as early as 180 m.

The two subjects who showed the greatest EEG modifications at the arrival at 450 m (increase in theta activity on the order of 1000%) were those who also showed the greatest EEG modification during test dives to 180 m (*Subjects B* and *E* of *Group* 2).

Five out of six subjects of the two other groups showed EEG modifications during compression and during the stage at 450 m, but the modifications were less important than those seen in the subjects of *Group* 2 (Fig. 2).

In two subjects of *Group* 0, one notes an increase of the power of the theta activity ranging between 100 and 200%; the EEG recordings of the third subject did not vary (*Subject A* [BA]).

In two subjects of *Group* 1 the power of the theta activity increased by 100 to 300%.

The subject of *Group* 1 (*Subject H* [PG]) who had shown important EEG modifications during the test dive to 180 m in He-N$_2$-O$_2$ also showed important modifications during the dive to 450 m: increase in theta activity to 700%. Classified in Group 1 with the He-O$_2$ mixture, this subject passed to *Group* 2 when breathing the He-N$_2$-O$_2$ mixture at 180 m and 450 m.

Finally, it must be noted that the maximum increase of theta activity was measured during compression in certain subjects, while in other subjects it occurred several hours after arrival at the bottom. During the stay at the bottom, the classification of the subjects remained the same despite the lessening of the degree of EEG modification found for all the subjects.

Performance (Table I)

Sensory-motor tests. Manual dexterity for our 8 subjects decreased by 2% between the surface and 180 m (extremes of +11 to −8%), and by 10% between the second reference test at 10 m and 450 m (extremes of −5 to −15%).

The performance of reaction time decreased by 3% at 180 m (+11 to −11%) and by 6% at 450 m (+6 to −15%). The most variation occurred at the individual level: certain subjects showed even better results at 450 m than at 180 m. It is thus impossible to predict the behavior of subjects at 450 m based on variations of performance noted at 180 m.

Intellectual tests. Number-order performance lessened for each group tested: by 2% at 180 m (+16 to −16%) and by 11% at 450 m (−4 to −16%). Performance on double sign barring increased at 180 m by 2% (+11 to −25%) and decreased to 2% at 450 m (+27 to −10%). At the individual
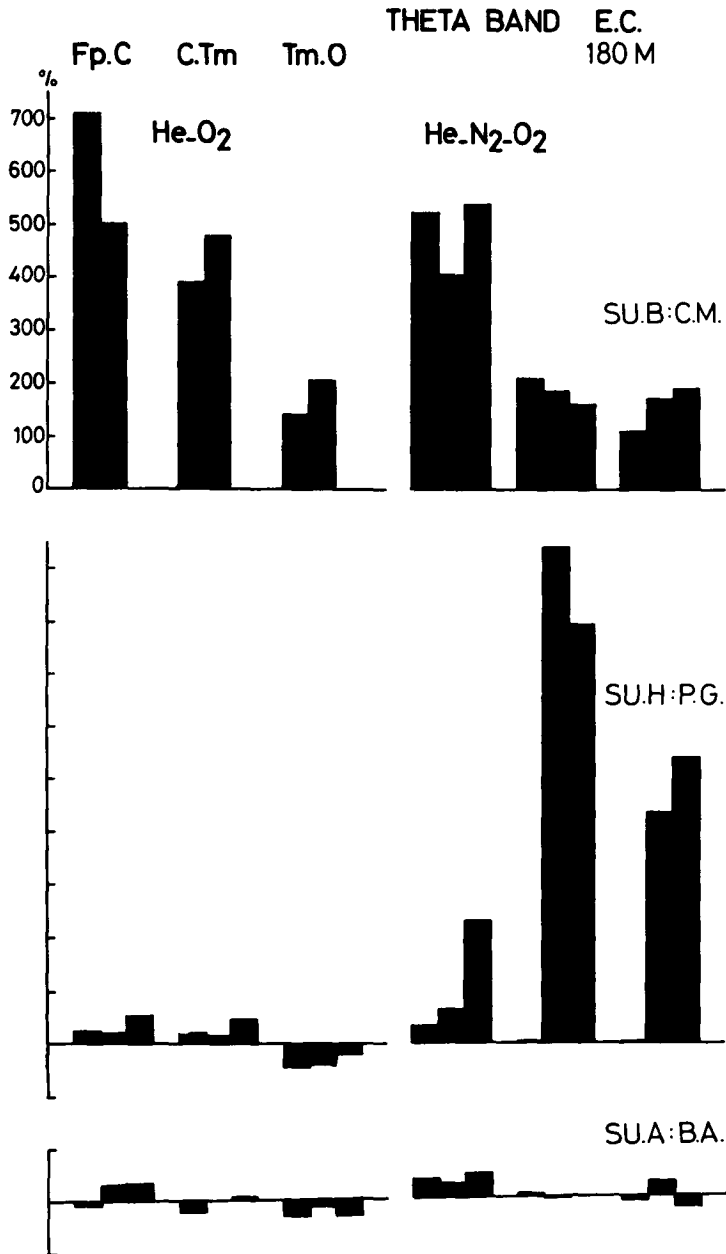
Fig. 1. Evolution of the power of EEG activities of the theta band frequency expressed in percentage of difference from mean value of surface. Three subjects are represented from top to bottom: *Group 2, Subject B* (CM); *Group 1, Subject H* (PG); *Group O, Subject A* (BA). For each subject results obtained with the He-O₂ mixture have been regrouped on the left-hand graph; the graph on the right shows results obtained with He-N₂-O₂. On each graph the variations are shown: *left*, Fp-C; *middle*, C-Tm; *right*, Tm-O. The evolution is represented for the different tests effected at 180 m (beginning, middle, and end of stay). Surface level is 0%: $\frac{(Vp-Vs)}{Vs} \times 100$.

THETA   BAND _ Fp.C _ E.C.
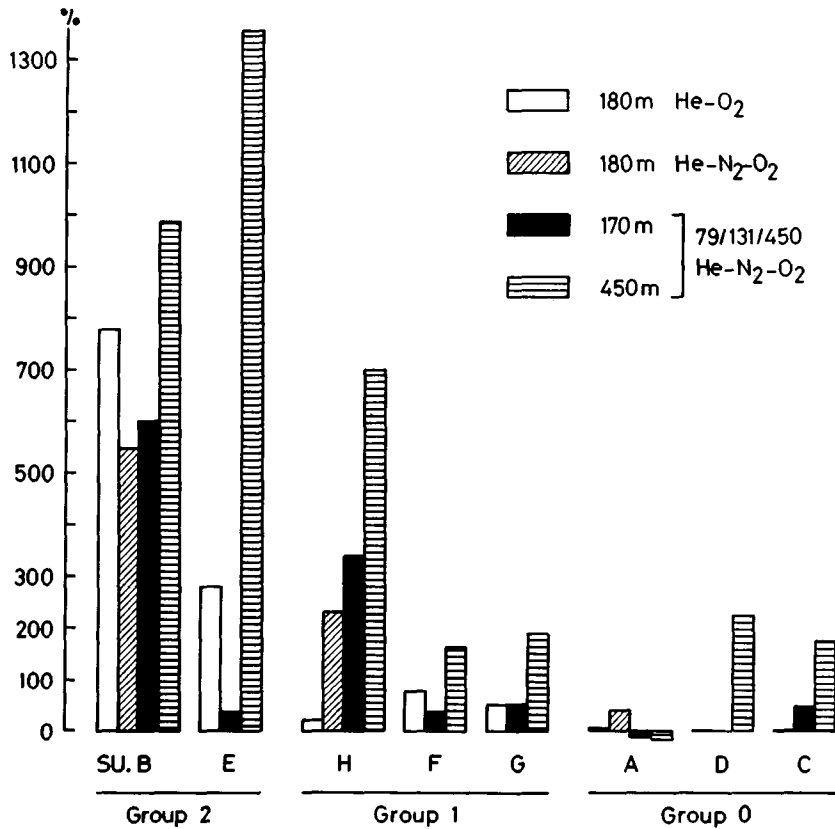
Fig. 2.   Eight subjects are represented and listed according to their classification by group. *Left: Group* 2, two subjects, *B* (CM) and *C* (MA); *center: Group* 1, three subjects *H* (PG), *F* (MT), and *G* (MM); *right: Group* O, three subjects, *A* (BA), *D* (GP), and *C* (DJM).   For each subject the histograms represent the increase in theta activity on the anterior region: at 180 m in He-O_2 (8 subjects); at 180 m in He-N_2-O_2 (3 subjects, *B, H, A*); during compression to 450 m, passage at 170 m, and upon arrival at 450 m (8 subjects).

level, the variation in performance did not necessarily depend on the depth, as it did for the sensory-motor tests.

Considering the absolute performance levels rather than the percentages of variation of performance by individual, and classing the subjects by order of performance, one notes that this order varies little between the surface, 180 m, and 450 m for each test (Table I) (*Subjects H* and *D* were not considered since they went through a different training period). If we give a grade to each subject according to his classification on each test and then establish a "general classification" for the whole of the tests, we note few modifications between the surface and 450 m. Only one subject showed a relative variation at 450 m (*Subject B*). Using the classification established from absolute values at the

TABLE I

Performances of Subject Divers at the Surface Before Each Dive at 180 m and at 450 m (explanation in text)

SURFACE	180 METRES	SURFACE	450 METRES
MANUAL DEXTERITY			
Su.G : MM 69	Su.G : MM 69	Su.G : MM 69	Su.G : MM 67
B : CM 68	E : MA 64	B : CM 68	B : CM 62
F : MT 66	F : MT 64	F : MT 66	E : MA 61
E : MA 66	B : CM 63	E : MA 66	A : BA 59
A : BA 64	C : DJM 61	A : BA 64	F : MT 57
C : DJM 55	A : BA 60	C : DJM 55	C : DJM 56
VISUAL CHOICE REACTION TIME			
Su.G : MM 37	Su.G : MM 35	Su.G : MM 37	Su.G : MM 35
A : BA 47	A : BA 40	A : BA 47	A : BA 45
E : MA 47	F : MT 50	C : DJM 47	C : DJM 47
C : DJM 47	E : MA 51	E : MA 47	B : CM 47
F : MT 51	C : DJM 54	F : MT 51	E : MA 51
B : CM 56	B : CM 61	B : CM 56	F : MT 52
NUMBER ORDINATION			
Su.E : MA 66	Su.E : MA 76	Su.E : MA 66	Su.F : MT 71
F : MT 64	F : MT 69	F : MT 64	E : MA 66
B : CM 64	B : CM 67	B : CM 64	B : CM 65
C : DJM 57	C : DJM 49	C : DJM 57	A : BA 53
G : MM 52	A : BA 49	G : MM 52	C : DJM 50
A : BA 50	G : MM 43	A : BA 50	G : MM 44
SYMBOL RECOGNITION			
Su.G : MM 5.50	Su.G : MM 7.10	Su.G : MM 5.50	Su.G : MM 5.00
F : MT 6.50	F : MT 7.20	F : MT 6.50	F : MT 6.00
A : BA 7.50	A : BA 7.30	A : BA 7.50	E : MA 6.40
E : MA 8.10	E : MA 7.30	E : MA 8.10	B : CM 6.40
B : CM 8.40	B : CM 9.00	B : CM 8.40	A : BA 6.55
C : DJM 10.50	C : DJM 10.20	C : DJM 10.50	C : DJM 7.10
TOTAL			
Su.G : MM 8	Su. G : MM 9	Su.G : MM 8	Su.G : MM 9
E : MA 10	F : MT 9	E : MA 10	B : CM 11
F : MT 12	E : MA 10	F : MT 12	E : MA 13
B : CM 15	A : BA 15	B : CM 15	F : MT 14
A : BA 16	B : CM 18	A : BA 16	A : BA 15
C : DJM 18	C : DJM 20	C : DJM 18	C : DJM 20

surface, we can then predict a classification of the subjects at 450 m using our compression methods.

DISCUSSION

A study of the EEG modifications in the eight subjects showed:

1) The subjects presenting the most marked EEG modifications at 180 m in He-O_2 (*Group* 2) likewise showed the greatest modifications at 450 m in He-N_2-O_2.

2) The subjects of the two other groups (0 and 1) showed average increase in their slow-wave activity at 450 m but their EEG recordings remained the least sensitive to the hyperbaric conditions.

3) The EEG of one subject varied in a different manner according to the breathing mixture: his EEG recordings showed average modification at 180 m in He-O_2, but significant modification at 180 m in He-N_2-O_2 and at 450 m in He-N-O_2.

This last result can be added to observations made during dives in He-N_2-O_2 concerning the reinforcement of theta activity in certain subjects when the mixture contains nitrogen (9,10). This poses the problem of the test dives: it would probably be preferable to carry out the tests at 180 m with a respiratory mixture analogous to that to be used during the very deep dive.

The latency of appearance of the EEG modifications varied from subject to subject. Certain subjects are more sensitive to compression, others to the composition of the gas mixture, and others to the pressure. The principal hyperbaric variables thus act independently on the structures of the nervous system that are responsible for the genesis of the EEG and are sensitive to it. This brings about variations in HPNS symptomatology depending upon the conditions of the dive and according to the subject (6).

For the psychometric tests, the classification of subjects established at the surface as a function of the absolute performance levels varied little at 180 and 450 m. At the group level, the average performance variations depended upon the depth and it was possible to predict a lessening of performance at 450 m. At the individual level, however, this prediction is not possible.

It must be noted that there is no strict relationship between the degree of psychometric deficiency and the increase in EEG modifications. This absence of correlation between the psychometric results and the EEG modifications, which has already been reported (11), brings up the problems of significance and importance of certain HPNS symptoms that we have considered in this study. However, a functional alteration of the nervous system can be masked by the effort made by the subject to accomplish a task. This possibility obliges us to be careful in the interpretation of the data in one direction as well as the other.

In conclusion, this first experimental approach destined to establish criteria for selection in deep diving has thus shown:

1) For the psychometric tests there is a significant interindividual variability at the surface and at 180 m, which will not allow one to predict the behavior of a subject at 450 m.

2) On the other hand, the EEG modifications can be predicted at 450 m from the data of a dive to 180 m effected with rapid compression, given an analogous respiratory mixture.

3) What remains to be defined is the characteristic that could be the most useful in selecting not only the best divers to already-explored depths, especially those between 300 and 600 m, but also those divers who would be most HPNS-resistant at greater depths. It would be tempting to ignore the EEG symptoms if the performance remained good; however, on the basis of data gathered from primates at great depths an epileptic seizure can be anticipated, and it is possible that the oncoming seizure would be detected only by the EEG signs and thereby prevented.

Acknowledgment

References

1. Brauer RW, Dimov S, Fructus X, Gosset A, Naquet R. Syndrome neurologique et électrographique des hautes pressions. Rev Neurol 1969;121:264–265.
2. Bennett PB, Towse EJ. Performance efficiency of men breathing oxygen-helium at depths between 100 feet and 1500 feet. Aerosp Med 1971;42:1147–1156.
3. Fructus X, Brauer RW, Naquet R. Physiological effects observed in the course of simulated deep chamber dives to a maximum of 36.5 atm in helium-oxygen atm. In: Lambertsen CJ, ed. Underwater physiology. Proceedings of the fourth symposium on underwater physiology. New York: Academic Press, 1971:545-550.
4. Rostain JC, Naquet R. Le Syndrome Nerveux des Hautes Pressions: caractéristiques et évolution en fonction de divers modes de compression. Rev EEG Neurophysiol 1974;4:107–124.
5. Rostain JC, Naquet R. Human neurophysiological data obtained from two simulated dives to a depth of 610 meters. In: Shilling CW, Beckett MW, eds. Underwater physiology VI. Proceedings of the sixth symposium on underwater physiology. Bethesda, MD: Federation of American Societies for Experimental Biology, 1978:9–19.
6. Rostain JC. Le Syndrome Nerveux des Hautes Pressions chez l'homme et le singe *Papio papio*. Thèse de doctorat es-sciences naturelles. Université d'Aix-Marseille I, 1980.
7. Rostain JC, Gardette B, Gardette MC, Dumas JC. HPNS of baboon Papio papio during slow exponential compression with N_2 injection to 1000 msw and beyond. Undersea Biomed Res 1979;6(Suppl):45.
8. Rostain JC, Gardette B, Gardette-Chauffour MC, Naquet R. HPNS in humans during 38 h compression to 450 m with N_2 injections. In: Program, abstracts, and mini-papers. The Undersea Medical Society annual scientific meeting (abstracts), 7th symposium on underwater physiology. Bethesda, MD: Undersea Medical Society, 1980:16.
9. Rostain JC, Naquet R, Fructus X. Study of the effects of "trimix" and "heliox" mixtures during rapid compression. Undersea Biomed Res 1976;3:A13–A14.
10. Rostain JC, Gardette-Chauffour MC, Naquet R. HPNS during rapid compression of men breathing He-O_2 and He-N_2-O_2 at 300 m and 180 m. Undersea Biomed Res 1980;7:77–94.
11. Rostain JC, Charpy JP. Effects upon the EEG of psychometric performance during deep dives in helium-oxygen atmosphere. Electroencephalogr Clin Neurophysiol 1976;40:571–584.

Part IV

OXYGEN SUFFICIENCY AND UTILIZATION WITHIN
THE CELL

CURRENT CONCEPTS OF OXYGEN SUFFICIENCY AND UTILIZATION WITHIN THE CELL

F. F. Jöbsis

The appropriate provision of oxygen to the human organism in stress or distress has been a central concern of many generations of athletes and their coaches, patients and their physicians, as well as assorted scientists and their sponsors. In no other situation is this concern more acute than in the underwater environment. What makes the issue especially complex is the realization, achieved some one hundred years ago, that administration of air under pressure could lead to serious pathological consequences. These were found to be at least twofold: the deleterious effects of pressure per se and those of elevated partial pressures of oxygen. The concept of oxygen toxicity led, of course, to twin questions about management and mechanism.

In practical terms too much oxygen is just as deleterious as too little. To date management towards appropriate oxygen provision is a health-care field of definite yet complex and somewhat unsatisfactory accomplishment, because our knowledge is almost totally based on empirical findings. Questions concerning the mechanism of oxygen toxicity are part of the larger question concerning the mechanism of the oxygen reactions in the body, specifically, the utilization at the cellular level in normoxia, hypoxia, and, conversely, in hyperoxia. It is somewhat disconcerting that several gaps exist in our understanding of these processes, especially at the intracellular level. Therefore, it is useful for us to survey the background information briefly, to delineate the status quo of the less well understood or totally unknown areas in the field, and to outline the possible directions to take towards a better understanding.

THE PHYSIOLOGICAL QUESTION

It is the purpose of this session to report on some of the more recent developments and achievements in our understanding of oxygen delivery and utilization in the intracellular milieu. Delivery is, of course, the *sine qua non* of the entire business of oxidative metabolism. Some of the work to be reported is of great beauty and importance: clearly, we are getting significantly closer to a detailed understanding of the events at the level of the capillary bed. We were and are still somewhat in the dark on this issue especially in terms of microvascular control mechanisms. But the new insights signify great strides in our understanding.

Nevertheless, we are stymied by two incontrovertible facts. First, in the management of the entire organism, especially human subjects, we cannot make these observations on capillary oxygen delivery routinely. More indirect data must be extrapolated for interpretation at that level. Commonly these data are bloodflow and oxygen extraction at the level of the entire organ or at best regions thereof; thus maladjustments in localized areas cannot be detected. Second and more fundamental, the appropriate *utilization* of oxygen, not its delivery, is physiologically more significant.

To illustrate by a few examples, we should consider the fact that the venous Po_2 of the effluent from most major organs is in the range of 30-40 Torr. Yet measurements with microelectrodes of the tissue Po_2 show a range of values under normoxic conditions from practically zero to those equalling the arterial Po_2. Hypoxic episodes result in a relative shift of the statistical distribution towards lower values. Thus the mixed venous Po_2 of the effluent is a very insensitive signal concerning the possible plight of micro or semimicro areas of the organ. In addition, many organs possess so-called shunt vessels, diverting part of the flow away from the cells. Changes in the fraction of the total blood supply flowing through these vessels will produce totally misleading conclusions concerning the adequacy of oxygen provision by sampling the venous efflux. Then there are the occurrences of toxic poisoning, such as by cyanide or carbon monoxide, of the enzyme(s) catalyzing the oxygen utilization reaction. Signals relevant to oxygen *delivery* are not germane in such cases.

As a final example consider the blood-flow approach. Much progress has been made in measuring regional blood flow noninvasively, specifically in the cerebral cortical circulation, by the radioactive Xenon technique. In this approach brief inhalation of Xe^{14} leads to radioactivity in the organ which can be monitored externally. The time course of its appearance and disappearance can be quantitatively related to the local blood flow. Conclusions concerning local oxidative metabolism are routinely made from such data. The reasoning is based on the assumption that autoregulation will adjust blood flow to provide sufficient oxygen delivery for varying levels of metabolism. Thus regional blood flow is used as an index to regional oxidative metabolism. This approach appears to be correct when all other parameters are constant and the subject is in good health. However, when the circulation is disturbed by high Pco_2 or Pa_{o_2} levels by whatever cause or when brain pathology is present, the

correlation between local circulation and metabolism breaks down. In these situations accurate information is essential.

The physiological question remains, "What is the condition of the oxidative metabolism as it is taking place in the intracellular milieu?" Although unanswerable by the classic methodologies, this question is emphatically the center of our concern. Therefore, we will review the status quo of our knowledge in this area and point to new techniques that promise to provide information in a more direct manner than heretofore.

THE BIOCHEMICAL BACKGROUND

The great majority of oxygen utilization in the animal organism is handled by the enzyme cytochrome c oxidase, also referred to as cytochrome a,a_3. This is the terminal member of a sequence of redox couples, enzymes which transfer electrons from the substrates to oxygen and finally result in the production of H_2O. A highly simplified diagram is shown in Fig. 1 (ref. 1). These redox components are systematically arranged on or within the inner membrane of the mitochondria, small intracellular granules found in practically all cells of animal organisms and in most plants. Within the respiratory chain, as this arrangement is called, electron transfer takes place from components with more negative redox potentials to more positive redox potentials until finally the span from minus 320 mV of the coenzyme nicotinamide adenine dinucleotide (NAD) to cytochrome c oxidase, at approximately 500 mV positive, has been traversed. The final reaction between the reduced, i.e., electron containing, cytochrome a_3 and oxygen spans the final 300 mV to the redox potential of oxygen at +800 mV. This array of components can be graphically arranged according to their redox potentials as shown in Fig. 2, which is taken from the clear and incisive review of Wilson et al. (2).

The overall reaction of the respiratory chain could be written O_2 + 4 H → $2H_2O$ or more correctly, O_2 + $4e^-$ + 4 H^+ → $2H_2O$ + energy. Both the electrons and the hydrogen ions are formally derived from the substrates, i.e.,
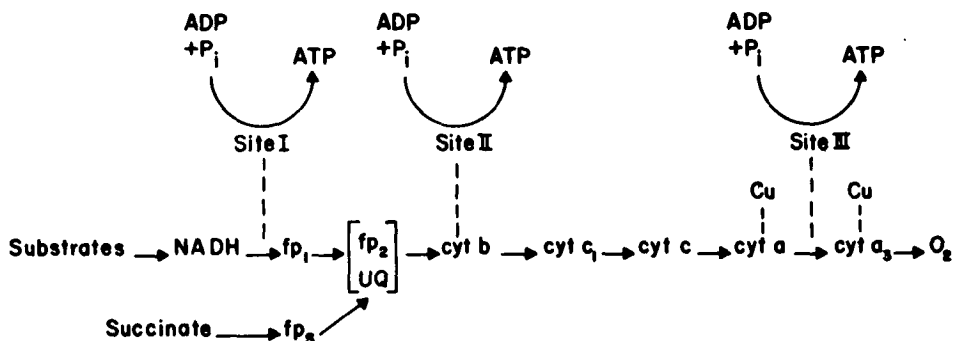

Fig. 1. The respiratory chain and oxidative phosphorylation sites; a simplified diagram (from ref 1; reprinted with permission from Am Rev Resp Dis).
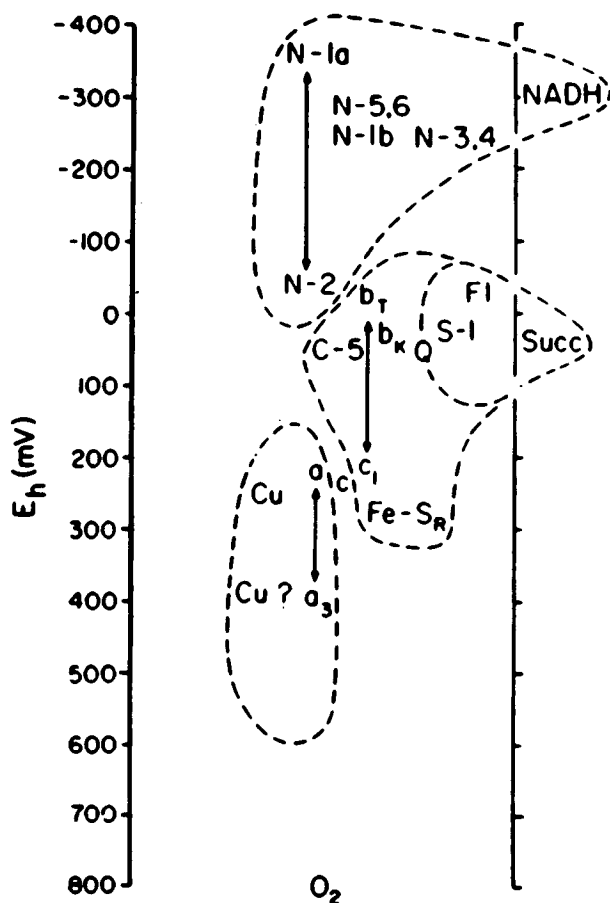
Fig. 2.   Redox potential range of the respiratory chain components, ranged in the three major subgroups (from ref 2; reproduced with permission, from the Ann Rev Biophys Bioeng, Vol. 3. Copyright 1974 by Annual Reviews Inc.).

breakdown products, of ingested foodstuffs. The free energy resulting from the difference in potential energy between the reduced form of NAD (NADH) and H_2O, the final product of the oxidative reaction, is conserved in a number of steps in the respiratory chain in a most complex manner. According to the current point of view, the passage of electrons down the respiratory chain is accompanied by extrusion of hydrogen ions from the intramitochondrial compartment to the extramitochondrial, i.e., cytoplasmic, compartment (3, 4). This activity produces an electrochemical gradient which is utilized in the formation of adenosine triphosphate (ATP) from adenosine diphosphate (ADP) and inorganic phosphate (P_i) (Fig. 3, ref. 5). Adenosine triphosphate, a so-called high-energy phosphate compound, travels by diffusion from the mitochondria to all parts of the cell and is utilized in the performance of physiological or biochemical work such as the contraction of muscles, the transport of ions, or the synthesis of cellular constituents. Adenosine diphosphate and P_i then return to the mitochondria and are rephosphorylated to ATP.

H⁺
NADH — S
2H — NAD⁺ — SH₂
2H⁺
2e
2H⁺
2H
2H⁺
2e
2H⁺
2H
2H⁺
2e
½ O₂ + 2H⁺
H₂O
F₁
o   i

MITCHELL 'LOOPS'

QH₂
2H⁺ — Q — 2e — b
2e
b — 2H⁺
Fe-S — 2e+2H⁺
2H⁺ — 2e+2H⁺
c₁
2H⁺ — c — 2e
F₁

FEASIBLE MITCHELL LOOP 2

o   i
F₁ — ATP
ADP+P₁
H⁺ — H⁺
e⁻ → O₂
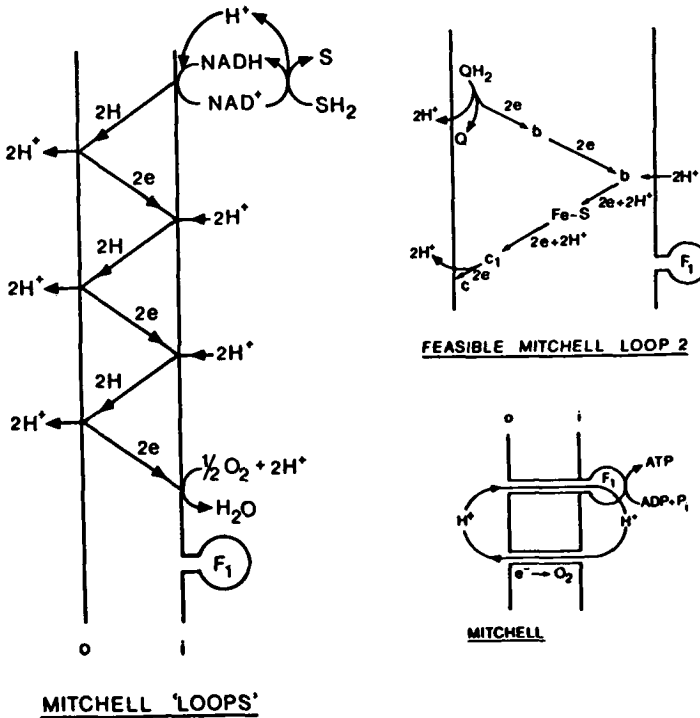
MITCHELL

Fig. 3. Simplified diagram of the chemiosmotic theory of Mitchell. *Left* and *upper right* depict possible mechanisms for respiratory chain transfer of hydrogen ions across the mitochondrial membrane.   *Lower right:* a hypothetical mechanism for phosphorylation of ADP through a coupling site (F_1) by means of a hydrogen ion gradient. (Adapted from Slater (5), reprinted with permission from Professional Information Library, Dallas, Texas.)

Although considerable work still needs to be performed to understand the exact mechanism of energy conservation, biochemists agree that most of the benefit for the energy economy of the cell is derived from these so-called oxidative phosphorylation reactions, perhaps as much as 95% of the total energy budget. This set of reactions is, therefore, the crux of the entire oxidative metabolic scheme. They are of the utmost importance for the function and survival of the cell.

Cytochrome c oxidase can perhaps be singled out as the most crucial enzyme and therefore is directly informative of oxidative metabolism. Aside from malfunction or the occurrence of Po_2 insufficient for the enzyme to function, evidence is accumulating that the reaction of cytochrome c oxidase with oxygen is sensitive to fluctuations in the oxygen supply; this sensitivity has been observed both in the range of conditions to which people might be exposed routinely and especially under hyperbaric conditions (6), even in the range where oxygen toxicity is not considered to occur. Therefore, the obvious need at the moment is to establish measurements of the behavior of the enzyme system in conditions of normoxia, hypoxia, or hyperbarically produced hyperoxia.

NONINVASIVE MONITORING OF INTRACELLULAR METABOLISM

What is needed then is a direct assessment of the functional state of the above metabolic pathways in the undisturbed intracellular milieu. The main constraint is the need to make the measurements in a totally noninvasive way, yet sufficiently specific for incisive conclusions and rapidly enough to provide opportunity for corrective action. As a further practical consideration some redundancy of signals would greatly boost confidence in the determination and would strengthen the conclusions.

At this time two methodologies appear promising. One of these, the nuclear magnetic resonance (NMR) technique, is able to provide information concerning the concentrations of certain cellular metabolites (7). Most importantly for our purposes, phosphate compounds such as ATP and ADP as well as P_i can be assessed by altering a powerful magnetic field surrounding the tissue, organ, or body part under investigation. The information is specific as to the identity of the molecule and its concentration and, in addition, the P_i signal provides an assessment of the intracellular pH condition, a parameter of some importance in pathological situations. Because the ATP falls and P_i rises when low oxygen levels prevent the occurrence of oxidative phosphorylation, the signal is highly relevant and specific. Hypoxia would also affect the concentrations of other detectable phosphate compounds, and their signals would provide useful redundancy. However, at the moment the time resolution is not rapid enough for optimal application to life-threatening situations or events, although theoretically this can be improved as required in further technological developments. More fundamental drawbacks are the large bulk of the magnets required for the measurements and the high cost of the instrumentation. It appears, however, that the NMR technique will be a useful research tool and may become extremely decisive as a diagnostic method for chronic or semi-chronic pathological conditions.

The other promising technique is an optical one that determines directly the redox state of cytochrome c oxidase and concomitantly provides information on the venous-arterial steady state of the blood and on the volume of blood in the organ under study. This redundancy, a time resolution of seconds or less and the modest size and cost in addition to the high specificity of the information concerning oxygen sufficiency make this approach a promising one for routine, bedside, or even ambulatory applications (8).

Since the first description of the cytochromes, researchers have taken advantage of the fact that these compounds absorb light differently when oxidized (not containing a free electron) than when reduced (containing an electron) (Fig. 4, ref 9). Spectrophotometric techniques have therefore been extremely useful in the assessment of cellular metabolism using monochromatic light as a probe (10). Until recently the technique was limited to exposed or excised organs. However, in 1977 it was found that signals can be obtained without surgical exposure by light in the near infrared range because of the deep penetration of this radiation into biological tissues. The primary signal for the new monitoring technique is related to the oxidation state of cytochrome a,a_3. The technique is founded on the fact that the enzyme absorbs
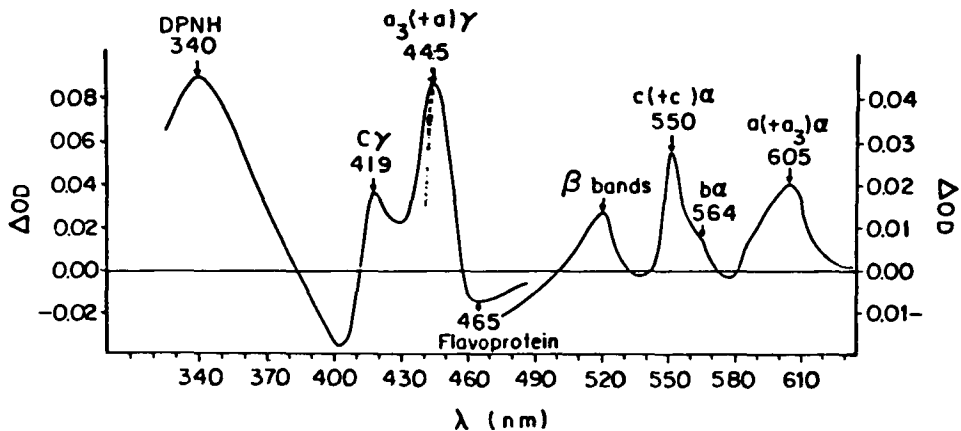
Fig. 4. Anoxic (N_2) minus oxygenated (100% O_2) difference spectrum from toad sartorius muscle at 20°C (from ref. 9; reprinted with permission from Jöbsis FF, J Gen Physiol 1963; 46:905–969).

light in the near infrared region when it is oxidized but not when it is reduced. Thus, the optical density of tissues is affected when insufficient oxygen produces an accumulation of electrons in the enzyme. When oxygen levels decline, more and more enzyme molecules in the tissue become reduced; the result is a decrease of optical density in the tissue, which is externally detectable using specific wavelengths of near-infrared light (8). In addition, hemoglobin also absorbs at somewhat different wavelengths in the same spectral region. Because these absorption bands also change depending on whether or not the hemoglobin is oxygenated, one can monitor the venous-to-arterial ratio and the total blood volume as ancillary information, which is useful in the interpretation of the cytochrome signals.

Most experimental results are presently limited to animal studies, although application to monitoring of healthy volunteers has been performed on a small scale with encouraging results (12). In the animal experiments the entire head is transilluminated from temple to temple while the animal is exposed to temporary hypoxia (Figs. 5 A & B, ref. 8), or hyperoxia with or without hypercarbia (Fig. 6, ref. 12). The results show the expected spectral changes for the redox variations of cytochrome c oxidase and hemoglobin oxygenation state. These results were satisfactorily supported by spectral analysis in the wavelength range of 720-880 nm during steady-state conditions. Ongoing studies with experimental stroke models show the applicability of the technique to pathophysiological situations.

Some preliminary results on human volunteers during hyperventilation and hyperoxia plus hypercarbia are shown in Figs. 7 and 8 (ref. 12). For these studies a reflection technique rather than transillumination was used. Further development of the technique toward instrumentation for experimental research and for routine applications for patient care is presently underway.

A

760-815 nm

↑HbO₂ disoxygenation

Respirator

↑Off   On↓   ┝─ 2 minutes ─┥   ↑
                                                                                  ΔAbs 40%
                                                                                       ↓

815 nm feedback

↑ Less blood in
  transilluminated field

                                                                  Blood pressure
                                                                  ─200 mm Hg

                                                                  ─80
                                                                  ─0

B

840-815 nm

↓a,a₃ reduction

              ↑Off   Respirator   On↓   ┝─ 2 minutes ─┥   ↑
                                                                       ΔAbs 10%
                                                                            ↓

815 nm feedback

↑ Less blood in
  transilluminated field

                                                                  Blood pressure
                                                                  ─200 mm Hg

                                                                  ─80
                                                                  ─40
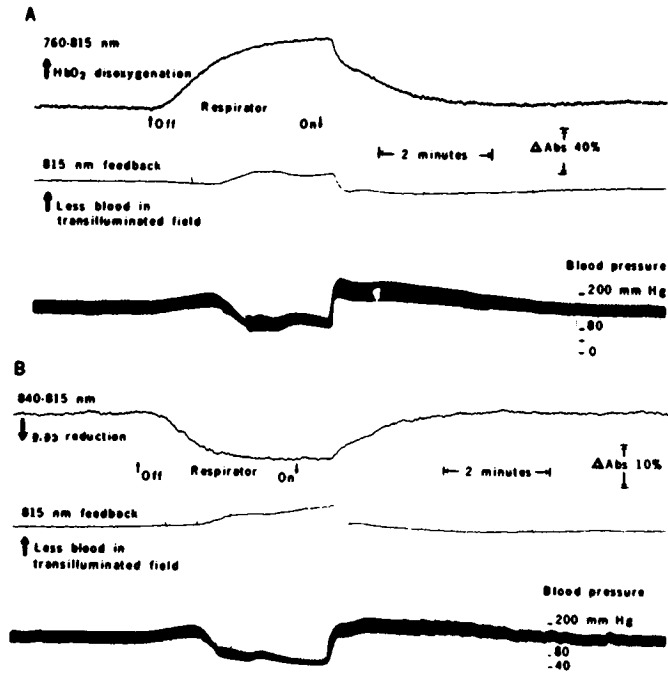
Fig. 5.   Time course of the responses to hypoxic episodes of intracranial hemoglobin and blood volume (A) and of cerebral cytochrome a,a_3 (B) in a transilluminated cat's head (from ref 8; reprinted from Jöbsis FF, Science 1977; 198:1264–1266. Copyright 1977 by the American Association for the Advancement of Science).
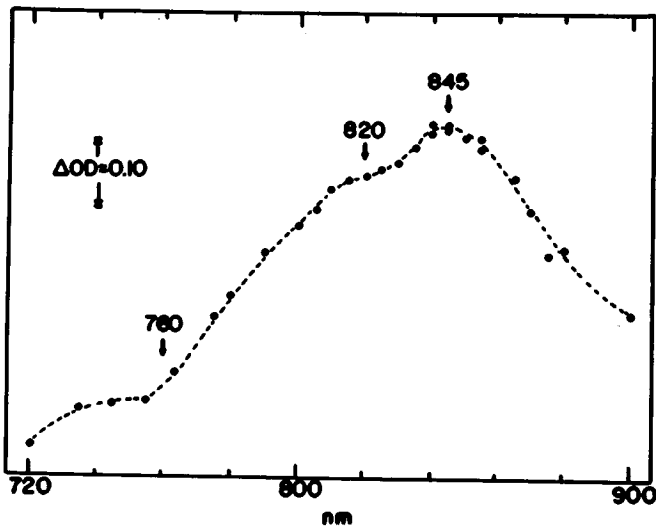
Fig. 6.   Oxidation of the copper bands, Cu_H at approx. 820 nm and Cu_L at approx. 845 nm, in an unexposed cat's brain. The spectrum is recorded as the difference between a hypercapnic, hyperoxic state as baseline and a hypocapnic normoxic state produced by hyperventilation with room air (from ref 12; reprinted from Jöbsis FF, Adv Neurol 1979:26;299–318, Raven Press, Publishers/New York).
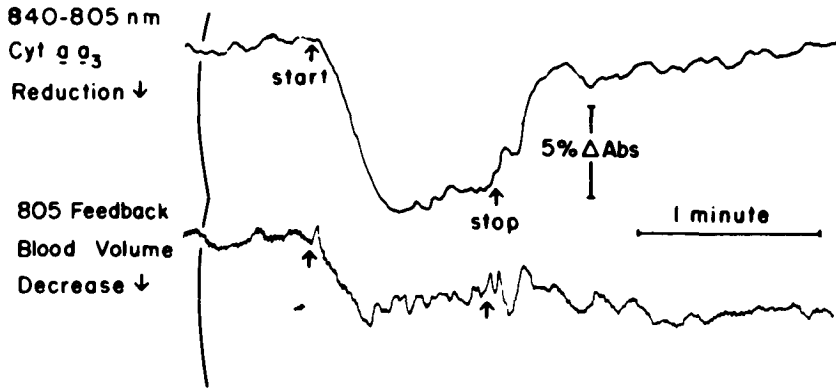
Fig. 7. Continuous monitoring of cytochrome c oxidase oxidation and blood volume decrease during voluntary hyperventilation by the healthy, volunteer subject. Reflectance mode using analog detection (from ref 12; reprinted from Jöbsis FF, Adv Neurol 1979:26;299–318, Raven Press, Publishers/New York).
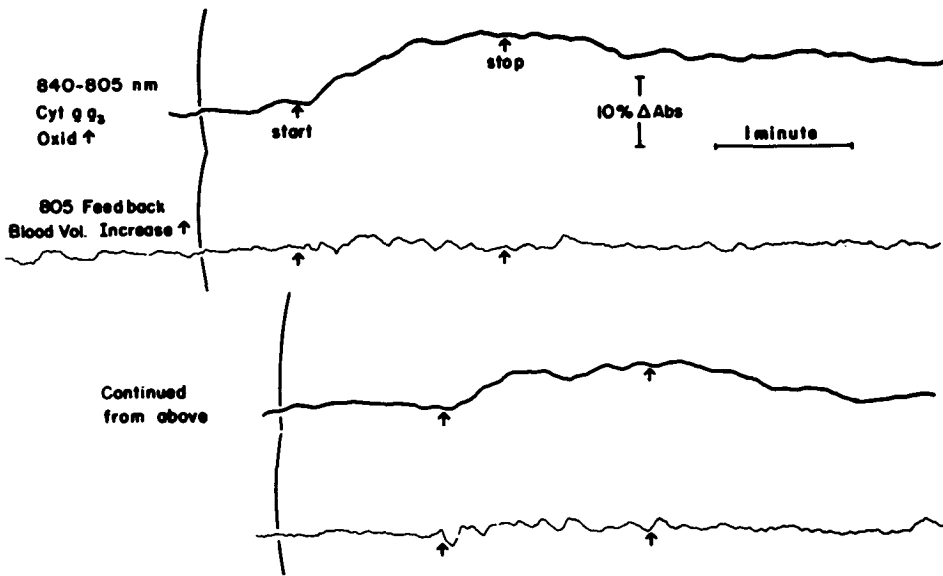

Fig. 8. Reflectance mode monitoring of the effects of inspiring 95% O_2 plus 5% CO_2 for two 90-s periods. During the control periods the subject breathed room air (from ref 12; reprinted from Jöbsis FF; Adv Neurol 1979:26;299–318, Raven Press, Publishers/New York).

CONCLUSION

At the moment it appears that emphasis may be shifting from studies of blood flow, arterial-venous differences, and respiratory variables toward direct observations on the metabolic pathways handling oxygen and producing free-

energy compounds for cell metabolism. The results of the old and new approaches can be expected to complement each other in our search for a better understanding of the role of oxygen for appropriate physiological function.

References

1. Jöbsis FF. Intracellular metabolism of oxygen. Am Rev Respir Dis 1974;6:58–63.
2. Wilson DF, Erecinska M, Dutton PL. Thermodynamic relationships in mitochondrial oxidative phosphorylation. Ann Rev Biophys Bioeng 1974;3:203–230.
3. Mitchell P. Coupling of phosphorylation to electron and hydrogen transfer by a chemi-osmotic type of mechanism. Nature 1961;191:144–148.
4. Mitchell P. Keilin's respiratory chain concept and its chemiosmotic consequences. Science 1979;206:1148–1159.
5. Slater EC. Energy conservation in the respiratory chain. In: Jöbsis FF, ed. Oxygen and Physiological Function. Dallas: Professional Information Library, 1977:39–53.
6. Rosenthal M, LaManna JC, Jöbsis FF, Levasseur JE, Kontos HA, Patterson JL. Effects of respiratory gases in intact cerebral cortex. Is there a critical Po_2? Brain Res 1976;108:143–154.
7. Radda GK, Seeley PJ. Recent studies on cellular metabolism by nuclear magnetic resonance. Ann Rev Physiol 1979;41:749–769.
8. Jöbsis FF. Noninvasive, infrared monitoring of cerebral and myocardial oxygen sufficiency and circulatory parameters. Science 1977;198:1264–1267.
9. Jöbsis FF. Spectrophotometric studies on intact muscle. J Gen Physiol 1963;46:905–969.
10. Chance B, Williams GR. Respiratory enzymes in oxidative phosphorylation. I. Kinetics of oxygen utilization. J Biol Chem 1955;217:383–393.
11. Wharton DC, Tzagolof A. Studies on the electron transfer system. LVII. The near infrared absorption band of cytochrome oxidase. J Biol Chem 1964;239:2036–2041.
12. Jöbsis FF. Oxidative metabolic effects of cerebral hypoxia. Adv Neurol 1979;26:299–318.

APPLICATIONS OF AORTIC BODY AND CAROTID BODY CHEMORECEPTORS AS INTERNAL PROBES TO MONITOR TISSUE OXYGENATION

S. Lahiri

It is often the inability of cells and tissues to use oxygen that leads to failure of their physiological functions under conditions of extreme environmental stress. Measurement of tissue oxygenation by both external and internal probes is a useful guide to the underlying mechanism of such failures. Oxygen-sensing receptors present in carotid and aortic bodies in mammals may be considered as a class of internal probes that generate nerve action potentials when arterial Po_2 decreases. To use the activity of these receptors as an index of tissue Po_2, one must document and understand the response patterns of these receptors to various forms of oxygen insufficiencies. This paper deals with some aspects of these properties of chemoreceptors in aortic and carotid bodies. The results show that chemoreceptors in the two locations as a rule respond differently to different forms of oxygen insufficiency: aortic body chemoreceptors respond to circulatory transport, whereas carotid body chemoreceptors respond to respiratory transport of oxygen. Accordingly, aortic chemoreceptors may monitor circulation and carotid chemoreceptors respiration.

METHODS AND MATERIALS

Anesthetized cats were used in this study of peripheral chemoreceptors as described previously (1,2). Briefly, cats were anesthetized with α-chloralose (60 $mg \cdot kg^{-1}$), paralyzed by gallamine (3 $mg \cdot kg^{-1}$), and ventilated artificially. The left carotid sinus nerve and left aortic nerve were exposed medially and cut. The peripheral ends of these nerves were desheathed, fine filaments separated, and chemoreceptor afferents identified by the specific tests (1,2). Single

457

or a few clearly identifiable receptors were monitored and counted. End-tidal P_{O_2} and P_{CO_2} were monitored and either maintained constant or altered by manipulating the inspired gases. Arterial blood pressure was measured continuously. A femoral venous catheter was used for saline and drug administration. In some animals a balloon catheter was introduced in the thoracic vena cava to block venous return partially.

While the activity of chemoreceptor afferents from aortic and carotid bodies was monitored, arterial oxygen flow was manipulated by one of four methods.

1) *Lowering* Pa_{O_2}. This reduced the dissolved and bound O_2.

2) *Carboxyhemoglobinemia*. This decreased oxygen bound to hemoglobin, increasing its affinity for oxygen at a given Pa_{O_2}.

3) *Anemia*. Anemia decreased red blood cell concentration and, hence, arterial oxygen content at a given Pa_{O_2}.

4) *Hypotension*. Lower blood pressure decreased arterial blood flow, and, hence, oxygen flow to the aortic and carotid bodies.

RESULTS

Figure 1 shows the effects of decreased $O_2Hb\%$ on chemoreceptor activity in aortic and carotid bodies. The discharge rates of aortic body and carotid body chemoreceptors were measured simultaneously under conditions of de-
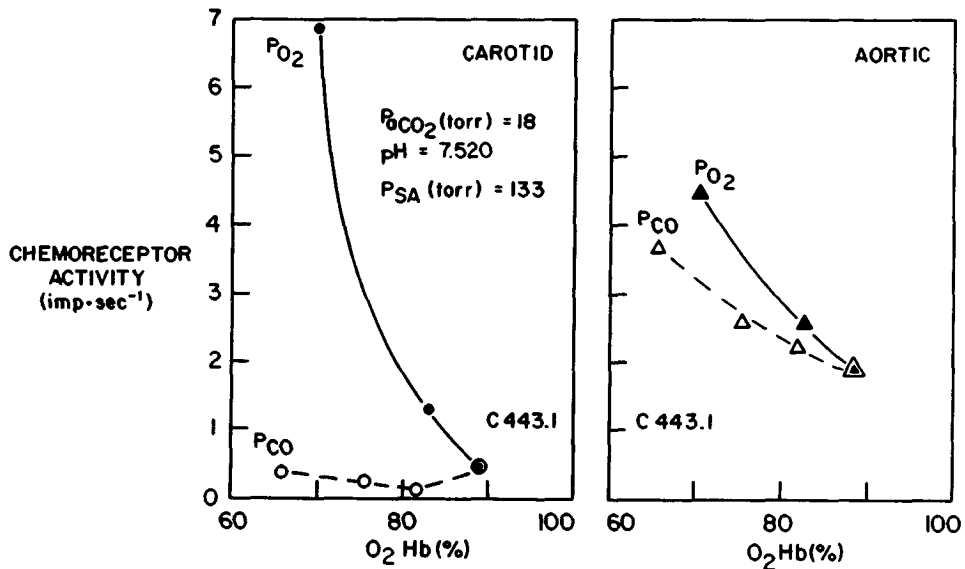
Fig. 1. The relative effects of $O_2Hb\%$ decrease by hypoxemia (P_{O_2} mediated) and carboxyhemoglobinemia (P_{CO} mediated) on aortic body and carotid body chemoreceptor activity.

creased Pa_{O_2} and increased PCO at a Pa_{O_2} of 80 Torr. In each case, single chemoreceptors were counted. Hypoxia-induced reduction of O_2Hb to 70% resulted in a sharp increase in carotid-chemoreceptor activity whereas a reduction to 66% by PCO caused no increase in the chemoreceptor activity. Thus, the carotid chemoreceptor tissue PO_2 was not altered by oxygen content, presumably because it was not constrained by oxygen delivery and was in dynamic equilibrium with the arterial PO_2. This demonstration leaves no doubt that it is the PO_2 not the $O_2Hb\%$ that is associated with carotid chemoreceptor stimulation. A decrease in $O_2Hb\%$ per se presumably did not lower tissue PO_2 to stimulate the receptors.

On the other hand, $O_2Hb\%$ reduction by both hypoxia and carbon monoxide stimulated aortic body chemoreceptors. For the same reduction of $O_2Hb\%$, however, the response to PO_2 was greater than that to PCO. Thus, $O_2Hb\%$ is not the common link between PO_2 and PCO for the chemoreceptor stimulation. However, a decrease in $O_2Hb\%$ presumably lowered aortic chemoreceptor tissue PO_2 because a high Pa_{O_2} attentuated the response at the same reduced $O_2Hb\%$. Nonetheless, there is a distinction between the phenomena in the two organs.

This distinction is further seen in the effects of isovolemic anemia on aortic and carotid chemoreceptor activity. A set of data on simultaneously measured aortic and carotid chemoreceptor activity is given in Table I. Hematocrit was decreased in successive steps from 43 to 13%. At each level of hemotocrit the activity during hypoxia ($Pa_{O_2} \simeq 50$ Torr) and hyperoxia ($Pa_{O_2} \simeq 400$ Torr)

TABLE I

Relationship between Hematocrit and Chemoreceptor
Discharge Rates

Pa_{O_2} (Torr)	Hematocrit (%)	Chemoreceptor Activity ($imp \cdot s^{-1}$)	
		Aortic	Carotid
50	43	2.10	4.05
450		0.00	0.10
50	33	2.05	4.10
450		0.03	0.15
50	21	2.50	4.00
450		0.05	0.10
50	17	2.60	3.80
450		0.15	0.15
50	13	3.65	3.5
450		0.20	0.2
50	10	5.55	3.20
450		0.50	0.20

is shown. Anemia did not stimulate carotid chemoreceptors at any of these levels of Pa_{O_2}, although hyperoxia diminished the activity. On the other hand, aortic chemoreceptor activity increased with anemia during hypoxia. Hyperoxia attenuated this response. Thus, unlike the carotid chemoreceptor, the aortic chemoreceptor was stimulated by a decrease in oxygen content. The effect of hyperoxia was, presumably, not due to an increase in the dissolved oxygen, but to an increase in tissue Po_2 in each case. This indicates that aortic body tissue Po_2 was diminished by a decrease in oxygen content.

From these observations and with certain assumptions regarding blood flow based on the previous reports (3–6), oxygen delivery to aortic body and carotid body chemoreceptors was calculated. The relationship between oxygen delivery and the respective chemoreceptor activity is depicted in Fig. 2. It shows that there is little increase in carotid chemoreceptor activity when oxygen delivery is reduced. Similar decreases in oxygen delivery at any Pa_{O_2} led to significant increases in the aortic chemoreceptor activity.

Thus, small decreases in oxygen flow caused by any of the above constraints stimulated aortic body chemoreceptors; this fact indicates that hemoglobin-bound oxygen participated in the maintenance of the receptor Po_2 level. All carotid body chemoreceptors were stimulated by a lowered Pa_{O_2} but most of them were not stimulated by moderate carboxyhemoglobinemia or anemia. These data indicate that a relatively large blood flow through the carotid body keeps the receptor Po_2 unchanged in spite of large decreases in the total oxygen delivery to the carotid body receptor tissue.

The idea regarding a difference in blood flow rate between the organs can be tested by recording the effect of arterial blood pressure changes on the respective chemoreceptor activity (shown in Fig. 3). The activities of aortic and carotid chemoreceptors were recorded simultaneously. The effects of blood gas changes induced by asphyxia were recorded first. The respirator was stopped for about 30 s, during which period Pa_{O_2} decreased and Pa_{CO_2} increased. Within 3 s carotid chemoreceptor activity increased, whereas about 13 s were required for the aortic chemoreceptors to show a response. With the reinitiation of respiration, carotid chemoreceptor activity began to decrease promptly but there was a delay in the aortic chemoreceptor response.

The longer latency of response of aortic body chemoreceptors to changes in the alveolar gas composition and blood chemistry is consistent with our earlier report (6). The same chemoreceptors showed a different response to hypotension: carotid chemoreceptor activity remained practically unchanged while aortic chemoreceptor activity began to increase immediately following hypotension, although alveolar Po_2 increased and Pco_2 decreased. After termination of hypotension, the aortic chemoreceptor activity diminished sharply and promptly. The systemic hypotension caused by a decreased venous return caused two major changes with respect to aortic and carotid bodies: a) a decreased perfusion pressure and, hence, a decreased blood flow; and b) a decrease in the arterial stimulus caused by a raised Po_2 and a lowered Pco_2. The lack of response of carotid chemoreceptors indicated that the opposite effects of blood flow and blood gas stimuli were equal. For aortic body chemorecep-

AORTIC CHEMORECEPTORS

CAROTID CHEMORECEPTORS
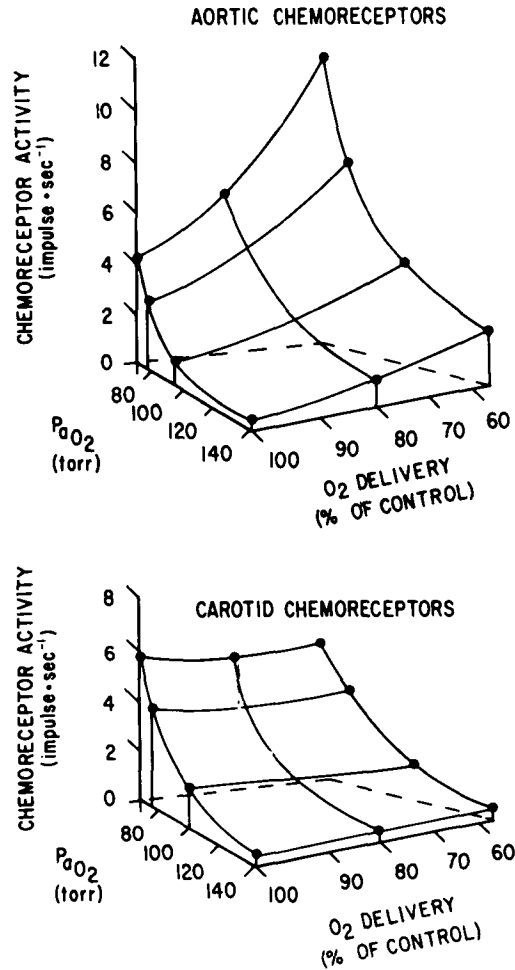
Fig. 2. The relative effects of arterial O_2 delivery on aortic body and carotid body chemoreceptor activity at various levels of Pa_{O_2}.

tors, blood flow stimulus dominated. This greater sensitivity of aortic chemoreceptors to hypotension than that of carotid chemoreceptors is consistent with our previous report (7) in that aortic chemoreceptors are endowed with constrained circulation.

In summary, as a rule carotid body chemoreceptors do not detect a moderate change in arterial oxygen content or minute oxygen flow because of changes in blood flow, but promptly recognize changes in arterial Po_2 and Pco_2 due to respiration. Aortic body chemoreceptors, on the other hand, respond to changes in minute arterial oxygen flow brought about by the changes
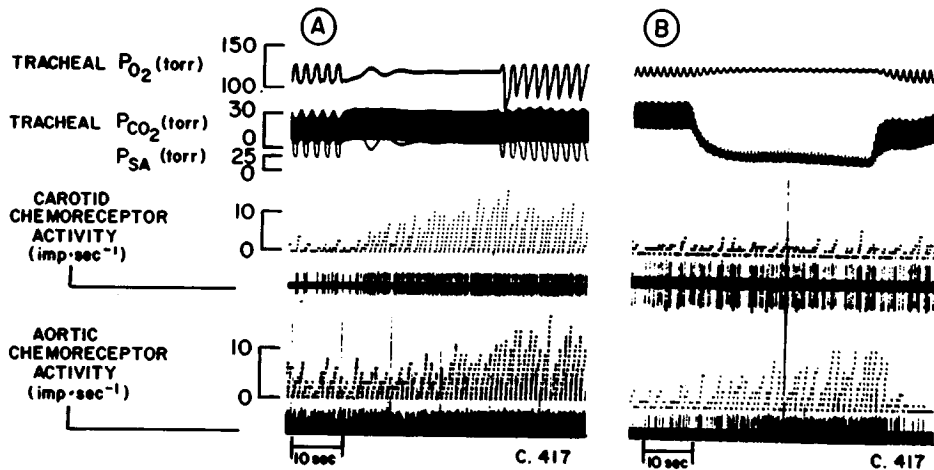
Fig. 3. Effects of asphyxia (*left-hand panel, A*) and ischemia caused by induced hypotension (*right-hand panel, B*) on the same carotid and aortic chemoreceptor activity measured simultaneously. Tracings from the top are tracheal Po_2, tracheal Pco_2, arterial blood pressure (P_{SA}), carotid chemoreceptor activity (counter output and action potentials), and aortic chemoreceptor activity (counter output and action potentials). Tracheal Pco_2 tracing is omitted in *panel B*.

in oxygen content or blood flow, or both. These receptors also respond to changes in Pa_{O_2} and Pa_{CO_2}, although to a lesser extent than do the carotid chemoreceptors. The exception to this rule is that 5–10% of the carotid chemoreceptors behave like aortic chemoreceptors.

DISCUSSION

It makes sense that when a carotid chemoreceptor does not respond to anemia and carboxyhemoglobinemia, it also does not respond to hypotension. Likewise, when an aortic chemoreceptor responds to one factor, it also responds to all of the factors that determine minute oxygen flow. The observations presented may help to sort out the current uncertainty in the literature. For example, Neil and his colleagues reported that carotid chemoreceptors were stimulated by hemorrhagic hypotension (8) but not by carboxyhemoglobinemia (9). Working with aortic chemoreceptors, Lee et al. (10) and Paintal (11) generalized that all chemoreceptors regardless of location were stimulated by hypotension. Biscoe et al. (5) found that carotid chemoreceptors did not respond to moderate hypotension during normoxia. Mills and Edwards (12) reported that carboxyhemoglobinemia stimulated both aortic and carotid chemoreceptors. Hatcher et al. (13) reported that carotid chemoreceptors were stimulated by anemia only after sympathetic nerves to the carotid body were cut, whereas intact aortic chemoreceptors were stimulated by anemia. We found that the differences between the chemoreceptors in the two locations followed a general pattern and were systematic.

The intriguing question is, What mechanism is responsible for the observed differences between the receptors in the two locations? We entertain the hypothesis that a difference in the blood flow characteristics might be critical (14). A simple interpretation is that a larger hydraulic-pressure drop occurs in the vascular bed of aortic bodies than in the carotid body. With the arterial hypotension, the aortic bodies suffer partial ischemia, the net effect of which is stimulatory. The observation that aortic chemoreceptor activity decreases sharply following a rise in blood pressure, in spite of a rise in the arterial chemical stimulus (see Fig. 3), suggests that the excitatory stimulus species in the aortic body at the termination of hypotension was greater than that in the inflowing blood. This stimulus was removed by the increased blood flow with the increased pressure. By the same token, a decrease in the carotid body blood flow did not cause a comparable ischemia and stimulation.

This line of argument emphasizes a different relationship between systemic aterial pressure and blood flow for aortic body and carotid body. Aortic body blood flow at a given pressure is expected to be lower than that of the carotid body. A possible low blood flow is likely to result not only in a low O_2 flow to the aortic body, but also in an accumulation of a local excitatory transmitter. The idea is also supported by the stimulation of aortic chemoreceptors by anemia and carboxyhemoglobinemia as well as the long latency of response to blood-borne chemical stimulus.

Regardless of the mechanism, it is clear that aortic chemoreceptors respond to changes in blood flow and oxygen delivery as well as to Pa_{O_2}. Aortic chemoreceptors are, therefore, suitable for monitoring changes in circulatory as well as respiratory constraints, whereas carotid chemoreceptors respond primarily to respiratory constraints. Thus, aortic chemoreceptors, as internal probes, depict physiological states of systemic circulation more accurately than carotid chemoreceptors. Indeed, the lack of carotid chemoreceptor response to a nonrespiratory insufficiency of oxygen delivery could be misleading to the biological system in the absence of aortic chemoreceptor input. The two receptor systems are potentially complementary. By virtue of their activity and responses, the aortic and carotid chemoreceptors provide the central nervous system with the input regarding the functional state of circulation and inspiration that leads to their possible integration. Aortic impulse traffic might not indicate insufficiency of oxygen flow to a particular microcirculatory bed, but the reflex action elicited by the aortic chemoreceptor activity would redistribute blood according to the preprogrammed mechanism.

The high pressure of the undersea environment, although not unusual for water-breathing organisms, provides an unusual environment for air-breathing man. Man encounters respiratory and circulatory constraints during his sojourn in the depths of ocean. Aortic and carotid bodies can monitor the functional states of these two systems for appropriate physiological responses. By monitoring the activity of the chemoreceptors in the two locations, we can study the mechanism of the effects of compression and decompression at the microcirculatory and cellular levels. Indeed, these well-defined oxygen sensors can be used as a model to investigate the mechanisms of high oxygen effects. There

is reason to believe that these organs will manifest oxygen toxicity at an early stage of high oxygen pressure because oxygen consumption and blood flow of carotid body and its tissue Po_2 are presumably higher than most tissues known.

It is perhaps in the world of underwater that these responses to oxygen first developed as a means of survival in the process of evolution of the animal organisms. An understanding of the mechanisms of these responses in the tissues of aortic and carotid bodies would no doubt provide further stimulus to the growth of underwater physiology.

Acknowledgments

References

1. Lahiri S, DeLaney RG. Stimulus interaction in the responses of carotid body chemoreceptor single afferent fibers. Respir Physiol 1975;24:249–266.
2. Lahiri S, Mulligan E, Nishino T, Mokashi A. Aortic body chemoreceptor responses to changes in Pco_2 and Po_2 in the cat. J Appl Physiol: Respirat Environ Exercise Physiol 1979;47:858–866.
3. Purves MJ. The effect of hypoxia, hypercapnia, and hypotension upon carotid body blood flow and oxygen consumption in the cat. J Physiol (Lond) 1970;124:395-416.
4. Daly MdeB, Lambertsen CJ, Schweitzer, A. Observations on the volume of blood flow and oxygen utilization of the carotid body in the cat. J Physiol (Lond) 1954;125:67–89.
5. Biscoe TJ, Bradley GW, Purves MJ. The relationship between carotid body chemoreceptor discharge, carotid sinus pressure and carotid body venous flow. J Physiol (Lond) 1970;208:99–120.
6. Lahiri S, Nishino T, Mokashi A, Mulligan E. Relative latency of responses of chemoreceptor afferents from aortic and carotid bodies. J Appl Physiol: Respirat Environ Exercise Physiol 1980;48:362–369.
7. Lahiri S, Nishino T, Mokashi A, Mulligan E. Relative responses of aortic body and carotid body chemoreceptors to hypotension. J Appl Physiol: Respirat Environ Exercise Physiol 1980;48:781–788.
8. Landgren S, Neil E. Chemoreceptor impulse activity following hemorrhage. Acta Physiol Scand 1951;23:158–167.
9. Duke HN, Green JH, Neil E. Carotid chemoreceptor impulse activity during inhalation of CO mixtures. J Physiol (Lond) 1952;118:520–527.
10. Lee KD, Mayou RA, Torrance RW. The effect of blood pressure upon chemoreceptor discharge to hypoxia and the modification of this effect by sympathetic-adrenal system. Q J Exp Physiol 1964;49:171–183.
11. Paintal AS. Mechanism of stimulation of aortic chemoreceptors by natural stimuli and chemical substances. J Physiol (Lond) 167;189:63–84.
12. Mills E, Edwards McIW Jr. Stimulation of aortic and carotid body chemoreceptors during carbon monoxide inhalation. J Appl Physiol 1968;25:494–502.
13. Hatcher JD, Chiu LK, Jennings DB. Anemia as a stimulus to aortic and carotid chemoreceptors in the cat. J Appl Physiol 1978;44:696–702.
14. Lahiri S. Role of arterial O_2 flow in peripheral chemoreceptor excitation. Fed Proc 1980;39:2648–2656.

HETEROGENEITY OF CAPILLARY DISTRIBUTION AND CAPILLARY CIRCULATION IN MAMMALIAN SKELETAL MUSCLES

E. M. Renkin, S. D. Gray, L. R. Dodd, and B. D. Lia

In evaluating effects of blood flow and arterial oxygen content on tissue oxygen supply, distribution of perfused capillaries is often represented by a mean capillary density or an average intercapillary distance, in a field of uniform oxygen utilization per unit mass (1–3). The morphology of many mammalian muscles suggests that neither capillaries nor oxygen utilization are evenly distributed. At least three fiber types are present in most muscles: FG (fast glycolytic), FOG (fast oxidative/glycolytic), and SO (slow oxidative). These differ in size, contraction velocity, capacity for oxygen uptake, and susceptibility to fatigue (4). Capillary supply to FOG and SO fibers is greater per unit fiber area, leading to clustering of capillaries around groups of these fibers (5,6). Uneven perfusion of the capillary network may lead to additional inhomogeneities within the diffusion field (7). Unless the distances between perfused capillaries are inversely related to the rates of oxygen uptake by intervening muscle cells, efficiency of oxygen transport will be reduced.

Honig and his colleagues (7) measured distances between blood-perfused capillaries of rat gracilis muscles by intravital microscopy. They reported variation from 0.1 to 3 times the mean values (6). The present study seeks to examine systematically, for representative mammalian skeletal muscles, the spatial distribution of a) all capillaries and b) perfused (or well-perfused) capillaries, and to relate their patterns of distribution to the arrangement of muscle fiber types.

I. Distribution of All Capillaries

Methods

Lower leg muscles of 2-kg female New Zealand white rabbits were used, because of the clear histochemical distinction between fiber types and staining of all capillaries by reaction for alkaline phosphatase (6). Measurements were made photomicrographically, on matched fields of serial frozen sections, of the following variables:

1) mean muscle fiber "diameter," (total section area ÷ number of fibers)$^{1/2}$;
2) fraction of each fiber type present;
3) capillary density (number of capillaries ÷ area in mm^2);
4) mean capillary diffusion radius ("Krogh radius" R_K) = (π × capillary density)$^{-1/2}$;
5) individual and mean intercapillary distances (ICD) within each field.

Intercapillary distances were measured by drawing lines from each capillary to surrounding capillaries on a tracing of the field to form a network of closed triangles with no lines crossing between points. The network was completed on the assumption that each field is a unit cell of a repeating two dimensional array. The locations of capillaries beyond two adjacent borders were marked, and the network of ICD's within the field boundary was completed with lines extending across the two borders to these capillaries, which correspond to those bounding the network on the opposite borders. An example of such a network is shown in Fig. 1, *I-A*. Graph *I-B* in this figure is the corresponding histogram, showing the distribution of individual ICD's.

Results

Parameters measured for six different leg muscles are listed in Table I. All were frozen at a fixed reference length (6). For each muscle, calculated R_K was almost exactly the same as mean ICD/2. Individual ICD's were distributed approximately in log-normal fashion with logarithmic standard deviations (S_{log}) between 0.19 and 0.22, which signifies that 95% of all values lay between ¼ and 4 times the means.

Inclusion of section area (equivalent to tissue mass) with respect to distance from the nearest capillary was evaluated by plotting contour intervals for each section in multiples of R_K (Fig. 1, *I-C*). The results are tabulated in the last four columns of Table I. With respect to the *entire* capillary bed, 0.64 to 0.76 of total section area was enclosed within R_K of the nearest capillary, 0.86 to 0.94 within 1.5 R_K. These values are lower than the predicted areas for a perfectly uniform array of capillaries: 0.91 and 1.00, respectively. Beyond 1.5 R_K, however, the enclosed area rapidly approaches unity, and only a minute fraction of tissue area falls beyond 2 R_K.
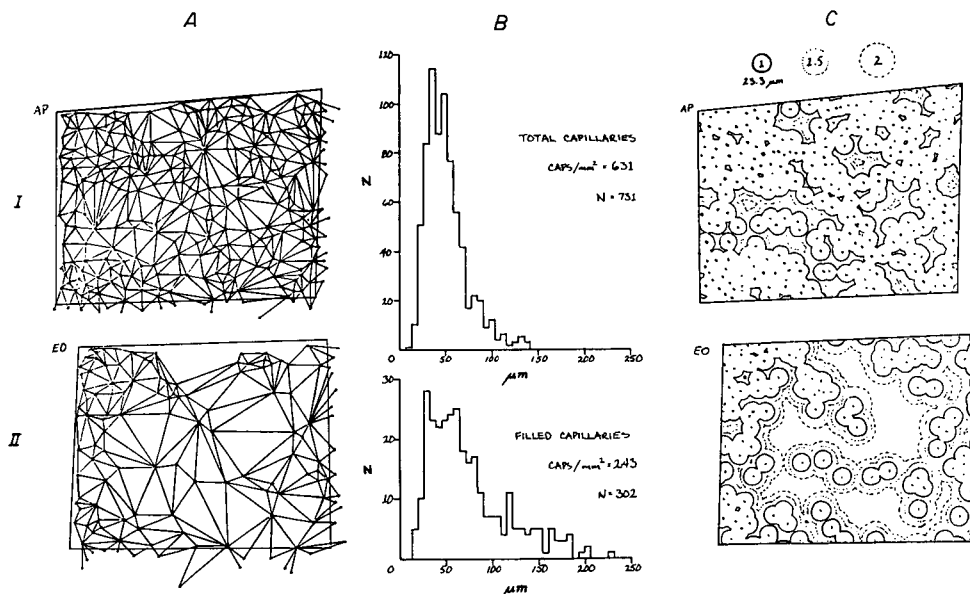
Fig. 1. Distribution of all capillaries (*Row I*, alkaline phosphatase stain, *AP*) and of ink-filled capillaries (*Row II*, eosin counter-stained adjacent section, *EO*) in the same 0.4 mm² cross-sectional field of a rabbit medial gastrocnemius muscle. This is a relatively "red" part of the muscle, with 29% FG fibers, 52% FOG, and 19% SO by area. *Column A*, network maps of intercapillary distances (ICD); *Column B*, equal-area histograms of ICD distributions; *Column C*, contour maps at multiple intervals of the average diffusion radius (R_K) for all capillaries; only R_K, 1.5 R_K, and 2.0 R_K contours are shown. Capillary/fiber ratio 1.44, total capillary density 613/mm², R_K = 23.3 μm. The fraction of capillaries filled with ink by 15 s perfusion was 0.40. Mean ICD_{total} = 47 μm, ICD_{open} = 71 μm. The distribution curves are approximately log-normal, with S_{log} = 0.20 and 0.28, respectively. Fractional tissue areas within the contour line at R_K (*solid line* in *column C*), between R_K and 1.5 R_K (*lightly dotted line*), between 1.5 and 2 R_K (*heavy dashed contour line*), and beyond 2 R_K are as follows: *Total* capillaries 0.76, 0.19, 0.04, 0.01; *open* capillaries 0.36, 0.21, 0.16, 0.27.

II. Distribution of Perfused Capillaries

Methods

To identify "open" or well-perfused capillaries in the total population, we perfused the lower leg with india-ink (diluted ½, dialyzed vs. Ringer's, and heparinized) for periods ranging from 3.5 to 90 s before removal, freezing, and sectioning the muscles. Perfusion pressures and flows were comparable to arterial pressures and blood flows just before perfusion, which was started immediately upon clamping the artery, via a T-cannula previously inserted. Ink spots were counted on a serial section counterstained with eosin, in fields matched to those used for counting total capillaries. Capillary densities, intercapillary distances, etcetera, were calculated for ink-filled capillaries exactly as for total capillaries. The reference R_K for both filled and total capillaries was taken as that calculated for the total population.

TABLE I

Fiber Composition and Capillary Distribution in Rabbit Skeletal Muscles

Muscle	Mean Fiber Diameter μm	Fiber Composition, Fractional Area				Caps mm²	R_K μm	$\overline{ICD}$ 2	ICD Log Normal S	Fraction of Section Area			
		FG	F?	FOG	SO					Within R_K	1–1.5 R_K	1.5–2 R_K	Beyond 2 R_K
Lat. gastroc.	54	0.66	0.03	0.24	0.07	363	30	28	0.20	0.64	0.26	0.08	0.01
Sartorius	62	0.65	0.02	0.34	0	221	38	38	0.22	0.65	0.22	0.11	0.02
Plantaris	70	0.64	0.00	0.28	0.08	243	36	36	0.20	0.70	0.24	0.05	0.003
Ext. dig. longus	53	0.57	0.04	0.37	0.02	416	28	28	0.22	0.64	0.22	0.12	0.02
Med. gastroc.	61	0.55	0.00	0.29	0.16	343	30	29	0.22	0.68	0.22	0.08	0.03
Ant. tibialis	52	0.50	0.04	0.40	0.08	540	24	24	0.19	0.75	0.20	0.05	0.01
Soleus	74	0	0	0.11	0.89	415	28	28	0.19	0.76	0.21	0.03	0.004

F? represents fibers apparently intermediate or in transition between FG and FOG. R_K = Krogh diffusion radius = $(\pi \times caps/mm^2)^{-\frac{1}{2}}$. ICD is intercapillary distance.

TABLE II

Fraction of Ink-Filled Capillaries

Perfusion	3.5 s	7.5 s	15 s	30 s	60–90 s
Med. gastroc.	0.18 ± 0.22 (39)	0.34 ± 0.17 (28)	0.39 ± 0.17 (28)	0.74 ± 0.21 (26)	0.74 ± 0.16 (29)
Soleus	0.12 ± 0.17 (19)	0.23 ± 0.09 (13)	0.26 ± 0.18 (13)	0.67 ± 0.23 (13)	0.80 ± 0.21 (13)

Values are mean ± SD (N fields counted). Data from ref. 8.

Results

The progression of ink filling in medial gastrocnemius and soleus muscles of resting rabbit legs perfused at an average rate of 4 mL/min × 100 g is shown in Table II. Between 7.5 and 15 s, the increment in $\bar{F}o$ was small, which suggests that these intervals characterize the filling of a population of well-perfused vessels (8) (a full report is in preparation). For the present study, Fo at 15-s perfusion was taken to represent this population, which we shall designate as open capillaries. Measurements were made on two fields each of six medial gastrocnemius and one field each of six soleus muscles. Although the mean values of Fo for these samples were close to the means listed in Table II (0.37 and 0.22, respectively), individual field Fo's varied over a wide range (Fig. 2).

Mean ICD between open capillaries was inversely related to Fo for that field. Distribution of individual ICD's were still close to the log normal pattern, and the variability parameter (S_{log}) increased as Fo fell. Figure 1 shows the patterns of capillary distribution (A), the variation of ICD's (B), and multiple R_K contours (C) for (Row I) all capillaries and (Row II) open capillaries at Fo = 0.40 for a single field of medial gastrocnemius. R_K (all capillaries) = 23 μm. Mean ICD/2 for all capillaries was 24 μm, for open capillaries, 36 μm. S_{log}'s were 0.20 and 0.28, respectively.

Tissue areas at different diffusion distances from open capillaries were measured with respect to multiples of total capillary R_K in order to provide an anatomically fixed reference for variability with Fo. Column C in Fig. 1 shows the contour maps for all capillaries (I) and for open capillaries (II). Fractional section area within the innermost contour around open capillaries is substantially diminished, and that beyond the 2 R_K contour is greatly increased. Figure 3 presents graphs of the areas included by contours at multiples of R_K for medial gastrocnemius (A) and soleus muscles (B) for different levels of Fo. At injection fractions below 0.25, a progressively larger fraction of total section area lies more than 4 times mean R_K or ICD/2 from the nearest open capillary.

DISCUSSION

The existence of substantial areas of tissue at such large distances from open capillaries may be responsible for the relatively high critical Po_2 levels observed for resting skeletal muscles (2), and for the discrepancy between capillary densities calculated from measurements of capillary filtration coefficient or permeability—surface area products and those calculated from critical Po_2's. The former depend on capillary surface only, while the latter depend both on surface and on intercapillary distance, and are strongly affected by extreme values of distance. The Krogh-Erlang equation provides a simple means for

MEDIAL GASTROC.   SOLEUS

NUMBER
OF
FIELDS

m=6   f=12   m=6   f=6

$\overline{F}_O = .37$ $\overline{F}_O = .22$

4
3
2
1

0 .1 .2 .3 .4 .5 .6   0 .1 .2 .3 .4

FRACTION OF CAPILLARIES FILLED (F_O)
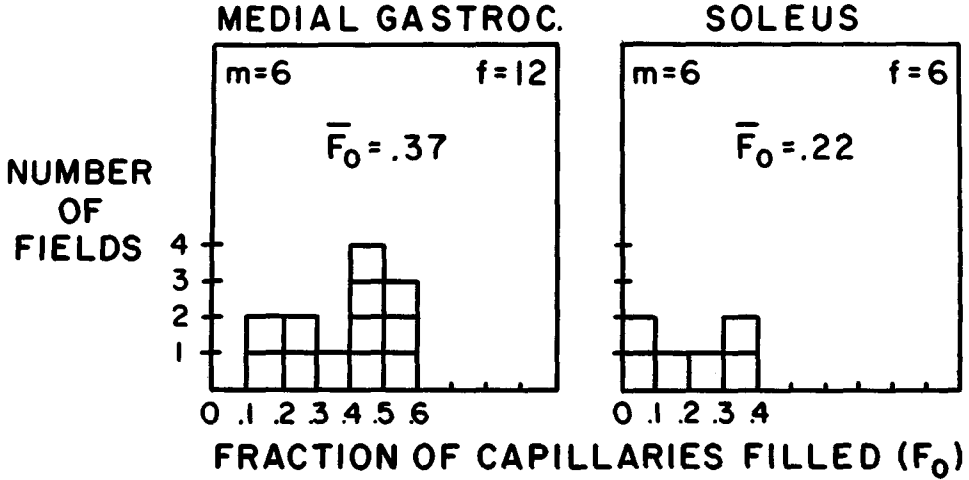
Fig. 2.   Variability of ink-filled fraction of capillaries (Fo) after 15-s perfusion at a flow rate of 4 mL/ min per 100 g. Six medial gastrocnemius muscles, two fields each; six soleus muscles, one field each. Mean Fo's for each group are close to those for the larger sample represented in Table I.

A. Medial Gastrocnemius   B. Soleus

R/R$_K$ CONTOUR   R/R$_K$ CONTOUR

FRACTION TISSUE AREA
WITHIN CONTOUR

1.0   1.0
.8   .8
.6   .6
.4   .4
.2   .2

0   .1   .2   .3   .4   .5   .6 0   .1   .2   .3   .4   .5

FRACTION OPEN CAPILLARIES
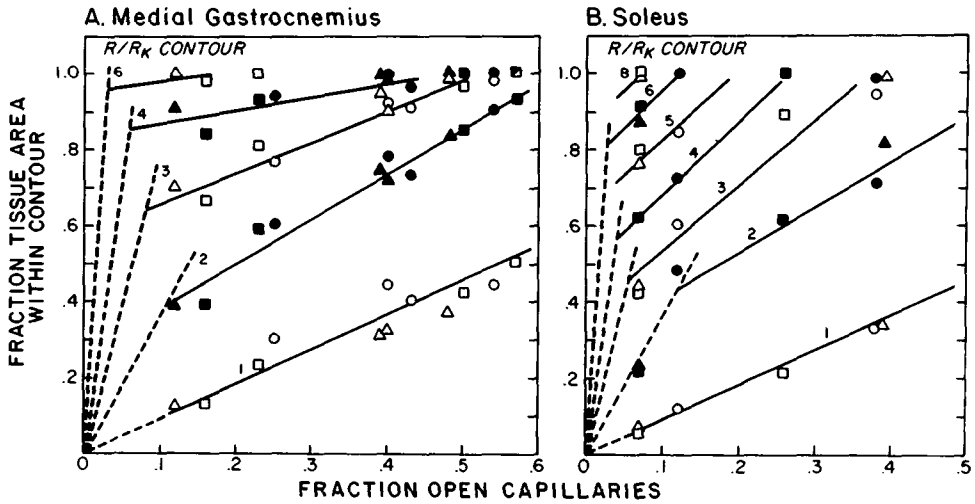
Fig. 3.   Partition of muscle cross-sectional area (equivalent to tissue volume) by radial distance contours from open capillaries, as a function of the fraction perfused. *A* medical gastrocnemius; *B* soleus. *Solid lines* are visual fits to experimental data obtained by planimetry of the contour graphs (Fig. 1, *Col. C*) or by summation of the ICD distributions (*Col. B*). The ordinate is area contained *within* the contour at the specified multiple of R$_K$, or *within* a distance equal to the specified multiple of ICD/2 for the total population. *Dashed straight lines* show partition of area by R$_K$ contours in a uniform array of capillaries. Deviations of the observed curves from these lines above a certain level of Fo is due to the uneven distribution of capillaries in the muscle sections. The *dashed line* corresponding to R/R$_K$ = 1.0 intersects the ordinate axis at 0.91 at Fo = 1. Observed data fall below the line above Fo = 0.7.

estimating oxygen tension gradients in a tissue field of uniform oxygen uptake and diffusibility (1):

$$\Delta P \, = \, \frac{\dot{V}O_2}{4\alpha D} \left[R^2 \, \ell n \left(\frac{R}{r} \right)^2 - (R^2 - r^2) \right]$$

where ΔP is the difference in Po_2 (in mmHg) between the capillary surface and a point in the tissue at distance R mm from the center of the capillary. The radius of the capillary itself is r, $\dot{V}O_2$ is the oxygen uptake (or uptake capacity) in mL/min per unit tissue volume, α is the solubility of oxygen in the tissue, and D the diffusibility of oxygen. If appropriate values are selected for r (2.5 μm), D (1.5 $\times$ 10^{-5} cm²/s), α (2.8 $\times$ 10^{-5} mmHg^{-1}) and $\dot{V}O_2$, it is possible to calculate ΔP for specified contours of R or of R/R_K as in Figs. 1 and 3. For resting medial gastrocnemius, if we take R_K = 30 μm, and $\dot{V}O_2$ = 0.3 mL/min per 100 g, the following values are obtained: for R/R_K = 4, ΔPo_2 = 29 mmHg; for R/R_K = 5, ΔPo_2 = 48 mmHg; for R/R_K = 6, ΔPo_2 = 73 mmHg; and for R/R_K = 7, ΔPo_2 = 103 mmHg. If the Po_2 of arterial capillary blood is 90 mmHg and of venous capillary blood is 40 mmHg, O_2 supply would start to show limitation at the R/R_K = 4.6 contour, and would be limited everywhere beyond the R/R_K = 6.6 contour. The corresponding levels of Fo are 0.30 and 0.10. Though these lie below the *average* $\bar{Fo}$ for resting medial gastrocnemius (0.39 in these muscles, Table II), nearly a third of the fields studied had filling fractions in this range (Fig. 2). If there is appreciable loss of oxygen from the arteriolar tree before the blood reaches the capillary network (9,10) and capillary Po_2's are lower than 90–40 mmHg, the critical contours will move closer to the capillary as tissue Po_2's fall. For soleus, if we take R_K = 30 μm and $\dot{V}O_2$ = 0.5 mL/min per 100 g the critical values of R/R_K are 3.7 and 5.2 for ΔPo_2's of 40 and 90 mmHg, respectively.

In contracting skeletal muscles, the entire capillary bed is believed to be open. If this is so, practically all of the tissue lies within 2 R_K of a perfused capillary: $\dot{V}O_2$ is of course higher, perhaps 3 mL/min per 100 g, while venous Po_2 is lower, around 20 mmHg. For a medial gastrocnemius with R_K = 30 μm, ΔPo_2 for the 1.5 contour will be 29 mmHg, which places more than 11% of tissue volume beyond the critical distance (according to the figures in Table I) for even this modest estimate of activity $\dot{V}O_2$. However, examination of the distribution of red muscle fibers, which have the higher oxygen uptake capacity, show that they are clustered around the capillaries, and fall largely within the R_K contour lines. This is shown in Fig. 4, by the distribution of FOG and SO fibers marked on the AP section (total capillaries).

In resting muscles with values of $\bar{Fo}$ substantially less than 1.0, as shown by the EO section in Fig. 4, FOG and SO fibers are present in comparable proportions in both inner and outer R_K contours. Thus, the anatomically defined association between these fibers and *all* capillaries does not carry over to the *open* capillaries. The mechanism for controlling distribution of blood flow does not appear to operate at an individual capillary level, but on the level of a larger array, which includes fibers of all types (8). For this reason, it seems
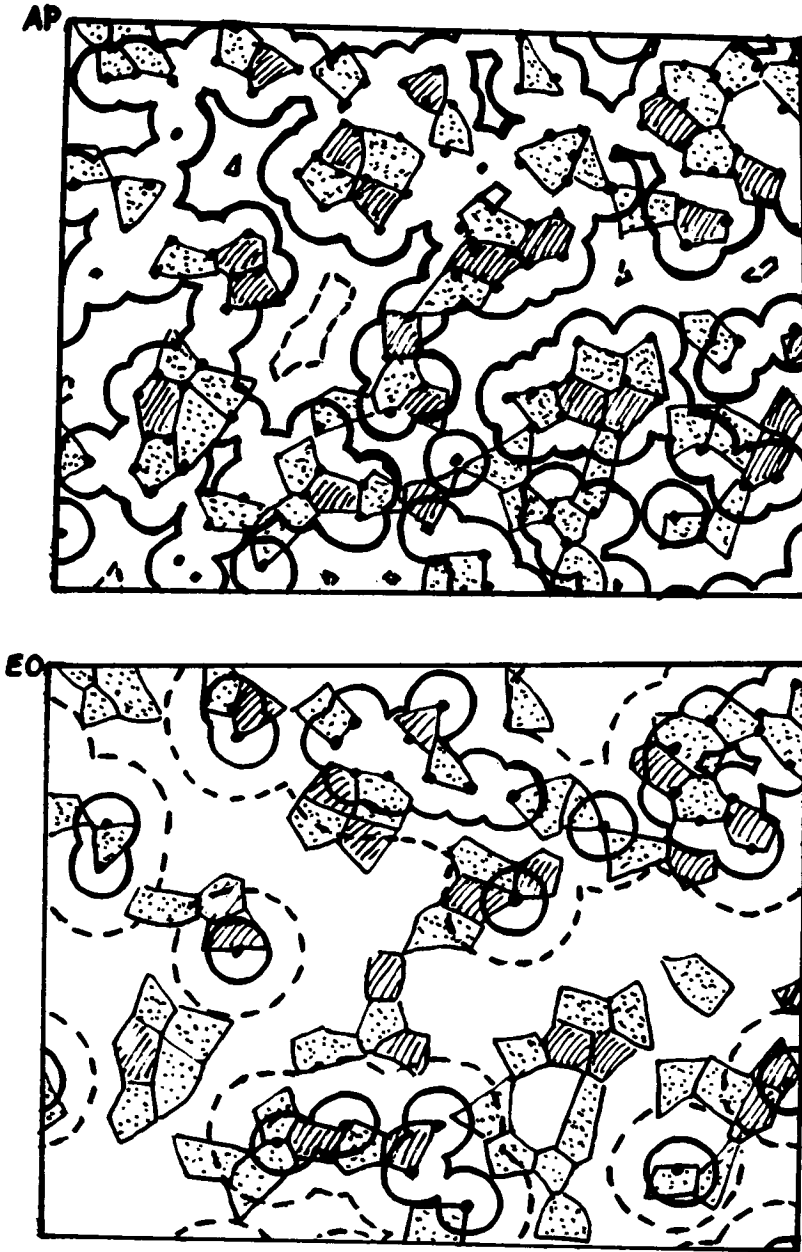
Fig. 4. Relation of red muscle fiber cross sections to total capillaries (*AP*) and ink-filled capillaries (*EO*) in a field of medial gastrocnemius with Fo = 0.25. Contours of 1.0 and 2.0 R_K are shown. *Stippled polygons*, FOG fibers; *hatched polygons*, SO. The rest of the area consists of FG and a few F? fibers. In the *AP section*, most of the FOG and SO fibers lie inside the R_K contour, i.e., the pattern of total capillaries follows the distribution of red fibers. In the *EO section*, however, several groups of red fibers lie in the poorly supplied regions outside the 2 R_K contour. Fiber type identification was made on the basis of two additional serial sections reacted for succinic dehydrogenase and myofibrillar ATP-ase (6).

feasible to model diffusion of oxygen from open capillaries as if the field of $\dot{V}o_2$ were uniform, as originally proposed by Krogh (1).

SUMMARY

1) Capillaries in skeletal muscles are not evenly distributed. In mixed muscles the capillary supply is denser to red, high-oxidative fibers. Nearly all tissue lies within twice the mean diffusion radius of a capillary.

2) Open or well-perfused capillaries may be identified by 15-s perfusion with india-ink. The mean fraction open in resting muscles was 0.39 for medial gastrocnemius and 0.26 for soleus, but individual 0.4 mm² fields showed wide variability of filling fraction.

3) As the fraction of well-perfused capillaries decreased and the mean distance between them increased, the heterogeneity of capillary distribution increased. Substantial fractions of tissue area lay at distances estimated to be close to critical with respect to oxygen supply even for resting muscles.

4) Tissue regions remote from open capillaries contained both white and red fibers, which is evidence that the mechanism controlling the distribution of blood flow in relation to local metabolism does not operate at the individual capillary level.

5) Nonuniformity of spatial distribution of well-perfused capillaries in resting muscles is probably responsible for the discrepancy between estimates of capillary density derived from critical Po_2 levels and those based on measurements of filtration coefficients or permeability—surface area products of nonmetabolized solutes. The former give values that are too low because they are sensitive to above-average intercapillary distances.

References

1. Krogh A. The supply of oxygen to the tissues and the regulation of capillary circulation. J Physiol (Lond) 1919;52:457–474.
2. Stainsby WN, Otis AB. Blood flow, blood oxygen tension, oxygen uptake, and oxygen transport in skeletal muscle. Am J Physiol 1964;206:858–866.
3. Grunewald WA, Sowa W. Capillary structures and O_2 supply to tissue. Rev Physiol Biochem Pharmacol 1977;77:149–209.
4. Burke RE, Levine DN, Tsairis P, Zajac FE. Physiological types and histochemical profiles in motor units of the cat gastrocnemius. J Physiol (Lond) 1973;234:723–748.
5. Romanul FCA. Capillary supply and metabolism of muscle fibers. Arch Neurol 1965;12:497–509.
6. Gray SD, Renkin EM. Microvascular supply in relation to fiber metabolic type in mixed skeletal muscles of rabbits. Microvas Res 1978;16:406–425.
7. Honig CR, Frierson SL, Nelson CN. O_2 transport and $\dot{V}o_2$ in resting muscle: significance for tissue capillary exchange. Am J Physiol 1971;220:357–363.

8. Gray SD, Renkin EM. Distribution of capillary transit times in mammalian skeletal muscle. In: Proceedings of the International Union of Physiological Sciences, Paris, July 18–23, 1977. Vol. XII. Publ. by Secretariat of the XXVIIth International Congress of Physiological Sciences, 1977.

9. Duling BR, Berne RM. Longitudinal gradients in periarteriolar oxygen tension. A possible mechanism for the participation of oxygen in local regulation of blood flow. Circ Res 1970;27:669–678.

10. Popel AS, Gross JF. Analysis of oxygen diffusion from arteriolar networks. Am J Physiol 1979;237:H681–H689.

RETINAL OXIMETRY WITH HYPERCAPNIA AND HYPERBARIC OXYGEN

F. G. Hempel, S. R. Burns, and H. A. Saltzman

Under hyperbaric conditions it is theoretically possible to raise the Po_2 of arterial blood to a level where oxygen dissociation from hemoglobin does not take place in the tissue and hemoglobin remains saturated in transit. The retina in particular lends itself to studies of this kind because of its high rate of oxygen extraction and its unique optical access.

Using a reflectance oximetric technique and pressures into the hyperbaric region, we investigated the effect of increased partial pressures of inspired oxygen on the hemoglobin saturation characteristics in the posterior pole of the rabbit eye, more specifically, the choroid. Essentially all of the oxygen supplied to the retina of this animal comes from the choroid; therefore our methods made it possible to approach that oxygen tension at which the metabolic needs of the retina were met by physically dissolved oxygen as we monitored the progression from mixed arterial-plus-venous blood to blood that had fully oxygenated hemoglobin. Furthermore, because hyperbaric experimentation permits the addition of sequentially greater carbon dioxide pressures without subtraction of oxygen, we also investigated the oximetric effect of increasing hypercapnia combined with a fixed normoxic or hyperoxic respiratory state. Finally, the effect of these unusual respiratory conditions on retinal function has not been fully explored before, nor has function been correlated with the oxygenation state of the perfusing blood. Therefore, additional observations were made on the electroretinographic (ERG) activity that accompanied these gas changes.

METHODS AND MATERIALS

Instrumentation for this study is illustrated in Fig. 1. The system is composed of a dual-wavelength spectrophotometer coupled to a conventional fundus (retinal) camera by means of fiber optics. The fundus camera was focused
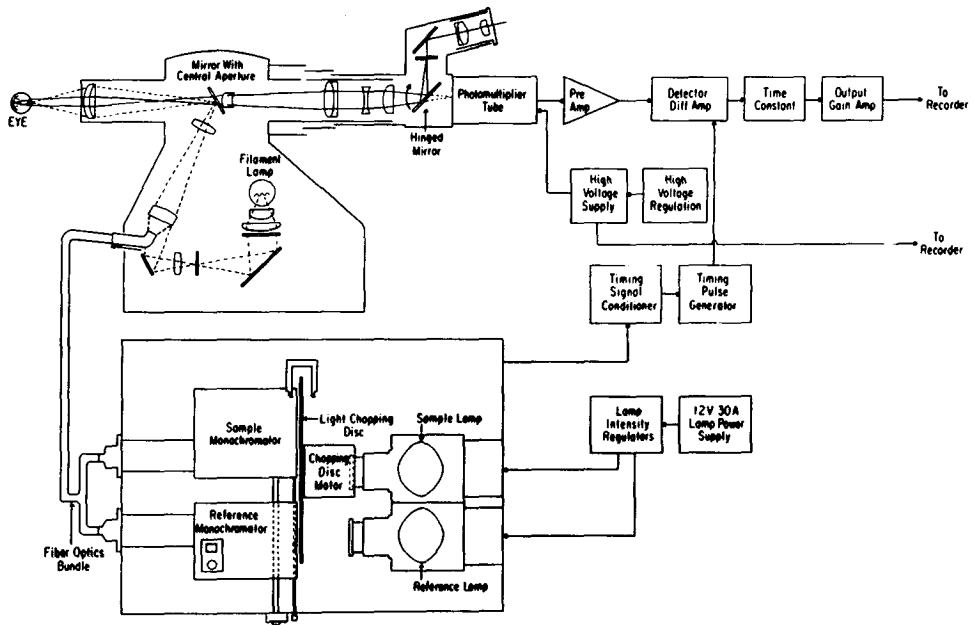
Fig. 1. Schematic diagram of the instrumentation for oximetric studies of the retina. A supply voltage to the photomultiplier tube is held constant by a regulation circuit during the interval when the 586-nm light is opened to the eye by the mechanical chopper. Adjustments in this high voltage provided an indication of changing blood volume in the retinal field.

on the retina just below and nasal to the optic disc. Monochromatic light from the spectrophotometer entered the eye through a dilated pupil, was reflected from the fundus, and was received on a photomultiplier tube. The sample, or oxygenation-dependent, wavelength for the oxy-deoxyhemoglobin transition was set at 577 nm. Absorbance was monitored relative to a reference at 586 nm, with the latter wavelength representing an isosbestic extinction point for these hemoglobin species. Each monochromatic beam was flashed onto the retina at 30 Hz, and the difference between the respective intensities of the reflected light, 577–586 nm, was displayed on a chart recorder along with a readout of the reference (586 nm) beam. Variations in the reflected reference light were used as an indicator of the relative blood volume in the retinal field. The entire optical apparatus was installed in a large walk-in hyperbaric chamber with appropriate penetrations through the chamber wall for electrical recording.

Rabbits were deeply anesthetized with repeated doses of pentobarbital and a tracheal tube was inserted. Paralysis was induced with gallamine triethiodide (Flaxedil) and the animals were artificially respired with a minute volume producing arterial Po_2 and Pco_2 values of 78 ± 11 and 20.6 ± 7.0 Torr, respectively, during air breathing. Animals were secured in a stereotaxic headholder. Premixed gases were administered from cylinders via the respirator.

The electroretinographic signal was evoked by a light flash delivered to the opposite eye and recorded from it with a corneal electrode of the low-vacuum type used clinically. Flashes were conducted to the eye from a commercial photic stimulator via a fiber optics bundle and presented at a rate of 15/min. The electroretinogram was displayed on a chart recorder and stored on tape for computer averaging.

RESULTS

The oximetric reaction of choroidal blood to increasing tensions of pure oxygen is summarized in Fig. 2A along with the corresponding changes that occurred in vascular volume. For these data, six animals were ventilated with oxygen in progressively greater fractions, up to 4 ATA. Zero oxygen measurement represents the oximetric response after 2 min of nitrogen ventilation. A characteristic oxygen saturation curve of hemoglobin is generated as the data are plotted up to 0.84 ATA O_2, and the additional observation is made that 2.0 and 4.0 ATA O_2 leads to small but distinct hemoglobin oxygenation increases. A decrease in regional blood volume accompanies each oxygen increment, with the net effect of this presumed vasoconstrictive response being an incomplete oxygen saturation in venous blood. Accordingly, oximetric changes were also monitored while vasodilation was induced in the animals by ventilating them with increasing carbon dioxide fractions in gas mixtures with a constant inspired oxygen fraction of 21%. Results of these experiments are shown in Fig. 2B. With each CO_2 increase up to 5% CO_2 at 4 ATA (equivalent to 20% CO_2 at sea level) there is a fall in the relative oxygenation of hemoglobin parallel with a substantial blood volume increase. A higher CO_2 fraction, 7.5% at 4 ATA, elicits a shift in the 577–586 signal toward greater oxygenation and at the same time the choroidal blood volume drops.

Electroretinographic signals recorded from the opposite eye during the hypercapnic series show that the c-wave is relatively unaffected by progressively greater carbon dioxide pressures, while the a-wave is reduced to an average of 68% of its control amplitude while the animal is breathing the highest (7.5%) CO_2 fraction. As shown in Fig. 3, this CO_2 tension, equivalent to 30% CO_2 at 1 ATA, led to a virtually extinguished b-wave (average amplitude = 3% of control) in the 6 animals tested. Pure oxygen at pressures up to 4 ATA produced no significant changes in the ERG during the short exposures employed here; thus, these signals were taken as controls.

DISCUSSION

The absence of vessels in the neural layers of the retina of the rabbit (1) and the total support of the retina by choroidal perfusion offers a simplified model system in which the oxygen saturation of choroidal hemoglobin can be examined alone. Present results clearly indicate the reactivity of the choroidal
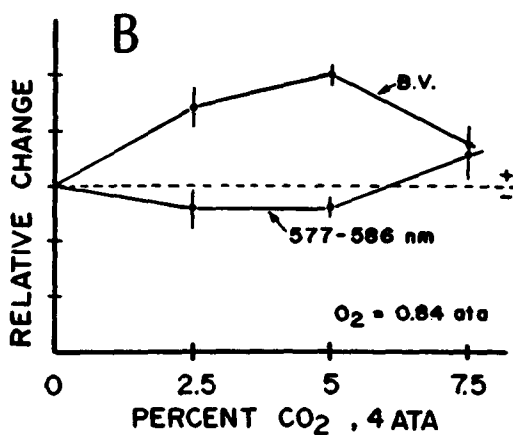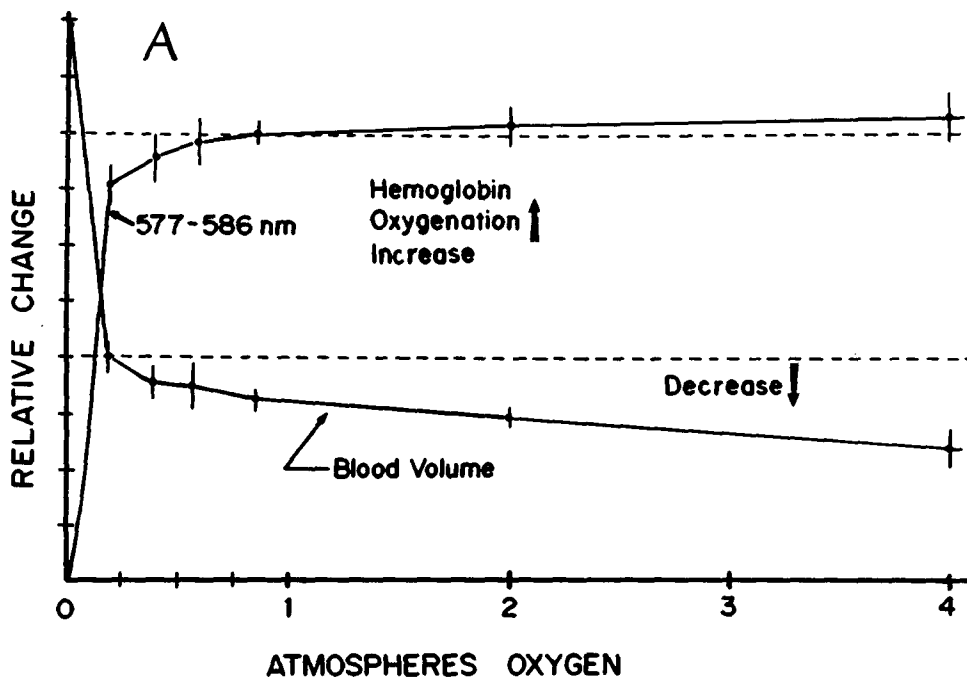
Fig. 2A. Increase in oxygen saturation of hemoglobin in rabbit choroid (577–586 nm) and decrease in blood volume, with atmospheres inspired oxygen. *Dashed line* of hemoglobin oxygenation trace intersects 0.84 ATA O_2 pressure; blood volume decrease is shown relative to control measurements with 0.2 ATA O_2 inspiration. Zero atm O_2 produced with 2-min N_2 ventilation.   *B*. Effects of increasing percentage of CO_2 at 4 ATA on blood volume (B.V.) and hemoglobin saturation (577–586 nm). Ordinate at same scale as *A* above. *Dashed line* indicates saturation and blood volume levels while breathing air at 4 ATA with no added CO_2; subsequent data were taken with a constant inspired O_2 pressure of 0.84 ATA. Points in *A* and *B* figures are means from 6 animals ± SEM.
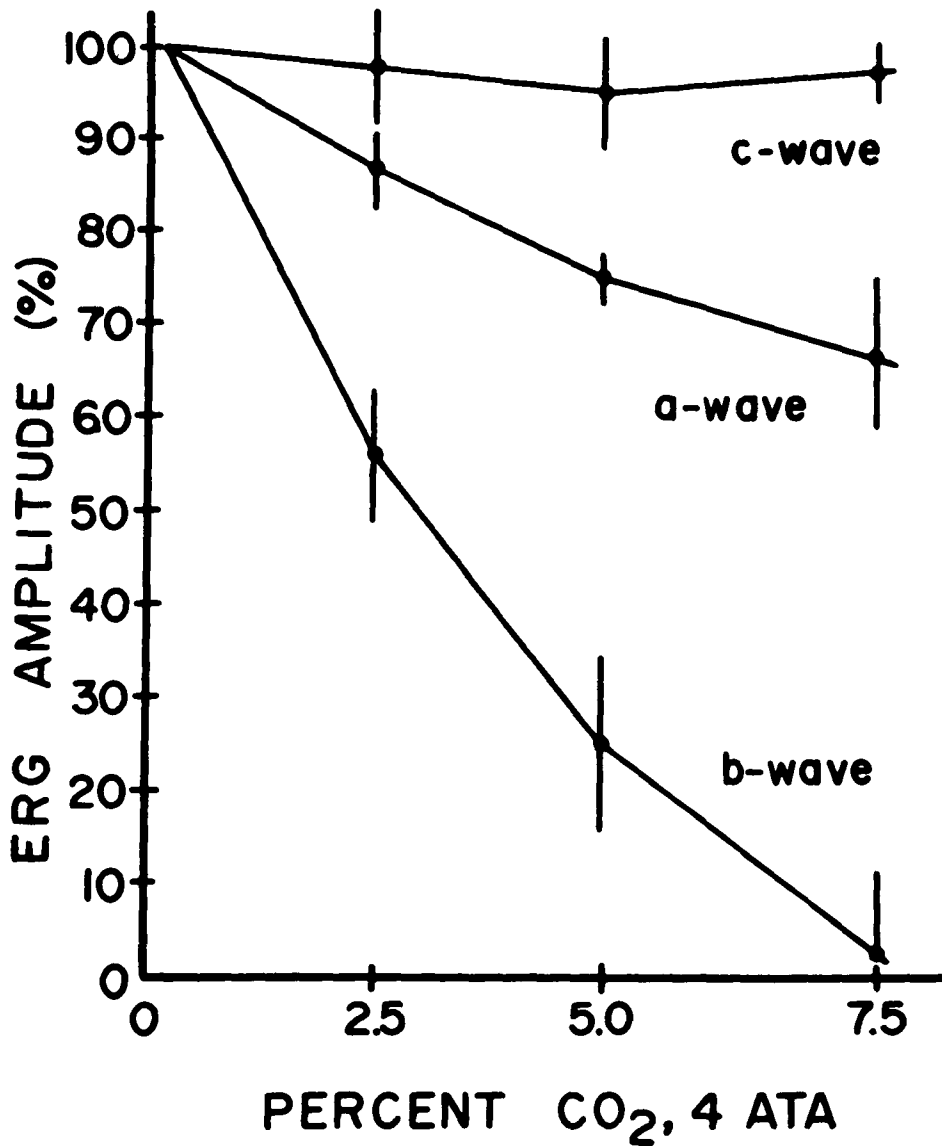
Fig. 3. Rabbit electroretinogram (ERG) wave amplitudes with percent CO_2 in 21% O_2 at 4 ATA. Data are means of 6 trials ± SEM.

vasculature to high oxygen pressures and to hypercapnia in the form of a decrease in blood volume with the first instance and a large increase in blood volume in the latter respiratory condition. A moderate vasodilatory response of the choroidal circulation to carbon dioxide has been shown before (2), but the vasoconstriction (decrease in blood volume) caused by hyperbaric oxygen is a unique observation in what was formerly believed to be a passive system with-

out autoregulation (3). Oxygenation was virtually complete in hemoglobin at 0.84 ATA pure O_2 (equivalent to air at 4 ATA), yet small increments in oxygen saturation were observed in 2.0 and 4.0 ATA O_2 pressures. These findings suggest that oxygen-induced vasoconstriction limits choroidal blood flow sufficiently to prevent full arterialization of the choroidal blood. A similar effect has been noted in the cerebral circulation where venous oxygen partial pressures do not reach a hemoglobin-saturating magnitude in 4 ATA O_2 (4). In this sense, it was not possible to achieve a partial pressure of oxygen in the retinal blood so high that some oxygen extraction from hemoglobin did not take place. In short, the provision of oxygen totally from physically dissolved oxygen was unattainable.

A decrease in oxygen saturation was noted when the carbon dioxide percentage in the inspired gas was raised from zero to 5%. At 4 ATA, the carbon dioxide level reached an equivalent of 20%. It was shown in Fig. 2A that the oxygen inspired in these experiments, 0.84 ATA, almost completely oxygenated hemoglobin. That this oxygen saturation fell is apparently a consequence of the Bohr shift, because concomitant blood volume increases presumably indicated a higher flow rate and a higher likelihood that the blood remained oxygenated in transit. Paradoxically, very high CO_2 levels, 7.5% CO_2 at 4 ATA, caused a drop in choroidal blood volume to an intermediate position along with raising the relative saturation of hemoglobin with oxygen. No reasons for these effects of very high hypercapnia are immediately apparent, but we may postulate that no further Bohr shift occurs and that blood flow remains high while the hypercapnia reduces the oxygen needs and extraction by the retina. Consequently, the arterial-venous oxygen difference would be smaller under these extreme conditions.

The striking effects of hypercapnia on the electroretinogram are likewise unique. Only with chemical uncoupling in the retina such as that after aspartate administration (5) has abolition of the b-wave combined with preservation of the a-wave been seen. Extreme hypercapnia (7.5% CO_2) has the most depressant effect. The survival of the a- and c-waves clearly indicates that the hypercapnic block of synpatic function or glial cell activity takes place at a point afferent to the receptor and pigment epithelial layers, because these regions give rise to the a- and c-waves, respectively, while the b-wave arises in the inner layers (6,7). For example, hypoxia caused by a Bohr shift can be ruled out because of the high oxygen saturation measured in hemoglobin simultaneous and because hypoxia typically reduces the c-wave of the rabbit before the a- or b-waves are substantially diminished, as observed in other experiments from this laboratory.

In summary, vasoconstriction limits the attainment of fully arterialized choroidal blood even with arterial Po_2 values grater than 2000 Torr, and the hypercapnia necessary to offset the vasoconstriction surely depresses retinal oxidative metabolism. Thus, achieving an equality between oxygen provision by the plasma and oxygen consumption in the retina is unlikely in the living eye.

Acknowledgment

References

1. Rohen J. Über das Gefässystem der Retina beim Kanichen. Ophthalmologica 1954;128:307–319.
2. Friedman E, Chandra SR. Choroidal blood flow: III. Effects of oxygen and carbon dioxide. Arch Ophthalmol 1972;87:70–71.
3. Alm A, Bill A. Ocular and optic nerve blood flow at normal and increased intraocular pressures in monkeys (*Macaca irus*): a study with radioactively labeled microspheres in brain and some other tissues. Exp Eye Res 1973;15:15–29.
4. Hempel FG. Oxygen tensions measured in cat cerebral cortex under hyperbaric conditions. J Appl Physiol: Respir Environ Exercise Physiol 1979;46:53–60.
5. Winkler BS. A role for metabolism in photoreceptor electrogenesis. Exp Eye Res 1978;26:107–110.
6. Oakley B. Potassium and the photoreceptor-dependent pigment epithelial hyperpolarization. J Gen Physiol 1977;70:405–425.
7. Rodieck RW. Components of the electroretinogram—a reappraisal. Vision Res 1972;12:773–780.

A MECHANISM FOR THE BENEFICIAL EFFECT OF HYPERBARIC OXYGEN ON STAPHYLOCOCCAL OSTEOMYELITIS

J. T. Mader and G. L. Brown

Hyperbaric oxygen (HBO) therapy is frequently used as adjunctive therapy in chronic osteomyelities (1–4). Previously we demonstrated that HBO used as the sole treatment modality was as effective as antibiotic (cephalothin) in the treatment of experimental *Staphylococcus aureus* osteomyelitis (5). Although HBO inhibits growth of most microorganisms including *S. aureus*, inhibition occurs at oxygen tensions higher than those found in tissue under standard HBO conditions (6–8). Our in vitro growth curves and kill curves using cephalothin and *S. aureus* under standard HBO conditions were identical to those obtained under ambient conditions (5). Since HBO did not per se inhibit or kill this strain of *S. aureus*, another mechanism was sought.

MATERIALS AND METHODS

A 16-gauge needle was inserted percutaneously into the left tibial metaphysis of a New Zealand white rabbit. One tenth mL 5% sodium morrhuate, 0.1 mL *S. aureus* (3×10^6 organisms), and 0.1 mL sterile saline were injected. The needle was removed, the infection was allowed to progress 3–4 weeks, a period during which osteomyelitis becomes well established by radiographic criteria (5,9).

Measurements of Blood Flow and Intramedullary Oxygen

The animal was anesthetized and a small hole was drilled into the shaft of the normal right tibia and the infected left tibia. If a bone fractured, the study

was aborted. A 16-gauge Teflon-coated mass spectrometer probe was inserted into the intramedullary canal, directed toward the tibial metaphysis, and the osteotomy was sealed with bone wax. The partial pressure of oxygen and argon were measured by a mass spectrometer (Chemtron, St. Louis, MO). Data were utilized from six rabbits that completed the entire study.

A tracheostomy was performed through which appropriate gases were administered according to these procedures:

1) The animal was breathing ambient air. The oxygen tensions were those found in normal and osteomyelitic bones under ambient conditions.

2) The inspired gas was changed from ambient air to 80% Ar and 20% O_2. This gas mixture was administered for 30 min and was the "argon wash-in phase." The argon-oxygen mixture was changed back to ambient air, allowing the accumulated argon to be "washed-out" of the tissues. The rate of argon wash-out allowed comparison of blood flow between normal and osteomyelitic bone.

3) After these measurements, the animal was pressurized to 2 ATA in a small hyperbaric chamber. The inspired gas was changed to 100% O_2 and the oxygen tension in normal and osteomyelitic bone was measured.

4) The chamber was decompressed to ambient conditions. A repeat argon wash-in and wash-out was accomplished. Blood flow between normal and osteomyelitic bone was compared after hyperbaric oxygen exposure.

We obtained bone pH measurements from normal and osteomyelitic bone using a tissue pH machine (Ionalyzer-801, Orion Research Inc., Cambridge, MA) by placing a flexible tissue pH probe (Microelectrodes Inc., Londonderry, NH) into the intramedullary canal and directing it into the tibial metaphysis area.

Phagocytic Killing of S. aureus Under Different Oxygen Tensions

S. aureus was grown overnight in trypticase soy broth, washed, and resuspended in Hanks balanced salt solution (HBSS). Rabbit peritoneal polymorphonuclear leukocytes (PMN) were harvested 3.5 h after intraperitoneal injection of 0.1% glycogen, washed 3 times, and resuspended in HBSS.

Three tubes were prepared for each time point (all studies were performed in duplicate). To the first tube was added 3×10^6 *S. aureus*, 3×10^6 PMN, and 10% pooled human serum (opsonin) to a total volume of 1 mL. Two control tubes were prepared for each time point—one without PMN and the other without opsonin. Hanks balanced salt solution and heat-inactivated fetal calf serum were substituted for PMN and opsonin, respectively. A small aliquot was taken from each tube, added to sterile water, and the number of colony-forming units (CFU) of *S. aureus* was determined.

The tubes were tumbled for 30 min at 4°C to provide optimal bacterial attachment to the PMN. The contents of each tube were then decanted into a polyethylene culture dish (35 × 10 mm). The resulting suspension was approximately 1 mm thick, so that optimal oxygen penetration was insured. Five different atmospheric conditions were studied. Dishes were placed in a 37°C

incubator (P_{O_2}, 150 mmHg, ambient conditions) or in a 37°C chamber in which the oxygen tension was either 23 mmHg (oxygen tension found in osteomyelitic bone under ambient conditions), 45 mmHg (oxygen tension found in normal bone under ambient conditions), 109 mmHg (oxygen tension found in osteomyelitic bone under our HBO conditions), or 760 mmHg (100% oxygen). At least six separate experiments were performed for each chamber oxygen tension and all six experiments were run in duplicate. A parallel ambient experiment was run for each chamber oxygen tension experiment. After 1 or 2 h, a dish representing each original tube was removed from the incubator or the chamber. An aliquot was taken from the plate and added to sterile water; the number of CFU of *S. aureus* was determined. The percentage of original inoculum was then calculated. The viability of the PMN was examined by the exclusion of trypan blue dye.

The data were analyzed by Student's unpaired *t*-test.

RESULTS

Oxygen tensions in normal and osteomyelitic bone are shown in Fig. 1. The partial pressure of oxygen in osteomyelitic bone under ambient conditions was 20.9 ± 1.7 mmHg, whereas the oxygen tension in normal bone was 44.7 ± 0.7 mmHg ($P < 0.001$). When the animals were placed under hyperbaric conditions, the oxygen tensions increased in both the osteomyelitic bone (104.0 ± 6.8 mmHg) and normal bone (321 ± 18.7 mmHg). This difference was statistically significant ($P < 0.001$).

Perfusion was decreased in osteomyelitic bone and was not acutely increased by HBO in either the normal or infected bone. The intramedullary pH was likewise decreased in osteomyelitic bone (6.85 ± 0.14), as compared to normal bone (7.21 ± 0.03). This difference was statistically significant ($P < 0.05$).

The phagocytic killing data are expressed as the percentage of surviving *S. aureus* (Fig. 2). The control tubes (*S. aureus* plus opsonin without PMN and *S. aureus* plus PMN without opsonin) showed a percentage of surviving *S. aureus* greater than 100% under all 5 oxygen tensions.

Phagocytic killing occurred only when *S. aureus*, PMN, and opsonin were in the in vitro test system. The greater survival (least killing) of *S. aureus* occurred at an oxygen tension of 23 mmHg (74.9 ± 8.6% and 88.2 ± 7.8% at 1 and 2 h, respectively. The increasing oxygen tensions resulted in progressively decreasing survival (greater killing) of *S. aureus*: 45 mmHg, 69.7 ± 7.1% (1 h) and 56.2 ± 3.5% (2 h); 109 mmHg, 65.6 ± 5.0% (1 h) and 49.3 ± 3.0% (2 h); 150 mmHg (ambient), 46.2 ± 2.6% (1 h) and 28.2 ± 2.9% (2 h); and 760 mmHg, 45.2 ± 5.7% (1 h) and 19.6 ± 6.8% (2 h).

Comparison of the differences in percent of survival of *S. aureus* at 2 h using any two oxygen tensions (23 mmHg, 45 mmHg, 109 mmHg, 150 mmHg, and 760 mmHg was significant ($P < 0.001$) except for the difference between 45 mmHg and 109 mmHg, and 150 mmHg and 760 mmHg ($P < 0.1$).

MASS SPECTROMETER OXYGEN DATA
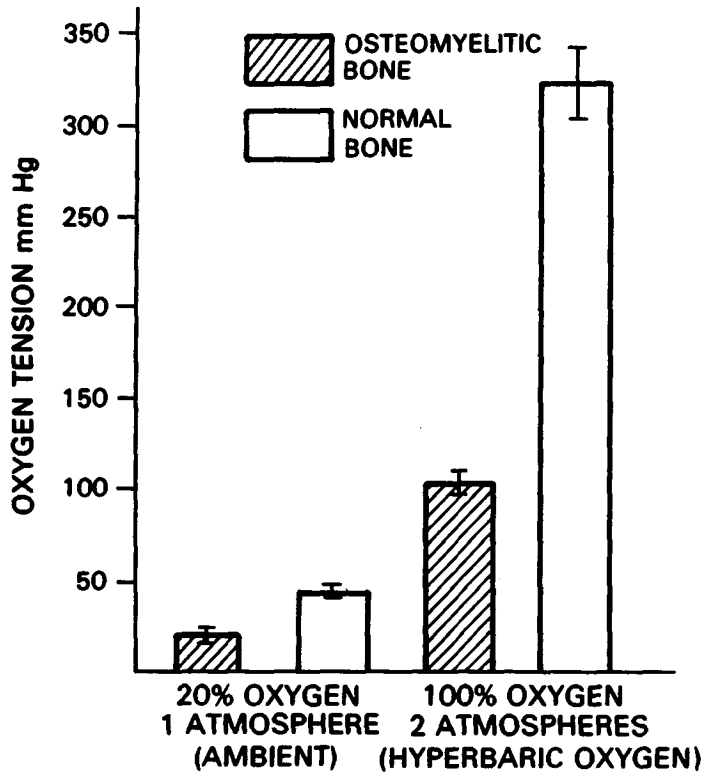
Fig. 1. Oxygen tensions in normal and osteomyelitic bone under ambient and hyperbaric oxygen (100% O_2 at 2 ATA. Oxygen tensions were measured simultaneously from normal and osteomyelitic bones by a mass spectrometer. Results are expressed in mmHg O_2. Brackets denote mean ± SE.

The viability of the PMN under all five oxygen tensions was greater than 95% at 2 h as shown by the exclusion of trypan blue dye.

DISCUSSION

Osteomyelitic bone in this model has a decreased blood flow, a decreased pH, and a markedly reduced partial pressure of oxygen. The oxygen tension in osteomyelitic bone (20.9 ± 1.7 mmHg) was significantly decreased compared to normal bone (44.7 ± 0.7 mmHg).

Hyperbaric oxygen failed acutely to influence blood flow in osteomyelitic bone. However, HBO increased the oxygen tension to supraphysiologic levels in osteomyelitic bone (104.0 ± 6.8 mmHg).

Phagocytic killing of this *S. aureus* was reduced markedly under oxygen tensions found in osteomyelitic bone. At decreased oxygen tensions a problem
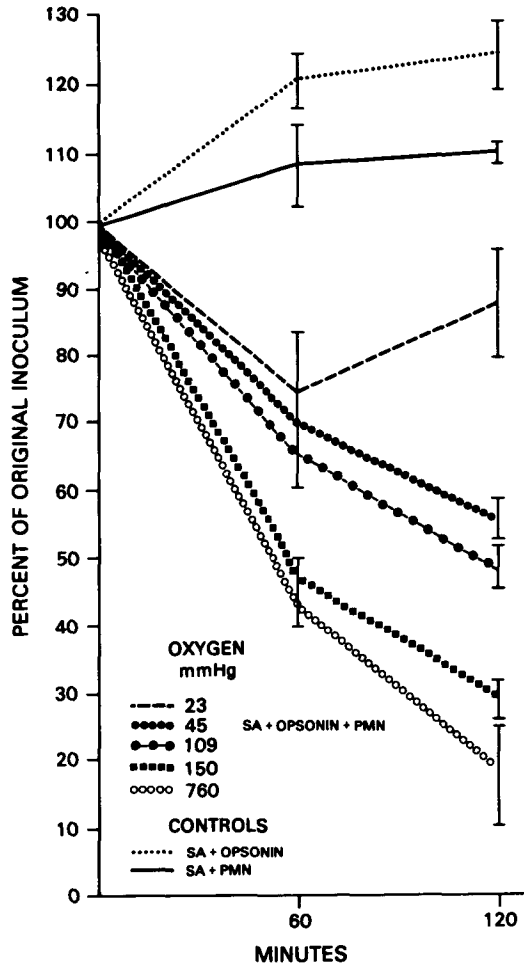
Fig. 2. .Phagocytic killing of *S. aureus* (SA) under different oxygen tensions (see text for procedures). Results are expressed as the percentage of the original inoculum of SA. Controls represent SA plus opsonin without PMN, or SA plus PMN without opsonin under the different oxygen tensions. Brackets denote mean ± SE.

exists in the ability of the phagocytic or intracellular killing mechanisms to handle pathogenic organisms (10,11). The cause of this difficulty is not clear from our studies; therefore we have used the broad term *phagocytic killing* to describe any breakdown in the process from ingestion to intracellular killing of *S. aureus*. However, Mandell (12) has shown *S. aureus* to be ingested normally but not totally killed under anaerobic conditions. Adequate oxygen tensions appear to be necessary for effective intracellular killing of this *S. aureus*.

    Under the oxygen tensions found in osteomyelitic bone treated with HBO, the phagocytic killing of this *S. aureus* returns to normal when compared to

the phagocytic killing found under the oxygen tensions in normal bone. Unfortunately, there is a tendency in the literature to equate phagocytic killing under ambient conditions to *normal phagocytic killing,* instead of phagocytic killing under oxygen tensions found within normal tissue. We believe phagocytic killing under tissue oxygen tensions is a more valid representation of normal phagocytic killing. Phagocytic killing can be enhanced by further increasing the oxygen tensions. Currently, the optimal oxygen tensions for phagocytic killing appear to be between 150–760 mmHg. However, phagocytic killing at higher oxygen tensions is yet to be explored.

Thus, intramedullary oxygen tension in osteomyelitic bone is insufficient to support normal phagocytic function. Reduced phagocytic cidal activity may explain, in part, both the chronicity of this infection and the effect of HBO. Hyperbaric oxygen therapy is effective in staphylococcal osteomyelitis because it increases the intramedullary tensions to levels where phagocytic killing may proceed optimally.

References

1. Slack WK, Thomas DA, Perrins D. Hyperbaric oxygenation in chronic osteomyelitis. Lancet 1965;1:1093–1094.
2. Depenbusch FL, Thompson RE, Hart GB. Use of hyperbaric oxygen in the treatment of refractory osteomyelitis: a preliminary report. J. Trauma 1972;12:807–812.
3. Davis JC. Refractory osteomyelitis of the extremities and axial skeleton. In: Davis JC, Hunt TK, eds. Hyperbaric oxygen therapy. Bethesda, MD: Undersea Medical Society 1977:217–227.
4. Morrey BF, Dunn JM, Heimbach RD, Davis J. Hyperbaric oxygen as an adjunct in the treatment of chronic osteomyelitis. Clin Orthop 1979;144:121–127.
5. Mader JT, Guckian JC, Glass DL, Reinarz JA. Therapy with hyperbaric oxygen for experimental osteomyelitis due to *Staphyloccus aureus* in rabbits. J Infect Dis 1978;138:312–318.
6. Ollodart, R, Blair E. High-pressure oxygen as an adjunct in experimental bacteremic shock. JAMA 1965;191:736–739.
7. McAllister TA, Stark JM, Norman JN, Ross RM. Inhibitory effects of hyperbaric oxygen on bacteria and fungi. Lancet 1963;2;1040–1042.
8. Hopkinson, WI, Towers AG. Effects of hyperbaric oxygen on some common pathogenic bacteria. Lancet 1963;2:1361–1363.
9. Crane LR, Kapdi CC, Wolfe JN, Silberberg BK, Lerner AM. Xeroradiographic, bacteriologic, and pathologic studies in experimental staphylococcus osteomyelitis. Proc Soc Exp Biol Med 1977;156:303–314.
10. Selvaraj RJ, Sbarra AJ. Relationship of glycolytic and oxidative metabolism to particle entry and destruction in phagocytosing cells. Nature 1966;211:1272–1276.
11. McRipley RJ, Sbarra AJ. Role of the phagocyte in host-parasite interactions. XI. Relationship between stimulated oxidative metabolism and hydrogen peroxide formation, and intracellular killing. J Bacteriol 1967;94:1417–1424.
12. Mandell GL. Bactericidal activity of aerobic and anaerobic polymorphonuclear neutrophils. Infect Immun 1974;9:337–341.

PART IV. DISCUSSION: OXYGEN SUFFICIENCY AND UTILIZATION WITHIN THE CELL

F. G. Hempel and F. F. Jöbsis, *Rapporteurs*

The noninvasive monitoring of cerebral oxidative metabolism uses the redox state of the heme Cu on cytochrome oxidase as an indicator of oxygen availability. In turn, availability is a reflection of the adequacy of blood flow and the density of the nutrient capillaries. The 850 nm absorbance band for the Cu on cytochrome oxidase is sufficiently specific for the determination of the redox state of the cytochrome. Cerebral metabolism, is best studied with the spectrophotometric probe being used in the reflectance mode rather than in the transillumination system. In such a way, light flux into and out of the cortex is considerably greater and much improves the signal quality of the spectrophotometric data. Indirectly, the carotid body serves also as an indicator of oxygen sufficiency. Its extremely high metabolic rate suggests that it first senses an oxygen deficit, or even oxygen toxicity. The receptor cells in the carotid body measure oxygen availability in relation to their own metabolism, and perhaps detect blood flow decrements to distant tissues such as skeletal or cardiac muscle by virtue of this oxygen sensitivity.

The geometric distribution of capillaries in any organ, particularly skeletal muscle, ultimately determines the oxygen gradient to the cell. Oxygen provision is dynamically uncertain, because at least four kinds of heterogeneity can exist at any instant. These are the heterogeneities in capillary distribution, in longitudinal patterns, in flow velocity, and in temporal arrangement. Some specialized tissues, such as the retina, are provided with oxygen from a more definable source. In the rabbit eye, oxygen provision to the retina is derived solely from the choriod, and thus the relationship between the oxygen source and consuming cells is well established. The choriodal vasculature displays a vigorous constrictive reaction to oxygen at high pressure, similar to the anterior retinal vessels in more complex ocular circulatory systems. The retina is especially sensitive to oxygen lack, as manifested by disruption of its electrical generating capacity and, moreover, shows a profound attenuation of activity in the presence of high carbon dioxide tensions. In the latter instance, a possible Bohr shift in hemoglobin binding affinity for oxygen may, in effect, mimic a hypoxemic condition in spite of high inspired oxygen tensions such as those achieved during air-breathing at 4 atm. Apparently, then, the oxygen affinity for hemoglobin at very high arterial partial pressures of oxygen ($>$ 400 Torr) may be markedly reduced by the formation of the carbamino species in hypercapnia.

Finally, oxygen tensions maximal for phagocytic killing in bone disease are far above these generally tolerable for other body tissues. Clearly, osteomyelitic bone suffers an oxygen embarrassment, and because of this cannot provide sufficient oxygen partial pressures for polymorphonuclear cells to act effectively. Whether a flow impairment exists or not has yet to be determined. If this were the case, perhaps stimulation of perfusion to a hypoxic bone core would be a beneficial adjunct to conventional antibiotic therapy and would, to some extent, replace the relatively short treatments presently administered via hyperbaric oxygen.

PART V

METABOLISM AND THERMAL PHYSIOLOGY

CURRENT CONCEPTS OF METABOLISM AND THERMOPHYSIOLOGY

P. Webb

The organizers of this symposium were wise to pair metabolism, the source of body heat, with thermophysiology, which deals with heat exchange. In this review of the literature from the past 5 or 6 years I have chosen whenever possible to first discuss findings from studies of hyperbaric gas environments where so many divers now live and work, then the results of experiments with direct cooling, as in water immersion.

The metabolic response to the dry, warm hyperbaric environment of saturation diving is disappointingly mild. I had hoped to find enough increase in 24-h metabolism to explain the weight loss commonly seen in these dives, a weight loss that prevails despite overeating. No explanation was found in either fluid balance or in poor absorption of food. The mystery remains. There is nice new work on the metabolic (shivering) response to cold-water immersion, resulting in sensible predictive equations. And we now know that the metabolic cost of cold exposure is an increment to the cost of swimming.

With the widespread use of saturation diving it has become painfully evident that precise thermal control of bells and chambers is critical. There are unpublished reports of deaths that sound much like heat stroke and hypothermia. How quickly an innocent-sounding temperature, like 27°C for gas at 18 ATA, causes sustained shivering, and how quickly unprotected men cool in hyperbaric heliox at 15, 20, and 25°C, is revealed in recent experiments. Also, there is new evidence that cold exposure increases the possibility of decompression sickness.

We seek a simple relationship between heat loss from the body and change in body temperature, but it appears to be a most complex connection. The rate of heat loss makes a critical difference, as do body size and fatness.

Experiments continue and summaries in the form of biothermal models appear. The knowledge will be valuable in the engineering design of thermal protection.

Rewarming from cold-water immersion continues to receive attention. A method suitable for certain field conditions is breathing hot saturated air, a method surprisingly effective in raising core temperature. In hospitals, peritoneal lavage with warmed fluids is found to be an effective treatment of profound hypothermia.

Finally, my review will touch on recent studies of human performance of the higher-order, cognitive variety, in underwater situations that produce mild hypothermia. Such studies are of great importance for the effectiveness and safety of the diver. I am sorry there are not more to report.

METABOLIC RESPONSE TO HYPERBARIC GAS

Several studies of thermally comfortable subjects in hyperbaric environments report small increases in metabolism. Raymond et al. (1) reported an increase of 8% at 14.6 ATA He-O_2. During a saturation dive to 18.6 ATA He-O_2, Webb et al. (2) reported a 12% rise in 24-h metabolism, based on continuous measurements of O_2, CO_2, and urinary nitrogen; the continuous 24-h measurement, using an open system, was confirmed by four times daily measurements with a Douglas bag and gas analysis. The rise in metabolism occurred principally during the hours awake. In this symposium, Garrard et al. (3) tell us that resting energy expenditure was highest at the greatest depth their divers reached and decreased during decompression, although basal metabolic rate was unchanged. Supporting data are found in the increase in thyroid hormone released from peripheral stores.

However, there are reports that show no increase in metabolic rate during thermally comfortable hyperbaric exposure. Timbal et al. (4), who measured metabolic rate from oxygen consumption for three 10-min periods at pressures from 1.5 to 30.8 ATA, found no increase, nor did Raymond et al. (5) in two men residing for 7 days in He-O_2 at 49.5 ATA. In this symposium, Nakayama et al. (6) report no significant change in the resting metabolic rate during a 14-day saturation dive at 31 ATA.

The disagreement may be simply the result of slightly lower than euthermic temperatures in those reports that show metabolic increase, because as little as ½°C makes a considerable difference in heat transfer in hyperbaric gas. Increased heat transfer may occur with warm skin temperatures and with very little if any decrease in core temperature. The metabolic rate increases that have been reported are small; therefore, they would not particularly influence food supply for saturation diving. There is no suggestion of a pharmacologic effect of helium, which once was thought to stimulate metabolism.

If thermal comfort is not maintained, the metabolic response is prompt. Webb et al. (2) reported there was a clear metabolic stimulus from living in cool hyperbaric gas during 3 cold days in which the He-O_2 at 18.7 ATA was 27°C instead of 31°C: 24-h metabolism was 26% higher than sea level control, while the daytime values alone were more than 50% higher.

WEIGHT LOSS IN SATURATION DIVING

The most likely explanation of the weight loss that accompanies most chamber saturation dives is increased heat loss, which might occur despite thermally comfortable temperatures. The fascinating thing is that the weight loss occurs in the face of high food intake. The magnitude of the weight loss correlates with the product of pressure and duration of exposure (2). Despite its plausibility the metabolic explanation of the weight loss, i.e., increased metabolism to match increased heat loss, is not supported by the studies of metabolic rate, referred to in preceding paragraphs. Other explanations of the weight loss include water loss, poor absorption of food, and atrophy of confinement with loss of tissue.

The case for water loss was made by Raymond et al. (7), who calculated fluid balance from liquid intake and urinary output and noted a fluid deficit roughly matching the weight loss of their subjects. However, they assumed that insensible and fecal water loss were of normal magnitude, roughly balancing the water in food and the water of oxidation. But insensible water loss is reduced during hyperbaric exposure (8). Further, the Raymond et al. (7) subjects did not recover their original weight during the long decompression, nor immediately after the dive. Urine output increases during saturation diving but, as shown in a comprehensive study of body fluid balance by Hong et al. (8), diuresis follows a suppression of antidiuretic hormone, which appears to result from the suppression of insensible water loss. Significantly, the diuresis and the weight loss occur while total body water remains nearly constant (2,8).

The possibility that food is poorly absorbed during hyperbaric exposure was eliminated in the detailed study by Webb et al. (2). We analyzed all the food by bomb calorimetry to eliminate the possibility that handbook values were a significant source of error, and all urine and feces were collected and analyzed for energy by bomb calorimetry. Absorption was a normal 92–94% of the food intake. In the same study, the question of atrophy of confinement seemed to be eliminated both by the fact that the men were in continuous positive nitrogen balance and by the studies of body composition before and after the dive, which showed no significant change in lean body mass. Incidentally, the food intake in our study increased the minute the chamber door was closed, even though the men then stayed for 3 days at sea-level pressure before chamber pressurization began; thus, the food drive was perhaps one of confinement and boredom rather than an effect of hyperbaric gas. Other studies (3,7) have specified particular food intakes and not allowed the men to overeat, but the weight loss persists.

No explanation for the weight loss of saturation diving has been found so far. Speculatively, there might still be a long, drawn-out excess loss of heat despite the sensation of thermal comfort and despite normal body temperatures. This would not necessarily be matched by an increase in metabolism. A parallel situation exists in the mild cold exposure we use to simulate the gradual but continuous heat loss of thermally protected underwater swimmers in swimmer delivery vehicles. By removing a net 0.5–1.0 kcal/min over many hours it is possible to reduce the body heat content by 200 or 300 kcal without

an increase in metabolism and with no great change in core temperature. If there is a similar situation in hyperbaric gas, it can only be measured by precise direct calorimetry. It may be a serious mistake to rely upon indirect calorimetry (measurement of metabolism) as the equivalent of direct calorimetry. The assumed equivalence of direct and indirect calorimetry is being seriously challenged by other studies in my laboratory (9).

METABOLIC RESPONSE TO COLD EXPOSURE

Shivering and increased metabolism are major responses to cold exposure that have traditionally interested thermophysiologists. Hayward et al (10) studied men and women wearing light clothing and life jackets immersed in the cold sea and described a relationship between metabolic rate and water temperature. At water temperatures between 5 and 18°C, metabolism increased to almost four times resting level at the coldest temperature, but in no case was the increase sufficient to prevent a fall in rectal temperature. In a second study, Hayward and colleagues (11) studied eight men wearing only bathing trunks and immersed in 10°C water. They developed equations to predict metabolic rate as a function of skin temperature and core temperature, measured either in the rectum or at the tympanic membrane. The subjects in both of these studies were young and relatively thin, and the predictions have yet to be tested for people with greater thicknesses of subcutaneous fat.

In a related study, Johnson et al. (12) found that the sympathetic nervous system responded quickly to cold. Two minutes after immersion in 10°C water, plasma norepinephrine doubled, then rose gradually as metabolism rose over the 60 min of immersion. Interestingly, plasma norepinephrine fell abruptly during the first 10 min of rewarming in 40°C water, at the same time that shivering stopped. Shivering, in these and other studies, is seen to stop quickly with rewarming, apparently as a result of a rise in skin temperature, even though the core temperature remains well below starting level.

Although exercise appears to inhibit shivering, the metabolic response to cold exposure adds to the metabolic cost of the exercise, as shown by Nielsen (13). Studying subjects swimming hard enough to give oxygen consumptions between 1.4 and 2.0 L/min, Nielsen has shown that cold water from 14 to 20°C causes an increase in metabolism above that needed for swimming as an inverse function of skin temperature. Nielsen also reported that during rewarming in air with bicycle exercise, shivering stopped as skin temperature rose despite a persistent low level of core temperature measured in the esophagus or rectum.

Shivering is not an easy phenomenon to study. Buguet et al. (14) found that shivering occurred when men were kept warm in sleeping bags but with their heads exposed to very cold air, so that shivering occurred despite generally comfortable skin temperatures. Marijuana, a common drug these days, also influences the shivering response. Hanna et al. (15) found that it increased shivering in standard exposures to cold air and cold water, and they suspected an involvement with the sympathetic nervous system.

Divers and underwater swimmers normally wear thermal protection and the cold exposures are not nearly so severe as those, for example, with nude men in 10°C water. In diving operations, shivering is generally a late symptom and it remains to be seen whether the shivering response can be predicted on models such as proposed by Hayward et al. (11).

THERMOPHYSIOLOGY IN HYPERBARIC GAS ENVIRONMENTS

For men to be thermally comfortable in hyperbaric gas, the temperature must be higher as the pressure increases and the band width of comfortable temperatures becomes progressively narrower. The comfort zone has been established both empirically and theoretically (1,2,4,5).

Exposure to temperatures only a little different from comfort leads rapidly to cold or heat exposure in hyperbaric environments. The rapidity of heat loss or heat gain has long been predicted and there have been deaths both from hypothermia and hyperthermia when the temperature control in bells and hyperbaric chambers was lost.

Experimental experience in noncomfort conditions has just begun. In *Hana Kai II*, a saturation dive at 18.6. ATA, we purposely lowered the chamber temperature from a comfortable 31 to 27°C for 3 days and nights (2). The subjects put on heavier clothing but were continually cold and increased their metabolism in response to the "cold stress" of 25°C. A more extensive study has been reported by Kuehn and Zumrick (16). Divers, clad only in shorts, were exposed for several hours to temperatures of 15, 20, and 25°C in helium-oxygen at pressures equivalent to depths up to 1400 ft. Skin temperatures dropped abruptly and rectal temperatures fell after an initial rise (as often seen in exposure to cold water), thus confirming the predicted rapid heat loss in hyperbaric gas. Additional measurements were made of heat flow with heat flux sensors applied to the skin. The subjects shivered violently. Tolerance times ranged from 60 to 158 min, with the shortest times generally those at the highest pressures and lowest temperatures.

Heat and cold stress also affect the washout of inert gas and therefore may increase the incidence of decompression sickness. This has been explored by Bove et al. (17) in studies of radioactive xenon gas exchange in rabbits. Dunford and Hayward (18) describe, in a current report, an increased formation of bubbles in no-decompression dives when the water is cold.

Bondi (19), in this symposium, offers a theoretical analysis of heat stress under hyperbaric conditions, which predicts heat storage and danger from hyperthermia or heat stroke as a function of chamber temperature and vapor pressure at various total pressures. It will be interesting to see how well empirical evidence matches these predictions.

BODY TEMPERATURE CHANGE AND HEAT LOSS IN DIVING

Direct measurements of body heat loss have been combined with the classic measurements of body surface and core temperatures, using both direct calorimetry and the measurement of surface heat loss with heat flux transducers

(20,21). Unfortunately, the relationship between heat loss and temperature change has proven not to be simple. In preliminary reports from my laboratory (22,23), the rate of cooling, body size, and body fat are important variables in predicting temperature change from heat loss. Slow cooling over a long period of time can result in large losses of heat, e.g., 300 kcal, with very little change in internal or surface temperature and little metabolic response. The same quantity of heat lost rapidly by direct immersion in cold water would cause a large metabolic response, a steep drop in skin temperature, and a rapidly falling rectal temperature. Also, as seems obvious, the larger the man the greater tolerance he has for a given heat loss and the smaller his body temperature change. Cooling rates much slower than experienced by men immersed nude in cold water are realistic in diving operations. Thermally protective clothing attenuates more or less effectively the cold exposure. Long, slow cooling may be a serious operational problem.

New and useful work continues to be done with direct immersion of unprotected men in cold water (10–13, 24). Boutelier et al. (24) have added significantly to the definition of convective heat transfer in water. Also interesting are the studies of which areas of the body lose heat most readily, using thermograms of the skin surface following immersion (25, 26).

The usefulness of various cooling experiments will be found in the engineering of better thermal protection for divers. Many of the cited papers offer predictive equations. Formal biothermal models are becoming more comprehensive and more widely applicable as laboratory data accumulates (23, 27–29).

REWARMING

In the recent literature two methods for rewarming have received the most attention. Inhalation warming is attractive because it promises to be useful as a field technique and because heat is added to the body core. Peritoneal lavage with warm saline is also a direct method of warming the core, but is suitable only in a hospital environment. There have been several studies comparing a number of rewarming methods on the same experimental subjects.

Hayward and Steinman (30) rewarmed subjects who had been acutely cooled in cold sea water by (a) immersing them in a hot bath and (b) by inhalation warming with moistened and heated oxygen. They observed rapid reversal of the downward trend of temperature in the esophagus and at the tympanic membrane when inhalation warming was used compared to the warming in a bath. The more slowly changing rectal temperature showed about the same amount of afterdrop with both methods. Morrison et al. (31) rewarmed subjects cooled in similar fashion, first by letting them breathe air heated to 45°C and saturated, then after a second exposure the subjects were caused to hyperventilate by rebreathing the hot saturated air to increase the respiratory exchange to 40 L/min. The rectal and tympanic temperatures increased more rapidly with the rebreathing technique. In his symposium, Conn et al. (32) compare rewarming by shivering alone, by breathing saturated air at 47°C at a spontaneous rate, and by breathing at 40 L/min through rebreathing of saturated hot

air at 47°C. They find that core temperature measured rectally and at the tympanic membrane is raised more effectively by both inhalation methods and suggest that metabolic heat production is only partially effective in raising internal temperature.

Treatment of a case of profound accidental hypothermia was accomplished effectively with peritoneal dialysis, as reported by Soung et al. (33). Using a dialysate at 38°C, they raised an initial rectal temperature of 28°C by 5° in the first hour, and by 4° more to 37°C in 2 more hours. Similarly, Jessen and Hagelsten (34) described successful rewarming by peritoneal dialysis of severely hypothermic youngsters who had been rescued from cold water. They recommend the treatment not only for core rewarming but also for the control of electrolyte imbalance and removal of possible toxic substances. Further evidence of the effectiveness of peritoneal lavage is reported by Bynum et al. (35), who found this the most effective way to recool dogs who had been made hyperthermic.

Laboratory comparisons have been made of various techniques for rewarming of subjects in early hypothermia. Marcus (36) found that rewarming in a hot bath was significantly more effective in raising deep body temperature than any other method, and that a water-heated tubing suit was more effective than inhalation rewarming or spontaneous rewarming in a sleeping bag. Harnett et al. (37) compared rewarming by eight different techniques, basing the comparison largely on the appearance of the afterdrop of rectal temperature. Various rewarming techniques were discussed thoroughly at a symposium at the RAF Institute of Aviation Medicine (38). While everyone agrees that rewarming is a medical necessity, there is considerable disagreement as to which technique is most appropriate for what situation. Further laboratory work and further experience will help to resolve the issues.

PERFORMANCE OF DIVERS IN COLD WATER

Studies of performance in the diving environment, including cold water, were reviewed recently in *The Underwater Handbook* (39). The well known peripheral effects of cold on dexterity, muscle strength, and sensation need not be reviewed again. The following studies were designed to look for the performance effects of general body cooling.

In a realistic cold exposure described by Vaughan (40), trained U.S. Navy men were studied in open-water trials of a two-man wet submersible vehicle in Puget Sound. The water temperature was 6°C. The divers wore their usual multiple layers of foamed neoprene wet suits, but in the 4- and 6-h trials, the men shivered and reported having painfully cold hands and feet. A single skin temperature, measured on the medial thigh, fell progressively from 28 to 22°C in 6 h. Rectal temperature fell only 1.2°C and tended to stabilize at 36.5°C. The long, slow cooling was physiologically tolerable, but it was surmised that the men lost a large amount of heat despite the small change in core temperature. The performance of the pilot in maintaining the depth of the vehicle remained good, but as time passed he made errors in keeping correct

headings. The second man, a sonar operator, found it difficult to concentrate on his task and to recall well-known procedure. The performance effects were response blocking and perseveration of nonadaptive responses.

Davis et al. (41) studied the performance of scuba divers wearing wet suits in 20°C and 5°C fresh water, taking measurements of five skin temperatures and of rectal temperature. In 5°C water, the men were cold and shivered within 10–15 min; 2 of the 15 divers could not complete the 40-min dive because of cold distress. A battery of tests—simple arithmetic, logical reasoning, word recall, word recognition, and manual dexterity—all showed immediate degradation in the cold, a distraction effect. Only one test, that of word recognition, worsened as rectal temperature fell.

The distracting effects of cold water were further emphasized by Vaughan (43) in a study of higher-order performance in trained men. In a simulated submersible vehicle in a temperature-controlled tank, the men detected peripheral targets and solved navigation problems. Water temperatures were 15.5 and 4.5°C. A full set of wet suits kept core and surface temperatures from falling greatly during 3-h exposures. Because task performance changed most in the first hour, and because second- and third-hour performances in cold water were similar to those at the more moderate water temperature, the performance decrements measured were not thought to be the result of body heat loss.

Nevertheless, performance decrement in the hypothermia of diving remains a concern. Perhaps the right laboratory studies have not yet been designed.

References

1. Raymond LW, Bell II WH, Bondi KR, Lindberg CR. Body temperature and metabolism in hyperbaric helium atmospheres. J Appl Physiol 1968;24:678–684.
2. Webb P, Troutman SJ Jr, Frattali V, Dressendorfer RH, Dwyer J, Moore TO, Morlock JF, Smith RM, Ohta Y, Hong SK. Hana Kai II: a 17-day dry saturation dive at 18.6 ATA. II. Energy Balance. Undersea Biomed Res 1977;4:221–246.
3. Garrard MP, Hayes PA, Carlyle RF, Stock MJ. The metabolic and thermal status of divers during simulated dives at 55 bar. In: Bachrach AJ, Matzen MM, eds. Underwater physiology VII. Proceedings of the seventh symposium on underwater physiology. Bethesda, MD: Undersea Medical Society, 1981:517–538.
4. Timbal J, Viellefond H, Guenard H, Varene P. Metabolism and heat losses of resting man in a hyperbaric helium atmosphere. J Appl Physiol 1974;36:444–448.
5. Raymond LW, Thalmann E, Lindgren G, Langworthy HC, Spaur WH, Crothers JH, Braithwaite WR, Berghage TE. Thermal homeostasis of resting man in helium-oxygen at 1–50 atmospheres absolute. Undersea Biomed Res 1975;2:51–67.
6. Nakayama H, Hong SK, Claybaugh J, Matsui W, Park YS, Ohta Y, Shiraki K, Matsuda M. Energy and body fluid balance during a 14-day dry saturation dive at 31 ATA (SEADRAGON IV). In: Bachrach AJ, Matzen MM, eds. Underwater physiology VII. Proceedings of the seventh symposium on underwater physiology. Bethesda, MD: Undersea Medical Society, 1981:541–554.
7. Raymond LW, Raymond NS, Frattali VP, Sode J, Leach CS, Spaur WH. Is the weight loss of hyperbaric habitation a disorder of osmoregulation? Aviat Space Environ Med 1980;51:397–401.
8. Hong SK, Claybaugh JR, Frattali V, Johnson R, Kurata F, Matsuda M, McDonough AA, Paganelli CB, Smith RM, Webb P. Hana Kai II: a 17-day dry saturation dive at 18.6 ATA. III. Body fluid balance. Undersea Biomed Res 1977;4:247–265.

9. Webb P. The measurement of energy exchange in man: an analysis. Am J Clin Nutr 1980;33:1299-1310.
10. Hayward JS, Eckerson JD, Collis ML. Thermal balance and survival time prediction of man in cold water. Can J Physiol Pharmacol 1975;53:21-32.
11. Hayward JS, Eckerson JD, Collis ML. Thermoregulatory heat production in man: prediction equation based on skin and core temperatures. J Appl Physiol: Respirat Environ Exercise Physiol 1977;42:377-384.
12. Johnson DG, Hayward JS, Jacobs TP, Collis ML, Eckerson JD, Williams RH. Plasma norepinephrine responses of man in cold water. J Appl Physiol: Respirat Environ Exercise Physiol 1977;43:216-220.
13. Nielsen B. Metabolic reactions to changes in core and skin temperature in man. Acta Physiol Scand 1976;97:129-138.
14. Buguet AGC, Livingstone SD, Reed LD, Limmer RE. Cold-induced shivering in men with thermoneutral skin temperatures. J Appl Physiol 1976;41:142-145.
15. Hanna JM, Strauss RH, Itagaki B, Kwon, WJ, Stanyon R, Bindon J, Hong SK. Marijuana smoking and cold tolerance in man. Aviat Space Environ Med 1976;47:634-639.
16. Kuehn LA, Zumrick J. Thermal measurements on divers in hyperbaric helium-oxygen environments. Undersea Biomed Res 1978; 5:213-231.
17. Bove AA, Hardenbergh E, Miles JA, Jr. Effect of heat and cold stress on inert gas ([133]xenon) exchange in the rabbit. Undersea Biomed Res 1978;5:149-158.
18. Dunford R, Hayward J. The effects of cold stress on venous gas bubble production in man following a no-decompression dive. In: Program, abstracts, and mini-papers. The Undersea Medical Society annual scientific meeting (abstracts), 7th Symposium on underwater physiology. Bethesda, MD: Undersea Medical Society, 1980:16.
19. Bondi KR. An analysis of heat stress under hyperbaric conditions. In: Bachrach AJ, Matzen MM, eds. Underwater physiology VII. Proceedings of the seventh symposium on underwater physiology. Bethesda, MD: Undersea Medical Society, 1981:503-507.
20. Kuehn LA. Assessment of convective heat loss from humans in cold water. Trans ASME, J Biomech Engin 1978;100:7-13.
21. Webb P. Calorimetric analysis of cold exposure in diving. In: Shilling CW, Beckett MW, eds. Underwater physiology VI. Proceedings of the sixth symposium on underwater physiology. Bethesda, MD: Federation of American Societies for Experimental Biology, 1978:107-113.
22. Webb P, Troutman SJ Jr, Annis JF. Heat loss and body temperature change during measured cooling. Undersea Biomed Res 1979;6(Suppl):27.
23. Troutman SJ Jr, Webb P, Annis JF. Estimating body heat loss from temperature changes during cooling. Undersea Biomed Res 1979;6(Suppl):27.
24. Boutelier C, Bougues L, Timbal J. Experimental study of convective heat transfer coefficient for the human body in water. J Appl Physiol: Respirat Environ Exercise Physiol 1977;42:93-100.
25. Hayward JS, Collis M, Eckerson JD. Thermographic evaluation of relative heat loss areas of man during cold water immersion. Aerosp Med 1973;44:708-711.
26. Wade CE, Veghte JH. Thermographic evaluation of the relative heat loss by area in man after swimming. Aviat Space Environ Med 1977;48:16-18.
27. Timbal J, Loncle M, Boutelier C. Mathmatical model of man's tolerance to cold using morphological factors. Aviat Space Environ Med 1976;47:958-964.
28. Gordon RG, Roemer RB, Horvath SM. A mathematical model of the human temperature regulatory system—transient cold exposure response. IEEE Trans Biomed Engin 1976;BME-23:434-444.
29. Wilcock S, Flook V. A computer model designed to make rapid predictions of diver temperature changes. In: Bachrach AJ, Matzen MM, eds. Underwater physiology VII. Proceedings of the seventh symposium on underwater physiology. Bethesda, MD: Undersea Medical Society, 1981:555-564.
30. Hayward JS, Steinman AM. Accidental hypothermia: an experimental study of inhalation rewarming. Aviat Space Environ Med 1975;46:1236-1240.
31. Morrison JB, Conn ML, Hayward JS. Thermal increment provided by inhalation rewarming from hypothermia. J Appl Physiol: Respirat Environ Exercise Physiol 1979;46:1061-1065.
32. Conn ML, Hayes PA, Morrison JB. Contribution of metabolic and respiratory heat to core temperature gain after cold water immersion. In: Bachrach AJ, Matzen MM, eds. Underwater physiology VII. Proceedings of the seventh symposium an underwater physiology. Bethesda, MD: Undersea Medical Society, 1981:509-516.
33. Soung LS, Swank L, Said RA, Goldman JW, Perez J, Geis WP. Treatment of accidental hypothermia with peritoneal dialysis. J Can Med Assoc 1977;117:1415-1416.

34. Jessen K, Hagelsten JO. Peritoneal dialysis in the treatment of profound accidental hypothermia. Aviat Space Environ Med 1978; 49:426–429.
35. Bynum G, Patton J, Bowers W, Leav I, Hamlet M, Marsili M, Wolfe D. Peritoneal lavage cooling in an anesthetized dog heatstroke model. Aviat Space Environ Med 1978;49:779–784.
36. Marcus P. Laboratory comparison of techniques for rewarming hypothermic casualties. Aviat Space Environ Med 1978;49:692–697.
37. Harnett RM, Sales FR, Jr, O'Brien EM, Pruitt JR. Resuscitation from hypothermia: experimental comparison of eight rewarming therapies. Preprints, Aerospace Medical Association Annual Meeting, 1979;167–168.
38. Marcus P. The treatment of acute accidental hypothermia: Proceedings of a symposium held at the RAF Institute of Aviation Medicine. Aviat Space Environ Med 1979;50:834–843.
39. Shilling CW, Werts MF, Schandelmeier NR, eds. The underwater handbook. New York: Plenum Press, 1976.
40. Vaughan WS, Jr. Diver temperature and performance changes during long-duration, cold water exposures. Undersea Biomed Res 1975;2:75–88.
41. Davis FM, Baddeley AD, Hancock TR. Diver performance: the effect of cold. Undersea Biomed Res 1975;2:195–213.
42. Vaughan WS, Jr. Distraction effect of cold water on performance of higher-order tasks. Undersea Biomed Res 1977;4:103–116.

AN ANALYSIS OF HEAT STRESS UNDER HYPERBARIC CONDITIONS

K. R. Bondi

Until recently, the recognition of *hyperthermia* as a potential hazard during hyperbaric operations has been totally ignored. The diving medical and scientific community was abruptly notified of such a danger when two North Sea divers lost their lives as a result of hyperthermic stress, and it was but a few months later that a seminar was convened to discuss thermal problems in diving, both hyperthermia and hypothermia (1). During this seminar several participants pointed out that there are virtually no data on hyperthermia during diving and stressed the need for such information. Furthermore, a recent study evaluating a portable recompression system (PRS) at the Naval Submarine Medical Research Laboratory showed that the most serious problem observed was that of thermal stress (2). The study indicated that the observed thermal stress might produce a significant safety problem and might compromise the adequacy of decompression treatment in a tropical climate.

The study also made us realize that predictions of thermal stress under hyperbaric conditions would have to be based on theory only, since no human laboratory experimentation under such conditions has been performed. Especially lacking in this regard was the effect of pressure on man's ability to dissipate heat by evaporation. Recently, Carlyle et al. (3) have shown that there is a 62% reduction in evaporative capacity at pressures ranging from 37–43 ATA. This reduction could be critical in man's ability to tolerate thermal stress at depth.

THEORY

Heat loss from the skin surface (H_{sk}) to the environment can be expressed in terms of the radiative, convective, and evaporative heat-transfer coefficients

(h_r, h_c, and h_e, respectively). The radiative and convective losses are governed by the differences in mean skin temperature ($\overline{T}_{sk}$) and ambient temperature (T_a), and the evaporative losses are a function of the difference between saturated skin vapor pressure ($P_{s,sk}$) and ambient vapor pressure (P_a), so that

$$H_{sk} = (h_r + h_c)\,(\overline{T}_{sk} - T_a) + wh_e\,(P_{s,sk} - P_a) \qquad (Eq.1)$$

where w = skin wettedness, a dimensionless factor describing the amount of sweat formation on the skin and ranging in value from 0.06, where the regulation of heat exchange by evaporation begins, to 1.0, the upper limit for evaporative regulation and where the skin is fully wet with sweat.

Equation 1 may be plotted on a psychrometric chart (temperature on the abscissa and water vapor on the ordinate) and will describe a straight line that passes through the two points [$P_{s,sk}(\overline{T}_{sk} - H_{sk}/(h_r + h_c)$] and ($P_a$, T_a) with a negative slope of [($h_r + h_c)/wh_e$] (ref. 4). This unique concept was extended by Nishi and Gagge (5) to include the hypo- and hyperbaric environments.

THE HYPERBARIC THERMAL WINDOW

It is well recognized that as pressure increases, not only must the ambient temperature increase to ensure that the divers remain in thermal comfort, but also tolerance for deviations from this comfort temperature progressively decreases. Using the works of Gagge and Nishi (4) and Nishi and Gagge (5), these concepts may now be graphically depicted. We have extended Nishi's predictions to include air pressures of 1, 2, 4, and 7 ATA, helium pressures of 10 and 50 ATA, and water immersion. Figure 1 depicts a comprehensive graphic presentation of the progressive narrowing of the "thermal window" with increasing pressure. The *dashed lines on the left* represent the limit for comfort where skin wettedness (w) equals 0.06 and regulation of heat exchange by sweating begins. The *solid lines on the right* represent the upper limit for evaporative regulation where w = 1. The *curved lines connecting dotted to solid lines* indicate specific ambient relative humidities. Each line was constructed according to the work of Nishi and Gagge with the following conditions and relationships: subject is nude and at rest (metabolic rate 58.2 Wm^{-2}); velocity of gas (v) = 0.1 ms^{-1}; $\overline{T}_{sk}$ = 34.0°C at limit for comfort and 36.5°C at maximum sweating; h_c, h_e, and h_r and respiration considerations were taken from Nishi (5).

Man's thermophysiological behavior in a warm-to-hot hyperbaric environment, graphically depicted in Fig. 1, has the following important features:

1) As pressure increases, the thermal window between comfort and heat stress progressively narrows. In air at 1 ATA and 30% RH this window has a range of 20°C. In helium at 50 ATA, the range is narrowed to about 3°C. As the density of gas (a fluid) increases to a theoretical limit of 1 (water environment) this window is narrowed to about 1°C (6).

2) This narrowing effect is greatest during the initial changes in pressure (1-7 ATA), i.e., at 30% RH the ambient temperature limit at 7 ATA (air) is
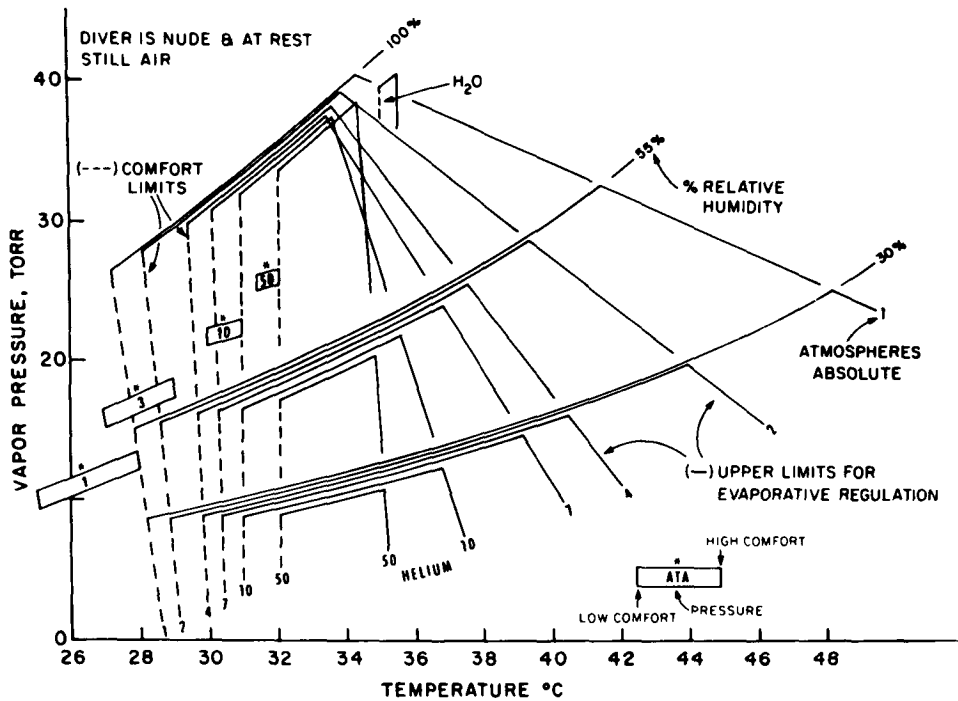
Fig. 1. The thermal window for warm comfort to heat stress is depicted by *the space between the dashed lines and solid lines* for any given pressure. The thermal window for warm comfort to cool comfort is represented by *boxes* and explained in the figure. The thermal limits of compressed gas diving approach that of a very dense gas (water) as shown by the H_2O *box* plotted in the figure.

9° lower than at 1 ATA (air), while the ambient temperature limit for 50 ATA (helium) is only 2°C lower than at 10 ATA (helium).

3) At high relative humidity, the upper limits for evaporative regulation are minimally affected by changes in pressure, while at mid to low relative humidity, these upper limits are greatly affected.

The thermal window from a low comfort temperature (below which divers would be uncomfortably cool) to a high comfort temperature (above which the divers would be uncomfortably warm) is also depicted in Fig. 1 using data from the literature for low comfort temperatures. For 1 ATA, a span of 3.4°C was taken, using the ASHRAE (American Society of Heating, Refrigerating and Air Conditioning Engineers) comfort zone as a guideline (7). The low comfort temperature for 3 ATA air was derived from 7 saturation dives at this pressure conducted at the Naval Submarine Medical Research Laboratory. The mean low comfort temperature for these dives was 26.8°C with an estimated CLO value of 0.3–0.4 (unpublished data). The low comfort temperature was adjusted up 3°C for inclusion in this example, where the CLO value is zero. The 10-ATA low comfort temperature was taken from a theoretical curve computed by Morlock (see Webb, 8). The low comfort temperature

for 50 ATA was taken from Raymond (9) and calculated to be about 31.5°C, a value that is slightly higher than the reported average comfort level, where the CLO value was probably in the 0.3 to 0.4 range. All high comfort temperatures were predicted from Eq. 1. The narrowing window as pressure increases is clearly depicted.

PRACTICAL CONSIDERATIONS

The above concepts were used to evaluate the thermal limits for a one-man portable recompression system developed by the Navy. The complete analysis was conducted at 4 ATA, but in practice a stage-wise decompression takes place from 4 ATA to 1 ATA according to Navy decompression treatment tables. A wide safety margin is therefore built into these limits. Figure 2
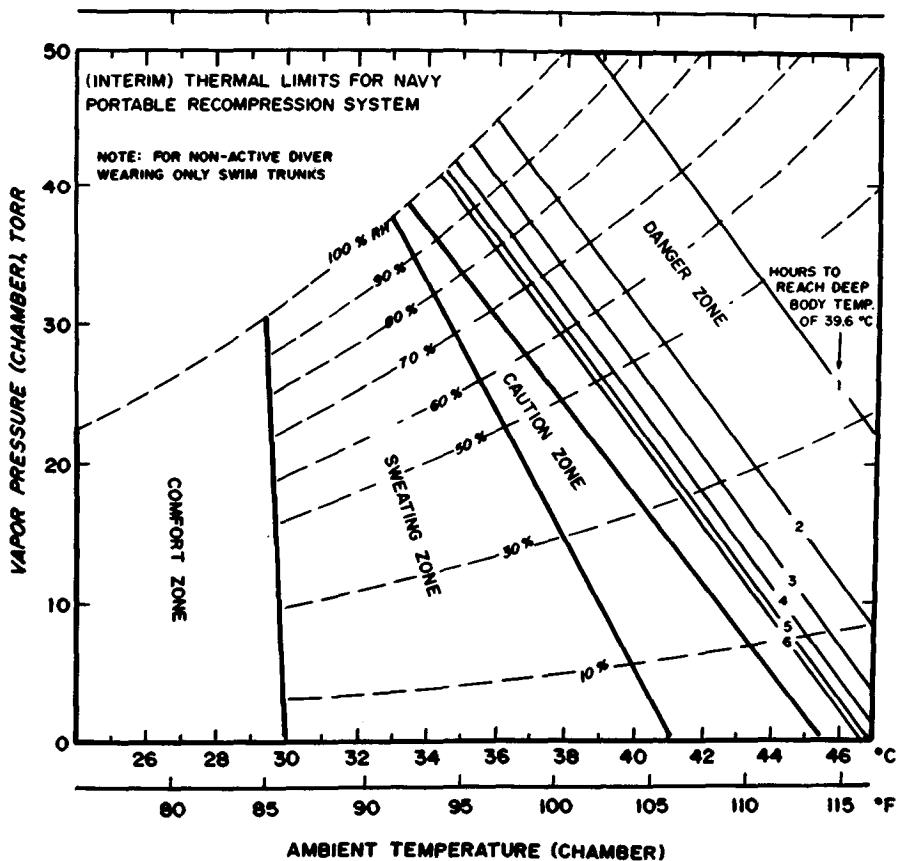
Fig. 2. Limit lines for 4 ATA were replotted in this figure to show practical use of such plots. Points falling in the danger zone indicate that a diver can no longer remain in thermal balance; thus lines to reach a critical body temperature of 39.6°C were calculated and plotted.

shows graphically the thermal limits for this system. The *solid lines* delineating the sweating zone and the upper limit of the caution zone are the same 4 ATA "comfort" and upper limit for evaporative regulation lines shown in Fig. 1 ($w = 0.06$ and 1, respectively). The line delineating the sweating zone and lower limit of the caution zone is for $w = 0.7$. At points above this $w = 0.7$ line a considerable amount of heat stress is incurred with profuse sweating and much uncomfort experienced by the diver or subject (10,11). Rectal temperature and heart rate will rise, but will reach a plateau. The danger zone, points above the $w = 1$ line, signifies that thermoregulation by sweating has reached a limit and that internal body temperature and heart rate will continue to rise until collapse. Body heat storage will increase at a rate computed from the metabolic heat production and the combined radiative and convective losses or gains. Rate of body temperature rise is then easily computed from standard physical characteristics. A body temperature of 39.6°C was chosen to represent that point where heat stroke occurrence will be greater than 1 in 100 (12). Hourly isopleths to reach this temperature are plotted in Fig. 2. Knowing the ambient temperature and relative humidity, a physician or technician in the field can now predict the thermal load expected and take the necessary precautionary measures. This chart must be termed "interim," because it is based on an analysis using physical principles with all empirical evidence collected at 1 ATA. Experiments are presently underway to verify these predictive methods in humans.

References

1. Egstrom GH, ed. Thermal problems in diving. Proceedings of a seminar held at Commercial Diving Center, Wilmington, CA. Wilmington, CA: Commercial Diving Center, 1977.
2. Hunter WL, Jr., Parker JW, Jordan JE, Biersner RJ, Gilman SC, Bondi KR. Evaluation of portable recompression system (PRS): life support schedule adequacy and human factors. New London, CONN: Naval Submarine Medical Research Laboratory, Report No. 876, 1978.
3. Carlyle RF, Garrand MP, Hayes PA. Insensible heat losses in man during simulated dives in helium-oxygen mixtures to a depth of 420 meters of sea water (43 bar). J Physiol 1979;295:39P.
4. Gagge AP, Nishi Y. 1977. Handbook of physiology. Section 9: reaction to environmental agents. Lee DKH, section ed. Bethesda, MD: American Physiological Society, Chapter 5, 1977:69-92.
5. Nishi Y, Gagge AP. Effective temperature scale useful for hypo- and hyperbaric environments. Aviat Space Environ Med 1977;48:97-107.
6. Craig AB Jr, Dvorak M. Thermal regulation during water immersion. J Appl Physiol 1966;21 (5):1577-1585.
7. American Society of Hearing, Refrigeration and Air Conditioning Engineers Standard 55-74.
8. Webb P, Troutman SJ Jr, Frattali V, Dressendorfer RH, Dwyer J, Moore TO, Morlock JF, Smith RM, Ohta Y, Hong SK. *Hana Kai* II: A 17-day dry saturation dive at 18.6 ATA. II. Energy balance. Undersea Biomed Res 1977;4(3):221-246.
9. Raymond LW, Thalmann E, Lindgren G, Langworthy HC, Spaur WH, Crothers J, Braithwaite W, Berghage TE. Thermal homeostasis of resting men in helium-oxygen at 1-50 atmospheres absolute. Undersea Biomed Res 1975;2(1):51-67.
10. Berglund LG, Gonzalez RR. Evaporation of sweat from sedentary man in humid environments. J Appl Physiol: Respirat. Environ Exercise Physiol 1977;42:767-772.
11. Gagge AP, Gonzalez RR. 1973. Physiological bases of warm discomfort for sedentary man. Arch Sci Physiol 1973;27:A409-A424.
12. Wyndham CH, Heyns AJ. The probability of heat stroke developing at different levels of heat stress. Arch Sci Physiol 1973;27:A545-A562.

CONTRIBUTION OF METABOLIC AND RESPIRATORY HEAT TO CORE TEMPERATURE GAIN AFTER COLD WATER IMMERSION

M. L. Conn, P. A. Hayes, and J. B. Morrison

Accidental hypothermia is a serious problem in cold air and water exposures. Inhalation warming is an attractive procedure for its treatment or prevention in remote or closed environments, where invasive core rewarming or hot bath peripheral rewarming is not practical. It supplies heat directly to the core area, is readily portable, and can be easily and safely administered. At present, controversy regarding the effectiveness of this technique is evident in the literature, and both animal and human studies are at variance (1–6). Disagreement exists over the quantity of heat delivered, its distribution and its significance relative to metabolic heat production.

In a comparative study using anesthetized hypothermic sheep, Lloyd et al. (1) found that hot bath rewarming was the most rapid method of elevating core temperature, and that inhalation rewarming offered considerable advantage over passive (metabolic) rewarming alone. They concluded, however, that the benefit of inhalation rewarming derived from elimination of respiratory heat loss rather than from added heat transfer to the core. Pavlin et al. (2) studied inhalation rewarming of anesthetized hypothermic dogs. Results showed that when ventilation was increased the rate of core rewarming measured at the pulmonary artery was enhanced, whereas removal of respiratory heat input resulted in a fall of core temperature. In a later study also with dogs, Auld et al. (3) showed no difference of core (esophageal) rewarming rates between passive rewarming and inhalation rewarming. Hot bath rewarming proved to be more rapid than the other treatments.

Hayward and Steinman (4) investigated hot bath and inhalation rewarming of mildly hypothermic humans. Results showed that whereas hot bath treatment gave a greater gain in rectal temperature, the gain in tympanic tempera-

ture was slightly less than that achieved by inhalation rewarming. In contrast, a similar study by Marcus (5) found that the effectiveness of inhalation rewarming in raising core (tympanic) temperature was not significantly different from shivering alone (passive rewarming), and both treatments were very much slower than hot bath rewarming. In a further study of inhalation rewarming using humans, Morrison et al. (6) found that an increase of ventilation resulted in greater core temperature gains measured at the rectal and tympanic sites. This finding thus confirmed the finding of Pavlin et al. (2) and opposed that of Auld et al. (3) and Marcus (3).

METHODS

The purpose of this study was to quantify the heat delivered by inhalation rewarming and its contribution to core temperature gain. To this end, mild hypothermia was induced in volunteer subjects who were then administered different levels of respiratory heat exchange during rewarming. Ten males were selected after medical examination and fitness testing. Hypothermia was induced on three occasions in the laboratory by immersion to the neck in 11.3°C water. Subjects wore no clothing and maintained a sitting posture with a minimum of movement. Rectal, tympanic, and skin temperatures were recorded at 2-min intervals and electrocardiographic recordings were monitored continuously. Subjects were removed from the water at a rectal temperature of 35.0°C, dried thoroughly, and placed supine in a sleeping bag for rewarming. In addition to the above measures, ventilation, inspired and mixed expired respiratory gas fractions, and inspired and expired gas temperatures were measured for a period of 60 min. Warming commenced 6 min after the signal to leave the water was given. All subjects were rewarmed on three occasions, once by metabolic heat alone (shivering) while breathing room air at 21°C, once by inhalation warming with spontaneous breathing of saturated air at 47°C (control), and once by inhalation warming with ventilation regulated at 40 L/min by respiring a controlled fraction of CO_2 (hyperventilation). In this manner, rewarming data were obtained for three distinct levels of respiratory heat exchange.

Respiratory heat transfer was calculated from minute ventilation, inspired and expired gas temperatures, gas fractions, specific heats, and the latent heat of condensation of water vapor. Respiratory gases were taken to be fully saturated with the exception of inspired air during shivering, when relative humidity of room air was derived from wet and dry bulb temperature readings. Oxygen uptake was calculated from inspired and expired gas fractions and temperatures and minute ventilation. Metabolic heat production was obtained by assuming a metabolic equivalent for oxygen of 4.8 kcal/L. Mean skin temperature was estimated from measures of arm, chest, thigh, and calf temperatures according to the weighted formula of Ramanathan (7). All temperature data were normalized relative to the temperature at the start of rewarming. The mean response of the 10 subjects to each treatment was then calculated.

RESULTS

There were no significant differences between the three treatments in the absolute values of rectal, tympanic, or skin temperatures measured at the commencement of rewarming (To). Core temperatures continued to decline after subjects left the water, and afterdrop was not arrested until after the rewarming treatment was well established.

The magnitude of the afterdrop in rectal temperature (see Fig. 1) was reduced by both the active rewarming treatments in comparison to shivering
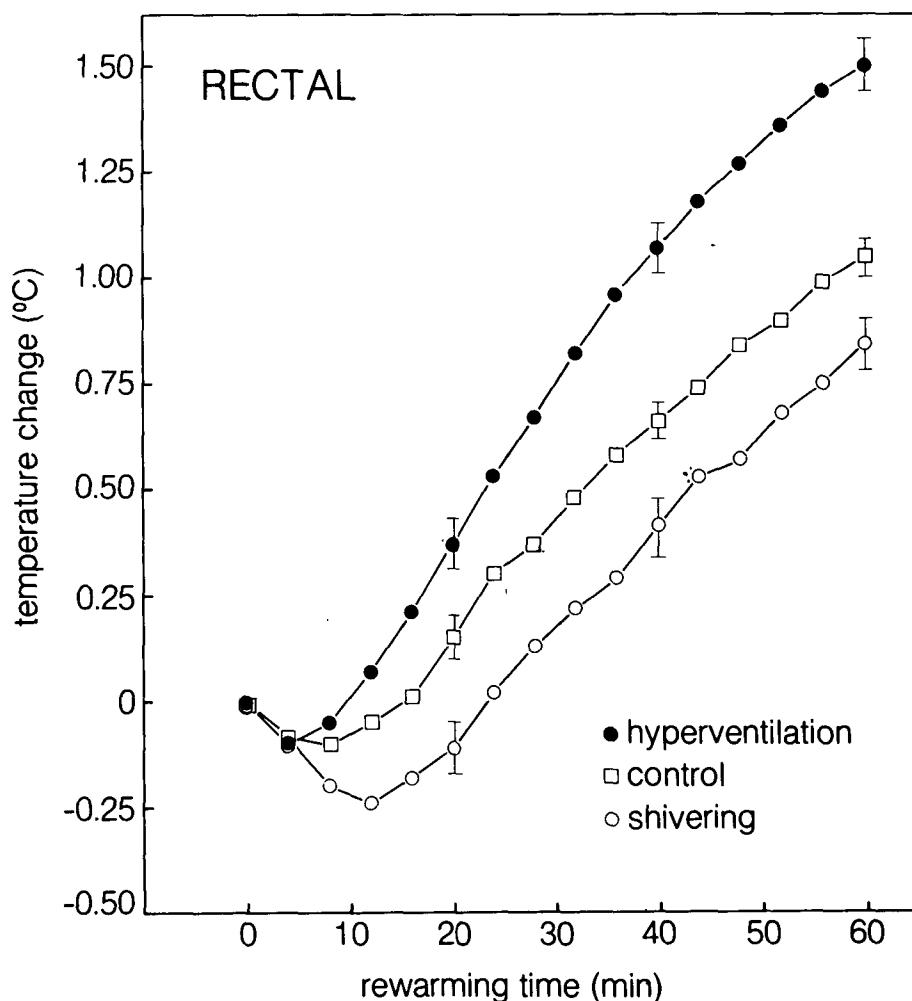
Fig. 1. Comparison of rectal temperature changes during rewarming from hypothermia by   a) inhalation rewarming with hyperventilation induced by rebreathing carbon dioxide (hyperventilation);   b) inhalation rewarming (control);   and   c) by shivering thermogenesis (shivering). Values are mean data of 10 subjects; *vertical lines* denote SEM.

($P < 0.05$). The time taken to recover to initial temperature T_{O_R} was also shortened ($P < 0.05$) from 23 min for shivering to 15 min for control and 10 min for hyperventilation. After 60 min of rewarming, hyperventilation and control gave greater net gains in rectal temperature (1.5 and 1.1°C, respectively) than did shivering (0.84°C). The afterdrop of tympanic temperature was small ($Ta_T < -0.2$°C) in all treatments and there were no significant differences. Shivering took longer to arrest afterdrop and to recover initial temperature ($P < 0.05$) than the other two treatments. The subsequent rate of rewarming was greatest for hyperventilation, which recorded a net temperature gain of 1.7°C compared with 1.4°C for the other two treatments.

There were no significant differences between procedures in the change of mean skin temperature although shivering recorded a slightly larger rise (9.1°C) than either control (8.3°C) or hyperventilation (8.7°C).

Subjects shivered rigorously in the early stages of rewarming. In the shivering treatment, oxygen uptake was greater after 2 min of treatment than in the other two rewarming methods (Fig. 2), and did not show a significant decrease until after 6 min. With active rewarming, oxygen uptake fell sharply from minute 2 onwards. In all treatments oxygen uptake decreased in response to core and skin temperature changes to reach a mean resting value of 0.3 L/min STPD at t = 60 min.

The mean values of respiratory heat exchange calculated for the three treatments are shown in Fig. 3. During shivering and control the respiratory heat transfer reflected change of metabolic rate and declined to a stable value towards the end of the rewarming period. With hyperventilation, respiratory heat exchange was maintained at an elevated level by a mean ventilation of 39.6 L/min BTPS.

Total metabolic heat production during the 60 min of rewarming was substantially reduced by inhalation rewarming ($P < 0.05$) from 218 kcal when shivering to 183 kcal (control) and 147 kcal when hyperventilating. The fall in metabolic heat production was greater than the corresponding respiratory heat gain, which increased from a loss of 10 kcal when shivering to gains of 20 kcal (control) and 40 kcal (hyperventilation).

DISCUSSION

As differences between treatments in the absolute values of mean skin temperature were small (<1.0°C) and not significant, we concluded that the fall in metabolic heat production in response to the two inhalation rewarming procedures must result from more rapid temperature gains at the central cold receptors. This conclusion is supported by the relative measures of rectal and tympanic temperatures. Calculations show that, on average, for each kcal of respiratory heat supplied 1.4 kcal of metabolic heat were forfeited. The fact that respiratory heating enhanced the recovery of core temperature implied that respiratory heat must be more efficient than metabolic heat in both arresting afterdrop and raising core temperature.
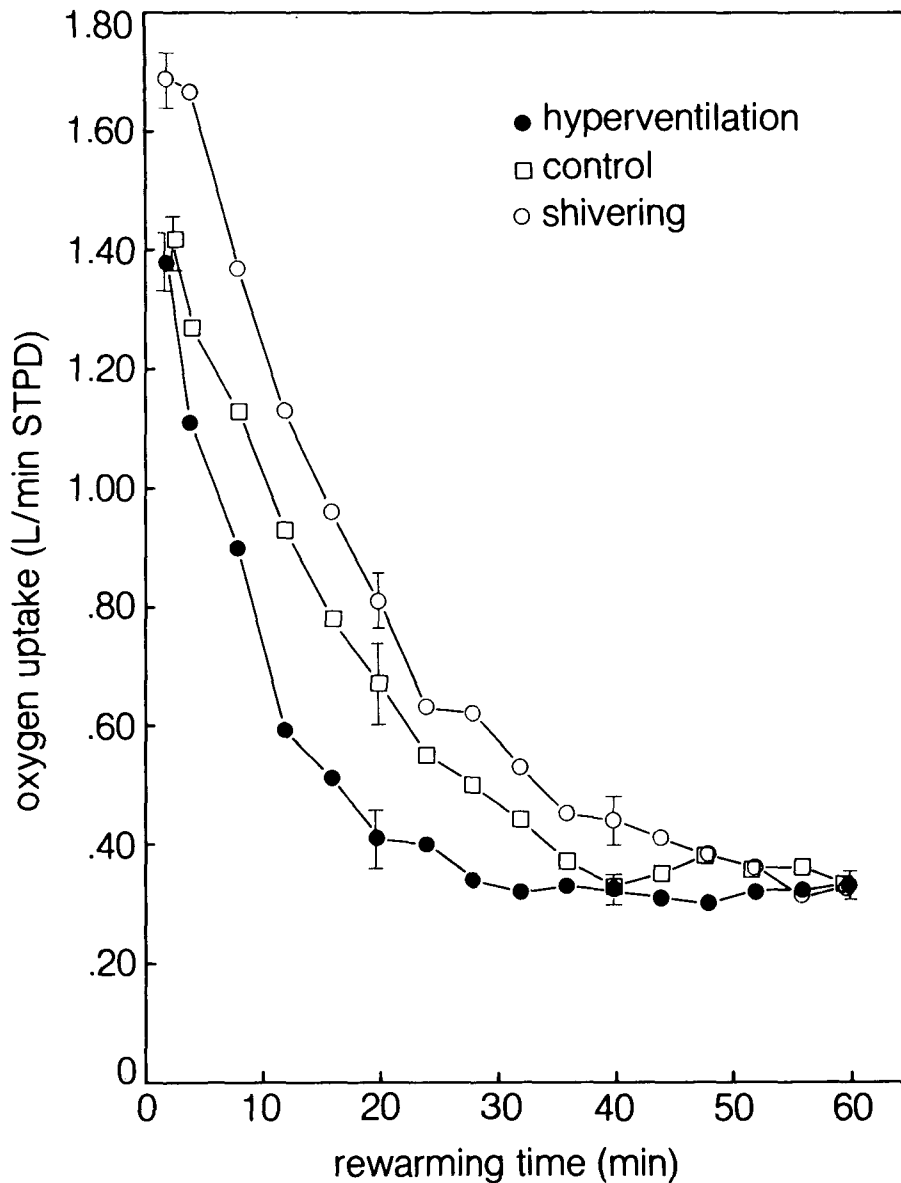
Fig. 2. Comparison of oxygen uptakes during rewarming from hypothermia by   a) hyperventilation,   b) control, and   c) shivering. Conditions are as in Fig. 1.

To quantify the above tendency, we calculated the fraction of the total heat input donated to core temperature gain using a core mass of 46% body mass (8) and rectal and tympanic temperature changes at t = 60 min. We obtained the change of core heat content using the two core temperature measures, with a weighting of 30% body mass at rectal temperature and 16% body mass at tympanic temperature, and a specific heat of tissue of 0.83
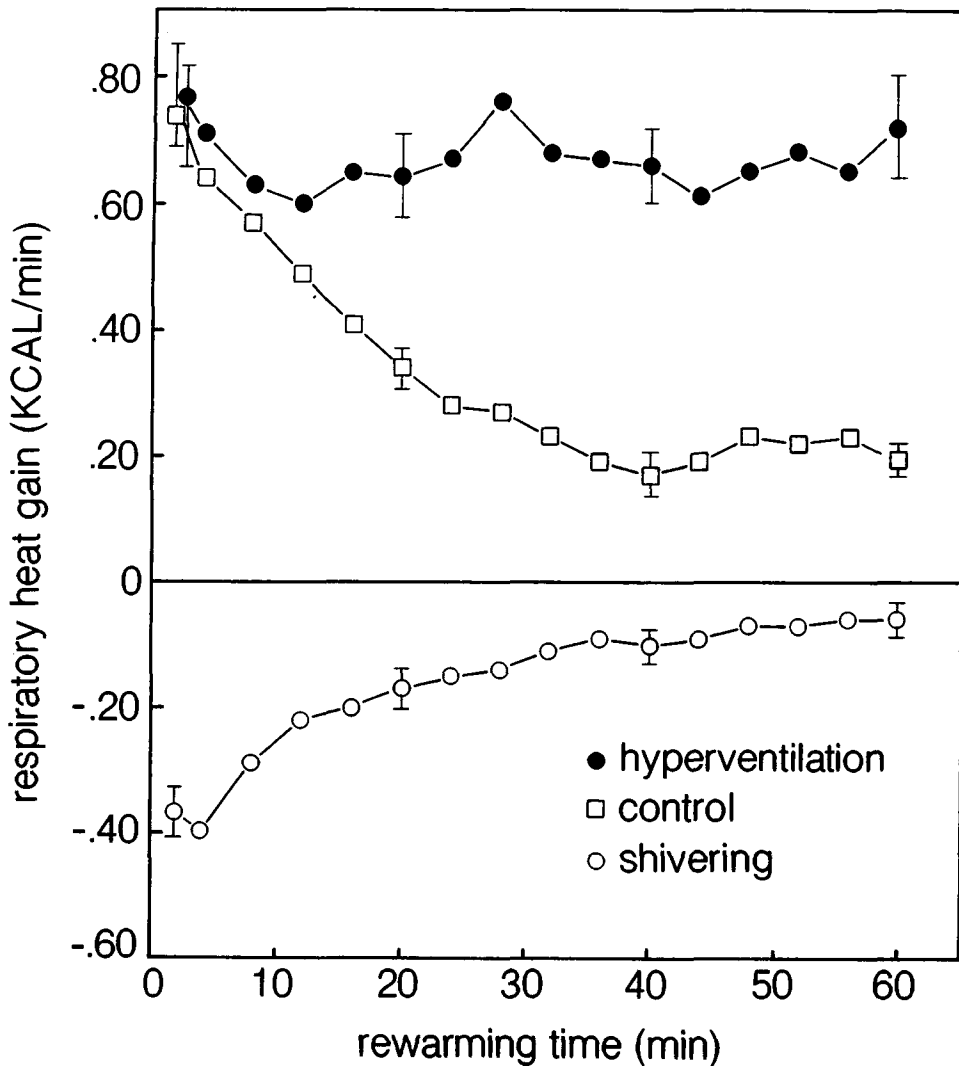
Fig. 3.   Comparison of respiratory heat exchanges during rewarming from hypothermia by   a) hyperventilation,   b) control, and   c) shivering. Conditions are as in Fig. 1.

kcal·°C^{-1}·kg^{-1}. Results shown in Table 1 indicate that the percentage of total heat donated to the core increased from 13% in shivering (i.e., metabolic heat alone) to 16% in control and 23% in hyperventilation. If one assumes that the fraction of metabolic heat donated to the core does not change significantly between treatments, it can be theorized that to produce the core temperature gains recorded with inhalation rewarming, approximately 42% to 60% of respiratory heat contributed to core temperature gain. Thus, although the absolute magnitude of respiratory heat was small, its efficiency as a source of core

TABLE I

Comparison of Heat Gains (kcal) and Core Temperature Increases (°C) after 60 Min of
Rewarming from Hypothermia   Values are mean ± SE.

	Shivering	Control	Hyperventilation
Respiratory Heat	−10±1	20±2	40±3
Metabolic Heat	218±6	183±5	147±5
Total Heat Input	218±6	203±6	187±7
Rectal Temperature Gain	0.8±0.2	1.1±0.1	1.5±0.2
Tympanic Temperature Gain	1.4±0.2	1.4±0.2	1.7±0.1
% Total Heat Input Donated to Core	13	16	23

heating was estimated to be three to five times greater than that of metabolic
heat production.

Respiratory heat loss is estimated to be 5–10% of metabolic heat produc-
tion in normal air environments. In divers breathing oxygen-helium mixtures
the greater thermal conductivity, specific heat, and density can result in sub-
stantial respiratory heat losses. Had the present study been repeated at 30 ATA
the estimates of Webb (9) predict that respiratory heat losses for the shivering
procedures would have been approximately 70 kcal, or 30% of metabolic heat
production. Respiratory heat gain from inhalation rewarming would also have
been enhanced.

This study disagrees with the conclusion of Lloyd et al. (1), Marcus (5),
and Auld et al. (3) that the heat donated by inhalation rewarming does not
significantly increase core temperature gain and supports the opposite conclu-
sions of Pavlin et al. (2), and Morrison et al. (6). It is difficult to explain the
disparity of results among authors, but the following factors may contribute to
differences reported. Rewarming rates are sensitive to variation of absolute
body temperatures and composition (10), and therefore comparative data must
be closely matched, or the results will be misleading. As the respiratory heat
gain is largely condensatory in nature, the effectiveness drops rapidly when
inspired gas is not 100% saturated. In animal studies, the use of anesthesia
and intubation may also interfere with the efficacy of the technique. Finally, as
shown in this study, the contribution of respiratory heat can be partly hidden
by a concomitant drop in metabolic heat production.

In conclusion, this study indicates that although inhalation warming in a
normal air environment provides 10% of total body heat input, it is more effi-
cient in terms of heat delivery to the core than shivering thermogenesis. Inhal-
ation warming is shown to be a practical method of treating or preventing hy-
pothermia. The potential benefits of this treatment will be enhanced when an
oxygen-helium gas mixture is breathed at increased pressure.

References

1. Lloyd EL, Mitchell B, Williams JT. Rewarming from immersion hypothermia: A comparison of three techniques. Rescuscitation 1976;5:5–18.
2. Pavlin E, Hornbein TF, Chaney R. Rewarming of hypothermic dogs with the use of heated nebulized ventilation. Proc Am Assoc Anesthesiol Ann Meet, San Francisco, 1976;105–106.
3. Auld CD, Light IM, Norman JN. Accidental hypothermia and rewarming in dogs. Clin Sci 1979;56:601–606.
4. Hayward JS, Steinman AM. Accidental hypothermia: An experimental study of inhalation rewarming. Aviat Space Envir Med 1975;46:1236–1240.
5. Marcus P. Laboratory comparison of techniques for rewarming hypothermic casualties. Aviat Space Envir Med 1978;49:692–697.
6. Morrison JB, Conn ML, Hayward JS. Thermal increment provided by inhalation rewarming from hypothermia. J Appl Physiol 1979;46(6):1061–1065.
7. Ramanathan NC. A new weighting system for mean surface temperature of the human body. J Appl Physiol 1964;19:531–533.
8. Burton AC. The average temperature of the tissues of the body. J Nutr 1935;9:261–280.
9. Webb P. Cold exposure. In: Bennett PB, Elliott DH, eds. The physiology and medicine of diving and compressed air work. London: Baillière Tindall, 1975:285–306.
10. Morrison JB, Hayward JS, Conn ML. Effect of body temperature and composition on recovery from hypothermia. In: Program, abstracts, and mini-papers. The Undersea Medical Society annual scientific meeting (abstracts), 7th symposium on underwater physiology. Bethesda, MD: Undersea Medical Society, 1980:19.

METABOLIC AND THERMAL STATUS OF DIVERS DURING SIMULATED DIVES TO 55 BARS

M. P. Garrard, P. A. Hayes, R. F. Carlyle, and M. J. Stock

Particular concerns of the diver working in United Kingdom waters are cold and the duration and depth of the saturation exposure he is likely to experience now and in the future. The purpose of this paper is to summarize part of the work carried out to investigate changes of metabolic and biochemical significance in the body in response to deep saturation diving, as well as to examine some of the thermal peculiarities of the operational-type diving environment. The particular topics covered are: the ionic, energetic, and nitrogen balances; blood chemistries and water losses; the measurement of local heat loss; the thermoregulatory responses to exercise; the perception of temperature; and respiratory heat transfer.

Individual investigations into the metabolic status of divers have not been extensive, but a large number of results have been presented from which only vague conclusions can be drawn. For example, a recent study (1) lists a plethora of physiological and biochemical variables measured in men down to 1600 fsw but ends with the comment that the bulk of the data could not be interpreted as it was "nonspecific and could be induced by a variety of conditions." In the studies presented below a great many controls were built into the experimental approach: maintaining the divers on a controlled dietary intake, taking blood samples at the same time each day, and adhering to a strict 24-h metabolic balance day, while keeping the divers in a comfortable condition. The attempted feeding of a totally fixed diet in *Dives 7, 8,* and *9B* (see later for explanatory code [Table I]) was a complete departure from standard practice and remains, to the best of our knowledge, the only examples of such a technique having been employed in hyperbaric human studies. The literature is not lacking in the estimates of food consumption (2) during dives to various depths, but is based primarily on ad libitum feeding experiments with divers

TABLE I

Profile of Dives

Dive No.	Compression Time (days)	Maximum Depth (msw)	Time (days)	Decompression Time (days)
7	9	420	2	16
8	7	420	3	16
9B	3.5	540	2.5	21
CD1	3	250	3	9

not in a sufficiently stable biochemical state for critical metabolic analysis to be performed.

It was against the stable dietary background that experiments could be carried out on ionic, energy, and nitrogen balances. Blood chemistry experiments could be performed with a constant nutritional intake, which greatly increased the validity of studies on heat loss (evaporation and convection) and thermal perception.

The thermoregulatory response to exercise was investigated down to 55 bars in relation to the changing physical characteristics of the environment affecting both insensible and sensible heat transfer mechanisms. The dives under discussion in this paper were coded as shown in Table I. The fourth dive (CD1) involving cold, wet excursions (approximately 4°C) to just over 250 m was conducted to measure respiratory heat transfer while divers were respiring gas at elevated temperatures and humidity.

METABOLIC BALANCES

The method employed in this study is a standard practice in clinical circumstances when determining the metabolic balance of ions. Adherence to this level of accuracy was also maintained for the energy, nitrogen, and water balances investigated. The dietary intake was kept constant during each 24-h period throughout the dives with a predive "run in" on each occasion. Meals were presented at the same time each day with an approximately even distribution of food bulk throughout the day. The amounts of the various constituents in each diet, e.g., total energy, protein, fat, carbohydrate, and calcium was based on the divers' normal surface daily requirement. This standardization enabled any deviation from the metabolic norm to be observed free from intake errors. If the divers at any time could not eat the prescribed diet because of nausea from the high pressure neurological syndrome (HPNS), then known supplementary diets were offered, usually in liquid form. Twenty-four-hour urine and fecal collections were made with the metabolic period running from 0800.

Ionic Balances

The results of the formal balances for calcium, phosphorous, and magnesium showed no appreciable mobilization of these from the body in four subjects down to 420 msw during *Dives 7* and *8*.

Energy Balance

To calculate the 24-h energy expenditure we used the diary-card method. For this, each 24-h period is divided into 5-min sections during which the divers record their activity. The categorized activities were: lying (L), sitting (S), reclining (R), kneeling (K), crouching (C), lying moving legs (Lm), sitting moving arms (Sm), kneeling moving arms (Km), and crouching moving arms (Cm). Energy expenditure was recorded for each activity at various depths on each dive during the compression, maximum depth, and decompression phases, and multiplied through the daily record; basal metabolic rate measurements, recorded on reveille, were used for the sleep record. During *Dive 7* the divers left the controlled dietary intake and from the 16th to 22nd day of decompression; the feeding was ad libitum and the composition of the diet was estimated from the McCance and Widdowson tables (3). With energy intake and fecal and urinary energy losses remaining constant on *Dive 7*, it is interesting to note the negative energy balance at 420 msw and for the first phase of decompression (Fig. 1A). This was due to an increase in energy expenditure at depth, which recovered to early compression levels by approximately 300 msw on *Dive 7* and 370 msw on *Dive 8*. The negative energy
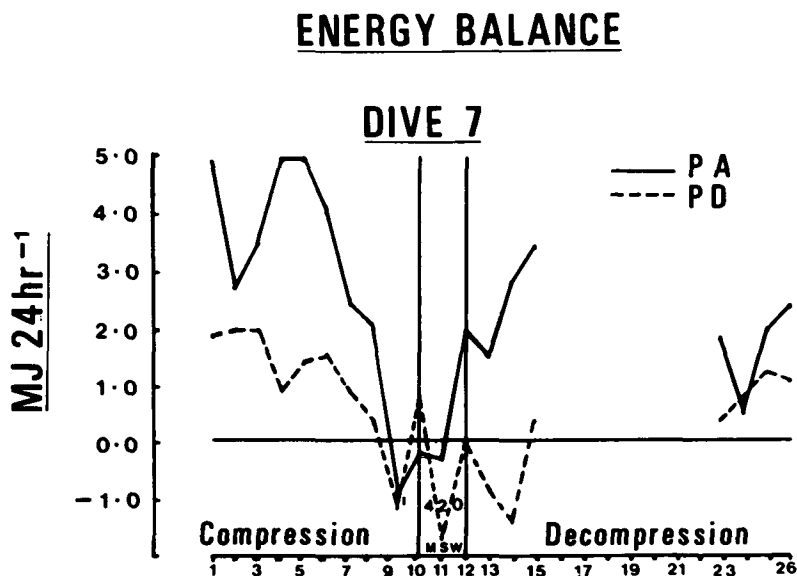
Fig. 1A.   Energy balance—*Dive 7*. Progressive approach to negative energy balance at 420 msw (43 bars).

balance was exaggerated on *Dive 8* (Fig. 1*B*) due to a decrease in food intake by both divers at 420 msw. However, after returning to the controlled dietary intake at the start of the decompression, the divers remained in negative energy balance and did not return to normal until reaching 370 msw.

Figure 2 shows clearly the trends involved for the mean energy expenditures for the same activities on *Dives 7* and *8*. In all four divers energy expenditure was maximal at 420 msw, decreasing during decompression to a
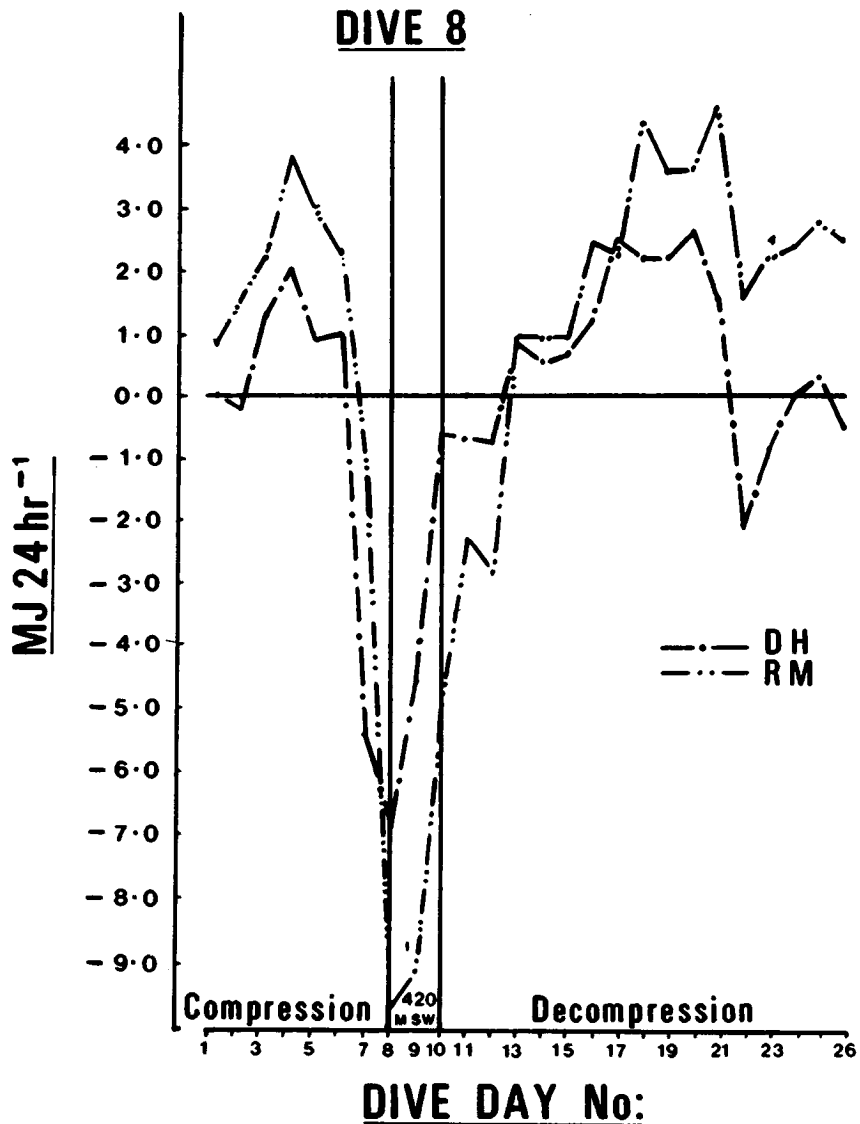
Fig. 1B.   Energy Balance—*Dive 8*. Negative energy balance at 420 msw (43 bars) maintained during the first phase of decompression while still in HPNS zone.
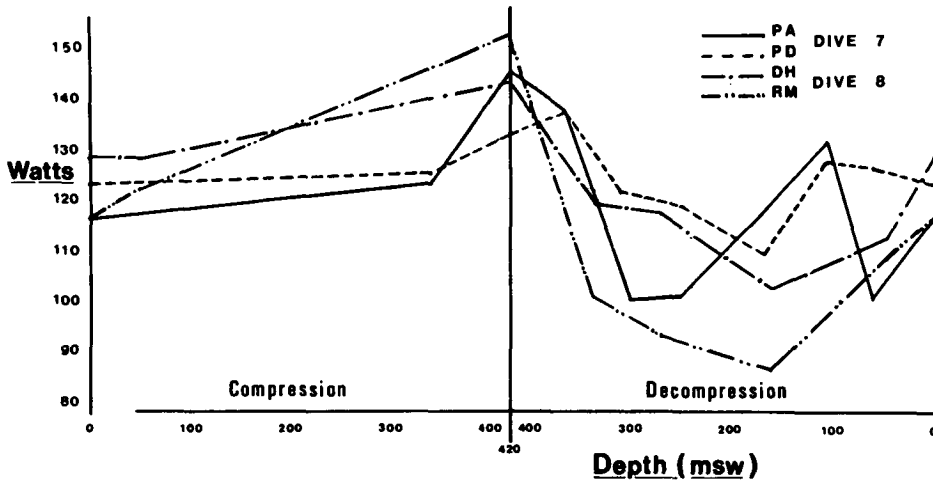
Fig. 2. Resting energy expenditures vs. depth—*Dives 7* and *8*. Mean of L, S, R, and C for each subject at specific depths.

minimum value between 300 and 150 msw, then increasing again to the sur-
face. The mean resting energy expenditure (MREE) for all four divers (the
mean of the energy ± expenditure measurements for the subject when L, S,
R, and C) was 143 W ± 7.7 at 420 msw, but decreased to 108.1 W ± 11.9
at 260 msw and further to 103.9 W ± 13.5 by 160 msw; the mean surface
value was 121.0 W ± 6.0. The MREE at 260 and 160 msw was significantly
lower ($P < 0.05$, $n = 4$) than at 420 msw; there was no significant difference
in the MREE between the surface and 420 msw, and the surface and 260/160
msw.

Basal metabolic rate (BMR) was measured on reveille at various depths
during *Dives 7, 8,* and *9B,* with no significant changes in the energy expendi-
ture of the divers recorded down to 540 msw (Fig. 3); mean skin temperature
and core temperature were measured simultaneously down to 420 msw with
similarly no significant changes.

Nitrogen Balance

Nitrogen balance proved a very interesting study. During *Dives 7, 8,* and
9B all the divers were in a state of negative nitrogen balance when they were
deeper than approximately 300 msw. Figure 4 illustrates the results from *Dive
7*: a progressive loss of nitrogen to 420 msw and a recovery to normal predive
levels during decompression. Fecal and dietary nitrogen remained virtually un-
altered leaving urinary nitrogen as the significant factor. Further analysis of the
urine revealed that the bulk of the increased urinary nitrogen was in the form
of urea with both uric acid and creatinine remaining constant.
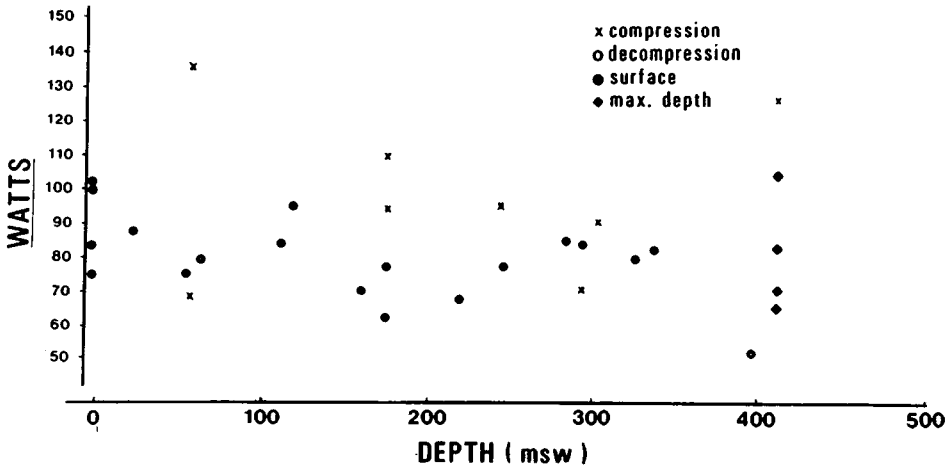
Fig. 3.   Basal metabolic rate measurements down to 540 msw (55 bars)—Dives 7, 8, and *9B*. *n* = 6 subjects.

Interestingly, at this state the excretion of these three key metabolic products occurred during the period that the divers on *Dive 7* were not on the controlled dietary intake. The trends shown at this stage were completely indefinable and any physiological changes in the levels we have observed could not have been detected without the control on dietary intake.
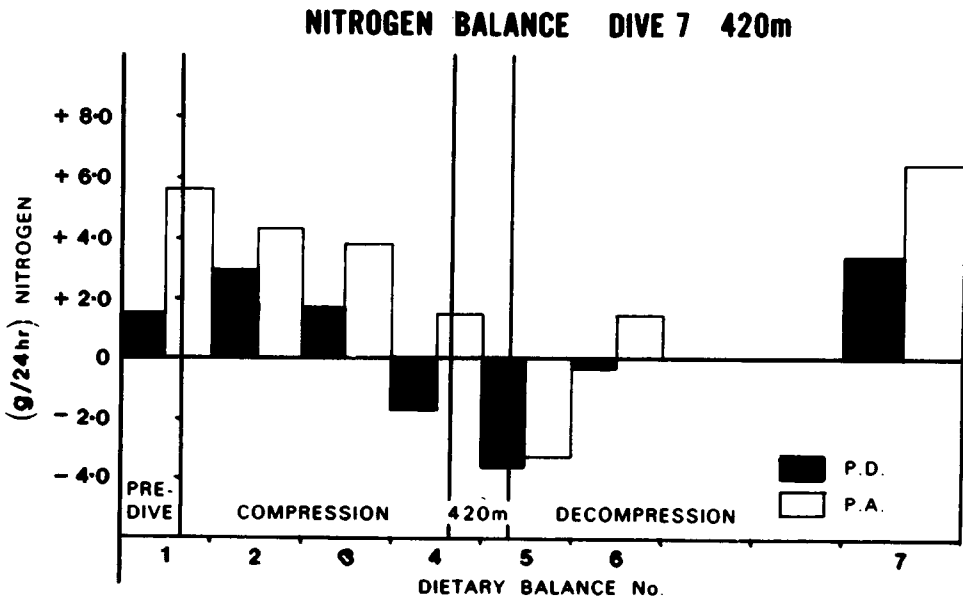
Fig. 4.   Nitrogen balance—*Dive 7* (420 msw [43 bars]). The dietary balance period was 3 days for balances 1–6 and 4 days for balance 7.

Many of the investigations carried out during *Dives 7* and *8* to 420 msw have reported (4,5) the conclusion that not only collagen metabolism but also the turnover of actin and myosin was normal. Analysis of the circulatory levels of amino acids on these dives showed increases in only glycine, valine, and lycine during the early stages of decompression. Further analysis of the results from *Dive 9B* and subsequent dives to 180 and 300 msw showed that there was a significant increase in total circulatory amino acid levels during this early phase of decompression. The evidence collected so far strongly suggests a preferential stimulation of specific pathways in protein catabolism on these dives, associated with HPNS. Moreover, it must be made clear that this negative nitrogen balance at depth is reversible by decompression and only occurs in the HPNS zone.

BLOOD CHEMISTRIES

During the period of each dive, venous blood was taken every 48 h at 0800; this included pre- and postdive samples. The thyroid hormone profile showed that although there was no change in the circulatory levels of triiodothyronine (T_3) (Fig. 5A) and T_3 resin uptake (taken to represent free thyroxine [6]), there was a significant increase in the levels of thyroxine (T_4) (Fig. 5B) and reverse T_3 (rT_3) (Fig. 5C) at the greatest depth of each dive. These increases were maximal during the early phase of decompression, with rT_3 returning to normal late in the decompression and T_4 returning to normal postdive. Thyroid-stimulating hormone (TSH) generally followed the T_4 trend, but no conclusive pattern emerged. It appears, therefore, that there is an increased conversion of T_4 to rT_3 with no complementary increase in the T_4 to T_3 conversion. As well as an increase in T_4 release from peripheral stores, the raised

Fig. 5A.   Serum 3, 3¹, 5-triiodothyronine (T_3) levels—*Dive 9B* (540 msw [55 bars]).
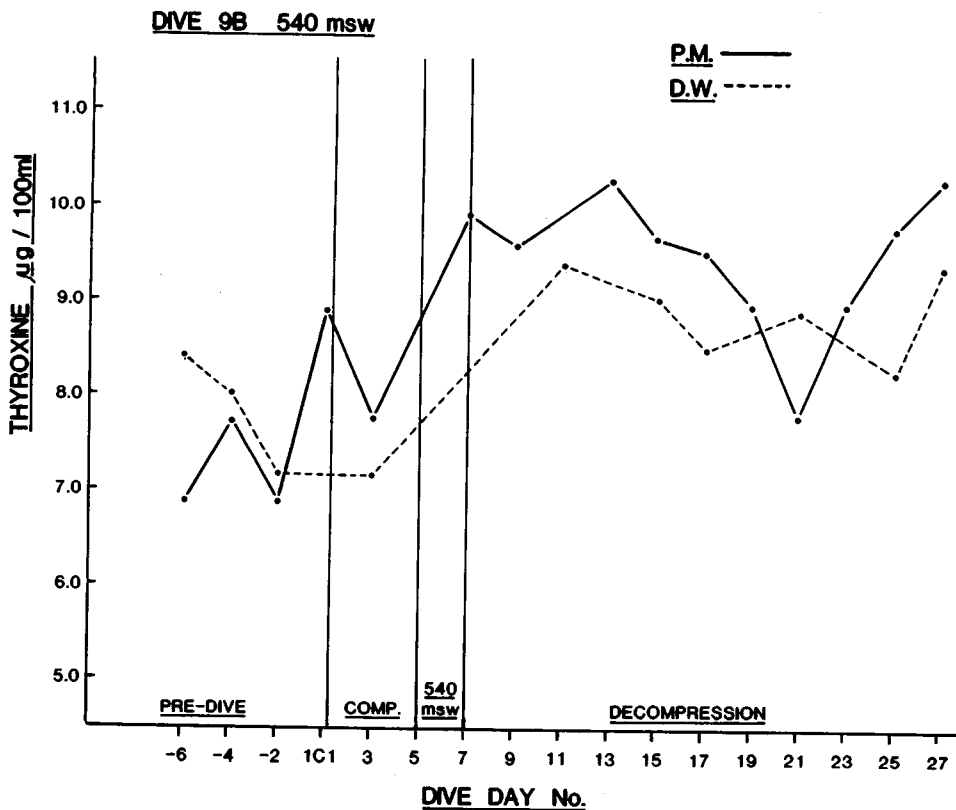
Fig. 5B.   Serum thyroxine (T₄) levels—*Dive 9B* (540 msw [55 bars]).

circulatory T_4 levels may have been caused by reduced bilary clearance, which in turn intimates an alteration in the conjunction of thyroxine to form sulphates and glucuronides in the liver. Thyroxine is also known to influence the peripheral nervous system and raised levels will shorten the reaction time of stretch reflexes; this is in accord with the observed hyperbaric hyper-reflexia in these divers (7).

There were no significant changes in the circulatory levels of free fatty acids (FFA), urea, glucose, serum osmolarity, and glucagon measured on these dives. Three of the divers showed definite decreases in insulin levels approaching 420 msw during *Dives 7* and *8*, recovering to normal during the decompression. The fourth diver maintained low levels until late in the decompression, when all the divers had an insulin peak, returning to normal levels postdive. Cortisol levels were raised at depth returning to predive levels before the end of the decompression; adrenocorticotropic hormone (ACTH) levels were, however, not increased on *Dive 9B*.

DIVE 9B 540 msw

P.M. ———

D.W. - - - - -
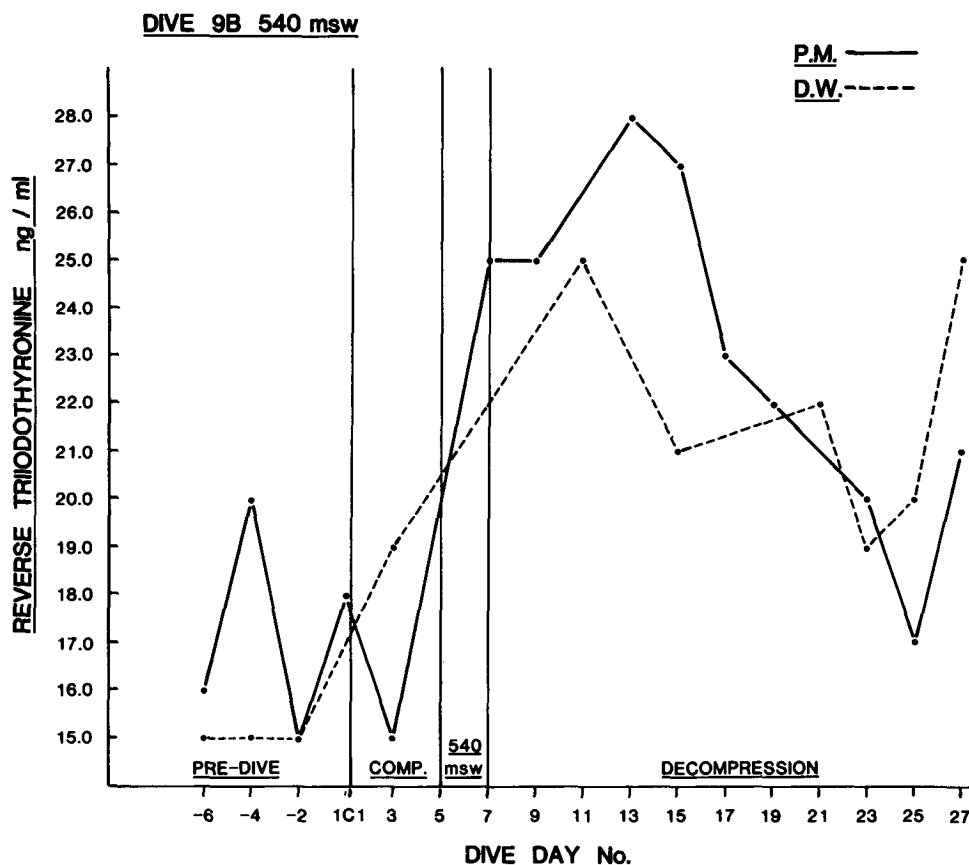
Fig. 5C. Serum 3, 3', 5'-triiodothyronine (reverse T₃) levels—*Dive 9B* (540 msw [55 bars]).   T₃ levels remained largely unaltered while rT₃ and T₄ increased, reaching peaks during the decompression phase.

DISCUSSION

Some of these results have been discussed in previous publications (4,5, 8,9), but recent work has cast more light on the etiology of the metabolic changes. The metabolic status of these divers is significantly different deeper than 300 msw; individual susceptibility influences the onset and recovery depth. All of the observed changes occur at the same time that the divers show HPNS symptoms, and it would not be incongruous to associate more closely the metabolic and neurological aspects of deep diving.

Increased glucocorticoid levels are known to decrease the anabolism and increase the catabolism of protein, as does T_4, and so produce a negative nitrogen balance. Furthermore, raised corticosterone levels accompanied by raised T_4 levels preferentially increase rT_3 rather than T_3 production from T_4 peripherally (10). It would appear therefore that the adrenal cortex and the thyroid are playing significant roles in the altered metabolic status of the divers. This specific stimulation of protein turnover by the diving environment raises questions

related to the consequences of long-term exposure to pressures greater than 31 bars.

EVAPORATION AND WATER LOSSES IN HYPERBARIC HELIUM

The hyperbaric environment often has a high absolute humidity (g_{H_2O} L^{-1}) and the evaporative heat loss can be limited by the reduced water concentration gradient from skin to gas. The efficiency of evaporation as a heat loss mechanism is also attenuated because of the reduction in mass transfer of water vapor from the skin. In addition, the high thermal conductivity and density of the surrounding medium would result in the diver being that much more susceptible to hyperthermia the deeper the dive. The diver would be ill-equipped to deal with any accidental overheating of the environment and body heat content would rise very quickly to a critical level.

Theoretical Considerations

The increase in pressure is likely to affect water vapor concentration at equilibrium as well as reduce the rate at which water vapor would attain that equilibrium condition. It is possible that the saturated vapor pressure at a given temperature may be greater at pressure than at 1 bar for two reasons. First, a direct effect of pressure on water in the liquid phase raises the vapor pressure, and, second, the nonideal quality of the tertiary mixture (He-O_2-H_2O) could further increase the vapor concentration. The total concentration of vapor in helium could be about 15% higher than that anticipated value at 50 bars (11). However, when the absolute humidity was measured in helium taken from a chamber under pressure but subsequently expanded, the helium appeared to hold less water than air for the same conditions (12), and less than the calculated value for normal conditions, e.g., at 43 bars the measured water at 30.8°C saturated was 25.7 mg L^{-1}, whereas the calculated value was 31.7 mg L^{-1}.

The rate limitation to evaporation is approximately inversely related to the density (ρ) where h_D, the mass transfer coefficient, varies as $\rho^{-0.5}$ where h_D appears in the equation:

$$E = h_D A_E L (c_s - c_\infty) \qquad (1)$$

where E is evaporative loss, watts; A_E is area of evaporation on the body; L is latent heat of evaporation; and c is vapor pressure concentration at the skin(s) and in the gas (∞).

From a consideration of the analogy between heat and mass transfer, h_D can be calculated using the Chilton-Colburn (13) correction to the Lewis relation:

$$h_D = h_c (Pr/Sc)^{0.667}/C_P \rho \qquad (2)$$

Pr and Sc are the Prandtl and Schmidt numbers, h_c is the convective heat transfer coefficient, and C_P is the specific heat. There is a reduction in the

coefficient h_D to 15% at 250 m and an average 12% in the range 360-420 m compared to its surface air value.

Measured Insensible Losses in Divers

Four divers were exposed to an oxyhelium environment containing 0.4 bar O_2. The maximum pressure reached was 43 bars. Subjects were fed a fixed and controlled diet, and water intake was measured. Water loss in the urine and feces was also measured and the combined respiratory and skin evaporative losses were deduced by subtraction. Insensible losses were computed over a 3-day balance period and are tabulated in Table II as grams per hour over each 3-day period.

Water losses at the surface were on average 30.3 $\pm$ 7.9 g h^{-1}, which represents a heat loss of about 21 W. Insensible losses decreased with depth to a mean of 8.5 $\pm$ 9.3 g h^{-1} between 37 and 43 bars during compression. This represents a fall in evaporative mass flux, caused by the pressure, of approximately 28% of the 1-bar level.

The negative values may indicate an over-compensating diuresis, which occurs to a minor degree in all divers. Alternatively, a 3-day period may not be sufficient to balance water input and output. Serum osmolarity and circulating ADH levels remained relatively constant throughout the dives. A graphical display of the data is shown in Fig. 6.

The reason that measured evaporative losses were reduced to only 28% when calculated values for h_D diminished to 12% is probably because the high level of skin wetness increased the vapor gradient ($c_s - c_\infty$) and thus was the driving force for evaporation. However, both theory and empirical determinations show a marked reduction in the rate at which water is capable of leaving the surface.

TABLE II

Insensible Losses Computed Over 3-Day Balance Period

Depth (msw)	PD	PA	RM	DH	Mean
Controls at Surface (predive)	32	39	30	20	30
0–180	17	7	5	9	10
180–360	8	1	−3	−30	−6
360–420	5	7	−10	15	4
420–360	7	9	13	22	13
360–300	8	3	—	—	6
360–250	—	—	4	11	8
250–170	—	—	1	18	10
170–80	—	—	8	22	15
80–0	13	19	14	31	19

Evaporative mass transfer gh^{-1}. Capital letters represent subject identification.
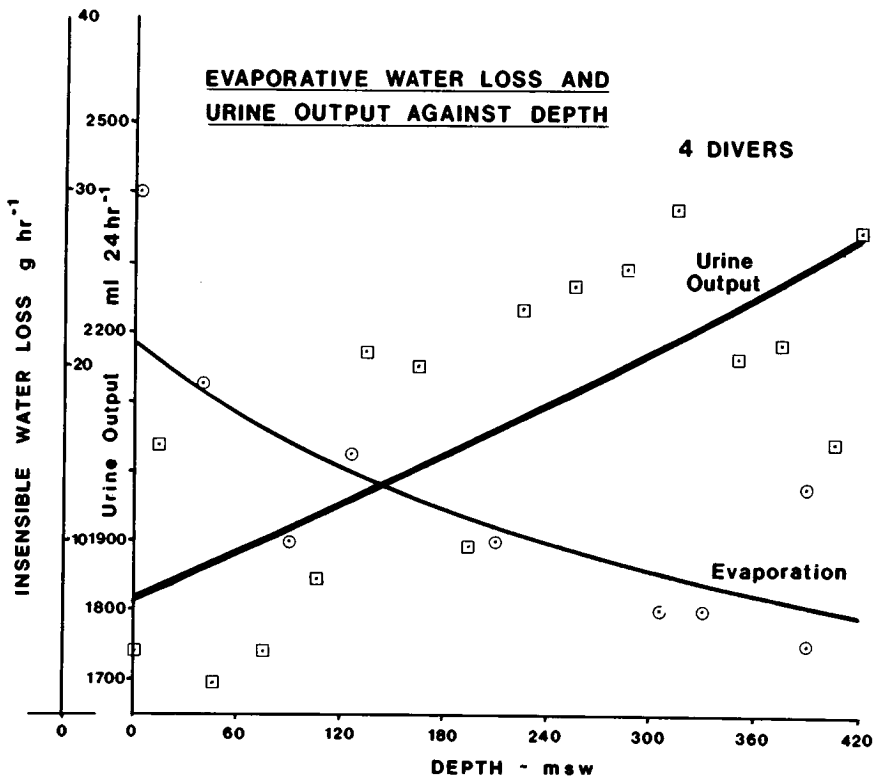
Fig. 6.   Change in the pattern of water loss as a function of depth.

The experimental data are largely an expression of general diffusion or perspiration loss as distinct from active sweating. The consequences of the reduction in evaporative efficiency are also likely to be encountered during exercise. Using Eq. 2, we computed the desired absolute humidity based on a minimal evaporative loss of 30 W and the figures were used as a guideline for chamber humidity when investigating the thermoregulatory response to exercise at depth (to be discussed).

REGIONAL LOSSES

Recently, a great deal of interest has been shown in the measurement of regional or local heat loss from divers both in dry and wet conditions. The technique is useful in assessing overall heat loss when the steady state condition required for partitional calorimetry cannot be guaranteed, especially in water. When one is unsure of the reliability of estimates of the rate of change of body heat content, direct surface measurements are a valuable alternative.

However, the integration of local measurements into an absolute value for the whole surface of the body still remains a problem.

We measured regional heat loss and associated skin temperatures on a number of divers in the dry comfortable condition using surface plate calorimeters (14). The calorimeters were placed on the forehead and thigh and on three points around the waist. At each depth the diver remained motionless in three different body positions while the average values for heat loss were recorded over the 5-min period. A typical change in the magnitude of total heat flux (radiation + convection) with depth is shown in Fig. 7 and displayed as a convective heat transfer coefficient in Fig. 8.

The development of the thermal boundary layer appears to be changed markedly with differences in posture, the influence being accentuated with depth. Each individual was comfortable over the measurement period with ambient temperature adjusted for the nude body, although the trend to increase heat loss is evident as the depth is increased. Convective heat loss becomes progressively more dominant at the expense of primarily evaporation and radiation. These data highlight the importance of the interrelation of body parts, and the consequences of the interruption of the convective flow pattern alter heat flux by a factor of 2:3 for the same site. The variation in heat transfer over relatively small areas presents difficulties in finding a local site of measurement representative of the average heat loss over a surrounding larger surface area of skin.

THERMOREGULATORY RESPONSE TO EXERCISE AT DEPTHS DOWN TO 55 BARS

The thermal response of the body to prolonged exercise at depth was tested to assess whether the change in convective and evaporative heat transfer altered the integration of peripheral and central inputs to the temperature control center. An underlying philosophy of most models of thermoregulatory control is that core and average skin temperature are integrated in some form, presumably at the hypothalamus, to initiate the controlled output. During exercise skin temperature is the function of the surrounding environmental temperature (external heat load). Core temperature is linearly related to oxygen consumption, being independent of the ambient conditions within limits and representing the internal heat load.

This hypothesis was tested initially with simple measurements of core and skin temperature and oxygen consumption during 25 min of work at rates of 40 and 80 W. Particular attention was paid to the level of humidity during the exercise periods in an attempt to compensate for the reduction in the mass transfer coefficient. Table III shows the level actually achieved, which was dependent upon the efficiency of the water scrubbing system, and a possible preferred level as calculated.

The results can be summarized as follows. Rises in core temperature are greater for 80 W than for 40 W; however, in the steady state the rise from
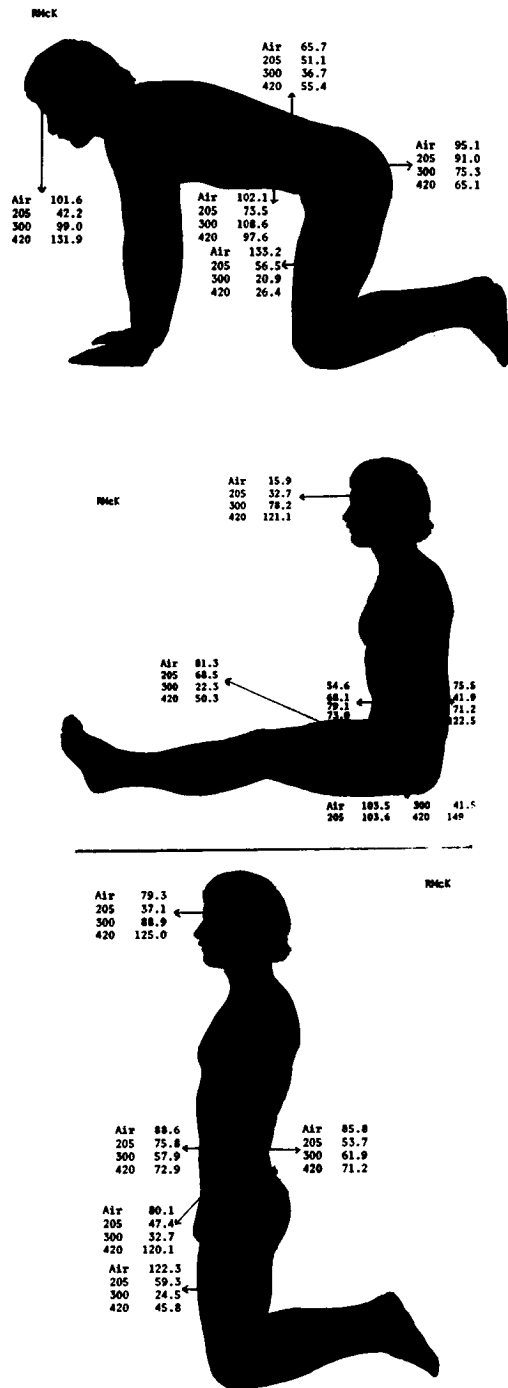
Fig. 7.   Total heat flux in different positions (W m⁻²) as a function of depth (msw); air at 1 bar.
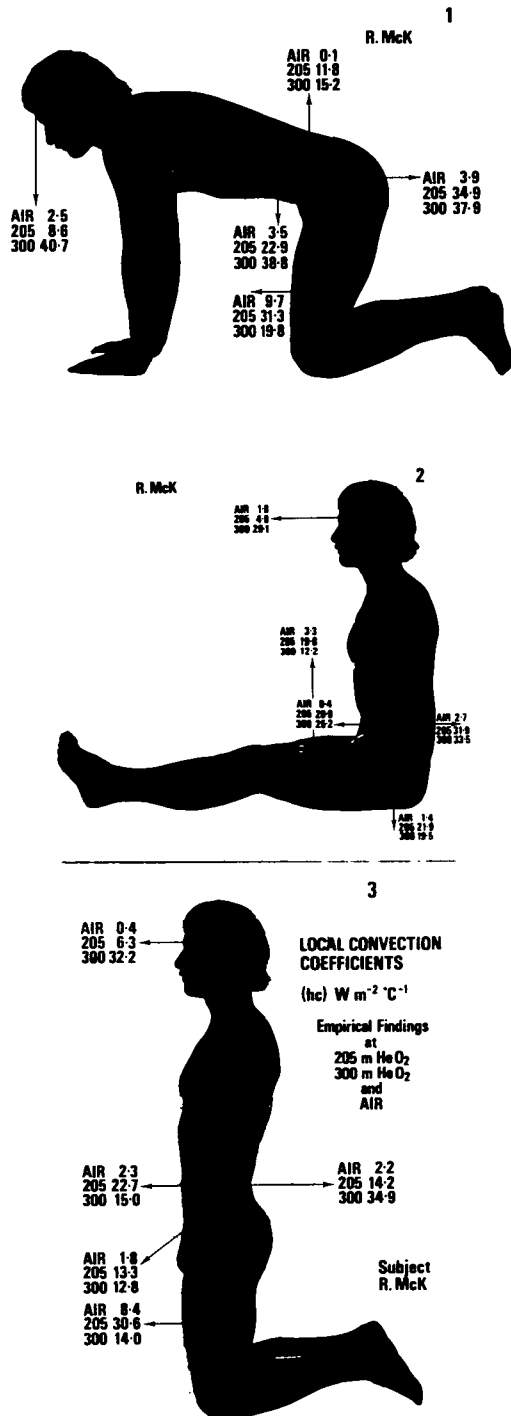
Fig. 8. Comparison of the measured values of the local heat transfer coefficient for different positions.

TABLE III

Level of Humidity During Exercise Periods

Depth (msw)	0	180	540	470	330	218
Absolute Humidity (mg L⁻¹)	12.0	11.8–12.1	3.7–4.7	8.1–8.4	14.2	15.5–16.4
*Preferred Level of Humidity (mg L⁻¹)		15.5	2.2	2.5	3.2	15.3

*Based on calculations.

resting levels appears reduced as the depth is increased. When actual heat production is plotted against depth, though, there is very little variation. There is a minor and not significant reduction in the heat produced for the same workload at intermediary depths (during decompression) compared to the bottom time value (at 55 bars) and the predive surface controls (Fig. 9). If rectal temperature did not rise so much, more heat would be lost, and one would anticipate a change in the core-to-skin gradient.

Usually, the skin temperature is determined by ambient temperature and the heat produced by the body while working is balanced by the increase in
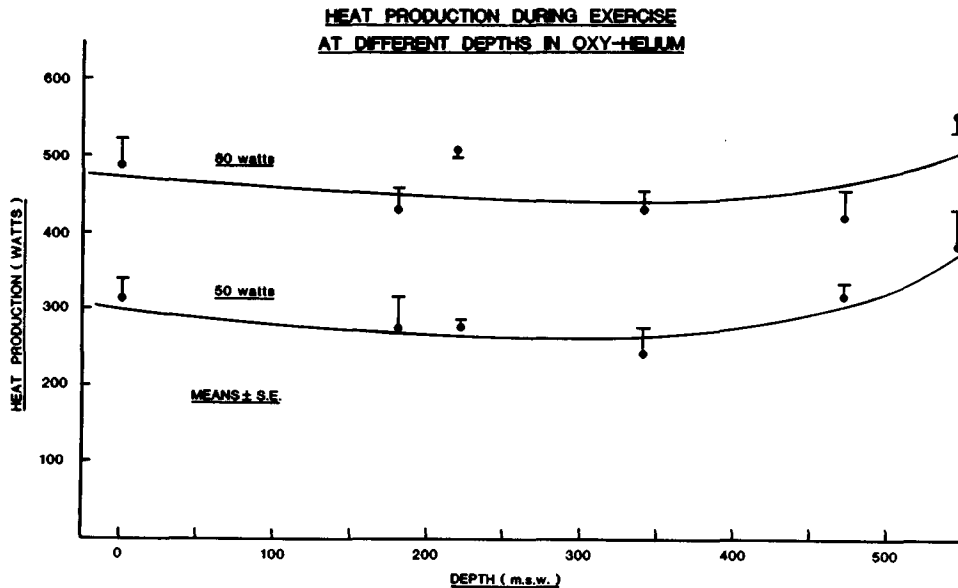
Fig. 9. Heat production for two workloads at various depths; steady state conditions after 23 min.

tissue conductance balanced in turn by the additional heat lost through sweating. At these comparatively low work rates there does appear to be some dependence of skin temperature on the workload, with the rise in mean skin temperature (ΔT_s) after 23 min greater for 80 W than for 50 W. The range of ΔT_s bar values was from -0.4 to $1.5°C$; the difference is only minor for both levels of exercise at all depths. Absolute levels at T_s at 50 and 80 W were significantly different ($P < 0.05$; $P < 0.05$) after the 23rd min. Separation of the data shows that the differences in workload are attributable primarily to surface data, and, in fact, the rise in skin temperature was less at depth for the same level of exercise ($P < 0.05$, paired t test; depths > 330 msw). The minimal rise in mean skin temperature at depth can be put down to the cooling effect of forced convection on the thighs and calves as the diver cycles on the ergometer. In many ways this is rather a reassuring phenomenum, as the extra convection transfer capability may compensate for the reduction in evaporative capacity. If the humidity is kept at a level compatible with comfort and comparative surface capability, there does not appear to be any thermal limitation in terms of excessive heat build-up, or surface discomfort, down to 55 bars with these chosen levels of work.

TEMPERATURE PERCEPTION

There have been a number of anecdotal accounts and some pictorial proof of divers being scalded in their hot water suits without any apparent realization at the time. In contrast, the measured core temperature while wearing the same type of suits shows that other divers become hypothermic without realization (15). One questions whether these divers show a certain temperature insensitivity or, alternatively, a predisposition to hypothermia, but the various merits or disadvantages of short-term adaptation or more long-term habituation may be involved.

Some aspects of sensitivity and the perception of temperature change in the saturation environment were studied using the psychophysical approach. A convenient index of sensation that can be used is the threshold value, and we analyzed temperature perception on a quantitative basis using this method. The actual recordable sensory observation was the first indication of a thermal transient occurring from a previously adapted level between 22 and 39°C. The transient stimulus was imparted to the skin by a Peltier module (6.25 cm^2) applied to the skin of the lower arm (16).

The skin was cooled from the adapted level (x) at a constant rate to the recognizable threshold level (y) and for 1 bar in air the relationship $y = 0.82 + 0.89\,x$ is remarkably linear ($r^2 = 0.99$). As the dives progressed the slope of the relationship gradually fell and by the third week of exposure $y = 5.57 + 0.74\,x (r^2 = 0.99)$. The change in threshold response was particularly noted over the range $x = 30$–$39°C$ ($P < 0.05$, paired t test) (Fig. 10). Upon return to living at 1 bar there was a gradual return to predive response levels that were only marginally different after 2 weeks ($0.05 < P < 0.1$) and were completely recovered after about a month.
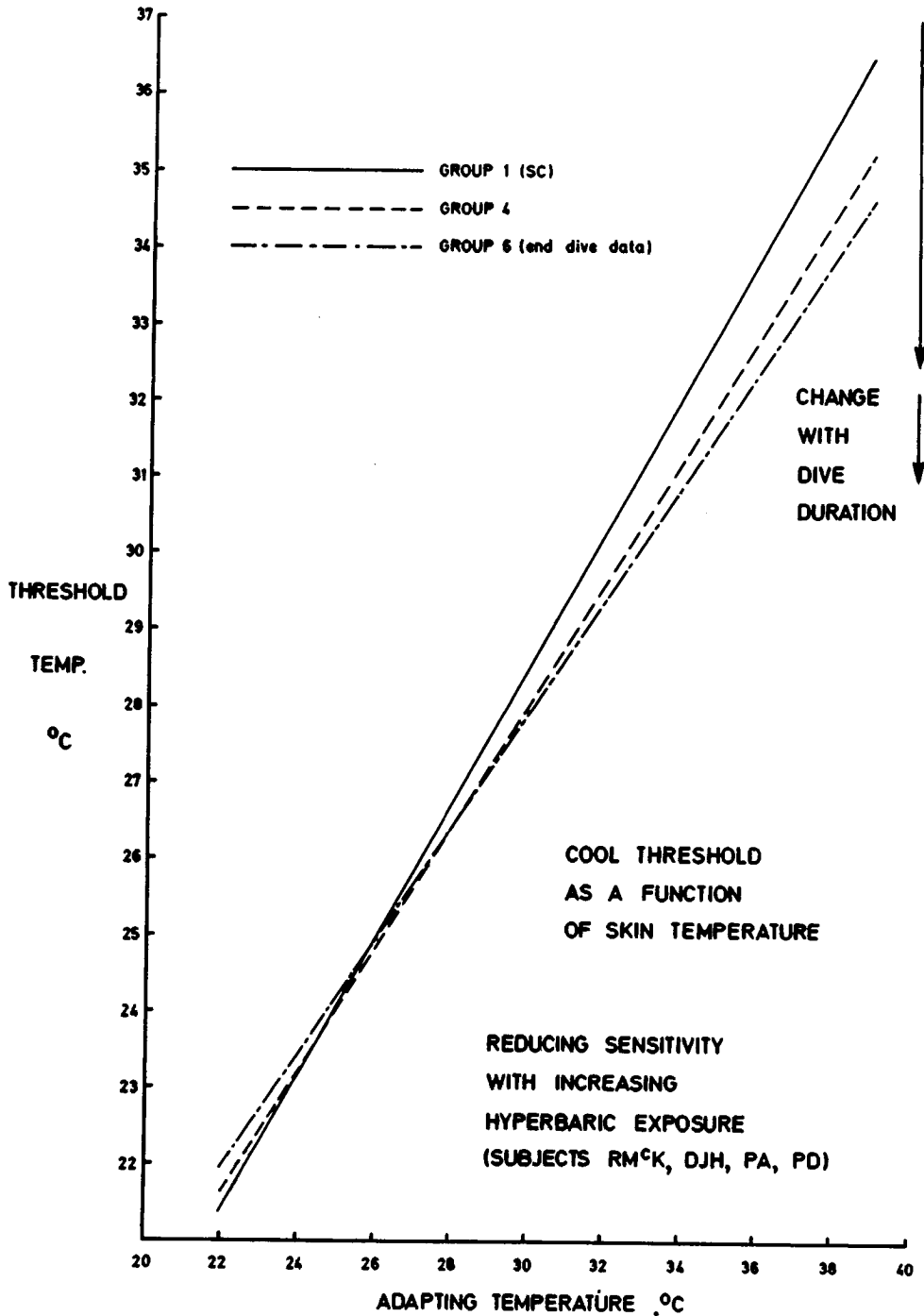
Fig. 10. Changes in temperature perception with duration of the dive.

The response to rate-of-change of cooling over the range 0.13-0.95°C/s is also susceptible to the duration of the dive, and although threshold recognition is still dependent upon initial starting temperature (x) there is evidence of a decreased sensitivity particularly at the higher temperatures of 34 and 38°C. The response to both warming from different temperatures and rate-of-change of warming appeared relatively unchanged throughout the dive: although no significant differences were found between predive and in-dive levels of response to a fixed rate of warming, there was some variability when warming at different rates from 28°C. Based on the analysis of receptor function by Kenshalo (17), a plausible inference is that the prolonged hyperbaric oxyhelium exposure may alter the temporal course of short-term temperature adaptation. The site of this change in perception is uncertain but is more likely to be central and interpretive rather than any change in the receptor itself.

It will be difficult to establish whether these minor changes in temperature perception are in any way involved in the problems of hot water suits. The cooling of divers while supplied with heat may be more satisfactorily explained on the basis of sustained and undetectable respiratory losses or an inability to reproduce the usual cold symptoms after repetitive exposures. However, the changes in sensitivity may add to the problems of recognition of thermal stress even though providing no great influence on their own.

RESPIRATORY HEAT TRANSFER

In the event that a diver becomes hypothermic in the cold water or cold gas conditions of the saturation system, there is little remedial action available at the present time. The possibility of using warm and humidified gas as a method of introducing heat into the body during respiration appears an attractive procedure. In any event, it will counteract high respiratory losses that might occur in the cold environment. The data and conclusions of Conn et al. (18) support the idea that the preferential deployment of heat to the body core would prevent further deterioration of the severely cold diver.

We performed an initial trial to assess the comfortable limits of breathing water-saturated oxyhelium at various densities. In addition, the rate of heat transfer and level of oxygen consumption were measured in divers after cold water excursions. Three divers performed alternating cycles of rest and work in water temperatures of 3-4°C at depths of 80, 180, and 250 m. Thermal protection consisted of a dry suit, woolly bear, and double-layer gloves. No attempt was made to heat or to particularly cool the gas delivered to the KMB10 mask. The average inspired gas temperature was 10 ± 4°C, depending upon the dwell time of the gas in the short umbilical length below the water. In all instances rectal temperature at the start of the cold water dive was above 37°C, reaching a maximum of 38.1°C while the diver dressed. During the subsequent cooling, rectal temperature fell a relatively minor amount, the maximum ΔT_R recorded was just over 1°C (to 36.03°C). However, there was

no mistaking the high level of discomfort and the limits of voluntary tolerance under these conditions. Two minutes after exit from the water, ventilation ($\dot{V}$) rates of the resting subject were 40-50 L min^{-1} (BTPS) and the afterdrop, which occurred in all cases, had a maximum value of about 0.31°C. The average time spent in the water was about 40 min and subjects tended to come out when the combined temperature of toe and finger fell below 16-18°C or when the temperature of either fell below 5°C. At 180 m the coldness of the breathing gas was noted and at 250 m subjects reported a definite feeling of cooling of the upper airways. Under these conditions rectal temperature appears to be a rather poor indication of "functional" core temperature pertaining to the level of stress.

During rewarming the heat transferred across the respiratory tract, that is, the net gain, varied from 4.5 to 15.5, 3.9 to 34.5, and 8.9 to 40.4 W for depths of 80, 180, and 250 m, respectively (Fig. 11). Average inspired temperatures recorded were in the range 38-43°C at all depths, and the gas was fully saturated. The greatest benefit of the warm gas, from a subjective point
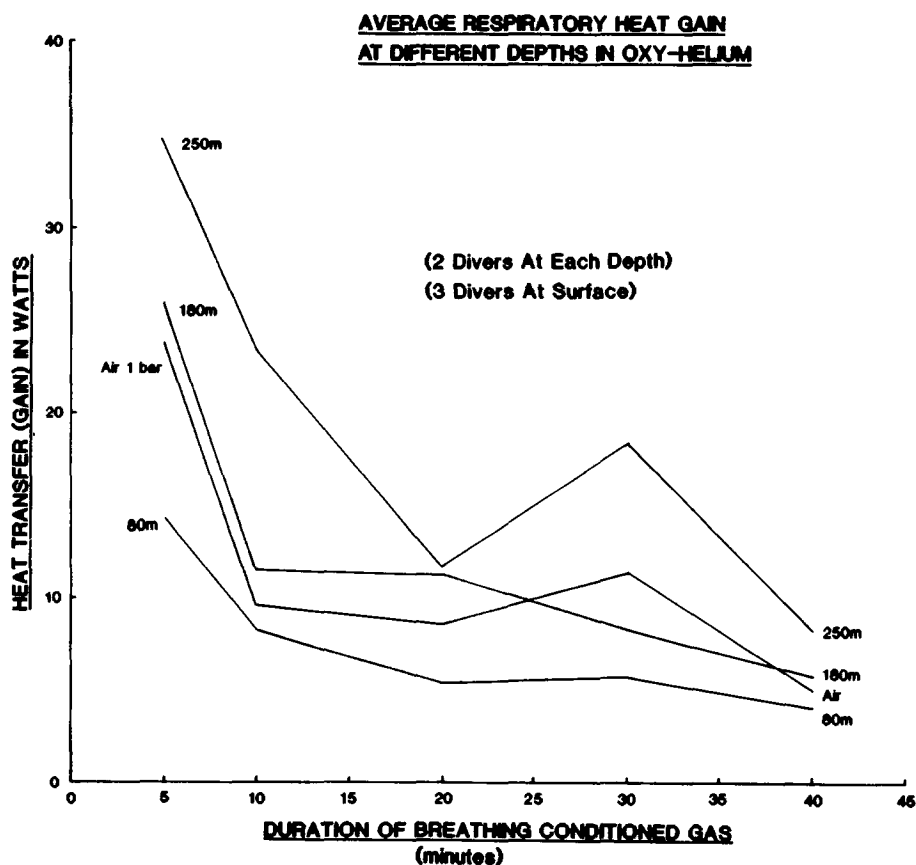
Fig. 11.   Respiratory heat gain—fluctuations with time following removal from cold water.

of view, occurred in the first 20 min of rewarming and at the greater depth. Usually by this time shivering had ceased, irrespective of rectal temperature; it returned intermittently at 80 m but not to such a marked degree at 180 m and even less at 250 m. The $\dot{V}o_2$ at the start of rewarming was about 0.75 L min^{-1} (STPD) at all depths, decreasing to 0.19, 0.21, and 0.35 L min^{-1} (mean, $n = 3$) after 40 min of rewarming for depths of 80, 180, and 250 m, respectively. Total heat available to the body from shivering thermogenesis and respiratory gain was over 300 W when $\dot{V}$ was more than 40 L min^{-1}. However, both sources diminished with the time of rewarming. In air about 86-88% of the heat transferred is attributable to latent heat, whereas about 95-97% is due to convection at 26 bars.

If inhalation rewarming had not been available to the diver breathing gas in a cold environment, the majority of heat generated from shivering could have been lost as a respiratory transfer deficit. These initial findings indicate that inhalation rewarming could be utilized as an immediate first aid treatment for the more severely chilled diver in an emergency situation.

CONCLUDING REMARKS

Certain aspects of metabolism change to varying degrees in subjects exposed to a hyperbaric He-O$_2$ environment in the HPNS zone. One of the most interesting findings has been the specific effect of increased pressure on nitrogen metabolism, resulting in a negative nitrogen balance.

The maintenance of BMR at normal predive levels down to 540 msw accompanied by a negative energy balance deeper than approximately 300 msw indicates an increase in the thermogenic or work components of total heat production or both. However, during controlled moderate exercise, total heat production did not significantly alter down to 540 msw. Nevertheless, inherent in the thermogenic component are two very important factors, namely, dietary-induced and thermoregulatory thermogenesis. Preliminary investigations on these two factors indicate that the former is increased and evidence has been presented that thermoregulation, is disturbed. The increased energy cost of everyday life in the hyperbaric environment, therefore, may be a result of a disturbance in thermogenic regulation. This change in thermoregulatory integrity is unlikely to interfere with any operational diving procedures or tasks. Perceptual quality may be altered, but there appears to be no reason why normal working dives should not take place considerably deeper than 300 m provided the supporting engineering can cope with the exacting physiological requirements. This is particularly true for environmental conditioning of chamber and umbilical gas.

References

1. Leach CS, Cowley JRM, Troell MT, Clark JM, Lambertsen CJ. Biochemical, endocrinological, and hematological studies. In: Lambertsen CJ, Gelfand R, Clark JM, eds. Predictive studies IV. Work capability and physiological effects in He-O$_2$ excursions to pressure of 400-800-1200 and 600 ft of sea

water. Philadelphia: Institute for Environmental Medicine, University of Pennsylvania Medical Center, 1978:E17–59.

2. Webb P et al. *Hana Kai* II: a 17-day dry saturation dive at 18.6 ATA II. Energy balance. Undersea Biomed Res 1977;4:221–246.

3. McCance RA, Widdowson EM. The composition of foods. Medical Research Council Series 297, London, UK: Her Majesty's Stationery Office, 1960.

4. Carlyle RF, Garrard MP. Further observations on nitrogen metabolism in man during simulated dives to 420 msw (43 bar) in helium-oxygen mixtures. In: Grimstad J, ed. Proceedings, European Undersea Biomedical Society, 5th Annual Scientific Meeting, July 1979, Norway: Bergen 1980: 222–240.

5. Carlyle RF, Collis S-A, Garrard MP, Hall GJ. Some aspects of calcium and collagen metabolism in men subjected to simulated dives of up to 420 msw (43 bar). J Physiol (London) 1979;293:79–80.

6. Hennemann G, Docter R, Krenning EP, Bos G, Otten M, Visser TJ. Raised total thyroxine and free thyroxine index but normal free thyroxine. Lancet 1979;1(8117):639–642.

7. Harris DJ. Some physiological studies of man at pressure. In: Hempleman et al. AMTE(PL) dives 7 and 8 report.Alverstoke, UK: Admiralty Marine Training Establishment Physiological Laboratory. (in press)

8. Carlyle RF, Garrard MP, Stock MJ. Observations on some metabolite and hormonal levels in the blood of men during simulated saturation dives to 420 msw (43 bar) in helium-oxygen mixtures. J Physiol (London) 1978;285:44.

9. Carlyle RF, Florio J, Garrard MP, Haynes PA, Stock MJ. Basal metabolite rate and resting energy expenditure of man during two simulated saturation dives, 420 msw (43 bar) in helium-oxygen mixtures. J Physiol (London) 1980;300:48.

10. Chopra IJ, Williams DE, Orgiazzi J, Solomon DH. Opposite effects of dexamethasone on serum concentrations of 3, 3^1, 5^1-tri-iodothyronine (reverse T$_3$) and 3, 3^1, 5-tri-iodothyronine (T$_3$). J Clin Endocrinol Med 1975;41(5):911–920.

11. Hayes PA. Some physiological studies of man at pressure. In: Hempleman et al. AMTE(PL) dives 7 and 8 report. Alverstoke, UK: Admiralty Marine Training Establishment Physiological Laboratory (in press).

12. Florio J, Towse J. Measurement of absolute humidity during a 420 m simulated saturation dive. AMTE(PL) Tech Memo, AMTE(E) TM 78–406, Alverstoke, UK: Admiralty Marine Training Establishment Physiological Laboratory, 1978.

13. Chilton TH, Colburn AP. Mass-transfer (absorption) coefficients. Prediction from data on heat transfer and fluid friction. Ind Eng Chem 1934;26:1183–1187.

14. Toy N, Cox RN. A surface plate calorimeter. J Phys E Sci Instrum 1973;6:702–704.

15. Keatinge WR, Hayward MG, McIver NKI. Hypothermia during diving in the North Sea. Br Med J 1980;280(6210):291.

16. Hayes PA. Psychophysical studies of thermoperception during prolonged hyperbaric oxyhelium exposures. J. Physiol (London) 1979; 293:80–81.

17. Kenshalo DR. Psychophysical studies of temperature sensitivity. Contri Sens Physiol 1970;4:19–74.

18. Conn ML, Hayes PA, Morrison JB. Contribution of metabolic and respiratory heat to core temperature gain after cold water immersion. In: Bachrach AJ, Matzen MM, eds. Underwater physiology VII. Proceedings of the seventh symposium on underwater physiology. Bethesda, MD: Undersea Medical Society, 1981:509–516.

PART V. DISCUSSION: METABOLISM AND THERMAL PHYSIOLOGY

G. Egstrom, *Rapporteur*

Central to the discussion of the Webb review paper were concerns about a need for more work on the effects of thermal stress upon bubble formation during decompression. Vann stated that "chilling" makes decompression stops longer while "warming" makes the stops shorter. A request for recommendations on rewarming brought comments related to the need for monitoring the temperature of circulating blood. Webb favored inhalation rewarming because he believes that warming the heart is enhanced. Bondi commented that an esophageal site looked promising in following the "afterdrop" phenomenon. Bondi's paper stimulated comments on the extreme care needed to maintain the rather narrow "comfort" band in chambers at depth. Webb expressed concern about the relative humidity and the need for forced convection in high pressure chambers. Morrison and coauthors stimulated a series of questions and comments which centered around a concern about tolerable temperatures in chambers. Hayes observed that there was not much change between 80 and 300 m with a temperature of 40°C ± 2°. Under full saturation this temperature was adequate although they found a fairly high heat transfer rate with some variation in their studies. Webb observed that a 50°C level was uncomfortable and that monitoring variations could be the cause of some of the differences. Morrison believed that hot showers could be dangerous, but a hot bath in a suit would be acceptable if the diver was conscious and in good shape.

Various concerns about the extrapolation of heat gain and loss for points other than where actual data exists reinforced earlier statements of concern about the specific nature of heat gain and loss in the working-diver environment.

Garrard's paper elicited a comment from Wissler about the relative importance of avenues of heat loss and the need to examine the physics of the system rather than the sensitivity.

Bondi questioned the measurement procedure in evaporative heat loss studies because most were not direct measures but, rather, were assumptions based upon assumed intake vs. output. This factor, he believes, may contribute to the apparent differences between experimental studies and data derived from working divers.

539

ENERGY AND BODY FLUID BALANCE DURING A 14-DAY DRY SATURATION DIVE AT 31 ATA (*SEADRAGON* IV)

*H. Nakayama, S. K. Hong, J. R. Claybaugh, N. Matsui, Y. S. Park,
Y. Ohta, K. Shiraki, and M. Matsuda*

Certain changes in energy and body fluid balance have been reported in divers exposed to hyperbaric environments for an extended period of time. For instance, a significant reduction in body weight despite a high energy intake (1), a slight increase in resting oxygen consumption in the absence of cold stress (2), and a significant increase in daily urine flow despite a slight decrease in the fluid intake (3,4) have been observed in previous dry saturation dives. However, the mechanisms underlying these changes have not been clearly elucidated.

The present study was undertaken to further document the pattern of energy and fluid exchange of divers exposed to a thermoneutral, 31 ATA He-O$_2$ environment for 14 days. The dive (code-named "*SEADRAGON IV*") was sponsored by and carried out at the Japan Marine Science and Technology Center (JAMSTEC) in July-September 1979, as a U.S.—Japan Cooperative Diving Research project.

METHODS

Subjects

Four Japanese male divers (*Subjects A, B, C,* and *D*) were selected on the basis of rigorous physical and psychological examinations. On the average, they were 29.7 (25-35) years old, 171.2 (167.7-180.5) cm in height, and 63.9

(59.5-73.3) kg in weight. All subjects were well-trained professional divers and were involved in earlier saturation dives carried out at JAMSTEC.

Dive Profile and Environmental Variables

The overall dive profile and some of the environmental variables (e.g., chamber temperature and chamber gas Po_2) are shown in Fig. 1. The divers entered the chamber at 1400 h on July 29, 1979 to become acquainted with the new environment before the predive control period that started at 0700 h on July 20 (*Dive Day 1*). Compression started at 1200 h on August 2 (*Dive Day 4*) with the divers breathing helium. The chamber pressure was first raised to 11 ATA in 10 h, and maintained at this level for 14 h. Using the identical schedule, we further increased the chamber pressure to 21 ATA and then to 31 ATA, completing the compression at 2200 h on August 4 (*Dive Day 6*). The pressure was kept at 31 ATA for 14 days; décompression was then carried out according to standard U.S. Navy schedules. Twelve days were required to complete the decompression. Divers were kept inside the chamber for 3 more days for postdive control studies. The chamber temperature was maintained at 26 ± 0.5°C at 1 ATA and 31.0 ± 0.2°C at 31 ATA. The Po_2 of the chamber
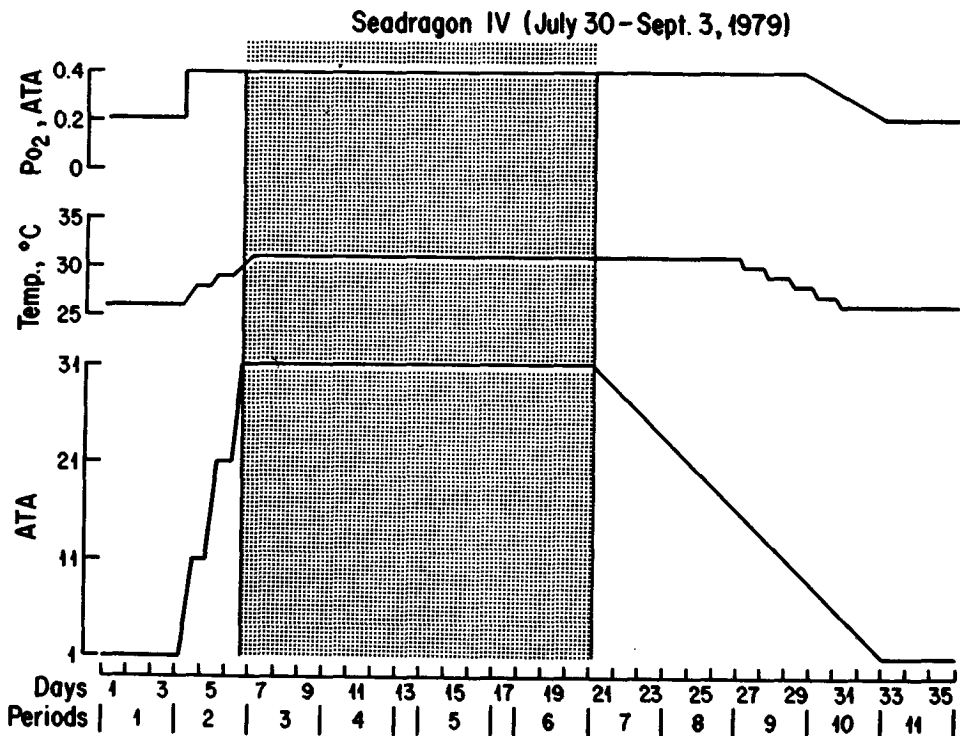
Fig. 1. Dive profile and chamber gas temperature and Po_2. Various dive periods are also indicated on the *abscissa*. Note that *Dive Days 13* and *17* are excluded from periods. ("Immersion" experiments were carried out on these days and thus the body fluid balance was sufficiently disturbed.)

gas was raised from 0.21 ATA at 1 ATA to 0.40 ATA at 31 ATA. The level of P_{CO_2} inside the chamber was kept below 0.004 ATA.

Energy Balance

Hot meals were provided three times a day. Each food item was weighed (to within ± 0.1 g) before it was sent in and after it was sent out of the chamber; in this way we obtained a complete record of all food actually consumed. We estimated the caloric intake as well as the amounts of carbohydrate, fat, and protein intake by using a Food Composition Table by Kagawa (5). The resting oxygen consumption was measured four times a day (0700, 1100, 1500, and 1900 h) by the usual Douglas bag method. The oxygen and carbon dioxide concentrations of the expired gas were determined by a mass spectrometer (Perkin Elmer Model MGA-1100) or a gas chromatograph (Quintron Model R), or both. The body weight was determined every day at 0700 h after voiding, but before eating or drinking. Reported weights have been corrected for the change in buoyancy that results from the increased density of the hyperbaric gas. The difference in gas density between hyperbaric He-O$_2$ (e.g., 6.097 g/L at 31 ATA) and 1 ATA air (1.189 g/L) was multiplied by the body volume of each subject in litres. The latter value was computed from the value of body density determined by the following formula (6):

Body density (kg/L) = 1.0872–0.00205 (mid-axil. skinfold thickness in mm).

We determined the mid-axillary skinfold thickness by using a skin caliper (National Institute of Nutrition, Tokyo). The weight correction factor for the 31-ATA condition varied from 273 g (*Subject A*) to 341 g (*Subject D*). Both the rectal and mean skin temperatures were also determined four times a day (oxygen consumption was indicated previously in this communication) with a telethermometer (Yellow Springs Instrument Co.)

Fluid Balance

The total fluid intake (drinks, water contained in food, and water of oxidation) was estimated on a daily basis. Each subject kept a complete record of all liquid consumption (other than that contained in food) in terms of type and quantity. The water content of food items was taken from a Food Table (5). Water of oxidation was calculated on the basis of 0.13 g/kcal (7). Both urinary and fecal water losses were determined daily. Each subject freely voided into a separate container during and at the end of each of the four collection intervals (0700–1200, 1200–1500, 1500–1900, and 1900–0700 h of the next day). The containers were locked out at the end of each interval, the volumes were recorded, aliquots for various analyses were obtained, and the remainder was then kept in a refrigerator. At 0700 h, a pooled urine sample for each subject was made from the four individual urine samples collected during the previous 24 h. Aliquots of individual and pooled samples were then frozen for later analyses. Each subject defecated into a plastic bag, which was locked out and weighed before and after overnight dessication in an oven (95°C).

Insensible water loss was determined by the measurement of body weight loss over a 3-h period (0900–1200 h), during which subjects were instructed to

avoid all intake of food and fluid and elimination of urine and feces. Weights were measured on a digital platform scale (DICIPE "T", Shinko Denshi Co., Model DBS). Repetitive weighings of objects in the 70-kg range gave standard deviations on the order of ± 9 g. Weight losses measured with the scale were corrected for gas exchange to give true insensible water loss, as described previously (3).

Blood Collection

Venous blood samples (20 mL) were drawn from each subject into separate heparinized syringes at 0630 h every 2–3 days (a total of 9 samples from each subject throughout the dive). Portions of these blood samples were drawn into capillary tubes for determination of hematocrit ratio inside the chamber. The rest of the samples were centrifuged to separate the plasma. The plasma sample was chilled on ice immediately; it was then locked out and frozen for later analysis.

Chemical Analysis

All urine samples were analyzed for osmolality (Fiske Model 230D) and for creatinine, urea, Na, and K by a Technicon Auto Analyzer (Model AAII). All plasma samples were analyzed for osmolality: they were then sent to the Clinical Chemistry Laboratory of the Tokai Medical Center for the complete chemical analysis with a 20-channel prototype SMAC sequential Multiple Analyzer plus Computer) (8). The following items were measured: glucose, urea nitrogen, creatinine, uric acid, Na, K, Cl, Ca, inorganic phosphate, total protein, albumin, SGOT, SGPT, LDH, CPK, alkaline phosphatase, total bilirubin, direct bilirubin, total cholesterol, and triglyceride.

Data Analysis

To avoid unnecessary confusion over the massive data, we present in this communication the mean and standard error for various experimental periods (each period consisting of 3 days, as indicated on the *abscissa* of Fig. 1). All blood and plasma data were compared with each other by paired t tests; other data were compared by unpaired t tests. A difference was considered significant if $P \leqslant 0.05$.

RESULTS

Energy Balance

Various functional measurements of energy exchange observed during the course of the dive are summarized in Table I. The daily caloric intake varied from 2,500 to 3,000 kcal throughout the dive without showing any consistent

TABLE I

Caloric Intake, Body Weight, Body Temperature, and O_2 Consumption during Various Periods of Dive

Dive Periods**	Caloric Intake (kcal/day)	Body Wt. (kg)	Rectal Temp. (°C)	Mean Skin Temp. (°C)	Mean Body Temp. (°C)	O_2 Consumption (mL/min STPD)
1	2,730±61	63.84±1.64	36.65±0.06	33.73±0.13	35.60±0.06	287±13
2	2,779±77	63.77±1.64	36.39±0.10*	32.25±0.19*	35.03±0.10*	—
3	2,523±112	63.14±1.69*	36.55±0.03	32.73±0.03*	35.31±0.05*	—
4	2,923±64*	63.29±1.65	36.63±0.03	32.82±0.05*	35.38±0.03*	302±25
5	2,757±111	63.12±1.62	36.66±0.03	32.76±0.04*	35.37±0.04*	283±14
6	2,825±74	63.35±1.61	36.73±0.04	32.88±0.04*	35.41±0.05*	259±18
7	2,904±124	63.16±1.56	36.63±0.07	32.87±0.05*	35.44±0.04*	265±13
8	3,049±112*	63.44±1.54	36.70±0.04	33.32±0.04*	35.59±0.03	241±13*
9	2,870±87	63.69±1.54	36.60±0.05	32.52±0.07*	35.27±0.03*	257±22
10	3,050±84*	64.13±1.55	36.69±0.06	33.23±0.15*	35.54±0.07	—
11	2,781±77	64.11±1.52	36.76±0.07	34.11±0.12*	35.89±0.06*	259±9*

Each number represents the mean ($\pm$ SE) of 12 values obtained from 4 subjects. Body temperature and O_2 consumption data represent the average of 4 daily measurements (see *METHODS*) on each subject at rest. *$P \leq 0.05$ compared to *Period 1* (paired t test for body weight and unpaired t test for others). **See Fig. 1 for the designation of each "*Period*."

effect of high pressure. Moreover, body weight was maintained remarkably well during the dive; the only significant change was noted during *Period 3* (first three days at 31 ATA) when it decreased by 700 g ($P < 0.05$).

The rectal temperature decreased by 0.26°C during *Period 2* (compression period) ($P < 0.05$), after which it returned to the predive control level. Despite the increase in the chamber temperature at high pressure (Fig. 1), the mean skin temperature (weighted average of 10 sites; see ref. 9) was significantly lower at high pressure ($P < 0.05$). Consequently, the mean body temperature [(0.65 × rect. tem) + (0.35 × mean skin temp.)] was also lowered significantly at high pressure. Subjectively, the divers complained of a mild cold sensation during the early compression phase but generally felt comfortable during the rest of the dive period. The oxygen consumption also remained fairly stable, again an indication that the hyperbaric environment is essentially thermoneutral.

Urinary Excretion of Water and Solutes

Urine flow (V) increased significantly from 1.42 ± 0.08 L/day at 1 ATA predive (*Period 1*) to 1.94 ± 0.08 L/day during the compression period (*Period 2*) ($P < 0.05$); it was maintained at the latter level throughout the subsequent 14 days at 31 ATA (Fig. 2). This diuresis was completely reversed during decompression. Although there was an inverse relationship between the changes in urine flow and urine osmolality, the osmolal clearance (C_{osm}) also increased significantly during 31-ATA periods (Fig. 2). On the other hand, the endogenous creatinine clearance, a measure of the glomerular filtration rate (GFR), decreased during exposure to 31 ATA (Fig. 2).

The daily excretion as well as the fractional excretion of filtered osmotic substances are summarized in Table II. Overall, the daily excretion of total osmotic substances increased significantly by 100–150 mOsm/day ($P < 0.05$) at high pressure, which could be accounted for mostly by the corresponding increase in excretion of urea, Na, and K (and attendant anions). The increase in the excretion of osmotic substances in the face of reduced GFR at high pressure resulted in a significant increase in the fractional excretion of Na, K, urea, and total osmotic substances. These results suggest that the tubular reabsorption of filtered osmotic substances is inhibited at 31 ATA.

Despite the significant increase in C_{osm} at 31 ATA the free water clearance (V − C_{osm}) remained at about −2.3 L/day throughout the dive. Therefore, the negative free water clearance to C_{osm} ratio decreased significantly from −0.61 ± 0.016 at 1 ATA predive to −0.55 ± 0.01 at 31 ATA ($P < 0.05$). These results indicate that the free water reabsorption is also inhibited at high pressure. In other words, the hyperbaric diuresis observed in this dive appears to have both osmotic and water diuresis components.

The most interesting finding in this study was a shift in the diurnal rhythm for urine flow. As shown in Fig. 3, the observed increase in the daily urine flow at high pressure was mostly due to the corresponding increase in overnight urine flow. Although the morning urine flow also increased at high
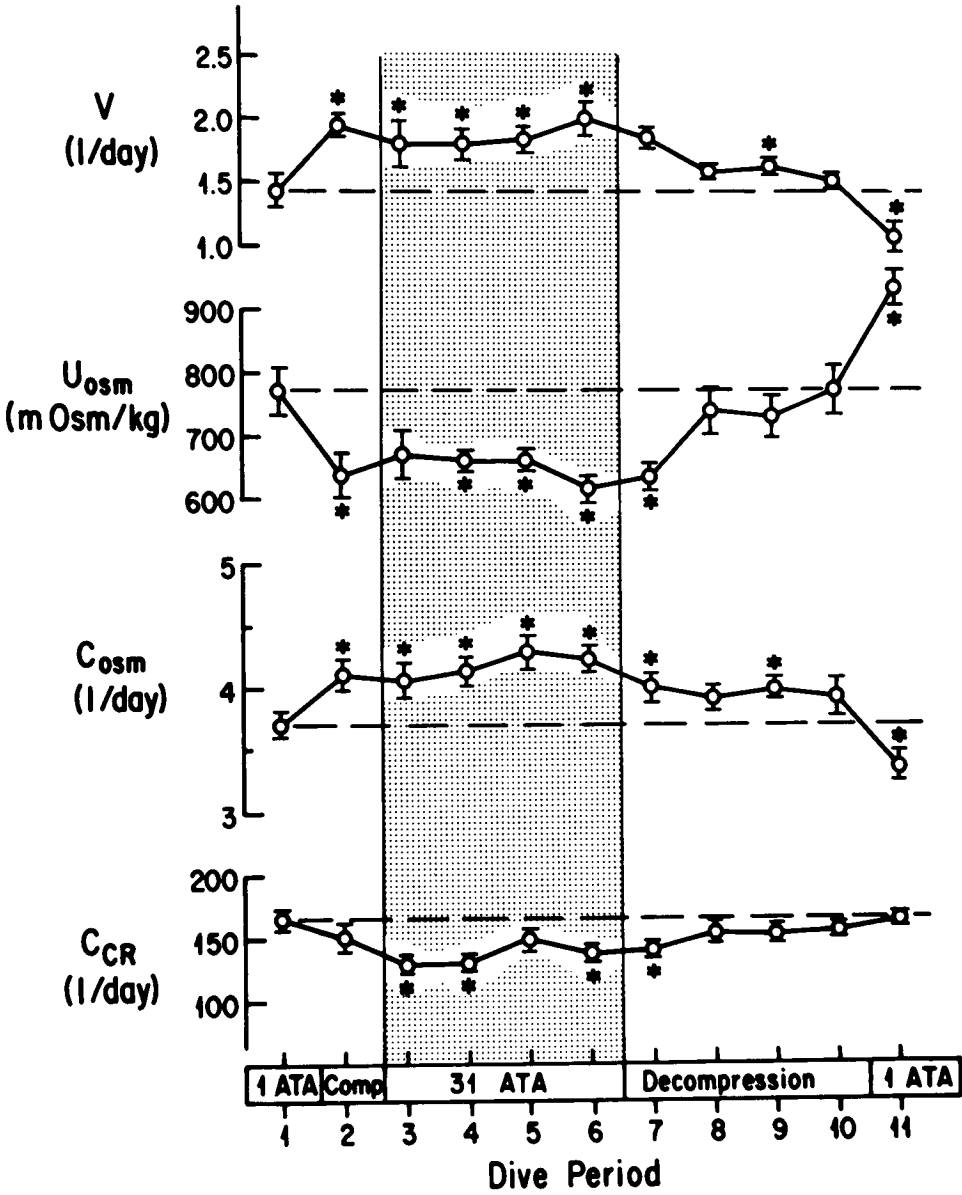
Fig. 2. Urine Flow (V), urine osmolality (U_{osm}), osmolal clearance (C_{osm}), and endogenous creatinine clearance (C_{cr}) during various dive periods. *$P \leq 0.05$ compared to *Period 1* (unpaired *t* test).

TABLE II

Daily and Fractional Excretion of Various Osmotic Substances During Various Periods of Dive.

Dive Periods	Daily Excretion (mOsm/day)				Fractional Excretion (%)**			
	Na	K	Urea	Tot. Osm.	Na	K	Urea	Tot. Osm.
1	265±16	52±3	404±15	1,065±28	1.18±0.10	7.3±0.4	52.8±2.8	2.28±0.11
2	316±10*	75±5*	381±25	1,210±37*	1.56±0.08*	11.4±0.9*	57.6±5.2	2.82±0.14*
3	267±12	77±7*	460±21*	1,177±41*	1.53±0.07*	15.1±0.04*	77.1±1.9*	3.24±0.13*
4	281±15	76±2*	490±14*	1,194±33*	1.60±0.14*	14.0±0.09*	72.9±4.9*	3.27±0.23*
5	312±18	83±3*	446±15	1,230±41*	1.55±0.12*	14.1±0.8*	60.7±3.0	2.99±0.20*
6	300±14	83±4*	448±16	1,232±28*	1.57±0.09*	14.6±0.8*	61.2±2.3*	3.09±0.12*
7	285±10	79±4*	415±13	1,170±26*	1.49±0.07*	13.9±0.7*	58.3±4.0	2.95±0.14*
8	263±9	57±2	407±12	1,149±29*	1.23±0.07	8.8±0.4*	50.4±2.1	2.58±0.13
9	290±9	62±2	398±7	1,162±22*	1.37±0.08	9.6±0.3*	50.1±1.7	2.66±0.15
10	297±13	58±2	376±13	1,124±38	1.34±0.08	8.8±0.4*	46.5±1.7	2.56±0.14
11	227±9*	56±3	362±15	973±34*	1.01±0.06	7.9±0.4	49.1±3.0	2.10±0.13

Each number represents the mean ($\pm$SE) of 12 values obtained from 4 subjects.   *$P \leqslant 0.05$ compared to *Period 1* (unpaired t test).

$$ ** \left(\frac{\text{urinary excretion}}{\text{filtered amount}} \times 100 \right) $$
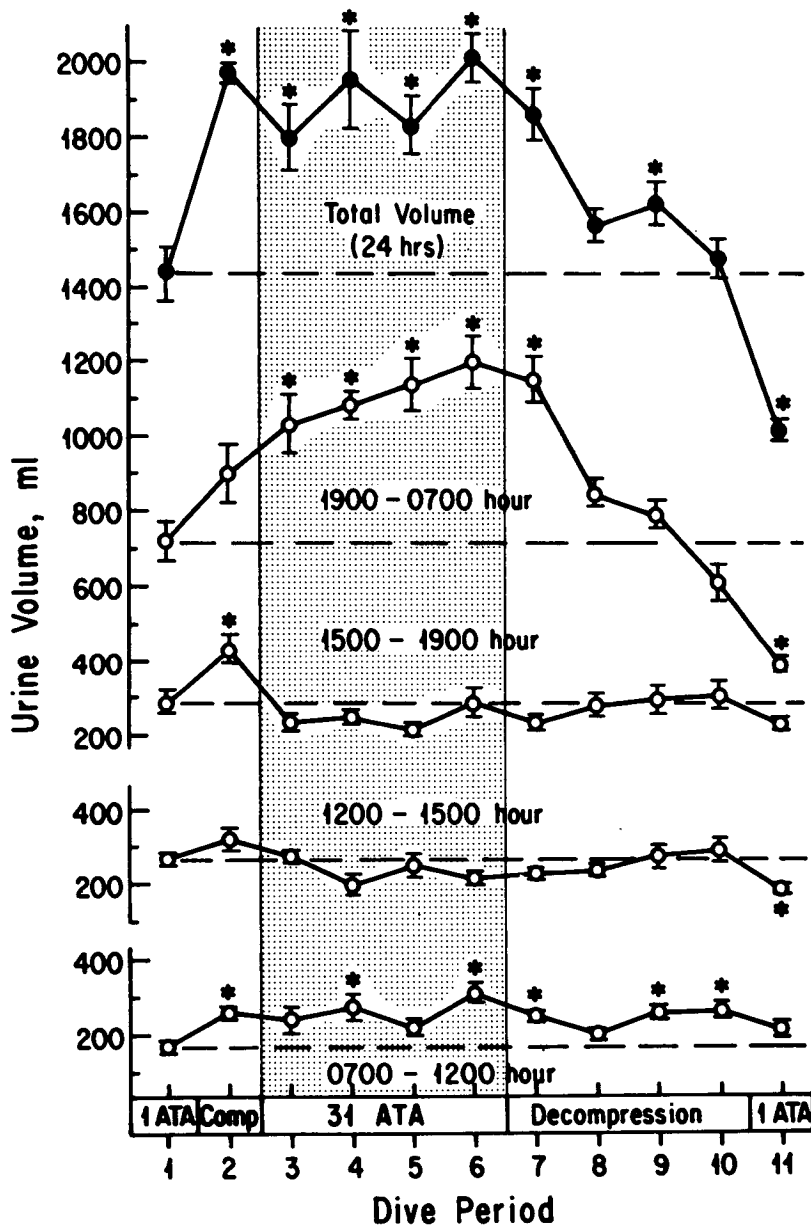
Fig. 3. Daily urine flow (top panel) and the volumes of urine collected during each of the four intervals during various dive periods. * P ≤ 0.05 compared to Period 1 (unpaired t test).

pressure, it was less consistent and small in magnitude as compared to the overnight flow. Moreover, the afternoon urine flow tended to decrease, if any, at high pressure. This hyperbaric nocturia was accompanied by increases in the rate of excretion of osmotic substances (Na, K, urea, and total osmotic substances) in the face of unchanged rate of creatinine excretion. As expected, the nocturia was accompanied by the significant increases in C_{osm} but the normalized negative free water clearance (i.e., the negative free water clearance to C_{osm} ratio) did not decrease significantly at 31 ATA. the presence of a water diuresis component noted above for the 24-h urine samples obtained at 31 ATA was mainly attributed to reduction in the normalized negative free water clearance during morning (0700–1200 h) and early afternoon (1200–1500 h).

Water Balance

Daily water exchanges via various avenues during the dive are summarized in Table III. Overall, the water intake (drinking plus water contained in food) decreased during exposure to high pressure while the water of oxidation remained fairly constant. Thus, the average total daily water input decreased by 260 mL at 31 ATA as compared to 1 ATA predive. On the other hand, the average daily urinary and fecal water output increased by 525 mL at 31 ATA as compared to 1 ATA predive. Thus, the daily sensible water balance decreased from 1,454 mL/day at 1 ATA predive to 676 mL/day at 31 ATA.

There is a remarkable agreement between the daily sensible water balance and the insensible water loss at both 1 and 31 ATA; the insensible water loss decreased from 1 ATA predive level of 0.84 ± 0.04 g/min (or 1,209 g/day) to 0.43 ± 0.05 g/min (or 620 mL/day) at 31 ATA ($P < 0.05$). This indicates that, despite the reduced water intake and the sustained diuresis at 31 ATA, the overall water balance seem to be well maintained.

Plasma Chemistry

Although there were minor variations in plasma osmolality and Na, K, and Cl concentrations during the dive, no consistent pattern was noted. On the other hand, the total plasma protein concentration increased significantly from 6.75 ± 0.25 g% at 1 ATA predive to 7.20 ± 0.12 g% ($P < 0.05$) during the first 5 days at 31 ATA, after which it returned to the predive level. The hematocrit ratio also increased significantly from 45.7 ± 1.7% at 1 ATA predive to 48. 2 ± 1.6% ($P < 0.05$) on the third day at 31 ATA. These findings suggest a reduction in the plasma volume during the early phase of exposure to 31 ATA. The magnitude of this reduction in plasma volume, estimated by the use of Van Beaumont's formula (10), was 9.31% ($P < 0.01$) and 4.54% ($P < 0.05$) on the third and sixth day, respectively, at 31 ATA. The plasma concentration of endogenous creatinine also increased significantly by 20–30% ($P < 0.05$) at 31 ATA, most probably because of reductions in glomerular filtration rate (previously mentioned). There were also interesting changes in other constituents of plasma, which will be published elsewhere.

TABLE III

Daily Water Exchange During Various Periods of the Dive (mL/day)

Dive Period	Water Intake (1)	Water of Oxidation (2)	Urine (3)	Fecal Water (4)	Sensible Water Balance (1 + 2-3-4)
1	2,673 ± 96	356 ± 9	1,419 ± 77	156 ± 22	1,454 ± 135
2	2,488 ± 51	359 ± 10	1,940 ± 77*	215 ± 26	707 ± 75*
3	2,279 ± 52*	328 ± 15	1,794 ± 89*	229 ± 23*	583 ± 87*
4	2,381 ± 33*	380 ± 8	1,812 ± 59*	229 ± 27*	721 ± 79*
5	2,290 ± 42*	358 ± 14	1,829 ± 76*	200 ± 21	619 ± 80*
6	2,653 ± 77	374 ± 9	2,020 ± 70*	225 ± 17*	781 ± 98*
7	2,374 ± 70*	377 ± 16	1,860 ± 70*	211 ± 33	681 ± 96*
8	2,476 ± 56	396 ± 15*	1,569 ± 38	209 ± 25	1,094 ± 93*
9	2,332 ± 32*	373 ± 11	1,625 ± 57*	202 ± 17	877 ± 65*
10	2,373 ± 47*	396 ± 11*	1,504 ± 55	219 ± 23	1,047 ± 72*
11	2,802 ± 42	361 ± 10	1,015 ± 30*	195 ± 23	1,953 ± 74*

Each value represents the mean (± SE) of 12 determinations in 4 subjects. * $P \leq 0.05$ compared to *Period 1* (unpaired t test).

DISCUSSION

In the present dive, 4 divers stayed 14 days in a thermoneutral, 31 ATA He-O$_2$ environment. Although there was a mild cold stress during the early compression period, the subjects felt comfortable during the remainder of dive periods. The mean skin temperature decreased by approximately 1°C at 31 ATA (Table I), but the resting oxygen consumption remained fairly constant. The caloric intake was approximately 30% higher than the energy expenditure based on the resting oxygen consumption. Because the divers were mostly engaged in physiological and psychomotor tests without involving prolonged, strenuous exercise, it was estimated that their daily caloric intake was adequate. Whether the small reduction in body weight (0.7 kg) observed during the early 31-ATA period (Table I) reflects a caloric deficit or a mild dehydration is difficult to assess in the absence of the data on total body water volume. However, the fact that the above reduction in body weight was accompanied by significant increases in both plasma protein concentration and hematocrit ratio strongly indicates a transient, dehydration-induced weight change. Regardless of the interpretation of the present data, it should be pointed out that the magnitude of the reduction in body weight observed in the present dive is much less than that observed in many previous dives where a reduction as large as 4.0 kg was observed (2). However, it is equally important to note that there was also a gain of body weight at least in one dry saturation dive at 31 ATA (11). The results obtained from the present dive certainly support a conclusion that human divers can maintain their energy balance in a thermoneutral 31-ATA environment for a period of 2 weeks without encountering any serious, adverse effects.

In practically all saturation dives carried out previously, a significant increase in urine flow was observed (12). In an attempt to elucidate the mechanism(s) underlying this hyperbaric diuresis, Hong et al. (3) carried out very comprehensive studies on 5 divers exposed to a thermoneutral 18.6 ATA He-O$_2$ environment for 17 days (*Hana Kai II*). They found that the increase in urine flow was accompanied by a reduction in urine osmolality, but not by any change in GFR and C$_{osm}$, indicative of a water diuresis. Based on these and other observations, these authors (3) concluded that the hyperbaric diuresis observed during steady state is primarily attributable to the inhibition of antidiuretic hormone (ADH) associated with the suppression of insensible water loss, and also that it does not induce dehydration. On the other hand, the diuresis observed during the early phase (i.e., first 4–5 days after the onset of compression) was independent of ADH, was osmotic in nature, and led to a transient dehydration. The mechanism of the diuresis observed in the present dive appears to be somewhat different. The diuresis was accompanied by an increase in the excretion of osmotic substances in the face of reduced GFR (Fig. 2), an indication that one mechanism for the diuresis is the inhibition of the tubular reabsorption of the filtered osmotic substances and water. However, the negative free water clearance/C$_{osm}$ ratio decreased, indicating that the

free water reabsorption independent of solute reabsorption is also suppressed at high pressure. The latter phenomenon is most likely related to the inhibition of ADH associated with the suppression of the insensible water loss also observed in the present dive. However, there is a similarity between the present and the *Hana Kai II* dives in that the overall water balance appears to have been well maintained at high pressure despite the sustained diuresis (owing to a reduction in insensible water loss) except during the early hyperbaric period when a transient, mild dehydration was observed.

The mechanism for the inhibition of the tubular reabsorption of osmotic substances observed in the present dive is not clear at present. At least in one dive reported by Neuman et al. (13), a small, consistent increase in the fractional excretion of osmotic substances was observed at 26.7 ATA. It is thus likely that the tubular transport of osmotic substances is pressure-sensitive. Recently, Goldinger et al. (14) reported a reversible inhibition of Na^+ efflux (i.e., Na^+ pump) from human erythrocytes under the influence of hydrostatic pressure, in which they observed about a 30% reduction at 30 ATA. Although the pressure sensitivity of the active Na^+ transport system in the renal tubule is not known, it is speculated that the active transport of Na across the tubular epithelium is subject to inhibition under the influence of higher pressure. Such an inhibition of Na reabsorption at pressure would also explain the increase in the fractional excretion of urea, K^+, and water, because the reabsorption of the latter substances is closely linked to the degree of Na reabsorption. However, as pointed out earlier, there is an additional mechanism for the inhibition of free water reabsorption at pressure. Likewise, the increase in the fractional excretion of K^+ also has an Na-independent component, because it has been observed in many previous dives to shallower depths where the Na^+ excretion is not affected (12).

The shift in diurnal rhythm for urine flow at 31 ATA (Fig. 3) is extremely interesting, although the underlying mechanism is not entirely clear. There was no significant change in the pattern of EEG during sleep at high pressure, and thus it is not likely that the alternations in CNS activities were in any way related to this shift. It is possible that the divers may have been subjected to a subtle cold stress during sleep at pressure, although they did not complain about it. However, the latter possibility is also unlikely because the observed nocturia was basically an osmotic diuresis; a cold-induced diuresis would more likely be a water diuresis (15). Another possibility is that the cardiovascular reflexes elicited by changes in posture may have been altered at 31 ATA. For instance, the assumption of a supine position at high pressure may have resulted in a greater pooling of blood in the thorax, thereby stimulating the volume receptors and activating a natriuretic factor to a greater extent. Lastly, there is the possibility of a shift in diurnal rhythm for the release of various hormones that are involved in body fluid regulation. Both plasma and urine samples obtained during the present dive are currently being analyzed for various hormones, and it is hoped that the hormone data provide some clue to the understanding of this interesting hyperbaric nocturia.

Acknowledgments

References

1. Webb P. The thermal drain of comfortable hyperbaric environments. Nav Res Rev 1973;26:1–7.
2. Webb P, Troutman SJ Jr, Frattali V, Dwyer J, Moore TO, Morlock JF, Smith RM, Ohta Y, Hong SK. *Hana Kai II*: a 17-day dry saturation dive at 18.6 ATA. II. Energy balance. Undersea Biomed Res 1977;4:221–246.
3. Hong SK, Claybaugh JR, Frattali V, Johnson R, Kurata F, Matsuda M, McDonough AA, Paganelli CB, Smith RM, Webb P. *Hana Kai II*: a 17-day dry saturation dive at 18.6 ATA. III. Body fluid balance. Undersea Biomed Res 1977;4:247–266.
4. Matsuda M, Nakayama H, Kurata FK, Claybaugh JR, Hong SK. Physiology of man during a 10-day dry heliox saturation dive (*Seatopia*) to 7 ATA. II. Urinary water, electrolytes, ADH, and aldosterone. Undersea Biomed Res 1975;2:119–131.
5. Kagawa A. Food composition table. Tokyo: Kagawa Nutritional College Press, 1979.
6. Nakamine S, Suzuki S. Anthropometry and body composition of Japanese young men and women. Human Biol 1964;36:8–15.
7. Muntwyler E. Water and electrolyte metabolism and acid-base balance. St. Louis: C.V. Mosby, 1968.
8. Schwartz M, Bethune VG, Fleisher M, Pennachia G, Menendez-Botel CJ, Lehman D. Chemical and clinical evaluation of the continuous-flow analyzer "SMAC." Clin Chem 1974;20:1062–1070.
9. Consolazio CF, Johnson RE, Pecora LJ. Physiological measurements of metabolic functions in man. New York: McGraw-Hill Book Co., 1963.
10. Van Beaumont W. Evaluation of hemoconcentration from hematocrit measurements. J Appl Physiol 1972;32:712–713.
11. Hempelman HV. Observations on man at pressures of up to 300 msw (31 bar). Alverstoke: Admiralty Marine Technology Establishment, 1978. (AMTE (E) R78401)
12. Hong SK. Body fluid balance during saturation diving. In: Hong SK, ed. International symposium on man in the sea. Bethesda, MD: Undersea Medical Society, 1975:127–140.
13. Neuman TS, Goad RF, Hall D, Smith RM, Claybaugh JR, Hong SK. Urinary excretion of water and electrolytes during open-sea saturation diving to 850 fsw. Undersea Biomed Res 1979;6:291–302.
14. Goldinger JM, Kang BS, Choo YE, Paganelli, CV, Hong SK. The effect of hydrostatic pressure on ion transport and metabolism in human erythrocytes. J Appl Physiol: Respirat Environ Exercise Physiol 1980; 49(2):224–231.
15. Segar WE, Moore WW. The regulation of antidiuretic hormone release in man. I. Effects of changes in position and ambient temperature on blood ADH levels. J Clin Invest 1968;47:2143–2151.

A COMPUTER MODEL DESIGNED TO MAKE RAPID PREDICTIONS OF DIVER TEMPERATURE CHANGES

S. Wilcock and V. Flook

Recent accidents in the North Sea that resulted in the loss of heat supplies to a diving bell have shown both the need to estimate diver survival time to allow planning of the rescue attempts within a realistic time scale and the need for emergency heat supplies. This paper reports a mathematical model of thermal balance designed to be used on-line to a computer so that a rapid estimate of rate of change of body temperature can be made once details of environmental conditions have been supplied. The program can also be used to produce tables relating body temperatures to a wide range of environmental conditions and to aid in the design of emergency heat sources.

It is not possible in the limited space available to present in detail all the equations used in the model; therefore, standard heat transfer equations are not included in this paper. Instead, the space has been used to summarize the choice and evaluation of the various physiological and physical parameters needed in the calculation.

The Mathematical Model

The model uses basic physical equations to describe the heat exchange processes between the body and the environment. This approach means that the model, once shown to be in agreement with experimental measurements, can be used to make predictions over a much wider range of conditions than could an empirical model.

The design allows separate calculation of heat loss from clothed and unclothed areas of the body with the facility to vary the proportion of the total body area that is clothed. The overall heat balance equation is therefore:

$$\dot{M} \pm \dot{S} - \dot{X} - (\dot{E}_R + \dot{C}_R) = \dot{K}_{(T)} = \dot{C}_u + \dot{R}_u + \dot{E}_u$$
$$+ \dot{K}_{(T+c)} = \dot{C}_c + \dot{R}_c \qquad (1)$$

555

$\dot{M}$ is metabolic heat production. $\dot{S}$ is changes in body heat stores, $\dot{X}$ is energy used in external work, and $(\dot{E}_R + \dot{C}_R)$ is respiratory heat loss. $\dot{C}$, $\dot{R}$ and $\dot{E}$ are convective, radiative, and evaporative heat loss, respectively, from the unclothed surface (u) and from the clothed surface (c). K is the heat conducted through the tissues to the body surface (T) and through the clothes (c). As yet there is no term accounting for the transfer of heat by conduction to the surrounding structures. Our present concern is with fully-shod divers standing in a bell and this term is very small under these conditions.

Changes in body heat stores ($\dot{S}$). We have evaluated changes in body heat stores using the results from our measurements on divers and they will be discussed later.

Energy used in external work ($\dot{X}$). There is little information about the energy cost of physical work in hyperbaric heliox. Our concern is with divers performing very little work other than standing, and our measurements were made on divers with similar levels of activity. In air at 1 ATA the energy cost of standing is about 1 Joule (J)/min and this value has been used. It will be necessary to give a more realistic value to $\dot{X}$ when considering the working diver.

Metabolic heat production ($\dot{M}$). The relationship between metabolic heat production and oxygen consumption ($\dot{V}O_2$) varies with respiratory quotient (RQ) and ranges from 19.6 to 21.05 J/mL O_2. For evaluation of the model this has been set to 20.1 J/mL corresponding to a "normal" value for RQ such as might be expected in the experimental divers who were on a "normal" mixed diet.

The relationship between oxygen consumption and ventilation ($\dot{V}_E$) has been derived from Astrand and Rodahl (1).

$$\dot{V}O_2 = -69.6 + 54.3 \, \dot{V}_E - 0.17 \, \dot{V}_E^2 \qquad (2)$$

Respiratory evaporative heat loss ($\dot{E}_R$). The heat required to vaporize the water added to the inspired gas in the respiratory tract is the respiratory evaporative heat loss. The mass of water inspired is calculated from the temperature and relative humidity of the inspired gas. Mass spectrometry measurements have shown that expired gas is fully saturated with water vapor at the temperature at which the gas leaves the mouth. The following relationship between inspired gas temperature and expired gas temperature in hyperbaric heliox has been drawn from the experimental work of Goodman et al. (2) and Hayes (3) for depths up to 300 m.

$$T_e = 23.85 + 0.337 \, T_i \qquad (3)$$

This equation is applicable for values of T_i from 2°C to 32°C and is statistically significant at $P < 0.001$.

Convective respiratory heat loss ($\dot{C}_R$). The heat required to warm the inspired gas to expired temperatures is the convective respiratory heat loss. The calculation uses the specific heat of the gas, and evaluation of this will be discussed in the section describing the evaluation of all the physical constants used.

Heat conducted through tissues to body surface ($\dot{K}_T$). The conduction of heat from the body core to the surface depends on the area of that surface, the temperature gradient from core to surface, and the conductivity of the tissue. Tissue conductivity depends on the degree of vasodilatation in the systemic circulation, and the best information about this is contained in a review by Benzinger (4). The "normal" level of tissue conductance has been calculated as 627 J/min·m² °C. This level increases under the influence of both core and skin temperature and begins to increase at exactly the same temperature at which sweating starts. The increase occurs at a rate of 950 J/min·m² °C for every 0.1°C rise in core temperature. It does not drop below the normal level even when core temperature has dropped by as much as 1°C.

Heat conducted through tissues to body surface and through clothes [$\dot{K}_{(T+c)}$]. For the clothed part of the body we are concerned with two rates of conduction—that from the core to the skin surface and that from the skin surface to the surface of the clothes. At equilibrium the two must be equal and depend on both temperature gradients, core-to-skin and skin-to-clothes surface.

Thus, at equilibrium the conductivity of the clothes G_c can be evaluated as

$$G_c = G_T \frac{(T_R - T_S)}{(T_S - T_c)} \tag{4}$$

where G_T is the tissue conductivity and temperatures (T) are rectal (R), skin (S), clothes surface (c).

Convective heat loss ($\dot{C}$). Convective heat loss is by "free" convection in conditions normally found in a diving habitat. It is dependent on the temperature gradient skin surface to environment for the unclothed areas and clothes surface to environment for the clothed areas. The coefficient of convective heat loss is determined by the expression $a\frac{(GR \times PR)^b}{L}K$, where GR is the Grashof number and PR the Prandtl number for the environmental gas. K is the thermal conductivity and L a characteristic dimension, in this model usually height. Constants a and b are dependent on the type of flow in the boundary layer; in this model the flow has been taken as laminar if GR × PR lies between 10^4 and 10^9 and turbulent if the product is greater than 10^9 according to Holland et al. (5).

Radiative heat losses ($\dot{R}$). The standard equation for radiative heat transfer using skin temperature or clothes temperature as appropriate is used for calculating radiative heat losses. No reliable information is available about the emissivity of chamber and diver surfaces, but the emissivity of an enclosed volume of gas is 1.0 unless that volume contains water vapor or carbon dioxide. Tables are available (5) to correct for the presence of these gases; however, a 5% error in the value used for the emissivity of the chamber causes an error in the radiative heat loss of less than 0.5% in the conditions applicable to diving habitats. A value of 0.95 has been taken as the emissivity of the diver surface; a 5% error in this results in almost 5% error in the calculated radiative heat loss.

Evaporative heat loss ($\dot{E}$). In this model evaporative heat loss has been considered to occur only from the uncovered area of the skin. This is a reasonable assumption for the evaluation of the model as the divers were not sweating heavily and their clothing was dry.

The general equation for evaporative heat loss from a nonsweating surface is from Flynn et al. (6).

$$E = L_{H_2O} \times h_E \times \text{area} \left[\frac{c\, C_{(H_2O)\, T_S} + h_E\, C_{(H_2O)\, T_a}}{c + h_E} - C_{(H_2O)\, T_a} \right] \quad (5)$$

$C_{(H_2O)}$ is the concentration of water vapor at ambient (T_a) or skin (T_S) temperature. L_{H_2O} is the latent heat of vaporization of water. The rate of transfer of water vapor through the skin is c and has been taken as the value quoted by Flynn et al. at 0.0143 m/min. The coefficient of evaporative heat transfer is h_E, given by

$$h_E = \left[\frac{Cp_d \times \rho_d \times D_{(H_2O)\, T_a}}{K} \right]^{\frac{2}{3}} \times \frac{h_c}{\rho_{moist} \times Cp_{moist}} \quad (6)$$

Cp and ρ are the specific heats and density of dry gas (d) and of the gas containing water vapor (moist). The convective heat transfer coefficient is h_c; K is the thermal conductivity; and $D_{(H_2O)}T_a$ is the diffusivity of water vapor in heliox at T_a.

Evaluation of Physical Constants

The specific heat of moist gas was calculated according to the equation

$$Cp_{moist} = \frac{Cp_d + W\, Cp_w}{1 + W} \quad (7)$$

where W is the mass of water/mass of dry gas and Cp_w the specific heat of water vapor (Rappe, 7).

The density of moist gas was calculated from

$$\rho_{moist} = \rho_d \frac{T1}{T_a} \left[\frac{P_B - \left(1 - \frac{Mw}{M_d}\right) P_{(H_2O)\, T_a}}{P1} \right] \quad (8)$$

The density of the dry gas at T1 and P1 is ρ; M is the molecular weight of water (w) and dry gas (d); P_B is the barometric pressure; and $P_{(H_2O)}\, T_a$ is the vapor pressure of water at T_a and the appropriate relative humidity (Humphrey, 8).

The diffusivity of water vapor in heliox was calculated from the diffusivity of water vapor in oxygen ($D_{(O_2)}$) and in helium ($D_{(He)}$) according to the equation

$$D_{(H_2O)} = \frac{D_{(He)} \times D_{(O_2)}}{F_{(He)} \times D_{(O_2)} + F_{(O_2)} \times D_{(He)}} \qquad (9)$$

$F_{(He)}$ and $F_{(O_2)}$ are the fractional concentration of oxygen and helium (Sibbons, 9).

The diffusivity values in helium and oxygen were corrected from the temperature at which they were measured (T_m) to ambient temperature (T_a).

$$.D_{T_a} = \left[\frac{273 + T_a}{273 + T_m}\right]^{\frac{1}{2}} \times D_{T_m} \qquad (10)$$

The molecular weight of the heliox mixture was calculated at each depth as weighted means of the molecular weight of helium and oxygen, weighted according to the fractional concentration.

Evaluation of the thermal conductivity of a gas mixture using a simple weighting according to concentration does not give values in agreement with experimentally measured values (Laby and Nelson, 10) and, therefore, the thermal conductivity of the heliox mixture has been determined at each depth according to the method of Lindsey and Bromley (11).

The specific heat and viscosity of the dry gas mixture has been calculated at each depth as weighted means, according to Ellenwood et al. (12). This gives close agreement with measured values.

Comings and Egly (13) have described the effect of pressure and temperature changes on thermal conductivity, viscosity, and specific heat of gases and gas mixtures as functions of reduced temperature and reduced pressure. Values for reduced temperature and pressure have been calculated for heliox at each pressure and 30°C; these are listed in columns 2 and 3 of Table I. Pseudocritical constants were calculated for the gas mixture at each pressure as weighted means of the critical constants of helium and oxygen. The reduced temperature and pressure values are such that according to Comings and Egly (13) the correction for effect of pressure per se on thermal conductivity, specific heat, and viscosity is less than 5%. As seen from Table I, the gas mixture is well above

TABLE I

Physical Constants for 0.4 ATA Oxygen + Helium at 30°C

1	2	3	4	5	6	7
			Thermal Conductivity	Viscosity	Specific Heat	
Pressure ATA	Reduced Temperature	Reduced Pressure	J/m °C s $\times 10^{-2}$	NS/M² $\times 10^{-6}$	J/kgm $\times 10^3$	Density kgm/m³
1	4.69	0.047	7.14	20.4	3.488	0.608
5	17.91	0.825	12.86	20.008	4.859	1.243
10	27.60	2.410	13.93	20.004	5.052	2.037
20	37.97	6.230	14.52	20.002	5.118	3.624
40	46.69	14.650	14.83	20.001	5.202	6.801
92	54.11	37.500	15.01	20.0004	5.244	15.63

critical temperature at all pressures; at the lower pressures, where critical temperature is highest, pressure is considerably below critical pressure. Columns 4, 5, and 6 of Table I list thermal conductivity, viscosity, and specific heat values that take account of the changing concentrations but have no allowance for the effect of pressure.

The density of the gas mixture was calculated as if the mixture were an ideal gas, i.e., making no allowance for compressibility. The justification for this approach is, again, that the reduced temperatures and pressures suggest that the mixture will behave as an ideal gas.

Experimental Results

Full details of the experimental work appear elsewhere (Wilcock and Flook, 14), but, in summary, recordings were made of six skin surface temperatures, rectal temperature, and environmental temperatures on 52 divers taking part in experimental dives. Recordings were made for up to 24 h and not less than 4 h. Figures 1 and 2 show some of the results of daytime temperatures averaged over a period of not less than 4 h. Figure 1 shows mean body temperatures against depth and Fig. 2 shows rectal temperatures against depth.

Evaluation of the Model

We evaluated the model using data from divers known to be in a steady state. The condition set was that mean body temperature had not changed for

Fig. 1 Averaged daytime mean body temperatures recorded in 52 divers. *Open circles* represent duplicate readings and were not used in statistical analysis.
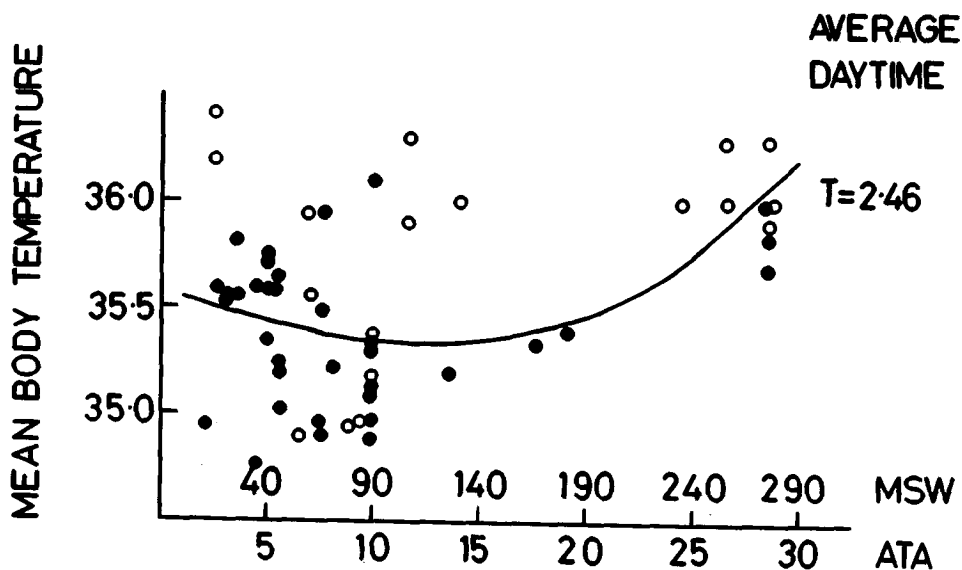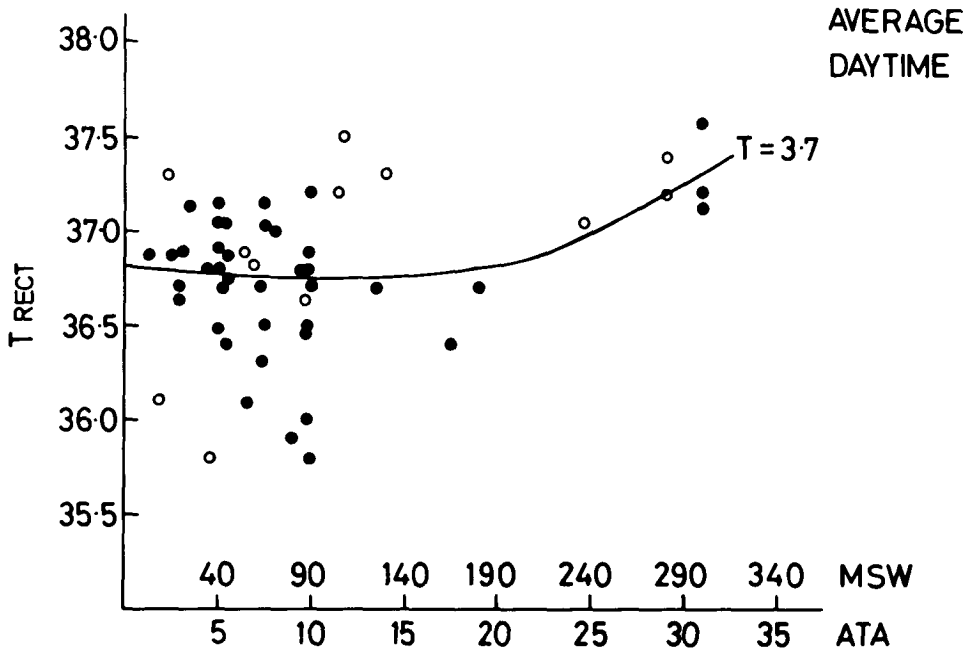
Fig. 2. Averaged daytime rectal temperatures recorded in 52 divers. *Open circles* represent duplicate readings and were not used in the statistical analysis.

at least 2 h and therefore changes in body heat stores could be assumed to be zero. From over 1700 data sets only 35 fulfilled this condition. All work with the model so far has been for a clothed area as 90% of body area which corresponds to head, neck, and hands uncovered.

The computer used iterative procedures to evaluate the ventilation required to balance the right- and left-hand sides of Eq. 1. None of the data sets used were from working divers and therefore ventilation levels should lie with a range 5–8 L/min. Table II shows the average values for heat losses, metabolic heat production, and ventilation calculated for the data sets at four depths.

Predictions from the Model

Development of the model as a means of predicting body temperature changes is at a very early stage but some interesting facts have come to light.

To estimate rates of change in body temperature one must give a value to $\dot{S}$, change in body heat stores. We did this by using 26 data sets each of which followed a "steady state" data set and which showed a change in mean body temperature. Assuming diver ventilation to be unchanged, we evaluated heat losses and metabolic heat production from each data set and the difference between the two sides of Eq. 1 set equal to $\dot{S}$. Thus, for each diver we have a

TABLE II

Average Values for Heat Losses, Metabolic Heat Production, and Ventilation Calculated for 4 Depths

| Depth msw | Heat Losses | | | | | | Metabolic Heat Production | Ventilation L/min |
| | Clothed Area | | Unclothed Area | | | | | |
	Convective	Radiative	Convective	Radiative	Evaporative	Respiratory		
40–45 (6 divers)	2637.2	1224.9	597.9	224.7	89.5	569.4	5293.5	6.26
85–90 (10 divers)	2593.5	910.0	467.6	161.1	79.1	544.8	4759.0	5.76
171 (1 diver)	3366.2	810.2	490.7	128.6	55.9	821.8	5650.1	6.6
300 (1 diver)	3437.7	671.3	516.7	113.7	58.6	1039.6	5859.0	6.8

All heats expressed in J/min. No data sets were from working divers; therefore ventilation levels should range from 5–8 L/min. See text for explanation.

value for change in body heat stores per degree change in mean body temperature.

The calculations were repeated for an inspired gas temperature 4°C with the environmental temperature and surface heat losses as for the experimental dives, i.e., the only increased heat loss is the respiratory heat loss. Under these conditions the average drop in mean body temperatures for 6 divers at 40–45 msw was estimated as 0.067 °C/h, for 9 divers at 85–90 msw 0.168 °C/h, and for 1 diver at 300 msw 0.8°C/h.

Respiratory heat loss has been evaluated as a percentage of metabolic heat production for inspired gas temperature equal to chamber temperature on the experimental dives, inspired gas temperature 4°C with the "normal" ventilation, and inspired gas temperature 4°C at four levels of increased ventilation. The results, shown in Table III, indicate that there is a benefit to be gained from shivering at depths up to 300 msw.

TABLE III

Respiratory Heat Loss as a Percentage of Metabolic Heat Production

Depth msw	T_i = Chamber Temperature Vent "normal"	T_i = 4°C				
		Vent "normal"	Vent + 10%	Vent + 50%	2 × Vent	3 × Vent
40–45	10.99	18.11	17.66	16.6	16.05	15.69
85–90	11.64	28.65	27.84	26.0	25.00	24.36
300 m	17.5	71	70.3	67.2	65.6	64.8

References

1. Astrand PO, Rodahl K. Textbook of work physiology. New York: McGraw-Hill Book Co, 1970.
2. Goodman MW, Smith NE, Colston JW, Rich EL. Hyperbaric respiratory heat loss study. Office of Naval Research, 1971 (N00014-71-C-0099). (AD 732, 039)
3. Hayes PA. Energy balance and heat loss during saturation diving. Alverstoke, UK: Royal Naval Physiological Laboratory, 1977, RNPL 2/77.
4. Benzinger TH. Heat Regulation: Homeostasis of central temperature in man. Physiol Rev 1969;49:671–759.
5. Holland FA, Moores RM, Watson FA, Wilkinson JK. Heat transfer. London: Heineman Education Books Ltd, 1970.
6. Flynn ET, Vorosmarti J, Modell HI. Temperature requirements for the maintenance of thermal balance in high pressure helium-oxygen environments. Washington DC: Navy Experimental Diving Unit 1974 (21–73).
7. Rapp GM. Convective mass transfer and the coefficient of evaporative heat loss from human skin. In: Hardy JD, Gagge AP, Stolwijk JAJ, eds. Physiological and behavioural temperature regulation. Springfield, IL: Charles C Thomas 1970: 55–80.
8. Humphreys WJ. Physics of the air. New York: McGraw-Hill Book Company, 1940.
9. Sibbons JLH. Coefficients of evaporative heat transfer. In: Hardy JD, Gagge AP, Stolwijk JAJ, eds. Physiological and behavioural temperature regulation. Springfield, IL: Charles C Thomas 1970:108-138.
10. Laby TH, Nelson EA. Thermal conductivity: Gases and vapors. Int Crit Tables 1929;213–215.
11. Lindsay AL, Bromley LA. Thermal conductivity of gas mixtures. Ind Eng Chem 1950;42:1508–1511.

12. Ellenwood FO, Kulik N, Gay NR. The specific heat of certain gases over wide ranges of pressures and temperatures. Cornell Univ Eng Exp Station 1942; Bulletin 30.
13. Comings EW, Egly RS. Viscosity of gases and vapours. Ind Eng Chem 1940;32:714–718.
14. Wilcock SE, Flook V. Environmental and body temperatures of 52 divers in hyperbaric heliox. Undersea Biomed Res 1980, 7(3): 225–239.

PART VI

MOLECULAR AND CELLULAR EFFECTS OF HYDROSTATIC PRESSURE

MOLECULAR AND CELLULAR EFFECTS OF HYDROSTATIC PRESSURE; A PHYSIOLOGIST'S VIEW

A. G. Macdonald

Our understanding of how hydrostatic pressure affects cells is advancing rapidly in some areas but not at all in others. Scattered along a very broad and erratically advancing front there are scenes of activity and progress which contrast with pockets of dormancy. The purpose of this paper is to outline the field in a way which makes sense to the nonspecialist and which might also stimulate further activity from the specialists.

An important long-term objective is the understanding of the stress which hydrostatic pressure imposes on the working diver, and allied to that is an appreciation of the stress which underwater animals in general sustain in their environment. The field necessarily entails the challenge of understanding the thermodynamics and kinetics of complex physiological reactions under pressure. This symposium should encourage us in our specialized interests and will also provide us with an opportunity to reflect on the wider significance of pressure physiology in contemporary biology generally, as well as its special role in the technology of human diving.

The paper begins with some observations on the structure and functions of cell membranes under pressure and then turns to some whole-cell functions. The second part deals with general questions, common to many fields of research, which will attempt to put our knowledge of hydrostatic pressure physiology in perspective.

Pressure over the range of several hundred atmospheres reduces the motional freedom of the fatty acid hydrocarbon chains within the bilayer structures of both artificial and natural membranes (1–3). It therefore resembles low

temperature in this respect. Both spectroscopic and thermodynamic techniques demonstrate that pressure favors an ordered gel state in artificial bilayers and it opposes the thermally driven endothermic phase transition, increasing the temperature required for the transition by an amount given by $\dfrac{dT}{dP} = \dfrac{\Delta VT}{\Delta H}$ (4–7). The direct ordering effect of pressure on bilayer structure may not be very drastic in the living cell, since the more important functions of membranes are not carried out by the bilayer as such. However, the indirect effects of an ordered bilayer may be highly significant. The normal functioning of membrane-bound enzymes, ion channels, and other functional units is, to varying degrees, thought to be dependent on the state of the bilayer. This phenomenon is a focal point of much membrane research, a recent and typical example being the demonstration that the activity of the Na-K-ATPase in a cultured mammalian cell is a direct function of the motional freedom of the acyl groups comprising the membrane in which the enzyme is located (8).

Pressure may also affect gross membrane organization and thereby function, by directly perturbing the structure and conformation of proteins, although the evidence that this actually happens is indirect and limited to the human erythrocyte, a rather unusual case (9). Pressure disturbs one of the main functions of plasma membranes, namely, the ionic regulation of cells and tissues, although the extent to which bilayer ordering is responsible is not yet clear in any one example (10).

In two cases, the fish gill epithelium and human erythrocytes, the passive permeability to Na^+ appears to be increased by moderate (100 atm) pressures (see 11,12,13), but note that the passive movement of ions through an epithelium may entail quite different mechanisms to those by which cations cross cell membranes. Input conductance measurements on pressurized neurones in snail ganglia also imply an increase in the passive permeability of the membrane to ions (14). Recent experiments with human erythrocytes have demonstrated that pressure (100–300 atm) in some way allows the concentration of intracellular sodium to rise but then to level off (13, Fig. 1). Much detail remains to be investigated (15), but the clear implication of this work is that the ionic regulation of the cells in animals or humans is disturbed by diving pressures, and perhaps an increased cation permeability incurs a small additional expenditure of metabolic energy at depth. It is conceivable that some of the neurological effects of pressure are caused, in part, by changes in the steady state intracellular concentrations of ions.

The long overdue investigation of neuronal excitability under pressure is now getting into its stride, yielding fundamental data which are difficult to interpret. Action potentials in such diverse cells as the squid giant axon, neurones in central ganglia in the snail *Helix,* and in the peripheral nervous system of the rat and frog are all slowed by pressures within the 200-atm range (10). The point of interest now shifts to the way pressure effects channel conductance and gating mechanisms (16). The decisive measurements are technically difficult, the molecular targets are still quite obscure, and interpretation of the results will not be easy.

A.

B.
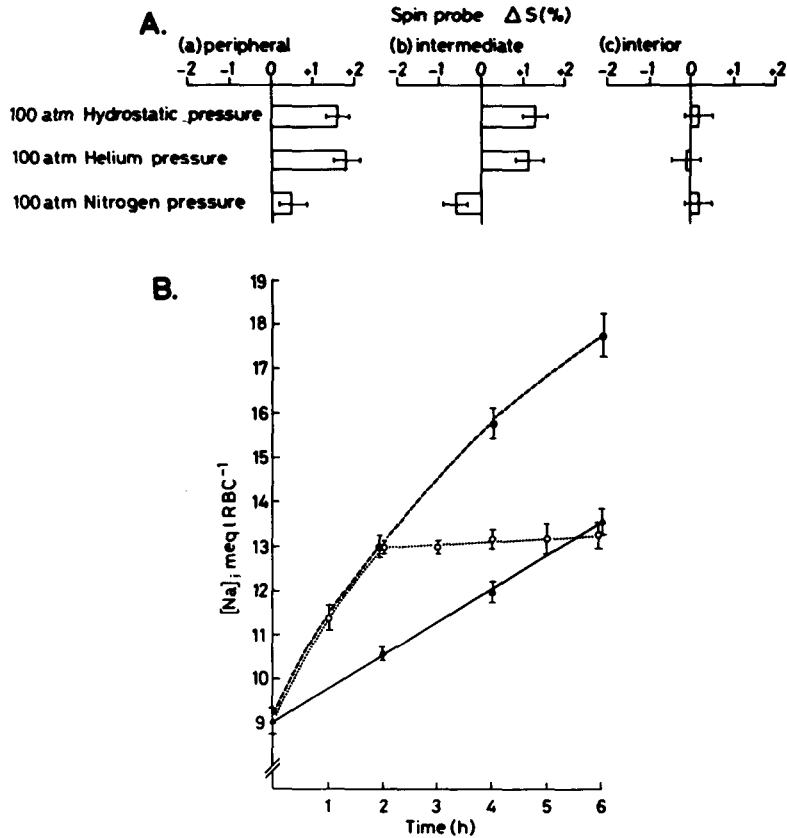
Fig. 1. Some unexpected effects of hydrostatic pressure and gas pressure on the membrane of the human erythrocyte. A. The effect of 100 atm on the order parameter (S) of ESR probes which report on the motion of different regions of the bilayer at 37°C. An increase in S indicates reduced motion, 100 atm N_2 appears to order the peripheral region and both hydrostatic and gas pressure have no effect on the bilayer interior (44). B. Increase in the internal concentration of Na^+ in human erythrocytes at 300 atm, 37°C. The data show that internal sodium increases for 2 h and then remains constant (O) and the Na^+ influx in the presence of $10^{-4}M$ ouabain at 300 atm (●) exceeds that occurring in ouabain-treated cells at atmospheric pressure (▲) (13).

The physiology of synapses under pressure has considerable importance in our eventual understanding of how pressure affects the activity of the integrated organism, and the hyperexcitable and other symptoms in human divers in particular. Although spontaneous action potentials have been reported in pressurized crustacean axons, and could conceivably be a means by which integrated functions are upset by pressure, most workers would probably envisage a major role for synapses in the origin of the high pressure nervous syndrome. Synapses are complex; their function involves membrane properties, "interior" cellular processes, and metabolic pathways. Isolated synaptic preparations are rewarding targets for electrophysiological pressure experiments, especially as some appear to be sensitive to pressures of less than 50 atm

(14,17–21). Pharmacological and biochemical methods may also be used to measure the response of receptors to transmitters at high pressure (22,23).

In synapse physiology under pressure, as in other fields, the inquiry is often a two-stage process. First, a detailed electrophysiological study of specific preparations is required, and is beginning with the squid giant synapse (18), the rat superior cervical ganglion (19), and the motor end plate in the frog (21). Generally, synaptic transmission is inhibited by pressure and both pre- and postsynaptic sites are implicated. It is an entirely different problem, however, to study the precise mechanism by which pressure acts in these synapses. Very detailed knowledge at both physiological and molecular levels is required to identify the direct effects of pressure on complex cells such as these. The classical approaches of describing pre- and postsynaptic effects and of conducting binding studies is an essential stage in the inquiry, and much remains to be understood at that level.

The cell interior is the environment which supports "soluble" enzyme chemistry and complex processes such as the highly structured chemistry of contraction and other types of motility, some of which are involved in synaptic function. Interestingly, research into muscular contraction under pressure is now nearly dormant whereas once it was an active field (20,24,25). Considerable progress is being made in understanding how enzymes respond to high pressure, a significant problem in deep sea biology no less than deep diving physiology (26). Pressure acts by disturbing enzyme-substrate or ligand equilibria, and inhibition is no more likely an effect of pressure than stimulation of enzyme activity.

Another major aspect of cell organization to be considered is inheritance, gene expression, and differentiation. It has been remarked that the peculiarly stable nature of DNA and the way moderate pressures act on molecules in solution leads to no interaction of interest between the two. However, the dynamic aspects of macromolecular synthesis are sensitive to pressure, and in human diving the whole question of the reversibility or otherwise of pressure symptoms has to be considered as thoroughly as possible. In the complex machinery of protein synthesis a variety of sites have been shown to be susceptible to several hundred atmospheres pressure (27). Genetic effects of pressure have so far only been demonstrated in microorganisms subjected to similarly high pressures (28). Viruses are favorable systems for study, and of intrinsic importance (29).

Knowledge of hydrostatic pressure physiology is reaching a state which encourages a forward-looking, predictive outlook which entails problems which are common to many fields of biological research. First, there is the difficulty of projecting conclusions from in vitro experiments to the whole organism, particularly the human diver. The details of reaction conditions, in particular the rate-determining step, are critical in determining how pressure affects a given reaction. In view of the "adaptive" changes which appear in the ionic regulation of erythrocytes under pressure it is clear that new steady state levels of critically important ions and other regulating molecules may be found in pressurized tissues in vivo (Fig. 1). One wonders how confident we should be

of predicting how cells in vivo will actually behave under pressure, a point which includes both the metabolic and the excitable behavior of cells (30).

A second, apparently easier problem of prediction is confined to the effects of pressure in single reactions in vitro. It is surely a sign of maturity in a field of research that testable predictions become more realistic and a theoretical approach to the subject emerges. Although certain molecular interactions are known to be particularly sensitive to pressure (such as ionization and hydrophobic interactions [31–33]), it is generally difficult (that is, impossible!) to predict the pressure-sensitivity of a given physiological process. The reason is that even if the presence of pressure-labile molecular targets are known their contribution will be obscured by a multitude of other unknown intervening factors. Nevertheless, with sufficient knowledge of simple systems it ought to be possible to predict their sensitivity to pressure, and in at least one case this has happened recently.

Much of the cell's biochemical activity, including ionic regulation, is carried out by membrane-bound enzymes, and, as already mentioned, the activity of these enzymes is often determined by the state of their surrounding bilayer lipids. The effect of membrane lipids on enzyme activity is manifest in Arrhenius plots which show a break at a characteristic temperature, sometimes thought to be the temperature at which the lipids undergo a phase transition. It was accordingly predicted that such enzymes would respond to high pressure with an increase in the temperature at which the break in the Arrhenius plot occurs. Independent studies have demonstrated that membrane-bound ATPases do in fact respond to pressure in this way, and there is some agreement between the dT/dP for the Arrhenius break point and typical dT/dP values for the phase transition temperature of membrane lipids (about $0.02°C$ atm^{-1} (34–36).

So simple is this prediction that some may argue that it has little significance, while others may question the success of the quantitative agreement between prediction and result. Another reservation is that although the thermodynamics of phase transition and break point phenomena may be fairly well understood, the kinetic aspects are not at all resolved. We do not know if a break point in an Arrhenius plot is shifted by high pressure to a higher temperature because of transition behavior in the enzyme's boundary lipid, or because lateral phase separation takes place, causing the enzyme to come under the influence of other interactions, or for other reasons.

The behavior of enzymes and other proteins such as ion channels and receptors in a lipid membrane phase at high pressure is a major problem. Much of our knowledge of how pressure affects proteins comes from experiments in aqueous solution, in which changes in hydration (either ionic or hydrophobic effects) cause volume changes and thereby determine the pressure-sensitivity of the molecule. What happens to proteins which are immersed in a heterogeneous lipid bilayer and compressed? Does the solvent lipid exert a dominant effect on the mobility and conformation of the protein? Does boundary lipid behave like solvent lipid or does it behave as part of an integral lipoprotein complex? Is there sufficient water of hydration within the membrane to enable the protein to respond as if it were in aqueous solution? These questions are

relevant to the kinetics of the action potential, the functioning of synapses, and the activity of many membrane-bound enzymes. In short, our thinking of how pressure affects physiological processes has to shift from the descriptive and thermodynamic to the detailed mechanistic level already achieved in the study of the kinetics of soluble enzymes.

A third general issue is specificity of action. In the integrated physiology of a cell it is often difficult to pin-point the site of action of a disturbance. Hydrostatic pressure, like other thermodynamic intensity parameters, is potentially capable of affecting many different sites, a problem mentioned in the case of synapses. Hydrostatic pressure can cause pH changes and alter the activity of solutes. It decreases the solubility coefficient of gases dissolved in water thereby increasing their activity slightly (37,38). The case of hyperbaric gases is more complicated. The solubility of oxygen in water exposed to high pressure oxyhelium corresponds to Henry's Law by virtue of a compensating shift in the fugacity of oxygen (39). The comparable effect in hydrophobic solvents in this respect are unknown.

Here, the specificity problem is illustrated by the case of pressure-labile microtubules in dividing cells, which have been studied for many years. It is well known that pressure, in the region of 200 atm depolymerizes various microtubules, of which the mitotic apparatus microtubules are the best understood (40). Pressure shifts the monomer = polymer equilibrium to the left, and apart from kinetic complications concerning nucleation steps it appears that pressure interferes with the interaction between tubulin subunits. However, in view of the way in which certain tubulin polymerization reactions are regulated by Ca^{++} and by a calcium-binding protein, it is conceivable that pressure acts on these regulators and not on the tubulin molecules themselves. The pressure-sensitivity of Ca^{++}-protein binding protein and other sequestering systems is important to know, not only in the case of microtubule assembly, but in synapses and in other cells. As with enzymes under pressure the physiological target which the experimenter has in mind may not be the sole one on which pressure acts directly.

In practical diving physiology we are always concerned with high partial pressures of inert gas, in conjunction with hydrostatic pressure. It has hitherto been acceptable to regard inert gases as extremely weak general anesthetics and in so far as they exert a bilayer-fluidizing effect and offset the ordering effect of hydrostatic pressure (41,42) this is reasonable. However, experiments with nitrogen have revealed results which should caution us. First, hyperbaric N_2 applied to multilamellar phospholipid liposomes increases the transition temperature by $0.006°C$ atm^{-1} demonstrating that hyperbaric N_2 favors the existence of a gel state bilayer, contrary to what various theories of inert gas narcosis would have predicted (43). Secondly, spin-labeled erythrocyte membranes subjected to hyperbaric (100 atm) N_2 reveal complex changes in the motional freedom of the bilayer which are also inconsistent with expectations (44, Fig. 1).

From all that we know of the diverse ways by which pressure perturbs the normal functioning of excitable membranes, synapses, and cells in general, we

would anticipate the central nervous system of an integrated organism would be stressed by pressure in various ways. And indeed this view is confirmed by the neurophysiological and behavioral effects seen under pressure. But we would not expect the symptoms to share a common primary mechanism, susceptible of a "single cure." It is therefore remarkable that addition of inert gas to the breathing mixture used by men in deep simulated dives apparently alleviates many of the symptoms caused by hydrostatic pressure. Our knowledge of the effects of pressure on isolated cells is meager enough but our knowledge of how pressure affects cells within the integrated organism is virtually nonexistent.

References

1. Trudell JR, Hubbell WL, Cohen EN. Pressure reversal of inhalation anaesthetic-induced disorder in spin labelled phospholipid vesicles. Biochim Biophys Acta 1973;291:328–334.
2. Stamatoff J, Guillon D, Powers L, Cladis P, Aadsen D. X-ray diffraction measurements of dipalmitoyl phosphatidylcholine as a function of pressure. Biochem Biophys Res Commun 1978;85:724–728.
3. Gause EM, Mendez VM, Rowlands JR. A spin label study of the effects of hydrostatic pressure and temperature on cellular lipids. Spectrosc Lett 1974;7:477–490.
4. Liu N, Kay RL. Redetermination of the pressure dependence of the lipid bilayer phase transition. Biochemistry 1977;16:3484–3486.
5. Macdonald AG. A dilatometric investigation of the effects of general anaesthetics, alcohols, and hydrostatic pressure on the phase transition in smectic mesophases of dipalmitoyl phosphatidylcholine. Biochim Biophys Acta 1978;507:26–37.
6. Mountcastle DB, Biltonen RL, Halsey MJ. Effect of anaesthetics and pressure on the thermotropic behaviour of multilamellar dipalmitoyl phosphatidylcholine liposomes. Proc Natl Acad Sci 1978;75:4906–4910.
7. Kamaya M, Ueda I, Moore P, Eyring H. Antagonism between high pressure and anaesthetics in the thermal phase-transition of dipalmitoyl phosphatidylcholine bilayer. Biochim Biophys Acta 1979;550:131–137.
8. Sinensky M, Pinkerton F, Sutherland E, Simon F. Rate limitation of $(N^+ + K^+)$-stimulated adenosine triphosphatase by membrane acyl chain ordering. Proc Natl Acad Sci 1979;76:4893–4897.
9. Hall AC, Macdonald AG. The effects of hydrostatic pressure on the osmotic fragility of erythrocytes and their protection by pentanol. J Physiol 1979;295:42–43P.
10. Wann KT, Macdonald AG. The effects of pressure on excitable cells. Comp Biochem Physiol 1980;66a:1–12.
11. Pequeux AJR. Effects of high hydrostatic pressures on Na^+ transports across isolated gill epithelium of sea water acclimated eels *Anguilla anguilla*. In: Bachrach AJ, Matzen MM, eds. Underwater physiology VII. Proceedings of the seventh symposium on underwater physiology. Bethesda, MD: Undersea Medical Society, 1981:601–609.
12. Brouha A, Pequeux A, Schoffeniels E, Disteche A. The effects of high hydrostatic pressure on the permeability characteristics of the isolated frog skin. Biochim Biophys Acta 1970;219:455–462.
13. Hall AC, Macdonald AG. Hydrostatic pressure alters the sodium content of erythrocytes. J Physiol (in press).
14. Wann KT, Macdonald AG, Harper AA. The effects of high hydrostatic pressure on the electrical characteristics of *Helix* neurones. Comp Biochem Physiol 1979;64A:149–159.
15. Goldinger JM, Kang BS, Morin RA, Paganelli CV, Hong SK. Effect of hydrostatic pressure on active transport, metabolism, and the Donnan equilibrium in human erythrocytes. In: Bachrach AJ, Matzen MM, eds. Underwater physiology VII. Proceedings of the seventh symposium on underwater physiology. Bethesda, MD: Undersea Medical Society, 1981:589–599.
16. Shrivastav BB, Parmentier JL, Bennett PB. A quantitative description of pressure-induced alterations in ionic channels of the squid giant axon. In: Bachrach AJ, Matzen MM, eds. Underwater physiology VII. Proceedings of the seventh symposium on underwater physiology. Bethesda, MD: Undersea Medical Society, 1981:611–619.

17. Akers TK, Carlson LC. The change in smooth muscle receptor coupling of acetylcholine and norepinephrine at high pressure. In: Lambertsen CJ, ed. Underwater physiology V. Proceedings of the fifth symposium on underwater physiology. Bethesda, MD: Federation of American Societies for Experimental Biology, 1976:587–593.

18. Henderson JV, Lowenhaupt MT, Gilbert DL. Helium pressure alteration of function in squid giant synapse. Undersea Biomed Res 1977;4:19–26.

19. Kendig JJ, Trudell JR, Cohen EN. Effects of pressure and anesthetics on conduction and transmission. J Pharm Exp Therapeutics 1975;195:216–224.

20. Kendig JJ, Cohen EN. Neuromuscular function at hyperbaric pressures: pressure-anesthetic interactions. Am J Physiol 1976;230:1244–1249.

21. Ashford MLJ, Macdonald AG, Wann KT. Moderate hydrostatic pressures reduce spontaneous release of transmitter in frog. J Physiol 1979;292:44P.

22. Sauter JF, Braswell L, Wankowicz P, Miller KW. The effects of high pressures of inert gases on cholinergic receptor binding and function. In: Bachrach AJ, Matzen MM. Underwater physiology VII. Proceedings of the seventh symposium on underwater physiology. Bethesda, MD: Undersea Medical Society, 1981:629–637.

23. Hochachka PW. Temperature and pressure adaptations of the binding site of acetylcholinesterase. Biochem J 1974;143:535–539.

24. Brown DES. Temperature-pressure relation in muscular contraction. In: Johnson FH, ed. Influence of temperature on biological systems. Washington, DC: American Physiological Society, 1957:83–110.

25. McWhirter J. The effect of helium pressure on guinea-pig isolated tracheal smooth muscle. J Physiol 1979;295:28–29P.

26. Low PS, Somers GN. Pressure effects on enzyme structure in vitro and under simulated in vivo conditions. Comp Biochem Physiol 1975;52B:67–74.

27. Pope DH, Connors NT, Landau JV. Stability of *Escherichia coli* polysomes at high hydrostatic pressure. J Bacteriol 1975;121:753–758.

28. Rosin MP, Zimmerman AM. The induction of cytoplasmic petite mutants of *Saccharomyces cerevisive* by hydrostatic pressure. J Cell Sci 1977;26:373–385.

29. Chastel C, Barthelemy L, Belaud A. Effects of hyperbaric conditions on the multiplication of Echo 11 and herpes simplex (type 1 and type 2) viruses in tissue culture. In: Bachrach AJ, Matzen MM, eds. Underwater physiology VII. Proceedings of the seventh symposium on underwater physiology. Bethesda, MD: Undersea Medical Society, 1981:577–588.

30. Wann KT, Macdonald AG, Harper AA, Ashford MLJ. Transient versus steady-state effects of high hydrostatic pressure. In: Bachrach AJ, Matzen MM, eds. Underwater physiology VII. Proceedings of the seventh symposium on underwater physiology. Bethesda, MD: Undersea Medical Society, 1981:621–627.

31 Bøje L, Huidt A. Volume effects in aqueous solutions of macromolecules containing non-polar groups. Biopolymers 1972;11:2357–2384.

32. Nemethy G, Scheraga HA. The structure of water and hydrophobic bonding in proteins. III. The thermodynamic properties of hydrophobic bonds in proteins. J Phys Chem 1962;66:1773–1789.

33. Neuman RC, Kauzmann W, Zipp A. Pressure dependence of weak acid ionization in aqueous buffers. J Phys Chem 1973;77:2687–2691.

34. De Smedt H, Borghgraef R, Ceuterick F, Heremans K. Pressure effects on lipid-protein interactions in $(Na^+ + K^+)$-ATPase. Biochim Biophys Acta 1979;556:479–489.

35. Ceuterick F, Peeters J, Heremans K, De Smedt H, Olbrechts H. Effect of high pressure, detergents, and phospholipase on the break in the Arrhenius plot of *Azotobacter* nitrogenase. Eur J Biochem 1978;87:401–407.

36. Macdonald AG, MacNaughtan W. The effect of high hydrostatic pressure on the membrane-bound ATPase of *Acholeplasma laidlawii* B. J Physiol 1979;296:105–106P.

37. Enns T, Scholander PF, Bradstreet ED. Effects of hydrostatic pressure on gases dissolved in water. J Phys Chem 1965;69:389–391.

38. Taylor CD. The effects of pressure upon the solubility of oxygen in water. Arch Biochem Biophys 1978;191:375–384.

39. Taylor CD. Solubility of oxygen in a seawater medium in equilibrium with a high-pressure oxy-helium atmosphere. Undersea Biomed Res 1979;6:147–154.

40. Salmon ED. Pressure-induced depolymerization of spindle microtubules II. Thermodynamics of in vivo spindle assembly. J Cell Biol 1975;66:114–127.

41. Chin JH, Trudell JR, Cohen EN. The compression-ordering and solubility disordering effects of high pressure gases on phospholipid bilayers. Life Sci 1976;18:489–498.

42. Mastrangelo CJ, Trudell JR, Cohen EN. Antagonism of membrane compression effects by high pressure gas mixtures in a phospholipid bilayer system. Life Sci 1978;22:239–244.

43. MacNaughtan W, Macdonald AG. Effects of gaseous anesthetics and inert gases on the phase transition in smectic mesophases of dipalmitoyl phosphatidyl choline. Biochim Biophys Acta (in press).

44. Finch ED, Kiesow LA. Pressure, anesthetics, and membrane structure: a spin probe study. Undersea Biomed Res 1979;6:41–45.

EFFECTS OF HYPERBARIC CONDITIONS ON THE MULTIPLICATION OF ECHO 11 AND HERPES SIMPLEX (TYPE 1 AND TYPE 2) VIRUSES IN TISSUE CULTURE

C. Chastel, L. Barthélémy, and A. Belaud

Previous observations led to the assumption that "per se" hydrostatic pressure or hyperbaric inert gases, or both, bring about biological effects by an impact on certain molecular structures. We tried to verify this hypothesis by using simple biological models: 1) a Picornavirus (Echo 11), one of the smallest and simplest RNA viruses; and 2) a more complex DNA virus (Herpes simplex virus, HSV_1 and HSV_2).

MATERIALS AND METHODS

Preliminary Experimentation

Preliminary work investigated per se hydrostatic pressure and the effects of hyperbaric partial pressures of the inert gases helium and nitrogen on cell cultures usually used in virology. Experimentation was carried out on WI 38 human diploid cells, primary Vervet monkey kidney cells, and cancerous HeLa cells (from BioMérieux, Marcy l'Etoile, France). These cells, cultivated by standard methods, were used when a layer of tissue culture was confluent. Eagle's medium containing 2% calf serum was used for each of these cells. Density was 2.10^5 cells for each mL of medium.

To investigate per se hydrostatic pressure action, we completely filled glass tubes (17.5 mL) with Eagle's medium; these tubes were closed at the

neck by a gas-tight flexible membrane, which allowed transmission of surrounding hydrostatic pressure to the enclosed liquid.

To investigate inert gas hyperbaric pressure actions, we partially filled glass tubes with the medium, which was separated from the hyperbaric atmosphere only by a sterile gauze to avoid contamination.

For every type of experimentation (per se hydrostatic pressure [P_H] or pressure saturated by the inert gases nitrogen [P_{N_2}], helium [P_{He}]), two tubes were taken as many times as there were different cells (WI 38, Vervet monkey kidney, HeLa): a total of 6 tubes.

Tubes were put in two 10-L hyperbaric chambers, supplied with compressed gases (N_2, He). The top of each hyperbaric chamber had a Plexiglas porthole; a tight passage for electric cables allowed temperature and pressure control within the chamber. The hyperbaric chambers were placed in a thermostated room. Temperature within the chamber was checked without interruption by electronic thermometers. Speed of compression was constant at the rate of 1 ATA · min^{-1}. Exposure duration was always 24 h.

Experimentation with Echo 11 Virus

Echo 11 virus cultivated on Vervet monkey kidney cells was investigated according to these procedures: The tubes containing tissue cultures were emptied of their medium and inoculated with 100 (50% cytotoxic) infectious doses (DITC 50) of Echo 11 virus (stock 35.11.115 from WHO Collaborating Center for Virus Reference and Research, Lyon, Pr M. Aymard). Each tube contained approximately 4.10^5 living cells (confluent layer).

Temperature was held at 36°C. After 1 h contact, the virus was discarded and, after rinsing, the cell contents of the tubes were completed with Eagle's medium.

Check samples were prepared identically and at the same time as the samples to be submitted to pressure; they were put in the thermostated chamber and kept under atmospheric pressure.

Hyperbaric conditions were the same as described above for the preliminary experimentation. Hyperbaric exposure duration was always 24 h. Four temperatures were investigated (26, 30, 33, and 36°C).

After decompression, the yield of virus was estimated by titration: first, on supernatant (except the P_H case); and second, on cells collected by scraping. We used decimal dilutions of supernatant or collected cells, or both, to inoculate Vervet monkey kidney cells at 36°C. Each of the dilutions (from 10^{-1} to 10^{-8}) was used to inoculate five test tubes. We estimated virus titration on the eighth day after inoculation, by looking for the cytopathogenic effect of Echo 11 virus. The DITC 50 was calculated by the Reed and Muench Method (1).

Multiplication curves were not established because it was impossible to take samples at regular time intervals from tubes placed in hyperbaric chambers. For this reason we chose to evaluate the global infectious yield of virus

obtained within 24 h under different experimental conditions, in comparison with infected check samples kept under barometric pressure.

Experimentation With Herpes Simplex Virus

Primary Vervet monkey cells, inoculated with 1000 DITC 50 of HSV_1 or HSV_2, (HSV_1, strain 10711; HSV_2, strain Bryan B'Mam, from WHO Center, Lyon, Pr M. Aymard) were submitted to per se hydrostatic pressure or inert gas pressure of 61, 51, 31, and 21 ATA, at a temperature of 36°C. The infectious yield of virus was estimated 48 h after decompression by virus titration as indicated previously. We carried out electron microscopy examinations to look for possible changes in cell and virus morphology and virus morphogenesis.

RESULTS

Preliminary Experimentation

Results including microscopic examination of cells and supernatant were evaluated according to the aspect of the layer of tissue culture obtained after 6 days of subculture in 20% of calf-serum Eagle's medium. Experimental conditions did not show alteration on WI 38 and HeLa cells either in morphology or in reproduction ability.

No modification was established on monkey kidney cells. Electron microscopy showed that any uninfected monkey kidney cells that had been submitted to pressure action had notable ultrastructural damage.

In particular, nucleus, cytoplasm, various organellae (mitochondria, for example), and membranes appeared to be normal. Because Echo 11 virus prefers to develop in simian cells, monkey kidney cells were chosen for hyperbaric experimentations.

Experimentation with Echo 11 Virus

Work on Vervet monkey cells infected by Echo 11 virus showed that whatever the applied hyperbaric conditions, the yield of virus is smallest for test tubes submitted to pressure compared to test tubes kept under the same conditions of temperature but under barometrical pressure (Table I). A linear relation can be established between the logarithm of virus titer (*log TV*) and the inverse ratio of absolute temperature to experiment (*log TV* $= f \frac{1}{T}$) (see Fig. 1a and 1b).

Experimentation with Herpes Simplex Virus

As for the Echo 11 virus, the yield of Herpes simplex virus obtained 48 h after decompression decreased in comparison to the control cultures. But contrary to the experiments on the Echo 11 virus, the inhibition of virus synthesis

TABLE I

Echo 11 Virus: Titration After an Hyperbaric Exposure Under Specified Conditions*

Pressure Conditions	51 ATA				31 ATA				21 ATA				11 ATA			
	C	HP	N_2	He	C	HP	N_2	He	C	HP	N_2	He	C	HP	N_2	He
36°C	$10^{3.3}$	$10^{4.0}$	$10^{4.7}$	$10^{3.5}$	$10^{4.8}$	$10^{4.4}$	$10^{4.0}$	$10^{3.2}$	$10^{3.5}$	$10^{2.7}$	$10^{3.5}$	$<10^{1}$	$10^{3.5}$	$10^{3.3}$	$10^{1.3}$	$10^{3.7}$
33°C	$10^{2.3}$	$10^{2.5}$	$10^{1.8}$	$<10^{1}$	$10^{3.3}$	$10^{3.4}$	$10^{3.5}$	$10^{2.5}$	$10^{3.2}$	$10^{4.3}$	$10^{3.0}$	$10^{3.5}$	$10^{4.0}$	$10^{2.5}$	$10^{3.7}$	$10^{2.5}$
30°C	$10^{3.6}$	$10^{2.2}$	$10^{2.6}$	$10^{2.5}$	$10^{4.0}$	$10^{2.2}$	$10^{2.5}$	$10^{2.5}$	$10^{2.3}$	10	$<10^{1}$	$10^{1.5}$	$10^{3.6}$	$10^{1.5}$	$10^{2.7}$	$10^{1.2}$

*C is control under barometric pressure; HP is per se hydrostatic pressure; N_2 is nitrogen pressure; He is helium pressure. Each of the hyperbaric conditions decreases the virus yield relative to control.
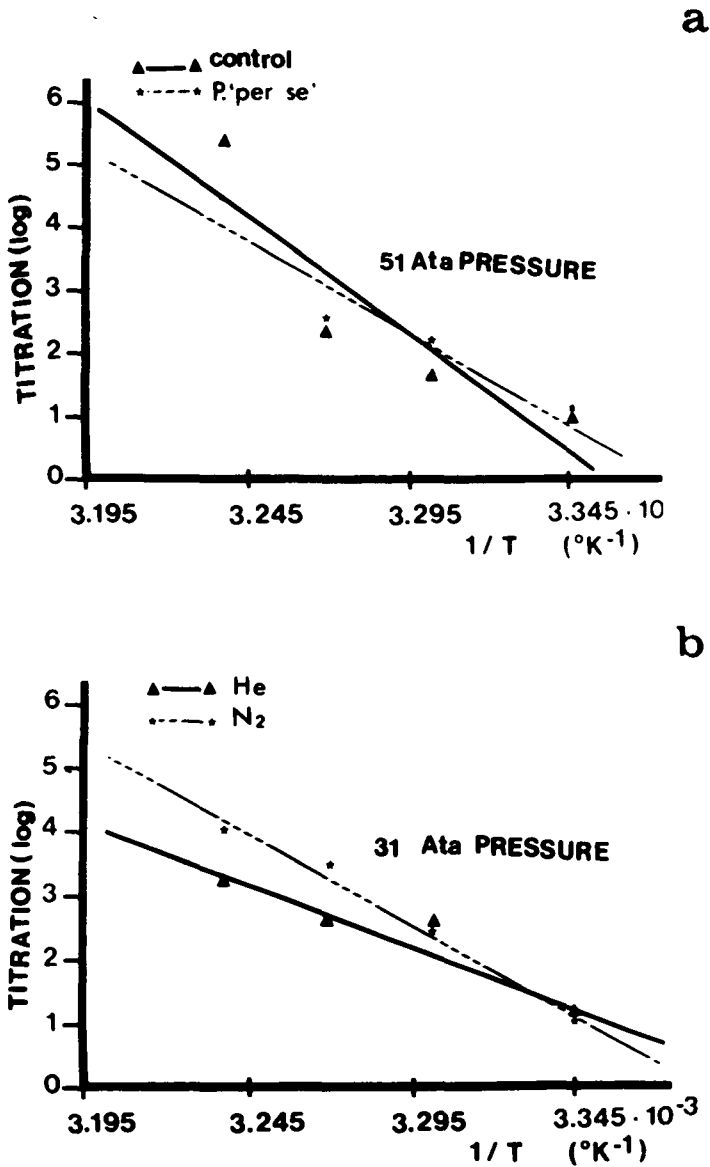
Fig. 1. Study of the regression of the Echo 11 virus yields logarithm onto inverse ratio of absolute temperature of experiment. Differences of slope and ordinate at the origin show the effects of pressure (hydrostatic pressure, inert gas partial pressures) on virus multiplication.

a. Linear relation of regression, showing 51 ATA per se hydrostatic pressure, is compared with that which shows the effects of barometric pressure (1 atm) under the same conditions of temperature (control). Linear regression equations are: *For control* (1 atm): $Y = 124.3\text{-}37.0\ X$; $r = 0.89$; $F = 7.9$.   *For 51 ATA per se pressure:* $Y = 97.4\text{-}28.9\ X$; $r = 0.96$; $F = 21.8$.

b. Experimental conditions reproduce the effects of nitrogen and helium hyperbaric partial pressures (31 ATA). Linear regression equations are: *For helium:* $Y = 65.1\text{-}19.1\ X$; $r = 0.95$; $F = 17.5$.   *For nitrogen:* $Y = 95.8\text{-}28.3\ X$; $r = 0.99$; $F = 92.9$.

was more significant under nitrogen or helium pressures than under the corresponding per se hydrostatic pressure (Table II). Moreover, maximum inhibition of virus synthesis was observed for 21 ATA pressure of nitrogen or helium (Table II).

Electron microscopy studies. The electron microscopy studies showed that the morphology and the morphogenesis of both HSV$_1$ and HSV$_2$ appeared normal for the hyperbaric condition under investigation: nitrogen, helium, or per se hydrostatic pressure. However, the results differed depending upon the type of HSV.

Electron microscopy study: HSV$_1$ multiplication. Because of the high titer of HSV$_1$ reached in infected cells under barometric pressure, the comparison between the morphological events of viral multiplication in these nonexposed cells and in exposed cells was easy.

In cells exposed to per se hydrostatic pressure, the number of cells exhibiting virus particles was the same as that for nonexposed cells. No obvious alteration of the virogenesis was found, including the envelopment of virus particles (Fig. 2a).

In cells exposed to N$_2$, the infected cells were reduced in number but the morphology and the morphogenesis of virus were apparently normal (Fig. 2b). On the other hand, in cells exposed to helium, both normal and atypical forms of virus were encountered. Synthesis of nucleocapsids (Fig. 2c) and envelopment (Fig. 3a) appeared quite normal, and a number of osmiophilic matrix containing atypical virus particles and covered by the same membrane occurred in the cytoplasm of infected cells (Fig. 3b). In addition, aberrant, giant, or irregular particles and duplicated membranous structures were found in the cytoplasm (Fig. 3c).

Electron microscopy study: HSV$_2$ multiplication. The relatively low titers exhibited by HSV$_2$ in nonexposed cells makes difficult the search for virus particles and the study of virogenesis in exposed cells: infected cells were rarely encountered and virus particles were never abundant here. As for HSV$_1$ multiplication, both normal morphological events and abnormal ones were seen after the different exposures.

Tubular structures, recently reviewed by Oda and Mori (2) and highly characteristic for HSV$_2$ replication, were seen in the nucleus of infected cells. Abnormal, giant virus particles and membrane duplication were seen mainly after nitrogen exposure.

DISCUSSION

We do not know of previous investigation of the effects of hydrostatic pressure or hyperbaric gas pressure on virus development, except for the study of a case of mumps during hyperbaric exposure by Danziger et al. (3) and a previous work in our laboratory by Chastel et al. (4).

TABLE II

Herpes Simplex Virus (Types 1 and 2): Titration After Hyperbaric Exposures Under Specified Conditions*

Pressure Conditions	61 ATA				51 ATA				31 ATA				21 ATA			
	C	HP	N_2	He	C	HP	N_2	He	C	HP	N_2	He	C	HP	N_2	He
HSV$_1$ 36°C	$10^{6.4}$	$10^{5.6}$	$10^{2.1}$	$10^{5.4}$	$10^{5.6}$	$10^{5.5}$	$10^{4.3}$	$10^{3.4}$	$10^{6.9}$	$10^{5.9}$	$10^{3.7}$	$10^{5.2}$	$10^{6.0}$	$10^{5.4}$	$10^{2.3}$	$10^{1.7}$
HSV$_2$ 36°C	$10^{5.0}$	$10^{2.9}$	$<10^{1}$	$10^{2.9}$	$10^{3.9}$	$10^{3.2}$	$10^{1.9}$	$10^{1.0}$	$10^{3.4}$	$10^{4.2}$	$10^{4.8}$	$10^{3.3}$	$10^{5.2}$	$10^{4.1}$	$<10^{1}$	$<10^{1}$

*C is control under barometric pressure; HP is per se hydrostatic pressure; N_2 is nitrogen pressure; He is helium pressure. The hyperbaric conditions (especially N_2 and He pressures at 21 ATA) decrease the virus yield.
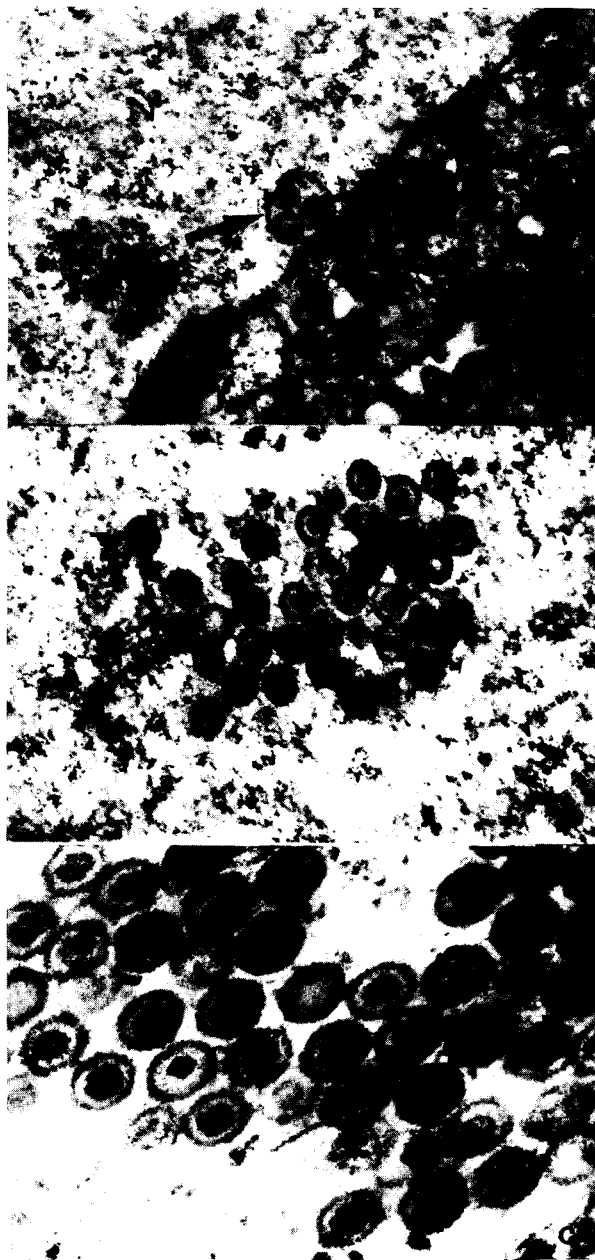
Fig. 2. Electron microscopy study of HSV multiplication.

  a. HSV$_1$-infected cell exposed to per se hydrostatic pressure of 31 ATA for 48 h. Complete virus particles (V) were seen outside the nuclear membrane and a virus particle is in the process of envelopment (arrow) from the inner leaflet of nuclear membrane (N) nucleus. 30 000 X.

  b. Nucleus of HSV$_1$-infected cell exposed to 31 ATA nitrogen for 48 h. Typical aggregate of nucleocapsids with dense or annular cores. 60 000 X.

  c. Nucleus of HSV$_1$-infected cells exposed to 31 ATA helium for 48 h. Accumulation of nucleocapsids exhibiting annular or dense cores. 100 000 X.

Fig. 3. Electron microscopy study of HSV multiplication.
  a. Cytoplasm of HSV$_1$-infected cell exposed to 31 ATA of helium for 48 h. Complete viral particles moving into cisternae of the endoplasmic reticulum. 84 000 X.
  b. Cytoplasm of HSV$_1$-infected cell exposed to 31 ATA of helium for 48 h, showing an osmiophilic matrix containing virus particles and covered by the same membrane.
  c. Cytoplasm of HSV$_1$-infected cell exposed to 31 ATA of helium for 48 h. Complete virus particule (V), aberrant form: viral ? (A) and duplication of membranous structures (arrow). 84 000 X.

On the other hand, some studies have dealt with the effects of P_H, P_{N_2}, P_{He} upon cells, essentially protozoa: Landau and Thibodeau (5) upon *Amoeba proteus;* Kitching (6,7) on *Spirostomum,* a ciliated protozoa; Zimmerman and Zimmerman (8) on *Tetrahymena pyriformis.* These various studies showed that a hydrostatic pressure (from 400 to 680 ATA) involved anomalies and changes in protoplasm consistency or inhibition of cell division, or both. These experimentations were carried out under pressures ranging from 140 to 680 ATA, which cannot be compared with those of the present experiment—purposely limited to pressures imposed upon divers in simulated and real-world dives.

Preliminary experimentation showed that different host cells used for virus development (WI 38, HeLa and monkey kidney primary cells), appeared morphologically undamaged and without obvious ultrastructural modifications. Therefore, in a first analysis, study of the effects of hydrostatic pressure or inert gas (N_2, He) partial pressures, or both, on virus development are proceeding from a direct impairment of the mechanisms of virus multiplication.

With respect to Echo 11 virus, linear curves established between *log TV* and 1/T, allow one to consider that the kinetics of multiplication of a virus in tissue culture obey a law identical to Arrhenius's one about the kinetics of chemical reaction. Arrhenius's model, completed with the Johnson and Eyring (9) model to take into account the actions of hydrostatic pressure upon chemical kinetics, was appropriate to explain the combined effects of both temperature and hydrostatic pressure upon various physiological processes. In accordance with Johnson and Eyring's concept (9), temperature and pressure may act jointly upon Echo 11 virus replication (Fig. 1).

When the experimental results (temperature and pressure combined) are added and when medium values of the yields of virus submitted to pressure are compared with the corresponding control value, it appears that experimental conditions of pressure (P_H, P_{N_2}, P_{He}) decrease virus multiplication in a significant way (Table I). Furthermore, no significant difference appears between the effects of hydrostatic pressure and the actions of the partial pressures of hyperbaric inert gases.

With respect to HSV, it is of interest to note that cytoplasmic osmiophilic matrix found in HSV_1 infected cells exposed to helium, originating probably in the nucleus, were previously described in HSV infection of FL cells by Nii (10). They were also seen with a particular frequency in different types of cells infected by other Herpes group virses, all sharing some degree of oncogenic potential: the Marek's disease virus by Ahmed and Schidlovsky (11); the Lucké frog renal adenocarcinoma virus by Stackpole (12); the *Herpesvirus sylvilagus* by Heine and Hinze (13); the *Herpesvirus saimiri* by Tralka et al. (14); and the *Herpesvirus ateles* by Luetzeler et al (15). Undoubtedly, these atypical findings may reflect some abnormal adaptation of these viruses to the cell. In addition, aberrant virus particles and membrane duplications resembling those we saw in the exposed cells were described by Nii (16) in Varicella-zoster virus infection of VERO cells.

So, in extreme environmental (hyperbaric) conditions, both HSV_1 and HSV_2 can well replicate the exposure to inert gases that leads more frequently

to the appearance of abnormal structures than does per se hydrostatic pressure. These morphological data correlated well with the observed yields of HSV_1 and HSV_2 after the corresponding exposures, as evidenced by virus titrations.

Different hypotheses can be suggested to explain the mechanisms of pressure (hydrostatic or inert gas pressures, or both) actions on virus development:

1) Pressure, as a thermodynamic agent, may modify the kinetics of chemical reactions and, thus, change the course of virus synthesis (replicase, polypeptidase, phosphorylase).

2) Pressure may modify the structure of one or several elements (macromolecules) interfering in one of these chemical reactions (sustratum, enzymes, activated complex . . .).

3) Pressure may also modify a structural compound of the virus: capsid proteins, nucleic acid.

4) Hyperbaric inert gas pressure (N_2, He) modifies the structure of the virus compounds by a specific action, which in some cases antagonizes the specific action of per se hydrostatic pressure. The effects of inert gases may be related to the amount of dissolved gas stored within the virus structures, and their consequent effect on virus development depends upon the complexity of the virus (size, number of macromolecules, presence of an envelope).

5) Another hypothesis deals with the modification of the host-cell during pressurization. If cells appear morphologically undamaged after decompression, nothing will prove that pressure did not involve physiological modification of these cells or a transient synthesis of interferon, reversible after decompression. Pressure effects upon cells can interact only with virus factors to change viral protein synthesis. For example, Landau (17) demonstrated that the synthesis of proteins by HeLa cells is precisely modified by a high hydrostatic pressure. Furthermore, 25 virus-induced proteins were found in cells infected by Picornavirus, and it is possible that many of these can have roles vital for virus replication (18); an influence of hydrostatic or inert gas pressure, or both, on the synthesis of these proteins can be involved.

In addition to an essential biological purpose, this experimentation presents an applied interest: when human dives become longer (several weeks) and deeper (from 400 to 600 m), it will be important to have evaluated the risks induced by viral illness and to have basic knowledge about their evolution under hyperbaric conditions.

References

1. Reed LJ, Muench HA. A simple method of estimating fifty per cent endpoints. Am J Hyg 1938;6:493–497.
2. Oda H. Mori P. Electron microscope observations on tubular structures in cells infected with Herpes Simplex Virus type 2. Arch Virol 1976;50:159–168.
3. Danzinger RE, Sallee TL, Vodin GE, Flynn ET, Alexander JM. Case of mumps during hyperbaric exposures. Aerosp Med 1971;42,12:1335–1337.
4. Chastel C, Barthélémy L, Balouet G. Effets des conditions hyperbares sur l'évolution de la chroioméningite lymphocytaire expérimentale de la souris. Path Biol 1977;25,5:307–313.
5. Landau JV, Thibodeau L. The micromorphology of Amoeba proteus during pressure induced changes in the sol-gel cycle. Exp Cell Res 1962;27:591–594.

6. Kitching JA. Effects of high hydrostatic pressure on the activity and behavior of the ciliate *Spirosto-mum*. J Exp Biol 1969;51;319–324.

7. Kitching JA. Some effects of high pressure on Protozoa. In: Zimmerman AM, ed. High pressure effects on cellular processes. New York: Academic Press, 1970:155–178.

8. Zimmerman SB, Zimmerman AM. Biostructural cytokinetic and biochemical aspects of hydrostatic pressure on Protozoa. In: Zimmerman AM, ed. High pressure effects on cellular processes. New York: Academic Press, 1970:179–210.

9. Johnson FH, Eyring H. The kinetics basis of pressure effects in biology and chemistry. In: Zimmerman AM, ed. High pressure effects on cellular processes. New York: Academic Press, 1970:1–44.

10. Nii S. Electron microscopic observations on FL cells infected with Herpes Simplex Virus. II Envelopment. Biken J 1971;14:325–348.

11. Ahmed M, Schidlovsky G. Electron microscopic localization of herpes virus-type particles in Marek's disease. J Virol 1968;2:1443–1457.

12. Stackpole CW. Herpes type virus of the frog renal adenocarcinoma. J Virol 1969;4:75–93.

13. Heine U, Hinze HC. Morphological studies on *Herpesvirus sylvilagus* in rabbit kidney cell cultures. Cancer Res 1972;32:1340–1350.

14. Tralka TS, Costa J, Rabson A. Electron microscopic study on *Herpesvirus saimiri*. Virology 1977;80:158–165.

15. Luetzeler J, Heine UI, Wendel E, Prasad U, Ablashi DV. Ultrastructural studies on the replication of *Herpesvirus ateles*-73 in owl monkey kidney cells. Arch Virol 1979;60:59–73.

16. Nii S. Aberrant forms of Varicella-zoster virus. Biken J 1973;16:173–176.

17. Landau JV. Hydrostatic pressure inhibition of ribonucleic acid synthesis in HeLa cells. In: Brauer RW, ed. Barobiology and the experimental biology of the deep sea, Chapel Hill, NC: University of North Carolina, 1972:106–114.

18. Sangar DV. The replication of Picornavirus. J Gen Virol 1979;45:1–13.

EFFECT OF HYDROSTATIC PRESSURE ON ACTIVE TRANSPORT, METABOLISM, AND THE DONNAN EQUILIBRIUM IN HUMAN ERYTHROCYTES

J. M. Goldinger, B. S. Kang, R. A. Morin,
C. V. Paganelli, and S. K. Hong

Pressure, in addition to being a thermodynamic state variable, constitutes an important environmental stress for organisms that live in water and for human beings engaged in diving. As such, its effects on membrane transport processes deserve attention both for what they can tell us about transport and for whatever information can be gained about physiological adjustment of animal organisms to life under hydrostatic pressure. The cation content of cells in a medium of fixed osmolality is a major determinant of cell volume. Cation content is in turn set by the relation between passive cation fluxes and the rates of cation pumping (1), which is dependent on the activity of the plasma-membrane-bound Na-K-ATPase found in many cell types, including red blood cells (2). Pressure may act on cell membranes by changing permeability (and thus passive flux), active transport, or both; changes in active transport may occur in response to alteration in Na-K-ATPase activity per se, or by alteration in metabolic supply of substrate in the form of ATP. Pressure may also change the degree of ionization of charged groups on intracellular macromolecules and small molecular weight buffers and so change the Donnan equilibrium across the cell membrane. The studies reported here describe some in vitro effects of hydrostatic pressure on Na^+ and K^+ transport, permeability properties, metabolic state, and Donnan equilibrium of the human red blood cell membrane.

METHODS

Flux and Permeability Measurements

The methods employed in this investigation are described in detail elsewhere (3). Briefly, active and passive Na^+ and K^+ transport were studied at pressures ranging from 1 to 400 ATA. Human erythrocytes were incubated in $^{24}NA^+$ or $^{42}K^+$, washed, and suspended in a tracer-free medium. The suspension was placed in a cylinder with no gas phase. One end of the cylinder consisted of a movable piston and pressure was transmitted to the suspension via this piston during incubation in a hyperbaric chamber. At various times pressure was released and an aliquot of the suspension was sampled. The cells and the medium were separated and the radioactivity appearing in the medium was measured. From the total radioactivity in the suspension and the radioactivity appearing in the medium at known times, the rate constant for sodium or potassium release was computed (3). Active and passive cation movements can be distinguished by measuring fluxes in the presence and absence of ouabain, a cardiotonic steroid that inhibits the Na-K coupled pump.

ATPase Measurements

ATPase activity was measured by chemically determining the amount of phosphate released from ATP by washed erythrocyte membranes (ghosts) during a 10-min incubation in the cylinder described above. Both total hydrolysis and the amount of hydrolysis that occurred in the presence of ouabain were measured. The second measurement yields Mg-ATPase and represents nonspecific ATPase activity of the membranes. The difference between total and Mg-ATPase activity can be attributed to Na-K-ATPase.

Metabolic Measurements

Glycolytic intermediates were determined in neutralized perchloric acid extracts of red cell suspensions after a 2.5-h incubation in the pressure chamber. Adenosine triphosphate, ADP, pyruvate, and lactate were determined by established enzymatic procedures involving stoichiometric oxidation or reduction of a pyridine nucleotide (4). Glucose was determined using glucose oxidase after zinc hydroxide extraction (4). The redox state was calculated according to Williamson et al. (5) from the lactate dehydrogenase equilibrium (3).

Donnan Equilibrium

The Donnan equilibrium was evaluated at pressure by measuring the $^{36}Cl^-$ distribution ratio between cells and medium in an erythrocyte suspension equilibrated at pressures of 1, 30, or 80 ATA. The cell and medium compartments

were separated at pressure using a filtration apparatus described in detail elsewhere (6). After decompression, both suspension and medium $^{36}Cl^-$ contents dre measured by liquid scintillation spectrometry and the Donnan ration calculated according to Reeves (7).

RESULTS

Fluxes and Permeability Measurements

The release of $^{24}Na^+$ from erythrocytes incubated at pressures from 1–400 ATA is shown in Fig. 1. Each sample of cells served as its own control, that is, the release of $^{24}Na^+$ from red blood cells was measured at 1 ATA for periods up to 1.5 h, then pressure was applied and efflux followed for a similar experimental period. In some cases, to test for reversibility, we applied pres-
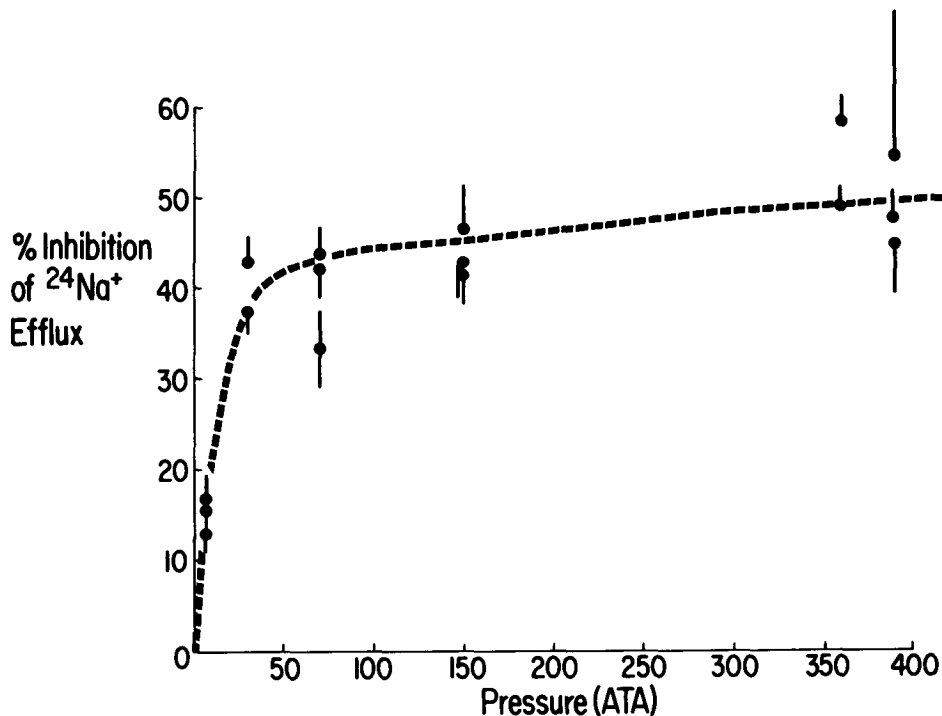
Fig. 1. Inhibition of $^{24}Na^+$ efflux from human erythrocytes as a function of pressure. Percent inhibition was computed as 100 × [1-(rate constant at pressure ÷ control (1 ATA) rate constant)]. Rate constants were determined from experiments described in the text. Individual experiments are shown. Each error bar represents ± 1 SD arising from combining the standard deviations of the rate constants at 1 ATA and pressure according to standard rules for propagation of error. (From Goldinger et al. (3) with permission from J Appl Physiol.)

sure measured $^{24}Na^+$ release, and then released pressure for subsequent flux determination at 1 ATA. Inhibition of $^{24}Na^+$ release from red blood cells was observed at all pressures tested. The relation between inhibition of efflux and pressure is roughly hyperbolic, rising very steeply between 7 and 30 ATA and then reaching a plateau. The effect of pressure was almost completely reversible.

The $^{24}Na^+$ efflux from red blood cells has two components, an active transport component via the sodium pump and a diffusional component. These two components were resolved by following the steady-state efflux of $^{24}Na^+$ in the presence and absence of ouabain both at 1 and 150 ATA. A test pressure of 150 ATA was chosen because it was well within the range of the maximum effect. As shown in Fig. 2, the rate constant $^{o}k_{Na}$ for active (ouabain-sensitive) sodium efflux comprised 74% of the rate constant for total release and was
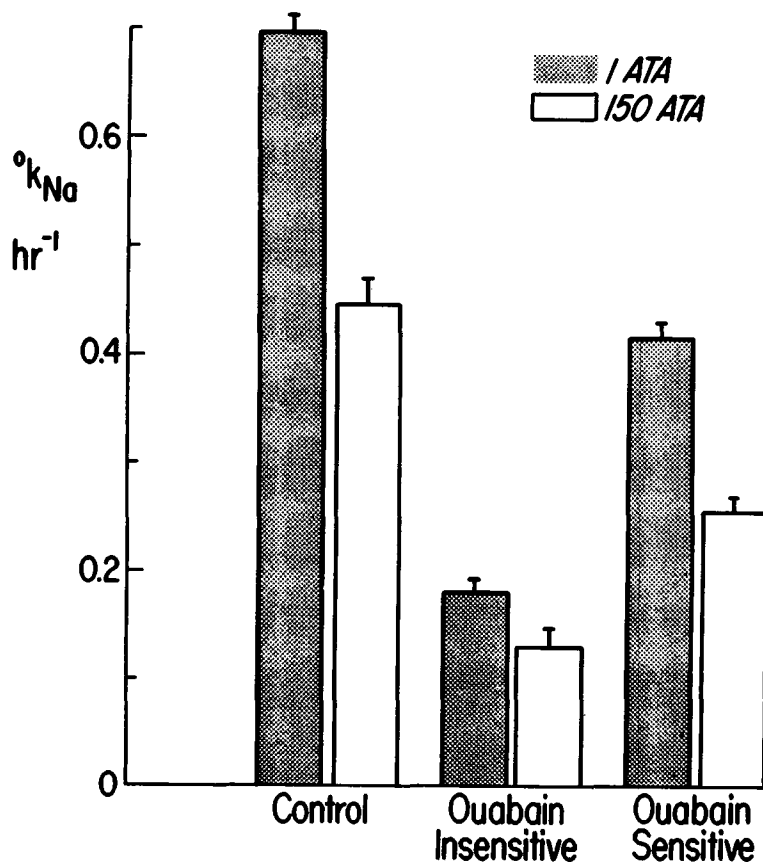
Fig. 2. Rate constants $(^{o}k_{Na})$ for total (control), ouabain-sensitive, and ouabain-insensitive sodium efflux from human erythrocytes at 1 and 150 ATA.   Each bar represents the mean ± SE of 4 experiments. Ouabain concentration was 10^{-4} M.

inhibited 38% by 150 ATA pressure. On the other hand, $°k_{Na}$ for the diffusional (ouabain-insensitive) efflux, which represents a much smaller proportion of the total, was also inhibited 30% by 150 ATA pressures.

Pressure inhibition of sodium efflux was found to be dependent on the internal sodium concentration. When cell sodium concentration was made artificially high (100 mM) or low (2 mM), pressure was found to have no inhibitory effect on $^{24}Na^+$ efflux.

ATPase Measurements

The enzymatic mediator of the sodium pump is widely considered to be the Na-K-ATPase. Na-K-ATPase activity can be differentiated from total ATPase activity by incubation in the presence of ouabain. Table I shows the various components of red cell membrane ATPase activity as a function of applied pressure. Compared to control activity at 1 ATA, pressure had a biphasic effect on the Mg-ATPase activity, first stimulating and then inhibiting. Within the range of pressures tested, however, Na-K-ATPase activity, computed from the difference between the total and Mg-ATPase activity, was stimulated by pressure. This stimulation was unexpected in view of pressure's inhibition of the Na pump in intact cells shown by the ouabain-sensitive $^{24}Na^+$ efflux measurements.

Metabolic Measurements

Active transport in intact cells is subject to many variables, including metabolic dependence. The results of experiments to test the effect of pressure on erythrocyte metabolism are shown in Table II. For the most part, pressure

TABLE I

Influence of Pressure on Human Erythrocyte ATPase Activity

Pressure	ATPase Activity (% of 1 ATA control)		
(ATA)	Total	Mg^{++}	Na^+,K
10	128.81* (16) ±14.98	143.99* (16) ±26.35	110.71 (16) ±6.44
20	143.47* (20) ±10.27	166.88* (20) ±19.40	104.45 (19) ±15.59
30	144.47* (7) ±7.35	152.83* (7) ±11.50	138.00* (7) ±5.62
150	110.58* (8) ±3.75	83.26* (8) ±11.67	141.25* (8) ±7.66

Values shown are means ± SE.The mean of each control value was taken to be 100. Number of experiments is shown in parentheses. All values except Na-K-ATPase activity at 10 and 20 ATA are significantly different from control as analyzed by the paired t test.   *$P < 0.05$.

TABLE II

Effect of Pressure on Human Erythrocyte Metabolism

Measurement	1 ATA	150 ATA
Glucose Utilization	1.12 ± 0.18	1.26 ± 0.17
Lactate Production	2.86 ± 0.33	2.50 ± 0.44
Glucose Util./Lactate Prod.	0.391 ± 0.06	0.504 ± 0.086
[2,3-Diphosphoglycerate]	3.39 ± 0.32	3.43 ± 0.26
[3-Phosphoglycerate]	0.052 ± 0.018	0.060 ± 0.017
[ATP] (without ouabain)	0.955 ± 0.021	1.136 ± 0.060*
[ATP] (with ouabain)	1.096 ± 0.074	1.253 ± 0.091*
[ADP] (without ouabain)	0.267 ± 0.019	0.196 ± 0.026*
$NAD^+/NADH$ (calc.)	321	133
pH (external)	7.20 ± 0.02	7.20 ± 0.01

Glucose utilization and lactate production are given in μmol mL RBC/h. All others have the units μmol/ mL RBC. Data were elevated using the paired t test. $*P < 0.05$.

had little effect. Glucose utilization, lactate production, 2,3-diphosphoglycerate, 3-phosphoglycerate, and the computed pyridine nucleotide ratio were unaffected by pressure. However, a consistent elevation of cellular ATP and depression of ADP were observed. The effect on ATP and ADP persisted even in the presence of ouabain, but the combined effect of both pressure and ouabain was less the sum of each agent alone.

Potassium Flux Measurements

To assess the effects of pressure on red cell membrane permeability, we measured $^{42}K^+$ efflux at 1 and 150 ATA. Figure 3 shows the logarithm of the fraction of $^{42}K^+$ remaining in the cells as a function of time under a variety of conditions. Normal cells are relatively impermeable to K^+; the efflux rate constant averaged 0.040 h^{-1} in four experiments. However, 150 ATA pressure significantly slowed $^{42}K^+$ to 0.021 h^{-1}, a reduction of almost 50%. (Compare *closed circles* and *open squares* in Fig. 3.)

It is well known that potassium permeability of human erythrocytes is dependent on internal Ca^{++} concentration (8). Raising the internal Ca^{++} level by any one of a number of methods produces a dramatic increase in K^+ permeability. One method of increasing intracellular Ca^{++} is by depletion of ATP (8). Presumably this raises the intracellular Ca^{++} by impairing the Ca^{++} pump as well as lowering levels of intracellular chelators such as ATP and DPG.

Figure 3 shows the increase in K^+ efflux that occurred when Ca^{++} was added to ATP-depleted cells at 1 ATA. (Compare x's and *open circles*.) Under these circumstances, application of 150 ATA (*closed squares*) dramatically increased K^+ permeability. Because increase in K^+ permeability is related to intracellular Ca^{++}, it is not clear whether pressure further increased K^+ permeability or whether intracellular Ca^{++} was simply higher under pressure. To clarify this point, we performed the same experiment in the presence of the
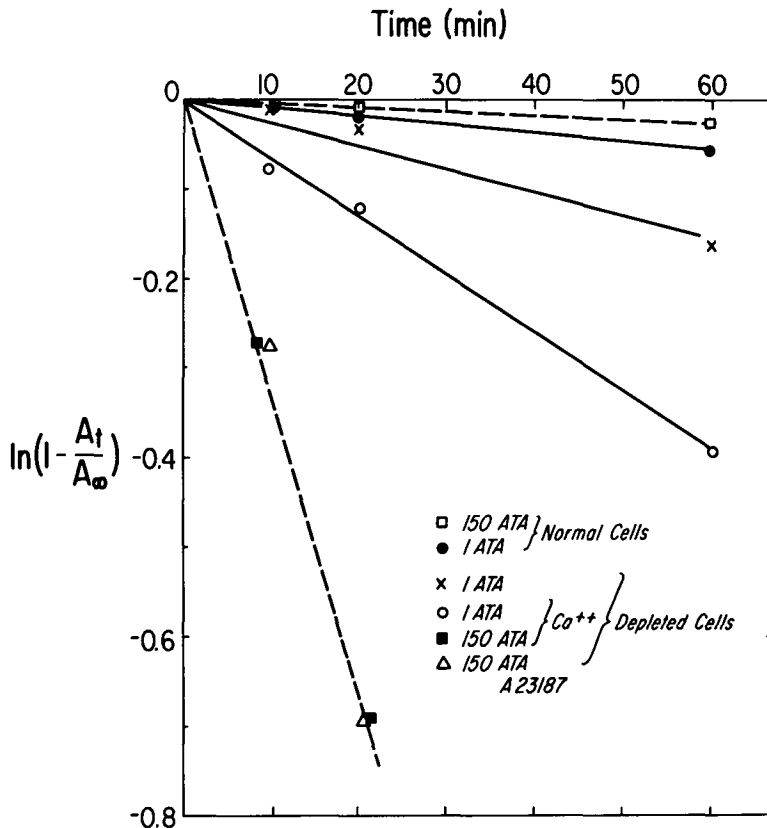
Fig. 3. Release of $^{42}K^+$ from energy replete and depleted human erythrocytes. The logarithm of the fraction of radioactivity remaining in the cells is plotted as a function of time under the conditions indicated on the graph. When present, the calcium and A23187 concentrations were 0.01 M and 8×10^{-6} M, respectively.

Ca^{++} ionophore, A23187 (*open triangles*). Under these circumstances pressure had no influence on K^+ permeability.

Donnan Equilibrium

The results of experiments designed to test the influence of pressure on the Donnan distribution of $^{36}Cl^-$ in red blood cells are shown in Table III. At 80 ATA of air pressure, the Donnan ratio (r_{Cl}) changed from 0.679 to 0.828. Similar results were obtained on compression with 80 ATA helium. Because the impermeant molecules 2,3-DPG and ATP make up a significant fraction of the intracellular charged species upon which the Donnan equilibrium depends, a similar experiment was done in cells depleted of 2,3-DPG and ATP, in which the only charged, impermeant molecular species present in significant quantity is hemoglobin. As shown in Table III, a pressure of 30 ATA still

TABLE III

Donnan Distribution of $^{36}Cl^-$ Under Pressure

Condition	1 ATA	30 ATA	80 ATA
Normal Red Cells—Air	0.679	—	0.828*
pH 7.4	±0.048	—	±0.048
Normal Red Cells—Helium	0.667	—	0.842*
pH 7.4	±0.042	—	±0.015
Depleted Red Cells	0.904	1.187	—
pH 7.4	±0.034	±0.030	—
Normal Red Cells	0.911	1.192	
pH 6.8	±0.038	±0.051	

Values are $\bar{X}$ ± SE; $n = 4$. Data were analyzed using the paired t test.   *$P < 0.05$.

caused r_{Cl} to increase. Pressure produced nearly the same increment in r_{Cl} when the pH of the incubation medium was initially 6.8.

DISCUSSION

Moderate pressure inhibits both active and passive sodium transport in human erythrocytes. Remarkably, the onset of inhibition is at pressures well within those experienced by diving man, and much less than those encountered by some diving mammals. The inhibition of active transport is not due to an effect of pressure on cell metabolism and hence a reduction in the energy supply needed to pump sodium. In fact, cell ATP level is consistently elevated by pressures that inhibit active sodium transport. Because the energy-producing reactions of glycolysis are relatively insensitive to pressures within the range tested, as indicated by nearly normal glucose utilization and lactate production, one must assume that elevated cellular ATP is due to diminished ATP utilization. Because the sodium pump normally uses about 30% of the cell's ATP production, it is tempting to suggest that the observed pressure inhibition of the pump results in the elevated ATP. However, this cannot be the sole reason, because cellular ATP levels are also increased under pressure in the presence of ouabain. Nevertheless, at least part of the elevated ATP must be caused by pump inhibition, because ATP levels are raised less in the presence of both ouabain and pressure than by either agent alone.

Although the metabolic data are consistent with observed pump inhibition at pressure, it is more difficult to fit stimulation of Na-K-ATPase activity into this framework. Part of the difficulty may arise from the different circumstances under which fluxes and Na-K-ATPase activity were measured. In the intact cell, active sodium and potassium transport are vectorial processes; the transport mechanism possesses a definite sidedness. However, ATPase activity is routinely measured in broken or open membranes, and is more properly considered a scalar process. Both sides of the membranes are in contact with

all substrates and products. It is conceivable that pressure would have quite different effects in an open system than in the intact cell. On the other hand, in the Na-K-ATPase results from open membranes are applicable to intact cells at pressure, then the data suggest an uncoupling of the pump from the enzyme. It is interesting to note that pressure activation of Na-K-ATPase has been observed in several other preparations, including fish gills (9), cardiac muscle and intestine (10).

We have shown that pressure will inhibit passive (ouabain-insensitive) Na^+ efflux and passive K^+ efflux, in addition to its inhibitory effects on active transport. If both active and passive fluxes are affected to the same degree, cell volume should not change under pressure. However, if pressure affects one process even slightly more than the other, some change in cell volume over the long term will occur. In vivo measurements of cell volume over a period of days at pressure would be necessary to provide information on this point.

The effect of pressure on the Ca^{++}-induced K^+ efflux is intriguing. A variety of unrelated agents selectively and markedly alter the red cell membrane permeability to K^+ but not Na^+, e.g., fluoride, iodoacetate and adenosine, energy depletion, propranolol, and Ca^{++} ionophore (8). The apparent common mode of action is increased intracellular Ca^{++} concentration, which is normally maintained very low by a Ca^{++}-activated ATPase (calcium pump) and intracellular chelators. In the present study pressure was found to enhance the Ca^{++}-induced K^+ efflux. The mechanism of enhancement does not appear to be an effect on K^+ permeability but rather an increase in intracellular Ca^{++}, either by increasing Ca^{++} permeability or reducing intracellular bound Ca^{++}. This conclusion comes from the fact that in the presence of the Ca^{++} ionophore A23187, which makes the membrane more permeable to Ca^{++} by several orders of magnitude, pressure does not increase K^+ loss further (11).

The increase in K permeability following a rise in intracellular Ca^{++} is not restricted to erythrocytes. The entry of Ca^{++} into liver cells makes the cells leaky to K^+ (12). Meech (13) has shown that injecting Ca^{++} into neurons increases K^+ permeability. Propranolol, an adrenergic β-receptor antagonist, is one of the agents that induces K^+ loss in human red cells, as mentioned previously. Red cells do not have adrenergic receptors but Manninen (14) suggested that the K^+ loss may be related to the drug's well-known anesthetic and antiarrhythmic properties. Glynn and Warner (15) discussed the possibility that the selective increase in K^+ permeability caused by propranolol in red cells, if produced in other tissues, could contribute to the drug's antiarrhythmic effects. They pointed out that the pacemaker potential of Purkinje fibers is very sensitive to changes in K^+ permeability. A 10% increase in resting K^+ permeability completely abolishes pacemaker activity in computed action potentials. Glynn and Warner (15) also calculated that a 10% increase in permeability roughly corresponds to the K^+ permeability change that Manninen (14) observed in red cells.

It is tempting to consider the Ca^{++}-induced K^+ channel in red cells as a possible model of the K^+ channel in excitable tissue. Pressure has been shown

markedly to affect ion-mediated events in excitable tissues. In fact, Örnhagen and Hogan (16) have pointed out that the primary action of elevated pressure on cardiac pacemaker function is to decrease the rate of diastolic depolarization.

Thus, the observation of apparent increased Ca^{++} in red cells under pressure may be relevant to pressure-induced cardiac chronotropic and inotropic effects. In addition, Spyropoulos (17) showed significant prolongation of the action potential by pressure in isolated nerve fibers from the toad. Henderson and Gilbert (18) described the effect of pressure on the kinetics of Na^+- and K^+-gating in voltage-clamped squid axons. The possible relevance of the red cell Ca^{++}-induced K^+ channel to excitable tissue alluded to by many investigators make the red cell an attractive tissue to study, particularly in light of the effects of pressure on nerves and the myocardium.

The erythrocyte is in Donnan equilibrium with respect to anions (19); therefore the distribution of anions across the membrane is related only to the concentration and net charge of the impermeant species inside the cell. In the erythrocyte these are principally hemoglobin and 2,3-DPG and ATP. Thus, any alteration in the net charge of these molecules, either by hydrogen ion titration, ligand binding, or conformational change will be directly reflected in the distribution of anions, i.e., a change in the Gibbs-Donnan equilibrium. The data in Table III show clearly that either air or helium at 80 ATA changed the equilibrium chloride distribution in human erythrocytes, and by implication that pressure alters the net change in impermeant anions within the erythrocyte. Our supposition is that pressure per se caused the observed change in Donnan distribution because helium produced the same effect as air. The oxygen and inert gas tensions are, of course, verty different under these two circumstances but hemoglobin is nearly saturated under both conditions. Three possible coclusions are that pressure results in 1) titration through acid production; 2) alteration of 2, 3-DPG or ATP binding, or both; or 3) a change in conformation. Acid titration seems unlikely because the principle source of acid is lactate and lactate production is invariant at pressure (Table II). Furthermore, the same change in r_{Cl} is observed at pressure at pH 6.8, where glycolysis is severely inhibited. Alteration in ATP or 2,3-DPG binding appear equally unlikely because the change in r_{Cl} is also observed in depleted cells. A tenable alternative is that pressure acts directly on hemoglobin conformation. By definition, a change in r_{Cl} must be accompanied by a change in pH (OH^- ions are also in Donnan equilibrium). This fact raises the question whether the other effects of pressure on glycolysis and transport have as their single cause a cellular pH change. In the case of transport, this appears unlikely because Na^+ pumping and Ca^{++}-induced K^+ leak are insensitive to changes in pH of the order of magnitude of 0.2 units. On the other hand, metabolism—particularly ATP/ADP ratios—may be in part affected by a pH change.

It is highly probable that the oxygen transport function of hemoglobin would be influenced by a 0.2-unit alkaline shift in pH. Moreover, the experiments of Chouteau (20) suggest behavioral modification at normal oxygen tensions at pressure. Finally, Kiesow (21) has shown a left shift of the oxygen dissociation curve at pressure. The extent to which the above observation may be related to a pH change in currently under investigation in this laboratory.

Acknowledgments

References

1. Tosteson DC, Hoffman JF. Regulation of cell volume by active cation transport in high and low potassium sheep red cells. J. Gen Physiol 1960;44:169–194.
2. Skou JC. Enzymatic basis for active transport of Na^+ and K^+ across cell membrane. Physiol Rev 1965;45:596–617.
3. Goldinger JM, Kang BS, Choo YE, Paganelli CV, Hong SK. The effect of hydrostatic pressure on ion transport and metabolism in human erythrocytes. J Appl Physiol 1980;49:224–231.
4. Marshall WE, Goldinger JM, Omachi A. The influence of anaerobiosis on human erythrocyte metabolism. Proc Soc Exp Biol Med 1977;154:356–359.
5. Williamson DH, Lund P, Kresb HA. The redox state of free nicotinamide-adenine dinucleotide in the cytoplasm and mitochondria of rat liver. Biochem J 1967;103:514–527.
6. Goldinger JM, Kang BS, Morin RA, Paganelli CV, Hong SK. A method for separating cells and suspending medium at high pressure. Undersea Biomed.Res 1981;8(1):59–62.
7. Reeves RB. Temperature-induced changes in blood acid-base status: Donnan r_{Cl} and red cell volume. J Appl Physiol 1976;40:762–767.
8. Knauf PA, Riordan JR, Schuhmann B, Wood-Guth I, Passow H. Calcium-potassium-stimulated net potassium efflux from human erythrocyte ghosts. J Membrane Biol 1975;25:1–22.
9. Pfeiler E. Effects of hydrostatic pressure on $Na^+ + K^+)$-ATPase and Mg^{2+}-ATPase in gills of marine teleost fish. J Exp Zool 1978;205(3):393–402.
10. Gottlieb SF, Koehler CJ, Rhodes LVG. An oxygen- and pressure-sensitive enzyme: Na,K adenosinetriphosphatase. In: Lambertsen CJ, ed. Underwater physiology V. Proceedings of the fifth symposium on underwater physiology. Bethesda, MD: Federation of American Societies for Experimental Biology, 1976:431–432.
11. Reed PW. Effects of the divalent cation ionophore A23187 on K permeability of rat erythrocytes. J Biol Chem 1976;25:3489.
12. van Rossum GDV. Relation of intracellular Ca^{2+} to retention of K^+ by liver slices. Nature (Lond) 1970;225:638–639.
13. Meech RW. Intracellular calcium injection causes increased potassium conductances in Aplysia nerve cells. Comp Biochem Physiol 1972;42a:493–499.
14. Manninen V. Movements of sodium and potassium ions and their tracers in propranolol-treated red cells and diaphragm muscles. Acta Physiol Scand (Suppl) 1970;355:1–76.
15. Glynn IM, Warner AE. Nature of the calcium dependent potassium leak induced by (+)-propranolol, and its possible relevance to the drug's antiarrhythmic effect. Br J Pharmacol 1972;44:271–278.
16. Örnhagen HCh, Hogan PM. Hydrostatic pressure and mammalian cardiac-pacemaker function. Undersea Biomed Res 1977;4(4):347.
17. Spyropoulos CS. The effects of hydrostatic pressure upon the normal and narcotized nerve fiber. J Gen Physiol 1957;40:849–857.
18. Henderson JV Jr, Gilbert DL. Slowing of ionic currents in the voltage-clamped squid axon by helium pressure. Nature 1975;258(5533):351–352.
19. Davson H. A textbook of general physiology. 2nd ed. Boston: Little, Brown, and Company, 1959.
20. Chouteau J, Corriol JH. Physiological aspects of deep diving. Endeavour 1971;30:70–76.
21. Kiesow LA, Bless JW, Shelton JB. Oxygen dissociation in human erythrocytes: its response to hyperbaric environments. Science 1971;179:1236–1238.

EFFECTS OF HIGH HYDROSTATIC PRESSURES ON Na⁺ TRANSPORTS ACROSS ISOLATED GILL EPITHELIUM OF SEA WATER-ACCLIMATED EELS *Anguilla anguilla*

A. J. R. Péqueux

When applied to isolated nonperfused gills of sea water-acclimated eels *Anguilla anguilla* L., hydrostatic pressure induces changes in tissue Na^+, K^+, and Cl^- contents (1,2). Upon incubation in artificial sea water (ASW), application of pressure steps higher than 250 atmospheres (atm) brings about a severe increase of the tissue Na^+ and Cl^- contents and a decrease of K^+, which are intensified the higher the pressure. Because pressure is known to affect the dissociation of weak electrolytes and the pH of natural sea water (3–7), the possibility that ionic changes observed under pressure could be indirect and only related to pressure-induced modifications in physical and chemical properties of the incubation medium has been considered. Experimental evidence has definitely shown that ionic changes were caused essentially by hydrostatic pressure itself.

Pressure effects on the tissular content of ions have appeared to be very complex and dependent on the pressure magnitude applied. As an example, all ions species, particularly Na^+ and Cl^-, are not affected in the same way by pressure, which raises the possibility that pressure could selectively act on the various transport mechanisms and indicates that Na^+ and Cl^- movements are governed by independent processes in teleostean gills.

Preliminary experiments done in ASW led to the conclusion that both an inhibition of Na^+ active extrusion processes and an increase of the passive Na^+ entrance along the concentration gradient might contribute to the pressure-induced increase of tissue Na^+ content observed upon compression at 500 atm

601

(2). However, both events resulting in a similar final effect in ASW cannot be discriminated easily.

Experiments were therefore initiated to bring more insight to the nature of the effects of high pressure on the various transport processes or components involved in Na$^+$ transfers at work in gill epithelium of ASW-acclimated eels.

The results reported in this paper deal particularly with the pressure sensitivity of passive transport processes. Discrimination between active and passive mechanisms was achieved by running incubations in a physiological saline isotonic to the blood. In such a medium where there is no concentration gradient across the epithelium, the active transport of Na$^+$ is indeed extremely reduced, or even abolished, as is demonstrated in this paper.

METHODS AND MATERIAL

Experiments were performed on isolated gills from European silver eels *Anguilla anguilla* L. adapted to natural sea water (521 meq/L Na$^+$; 19 meq/L K$^+$; 610 meq/L Cl$^-$; pH 7.8, t° 15°C).

Single gills isolated by dissection were incubated at atmospheric pressure and under high hydrostatic pressures in a pressure vessel designed to avoid the presence of any gas phase (see description and details in previous papers: 1,8,9).

At the end of the incubation period, gill filaments were cut off the gills; they were blotted on filter paper, weighed, and dried at constant weight in an oven at 110°C for dry weight measurements. Inorganic ions were extracted after treatment with HNO$_3$ O.1 N for 48 h. Determinations of Na$^+$ and K$^+$ were made by flame photometry and Cl$^-$ content was estimated with a Buchler-Cotlove chloridometer. Results were expressed in μeq/tissue wet weight. Ion fluxes were estimated by measuring net changes of the total tissue ion contents. Compartmental analysis and radiosodium effluxe measurements were made on the basis of typical washout experiments of pieces of gill tissue preloaded for 45 min in radioactive saline (20μC$_i$ Na^{24}/mL). Results were expressed in μeq/gww on the basis of the specific radioactivity of the incubation medium. The so-called "saline isotonic to the blood" contained 170 mM/L NaCl, 5 mM/L KCl, 2.6 mM/L CaCl$_2$, 4.1 mM/L MgSO$_4$, buffered at pH 7.6 by means of 10 mM/L tris buffer.

RESULTS AND DISCUSSION

Experiments carried out *at atmospheric pressure* in the so-called "saline isotonic to the blood" (i.e., in a physiological medium in which the concentration gradient across epithelium is considerably reduced or even abolished) show that the tissue water and ion content remain almost unchanged for more than 60-min incubation (Table I). At variance with the results obtained upon incubation in ASW, application of active transport inhibitors like ouabain, 2–4

TABLE I

Ions and Water Contents of Gill Filaments from ASW-Acclimated Eels *Anguilla anguilla* Before and After Incubation Under Various Conditions at Atmospheric Pressure and Upon Application of a Pressure Step of 500 atm

Incubation Conditions	Na⁺	K⁺ μeq/gww	Cl⁻	H₂O g/gww
t₀ (not treated)	64.5 ± 4.0	84.1 ± 3.0	53.0 ± 4.3	0.795 ± 0.004
60 min at atm pressure	61.0 ± 2.2	80.1 ± 3.9	54.4 ± 1.6	0.801 ± 0.005
Anoxy; 60 min at atm pressure	69.9 ± 1.9	78.4 ± 3.1	59.8 ± 3.5	0.798 ± 0.005
10⁻³M ouab.; 60 min at atm pressure	69.6 ± 9.3	75.1 ± 6.3	53.9 ± 10.9	0.796 ± 0.009
5.10⁻⁴M DNP; 60 min at atm pressure	64.5 ± 6.7	69.1 ± 0.7	55.1 ± 3.0	0.816 ± 0.001
60 min at 500 atm	80.4 ± 3.4	64.1 ± 4.0	56.6 ± 3.1	0.789 ± 0.006

Mean data ± SD (four experiments).

(α) dinitrophenol (DNP) and anoxy does not result in any significant effect (Table I). In such conditions, it can therefore be reasonably concluded that the activity of "pumping" mechanisms must be reduced so much as to be practically undetectible. The same holds true for diffusional movements from environment towards blood.

Results of Table I show that in identical-incubation conditions *application of a pressure step of 500 atm induces* a mean increase of tissue Na⁺ content of about 25% (individual data sometimes rising 40%). Concomitantly and despite the absence of detectible active components, there is a decrease in K⁺ content (23%), but Cl⁻ content does not appear to be significantly modified. Upon decompression, Na⁺ and K⁺ contents have been observed to resume their initial level within 30–40 min, which indicates that pressure-induced variations are fully reversible.

In consideration of the conclusions drawn from the experiments done at atmospheric pressure, the pressure-induced increase in Na⁺ content can be reasonably ascribed essentially to an effect on Na⁺ passive permeability. This conclusion is in full agreement with my results obtained by incubating gills in Na⁺-free sea water (2). It must also apply to the drop in tissue K⁺ content that occurs at 500 atm. As the supposed Na⁺/K⁺ coupled transport has to be considered as ineffective, any effect of pressure on an eventual active component also must be discarded. As far as K⁺ transport across gill epithelium is concerned, the problem up to now is far from being solved even at atmospheric pressure.

According to Bellamy (10), the gill epithelium has little permeability to K^+ ions. On the other hand, a lack of K^+ in the surrounding medium severely disturbs the maintenance of Na^+ balance of blood (11,12). That K^+ ions may be involved in active exchange processes against Na^+ appears therefore as very likely, but the importance and the exact modalities of the procedure remain to be established. At this step of investigation on pressure effects and in consideration of the results presented in this paper, it thus seems to be more reasonable to consider that high pressures act by enhancing the passive K^+ permeability. In that view, it is worth noticing that conclusive evidence concerning the pressure sensitivity of K^+ passive movements have been obtained with human red blood cells more accessible to experimentation under pressure. It has been indeed been demonstrated that the net K^+ efflux from human erythrocytes essentially to be considered as passive, increases gently but almost linearly with pressure until 600–700 atm, while above that pressure range, a very pronounced increase in membrane K^+ permeability occurs (13,14).

If the results presented in Table I suggest that active transport activity falls to negligible values when gills are transferred into physiological medium, they also suggest that passive diffusion from outside towards body fluids is very low too. This could be compared to observations done by Motais et al. (15) that Na^+ or Cl^- influx is instantaneously reduced to very low levels when sea water-acclimated fishes are suddenly transferred into fresh water. In this latter case, Motais et al. (15) interpreted such flux readjustments in terms of the possible occurrence of an exchange-diffusion mechanism.

Investigations on the effects of pressure on exchange-diffusion appears almost impossible without the help of isotopic tracers. Because the difficulty to obtain a functional perfused preparation of fish isolated gill, which is further susceptible to work under pressure, it has been preferred to adapt the washout method of a Na^{24} preloaded piece of tissue to the peculiar pressure techniques in use (compartmental analysis).

By that method, three compartments, A, B, and C, have been identified in gills from ASW-acclimated eels incubated at atmospheric pressure in isotonic saline (Fig. 1 and Table II). Compartment B is considered to correspond to the Na^+ fraction contained in cell epithelium, while A and C are considered to correspond to the outside facing extracellular space and to the body fluids reservoir.

The effects of 15-min pressure application on Na^{24} efflux have been investigated after 15 min prewashing to avoid any interference due to Na^{24} from compartment A. Pressure effects were evaluated by comparing ion content, radiosodium content, and specific radioactivity of gill epithelium before and after pressure application.

Results shown in Table III indicate a slight but not yet significant increase of tissue Na^+ content measured by flame photometry in gills submitted to 500 atm. Concomitantly, there was less radioactive Na^+ remaining in compressed gills than in controls incubated at atmospheric pressure, and specific radioactivity in compressed gills appears as to have been significantly lower (Student's

TABLE II

Na[24] Washout Kinetics of Isolated Gills from ASW-Acclimated Eels *Anguilla anguilla*

Compartment	Radiosodium %	Rate Constant k_i	Half Life Time
A	10.6 ± 2.5	1.05 ± 0.44	45″ ± 17″
B	8.2 ± 4.5	0.11 ± 0.06	8′22″ ± 4′52″
C	81.2 ± 4.2	0.007 ± 0.001	106′55″ ± 18′00″

Data result from graphical analysis of complex exponential curves. Mean data ± SD (four experiments).
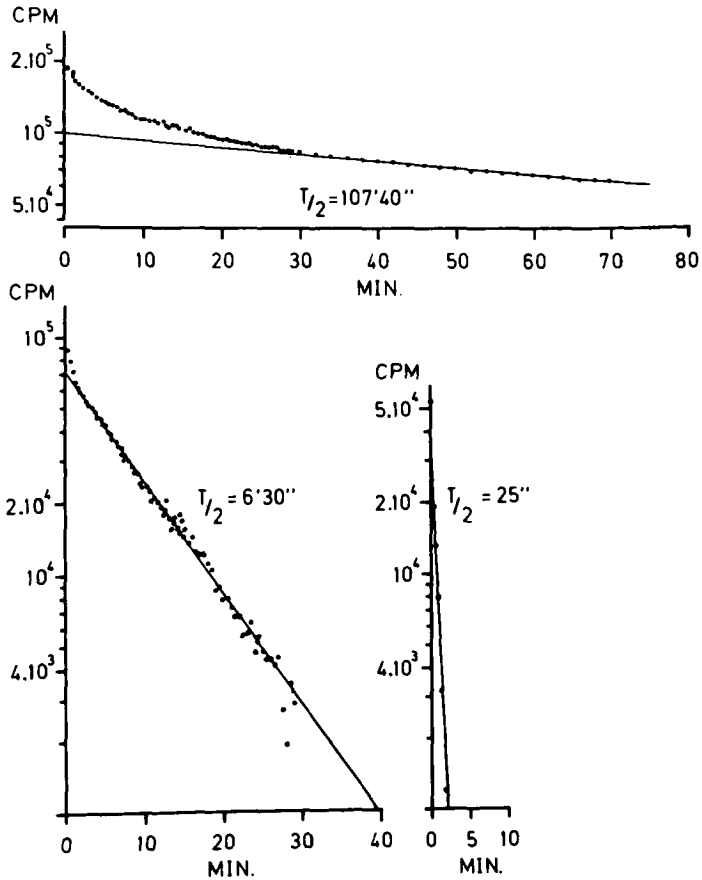
Fig. 1.   Graphical analysis of a Na[24] washout experiment in isotonic saline of an isolated gill of ASW-acclimated eel. The tissue has been preloaded for 45 min in radioactive saline (20μCi Na[24]/mL).   *Ordinate:* residual radioactivity in the gill, expressed in CPM.   *Abscissa:* washing time in minutes.   T/2 = half life of corresponding compartment (minutes, seconds).

TABLE III

Effects of 500-atm Pressure on Total Na$^+$, K$^+$, Cl$^-$ Content and on Na^{24} Efflux of Gill Filaments from ASW-Acclimated Eels
Anguilla anguilla

Incubation Conditions	Na$^+$ Content (μeq/gww) Chemical Determination	Na^{24} Content Isotopic Determination	Specific Radioactivity	K$^+$ (μeq/gww)	Cl$^-$ (μeq/gww)	Water (g/gww)
t$_0$ (n = 6)	58.7 ± 7.2	18.34 ± 4.05	0.313 ± 0.047	69.7 ± 2.0	50.7 ± 7.6	0.821 ± 0.010
500 atm for 15' (n = 5)	64.0 ± 5.4	13.77 ± 2.57	0.226 ± 0.032	62.5 ± 2.2	48.2 ± 6.0	0.813 ± 0.007
Control atm pressure for 15' (n = 5)	60.4 + 6.8	16.47 ± 2.43	0.285 ± 0.029	69.3 ± 2.4	49.9 ± 6.4	0.815 ± 0.005

Mean results ± SD of n washout experiments in isotonic saline of gill pieces preloaded for 45 min in radioactive saline (20μCi Na^{24}/mL).

96

test: $0.02 < P < 0.05$). On the other hand, much more radioactivity appeared in incubation medium under pressure than at atmospheric pressure. By comparison with control data, Na^{24} efflux increased about 140% at 500 atm (Fig. 2).

According to observations and conclusions reported above, the possibility of a pressure-induced increase of active Na$^+$ efflux cannot be considered. Such an effect should induce a decrease in tissue Na$^+$ content in opposition to what occurs and, moreover, pressure steps of that magnitude are known to directly inhibit active transport processes (1,2,16). It is therefore more reasonable to consider that the observed increase of radiosodium efflux without concomitant decrease of tissue Na$^+$ content reflects a pressure-induced stimulation of exchange-diffusion processes Na$^+$-Na$^+$. As increased exchange-diffusion Na$^+$-Na$^+$ does not result in any net variation of tissue Na$^+$ content, the pressure induced-increase of tissue Na$^+$ content thus appears to have been caused an effect on the Na$^+$ passive diffusion from the environment towards body fluids.
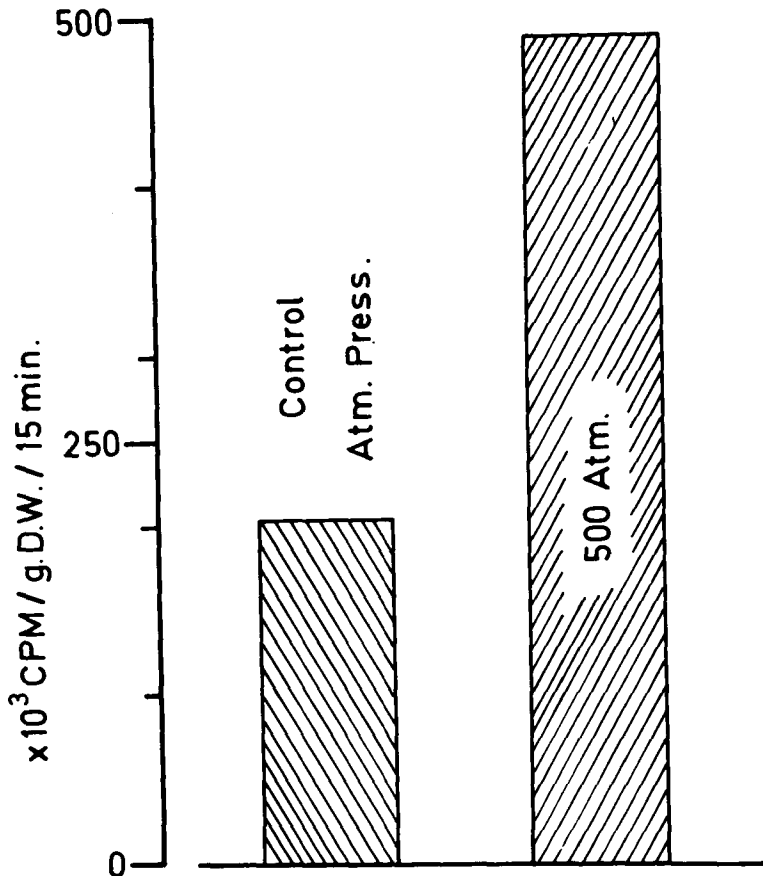
Fig. 2. Na^{24} efflux from isolated gills of ASW-acclimated eels, incubated at atmospheric pressure and at 500 atm in isotonic saline. Typical result of one experiment.

When isolated gills are incubated under pressure in sea water, it is likely that in addition to both inhibition of the Na^+ pump and enhancement of Na^+ passive permeability that contributes to pressure-induced changes of tissue Na^+ content (reported in previous papers, 1,2), exchange-diffusion Na^+-Na^+ also must be pressure activated, although it does not result in net variation of tissue Na^+. Experiments with isotopic tracers are under investigation to test that hypothesis.

Results presented in this paper also corroborate the idea that pressure acts differently and selectively on Na^+ and Cl^- transports in agreement with observations reported previously and subsequent conclusions on the relationships binding both mechanisms (1,2). Results shown in Table I indeed indicate that tissue Cl^- content remains unaffected by 1-h pressure application. That observation obviously does not infer that all possible components of Cl^- transports are insensitive to pressure. Experiments using radioactive Cl^- are now being carried out to bring more insight to that question.

It is now clear that hydrostatic pressure affects the functioning of biological membranes by modifying selectively their properties of passive and active ion transports in a way depending upon the magnitude of the applied pressure.

At the present time, little can be said about the molecular aspect of pressure-induced disturbances. Nevertheless, several pieces of evidence prompt us to explain such effects in terms of phase transitions in the lipidic components of the membrane affecting the conformation of the enzyme proteins associated with the active processes and of the pathways specifically involved in passive ionic transports.

It is evident that knowledge of how hydrostatic pressure affects membrane processes is a fundamental problem in the biology of marine organisms and is essential to a thorough understanding of underwater physiology. According to that view, investigations on the effects of hydrostatic pressure on ion transport across fish gill epithelium might contribute efficiently to development of undersea biomedical sciences.

References

1. Péqueux A, Gilles R. Effect of high hydrostatic pressures on the movements of Na^+, K^+, and Cl^- in isolated eel gills. Experientia 1977;33:46–48.
2. Péqueux A. effects of high hydrostatic pressures on ions permeability of isolated gills from sea water acclimated eels Anguilla anguilla. In: Gilles R, ed. Animals and environmental fitness. Abstracts volume. Oxford-New York: Pergamon Press, 1979:127–128.
3. Distèche A. pH measurements with a glass electrode withstanding 1,500 kg/cm² hydrostatic pressure. Rev Sci Instrum 1959;30:474–478.
4. Distèche A. Nouvelle cellule à électrode de verre pour la mesure directe de pH aux grandes profondeurs sous-marines. Bull Inst Oceanogr (Monaco) 1964;64:1–10.
5. Distèche A. Effects of pressure on the dissociation of weak acids. In: The effects of pressure on organisms. Symposia of the Society for Experimental Biology. New York: Cambridge Univer Press 1972;26:27–60.
6. Distèche A, Distèche S. The effect of pressure on the dissociation of carbonic acid from measurements with buffered glass electrode cells. The effect of NaCl, KCl, Mg^{2+}, Ca^{2+}, SO_4^{2-} and boric acid with special reference to sea water. J Electrochem Soc 1967;114:330–340.

7. Distèche A., Dubuisson M. Mesures directes de pH aux grandes profondeurs sous-marines. Bull Inst. Oceanogr (Monaco) 1960;57:1–8.

8. Péqueux A. Polarization variations induced by high hydrostatic pressures in the isolated frog skin as related to the effects on passive ionic permeability and active Na$^+$ transport. J Exp Biol 1976;64:587–602.

9. Péqueux A. Effects of pH changes on the frog skin electrical potential difference and on the potential variations induced by high hydrostatic pressures. Comp Biochem Physiol 1976;55A:103–108.

10. Bellamy D. Movements of potassium, sodium, and chloride in incubated gills from the silver eel. Comp Biochem Physiol 1961;3:125–135.

11. Maetz J. Sea water teleosts: evidence for a sodium-potassium exchange in the branchial sodium-excreting pump. Science 1969;166:613–615.

12. Kamiya M, Utida S. Changes in activity of sodium-potassium-activated adenosinetriphosphatase in gills during adaptation of the Japanese eel to sea water. Comp Biochem Physiol 1968;26:675–685.

13. Péqueux A, Gilles R, Pilwat G, Zimmermann U. Pressure induced variations of K$^+$ permeability as related to a possible reversible mechanical breakdown in human erythrocytes. Experientia (in press).

14. Zimmermann U, Pilwat G. Péqueux A, Gilles R. Electromechanical properties of human erythrocyte membranes: the pressure-dependence of potassium permeability. J Membr Biol 1980;54:103–113.

15. Motais R, Garcia-Romeu F, Maetz J. Exchange diffusion effect and euryhalinity in teleosts. J Gen Physiol 1966;50:391–422.

16. Péqueux A, Gilles R. Effects of high hydrostatic pressures on the activity of the membrane ATPases of some organs implicated in hydromineral regulation. Comp Biochem Physiol 1978;59B:207–212.

A QUANTITATIVE DESCRIPTION OF PRESSURE-INDUCED ALTERATIONS IN IONIC CHANNELS OF THE SQUID GIANT AXON

B. B. Shrivastav, J. L. Parmentier, and P. B. Bennett

The effects of increased hydrostatic pressure on animals are varied. These effects on different organs are manifestations of physico-chemical and structural changes in individual cells and their relationship to each other. Pressure effects appear in the nervous system as a generalized hyperexcitability known as high pressure nervous syndrome (HPNS) (1,2,3). In animals HPNS develops as tremors in the pressure range of 70 ATA. Further increase in pressure to 90–100 ATA produces convulsions and respiratory distress, eventually resulting in muscle contraction, paralysis, and death.

An action potential in a nerve fiber is a transient but specific change in membrane polarization which is brought about by breakdown of membrane permeability barriers to sodium and potassium ions. This change results in inward flow of Na^+ and outward flow of K^+ down their respective electrochemical gradient (4). It is almost certain that these ions flow through specific pathways in the membrane known as ionic channels (5,6). Although the membranes are composed of almost equal amounts of lipids and proteins by weight, the ionic channels are probably protein molecules imbedded in the lipid matrix (7,8). The opening and closing of these channels is voltage and time dependent; once the membrane is depolarized to its threshold potential, these channels open and close to allow Na^+ and K^+ to flow and this produces the action potential (9).

The primary objective of this paper is to summarize our data on the effects of increased hydrostatic pressure and temperature on the action potential and the ionic currents in the membrane of the squid giant axon.

Hodgkin-Huxley Model for the Ionic Currents in the Excitable Membrane

Hodgkin and Huxley (9) pioneered the voltage clamp technique to analyze the sodium and potassium currents in the squid giant axon. The change in sodium and potassium conductances are respectively described by the following empirical equations:

$$g_{Na} = \bar{g}_{Na} m^3 h \tag{1}$$

$$\frac{dm}{dt} = \alpha_m (1 - m) - \beta_m m \tag{2}$$

$$\frac{dh}{dt} = \alpha_h (1 - h) - \beta_h h \tag{3}$$

$$g_K = \bar{g}K^{n4} \tag{4}$$

$$\frac{dn}{dt} = \alpha_n (1 - n) - \beta_n n \tag{5}$$

Where g_{Na} and g_K are time and voltage dependent sodium and potassium conductances, $\bar{g}_{Na}$ and $\bar{g}_K$ are constants and represent the maximum sodium and potassium conductances respectively. The parameters m, h, and n are variable from 0 to 1, and are time and voltage dependent. The α's and β's are the forward and backward rate constants and are voltage dependent.

These equations, with little modification, have also been applied to account for excitability phenomenon in other tissues including the node of Ranvier in myelinated fibers (10), Myxicola giant axon (11), and frog muscle (12).

When one considers the excitability phenomenon in the nerve fiber, two properties of the ionic channel system are important. The first is the mechanism of channel opening following membrane depolarization. This has been termed as channel gating (13,14). The mechanism of gating of a particular channel system has been considered to be the transfer or movement of charged particles upon membrane depolarization from an inactive to an active state and vice versa (9,15,16). The active state is related to the opening of the channel. The gating particle transfer, therefore, may be considered as a chemical reaction represented by the equation

$$(1 - A) \underset{\beta}{\overset{\alpha}{\rightleftharpoons}} A \tag{6}$$

in which A represents the active state of the channel gating particles; α and β are the forward and reverse rate constants respectively from inactive to active state. The rate of change of the active state is given by

$$\frac{dA}{dt} = \alpha (1 - A) - \beta A \tag{7}$$

The second property of the ionic channel system is its selectivity for a particular ion. This function is said to be performed by the selectivity filter of the channel. Hille proposed a model for the selectivity mechanism of the sodium channel, in which the high negative field caused by the presence of ionized acid groups within the sodium channel controls the ionic selectivity of the sodium channel (5,17,18).

Equation (7) is analogous to Eqs. 2, 3, and 5. Therefore, the change to active from inactive state upon depolarization of the potassium gating system particle may be considered as charged particles which either realign themselves or make or break chemical bonds. Statistically, the probability that these particles will be in the active state is n. Thus Eq. 5 describes the rate of transfer of these particles to the active state. The α_n and β_n are the voltage dependent rate constants of the transfer reaction. Furthermore, n^4 which has been empirically fitted to the potassium conductance curves because of its sigmoidal initial rise (9) represents the probability of the potassium channels in the active or open state. In such a transfer system, as defined by Eq. 5, the rate of rise of n will be exponential to its steady state value. This steady state value of n and its time constant for the exponential rise, τ_n, therefore may be given by

$$n_\infty = \alpha_n \, (\alpha_n + \beta_n)^{-1} \tag{8}$$

$$\tau_n = (\alpha_n + \beta_n)^{-1} \tag{9}$$

In similar considerations, the sodium channel gating system may be represented by two similar reactions operating in opposite directions. For this system the two parameters are m for activation and h for inactivation of the channel. These two parameters have been implicated to be independent of each other, but other workers have presented m and h as being coupled to each other (19,20,21). As presented in Eq. 1, the conducting state of the sodium channel is empirically represented by m^3h; implying that three m particles and one h particle have to be in the right or active position for the channel to be in the open state.

Taking α_m, β_m and α_h, β_h as the respective rate constants for the activation and inactivation of the sodium channel, the change of m and h to their steady state values, and the time constants for their exponential change may respectively be given by

$$m_\infty = \alpha_m \, (\alpha_m + \beta_m)^{-1} \tag{10}$$

$$\tau_m = (\alpha_m + \beta_m)^{-1} \tag{11}$$

and

$$h_\infty = {}_h \, (\alpha_h + \beta_h)^{-1} \tag{12}$$

$$\tau_h = (\alpha_h + \beta_h)^{-1} \tag{13}$$

Absolute Rate Theory

On the basis of the Absolute Rate Theory, the effect of pressure, P, on the forward rate constant α, for a chemical reaction can be expressed by the equation (22)

$$\alpha_2 = \alpha_1 \, e^{\dfrac{-\Delta V^* \, (P_2-P_1)}{RT}} \tag{14}$$

Where R and T have usual meaning. The quantity ΔV^* is the volume charge of activation. Increase in pressure below 1000 atm promotes the formation of hydrogen bonds and ruptures ionic bonds or hydrophobic interactions (23,24,25).

MATERIAL AND METHODS

The squid giant axons from "Loligo pealei" were used in these studies. These giant axons were isolated, cleaned, and cannulated. For each experiment, an axon was hung vertically in a pool of sea water, with cannula clamped on a stand. The "piggy back" electrode system, consisting of a platinized platinum wire and a quartz capillary each of 75 μ in diameter, was brought vertically by a micromanipulator to go through the cannula into the vertically hanging axon. The electrode was very carefully inserted inside the axon until it was about 4.5 to 6 cm inside the fiber. The resting potential and the action potential of the fiber were measured. The experiment was continued only if the action potential was 100 mV or above. The axon with the electrode system in it was then carefully transferred to a vial, which was 1.5 cm in diameter and 5 cm high. This vial contained artificial sea water with either 300 nM tetrodotoxin or 100 μm 3,4-Diaminopyridine (26) to respectively suppress either sodium or potassium currents. The inside of the vial was also fitted with a platinized platinum foil ring of 4 mm width, surrounded by two similar rings as guard electrodes. With the cannula holder in place at the top of the vial, the tip of the potential measuring capillary of the electrode system reached the mid-horizontal plane of the current-measuring platinum ring. The reference electrode was made of Ag-AgCl and was also hung inside the vial. The vial was then transferred to the unassembled Wilson high pressure chamber, which has been described elsewhere (27). Connections for the measurement of the potential and ionic currents were made through the wall of the pressure chamber. The cooling system was made of stainless steel tubing coil in contact with the vial and was connected through the base of the chamber to a Lauda circulating bath. The temperature inside the vial was continuously monitored. The experiments were conducted between 6.4°C and 10.5°C. However, the temperature in each experiment was maintained constant within 0.1°C. The chamber was filled with mineral oil, and the pressure inside the chamber was exerted by helium from a commercially available 3500-lb helium tank. The compression rate was controlled by a micrometer and was monitored by a transducer and recorded by chart recorder.

The voltage clamp of the nerve fiber was achieved in the conventional manner. The holding potential was kept at -80 mV. The leak currents were measured at -100, -120, and -140 mV of membrane potentials. The series resistance was compensated by a feedback system. The experiments were performed at 1, 100, and 150 atm. The families of the sodium and potassium currents were obtained over the range of -60 to $+80$ mV of the membrane potential in steps of 5 or 10 mV. Measured leak current was subtracted from each of the current traces for data analysis. The membrane potentials were corrected for 10 mV junction potential (28). The ionic currents for both sodium and potassium were analyzed (29) for calculation of the rate constants α's and β's of the Hodgkin-Huxley equations (9). A limited number of experiments were performed in which the decreased rate of rise of the ionic currents at increased hydrostatic pressures was compensated for by increasing the temperature of the sea water bathing the axon.

The sea water used in these experiments had the following composition: Na^+ 400 mM; K^+ 10 mM; Ca^{++} 10 mM, Mg^{++} 50 mM; Cl^- 530 mM Hepes or tris 5 mM at pH 8.0.

RESULTS

Figure 1 shows three superimposed action potentials from one axon: at 1 atm and 8.4°C, at 100 atm and 8.4°C, and at 100 atm and 13.4°C. With the temperature held constant, 100 atm of pressure caused a decrease in both the rise and fall of the action potential. When the temperature was slowly increased to 13.4°C and the pressure was held constant at 100 atm, the rate of rise matched the rate of rise at 1 atm and 8.4°C. The rate of fall, which was also increased by the increase in temperature, however, did not match the rate of fall at 1 atm and 8.4°C. Figure 2 shows ionic currents under voltage-clamped conditions at 1 and 100 atm.

Increased pressure up to 150 atm had no effect on the maximum value of the potassium conductance $\overline{g}_K$. However, the steady-state value of the activation parameter, n_∞ shifted towards a more positive membrane potential by about 5 mV at 100 atm and about 7 mV at 150 atm. Pressure also increased the time constant τ_n by 17.5 ± 3.2 and $29.6 \pm 5.5\%$ at 100 and 150 ATA, respectively.

Hydrostatic pressure up to 100 atm had no effect on the maximum conductance g_{Na} recovered to the control value of 1 atm. The steady state sodium conductance was calculated and was plotted against the membrane potential. Increased pressure to 100 atm shifted the conductance curve towards more positive membrane potentials by about 4 to 6 mV. Further, the time constant τ_m and the value of m_∞ were calculated. Pressure at 100 and 150 atm increased τ_m by 13.7 ± 4.5 and $21.1 \pm 5.2\%$, respectively. The value of τ_m and m_∞ were used in the calculation of the rate constants α_m and β_m. Increased pressure decreased α_m while the effect of pressure on β_m was too small to detect.

7-31-79

1 ATM, 8.4°C
100 ATM, 8.4°C
100 ATM, 13.4°C

20mV

0.5 msec
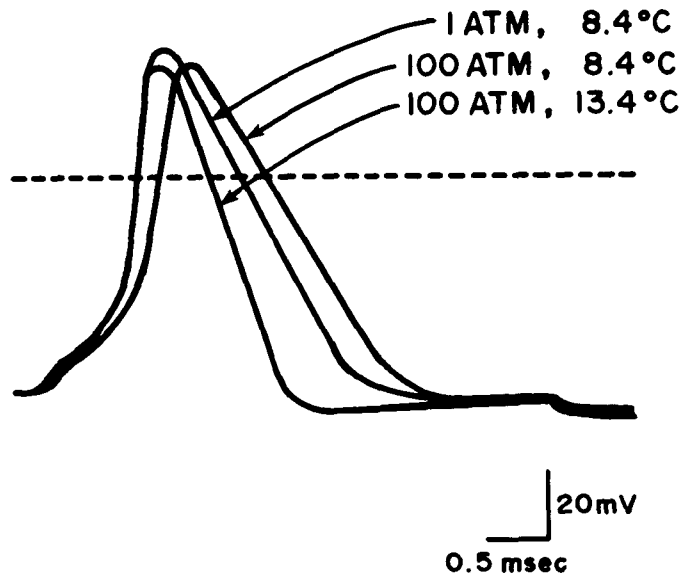
Fig. 1. Superimposed action potentials at varying pressures and temperatures. Increased pressure (100 atm) slowed both the rising and falling phases of the action potential. Subsequent rise of temperature (5.0°C) restored the rising phase to the control levels while overcompensating for the falling phase.

7-31-79
8.4°C

mV
60
40
20
0
-20
-40

100mV

0.5 msec
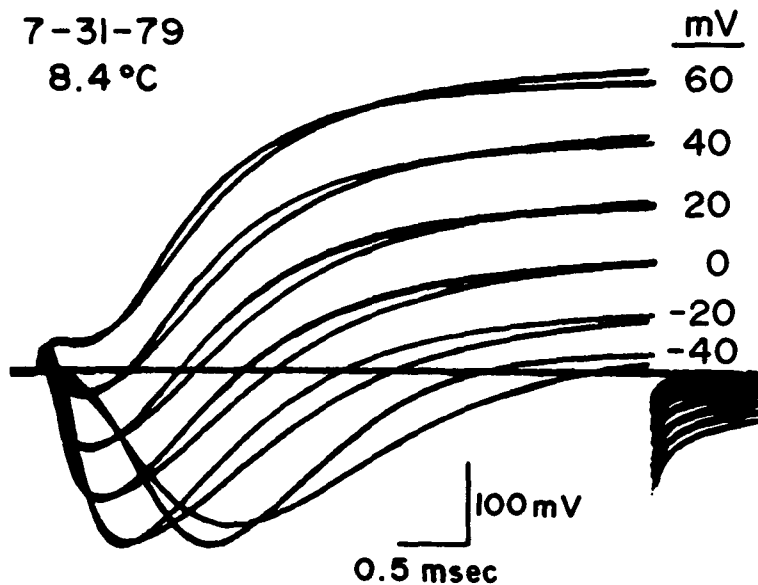
Fig. 2. Superimposed ionic currents measured at 1 and 100 atm. Increased pressure slowed the rising phase of both the sodium and potassium currents. The slow kinetics at 100 atm that caused less accumulation of potassium in the Hodgkin-Huxley space is responsible for the increase in the steady state currents seen at the positive membrane potentials.

Separate experiments were performed to measure h. Pressure up to 100 atm had no effect on the h_∞ (V) curve. Estimates were made for the effect of pressure on τ_h. Pressure of 100 and 150 atm increased τ_h about 15 and 26%, respectively.

DISCUSSION

Hydrostatic pressure mainly decreased both the rate of rise and the rate of fall of the action potential in the squid giant axon. The falling phase is more affected than the rising phase. Consequently, the action potential is prolonged by increased pressure. The observation that increased temperature will compensate the pressure-slowed rate of rise suggests that in an axon the pressure and the temperature primarily operate on the kinetics of the gating mechanism so that the slowing effects on the rising phase of the action potential by increased pressure to 100 atm are almost counter-balanced by a 5°C increase in temperature. Figure 2 demonstrates that the increased pressure slowed the rise of the ionic currents.

Increased pressure below 1000 atm promotes formation of hydrogen bonds. The volume of activation associated with this process is about -5 mL/mol. On the other hand, an increase in pressure helps to rupture ionic bonds and hydrophobic interactions. The volume of activation associated with these processes is about -21 and -17 mL/mol, respectively (23,24,25).

The calculated mean volume of activation ΔV^* associated with the reactions involved in activation of the sodium channels is about 30 mL/mol. Similar calculations for the volume of activation associated with the inactivation process of the sodium channel provide ΔV^* to be about 35 to 40 mL/mol. The volume of activation associated with the inactivation process is substantially higher than that of the activation process. This strongly supports the notion that the activation and inactivation processes are not coupled to each other (9).

Since the pressures of a few hundred atmospheres affect only noncovalent bonds, and further considering that the opening of the sodium channel is a two-step function, we can compare ΔV^* associated with the opening of the channel to ΔV^* for the breakdown of hydrogen bonds. We conclude that the opening of the sodium channel may be related to breakdown of about 5 to 6 hydrogen bonds in the channel protein.

Similar considerations regarding the inactivation process suggest that *either* the formation of hydrophobic interactions *or ionic bonds* are involved in the inactivation process.

The activation mechanism of the potassium channel also is slowed by the increased hydrostatic pressure. The ΔV^* calculated for the activation of the potassium channel is about 40 mL/mol. We therefore conclude that the opening of the potassium channel is associated with the formation of either ionic bonds or hydrophobic interactions. Armstrong (30), on the basis of the effects of tetraethylammonium compounds on the potassium currents has proposed an involvement of hydrophobic interactions in the potassium current gating mechanism.

The separate mechanisms of activation of the sodium and the potassium channel systems reaffirm the notion that these two channels are separate identities in the excitable membranes.

The effects of pressure on the rising phase of the action potential can be accounted for by the increase in τ_m. While the decrease in the rate of fall of the action potential, which is always larger than the decrease in the rate of rise at increased pressure, can be accounted for by increases in both τ_h and τ_n, the time constant for the sodium channel inactivation and the time constant for the activation of the potassium channel, respectively.

In summary, we would like to conclude that these features of channel architecture that we have just suggested only become experimentally apparent through the use of hydrostatic pressure to alter the physical environment of the activation and inactivation processes. By measuring quantitatively the changes of reaction rate for both sodium and potassium ions under pressure, we were able to understand the process of neural excitation in normal (1 atm) conditions and its function under increased pressure. These results demonstrate the value of hydrostatic pressure as an experimental factor in the study of membrane physiology.

Acknowledgments

References

1. Bennett PB. Performance impairment in deep diving due to nitrogen, helium, neon, and oxygen. In: Lambertsen CJ, ed. Underwater physiology. Proceedings of the third symposium on underwater physiology. Baltimore: William & Wilkins, 1967:327–340.
2. Zaltsman GL. Obschchiye cherty epilepticheskovi narkoitcheskovo lipore raspada funksii tsentralnoi nervnoi systemy. In: Zaltsman GL, ed. Giperliaricheskive Epilipsia; narcos. Moscow: Izdat Nauke, 1968:243.
3. Brauer RW, Goldman SM, Beaver RW, Sheehan ME. N_2, H_2, and N_2O antagonisms of high pressure neurological syndrome in mice. Undersea Biomed Res 1974;1:59–72.
4. Hodgkin AL, Katz B. The effect of sodium ions on the electrical activity of the giant axon of the squid. J Physiol 1949;108:37–77.
5. Hille B. The permeability of the sodium channel to metal cations in myelinated nerve. J Gen Physiol 1972;59:637–658.
6. Armstrong CM. Ionic pores, gates, and gating currents. Rev Biophys 1974;7:179–210.
7. Tanford C. The hydrophobic effect and the organization of living matter. Science 1978;200:1012–1018.
8. Singer SL, Nicolson GL. The fluid mosaic model of the structure of cell membranes. Science 1972;175:720–731.
9. Hodgkin AL, Huxley AF. A quantitative description of membrane currents and its application to conduction and excitation in nerve. J Physiol 1952;117:500–544.
10. Frankenhaeuser B. A quantitative description of potassium currents in myelinated nerve fibers of xenopus laevis. J Physiol 1963;169:424–430.
11. Goldman L, Schauf CL. Quantitative description of sodium and potassium currents and computed action potentials in Myxicola giant axons. J Gen Physiol 1973;61:361–384.

12. Adrian RH, Chandler AL, Hodgkin AL. Voltage clamp experiments in striated muscle fibers. J Physiol 1970;208:607–644.
13. Armstrong CM, Bezanilla F. Charge movement associated with the opening and closing of the activation gates of the Na channel. J Gen Physiol 1974;63:533–552.
14. Keynes RD, Rojas E. Kinetics and steady-rate properties of the charged system controlling sodium conductance in the squid giant axon. J Physiol 1974;239:393–434.
15. Hodgkin AL. Excitation and conduction in nerve. Quantitative analysis (Noble Lecture). Science 1964;145:1154–1159.
16. Noble D. Application of Hodgkin-Huxley equations to excitable tissues. Physiol Rev 1966;46:1–50.
17. Hille B. The permeability of the sodium channel to organic cations in myelinated nerve. J Gen Physiol 1971;58:599–619.
18. Hille B. Ionic selectivity of Na and K channels of nerve membranes. In: Eisenman G, ed. Membranes Vol. 3. New York: Dekkar, Marcel, Inc., 1975:256–323.
19. Hoyt RC. Sodium inactivation in nerve fibers. Biophy J 1968;8:1074–1097.
20. Peganov E, Timin E, Khodorov B. Interrelationship between the progress of sodium activation and inactivation. Bull Exp Biol Med USSR 1973;10:7–11.
21. Goldman L. Kinetics of channel gating in excitable membrane. Rev Biophy 1976;9:449–526.
22. Johnson FH, Eyring H, Stover BJ. The theory of rate processes. In: Biology and Medicine. New York: John Wiley & Sons, Inc. 1974.
23. Suzuki K, Taniguchi Y. The effect of pressure on biopolymers and model systems. Symp Soc Exp Biol 1972;26:103–124.
24. Davis JS, Gutfreund H. The scope of moderate pressure changes for kinetic and equilibrium studies of biological systems. Fed Exp Biol Soc Lett 1976;72:199–207.
25. Shrivastav BB, Parmentier JL. Hydrostatic pressure as a tool in electrophysiology. In: Fink BR, ed. Molecular mechanism of anesthesia (Progress in anesthesiology) Vol. 2. New York: Raven Press, 1980:297–304.
26. Kirsch GE, Narahashi T. 3,4-Diaminopyridine: a potent new potassium channel blocker. Biophys J 1978;22:507–512.
27. Parmentier JL, Shrivastav BB, Bennett PB, Wilson KM. A versatile high pressure chamber for electrophysiological measurements. J Appl Physiol 1980;48(3):562–566.
28. Cole KC, Moore JW. Liquid junction and membrane potential of the squid giant axon. J Gen Physiol 1960;43:971–980.
29. Hille B. A pharmacological analysis of ionic channels of nerve. Ph.D. Thesis, New York: The Rockefeller University, 1967.
30. Armstrong CM. Interaction of tetraethylammonium ion derivatives with the potassium channels of giant axons. J Gen Physiol 1971;58:413–437.

TRANSIENT VERSUS STEADY-STATE EFFECTS OF HIGH HYDROSTATIC PRESSURE

*K. T. Wann, A. G. Macdonald, A. A. Harper,
and M. L. J. Ashford*

The effects of high hydrostatic pressure on the electrical activity of a variety of excitable cells have now been described (1). The basis of pressure-induced changes in the properties of excitable cells is, however, not well understood. In this paper we draw attention to the possibility that in many experiments high pressure simultaneously affects several cellular activities with the consequence that the cell's electrical response to pressure is not a simple one. In particular, we distinguish between the transient and the steady-state effects of high pressure which we have observed. We have not sought to investigate systematically the transient effects. Indeed, in some studies the nature of the pressure profile or the temperature changes associated with pressurization have made it impossible to determine whether transient effects do occur. Pressurization produces small transient temperature changes ($\sim$ 1°C) in the experiments to be described, and, regrettably, there are very few Q_{10} data at pressure to enable the appropriate corrections to be made. Such small temperature changes still complicate the interpretation of any transient changes in electrical activity produced by high pressure, and are therefore discussed where relevant.

METHODS AND MATERIALS

The studies described here have been performed with in vitro preparations. Many data have been obtained from the neurones of the suboesophageal ganglionic mass of the snail *Helix pomatia* or *aspersa*, but we also describe

experiments recording miniature end-plate currents (MEPCs) or miniature end-plate potentials (MEPPs) from the sartorius muscle of the frog *Rana temporaria* or *pipiens*. Our pressure techniques have been described in detail elsewhere (2). In all of the experiments hydrostatic pressure was used, the compressium medium being light mineral oil, and pressure was usually applied in steps of 5.2 MPa every 5 min. In the end-plate studies steps of 1.03 MPa were applied at 1-min intervals.

RESULTS

Hydrostatic pressure produces significant changes in the passive electrical characteristics of *Helix* ganglion cells. Over the pressure range 0.1–35.8 MPa depolarization and a concomitant reduction in input resistance are observed. What is additionally interesting is that at normal temperature ($\sim$ 20°C) the initial depolarization is maximum within seconds of applying the pressure step, and during a 5-min period at pressure the resting membrane potential partially recovers to its precompression value. Such overshoot behavior is most commonly seen at higher pressures (> 10.4 MPa) and the time constant of the recovery is typically 2–3 min at temperatures of 18°–24°C. The steady-state depolarization observed after 5 min at the new pressure is variable and in quiescent cells a maximum depolarization of approximately 15 mV is produced by 35.8 MPa. On compression at lower temperatures (< 7°C) we find that the transient resting membrane potential changes are absent and the steady-state depolarization is close to the steady-state level observed with compression at higher temperatures.

We have not measured changes in input resistance of *Helix* neurones immediately after applying pressure so we do not know whether transient changes in this parameter occur. In both single and twin microelectrode studies where measurements were taken after 2–10 min at pressure (10.4–20.8 MPa), we have found that high pressure reduces the input resistance. From voltage-clamp experiments it is clear that high pressure increases the leakage conductance of *Helix* neurones, in confirmation of our input resistance data. These results contrast with previous findings with lobster fibers and the squid axon (3,4).

We tentatively conclude that although the depolarization of *Helix* ganglion cells is produced by an increase in the somatic membrane permeability, secondary changes in the cell could be responsible for the recovery phase. One possibility is that small changes in ionic balance occur which subsequently offset the initial effect of pressure on the resting membrane potential.

Higher pressures (> 10.4 MPa) produce variable effects on the electrical threshold of *Helix* ganglion cells. This has been assessed in single microelectrode studies by injecting depolarizing currents of 50–500 ms duration across the cell membrane. Pressure often depresses excitability and, again, its effect is greatest initially on compression, and excitability can return to precompression values during a 1½ to 2-min stay at pressure. The temperature increment associated with pressurization in these experiments is <1°C.

In experiments with cells which are not isolated from synaptic input it might be argued that the effects of pressure on excitability are due to altered synaptic bombardment of the impaled cell. However we find that pressure depresses fast excitatory synaptic transmission in *Helix* neurones without any obvious transient or overshoot effects.

In view of these effects of pressure on resting membrane potential, input resistance, threshold and synaptic transmission, it is not surprising that the pattern of spontaneously generated action potentials of many ganglion cells is altered in an erratic way by pressure. We distinguish four types of behavior.

Firstly, high pressure can convert a rhythmically discharging firing pattern into a periodic bursting pattern. With increased pressure there is a gradual transition from one type of activity to the other. The total action potential output of the cell remains at about control value.

Secondly, the firing frequency of cells which are synaptically driven is decreased by high pressure (> 5.2 MPa), but the firing pattern remains regular. In this case, however, both transient and steady-state effects are observed following both compression and decompression (Fig. 1). This behavior is reminiscent of the effects of hydrostatic pressure on ciliary frequency (5,6). An additional point of interest is that the time course of the overshoot on compression approximately corresponds to the time course of the threshold changes described above.

Thirdly, the firing frequency of pacemaker cells in increased by high pressure (> 5.2 MPa). Again, the firing remains rhythmic and is characterized by an initial rise in frequency followed by a decline to the steady-state level. In this case the changes in firing frequency match the resting membrane potential changes described above.

Finally, high pressure may have a variety of effects on the firing pattern of a nerve cell. Figure 2 shows the complicated response of an unidentified *Helix* nerve cell to three pressure steps. When pressure is applied (0.1–5.2 MPa) there is little effect initially, then the frequency declines to below control value (A). A second pressure step (5.2–10.4 MPa) accelerates firing transiently, then the frequency of firing drops further below the control level (B). Note, however, that the frequency returns to the level prior to the second pressure step after 5 min (beginning of C). The third pressure step from 10.4–15.6 MPa halts firing transiently, then the firing frequency returns to the level recorded before the third step.

This experiment illustrates that high pressure can produce a variety of transient effects and that these can be either excitatory (B) or depressant (C).

One last general point is that the magnitude of the transient effects described for all parameters in *Helix* neurones is a function of the rate of compression and the magnitude of the pressure step. Thus transient effects are more pronounced if compression is applied rapidly and the compression step is large.

Other experiments using the amphibian neuromuscular junction have confirmed that the transient responses to compression are not only confined to electrophysiological measurements with *Helix* nerve cells. The processes con-
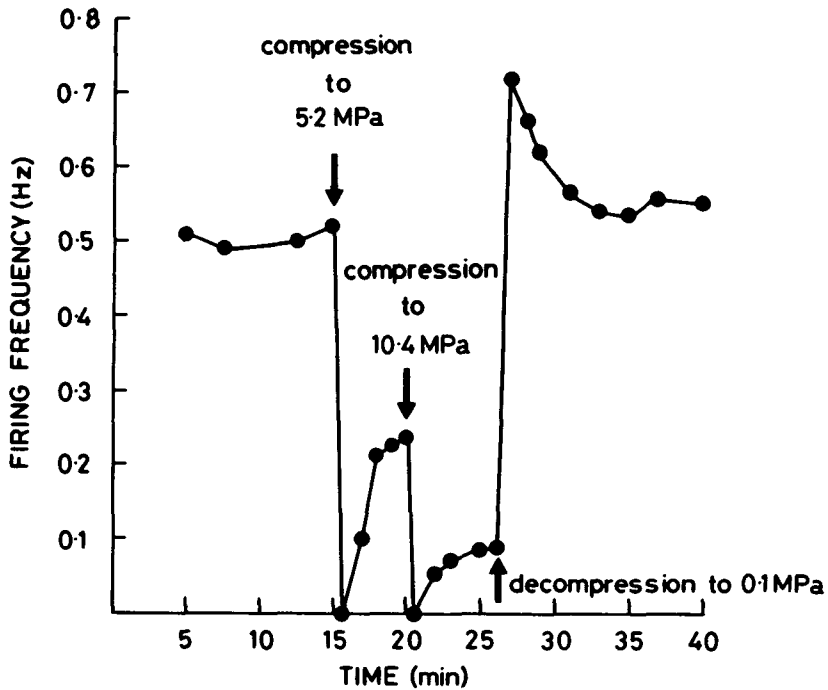
Fig. 1. The effects of hydrostatic pressure on the firing frequency of a synaptically driven *Helix* ganglion cell. Overshoot was observed on both compression and decompression.
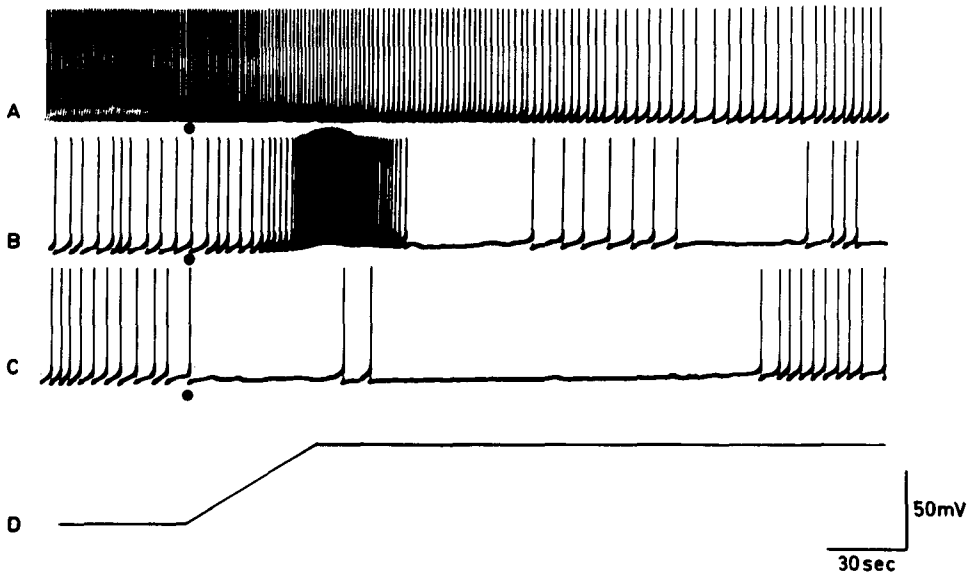
Fig. 2. The effect of hydrostatic pressure on the firing frequency of a *Helix* ganglion cell. The pressure steps were applied at the times indicated by ●. The steps were (*A*) 0.1–5.2 MPa, (*B*) 5.2–10.4 MPa, (*C*) 10.4–15.6 MPa. The pressure "profile" for each step is shown in *D*.

trolling transmitter release are very sensitive to pressure and at 10.4 MPa the quantal release of transmitter is almost entirely abolished (7). In some experiments the response to pressure is more complex, however, and MEPC or MEPP frequency recovers to a value closer to precompression levels after a short stay at pressure. Figure 3 shows an example of such overshoot behavior. A small pressure step (1 MPa) applied during the recovery period causes once again a reduction in frequency. On decompression the frequency can also overshoot the control value. These overshoot effects resemble the results obtained with rhythmically firing *Helix* ganglion cells (Fig. 1).

DISCUSSION AND CONCLUSION

There are clearly several transient effects of pressure on the electrical properties of the two preparations discussed. Previously, it has been observed that high pressure can produce transient changes in ciliary beating (5), cardiac beating frequency (8,9), and the evoked luminescence of *Chaetopterus* (10). In attempting to interpret such behavior we must be aware of the possibility that small temperature fluctuations associated with compression and decompression will complicate the picture. In the more recent experiments we can be more certain of such temperature changes (e.g., 9). We believe that the overshoot
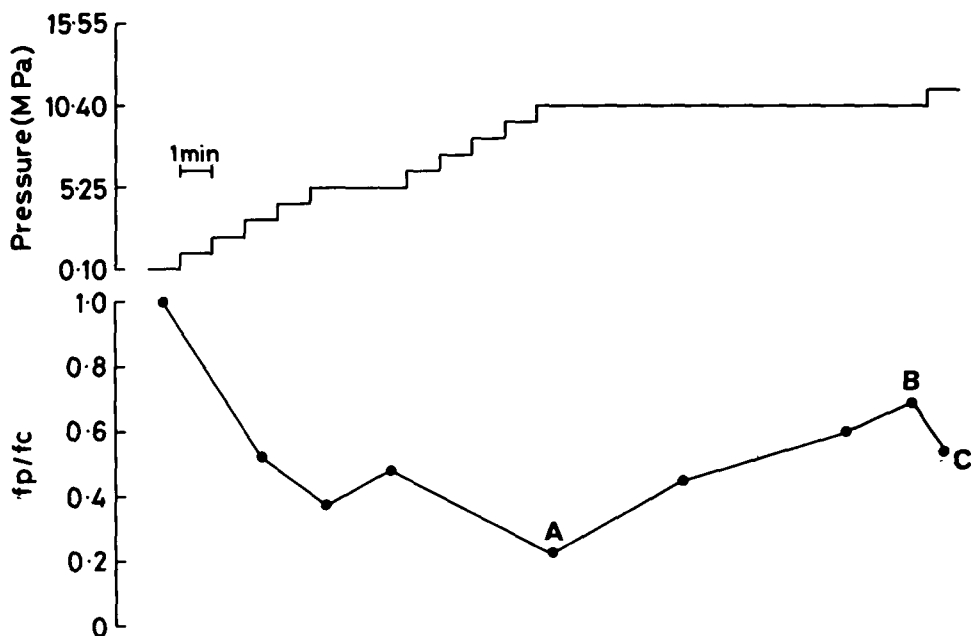
Fig. 3.   The effect of hydrostatic pressure on MEPC frequency recorded at the frog neuromuscular junction. Frequency was measured at 1 atm or 0.1 MPa (fc) and at pressure (fp) and the data are presented as the ratio fp/fc. Note the recovery between *A* and *B* and the effect of a small pressure step during this period (*C*).

effects on compression which have been discussed in our experiments are un-likely to be due to the small temperature increment. An increase in tempera-ture generally produces hyperpolarization and an increase in excitability of *He-lix* ganglion cells. In our studies high pressure, with the associated small temperature increase, depolarizes and reduces the excitability of *Helix* ganglion cells. The temperature change is also too small to account for the partial re-covery of the resting membrane potential or excitability observed at pressure. Similarly, the temperature increase is too small to account for the increase in MEPC frequency observed after a period at pressure (Fig. 3).

How do we explain the transient effects produced by pressure? It has been suggested that the changes in ciliary activity following pressurization can be explained if it is assumed that the activity is dependent on the rate of two consecutive reactions (11). This approach is difficult to apply to excitable cells since little is known about the chemical reactions controlling the electrical be-havior of neurones. Interestingly, it has been argued that the discharge fre-quency of invertebrate neurones can be modulated by the activity of two mem-brane-bound enzymes, phosphofructokinase (PFK) and fructose-1, 6-diphosphatase (FDPase) (12). These enzymes determine the rate and direction of gluconeoge-nesis and glycolysis, respectively. Associated with the PFK-FDPase cycle are oscillations in membrane potential. In view of the effects of high pressure on the firing pattern of *Helix* neurones it may prove interesting to examine the effects of pressure on the PFK-FDPase cycle.

The initial depolarization of *Helix* neurones by high pressure is due to a passive permeability increase and we presume that Na^+ ions are involved. The recovery observed at normal temperatures may be due to activation of the elec-trogenic Na pump following the small amount of Na loading. The finding that such recovery is absent when the experiment is carried out at low temperature is consistent with this notion. It is necessary, however, to measure the ionic balance of these cells at pressure. The increase in MEPC frequency following the initial drop at pressure could conceivably be due to the same Na loading phenomenon. We are at present checking these possibilities.

The time course of the transient changes in activity should provide some clue to their basis. In our experiments the system often "relaxes" to a new equilibrium with a time constant of several minutes. Such behavior seems in-compatible with the view that high pressure is affecting only membrane struc-ture, e.g., ion channels.

We should ask why in certain cases high pressure produces no transient effect. For example, in experiments with *Helix* ganglion cells where the action potential shape has been monitored continuously during pressurization, there is no indication that there are transient changes (13). Also, at the amphibian end-plate high pressure prolongs the MEPC decay and no transient changes in this parameter are observed (7). Perhaps in these latter experiments at least the processes being studied are rate limited by one factor, e.g., the microviscosity of the membrane lipid. If pressure affects the microviscosity in a simple way then transient changes in decay rate might not be produced.

In our experiments we have used simple in vitro preparations. If our observations can be extended to more complex systems then it is clear that the analysis of the effects of high pressure on central nervous system function or whole animal behavior will be made all the more difficult. This must be particularly true when the rate of compression is being examined.

Acknowledgments

References

1. Wann KT, Macdonald AG. The effects of pressure on excitable cells. Comp Biochem Physiol 1980;66A(1):1–12.
2. Wann KT, Macdonald AG, Harper AA, Wilcock SE. Electrophysiological measurements at high hydrostatic pressure: methods for intracellular recording from isolated ganglia and for extracellular recording in vivo. Comp Biochem Physiol 1979;64A:141–147.
3. Campenot RB. The effects of high hydrostatic pressure on transmission at the crustacean neuromuscular junction. Comp Biochem Physiol 1975;52B:133–140.
4. Spyropoulos CS. The effects of hydrostatic pressure upon the normal and narcotized nerve fiber. J Gen Physiol 1957;40:849–857.
5. Peace DC, Kitching JA. The influence of hydrostatic pressure upon ciliary frequency. J Cell Comp Physiol 1939;14:135–142.
6. Coakley CJ, Holwill MEJ. Effects of pressure and temperature changes on the flagellar movement of Crithidia oncopelti. J Exp Biol 1974;60:605–629.
7. Ashford MLJ, Macdonald AG, Wann KT. Moderate hydrostatic pressures reduce the spontaneous release of transmitter in the frog. J Physiol 1979;292:44P.
8. Landau J, Marsland D. Temperature–pressure studies on the cardiac rate in tissue culture explants from heart of the tadpole (Rana pipiens). J Cell Comp Physiol 1952;40:367–381.
9. Ornhagen HCh, Hogan PM. Hydrostatic pressure and mammalian cardiac-pacemaker function. Undersea Biomed Res 1977;4:347–358.
10. Sie HC, Chang JC, Johnson FH. Pressure temperature-inhibitor relations in the luminescence of Chaetopterus variopedatus and its luminescent secretion. J Cell Comp Physiol 1958;52:195–225.
11. Johnson FH, Eyring H, Stover BJ. The theory of rate processes in biology and medicine. New York: Wiley-Interscience 1974:315–317.
12. Chaplain RA. Metabolic control of neuronal pacemaker activity and the rhythmic organization of central nervous functions. J Exp Biol 1979;81:113–130.
13. Harper AA, Macdonald AG, Wann KT. The action of high hydrostatic pressure on voltage-clamped Helix neurones. J Physiol 1977;273:70–71P.

THE EFFECTS OF HIGH PRESSURES OF INERT GASES ON CHOLINERGIC RECEPTOR BINDING AND FUNCTION

J. F. Sauter, L. Braswell, P. Wankowicz, and K. W. Miller

The ability of pressure to excite animals has been known for about a hundred years (1). Nonetheless, little detailed progress has been made towards understanding the underlying events. Recently a number of workers have begun to explore the electrophysiological changes which occur when pressure is raised. (These studies have been reviewed recently by Wann and Macdonald [2].) In addition to these pioneering studies, neurochemical data will be required if a complete description is to be arrived at. Such studies can directly answer questions such as, What is the effect of pressure on neurotransmitter release and binding, on cyclase activation, and so on?

One advantage of such studies would be that they can be readily applied to the central nervous system of animals. Because many of the manifestations of pressure excitability are thought to be central in origin, and because electrophysiological studies in the brain are difficult, one would expect a neurochemical approach to be particularly fruitful. Nonetheless, few such studies have been undertaken (3) and little has been done towards developing techniques. In this paper we examine the effects of pressure on [³H]-acetylcholine binding to the acetylcholine receptor using apparatus we have developed for performing filtration assays. Although we have applied this technique here to a peripheral synapse (to be described), with minor adaptions it could be used to study a wide variety of central receptors.

For these studies we chose the nicotinic cholinergic receptors that can be isolated from the electroplaque of certain electric fish. This synaptic membrane can be obtained in high yield and specific activity and offers the best model for studies on the postsynaptic mechanisms of action of pressure. Furthermore,

because electric tissue was developed from muscle cells, this synapse has many of the characteristics of the neuromuscular junction. Thus, the most powerful electrophysiological and biochemical techniques can both be brought to bear on the problem.

The effects of pressure on the neuromuscular junction have been studied. Campenot (7) found that end-plate potentials in lobster and crab neuromuscular junction were depressed by hydrostatic pressure (200 atm). In the crab this effect was overcome when higher stimulation frequencies were employed. Kendig and Cohen (4) showed that 137 atm of helium had no effect on the indirectly elicited electromyogram (EMG) of rat diaphragm unless the calcium concentration in the bath was lowered. They too believed pressure was exerting a presynaptic effect. More recently Wann et al. (5) have made more detailed studies of the frog neuromuscular junction. They found that hydrostatic pressure caused a marked reduction in miniature end-plate current (MEPC) frequency at 102 atm; a finding that indicates a reduction in transmitter release. At higher pressures the decay phase of the MEPC was lengthened from a control value of 1.5 ms to a value of 2.1 ms at 153 atm. Their results suggested that the rate process governing decay has an activation volume of 56 mL mol^{-1}.

METHODS

Preparation of Acetylcholine Receptor-Rich Membranes

The method outlined here was adapted from Cohen et al. (7). Briefly, 100 g of fresh skinned electric tissue, dissected from a chilled *Torpedo californica* immediately upon receipt, is minced and added to 200 mL of cold azide water, homogenized on a Vertis apparatus at full speed for 3 min, briefly sonicated and centrifuged at 5,000 xg for 10 min. The supernatant is filtered and centrifuged at 15,000 xg for 90 min. This pellet is resuspended in distilled water and centrifuged through a 1.08 M sucrose cushion at 80,000 xg for 90 min; this step removes much acetylcholinesterase. The soft pellets are resuspended in water and the hard pellet discarded. The resuspended pellet is placed on a sucrose gradient, consisting of equal volumes of 1.5, 1.4, 1.3, 1.2, 1.1, and 0.8 M sucrose and centrifuged at 80,000 xg for 4½ h. Fractions of 1 mL are fractions collected from the bottom and assayed for acetylcholine receptors (AchR) using a tritiated snake toxin (a kind gift to us from J.B. Cohen), acetylcholinesterase (AchE), protein, and sucrose.

The sucrose gradient profile from an experiment is shown in Fig. 1. The specific activity in the pooled receptor peak is usually 1–3 μmol AchR/g protein. Receptor is stored at 4°C as collected. For critical use it is used within 3 weeks, but activity is usually present even after several months. The membranes may also be frozen and later thawed on ice as required.

Distribution of $[^3H]$ α-Toxin, Acetylcholinesterase and Protein in a Sucrose Gradient after Ultracentrifugation of a Homogenate of <u>Fresh</u> Torpedo California Electric Organ.
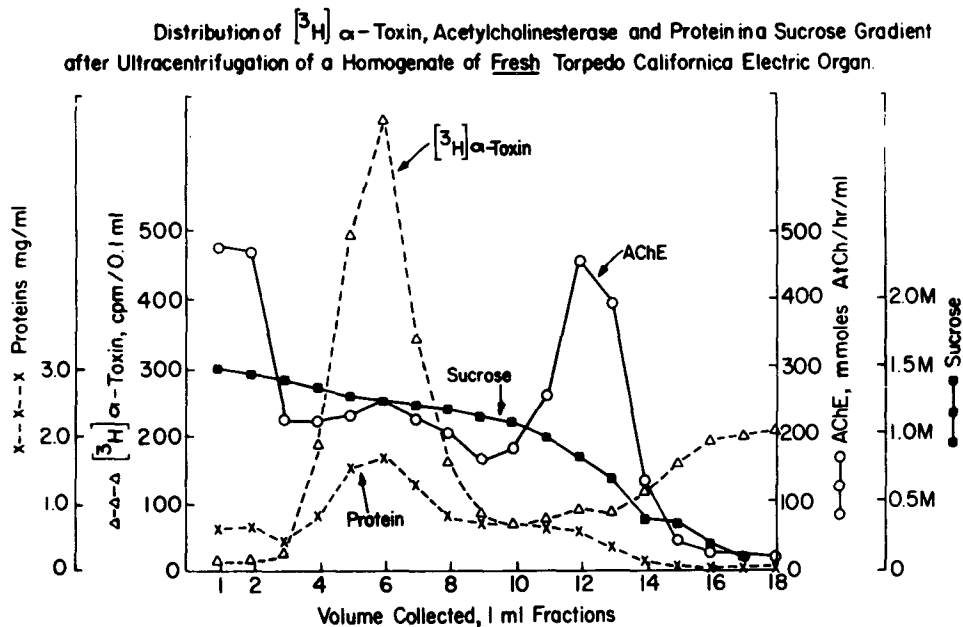
Fig. 1.   Profile of a sucrose density gradient used in the final step of the isolation of acetylcholine receptor-rich membranes from *Torpedo californica*. The α-toxin marks the position of the receptor containing membranes.

Binding of [³H]-Acetylcholine to Membranes

The equilibrium binding of [³H]-acetylcholine (Amersham-Searle, Arlington Heights, IL) to receptor containing membranes was determined by filter assay. Whatman GFF glass fiber filters are used to separate the membranes from the buffer once the equilibrium is attained. The amount of acetylcholine bound is determined from the difference between total counts and the counts in the filtrate. The difference between the amount bound in the presence and absence of excess α-bungarotoxin is defined as *specific binding*. This correction is only a few percent of the bound ligand. Because AchE is present (Fig. 1), its activity must be inhibited with di-isopropylfuorophosphate (DFP). Typically, 1.2 mL of AchR stock solution (3μM, in sucrose) is diluted to 13.5 mL with Torpedo Ringer (250 mM NaCl, 5 mM KCl, 3 mM CaCl₂, 5 mM sodium phosphate, pH 7) and mixed with 1.5 mL of 10⁻³M DFP. Controls show these conditions block all the AchE activity after 30 min incubation. Finally, this preparation is split into aliquots and diluted to give the final AchR concentrations noted in results. These are usually in the range of 20–50 nM. [³H]-acetylcholine is allowed to equilibrate with the membranes for 30 min before filtration.

The kinetics of acetylcholine binding to its receptor were determined similarly except that equal aliquots of receptor suspension and of [^{3}H]-acetylcholine are mixed rapidly at zero time and the amount of binding determined as a function of time.

Filtration Assays at Pressure

Work in hyperbaric gaseous environments is carried out in an 8-inch diameter steel chamber capable of working to 300 atm. Twelve filtration units are mounted on a turntable in the chamber. They may be moved in turn to a position where they may be remotely connected to the outside of the chamber thus providing suction. This process is operated and timed by a microprocessor that gives smooth, reproducible filtering. Solutions to be filtered may be placed above the filters on diaphragms that rupture at the commencement of filtration, or may be delivered from motor-driven syringes. Incubating mixtures may be stirred magnetically. A more detailed description of this apparatus has been given (8).

RESULTS

We first determined whether exposure to 300 atm of helium caused irreversible effects on the receptor containing membranes. The incubation wells of the 12 filtration units were filled with receptors and [^{3}H]-acetylcholine. Six units were filtered in the chamber at 10 atm of helium. (A small amount of pressure is necessary to ensure filtration. The remaining receptors were compressed to 300 atm, held for 30 min, and slowly decompressed to 10 atm, where they were filtered. The amount of acetylcholine bound was the same in both sets of filters.

We next examined the effects of helium pressure on binding. A simple assay was used in which the incubation mixture contained sufficient [^{3}H]-acetylcholine to half-saturate the receptor sites. The ratio of the concentration of bound acetylcholine to that of free acetylcholine changed from 1.0 to 0.71 at 300 atm. A similar effect was observed with the antagonist [^{3}H]-d-tubocurarine. The cause of this decrease could either be loss of receptor sites or a reduction in affinity, that is, an increase in dissociation constant, K_d. Accordingly, receptor containing membranes were equilibrated with a wide range of [^{3}H]-acetylcholine concentrations. The receptor sites were progressively saturated as the [^{3}H]-acetylcholine concentration was raised. On the bench filtration assays typically yield binding curves that exhibit positive co-operativity with a Hill coefficient of about 1.5 and a Hill dissociation constant of 20 $\pm$ 9 nM, where the variation reflects the difference between different batches of receptor and not the experimental error. In one experiment shown in Fig. 2, the Hill dissociation constant, K_d, decreased from 16 $\pm$ 2.2 nM at 5 atm to 23 $\pm$ 3.2 nM at 275 atm of helium, whereas the Hill coefficient, n_H, which was 1.5, did not change. Two such experiments have been performed up to this time and the mean ratio of the K_d at high pressure to that at low pressure was 2.6 $\pm$ 0.7. The binding of acetylcholine is a complex process, but if we make
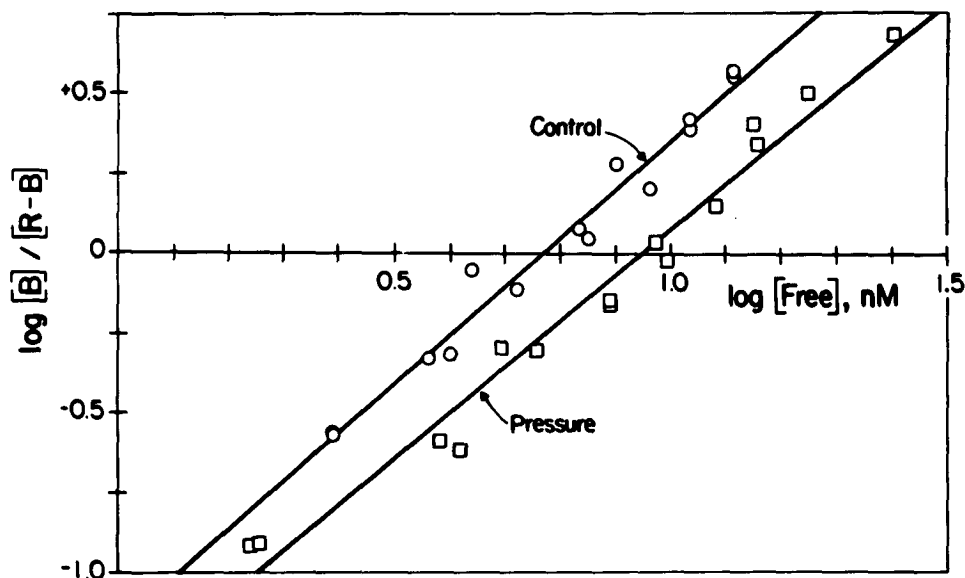
Fig. 2. Hill plot of the effect of pressure (275 atm) on specific [³H]-acetylcholine binding to *Torpedo* membranes. B is bound acetylcholine and R is the total receptor binding sites (~30 nM). Pressure decreases the binding affinity without changing the slope.

the simplifying assumption that the K_d represents an equilibrium we may calculate thermodynamically that a volume change of 80 ± 30 mL/mol is involved in the overall processes involved in acetylcholine binding.

To understand the origins of the effects of pressure on acetylcholine binding, detailed kinetic experiments will be required. These are technically very demanding and only preliminary results are available at pressure. The binding of [³H]-acetylcholine is biphasic. An initial rapid binding step, which is too fast to follow experimentally, is followed by a slow phase with a time constant of a few minutes (Fig. 3). This second step can be characterized kinetically. The observed rate constant is usually in the range 5-8 × $10^{-3}s^{-1}$. Figure 3 shows a pair of experiments conducted within a few days of each other on the same membrane preparation. The rate constant at 300 atm is decreased relative to that at 10 atm by by a factor of 1.6, but the value at pressure is close to the range of values generally obtained on the bench. Thus, further work will be required to establish the significance of the change seen here. In addition, if the slow phase extrapolated back to zero time, the intercept yields an estimate of the amplitude of the fast phase. This is slightly decreased by pressure.

It is of interest to ask if the other diving gases cause effects similar to those of helium. Our preliminary data show that in fact they cause changes in the opposite direction. After 30 min stirring to equilibrate with the gaseous atmosphere, both nitrous oxide (3.5 and 6 atm) and argon (100 atm) caused increases in [³H]-acetylcholine binding (Table I).
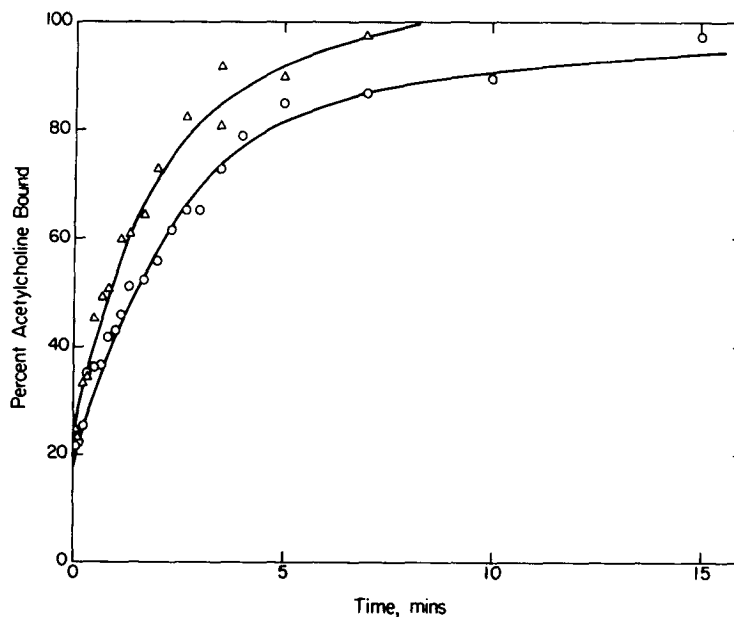
Fig. 3. The kinetics of binding of [³H]-acetylcholine to *Torpedo californica* receptor-rich membranes. Both experiments were carried out in the pressure chamber.   Δ: 5 atm of helium, [AchR] = 25 nM, [Ach] = 48 nM; rate constant = 7.7 ± 0.84 × $10^{-3}s^{-1}$.   O: 300 atm of helium. [AchR] = 27 nM, [Ach] = 50 nM; rate constant = 4.7 ± 0.17 × $10^{-3}s^{-1}$.

TABLE I

Change in [³H]-Acetylcholine Binding to *Torpedo californica* Receptor-Rich Membranes After Exposure to Inert Gases for 30 Min

Gas	Pressure (ATA)	[Bound Acetylcholine]/[Free Acetylcholine]
Air	1	1.00
Helium	300	0.75
Argon	100	1.37
Nitrous Oxide	3.5	1.25
Nitrous Oxide	6.0	2.04

DISCUSSION

Although this research is ongoing and much of the quantitative data are still incomplete, certain qualitative conclusions stand out. First, the effects of inert gases on the binding of [³H]-acetylcholine to its receptor follow a similar pattern to that observed in the behavior of animals. In animals helium at pressure causes excitation while argon and nitrous oxide cause depression and general anesthesia (9,10). The sign, or direction, of the effect changes when helium is compared to the other gases. Similarly, the direction of the effect on

acetylcholine binding changes. Binding decreases with helium, whereas it in-creases with argon and nitrous oxide. When the underlying mechanisms of these effects are finally established it is possible that they will bear some simi-larities to the events occurring in vivo.

The effects of helium pressure we have investigated in some detail. The binding of acetylcholine to its receptor is a complex process, which may be represented approximately as

$$A + R \rightleftharpoons AR_o$$
$$\updownarrow \qquad \updownarrow$$
$$A + R' \rightleftharpoons AR'$$
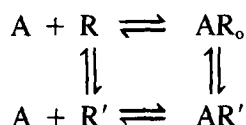
where A is acetylcholine, R is resting receptor, R_o is receptor associated with an open channel, and R' is desensitized (that is, inactive) receptor (11). Thus, the overall equilibrium measured for acetylcholine binding represents the sum of several processes (12,13). Our results show that pressure changes the over-all dissociation constant without changing the cooperativity of binding (Hill coefficient). Such cooperativity suggests that more than one acetylcholine mol-ecule binds to each receptor molecule. Available data suggest there are two acetylcholine binding sites per receptor complex (14,15). Thus, pressure has no effects on the allosteric interactions between these sites.

To define which steps in the cyclic scheme above are effected by pressure requires more detailed kinetic studies. Our studies up to this time (Fig. 3) uti-lize the fact that R binds acetylcholine with much lower affinity than R' and also that the vertical equilibria are slow and the horizontal ones very fast. Therefore, the initial concentration of acetylcholine can be adjusted so that ini-tially all R' is bound rapidly but no R binds. Then, as R $\longrightarrow$ R', attempting to re-establish the equilibrium, more acetylcholine will bind at a rate representing the rate of formation of R'. This is the situation shown Fig. 3. This single experiment, which requires confirmation, suggests that the resting amount of R' is slightly reduced by pressure while, consistently, the rate of R $\longrightarrow$ R' is reduced. These effects are small but, if confirmed, would suggest that pressure does not act only at this step because the change in overall dissociation con-stant is too large. In particular, one might expect that if the binding of acetyl-choline (a cation) to R' involves any charge neutralization, a positive volume change would occur because of the release of electrostricted water (16). The dissociation constant for this step would also be increased. If this turns out to be true, then pressure acts both on R $\longrightarrow$ R' and A + R' $\longrightarrow$ AR'.

It is important to realize that the most critical reason why our results on the effects of pressure are tentative is that the effects in the pressure range studied (up to 300 atm) are fairly small and therefore require accurate quantita-tion. We can say from Fig. 3 that the conformational change R $\longrightarrow$ R' is af-fected little by pressure, even though several more experiments will be re-quired before we can be certain how small the effect is. The rate of decay of

MEPCs in frog is also decreased only 1.4 fold by 154 atm (5). This can approximately be taken as a measure of the effects of pressure on $AR_o \longrightarrow AR'$. Our results for $R \longrightarrow R'$ yield an activation volume of 45 mL/mol, whereas the latter data for $AR_o \longrightarrow AR'$ yield 56 mL/mol. Thus, both conformation changes in this membrane protein are associated with similar volume changes.

We have not yet investigated in detail how the effects of other gases, such as argon, are brought about. What we know so far suggests they act in a similar manner to the volatile anesthetics (17,18). These agents increase acetylcholine binding and can increase the proportion of R' in the resting state.

This work clearly demonstrates that biochemical techniques can be applied to the study of ligand binding to postsynaptic membranes in hyperbaric gaseous environments. The data reported here concern a peripheral synapse from a fish adapted to moderate pressures. Nonetheless, it exhibits many of the expected properties. It thus serves as a useful model for the detailed elucidation of the underlying mechanisms. These techniques can also be applied, though not in such a detailed manner, to central mammalian synaptic membranes. It remains to be seen whether the effects of pressure on these will be more profound.

References

1. Regnard P. Recherches experimentals sur les conditions physiques de la vie dans les eaux. Paris: Masson, 1891.
2. Wann KT, Macdonald AG. The effects of pressure on excitable cells. Comp Biochem Physiol 1980; 66A:1-12
3. Fish E, Shankaran R, Hsia JC. High pressure neurological syndrome: antagonistic effects of helium pressure and inhalation anesthetics on the dopamine sensitive cyclic AMP response. Undersea Biomed Res 1979;6:189-196.
4. Kendig JJ, Cohen EN. Neuromuscular function at hyperbaric pressures: pressure-anesthetic interactions. Amer J Physiol 1976;230:1244-1249.
5. Wann KT, Ashford M, Macdonald AG. The effect of alcohol anaesthetics and high hydrostatic pressure on spontaneous activity at the neuromuscular junction. J Physiol (in press).
6. Miller KW. The role of the critical volume theory. In: Daniels S, Little HJ, eds. The effects of pressure and the use of pressure in studies on anaesthesia, Oxford: 1978:60-63.
7. Cohen JB, Weber M, Huchet M, Changeux J-P. Purification from *Torpedo marmorata* electric tissue of membrane fragments particularly rich in cholinergic receptor protein. FEBS Letters 1972;26:43-47.
8. Sauter J-F, Wankowicz PG, Miller KW. An apparatus for performing filtration assays in hyperbaric atmospheres. Undersea Biomed Res 1980;7:257-263.
9. Brauer RW, Goldman SM, Beaver RW, Sheehan ME. N_2, H_2 and N_2O antagonism of high pressure neurological syndrome in mice. Undersea Biomed Res 1974;1:59-72.
10. Miller K. The opposing physiological effects of high pressure and inert gases. Fed Proc 1977;36:1663-1667.
11. Katz B, Thesleff S. A study of the desensitization produced by acetylcholine at the motor end-plate. J Physiol 1957;138:63-80.
12. Sugiyama H. The mode of action of the nicotinic cholinergic receptor protein in the postsynaptic membrane. Adv Biophys 1978;10:1-25.
13. Cohen JB, Boyd ND. Conformational transitions of the membrane-bound cholinergic receptor. In: Pullman B, Ginsgurg D, eds. Catalysis in chemistry and biochemistry. Dordrecht: Reidel, 1979:293-304.

14. Karlin A, Damle V, Hamilton S, McLaughlin M, Valderamma R, Wise D. Acetylcholine receptors in and out of membranes. In: Ceccarelli B, Clementi F, eds. Advances in cytopharmacology, 3. New York: Raven Press, 1979:183–189.

15. Neubig RR, Cohen JB. Equilibrium binding of tubocurarine and acetylcholine by Torpedo postsynaptic membranes: stoichiometry and ligand interactions. Biochem 1979;18:5464–5475.

16. Hills G. The physics and chemistry of high pressures. In: Sleigh MA, MacDonald AG, eds. The effects of pressures on organisms. Cambridge: University Press, 1972:1–26.

17. Sauter J-F, Braswell LM, Miller KW. Action of anesthetics and high pressure on cholinergic membranes. In: Fink BR, ed. Molecular mechanisms in anesthesia. Vol. 2. New York: Raven Press, 1980:191–207.

18. Young AP, Sigman DS. Allosteric facilitation of in vitro desensitization of the acetylcholine receptor by volatile anesthetics. In: Fink BR, ed. Molecular mechanisms in anesthesia. Vol. 2. New York: Raven Press, 1980:209–228.

PART VI. DISCUSSION: MOLECULAR AND CELLULAR EFFECTS OF HYDROSTATIC PRESSURE

A. G. Macdonald, *Rapporteur*

Each paper in this session prompted a number of questions but they varied considerably and no particular theme emerged in a coherent discussion. This indicates the extremely primitive state of knowledge in the field and the wide range of phenomena described. Virus multiplication, ionic regulation, membrane currents, transmitter release, and binding studies are all well-developed fields of research, and to study the effects of high pressure on these phenomena at a level which leads to satisfactory conclusions involves a great deal of advanced work. It is encouraging to see that this is being recognized and that specialists from the various branches of physiology are being attracted to the field of molecular and cellular pressure physiology.

A disconcerting feature, apparent in the comments of other speakers in other Sessions, was the premature acceptance of some generalizations about the effects of pressure. Thus, the last paper in the symposium, "The Efficacy of Spinal Anesthesia at High Pressure," was based on the assumption that if pressure modified the effect of the spinal anesthetics then it would diminish their effects. In fact, pressure-anesthetic interactions in synaptic preparations have been described in which pressure potentiates the action of the anesthetics, the reverse of what is seen in several whole-animal experiments. In such a potentially important clinical problem as spinal anesthesia in hyperbaric conditions, it is surely important to be alert to the possibility that pressure may enhance or reduce anesthetic potency and to design the experiments accordingly. The complexity of the effects of hydrostatic pressure has yet to be accepted by hyperbaric physicians and human physiologists.

A STUDY OF THE SPECIFIC ACTION OF "PER SE" HYDROSTATIC PRESSURE ON FISH CONSIDERED AS A PHYSIOLOGICAL MODEL

L. Barthélémy, A. Belaud, and A. Saliou

As a water-breather, the fish can be submitted either to the specific action of "per se" hydrostatic pressure (when compressed in a closed, soft chamber entirely filled with water) or to the influence of both pressure and hyperbaric inert gas tensions (when compressed in an open aquarium where bubbling achieves gas equilibration of the water and fish body compartments). In the latter condition, the density of the water remains unchanged whatever the nature or the pressure of inert gas. Hence, contrary to gas-breathers, the fish is not affected by changes in the mechanics of breathing.

Physiological modifications were observed in eels exposed to a 101 ATA hydrostatic pressure: increased activity, hyperventilation, increased metabolic rate, hemodynamical changes, tachycardia, EEG disorders (1). The purpose of the present investigation was a) to state the effects of "per se" hydrostatic pressure up to 151 ATA, and b) to investigate the combined actions of either inert gases or anesthetic drugs with the effects of hydrostatic pressure.

MATERIAL and METHODS

Rainbow trout (*Salmo gairdneri R.*), weighing between 100 and 200 g, were chronically implanted with opercular electrodes (for recording of ventilatory activity [2]), and with electroencephalographic electrodes (for recording spontaneous electrical activity from the *opticum tectum* and for obtaining visual evoked potentials (VEP)(3). Pressurization was obtained in a 130-L chamber, the portholes of which allowed visual observation of experimental fish kept in different aquariums according to the two devised hyperbaric conditions:

1) For per se hydrostatic pressure investigations, a 3-L glass container was completely filled with water and the large neck was covered by a gas-proof soft rubber membrane (Fig. 1A).

2) For combinations of inert gas tension (IGT) with hydrostatic pressure (HP), identical glass-containers were covered by a rubber membrane opening into a latex gas sock (Fig. 1B). The compressed gas mixture was passed through porous stone diffusers at a rate controlled by valves outside the chamber. The excess gas collected under the membrane and escaped through the latex gas sock. In the absence of gas admission the airtightness of the container was re-established because the latex lay flat on the rubber membrane. This container (represented in Fig. 1B) allowed either complete water saturation by gases when gas admission was maintained throughout the hyperbaric exposure, or partial equilibration by opportunely stopping the gas admission. A required IGT was reached in a given period of gas admission, which was calculated according to the previous measured time constant for gas equilibration in the container, composition of the gas mixture, and HP value. The experimental aquarium (Fig. 1B) offered the possibility of adding a given partial pressure of inert gas (less than ambient hydrostatic pressure) at any moment of the hyperbaric exposure.

The temperature was kept constant within the range 10–15°C, the oxygen partial pressure in water was initially 1 ATA and the compression rate was 10 atm·mn^{-1}.
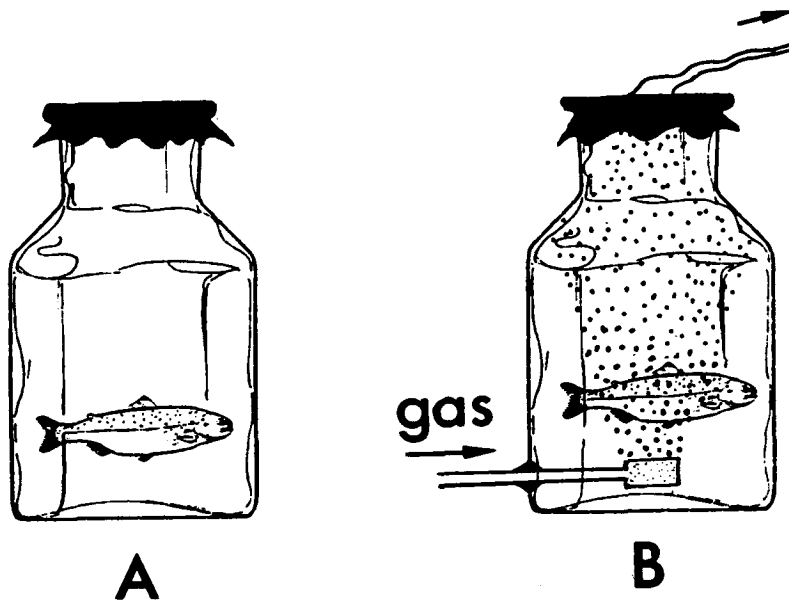
Fig. 1. Schematic representation of the two different kinds of hyperbaric conditions for the fish. A: Conditions of "per se" hydrostatic pressure; B: Combination of hydrostatic pressure action with gas effects (explanations in MATERIAL AND METHODS).

Anesthesia was induced either by methane tricaine sulfonate (MS_{222}) at a concentration of 35 mg·L^{-1} in water, or by pentobarbital (Nembutal) intraperitoneally injected with a 45 mg·kg^{-1} dosage and dissolved in water at the same concentration. These treatments led to a light anesthesia depth, i.e., motionless and feeble ventilatory activity that necessitates artificial assistance provided by an immersed pump.

RESULTS

Effects of "Per Se" HP on Unanesthetized Trout

Above a pressure threshold of about 20 ATA, the trout became more and more restless as the HP value increased; the eyes began a pendulous movement. The state of excitation was maximal at about 101 ATA. For higher pressures, the fits of restlessness and sudden starts were interrupted by periods of motionless and lack of equilibration in water, these periods were progressively preponderant. Under 151 ATA HP, the trout body was motionless and rigid, the eye movements lasted for a few minutes, and opercular movements ceased after about 5 min of exposure. The mean survival time under 151 ATA HP was 9 min (Table I). The trout examined after decompression were rigid, the gill covers were open, and large skin areas were discolored. The recordings of ventilatory activity showed, above 81 ATA, a progressive disorganization in the magnitude and pattern of opercular movements. Above 131 ATA, ventilatory frequency also became irregular. Anomalies in spontaneous electrical activity from *opticum tectum* were noticed above 51 ATA. They were slow (5 cps^{-1}), large waves, which appeared first as separated bursts and which tended to be predominant for higher pressures. The EEG activity progressively disappeared within the first 10 min of the 151 ATA hyperbaric stay. The magnitude of VEP decreased between 1 and 101 ATA while the latency period decreased. Between 101 and 151 ATA, the decrease in VEP magnitude was associated with an increase in latency duration. The VEP disappeared after 5 min of 151-ATA HP exposure.

Complementary investigations into the role of compression rate, oxygen partial pressure, metabolic rate, and the like were undertaken. A 3-h interruption in compression at 51 ATA allowed the fish to return to a calm state, but restlessness reappeared as soon as the compression was continued. A second interruption at 81 ATA for 5 h did not stop the fish excitation; under 151 ATA HP the survival time was identical to that of trout compressed without interruption. In some experiments, provision of oxygen to the trout was facilitated either by an intense artificial ventilation or by increasing the initial oxygen tension in water up to 2 ATA, but the compression syndromes and survival time under 151-ATA HP remained identical to those described before these complementary investigations. The fish reactions to HP were also unchanged in conditions of adaptation at 4°C, which decreased the metabolic rate. The ablation

TABLE I

Mean Survival Time (*expressed in hours*) in Trout, According to Different Hyperbaric Conditions

Conditions \ TEP	101 ATA	121 ATA	151 ATA
"Per se" HP (IGT = 0 ATA)	1.0 ± 0.5 (n = 15)	0.2 ± 0.05 (n = 8)	0.15 ± 0.1 (n = 10)
Saturation with He (IGT = TEP)	22.0 ± 4.0 (n = 5)	6.2 ± 2.0 (n = 4)	3.75 ± 0.9 (n = 5)
Saturation with N_2 (IGT = TEP)	1.55 ± 1.2 (n = 3)	< 0 (n = 3)	< 0 (n = 3)
"Per se" HP (Nembutal–anesthetized)			1.5 ± 0.5 (n = 9)
"Per se" HP (MS_{222}–anesthetized)			0.7 ± 0.2 (n = 8)
11 ATA N_2, then 140 ATA HP (IGT = 11 ATA)			0.1 ± 0.05 (n = 4)
30 ATA HP, then 11 ATA N_2, then 110 ATA HP (IGT = 11 ATA)			0.5 ± 0.2 (n = 5)
50 ATA HP, then 11 ATA N_2, then 90 ATA HP (IGT = 11 ATA)			1.0 ± 0.5 (n = 5)
80 ATA HP, then 11 ATA N_2, then 60 ATA HP (IGT = 11 ATA)			0.5 ± 0.3 (n = 5)

Values are means ± SE. TEP is total experimental pressure; HP is hydrostatic pressure; IGT is inert gas tension; n is number of subjects.

of the swim bladder or the implantation of tubes to equilibrate the pressure between the ambient water and the abdominal cavity were also without influence on the reactions to HP.

Effects of "Per Se" HP on Anesthetized Trout

The anesthetized trout were motionless, except for ventilatory activity that decreased in frequency and magnitude. As previously described (3), the spontaneous EEG activity slowed down and decreased in magnitude; the VEP were maintained but their morphology was simplified in relation to untreated trout.

In MS_{222}-anesthetized trout, the fits of restlessness and sudden starts appeared above 41 ATA and intensified under higher HP. Convulsive movements of fins or of the whole body were observed throughout the 151-ATA hyperbaric stay. The mean survival time was 42 min (Table I), i.e., greater than

that of untreated trout. The EEG activity decreased in magnitude and fre-
quency during compression. Under 151-ATA HP, the electrical activity from
opticum tectum progressively decreased in frequency. The VEP did not notice-
ably change during hyperbaric experimentation.

In Nembutal-treated trout, the compression did not develop any restless-
ness or convulsive movement. The mean survival time under 151 ATA was 90
min (Table I). The EEG activity was temporarily activated at the end of the
compression stage, as previously described (3).

Effects of Inert Gases Combined With Those of HP

Helium. In conditions of helium-equilibrated water under HP up to 151
ATA, the compression developed a) a phase of restlessness during compres-
sion, then a return to a calm state during the hyperbaric stay; b) a progressive
disorganization of ventilatory activity (changes in opercular movement pattern
that left magnitude or frequency unaffected); c) a slowing down in EEG mag-
nitude and rhythm beyond 6 h of exposure; d) a reversible decrease in VEP
magnitude during compression, followed by a biphasic evolution during the
hyperbaric exposure: first, an increase in magnitude, then a progressive de-
crease beyond 4 h of HP exposure. The VEP disappeared before ventilatory
and EEG arrest. Trout that died under high helium pressure were rigid but the
skin was not discolored. The survival time in helium-saturated water lay be-
tween 10 and 30 h under 101 ATA and between 1 and 5 under 151 ATA, i.e.,
greater than the survival time observed under "per se" HP (Table I).

The experimental aquarium allowed investigations into the mean survival
time under a given total experimental pressure (TEP) and in relation to the
inert gas tension (IGT). The results given in Table II show that the survival
time in every case increased proportionately to IGT value.

Nitrogen. In conditions of nitrogen-equilibrated water, the compression
induced a short phase of restlessness without sudden starts up to 71 ATA. For
higher pressure values, ventilatory activity decreased and the ventilatory rhythm
and pattern was disorganized. Under 101-ATA pressure, first the VEP and
then the spontaneous EEG activity disappeared within the first 30 min of hy-
perbaric stay. If the compression continued up to 151 ATA, the trout died be-
fore the end of the compression phase. The trout that died under such condi-
tions were not rigid or discolored.

In conditions of partial equilibration of water by nitrogen, for a given
TEP the increase of IGT lengthened the survival time as long as IGT remained
lower than 71 ATA. For higher IGT values, the survival time was reduced in
relation to "per se" HP conditions. The complete results are reported in Table
III, which indicates for each TEP value the most suitable combination TEP–IGT
for trout survival.

Table I indicates that the compression stage during which an 11-ATA ni-
trogen dosage was administered influenced the results. The most suitable mo-
ment of nitrogen administration for the survival of trout corresponds to the
pressurization stage of 51 ATA. The addition of nitrogen may either increase

TABLE II

Mean Survival Time (*expressed in hours*) of
Unanesthetized Trout Submitted to a TEP
and to a Helium IGT Administered at the Beginning of
Compression

IGT (ATA) / TEP	101	121	151
0 "per se" HP	1.00 ± 0.5 (n = 6)	0.2 ± 0.05 (n = 4)	0.1 ± 0.1 (n = 9)
11	4.25 ± 0.5 (n = 4)	2.0 ± 1.00 (n = 4)	0.3 ± 0.1 (n = 5)
71	—	3.5 ± 0.8 (n = 3)	0.98 ± 0.5 (n = 4)
101	22 ± 4.0 (n = 5)	—	—
121	—	6.2 ± 2.0 (n = 4)	—
151	—	—	3.75 ± 0.9 (n = 5)

Values are means ± SE. TEP is total experimental pressure; IGT is inert gas tension; HP is hydrostatic pressure; n is number of subjects. There was an increase of survival time proportional to IGT values.

or decrease the tolerance of trout exposed to HP, according to the amount of nitrogen and the moment of its administration.

DISCUSSION

Effects of "Per Se" HP

Two kinds of hypotheses can be considered to explain the effects of "per se" HP: a) hypotheses in which HP would stimulate the barosensitive organs of the fish, and b) hypotheses in which HP could be assimilated to a thermodynamic factor acting on the structures and functions of various cellular or subcellular elements. The barosensitivity of fish principally involves the swim bladder (4,5), which constitutes the main gaseous compartment of the fish body. As the results obtained either in cystectomized fish or in trout equipped

TABLE III

Mean Survival Time (*expressed in hours*) of
Unanesthetized Trout Submitted to a TEP
and to a Nitrogen IGT Administered at the Beginning of
Compression

TEP (ATA) / IGT (ATA)	101	121	151
0 ("per se" HP)	1.00 ± 0.5 (n = 6)	0.2 ± 0.05 (n = 4)	0.1 ± 0.1 (n = 9)
11	6.75 ± 0.5 (n = 4)	1.45 ± 0.3 (n = 4)	0.01* (n = 4)
41	8.5 ± 2 (n = 3)	1.5 ± 0.5 (n = 4)	0.8 ± 0.5 (n = 5)
61	12 ± 4 (n = 5)	1.55 ± 0.9 (n = 4)	0.16 ± 0.2 (n = 4)
101	1.55 ± 1.2 (n = 3)	< 0	< 0

Values are means ± SE. TEP is total experimental pressure; IGT is inert gas tension; HP is hydrostatic pressure; n is number of subjects. A nitrogen dosage lower than 61 ATA increased the survival time relative to "per se" HP conditions (IGT = 0). A nitrogen dosage of 61 ATA and more decreased the survival time.

with tubes for abdominal pressure equilibration are identical to those concerning intact trout, the first kind of hypothesis is not supported by the present investigation. The second kind of hypothesis involves the thermodynamic properties of HP: changes in structure of certain molecules resulting in changes in the chemical kinetics of metabolic chains (6,7); changes in protoplasmic consistence (8); and, particularly, changes in membrane functional properties because HP first affects the excitable cells (9,10). Miller (11) has stated that HP decreases the membrane volume (VM) and that functional troubles would occur when the decrease in VM is 1% higher than the initial VM value. So, this previously suggested hypothesis could explain the restlessness of the trout, the EEG and ventilatory disorders, and the discoloration phenomenon (cf. RESULTS).

Effects of HP Under Anesthesia

It is generally accepted that anesthetic drugs act principally at membrane level. The VM value increases in the presence of anesthetic drugs (11,12,13)

and anesthesia develops beyond a drug-concentration threshold, which pro-
vokes a membrane inflation above a critical volume. The increase in V_M is
tenfold greater than the volume of the drug itself, so the presence of the drug
modifies the molecular structures in the membrane, and results in membrane
distension.

Anesthetic drugs and HP each seem to act on the same structures, but in
an opposite direction if we consider only the changes in V_M. The above results
demonstrate that in trout anesthetic administration before compression in-
creases the survival time under pressure and reduces restlessness during
compression in relation to untreated fish. Hence, HP and anesthetic drugs act
in opposite directions on the trout body as a whole.

Combined Effects of HP and IGT

In fish, gas dissolution in water does not alter the mechanics of breathing,
(whatever the nature) or the pressure of the dissolved gases.

As anesthetic drugs, helium and nitrogen (in certain conditions of admin-
istration for nitrogen) may extend the survival time under HP. This similitude
in action between anesthetics and inert gases leads to the consideration that
helium and nitrogen both exhibit "narcotic" properties that antagonize the HP
action. Helium antagonizes the HP action at every IGT value up to 151 ATA
and proportionately to IGT. On the contrary, nitrogen increases the survival
time in low dosages and exhibits a narcotic effect in higher dosages. These
differences between helium and nitrogen effects may result from differences in
the action threshold or efficiency, or both, of these two inert gases.

At molecular level, inert gases can interact with other molecules by
means of Van der Walls' forces or allosteric influences. They may also gener-
ate hydrates or clathrates (14) that alter the properties of cell membranes and
protoplasm. Without chemical binding, inert gases can physically influence
membranal properties, enzyme functions, metabolic reactions, and the like,
and their effects can be predicted according to their physical properties.

These models of molecular actions of HP, IGT, and anesthetics can facili-
tate comprehension of the effects observed on the trout. As a simplification of
these complex phenomena, we can only consider in this discussion the results
of Miller (11) about membrane volume value V_M, which is increased by anes-
thetics and decreased by HP. Considering both helium and nitrogen as "nar-
cotics," it can be supposed that they tend to increase V_M. The quantitative
differences between helium and nitrogen effects may result from a difference
in the ability of each of these inert gases to increase V_M, nitrogen being more
efficient than helium. Low dosages of nitrogen counterbalance the HP-induced
decrease in V_M; for higher nitrogen dosages, the increase in V_M attributable to
nitrogen is greater than the decrease in V_M caused by HP; the resultant effect
is an increase in V_M. In helium administration, up to 151 ATA the decrease in
V_M due to HP is incompletely counterbalanced by the increase in V_M attribut-
able to the specific action of helium. These examples of differences between
helium and nitrogen actions in combination with HP effects at molecular level

may explain the differences in symptomatology found in trout exposed to the different inert gases.

Acknowledgment

References

1. Balouet G, Barthélémy L, Belaud A. Etude, à partir d'un vertébré aquatique, des effets spécifiques de la pression hydrostatique "per se". Proceedings of the 1st Sci. Meet. of the E.U.B.S., Swedish J. of Defense Med., Försvarmedicin 1973;9:483–489.
2. Belaud A, Peyraud-Waitzenegger M, Peyraud C. Techniques originales de prélèvement des paramètres physiologiques sur le congre (Conger conger L.) libre de ses déplacements. I. Electrocardiogramme et activité respiratoire. Hydrobiologia 1971;38:49–59.
3. Belaud A, Barthélémy L. Rôle de la pression hydrostatique "per se" sur l'action des substances anesthésiques du poisson. Proceedings of the 4th Sci. Meet. of the E.U:B.S. Méd Aéronaut Spat Med Subaquat Hyp 1977;16(63):280–283.
4. Jones FRH, Marshall NB. The structure and function of the teleostean swimbladder. Biol Rev 1953;28:16–83.
5. Qutob Z. The swimbladder of fishes as a pressure receptor. Arch Néerl Zool 1962;15:1–67.
6. Johnson FH, Eyring H. The kinetic basis of pressure effects in biology and chemistry. In: Zimmerman AM, ed. High pressure effects on cellular processes. New York: Academic Press, 1970:1–44.
7. Belaud A, Barthélémy L, Le Saint J, Peyraud C. Trying to explain an effect of "per se" hydrostatic pressure on heart rate in fish. Aviat Space Environ Med 1976;47(3):252–257.
8. Brown DE, Marsland DA. The viscosity of Amoeba at high hydrostatic pressure. J Cell Comp Physiol 1936;8:159–165.
9. Flügel H, Schlieper C. The effects of pressure on marine invertebrates and fishes. In: Zimmerman AM, ed. High pressure effects on cellular processes. New York:Academic Press, 1970:211–234.
10. Spyropoulos CS. The response of single nerve fibres at different hydrostatic pressures. Am J Physiol 1957;189:214–218.
11. Miller KW. Inert gas narcosis, the high pressure neurological syndrome, and the critical volume hypothesis. Science 1974;185:867–869.
12. Seeman P, Roth S. General anaesthetics expand cell membranes at surgical concentrations. Biochem Biophys Acta 1972;255:171–177.
13. Macdonald AG. A dilatometric investigation of the effects of general anaesthetics, alcohols and hydrostatic pressure on the phase transition in smectic mesophages of DPPC. Biochem Biophys Acta 1978;507:26–37.
14. Pauling I. A molecular theory of anesthesia. Science 1961;134:15–21.

OSMOTIC FRAGILITY OF ERYTHROCYTES: EFFECTS OF HYDROSTATIC PRESSURE AND PENTANOL

A. C. Hall and A. G. Macdonald

Although hydrostatic pressure has been shown to order lipid bilayers and dissociate protein polymers, the effects being enhanced at low temperature (1,2), its actions on the mechanical properties of cell membranes are difficult to predict. The red blood cell is excellent for investigating this problem since when a population of erythrocytes is subjected to an osmotic shock, the amount of hemolysis is determined by the mechanical state of the cells; the more fragile the cells are, the more hemolysis occurs.

The fragility of red cells to a rapid osmotic shock is affected by altering the initial cell shape of the normal biconcave disc, or the critical hemolytic volume (Vc) of the fully swollen spherical cell (3). Alterations to the kinetics of water movement will be insignificant because of the rapidity of swelling and hemolysis (3). Preswelling cells in a slightly hypotonic solution will increase the initial cell volume (Vo) and hence fragility since their potential for swelling during osmotic shock will be less (4). Decreasing the membrane surface area makes the cells more spherical; it decreases the Vc and thus they are more fragile (5). On the other hand, agents like alcohols and other anesthetics are thought to protect erythrocytes by increasing the Vc and thus fewer cells in the red cell population lyse because they can swell to a larger volume (6).

The effect of pressure on the mechanical state of the erythrocyte may be reflected in its osmotic fragility. For example, if cells are more fragile under pressure then it is likely that they are more spherical or Vc is decreased, or both. If the cell becomes more spherical then it is possible that the factors which maintain the red cell in its characteristic shape, the most important of which appears to be the peripheral protein cytoskeleton (7), have been affected in some way. Additionally, it is of interest to know if the osmotic protection

(Vc increase) induced by alcohols is affected by pressure because it might then be possible to deduce how pressure is acting on the treated membrane.

Finally, a number of hemolysis experiments have been reported, the results of which appear to contain limitations in both technique and interpretation. The data obtained from the osmotic-hemolysis pressure experiment described in this report have considerably clarified the position. This equipment enables red cells equilibrated at selected temperatures and pressure to be subjected to an osmotic shock (with or without an alcohol), after which the unlysed cells are fixed, decompressed, and the extent of the hemolysis determined. The results show that pressure increases red cell fragility, particularly at low temperatures. It will be reasoned that the dominant effect of pressure on the membrane is probably a weakening of the protein network, perhaps in a way similar to its well-known effects on structural proteins. Furthermore, the action of pressure appears to be at a site distinct from that of an alcohol, n-pentanol. In this paper we also attempt to resolve some discrepancies in the literature.

MATERIALS AND METHODS

Fresh heparinized human and bovine red cells were used. At the start of a day's experiments red cells were washed in isotonic (0.9%) NaCl and the packed cells added to a series of hypotonic NaCl solutions in the range 0.3-0.6% NaCl and maintained at the experimental temperature. After 5 min the sample was centrifuged, and the amount of hemolysis in the supernatant was determined using an Unicam SP500 spectrophotometer, reading hemoglobin release at 540 nm against a distilled water blank. A fragility curve was constructed and the NaCl concentration, which gave 50 ± 10% hemolysis, was noted. This NaCl solution called H50, overcomes the problem of heterogeneity of cell ages and ensures that only the mature erythrocytes were studied. Osmotic lysis was carried out under high pressure by a special mixing apparatus within a thermoregulated pressure vessel ($\pm 0.5°C$) pressurized with water. Lysis was caused by injecting the H50 solution into an appropriate volume of blood (Fig. 1). After 10 min the suspension of partially hemolysed red cells was prevented from further hemolysis by fixing with 2% glutaraldehyde, or mixing with 0.9% NaCl. Pressure was generated by a hand pump and measured to $\pm 1\%$. Syringe 1 ($S1$) (Fig. 1) contained the H50 solution (with or without pentanol); by turning the handle (H) clockwise, tne cam (C) moved up the central threaded rod and thus delivered tne contents (normally 6 mL) to syringe 2 ($S2$). The two-way valve (V) prevented leakage of the saline solution to syringe 3 ($S3$). Syringe 2 ($S2$) contained 0.5 mL of packed red cells in isotonic saline on plasma and a mixing disc; the red cells + H50 solution were mixed frequently to minimize sedimentation. After a 10-min reaction time the handle was turned in the opposite direction and the red cell suspension injected into $S3$, which contained the fixing solution. Leakage back to $S1$ was avoided
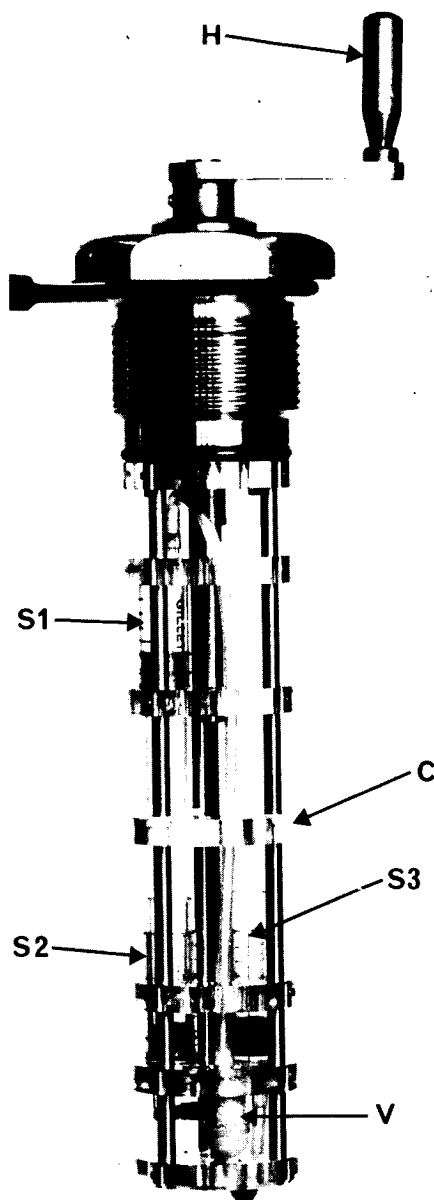
Fig. 1. Hemolysis equipment.   *Syringe* 1 (*S1*) contained H50 NaCl; *syringe* 2 (*S2*) contained red blood cells + mixing disc; *syringe* 3 (*S3*) contained fixative.   *H* is the brass handle; *C* is the perspex cam; *V* is the 2-way valve.   The threaded rod (stainless steel, 6 mm dia.) was rotated at 2 r/s and the delivery of 6 mL H50 NaCl to *S2* took 15 s. After the osmotic shock the cell suspension was thoroughly mixed using disc in *S2*. Before the fixation of the red cells the cam was lowered until it was just touching the extended plunger of *S2*. The delivery of the partially hemolyzed red cell suspension in *S2* to *S3* for fixation also took 15 s. The rotating shaft was centered by a bearing and sealed by means of a lip-seal mounted within the pressure vessel end-plug.

by the value (*V*). The pressure vessel was then decompressed and the hemo-globin released by hemolysis assayed colorimetrically.

Compression and decompression rates were found to be unimportant and samples rapidly compressed to 300 atm, decompressed, and the hemolysis car-ried out at atmospheric pressure showed no difference from unpressurized controls.

RESULTS

Figure 2 shows that pressure increases the osmotic fragility of human red cells. At all pressures red cell fragility is greatest at 5°C and there was no significant difference between the results at 21°C and 37°C.

Figure 3 shows the results obtained from bovine red cells at 5°C equili-brated at pressure and then subjected (*A*) to a standard osmotic shock and (*B*) to a standard osmotic shock with pentanol in the H50 giving a final concentra-tion of 100 mM pentanol. The fragility of bovine red cells at 5°C under pres-sure is similar to that of human red cells under the same conditions. There-fore, pressure appears to exert the same effect, but it should be noted that at atmospheric pressure bovine red cells are more fragile with an H50 of 0.53% compared to 0.425% for human cells.

Hemolysis in the presence of 100 mM pentanol is reduced by 60% (Fig. 3*B*, and see ref. 8). The results also show that above 100 atm the fragility of pentanol-treated cells is affected by pressure to the same extent as untreated cells, but there is an interesting change in slope at 100 atm.

DISCUSSION

Pressure may increase red cell fragility either by an effect on the ionic balance of the cell in such a way as to change the initial cell volume (Vo) and hence fragility, or by a direct action on the cell membrane, either by increas-ing Vo and hence cell shape and/or decreasing Vc. However, if red cells are incubated at 300 atm at 5°C for 30 min and then hemolyzed at atmospheric pressure, no change in hemolysis is noted. Thus, it seems unlikely that a pres-sure-induced ionic imbalance can explain the results presented here.

It is therefore probable that pressure increases fragility by a direct action on the cell membrane. Pressure may have a direct effect on the various mem-brane components, and alterations to the individual constituents of the mem-brane should change the osmotic fragility of intact red cells, the extent being determined by the relative contribution of the affected component. The domi-nant action may be to "order" the lipid bilayer component of the membrane (1), an effect which would be expected to be enhanced at low temperatures (9). Ordering the membrane bilayer will decrease its area. A decrease in mem-brane area would be expected to alter cell shape and make it more spherical and decrease the Vc (5). On the other hand, pressure might affect the mem-brane protein network, alter cell shape or Vc, or both, and hence alter fragil-ity. These two alternatives, i.e., lipid or protein targets, will now be considered.
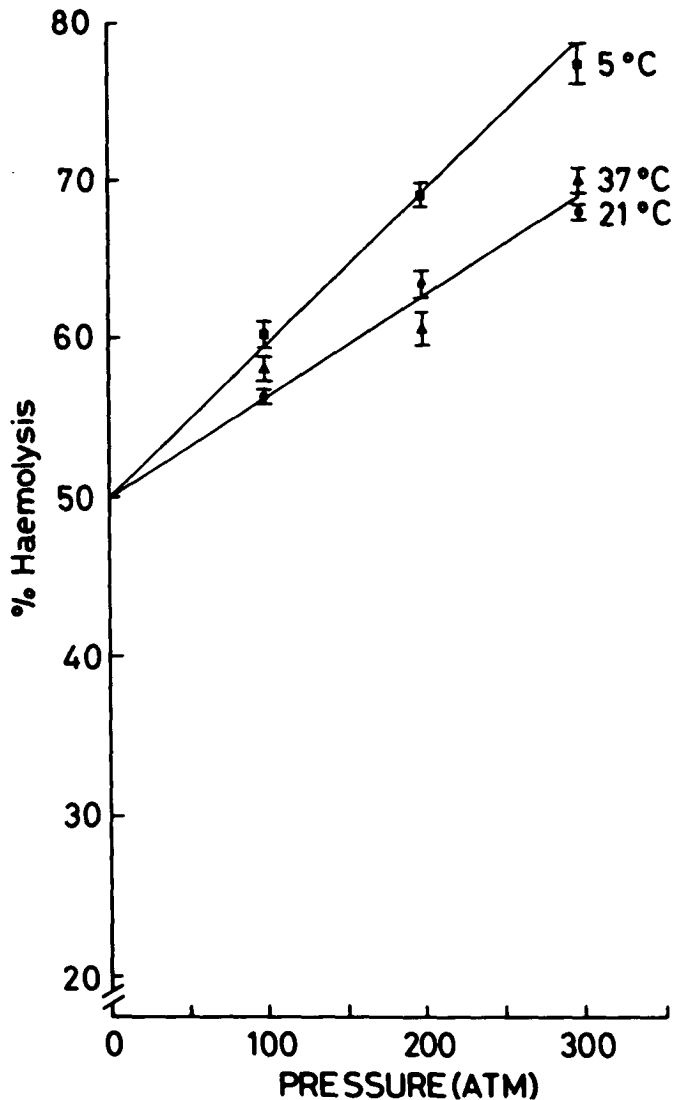
Fig. 2. Human red cells equilibrated at 5°C (■), 21°C (●), and 37°C (▲) and at pressure subjected to an osmotic shock of H50 NaCl.   Results are means ± SE for a minimum of 3 experiments. The hemolysis produced by the H50 NaCl solution at the experimental temperature and atmospheric pressure was normalized to 50%.

Results presented by Aloni et al. (10) show that the intact red cell is more fragile as the temperature is lowered, whereas liposomes made from red cell lipids become less fragile with decrease in temperature, despite the increase in microviscosity in the membranes of both (11). The mechanical state of the lipid bilayer is therefore not simply the site for the temperature effect in intact membranes, and membrane proteins are presumably involved. This conclusion
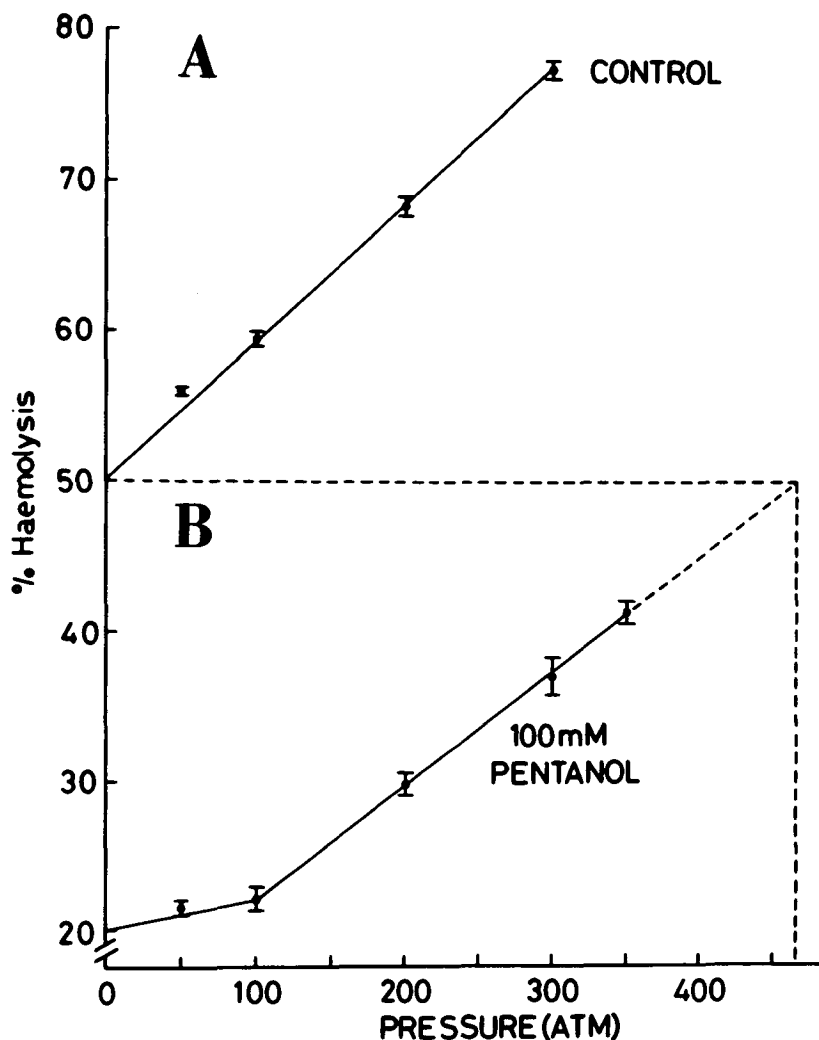
Fig 3. Bovine red cells equilibrated at 5°C and at pressure subjected to an osmotic shock of H50 NaCl with or without 100 mM *n*-pentanol.   Results are means ± SE for a minimum of 4 experiments. The hemolysis produced by the H50 NaCl of the untreated cells at 5°C and atmospheric pressure was normalized to 50%. Pentanol treatment consistently reduced the fragility by 60%; therefore the hemolysis has been normalized to 20%.

is reinforced by the observation that liposomes made from human and camel erythrocyte lipids respond very similarly in terms of other osmotic fragility at different temperatures despite the unique osmotic stability of camel red cells (10,12).

In view of the similar bilayer-ordering effects of high pressure and low temperature it is likely that pressure increases fragility by affecting some membrane component other than the lipid bilayer, perhaps the peripheral protein

complex (13). There is substantial evidence to show that the protein network has a major role in determining structural strength of red cell membrane and hence cell shape and deformability (13). For example, reduction in the membrane-spectrin content appears to reduce hyperelasticity and tensile strength, whereas removal of an integral protein such as glycophorin has no effect (14). The possibility that the pressure effects are mediated by changes in, for example, intracellular Ca^{++} concentration and binding or intracellular ATP rather than a direct effect on protein structure, must remain open.

It is well known that pressure depolymerizes protein polymers (2), and its action may be similar to those drugs (e.g., vinblastine) which disrupt microfilamentous proteins purified from human red cell membranes. These drugs decrease membrane structural strength, cause a reversible increase in osmotic fragility and deformability, probably by dissociating membrane structural proteins (15).

The observation (see Fig. 3) that pressure above 100 atm does not alter the antihemolytic effect of pentanol is consistent with each having different sites of action, that is, pressure does not affect the pentanol-induced increase in Vc. Thus, we suggest that pressure alters the shape of the cell by acting primarily on the protein network underlying the membrane, an effect which is sensitive to temperature (Fig. 2).

Note in Fig. 3 that from 100-300 atm the protection afforded by pentanol is constant. Below 100 atm there is a change in the slope obtained with treated cells, the osmotic protection conferred by pentanol at 100 atm being greater than at atmospheric pressure. The reasons for this are obscure. Finally, the extrapolated percent hemolysis of treated cells at 475 atm equals that of untreated cells at atmospheric pressure (Fig. 3).

PREVIOUS EXPERIMENTS

The first studies on the effects of pressure on red cells (16) showed that there was no spontaneous hemolysis of human erythrocytes in isotonic media exposed to 2000 atm, but the cells lost their biconcave shape and became spherical. Haubrich (17) confirmed this but found that the treated cells were more fragile in subsequent experiments. Thus, the spherical cells seen by Ebbecke may be caused by extensive disruption of the protein network, presumably irreversibly, in view of Haubrich's observations. At these very high pressures there may be additional problems of interpretation due to temperature changes on compression and alterations to red cell ionic composition.

Bernardini and Pryer (18) observed that 2–3 atm of air (exact composition not given) decreased the hemolysis in hypotonic solutions containing 0.36–0.48% NaCl; the experimental temperature was not mentioned. Fenn and Boschen (19) studied the effects of pressures of nitrogen and helium up to 41 atm on hypotonic hemolysis (presumably at room temperature) and reported that with their techniques (which enabled hemolysis to be monitored at pressure) no significant increase could be detected. However, after 16 h at pressures of up to

540 atm they found that there was more spontaneous hemolysis of red cells in isotonic saline at 6°C than at 25°C. Finally, Brewster et al. (20) investigated the effects of helium pressures of up to 130 atm on hypotonic hemolysis of human erythrocytes at 21°C and observed that pressure did not potentiate the hemolysis seen at atmospheric pressure. One possible reason for this lack of effect is that the atmospheric pressure control experiment gave 80% hemolysis. Thus, these authors were using cells whose fragility was much less than those described in this report. The H50 technique ensures that only the mature erythrocytes are studied, and their fragility is proportional to the osmotic or mechanical stress applied to them, unlike cells at either end of the sigmoid fragility curve (21).

OTHER STRUCTURALLY RELATED PHENOMENA

Normal red cells treated with vinblastine and other drugs demonstrate very similar properties to those shown in hereditary spherocytosis (HS) red cells. These include a decreased membrane structural strength, a reversible increase in osmotic fragility and rigidity, and an increased passive influx of Na^+. It has been proposed that a common defect in membrane microfilamentous proteins underlies this similarity (22). In view of the conclusions from the present work and the fact that hydrostatic pressure increases ouabain-insensitive Na^+ influx (23), it is tempting to speculate that the fault in HS cells and the pressure effects are linked in some way. Finally, changes in the morphology of red cells from men decompressed from hyperbaric (31 atm) helium-oxygen environments have been reported (24). Abnormal red cells were not observed during the simulated dive, however.

CONCLUSIONS

1) The osmotic fragility of human and bovine erythrocytes is increased by hydrostatic pressure over the range 1–300 atm, being greatest at 5°C.

2) The most likely target for the pressure effect is the protein network underlying the erythrocyte membrane in contrast to the lipid bilayer which is thought to be the site of action of pentanol (6).

3) Thus pressure reverses, not antagonizes, the osmotic protection conferred by pentanol, and the increased Vc induced by pentanol is not altered by pressure.

Acknowledgments

References

1. Trudell JR, Hubbell WL, Cohen EN. Pressure reversal of inhalation anesthetic-induced disorder in spin-labelled phospholipid vesicles. Biochim Biophys Acta 1973;291:328–334.
2. Zimmerman AM. High pressure effects on cellular processes. New York: Academic Press, 1970.
3. Ponder E. Hemolysis and related phenomena. New York: Grune & Stratton, 1948.
4. Castle WB, Daland GA. Susceptibility of erythrocytes to hypotonic hemolysis as a function of discoidal form. Amer J Physiol 1937;120:371–383.
5. Weed RI, Reed CF. Membrane alterations leading to red cell destruction. Amer J Med 1966;41:681–698.
6. Seeman P, Kwant WO, Sauks T, Argent W. Membrane expansion of intact erythrocytes by anesthetics. Biochim Biophys Acta 1969;183:490–498.
7. Kirkpatrick FH. Spectrin: current understanding of its physical, biochemical, and functional properties. Life Sci 1976;19:1–18.
8. Seeman P. The membrane actions of anesthetics and tranquilizers. Pharmacol Rev 1972;24:583–655.
9. Jost P, Libertini LJ, Herbert VC. Lipid spin labels in lecithin multilayers. A study of motion along fatty acid chains. J Mol Biol 1971;59:77–98.
10. Aloni B, Eitan A, Livne A. The erythrocyte membrane site for the effect of temperature on osmotic fragility. Biochim Biophys Acta 1977;465:46–53.
11. Aloni B, Shinitzky M, Livne A. Dynamics of erythrocyte lipids in intact cells, in ghost membranes and in liposomes. Biochim Biophys Acta 1974;348:438–411.
12. Ralston GB. The isolation of aggregates of spectrin from bovine erythrocyte membranes. Aust J Biol Sci 1975;28:259–266.
13. Lux SE. Spectrin-actin membrane skeleton of normal and abnormal red blood cells. Semin Hematol 1979;16:21–51.
14. Heusinkveld DS, Goldstein DA, Weed RI, LaCelle PL. Effect of protein modification on erythrocyte membrane mechanical properties. Blood Cells 1977;3:175–182.
15. Jacob H, Amsden T, White J. Membrane microfilaments of erythrocytes: alterations in intact cells reproduces the hereditary spherocytosis syndrome. Proc Natl Acad Sci 1972;69:471–474.
16. Ebbecke U. Über plasmatische Kontraktionen von roten Blutkörperchen, Paramäcien und Algenzellen unter der Einwirkumg hoher Drucke. Pflüg Arch Ges Physiol 1936;238:452–466.
17. Haubrich R. Über die Druckresistenz der Erythrocyten. Pflüg Arch Ges Physiol 1937;239:304–313.
18. Bernardini AT, Pryor WH. Initial observations on the effects of hypobaric and hyperbaric pressure on cell permeability. Tech Rpt 66-108, Brooks USAF Sch Aerosp Med AF Base TX: 1966.
19. Feen WO, Boschen VP. Hemolysis under high hydrostatic pressure. Proc Soc Exp Biol Med 1971;137:847–851.
20. Brewster E, Collins S, Furnell GR, Smith EB. The effect of high pressure on the hemolysis of red blood cells. Undersea Biomed Res 1976;3:151–155.
21. Dacie JV, Vaughan JM. The fragility of red blood cells; its measurement and significance. J Path Bact 1938;46:341–356.
22. Jacob HS. The abnormal red-cell membrane in hereditary spherocytosis: evidence for the casual role of mutant microfilaments. Br J Haematol (Suppl) 1972;23:35–44.
23. Hall AC, Macdonald AG. Hydrostatic pressure alters the sodium content of human erythrocytes. Proceedings of the Physiological Soc. J Physiol 1980;305:108P.
24. Carlyle RF, Nichols G, Paciorek JA, Rowles P, Spencer N. Changes in morphology and carbonic anhydrase content of red blood cells from subjected to simulated dives. J Physiol 1979;292:34P.

A MATHEMATICAL ANALYSIS OF HIGH PRESSURE AND ANESTHETIC EFFECTS

*M. J. Halsey, A. F. Mott, C. C. Spicer,
and B. Wardley-Smith*

The pressure reversal of anesthesia is a well established phenomenon that has been quantitated in luminous bacteria (1), amphibians (2,3), and rodents (4). It has recently been studied with one agent Althesin, in man (5). Since 1971 the quantitative data on the decrease of anesthetic potency with increasing pressure have usually been analyzed in terms of the critical volume hypothesis. It was postulated that the critical stage of anesthesia is accompanied by a critical increase in membrane volume. This may be achieved either by anesthetic alone or by a combination of a higher dose of anesthetic (expanding more) with hydrostatic pressure (compressing). The detailed mathematical model of this concept was reported in 1973 (6), and it was predicted that there should be a universal linear relationship between the fractional increase in anesthetizing partial pressure of any agent and the increase in pressure over and above that of the anesthetic itself. This increase in pressure was usually that of helium, which was used as the "inert" gas. It had been demonstrated in newts that the use of high pressures of helium was equivalent to hydrostatic pressure per se (7). In mice helium does appear to have a weak inherent anesthetic potency (8), which is masked by the effects of pressure. However, this only alters the slope of the predicted linear relationship.

There has been considerable discussion as to whether the universal linearity prediction of the critical volume hypothesis is proven or not. The original workers established the relationship for four gases using newts (6). However, the earlier studies on luminous bacteria (1) contradict the prediction. At the time the data were not analyzed in terms of the critical volume hypothesis, but

a review of the paper indicates that the pressure dependencies of narcotic potency are clearly more complex. The potencies of some agents (such as chloroform and ethyl carbamate) have a nonlinear pressure dependence, whereas those of others (such as sodium-barbital and chloral hydrate) have little or no pressure dependency. A later experiment (9) with the homologous series of carbamates demonstrated that, although pressure reduces the inhibition by lower members of the series, this effect becomes progressively less with increasing length of the aliphatic chain until finally there is evidence of an increase in the amount of inhibition under pressure. It is interesting to note that in spite of the fact that narcotic actions on luminous bacteria do not even approximate the critical volume hypothesis, the organism has continued to be regarded as a useful model system for general anesthesia.

The pressure-reversal data in rodents are also in conflict. A summary of all the rodent studies was presented in a 1979 review (10). For example, detailed studies with nitrogen and argon in mice indicate that pressure reversal is nonlinear (11), but this is disputed by one group of workers (12). There have been fewer studies with intravenous agents but there does appear to be agreement that their degree of pressure reversal is different from that for the inhalational agents (4,12). However, these last two studies disagree as to whether the reversal is linear.

The issue of universal linearity is particularly important because it is the major prediction of the unitary critical volume hypothesis. One alternative is the multi-site hypothesis, which postulates different molecular sites with limited degrees of occupancy (4). In view of this importance it seemed appropriate to attempt to analyze the available data in terms of a mathematical model. We formulated three specific questions:

1) Are the percentage increases in anesthetic requirements unequivocally nonlinear when all experimental errors are included?

2) If they are nonlinear, do they fit a mathematical model based on a simple saturation of the molecular sites—analogous to the Langmuir adsorption isotherm (13)?

3) Alternatively, do they have to be fitted to a more complex model which would predict additional effects as the pressure is increased?

In our preliminary analysis we have used the data obtained for the pressure reversal of the intravenous agents (4) because the individual values of the variables were available to us. In these experiments anesthetic potencies were determined in terms of infusion rates under steady-state conditions. Technical limitations prevented us from directly measuring the anesthetic concentrations in the serum while the animals were at pressure. However, the potencies of the agents are expressed as percentage increases relative to the control period at normal pressure rather than as absolute values. We were concerned about the theoretical possibility of the rates of metabolism or excretion changing with pressure. We therefore established a stable and defined level of anesthesia and measured waking times after the infusion was switched off. For all the agents so far studied, there were no significant differences in the waking times between the control and high pressure conditions.

In answer to the first question, we have established that the pressure-reversal curves based on all the individual data values for althesin, thiopentone, propanidid, and ketamine are significantly nonlinear.

The departures from a linear relation between ambient pressure and inhibition of anesthetic effect suggested that an expression of the following form might be suitable:

$$y = \frac{p}{a + bp + cp^2} \tag{1}$$

where y = % inhibition of anesthetic potency; p is pressure above atmospheric; and a, b, c are constants.

This curve has a maximum at $\sqrt{\dfrac{a}{c}}$ and declines to zero at p = O and $+\infty$.

When a and b are positive and c = 0, it is identical to a Langmuir adsorption curve. The functional changes in y and p are related by the equation:

$$\frac{dy}{y} = \frac{dp}{p} - \frac{df}{f} \tag{2}$$

where $f(p) = a + bp + cp^2$ in the present case. The values of the parameters (with their standard errors) for the four anesthetics are shown in Table I. The standard errors indicate that in some cases the parameters are not significantly different from zero. However, in all cases fitting the parameters in turn resulted in a decrease in the deviance.

It will be seen that the b's are negative and these quadratics have imaginary roots. Their values are everywhere positive. Consequently, the effect of pressure in the second form of Eq. 2 is always opposed to that in the first. Figure 1 illustrates the computed curves up to a pressure of 250 atm. It is interesting that the observed data, which is limited to a maximum pressure of 60–100 atm, predicts curves with maxima in all cases. For example, although

TABLE I

Parameters of Equation 1 Relating Anesthesia Inhibition
to Pressure Without Assuming Linearity

	a	b	c
Althesin	1.952 (0.440)	−0.0395 (0.0196)	0.000341 (0.000201)
Thiopentone	2.937 (0.226)	−0.0359 (0.0084)	0.000154 (0.000066)
Propanidid	4.835 (1.354)	−0.1136 (0.0575)	0.00132 (0.00060)
Ketamine	7.841 (3.554)	−0.1150 (0.1374)	0.000923 (0.001144)
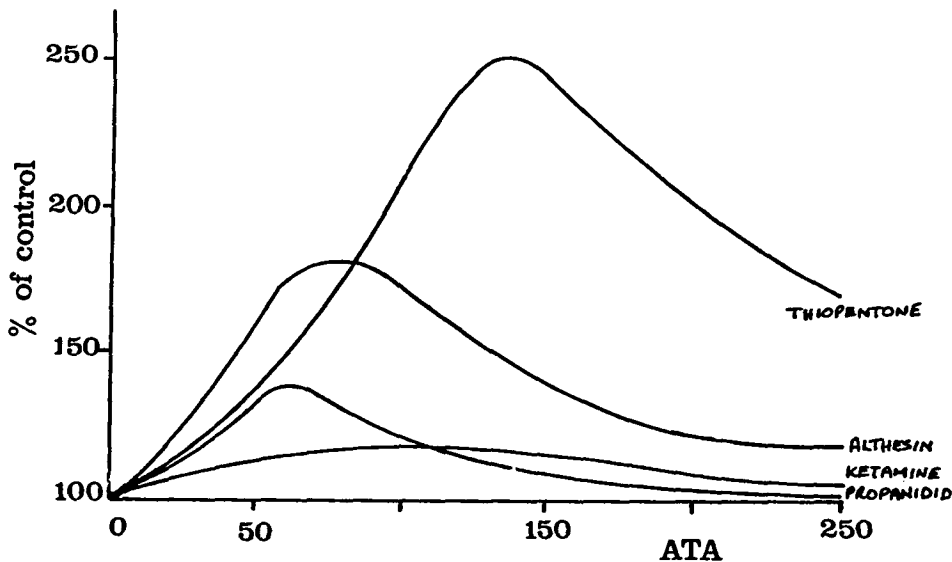
Fig. 1. The computed curves for the relationship of anesthetic potency (expressed as % of control) versus total pressure in atmospheres absolute (ATA). These curves are derived from Eq. 1 with the parameters specified in Table I.

the thiopentone indicated an apparent upswing in the pressure-reversal curve of the observed data, the computed curve has a maximum at 138 atm.

If the term in p^2 is omitted and the data are fitted to the equation, then

$$y = \frac{x}{a + bx} \qquad (3)$$

The values of a and b (with their standard errors) are shown in Table II. Again, all the b's are negative and the equation is not a Langmuir curve but

TABLE II

Parameters of Equation 3 Relating
Anesthetic Inhibition to Pressure

	a	b
Althesin	1.33	−0.0064
	(0.27)	(0.0047)
Thiopentone	2.52	−0.0175
	(0.17)	(0.0021)
Propanidid	0.92	−0.0029
	(0.78)	(0.0161)
Ketamine	5.29	−0.0056
	(1.36)	(0.0214)

one that increases steadily with pressure and becomes *infinite* at a pressure given by $p_\infty = a/b$.

What seems to be happening is that the data are essentially concave upward at lower pressures and cannot be fitted to an adsorption type of model. The other implication is that the antagonistic effect is not uniform at all pressures but goes through a minimum at a pressure $P_{min} = -b/2c$.

The differences between the parameters for the different agents is in accord with their acting at different sites. However, the nature of the results is so consistent in the four separate series of experiments that we believe it must reflect some underlying general mechanism at these sites. A possible mechanism is that there are two effects operating, one is strong at low pressures and dies away and the other is weak at low pressures and increases with pressure. Alternatively, the combination of these two effects predicts that the inhibition would first decline with pressure and then increase. This at first sight appears unlikely, but it is known that the effects of pressure on the unfolding and folding of proteins can behave in this way. Lipids are compressible but do not show this biphasic response to pressure (see 14). Thus, the mathematical analysis of our data for the intravenous agents provides unexpected support for the postulate that the sites of action of at least some anesthetics are hydrophobic areas of proteins.

References

1. Johnson FH, Brown DES, Marsland DA. Pressure reversal of the action of certain narcotics. J Cell and Comp Physiol 1942;20;269–276.
2. Lever MJ, Miller KW, Paton WDM, Smith EB. Pressure reversal of anesthesia. Nature 1971;231;368–371.
3. Halsey MJ, Wardley-Smith B. Pressure reversal of narcosis produced by anesthetics, narcotics and tranquillizers. Nature 1975;257;811–813.
4. Halsey MJ, Wardley-Smith B, Green CJ. Pressure reversal of general anesthesia—a multi-site expansion hypothesis. Br J Anaesth 1978;50;1091–1097.
5. Dundas CR. Alphaxalone/alphadolone in diving-chamber anaesthesia. Lancet 1979;i:378
6. Miller KW, Paton WDM, Smith RA, Smith EB. The pressure reversal of anesthesia and the critical volume hypothesis. Mol Pharmacol 1973;9;131–143.
7. Miller KW, Paton WDM, Smith EB, Sreet WB. Animals at very high pressures of helium and neon. Science 1967;157;97–98.
8. Halsey MJ. Structure-activity relationships of inhalational anesthetics. In: Halsey MJ, Millar RA, Sutton JA, eds. Molecular mechanisms in general anesthesia. Edinburgh: Churchill Livingstone, 1974;3–14.
9. Johnson FM, Flagler EA, Simpson R, McGeer K. The inhibition of bacterial luminescence by a homologous series of carbamates. J Cell Comp Physiol 1951;37;1–14.
10. Wardley-Smith B, Halsey MJ. Recent molecular theories of general anesthesia. Br J Anaesth 1979;51;619–626.
11. Smith RA, Smith M, Eger EI, Halsey MJ, Winter PM. Non-linear antagonism of anesthesia in mice by pressure. Anaesth Analg 1979;58;19–22.
12. Miller KW, Wilson MW. The pressure reversal of a variety of anesthetic agents in mice. Anesthesiology 1978;48:104–110
13. Glasstone S. Textbook of physical chemistry. London: Macmillan, 1946.
14. Halsey MJ, Brown FF, Richards RE. Perturbations of model protein systems as a basis for the central and peripheral mechanisms of general anesthesia. In: Molecular interactions and activity in proteins. Amsterdam: Ciba Foundation Symposium 60, Excerpta Medica, 1978;123–136.

CONTRASTING ACTIONS OF HYDROSTATIC PRESSURE AND HELIUM PRESSURE ON GROWTH OF *Saccharomyces cerevisiae*

S. R. Thom and R. E. Marquis

It has been known since the work of Claude Bernard that cell growth can be inhibited by anesthetics. The response seems to be a universal one of plant, animal, and microbial cells. There has been renewed interest in the response in the past few years because of advances in deep diving with addition of nitrogen and argon to breathing mixtures for divers and because of a number of provocative studies such as those showing that nitrous oxide can suppress growth of leukemia cells in man (1).

The growth-inhibitory action of anesthetics is generally viewed as a narcotic action. However, our recent investigations of growth inhibition by anesthetic gases have led to the conclusion that microbial growth modification cannot really be considered as a narcotic effect and certainly cannot be interpreted in terms of the critical volume hypothesis.

The actions of helium are particularly indicative of the difference between narcosis and growth modification. Brauer and Way (2) found that helium in combination with other gases actually had a negative narcotic potential in that it antagonized the anesthetic actions of gases such as nitrous oxide for mice. Helium is commonly used as a convenient vehicle for applying hydrostatic pressure to biological systems, especially to gas-breathing animals, and this use is based on the view that helium is non-narcotic. Another proposed biological use for high-pressure helium has to do with the retrieval and culture of bacteria from the deep sea. Jannasch and Wirsen (3) have developed apparatus for isobaric retrieval and transfer of deep-sea samples. Taylor (4) has explored the possibility of using compressed helium for pressure chambers which would have a gas phase and in which barophilic bacteria could be streak-plated or

667

otherwise manipulated without the need for an all-liquid environment. Clearly, it is desirable for this sort of use that helium be without specific biological effect. However, the results of our experiments over the past few years do not support the view that helium pressures are equivalent to hydrostatic pressures. Instead, it appears that the helium itself has significant effects on microbial growth.

METHODS AND MATERIALS

A haploid strain of *Saccharomyces cerevisiae* was obtained from Dr. R. Christensen of this Institution. The organism was grown in a complex medium described previously (5), which contains tryptone, glucose, and yeast extract. Ampicillin (162 μg/mL) was added, and cultures were inoculated with a 5% inoculum of an overnight culture. The growth temperature was 24°C.

For application of hydrostatic pressure, cultures were placed in plastic syringes of the type we have used previously and compressed in standard pressure chambers (6). For application of helium pressure, cultures were placed in flasks containing teflon-coated, magnetic stirring bars, and the flasks were placed in standard pressure chambers. The chambers were connected to cylinders of compressed helium and pressurized. The cultures were stirred initially with the magnetic bars to speed up gas transfer. In these experiments, air was not flushed from the chambers, but air removal was found not to affect experimental results. For absorbancy determinations, cultures were decompressed slowly to avoid excessive cooling, sampled, and immediately recompressed. Absorbancy was assessed with a Beckman DU spectrophotometer set for 700 nm light.

Cultures were exposed to helium-nitrous-oxide mixtures as described previously (7). Cultures were exposed to nitrous oxide or oxygen at high hydrostatic pressure by placing them in gas-tight syringes (Glenco Scientific Co.) with the proper amount of nitrous oxide or oxygen and then compressing the syringes in standard pressure chambers. The amounts of nitrous oxide required were calculated by use of the Ostwald coefficients presented by Wilhelm et al. (8), and the amounts of oxygen by use of the data of Taylor (9).

RESULTS AND DISCUSSION

The data presented in Fig. 1 show major differences in the effects of hydrostatic pressure and helium pressure on the extent of growth of *Saccharomyces cerevisiae*. A similar picture was obtained for growth rate. It is readily apparent that hydrostatic pressure is a more potent growth inhibitor than is helium. This finding basically agrees with the findings of Macdonald (10) for *Tetrahymena* cell division. *Saccharomyces cerevisiae* is very sensitive to pressure compared to the bacteria with which we have worked previously, and so it is possible to carry out these experiments with compressed helium from
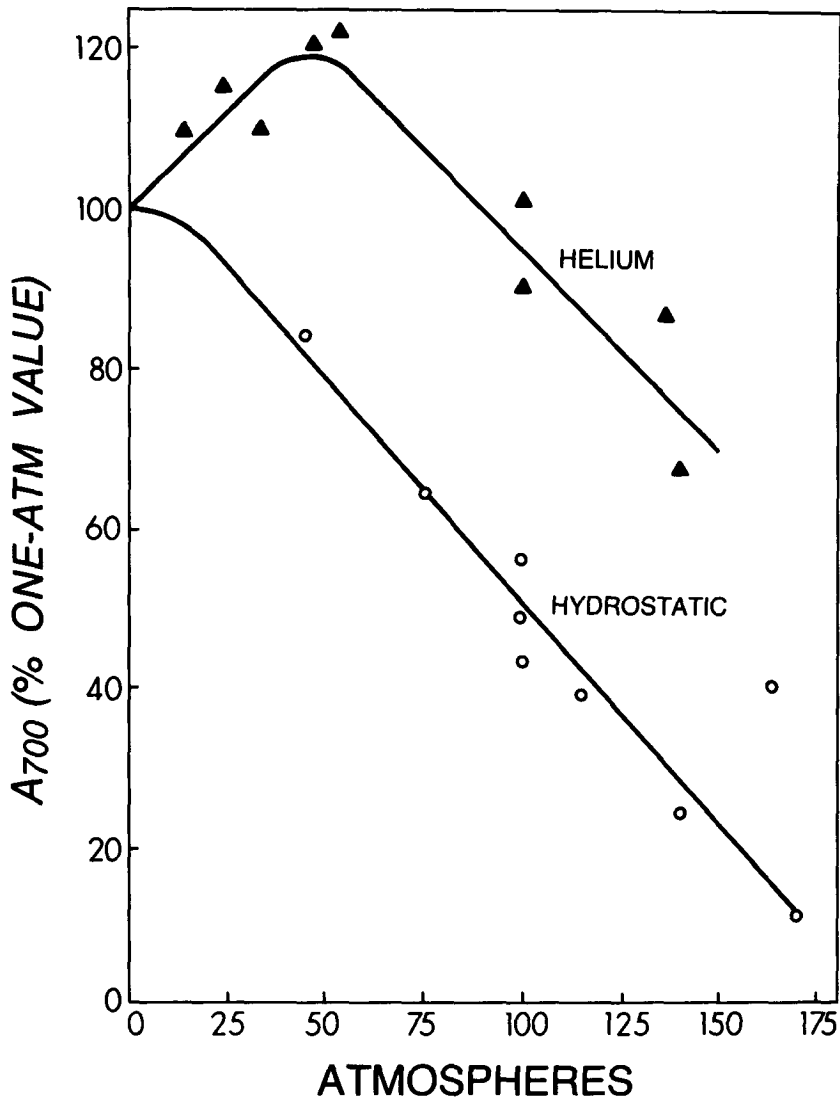
Fig. 1. Comparative effects of hydrostatic pressure (●) and helium pressure (▲) on growth of *S. cerevisiae*. The values indicated are for maximal absorbancy.

commercial tanks of the gas. Taylor (4) used a system in which helium from a 100-atm source was further compressed to 500 atm. His data for a marine bacterium EP-4 show that 500 atm helium was much less inhibitory for growth than was 500 atm hydrostatic pressure. In essence, it appears that helium, to a degree, reverses the growth-inhibitory action of hydrostatic pressure. In our experiments, the difference between helium pressure and hydrostatic pressure could not be related to air contamination of the helium since addition of even

as much as 0.5 atm oxygen to the cultures through the vehicle of FC-80 fluorocarbon liquid did not reduce the sensitivity of the organism to pressure. Moreover, nitrogen or argon at pressures as high as 100 atm also proved to be less inhibitory for growth than was hydrostatic pressure. Xenon was as inhibitory as nitrous oxide, and 20 atm xenon could completely stop growth.

As mentioned, helium is generally considered to have negative narcotic potency and it antagonizes the narcotic actions of nitrous oxide. In contrast, we found that helium acts to potentiate or enhance the growth inhibitory actions of nitrous oxide for bacteria (7). The data presented in Fig. 2 indicate
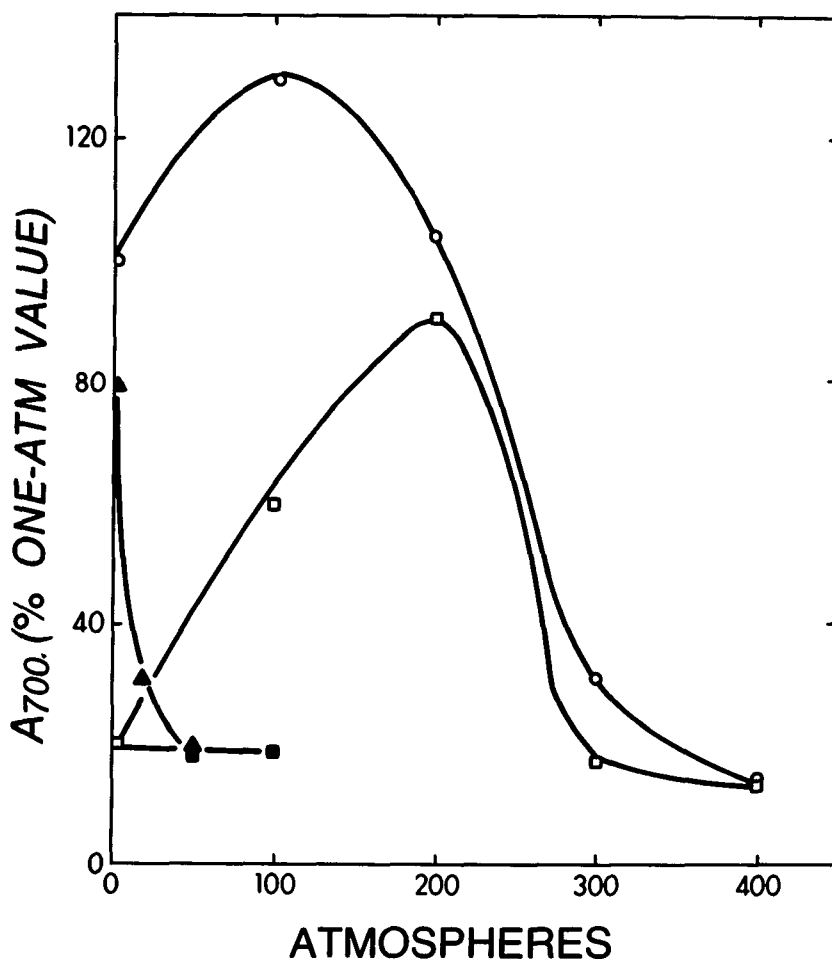
Fig. 2. Potentiation by helium and reversal by hydrostatic pressure of the growth-inhibitory action of nitrous oxide for *S. cerevisiae* growing in tryptone-glucose-yeast-extract medium at 24°C.   Data are presented for the effects of hydrostatic pressure on cultures exposed to 3.3 atm nitrous oxide (O) or 16.4 atm nitrous oxide (□) and of helium pressure on cultures exposed to nitrous oxide at pressures of 10 (▲) or 16.4 (●) atm.   The *abscissa scale* indicates pressure in addition to that due to nitrous oxide.

that helium also enhances the inhibitory effect of nitrous oxide on yeast growth. Other experiments indicated a similar enhancing effect for nitrous oxide inhibition of growth of *Tetrahymena thermophila*. Even though high-pressure helium enhances growth inhibition, hydrostatic pressure acts to reverse the inhibition, as it acts to reverse narcotic responses. As shown in Fig. 2, 16.4 atm of nitrous oxide almost completely suppressed growth of *S. cerevisiae*. However, application of 200 atm hydrostatic pressure to the culture nearly completely reversed the effect of nitrous oxide, even though 200 atm hydrostatic pressure alone also almost completely stopped growth. Here, the antagonistic actions of nitrous oxide and hydrostatic pressure are clear. At a lower level of 3.3 atm of nitrous oxide, it was possible, by application of 100 atm hydrostatic pressure, to obtain better growth than at 1 atm in the absence of nitrous oxide.

Differences between helium pressure and hydrostatic pressure were apparent also in relation to oxygen toxicity. The data presented in Table I indicate that compressed helium acts to potentiate the growth inhibitory action of hyperbaric oxygen for *S. cerevisiae*. Here, 2 atm of oxygen in the presence of air (final oxygen concentration of ca. 88 μg/mL) caused an inhibition of growth of some 36%. Addition of 10 atm of helium increased inhibition, and addition of 20 atm He resulted in essentially complete inhibition. Hydrostatic pressures of 10 or 20 atm had no effect on oxygen toxicity. As shown by the data, a hydrostatic pressure of 100 atm in addition to 2 atm of oxygen in the presence of air also resulted in no increase in growth inhibition. In fact, the level of inhibition was essentially equal to that produced by either agent alone,

TABLE I

Comparison of the Effects of Helium Pressure and Hydrostatic Pressure on the Sensitivity of *Saccharomyces cerevisiae* to Oxygen

Oxygen Concentration (μg/mL)*	Helium Pressure (atm)	Additional Hydrostatic Pressure (atm)	$A_{700}^{max\dagger}$	
			$A_{700}^{max\dagger}$	% 1-atm Control
8	0	0	0.480	100
8	20	0	0.500	104
8	0	100	0.245	51
88	0	0	0.308	64
88	10	0	0.228	48
88	20	0	0.032	7
88	0	100	0.318	66

*It was assumed that the culture medium in equilibrium with air at 24°C contained 8 μg O_2 per mL, and that when 2 atm O_2 was added to the air, the oxygen concentration increased to 88 μg/m. Hydrostatic pressure acts to decrease the solubility of oxygen in water. At 100 atm, the reduction would be only about 12%, according to Taylor (9), and allowance was made for this change in calculating the required volume of oxygen.

$\dagger A_{700}^{max}$ refers to the maximum absorbancy of the culture assessed with light of 700 nm wavelength.

and the net conclusion is that the two are antagonistic. These results were obtained repeatedly, and they are in contrast to the findings reported by ZoBell and Hittle (11) of enhanced toxicity of oxygen for bacteria caused by hydrostatic pressure.

It seems clear from the data presented that the growth responses of yeast to pressure imposed by use of compressed helium are very different from those imposed purely by hydrostatic pressure. Other work in this laboratory has led to the same conclusion for bacteria and *Tetrahymena*. The net conclusion is that helium must have specific effects on cell growth, separate from those caused simply to pressure. Previously, Schlamm et al. (12) showed that helium can enhance iron uptake by bacteria in iron-deficient media. This enhancement was not important in our experiments with complex, iron-sufficient media. However, it is still clear that helium must specifically affect some reactions involved in the growth of cells and compressed helium should not be used as a means to apply hydrostatic pressure to microbial cultures unless some gas-impermeable barrier is interposed between the helium and the culture. It is clear also that the interactions of helium and nitrous oxide affecting microbial growth are very different from their interactions in relation to narcotic responses. Again, the net conclusion is that growth modification by anesthetic gases is a non-narcotic response and not related to narcosis as we had previously supposed it to be (13).

Acknowledgments

References

1. Lancet editorial. Nitrous oxide and the bone marrow. Lancet 1978;ii:613–614.
2. Brauer RW, Way RO. Relative narcotic potencies of hydrogen, helium, nitrogen, and their mixtures. J Appl Physiol 1970;29:23–31.
3. Jannasch HW, Wirsen Co. Retrieval of concentrated and undecompressed microbial populations from the deep sea. Appl Environ Microbiol 1977;33:642–646.
4. Taylor CD. Growth of a bacterium under a high-pressure oxy-helium atmosphere. Appl Environ Microbiol 1979;37:42–49.
5. Marquis RE, Porterfield N, Matsumura P. Acid-base titration of streptococci and the physical states of intracellular ions. J Bacteriol 1973;114:491–498.
6. Marquis RE. High-pressure microbial physiology. Adv Microbial Physiol 1976;14:159–241.
7. Marquis RE, Thom SR, Crookshank CA. Interactions of helium, oxygen, and nitrous oxide affecting bacterial growth. Undersea Biomed Res 1978;5:189–198.
8. Wilhelm E, Battino R, Wilcock RJ. Low-pressure solubility of gases in liquid water. Chem Rev 1977;77:219–262.
9. Taylor CD. The effect of pressure upon the solubility of oxygen in water. Arch Biochem Biophys 1978;191:376–384.

10. Macdonald AG. The effect of helium and of hydrogen at pressure on the cell division of *Tetrahymena pyriformis* W. J Cell Physiol 1975;85:511–528.
11. ZoBell CE, Hittle LL. Some effects of hyperbaric oxygenation on bacteria at increased hydrostatic pressures. Can J Microbiol 1967;13:1311–1319.
12. Schlamm NA, Perry JE, Wild JR. Effect of helium gas at elevated pressure on iron transport and growth in *Escherichia coli*. J Bacteriol 1974;117:170–174.
13. Fenn WO, Marquis RE. Growth of *Streptococcus faecalis* under high hydrostatic pressure and high partial pressures of inert gases. J Gen Physiol 1968;52:810–824.

EFFECTS OF DIFFERENT NORMOXIC HYPERBARIC EXPOSURES ON GLUCOSE, LACTATE, AND GLYCOGEN BRAIN CONCENTRATIONS

T. Obrénovitch and F. Brue

During a prior experiment (1,2) dealing with modifications of brain glucidic metabolism in mice breathing 6 ATA of either pure oxygen or a normoxic breathing mixture, we found a) an increase in brain glucose in all exposed animals regardless of the inhaled partial pressure of oxygen (PI_{O_2}); b) a decrease in brain lactate in animals exposed to hyperbaric normoxic environments; and c) a decrease in brain glycogen, which appears only in mice submitted to hyperbaric oxygen. Nolan and Faiman (3) had previously observed in mice exposed to 6 ATA of pure oxygen: a) a nonsignificant decrease in brain lactate at the end of the compression followed by a significant increase as compared to the level reached at the end of the compression period, and b) an increase in brain glucose in mice exposed during 18 min at 6 ATA of pure oxygen. According to recent results obtained by these same authors, only oxygen would be responsible for the brain glucose increase (4).

In experiments here reported to study more precisely the specific modifications resulting from normoxic hyperbaric exposures, we measured brain concentrations of glucose, lactate, and glycogen in mice exposed to various hyperbaric situations ($N_2 + O_2$ 6 and 11 ATA, $He + O_2$ 21 ATA). Blood concentrations of glucose and lactate also have been measured because of their possible interference with brain levels.

METHODS AND MATERIALS

Animal Exposures

Five series each consisting of 15 male mice (mean weight = 30 g, water and food ad libitum) were used for our investigation. We performed all exposures in the morning to avoid the dispersion of results caused by circadian rhythms, particularly those of brain glycogen (5). To minimize artifactual changes in brain substrates, we subjected the animals to euthanasia under pressure by rapid freezing in liquid nitrogen using a previously described technique (6).

The four diving profiles considered are shown in Fig. 1.

To discriminate compression effects from hyperbaric exposure effects in the two series of animals exposed to 6 ATA, one series of animals was sacrificed just after the end of compression (series $N_2 + O_2$ 6 ATA); the other series was sacrificed at the 60th min (series $N_2 + O_2$ 6 ATA 60 min).

We compressed animals to 11 ATA with $N_2 + O_2$ to determine any correlation between nitrogen narcosis and biochemical modifications (series $N_2 + O_2$ 11 ATA). To study the effects of a fast compression combined with a different diluent gas, we compressed animals to 21 ATA with a helium-oxygen mixture (series $He + O_2$ 21 ATA).

Each exposure was preceded by a 5-min ventilation of the pressure chamber with a normoxic mixture; the diluent gas was the same as the one used
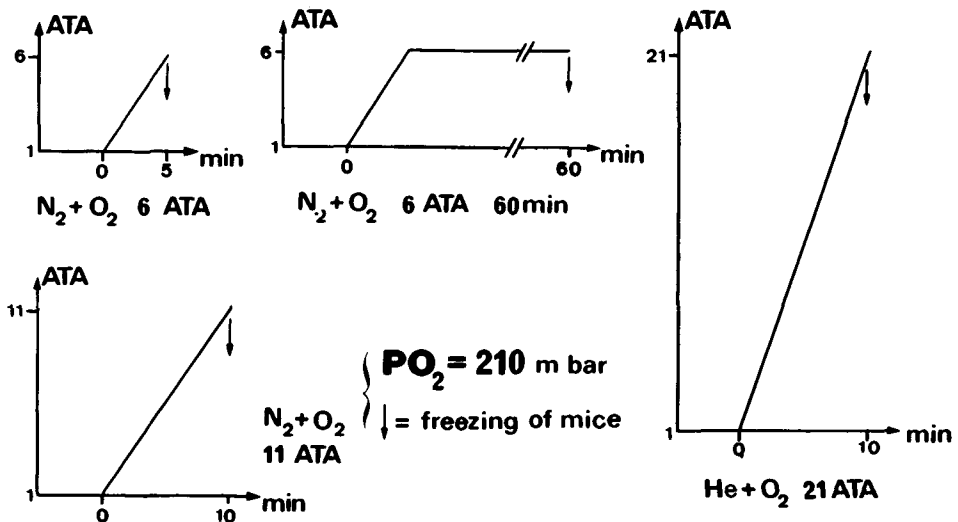
Fig. 1.   Hyperbaric exposure profiles.

during the corresponding hyperbaric exposure. During the exposure, the temperature of the cage was regulated at 27°C, PI_{O_2} was maintained between 200 and 250 mbar, and CO_2 was removed.

Blood and Brain Analysis

After the mice were sacrificed by immersion in liquid nitrogen, the chamber was decompressed and the mice removed. Dissection was performed at about -20°C on frozen animals; the brain was taken first, then approximately 150 mg of frozen blood was carefully removed from the vena cava and cardiac ventricles. Tissue samples were stored at -80°C until their analysis.

Brain glucose and lactate were estimated enzymatically on neutralized perchloric-acid extracts of a cerebral hemisphere (7). The other hemisphere was used for the glycogen analysis (5). We checked the level of these substrates and found them to be the same in the two hemispheres.

Blood glucose and lactate were also measured in aliquots of neutralized perchloric-acid extracts, according to the method recommended by Boehringer (Mannheim), slightly modified.

Enzymes, cofactors, and substrates were purchased from Boehringer (Mannheim). Other chemicals used were of reagent grade.

All data were compared by Student's t test.

RESULTS

Behavior of Exposed Animals

Mice exposed to 6 ATA with a nitrogen-oxygen mixture behaved normally during the whole exposure. On the other hand, those compressed up to 11 ATA showed a specific narcotic behavior (hyperactivity and staggering); some animals presented such a behavior as early as 8 ATA.

Animals submitted to heliox at 21 ATA did not show any of the behavioral changes designated as the high pressure neurological syndrome (HPNS), changes characterized by locomotor disturbances, tremors, and then convulsions. This fact appears quite normal if we refer to the recent work reported by Brauer et al. (8), who showed that a 120 atm/h (the compression rate we used), the convulsion threshold pressure for mice is 80 ATA. We intended to reach such pressures in the plan for this study; unfortunately, because of the use of liquid nitrogen under pressure, it was impossible to work deeper than 21 ATA (9).

Effects of Hyperbaric Normoxic Exposures on Blood Glucose and Lactate, Brain Glucose, Lactate, and Glycogen

The results are tabulated in Table I and presented as percent of controls in Fig. 2.

TABLE I

Effects of Several Hyperbaric Normoxic Exposures on Blood Glucose and Lactate and Brain Glucose, Lactate, and Glycogen

Series	Blood Glucose	Blood Lactate	Brain Glucose	Brain Lactate	Brain Glycogen
	(μmol/mL)			(μmol/g)	
Control	9.58*	7.35	1.81	2.34	3.23
	0.24†	0.21	0.08	0.08	0.09
	(15)	(15)	(15)	(15)	(14)
6 ATA	9.79	7.04	2.04	1.89	3.60
$N_2 + O_2$	0.32	0.26	0.06	0.08	0.12
	(15)	(15)	(15)	(15)	(15)
6 ATA	9.26	6.16	1.92	1.80	3.77
$N_2 + O_2$	0.18	0.18	0.09	0.09	0.12
60 min	(15)	(15)	(15)	(15)	(15)
21 ATA	9.47	7.32	2.20	1.86	3.82
$He + O_2$	0.26	0.26	0.10	0.08	1.10
	(15)	(15)	(15)	(15)	(15)
11 ATA	9.68	6.56	2.19	2.16	3.56
$N_2 + O_2$	0.29	0.20	0.05	0.07	0.13
	(15)	(15)	(15)	(15)	(15)

* = mean; † = standard error; number of mice are in parentheses; these designations apply to all columns.   For details concerning exposure profiles, see Fig. 1.
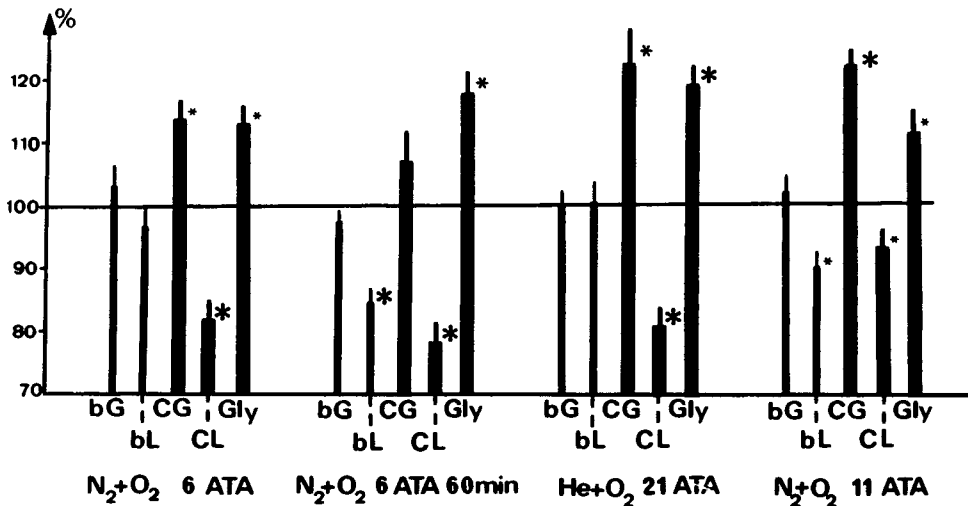
Fig. 2. Effects of different normoxic hyperbaric exposures on blood glucose and lactate, brain glucose, lactate, and glycogen expressed as percent of controls. bG is blood glucose; bL is blood lactate; CG is cerebral glucose; CL is cerebral lactate; Gly is cerebral glycogen.   *P < 0.05; *p ⪝ 0.005; *P⪝ 0.0005 (Student's t test).

Blood glucose was not modified by any of the tested exposures. Blood lactate level was significantly decreased in animals exposed to either 6 ATA for 60 min (series $N_2 + O_2$ 6 ATA 60 min) or 11 ATA compression alone (series $N_2 + O_2$ 11 ATA).

The compression up to 6 ATA (series $N_2 + O_2$ 6 ATA) induced a significant increase in brain glucose ($+13\%$). This increase was more significant ($+21\%$) for the mice compressed up to a higher pressure (series $N_2 + O_2$ 11 ATA and $He + O_2$ 21 ATA). This increase was not significant for the mice exposed during 55 min at a constant pressure (series $N_2 + O_2$ 6 ATA 60 min).

Results of all compressed animals are characterized by a significant decrease in brain lactate. This decrease holds up in the course of a long exposure (series $N_2 + O_2$ 6 ATA 60 min). The brain lactate decrease is less important in animals that showed nitrogen narcosis symptoms (series $N_2 + O_2$ 11 ATA). For those mice, the brain lactate level decreased significantly compared to the controls and increased significantly compared to animals compressed to a non-narcotic pressure of nitrogen (series $N_2 + O_2$ 6 ATA).

All the tested exposures induced an increase in the brain glycogen level. This increase was less important but still significant in animals exposed to a narcotic pressure of nitrogen (series $N_2 + O_2$ 11 ATA).

DISCUSSION

Validity of the Results Obtained with Mice Sacrificed Under Pressure by Rapid Freezing

For substrates that have a fast rate of synthesis or catabolism, or both, measured tissue levels are conditioned by the rate at which the tissue metabolism has been blocked (10–12). We recently showed (9) that the cooling rate of a body dropped in liquid nitrogen slows down when the surrounding pressure increases (increase of the freezing threshold: 3.3% at 6 ATA, 6.3% at 11 ATA, 15.2% at 21 ATA). These two data suggest that some biochemical modifications observed in animals sacrificed under pressure by immersion in liquid nitrogen could be artifacts because of slower freezing rate of animals.

In animals immersed in liquid nitrogen, blood flow stops before the freezing of some brain regions (13). Because of the slower freezing rate under pressure, one can suppose that this short ischemic period is slightly lengthened in exposed animals, particularly those sacrificed at 21 ATA. Cerebral ischemia induced a quick decrease of brain glucose and glycogen combined with an increase of lactate (14–17). These effects are diametrically opposed to those shown in animals exposed to hyperbaric conditions: thus, the latter effects are not artifacts caused by different freezing rates.

Effects of Several Hyperbaric Normoxic Exposures on Brain Metabolism

Brain Glucose. During this experiment, a compression up to 6 ATA with a nitrogen-oxygen mixture induced a significant increase in cerebral glucose

($+13\%$). This observation confirms our previous results (1,2), which seem to be inconsistent with those of Nolan et al. (4). These authors also studied brain metabolism on mice killed under pressure by rapid freezing in liquid nitrogen. They found a significant increase ($+64\%$) of brain glucose in animals exposed during 10.5 min at 6 ATA of pure oxygen (compression period included). Comparing this result with another obtained with mice exposed at the same pressure but with a nontoxic PI_{O_2} (3 bar), these authors concluded that only oxygen was responsible for this alteration. In fact, animals of this last series presented a nonsignificant increase of brain glucose ($+12\%$) in comparison to controls; the nonsignificance of this result could be explained by the small number of animals that constituted their different series (6 mice per series).

Thus, it appears that a hyperbaric exposure either normoxic or with a high but not toxic PI_{O_2} because of the exposure duration probably induces an increase of cerebral glucose, which appears as early as 6 ATA either with nitrogen or helium as diluent gas; thus, this alteration could be due only to the increased pressure. However, this brain glucose level increase is more important when animals are submitted to oxygen at high pressure (OHP) (1,4). It is logical to hypothesize that one part of this modification is due to pressure, the other might be specific to oxygen toxicity.

The 13% increase in brain glucose in mice compressed up to 6 ATA with a nitrogen-oxygen mixture (series $N_2 + O_2$ 6 ATA) seems to diminish in animals remaining a long time at this pressure ($N_2 + O_2$ 6 ATA 60 min). A more important increase has been found in animals compressed up to 11 ATA (series $N_2 + O_2$ 11 ATA), which suggests that this alteration increases with pressure.

This increase of brain glucose cannot be due to an increase of the blood level: we observed that blood glucose was not changed by any of the exposures tested. Also, it cannot be the consequence of a glycogenolysis activation because a brain glycogen increase has been observed in all exposed animals. Thus, only a decrease of glucose consumption or an increase of glucose transport across the blood-brain barrier (BBB) can be considered.

An increase of glucose transport across BBB induced by an intravascular injection of hypertonic solution (18,19) has been found; it probably leads to an increase in brain glucose (20,21). A compression, by setting up a gradient of diluent gas concentrations between blood and brain tissue, should induce a similar phenomenon; previously, it has been shown (22–24) that gas can induce osmotic phenomenon. However, several elements disagree with this hypothesis: gas osmotic forces are very weak and such a mechanism could not explain the combined brain lactate decrease.

In normal situations, glucose is the only fuel for brain tissue. However, in some conditions such as hypercapnia, a decrease of glucose consumption with little or no change of oxygen consumption has been observed; this result could be explained by oxidation of other endogenous substrates such as lactate and glutamate (25). It appears logical to hypothesize that our results could be induced by such a mechanism, even by a tissue CO_2 retention under pressure (26).

We recently checked these two hypotheses by studying brain uptake of 2-deoxyglucose, 3-O-methylglucose, and cerebral phosphorylation of 2-deoxyglucose (27). Results obtained during this experiment show that glucose transport across BBB is not affected by a hyperbaric exposure and support the concept of a decrease of brain glucose consumption under pressure. Previous results obtained by measurement of arteriovenous differences across the brain of rabbits exposed to pressure also support this hypothesis (28).

Brain Glycogen. Brain glycogen was significantly increased in all exposed animals, whatever the hyperbaric exposure tested. Nelson et al. (29) showed that the brain glycogen increase induced by different factors generally goes with an increase in the brain/blood glucose ratio. This modification should result from a combined effect of glycogen synthesis activation plus glycogen degradation decrease. In animals exposed to a hyperbaric environment, one can also suppose that the brain glycogen increase is a consequence of the brain glucose increase.

It seems interesting to recall here that brain glycogen rapidly decreases in mice submitted to OHP (1,2,30,31). This decrease appears to be specific to OHP toxicity.

Brain Lactate. The different hyperbaric exposures tested significantly decreased the brain lactate level: this modification appeared early (series $N_2 + O_2$ 6 ATA) and held on during the whole exposure under pressure series $N_2 + O_2$ 6 ATA 60 min). Previously, it has been shown that normoxic exposures with either a nitrogen-oxygen or an helium-oxygen mixture both induce such a modification (1,2). This result is supported by the brain lactate decrease observed in mice by Nolan et al. (3) at the end of a compression up to 6 ATA with pure oxygen. In that case (OHP toxicity), brain lactate level then increased to reach a level slightly higher than controls: this last phenomenon appears to be specific to toxic partial pressures of oxygen.

Brain lactate decrease is less important in animals exposed to a narcotic nitrogen pressure (series $N_2 + O_2$ 11 ATA) than in the other hyperbaric exposures tested. Other results recently obtained in our laboratory with mice exposed at 1-ATA narcotic breathing mixtures (nitrous oxide-oxygen; xenon-oxygen) support the concept that this difference is a consequence of the narcotic potency of nitrogen at such a pressure (Fig. 3) (32); increase of pressure decreases brain lactate but "inert" gas narcosis increases it. Those two factors probably act at different levels and involve different mechanisms.

A significant blood lactate decrease was found in series $N_2 + O_2$ 6 ATA 60 min and $N_2 + O_2$ 11 ATA. During our experiments, heliox-compressed animals did not present any blood lactate modification; however, a recent experiment (27) showed that a blood lactate decrease can also appear in such conditions (He + O_2 11 and 21 ATA). Hanson et al. (33) have found a nonsignificant blood lactate decrease in rats at rest and exposed during 30 min at 5 or 6.8 ATA of air; this decrease becomes significant in exercising rats. All of these data tend to demonstrate that pressure can induce a decrease of blood lactate regardless of the breathing gas mixture. This blood lactate decrease should be combined with a pyruvate decrease; then the lactate/pyruvate ratio would not
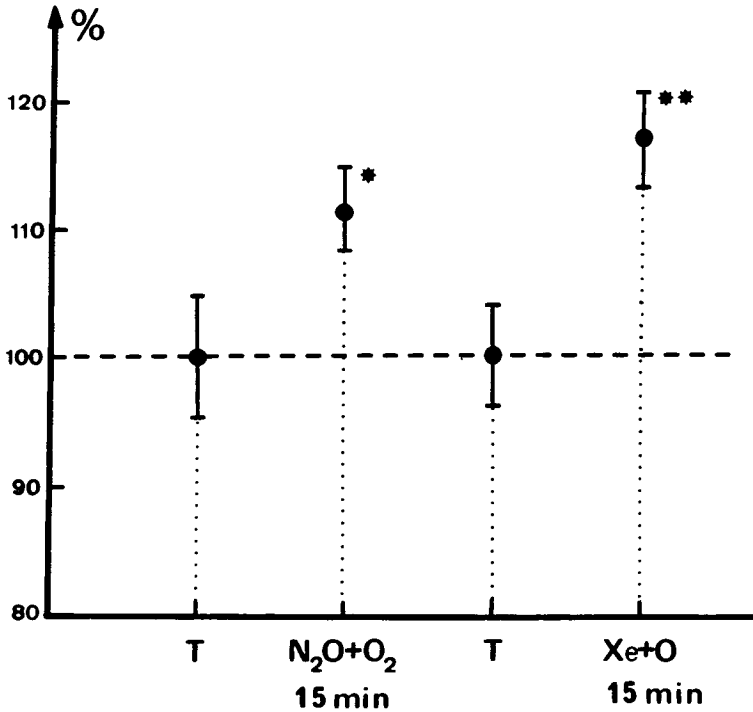
Fig. 3.   Effects of narcotic normoxic breathing mixtures at 1 ATA on the brain lactate level of mice. The results have been previously reported (32); they are here presented as percent of controls.   Xe + O_2 is xenon + oxygen; $N_2O + O_2$ is nitrous oxide + oxygen.   *P < 0.05;   ** P < 0.005   (Student's t test).

be modified (33), and this lactate decrease would not be a consequence of an altered blood oxygenation.

A blood lactate modification can interefere on the brain level (34). However, the fact that a more important decrease generally appears at the cerebral level (except in the case of narcosis), supports another mechanism: the inhibition of lactate production and, eventually, consumption of lactate as an energetic substrate.

CONCLUSIONS

The different hyperbaric normoxic exposures that we tested induced at the cerebral level an increase of glucose and glycogen combined with a decrease of lactate. Those alterations appeared early, regardless of the inhaled gas mixture, in animals without any symptoms either of nitrogen narcosis or HPNS. Mice exposed to a narcotic pressure of nitrogen showed a brain lactate decrease less important than mice exposed to heliox or to a non-narcotic pressure

of nitrogen. Results obtained at 1 ATA with narcotic gas (nitrous oxide and xenon) support the concept that this discrepancy is due to the narcotic potency of nitrogen in such conditions ($N_2 + O_2$ 11 ATA normoxia): an increase in high pressure decreases brain lactate level while gas narcosis appears to increase it. This fact leads to great caution in interpreting results with hyperbaric exposure effects because of the numerous factors involved.

Alterations here reported are induced by hyperbaric exposures corresponding to common dives. It would be interesting to understand by which mechanism they are induced. Complementary studies presently undertaken and dealing with brain glucose transport and phosphorylation will contribute to a better understanding of those pressure effects.

Acknowledgments

References

1. Brue F, Obrénovitch T. Effets de l'oxygène, de l'azote et de l'helium hyperbares sur les concentrations cérébrales en glucose, lactate et glycogène. Med Aeronaut Spat Med Subaquat Hyp 1977;16(61):62–65.
2. Brue F, Obrénovitch T, Dumas C. Effects of hyperbaric (6 ATA) nitrogen, helium and oxygen on cerebral levels of glucose lactate and glycogen. Undersea Biomed Res 1977;4(1):A-42.
3. Nolan RJ, Faiman MD. Brain energetics in oxygen-induced convulsions. J Neurochem 1974;22:645–650.
4. Nolan RJ, Dodd DE, Faiman MD. Cerebral and blood glucose in central oxygen poisoning. Undersea Biomed Res 1978;5(1):87–93.
5. Hutchins DA, Rogers KJ. Physiological and drug-induced changes in the glycogen content of mouse brain. Br J Pharmacol 1970;39:9–25.
6. Obrénovitch T, Brue F. Congélation de petits animaux en ambiance hyperbare: étude théorique et réalisation pratique. Med Aeronaut Spat Med Subaquat Hyp 1976;15(6)):271–274.
7. Taberner PV. Effects of gamma hydroxybutyric acid and other hypnotics on glucose uptake in vivo and in vitro. J Neurochem 1973;20:669–680.
8. Brauer RW, Mansfield WM, Beaver RW, Gillen HW. Stages in development of high-pressure neurological syndrome in mouse. J Appl Physiol: Respir Environ Exercise Physiol 1979;46(4):756–765.
9. Obrénovitch T, Brue F. Congélation de petits animaux isolés en ambiance hyperbare: étude expérimentale du refroidissement d'un corps plongé dans l'azote liquide a différentes pressions. Toulon, France: Centre d'Etudes et de Recherches Biophysiologiques Appliquées à la Marine, 1979. (CERB-79-05).
10. Swaab DF. Pitfalls in the use of rapid freezing for stopping brain and spinal cord metabolism in rat and mouse. J Neurochem 1971;19:2085–2092.
11. Faupel RP, Seitz HJ, Tarnowski W. The problem of tissue sampling from experimental animals with respect to freezing technique, anoxia, stress and narcosis. Arch Biochem Biophys 1972;148:509–522.
12. Miller AL, Shamban A. A comparison of methods for stopping intermediary metabolism of developing rat brain. J Neurochem 1977;28:1327–1334.
13. Ponten U, Ratcheson RA, Siesjo BK. Metabolic changes in the brain of mice frozen in liquid nitrogen. J Neurochem 1973;21:1121–1126.
14. Lowry OH, Passonneau JV, Hasselberger FX, Schulz DW. Effects of ischemia on known substrates and cofactors of the glycolytic pathway in brain. J Biol Chem 1964;239(1):18–30.

15. Yashon D, Wagner FC, Demian YK, White RJ. Cerebral lactate accumulation and glucose exhaustion during circulatory arrest. Proc Soc Exp Biol Med 1970;133:728–730.
16. Nilsson B, Norberg K. Siesjo BK. Biochemical events in cerebral ischemia. Brit J Anaesth 1975;47:751–760.
17. Kobayashi M, Lust WD, Passonneau JV. Concentrations of energy metabolites and cyclic nucleotides during and after bilateral ischemia in the gerbil cerebral cortex. J Neurochem 1977;29:53–59.
18. Spatz M, Rap ZM, Rapoport SI, Klatzo I. The effects of hypertonic urea on the blood-brain barrier and on the glucose transport in the brain. In: Reulen HJ, Schurmann K, eds. Steroids and brain oedema. Berlin: Springer-Verlag, 1972:19–27.
19. Pollay M. Effect of hypertonic solutions of the blood-brain barrier. Neurology 1975;25(9):852–856.
20. Obrénovitch T, Brue F. A propos d'une action osmotique éventuelle des fortes pressions de gaz: I—Effets de l'injection d'une solution hypertonique d'urée sur les gradients hémato-tissulaires en glucose et lactate au niveau du cerveau du foie et du muscle chez la souris. Toulon, France: Centre d'Etudes et de Recherches Biophysiologiques Appliquées à la Marine, 1980. (CERB-80-02).
21. Obrénovitch T, Brue F. A propos d'une action osmotique éventuelle des fortes pressions de gaz: II—Effets de l'injection d'une solution hypertonique d'urée sur le transport et la phosphorylation du glucose dans le cerveau, le foie et le muscle chez la souris. Toulon, France: Centre d'Etudes et de Recherches Biophysiologiques Appliquées à la Marine, 1980. (CERB-80-02).
22. Kylstra JA, Longmuir IS, Grace M. Dysbarism: osmosis caused by a dissolved gas? Science 1968;161:289.
23. Hills BA. Osmosis induced by nitrogen. Aviat Space Environ Med 1971;42(6):664–666.
24. Hills BA. Gas induced osmosis in the lung. J Appl Physiol 1972;33(1):126–129.
25. Miller AL, Hawkins RA, Veech RL. Decreased rate of glucose utilization by rat brain in vivo after exposures to atmospheres containing high concentrations of CO_2. J Neurochem 1975;25:553–558.
26. Obrénovitch T, Brue F. Effets d'une exposition à un melange respiratoire hypercapnique ou de densite élevée a la pression atmospherique, sur les concentrations sanguines at cérébrales de glucose et de lactate. Toulon, France: Centre d'Etudes et de Recherches Biophysiologiques Appliquées à la Marine, 1979 (CERB-79-16).
27. Obrénovitch T, Brue F. Effets d'une exposition hyperbare normoxique sur le transport et la phosphorylation du glucose au niveau du cerveau, du foie et du muscle. Toulon, France: Centre d'Etudes et de Recherches Biophysiologiques Appliquées à la Marine, 1980 (CERB-80-04).
28. Obrénovitch T, Brue F. Prélèvements de sang arteriel et de sang veineux cérébral chez l'animal en atmosphere hyperbare. Application aux effets de l'oxygène et de l'azote hyperbares sur la consommation cérébrale de glucose. Agressologie 1977;18(1):39–45.
29. Nelson SR, Schulz DW, Passonneau JV, Lowry OH. Control of glycogen levels in brain. J Neurochem 1968;15:1271–1579.
30. Segerbo BE. Degradation of brain glycogen during influence of oxygen high pressure and prevention by hyperosmolar glucose of acute hyperbaric oxygen toxicity. Undersea Biomed Res 1976;3:A–45.
31. Segerbo BE. Alterations in seizures mechanisms caused by oxygen high pressure, 1,1-dimethyl-hydrazine and pyridoxine. Undersea Biomed Res 1979;6(2):167–174.
32. Obrénovitch T, Brue F. Gaz "inertes" et métabolisme cerebral: effets de gaz narcotiques (xenon et protoxyde d'azote) sur les concentrations sanguines at cérébrales de glucose et de lactate. Toulon, France: Centre d'Etudes et de Recherches Biophysiologiques Appliquées à la Marine, 1979 (CERB-79-12).
33. Hanson RdeG, Gray R. Smythe P, Alberti KGMM. Blood metabolites in the rat at rest and after exericse in air at different pressures. Med Aeronaut Spat Med Subaquat Hyp 1977;16(63):257–259.
34. Oldendorf WH. Blood brain permeability to lactate. Eur Neurol 1971–1972;6:49-55.

Part VII

INERT GAS EXCHANGE AND DECOMPRESSION

CURRENT CONCEPTS OF INERT GAS EXCHANGE AND DECOMPRESSION

P. K. Weathersby and L. D. Homer

Gas exchange and decompression are venerable topics with a rich history of scientific and empirical development. In this short review, our focus will be on following the path of inert gas molecules that have reached the first barrier to entry into the body (the alveolar membrane) and follow the molecules as they move through the body. Intrapulmonary and transcutaneous gas exchange will be neglected.

MODELS OF INERT GAS EXCHANGE

Once the gas molecules have dissolved in the pulmonary circulation, they are carried through the arterial circulation before arriving at the tissues. In the major arteries little gas is lost through the vessel walls, but the molecules have been dispersed somewhat along the length of the arteries (1). This dispersion, however, does not contribute a large term to the total circulation time of mole-cules that will spend a substantial time in the capillaries. As the arteries de-crease in caliber, however, gas loss should increase. Recent calculations indi-cate that arterioles play a significant role in the exchange of oxygen (2), and the same mechanisms probably exist for the inert gases.

The major exchange of gases occurs at the level of individual capillaries, because of the very large surface area of thin wall channels. Most mathemati-cal modeling of small solute exchange has consequently focused on the capil-laries. The unit most studied in capillary modeling is the right circular cylinder with a single capillary on the axis named after its first user, A. Krogh (3). Possible gas movements in a Krogh cylinder include convective flow, barrier penetration, diffusion perpendicular to the flow axis (radial diffusion), and diffusion parallel to the flow axis (axial diffusion) as shown in Fig. 1. Two other features of the cylinder

THE JOURNEY OF A TRACER PARTICLE
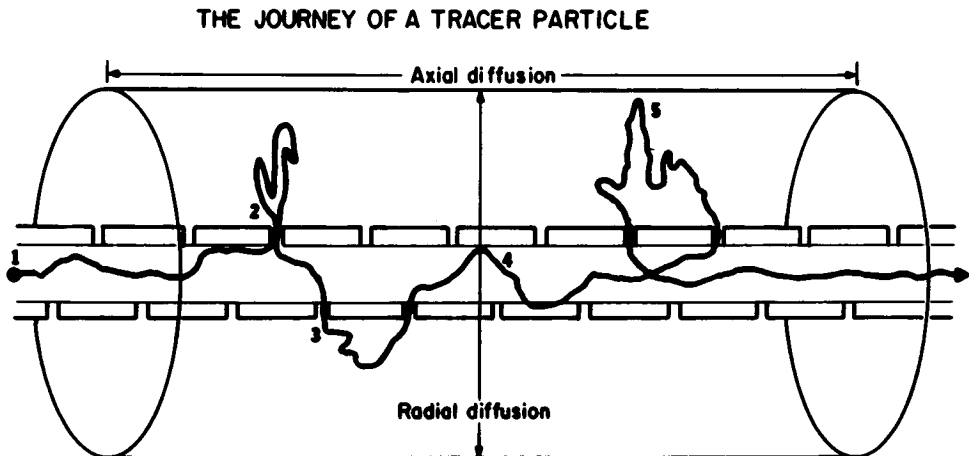
Fig. 1. Schematic diagram of Krogh capillary-tissue cylinder illustrating the possible movement of gas molecules: convective flow in the capillary, endothelial barrier transit, diffusion axially and radially in the tissue space.

must be addressed: whether gas molecules are allowed to traverse the ends of the cylinder while in the tissue space, and what happens to molecules along the outer tissue boundary. The latter consideration is the major factor in capillary-capillary interaction. The set of differential equations that describe the movements of gas within the Krogh cylinder with any boundary conditions have never been solved. The mathematical problems and approaches have been summarized by Leonard and Jorgensen (4), and a shorter summary of the resulting models was presented by Hennessy (5).

Unlike blood cells and large proteins that cannot readily leave the capillary, gas molecules will wander through the tissue and be delayed in exiting. For nonpolar molecules such as the inert gases, a common simplifying assumption is that the capillary endothelial wall is freely permeable to the gas molecules. This assumption avoids many of the barrier treatments necessary to describe the movements of charged molecules (6). The most common model of tissue exchange assumes that no diffusion gradients exist and the entire cylinder is well mixed (7). This model predicts a single exponential response to step- or pulse-input of gas. Of the thousands of curves we have examined in our own work and in reviewing the literature, we have found exactly one curve that appears to be truly exponential over more than two orders of magnitude in concentration (8).

Several models of Krogh cylinders with totally closed boundaries combine flow with a single direction for tissue diffusion. The simplest is a "lumped" diffusion barrier between capillary and tissue, both of which are considered well mixed (9). This model leads also to a prediction of exponential kinetics, but with the half-time decreased as the diffusion coefficent increases. Experimental evidence against this model is strong (9, 10).

Another model assumes that only tissue diffusion in the axial direction is significant (11). This model has recently been applied specifically to the washout of inert gases (12). For very large values of the diffusion coefficent, this model leads to the well-stirred compartment with exponential kinetics.

A fourth model follows from an'assumption that only diffusion radially in tissue is important. Such a model was proposed by Hills (13) and useful solutions were obtained by Hennessy, who provided both a full solution for diffusion into a solid tissue cylinder bathed on the outside with a well-mixed fluid (14), and a Laplace transform solution of the Krogh geometry useful for numerical inversion and moment evaluation (5).

The closed radial boundary models described above make no provision for gas movement between capillaries, and this assumption is appropriate if all the capillaries are parallel, have cocurrent flow, and have arterial and venous ends aligned. A fifth gas exchange model has been proposed that approaches an open radial boundary—the diffusion slab used by Hempleman (15). The slab model as used was finite in extent, though it was intended to imply a very "deep" tissue. This and other pure diffusion models require the physically unrealistic boundary condition that the face of the tissue slab must instantaneously equilibrate with arterial blood. This leads to the paradox of having a zero average residence time of gas molecules in the tissue.

Two models deal with a Krogh cylinder that has closed radial boundaries but open axial boundaries; that is, gas molecules are allowed to diffuse backward in the tissue space into arteriolar spaces and forward into the area of venules. The random walk with imposed drift model of Feller is the appropriate combination of flow and axial diffusion (16). We have recently combined barrier limitations, flow, axial diffusion, and radial diffusion in a single stochastic model that evaluates the first two moments of the residence time distribution without specifically obtaining the analytic solution to the set of differential equations (17). The general solution has additive terms for the residence time variance for each of the transport modes. The form of the combined variance expression is similar to the result of Aris (18) for spatial moments of chromatographic peaks, where the solute is subject to flow and two-dimensional diffusion with closed radial and open axial boundaries. Levitt has applied parts of the Aris approach to capillaries (19).

Most of these models produce complicated equations that have the same general shape. To obtain a unified approach to the models, we have proposed that the models be summarized in terms of their moments. Moments are weighted averages of the variable times that gas molecules reside in tissue. The first two moments are the well-known mean and the variance (square of the standard deviation). In most models, the mean depends only on blood flow and gas solubility; the variance includes the actual model interpretation of capillary mechanisms. Small variance corresponds to rapid dispersion, and large variances to slower dispersion (20).

The appropriate formulation of the variance in terms of the model parameters are tabulated in Table I. Summarizing experimental data in terms of these moments is also readily accomplished (21). Note that the radial and axial diffusion models predict the inverse dependence of kinetics on gas diffusion coefficient. The radial diffusion models predict that gas washout from tissue should be more rapid with a large diffusion coefficient than with a small one. The axial diffusion models predict the reverse: gas washout is more rapid for the gas with the smaller diffusion coefficient. Accurate information on tissue diffu-

TABLE 1

Capillary Gas Exchange Models

Model	Boundaries		Flow	Axial	Radial	Diffusion Barrier	Variance
	Axial	Radial					
Well Mixed (7)	closed	closed	yes	no	no	no	M^2
Lumped Barrier (9)	closed	closed	yes	no	no	yes	M'^2
Perl-Chinard (11)	closed	closed	yes	yes	no	no	$2M^3D/L^2 (1 - [MD/L^2] [1-\exp(-L^2/MD)])$
Hennessy (5)	closed	closed	yes	no	yes	no	$M'' A(r) / D$
Hempleman (15)	closed	closed	no	no	yes	no	—
Feller (16)	open	closed	yes	yes	no	no	$2 M^3 D / L^2$
Homer (17)	open	closed	yes	yes	yes	yes	$V(rad) + V(ax) + V(bar)$

Numbers in parentheses under models are references in text.   M is mean residence time $= V \lambda /F$;   V is volume of tissue cylinder; λ = tissue/blood partition coefficient;   F is capillary flow rate;   M', M'' are adjusted mean residence times;   D is gas diffusion coefficient;   L is length of tissue cylinder;   A(r) is numerical constant dependent on radius.   V(i) is variances for radial, axial, and barrier diffusion: V(rad) is numerically close to result of Hennessy (5);   V(ax) is numerically close to Feller (16);   V(bar) is numerically close to Goresky (6).

sion coefficients and capillary dimensions is needed to help sort out these different models.

Our combined model indicates that Hennessy's radial diffusion model should be appropriate for diffusion coefficients smaller than 10^{-8} cm²/s. If the diffusion coefficients are about 10^{-6} cm²/s or greater then radial diffusion is relatively unimportant, and we should consider one of the two axial models. For large diffusion coefficients the axial model of Perl and Chinard (11) approaches the well-mixed single exponential model. To date the variances we have estimated seem to favor the random walk model with open ends rather than the Perl-Chinard model.

The basic physiologic parameters to be used in the tissue exchange models are difficult to find in the literature. Tissue gas solubilities and partition coefficients recently have been tabulated (22). Measurements of gas diffusion coefficient are scarce. Hills's claim that the tissue value is lower than usual aqueous values by 3 to 5 orders of magnitude (13,23) has serious implications in tissue gas exchange—that is, radial diffusion in the tissue will be more important in controlling kinetics than even the blood flow. However, the bulk of the evidence, including recent measurements on rat liver cells (24), muscles (25,26), and eye tissues (27) all point to diffusion coefficients between one-fifth and one-half of the usual values in water. This suggests we should give primary attention to axial diffusion models.

All models described so far focus on an individual "typical" capillary. Obviously, the body has many different vascular beds (28) and we do not expect a single capillary model to describe, say, whole-body washout. Years ago Behnke proposed a two-tissue model of the whole body that used two well-mixed compartments to account for the two "solvents"—oil and water—that comprised an entire organism (29). This concept was a very reasonable assumption at the time since it explained the apparently two-exponential form of experimental washout data in a manner testable by independent measures of body composition in terms of fat and lean tissues. However, these prospects failed and more recent combinations of well-mixed compartments have simply proliferated the number of compartments and adjustable parameters far beyond the point of any reconciliation with the actual physiology. One exception was the model of Perl et al. (30) that fitted data from a two-gas experiment (31) to a two-compartment model with a direct diffusion connection.

A treatment of capillary beds that attempts to deal with staggered but still cocurrent capillaries has been proposed by Levitt (32). His solution is intermediate between the Perl-Chinard and the well-mixed models as would be expected for these closed axial boundary approaches. Extension of any of these analytic models to account for countercurrent capillary flows would be useful but does not appear to be available. Strong experimental evidence exists for effective countercurrent behavior: when dissolved inert gas and blood cells are simultaneously injected into an artery, the gas appears in venous blood before the cells (33). Some numerical work on simulating capillary networks with combinations of cocurrent and countercurrent features has been published for

oxygen transport (34,35). The results of such studies are numerical rather than parametric, and since the original equations with oxygen have a strong consumption term, extension to inert gases is not direct.

Another approach to heterogeneity is suggested by statistical approaches. If one can relate gas exchange properties of a single type of capillary bed to its capillary parameters, then the whole tissue response can be obtained by using the distribution of capillary parameters, e.g., the flow rates, across all capillary types found in the tissue. Combining such distributions was proposed by Macey (36). Moments are particularly convenient parameters for combining results from many tissues and experiments since straight-forward formulas exist for combining moments from serial or parallel vascular beds. Formulas also exist for computing the effects on moments of variations of a parameter with a single capillary (37). At this time, reliable information on the distribution of capillary parameters across organs is even rarer than good mean values. Studies such as those reported by Renkin at this symposium (38) are critically needed.

Some phenomena are not systematically included in any models. Hills has recently raised the possibility that blood flows in some tissues may be so unsteady in time as to confound the present assumptions of time stationarity (39). The linearity assumption may be violated following decompression. Several experimental studies have concluded that gas exchange may be enhanced (40) or retarded (41,42) after significant decompressions. The changes are most frequently interpreted as due to intravascular or tissue gas bubbles (43). The possibility that less pathological effects, such as altering local blood flow (44), has not been sufficiently examined.

DECOMPRESSION MODELS

All present methods for calculating decompression schedules presume that gas bubbles must be avoided, or at least not permitted to get numerous or large. This aspect of decompression is easy to formulate physically and mathematically, but difficult to evaluate experimentally. Since Haldane (45), the most common supposition was that a finite degree of tissue supersaturation— defined as the amount of gas held in tissue in excess of the amount possible by equilibrium solubility—could be tolerated without the formation of bubbles. Decompression calculations would then proceed to recommend a rate of decompression that did not have a calculated tissue gas quantity in excess of this supersaturation. Haldane's original rule was to allow 100% supersaturation; subsequent extensions of that work produced a large number of allowable figures from 35% to over 200% (46).

The work of Harvey and colleagues (47) concluded that actual gas nucleation in vivo was impossible unless decompressions of hundreds of atmospheres were experienced. Yount's recent review of nucleation theory reaches the same conclusion (48). Their objections to homogeneous nucleation appear to be based on calculations for nucleation of pure water. Examination of the nucleation equations (49) lead one to expect less severe decompression to be required

with physiological parameters. This is partly because surface tensions will be lower in the body than in pure water, and partly because of the opportunity for nucleation to occur at more favorable surfaces. Initial formation of gas bubbles at an interface between two substances, called heterogeneous nucleation, has been recognized as occasionally an easier site for nucleation, but systematic exploration of this topic has not been undertaken. In any case, the theory leads to risk estimates proportional to the difference between ambient and dissolved pressures, not the ratio. Thus discussions of "critical supersaturation ratios" are inconsistent with a belief in nucleation as the precipitating event in decompression sickness (DCS).

A second school of thought supposes that no finite supersaturation can be tolerated without bubble formation. The only means to avoid bubbles by this view is to match decompression rate with gas kinetics to use the "oxygen window": tissue gas tension at steady state is assumed to be appreciably lower than ambient because of the nonlinear oxyhemoglobin dissociation curve and the high solubility of carbon dioxide (23,50). If bubble formation is deemed unavoidable, some other aspects of the bubble must be damaging. Hennessy has examined the possibility that a certain volume of gas phase is necessary for symptoms (51). This approach predicts DCS to occur with tissue pressure and ambient pressure related by a straight line with a non-zero slope and non-unity intercept. Hills has achieved the same mathematical result with a model invoking a critical degree of tissue elastic deformation (52).

Others believe that not only do bubbles form easily they are always present in tissue. Deformation of elastic tissues is the basis for such a development by Vann and Clark (53), which invokes arguments used in analyzing rubber behavior. Starting from a large series of experiments with gelatin, Yount has developed a mathematical description of DCS that expresses risk as a function of the number of bubbles present (54). His original predictions matched the straight line of other theories, and has recently been extended to allow curvature by positing special behavior of interfacial molecules (55).

If bubbles actually form, some quantitative treatment is needed for the kinetics of bubble growth and shrinkage. Large bodies of engineering and physiological literature are available on this problem. The partial differential equations in general are complex (56), but can be simplified immediately by the the physiologically realistic assumptions of constant temperature, slowly varying pressure, and ideal gas behavior (57). Problems in the solution come not from dealing with the bubble itself, but from setting boundary conditions according to the expected physiologic state of nearby tissue. Van Liew has studied and modeled the case of large chronic gas pockets (58) where a thin diffusion barrier is appropriate. Solutions for a uniformly distributed "sink" of intact blood vessels (59), and for small bubbles in the middle of large diffusion fields have also been published (60). The various models disagree on the importance of tissue diffusion coefficient and on the dependence of bubble radius with time: both linear and square-root relations may be appropriate.

The interaction of nucleation theories with theories of gas washout poses some interesting possibilities. If we assume the blood-tissue partition coefficients are about the same for nitrogen and for helium, then the axial diffusion

models predict that nitrogen will be washed out of tissue more rapidly than helium. The peak supersaturations, however, following a decompression maneuver after saturation should be greater and more prolonged for nitrogen than for helium. The consequence is that for theories stating that bubbles are easily formed, or always present, nitrogen should lead to fewer cases of decompression sickness than helium following similar decompression maneuvers from saturation dives. If nucleation, on the other hand, is a relatively rare event, but nearly always leads to symptoms when it occurs, then nitrogen should be more often associated with decompression sickness than helium in saturation dives. The transient situations on dives far short of saturation will be more complicated as we may expect tissue accumulation of nitrogen to be the more rapid.

DECOMPRESSION EXPERIMENTS

We now pose the crucial question: Is inert gas, and especially bubbles of inert gas, responsible for human DCS? Though a nearly universal assumption, the chain of inference is incomplete. Very pure water will form bubbles after decompression from several hundred atmospheres of excess dissolved gas pressure (61). Less pure aqueous liquids will form bubbles after much less exposure; perhaps only a fraction of an atmosphere (23,54). Unicellular organisms may not show bubbles until more than 100 ATA decompression are exceeded (62,63), but excised animal tissues appear to be much more vulnerable (47,63). Numerous studies have reported that severely decompressed animals will have visible bubbles present at autopsy.

The recent proliferation of Doppler ultrasonic detectors has given rise to numerous reports of decompression-associated signals. This usage has sprung up largely without quantitative analysis of the highly transformed and filtered signals. Perhaps it is not surprising that the only double-blind study with which we are familiar reports basically a random association of Doppler events and clinical DCS (64). More direct quantitative ultrasonic devices (65,66) appear to be ready to answer some of the crucial questions: Where do bubbles appear and what do they do? The Oxford device, described elsewhere in this Symposium, in particular appears to be capable of providing this data. Despite the comprehensive work of Hallenbeck in determining the natural history of serious spinal cord DCS (67), no link has ever been shown between the much more common limb bends and any bubble event.

The probabilistic nature of DCS has been underemphasized. Experimental studies of nucleation show random generation of bubbles, and gas exchange can be viewed as a statistical process. Certainly, decompression trials (68,69) are tests of a random event and more use can be made of dose-response curves (68,70,71) than estimation of a midpoint.

What links with gas events are available from experimental decompression? The near linear dependence of saturation (i.e., tissue) pressure and post-decompression (ambient) pressure has been well established for rats (72), and men (73,74). As already seen, numerous theories can account for this relation-

ship. In small-animal decompression studies, the effects of carbon dioxide (75) and oxygen (76) are not negligible as assumed by the oxygen window approach. Temperature also appears important (77). The advantage of one gas over another is not straightforward. Nitrogen appears to be safer for short pressure exposures, and helium seems safer at nearly steady-state (71,78). Animal work with other inert gases provides a wider data base even though the resulting symptoms can point toward other disease processes (79,80). A fast pressure spike decreases subsequent DCS incidence (81,82). This phenomenon is interpreted physically as "crushing" existing bubbles, but physiological explanations, such as diminution in tissue blood flow, have not been explored.

CONCLUSION

Decompression sickness as an occupational disease has been approached by a long empirical development. The premise behind modification of procedures has been concepts of inert gas exchange and bubble mechanics. The experimental and theoretical evidence for such a hypothesis is strong but not conclusive. Many physical and physiological principles are involved; the quantitative application of them remains to be accomplished.

Acknowledgments

References

1. Bassingthwaighte JB, Ackerman FH. Mathematical linearity of circulatory transport. J Appl Physiol 1967;22:879–888.
2. Popel AS, Gross JG. Analysis of oxygen diffusion from arteriolar networks. Amer J Physiol 1979;237:H681–H689.
3. Krogh A. The number and distribution of capillaries in muscles with calculation of the oxygen pressure head necessary for supplying the tissue. J Physiol 1919;52:409–415.
4. Leonard EF, Jorgensen SB. The analysis of convection and diffusion in capillary beds. Ann Rev Biophys Bioengr 1974;3:293–339.
5. Hennessy TR. The interaction of diffusion and perfusion in homogenous tissue. Bull Math Biol 1974;36:505–526.
6. Goresky, CA, Ziegler WH, Bach GG. Capillary exchange modeling: barrier limited and flow limited distribution. Circ Res 1970;27:739–764.
7. Kety SS. The theory and application of the exchange of inert gas at the lungs and tissues. Pharmacol Rev 1951;3:1–41.
8. Sejrsen P.\Measurement of cutaneous blood flow by freely diffusible radioactive isotopes. Danish Med Bull 1971;18 Suppl 3:3–38.

9. Ohta Y, Song SH, Groom AC, Farhi LE. Is inert gas washout from tissues limited by diffusion? J Appl Physiol 1978;45:903–907.

10. Ohta Y, Fahri LE. Cerebral gas exchange: perfusion and diffusion limitations. J Appl Physiol: Respirat Exercise Environ Physiol 1979;46:1164–1168.

11. Perl W, Chinard FP. A convection-diffusion model of indicator transport through an organ. Circ Res 1968;22:273–298.

12. Tepper RS, Lightfoot EN, Baz A, Lanphier EH. Inert gas transport in the microcirculation: risk of isobaric supersaturation. J Appl Physiol:Respirat Exercise Environ Physiol 1979;46:1157–1163.

13. Hills BA. Diffusion versus perfusion in limiting the rate of uptake of inert nonpolar gases by rat skeletal muscle. Clin Sci 1967;33:67–87.

14. Hennessy TR. Inert gas exchange in heterogeneous tissue. II. With perfusion. Math Biophys 1971;33:249–257.

15. Hempleman HV. British decompression theory and practice. In: Bennett PB, Elliott DH, eds. The physiology and medicine of diving and compressed air work. Baltimore: Williams & Wilkins, 1969:331–347.

16. Feller W. An introduction to probability theory and its applications, Vol. 1, 2nd ed. New York: Wiley, 1968: Chapter 14.

17. Homer LD, Weathersby PK. The variance of the distribution of traversal times in a capillary bed. J Theor Biol 1980;87:349–377.

18. Aris R. Compartmental analysis and the theory of residence time distributions. In: Warrent KB, ed. Intracellular transport. Symposia of the International Society for Cell Biology 1966;5:167–197.

19. Levitt DG. Capillary-tissue exchange kinetics; an analysis of the Krough cylinder model. J Theor Biol 1972;34:103–124.

20. Homer LD, Small A. A unified theory for estimation of cardiac output, volumes of distribution, and renal clearances from indicator dilution curves. J Theor Biol 1977;64:535–550.

21. Weathersby PK, Barnard EEP, Homer LD, Mendenhall KG. Stochastic description of inert gas exchange. J Appl Physiol: Respirat Environ Exercise Physiol 1979;47:1263–1269.

22. Weathersby PK, Homer LD. Solubility of inert gases in biological fluids and tissues. Undersea Biomed Res 1980;7:277–296.

23. Hills BA. Decompression sickness. Vol. 1: The biophysical basis of prevention and treatment. New York: John Wiley & Sons, Inc. 1977.

24. Evans AL, Busuttil A, Gillespie FC, Unsworth J. The rate of clearance of Xenon from rat liver sections in vitro and its significance in relation to intracellular diffusion rates. Phys Med Biol 1974;19:303–316.

25. Kawashiro T, Carles AC, Perry SF, Piiper J. Diffusivity of various inert gases in rat skeletal muscle. Pflugers Arch 1975;359:219–230.

26. Unsworth J, Gillespie FC. Diffusion coefficients of xenon and krypton in water from 0°C to 80°C and in biological tissue at 37° C. In: Sherwood JN, Chadwick AV, Muir WM, Swinton FL, eds. Diffusion processes. New York: Gordon and Breach, 1969:599–608.

27. Strang R. The determination of the diffusion coefficent of krypton in rabbit ocular tissues. Invest Opthmalmol Visual Sci 1977;16:83–86.

28. Goresky CA, Goldsmith HL. Capillary-tissue exchange kinetics: diffusional interactions between adjacent capillaries. In: Bruley DF, Bicher HI, eds. Oxygen transport to tissue, International Symposium on. Vol. 2 New York: Plenum, 1973:773–782.

29. Behnke AR, Thomson RM, Shaw LA. The rate of elimination of dissolved nitrogen in man in relation to the fat and water content of the body. Amer J Physiol 1936;114:137–146.

30. Perl W, Rackow H, Salanitre E, Wolf GL, Epstein RM. Intertissue diffusion effect for inert fat-soluble gases. J Appl Physiol 1965;20:621–627.

31. Rackow HL, Salanitre E, Epstein RM, Wolf GL, Perl W. Simultaneous uptake of N_2O and cyclopropane in man as a test of compartment model. J Appl Physiol 1965;20:611–620.

32. Levitt DG. Theoretical model of capillary exchange incorporating interactions between capillaries. Amer J Physiol 1971;220:250–255.

33. Sejrsen P. Convection and diffusion of inert gases in cutaneous, subcutaneous, and skeletal muscle tissue. In: Crone C., Lassen NA, eds. Capillary permeability. Proceedings of the Alfred Benzon Symposium II. New York: Academic Press, 1970:586–602.

34. Metzger H. Distribution of oxygen partial pressure in a two-dimensional tissue supplied by capillary meshes and concurrent and countercurrent flow. Math Biosci 1969;5:143–154.

35. Gruenwald WA, Sowa W. Capillary structure and O_2 supply to tissue. An analysis with a digital diffusion model as applied to the skeletal muscle. Rev Physiol Biochem Pharmacol 1977;77:149–209.

36. Macey R. A probabilistic approach to some problems on blood-tissue exchange. Bull Math Biophys 1956;18:205–217.

37. Kendall MG, Stuart A. The advanced theory of statistics. 2nd ed, Vol III, New York: Hafner, 1968.

38. Renkin EM, Gray SD, Dodd LR, Lia BD. Heterogeneity of capillary distribution and capillary circulation in mammalian skeletal muscles. In: Bachrach AJ, Matzen MM. Underwater physpology VII. Proceedings of the seventh symposium on underwater physiology. Bethesda, MD: Undersea Medical Society, 1981: 465–475.

39. Hills, BA. Intermittent flow in tendon capillary bundles. J Appl Physiol: Respirat Environ Exercise Physiol 1979;46:696–702.

40. Kindwall E, Lightfoot EN, Lanphier EN, Seirig E. Nitrogen elimination in man during decompression. Undersea Biomed Res 1975;2:285–297.

41. D'Aoust BG, Smith KH, Swanson HT. Decompression induced decrease in nitrogen elimination rate in awake dogs. J Appl Physiol 1976;41:348–355.

42. Hills BA. Effect of decompression per se on nitrogen elimination. J Appl Physiol: Respirat Environ Exercise Physiol 1978;45:916–921.

43. Lightfoot EN, Baz A, Lanphier EH, Kindwall EP, Seireg A. Role of bubble growth kinetics in decompression. In: Shilling CW, Beckett MW, eds. Underwater physiology VI. Bethesda, MD: Federation of American Societies for Experimental Biology, 1978:449–457.

44. Bove AA, Famiano FC, Levin LL, Carey RA, Pierce AL, Lynch PR. Alterations in long-bone regional blood flow associated with inadequate decompression in dogs. Undersea Biomed Res 1977;4:169–182.

45. Boycott AE, Damant GCC, Haldane JS; The prevention of compressed air illness. J Hyg Ca. b) 1908;8:342–443.

46. Workman RD. Nitrogen-oxygen and helium-oxygen dives. Research Rpt 6–65. US Naval Experimental Diving Unit, Washington DC, 1965.

47. Harvey EN, Barnes DK, McElroy WD, Whiteley AH, Pease DC, Cooper KW. Bubble formation in animals. I. Physical factors. J Cell Comp Physiol 1944;24:1–22.

48. Yount DE. Decompression sickness. In: International symposium on man in the sea. Chapt. V. Bethesda, MD: Undersea Medical Society, 1974.

49. Blander M, Katz JL. Bubble nucleation in liquids. Am Inst Chem Eng J 1975;21:833–848.

50. Behnke AR. The isobaric (oxygen window) principle of decompression. In: The new thrust seaward. Washington: Marine Technology Society. 1967:213–230.

51. Hennessy TR. An examination of the critical released gas concept in decompression sickness. Proc Roy Soc (Lond) 1977;B197:299–443.

52. Hills BA. A quantitative correlation of conditions for the occurrence of decompression sickness for aerial and underwater exposures. Rev Subaquat Physiol Hyperbaric Med 1969;1:249–254.

53. Vann RD. Clark HG. Bubble growth and mechanical properties of tissues in decompression. Undersea Biomed Res 1975;2:185–194.

54. Yount DE, Strauss RH. Bubble formation in gelatin: a model for decompression sickness. J Appl Physics 1976;47:5081–5088.

55. Yount DE. Skins of varying permeability: a stabilization mechanism for gas cavitation nuclei. J Acoust Soc Amer 1979;65:1429–1439.

56. Scriven LE. On the dynamics of phase growth. Chem Eng Sci 1959;10:1–13.

57. Rosner DE, Epstein M. Effects of interface kinetics, capillarity, and solute diffusion on bubble growth rates in highly supersaturated liquids. Chem Eng Sci 1972;27:69–86.

58. Van Liew HD. Coupling of diffusion and perfusion in gas exit from subcutaneous gas pockets. Amer J Physiol 1968;214:1176–1185.

59. Hlastala M, Van Liew HD. Absorption of in-vivo inert gas bubbles. Respir Physiol 1975;24:147–158.

60. Epstein PS, Plesset MS. On the stability of gas bubbles in liquid-gas solutions. J Chem Physics 1950;18:1505–1509.

61. Hemmingsen EA. Cavitation on gas-supersaturated solutions. J Appl Physics 1975;36:213–218.

62. Hemmingsen EA, Hemmingsen BB. Lack of intracellular bubble formation in microorganisms at very high gas supersaturations. J Appl Physiol: Respirat Environ Exercise Physiol 1979;47:1270–1277.

63. Harvey EN, Whiteley AH, Cooper KW, Pease DC, McElroy WD. The effect of mechanical disturbance on bubble formation in single cells and tissues after saturation with extra high gas pressures. J Cell Comp Physiol 1946;28:325–337.

64. Bayne CG, Hunt WS, Bray PG, Johanson DC. A prospective clinical trial in human decompression sickness. Undersea Biomed Res 1979;6 Suppl 1:17a (Abstr).

65. Rubissow GJ, Mackay RS. Decompression study and control using ultrasonics. Aerosp Med 1974;45:476–478.

66. Daniels S, Paton WDM, Smith EB. Ultrasonic imaging system for the study of decompression-induced gas bubbles. Undersea Biomed Res 1979;6:197–207.

67. Hallenbeck JM, Bove AA, Elliott DH. Mechanisms underlying spinal cord damage in decompression sickness. Neurology 1975;25:308–316.

68. Buckles RG, Hardenbergh E. The role of inert gas exchange and population statistics in studies of decompression sickness. In: Reneau DD, ed. Chemical engineering in medicine. Advances in Chemistry Series 118. Washington: American Chemical Society, 1973:17–34.

69. Berghage TE, Woolley JM, Keating LJ. The probabilistic nature of decompression sickness. Undersea Biomed Res 1974;1:189–196.

70. Berghage TE, Armstrong FW, Conda KJ. Relationship between saturation exposure pressure and subsequent decompression in mice. Aviat Space Environ Med 1975;46:244–247.

71. Flynn ET, Lambertsen CJ. Calibration of inert gas exchange in the mouse. In: Lambertsen CJ, ed. Underwater physiology. Proceedings of the fourth symposium on underwater physiology. New York: Academic Press, 1971:179–191.

72. Berghage TE, Gomez JA, Roa CE, Everson TR. Pressure-reduction limits for rats following steady-state exposures between 6 and 60 ATA. Undersea Biomed Res 1976;3:261–271.

73. Barnard EEP. Fundamental studies in decompression from steady-state exposures. In: Lambertsen CJ, ed. Underwater physiology V. Proceedings of the fifth symposium on underwater physiology. Bethesda, MD: Federation of American Societies for Experimental Biology, 1976:263–271.

74. Spaur WH, Thalmann ED, Flynn ET, Zumrick TW, Reedy TW, Ringelber JM. Development of unlimited duration excursion tables and procedures for helium-oxygen saturation diving. Undersea Biomed Res 1978;5:159–177.

75. Berghage TE, Keating LJ, Woolley JM. Decompression sickness in rats and mice rapidly decompressed after breathing various concentrations of carbon dioxide. In: Lambertsen CJ, ed. Underwater physiology. Proceedings of the fourth symposium on underwater physiology. New York: Academic Press, 1971:485–496.

76. Berghage TE, McCracken TM. Use of oxygen for optimizing decompression. Undersea Biomed Res 1979;6:231–239.

77. Tobias CA, Loomis WF, Lawrence JH. Studies on skin temperature and circulation in decompression sickness. Amer J Physiol 1947;149:626–633.

78. Berghage TE, Donelson C IV, Gomez JA. Decompression advantage of trimix. Undersea Biomed Res 1978;5:233–242.

79. Lever MJ, Paton WDM, Smith EB. Decompression characteristics of inert gases. In: Lambertsen CJ, ed. Underwater physiology. Proceedings of the fourth symposium on underwater physiology. New York: Academic Press, 1971:123–136.

80. Daniels S, Paton WDM, Smith EB. Use of exotic gases for the study of decompression sickness. In: Lambertsen CJ, ed. Underwater physiology. Proceedings of the fourth symposium on underwater physiology. New York: Academic Press, 1971:475–484.

81. Vann RD, Grimstad J, Nielsen CH. Evidence for gas nuclei in decompressed rats. Undersea Biomed Res 1980;7(2):107–112.

82. Evans A, Walder DN. Significance of gas micronuclei in the aetiology of decompression sickness. Nature 1969;222:251–252.

SPECIES INDEPENDENT MAXIMUM NO-BUBBLE PRESSURE REDUCTION FROM SATURATION DIVE

Y. C. Lin

Construction of a decompression table is based on the fact that animal tissue can tolerate a certain degree of supersaturation without forming bubbles. Formulation of an efficient decompression table depends on determination of pressure reduction (ΔP) from a saturation pressure (P_1) to a lower pressure (P_2) and depends on determination of the duration required at P_2 before subsequent pressure reduction can be made. The duration required at each stage of decompression is a function of the rate of inert gas elimination and thus is species-dependent (1), and metabolic state-dependent (1,2). On the other hand, the maximum ΔP without forming bubbles is determined by the physics of bubble formation in a given liquid and thus may not be species- and metabolic state-dependent. The objective of this study was to determine and to compare the maximum ΔP allowable from a saturation dive without forming intravascular bubbles in rats, cats, and dogs.

The decompression schedules currently in use are mainly a result of empirical trials, and to a lesser extent rely on extrapolation from animal models. Animal models should be useful for testing new decompression tables derived theoretically, and for improving existing tables, if interspecies correlation can be made. The convenience of using laboratory animals is often offset by the difficulty in assessing decompression stress, which is less than debilitating or fatal. Evaluation of decompression stress by symptomatic or behavioral observation, or both, in animals is relatively imprecise. Because observed symptoms are results of a major decompression stress and are evaluated subjectively in most cases, it is therefore desirable to determine some presymptomatic parameters by means of an objective criterion. This paper is such an attempt, by monitoring the threshold of intravascular bubble formation. The threshold of

decompression-induced intravascular bubbles was detected by an ultrasonic Doppler flowmeter.

MATERIALS AND METHODS

Rats (Male Wistar) weighing 475 ± 25 g were anesthetized with pentobarbital sodium (40 mg/kg) and surgically prepared by implanting a 2- to 3-mm diameter perivascular Doppler probe (Parks Electronics, Beaverton, OR) on the posterior vena cava caudad to the renal veins (3). This chronic preparation was chosen over an external probe to eliminate the necessity of anesthetizing the animal during compression and subsequent decompression. The wire leads from the probe were run subcutaneously to the top of the head between the two ears.The flowmeter probes with frequencies of 8.0–10.0 MHz were tested for bubble-detecting ability in vitro before implantation by introducing bubbles into water flowing through a polyethylene tubing. The ability to detect bubbles in vivo was again confirmed following surgical preparation by injecting small volumes of air through a 25-G needle into the femoral vein. Rats were allowed to recover for at least 24 h before experimentation.

Dogs weighing between 18.0 and 22.0 kg were also surgically prepared in a way similar to the rat by use of 16- to 20-mm diameter flowmeter probes; however, the probe was located on the posterior vena cava between the heart and the diaphragm. Two weeks were allowed for recovery following surgery. The bubble-detecting ability of the implanted probes was also tested by injecting small amounts of air through a superficial vein in the hind leg.

Cats of either sex weighing between 2.3 and 3.2 kg were anesthetized with 50–60 mg/kg sodium pentobarbital. A 3-mm Doppler perivascular flow probe was implanted on the vena cava caudad to the renal veins and the connecting wires exteriorized. The cat was placed in the chamber on its side under anesthesia. The bubble-detecting ability of the probe was tested in a way similar to that of the dog.

Detection of intravascular bubbles was made by a Parks Electronics Doppler Flowmeter Model 803 with the output signal fed to an audio amplifier, a cassette tape recorder, and a pen-writing oscillographic recorder. The bubbles can be detected by the distinct Doppler-shifted chirping sounds, or from recorded traces.

Animals were subjected to a step increase in ambient pressure (P_1) under these conditions: unanesthetized rats in a 1-L chamber for 1 h, anesthetized cats in a 50-L chamber for 4 h, and dogs in a human hyperbaric chamber (Hahn and Clay, Houston, TX) for 6 h. Following these exposures, pressure reduction was carried out as rapidly as the system permitted to a predetermined lower pressure (P_2). If there was no indication of bubbles within 1 h, the decompression was considered bubble-free. For each saturation pressure (P_1), an increasing pressure difference (ΔP) to a lower pressure (P_2) was tried on each exposure until the threshold for bubble detection was found. In the rat, repeat exposures were at least 24 h but no longer than 4 days after first

exposures. For the dog, the repeat compression-decompression exposures were made weekly. No repeat exposure was made on the cat. Compressed air was used in all experiments.

RESULTS

Rat A total of 54 decompression trials were made on 39 rats. The data shown on Fig. 1 are the greatest ΔP values not producing bubbles and the smallest ΔP values where bubbles were detected during the first pressure exposures. Each point represents one rat for one pressure exposure. Trial points with values greater than the lowest ΔP with bubbles (*circles*) and less than the highest ΔP without bubble (*squares*) have been omitted. The true threshold for Doppler-detected intravascular emboli can be considered to lie between the paired bubble and no-bubble lines. *Upper dashed lines* indicate incidence levels for decompression sickness based on behavioral observations of Berghage et al. (4). Data on the repeat pressure exposures for the rat are similarly summarized in Fig. 2. The *paired lines without data points* indicate the regression lines of the first exposure results as seen in Fig. 1. It is important to note that
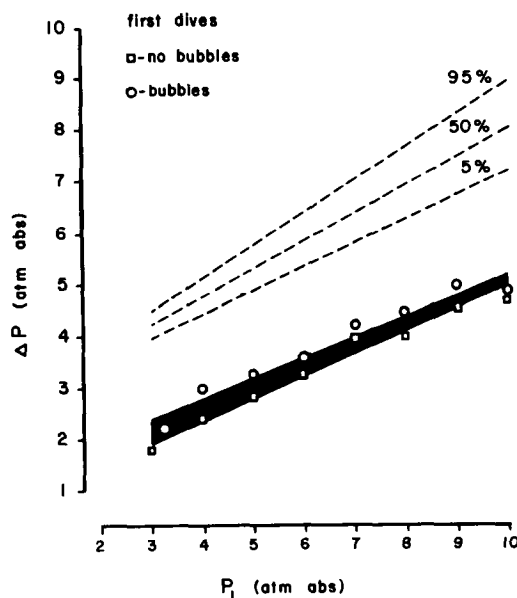
Fig. 1. Doppler-determined decompression sickness thresholds based on the detection of venous gas emboli in the rat during the first pressure exposure. *Circles* represent the minimum pressure reduction from from saturation that produces intravascular bubbles. *Squares* represent the maximum pressure reduction from saturation that produces no intravascular bubbles. The true decompression-induced bubble threshold can be considered to lie between the bubble and no-bubble regression lines. P_1 is the saturation pressure, ΔP the pressure reduction from P_1 to a predetermined lower pressure P_2. *Upper dashed lines* indicate incidence levels for decompression sickness based on behavioral observation by Berghage et al. (4).
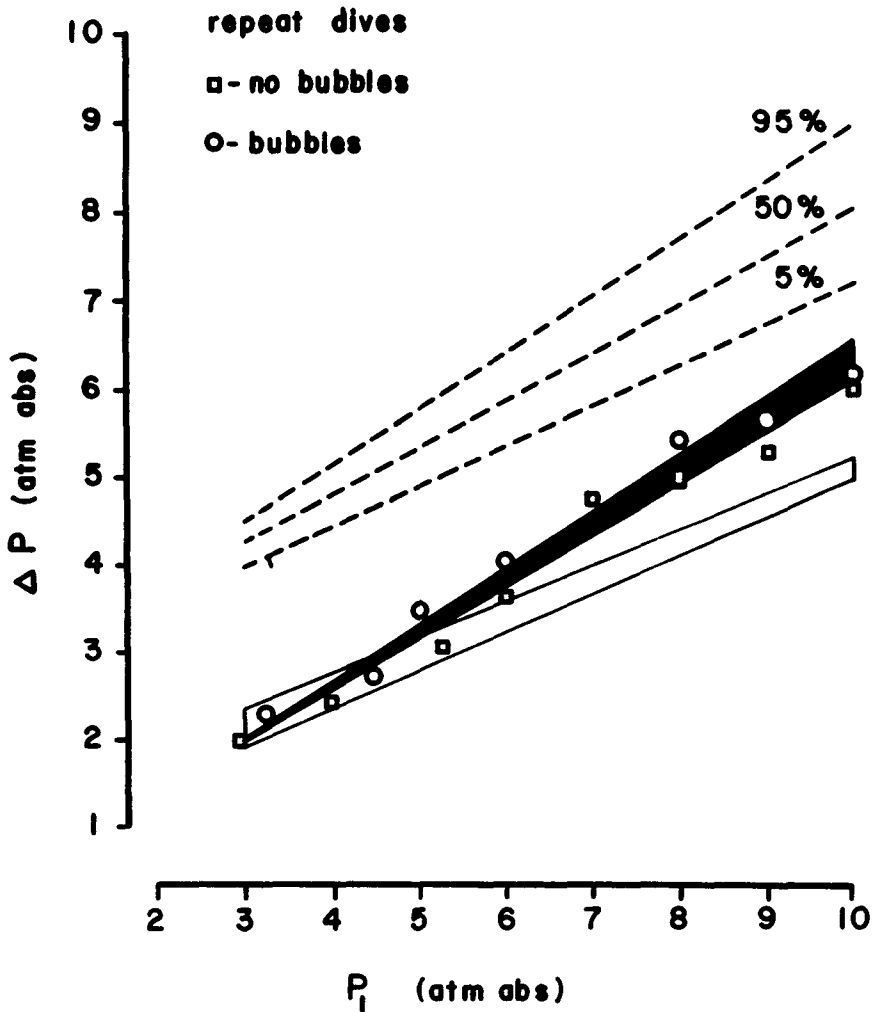
Fig. 2.   Doppler-determined decompression sickness thresholds based on the detection of venous gas emboli in the rat during repeat exposures.   The *blank rectangular area* represents the bubble threshold for the first exposure experiments as shown in Fig. 1. For further explanation. see legend for Fig. 1.

no animals represented by the threshold boundary lines exhibited any overt signs or behavioral changes indicating decompression sickness, even if intravascular bubbles were detected.

The thresholds of intravascular bubble detection by the present method can be represented by a linear equation of the form $P_1 = a P_2 + b$ where P_1 is saturation pressure and P_2 the reduced pressure. Regression equations describing the threshold lines (Table I) show a greater slope value for repeat exposures, indicating that an increased pressure differential is tolerable without forming bubbles upon repeat exposures.

TABLE I

Regression Equations Describing Bubble Detection Thresholds

Exposure	No Bubble	Bubbles
First	$P_1 = 1.71 P_2 + 1.25$ $r = 0.99, P < 0.001, n = 8$	$P_1 = 1.57 P_2 + 2.21$ $r = 0.99, P < 0.001, n = 8$
Repeat	$P_1 = 2.34 P_2 + 0.77$ $r = 0.97, P < 0.001, n = 8$	$P_1 = 2.51 P_2 + 0.61$ $r = 0.99, P < 0.001, n = 7$

The experimental points included in the calculation of the regression lines are the least pressure reduction that produced bubbles and the largest pressure reduction that produced no bubbles. See text for further explanation.

Dog. Sixteen compression-decompression experiments were performed in three surgically prepared dogs. Experimental protocols were similar to those for the rat. The first trial began with the average critical pressure for humans (5), in which the ΔP was much smaller than for the rat as presented above (Fig. 3, *line C*). It became apparent that intravascular bubbles do not form for this small ΔP. We made subsequent trials using the first exposure bubble threshold line of the rat and detected no bubbles in all trials in dogs (Fig. 3, *line B*). However, use of the repeat rat pressure exposure line in two out of four exposures in the dogs resulted in intravascular bubbles, although no observable symptoms appeared (Fig. 3, *line A*).

Cat. The results of six trials on six anesthetized cats are presented in Fig. 3. There were no bubbles detected in all four trials using the first exposure schedule for the rat. In two cats decompressed by the repeat exposure schedule, intravascular bubbles were detected. Both cats died shortly (within 10 min) following detection of bubbles.

DISCUSSION

The results of this investigation demonstrate the feasibility of using an implanted Doppler probe in laboratory animals of varying sizes for detection of decompression-induced intravascular bubbles. The intravascular bubble thresholds indicate a mild, previously undetectable level of decompression sicknesses in animals. Thus, the present method offered a clear and non-subjective criterion for detection of the onset of decompression sickness which is still sub-symptomatic. At the threshold of intravascular bubble formation induced by decompression, the rat and the dog showed no indication of decompression sickness. This procedure is clearly more sensitive and advantageous than the behavioral determination of decompression sickness.

The ultrasonic Doppler flowmeter has been used to detect intravascular gas emboli induced by decompression in both animals and man. Larger animals, such as swine (6–7), and sheep (8) have had Doppler probes implanted directly on the vessels; it has been necessary to use external probes on small
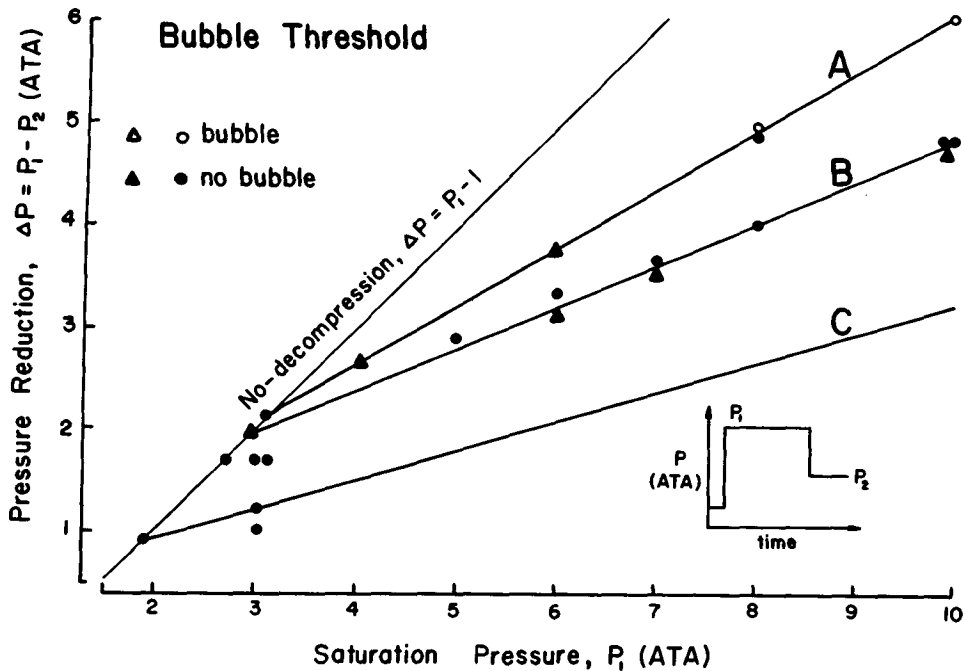
Fig. 3. Doppler-determined decompression sickness threshold based on the detection of venous gas emboli in the unanesthetized dog at weekly exposures, and in the anesthetized cat.   *Lines A* and *B* are the bubble threshold regression lines for the rat at the repeat exposure and at the first exposure, respectively (Figs. 1 and 2 and Table I).   *Line C* is the averaged critical reduction pressure for humans according to Yount (5).   Solid circles represent no bubbles (●), and *open circles* indicate detection of intravascular bubbles (○) during decompression in the dog.   Solid triangles represent no bubbles (▲), and *open triangles* indicate detection of intravascular bubbles (△) during decompression in the cat.

animals (10–11), a technique that requires anesthesia or restraint. The present method of Doppler bubble detection in small laboratory animals, as described in this paper, is an improvement over past methods in that it allows a sensitive determination of decompression sickness thresholds based on a well-defined, objective endpoint; it can be used on awake unrestrained animals; and it does not result in debilitation or death, and thereby allows repeat studies on the same animal. Repetitive measures of decompression sickness in the same animal provide direct evidence for many past observations and speculations that greater pressure reductions can be tolerated on repeat dives than on first dives (12–15). The most likely explanation may be that pressurization alters the number, conformation, or distribution of gas micronuclei shown to be necessary for bubble formation upon decompression (16). Two out of four trials on dogs pressurized 1 week apart showed intravascular bubbles by using the repeat schedule for the rat. It may be that the regeneration of micronuclei requires less than 1 week.

The results of the present study indicate that the maximum ΔP without forming intravascular bubbles is the same in the dog, the cat, and the rat, which represents a significant finding. Dogs and rats differ in body weight by

a factor of about 40, yet according to our criterion the maximum ΔP was the same in these two species. However, according to behavioral criteria, species differences in maximum allowable pressure from saturation exist and, in general, a larger animal tolerates a smaller magnitude of pressure reduction from saturation (1). Methodological differences in determining decompression sickness may be of fundamental importance and should be resolved by further experimentation.

When the pressure reduction from saturation is less than maximum, there will be infinite decompression pressure-time combinations. Consequently, comparisons of decompression tables are extremely difficult. The present study suggests that decompression from saturation be made with a maximally-allowable pressure difference, then it becomes a matter of determining the duration to reach equilibrium at the lowered ambient pressure. This duration is, of course, a function of inert gas elimination, and is species-dependent as well as metabolic state-dependent. Extrapolation of experimental data between species becomes less burdensome in this single-variable approach as compared to the multiple-variables scheme currently in use.

In summary, the results of this investigation demonstrate the feasibility of using an implanted Doppler probe in laboratory animals of varying sizes for detection of decompression-induced intravascular bubbles. These intravascular bubbles indicate a mild, previously undetectable level of decompression sickness in the rat and in the dog. The findings showed that the maximum no-bubble pressure reduction from a saturation dive appears not to be a species-dependent phenomenon. We anticipate that this finding will facilitate the extrapolation of decompression schedules among species, since only the consideration of a species-specific parameter is required, namely, the rate of inert gas elimination.

Acknowledgment

References

1. Berghage TE, David TD, Dyson CV. Species differences in decompression. Undersea Biomed Res 1979;6:1–13.
2. Groom AC, Song SH, Ohta Y, Farhi LE. Effect of anesthesia on the rate of N_2 washout from body stores. J Appl Physiol 1974;36:219–223.
3. Watt DG, Lin YC. Doppler detection of thresholds for decompression-induced venous gas emboli in the awake rat. Aviat Space Environ Med 1979;50:571–574.
4. Berghage TE, Gomez JA, Roa CE, Everson TR. Pressure reduction limits for rats following steady state exposures between 6 and 60 ATA. Undersea Biomed Res 1976;3:261–272.

5. Yount DE. Application of a bubble formation model to decompression sickness in rats and humans. Aviat Space Environ Med 1979;50:44–50.

6. Gillis MF, Peterson PL, Karagianes MT. *In vivo* detection of circulating gas emboli associated with decompression sickness using the Doppler flowmeter. Nature 1968;217:965–967.

7. Powell MR. Doppler ultrasound monitoring of venous gas bubbles in pigs following decompression with air, helium, or neon. Aerosp Med 1974;45:505–508.

8. Smith KH, Spencer MP. Doppler indices of decompression sickness: their evaluation and use. Aerosp Med 1970;41:1396–1400.

9. Spencer MP, Johanson DC, Campbell SD. Safe decompression with the Doppler ultrasonic blood bubble detector. In: Lambertsen CJ, ed. Underwater physiology V. Proceedings of the fifth symposium on underwater physiology. Bethesda, MD: Federation of American Societies for Experimental Biology, 1976:311–325.

10. Powell MR. Leg pain and gas bubbles in the rat following decompression from pressure: monitoring by ultrasound. Aerosp Med 1972;43:168–172.

11. Ulrich WD, Fine RM. Respiratory signs and ultrasonic detection of bubbles in hamsters with severe decompression stress. Aerosp Med 1974;45:171–175.

12. Elliott DH. Some factors in the evaluation of oxygen-helium decompression schedules. Aerosp Med 1969;40:129–132.

13. Elliott DH, Hallenbeck JM. The pathophysiology of decompression sickness. In: Bennett PB, Elliott DH, eds. The physiology and medicine of diving and compressed air work. Baltimore, MD: Williams & Wilkins, 1975:442.

14. Hempleman HV. Decompression theory: British practice. In: Bennett PB, Elliott DH, eds. The physiology and medicine of diving and compressed air work. Baltimore, MD: Williams & Wilkins, 1975:338–343.

15. Walder DN. The prevention of decompression sickness. In: Bennett PB, Elliott DH, eds. The physiology and medicine of diving and compressed air work. Baltimore, MD: Williams & Wilkins, 1975:460.

16. Yount DE, Strauss RH. Bubble formation in gelatin: a model for decompression sickness. J Appl Physics 1976;47:5081–5089.

DETERMINATION OF SAFE TISSUE TENSION VALUES DURING THE SURFACE INTERVAL IN SURFACE DECOMPRESSION SCHEDULES FOR HELIUM-OXYGEN DIVES

P. O. Edel

Although the safe inert supersaturation levels for nitrogen in man during brief surface intervals in surface decompression air dives have been determined through empirical testing by Van Der Aue et al. (1), no equivalent experiments have been conducted for limiting gas tissue tensions following helium-oxygen exposures. Since use of helium-oxygen is very advantageous beyond the practical limits of air decompression tables, surface decompression techniques obviously would be more beneficial for use with helium-oxygen tables than with air schedules. Accordingly, a modification of the helium-oxygen tables computed by Momsen (2) was developed, which permitted the diver to surface for a brief interval following the final water decompression stop at 40 fsw on oxygen before completing his oxygen decompression in a surface chamber. This alternate form of decompression, using the surface-supplied helium-oxygen diving tables included in the *U.S. Navy Diving Manual* (3), is so advantageous by comparison with conventional in-water decompression, that this alternative is used almost exclusively today with Momsen's schedules.

Unfortunately, the lack of empirical data with respect to physiological limits which may be applied to a brief surface interval, following a helium-oxygen exposure and before recompression in a surface chamber, precludes the extrapolation of this method for depth-time combinations beyond present experience. Further, there was no assurance that tissue tensions developed at the point at which the final water stop was terminated represented actual physiological limitations for a brief surface exposure before recompression and subsequent decompression in a surface chamber. However, some evidence suggested the possible use of much higher quantities of inert gas levels in slower tissue half-time compartments than those in current use in military and commercial surface decompression schedules. In tests to develop an emergency surface decompression schedule following profiles (simulating a total saturation

707

exposure at 42 fsw breathing a 91% N_2–9% O_2 mixture) for project TEKTITE I, subjects were exposed to surface intervals of 10, 15, and 20 min in successive tests following exposures in which the subject's slowest tissue compartments were computed to be at equilibrium with the nitrogen partial pressure in a normoxic nitrogen-oxygen atmosphere at 42 fsw (4). Following the surface interval, the subjects were then recompressed to 55 or 60 fsw and were then decompressed on an air, or intermittent air-oxygen, schedule. The two divers exposed to a 10-min surface interval and the six divers exposed to a 15-min surface interval showed no symptoms of decompression sickness during the interval at surface pressure before recompression. Likewise, one of the two divers exposed to a 20-min surface interval was free of symptoms during this period. The other subject experienced serious symptoms in the 19th min of the surface interval. However, it was not the decompression sickness as such, but the nature of the symptoms which was not anticipated.

As shown in Fig. 1, all bodily tissue half-time compartments between 5 and 360 min (the latter at that time thought to represent the slowest tissue half-time compartment in man) were at an approximate state of equilibrium with
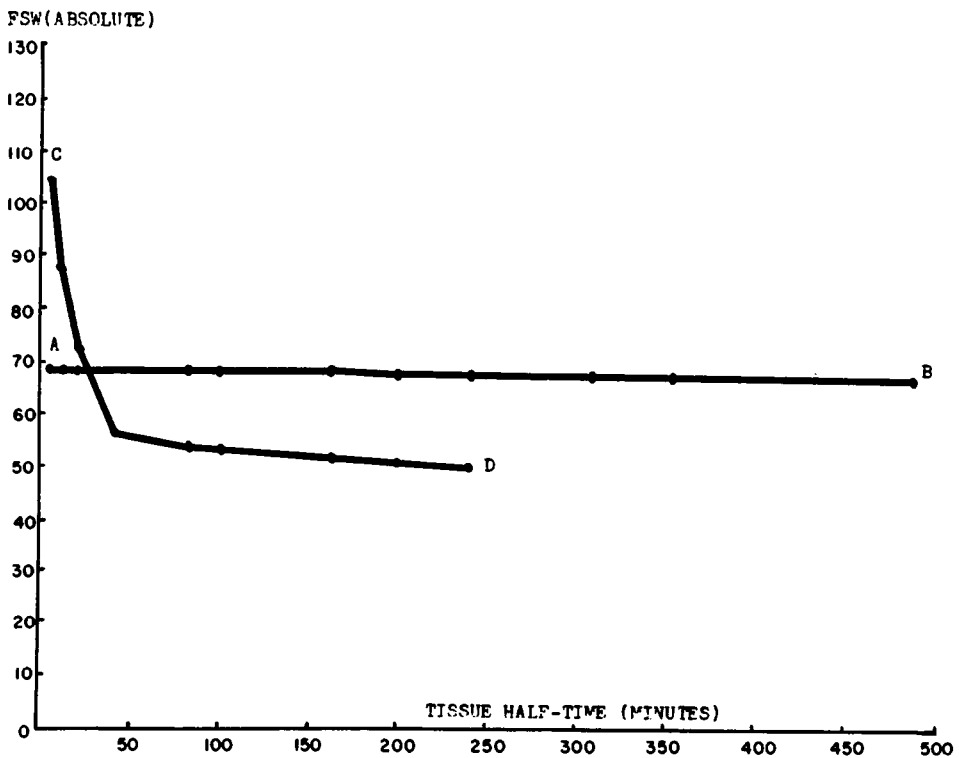
Fig. 1. Tissue tensions compared with Workman's M-values upon direct ascent to surface following a saturation exposure at 42 fsw with a 9% O_2–91% N_2 breathing mixture. *A-B* = half-time tissue tensions upon arrival at surface. *C-D* = Workman M-value limits for arrival at surface pressure.

the nitrogen partial pressure of the breathing medium (68.25 fsw) as indicated by the *horizontal line*. The *intersecting line* shows Workman's (5) M-values for nitrogen which permit a safe ascent to sea-level pressure. As shown, tissue compartments with half-times of from 5 to 20 min do not involve violations of accepted safe criteria for an indefinite period of residence at sea-level. Beyond the 20-min half-time compartment, the degree of inert gas loading, in excess of the indicated safe limit, increases with tissue half-time. Hence, the slowest tissue half-time compartments have the greatest degree of gas in excess of the accepted safe criteria and probably would be the most limiting and, therefore, the most likely areas of initial symptoms of decompression sickness. The actual symptoms, however, were not the characteristic "knee bends" associated with the slowest tissue but rather a type associated with much faster tissue half-time compartments. This suggested a response more directly associated with bubble growth as opposed to excess inert gas loading per se. Assuming the foregoing to be true, surface decompression schedules, which maintained the tissue tension of the faster half-time compartments within accepted safe criteria at the time wherein the diver is exposed to surface pressure for a brief interval, could be modified to permit much greater inert gas loading in the slowest half-time tissue compartments.

This study was undertaken to provide the empirical data necessary to determine the inert gas loading limits for the surface interval following an exposure with helium-oxygen breathing mixtures.

METHOD

A computer was used to construct pressure profiles in which the slowest bodily tissue compartment would control, or limit, decompression before arrival at the final water decompression stop, where, in all schedules, sufficient oxygen was used to bring the faster tissue half-time compartments within acceptable limits for a brief surface interval. These profiles were used in experiments conducted in a dry test chamber, in which human volunteers were exposed for 4 h to 150 fsw breathing helium-oxygen mixtures. At the end of this period the computer schedule was used to control the simulated water decompression phase of helium-oxygen and, on their final water stop, the subjects breathed pure oxygen. Following this they were brought to the surface within either 1 or 2 min. They then left the chamber to remain on surface for periods that varied from 5 to 15 min, after which they were recompressed to 70 fsw. On arrival at this pressure, they began a 10 min oxygen breathing period, after which they were shifted to air and brought to 60 fsw. The decompression was completed in accordance with the appropriate computer-generated schedule in which the subjects ascended to the surface in 10-fsw stages, breathing intermittent air-oxygen mixtures. All tests involved four subjects who were exposed in pairs for each pressure profile used. Subjects were restricted to one exposure per week to prevent any possible acclimatization from previous exposures.

In the initial experiment, the computed tissue tensions in the slowest bodily tissue half-time compartment at the time of arrival at sea-level pressure for the surface interval were limited to a value which is presently in use in many tables for surface decompression dives following helium-oxygen exposures. As shown in Fig. 2, the subjects were surfaced from point A after a period of time breathing oxygen at 40 fsw. In succeeding experiments the tissue tension levels were elevated in gradual stages to permit increased inert gas loading in the slowest tissue half-time compartment. This was accomplished by deleting only the final portion of the water decompression profile as indicated in Fig. 2; the points from which the subjects surfaced are indicated by the letters B, C, D, and E. As shown, the progression of the experimental plan required surfacing from a final water stop of 50 fsw in later dives and ultimately from a final water stop of 60 fsw in the last dive in this test series. In all tests oxygen was used for all or part of the time spent at the final water stop before ascent for the surface interval phase to reduce the inert partial pressure in the faster tissue half-time compartments to levels found safe in standard surface decompression schedules.

In one test it was desired to surface the subjects from a 50-fsw level with greater tissue tensions than would develop through use of the planned profile
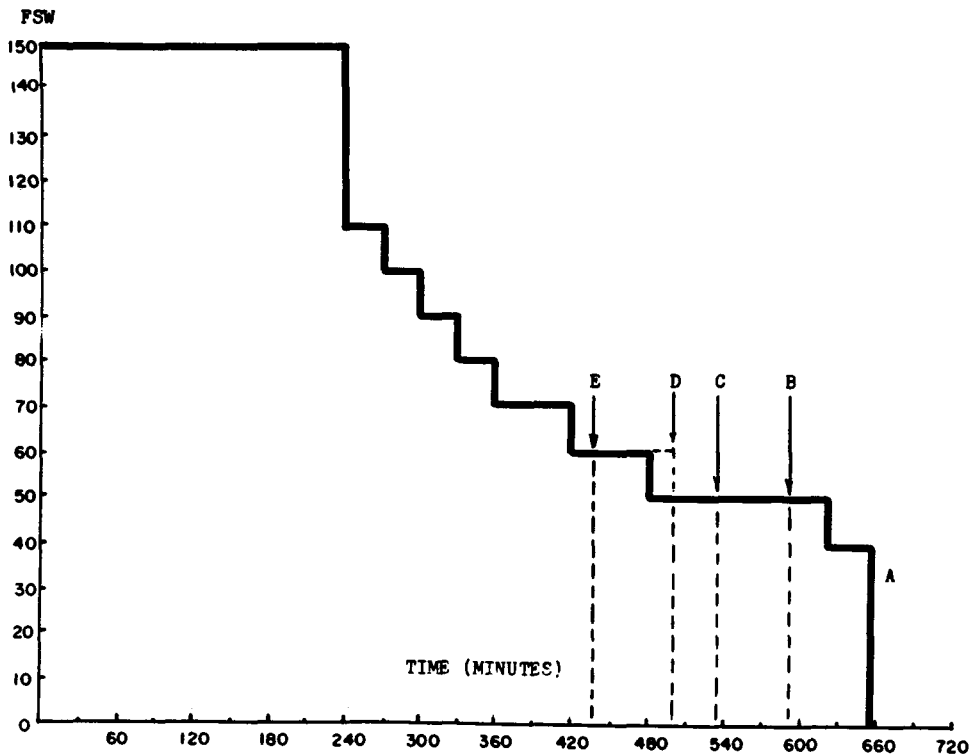
Fig. 2. Experimental profiles to determine the maximum safe tissue tensions in the slowest bodily half-time compartment for a 5-min surface interval.

that used the standard 90% He–10% O_2 breathing mixture at 150 fsw. The planned dive profile was submitted to the computer for dive analysis before testing. The "AUTODEC" analysis showed that technical (or minor) compartment violations during the water decompression phase would result from use of this mixture with the "standard" profile chosen. As such schedules with "technical" violations characteristically produce only a small percentage of decompression sickness in normal usage, it was decided to use this schedule. Accordingly, two subjects were exposed to this profile, which resulted in the same tissue tensions upon arrival at surface pressure for the surface interval phase as had resulted from the exposure in which the subjects terminated the water decompression phase at the point marked C in Fig. 2.

RESULTS

The results of this study are shown in Table I. As indicated, no symptoms of decompression sickness occurred in any schedule in which the 90% He–10% O_2 breathing mixture was used at 150 fsw. The one exposure in which the 95% He–5% O_2 mixture was used resulted in bilateral knee pain, which began approximately 3 min after arrival at surface pressure for the surface interval phase of the dive. The symptoms were completely relieved during the recompression to 70 fsw. As the planned surface decompression profile offered more oxygen than the standard table 6, it was used to decompress both subjects to surface pressure. There was no recurrence of symptoms in the affected subject, and the subject's test partner was asymptomatic throughout the profile and postdive period.

TABLE I

Decompression Sickness During Surface Interval Following Dive for All Exposures

Test No.	Mixture	Final Depth†	Water Stop Time†	Surface Interval (min)	Decompression Sickness* (During SI/Following Sur. Dec.)	
1	90% He-10% O_2	40	35	7	0	0
2	90% He-10% O_2	40	35	10	0	0
3	90% He-10% O_2	50	100	7	0	0
4	90% He-10% O_2	50	100	10	0	0
5	90% He-10% O_2	50	30	14	0	0
6	90% He-10% O_2	50	30	17	0	0
7	95% He- 5% O_2	50	30	7	1	0
8	90% He-10% O_2	60	70	7	0	0
9	90% He-10% O_2	60	70	11	0	0
10	90% He-10% O_2	60	15	8	0	0
11	90% He-10% O_2	60	15	9	0	0

*Two subjects per test.　　†Depth in fsw, time in min.　　SI is surface interval.

DISCUSSION

The ability of the subjects to remain symptom-free for surface intervals well in excess of the standard 5-min value in the earlier experiments shown in Table I indicates the conservatism of the conventional surfacing criteria for limited duration at sea-level pressure when applied to in-water decompression which does not violate tissue compartment limits. The duration of the symptom-free period also indicated that significant increases in tissue tension values in the slowest compartments could be applied for a 5-min surface interval. The importance of adequate water decompression before ascent for the surface interval phase was dramatically illustrated by the single incident of decompression sickness resulting from use of a profile in which only minor tissue compartment violations had occurred, according to computer analysis, during the water decompression phase of the dive. An asymptomatic dive by the same subject in a subsequent schedule that involved higher inert gas partial pressures in the slowest tissue half-time compartment, but without any compartment violations during the water phase of the test, showed the previous problem had not occurred because of the amount of inert gas in the slowest bodily tissue compartment per se. The result of this dive confirmed the opinion that the inadequate water decompression was responsible for the problem. Further, the nature of the symptoms (knee pain) associated with the slowest bodily tissue compartment strongly indicated that the earlier problems of type II decompression sickness resulting from surface decompression tests with the Project TEKTITE I schedule had been solved by the use of oxygen to maintain tissue tensions in the faster compartments to within accepted safe levels during the surface interval. The difference in the type of symptoms in this experiment as compared with the TEKTITE I tests re-emphasized the need for proper control of the fast tissue compartment before ascent for the surface interval for safe use of these schedules.

Table II shows the tissue tensions which resulted from the tests accomplished in this series. The tissue tension shown used the Workman model (5) which used a 240 min half-time value for both helium and nitrogen in the slowest bodily tissue compartments. The next column uses the same values for helium with a value of 480 min for nitrogen in the slowest half-time compartment. The latter value for nitrogen is in closer agreement with the mathematical assumptions shown to be necessary for adequate prediction of the decompression obligation following total saturation from depth with nitro-oxygen mixtures in the TEKTITE II project (6). Use of the latter values accomplished an increase of the tissue tensions in the slowest tissue compartment upon ascent for the surface interval phase of 26.3% as compared with the conventional values used in contemporary surface decompression tables. Through use of the Workman method in its original form, an increase of 28.6% was achieved, as compared with values used in contemporary schedules.

Perhaps of greater interest with respect to potential applications is the possible reduction of decompression time which may be achieved by this method. As can be seen in Table II, the water decompression time achievable

TABLE II

Tissue Tensions Resulting from Tests in This Series

Test No.	Final Depth (fsw)	Water Stop (Time min)		Slowest Tissue Tension on Arrival for S.I. (240 He–240 N₂/ 240 He–480 N₂)	Decompression Time		Reduction From Test No. 1	
		He-O₂	O₂	(240 He–240 N₂/ 240 He–480 N₂)	In Water	Total	Water Dec. %	Total Dec. %
1,2	40	0	35	77.8 84	423	711	0	0
3,4	50	70	30	82.7 89.1	347	665	18	6.5
5,6	50	0	30	87.3 93.8	277	615	34.5	13.5
8,9	60	50	20	92.1 97.0	256	604	39.5	15
10,11	60	5	10	103.9 104.1	201	574	52.5	19.3

SI is surface interval.

by standard procedures was 423 min. This was reduced to 201 min in the final table: a reduction of over 50% of the standard water decompression from this exposure. Since surface-supplied tables are limited to the practical exposure limits in the water, a reduction of water decompression increases the possible total working time of the diver at maximum depth and, hence, increases the amount of useful work per diver in a surface-supplied dive. A comparison of the initial and final decompression schedules used in this experimental series is shown in Table III.

In general, the experiments showed it is possible to permit a replacement of 50% of the water decompression time to decompression time in the surface chamber. The mathematical equations show, as would be expected, a transferral of decompression time from water to chamber with no net gain as compared to the total decompression requirement which remains constant. The advantage is in transferring the decompression process from a less desirable (water) to a more desirable (chamber) location. However, as can be noted

TABLE III

Comparison of Initial and Final Experimental Schedules Following a 4-h Exposure at 150 ft with a 90% Helium–10% Oxygen Breathing Mixture

Initial Schedule			Final Schedule		
Depth (fsw)	Time (min)	Mixture	Depth (fsw)	Time (min)	Mixture
Water Decompression Schedule					
110	30	90% He-10% O_2	110	30	90% He-10% O_2
100	30	90% He-10% O_2	100	30	90% He-10% O_2
90	30	90% He-10% O_2	90	30	90% He-10% O_2
80	30	80% He-20% O_2	80	30	80% He-20% O_2
70	60	80% He-20% O_2	70	60	80% He-20% O_2
60	60	80% He-20% O_2	60	5	80% He-20% O_2
			60	10	Oxygen
50	140	80% He-20% O_2			
40	35	Oxygen			
Chamber Decompression Schedule					
70	10	Oxygen	70	10	Oxygen
60	5	Air	60	5	Air
60	20	Air	60	20	Oxygen
60	5	Air	60	5	Air
50	30	Oxygen	50	30	Oxygen
40	10	Air	40	10	Air
40	40	Oxygen	40	40	Oxygen
40	10	Air	40	10	Air
30	40	Oxygen	30	50	Oxygen
20	15	Air	20	15	Air
20	40	Oxygen	20	60	Oxygen
20	15	Air	20	15	Air
10	60	Oxygen	10	70	Oxygen
			10	20	Air
			10	10	Oxygen

from the last columns in Table II, a reduction of total time was apparently achieved in the later experiments in which the total decompression time was 1 h less than that of the initial table. The apparent gain was due to the replacement of helium-oxygen breathing in the water with oxygen breathing in the chamber. The increased efficiency of oxygen in elimination of inert gas resulted in a small reduction of the total decompression time, although the surfacing criteria, as such, remained unchanged.

The depth increase in the final water stops was a requirement of the mathematical model used to construct these profiles. For example, in the final exposure the AUTODEC computer program (7) used to generate these profiles would not permit an ascent to 50 fsw before the time it was programmed to start ascent to sea level for the surface interval. The paradox is more apparent than real. The process of surface decompression assumes that the duration at sea level will not be indefinite during the surface interval. This eliminates the requirement for M-values which permit ascent that will not produce symptoms, regardless of the period of residence at the next pressure level, and which permit use of values that will allow the subject to remain symptom-free for the designated period but will result in symptoms if the period is extended. The values used for arrival at sea level pressure are of the latter form, whereas the values for arrival at 50 ft are predicated on the assumption that decompression sickness will not be produced regardless of the time spent at that pressure level.

In theory, permitting a compartment violation before surface decompression will prohibit or endanger a subsequent attempt to use the surface decompression mode. The violation, if significant, will produce bubble formation. Upon subsequent pressure reduction to the surface, the existing bubble will rapidly increase in size, producing symptoms soon after arrival at surface pressure. In cases where the previous compartment violations have been excessive, symptoms may even develop during the ascent to surface. Such a condition would seem to be the logical explanation for the single incidence of decompression sickness occurring during this experimental series. The degree of the compartment violation, as analyzed by the AUTODEC system, was similar to the values occurring in commercial diving operations, wherein a decompression sickness resulted in about 1% of the exposures. Further, such problems characteristically occurred an hour or more after the termination of the decompression. In this case the symptoms manifested themselves within 3 min after arrival at surface, which suggests a bubble with very rapid growth characteristics (not compatible with the anatomical site of the symptoms) or a preexisting condition which was exacerbated by the ascent. The subsequent test, in which the subject remained symptom-free in spite of much greater tissue tensions in the slowest tissue compartment at the time of the start of the surface interval, seems to be additional confirmation of the latter explanation.

The figures of Table II for the tissue tensions (in the slowest bodily tissue) in the terminal dive of this series (which did not result in decompression sickness) result in more than twice the tissue tensions which are permissible for an indefinite period of residence at sea level. If we compare this excess gas

loading (beyond the accepted safe criteria) with that occurring in the faster tissue compartments during the surface interval in the TEKTITE I experiment, it appears obvious that excess gas alone cannot explain the symptoms that occurred. The only logical explanation available at present is in relation to the compartment half-times according to bubble growth formula.

References

1. Van Der Aue OE, Brinton ES, Kellar RJ. Surface Decompression, derivation, and testing of decompression tables with safety limits for certain depths and exposures. Research Project X-476, Research Rpt. 1. Washington DC: U.S. Navy Experimental Diving Unit, 1945.
2. Momsen CB, Wheland KR. Report on use of helium-oxygen mixtures for diving. (Revised 1942). Washington DC: U.S. Navy Experimental Diving Unit, 1939.
3. U.S. Navy Diving Manual (NAVSHIPS 0094-001-9010) Washington DC: U.S. Government Printing Office, 1970.
4. Edel PO. Delineation of emergency surface decompression and treatment procedures for PROJECT TEKTITE Aquanauts, Aerosp Med 1971:42:616–621.
5. Workman RD. Calculation of decompression schedules for nitrogen-oxygen and helium-oxygen dives. Research Rpt 6–65. Washington DC: U.S. Navy Experimental Diving Unit, 1965.
6. Edel PO. Experiments to determine decompression tables for TEKTITE II 100 fsw mission, Report to the Department of the Interior, Pasadena, TX: J & J Marine Diving Company, March 31, 1971.
7. Edel PO. Analysis of decompression tables calculated by non-U.S. Navy methods. Report to the Office of Naval Research, Harvey, LA: Sea-Space Research Company, Inc. March 31, 1980.

ASSESSMENT OF DECOMPRESSION PROFILES AND DIVERS BY DOPPLER ULTRASONIC MONITORING

R. Y. Nishi, K. E. Kisman, B. C. Eatock,
I. P. Buckingham, and G. Masurel

Historically, decompression profile testing and evaluation have been based on the degree of incidence of decompression sickness incurred in experimental dive profiles. A very large number of man-dives was necessary to validate a profile or profiles as safe, depending on the acceptable incidence of decompression sickness, the acceptable variability around this incidence level, and the confidence limits desired (1). An alternative method for evaluating the stress of a decompression profile is the use of the Doppler ultrasonic bubble detector (2,3). In this method, the end point is not whether the profile results in any incidence of decompression sickness, but on the number of venous gas emboli produced by that profile during and after decompression. Profiles that produce many bubbles can be considered to be more severe in terms of decompression stress than those that produce fewer bubbles.

By monitoring a number of dives in which decompression incidents occur, one can determine a correspondence between the level of detected bubbles and the incidence of decompression sickness. Once this correspondence is determined, the bubble information alone could be used to assess the severity of dive profiles and whether potential problems could result. This procedure tends to be more objective than that in which a diver reports subjective feelings of pain or other symptoms of decompression sickness. Hence, with this method, not as many man-dives may be required to determine safe decompression profiles. The Doppler method can also be used to assess which divers are more susceptible or vulnerable to "bubbling," and presumably, therefore, to suffering from decompression sickness. This paper describes the use of the Doppler

technique for assessing and comparing compressed air dive profiles generated by a decompression computer, and for assessing divers and their tendency to produce gas bubbles after diving.

METHODS

Twenty-seven bounce dives (172 man-dives) in the depth range from 30 to 75 metres of seawater (msw), with bottom times from 10 to 55 min, were performed on compressed air. Decompression was controlled on-line by the XDC-2 digital decompression computer (4), which is a microprocessor-controlled real-time dive monitor. It is based on the Kidd-Stubbs decompression computer model (5), which, in several hardware configurations, has been in use at the Defence and Civil Institute of Environmental Medicine for a considerable number of years for controlling decompression from experimental, operational, and training dives. The aim of these dives was to determine the operational bottom-time limits at different depths and to assess the severity of the profiles generated by the XDC-2 computer. The dive program was divided into two phases.

In *Phase I*, the average descent rate to bottom depth was about 13 msw/min, and in *Phase II*, about 19 msw/min. The initial ascent rate during decompression to the computed safe depth was 18–35 msw/min and then slowly decreased to about 5 to 10 msw/min (because the dives were done in a hyperbaric facility designed for saturation diving and maximum venting rates were limited by the size of the gas lines and valves). After the safe ascent depth was reached, we controlled decompression by following the safe depth exactly as displayed on the computer until 3 msw. The depth was then maintained at 3 msw until the computer showed that it was safe to surface. Figure 1 gives an example of the depth-time profile for one of these dives. Table I shows the decompression times for the dives performed with the corresponding U.S. Navy (6) and Royal Navy (7) decompression times shown for comparison.

Each dive involved 6 divers: two wet working divers wearing standard foam neoprene wet suits and either KMB-9 breathing apparatus or Superlite-17 helmets, two dry attendants performing a light workload to support the wet divers, and two dry nonworking divers. The two wet divers took turns, as time permitted, working on a submerged exercise ergometer set at 50 watts, and performing a workload estimated to be 100 watts. The water temperature was between 18 and 23°C for all dives. Two teams of divers were used, each team diving on alternate dive days. In *Phase I*, Team A consisted of 6 divers divided into 3 pairs who were rotated among the three dive positions (from dive to dive). Team B came from a pool of 18 divers from which 6 were selected each diving day according to availability. Divers were from both civilian and military backgrounds and all were qualified Ship's Divers or Clearance Divers. The average age was 33 years. In *Phase II*, the subjects were 11 civilian student divers and one civilian instructor, the average age was 24 years. Two teams of six divers were used; each team was kept intact for the duration of
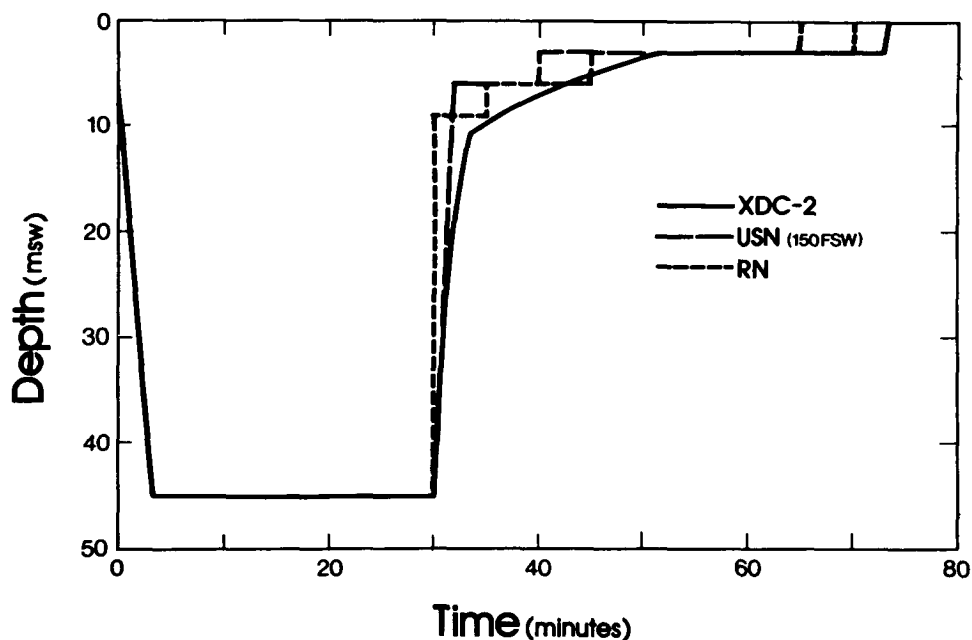
Fig. 1.   Example of a dive profile generated by the XDC-2 decompression computer—45 msw for 30 min. The corresponding profiles from the U.S. Navy (USN) and Royal Navy (RN) diving tables are shown for comparison.

the dives. A seventh dry diver participated on each team as a dive supervisor. Two of the dives in this phase were similar to dives in *Phase* I.

All divers were monitored with the Doppler Precordial Bubble Detector developed by the Centre d'Étude et de Recherches Techniques Sous-Marines and the Institut National de Sciences Appliquées in France and manufactured by Sodelec S.A. This instrument is a 5-MHz CW (continuous wave) unit with a deep focusing precordial detector and can be used inside a hyperbaric chamber. A reference signal was recorded for each diver one-half hour before the dive began. The four dry subjects were monitored at approximately 15-min intervals during decompression in the chamber. All divers had been instructed previously on how to place the probe over the precordial region of the chest. On reaching surface, the wet divers were monitored immediately, followed by the dry divers. Two Doppler monitoring teams were used. After leaving the chamber area, all divers were monitored periodically while relaxing in a nearby resting area for at least 3 h and in some cases up to 9 h after the start of decompression.

Both precordial (right ventricle and/or pulmonary artery) and subclavian (right and left shoulders) sites were monitored. The precordial signal was obtained for two conditions, first with the diver standing at rest, and second, with a specified movement consisting of a deep knee bend. The subclavian vein signal was similarly obtained with the subject standing at rest, and then with a movement consisting of clenching of fist. The purpose of the movement

TABLE I

Decompression Times for the Dive Profiles Evaluated with those of the U.S. Navy (USN) and Royal Navy (RN) Air Diving Tables

Depth (msw)	Bottom Time* (min)	Ascent Time to 3 msw (min)	Stop Time at 3 msw (min)	Total Ascent Time (min)	Ascent Time (min)	
					USN	RN
Phase I						
36	30	14	15	29	16	20
36	40	18	20	38	32	35
36	50	22	31	53	48	50
45	20	15	14	29	12	20
45	25	19	16	35	24	30
45	30	22	21	43	35	40
54	15	16	13	29	12	20
54	20	22	16	38	26	30
54	25	27	24	51	40	45
Phase II						
30	55	16	22	38	38	35
54	20	22	17	39†	26	30
54	25	27	26	53†	40	45
66	10	15	13	28	11	‡
66	15	24	17	41	27	‡
75	10	20	14	34	16	‡

*Bottom time includes descent time from surface. Average descent rate for *Phase II* was faster than in *Phase I*. For example, average descent rate to 54 msw was 13 msw/min for *Phase I* and 19 msw/min for *Phase II*.   †Difference in decompression times from *Phase I* is accounted for by the faster descent rate to depth.   ‡Not allowed in RN air tables.

condition (knee bend or clenching of fist) was to help identify the bubbles, to confirm the bubble signals measured at rest, and to predict when bubbles should appear at rest because bubbles often appeared first following movement.

All blood flow and bubble signals were assessed aurally at the time of monitoring and recorded on magnetic tape for later reference or verification. Bubbles were assessed according to the Kisman-Masurel code (8), which breaks up the bubble signals into three distinct parameters: bubble frequency (per cardiac cycle); bubble duration (as a function of the number of cardiac cycles); and bubble-signal amplitude. From the resulting three-digit code, bubbles were graded on a scale from 0 to 4, similar to that developed by Spencer (2), but with finer steps.

Divers were instructed to report any symptoms of decompression sickness. Initiation of treatment was not based on bubble-grade results but on reported symptoms only, although the bubble results were used by the diving medical officer for supplementary information. No automatic recompression

therapy or surface oxygen was given for subjects showing high bubble grades if these bubbles were asymptomatic.

RESULTS

Figure 2 *A* to *D* show examples of the bubbles detected from the precordial region. At rest bubble evolution in most individuals in which many bubbles were detected usually reached a maximum between 1 and 2 h after the start of decompression, and remained at this level for some time before disappearing 4 or 5 h after the start of decompression. Bubbles detected following movement generally occurred earlier than those detected at rest; in severe dive profiles, bubbles were detected at depth during decompression. Bubble grades observed were usually higher for movement and persisted for a longer period of time than for bubbles at rest. In one case, bubbles were still detected following movement 9 h after the start of decompression with no concurrent symptoms of decompression sickness.

Figures 2 *E* and *F* show examples of the results obtained from the right and left subclavian veins in one subject. Figure 2*D* shows the corresponding results for the precordial region. In many instances, as shown in this example, bubbles could be detected in the subclavian sites well after bubbles were no longer

---

A. 36 MSW/50 Min.   DIVER RL(PR)

Move 2 2 2 3+ 4   4 3+   3+   3   3

Rest 0 0 0 3 3 3 1+   0   0   0

(Time axis: 0 1 2 3 4 5 6; s at ~1)

B. 36 MSW/50 Min.   DIVER AK(PR)

Move 0 3 3 4 4 4 4 3+3   3   2

Rest 0 1 1 3+ 3+3 3- 1 0   0   0

(Time axis: 0 1 2 3 4 5 6; s at ~1)

C. 36 MSW/50 Min.   DIVER RMc(PR)

Move 0 1 0 0 3 3 3 1   1   0   0

Rest 0 0 0 0 1 0 0 1 0   0   0

(Time axis: 0 1 2 3 4 5 6; s at ~1)

D. 66 MSW/10 Min.   DIVER DB (PR)

Move 0 3 0   0   0 0 0

Rest 0 3-0   0   0 0 0

(Time axis: 0 1 2 3 4 5 6; s at ~0.5)

E. 66 MSW/10 Min.   DIVER DB (RS)

Move   4 3-   3- 2 1   1+

Rest   2 2   2 2 1+   0

(Time axis: 0 1 2 3 4 5 6; s at ~0.5)

F. 66 MSW/10 Min.   DIVER DB(LS)

Move   3- 3   3+ 2+ 3- 2

Rest   3 3   2 3- 2 2

(Time axis: 0 1 2 3 4 5 6; s at ~0.5)

Time (hours)   Time (hours)

Fig. 2. Examples of the bubble grades observed at rest and their movement as a function of time after the start of decompression. The letter s indicates when surface was reached.   A to C: Results obtained in the precordial region (PR) for three of the subjects in the dive to 36 msw for 50 min. Diver AK incurred type II decompression sickness.   D to E: Results for diver DB from precordial (PR) right subclavian vein (RS), and left subclavian vein (LS).

detectable in the precordial region. In other instances, bubbles were not observed in the precordial region but were observed in significant amounts in one or both of the subclavian sites. Alternatively, there were many instances in which bubbles were detected in the precordial region but no bubbles were observed in the subclavian sites.

Table II presents a summary of all dives, showing the number of man-dives for each profile, the maximum bubble grades observed at rest and after movement in the precordial region, the number of bends observed, and the bubble grades at rest associated with these bends. No consideration was given to diver role, i.e., whether wet working, dry nonworking, or attendant, because no obvious relationship could be determined between diver role and bubble results in this study. A difference in diver population was observed, the divers in *Phase II* were less prone to bubbling than those in *Phase I*. This difference can be observed in the two dives to 54 msw for 20 and 25 min; it was common to the two phases. In *Phase I*, 11 out of 24 man-dives resulted in grade 3 or 4 bubbles, whereas in *Phase II*, only one in 14 showed grade 3 bubbles.

Seven incidences of decompression sickness occurred in *Phase I* and were treated by recompression therapy. Two others (at 54 msw for 25 min in *Phase*

TABLE II

Maximum Bubble Grades Observed in the Precordial Region

Depth (msw)	Bottom Time (min)	No. Man Dives/ Phase	Man-Dives with Maximum Bubble Grade At Rest					After Movement					No. of Bends	Bubble Grade at Rest for Bend
			0	1	2	3	4	0	1	2	3	4		
30	55	14/II	2	4	4	4	0	2	3	1	7	1	0	
36	30	12/I	5	3	3	1	0	5	1	1	4	1	0	
36	40	12/I	2	2	3	5	0	1	1	0	3	7	1	3
36	50	6/I	0	1	0	5	0	0	0	0	3	3	3	3
36	50+02	6/I	5	1	0	0	0	6	0	0	0	0	0	
45	20	6/I	2	3	1	0	0	3	0	0	3	0	0	
45	25	12/I	5	4	3	0	0	3	3	4	2	0	0	
45	30	12/I	3	4	2	3	0	2	1	2	6	1	2	3
54	15	12/I	7	2	2	1	0	6	2	1	3	0	1	2
54	20	12/I	3	1	3	4	1	3	1	0	5	3	0	
		7/II	5	1	0	1	0	2	1	2	2	0	0	
54	25	12/I	1	1	4	5	1	1	0	2	7	2	*	
		7/II	3	0	4	0	0	3	0	3	1	0	0	
66	10	14/II	12	1	0	1	0	10	2	0	2	0	0	
66	15	14/II	6	3	0	5	0	4	3	1	6	0	0	
75	10	14/II	8	1	2	3	0	8	0	2	3	1	0	
	Totals	172	69	32	31	38	2	59	18	19	57	19	7	

*Two probable cases of decompression sickness, but not treated. Maximum bubble grades observed in these two individuals were grades 3 and 4.

I) may have been cases of decompression sickness but were not treated. No decompression sickness incidences occurred in *Phase II*. The nine incidents in *Phase I* involved six divers. The two probable cases were individuals who had incurred decompression sickness previously. One treated incident was associated with grade 2 bubbles in the precordial region at rest. The symptoms were a vague feeling of discomfort in the right shoulder and vague feelings of malaise. The subject felt better after a trial recompression to 18 msw on oxygen, and a full U.S. Navy Table 5 treatment (6) was given. This incident may indicate that there is a small probability that grade 2 bubbles could result in decompression sickness.

Six of the seven cases treated and one of the probable cases were associated with grade 3 bubbles at rest. The other probable case had grade 4 bubbles at rest. Hence, grade 3 and grade 4 bubbles observed in the precordial region at rest definitely indicate some hazards in terms of decompression safety. Two of the bends were type II decompression sickness and involved the same individual. The Doppler results of his first dive (36 msw for 50 min) is shown in Fig. 2*B*. Symptoms occurred 18 h after the dive. On his second dive (45 msw for 30 min), symptoms occurred approximately 13 h after the dive. In both cases, pain was associated with his left leg which had been injured many years previously. This individual was also the oldest diver at 47 years of age, and was slightly over his recommended weight range based on skinfold measurements. All other bends resulting from grade 3 bubbles were type I (pain symptoms only) and occurred immediately or within a few hours after surfacing except for one that occurred 18 h later (36 msw for 50 min). Subclavian monitoring on divers who reported pain in the arm or shoulder generally showed at least grade 3 bubbles at rest.

Because of the large number of bends on the dive to 36 msw for 50 min, this dive was repeated with oxygen used during decompression from 10 msw. The use of oxygen resulted in only one diver showing grade 1 bubbles at rest in the precordial region for one period of monitoring only. However, three of the six divers had some bubbles in the subclavian veins.

Maximum bubble grades detected as shown in Table II, although convenient indicators, are misleading to some extent in indicating the severity of the dives because they do not indicate the duration of bubbling at the maximum bubble grade or the time distribution of bubble grades observed. For example, in Figs. 2*C* and *D*, both divers showed a maximum of grade 3 bubbles after movement. However, considerably more bubbles were detected for the subject in Fig. 2*C*. An index of severity, *S*, has been devised, which integrates the amount of bubbles detected over a period of time (9):

$$S = \{100/4^\alpha(t_j - t_o)\} \sum_{i=1}^{j} [(t_i - t_{i-1})(d_i^\alpha + d_{i-1}^\alpha)/2]$$

where d_i is the bubble grade observed at time t_i ($d_o = t_o = 0$), j is the number of observations, t_j is the time of the last observation, and α is a parameter that takes into account that the bubble grade is not a linear measure of bubble quantity. (Kisman et al. (9) have assumed $\alpha = 3$.) For these dives, t_j was taken to be 5 h, because except for about four man-dives, bubbles were no

longer detectable by this time or were considered insignificant for these calculations. The index is normalized for grade 4 bubbles over the entire measurement period.

These calculations showed that for each dive profile, the divers could be divided into three groups representing high, moderate, and low "bubblers," depending on the value of S. Table III shows the means and standard deviations (SD) of S for the three groups. The number of times each diver fell into the high, moderate, or low categories was rated, and an assessment was made as to which category each diver would belong on the average. Of the 36 divers (mean age 30 ± 8 years) involved in both phases, 13 divers (mean age, 33 ± 9 years) were classed as high bubblers, 12 divers (mean age, 30 ± 8 years) as moderate bubblers, and 11 divers (mean age, 25 ± 4 years) as low bubblers. Most of the *Phase 1* divers were either high or moderate bubblers, 10 were high (mean age, 36 ± 8 years), and 9 were moderate (mean age, 33 ± 8 years). This would indicate that older divers are more susceptible to bubbling and should avoid high-stress dives. Of the 6 divers who incurred decompression sickness, 4 were high bubblers, 1 was a moderate bubbler, and 1 was a

TABLE III

Means and Standard Deviations (SD) for the Index of Severity, S, for High, Moderate, and Low Bubblers Based on 5 h of Monitoring the Precordial Region at Rest

Profile	High Bubblers		Moderate Bubblers		Low Bubblers	
	No. of	S	No. of	S	No. of	S
msw/min	Divers	Mean SD	Divers	Mean SD	Divers	Mean SD
30/55	2	16.8 ± 8.8	6	4.0 ± 1.9	2	0
					4	0.3 ± 0.1
36/30	4	3.5 ± 1.4	3	0.3 ± 0.1	5	0
36/40	6	14.4 ± 3.7	2	4.2 ± 2.3	2	0
					2	0.3 ± 0.2
36/50	3	17.0 ± 3.1	1	6.8	1	0.5
	1	36.6				
45/20	1	1.6	3	0.5 ± 0.2	2	0
45/25	3	3.0 ± 2.4	4	0.4 ± 0.2	5	0
45/30	3	11.7 ± 3.2	4	1.7 ± 0.9	3	0
					2	0.1
54/15	3	4.2 ± 2.0	2	0.2 ± 0.1	7	0
54/20	4	15.9 ± 3.3	4	4.1 ± 1.6	8	0
	1	34.0			2	0.4 ± 0.3
54/25	4	17.2 ± 5.0	9	3.6 ± 1.9	4	0
	1	45.3			1	0.5
66/10	1	4.0	1	0.7	12	0
66/15	3	19.5 ± 2.0	2	9.3 ± 0.1	6	0
					3	0.3 ± 0.1
75/10	2	19.1 ± 3.7	3	4.5 ± 2.4	8	0
					1	0.3

low bubbler. The low bubbler was extremely active immediately after surfacing and this was probably the contributing factor for the bend.

Table III shows that, for each depth, the decompression stress *increases* (larger values of *S*) as the bottom time increases. Figure 3 shows *S* for high bubblers for each dive profile and a limiting bottom-time line. For dives with bottom times less than the limiting values, the dives should result in grade 2 bubbles or less. High bubblers should avoid diving at or near the limiting values because grade 3 bubbles would result. With the exception of the bend resulting from grade 2 bubbles, all cases of decompression sickness occurred for bottom times greater than the limiting values. Moderate bubblers should be safe at or near the limiting values with grade 2 bubbles. Only low bubblers should dive beyond the limiting values. It is interesting to note that the Royal Navy limiting line for air dives, beyond which the risk of decompression sickness increases (7), is near the limiting values determined for the decompression computer dives.
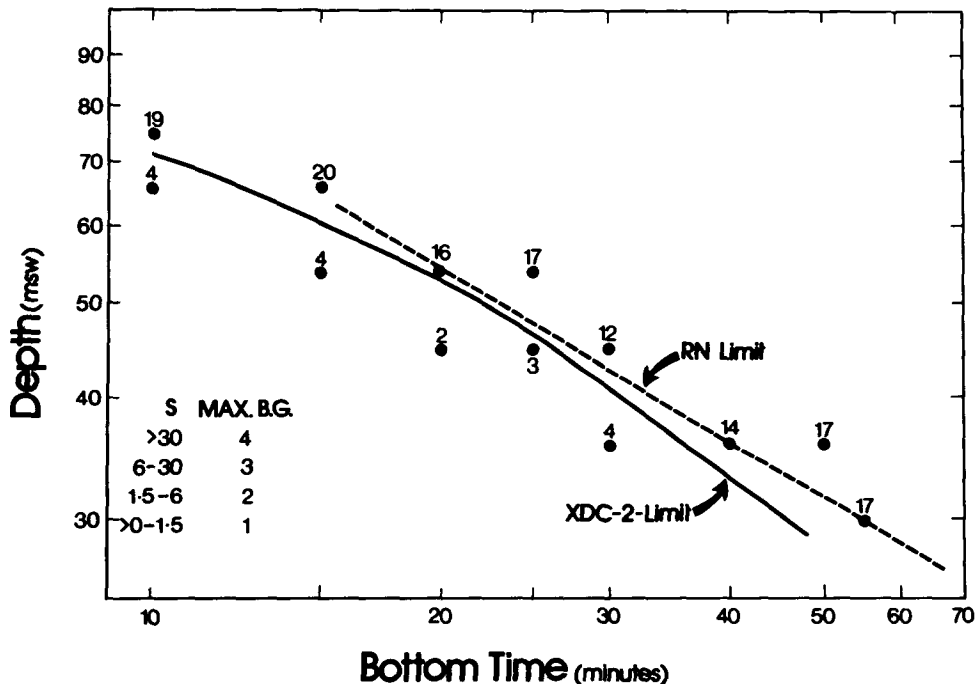
Fig. 3. Severity of the dive profiles generated by the XDC-2 decompression computer. Data points indicate the dive profiles tested. The *index of severity, S,* is shown for high bubblers besides each depth and bottom time. Maximum bubble grades (B.G.) corresponding to ranges of *S* are indicated. An empirical limiting bottom-time line (*solid line*) for high bubblers is indicated. High bubblers should avoid diving at or near this limiting line because of increased decompression stress. Also shown for comparison is the Royal Navy limiting line (*dashed line*) for compressed air dives.

DISCUSSION

Bubble results obtained during this investigation showed that bubbles often did not occur during or immediately after decompression but occurred some time after surfacing, reaching a maximum between 1 and 2 h after the start of decompression. In many cases, bubbles were found to persist for a period of many hours after the dive, and could be observed particularly after a movement. The fact that bubbles can persist for so long after a dive can have severe consequences, particularly for individuals who fly after diving. The results also showed that many high bubblers could tolerate a high degree of bubbles with no apparent ill effects.

Bubbles observed in the precordial region were only those that were detectable. Bubbles must be above a certain size (estimated to be about 100 μm in diameter [2,10]) to be detectable above the background noise level caused by the blood flow and other signal sources in the precordial region with transducers operating at 5 MHz. In the subclavian region, the background blood flow signal was much lower and as a result, bubble signals in this region were clearer and much smaller bubbles could be detected. These bubbles may not have grown sufficiently by the time the heart was reached to be detectable there, and this would explain why bubbles can be detected in the subclavian veins in the absence of bubbles in the precordial region. Hence, failure to detect bubbles in the precordial region does not imply that bubbles do not exist.

The best and most convenient criterion for indicating the severity of a dive profile appears to be the maximum bubble grade observed at rest in the precordial region because the entire venous system drains through this site. Dive profiles that produce a maximum of grade 3 or grade 4 bubbles at rest indicate a definite hazard in terms of decompression safety. Any decompression profiles found to be safe for high bubblers within some acceptable level of risk should be safe for moderate or low bubblers with little risk. Attempting to develop safe profiles with low bubblers could result in decompression tables or profiles that could be hazardous for high bubblers.

In summary, the results of this investigation have shown that the use of the Doppler ultrasonic bubble detector provides a convenient and valuable method for assessing the safety or severity of decompression profiles. Moreover, it is a more reliable and more acceptable method than the traditional method of performing a larger number of dives and provoking bends. In addition, the Doppler method provides a method of assessing divers as to their susceptibility to decompression sickness.

References

1. Berghage T, Heaney D. How many subjects are enough? Pressure 1976;5(4):4–5.
2. Spencer MP. Decompression limits for compressed air determined by ultrasonically detected blood bubbles. J Appl Physiol 1976;40:229–235.
3. Pearson R, ed. Early diagnosis of decompression sickness. Proceedings of the Twelfth Undersea Medical Society Workshop, Toronto, Ontario. Report No. UMS 7-30-77. Bethesda, MD: Undersea Medical Society, 1977.
4. Nishi RY. Real-time decompression monitoring by computers. In: Johnson CE, Nuckols ML, Clow PA, eds. Hyperbaric diving systems and thermal protection. OED-Vol. 6. New York: The American Society of Mechanical Engineers, 1976:25–38.
5. Kidd DJ, Stubbs RA. The use of the pneumatic analogue computer for divers. In: Bennett PB, Elliott DH, eds. The physiology and medicine of diving and compressed air work, Baltimore: Williams & Wilkins Company, 1969:386–413.
6. U.S. Navy. U.S. Navy Diving Manual, Vol. 1, Air Diving. NAVSEA 0994-LP001-9010, Washington DC: U.S. Navy Department, 1973.
7. Royal Navy. Diving Manual, B.R. 2806. Ministry of Defence (Navy), London: Her Majesty's Stationary Office, 1972.
8. Kisman KE, Masurel G, Guillerm R. Bubble evolution code for Doppler ultrasonic decompression data. Undersea Biomed Res 1978; 5(1) (Suppl):28 (Abstr).
9. Kisman KE, Masurel G, Lagrue D, Le Pechon JC. Évaluation de la qualité d'une décompression basée sur la détection ultrasonore de bulles. Médecine Aéronautique et Spatiale, Médecine Subaquatique et Hyperbare 1978;17:293–297.
10. Nishi RY. Problem areas in ultrasonic detection of decompression bubbles. In: Pearson R, ed. Early diagnosis of decompression sickness. Proceedings of the Twelfth Undersea Medical Society Workshop. Report No. UMS 7-30-77, Bethesda, MD: Undersea Medical Society, 1977:50–68.

MONITORING BUBBLE FORMATION WITH AN INTEGRATING PULSE-ECHO ULTRASONIC METHOD

S. Daniels, J. M. Davies, K. C. Eastaugh,
W. D. M. Paton, and E. B. Smith

Gas bubbles formed in blood and tissues during or after decompression are now generally recognized to be the cause of the signs of decompression sickness. This fact has prompted a considerable amount of research into methods of observing bubble formation in vivo. In the first instance optical methods dependent on surgical intervention were used (1–4). These methods are, however, open to the criticism that the surgical intervention may itself alter gas separation or transport sufficiently to distort the normal in vivo pattern of bubble formation. Accordingly, a noninvasive method was sought which would allow in vivo bubble formation to be followed. Methods that use the degree of interaction between a gas bubble located in tissue and a sound wave have been widely investigated by both transmission (5–8) and reflection (9) techniques. The technique that has received the greatest attention relies on the shift in frequency of a sound wave reflected from a moving target (the Doppler shift) (10,11).

The Doppler method originally demonstrated used transducers surgically implated around an appropriate blood vessel, but this was rapidly superseded by transcutaneous devices (10,12,13). These became generally adapted to detect bubbles occurring in the total venous return to the heart (precordial monitoring) (14). A number of limitations are apparent with this technique: first, the nature of the method precludes the detection of fixed bubbles; second, observation is restricted to a particular site; and third, the interpretation of the Doppler signals is complex and unreliable, although improvements have been made by the use of advanced signals processing techniques (15,16). Recent work has shown that after certain types of dive profiles no reliable correlation

can be found between the incidence of decompression sickness and the intensity of Doppler signals (17).

In 1963 it was suggested that the limitations imposed by Doppler monitoring could be avoided by the use of Pulse-Echo Ultrasonic Imaging (18). This method relies only on the reflection of a sound wave and would thus respond equally well to a fixed or moving bubble. Furthermore, by scanning the transmitting and receiving transducer across an area of tissue, a two-dimensional image of that area could be displayed, within which any bubbles could be located. This was demonstrated by use of 7.5 MHz ultrasound to visualize the cross-section of a guinea-pig leg (19–21).

Subsequently, a high resolution Pulse-Echo Imaging system was developed in Oxford for study of the distribution and fate of gas bubbles within small rodents (22,23). This system employs 8 MHz ultrasound capable of detecting 10-μm diameter bubbles, and results from simulated dives using guinea pigs have been reported (24–26). The analysis of the distributions in time and space of the bubbles formed is, however, exceedingly complex and time consuming. Thus, although the method is suitable for assessing the fundamental role of gas bubbles in the etiology of decompression sickness, it is not applicable as an on-line monitor of bubble formation during decompression.

This difficulty has been overcome by adoption of an additional, new approach for processing the signals generated by Pulse-Echo Imaging (27). This approach involves an analogue-to-digital conversion of each image that results in a series of numbers that are equivalent to the total number of echoes in each successive two-dimensional image. These numbers are then normalized relative to the predecompression controls from each experimental subject. Thus the final output always represents the total number of echoes on each scan because gas bubbles are present within the area of tissue under study. Normalization is achieved, during the predecompression control period by electronic subtraction from each separate digital quantity a constant number sufficient to leave a small, non-zero remainder. Stationary bubbles within the area studied produce a fixed increase in the output level, whereas moving bubbles produce a transient increase.

This new approach primarily has been tested in conjunction with the complete Pulse-Echo Imaging system for study of bubble formation in guinea pigs after saturation air dives. However, a new system is currently under development for the study of bubble formation in humans, and a number of pilot experiments that have been performed in cooperation with the Admiralty Marine Technology Establishment Physiological Laboratory will be described.

METHODS

Small-Animal Experiments

The Pulse-Echo Imaging system is based on two units manufactured by Kretztechnik; a SHB4100MGB and a SHB4100MG Combison. These units have been modified to provide, in conjunction with a 8-MHz focused 5-mm

diameter PZT-5A transducer the basic amplitude and brightness-modulated display using a pulse repetition frequency of 2 kHz and electronic magnification up to ×4. Scanning is achieved mechanically with a sin/cos potentiometer providing the angular position of the transducer. The ultrasound image is displayed on a Hewlett-Packard 1331A oscilloscope. Each image is recorded automatically by a Grass C4H oscilloscope recording camera and is identified by a digital time display. The amplitude-modulated signal is additionally fed to the integrating unit. This unit consists of a pulse shaper and interface buffer, a gate and control circuit, the subtraction unit, and the output displays. The time over which echoes are counted is controlled by an internal clock, which is set to correspond to the scan frequency used (typically 1 Hz). This clock is triggered by a signal derived from the sin/cos potentiometer via a delay unit, so that the counting period coincides with passage of the transducer across the target area. The number of pulses to be subtracted is determined by inspection of the total count during the control period, as described previously. The remaining count (or, without subtraction, the total count) is displayed digitally and also is fed to a chart recorder via a digital-to-analogue converter.

Control experiments have shown that this system responds in a predictable fashion to targets of 10-μm diameter and upwards; there is no response to rapid cycling of pressure on the transducer; and a stable output is obtained from scanning a guinea pig leg, at a constant pressure and temperature, over a 2-h period.

The experiments, performed in a 351 pressure chamber, involved exposure of guinea pigs to air (medical grade) pressures ranging from 2.8 bars gauge to 8.3 bars gauge for 90 min followed by decompression in 1 min to surface. Compression was always at approximately 5 bars·min^{-1}. Pressure was maintained by a spring-loaded diaphragm-reduction gauge and monitored by a Bourdon tube pressure gauge. The chamber gases were mixed by a fan that assisted in the removal of carbon dioxide by renewable soda lime scrubbers. The air temperature inside the chamber was monitored with a thermistor and maintained at 30 ± 2°C by an external water jacket.

Before each experiment the guinea pigs (male, Duncan Hartley-derived, supplied by the University Park Farm, Northmoor, Oxford) were weighed and anesthetized with urethane (1.5 g/kg body weight, i.p.). The left hind limb was chosen for study and prepared by shaving and applying depilatory cream to remove all hair. Electrocardiogram electrodes were placed over the heart and at the back of the neck and the guinea pig was placed prone inside a perspex holder with the left hind limb extended downwards in the vertical plane and secured in place. The holder was positioned within the scanning tank, which carried the ultrasonic transducer, sin/cos potentiometer, and scan drive system, such that the leg was 15 mm in front of the transducer. Acoustic coupling between the leg and the transducer was achieved with use of a salt solution thermostated to 37 ± 0.5°C. Ultrasonic surveillance was begun 20 min before decompression so that the equipment could be adjusted. Recording was begun 1 min before decompression and continued for up to 2 h after decompression. To assess its therapeutic efficacy and to test the response of the

integrating system, we applied recompression at various times after the decompression. The onset of decompression sickness was taken as the time at which the first ECG arrhythmia occurred. Death was judged by the disappearance of both respiration and functional cardiac activity.

Experiments on Bubble Formation in Large Animals and Humans

For these experiments a new integrating system was constructed based upon an ADR 2130 Real Time Scanner (RTS) and a 5-MHz, 64-element cophased linear array transducer. The integrator presently in use is similar to that described previously. The major difference is the interface buffer and the analogue-to-digital converter. The signal obtained from the RTS is a full gray scale video signal, which is presently being digitalized using a high speed voltage comparator. The RTS was operated at 20 frames $\cdot$ s^{-1} (120 lines) and the integrator was counted for 250 ms with a counting cycle initiated every 300 ms. In addition, the ultrasound images can be recorded by a Polaroid camera.

Experiments on human subjects exposed to simulated air dives using both the R.N.P.L. tables and the U.S.N. tables, have been performed at the Admiralty Marine Technology Establishment Physiological Laboratory. Each experiment comprised two subjects; one was ultrasonically monitored and the other acted as attendant. Throughout the experiments normal chamber communications were maintained between the divers and the chamber operator. Additional communication between the subject under surveillance and the ultrasound operator was available if required. Any problems encountered were reported directly to the chamber controller. With the subject seated, the ultrasound transducer was positioned midway between the groin and knee and oriented to give an image corresponding to a transverse section through the thigh. A small quantity of "Aquagel," acoustic coupling gel, was applied to the thigh to provide acoustic contact between the skin and transducer. The transducer was positioned with a specially designed aluminium cradle fitted with rubber straps. A foam pad acted to cushion the transducer and prevent lateral rocking. All subjects reported this arrangement comfortable for periods up to 2 h.

Compression was at a rate of 3 bars $\cdot$ min^{-1} and decompression at 1.5 bars $\cdot$ min^{-1} without interruption. During these periods of changing pressure, transient fluctuations in the ambient temperature occurred. After surfacing, the subject remained seated for at least 30 min, during which time ultrasonic surveillance was continued.

RESULTS

Small-Animal Experiments

A total of 50 guinea pigs have been used in simulated air dives to 2.8, 4.1, 5.5, 6.9, and 8.3 bars gauge. All dives were of 90-min duration followed by decompression in 1 min. After the more severe decompressions, death almost invariably followed the onset of cardiac arrhy* _.iias. A summary of the results is given in Table I.

TABLE I

Summary of Response of Integrating Pulse-Echo Imaging after Air Dives of 90 min Duration Using Guinea Pigs

| | Exposure Pressure (bars gauge) | | | | |
	2.8	4.1	5.5	6.9	8.3
Incidence of Decompression Sickness	0%([0]/10)	10%([1]/10)	40%([4]/10)	79%([12]/14)	100%([6]/6)
Mean Time to First Cardiac Arrythmia (min ± SE)	—	33.8 ($n=1$)	24.4 ± 5	11.5 ± 1.2	6 ± 0.5
Mean Integrator Count Above Control at Time of First Cardiac Arrhythmia (± SE)	—	396 ($n=1$)	843 ± 341	526 ± 125	143 ± 91

Two different responses are identifiable on the integrator output: a) a long-term increase in the number of counts (associated with stationary bubbles), and b) transient responses seen as increases in variability (associated with bubbles passing through the plane of scan). An example of the integrator output is shown in Fig. 1.
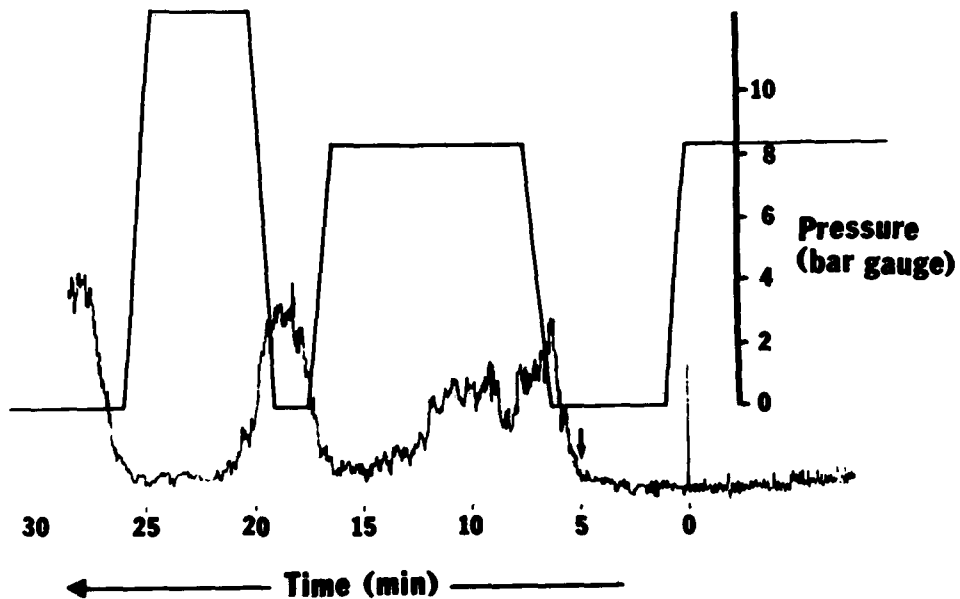
Fig. 1. Example of integrator output recorded after an 8.3-bar decompression. On the same time scale, the pressure profile after initial 90 min at 8.3 bar is shown. The *arrow* denotes the cardiac arrhythmia.

Average integrator outputs were constructed from the individual records for each of the 8.3-, 6.9-, and 5.5-bar dive series, in which long-term rises were always observed in addition to periodic increases in variability. The time elapsed before a significant rise in the average output (> 3 SD above control) was found to be 5, 8, and 15 min after 8.3-, 6.9-, and 5.5-bar decompressions, respectively.

After the 4.1-bar decompressions, 3 of the 10 integrator records showed no significant sustained increase in signal and no symptoms were observed. Of these three records, two showed considerable transient activity. Of the seven remaining records, three showed a rise in output followed by a gradual return to control levels, again with no symptoms observed. Of the remaining four records; one was associated with the appearance of cardiac arrhythmias, and recompression to the exposure pressure was both therapeutic and returned the integrator count to control values; two, not associated with symptoms, showed a rise that had not begun to fall after 60 min, and recompression returned the integrator count to control values in both cases. The remaining record showed a biphasic response with an initial rise and fall over 36 min, followed by a second rise that did not fall within 128 min, again no symptoms were observed.

After the 2.8-bar decompressions, none of which were associated with symptoms, 3 of the 10 integrator records again showed no significant rise but in this case only 1 of these showed appreciable transient activity. Of the remaining seven records; four showed a gradual rise followed by a return to control; two showed a rise with no reduction after 60 min, and recompression to the exposure pressure returned the count to the control value; the last showed a biphasic response with an initial rise and fall in 25 min, followed by a second rise that had not returned to the base line after 85 min.

Table II gives an analysis of those runs, 3 at 4.1 bars and 4 at 2.8 bars, when there were positive signals but no symptoms, so that subsequent events were not distorted by recompression. Because the later course of the counts may represent natural recovery from a period of bubble formation, the mean time for return to control values has been calculated and is given together with the average maximum count.

In all experiments involving recompression it was observed that subsequent decompression produced more rapid increases in integrator output than observed after the initial decompression.

To test the sensitivity of the integrator we have made a number of comparisons between the output and the number of bubbles per frame. The bubbles were identified from a full frame-by-frame spatial and temporal analysis of the ultrasound images. An example of this comparison is shown in Fig. 2.

Experiments Using Human Subjects

Preliminary experiments have been performed using two different exposures to 3 bars gauge air with "no stop" decompression: the first, according to the BSAC/RNPL 1976 (BR2806 Table II) schedules, and the second, according to the U.S. Navy Standard Air Decompression Table, which allows a maximum of 20 and 25 min bottom time, respectively. Ten different subjects were

TABLE II

Time Course for Return of Individual Integrator Outputs to Control Values after
Asymptomatic Decompressions

| | 4.1 bars | | 2.8 bars | |
	(min)	(counts)	(min)	(counts)
Time to Return to Control (min) and	24	384	53	480
Maximum Count Above Control	48	288	34	160
	55	304	43	448
			40	480
Mean ± SE	42 ± 9 min	325 ± 29 counts	42 ± 4 min	392 ± 77 counts
		(n = 3)		(n = 4)

used and a minimum of 2 days separated repeat exposures, with the exception
of one subject who had sport-dived on the day before an experiment. The re-
sults are summarized in Tables III and IV and four examples of the integrator
traces are shown in Fig. 3.

DISCUSSION

The results from the small-animal experiments, in which the incidence of
decompression sickness varied from 100 to 0% can now be used to gauge the
limitations to the application of Integrating Pulse-Echo Imaging to monitoring
bubble formation in humans.

There are two main requirements by which the success of any monitoring
method may be judged: first, as large a time interval as possible between a
positive response by the monitor and the onset of symptoms, and second, an
unambiguous and, preferably, quantitative signal from the monitor. The exper-
iments using guinea pigs have shown that Integrating Pulse-Echo Imaging
gives separations in time between symptoms and a positive response of up to
9.5 min after 5.5-bar decompressions. The observed trend, that this separation
was greater after the least severe decompressions, was confirmed by the single
symptomatic 4.1-bar decompression where the separation was 12.3 min. With
severe decompression associated with a short warning period, the amplitude of
the maintained signal may not be well developed at the time symptoms appear.
Because full analyses of such decompressions have shown that the early stages
of the response are marked by a considerable number of transient signals, it is
thought that as a result a large number of bubbles could arrive at the heart
within a short time. This concern should not prevent the application of the
technique in humans because such severe decompressions would only arise by
accident. The magnitude of the response before symptoms occur has always
been found sufficiently large to allow positive prediction, and symptoms have
never been observed without a positive response.
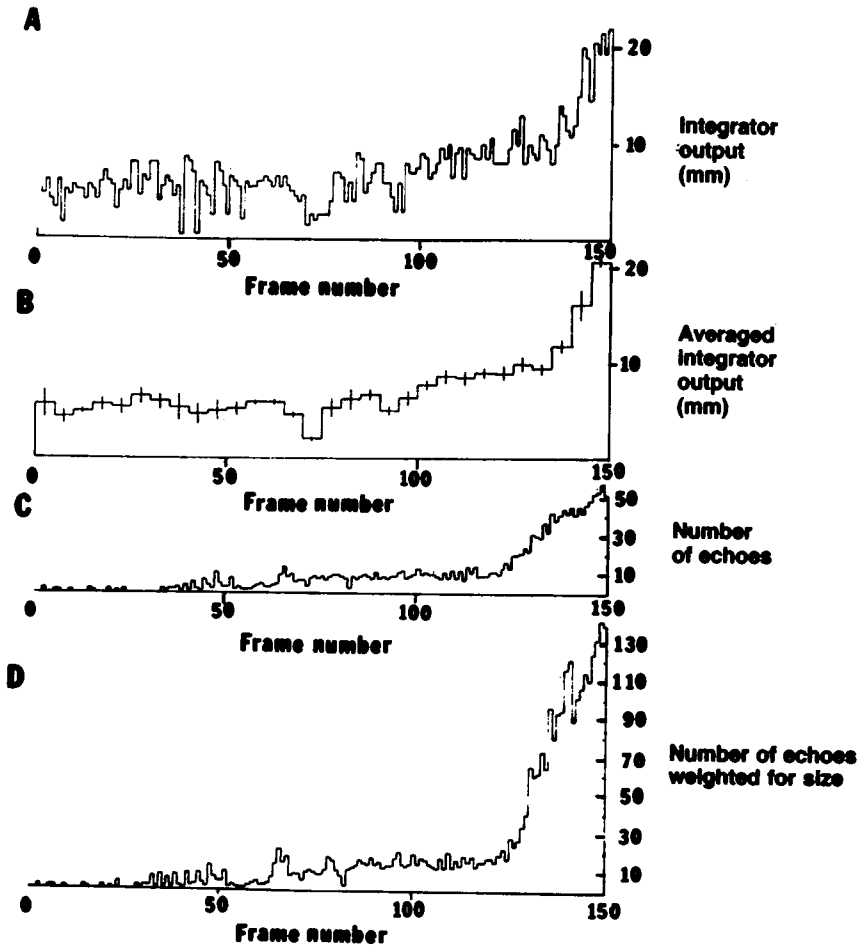
Fig. 2. Comparison of integrator output and number of echoes per frame, identified from a full spatial and temporal analysis of the ultrasound images, after decompression of a guinea pig from a 90-min exposure to 8.3-bars gauge air. Time is shown, on the horizontal axis, as frame number, corresponding to intervals of 2 s.   A. Integrator output expressed in millimeters (mm) above base line for the first 5 min after the beginning of decompression.   B. Integrator output averaged over 5 frame (10-s) intervals, with *vertical bars* denoting SD. The *vertical scale* is again in mm above the base line.   C. Number of echoes per frame identified by image analysis.   D. Number of echoes per frame weighted for size variation. Weighting factors were 1, 3, and 5 for images corresponding to bubbles < 100 μm in diameter, bubbles between 100 μm and 500 μm in diameter, and bubbles > 500 μm in diameter, respectively.

The comparison of the integrator outputs from those 4.1- and 2.8-bar decompressions a) were asymptomatic, b) showed a rise in the output, and c) where recompression was not applied, showed that the mean time for the response to return to the base line was the same for both exposures and the mean maximum integrator level was also the same. The time for return to control level, 42 min, is about 40% longer than the estimated half-time for gas uptake.

TABLE III

Results of Monitoring Divers Subjected to 30-msw Simulated Dive Following BSAC/
RNPL 1976 Table for 20-min No-Stop Time, with Integrating Pulse-Echo Imaging

Subject	Integrator Output	Subjective Assessment
JT	Small sharp rise 30 s after surfacing lasting 6.5 min followed by a smooth rise lasting 9 min	OK
*ME	Smooth rise 8 min after surfacing lasting 10 min	OK
*DWB	Sharp rise 12.5 min after surfacing lasting 5.5 min	Reported "sick and hazy" 19.6 min after surfacing
DM	No change	OK
PW	Slow rise 8 min after surfacing lasting 18 min	OK
*TRH	Small rise 5 min after surfacing lasting 5 min	OK
DE	Sharp rise 4.5 min after surfacing lasting 3.5 min	OK
PT	No change	OK
*JF	No change	OK
RM	No change	OK

*Integrator outputs shown in Fig. 3.

TABLE IV

Results of Monitoring Divers Subjected to 30-msw Simulated Dive Following U.S. IV
Standard Air Decompression Table for 25-min No-Stop Time with Integrating Pulse-
Echo Imaging

Subject	Integrator Output	Subjective Assessment
JT	Smooth rise 21 min after surfacing lasting 5 min	OK (Subject observed to be restless)
ME	No change	OK
DWB	Small rises 4, 16, and 19.5 min after surfacing, each lasting 2 min	OK
DM	No change	OK
PW	Small rises 8, 11.5, and 19 min after surfacing, each lasting 3.3, 3.3, and 4 min, respectively	OK

It was found on symptomatic dives that recompression to the exposure pressure had to be applied very shortly after the onset of cardiac arrhythmias for it to be therapeutic. If recompression was delayed, it was necessary to go beyond the exposure pressure to obtain relief. One could anticipate that recompression as soon as positive signals appear, and before any symptoms develop, would be still more effective therapeutically. As expected, very late
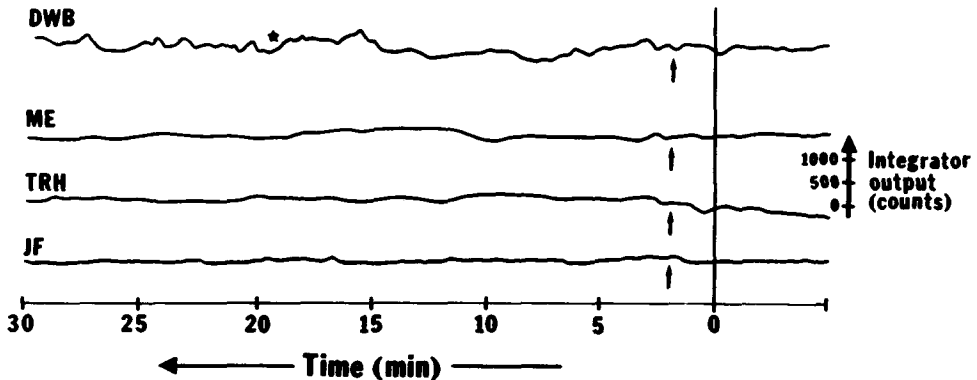
Fig. 3.   Integrator outputs after "no-stop" decompression from 20-min exposures to 30 msw for four subjects using the Real-Time Scanner in conjunction with the integrator. Dives involving Subjects ME, TRH, and JF were reported symptomless. Subject DWB reported feeling sick and hazy at the time indicated by the *.   In all cases the *vertical axis* represents number of counts. The decompressions began at time 0 and surfacing is denoted by the *arrows*.

recompression was not always fully therapeutic even though the integrator count was returned to control values.

The comparison of the integrator count with the number of bubbles per frame, as identified by a full spatial and temporal analysis of the images, was good. A little sensitivity may be lost (Fig. 2) in the response to a small number of transient bubbles, because such changes cannot be distinguished by the integrator from minor variations caused by animal movement. However, this does not appear to present any major problems with regard to the predictive value of the integrator.

In view of these results, the new equipment is being developed and tested with human subjects. The reduction in operating frequency (from 8 MHz to 5 MHz) provides a greater penetration and is fully capable of allowing imaging through the thigh of a human adult. At present an output is obtained every 0.3 s (cf: small animal equipment—output every 2 s). It is expected that the high rate of acquisition of data will allow a running average to be made, and thus reduce the effect of small movements. The equipment has proved acceptable to experimental subjects, being comfortable to wear over a period of 2 h. Stable outputs are obtained with the extremely simple method of attachment, although it remains to be determined if the transducer can be removed for periods and then replaced with the same base line obtained.

The experiments with the new integrating system using human subjects have to date proved promising, with some evidence for minor bubble formation being detected in 9 of the 15 dives. The only subject to report any feeling of malaise did so 7 min after a small rise in the integrator level, which lasted 5.5 min. Similar sharp rises were observed in two other experiments without any reported symptoms. Restlessness was noted for one subject, but he reported that he felt well and did not attribute the restlessness to the decompression; some rise in the integrator level was observed.

Before firm conclusions can be drawn regarding the suitability of Integrating Pulse-Echo Imaging for monitoring bubble formation during decompression, more severe human dives must be completed in which definite bends are obtained, so that amplitude and time course may be fully calibrated. Finally, it may be of importance to note that if these results are substantiated, evidence for bubble formation will have been obtained after decompressions that amateur sports divers universally regard as safe.

Acknowledgments

References

1. Harvey EN. Animal experiments on bubble formation. In: Fulton JF, ed. Decompression sickness. Philadelphia and London: W. B. Saunders Co, 1951:115–165.
2. Buckles RG. The physics of bubble formation and growth. Aerosp Med 1968;39:1062–1069.
3. Lever MJ, Miller KW, Paton WDM, Smith EB. Experiments on the genesis of bubbles as a result of rapid decompression. J Physiol 1966;184:964–969.
4. Gait DJ, Miller KW, Paton WDM, Smith EB, Welch B. The redistribution of vascular bubbles in multiple dives. Undersea Biomed Res 1975;2:42–49.
5. Manley DMJP. Ultrasonic detection of gas bubbles in blood. Ultrasonics 1969;7:102–105.
6. Powell MR. Leg pain and gas bubbles in the rat following decompression from pressure: monitoring by ultrasound. Aerosp Med 1972;43:168–172.
7. Walder DN. Ultrasonics in the detection of intravascular bubbles. Can Med Assn J 1967;96:1233–1234.
8. Welsby VG. Acoustic detection of gas bubbles in liquids. I.E.R.E. Conference Proceedings, 1969;16:97–108.
9. Franklin DL, Schlegel W, Rushmer RF. Blood flow measured by Doppler shift frequency of back-scattered ultrasound. Science 1961;134:564–565.
10. Gillis MF, Peterson PL, Karagianes MT. In vivo detection of circulating gas emboli associated with decompression sickness using the Doppler flowmeter. Nature 1968;217:965–967.
11. Spencer MP, Campbell SD. The development of bubbles in the venous and arterial blood during hyperbaric decompression. Bull Mason Clin 1968;22:26–32.
12. Evans A, Walder DN. Detection of circulating bubbles in the intact mammal. Ultrasonics 1970;8:216–217.
13. Spencer MP, Simmons N, Clarke HF. A precordial transcutaneous cardiac output and aeroembolism monitor. Fed Proc 1971;30:703.
14. Spencer MP, Clarke HF. Precordial monitoring of pulmonary gas embolism and decompression bubbles. Aerosp Med 1972;43:762–767.
15. Belcher EO, Ehrenberg JE, Lytle DW. Adaptive embolic detection and quantification in man during decompression. In: Early diagnosis of decompression sickness; Twelfth Undersea Medical Society Workshop. Bethesda, MD: Undersea Medical Society, 1977:118–139.
16. Kisman K. Spectal analysis of Doppler ultrasonic decompression data. Ultrasonics 1977;15:105–110.
17. Gardette B. Correlation between decompression sickness and circulating bubbles in 232 divers. Undersea Biomed Res 1979;6:99–107.
18. Mackay RS. Discussion remarks. In: Lambertsen CJ, Greenebaum LJ, eds. Proceedings of second symposium on underwater physiology. Washington, DC: Nat. Acad. Sci.-Nat. Res. Counc 1181, 1963:41.
19. Mackay RS, Rubissow GJ. Ultrasonic imaging of in vivo bubbles in decompression sickness. Ultrasonics 1971;9:225–234.

20. Rubissow GJ, Mackay RS. Decompression study and control using ultrasonics. Aerosp Med 1974;45:473–478.
21. Mackay RS, Rubissow GJ. Decompression studies using ultrasonic imaging of bubbles IEEE Trans 1978;BME25(6):537–544.
22. Daniels S, Paton WDM, Smith EB. An ultrasonic imaging system for the study of decompression induced gas bubbles. Undersea Biomed Res 1979;6:197–209.
23. Beck TW, Daniels S, Paton WDM, Smith EB. Detection of bubbles in decompression sickness. Nature 1978;276:173–174.
24. Daniels S, Paton WDM, Smith EB. Ultrasonic imaging of bubble formation from sub-lethal decompressions. In: Early diagnosis of decompression sickness; Twelfth Undersea Medical Society Workshop. Bethesda, MD: Undersea Medical Society, 1977;81–95.
25. Daniels S, Paton WDM, Smith EB. Bubble formation investigated by ultrasonic imaging. In: Medical aspects of diving accidents. Luxembourg E.C.S.C., E.E.C., E.A.E.C. 1979;99–106.
26. Daniels S, Davies JM, Paton WDM, Smith EB. The detection of gas bubbles in guinea pigs after decompression from air saturation dives using ultrasonic imaging. J Physiol 1980;308:369–383.
27. Daniels S. An integrating pulse-echo ultrasonic bubble detector for use during decompression procedures. Patent Application No. 40103/73, 1978: superceded by No. 7934423, 1979.

MIGRATION OF LUNG SURFACTANT TO PULMONARY AIR EMBOLI

B. A. Hills and B. D. Butler

While minimal arterial gas embolism can lead to permanent neurologic injury or death, venous air, by contrast, usually remains asymptomatic—at least, it does so in the volumes produced by decompression. As a comparison, some dogs have survived as much as 1 litre (L) of air infused into the venous system (1) and yet only 0.5 mL injected into the arterial system has proved fatal (2)—or only 0.025 mL if injected directly into the coronary circulation (3).

In view of the very common occurrence of venous bubbles during decompression as detected by precordial monitoring of the pulmonary artery by Doppler ultrasound (4) and frequent cases of venous air introduced following surgery (5), there is little doubt that the lungs are normally most effective in trapping bubbles. A recent study (6) has shown that they not only trap boluses of gas, but can filter microbubbles of 21 μm diameter or less out of the circulating blood just as they remove thrombi, platelet aggregates, and other potential infarcting agents. Indeed, the secondary role of the lungs as a blood filter under normal conditions is now well established (7).

The concept of asymptomatic bubbles was first postulated by Haldane and co-workers (8) to try to correlate clinical symptoms of decompression sickness with their pathological findings and was further emphasized by Behnke (9) who gave them the popular name of "silent" bubbles. The propensity of the venous bubbles formed during decompression and his appreciation of the potential danger of their release into the arterial system led Walder, in 1948, to perform a most pertinent calculation (10). He argued that, for any gas to escape from the venous system into the arterial system in the absence of lung shunts, it would need to pass through pulmonary capillaries, which could be as

large as 10 μm in diameter, but would be held back by capillarity in attempting to do so. This retarding pressure (ΔP) was estimated using the following equation:

$$\Delta P = 2\,\gamma/r \qquad (1)$$

where γ is the plasma surface tension and r is the capillary radius. Taking a value of 50 dyne/cm for γ and r = 5 μm, Eq. 1 gives ΔP = 150 mmHg. Thus, Walder argued that pulmonary arterial pressure would need to reach a value of 150 mmHg before the blood-air interface would recede and enable air to reach the arterial system. Since this level of pulmonary hypertension is virtually impossible, it was further argued that it was most unlikely that venous bubbles could become arterial emboli, and interest in this subject was not revived until quite recently (1). It was then pointed out that the value calculated for ΔP depends markedly upon the value used for γ and whether there was a finite contact angle (θ) at the endothelial-air interface, in which case the full equation for capillarity should be used, viz,

$$\Delta P = 2\,\gamma\cos\,(\theta)/r \qquad (2)$$

Appreciating the full significance of Walder's original calculation, it was also pointed out (11) that surfactants are normally present in the lung. Some of those, e.g., dipalmitoyl lecithin (DPL), can greatly reduce surface tension; even lung extracts can give values as low as 2 dyne/cm when their films are compressed in vitro (12). Recently, it has also been shown (13) that DPL can induce a contact angle at pulmonary epithelial surfaces of up to 70°. If these values are now substituted in Eq. 2, a value of less than 3 mmHg is obtained for ΔP. Since pulmonary arterial pressure lies intermediate between this value and Walder's original estimate of the resistance to capillary flow offered by the trapped bubble, the degree of modification of surface properties by surfactant could determine whether or not flow occurs. Hence, the extent of recruitment of surface active agents could determine whether the embolus is ejected into the arterial system. Thus, it is imperative to find out whether, in fact, pulmonary surfactants actually reach the surface of bubbles trapped in the pulmonary circulation.

Theoretically, surfactant molecules have a great affinity for any gas-aqueous interface where they orientate themselves with the hydrophylic group in the aqueous medium and their hydrophobic "tails" in the air. As far as surface thermodynamics are concerned, they would be equally attracted to locate at the air-aqueous surface of a bubble trapped in a pulmonary capillary as they would at the alveolar-air interface where their presence has long been recognized (14). Hence, this study has been designed to attempt to detect any tendency for surfactant molecules to migrate to the surfaces of trapped pulmonary bubbles.

MATERIALS AND METHODS

Principle

The method adopted was one of embolizing the lung with a large number of microbubbles to provide a large surface area and, hence, a large "sink" for any migrating surfactant. The animal was subjected to euthanasia immediately after embolization to prevent the subsequent dilution of any migrated surfactant that would occur if blood were flowing and to avoid its removal from the lung as each bubble dissolved. After allowing adequate time, we back-flushed the lungs and assayed the washings for surfactant by obtaining surface tension vs. surface area loops on the same Wilhelmy balance used as standard equipment for estimating and studying DPL, lung washings, lung extracts, and the like (12).

Apparatus

The apparatus used for assay of the surfactant was a Langmuir-type trough (Kimray-Greenfield surfactometer) in which 32 mL from each aliquot of lung back-flushings provided the pool. The Teflon trough was fitted with a moveable barrier, which was programmed to cycle between 100% and 15% of initial area every 3 min. Surface tension was monitored continuously during each cycle by means of a platinum flag partially immersed in the pool and suspended from the arm of a force transducer, i.e., using the Wilhelmy principle (12).

Procedure

Nine mongrel dogs were used. Each was anesthetized with sodium pentobarbital (30 mL/kg i.p. Nembutal) and intubated to permit external ventilatory assistance. Cannulae (7 Fr.) were inserted into the right ventricle and abdominal aorta for drug infusions and blood sampling. Sodium heparin (10,000 units) was administered intravenously before collecting blood samples for surface tension measurements.

Fifty mL of whole blood (arterial) was collected and centrifuged, and the plasma was mixed with an equal volume of heparinized Ringer's solution to produce the medium in which the microbubbles were produced by direct mixing with air.

Each animal was embolized over a period of 5 min by infusion into the right ventricle the 12 mL of the medium mixed with 12 mL of air microbubbles. Immediately post embolization, each dog was subjected to euthanasia with an overdose of pentobarbital and the thoracic cavity was exposed. The pulmonary circulation was then isolated by ligation of the superior vena cava,

the inferior vena cava above the diaphragm, and the azygous vein adjacent to the right atrium, while the ascending aorta was clamped. To facilitate subsequent back-flushing of the pulmonary capillaries, we inserted a silastic cannula (24 Fr.) just inside the left ventricle through an incision in the left atrial appendage, while the main pulmonary arterial trunk was cannulated for ·collection. In this latter procedure the base of the pulmonary artery trunk was ligated, thus right ventricular blood was separated from that sampled.

After separation of the ribs, the surfaces of the lungs were kept moist with gauze soaked in Ringer's solution and ventilated on a Harvard ventilator at 16 cycles/min at normal tidal volumes with 4 cm w.g. end-expired pressure. After 1 h, we back-perfused the lungs using 300 mL of the flush solution from a reservoir in which the fluid level gave a "head" not exceeding 30 cm w.g. Back-flushings were collected as three consecutive 75 mL aliquots, changing from red to pinkish as pulmonary capillary blood was progressively diluted.

An identical procedure was used for the control animal except that the microbubbles were omitted from the initial infusate.

From each aliquot, a 32 mL sample was placed in the Langmuir trough described above and allowed to stand for 5 min—the time generally allowed in studies of lung extracts (15) for surfactant molecules to locate at the air-aqueous interface. Surface tension vs. pool area loops were recorded continuously for 15 min at 25°C.

RESULTS

The plots of surface tension vs. surface area all displayed loops that changed little after the third cycle, including controls taken for both the embolized animals and the nonembolized animal. Data for the first cycle are given in Table I and for the fifth cycle in Table II.

The loops for the embolized animals are plotted in Fig. 1, where it can be seen that they display the relationships characteristic of lung surfactants measured on the same instrument (12,15). These loops differ markedly from those of the nonembolized animal (Fig.2) and, to a lesser extent, from the individual controls (Fig.3) in the magnitude of reduction of surface tension at maximum film compression.

The mean surface tension for maximum compression of the first loop was 31.9 dynes/cm for the first aliquot, 31.2 for the second, and 28.3 for the third, compared with a control value of 33.80 dynes/cm. These values represent decreases of 4.8, 7.8, and 16.4%, respectively, from the control.

The fifth loop may provide a better assay because later cycles are generally considered to offer more opportunity for the pool surface to recruit surfactants from the underlying hypophase (15). For the fifth loop, mean surface tension values were 31.9 dynes/cm for the first aliquot, 29.3 for the second, and 27.2 for the third by comparison with 35.7 dynes/cm for the control, i.e., mean decreases of 11, 18, and 24%, respectively. A statistical analysis was performed for all data and the results are included in Tables I and II. Essentially, this analysis showed that the likelihood that the bubble injection procedure was responsible for the reduction in surface tension for maximal film

Table I

SURFACE TENSION MEASUREMENTS FROM PULMONARY
CAPILLARY BLOOD FOLLOWING EMBOLIZATION
(FIRST COMPRESSION)

COMPRESSION AREA	SAMPLE NO. 1 FIRST COMPRESSION	% CHANGE FROM CONTROL (Control vs. No. 1)	P VALUE	
100	51.92 ± 2.31	5.82	0.01	n=4
90	50.58 ± 1.83	6.76	0.05	n=4
80	49.0 ± 1.61	5.55	0.05	n=4
70	48.33 ± 1.51	4.54	0.10	n=4
60	47.25 ± 1.21	4.55	0.05	n=4
50	45.92 ± 1.43	5.51	0.05	n=5
40	43.83 ± 1.47	5.94	0.10	n=5
30	40.0 ± 2.32	8.47	0.05	n=5
20	34.50 ± 4.34	7.01	0.25	n=5
15	32.17 ± 4.30	4.82	0.25	n=5

COMPRESSION AREA	CONTROL FIRST COMPRESSION		SAMPLE NO. 2 FIRST COMPRESSION	% CHANGE FROM CONTROL (Control vs. No. 2)	P VALUE	
100	55.13 ± 3.97	100	53.0 ± 4.15	3.86	0.25	n=6
90	54.25 ± 3.85	90	51.08 ± 3.07	5.85	0.10	n=6
80	51.88 ± 3.12	80	49.42 ± 2.42	4.74	0.10	n=6
70	50.63 ± 2.84	70	48.0 ± 2.10	5.19	0.10	n=6
60	49.50 ± 2.45	60	47.08 ± 2.08	4.89	0.10	n=6
50	48.60 ± 2.86	50	45.83 ± 2.71	5.70	0.10	n=6
40	46.60 ± 3.80	40	43.92 ± 3.29	5.75	0.25	n=6
30	43.70 ± 4.15	30	40.67 ± 3.57	6.93	0.25	n=6
20	37.10 ± 4.74	20	34.75 ± 3.47	6.33	0.25	n=6
15	33.80 ± 5.37	15	31.17 ± 3.27	7.78	0.25	n=6

	SAMPLE NO. 3 FIRST COMPRESSION	% CHANGE FROM CONTROL (Control vs. No. 3)	P VALUE	
100	51.88 ± 2.72	5.90	0.25	n=4
90	50.13 ± 2.29	7.59	0.10	n=4
80	48.50 ± 1.08	6.52	0.05	n=4
70	47.38 ± 1.03	6.42	0.05	n=4
60	45.50 ± 1.08	8.08	0.01	n=4
50	43.63 ± 1.89	10.23	0.025	n=4
40	41.13 ± 2.39	11.74	0.025	n=4
30	36.75 ± 2.75	15.90	0.025	n=4
20	31.0 ± 3.03	16.44	0.05	n=4
15	28.25 ± 2.75	16.42	0.10	n=4

compression exceeded the 90% significance level for comparison of second and third aliquots.

In the nonembolized dog the first loop showed a surface tension for maximum compression of 33 dynes/cm for the first aliquot and 37 for the second compared with 33.8 dynes/cm for its own control.

DISCUSSION

The statistical significance of the decreases in the surface tension of blood samples back-flushed from the lungs of the embolized dogs strongly suggests the recruitment of surface-active molecules to the bubble surface. Moreover, the similarity of the surface tension/area loops with those of lung extracts and lung washings further suggests that some of those molecules are surfactants known to be present at the air-alveolar interface (12,16).

This conclusion is supported by the further decrease in surface tension recorded for successive aliquots of back-flushings, i.e., as a higher percentage of

Table II

SURFACE TENSION MEASUREMENTS FROM PULMONARY
CAPILLARY BLOOD FOLLOWING EMBOLIZATION
(FIFTH COMPRESSION)

COMPRESSION AREA	SAMPLE NO. 1 FIFTH COMPRESSION	% CHANGE FROM CONTROL (Control vs. No. 1)	P VALUE	
100	55.83 ± 3.14	4.29	0.05	n=6
90	54.08 ± 3.22	5.82	0.025	n=6
80	52.17 ± 2.50	6.00	0.025	n=6
70	50.83 ± 2.02	6.96	0.025	n=6
60	49.25 ± 1.51	4.52	0.025	n=6
50	48.17 ± 1.03	3.49	0.025	n=6
40	46.67 ± 1.37	4.60	0.01	n=6
30	43.67 ± 2.16	6.75	0.01	n=6
20	37.75 ± 4.86	8.11	0.10	n=6
15	31.92 ± 3.92	10.51	0.10	n=6

COMPRESSION AREA	CONTROL FIFTH COMPRESSION	SAMPLE NO. 2 FIFTH COMPRESSION	% CHANGE FROM CONTROL (Control vs. No. 2)	P VALUE	
100	58.33 ± 1.21	57.42 ± 1.96	1.56	0.25	n=6
90	57.42 ± 1.43	55.67 ± 2.66	3.05	0.10	n=6
80	55.50 ± 1.67	53.17 ± 2.86	4.20	0.10	n=6
70	54.63 ± 1.86	50.25 ± 3.68	8.02	0.05	n=6
60	51.58 ± 1.43	48.83 ± 3.08	5.33	0.05	n=6
50	49.92 ± 1.59	48.58 ± 1.20	2.68	0.10	n=6
40	48.92 ± 1.43	46.92 ± 1.36	4.09	0.025	n=6
30	46.83 ± 1.69	43.50 ± 1.70	7.11	0.005	n=6
20	41.08 ± 2.89	34.42 ± 3.56	16.21	0.005	n=6
15	35.67 ± 4.63	29.25 ± 2.77	18.00	0.01	n=6

	SAMPLE NO. 3 FIFTH COMPRESSION	% CHANGE FROM CONTROL (Control vs. No. 3)	P VALUE	
100	56.67 ± 1.89	2.85	0.10	n=3
90	54.33 ± 3.06	5.38	0.05	n=3
80	51.50 ± 3.97	7.21	0.05	n=3
70	49.33 ± 4.25	9.70	0.05	n=3
60	47.67 ± 4.48	7.58	0.05	n=3
50	46.17 ± 5.39	7.51	0.10	n=3
40	44.33 ± 5.92	9.38	0.05	n=3
30	40.67 ± 6.64	13.15	0.05	n=3
20	32.83 ± 6.83	20.08	0.025	n=3
15	27.17 ± 1.89	23.83	0.025	n=3

the collected blood was derived from pulmonary capillaries as opposed to pulmonary arteries. There is little doubt that some of the blood was derived from regions adjacent to trapped bubbles because many of these were seen in the back-flushings.

The extent of recruitment of surfactant onto the surfaces of trapped bubbles is particularly difficult to estimate because of the enormous dilution that must occur upon back-flushing. Any degradation of surfactant during the ventilation or measurement periods would have increased surface tension, so that the true extent of recruitment would tend to be underestimated by this assay. Any change in the permeability of pulmonary endothelium to surfactant is likely to be no different in this model to that found following air embolism in vivo (16). In fact, the ventilated isolated lung preparation has been used (17) as a model for studying capillary permeability changes leading to pulmonary edema. However, whatever the extent of recruitment of surfactant to the surfaces of pulmonary air emboli, this study is strongly suggestive that such transfer does occur.
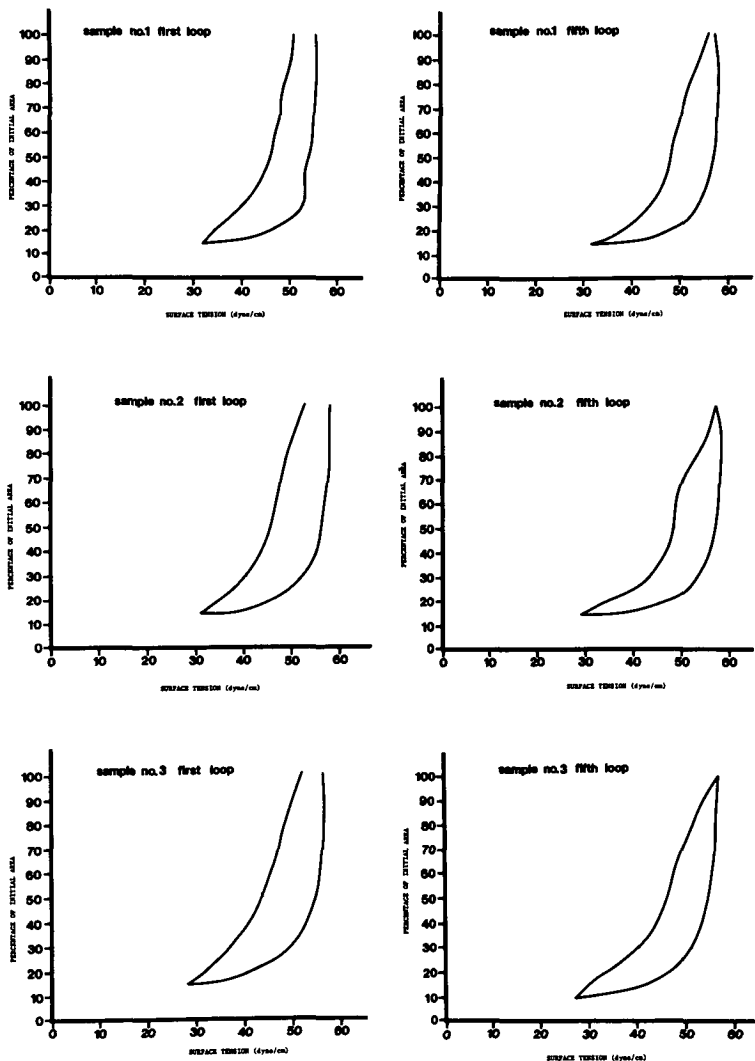
Fig. 1. Surface tension vs. surface area relationships showing the first and fifth loops for samples from all three aliquots taken when back-flushing lungs from the same dog previously embolized with 12 mL of air.

It is interesting but somewhat academic to speculate whether the surface-active substances attracted by the pulmonary air emboli were recruited from adjacent blood or from interstitium or from the alveolar surface or even direct from the granular pneumocytes (Type II cells) known to secrete surfactants on to the alveolar surface (15).

The physiological and clinical implications of the recruitment of surfactant to pulmonary air emboli are not so obvious. Even the most potent lung surfactants such as DPL applied to a plasma surface do not cause an appreciable
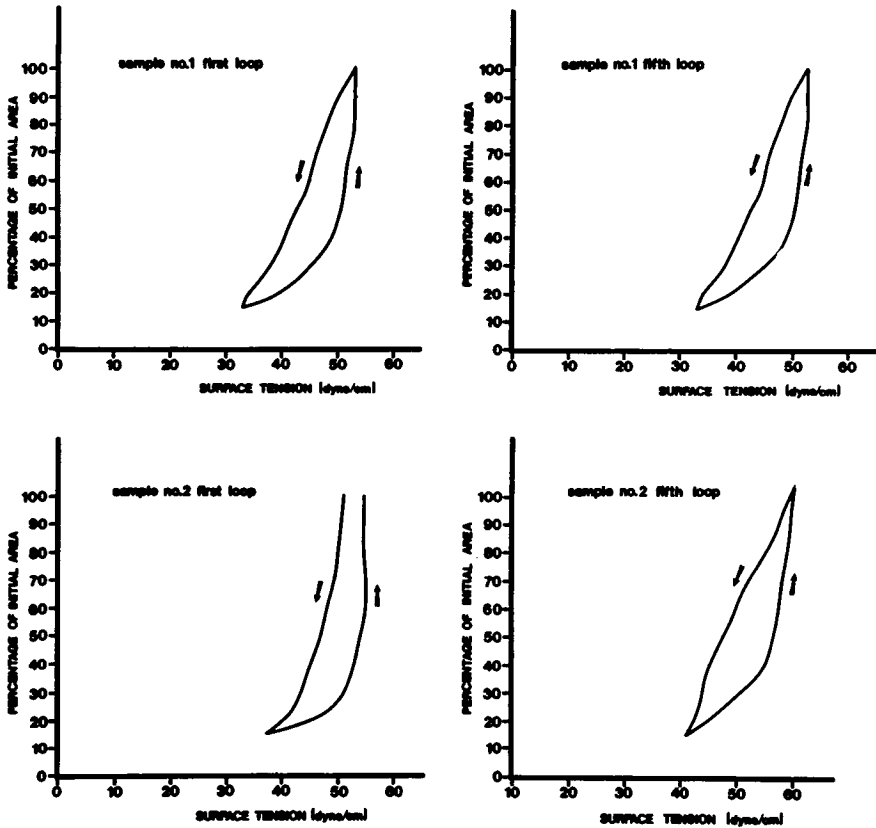
Fig. 2. Surface tension vs. surface area relationships showing the first and fifth loops for samples from two aliquots taken when back-flushing the lungs of a nonembolized "control" dog.

reduction in surface tension nor do they induce an appreciable contact angle (18) unless the surface area is reduced following its deposition. Now, any gas embolus in the lung will gradually dissolve and, in so doing, would be expected to reduce its surface area. The requirement to reduce surface area before there is any appreciable reduction in surface tension could explain the characteristic delay (6) of 10–90 min in the appearance of arterial bubbles following venous embolization in cases where the filtering capability of the lungs has been compromised by one of several known factors. On this basis, however, it could also be argued that any bubble trapped in the lung could be expected to escape into the arterial system if allowed to shrink far enough, but arterial embolism would then be expected much more often than observed clinically, unless such bubbles had become too small to produce acute symptoms.

The real question concerns whether the plateau values for surface tension reached upon film compression are low enough to reduce the capillary resistance (ΔP) to a level at which it can be exceeded by the pulmonary arteriovenous pressure difference. It is again difficult to know what values to use for γ
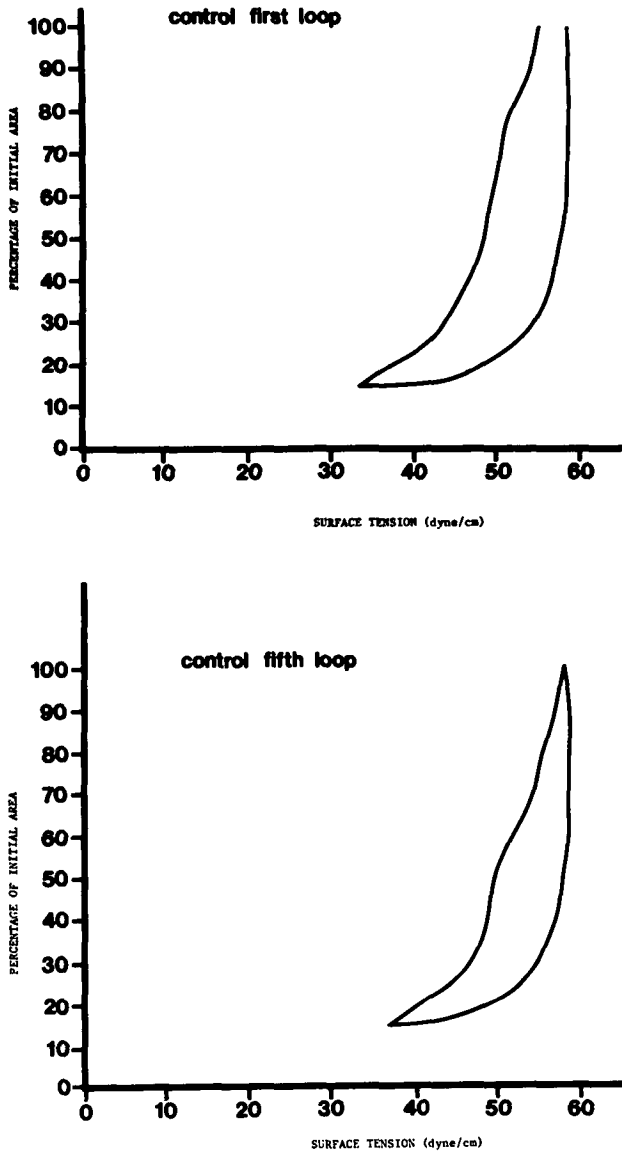
Fig. 3. Surface tension vs. area relationships for the first and fifth loops for arterial blood taken prior to embolization from the same dog as shown in Fig. 1.

in Eq. 2 since many standard studies in pulmonary mechanics quote values in the region of 2 dyne/cm (12,15) and yet a recent study (18) has indicated a value closer to 20 dyne/cm when conditions in vitro comply more closely with those in vivo, e.g., the air is humidified at body temperature, etcetera. Substitution of these values in Eq. 2 gives ΔP values ranging from 3 mmHg (for standard literature γ plus a contact angle) to 60 mmHg (for a "physiological"

γ value and no contact angle). Even a minimal contact angle of 43° reduces ΔP to 44 mmHg, a mean value to which pulmonary arterial pressure can easily be elevated following venous embolism (19). This fact indicates that the release of trapped pulmonary bubbles into the arterial system would be facilitated by surfactant and could occur in conjunction with appreciable pulmonary hypertension.

The next question concerns the degree of film compression needed to reach minimal surface tension of the trapped bubble. This is of particular interest in treating a diver with the bends by recompression, which not only reduces bubble volume but surface area also and might therefore facilitate the release of hitherto "silent" venous bubbles into the arterial system. In this situation we are now concerned with the first compression of the film—unlike normal pulmonary mechanics—where surface area reductions of only 40% for DPL films of 60% for lung washings are now needed to reach minimal γ values. These correspond to volume reductions of 54 and 75% which, on a simple Boyle's Law basis, would be attained for compressions from the surface to 39 ft and 99 ft, respectively. Since these depths are less than those recommended in certain treatment tables, e.g., 165 ft for CNS problems, this work would add support to the recommendation in the *U.S. Navy Diving Manual* (20) of not treating a limb bend by taking the diver deeper than 60 ft—as recommended in Tables 5 and 6—for fear of liberating trapped pulmonary bubbles with the risk of inducing neurologic decompression sickness. Such symptoms have been induced upon deeper compression (21). In fact, this work raises the old question of whether to take a case of limb bends just to the depth of relief, which is often less than 60 ft.

Acknowledgment

References

1. Durant TM, Long JM, Oppenheimer MJ. Pulmonary (venous) air embolism. Am Heart J 1947;33:269–281.
2. Kent EM, Blades B. Experimental observations upon certain intracranial complications of particular interest to the thoracic surgeon. J Thorac Surg 1942;11:434–445.
3. Durant TM, Oppenheimer MJ, Webster MR, Long J. Arterial air embolism. Am Heart J 1949;38:481–500.
4. Spencer MP, Oyama Y. Pulmonary capacity for dissipation of venous gas emboli. Aerosp Med 1971;42:822–827.
5. Chang KS, Yang WJ. Survey of literature related to the problems of gas embolism in the human body. J Biomech 1969;2:299–312.
6. Butler BD, Hills BA. The lung as a filter for microbubbles. J Appl Physiol 1979;47:537–543.
7. Heinemann HO, Fishman AP. Nonrespiratory functions of the mammalian lung. Physiol Rev 1969;49:1–17.
8. Boycott AE, Damant GCC, Haldane JS. Prevention of compressed air illness. J Hyg Camb 1908;8:342–443.

9. Behnke AR. Decompression sickness following exposure to high pressures. In: Fulton JF, ed. Decompression sickness. Philadelphia and London: W.B. Saunders Co, 1951:53–89.

10. Walder DN. Serum surface tension and its relation to the decompression of aviators. J Physiol 1948;107:43P.

11. Hills BA. Decompression Sickness. Vol. I: The biophysical basis of prevention and treatment. New York: John Wiley & Sons, 1977:66.

12. Radford EP. Static mechanical properties of mammalian lungs. In: Fenn WO, Rahn H, eds. Handbook of physiology, Vol. 2: Respiration. Washington DC: American Physiological Society, 1954:429–449.

13. Hills BA, Barrow RE. The contact angle induced by DPL at pulmonary epithelial surfaces. Respir Physiol 1979;38:173–183.

14. Pattle RE. Surface lining of lung alveoli. Physiol Rev 1965;45:48–79.

15. Scarpelli EM. Surfactant system of the lung. Philadelphia: Lea & Febiger, 1968.

16. Perschau RA, Munson ES, Chapin JC. Pulmonary interstitial edema after multiple venous air emboli. Anesthesiology 1976;45:364–368.

17. Staub NC. Pulmonary edema. Physiol Rev 1974;54:678–811.

18. Barrow RE, Hills BA. Surface tension induced by dipalmitoyl lecithin in vitro under physiological conditions. J Physiol 1979;297:217–227.

19. Josephson S. Pulmonary hemodynamics during experimental air embolism. Scand J Clin Lab Invest 1970;26 (Suppl):115.

20. U.S. Navy. Diving manual. NAVSHIPS 0994-001-9010. Washington DC: U.S. Government Printing Office, 1974.

21. Hallenbeck JM, Bove AA, Elliott DH. Decompression sickness studies. In: Lambertsen CJ, ed. Underwater physiology V. Proceeding of the fifth symposium on underwater physiology. Bethesda, MD: Federation of American Societies for Experimental Biology, 1976:273–286.

AMELIORATION OF DECOMPRESSION SICKNESS BY COMBINED AMPHETAMINE-CYPROHEPTADINE TREATMENT

C. Chryssanthou, L. Rodriguez, and P. Branden

Previous studies conducted in our laboratories in the last 15 years strongly suggest that smooth muscle stimulating factors are implicated in the pathogenesis of decompression sickness (DCS).

The following are some of our observations that lend support to this concept:

1) Several pathological alterations in DCS are similar to those seen in bradykinin-treated animals (1).

2) Smooth muscle stimulants, such as bradykinin and smooth muscle acting factor (SMAF), increase susceptibility of animals to DCS (1,2).

3) SMAF is released or activated in DCS (3,4).

4) Decompression or nitrogen bubbling of blood in vitro generates smooth muscle stimulating activity (4,5).

5) Smooth muscle stimulating substances could account for several clinical manifestations and pathologic alterations in DCS (6,7).

6) Compounds which combine activities against histamine, bradykinin, and 5-hydroxytryptamine prevent or at least ameliorate DCS in mice (1,7,8). The latter observation was confirmed by other investigators working with hamsters and dogs (9,10). Dimethothiazine and cyproheptadine are among the compounds which exhibit an appreciable DCS preventing effect as evidenced by a significant reduction in morbidity and mortality (7,8).

The fact that all compounds in our studies prevented DCS-produced sedation, probably because of their antihistaminic activity, raises the question of this central depressant action playing a role in the prophylactic effect of these compounds.

The present communication deals with experiments designed to determine whether drugs that ameliorate DCS retain their protective effect when their sedative action is neutralized or counteracted. Elucidation of this question is important not only from a theoretical point of view but also for practical reasons because it would not be advisable to administer to divers or compressed air workers DCS-preventing drugs that cause drowsiness.

Two series of experiments were conducted. The first series determined the minimum amount of amphetamine required to antagonize the sedative effect of dimethothiazine and cyproheptadine at doses which ameliorate DCS in mice. The second series of experiments assessed the effectiveness of optimum amphetamine-cyproheptadine combinations in the amelioration of DCS.

MATERIAL

Animals. C57BL/6J mice (Jackson Memorial Laboratories, Bar Harbor, ME), weighing 22–38 g, were used in the first experimental series and their obese littermates (C57BL/6J-ob), weighing 40–78 g, were used in the second series. The reason for using both thin and obese mice is that thin animals are better suited than obese for experiments on the effects of drugs on locomotor activity (obese are too inactive for such studies). Obese mice, on the other hand, are preferable for studies on DCS because of their greater susceptibility to the disease as compared to their thin littermates (11). Only male animals were used as subjects because their activity is not influenced by cyclic changes as in females.

Drugs. The compounds used in these investigations were: dimethothiazine (Migristene, Rhône-Poulenc-Special), cyproheptadine (Periactin, Merck Sharp & Dohme), pseudoephedrine HCL (Chromalloy Pharmaceuticals), and *dl*-amphetamine sulfate (Amend). All solutions for injection were made in sterile normal saline.

Revolving wheel cage. A revolving drum, 18 cm in diameter and 11.5 cm in width, were used. Friction was minimized by ball bearings and thus locomotion of the animals by even a fraction of an inch caused partial rotation of the drum. The revolving drum measured only lateral movement; vertical movement (standing on hind legs and jumping) or leaning and turning could not be measured. A mechanical counter connected to the revolving drum responded to every one-half rotation in either direction and counted once every two such one-half rotations.

Hyperbaric chamber. A Model 1836HP Bethlehem Corporation chamber with controlled temperature and humidity was used. The chamber was pressurized with air (dry air cyclinders, Matheson Company, Inc.).

METHODS

The animals were kept in metal cages in rooms with controlled temperature (22 ± 2°C) and relative humidity (50%) for a 2–3 week stabilization period.

They were fed Wayne Lab-Blox and water ad libitum.

The degree of sedation produced by dimethothiazine and cyproheptadine and the only antagonistic effect of pseudoephedrine and amphetamine were measured in thin mice in the first experimental series. The central depressant or stimulant effect of the drugs on the animals was expressed in terms of changes in spontaneous locomotor activity measured by the revolving wheel cage.

The effectiveness of the optimum cyproheptadine-antagonist combination in preventing DCS was tested in obese mice in the second series of experiments.

Measurement of spontaneous locomotor activity. These measurements, which were assumed to reflect drug-induced sedation or stimulation of the animals, were made in a dark quiet room so that visual and auditory stimuli were eliminated. Temperature ranged between 22° and 26°C. Variations of temperature within 5°C have a negligible effect on locomotor activity (12). The previously described revolving wheel cage was used to record locomotion. Because of minimal friction between the wheel and the horizontal axis, the animals did not use extra effort to rotate the wheel and were thus not discouraged from walking or running. No food or water was available to the animals during the recording period. They were given Lab-Blox and water ad libitum before and after testing.

Each animal served as its own control because of great variations in locomotor activity even among littermates of the same sex under the same experimental conditions (12). Activity was recorded every 15 min during a 4-h run, which was conducted once a day every other day for a total of 5 runs. The test substances were injected subcutaneously following the first 2 h of activity in the wheel cage. Normal saline was administered to all animals in the first three runs to establish base-line (control) levels of activity. The same animals received dimethothiazine (40 mg/kg) or cyproheptadine (5 mg/kg) in the 4th run. Administration of the same drugs in the same dose to the same animals was repeated in the 5th run 15 min after a subcutaneous pseudoephedrine or amphetamine (1–10 mg/kg) injection. Activity was expressed as mean rotations per hour (RPH). The results were statistically evaluated by the Student's *t*-test for paired observations.

Testing effectiveness of drug combinations on DCS. Decompression sickness was produced in obese mice by exposure to 6.12 ATA (90 psi) absolute air pressure for 6 h followed by decompression to sea level within 1 min (usually 30 s). This simulated dive profile has been previously shown to produce DCS in obese mice with approximately 60–80% mortality rate. A total of 64 mice were used in 4 experiments. The animals were divided into one control and one experimental group of corresponding weights. In each experiment eight animals from each group were placed in the chamber at the same time and subjected to the above dive profile simultaneously to ensure exposure of control and experimental animals to identical dysbaric conditions. No food or water were available to the animals during dysbaric exposure. Immediately before compression, the experimental animals received a subcutaneous injection of the optimum amphetamine-cyproheptadine combination. Normal saline was

administered to the control mice in a volume equal to that of the drug injections. The effect of amphetamine alone on DCS was tested on 16 additional animals in 2 preliminary experiments.

Following decompression, the animals were taken out of the chamber and observed for at least 60 min for clinical manifestations of DCS. Animals that succumbed were immediately autopsied and representative tissues were removed for histologic examination. Postdecompression survival times were recorded. Autopsies and histologic examinations were also performed on a few animals which were subjected to euthanasia at various intervals after decompression. These animals were not included in the mortality statistics. The results were statistically evaluated by the chi-square test with Yates correction.

RESULTS

First Experimental Series: Effect of Drugs on Spontaneous Locomotion

Both cyproheptadine and dimethothiazine caused a dramatic reduction in spontaneous locomotor activity. Within 15 min following drug administration locomotion began to decrease precipitously and 1 h after injection most animals exhibited minimal or no activity (Fig. 1). In one group of 19 animals locomotor activity of 211 RPH during the control run (following saline administration) was reduced to 47.5 RPH after an injection of 5 mg/kg cyproheptadine (Table I). Similarly, dimethothiazine administered to another group of 12 animals lowered activity from a control level of 257 RPH to only 35 RPH (Table II).
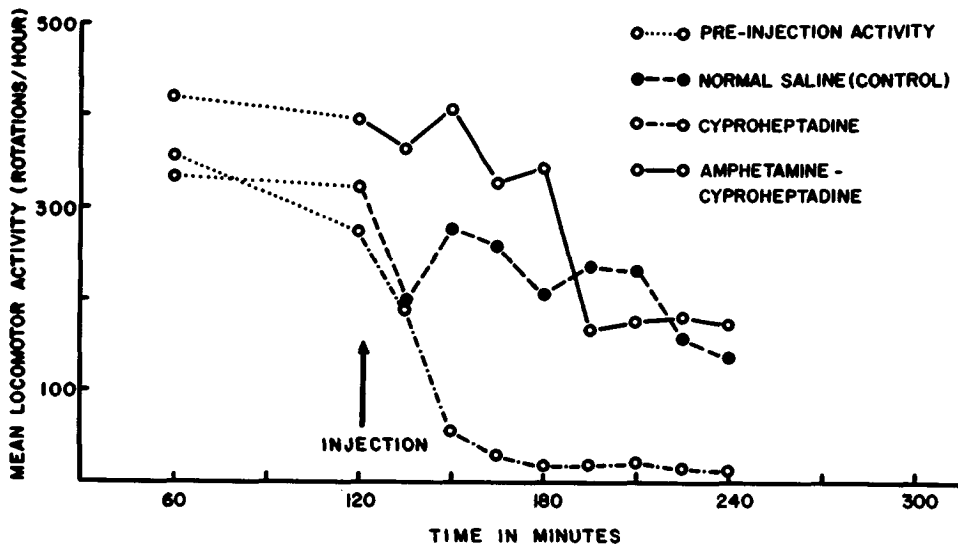
Fig. 1. Time-course of spontaneous locomotor activity of mice treated with cyproheptadine alone and in combination with amphetamine.

TABLE I

Effect of Cyproheptadine and Amphetamine-Cyproheptadine on Spontaneous Locomotor Activity of Mice

Animal No.	Rotations per hour		
	Control (Normal Saline)	Cyproheptadine (5 mg/kg)	Amphetamine (7.5 mg/kg) plus Cyproheptadine (5 mg/kg)*
1	319.5	62.0	301
2	380.5	40.5	342
3	38	14.5	20.5
4	263.5	47.5	123.5
5	155.0	56.5	400.0
6	394.0	44.0	221.5
7	105.0	92.0	408.0
8	52.5	21.5	140.0
9	2.5	5.5	232.0
10	287.5	82.5	329.5
11	112.5	56.5	226.0
12	452.0	96.5	402.5
13	31.5	26.5	175.5
14	83.5	23.5	179.0
15	502.5	72.5	330.0
16	70.5	102.0	251.0
17	408.5	35.0	424.0
18	172.5	14.5	335.5
19	185.5	9.0	219.5
Mean ± SE	211.4 ± 36	47.5 ± 7	266 ± 25

* Cyproheptadine was administered 15 min after the amphetamine injection.

TABLE II

Effect of Dimethothiazine and Amphetamine-Dimethothiazine on Spontaneous Locomotor Activity of Mice

Animal No.	Rotations per hour		
	Control (Normal Saline)	Dimethothiazine (40 mg/kg)	Amphetamine (7.5 mg/kg) plus Dimethothiazine (40 mg/kg)*
1	488.5	49.5	305.5
2	357	98	666
3	427.8	13	122
4	91.5	24.5	314
5	133.1	26.5	46.5
6	475.5	28.5	144.5
7	135.5	30	185.5
8	96.5	49	132.5
9	353.8	35.5	21.5
10	180.5	23.5	200.5
11	196	38	130.5
12	121	16.5	156
Mean ± SE	257.28 ± 41	35.07 ± 6	198.42 ± 45

*Dimethothiazine was administered 15 min after the amphetamine injection.

Pseudoephedrine (10 mg/kg) administered to 10 animals 15 min before or after a cyproheptadine (5 mg/kg) or dimethothiazine (40 mg/kg) injection did not influence the depressant effect of the latter compounds on locomotor activity.

Amphetamine, on the other hand, significantly antagonized the sedative action of both cyproheptadine and dimethothiazine (Fig. 2). The time-course of the depressant action of cyproheptadine and the antagonistic effect of amphetamine is illustrated in Fig. 1. Table I shows that 5 mg/kg cyproheptadine, when administered alone, lowered mean locomotor activity from a control level of 211 RPH to 47.5 RPH and did not depress locomotion when preceded by an injection of 7.5 mg/kg amphetamine as evidenced by a mean locomotor activity of 266 RPH. In fact, all animals exhibited a significantly greater locomotor activity when amphetamine preceded cyproheptadine administration. Likewise, Table II indicates that the sedative effect of 40 mg/kg dimethothiazine reflected in the reduction of locomotion from 257 to 35 RPH, was counteracted by 7.5 mg/kg amphetamine, which increased mean locomotor activity to 198 RPH when administered 15 min before dimethothiazine. These results are statistically significant at high levels of confidence ($P<0.001$). Lower doses of amphetamine did not sufficiently antagonize the sedative effect of cyproheptadine or dimethothiazine; higher doses produced stimulation resulting in locomotor activity much higher than base line levels.
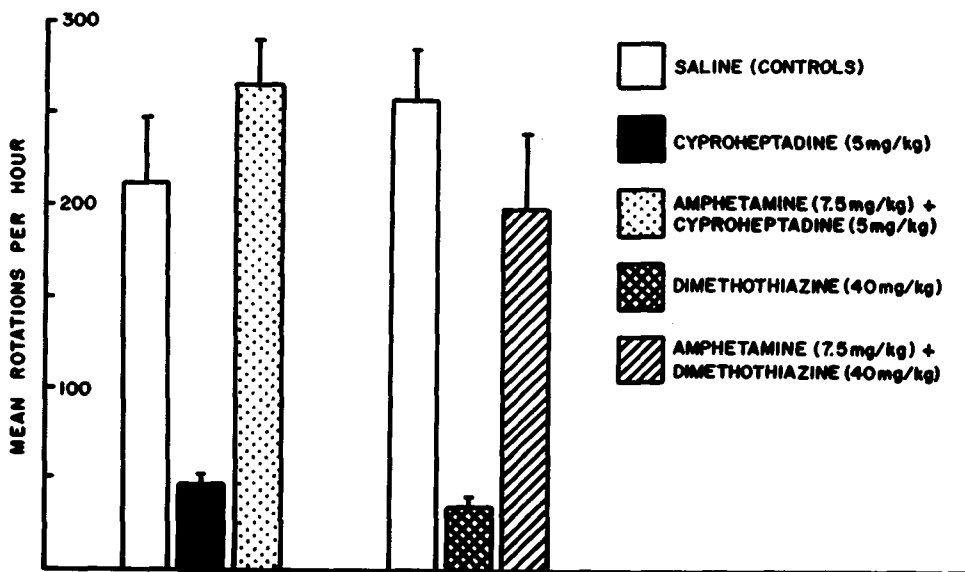
Fig. 2. Amphetamine antagonism of the inhibitory effect of cyproheptadine and dimethothiazine on spontaneous locomotor activity in mice. Height of columns represents mean revolutions per hour of all animals in the group during the entire test period. *Vertical lines* represent SEM.

Second Experimental Series: Effect of Amphetamine-Cyproheptadine on DCS

Animals that developed DCS, as a result of their exposure to the previously described dive profile, began to exhibit signs of the disease soon after decompression. Clinical manifestations of DCS included scratching (possibly because of the formation of subcutaneous gas bubbles), reduced locomotion, chokes, and convulsions. Almost all control animals exhibited these signs and the majority of them succumbed in less than 1 h following decompression; their death was preceded by twitching and severe respiratory distress with gasping and hiccough-like spells.

In the groups that received the combined amphetamine-cyproheptadine treatment before compression, a smaller number of animals manifested signs of DCS than in corresponding control groups. Table III shows that in all experiments fewer animals died in the groups treated with amphetamine-cyproheptadine than in controls. The overall mortality decreased from 83.8% to 51.7%, a reduction of 38.3%, which is statistically significant ($0.02 < P < 0.01$).

Autopsies of animals that succumbed to DCS revealed the previously described gross alterations (1,11). Most striking were the abdominal enlargement caused by gaseous distention of the gastrointestinal tract and the presence of grossly visible gas bubbles in the vena cava, the subcutaneous and intra-abdominal adipose tissue, and, in some cases, in the adrenals and spleen.

Histologic examination showed perivascular edema in the lungs, severe congestion of the bone marrow, rouleaux formation, and the presence of gas bubbles in various tissues and organs including the lung, spleen, adrenal

TABLE III

Effect of the Combined Amphetamine-Cyproheptadine
Treatment on Mortality of Obese Mice in Decompression
Sickness

Experiment No.	Mortality %	
	Controls	Amphetamine (7.5 mg/kg) plus Cyproheptadine (5 mg/kg)*
1168	87.5(7/8)†	62.5(5/8)
1171	100(8/8)	62.5(5/8)
1172	62.5(5/8)	25.0(2/8)
1177	85.7(6/7)	37.5(3/5)
Total	26/31(83.8%)	15/29(51.7%)

* Cyproheptadine was administered 15 min after the amphetamine injection.   † Number of dead animals/total number of animals in group.

(Fig. 3A), skin, bone, adipose tissue, and less frequently, liver, pancreas, and heart (Fig. 4A). It was not always easy to determine whether the gas bubbles were intravascular or in tissue spaces. Sometimes serial sections revealed that bubbles which on coarse examination appeared extravascular, were continuous with the lumen of a blood vessel. Not infrequently, widely separated nuclei of flattened endothelial cells were observed around such bubbles. Gas accumulations were particularly numerous in the spleen and adrenals giving these organs a spongy appearance (Fig. 3A).

The above histologic alterations were more frequent and more severe in control animals than in those treated with amphetamine-cyproheptadine. Surviving animals that were subjected to euthanasia at intervals after decompression revealed minimal or no changes (Fig. 3B and 4B).

Amphetamine administered alone did not reduce morbidity or mortality in DCS. In fact, in one group treated with amphetamine alone, mortality was higher than in corresponding controls. The number of animals in this group, however, was not sufficient to allow statistical evaluation of this effect.
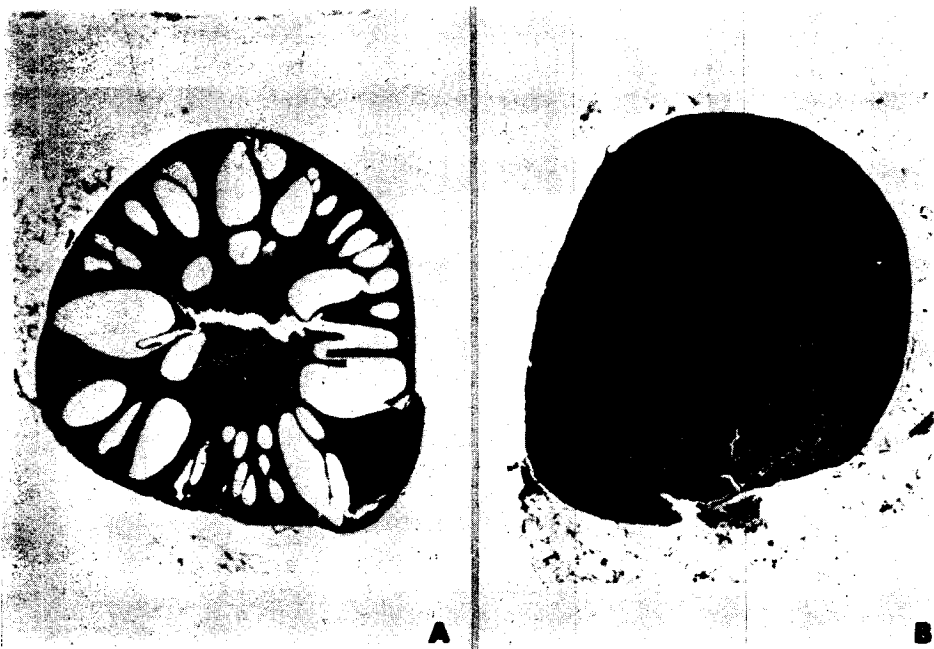
Fig. 3. A. Adrenal from control animal (subjected to compression-decompression without drug treatment), which died 40 min after decompression. The organ has a sponge-like appearance because of numerous gas bubbles of varying size located predominantly in the cortex.   B. Corresponding adrenal from animal treated with amphetamine-cyproheptadine, which was subjected to euthanasia 60 min after decompression. Both the cortex and the medulla are free of gas bubbles.   (Stained with hemotoxylin and eosin. Original magnification 7.8 X.)
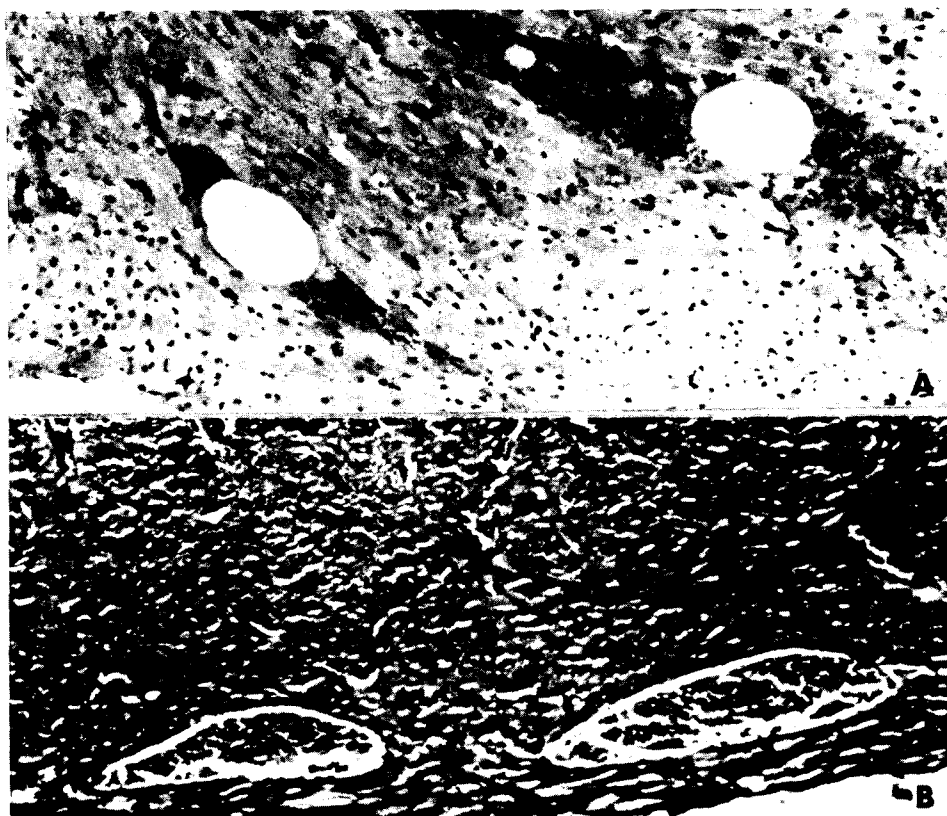
Fig. 4. *A*. Myocardium from a control animal (subjected to compression-decompression without drug treatment) showing intravascular gas bubbles. *B*. Corresponding tissue from animal that was treated with amphetamine-cyproheptadine before compression. No gas bubbles are present. (Stained with hematoxylin and eosin. Original magnification 25 X.)

DISCUSSION

The first series of experiments demonstrated a central depressant effect of cyproheptadine and dimethothiazine as well as antagonism of this effect by amphetamine. Evaluation of the depressant or stimulant action of the drugs was based on measurements of spontaneous locomotor activity, which is easily quantitated and expressible in simple units (13). This method obviously does not measure all the complex behavioral changes produced by compounds with sedative or excitatory effects. It does, however, provide a consistent measure of an important parameter of psychomotor activity, and it was therefore assumed to reflect with a reasonable degree of reliability the central depressant or stimulation action of the drugs. Measurements of locomotor activity have

already been used in many studies of behavioral changes induced by a variety of drugs (14,15).

It is evident from Figs. 1 and 2 and from Tables I and II that 7.5 mg/kg amphetamine sulfate counteracted the depressant effect of 5 mg/kg cyproheptadine and 40 mg/kg dimethothiazine. The doses of the latter drugs were those which were previously shown to ameliorate DCS (7,8). Consequently, the combination amphetamine-cyproheptadine in the above doses were used to test the effectiveness of cyproheptadine in ameliorative DCS when its sedative action is counteracted.

The results indicate that the combined amphetamine-cyproheptadine treatment decreased the incidence and severity of clinical manifestation and histologic alterations and reduced mortality by 38.3%, as seen in Table III. This decrease in mortality does not significantly differ from the 44.4% reduction obtained when the same dose of cyproheptadine was administered alone in previous studies (16). Because the pharmacologic effects of dimethothiazine are similar to those of cyproheptadine, it is reasonable to expect that dimethothiazine will also retain the DCS-ameliorating effect when its sedative action is counteracted. This, however, will remain a speculative extrapolation until further experimentation explores the effect of the combined amphetamine-dimethothiazine administration on DCS.

The observations of these investigations leads to the conclusion that the DCS-ameliorating effect of cyproheptadine, and conceivably of dimethothiazine, is independent of the sedative action of the compounds. The observation that sedation is not responsible for the protection against DCS is consistent with the reported failure of hypnotics (chloralose) to prevent DCS (10).

As mentioned earlier, demonstration of the ability of cyproheptadine to decrease morbidity and mortality in DCS when its central depressant effect is counteracted is of theoretical as well as practical importance. From a theoretical point of view, the results of the present investigation suggests that the DCS-ameliorating effect of cyproheptadine is related to its activity against bradykinin, histamine, and serotonin rather than to the central depressant action of the compound. This in turn supports the previously proposed implication of smooth muscle stimulating substances in the pathogenesis of DCS (1–7). The practical aspect of the study is related to the obvious problems with the use of DCS-ameliorating drugs that produce sedation and drowsiness. Such effects could impair performance of divers and compressed air workers and, in extreme situations, jeopardize their missions and even their safety. Elimination of the undesirable sedative effect of cyproheptadine and dimethothiazine by the use of psychomotor stimulants, such as amphetamine, alleviates these difficulties and provides an attractive and promising pharmacologic approach for the amelioration of DCS in humans.

Acknowledgments

References

1. Chryssanthou C, Kalberer J, Kooperstein S, Antopol W. Studies on dysbarism II. Influence of bradykinin and "bradykinin-antagonists" on decompression sickness. Aerosp Med 1964; 35:741–746.
2. Chryssanthou C, Teichner F, Antopol W. Studies on dysbarism IV. Production and prevention of decompression sickness in "non-susceptible" animals. Aerosp Med 1971;42:864–867.
3. Chryssanthou C, Teichner F, Goldstein G, Kalberer J Jr, Antopol W. Studies on dysbarism III. A smooth muscle acting factor (SMAF) in mouse lungs and its increase in decompression sickness. Aerosp Med 1971; 41:864–867.
4. Chryssanthou C, Humoral factors in the pathogenesis of decompression sickness. In: Ackles KN, ed. Blood bubble interaction in decompression sickness. DCIEM Conference Proceedings No. 73-CP-960. Downsview, Ontario: Defense and Civil Institute of Environmental Medicine, 1974;165–170.
5. Chryssanthou C, Waksman M, Koutsoyiannis M. Generation of SMAF activity in blood by gas bubbles. Undersea Biomed Res 1974;1:49.
6. Chryssanthou C, Pathogenesis and treatment of bends. New York J State Med 1974;74:808–812.
7. Chryssanthou C, Teichner F, Koutsoyiannis M. Studies on dysbarism V. Prevention of decompression sickness in mice by dimethothiazine. Aerosp Med 1974;45:279–282.
8. Chryssanthou C, Teichner F, Graber B. Prophylaxis against decompression sickness by cyproheptadine. Undersea Biomed Res 1978;5:27.
9. Fructus X, Lemaire C, Sicardi F, Gardette B. Influence de l'exercise et effect d'un anti-histaminique sur la decompression. Étude preliminaire chez le chien. Bull MEDSUBHYP 1975;12:87–94.
10. Urlich W, Smith B, Fine R. Acoustical-optical detection of decompression sickness in hamsters. Bethesda, MD: Naval Medical Research Institute, 1972;1–20.
11. Antopol W, Kalberer J, Kooperstein S, Chryssanthou C, Studies on dysbarism. I. Development of decompression sickness in genetically obese mice. Am J Pathol 1964;45:115–127.
12. Shirley M. Studies of activity. I. Consistency of the revolving drum method of measuring the activity of the rat. J. Comp Psychol 1928;8:23–38.
13. Skinner BF. The measurement of "spontaneous activity." J Gen Psychol 1933;9:3–23.
14. Glick SD, Zimmerberg B, Greenstein S. Individual differences among mice in normal and amphetamine-enhanced locomotor activity: relationship to behavioral indices of striatal asymmetry. Brain 1976;105:362–364.
15. Irwin S. Behavioral effects of chronic iproniazid administration. Fed Proc 1959;18:406.
16. Chryssanthou C, Rubin L, Graber B. Amelioration of decompression sickness in mice by treatment with cyproheptadine. Undersea Biomed Res 1980;7:321–329.

PART VII. DISCUSSION: INERT GAS EXCHANGE AND DECOMPRESSION

K. D. Reimann, *Rapporteur*

Remarks after the review paper by Weathersby pointed out that Berghage's data would not fit these findings and questioned the use of equations for calculation of the presented models. Further comments included: changes in body fat during investigations could have influenced the findings, and the technique of "no bubble decompression from saturation" might not be the best because tissue can remain supersaturated without bubbling.

Warnings were issued by Lambertsen, Smith, and others when Edel presented his short-cut decompression schedules according to the tendency of commercial companies. Despite Edel's 7 years of experience in surface decompression, severe cases were cited and hidden dangers and permanent lesions announced. This was particularly pointed out for tables using oxygen during chamber tests, which probably could not be extrapolated to open water dives.

The presentations of Nishi and Daniels caused new controversial remarks on Doppler technique such as: symptoms produced by extravascular bubbles could not be detected, or bubbles might be formed at places of surgical intervention or by anesthesia.

The speakers thought ultrasonic methods in the present form not to be very good indicators of decompression sickness but agreed on the scientific value of ultrasound for bubble-detection and investigation of bubble size, quantity, and the like.

Discussion on the last presentation focused on mechanisms and further pharmacological effects of cyproheptadine, which Chryssanthou said were not yet investigated. He thought cyproheptadine might decrease bloodflow, so that gas uptake might be reduced. Another explanation of its mechanism might be the cutting of the bradykinin chain. Further investigation on this interesting substance is needed.

STUDY ON DEFINITION OF MAXIMUM PERMISSIBLE GAS FLOW IN LUNGS DURING DECOMPRESSION

J. Parc, M. Monti, and J. Le Chuiton

During decompression of animals after 1,000-m exposure, we observed respiratory frequency increases from 15 to 120. At this time, if decompression was not stopped, the animal died, and death was attributed to decompression sickness. But, if decompression was stopped immediately when respiratory frequency began to increase and before it reached 70 movements per minute, then frequency quickly returned to normal, after a delay of 10 to 30 min. About a 1-h stop was needed before normal decompression could be started again.

We hypothesized that during a fast decompression, gas volume coming from tissues and arriving at the lungs might be too much for the alveolae filter. The excess gas would increase the vascular pressure on the vessel walls, and hyperpnea would begin by way of a reflex from the venous walls and pulmonary vascular reflex (1). The gas flow between venous blood and alveolae might therefore be a limiting factor of decompression rate. In these conditions a decompression stop might decrease the gas volume in the lungs and decrease the stimulation of reflexes. Therefore, in this study we have tried to define the maximum permissible gas flow level for the pulmonary barrier.

METHOD

We have worked with bounce dive schedules. Our model was based on the Haldane formula with eight tissues. The ascent criterion is the supersaturation ratio; for each tissue we have:

$$\frac{da}{dt} = k \, (nH - a) \text{ and } a \leqslant ch \tag{1}$$

767

where H is hydrostatic pressure, a is inert gas tissue tension, n is inert gas percentage in mixture gas, c is tissue supersaturation ratio, k is $\dfrac{\text{Log } 2}{T}$, and T is tissue half-time.

For the bounce-dive schedule calculation, we used eight tissues that were slightly different for descent and ascent:

Tissue number	1	2	3	4	5	6	7	8
Descent half-time (min)	5	10	20	40	80	160	200	240
Ascent half-time (min)	10	20	40	80	120	160	200	240

To measure inert gas flow in lungs during decompression, we must calculate the gas quantity dissolved in each tissue.To do this, we need to know the inert gas solubility in tissues, the weight of each tissue in the organism, and the percentage of water and fat in each tissue.

In their study on inert gas solubility in pure water, David and Gelot (2) stated:

> For helium between 1 and 100 ATA, Henry's law is valid. For nitrogen and hydrogen there are some deviations which depend from the gas nature. But deviations are less than 16 percent. . . . We can liken blood to water with 8 g NaCl per kilogram of saline solution . . . and the high pressure effects, for both pure gas and mixture, are the same than those observed on gas solubility in pure water. . . . (2)

Therefore, to know the gas solubility in tissues, we can use Henry's law: "The gas quantity dissolved in a liquid is proportional to the gas partial pressure upon the liquid."

The proportionality coefficient represents a partition factor, which is defined as the inert gas quantity contained in a tissue when inert gas is breathed at a partial pressure of 1 ATA. This coefficient depends upon the nature of gas and tissue and the solubility coefficient.

To simplify, we have reduced an organism to four tissue groups (muscle, organs, fat, bones), and we have given them half-times used in diving schedule calculation.

Tissue number	1	2	3	4	5	6	7	8
Half-time (min)	10	20	40	80	120	160	200	240
Tissue group	Muscles			Organs		Fat		Bones

The gas quantity calculation has been made for a man weighing 80 kg with muscles, organs, fat, and bones, and a certain percentage of water and fat in each group (3–4).

The nitrogen solubility coefficients are S_w = 0.013 gas litre per water litre; S_f = 0.067 gas litre per fat litre.

The amount of gas, CR, contained in a tissue under 1 ATA pressure of this gas is computed by this formula:

$$CR = \alpha \cdot P \cdot S_w + 0.8 \ \beta \cdot P \cdot S_f \qquad (2)$$

in which P is tissue weight, α is tissue water percentage, β is tissue fat percentage, and 0.8 is fat density.

This amount of gas represents the partition factor of this gas in the tissue. The total nitrogen amount dissolved in a man weighing 80 kg breathing air at atmospheric pressure is about 1 L (5). The nitrogen amount corresponding to a 1-ATA nitrogen partial pressure is

$$\Sigma \ CR = \frac{1}{0.8} = 1.34 \qquad (3)$$

which is the sum of the whole partition factors. Table I shows the tissue content and partition factors in an 80-kg man.

During bounce-dive decompression, the gas flow concept is concerned with an instantaneous gas flow of one tissue and a mean gas flow during a step. Instantaneous gas flow GF_i is calculated by the product of instantaneous tension variation $\frac{da}{dt}$ and partition factor CR:

$$GF_i = \frac{da}{dt} \times CR. \qquad (4)$$

TABLE I

Tissue Content and Partition Factors in a Man Weighing 80 kg

Tissue Number	Half-Time	Water α (%)	Fat β (%)	Body Weight (%)	Tissue Weight (kg)	Partition Factor
1	10	100	0	16.66	13.32	0.173
2	20	100	0	16.66	13.32	0.173
3	40	100	0	16.66	13.32	0.173
4	80	80	20	12	9.6	0.203
5	120	80	20	12	9.6	0.203
6	160	66	33	7	5.6	0.148
7	200	66	33	7	5.6	0.148
8	240	100	0	12	9.6	0.125

Note: Tissue half-time difference between number 1 and number 8 tissues, which have the same water and fat content in the table, is due to blood perfusion difference.

Mean gas flow during a step is calculated as a) gas amounts A1 and A2 contained in tissue at the beginning and the end of step; b) the gas amount A1 − A2, which left the tissue during the time (t) of step and the mean gas flow during the step

$$GF_m = \frac{A1 - A2}{t} \tag{5}$$

RESULTS

Diving Schedules Without Bends

Results obtained with schedules that did not cause bends are shown in Fig. 1. Minimum and maximum gas flow for five dives between 110 and 150 m without bends are shown in Table II.

Minimum and maximum gas flow for five dives between 110 and 150 m without bends are shown in Table II.

Diving Schedules That Caused Bends

Results obtained with schedules that caused bends are much greater than those with schedules without bends. For example, for a 60-min dive at 110 m,
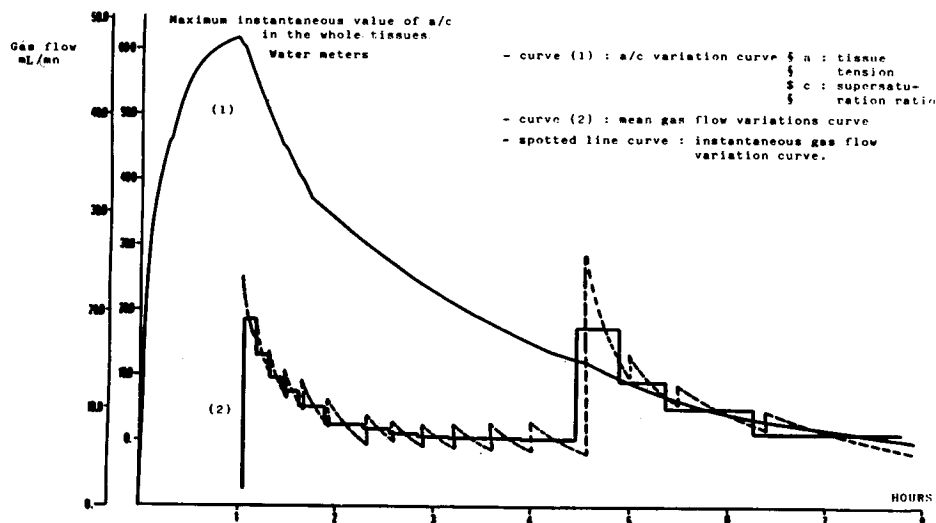
Fig. 1.   Bounce dive without bend: 60 min at 110 m with trimix (15% O_2, 40% N_2, 50% He). The increase of the two gas flow curves 4½ h after the beginning of decompression corresponds to step with superoxygenated mixture.

TABLE II

Minimum and Maximum Gas Flow for Five Dives Between 110 and 150 m Without Bends

Depth (m)	Bottom Time (min)	Mean Gas Flow		Instantaneous Gas Flow	
		Minimum	Maximum	Minimum	Maximum
110	60	3.3	18	2.7	21
120	20	5	20	3	23
120	30	5	19.5	3	21
150	20	5	19.5	3.3	21
150	30	5	17	2.7	20

Note: Maximum mean gas flow (mL/min) was 18.8 ± 1.25 SD.   Maximum instantaneous gas flow (mL/min) was 21.2 ± 1.09 SD.

which caused a bend at 23 m, we found these values (see Fig. 2): maximum mean gas flow was 22 mL/min about 1 h before bend; maximum instantaneous gas flow was 25 mL/min at the same time. The difference between these values and means of schedules without bends is greater than 3 SD.

One can see in Fig. 2 (schedule with bends) that instantaneous gas flow variations are irregular with two peaks at 25 mL/min at the beginning of the
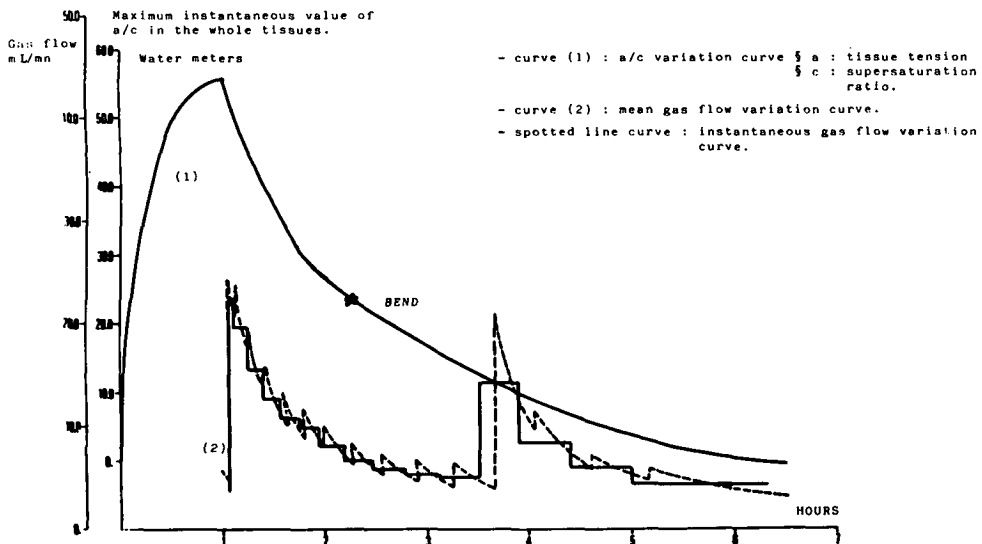
Fig. 2. Bounce dive with bends: 60 min at 110 m with trimix (15% O_2, 40% N_2, 50% He). The two gas flow curves show peaks in a short time and great values; bend occurred about 1 h later. The second increase of the gas flow curves corresponds to steps with superoxygenated mixture.

curve. Mean gas flow increased concurrently. Table III shows minimum and maximum gas flow for five dives that caused bends.

DISCUSSION

This study is based upon two hypotheses of Henry's law validity and inert gas flow relation with pressure gradient; a choice of an organism composition and an inert gas partition in different tissues; and an arbitrary definition of organism tissues and half-times used in schedule calculation.

The Validity of Henry's Law

The results of David and Gelot (2) on gas solubility in pure water have been extrapolated to organic tissues. But gas solubility might vary with salinity or with pressure. Battino and Clever (6) wrote ". . . the dissolved gas molecules transform some 'liquid' water molecules to 'icelike' molecules."

A change of water structure at high pressure surely induces physical characteristic variations in water. For example, sound speed in water increases by 1 m/s at 6.5 ATA. So, gas solubility in organic tissues is probably altered at high pressure. It would be very useful for other studies to determine such variations of gas solubility under pressure.

Pressure Gradient

When a pressure gradient is established during a bottom time at constant pressure, the work of Giry et al. (7) has shown that we observe the following

TABLE III

Minimum and Maximum Gas Flow for Five Dives That Caused Bends

		Gas Flow (mL/min)			
Depth (m)	Bottom Time (min)	Mean Gas Flow During a Step		Instantaneous Gas Flow	
		Minimum	Maximum	Minimum	Maximum
110	60	3	22	4	25
120	20	2.1	30.5	3.3	35
120	30	3.8	27.7	4.2	34
150	20	1.4	28.8	3.4	33
150	30	3.2	20.2	4	24

Note: Maximum mean gas flow (mL/min) was 24.5 ± 4.5 SD.   Maximum instantaneous gas flow (mL/min) was 28.4 ± 5.0 SD.

facts: a) after a delay of about 1 min, an inert gas flow begins between pulmonary blood and alveola, and b) this gas flow increases rapidly until it reaches a maximum value and then decreases slowly following an exponential curve. This curve follows the same variations as a pressure gradient decrease.

The instantaneous gas flow variation curves that we did for bounce dives have the same morphology. We can see on these curves a certain delay to reach maximum instantaneous gas flow after the beginning of the step. This delay corresponds to circulation time and to gas flow starting from blood. Then the curve corresponds to gas flow from tissue. At each step there is a new pressure gradient, and we have the following sequence: a) a delay to start instantaneous gas flow, b) a delay to reach maximum instantaneous gas flow, and c) an exponential curve decreasing gas flow.

Compared to Fig. 1, Fig. 2 shows at the beginning of a curve a greater number and a greater frequency of variations of instantaneous gas flow, with greater mean gas flow values. This diving profile induced a bend. Of the two criteria, instantaneous gas flow represents more accurately what happens in tissues. Then, this criteria could be a decompression-limiting factor to be held in consideration with a supersaturation coefficient for diving schedule calculation.

The tissue composition of an organism and the water and fat tissue composition were chosen from works (refs. 3 & 4) so that the sum of partition factors is equal to the total inert gas amount contained in an organism for an inert gas partial pressure of 1 ATA. To simplify calculation, we used only the nitrogen values, although the two types of dives (with and without bends) were done with trimix. This introduces an error in the absolute values calculated, but we think that comparison between the two groups of schedules remains valid.

CONCLUSION

One should not conclude with only a few cases. Nevertheless, the great differences observed between normal schedules and schedules with bends, and the presence of bends when there are large gas flow values, suggest to us that we carry on further work to develop and improve the method.

Tissue tension variations depend upon hydrostatic pressure variations. But when we change breathing gas at constant pressure, e.g., during a step while subjects are breathing a special mixture, the supersaturation coefficient is not affected, but the pressure gradient and gas flow are greatly and suddenly modified. Inert gas flow between tissues and lungs appears to be a concept that must be considered with supersaturation ratio in diving schedule calculation.

References

1. Comroe JH. Réflexes d'origine pulmonaire. In: Comroe JH, ed. Physiologie de la respiration. Paris: Masson et Cie, 1972:71–83.

2. David M, Gelot JL. Solubilité des gaz respirables à haute pression dans les liquides polaires. Rapport S.E.P.G Air liquide. 2/026 juillet 1972. Contrat DRME n 71.34.112.00.480.75.01.
3. Chevrier A. Etude de plongées profondes (1100 m) à saturation chez le mini porc. Thèse de doctorat vétérinaire. Lyon, France: Université Claude Bernard, 1975.
4. Diem K. Composition chimique du corps et de quelques organes. In: Documenta Geigy. Basle: J.R. Geigy, 1963:530.
5. Farhi LE, Rahn H. A theoretical analysis of the alveolar-arterial O_2 difference with special reference to the distribution effects. J Appl Physiol 1955;7:699–703.
6. Battino R, Clever HL. The solubility of gases in liquids. Chem Rev 1966;395–463.
7. Giry P, Servantie B, Meliet JL, Burnet H, Tournier JM, Broussolle B. Tentatives de modélisation de l'évolution des pressions partielles artérielles de gaz inerte en hyperbarie. Med Aéro Spa Med Sub Hyp 1979;18:225–229.

EVALUATION OF DECOMPRESSION TABLES BY A MODEL DESCRIBING BUBBLE DYNAMICS IN TISSUE

S. Meisel, Y. Talmon, and D. Kerem

Decompression following a hyperbaric exposure may cause formation of gas bubbles in tissue and blood. It is widely accepted that this gas phase is the cause of marginal symptoms of decompression sickness. It has been suggested that the formation of bubbles in tissue could also occur during symptomless decompression carried out by following conventional diving tables, in which case the bubbles are termed "silent."

We believe, as do others (1–3), that bubble formation in some critical tissue and its dynamics are the key to a correct rationale in computing decompression tables. To pursue this concept further, we have developed a mathematical model, briefly reviewed in this paper, which describes bubble dynamics in tissue in relation to environmental variables characteristic of a dive, such as bottom-time and depth. In addition, we demonstrate in this paper the use of this model for evaluating existing decompression profiles, and as an aid for devising innovative decompression procedures.

MODEL

We assume that a gas phase is already present in the tissue undergoing decompression, and probably exists as nucleates even under normal conditions resulting from the heterogeneous nature of the tissue (4). This gas phase is considered to be finely dispersed in the tissue as minute bubbles that grow upon decompression by physical expansion and by inward diffusion of inert gas from the surrounding supersaturated tissue. At the same time blood flowing in capillaries absorbs inert gas from the tissue. Bubble resolution will

eventually take place because of surface tension, tissue elasticity, and inherent unsaturation (5), which establish a tension gradient favoring inert gas efflux.

We surmise the bubbles to be spherical and so dispersed as to be considered situated in an infinite medium of perfused tissue. Perfusion is taken into account as a uniformly distributed mass sink. A mass balance on the bubble yields (after deleting a convective term found to be of minor significance) an expression that can be written in a dimensionless form as

$$\frac{\partial \Phi}{\partial \tau} = \frac{1}{\rho^2} \frac{\partial}{\partial \rho} \left(\rho^2 \frac{\partial \Phi}{\partial \rho} \right) - \lambda^2 \Phi \qquad (1)$$

with the following boundary conditions:

$$\Phi(\rho, 0) = 1 \qquad (2)$$

$$\Phi(\varepsilon, \tau) = \Phi_B \qquad (3)$$

$$\left. \frac{\partial \Phi}{\partial \rho} \right|_{\rho \to \infty} = 0 \qquad (4)$$

where $\Phi(\rho, \tau)$, a dimensionless pressure of inert gas in tissue, is defined as $\Phi = \dfrac{P - P_a}{P_0 - P_a}$. P denotes partial pressure of inert gas in tissue, P_0 initial arterial partial pressure, and P_a the arterial partial pressure of the inert gas after the pressure step. We define the following dimensionless variables as

a dimensionless time,

$$\tau \equiv \frac{Dt}{R_{B0}^2} \qquad (5)$$

where t is time, D is the diffusivity, and R_{B0} is the initial bubble radius,

the ratio of bubble radius to its initial value,

$$\varepsilon \equiv \frac{R_B}{R_{B0}} \qquad (6)$$

and a dimensionless radial-coordinate,

$$\rho \equiv \frac{r}{R_{B0}} \qquad (7)$$

We also define a dimensionless perfusion modulus

$$\lambda^2 \equiv \frac{R_{B0}^2 \, \alpha_b Q}{\alpha_t D} \qquad (8)$$

where α and Q are the solubility coefficient and the perfusion rate. The subscripts b and t denote blood and tissue-related parameters.

Equations 2 and 3 are equivalent to stating that the initial gas tension in the tissue is uniform and that inert gas tension at the tissue bubble interface is

equal to inert gas partial pressure in it. Equation 4 stems from the assumption that far away from the bubble, inert gas tension is determined by perfusion only.

The dimensionless pressure in the bubble is given by

$$\Phi_B = \frac{\Delta P + 4\pi K\, R_B^3/3 + 2\gamma/R_B}{P_0 - P_a} \qquad (9)$$

where the three terms in the numerator stand for the inherent unsaturation, tissue elasticity, and the surface tension. K is the elastic modulus of the tissue and γ is the surface tension.

An expression for ΔP, in case of air breathing, is obtained from Hills and LeMessurier (5):

$$\Delta P = 0.24(\pi_{amb} - 400) \qquad (10)$$

where π_{amb} denotes ambient pressure.

Equation 1 is given a Cartesian form, by applying the transformation $U = \Phi \rho e^{\lambda^2 \tau}$, and solved according to Carslaw and Jaeger (6). The solution is then substituted in a dimensionless Fick's law, and the result, an expression for bubble radius rate of change, is finally given by

$$\frac{d\varepsilon}{d\tau} = (P_0 - P_a)\frac{\alpha_t}{\varepsilon^2}\left(\frac{\pi_n}{\pi_B}\right)\left\{ e^{-\lambda^2\tau}\left(1 + \frac{\varepsilon}{\sqrt{\pi\tau}}\right) - \Phi_B\left(1 + \frac{e^{-\tau}}{\sqrt{\pi\tau}}\right)\right\}. \qquad (11)$$

π_n and π_B denote standard and internal bubble pressure.

Inert gas tension in tissue before decompression, P_{ti}, is determined by bottom time. It reaches a constant value $(P_0)_s$ only upon saturation (or more accurately, steady state). The degree of saturation, if saturation is not achieved, is characterized by

$$f_s = \frac{P_{ti} - P_a}{(P_0)_s - P_a}. \qquad (12)$$

After choosing a proper inert gas tissue-uptake function into which bottom time is substituted, P_{ti} can be calculated and serves as P_0 in Eq. 11 for situations of partially-saturated tissue. Otherwise $(P_0)_s$ is taken as P_0.

Numerical integration of Eq. 11 yields $\varepsilon(\tau)$ for a step change in alveolar inert gas partial pressure, assuming steady state values of $P_0 - P_a$.

A detailed description of the derivation of the model is given elsewhere (7).

This model can predict the behavior of a decompressed bubble for various depths and saturation fractions (f_s), and for different breathing gas mixtures.

Stage decompression is characterized by a series of consecutive pressure steps. So, a serial application of the basic model to each of these steps will yield a bubble growth pattern that follows the decompression profile. Since our basic model infers a uniform initial gas tension in tissue, steady state is assumed in the system before any further step can take place. We postulate that the tension gradient in the tissue after a pressure step can be considered uni-

form after some time has elasped, without introducing a significant error. Perfusion that determines inert gas tension in most of the tissue establishes a uniform tension profile. The nonuniform tension gradient near the bubble is due to diffusion, but because its effect is limited, the above assumption is a reasonable one. Following this rationale we have written a computer program for calculating $\varepsilon(\tau)$ for any given decompression profile. We call this model "the multistage model."

As mentioned before, we assume stable nuclei to exist in the tissue even under normal conditions. This led us to implement in the computer program a lower bound for bubble radius; whenever the calculations result in a bubble radius smaller than the initial value, the bubble is assumed to be of the initial size. The final radius obtained in the previous step is taken as the initial bubble radius for the next step, after correcting for physical expansion by Boyle's law.

We have adopted the hypothesis that marginal symptoms become overt when pressure in a semi-rigid tissue exceeds a certain critical value (3). This value pertains to a local pressure differential which can bend a nerve ending beyond its pain-provoking threshold. This assumption enabled us to base predictions of any clinical manifestation of decompression sickness on results of the physical model. If F_D is the concentration of nucleates in the tissue, and δ is the excess pressure caused by the gas phase in tissue, then we have (Nims, 2)

$$\delta = \frac{4\pi}{3} F_D K(R_{B0} \varepsilon)^3. \tag{13}$$

To facilitate the mathematical treatment, we assumed nucleates to be of uniform radius. If the critical δ for inducing symptoms is 11 mmHg (8), then ε_{cr} can be easily estimated.

Thus, bubble radius changes following a stage decompression can be calculated and symptoms can be expected when ε exceeds ε_{cr}.

RESULTS

A typical plot obtained by applying the basic model to a pressure step is shown in Fig. 1. If α_b is approximately equal to α_t (3), Q for an averagely perfused tissue is on the order of 10^{-4} mL/mL tissue·s and D is on the order of 10^{-7} cm²/s, then λ, the perfusion modulus, is about 0.02–0.04. The plot shows $\varepsilon(\tau)$ for surfacing after saturation at various depths. As the bubble approaches total resolution the process accelerates considerably. This is due to surface tension, which is inversely proportional to bubble radius, and thus increases significantly.

Figure 2 shows bubble radius changes after surfacing from a 30 m exposure for saturation fractions of 0.15 and 0.3 with $\lambda = 0.02$. The issue of a proper uptake function is avoided by simply choosing f_s values. The first stages of the decompression reveal bubble resolution because of the low degree of supersaturation, but upon further decompression bubble growth takes
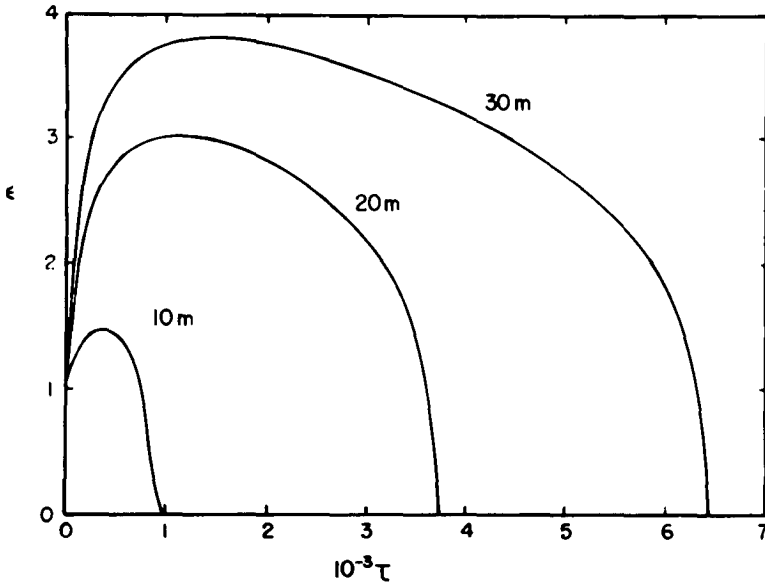
Fig. 1. $\epsilon(\tau)$ after saturation at various depths for $\lambda = 0.04$.
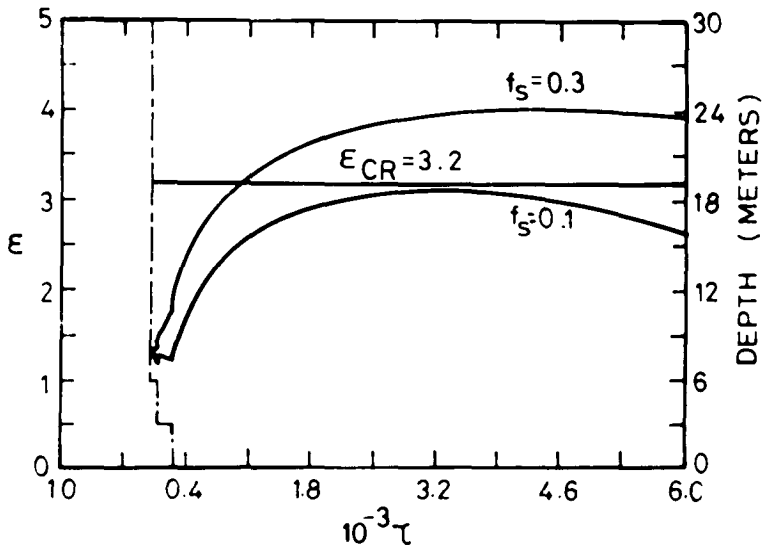
Fig. 2.   Change of bubble size (solid curves) for a given decompression profile (dotted line) for saturation fractions of 0.1 and 0.3 at 30 m.

over. This decompression profile includes stops at 7 m and 3 m with more time spent at the shallower stop. This is typical of conventional decompression tables. It must be kept in mind that the saturation fraction values relate to the first decompression stop only and require adjustment if the surface is considered as reference.

As another example, we have chosen to evaluate the decompression schedule advocated by standard U.S. Navy tables for an air exposure of 100 ft/720 min. Time was rendered dimensionless by the simple expression $\tau = t/10$ obtained by substitution of $D = 10^{-7}$ cm²/s and $R_B = 10^{-3}$ cm in Eq. 5. Substitution of 1500 mmHg·mL tissue/mL gas for K and 15625(25^3) nucleates/mL tissue for F_D in Eq. 13 give $\varepsilon_{cr} = 3.2$. Calculation with these parameters gives an initial gas phase volume in the tissue on the same order of magnitude as the results of Aggazzotti and Ligabue as cited by Albano (4). After a 720-min exposure at 30 m depth the critical tissue was considered to be "saturated," thus $f_s = 1$. Figure 3 depicts the decompression profile and the resulting bubble growth pattern. As expected, the maximal bubble radius obtained ($\varepsilon_{max} = 2.8$) is lower than the critical value.

To demonstrate an unconventional approach to decompression, we consider a "linear" profile where consecutive pressure steps follow a line of constant negative slope. Results are plotted in Fig. 4. The model predicts no bubble growth during the first stops, because physical expansion is limited, and the degree of supersaturation is not sufficient to override the effects of surface tension and perfusion. The maximal bubble radius obtained is close to the critical value, but about 20% less time was spent on total decompression than in
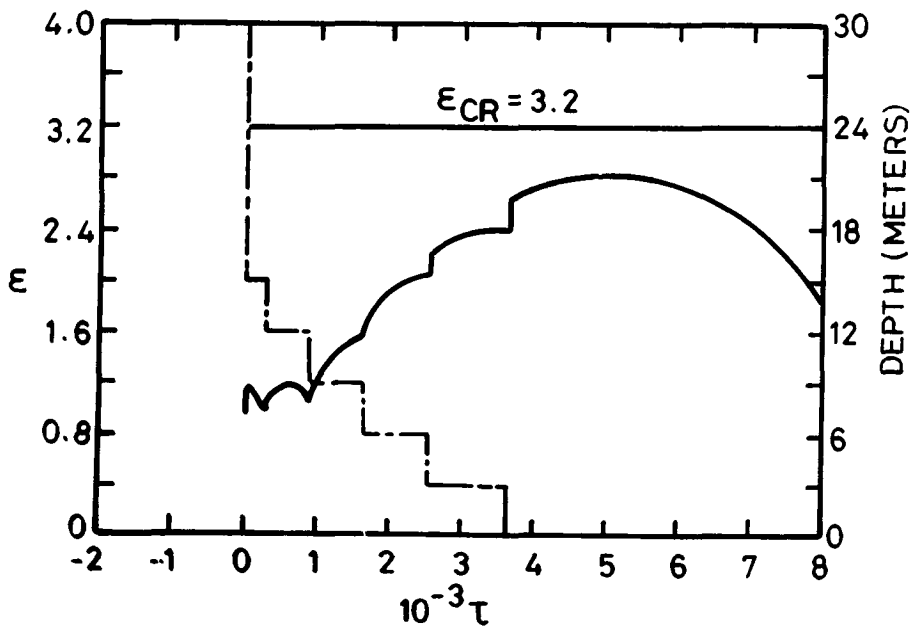
Fig. 3. Decompression profile and bubble growth pattern for U.S. Navy 100 ft/720 min schedule.
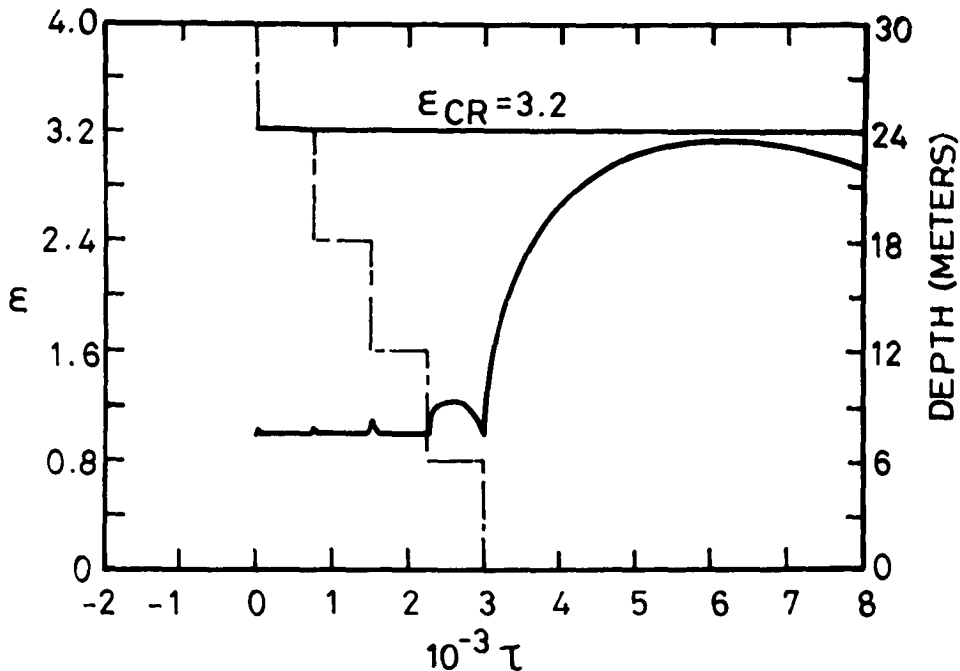
Fig. 4. A "linear" decompression profile after saturation at 100 ft.

the previous case (Fig. 3). If one defines "the most efficient profile" as the one that leads to a given maximal bubble radius in the shortest total decompression time, then our calculations indicate that a linear profile is more efficient than the conventional ones. These results support the theory of several workers (3) that a long "pull" towards the surface when a gas phase exists in tissue is a wrong policy, because not only does physical expansion occur, but the driving force for inert gas elimination is reduced.

In contrast to the previous profile where decompression was carried out by constant 5 m intervals, we have evaluated a profile where the first step is of 10 m and the following steps gradually decrease in magnitude to a final value of 1 m. Time spent at decompression stops also decreases with decreasing depth. Results are plotted in Fig. 5; a value of ε_{max} = 2.5 was obtained. Though total decompression time is equal to that in the former profile, ε_{max} obtained is significantly smaller. This agrees with an observation made by Berghage et al. (9), that the degree of decompression tolerated by the critical tissue decreases as the exposure pressure decreases.

CONCLUSIONS

In this paper we have demonstrated the use of a mathematical model, the multistage model, for the evaluation of decompression profiles and for the prediction of marginal symptoms. The multistage model is based on a model that
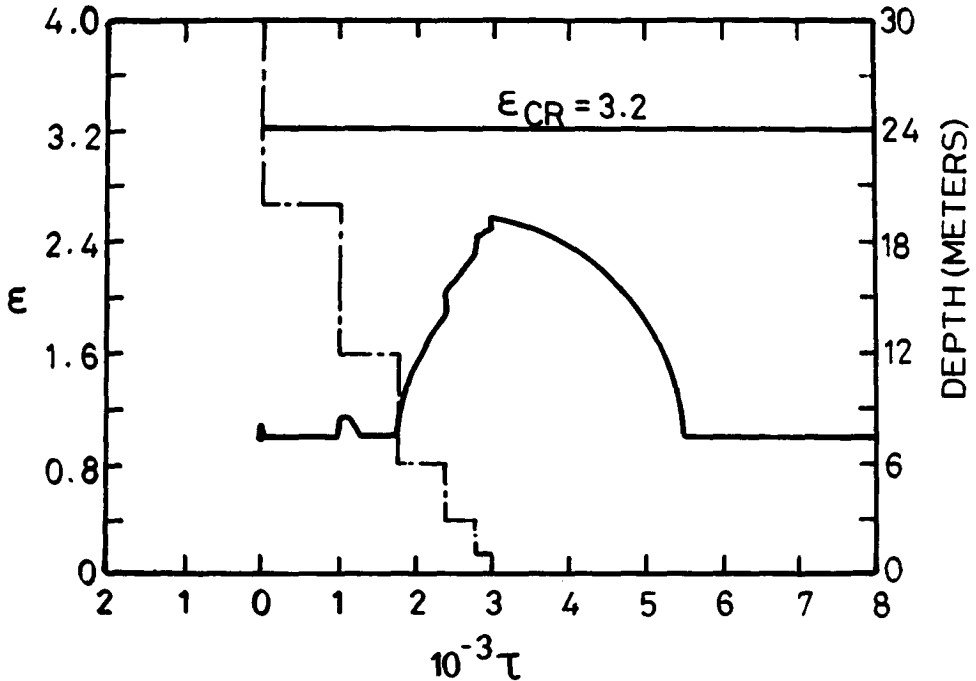
Fig. 5.   A varying step "linear" decompression profile after saturation at 100 ft (λ = 0.02 and f_s = 1).

describes the dynamics of a stationary bubble in perfused tissue that is undergoing a step pressure change.

It must be remembered that when evaluating decompression profiles with stops of short duration, the credibility of the results is affected, since the "steady state" postulate is violated to some extent. However, we strongly believe that these results enable us to compare the efficiency of decompression schedules and give a clear indication how to devise more efficient innovative decompression profiles, such as the "linear" profile of this paper.

The multistage model could be further applied to the optimization of recompression practices where it is essential to treat bubbles in the blood and tissue of a patient and yet avoid as much as possible inert gas uptake. The model in its present form can accommodate air, oxygen, or any other breathing medium. Intermittent breathing of different gas mixtures during various stages of the recompression requires model modifications.

References

1. Bateman JB. Preoxygenation and nitrogen elimination. In: Fulton JF, ed. Decompression sickness. Philadelphia: Saunders, 1951:242–277.
2. Nims LF. Environmental factors affecting decompression sickness. Part I. A physical therapy of decompression sickness. In: Fulton JF, ed. Decompression sickness. Philadelphia: Saunders, 1951:192–222.

3. Hills BA. Decompression sickness. Vol. 1. New York: John Wiley and Sons, 1977.
4. Albano G. Principles and observation on the physiology of the scuba diver. Arlington, VA: Office of Naval Research, 1970 (ONR Rep. DR-150).
5. Hills BA, LeMessurier DH. Unsaturation in living tissue relative to the pressure and composition of the inhaled gas and its significance in decompression theory. Clin Sci 1969;36:185–195.
6. Carslaw HS, Jaeger JC. Conduction of heat in solids. 2nd ed. Oxford: University Press, 1959.
7. Meisel S, Nir A, Kerem D. Bubble dynamics in perfused tissue undergoing decompression. Respir Physiol (in press).
8. Inman VT, Saunders JB. Referred pain from skeletal structures. J Nerv Ment Dis 1944;99:660–667.
9. Berghage TE, Gomez JA, Roa CE, Everson TR. Pressure-reduction limits for rats following steady state exposures between 6 and 60 ATA. Undersea Biomed Res 1976;3:261–271.

COMPUTER SIMULATION OF DIFFUSIVE GAS MIXING IN THE LUNG AT 10 ATA

H. D. Van Liew

Mixing between inspired gas and resident gas in the lungs, an essential step for exchanges of oxygen and carbon dioxide, can be expected to be poor at high pressure. Gas-phase diffusivity is inversely proportional to gas density (1); diffusive mixing should be slowed by a factor of 10 when a person breathes air at 10 ATA. Convective mixing should also suffer at high pressure whenever there are increased turbulent flow patterns. However, it is known that short exposures to 10 ATA of air do not cause severe gas exchange impairment. In experiments at 9.5 ATA (2), a heavy gas, SF_6, was clearly not as well mixed in the lung as it had been at 1 ATA, but the decrease was far less than the approximately tenfold decrease of diffusivity.

The commonplace result of observations of expired gas in normal environments is that mixing is very effective, so that for most purposes the lung can be assumed to be a single well-mixed "alveolar" compartment in series with a completely unmixed "dead" space. To study the mixing processes where and when they occur, investigators have sampled gas from within airways as deep in the lungs as sampling devices could go (3–5), and other investigators have resorted to mathematical simulations of the mixing processes.

The advent of computers made it feasible to combine rather complex considerations concerning lung anatomy (6,7) with physical laws of diffusion and of diffusion/convection interactions (8–13), with the result that mathematical simulations have shed new light on the division between dead space gas and alveolar gas at normal pressures:

1) The several most peripheral (lower) generations along any path are essentially at diffusion equilibrium with each other because the airways are so short. The lower airways and the alveoli they serve account for almost all of the lung volume.

2) At some location along the airways, there is a steep concentration gradient between the well-mixed gas in lower airways and unmixed inspired gas in upper airways.

3) During inspiratory flow, convection pushes the gradient region peripherally.

4) Whenever flow slows or stops, diffusive discharge from upper to lower airways causes the gradient region to move mouthward.

There are two aspects to the explanation of why the lung is so insensitive to the density of the environment. The first is the logical outcome of the way gas mixes in the particular geometric configuration of the lung that was briefly described above: A decrease of mixing moves the gradient region deeper into the lung (13), but the regions in which this occurs are of small volume, so a fairly large linear displacement of the gradient region makes little difference to the volume of inspired gas that becomes mixed with gas in the functional residual capacity (FRC).

The second aspect of the lung's insensitivity to environmental density is that in the lung molecular diffusivity seems to be enhanced by convective processes such as agitation by the heart (3–5,14).

To explore these matters further, I simulated diffusive mixing in the lung at 10 ATA with a computer program and compared the results with experimental results from a person breathing air at approximately 10 ATA.

METHODS

The program uses Weibel's morphometric equations "A" for a dichotomously branching airway tree (6) to generate a lung of desired size consisting of 24 compartments, 1 for the trachea and 1 each for the sum of all airways in each of 23 generations of branching.

The simulation of diffusion alone consists of allowing an indicator gas to move between the gas volumes (alveoli plus airways) of adjacent compartments. The rate of movement between a compartment and its neighbor is caused to be directly proportional to summed cross-sectional area of all airways in that generation, to gas-phase diffusivity, and to the concentration difference between the compartments; rate is inversely proportional to length of the airways in the generation. Movement occurs between each pair of compartments for a short time interval. At the end of the interval, the new concentration in each compartment is calculated and then another interval is allowed to occur.

The simulation of diffusion plus convective addition of inspired gas into the lung consists of the above process plus addition of an appropriate amount of indicator gas during each time interval. The gas is added into the particular generation in which diffusive conductance just equals the desired convective flow; in effect, all the gas that enters the appropriate compartment by convection can leave it by diffusion.

Experimental Data

Men took single breaths (inspire from FRC, expire to RV) of a mixture of indicator gases, and patterns and amounts of indicator were calculated from continuous analysis of expired gas at the mouth by mass spectrometer, as described before (2), except that addition of a bag-in-box system allowed continuous measurements of expired volume. The mixture contained low concentrations (4–6%) of He, Ne, Ar, and SF$_6$, N$_2$ that was lower than air N$_2$; and O$_2$.

RESULTS

The *upper panel* of Fig. 1 shows simulated concentration of an indicator gas that has the diffusivity of oxygen or nitrogen in air inside a lung that originally contained no indicator. The computations are for the end of 3 s of inspiration of indicator at a constant flow rate of 0.33 L/s, equivalent to the end of
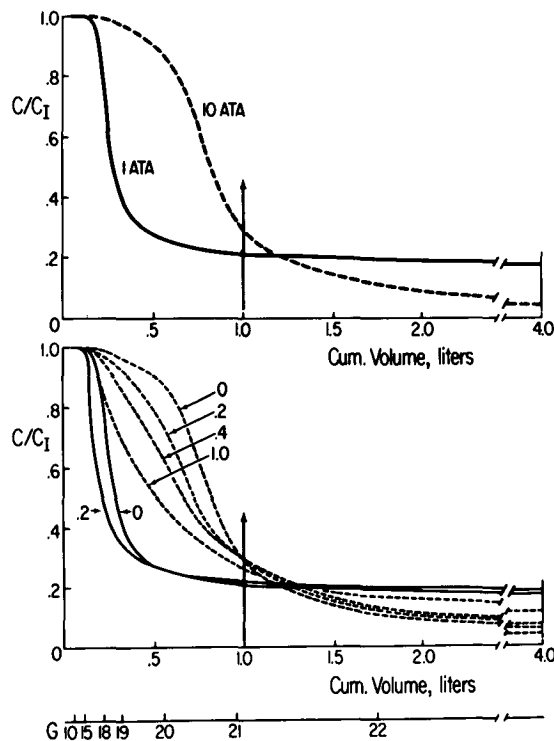
Fig. 1. *Upper panel:* Simulated profiles of indicator gas concentration (relative to inspired concentration) vs. cumulative volume inside the lung after 3 s of constant inspiratory flow. *Lower panel:* Change of profiles caused by breathholds in the inspiratory position for various time (s); profiles from *upper panel* labeled zero. *Solid curves* = 1 ATA; dashed = 10 ATA. Midpoints of the various generations of branching of the Weibel morphometric model (6) are on the lowest axis.

a 1.0 L inspiration. The concentration is displayed as a profile of C/C_I (concentration relative to inspired concentration) vs. cumulative lung volume along the airway starting at the top of the trachea. The gas to the left of the *vertical arrow* will be exhaled, and if there were no further mixing, the profile shown would be traced out in the exhaled gas; for the 1 ATA simulation (*solid*), about 200 mL of high-concentration indicator would be exhaled as the upper airway dead space followed by a sloping alveolar plateau that has C/C_I of 0.28 to 0.22. The gas in the FRC (3 L to the right of the *vertical arrow*) would not be exhaled; the FRC concentration is almost level at C/C_I of about 0.18. The 10 ATA profile (*dashed*) in Fig. 1 (*upper*) is considerably different; there is no plateau in the gas that will be expired and there is a gradient from C/C_I of 0.28 to 0.04 within the FRC. The computations showed that for the 1 ATA case of Fig. 1 (*upper*), 550 mL of indicator was in the FRC, whereas the value was only 245 mL at 10 ATA.

To simulate the additional mixing that occurs during the slowing, stopping, and reversing of flow at the end of inspiration of a real breath, I allowed diffusion to occur as it would during a breathhold. For the 1 ATA case, after only 0.2 s of this breathhold mode of diffusive mixing, the steep gradient has moved mouthward so that a Fowler dead space estimate would be about 150 mL (*lower panel,* Fig. 1). The process is much slower at 10 ATA; in 1 s the profile is still to the right of the beginning 1 ATA profile. After 1 s at 10 ATA, dead space is about 400 mL.

Figure 2 contrasts simulated profiles of the kind seen in Fig. 1 with measured results from a man's breath at 9.5 ATA. The simulations were for a lung of the same size as that of the subject. The experimental breath consisted of a phase of approximately constant inspiratory flow lasting 2 s and an inspiratory pause of 0.4 s.

Figure 3 contrasts measured amount of each of the indicators that was retained in the FRC (*points* and *solid line segments*) with amounts predicted by simulations. Because the *abscissa* is the reciprocal of the molecular diffusivity, high resistance to diffusive mixing is to the right on the graph. The additional breathhold time required to match simulation with data is not constant for different gases; whereas it took 4.0 s for SF_6 to reach the measured A_{FRC}/A_I value, the time for helium was only about 1.8 s.

DISCUSSION

The experimental breath shows much better mixing than the simulated profiles for 0.4 s of inspiratory pause, not only for the heavy gas, SF_6 (*lower panel,* Fig. 2), but also for N_2 (*upper panel,* Fig. 2). However, when the simulations were run for much longer times than were actually observed in the breath, the simulated profiles are a surprisingly good match for the measured patterns. One could obtain equally good matches by using high diffusivity instead of long time in the simulations.

Possibly the discrepancy between simulation and experiment is a consequence of the oversimplification of lung geometry embodied in the Weibel
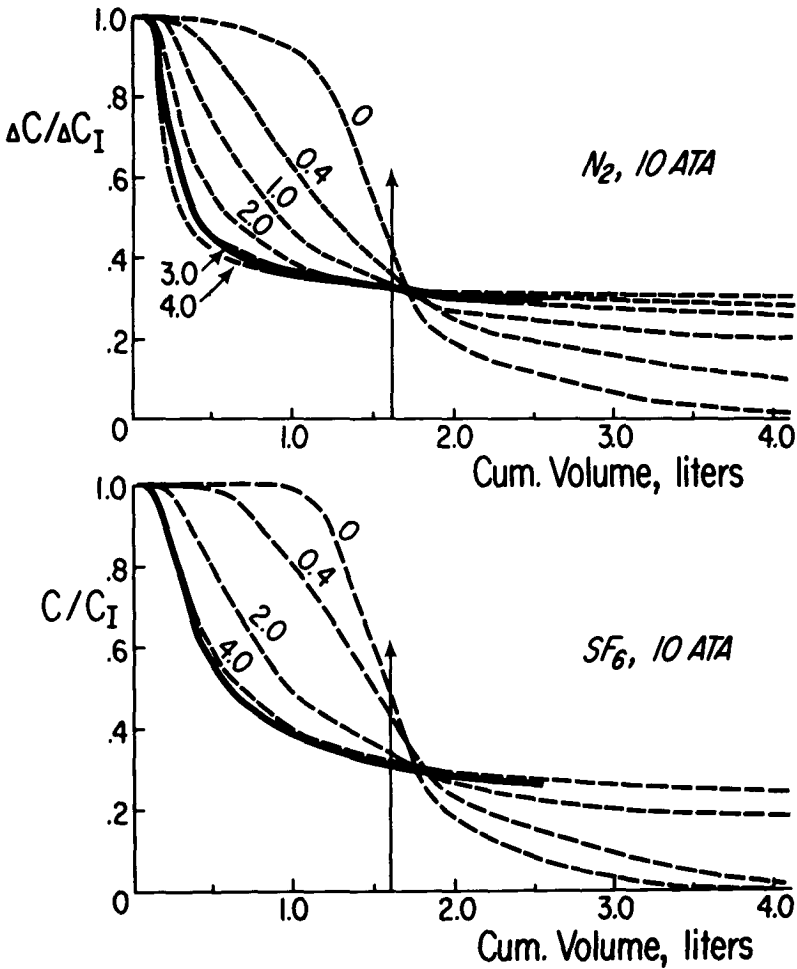
Fig. 2. Comparison of simulated results (*dashed*) with expired concentrations from a real breath at 9.5 ATA (*solid*) for N_2 (*upper*) and SF_6 (*lower*). Labels on the *dashed curves* show time in seconds allowed for an inspiratory pause (breathhold in the inspiratory position) for the simulations. Since N_2 was low in the inspirate and high in the lung gas, its measured profile was inverted. The *ordinate* value for N_2, $\Delta C/\Delta C_I$, is $(C - C_0)/(C_I - C_0)$, where concentrations are C, measured at any volume; C_0, in the lung before the breath; and C_I, inspired.

model. The Hansen et al. data (7) show a more rapid divergence of airway cross-sectional area along the bronchial tree, and work of Horsfield and Cumming (15) questions the dichotomous branching assumption. However, it seems more likely that the "effective diffusivity" is indeed several times larger than molecular diffusivity because of convective processes, as suggested by other experimental approaches (3–5, 14). If so, our findings show that the convective mixing operates in the same way as diffusive mixing, since the patterns of total mixing could be closely matched by manipulation of time or diffusivity in a model that was originally intended to account for molecular diffusion alone.
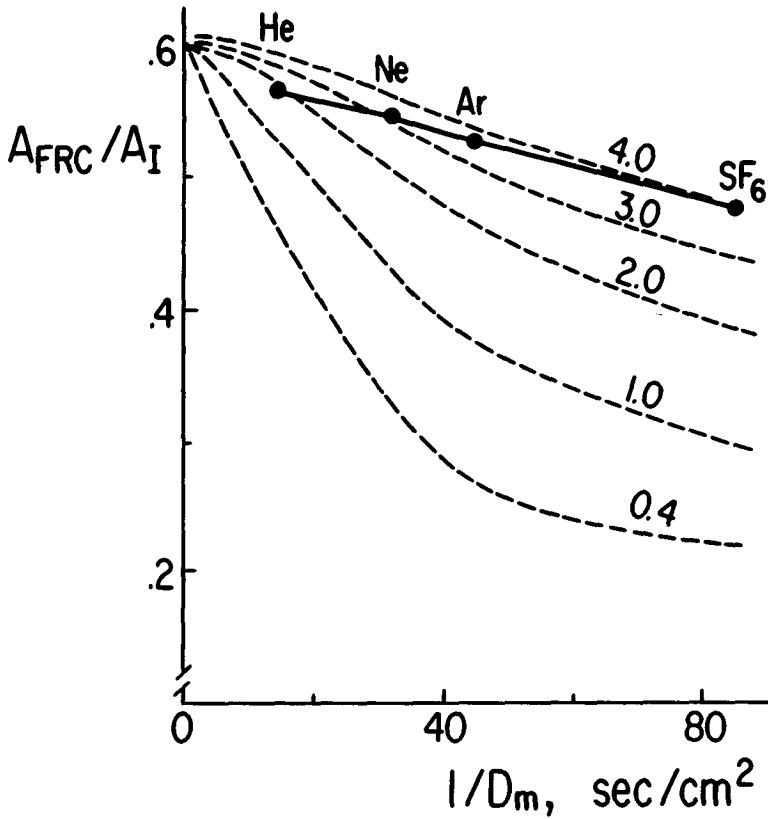
Fig. 3. *Points* are measured retention data obtained from inhalation of a mixture of indicators in one breath; *dashed curves* are from computer simulations based on the same breath size and lung volume as the measured breath. *Ordinate* is fraction of inspired amount of indicator gas that is retained in the FRC after expiration of the tidal breath. *Abscissa* is the reciprocal of molecular diffusivity. *Labels* show time in seconds allowed for diffusion in an inspiratory breathhold.

Acknowledgments

References

1. Paganelli CV, Kurata FK. Diffusion of water vapor in binary and ternary gas mixtures at increased pressures. Respir Physiol 1977;30:15–26.
2. Van Liew HD, Thalmann ED, Sponholtz DK. Diffusion dependence of pulmonary gas mixing at 5.5 and 9.5 ATA. Undersea Biomed Res 1979;6:251–258.
3. Engel LA, Menkes H. Wood LDH, Utz G. Joubert J, Macklem PT. Gas mixing during breath holding studied by intrapulmonary gas sampling. J Appl Physiol 1973;35:9–17.
4. Engel LA, Wood LDH, Utz G, Macklem PT. Gas mixing during inspiration. J Appl Physiol 1973;35:18–24.

5. Fukuchi Y, Roussos CS, Macklem PT, Engel LA. Convection, diffusion, and cardiogenic mixing of inspired gas in the lung; an experimental approach. Respir Physiol 1976;26:77–90.
6. Weibel ER. Morphometry of the human lung. New York: Academic Press, 1963.
7. Hansen JE, Ampaya EP, Bryant GH, Navin JJ. The branching pattern of airways and airspaces of a single human terminal bronchiole. J Appl Physiol 1975;38:983–989.
8. LaForce RC, Lewis BM. Diffusional transport in the human lung. J Appl Physiol 1970;28:291–298.
9. Cumming G, Horsfield K, Preston SB. Diffusion equilibrium in the lungs examined by nodal analyses. Respir Physiol 1971;12:329–345.
10. Scherer PW, Shendalman LH, Green NM. Simultaneous diffusion and convection in single breath lung washout. Bull Math Biophys 1972;34:393–412.
11. Paiva M. Gas transport in the human lung. J Appl Physiol 1973;35:401–410.
12. Baker L, Ultman JS, Rhoads RA. Simultaneous gas flow and diffusion in a symmetric airway system: a mathematical model. Respir Physiol 1974;21:119–138.
13. Nixon W, Pack A. Effect of altered gas diffusivity on alveolar gas exchange—a theoretical study. J Appl Physiol: Respir Enviror Exercise Physiol 1980;48:147–153.
14. Haselton FR, Scherer PW. Bronchial bifurcations and respiratory mass transport. Science 1980;208:69–71.
15. Horsfield K, Cumming G. Morphology of the bronchial tree in man. J Appl Physiol 1968;24:373–383.

SOME RECENT EXPERIMENTS ON BUBBLE FORMATION IN SUPERSATURATED GELATIN

D. E. Yount, C. M. Yeung, and T. D. Kunkle

Previous experiments on bubble formation in supersaturated gelatin (1–5) were carried out mainly with rectangular pressure schedules consisting of a rapid compression, equilibration of the sample at some increased pressure, and a rapid decompression. This simulates a dive profile from which pressure-reduction limits can be determined as a function of saturation pressure. For this class of schedules, the results in vitro are quite similar to those in vivo, and a mathematical model developed to describe bubble nucleation in gelatin (6,7) has been found to be in remarkably good agreement with decompression data obtained from rats and humans (8). More specifically, isopleths of constant bubble number N in gelatin are similar to those in rats (9), and they are also of the same mathematical form as the lines of constant effective dose in rats (10), and as the pressure-reduction limits in humans (10,11).

The gelatin experiments reported here extend the isopleths of constant bubble number into a new pressure region, thereby simulating conditions that would be experienced, for example, by humans exposed to high altitude or to isobaric countercurrent diffusion. The new region can also be explored by using slow compressions which permit a significant rise in the dissolved gas tension τ while the ambient pressure p_{amb} is still increasing. Thus, whereas conventional rectangular schedules satisfy the condition that the initial compression is greater than or equal to the final decompression, the reverse is true for the schedule shown in Fig. 1.

The new pressure region can be characterized mathematically by the inequality

$$p_{ss} > p_{crush},\qquad(1)$$

where

$$p_{crush} = (p_{amb} - \tau)_{max} \tag{2}$$

is the maximum overpressure or crushing pressure achieved during compression and where

$$p_{ss} = (\tau - p_{amb})_{max} \tag{3}$$

is the maximum supersaturation achieved during decompression. For the schedule shown in Fig. 1, the maximum overpressure occurs on the first step and is simply the magnitude of the initial compression, 4.1 atm. The maximum supersaturation is
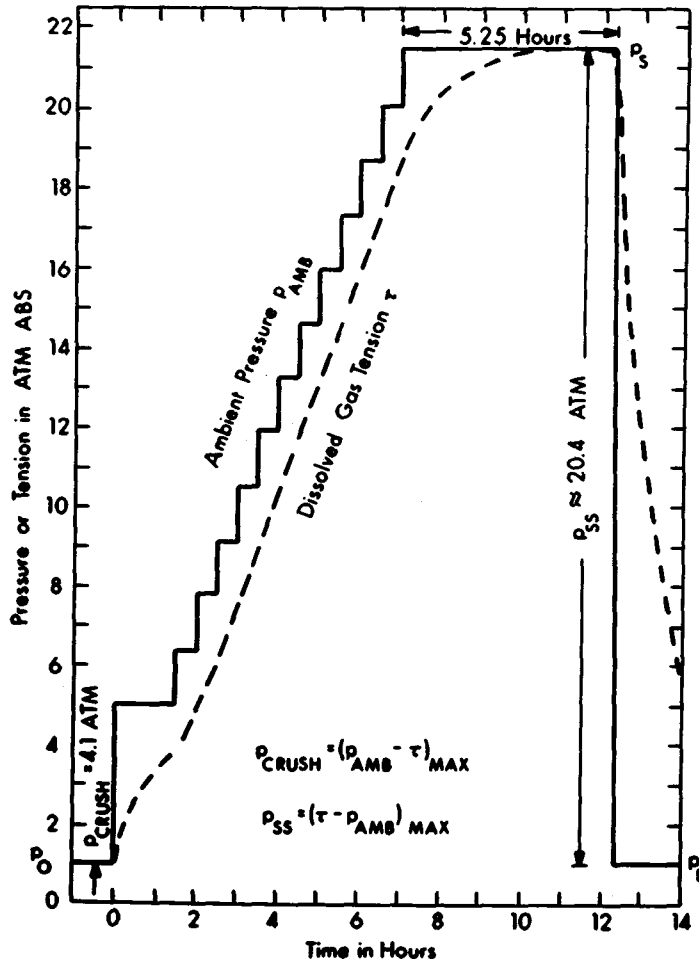
Fig.1. Stepped compression schedule used to limit the overpressure p_{crush} without affecting the supersaturation p_{ss}.

$$p_{ss} = p_s - p_f, \tag{4}$$

where p_s is the saturation or equilibration pressure and p_f is the final pressure at which the bubble counts are made. The magnitude of p_{ss} in Fig. 1 is 20.4 atm, which is much larger than $p_{crush} = 4.1$ atm.

Our interest in the variables p_{ss} and p_{crush} is due in part to the experimental observation (4) that bubble counts in gelatin subjected to a rectangular pressure schedule depend only upon these pressure differences and not upon the absolute pressure per se. Furthermore, since p_{crush} is determined in a stepped compression by that increment which has the largest overpressure, any other increments, whether they precede or follow the largest, will have no effect. These ideas are implicit in the nucleation model with which we shall be comparing our data.

THE VARYING-PERMEABILITY MODEL

According to the varying-permeability model (6,7), bubble formation in aqueous media is initiated mainly by spherical gas nuclei that are stabilized by elastic skins or membranes composed of surface-active molecules. Essentially, the model is a description of the way nuclear radii respond to changes in ambient pressure. For a given pressure schedule, one can calculate an initial minimum radius r_0^{min} above which all nuclei originally present in the sample will ultimately grow to form macroscopic bubbles. Nuclear skins are ordinarily gas-permeable and become impermeable only for values of p_{crush}, which are both large in absolute magnitude and large relative to p_{ss}—conditions which are not satisfied by any of the data points reported here. The mechanical strength of the surfactant membrane is represented by the crumbling compression γ_C, which must exceed the surface tension γ for permeable nuclei to survive. It follows in the ever-permeable region of the model that the number of bubbles N is uniquely associated with a radius r_0^{min} and crumbling compression γ_C. The isopleths of constant N are then described by (6,7)

$$p_{ss} = [2\gamma(\gamma_C - \gamma)/r_0^{min}\gamma_C] + [p_{crush}(\gamma/\gamma_C)]. \tag{5}$$

A breakdown of the varying-permeability model has already been reported (4,5,7). This breakdown is associated with small values of the minimum radius r_m^{min} at the pressure p_m defined by $p_{crush} = p_m - p_0$, and it has been suggested that it results from the fact that the finite thickness of the nuclear membrane has not been taken into account (7). To remedy this situation, we shall use the model equations for a permeable compression from p_0 to p_m (7),

$$p_{crush} = 2(\gamma_C - \gamma)[(1/r_m^{min}) - (1/r_0^{min})], \tag{6}$$

to eliminate $p_{crush} = p_m - p_0$ in Eq. 5. The result is

$$p_{ss} = (\gamma/\gamma_C)[(2\gamma_C/r_m^{min}) - (2\gamma/r_m^{min})]. \tag{7}$$

We now assume that at pressure p_m the membrane is characterized by a radius r_m^{min}, while the reservoir or surrounding liquid is characterized by a radius r_m^{min}

+ δ, where δ is the effective skin thickness. Equation 7 should then be corrected to give

$$p_{ss} = (\gamma/\gamma_C) \{(2\gamma_C/r_m^{min}) - [2\gamma/(r_m^{min} + \delta)]\}, \qquad (8)$$

where γ_C and r_0^{min} can be determined from data in the region where Eq. 5 is valid and r_m^{min} can be calculated from Eq. 6. The effective skin thickness is expected to be independent of p_{ss} and p_{crush}, and it can be evaluated by using Eq. 8 to describe the data in the region where Eqs. 5 and 7 are breaking down. Two important goals of this experiment are therefore to investigate the breakdown phenomenon in more detail and to determine the effective skin thickness δ.

METHODS, MATERIALS, AND RESULTS

The apparatus and procedures used in studying bubble formation in supersaturated gelatin are described elsewhere (4). We mention here only the salient features and those respects in which the present experiment differs from those reported previously (1–5).

For this series of runs, a new batch, gelatin batch E, was prepared and stored in individual 10-mL aliquots by freezing. Bubble counts from a given batch are ordinarily reproducible within statistical errors calculated from the square root of the number of bubbles, but significant differences have been noted between batches, even those mixed with the same stock of gelatin crystals (1,4,5). Qualitatively, batch E is similar to batch A (1–4) and to batch D (5), but there are some quantitative differences. Like batch D (5), batch E was blended from high-yield and low-yield crystals. In this case a low-yield mixture was selected because the region $p_{ss} > p_{crush}$ is associated with small initial radii, and some of the schedules of interest would otherwise produce bubbles too numerous to count.

Shortly before each run, the contents of one aliquot were thawed and pipetted into four separate glass counting chambers. The four samples, initially free of visible bubbles, were then subjected simultaneously to a particular pressure schedule causing macroscopic bubbles to form. The samples were 4 mm deep, and bubbles were counted in the lower 3 mm. This results in a fiducial volume of about 0.4 mL per sample. The raw data thus consist of the bubble counts N and their respective pressure schedules. A small correction was made for the measured differences in fiducial volume among the counting chambers (5).

The mean number of bubbles per sample is plotted in Fig. 2 for the various combinations of p_{crush} and p_{ss} as defined, respectively, by Eqs. 2 and 3. The error bars indicate standard deviations from the mean and were calculated by combining in quadrature the square roots of the bubble counts for the individual samples.
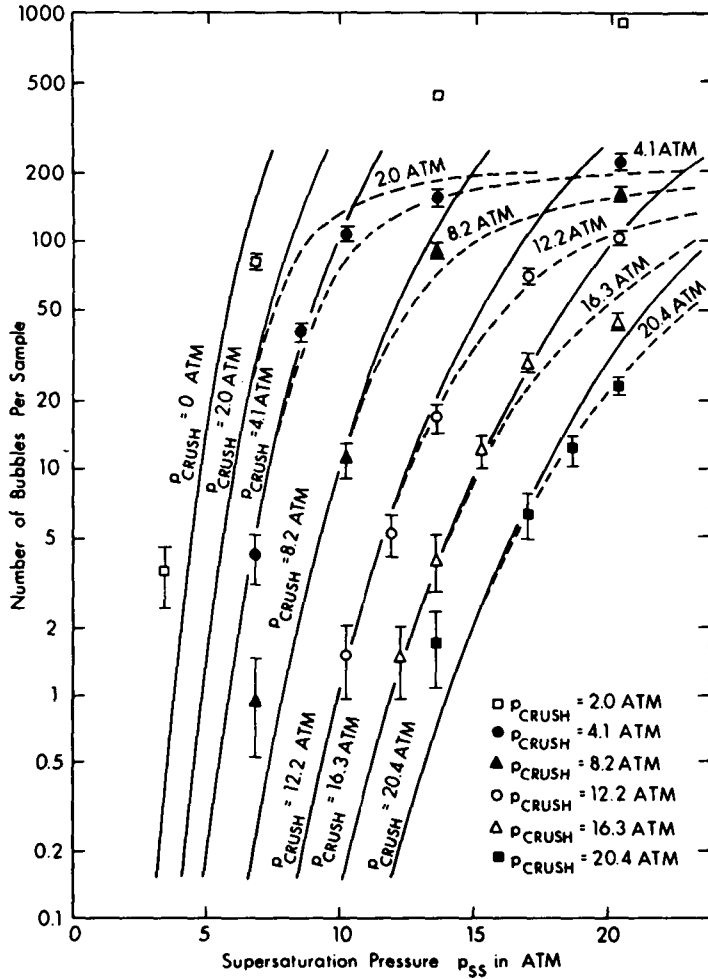
Fig. 2. Number of bubbles per 0.4-ml sample vs. supersaturation pressure p_{ss} for six values of the maximum overpressure p_{crush}. The solid curves, obtained from Eq. 5 or Eq. 7, correspond to a skin thickness of $\delta = 0$. The dashed curves, calculated from Eq. 8, correspond to a skin thickness of $\delta = 2.5$ Å. Evidently, the discrepancies which remain at $p_{crush} = 2.0$ atm are not related to the finite skin thickness.

Comparison with the Varying-Permeability Model

In this section we compare the experimental data plotted in Fig. 2 with the varying-permeability model given by Eq. 5 and extended by Eq. 8. The first step is to obtain from Fig. 2 combinations of p_{crush} and p_{ss} that give fixed bubble numbers, such as N = 1, 3, 10, 30, 50, 100, 200, and 500 (5–7). The results are replotted in Fig. 3 to yield p_{ss} vs. p_{crush} for each of the values of N selected. Evidently, most of the data points lie in the new region $p_{ss} > p_{crush}$, and the isopleths for constant N traverse the boundry $p_{ss} = p_{crush}$ without incident. The hypothesis (4) that the bubble counts N depend only upon p_{crush} and

p_{ss} seems still to be viable, and our interpretation of p_{crush} as the maximum overpressure appears also to be valid.

All of the data points in the old region of Fig. 3 and many of those in the new can be described by a family of straight lines. This is the behavior predicted by Eq. 5, and hence the next step in the analysis is to draw a set of straight lines through the suspicious points. The combinations of γ_C/γ and r_0^{min} found for each N can be summarized by another straight line,

$$\gamma_C/\gamma = 1 + (7.5 \, r_0^{min}/\mu m), \tag{9}$$

which is of the same form as that predicted from thermodynamic considerations (7). The surface tension measured in previous gelatin experiments is (4,5)
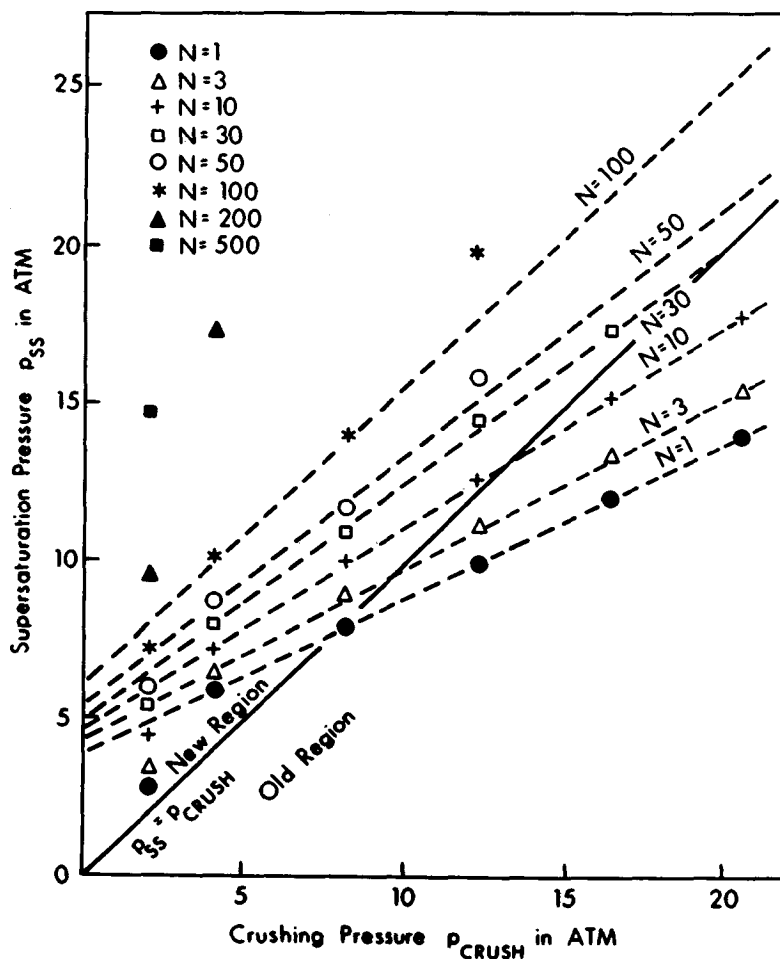
Fig. 3. Plot of p_{ss} vs. p_{crush} for various numbers of bubbles N. In and near the old region the data points for the various bubble numbers seem to trace out straight lines that extend well into the new region.

$$\gamma = (51 \pm 5) \text{ dyn/cm.} \tag{10}$$

The initial radial distribution, determined in the region where Eq. 5 is valid, is

$$N(r_0 \geq r_0^{min}) = 265 \exp(- r_0^{min}/0.0237 \ \mu m). \tag{11}$$

We apply Eq. 8 to the present data sample as follows. First, we assume that the initial radial distribution is that given by Eq. 11. Since data in the model breakdown region were not used in extracting Eq. 11, the empirical function $N(r_0 \geq r_0^{min})$ is insensitive to a finite skin thickness δ. The same argument holds for γ_C in Eq. 9. In other words, $N(r_0 \geq r_0^{min})$ in Eq. 11 and γ_C in Eq. 9 are regarded as "primordial" functions that characterize the nuclei in batch E before samples are subjected to various pressure schedules, and any discrepancies revealed later are interpreted as artifacts of our experimental and analytical techniques.

We next choose a value of N that is less than or equal to $N_0 = 265$ and calculate the corresponding values of r_0^{min} from Eq. 11 and γ_C from Eq. 9. We then select a value of p_{crush} and calculate r_m^{min} from Eq. 6. The corresponding uncorrected value of p_{ss} is obtained from Eq. 5 or Eq. 7, and the value of p_{ss} for a given skin thickness δ is found from Eq. 8. This procedure is repeated for different N and p_{crush}, and an attempt is made to describe all of the data points with the same δ. The results for $\delta = 0$ and for $\delta = 0.00025 \ \mu m = 2.5$Å are indicated by the solid and the dashed lines, respectively, in Fig. 2.

It is evident from Fig. 2 that a finite skin thickness has very little effect at modest values of p_{ss} and p_{crush}. It cannot, for example, explain the discrepancies at $p_{crush} = 2.0$ atm. In the model breakdown region, however, the difference between the *dashed* and the *solid curves* becomes quite large, approaching 10 atm in p_{ss} for $p_{crush} = 4.1$ atm. This resolves the disagreement between theory and experiment in this region, and a satisfactory description of all of the data above $p_{crush} = 2.0$ atm is now provided by Eq. 8 with $\delta = 2.5$ Å. It is, in fact, quite remarkable that so much has been gained by the introduction of a single parameter and parameter value. Furthermore, the manner in which δ has been introduced is both plausible and elementary in the context of the varying-permeability model.

DISCUSSION

The distinctive feature of this experiment is the use of slow or stepped compressions which limit the maximum overpressure p_{crush} without affecting the maximum supersaturation p_{ss}. Pressure schedules of this type are of particular interest in cavitation theory because they can be used to investigate gas nuclei of unusually small size. This has permitted a systematic study of a breakdown of the varying-permeability model, including a demonstration that the model works well, even in the breakdown region, when the effective skin thickness δ is taken into account. In other words, "breakdown" nuclei are also surfactant nuclei, and an elementary extension of the varying permeability model suffices to describe them.

We have referred to δ as the "effective" skin thickness since its experimental value of about 2.5 Å seems too small to be the length of an aligned surfactant molecule in situ. On the other hand, 2.5 Å could plausibly represent the half-width of a spherical-shell potential-well whose minimum defines the effective nuclear radius. An outward displacement of 2.5 Å might then suffice to liberate a bound surfactant molecule by dislodging its polar head from the potential-well. Similarly, since the polar heads would be pointing outward, it is plausible that the external surface pressure $2\gamma/r$ is transmitted through the reservoir or liquid phase to within 2.5 Å of the effective radius, while the aligned carbon tails, pointing inward, passively convey the internal gas pressure to the same region.

Whereas the model breakdown in previous experiments (4,5,7) appears to have been resolved by our data and by the introduction of the effective skin thickness δ, an entirely different aberration has been revealed at $p_{crush} = 2.0$ atm. The salient features are as follows. First, the bubble counts are all much higher than the model extrapolations derived from the rest of the data points. Second, the bubble counts at $p_{ss} = 13.6$ atm and at $p_{ss} = 20.4$ atm (430 and about 900, respectively) are much higher even than $N_0 = 265$ bubbles or nuclei per 0.4-mL sample. Third, if we subtract from the observed bubble counts at $p_{crush} = 2.0$ atm the number expected from our analysis, we obtain a "radial distribution" for the "surplus" nuclei that is not of an exponential form analogous to Eq. 11. Fourth, the data points at $p_{crush} = 2.0$ atm are well inside the new region $p_{ss} > p_{crush}$, and hence they would not have been observed in previous gelatin experiments. These observations suggest that we may be dealing with a different type of nucleus to which the usual model equations do not apply. The "surplus" nuclei are easily crushed and must therefore be gas-filled and rather fragile. One class of objects that might fit this description is gas-filled crevices in suspended dust particles. Other types of surfactant nuclei could also be involved.

A comparison of the varying-permeability model with data on decompression sickness in rats and humans has already been reported (8). We shall end this section by mentioning several other in vivo applications. The first concerns dive profiles in which, for some reason, a slow or stepped compression has been used. In the *Hana Kai II* dive (12), for example, compression was halted at 5.5 atm abs for 90 min, at 12.3 atm abs for 30 min, and at 14.4 atm abs for 30 min to permit measurements of thoracic impedance. Full compression to 18.6 atm abs required 14 h and 9 min, which is slow. After 16 days, 9 h, and 51 min at 18.6 atm abs, decompression was initiated according to a standard U.S. Navy schedule. This schedule was subsequently modified to treat decompression sickness which occurred at 6.5, 5.6, 1.8, and 1.5 atm abs, respectively, in four of the five subjects. Our interpretation of these results is that the supersaturation which subjects could tolerate during decompression was much less than expected because the maximum overpressure p_{crush} was of order $(12.3-5.5) = 6.8$ atm or less, rather than $(18.6-1.0) = 17.6$ atm, as tacitly assumed.

In the experiment of Cowley et al. (13), the ears of New Zealand White rabbits were subjected to isobaric counterdiffusion at 1 atm abs. The rabbits breathed a mixture of 80% N_2O and 20% O_2 while their ears alone were surrounded by helium. Bubble formation was detected by monitoring the pressure changes in a subcutaneous fluid-filled needle inserted into the external ear and attached to a transducer-recorder system. Whereas the maximum supersaturation was only 0.3–0.4 atm, bubbles formed readily because p_{crush} was equal to zero.

In the experiment reported by Lambertsen and Idicula (14), compression stops lasting from 2 to 5 days were made at 13.1, 22.2, and 28.3 atm abs on route to a maximum depth of 37.4 atm abs. The purpose of these stops was to permit an investigation of the effects of various respired gas mixtures as a function of depth. It follows that the value of p_{crush} for this profile was only about 12.1 atm, rather than 36.4 atm, and hence the allowed supersaturation was much less than it would have been for a continuous rapid compression to 37.4 atm abs. A second observation is that the skin and certain other tissues were exposed to the ambient atmosphere during compression, implying that their dissolved gas tensions τ were at all times near ambient and that the maximum overpressure p_{crush} was small. During the gas switching experiments, three of the four subjects developed visible skin lesions. At 37.4 atm abs, three of the four subjects had vestibular dysfunction, and two experienced severe nausea, vomiting, and incapacitating vertigo while breathing nitrogen-oxygen or neon-oxygen in the helium-oxygen environment. The prediction that the supersaturation tolerance of a subject should depend strongly upon compression rate as well as compression magnitude follows directly from nucleation theory and cannot be derived from conventional analyses of inert-gas exchange.

Acknowledgments

References

1. Strauss RH. Bubble formation in gelatin: implications for prevention of decompression sickness. Undersea Biomed Res 1974;1:169–174.
2. Strauss RH, Kunkle TD. Isobaric bubble growth: a consequence of altering atmospheric gas. Science 1974;186:443–444.
3. Kunkle TD, Yount DE. Gas nucleation in gelatin. In: Shilling CW, Beckett MW, eds. Underwater physiology VI. Proceedings of the sixth symposium on underwater physiology. Bethesda, Md. Federation of American Societies for Experimental Biology, 1978:459–467.

4. Yount DE, Strauss RH. Bubble formation in gelatin: a model for decompression sickness. J Appl Physiol 1976;47:5081–5089.

5. Yount DE, Yeung CM, Ingle FW. Determination of the radii of gas cavitation nuclei by filtering gelatin. J Acoust Soc Am 1979;65:1440–1450.

6. Yount DE, Kunkle TD, D'Arrigo JS, Ingle FW, Yeung CM, Beckman EL. Stabilization of gas cavitation nuclei by surface-active compounds. Aviat Space Environ Med 1977;48:185–191.

7. Yount DE. Skins of varying permeability: a stabilization mechanism for gas cavitation nuclei. J Acoust Soc Am 1979;65:1429–1439.

8. Yount DE. Application of a bubble formation model to decompression sickness in rats and humans. Aviat Space Environ Med 1979;50:44–50.

9. Watt DG, Lin YC. Doppler detection of thresholds for decompression-induced venous gas emboli in the awake rat. Aviat Space Environ Med 1979;50:571–574.

10. Berghage TE, Gomez JA, Roa CE, Everson TR. Pressure reduction limits for rats following steady-state exposures between 6 and 60 ATA. Undersea Biomed Res 1976;3:261–272.

11. Hennessy TR, Hempleman HV. An examination of the critical released gas volume concept in decompression sickness. Proc R Soc Lond 1977;B197:299–313.

12. Hong SK, Smith RM, Webb P, Matsuda M: *Hana Kai II*: a 17-day dry saturation dive at 18.6 ATA. I. Objectives, design, and scope. Undersea Biomed Res 1977;4:211–220.

13. Cowley JRM, Allegra C, Lambertsen CJ. Measurement of subcutaneous tissue pressure during superficial isobaric gas counterdiffusion. J Appl Physiol: Respir Environ Exercise Physiol 1979;47:224–227.

14. Lambertsen CJ, Idicula J. A new gas lesion syndrome in man, induced by "isobaric gas counterdiffusion." J Appl Physiol 1975;39:434–443.

Part VIII

HEALTH HAZARDS

The first eight papers and the discussion thereof were presented at the
European Undersea Biomedical Society Meetings in Conjunction with the
Seventh Symposium on Underwater Physiology

INNER EAR INJURIES IN DIVING—DIFFERENTIAL DIAGNOSIS OF INNER EAR DECOMPRESSION SICKNESS AND INNER EAR BAROTRAUMA

J. C. Farmer, Jr.

Previous literature concerning otologic problems in diving has emphasized middle ear barotrauma. With recent increases in commercial, military, and sport diving to deeper depths, inner ear injuries have been noted more frequently and have been reviewed in previous publications (1,2). Studies of these injuries indicate that the causes and treatment of these problems differ depending upon the phase and type of diving. Thus, inner ear injuries in diving have been classified as follows:

1) Inner ear barotrauma and labyrinthine window rupture.
2) Inner ear injuries occurring at stable deep depths.
3) Inner ear decompression sickness.
4) Sensorineural deafness to high background noise during diving conditions.

Inner ear injuries occurring at stable deep depths have been documented on one occasion and occurred shortly after the onset of breathing a different inert gas by mask while the chamber remained at a stable pressure with the original helium-oxygen atmosphere (3). Injuries related to high background noise have been suggested (4). The exact frequency of these injuries is not known.

Most divers who suffer inner ear injuries related to diving have inner ear barotrauma with probable labyrinthine window rupture or inner ear decompression sickness with bubble formation and hemmorhage in the labyrinthine fluid spaces or vasculature, or both. In some instances the differential diagnosis of inner ear barotrauma and inner ear decompression sickness is difficult. Some of the related dives are air exposures close to the no-decompression limits. Divers occasionally do not know when during the dive the symptoms began. Also, signs of middle ear barotrauma suggesting the possibility of inner ear

barotrauma or other systemic signs suggesting decompression sickness may not be present. Indeed, recent work (2) has indicated that inner ear injuries can be the only manifestation of decompression sickness.

An accurate, prompt diagnosis is important, for the likely mechanism of such injuries strongly indicate that recompression would be an inappropriate treatment for inner ear barotrauma and labyrinthine window rupture. Conversely, bed rest and possible middle ear surgery and/or unnecessary delay in recompression therapy for those cases of inner ear decompression sickness can increase the likelihood of permanent deficits (2). Therefore, the following review of the differential diagnosis of these two types of inner ear injuries in diving is presented.

INNER EAR BAROTRAUMA

Inner ear injuries occurring after relatively shallow diving or with symptom onset during the compression phase in deeper diving have been termed *inner ear barotrauma*. Such injuries were first documented and named by Freeman and Edmonds in 1972 (5) and have been related to labyrinthine window ruptures (6). Implosive and explosive mechanisms for such ruptures have been postulated by Goodhill et al. (7). The explosive mechanism suggests that with inadequate middle clearing during descent, intracochlear pressure as well as ambient pressure increases relative to middle ear pressure. With straining or a Valsalva maneuver, a further increase in this pressure differential occurs with rupture of the round window or oval window membrane into the middle ear and a subsequent perilymph fistula. The implosive mechanisms suggest that with a sudden Valsalva maneuver that does result in middle ear ventilation, the rapid increase in middle ear pressure results in rupture of the round window or oval window into the intracochlear space. Another suggested implosive-like mechanism involves the inward displacement of the ear drum, ossicular chain, and stapes footplate with subsequent subluxation of the footplate into the vestibule resulting from a large pressure differential between the ear drum and middle ear caused by continued descent with no middle ear pressure equilibration. Simmons (8) has suggested that the pressure changes encountered with inadequate middle ear pressure equilibration during the descent phase of diving may result in membrane breaks within the inner ear without specific labyrinthine window rupture. Which of these mechanisms is more often the cause of middle ear injuries during the compression phase of diving as well as the overall frequency of such injuries during diving has not yet been established. Most of the described cases of labyrinthine window rupture in association with diving have involved round window ruptures. A few cases have been noted to have oval window ruptures (9).

Treatment principles for inner ear barotrauma include the following:

1) The best treatment is prevention. Descent or compression should be avoided when middle ear pressure equilibration problems exist. Ascent until adequate middle ear clearing occurs, even if the dive must be terminated,

should be practiced. Forceful Valsalva maneuvers in an attempt to clear ears at depth should be avoided.

2) Recompression therapy should be avoided for cases of inner ear barotrauma since such therapy exposes the divers to conditions similar to those which resulted in the injury.

3) A complete otologic evaluation by a knowledgeable physician should be accomplished as soon as possible.

4) Until such an evaluation can be obtained and appropriate treatment measures initiated, maneuvers which may result in an increase in cerebrospinal fluid or perilymphatic pressure should be avoided; this includes the avoidance of coughing, straining, or exertion. Bed rest with head elevation is indicated.

5) Drugs which supposedly increase inner ear blood flow are generally not effective and may indeed result in a decrease of intracranial and inner ear perfusion from shunting of the axial circulation to other body regions. Also, anticoagulants should be avoided because of possible hemorrhage from traumatized tissues. Indeed, the pathophysiological mechanisms responsible for this type of inner ear injury in diving strongly indicate that inadequate blood flow to or intravascular clotting in the inner ear are not major problems.

6) The need for immediate exploratory tympanotomy is controversial. Some authors have advocated immediate exploratory surgery in all suspected cases (10). Others have suggested reserving surgery for those who do not improve after 48–72 h of bed rest with head elevation. Singleton et al. (11), in a review of 34 cases of labyrinthine window fistulas, many of which were not associated with diving, noted better recovery after 5 days of conservative therapy than with surgical intervention. Caruso et al. (9) state that although the majority of otologic membrane ruptures may heal spontaneously with conservative treatment, such treatment may be associated with progressive hearing loss. They suggest that when the diagnosis is fairly certain, surgery be performed without delay to prevent further hearing deterioration which may be permanent. We advise treating these cases conservatively and reserving exploratory surgery for those who demonstrate no improvement after 4 to 5 days or worsening hearing after 48 h of conservative treatment, or both.

INNER EAR DECOMPRESSION SICKNESS

During the past decade, isolated symptoms of inner ear dysfunction occurring during or shortly after decompression from dives in which decompression sickness is possible have been associated with inner ear decompression sickness (2). Animal studies have demonstrated bubble formation or hemorrhage into inner ear fluid spaces, or both (12), and human investigations have shown a significant correlation between prompt recompression treatment and recovery (2). This entity appears to be more common with decompression from deep helium-oxygen exposures, particulary those involving changes to air during the latter stages of decompression. Cases have also been noted to occur during or shortly after air dives requiring staged decompression. The following

principles of management of inner ear decompression sickness were proposed in 1976 (2) and, thus far, appear to be effective:

1) Vertigo, nausea, vomiting, tinnitus, and/or hearing loss beginning during or shortly after the decompression phase of dives in which decompression sickness is possible should be considered forms of decompression sickness and recompressed promptly. Divers who experience such symptoms during or shortly after a switch to an air environment during decompression from a deep helium-oxygen exposure should be switched back to the presymptom helium-oxygen atmosphere and recompressed promptly.

2) The optimum treatment depth or depth of recompression still has not been established. Theoretically, the optimum recompression depth is the lesser of the depth of relief or the bottom depth. However, labyrinthine trauma resulting from inner ear bubble formation may result in hemorrhage or structural deformities, and prompt relief will not be seen even though an adequate depth of recompression to drive the bubbles back into solution is achieved. Also, returning to the bottom depth in some situations may be hazardous or impractical. Therefore, we arbitrarily suggest that the optimum treatment depth in these situations should be at least 3 atm deeper than the depth of symptom onset. Whether or not a lesser treatment depth will suffice has not been established.

3) Drugs which supposedly increase intracranial and inner ear blood flow are generally not effective and may result in shunting of blood to the periphery. Also, if labyrinthine hemorrhage has occurred as indicated by animal studies, anticoagulants may result in additional intracochlear bleeding. Thus, these agents are considered potentially harmful and not recommended. Diazepam, 5–15 mg given intramuscularly, has been noted to result in significant relief of vertigo, nausea and vomiting during otologic decompression sickness. This drug can suppress the nystagmus accompanying such injuries and thus mask a sign of optimum treatment. However, in many cases the symptoms are so severe that relief is desired. Fluid replacement and other measures, such as administration of oxygen-enriched breathing gases advocated in the treatment of general decompression sickness, are indicated.

DIFFERENTIAL DIAGNOSIS OF INNER EAR BAROTRAUMA AND INNER EAR DECOMPRESSION SICKNESS

The most important factors in accurate differentiation of inner ear barotrauma and inner ear decompression sickness include a) the knowledge that such injuries can occur in diving, b) familiarity with the likely pathophysiological mechanisms, and c) the obtaining of an accurate history and physical examination. Other factors to be considered in this differential diagnosis include the following:

1) The time of symptom onset is important. Divers who indicate that their symptoms started during compression are likely to be suffering from inner ear barotrauma whereas divers whose symptoms start during or shortly

after decompression are likely to be suffering from inner ear decompression sickness.

2) Knowledge of the dive profile is important. Symptoms of inner ear dysfunction associated with shallow dives which do not approach the no-decompression limits and in which decompression sickness is unlikely should not be suspected of resulting from decompression sickness. Inner ear barotrauma is certainly more likely in these instances. Also, dives associated with rapid descents are more likely to result in inadequate middle ear pressure equilibration during compression, especially with inexperienced divers, and subsequent inner ear barotrauma.

3) The presence or absence of associated symptoms should be noted. Divers experiencing ear pain or blockage or fullness during compression are more likely to develop inner ear barotrauma. Freeman (13) notes that the common factor in his series of labyrinthine window ruptures in divers is difficulty in clearing the ears when descending. However, divers who note symptoms suggestive of decompression sickness involving other organs or tissues certainly should be suspected of having their inner ear symptoms secondary to bubble formation of the inner ear structures or vasculature, or both.

4) The presence or absence of associated physical findings is important. Divers who exhibit physical findings compatible with middle ear barotrauma, such as a retracted, hemorrhagic, or ruptured ear drum, should certainly be suspected of having a possible labyrinthine window rupture as an explanation of their inner ear symptoms. Divers who exhibit other signs of decompression sickness, such as neurological deficits, should be suspected of having their inner ear symptoms on the basis of inner ear decompression sickness.

An accurate differential diagnosis can be difficult in those cases in which inner ear symptoms are first noted after no-decompression dives close to the no-decompression limits or deeper dives in which apparently adequate decompression schedules were followed and in which the divers can not recall the time of symptom onset. In these instances, other factors such as associated signs and symptoms should be considered. Divers who have associated symptoms or signs of middle ear barotrauma, or both, should be suspected of having inner ear barotrauma and possible labyrinthine window ruptures. For divers without these signs or symptoms, additional factors to be considered would be the presence or absence of other signs or symptoms suggestive of decompression sickness or air emboli. If these are absent, and if none of the above factors are helpful in arriving at a diagnosis, the overall type of diving should be considered. Such cases associated with air diving in which proper decompression procedures were followed are more likely to represent inner ear barotrauma since isolated inner ear decompression sickness seems to be more common with deeper helium-oxygen exposures. Fortunately, in most cases, an adequate determination of the time of symptom onset, dive profile, and the presence or absence of other signs and symptoms is possible and an accurate diagnosis can be made.

All cases of inner ear injury during diving should have a complete, follow-up otoneurological evaluation after treatment. This should be done even

though symptom relief has occurred. Individuals who exhibit permanent inner ear deficits should not be returned to diving because future injury, especially to the uninvolved inner ear, is likely to result in significant permanent disability.

In summary, an accurate diagnosis is essential for the proper management of individuals suffering inner ear symptoms related to diving. Usually, it is not difficult to differentiate a) inner ear barotrauma and possible labyrinthine window ruptures related to middle ear pressure equilibration problems during compression, b) inner ear symptoms associated with inert gas exchanges at stable deep depths, c) inner ear decompression sickness, and d) inner ear injuries resulting from excessive noise exposure during diving. However, confusion as to the differentiation of inner ear barotrauma from inner ear decompression sickness has occasionally occurred. In these cases, major consideration should be given to the depth of dive, rate of descent, the breathing mixture used, the time of symptom onset, and the presence or absence of other associated signs or symptoms.

References

1. Farmer JC. Diving injuries to the inner ear. Ann Otol Rhinol Laryngol 1977;86(Suppl36):1–20.
2. Farmer JC, Thomas WG, Youngblood DG, Bennett PB. Inner ear decompression sickness. Laryngoscope 1976; 86:1315–1327.
3. Lambertsen CJ. Collaborative investigation of limits of human tolerance to pressurization with helium, neon, and nitrogen. Simulation of density equivalent of helium-oxygen respiration at depths of 2000. 3000, 4000 and 5000 feet of sea water. In: Lambertsen CJ, ed. Underwater physiology V. Proceedings of the fifth symposium on underwater physiology. Bethesda, MD: Federation of American Societies for Experimental Biology, 1976:35–48.
4. Summit J, Reimers J. Noise: a hazard to divers and hyperbaric chamber personnel. Aerosp Med 1971;42:1173–1177.
5. Freeman P, Edmonds C. Inner ear barotrauma. Arch Otolaryngol 1972;95:556–563.
6. Edmonds C, Freeman P, Tonkin F. Fistula of the round window in diving. Trans Am Acad Ophthalmol Otolaryngol 1974;78:444–447.
7. Goodhill V, Harris I, Brockman S. Sudden deafness and labyrinthine window ruptures. Ann Otol Rhinol Laryngol 1973;82:2–12.
8. Simmons FB. Fluid dynamics in sudden sensorineural hearing loss. Otolaryngol Clin North Am 1978;11:55–61.
9. Caruso BG, Winkelmann PE, Correia MJ, Miltenberger GE, Love JT. Otologic and otoneurologic injuries in divers: clinical studies on nine commercial and two sport divers. Laryngoscope 1977;87:508–521.
10. Pullen FW, Rosenberg GJ, Cabeza CH. Sudden hearing loss in divers and fliers. Laryngoscope 1979;89:1373–1377.
11. Singleton GT, Karlan MC, Post KN, Bock DG. Perilymph fistulas. Diagnostic criteria and therapy. Ann Otol Rhinol Laryngol 1978;87:797–803.
12. McCormick JG. Sudden hearing loss due to diving and its prevention with heparin. Otolaryngol Clin North Am 1975;8:417–430.
13. Freeman P. Rupture of the round window membrane. Otolaryngol Clin North Am 1978;11:81–93.

MECHANISMS OF AURAL BAROTRAUMA

J. M. Miller, A. Axelsson, D. McPherson, and W. Potter

Middle ear (ME) changes with barotrauma include development of effusions, vascular hemorrhage, tympanic membrane perforations, and disarticulation of the ossicles (1–6). Suggested inner ear changes have included membraneous labyrinth distortion and rupture, round window perforation, and hemorrhage (7–10). The majority of these suggested and observed changes derive from observations in man. On the basis of animal studies, some of them, including inner ear changes, have been confirmed (12,13). For the most part, these animal investigations have been performed under conditions of whole-body hyperbarotrauma or local static ME pressure changes. We have initiated studies to evaluate the effects of various ME pressure changes, among them phasic pressure changes. This aspect of our program is aimed at evaluating the structural and physiological mechanism underlying phasic barotrauma. This report will describe the chronic effects on middle and inner ear structures of phasic pressure change. We will also describe acute changes in middle and inner ear structures and associated changes in ME transmission and inner ear electrophysiological response immediately following phasic ME pressure change.

METHODS

A total of 94 guinea pigs were used in this investigation. In each animal one ear was randomly designated "control" the other "experimental." Following the exposure of the bulla of both ears, sealing of a Teflon cannula through the bulla, the experimental ear was exposed to a positive or negative phasic pressure change with rapid rise/fall times, 1–2 s in duration, ranging in magnitude from 1000 to 6000 mm H_2O. Details of the exposure are described elsewhere (14,15). Following pressure exposure in 20 animals, the incisions

were closed and the subjects treated with antibiotics. These animals were subjected to euthanasia following three-week survival for anatomical study. Seventy-four animals were used in acute studies of immediate structural ($n = 56$) and physiological ($n = 18$) changes.

Histological study included evaluation of drum and ME structures with the aid of the operating microscope, followed by light and phase-contrast microscopic study of inner ear sensory neuroepithelium and vasculature. Histological preparation of inner ear structures was based upon soft surface preparation procedures (16,17) in 52 animals and serial paramodiolar sectioning of cellodin embedded material in 22 animals. Surface prepared tissue was stained with osmic acid. Serially sectioned material was stained with Hematoxyline and Eosia. Physiological study included evaluation of phasic ME pressure-induced changes in absolute and relative ME input impedance and a measure of cochlear impedance derived from cochlear microphonic activity, after Møller (18) for frequencies from 200 to 20,000 Hz (19).

RESULTS

Anatomical Observations

Primary ME structural changes in both acute and chronic animals included distortion and perforation of the tympanic membrane (TM) and vessel distention and hemorrhage. Figure 1 shows the percent occurrence of these pathologies. Tympanic membrane and vessel pathology were similar in both acute and chronic animals. Thus, the data of Fig. 1 are based upon all experimental ears studied anatomically. The changes observed were correlated with direction and magnitude of applied pressure. Tympanic membrane perforations were most frequently observed with negative pressures of high value. Vessel pathology was most common with high positive pressure.

The presence of serosanguineous effusion was equally common in ears exposed to positive and negative pressure. Thus, while its occurrence was related to magnitude of applied pressure, it was not dependent upon direction of pressure change. The frequency with which serosanguineous effusions were observed varied significantly between acute and chronic animals. In acutely exposed and studied ears, it was observed in 19% of the material. In chronically studied ears, it was observed with a frequency of 56%. In these chronic ears, the frequency of this pathology was related to the presence of infection.

The presence of serous fluid was similar to that seen with serosanguineous effusions in acutely studied material. In chronically studied experimental ears with no infection, serous fluid was not observed in ears exposed to positive pressure and was observed with a frequency of 83% in ears exposed to negative pressure.
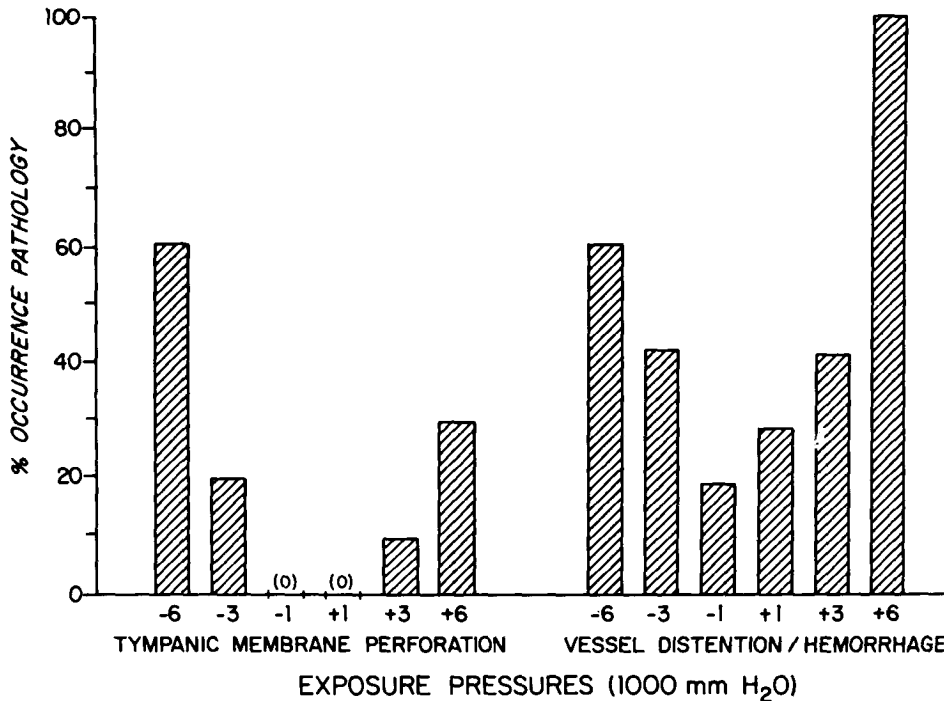
Fig. 1. Percent occurrence of tympanic membrane perforations and vessel distention and hemorrhage in acutely and chronically studied experimental ears. Tympanic membrane perforations were primarily related to high-negative pressures. Vessel distention and hemorrhage was primarily related to high-positive pressures.

No round window perforations were observed in acutely studied ears. In the chronic study, 6 of 19[1] exposed ears demonstrated round window perforations. Of those exposed to the higher pressure (± 6000 mm H_2O) the frequency was 56%. Each of these ears exhibited a ME infection demonstrated by the presence of perulant material. Round window perforations were not observed in control infected ears of chronic animals.

Physiological Observations

Phasic pressure change exhibited relatively consistent acute effects on input impedance to the ME and a derived value of equivalent cochlear impedance.[2] Figure 2 shows the change in these two impedance values immediately following exposure to a phasic pressure of ± 4000 mm H_2O. Input impedance changes to the ME were observed at low frequencies, below approximately 600 Hz. The decrease in impedance observed was less than 10 dB. On the

[1]One subject did not survive the 3-week recovery period.

[2]This equivalent cochlear impedance was derived from a measure of 1 divided by transmission; transmission was based upon cochlear microphonic recorded activity (18).
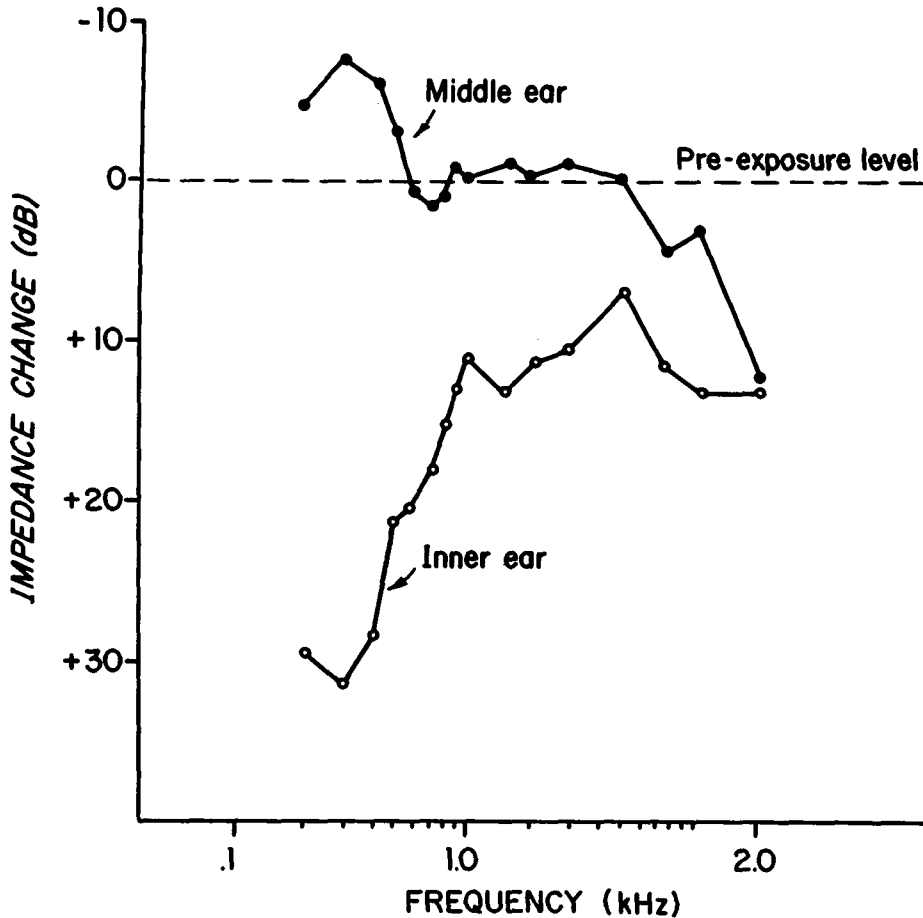
Fig. 2. Change in input impedance to the middle ear and equivalent cochlear impedance following exposure to a phasic pressure change of ±4000 mm H₂0. Middle ear impedance decreased for low-frequency signals and increased for high-frequency signals (see discussion in text). Cochlear impedance showed an increase for all frequencies tested. The dominant affect was for low-frequency signals.

basis of cochlear recorded activity, inner ear changes were far greater. They were most significant at low frequencies (below 1 kHz), demonstrating an increase in equivalent cochlear impedance as high as 30 dB. However, the effect extended to over 5 kHz. Through this frequency range for the inner ear, positive pressure demonstrated a somewhat greater effect than negative pressure. Also, second-order distortion was produced in the inner ear response in a manner following the change in cochlear impedance. For both ME and inner ear measures, an increase in impedance was observed for frequency values greater than 5 kHz.

DISCUSSION

Observations in both acute and chronic guinea pigs of phasic ME pressure change are consistent with observations in man. Acutely, we may expect TM distention and rupture and effusions (serous, serosanguineous, and hemorrhagic) to be associated with barotrauma. While TM perforations and serous fluid (in the absence of infection) are primarily dependent upon negative pressure changes, vessel hemorrhage and distention is primarily dependent upon positive pressures. A rebound effect of the pressure change on the membranes of the vessel walls may underlie this sensitivity to high positive pressures. This potential pathophysiological mechanism has been discussed further elsewhere (14,15).

Inner ear changes consist primarily of hemorrhage. In our animal model, significant round window perforations were not observed acutely. Our observations do not, however, rule out the presence of acute microscopic perforations. Chronically, round window perforations were clear, but only in association with ME infections. Our findings indicate that even in the absence of obvious round window perforations, the barotrauma may interact with infection to influence the integrity of this membrane. In the absence of infection, all pathologies were significantly reduced in the chronic series as compared to the acute series. In our experimental models, pathologies resulting from infection showed no relationship to magnitude or direction of pressure change and were observed in control material. Without this observation in chronic material, it would not be possible to evaluate infection-dependent effects from barotrauma effects. (As emphasized in our previous work (14), the value and need for control observations in investigations such as this cannot be overemphasized.)

Physiological changes observed are consistent with the varied ME and inner ear pathology found. They indicate that ossicular changes are produced by the phasic pressure change. The low-frequency decrease in input impedance to the ME is consistent with a partial disarticulation of the ossicular chain, resulting in an apparent unloading of the system. Our anatomical methods in the ME were not sensitive to small changes in the ossicles and their articulations, which could be of functional significance. The increased cochlear impedance at low frequency probably reflects in part the change in ME impedance. However, at frequencies above approximately 600 Hz, this change in cochlear function must reflect other mechanical and, perhaps, transduction changes probably caused by fluid changes (hemorrhage) or membrane changes not observable with our anatomical techniques. The further increase in inner ear impedance at values over 5 kHz appears to reflect quite closely a ME impedance change; however, both may reflect a difficulty in performing these measures and calibration of our measuring equipment at higher frequencies.

Acknowledgment

References

1. Fields JA. Skin diving, the physiological and otolaryngological aspects. Arch Otolaryngol 1958;68:531–541.
2. Goodhill V. Sudden deafness and round window rupture. Laryngoscope 1971;81:1462–1474.
3. Edmonds C, Thomas RL. Medical aspects of diving, Part 3. Med J Aust 1972;2:1300–1304.
4. Goodhill V, Brockman SJ, Harris I, Hantz O. Sudden deafness and labyrinthine window ruptures. Ann Otol Rhinol Laryngol 1973;82:2–12.
5. Beasly JW. Inner ear damage due to barotrauma. Wis Med J 1974;73:143–145.
6. Compere WE. Otolaryngologic problems encountered in scuba divers. ORL Digest 1974;21–28.
7. Vail HH. Traumatic conditions of the ear in workers in an atmosphere of compressed air. Arch Otolaryngol 1929;10:113–126.
8. Simmons BF. Theory of membrane breaks in sudden hearing loss. Arch Otolaryngol 1968;88:41–74.
9. Farmer JC. Diving injuries to the inner ear. Ann Otol Rhinol Laryngol 1977;86(Suppl 36):1–20.
10. Freeman P, Edmonds C. Inner ear barotrauma. Arch Otolaryngol 1972;95:556–563.
11. Harker LA, Norante JD, Ryu JH. Experimental rupture of the round window membrane. Trans Am Acad Ophthal Otol 1974;78:ORL 448–452.
12. McCormick JG, Philbrick T, Holland W, Harrill JA. Diving induced sensorineural deafness: prophylactic use of heparin and preliminary histopathology results. Laryngoscope 1973;83:1483–1500.
13. Lamkin R, Axelsson A, McPherson D, Miller J. Experimental aural barotrauma: electrophysiological and morphological findings. Acta Otolaryngol 1975; (Suppl 335):1–24.
14. Axelsson A, Miller J, Silverman M. Anatomical effects of sudden middle ear pressure changes. Ann Otol Rhinol Laryngol 1979;88:368–376.
15. Miller JM, Axelsson A, Potter W. Chronic effects of phasic middle ear pressure changes. Ann Otol Rhinol Laryngol (in press).
16. Axelsson A, Miller J, Holmquist J. Studies of cochlear vasculature and sensory structures: a modified method. Ann Otol Rhinol Laryngol 1974;83:537–550.
17. Axelsson A, Miller J, Larsson B. A modified "soft surface specimen technique" for examination of the inner ear. Acta Otolaryngol 1975;80:362–375.
18. Møller AR. An experimental study of the acoustic impedance of the middle ear and its transmission properties. Acta Otolaryngol 1965;60:129–149.
19. McPherson DL, Miller JM, Axelsson A. Middle ear pressure: effects on the auditory periphery. J Acoust Soc Am 1976;59:135–142.

WATER-BORNE MICROBIAL PATHOGENS: POTENTIAL HUMAN HEALTH HAZARDS IN MARINE ENVIRONMENTS

O. P. Daily, S. W. Joseph, J. D. Gillmore, R. J. Seidler, D. A. Allen, and R. R. Colwell

Public health specialists have long recognized that serious diseases, such as cholera, shigellosis, and typhoid fever, are associated with contaminated drinking water. More recently, they have become concerned with exposure to polluted waters via water-related recreation or occupations, or both (1–4). Global documentation of increasingly higher levels of pollution in coastal waters has prompted various agencies, such as the United Nations, National Oceanic and Atmospheric Administration (NOAA), Environmental Protection Agency (EPA), and the U.S. Navy, to expand efforts designed to assess and control public health problems associated with polluted waters.

Since a significant number of commercial and military diving operations are conducted in heavily polluted waters, notably major harbor areas, there is a potential for increased health hazards because of exposure to water-borne microbial pathogens. In the past decade, the presence of a number of water-borne pathogens in polluted waters has been established (3, 5–23). Infections caused by members of the genus *Vibrio* (especially *V. parahaemolyticus, V. alginolyticus,* lactose positive vibrios and *Vibrio cholerae), Campylobacter, Aeromonas, Legionella, Plesiomonas,* and *Yersinia* spp. following contact with polluted waters have been documented in various locations throughout the world (1–23).

We are currently studying water-borne pathogens isolated from locations where diving operations are ongoing in the Anacostia River, Washington, D.C., site of the U.S. Naval School, Diving and Salvage, and the New York Bight, site of NOAA diving operations.

817

Our first encounter with a water-borne infection resulted when a U.S. Navy diver suffered a leg puncture wound while conducting night scuba operations in the Anacostia River. The diver developed an infection from which two species of *Aeromonas, A. hydrophila* and *A. sobria,* subsequently were isolated (15).

ISOLATION AND IDENTIFICATION OF PATHOGENS

A study designed to identify, enumerate, and characterize water-borne pathogens in the Anacostia River and the New York Bight revealed a large number of major types of potentially pathogenic microorganisms to be present at both locations, where the incidence varied seasonally and geographically. Of the microorganisms listed in Table I, *Aeromonas* spp. were present in consistently larger numbers than were coliforms in the Anacostia River. *Vibrio parahaemolyticus, V. cholerae, E. coli, Klebsiella, Salmonella,* and *Enterobacter* were also isolated. Isolates from water samples collected in the New York Bight included group F vibrio, a potentially highly virulent water-borne pathogen (12).

The numbers of obligate anaerobes appeared to be related to temperature and dissolved oxygen (dO_2) concentration, with the highest numbers of obligate anaerobes occurring in the warmer months, when the water temperature reached 28°C and the dO_2 concentration was lowest. Of particular interest at both sampling sites was the occurrence and distribution of two genera of obligately anaerobic bacteria, *Bacteroides* and *Clostridium,* commonly recognized

TABLE I

Microbial Parameters and Potential Pathogens Isolated from Polluted Waters

Isolates	Concentrations per 100 mL water	
	Anacostia River	New York Bight
Total Viable Count	$2 \times 10^6 – 2 \times 10^7$	700–76,000
Total Coliforms	3,000–28,000	4–800
Total Fecal Coliforms	100–4,900	0–90
Total Anaerobic Count	0–10,000	0–48,000
Aeromonas spp.	1,000–50,000	0–10
Bacteroides spp.	✔	✔
Clostridium spp.	✔	✔
Enterobacter spp.	✔	✔
Escherichia coli	✔	✔
Klebsiella spp.	✔	✔
Salmonella spp.	✔	✔
Vibrio cholerae	✔	0
Vibrio parahaemolyticus	✔	✔
Group F. Vibrio	0	✔

✔ is detectable levels present;   0 is not detected.

as significant pathogens. The majority of the *Bacteroides* spp. were isolated throughout the water column, whereas *Clostridium* spp. were usually found in the sediment. Several of these anaerobes were cytotoxic for Y-1 adrenal cells.

Figure 1 illustrates the seasonal fluctuation of the total viable count, total and fecal coliforms, and *Aeromonas* at the Anacostia River sampling site from July 1978 to June 1979. In general, the numbers of *Aeromonas* spp. decreased from a maximum of 5 × 10⁴ cells/100 mL of water in August 1978, to a minimum of 1 × 10³ cells/100 mL of water in February 1979. An excellent correlation between the total numbers of *Aeromonas* ssp. in the Anacostia River
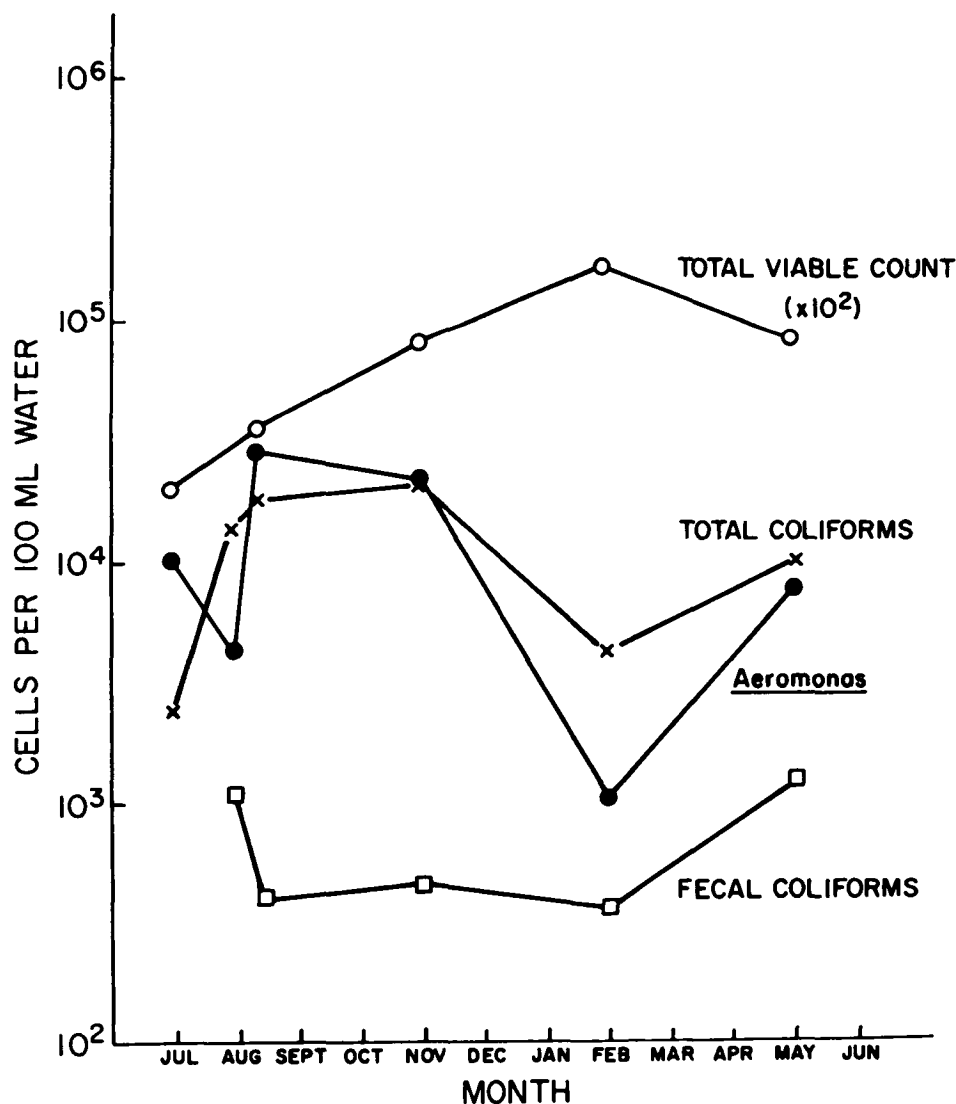
Fig. 1. Seasonal distribution of total viable count, total and fecal coliforms, and *Aeromonas spp.* in the Anacostia River.

water and temperature was obtained wherein a significant reduction in bacterial numbers occurred when the water temperature dropped to 15°C or below.

Total coliforms also showed seasonal fluctuation, i.e., the number of coliforms in the Anacostia River dropped significantly during the winter months. Fecal coliforms ranged from 1×10^2 to 5×10^3 cells/l00 mL, indicating a significant level of pollution. The total viable count remained relatively constant during the sampling period (Fig. 1).

TOXIGENICITY OF *Aeromonas* AND GROUP F VIBRIO

The high incidence of *Aeromonas* spp. in the Anacostia River and the presence of *Aeromonas* spp. and Group F vibrio in the New York Bight suggested a possible human health hazard. To further investigate the potential pathogenicity of these microorganisms, we assayed a number of isolates for cytotoxic and cytotonic (enterotoxic-like) effects for Y-1 adrenal cells, and for enterotoxin-mediated fluid accumulation in rabbit ligated ileal loops (15). In addition, *Aeromonas* isolates from environmental and clinical sources were speciated to either *A. hydrophila* or *A. sobria* and characterized for the presence of these virulence factors (Table II). Although *A. sobria* appeared to be the more frequently isolated species from clinical specimens, it comprised only about 10% of the *Aeromonas* isolated from the Anacostia River and only 3% of those from the New York Bight. Approximately 38% of the *A. sobria* and *A. hydrophila* isolates from the environment were cytotoxic for Y-1 adrenal cells, as compared with 77–100% of the clinical *Aeromonas*. An enterotoxin-like effect in rabbit ligated ileal loops was observed more frequently with clinical *Aeromonas* isolates (50–80%) than with environmental *Aeromonas* spp. (20–55%). Cytotonic activity by the environmental isolates in Y-1 adrenal cells ranged from 3 to 6% (Table II).

Group F vibrio, a highly virulent organism requiring NaCl for growth but otherwise biochemically similar to *Aeromonas*, was not isolated from the Anacostia River but was present in detectable levels in the New York Bight. Approximately 50% of these isolates were cytotoxic or cytotonic for Y-1 adrenal cells and caused fluid accumulation in rabbit ligated ileal loops.

ANTIBIOTIC SUSCEPTIBILITY OF *Aeromonas* FROM THE ENVIRONMENT

Multiple antibiotic resistance patterns were observed in several of the *Aeromonas* isolates. In general, both *A. hydrophila* and *A. sobria* were resistant to ampicillin (183/190 strains). Sixteen strains of *A. hydrophila* isolated from water samples were also tetracycline-resistant and four were resistant to several antibiotics (three to tetracycline, erythromycin, and ampicillin, and one to tetracycline, nalidixic acid, and erythromycin). Only 1 of 21 strains of *A. sobria* was multiply-resistant, i.e., ampicillin, tetracycline, and kanamycin.

TABLE II

Cytotoxicity and Enterotoxicity of *Aeromonas* and Group F Vibrio

Strain Identification	No. of Isolates	Response in Y-1* Adrenal Cells		Enterotoxicity* in Ligated Rabbit Ileal Loops
		Cytotoxic	Cytotonic	
A. sobria:				
- Clinical	13	10/13 (77%)	N.D.	4/5 (80%)
- Environmental (Anacostia River & New York Bight)	35	13/35 (37%)	1/35 (3%)	5/9 (55%)
A. hydrophila:				
- Clinical	2	2/2 (100%)	N.D.	1/2 (50%)
- Environmental (Anacostia River & New York Bight)	330	123/330 (39%)	20/330 (6%)	1/5 (20%)
Group F Vibrio (New York Bight)	16	9/16 (56%)	9/16 (56%)	8/16 (50%)

*No Positive/number tested;   N.D. is not determined.

MICROBIOLOGICAL HAZARDS FOR DIVERS

Because there were large numbers of *Aeromonas* isolated from Anacostia River water samples, experiments were designed to determine if colonization of divers by *Aeromonas* were possible. Ears, noses, throats, and the equipment of divers were examined following a 30-min exposure in the Anacostia River. Samples were taken with saline-wetted sterile swabs, placed in 2 mL of sterile saline, immediately transported to the laboratory, inoculated on an appropriate medium, incubated for 24 h at 37°C and *Aeromonas spp.* were enumerated and isolated for further study. Figure 2 shows the results of two such surveys. The first survey, conducted in August 1978, when the *Aeromonas* counts were 300/ mL and the water temperature was 28°C, indicated that approximately 90% of the divers' ears and masks were contaminated with *Aeromonas* after exposure to the polluted water. Colonization was approximately 7% in noses and 27% in throats. The second survey, conducted in October 1978, when the *Aeromonas* counts in the water were 50/mL and the temperature was 13°C, showed generally lower colonization rates, except for the divers' ears which were again about 90% colonized.

The results of these experiments indicated that it was, indeed, possible for divers to become colonized with *Aeromonas spp.*, even when the numbers of *Aeromonas* in the water were as low as 50/mL. The total number of *Aeromonas* and coliforms isolated from each positive swab averaged 130/mL. Exposure to polluted water for as little as 30 min significantly altered the composition of the skin microflora to an extent resembling that of the diving environment. Although the number of *Aeromonas* required to establish a

Fig. 2.   Colonization of divers and equipment with *Aeromonas* after exposure to Anacostia River Water.

wound infection or a gastrointestinal disorder is not known, a short period of exposure may facilitate pathogenesis, i.e., attachment of microorganisms to the skin surface as the first step in the disease process.

CONCLUSIONS

To date results of our studies of water-borne pathogens indicate that polluted water, i.e., water containing fecal coliforms in numbers greater than 1/100 mL or total coliforms in numbers greater than 200/100 mL, contain many potentially pathogenic species in significant numbers (Table I). Several of these organisms produce cytotoxins or enterotoxins, or both. Exposure to these organisms has been shown, in reports from our laboratories and elsewhere, to be capable of causing wound infections or gastrointestinal disease, or both. Thus, it can be concluded that presence of these organisms poses an additional health risk associated with diving operations in polluted waters.

Diving Medical Officers should be aware of the potential health problems presented by water-borne pathogens and provide complete clinical documentation through accurate recording of infectious disease occurrences within the diving community. Without proper documentation it is difficult to assess the magnitude of such risks. Because some of the water-borne microorganisms are only now becoming recognized as significant pathogens, it is imperative that Diving Medical Officers or attending physicians, who are involved in treatment of infectious disease problems of divers, become familiar with these recently described pathogens associated with polluted waters.

Acknowledgments

References

1. Black RE, Craun GF, Blake PA. Epidemiology of common-source outbreaks shigellosis in the United States, 1961–1975. Am J Epidemiol 1978;108:47–52.
2. Colwell RR, Kaper J, Joseph SW. Vibrio cholerae, Vibrio parahaemolyticus, and other vibrios: Occurrence and distribution in Chesapeake Bay. Science 1977;198:394–396.
3. Feldman RE, Baine WB, Nitzkin JL, Saslaw MS, Pollard RA, Jr. Epidemiology of Salmonella typhi infection in a migrant labor camp in Dade County, Florida. J Infect Dis 1974;130:334–342.
4. Kaper J, Lockman H, Colwell RR, Joseph SW. Ecology, serology, and enterotoxin production of Vibrio cholerae in Chesapeake Bay. Appl Environ Microbiol 1979;37:91–103.
5. Blake PA, Merson MH, Weaver RE, Hollis DC, Heublein PC. Disease caused by a marine vibrio. New Engl J Med 1979;300:1–5.
6. Caprioli T, Drapeau AJ, Kasatiya S. Yersinia enterocolitica: serotypes and biotypes isolated from humans and the environment in Quebec, Canada. J Clin Microbiol 1978;8:7–11.

7. Carpenter CCJ. More pathogenic vibrios. New Engl J Med 1979;300:39–41.

8. Ciznar I, Hostacka A, Urgeova E, Majtan V, Karolceks J. Physico-chemical and biological properties of enterotoxins from NAG vibrio, *Aeromonas hydrophila* and *Plesiomonas shigelloides*. Toxicon 1979;17(Suppl 1):27.

9. Felsenfeld O. Present status of the el tor vibrio problem. Bacteriol Rev 1964;28:72–86.

10. Fliermans CB, Cherry WB, Orrison LH, Thacker L. Isolation of *Legionella pneumophila* from nonepidemic related aquatic habitats. Appl Environ Microbiol 1979;37:1239–1242.

11. Fraser DW, Deubner DC, Hill DL, Gilliam DK. Nonpneumonic, short-incubation-period Legionellosis (pontiac fever) in men who cleaned a steam turbine condenser. Science 1979;205:690–691.

12. Furniss AL, Lee JV, Donovan TJ. Group F, a new vibrio? Lancet 1977;2:565–566.

13. Hanson PG, Standridge J, Jarrett F, Maki DG. Freshwater wound infection due to *Aeromonas hydrophila*. JAMA 1977;238:1053–1054.

14. Hazen TC, Fliermans CB, Hirsch RP, Esch GW. Prevalence and distribution of *Aeromonas* hydrophila in the United States. Appl Environ Microbiol 1978;36:731–738.

15. Joseph SW, Daily OP, Hunt WS, Seidler RJ, Allen DA, Colwell RR. *Aeromonas* primary wound infection of a diver in polluted waters. J Clin Microbiol 1979;10:46–49.

16. Kohl S. *Yersinia enterocolitica:* a significant "new" pathogen. Hosp Pract 1978;13:81–85.

17. Mertens A, Nagler J, Hansen W, Gepts-Friedenreich E. Halophilic, lactose-positive *Vibrio* in a case of fatal septicemia. J Clin Microbial 1979;9:233–235.

18. Olsen H. *Vibrio parahaemolyticus* isolated from discharge from the ear in two patients exposed to sea water. Acta Path Microbiol Scand 1978;86(Sect. B):247–248.

19. Prociv P. *Vibrio alginolyticus* in western Australia. Med J Aust 1978;2:296.

20. Rippey SR, Cabelli VJ. Membrane filter procedure for enumeration of *Aeromonas hydrophila* in fresh waters. Appl Environ Microbiol 1979;38:108–113.

21. Seidler RJ, Allen DA, Lockman H, Colwell RR, Joseph SW, Daily OP. Isolation, enumeration and characterization of *Aeromonas* from polluted waters encountered in diving operations. Appl Environ Microbiol 1980;39:1010–1018.

22. Smibert RM. The Genus *Campylobacter*. Ann Rev Microbiol 1978;32:673–709.

23. Walker ARP, Walker BF. Pure water and infections in Africa. Lancet 1978;2:639.

MANAGEMENT OF HEALTH HAZARDS ASSOCIATED WITH THE SALVAGE OF TOXIC CHEMICALS USING A SATURATION DIVING TECHNIQUE

A. Marroni, J. Gething, and D. Zannini

On 14 July 1974 a collision occurred between the M.V. CAVTAT and the steamship LADY RITA. The M.V. CAVTAT was badly damaged amidships and sank in 95 m of water. The M.V. CAVTAT was carrying a general cargo, but of special interest was 900 drums of antiknock compound. The drums contained tetramethyl lead (TML) and tetraethyl lead (TEL) or a mixture of the two compounds. Antiknock compounds are heavy, volatile liquids, virtually insoluble in sea water.

This paper deals with the problems of salvage of toxic compounds from a depth of 95 m and the various safety and medical recommendations that were made to ensure that the operation could be successfully completed.

TOXIC EFFECTS OF LEAD ALKYL COMPOUNDS

Absorption of lead alkyl compounds can occur a) through the respiratory tract by inhalation of the vapor, b) through the skin from contact with the liquid, and c) through the alimentary tract by ingestion of the liquid. Of these three routes inhalation of the vapor is the most important, although skin absorption can be significant if contact is long enough (1). The clinical effects of exposure to tetraethyl lead and tetramethyl lead are the same. Symptoms may follow one brief, severe exposure or repeated mild exposures.

The early symptoms are related to the central nervous system, and include sleep disturbance, unpleasant dreams, anorexia, nausea and vomiting, and irritability. Later symptoms include intense anxiety and "nervousness," nightmares, and muscular weakness. Following severe exposure and a high level of

absorption, the symptoms can progress to disorientation, mania, hallucinations, and eventually lead to coma and death (2,3).

Following absorption, lead alkyls are broken down in the liver to tri-alkyl compounds which represent the toxic agent. Further de-alkylation takes place in the liver and eventually the majority of the lead is excreted in the urine. Lead alkyl compounds do not interfere with hemoglobin synthesis as do inorganic lead compounds, and some of the tests used in controlling exposure to inorganic lead are of no value in monitoring exposure to lead-alkyls (3). The most important single test for biological monitoring is the level of lead in urine.

MATERIALS AND METHODS

Diving Procedures

Saturation diving techniques were adopted for the task; the deck decompression chamber (DDC) was compressed in air to an equivalent depth of 6.5 msw, then in helium to the saturation depth. The P_{O_2} was maintained at 330 mbar ± 80, P_{N_2} at an average of 1,330 mbar, and relative humidity in the 50-75% range (4) throughout the 23 saturation periods accounting for 33,474 saturation man-hours.

The 35 divers employed on this task spent 1,235 h working on the CAVTAT wreck and performed a total of 247 no-decompression saturation excursion dives of an average duration of 5 h each (see Table I).

The problem of a possible contamination of the saturation habitat by a volatile and extremely toxic pollutant was considered most important in this situation. Lead alkyl TLV is normally considered to be 100 μg Pb/m³ of gas for an exposure of 8 working hours (1–3); as saturation divers work and live in a confined habitat 24 h a day, the TLV should be, in this case, 23.8 μg Pb/m³ of gas. This quantity would correspond to the evaporation of a lead alkyl droplet of a radius less than 0.01 mm. Considering this and the total lack of information (and experience) about toxic effects of lead alkyl under increased hydrostatic pressure conditions and the extreme difficulty involved in excluding

TABLE I

Diving Operations

Saturation periods	23
Saturation days	389
Saturation man-hours	34,128
Bottom-time hours	1,235
Saturation-excursion dives	247
Average duration of excursion (h)	5

Dates: March 3, 1977–April 25, 1978.

the possibility that such a small quantity of lead alkyl compound was not taken into the habitat, we considered the limit of 20 μg Pb/m³ an emergency threshold and aimed for the total absence of lead alkyl vapor in the DDC atmosphere. Therefore, the divers were all submitted to a step-by-step decontamination procedure, which assumed the diver, the bell, and the transfer lock were contaminated until the contrary was proven by the testing.

To prevent skin absorption the diver was provided with a PVC suit and gloves in addition to his normal hot water diving suit; when he returned to the diving bell he removed the PCV suit and gloves and the flippers which were left in a basket outside the bell, or abandoned. The umbilical was designed to be relatively buoyant, to prevent contamination on the sea bed.

Should contamination have occurred the umbilical was cleaned before the diver entered the bell. Entering the bell after a dive, both the divers and the tender breathed through a mask to prevent possible exposure to lead alkyl vapor in the bell. The diving bell was fitted with an activated charcoal filter to remove lead alkyl vapor. After the bell reached the surface and was connected to the transfer lock, its outlet valve was opened to ensure a light but constant gas flow from the transfer lock to the bell, which would prevent the passage of lead vapor from the bell to the transfer lock. The divers then stripped and transferred to the interlock, where they showered while continuing the "mask-on" system. Only when the analytical results of the gas were shown to be within normal limits did the divers transfer to the living chamber and were given the "mask off" order.

The saturation habitat life-support system was equipped with additional activated charcoal filters as a final precaution. In case of persistent contamination of the bell and the transfer lock, the bell was detached, depressurized, and thoroughly cleaned while the activated charcoal filtering system was shifted to the transfer lock. If this procedure proved insufficient, the divers were isobarically transferred to the living chamber and the "mask-on" order was given to all occupants of the DDC; the transfer lock was depressurized, cleaned, and repressurized; all the divers were then transferred to the interlock and the procedure repeated for the living chamber. At the end of this emergency procedure, which was used once, the whole saturation system atmosphere had been changed and the chambers had been cleaned without decompressing the divers.

Biological Monitoring of the Divers

At the onset of the operation each of the divers had a complete physical examination and a full blood count. During the working period urinary lead levels were checked weekly. At the end of the diver's tour of duty he had a further medical examination and estimations for blood lead and urinary lead; while under saturation, a diver's behavior was constantly observed by a physician. According to SAIPEM's saturation diving procedure, the divers filled in a medical form daily, which logged body temperature, heart and respiratory rate, blood pressure, bowel function, urinary output, sleep, eating habits, work

shifts, mood, and personal comments (4,5). In addition to these usual questions a few new ones were added regarding disturbed sleep, nightmares or disagreeable dreams, unusual anxiety, or a metallic taste (1–3).

Normal levels of urinary lead in subjects with no previous occupational exposure vary between 0 and 80 μg Pb/L (1–3). Symptoms following exposure to tetraethyl lead had been reported for levels below 200 μg lead/L of urine, (2,3), and it was decided for this salvage operation to regard 120 μg lead/L of urine as an "alert" level for immediate further investigation on safety procedures and biological monitoring.

Determination of Lead in Urine

The urine samples were collected in lead-free containers, and these containers were flown to the Octel Company's Analytical Laboratory in the United Kingdom. No correction was made for specific gravity, but samples of low gravity (below 1010) and high gravity (over 1030) were discarded and repeat samples requested. The urinary lead content was determined by Atomic Absorption Spectrophotometry, using electrothermal atomization.

Determination of Organic Lead in Gas

A measured volume of gas is passed through a glass filter-carbon paper, impregnated with iodine. The organic lead retained by the paper is then extracted by iodine solution converted to inorganic lead by the use of "Telmatic" lead-in-air reagents and colorimetrically determined using dithizone. A total of 465 lead-in-gas tests were made, 241 in the bell and 224 in the transfer lock. Of the 241 lead-in-gas tests in the bell, 149 were above 40 μg Pb/m³, 81 of which were above 120 μg Pb/m³, and 42 above 300 μg Pb/m³. Only 22 lead-in-gas tests performed in the transfer lock were above 40 μg Pb/m³, and none were above 300 μg/Pb/m³ (see Fig. 1).

RESULTS AND DISCUSSION

From March 1977 to April 1978 medical surveillance was carried out on 35 divers who were working on the recovery of drums from the M.V. CAVTAT. As can be seen from the lead-in-urine results, the vast majority of these were within the prescribed "alert" level of 120 μg lead/L urine (see Fig. 2). At the end of saturation number 6, the urinary lead test performed after decompression for one diver showed a lead-in-urine level of 160 μg/L. Subsequent investigation revealed he had not worn his mask while in the bell and inspection of the lead levels in the bell atmosphere showed levels up to 500 μg Pb/m³. In saturation number 12, two divers became contaminated by a compound that spilled over them while working on the side of the wreck. The compound was lying loose trapped in an angle of metal. The test results for these two men showed a slight rise of urinary lead and normal values for the other two saturated divers.
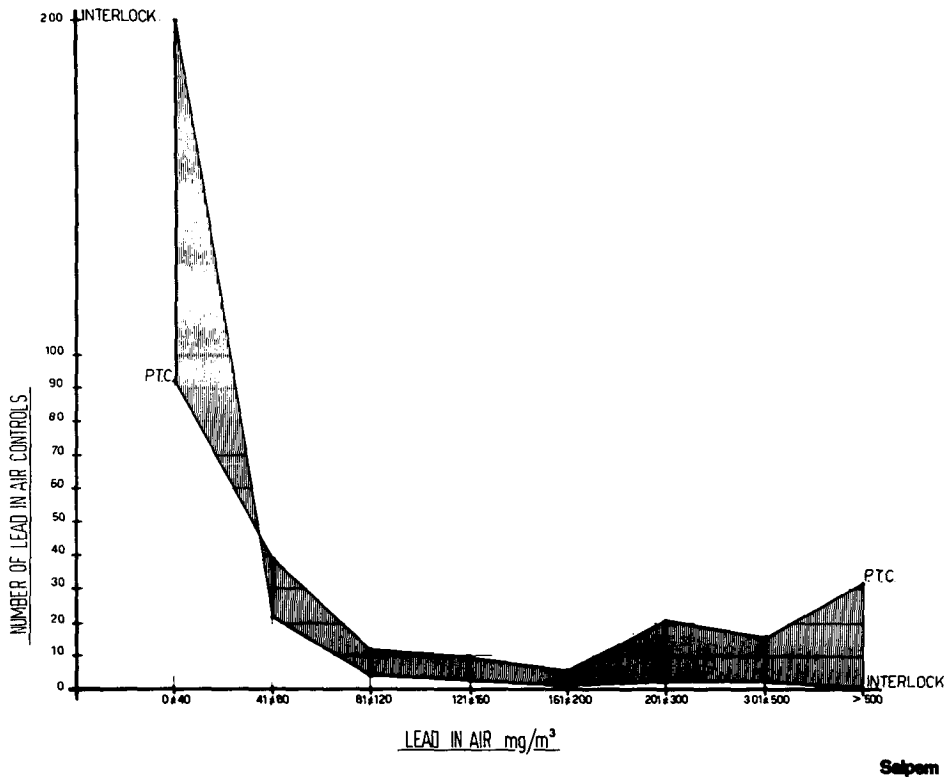
Fig. 1. Number of lead-in-air controls in PTC and INTERLOCK showing efficacy (*shaded area*) of PTC to INTERLOCK decontamination step.

The last saturation period, number 23, had the highest lead-in-urine levels (see Fig. 2). The divers employed at the time were very experienced and were working hard to finish the job. The mean level may be distorted by two high figures from two men, one of 380 μg and one of 365 μg. It was found that the umbilical in use by these two divers was contaminated by compound and a "bag-test" gave a lead-in-air level of 714 μg/m³. For this test the umbilical was placed in a sealed plastic bag for 24 h and then the level of the lead in the air in the bag was determined. Because of this high level it was considered possible that compound may have penetrated through the walls of the umbilical to contaminate the gas mixture supplying the divers. The umbilical is carried into the bell, and contamination to this degree would result in high lead level in the bell. No symptoms were reported but urine samples were collected daily during the last 12 days of the saturation period and the umbilical was changed. The other two divers showed normal urinary lead levels and the samples for the following days for the two men who had shown high levels earlier showed a fall in urinary lead levels.

The described procedure and the "mask-on" system used in the bell and the interlock were designed to provide a closed system of respiration for the divers in a potentially contaminated environment of the bell and the interlock.
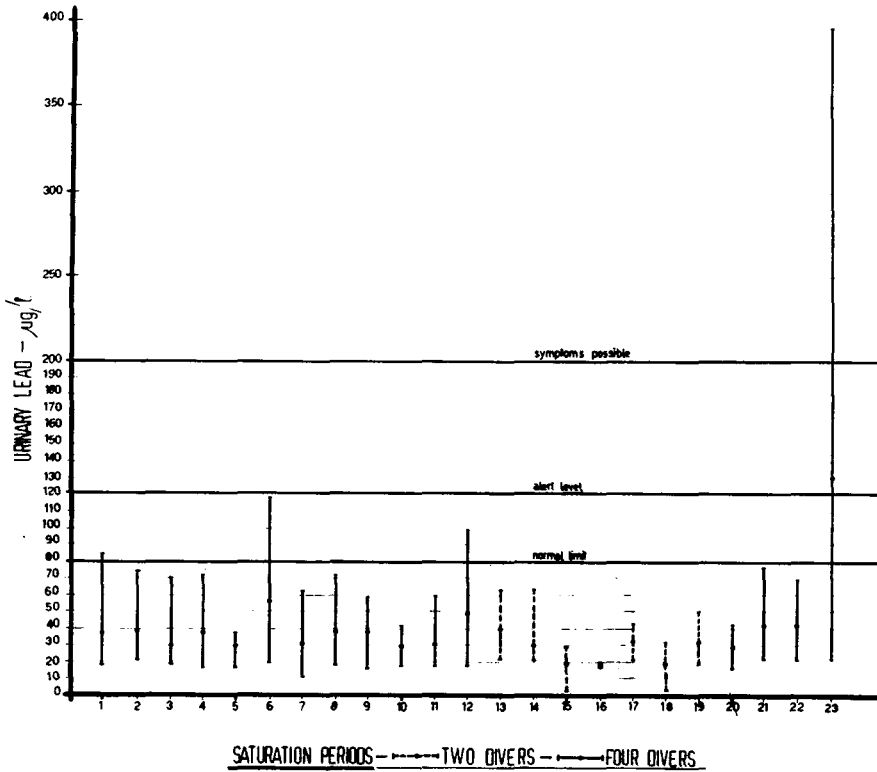
Fig. 2.   Mean urinary lead and range (µg/L) for each saturation period.

The constant DDC-to-PTC gas flow kept during the transfer of the divers from the bell to the habitat and the strip-and-shower procedure described previously also proved efficient as shown by the lead-in-gas values in the PTC compared to the ones in the transfer lock (see Fig. 1).

The lead-in-urine results compared to the lead-in-gas values in the bell show that this concept was successful, and on the occasions when the lead-in-urine levels showed a rise in absorption of lead alkyls this was due to a failure in the safety system. The most common failure was due to the nonwearing of masks, either in the bell or the interlock, but contamination of the umbilical was also an important factor. In the last saturation period a combination of these two factors, that is, contamination of the umbilical wall causing lead alkyl vapor to contaminate the breathing system, and contamination from outside the umbilical causing raised lead in air levels in the bell, caused fairly significant levels of lead in urine in the divers. These raised levels only occurred for a few days, and none of the divers had any untoward symptoms. The blood lead levels for all saturation divers showed no significant variation from normality (see Table II).

TABLE II

Blood Lead for all Saturation Divers Showing
No Significant Variation from Normality

	Blood Lead ($\mu g/100$ mL)	Range
Mean at Start	22.46	12–32
Mean At Finish	25.9	11–42
Mean Overall	23.7	11–42

The results show that by applying stringent safety controls (including the step-by-step decontamination procedure described previously) backed up by adequate biological monitoring, salvage of potentially toxic volatile chemicals such as tetraethyl lead and tetramethyl lead can be carried out safely despite the use of saturation-diving techniques, which allow for minimal variations in microclimatic conditions with little modification of routine saturation diving procedure.

References

1. Plunkett ER. Handbook of industrial toxicology. New York: Heyden-Chemical Publishing Co., 1976.
2. Rubino GF, Pettinati L. Intossicazione professinonale da piombo tetraetile. In: Elementi di medicina del lavoro. Minerva Med 1979:135–137.
3. Caccuri S. Piombo tetraetile. In: Medicina del lavoro. Indelson Napoli, 1977:155.
4. Zannini D, Marroni A, Canepa E. Physiologic check-list during saturation diving. Ann Med Nav 1979;84(1):41–56.
5. Zannini D, Marroni A, Canepa E. Physiologic check-list during saturation diving (a comprehensive method for the control of divers's fitness). In: Abstracts of the sixth symposium on underwater physiology, San Diego, CA., July 6–10, 1975:89.

THE PRESENT STATUS OF BONE NECROSIS RESEARCH

D. N. Walder

At present (April 1980) the M.R.C. Decompression Sickness Central Registry in Newcastle upon Tyne has the radiographs of the bones of about 4,900 professional divers. Of these persons nine are known to have juxta-articular (A) lesions with broken joint surfaces (the most serious outcome of bone necrosis). A further 50 have unbroken juxta-articular (A) lesions that are potentially disabling, and 140 more have the head, neck, and shaft (B) lesions that have not, so far, been considered to be of any significance to the health or efficiency of the subject concerned.

In addition, we have noted in our records that 35 divers have suspected juxta-articular lesions and 30 divers have suspected head, neck, and shaft lesions. From experience we know that some of these suspected lesions will become definite in a year or so.

In terms of an overall problem, bone necrosis in divers does not appear to be overwhelming. However, because the management of the condition is so difficult, it does seem to be important to try to understand why it occurs and what its natural history is so that we can either stop its occurring or select the optimum time for treatment.

Ultimately, the aim must be to avoid the condition altogether. Most decompression tables in use at present are presumably believed, at least by those who use them, to be satisfactory. This, I suggest, means that they will be safe for most (say, for example, 99%), but not all, of the population at risk. It now transpires that bone necrosis can occur in the absence of previous attacks of decompression sickness, although a history of such attacks does increase the likelihood of bone necrosis occurring. It therefore now appears that there may be some additional factor independent of the decompression which makes a diver susceptible to bone necrosis.

Research into bone necrosis following hyperbaric exposure has been proceeding simultaneously along several avenues and although at first sight they may appear to be unrelated, they are in fact all directed towards the development of an integrated picture of the total problem.

EPIDEMIOLOGY

First, I would like to express my thanks to all those radiologists in every part of the world who have followed the M.R.C. Decompression Sickness Panel's system of radiological skeletal survey and classification of bone lesions and who have thereby enabled us to build up a clear idea about the overall problem that would otherwise not be possible.

In addition to obtaining some idea about the prevalence of bone necrosis in North Sea divers, it has also been possible to study the influence on the prevalence of the condition of a) the type of diving carried out (for instance, there seems to be a critical limit for combined depth and time short of which bone damage does not occur); b) decompression sickness; and c) some personal factors, such as weight.

A question currently being asked is whether or not the appearance of a B lesion is an indication that the individual is more likely than a normal person to develop an A lesion if he continues to dive. This question has proved difficult to answer. The crux of the problem lies in finding men with a complete history and comparable hyperbaric experience. At the Newcastle Central Registry we have recently reviewed all of our data, including that from compressed-air workers as well as that from divers, and can find no statistically justifiable conclusion one way or the other.

ANIMAL MODELS

Bone necrosis research has proceeded slowly over the years because it has been difficult to find a satisfactory animal model. Many laboratory animals can be shown to develop microscopic evidence of necrotic bone when examined after severe decompressions, but under realistic conditions of depth, duration of exposure, and decompression, only the minipig develops macroscopic lesions similar to those seen in man.

An interesting alternative model system which we have used successfully has been the simulation in rabbits of bubble emboli by glass spheres. After these particles had been injected into the arterial circulation, the rabbits developed both shaft and juxta-articular lesions, which appear to be identical with those seen in man after hyperbaric exposures.

THE DEVELOPMENT OF DIAGNOSTIC TECHNIQUES

One of the practical problems in dealing with divers is to relate any bone lesion which may appear to the causal incident. As diagnosis by radiography cannot be immediate and usually requires a period of at least 3 months between the initiating insult and the development of changes sufficient to be seen

on a radiograph, efforts have been made to seek more sensitive but nonetheless practical indicators. So far, the most encouraging and conveniently detectable sign of incipient bone damage appears to be a rise in the serum ferritin level. This is, of course, a nonlocalizing sign and when positive has to be followed up with a bone-seeking radioisotope scan to identify the site of the abnormality.

This is a very sensitive technique and one of the dangers with any such method is that it may be too sensitive and detect lesions which will in any case heal spontaneously. It is therefore important to gain more experience in this area before concluding that all positive serum ferritin results will necessarily end up as definite bone lesions.

A PREDISPOSING FACTOR

Bone lesions occur mainly in a few well-known sites in the skeleton. As there is no absolute relationship between being treated for decompression sickness and subsequently developing bone necrosis, this raises the question as to whether there is some additional predisposing factor which has so far not been considered. Recently, we have been studying in animals the clearance of radioisotopes from bone marrow before, during, and after decompression from simulated dives. As will be reported elsewhere at this meeting, it does look as though there are times when the marrow circulation is embarrassed and would be more than usually vulnerable to transient ischemic episodes. Should the cause for this diminution in clearance rate be one which could be controlled, it might be possible to minimize the damage to bone marrow and bone during compression.

TREATMENT

Unfortunately, the treatment of juxta-articular lesions once the joint surface has broken is unsatisfactory. Essentially, the choice lies between arthrodesis and the replacement of the damaged joint by a prosthesis. While one or the other of these options may be perfectly acceptable for patients at the end of an active life, neither is desirable in young and otherwise fit men.

Post-mortem studies of juxta-articular lesions have provided evidence that almost always the body makes a considerable effort to repair the damaged area of bone but rarely succeeds completely. In most cases the healing process comes to a halt just short of the articular surface to leave a saucer of dead bone at this crucial point. It transpires that the explanation for this failure to repair totally lies in the fact that the repair process involves the deposition of new bone on the dead trabeculae. These eventually become so thick that where they lie close together the spaces between them are occluded and this prevents the forward progress of new capillaries and deprives the tissue beyond of a blood supply. The repair process stops. Now that this mechanism is appreciated, possible ways in which the difficulty could be overcome are clear and can be tested.

ABNORMAL BONE AND CARTILAGE COLLAGEN METABOLISM IN EXPERIMENTALLY INDUCED DYSBARIC OSTEONECROSIS

D. Brickley-Parsons and M. E. Bradley

Dysbaric osteonecrosis is a debilitating, chronic disease found in certain individuals exposed to changes in ambient pressure. Yet the very survival of man dictates the expansion of undersea and space exploration. One can hardly recommend that such exploration cease; yet neither can one ignore the inevitable increase in the incidence of destructive bone lesions in those afflicted with dysbaric osteonecrosis.

Despite interest, concern, and study during the last half century, the etiology and pathogenesis of dysbaric osteonecrosis remains an enigma. Clearly, important fundamental problems involving the predisposing factors and the sequence of biochemical events leading to bone necrosis must be fully probed. In addition, new techniques must be developed to detect early lesions and thus prevent disease·progression.

The main functions of the skeletal tissues, bone, and cartilage are to provide the body with mechanical support and motion. Mineral formation and resorption, as well as the quality and quantity of the structural protein collagen, play crucial and critical roles in carrying out these functions and in doing so efficiently. In recent years it has become increasingly apparent that collagen exhibits an extensive heterogeneity (1–3). At least some of this molecular polymorphism reflects the biological adaptation of basic molecules for special tissue requirements. Thus, for example, cartilage contains a type of collagen that is genetically distinct from that of bone; yet the collagens of bone and cartilage both contain intermolecular crosslinks that display similar distinctive features (4,5). Such unique chemical components equip the tissue with the special properties that are important to its physiological functions. Thus, it seems reasonable to assume that the skeletal deterioration observed in dysbaric osteonecrosis may indeed be linked to abnormalities in collagen metabolism.

Richmond et al. (6) examined the femurs from swine in which dysbaric osteonecrosis associated with inadequate decompression had been induced. Their results demonstrated a greater content of unsaturated crosslinks in the collagen of experimental animals than in control animals. This would suggest an enhanced ability to remodel collagen, which would be consistent with the histological observation of increased derangement of collagen fiber in experimental bone samples (7). Over the past 2 years, our laboratories have been extensively involved in studying collagen synthesis, maturation, and degradation of bone and cartilage in the early, intermediate, and latent stages of induced dysbaric osteonecrosis. Our studies using the experimental mouse model of Chryssanthou (8) revealed a number of striking changes in the composition of bone and cartilage at the molecular level.

MATERIALS AND GENERAL METHODS

Four groups of male, genetically-obese hyperglycemic mice (Jackson Labs, Bar Harbor, ME) were subjected to 75 psig air pressure in a pressure chamber for 3 h. The compression was either rapid (75 psig in 60 s) or slow, staged. The slow, staged compression involved stops at 15 psig (10 min), 30 psig (20 min), 45 psig (10 min), and 60 psig (20 min). All decompression was staged with stops at 50, 40, 30, 20, and 10 psig for 5, 25, 35, 75, and 120 min, respectively. Two groups of mice were subjected to either rapid or slow staged compression for 3 times per week; two other groups were exposed 7 times per week. A fifth group of mice was not subjected to hyperbaric exposure and served as age and site matched controls.

Bone from the epiphyses of the proximal femur, distal femur, proximal tibia and humerus, and the mid-shafts of the femur, tibia, and humerus were divested of periosteum and marrow, dried, pulverized, demineralized in 0.5M EDTA, pH 7.2, and washed thoroughly with distilled, demineralized water. Cartilage from the femoral and humeral head and the knee joint were freed of all extraneous material, finely minced by hand, dried, and pulverized. All control and experimental bone and cartilage samples at each stage of induced dysbaric osteonecrosis were analyzed chemically. These determinations included amino acid analysis (9), crosslink profile (10), hydroxylysine glycosylation (11), gel electrophoresis (12), and cyanogen bromide digestion of whole tissue followed by phosphocellulose chromatography of collagen-specific peptides (13).

Specific Biochemical Procedures

Amino Acid Analyses

Conventional amino acid analyses of 1 mg aliquots of bone and cartilage were carried out after hydrolysis in triply distilled 6N HCl at 105°C for 24 h, using a commercial amino acid analyzer adapted to the single column method.

Crosslink Profile

All samples were reacted with tritiated sodium borohydride (10 μC/mol, 0.01 mmol/10 mg tissue) in 0.1M phosphate buffer, pH 7.4, for 1 h. Excess borohydride was destroyed by the addition of glacial acetic acid to pH 3.0. The samples were washed with water, lyophilized, and hydrolyzed in 3N HCl at 105°C for 48 h. All hydrolysates were dried, dissolved in 0.2M sodium citrate, pH 2.2, and analyzed by elution from a 60 cm column of an amino acid analyzer with a single buffer of 0.35M sodium citrate, pH 5.28. The flow rate was maintained at 60 mL/h and the column temperature at 57°C. The total effluent was collected in 2.7 mL fractions for measurement of radioactivity. The activity of ^{3}H in the column effluents was measured after mixing 2 mL of sample fraction with 10 mL Aquasol. To prevent phasing, we added 0.2 mL of water. The samples were counted in a liquid scintillation spectrometer.

Hydroxylysine Glycosylation

Samples of known weight (3-5 mg) were hydrolyzed in 2N NaOH at 105°C for 24 h, neutralized, and washed. The hydroxylysine and hydroxylysine-glycoside fractions were eluted from a P-2 desalting column and analyzed for content on the amino acid analyzer.

Gel Electrophoresis

Sodium dodecylsulfate-polyacrylamide electrophoresis using 7.5% acrylamide gels was carried out on all samples for 4 h using a current of 4 mA/tube. The gels were stained with Comassie-Brilliant Blue.

Cleavage with Cyanogen Bromide (CNBr)

Aliquots of all samples were suspended in 70% formic acid (0.25 gm/50 mL) and flushed with nitrogen; a weight of CNBr equal to two times the weight of the sample was added. Digestion proceeded for 4 h at 30°C with gentle stirring. All samples were centrifuged for 10 min at 40,000 g and the supernatant containing the liberated peptides was lyophilized after a tenfold dilution with cold distilled, demineralized water.

Phosphocellulose Chromatography (P-11)

The CNBr peptides of all samples were dissolved in starting buffer (1 mM sodium acetate, pH 3.6) and applied to a P-11 column (1.5 × 10 cm) equilibrated with the same buffer and maintained at 43°C. The peptides were eluted with a linear gradient of 0-0.3M NaCl forced between 400 mL each of starting buffer and limit buffer (1 mM sodium acetate/0.3M NaCl, pH 3.6). A flow rate of 70 mL/h was used and the effluent was continuously monitored at

230 nm. The specific CNBr peptides, $\alpha 1(I)CB2$ characteristic of Type I collagen and $\alpha 1(II)CB6$ characteristic of Type II collagen, were isolated and characterized by their amino acid content. The relative proportions of the parent Types I and II collagens were calculated from the molar ratio of their characteristic peptides.

RESULTS

Samples from of 480 mice were analyzed biochemically to determine the heterogeneity and crosslinking of bone and cartilage collagen as a function of the development of osteonecrosis induced by hyperbaric exposure. Table I shows the incidence of osteonecrosis induced by exposure to hyperbaric conditions as diagnosed by abnormal collagen composition present in individual samples. These data clearly demonstrate that with daily exposure to rapid compression, the incidence of abnormal alterations in collagen metabolism is greater and the latent period shorter than with 3 exposures per week or with slow, staged compression.

BONE

Table II shows a striking, temporal correlation between the rate of compression and the content of hydroxylysine in the collagens analyzed. Amino acid analyses of bone collagen from the epiphyses of the proximal femur and tibia revealed a marked increase in the hydroxylysine content as a function of daily exposure to rapid compression. The increased hydroxylysine content in the epiphyses of the distal femur and proximal humerus demonstrated that those areas were the least affected by exposure to either rapid or slow staged compression, with hydroxylysine values only slightly higher than the age-matched controls. The hydroxylysine content of the collagen of the

TABLE I

Influence of the Rate of Compression and the Frequency and Duration of Hyperbaric Exposure on the Incidence of Abnormal Collagen in Obese Mice

Exposure Duration (months)	Rapid Compression		Slow, Staged Compression	
	Daily	3/Week	Daily	3/Week
3	60% (12/20)	35% (7/20)	— (0/20)	— (0/20)
6	70% (14/20)	40% (8/20)	— (0/20)	— (0/20)
9	85% (17/20)	55% (11/20)	15% (3/20)	5% (1/19)
12	90% (18/20)	68% (13/19)	21% (4/19)	10% (2/20)
15	93% (14/15)	80% (12/15)	32% (6/19)	11% (2/18)
18	100% (16/16)	81% (13/16)	33% (5/15)	20% (4/20)
20	100% (12/12)	87% (14/16)	47% (8/17)	22% (2/18)

TABLE II

Alterations in the Hydroxylysine Content of Bone Collagen as a Function of Daily
Exposure to Hyperbaric Conditions

(Values expressed as Residues of Hydroxylysine/Collagen Chain)

Exposure Duration (months)	Epiphysis				Mid-Shaft	
	PX Tibia	PX Femur	DS Femur	PX Humerus	Tibia	Humerus
RAPID COMPRESSION						
3	8.4	6.9	6.5	6.2	5.2	5.2
6	10.6	8.4	7.6	6.2	5.2	5.1
9	12.7	10.3	8.3	7.2	5.3	5.3
12	14.4	12.6	8.5	7.7	5.3	5.2
15	13.2	11.1	7.7	6.3	5.2	5.3
18	13.6	11.4	7.5	6.4	5.1	5.2
20	13.4	11.5	7.5	6.8	5.2	5.3
SLOW, STAGED COMPRESSION						
3	6.5	6.5	6.4	6.2	5.2	5.2
6	6.6	6.4	6.3	6.2	5.3	5.1
9	7.3	6.4	6.8	6.3	5.2	5.1
12	8.9	7.8	6.9	6.4	5.1	5.2
15	9.2	8.3	7.2	6.8	5.2	5.3
18	9.7	8.6	7.4	6.9	5.2	5.3
20	10.5	10.1	8.9	6.7	5.2	5.2
CONTROL (all ages)	6.5	6.4	6.4	6.2	5.2	5.2

mid-shafts of all experimental bones was identical to the control, which suggests the absence of collagen abnormality or necrosis in those areas. No changes were observed in the epiphyses of the proximal humerus, distal femur, or mid-shafts of all experimental tissues exposed to hyperbaric conditions for 3 times per week. However, the epiphyseal bone of the proximal femur and tibia in those mice exposed to either rapid or slow staged compression for 3 times per week showed an increasing hydroxylysine content. The time factor required to detect these changes was greater than 9 months using rapid compression and greater than 12 months using slow, staged compression.

These data strongly suggest that bone cells, in response to injury by repeated hyperbaric exposure, synthesize an embryonic, hyperhydroxylated collagen similar to that repair collagen synthesized in the healing of bone fracture.

Further evidence for the synthesis of a repair collagen is demonstrated in the reducible crosslink profile (Table III). In all control mice, a decrease in the amount of reducible crosslinks, hydroxylysinohydroxynorleucine (HylOHNLe) and hydroxylysinonorleucine (HylNLe), and precursor aldehydes as a function of age was observed. However, in all experimental bone, particularly those exposed to rapid compression, increasing amounts of HylOHNLe, HylNLe, and

TABLE III

Changes in the Ratios of Reducible Crosslink Precursors and Reducible Crosslinks of
Bone Collagen Based on Percent Activity (^{3}H/mg bone)

No. of Months	Precursor Aldehyde HylOHNLe + HylNLe	HylOHNLe : HylNLe
RAPID COMPRESSION		
3	10.2	8.2
6	12.5	8.7
9	15.6	9.8
12	15.8	9.8
15	16.2	10.3
18	17.5	10.6
20	18.8	11.1
SLOW, STAGED COMPRESSION		
3	8.6	6.8
6	8.8	6.9
9	10.5	6.9
12	12.1	7.2
15	13.3	7.5
18	14.6	9.2
20	16.1	9.9
CONTROL (all ages)	8.3	6.3

precursor aldehydes were consistently observed. Moreover, ion-exchange chromatography on selected samples for detection of collagen type showed the bone at both normal and elevated levels of hydroxylysine to be composed solely of a Type I bone collagen. No Type II cartilage collagen was detected.

Cartilage

Phosphocellulose chromatography of CNBr digests of cartilage samples demonstrated that the ratio of Type I to Type II collagen in selectively pooled samples of femoral head and knee cartilage increased dramatically with time in those mice exposed daily to rapid compression (Fig. 1). Approximately 20% of the cartilage was Type I after exposure for 3 months. At 6 months, the Type I collagen increased to 33%, at 9 months to 41%, at 12 months to 49%, and at 15, 18, and 20 months over 75% of the collagen was Type I. Age-matched controls consistently gave values of 15 to 20% Type I collagen. Identical cartilage samples taken from mice exposed to slow, staged compression exhibited only a slightly increased molecular polymorphism. Samples of humeral cartilage from mice exposed to either rapid or slow staged compression at all time intervals showed no increase in polymorphism over the age-matched controls.

Further support for an abnormal distribution of collagen Type as a function of daily exposure to rapid compression was provided by determination of
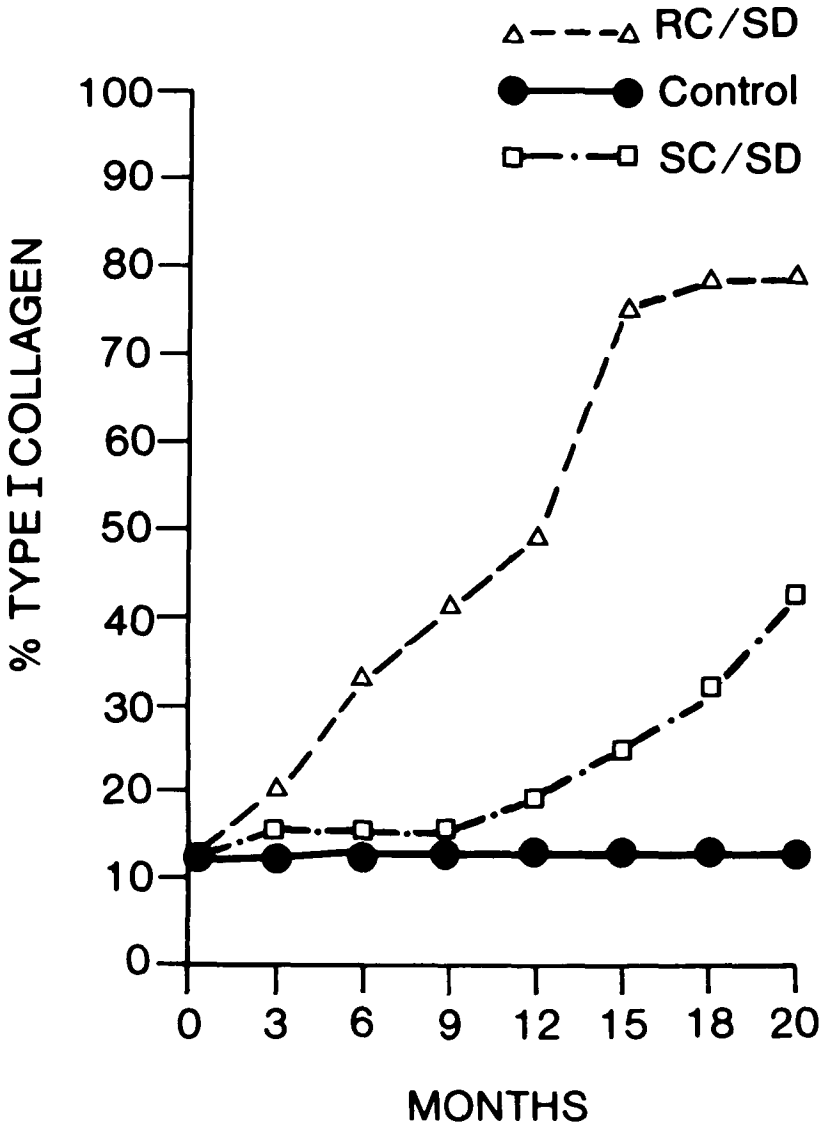
Fig. 1. Percent Type I collagen in femoral head and knee articular cartilage as a function of daily exposure to dysbaric conditions.

the hydroxylysine content of 50 micron serial sections of femoral head cartilage (orientation, surface to depth). Table IV clearly demonstrates a temporal correlation between the duration of exposure and the hydroxylysine content in cartilage sections. This phenomenon was corroborated by determination of the percentage of hydroxylysine glycosylation (Table V). The high levels of hydroxylysine and hydroxylysine glycosylation typical of a Type II cartilage collagen were severely diminished or absent in femoral cartilage exposed to daily

TABLE IV

Alterations in the Hydroxylysine Content of Cartilage Collagen as a Function of Daily
Exposure to Rapid Compression

(Values expressed as Residues of Hydroxylysine/Chain)

Depth—Microns	3	6	9	Months 12	15	18	20	Control (all ages)
1-50	24.2	22.5	18.6	15.6	13.6	13.3	13.0	25.8
51-100	23.6	22.3	18.7	14.8	13.2	13.0	12.9	24.5
101-150	22.8	22.4	16.8	13.6	13.4	12.8	12.7	23.7
151-200	22.4	21.8	14.7	13.4	13.2	12.7	12.8	22.5
201-250	17.4	16.4	14.5	12.8	12.8	12.5	12.4	18.7
251-300	15.7	15.3	13.7	12.6	12.6	12.5	12.3	12.1
301-400	14.9	13.7	13.5	12.5	12.5	12.4	12.2	8.7
401-500	11.8	11.2	13.4	12.3	12.5	12.2	11.9	6.9

TABLE V

Alterations in the Glycosylation of Hydroxylysine Residues in Cartilage Collagen as a
Function of Daily Exposure to Rapid Compression

(Values expressed as Percent Hydroxylysine Glycosylated per Total Hydroxylysine
Residues/Collagen Chain)

Depth—Microns	3	6	9	Months 12	15	18	20	Control (all ages)
1-50	62	61	54	46	31	24	19	63
51-100	60	60	54	41	29	22	18	62
101-150	58	60	43	36	24	20	17	62
151-200	56	58	42	28	20	18	17	60
201-250	54	41	39	25	19	18	17	59
251-300	30	27	26	20	18	17	17	38
301-400	23	20	19	18	18	17	17	25
401-500	18	17	18	18	18	18	17	19

rapid compression for 9 months or more. A similar pattern of changing hy-
droxylysine and hydroxylysine glycosylation was demonstrated in those tissues
exposed to slow, staged compression (Table VI). However, a considerably
longer time period of exposure to hyperbaric conditions was necessary to pro-
duce these changes.

Electrophoresis of the collagen CNBr peptides of consecutive slices of
femoral cartilage from mice exposed to rapid compression for 3, 6, and 9
months showed that the Type II collagen was predominantly at the surface and
the Type I collagen was in the deeper layers adjacent to the epiphysis. How-
ever, samples taken after 12 and 15 months of exposure times revealed a shift

TABLE VI

Alterations in the Hydroxylysine Content and in the Glycosylation of Hydroxylysine Residues in Cartilage Collagen as a Function of Daily Exposure to Slow, Staged Compression

(Values expressed as Residues of Hydroxylysine/Collagen Chain Percent Hydroxylysine Glycosylated/Hydroxylysine)

Depth—Microns	Hydroxylysine				% Glycosylation			
	15	18	20	Control	15	18	20	Control
1-50	23.8	23.6	17.3	25.8	54.2	54.1	32.1	63.7
51-100	23.4	22.4	15.5	24.5	51.3	49.3	28.6	62.8
101-150	21.8	20.6	14.7	23.7	34.8	29.7	26.8	62.5
151-200	20.8	20.2	13.9	22.5	31.4	30.1	20.4	60.3
201-250	18.0	18.3	13.7	18.7	30.0	27.6	19.6	59.6
251-300	15.6	15.8	13.2	12.1	29.6	24.3	19.3	38.2
301-400	12.6	12.9	12.8	8.7	26.2	21.4	18.5	25.8
401-500	13.3	13.7	12.6	6.9	18.4	17.2	18.1	19.2

in the distribution of collagen with the Type I collagen detected closer to the surface. In 6/16 mice exposed to rapid compression for 18 months, marked concave defects were noted in the articular surface. Electrophoresis of consecutive slices of these samples showed that the Type I collagen was the sole collagen at the surface, with a mixture of Types I and II collagens in the deeper layers. This finding was supported by increased hydroxylysine content of the tissue with depth. Amino acid analyses of surface slices from two such mice clearly demonstrated that the Type I collagen was hyperhydroxylated with a hydroxylysine value calculated at 12.7 and 13.4 residues/chain, respectively.

CONCLUSION

The present study demonstrates that marked changes in collagen synthesis, crosslinking, and distribution of genetic types accompany the onset, progression, and severity of bone and cartilage necrosis induced by exposure to hyperbaric conditions. Although decompression sickness was not observed in any of the experimental mice used in this study, the rate of compression and the frequency of exposure clearly influenced the appearance and progression of abnormal alterations in collagen metabolism.

The most dramatic abnormalities observed in bone collagen were an increased hydroxylysine level and an increase in the amount of reducible crosslinks and precursor crosslinks in the epiphysis. The epiphyses of the proximal femur and tibia were the areas most strikingly affected by exposure to hyperbaric conditions, whereas the epiphyses of the distal femur and the proximal and distal humerus were only slightly affected. The cartilage of the femoral head and knee showed a striking increase in collagen polymorphism caused by the marked synthesis of a Type I collagen.

We suggest that a repair, hyperhydroxylated Type I collagen is synthesized in response to exposure to hyperbaric conditions. However, unlike repair collagen that is synthesized and then resorbed after fracture healing, the collagen synthesized in response to injury by hyperbaric exposure fails to be contained at the bone-cartilage junction and continues to invade the overlying articular cartilage.

It was apparent that in the early stages, collagen metabolism in the articular cartilage remained viable and functioned normally despite the development of necrosis in the epiphyseal bone. Thus, the findings of this study strongly suggest that the initial response to connective tissue injury by hyperbaric exposure is the synthesis of a repair tissue containing hyperhydroxylated Type I collagen. In addition to resorbing and destroying the epiphyseal bone, the invasion of this repair tissue into the cartilage contributes to the development of osteoarthritis and ultimate destruction of the adjacent joint.

Although extrapolation of the findings of this small animal study must be made cautiously, the synthesis and fate of an abnormal repair tissue may have potentially serious implications for human connective tissue function in individuals subjected to hyperbaric exposure.

Acknowledgment

References

1. Grant ME, Prockop DJ. The biosynthesis of collagen. N Engl J Med 1972:286–294.
2. Kivirikko KI, Risteli L. The biosynthesis of collagen and its alterations in pathological states. Med Biol 1976;54–159.
3. Prockop DJ, Kivirikko KI, Tuderman L, Guzman NA. The biosynthesis of collagen and its disorders. N Engl J Med 1979;301–313.
4. Brickley-Parsons DM, Glimcher MJ. Reducible crosslinks of type I and type II collagens of chicken cartilage. FEBS Lett 1976;65:373.
5. Eyre DR, Brickley-Parsons DM, Glimcher MJ. Predominance of type I collagen at the surface of avian articular cartilage. FEBS Lett 1977;85:259.
6. Richmond V, Miller BS, Stegall PJ, Smith KH. Bone collagen in dysbaric osteonecrosis. Clin Orth 1977;126–292.
7. Smith KH. Investigations of hematologic and pathologic response to decompression. Final Technical Report, Office of Naval Research, 1978.
8. Chryssanthou CP. Experimental dysbaric osteonecrosis. Undersea Biomed Res 1976;3–67.
9. Piez KA, Weiss E, and Lewis MS. Separation and characterization of the α and β components of calf skin collagen. J Biol Chem 1960;235–1987.
10. Brickley-Parsons DM, Glimcher MJ. The biosynthesis of collagen crosslinks in vitro. In Proceedings of 2nd annual workshop on vitamin D. Weisbaden, Germany: Walter DeGruter Co, 1975:1–24.
11. Eyre DR. Collagen heterogeneity. In Burleigh PMC, Poole AR, eds. Dynamics of connective tissue macromolecules. Amsterdam: North Holland, 1975:394.
12. Smith CN, Linsenmayer TF, Newsome DA. Synthesis of type II collagen in vitro by embryonic chick neural retina tissue. Proc Nat Acad Sci USA. 1976;73:4420.
13. Eyre DR, Muir H. Collagen polymorphism: two molecular species in pig intervertebral disk. FEBS Lett 1974;42–192.

A DETAILED HISTOLOGICAL AND RADIOLOGICAL CONTROLLED STUDY OF SELECTED BONES FROM DIVERS

C. R. Weatherley, W. M. Park, M. Haddaway, and I. Calder

Inadequate decompression may give rise to decompression sickness and dysbaric osteonecrosis, and for this reason an accurate record of both conditions forms a valuable index of the safety of the decompression procedures being used. There are, however, recognized difficulties in recording the true incidence of both conditions, and in type 1 decompression sickness not the least of these is the transient and sometimes trivial nature of the symptoms experienced. By contrast, the lasting nature of the changes that may be produced in bone are at least, when present, definitive. Collection of data on the incidence of dysbaric osteonecrosis combined with particulars of diving experience is, therefore, at the present time an important aspect of the safety of deep diving.

In England details of the diving history and medical records of many divers are contained in the M.R.C. Central Registry in Newcastle-Upon-Tyne and are updated each year from forms completed at the time of each diver's obligatory medical examination for fitness to dive. At these medical examinations a full radiographic skeletal survey is also made, as recommended by the M.R.C., of those areas of the skeleton which it is known may be affected by dysbaric osteonecrosis. Subject to the radiographs being of good quality they are then viewed by a panel of radiologists experienced in the interpretation of such radiographs. Even with such a planned approach to the detection of dysbaric osteonecrosis, the recorded incidence of the condition can be only as accurate as the method used for its diagnosis, which at the present time is radiology.

It is known that the characteristic radiological changes of bone necrosis from whatever cause may take some months to develop but it is also possible

that in some cases they never appear. In this context it is of interest that in one study, scanning changes were reported immediately postdive in 6 out of 14 divers, although subsequently only one man developed radiological evidence of dysbaric osteonecrosis (1). It is also reported that in conditions of chronic limb ischemia in man, massive bone necrosis may be found on histological examination in the presence of normal radiographs (2). While acute ischemia in a previously healthy limb may be a different entity from chronic ischemia, nonetheless, extensive cortical necrosis has been found in the long bones of minipigs subjected to rapid decompressions and in which the radiographs were normal (3) (Fig. 1).

Cognizant of the limitations of conventional radiology, recent research has considered the possible role of biochemical methods of detecting bone necrosis (4,5). The possible value of such methods, however, would in part be related to the extent of bone involved, be it cortical, intramedullary, or both. For this reason and the others that have been summarized, a controlled histological and radiological comparative study has been carried out on bones obtained from divers at autopsy examination, and particular attention has been paid to the subject of possible cortical changes. Finally, the complete findings have been reviewed and related to the diving history of the men involved.
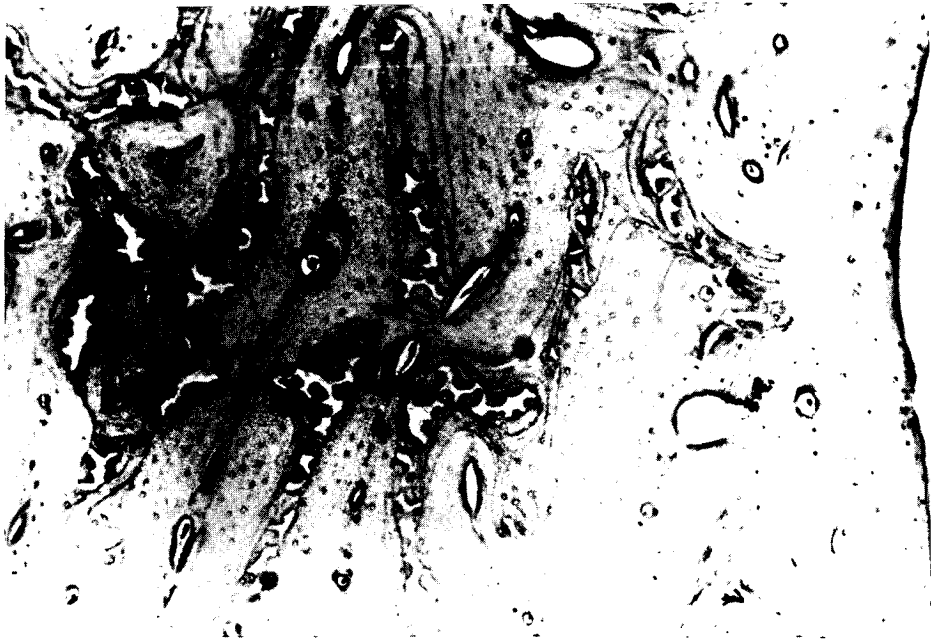
Fig. 1.   Photomicrograph of a transverse section of the femoral cortex in a minipig subjected to rapid decompressions. There is a confluent and almost complete absence of osteocytes except at the endosteal border.

MATERIALS AND METHODS

In this initial report on what is a continuing study, selected bones obtained from three divers at autopsy examination have been the subject of detailed studies. Bones from two other men, with no history of exposure to pressure and of similar age and physique, have been used as controls. One femur from each of the five men has been examined together with a humerus in one diver and a humerus and a tibia in the controls.

The three divers all had current medical certificates of fitness to dive and no evidence of dysbaric osteonecrosis on their last skeletal survey; all died as a result of diving accidents. Some details of the diving history of each of these men was available through the M.R.C. Central Registry in Newcastle-Upon-Tyne. Both controls in life had been regarded as fit men and neither had a history of serious illness. One died from a head injury sustained in a car accident and the other died suddenly from what was diagnosed at post-mortem as a myocardial infarction. In the absence of ante-mortem evidence of bone pathology in either the divers or the controls, the side of the femur and the other bones was selected at random. A summary of the salient facts in these cases is given in Table I.

All bones were preserved in formalin and subjected to the same sequence of investigations. This began with an antero-posterior and a lateral radiograph following which the total length of each bone was measured. Four transverse sections, 7-mm thick, were then cut at distances of 20, 40, 60, and 80% along the shaft of the bone and a longitudinal section, also 7-mm thick, was cut from the intervening lengths of bone. This gave a total of nine sections for

TABLE I

Summary of Subjects and Bones Examined

Subjects	Age	Cause of Death	Bones Examined	Diving Experience
Diver 1	28	diving accident	femur humerus	2 years saturation diving; maximum recorded depth, 183 m; history of type 1 DCS.
Diver 2	42	diving accident	femur	18 years; 608 hours in saturation (3 dives); maximum recorded depth, 130 m; no history of DCS.
Diver 3	35	diving accident	femur	15 years; no history of DCS.
Control 1	22	head injury	femur tibia	None
Control 2	40	myocardial infarction	femur humerus	None

DCS is decompression sickness.

each bone, each of which was subjected to microfocal radiography. In addition to the total length of each bone, measurements were also made of the thickness of the cortex and the overall diameter of the bone at the levels of the transverse sections. In this way it was hoped to exclude abnormal cortical thickening which might have been missed on radiological examination. The sections were prepared for histological examination by first decalcifying them with Custers fluid, using radiology to determine the completeness of the process. Each bone section was then cut into technically manageable sizes and embedded in paraffin wax; histological sections, which were 6–8 microns in thickness and were stained with hematoxylin and eosin, were prepared for examination.

RESULTS

All bones appeared normal on naked eye examination as did the cut surfaces of the cortex and marrow after the bones had been sectioned. The articular cartilage in both divers and controls was of equal thickness and no abnormality was detected on cortical measurement. The only abnormalities found on radiological examination were a cyst in the femoral neck of *Diver 1* and a bone island in the femoral neck of *Diver 2*. On histological examination both these structures were identified and in each case the surrounding bone appeared normal. In both divers and controls, scattered osteocyte loss was seen in both cortical and cancellous bone (Fig. 2). Thrombosis and recanalization of
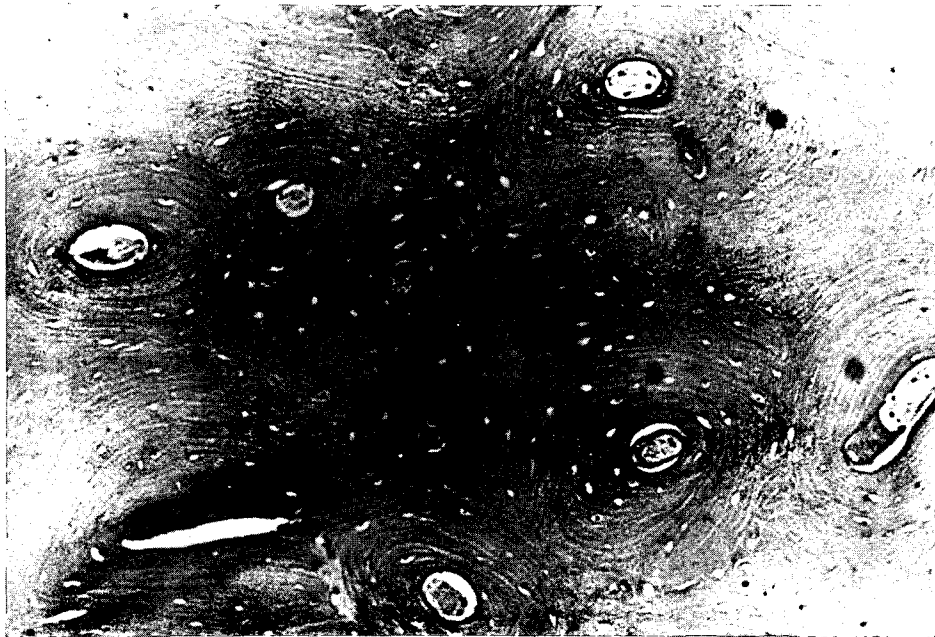
Fig. 2. Photomicrograph of a transverse section of the femoral cortex in *Diver 1*. Osteocyte loss is scattered and does not conform to any clear anatomical distribution (X125).

a few vessels was found in the cortex of *Diver 1* and in *Diver 2* certain of the vascular spaces appeared to contain micro-organisms. While the former changes were clearly ante-mortem, the latter were believed to represent changes occurring at, or soon after, death.

DISCUSSION

With the exception of a bone cyst in the femoral neck in *Diver 1* and a bone island in the femoral neck of *Diver 2*, no difference was found on radiological examination between the bones of the three divers and those of the two controls. The question of whether bone cysts and bone islands represent a manifestation of dysbaric osteonecrosis has previously been a matter of some controversy. However, in a most comprehensive study on this subject, comparing 100 British Royal Navy divers with 100 nondived controls, such lesions were found with equal frequency in both groups and were considered, therefore, not to represent evidence of dysbaric osteonecrosis (6).

Apart from confirming the presence of the bone cyst and the bone island, histological examination of the bones in this study did not reveal any marked difference between divers and controls. Thrombosis of small vessels may be found in many tissues and is not unusual in cortical bone. The presence of what would appear to be micro-organisms is unusual, but in this case may reflect delays in fixation of the tissue following death. The osteocyte loss noted particularly in the cortex of the bones of both groups was not associated with evidence of marrow infarction, new bone formation, or structural changes. This and the nondiscrete and nonanatomical nature of the loss would not appear, therefore, to support a specific ischemic etiology other than perhaps that normally occurring with age (7).

Whether cortical necrosis of an abnormal degree may occur in divers and be present in the absence of radiological changes has not, therefore, been resolved by these studies. However, such a condition might, at least in some cases, offer a reasonable explanation for the known discrepancies which may occur between the results of bone scanning and radiography. For this reason, further studies are in progress and particular attention is being paid to bones with known lesions of dysbaric osteonecrosis. From these additional studies it would be hoped that a constructive appraisal could be made of the value of biochemical indicators of bone necrosis, which, in the absence of changes in this study, has not been possible.

In conclusion, the results of the histological examination of selected bones from the divers in this study was not at variance in any way with the results of the radiological assessment. Insofar as this might apply to the other bones of these divers, which were not examined histologically but were assessed as radiologically normal, we may infer that a diving history of up to 18 years and a history of saturation exposure is not incompatible with at least no permanent extensive skeletal damage.

References

1. Harrison JAB, Pearson RR, MacLeod MA. Radioisotopes as an aid to the study of dysbaric osteone-crosis. In: Early diagnosis of decompression sickness. Report No. UMS 7–30–77. Bethesda, MD: Undersea Medical Society, Inc., 1977:227–298.
2. Sherman MS, Selakovich WG. Bone changes in chronic circulatory insufficiency. J Bone J Surg 1957;39A:892–901.
3. Weatherley CR, Gregg PJ, Walder DN. Dysbaric osteonecrosis-experimental studies with the minipig. Med Aeronaut Spat Med Subaquat Hyp 1977;64:399–40.
4. Gregg PJ, Walder DN. Early diagnosis of dysbaric osteonecrosis. In: Early diagnosis of decompression sickness. Report No. UMS 7–30–77. Bethesda, MD: Undersea Medical Society, Inc., 1977:268–276.
5. Weatherley CR. Hydroxyproline excretion in the early detection of bone necrosis. In: Evans A, Walder DN, eds. Aseptic bone necrosis—proceedings of a symposium. London: CIRIA, 1977.
6. Davidson JK, Harrison JAB, Jacobs P, Hilditch TE, Catto M, Hendry WT. The significance of bone islands, cystic areas and sclerotic areas in dysbaric osteonecrosis. Clin Radiol 1977;28:381–393.
7. Frost HM. In vivo osteocyte death. J Bone J Surg 1960;42A:138–143.

THE EFFICACY OF SPINAL ANESTHESIA AT HIGH PRESSURE

H. F. Nicodemus, H. McElroy, and R. Levy

Pressure antagonizes general anesthesia induced with inhaled anesthetic gases or with intravenous agents that are widely varied in nature. Antagonism is manifested by increased requirements or shortened duration of effect, or both. Similarly, pressure also antagonizes the nerve conduction block caused by some local or general anesthetics (1,2). It is therefore important to determine how much pressure may influence the dose requirement and the duration of the block if spinal anesthesia is to remain a viable alternative to general anesthesia under pressure.

MATERIALS AND METHODS

Male guinea pigs (300–500 g) were employed in this study. Spinal anesthesia was induced with tetracaine hydrochloride crystals dissolved in 5% dextrose in lactated Ringer's solution. Under clinical conditions, to make the anesthetic solution heavier than cerebrospinal fluid, one uses 5% dextrose in water as the vehicle for the active ingredients. Instead, we used 5% dextrose in lactated Ringer's solution because we feared that solutions with electrolyte contents too different from that of the plasma or cerebrospinal fluid might influence ionic transfer across the nerve membrane, especially during hyperbaria, and therefore change the recovery time. To assure the same quality of the anesthetic, we prepared from the same parent solution aliquots of 5 mg/mL, 2.5 mg/mL, 1.25 mg/mL, and 0.625 mg/mL in equal volumes. To each 4 mL of the solution, we added 0.2 mL of 1:1000 epinephrine. The concentration of the anesthetic solution was not known at the time of use. Each concentration was studied in groups of four guinea pigs at a time, either at 1 ATA of air (surface control) or at 32 ATA helium with 0.35 O_2.

Lumbar puncture was performed under general anesthesia (halothane-air) at the first or second lumbar vertebral interspaces. A 2-cm 23 G needle was introduced into the spinal canal at 1 cm depth where 0.1 mL of the anesthetic solution was injected. We made no attempt to obtain cerebrospinal fluid. The onset of the spinal block was instantaneous, manifested by loss of abdominal muscle tone and loss of urinary sphincter tone. Within minutes, the animals emerged from the general anesthesia. Only those with bilateral motor blocks were included in the study.

To evaluate recovery of muscle function, we placed blocked animals in an electrically driven drum that rotates at 4–5 rpm when activated. The drum, divided into sections, was located inside a 180-L hyperbaric chamber. Evaluations were carried out at 5- to 10-min intervals. The recovery was considered complete when three criteria were satisfied: (a) motor function—ability to sustain posture for at least one rotation, (b) strength—ability to lift and support caudal half of the body off the floor of the rotating drum, and (c) proprioception—ability of the hind extremities to follow the rotation by taking alternate steps, as in normal gait.

The experimental conditions, except for the pressure, were similar for both groups. For the control group, the door of the chamber was left slightly ajar, and the fan for the carbon dioxide scrubber was kept running to simulate the noise of the compression. In addition, short bursts of oxygen under pressure were allowed to flow into the chamber periodically. Two days after the controls' recovery from the initial spinal block, the animals were reblocked and compressed. The groups studied under pressure were compressed at 3 ATA/min as previously described (3). When all of the animals had recovered function, or after 3 h at 32 ATA, they were subjected to euthanasia by rapid decompression.

Statistical handling of the data required natural log transformation of the variables (duration and doses) to make the distribution more homoscedastic. Comparison of the duration was by S-test derived from the regression analysis.

RESULTS

A total of 113 observations were made. The mean duration of spinal block in each dose (concentration) and condition are presented in Table I. Increasing the dose of anesthetic agent consistently produced longer-duration

TABLE I

Duration of Spinal Block

Concentration (mg/mL)	Mean Duration (min ± SE)	
	Surface Control	32 ATA
0.625	63.1 ± 4.5	55.8 ± 5.1
1.25	76.8 ± 4.7	72.4 ± 13.4
2.5	92.4 ± 4.8	89.6 ± 4.5
5.0	118.0 ± 8.4	125.2 ± 6.2

spinal block. The effect of pressure was not clinically or statistically signifi-
cant, $P > 0.3$. Up to 32 ATA, durations of spinal anesthesia induced with the
same doses were close to or identical with those on the surface. Figure 1 is a
graphic presentation of the effect of doubling the concentration of the solution
on the duration of spinal block.

DISCUSSION

The anesthesia induced in the experimental animals was patterned as
closely as possible to clinical practice. Recovery was surprisingly complete for
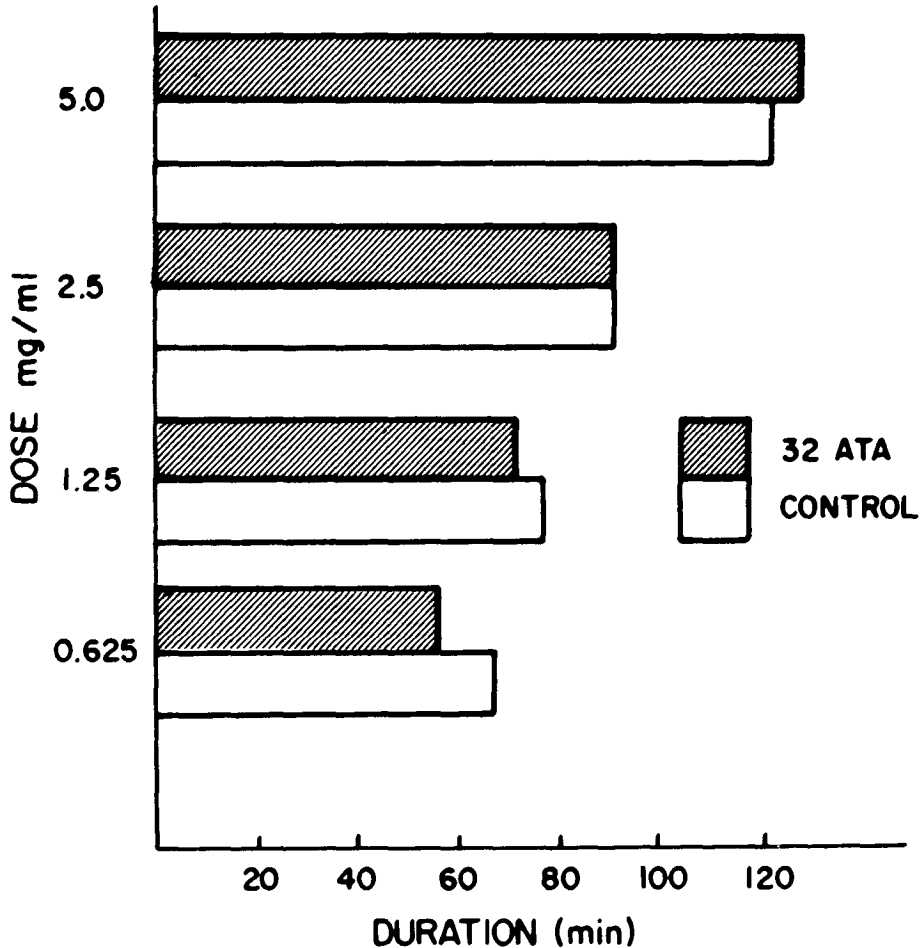
Fig. 1.   The effect of doubling the dose (concentration) of the drug on the duration of spinal bloc.

most of the guinea pigs except for four that showed residual nerve damage (poor rectal sphincter control), either from trauma during the lumbar puncture or infection. These four animals were not reused.

Our findings show that spinal anesthesia is a practical alternative to general anesthesia under hyperbaric conditions. There is neither an increase in requirements nor a change in the duration of the block. We suspected that spinal and other techniques of conduction anesthesia that bathe the nerves in the anesthetic solution would be effective under pressure. We reasoned that the concentrations of the drug employed for any of these techniques are much larger than those required to cause nerve block. The concentrations employed should mask whatever increased requirement high pressure might induce.

The findings reported here are not necessarily at variance with those of Kendig et al. (1) and Roth et al. (2) because the experimental methods are different. These investigators used isolated nerve preparations, whereas we used intact animals with more complicated pharmacodynamics. The end-point in their studies was a return of electrical conduction toward base line to show antagonism, whereas, our criteria may have been too strict to show similar grades of pressure antagonism. Neural conductivity may have recovered long before muscular strength and proprioception, because these functions require a more refined modulation of nerve impulse through a system of feedback mechanisms.

Based on our data, we conclude that spinal anesthesia with tetracaine, as clinically practiced, is not antagonized by pressure up to 32 ATA and therefore is applicable to surgical procedures that are usually performed under spinal anesthesia at surface conditions. Based on the obtained data, we cannot make specific recommendations about the safety of spinal block under pressure.

Acknowledgments

References

1. Kendig JJ, Cohen EN. Pressure antagonism to nerve conduction block by anesthetic agents. Anesthesiology 1977;47:6–10.
. Roth SH, Smith RA, Paton WDM. Pressure antagonism of anesthetic-induced conduction failure in frog peripheral nerve. Br J Anaesth 1976;48:621–628.
3. McCracken LE, Nicodemus HF, Tobey RE, Bailey RC. Ketamine and thiopental sleep response in hyperbaric helium oxygen in guinea pigs. Undersea Biomed Res 1979;6(4):329–338.

PART VIII. DISCUSSION: HEALTH HAZARDS

D. H. Elliott, *Rapporteur*

Together with the "Health Effects" poster presentations this clinical session provided a particularly broad range of topics, which are reflected in the variety of subjects discussed.

It was confirmed by Dr. Miller that the antibiotics used in their study were not oto-toxic. Microphonics and click stimuli were among other parameters studied but it was agreed that different techniques would have been needed to pinpoint the damage to hair cells.

Dr. Daily recommended that samples of water be taken before any diving operations begin in polluted water. Knowledge of the antibiotic sensitivities of the pathogens found could be invaluable should a diver subsequently become infected. He stated that colonization of the diver might persist for some hours postdive, but probably would become important only in the case of some skin wound or a ruptured tympanic membrane.

Dr. McCallum commented on the importance of the unusual experiences associated with the salvage of toxic organic-lead by saturation divers. Dr. Marroni confirmed that all surface personnel on this project also underwent appropriate health monitoring and that the Italian National Research Council had found no significant quantities of lead in the sea water around the wreck.

Dr. Parsons stressed that their findings in mice were not necessarily relevant to pathogenesis in man.

Dr. Nicodemus stated that their experiment was not designed to investigate temperature effects nor specifically to look for any increased anesthetic function.

Discussion on other papers was curtailed by lack of time.

857

MICROBIOLOGICAL STUDIES ON ACUTE OTITIS EXTERNA IN SATURATION DIVERS

S. R. Alcock

A saturation dive establishes a uniform pressure system between a diver's living quarters and the depth at which he works. Typically, a team of divers live on the surface in a complex of several linked pressure chambers, and a detachable pressurized diving bell transports them to and from the sea bed as required. A diver may live for several weeks within the complex before his eventual decompression.

Otitis externa is the major infection problem associated with all forms of diving (1,2). It is probably the commonest cause of morbidity during saturation dives, and in this environment the symptoms are frequently incapacitating (2-4).

Local trauma, depletion of skin lipids, and prolonged exposure to high humidity and temperature are all thought to predispose to otitis externa; high humidity is particulary important (5-7). A critical factor in the pathogenesis of the disease appears to be the ratio of gram-positive to gram-negative bacteria in the ear canal. The normal flora is predominantly gram-positive—mainly staphylococci and *Corynebacteria;* that in otitis externa is predominantly gram-negative, mainly Enterobacteriaceae and *Pseudomonas aeruginosa* (8-10). Hydration of the skin of the ear canal probably predisposes to this change (7,11). *P. aeruginosa* is the gram-negative species most often implicated in overt disease (8,9).

During 1974-75 two saturation dives in the North Sea were terminated because of outbreaks of incapacitating otitis externa, and others were disrupted. This paper discusses data obtained during seven subsequent dives subjected to microbiological monitoring and control.

METHODS AND MATERIALS

Chamber Complexes

Two complexes (Fig. 1, *T* & *R*) situated on different ships were studied at different times. Individual chambers were named after their diameter in milmeters. Each chamber had an "S.A.S." area, which contained the lavatory, shower, and wash-basin for that chamber and was very cramped. In the *R* complex this area was separated from the rest of a chamber by an air lock (usually open during the dives). In the *T* complex there was no separation in the 1500 chamber and only a loose-fitting screen in the 2500. In both complexes the 2500 was the main living chamber and housed 6–7 divers. An oxyhelium atmosphere (Po$_2$ 400 mbar) was maintained at 35°C, and recycled over 7–8 min through tanks of silica gel, carbon, and soda-lime,

Dive Monitoring and Control

Four dives (*T*$_1$–*T*$_4$) lasting 10, 5, 9, and 30 days and involving a total of 25 divers were monitored in the *T* complex. Three dives (*R*$_1$–*R*$_3$) lasting 26, 9,
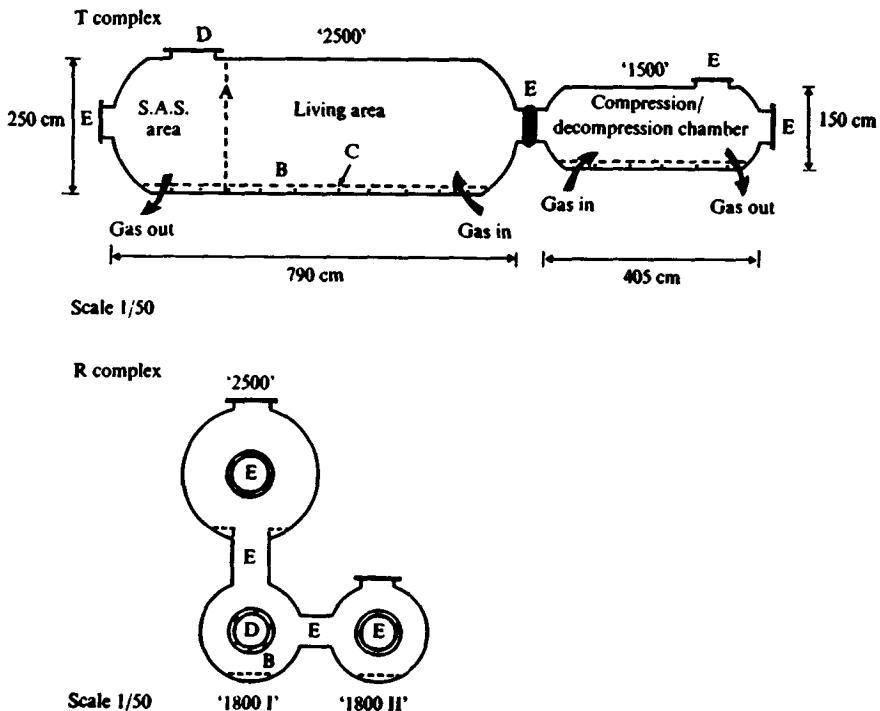
Fig. 1. Arrangment of pressure chambers in the *T* and *R* living complexes. *A, T complex*: partition with loose-fitting door; *B*, false floor; *C*, heating elements; *D*, diving bell keys on here; *E*, air locks.

and 30 days and involving a total of 33 divers were monitored in the R complex. At any one time, a chamber complex housed from 5–8 divers. Work was at a depth of 75–85 m and divers spent 4–8 h each day on the sea bed for about 9 of every 14 days in saturation. Decompression occupied 50 h.

The divers' ears and the chamber complex were swabbed before each dive and at least every 2 days thereafter. Divers were not admitted to the dives if gram-negative bacilli were isolated from their ears in the predive screen. In T_1, however, one diver, from whose ears P. $aeruginosa$ had been grown, was inadvertently allowed into the complex and not removed for 3 days.

During a dive, those divers from whose ears gram-negative bacilli had been isolated were treated every 8 h with ear drops containing gentamicin sulphate 0.3% (w/v) and polymyxin B sulphate 0.5% (w/v). In dive T_1 only, a cream was used containing the same antibiotics at the same concentration. Infected divers were decompressed as soon as operational needs allowed.

A high standard of personal and chamber hygiene was enforced during the dives. During T_1 and T_2 Savlon (Imperial Chamicals Industries Ltd., England) was used to disinfect the chambers, thereafter Panacide (dichlorophen; B.D.H. Chamicals Ltd., England) 200 parts of million was used. In all the dives except T_1, sheets and towels were changed every 2 days.

In the R system only, divers routinely used prophylactic ear drops containing boric acid, alcohol and glycerol.

Bacteriological Techniques

Swabs were plated out, before and after incubation for 12 h in thioglycollate broth, using heart infusion agar (Difo) + 10% horse blood, and Mac-Conkey's agar (Oxoid). Only swabs from T_1 were cultured for fungi. Pseudomonads were identified after Cowan and Steel (12), with additional tests for growth on milk agar (13), 6% sodium chloride, and 1% tetrazolium chloride (14). Nonpseudomonad isolates were fully identified in T_1, but thereafter were classified on the basis of colonial appearance and growth characteristics. All nonlactose fermenting gram-negative bacilli were regarded as putative pseudomonads. Antibiotic sensitivities were determined by the disc method on Mueller Hinton agar of calcium and magnesium content 75 mg/L and 32 mg/L, respectively (15,16). Oxoid discs containing 10μm of gentamicin or colomycin (Polymxin E) were used, and a zone of inhibition of less than 2 mm diameter on either side of the disc was taken to indicate resistance.

RESULTS

Divers' Ear Swabs

The pattern of data illustrated in Fig. 2 is representative of that obtained in all of the dives studied. Many divers had used prophylactic or antibiotic ear

Divers	Ear L or R	Pre-dive	1	2	3	4	5	6	7	8	9
				Duration of Saturation (days)							
A	L	+		+		+	TREAT*	●	N		OUT
A	R	+		+		▲	TREAT	●	N		OUT
B	L	+		+		+	TREAT	N	OUT		
B	R	N		+		●	TREAT	+	OUT		
C	L	+		+		●	TREAT	N	OUT		
C	R	+		+		●	TREAT	N	OUT		
D	L	+		+		+		+	OUT		
D	R	+		+		+		+	OUT		
E	L	+		+		+ ▲	TREAT			OUT	
E	R	+		+		+ ●	TREAT			OUT	
F	L					+	IN		+ ●	TREAT	OUT
F	R					+	IN		+ ●	TREAT	OUT
G	L					N	IN		●		TREAT OUT
G	R					N	IN		+		TREAT OUT

Fig. 2. Ear flora of divers during dive R_2: +, normal gram-positive flora; ▲, nonpseudomonad gram-negative bacilli; ●, *Pseudomonas aeruginosa*; N, no bacteria isolated; L, left; R, right; *begin 7 days treatment with antibiotic drops.

drops, or both, during previous dives. Most had been subjected to earlier bacteriological sudies, and divers were not considered for saturation work while gram-negative bacilli could be isolated from their ears.

Divers entered saturation with either normal or no detectable ear flora (Table I). Staphylococci predominated, and all 29 isolations of this organism sampled before T_1–T_3 were coagulase negative.

During saturation, gram-negative bacilli were isolated from the ears of 72% of the 54 divers who lived in either the T or R complexes for at least 7 days, or who were decompressed within this period because of abnormal ear flora. (The corresponding figure if all divers are considered irrespective of their time in saturation is 67%.) The ears of 85% of infected divers became colonized with gram-negative bacilli within the first 6 days of the dive. In 46%

TABLE I

Ear Flora of 57 Divers Swabbed Before Entering Saturation

Bacterial Genus	Isolation Rate* %
Staphylococci	60
Corynebacteria	6†
Pseudomonas	2‡
No detectable flora§	38

*Expressed as a percentage of the number of swabs cultured (114).   †Mixed growth with staphylococci.   ‡ One diver admitted to T_1 in error.   §No colonies observed after plating out swabs incubated in thioglycollate broth for 12 h.

of infected divers the initial isolations were made from both ears, and in 89% of these the two ears were colonized with similar bacteria.

P. aeruginosa was isolated at some time from 84% of infected divers, and was the first isolation of gram-negative bacilli in 50% of cases. Nonpseudomonad gram-negative bacilli isolated from divers' ears (and from the chambers) contained a high percentage of members of the Enterobacteriaceae (Table II).

TABLE II

Gram-Negative Bacilli Other Than Pseudomonas aeruginosa Isolated from Divers and Saturation Chambers

Saturation Complex and Dive	Site Swabbed	Number of Isolations	Percentage Distribution of Isolations According to Family and Genus					
			Enterobacteriaceae				Alcaligenes*	Unidentified N.L.F.
			Escherichia	Klebsiella	Proteus	Enterobacter		
T_1†	Divers' Ears	13	0	8	23	0	61§	8
	Chamber	30	13	13	7	30	3	33
R_1–R_3‡	Divers' Ears	37	24	19	22	—	—	35
	Chamber	74	38	26	3	—	—	34

N.L.F. is nonlactose fermenting organism;   *As defined by Cowan and Steel (12);   †Identified culturally and biochemically as described in Methods;   ‡Identified by growth and colonial characteristics only;   §Isolated from the ears of 4 of the 6 divers who participated in T_4.

There appeared to be no significant difference in results between divers using the two complexes, and between divers entering the chambers at the beginning of a dive and those who entered during a dive. Gram-positive ear flora detected in the predive screen was usually retained during the dive, irrespective of subsequent colonization with gram-negative bacilli. An absence of detected ear flora in the predive screen did not predispose to infection.

Seven divers never entered the water but remained in the chambers as tenders. Three became infected, two with *P. aeruginosa*. Actual diving with direct wetting of the ear canal was thus not essential for infection, although it may have been a contributory factor.

Gram-negative bacilli were not isolated from the ears of 9 divers using the *T* complex and 10 using the *R* complex. The ear floras identified in these divers before they entered saturation showed no change during the dives, and were similar to the predive floras of divers who subsequently became infected. The absence of detected gram-negative colonization was not due to unusually short periods of exposure to the saturation environment: 12 divers spent 9 or more days and 9 spent 14 or more days in saturation.

Ear Pain

Five (25%) of the divers using the *T* complex and five (15%) of those using the *R* complex developed ear pain. Gram-negative bacilli were isolated from the ears of all these divers, and *P. aeruginosa* from eight of them. The pain developed within zero to 4 days of taking the ear swab from which gram-negative bacilli were isolated for the first time and only affected two divers already under treatment, both within 24 hours of starting therapy. It was managed by mild analgesics, antibiotic ear drops, and prompt decompression; it was never incapacitating.

Twenty-one divers (54% of all infected divers) did not start decompression for 5 or more days after taking the ear swabs from which gram-negative bacilli were first isolated. All but two of them were treated, and only one (who was treated) suffered pain. These data, combined with the finding that only two of all treated divers suffered pain, suggest that, with treatment, infected divers can remain in saturation and incur little risk of pain.

Effect of Treatment on Ear Flora

Of the infected divers 35 (90%) were treated, 34 within 12–48 h of taking the diagnostic swab. Most were treated for 8–10 days and decompressed within 2–8 days. No bacteria were isolated from 28 of 34 swabs taken about 24 h after beginning treatment and 7 h after an application of antibiotic ear drops. A similar result was obtained from swabs taken throughout the courses of treatment. (All of these swabs were probably contaminated with antibiotics from the ear canal.) Sampling thereafter was unsatisfactory, but data from 19 divers suggested that after treatment, and without further diving, ears remained free of detectable gram-negative bacilli.

Resistance to gentamicin and polymyxin was not a problem in the dives where antibiotic drops were used. However, in the Dive T_1, where the same antibiotics were administered as a cream, 3 of the 25 ear isolations of *P. aeruginosa* were resistant to gentamicin. These resistant strains were isolated from 2 divers and were all of serotype 11. In one diver, the first resistant isolate was made after 2 days of treatment for an ear infection with *P. aeruginosa*, also of serotype 11, and originally sensitive to gentamicin. The other had had no previous isolations of *P. aeruginosa*, but had been treated for 5 days for a nonpseudomonad ear infection.

The routine use of prophylactic ear drops by divers in the R complex failed to prevent either changes in ear flora or the occasional case of pain.

Chamber Swabs

During the dives, 377 swabs were taken from the main living (2500) chambers of T and R complexes. The pattern of contamination of these chambers with gram-negative bacilli is shown in Fig. 3. The S.A.S. regions of the chambers (lavatory, wash basin, shower, and the adjacent chamber) showed
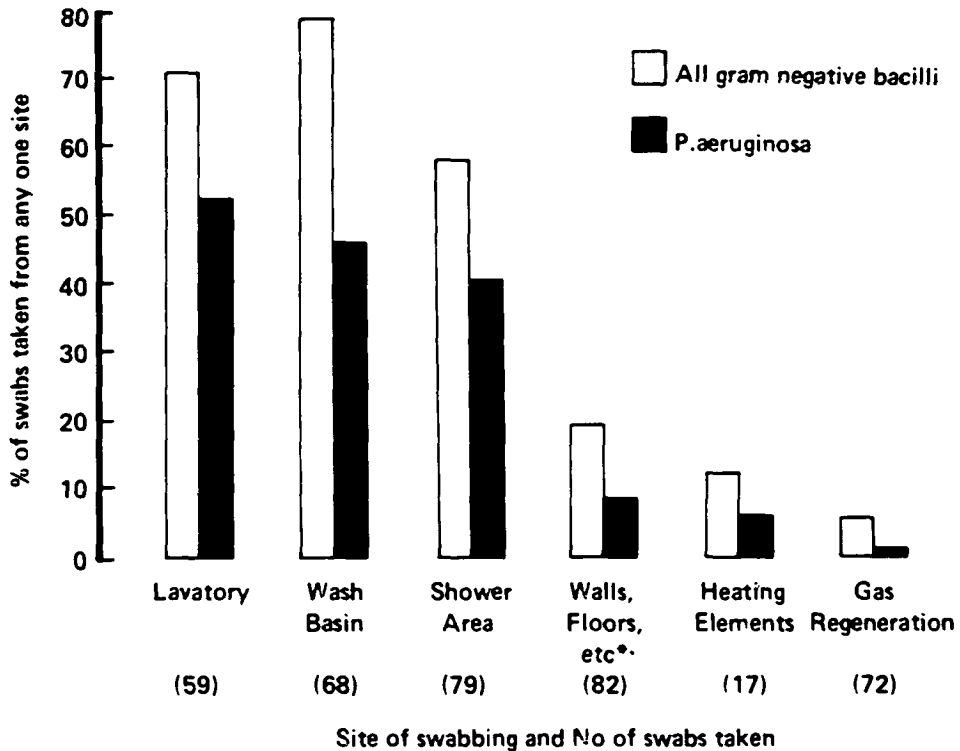
Fig. 3. Isolations of gram-negative bacilli from the 2500 chambers of the T and R complexes. *Excludes swabs from the S.A.S. area.

heavy contamination with *P. aeruginosa* and other gram-negative bacilli within 1–2 days of starting a dive and continuously thereafter. Elsewhere only scattered isolations were made, the gas regeneration systems remaining particularly clear. The same pattern was observed in the smaller chambers when divers were living in them. In the *Dive* T_1, the mens' bedding showed a mixed flora of gram-negative bacilli after 4 days in saturation; in subsequent dives bedding was changed every 2–3 days.

Throughout any one dive either Savlon or Panacide was used to disinfect the chambers. Neither regime reduced contamination of the S.A.S. areas to acceptable levels, although Panacide proved more effective than Savlon.

Scattered isolations of staphylococci and, less commonly, aerobic spore bearers were made at all sites in the chambers throughout the dives. In T_1 only, swabs were cultured for yeasts and fungi, and occasional isolations were made from the chamber walls and the divers' bedding.

Limited sampling of diving suits and hoods showed scattered contamination with *P. aeruginosa* and other gram-negative bacilli; washing with Panacide did not eliminate this.

Serotypes and Phage Types of *Pseudomonas Aeruginosa*

Isolations of *P. aeruginosa* from *Dives* T_1 and R_1–R_3 were serotyped (17) and phage typed at the Central Public Health Laboratory, Colindale, London. Chamber contamination with *P. aeruginosa* was not detected before *Dive* T_1. One diver (*H*) entered with two strains (of serotypes 11 and 2b/5c) in his ears, and he was not removed for 3 days. The 2b/5c strain later became predominant in his ears, but type 11 strains accounted for 16 of 18 isolations of *P. aeruginosa* from the ears of the other 5 divers, for 11 of 12 isolations from the chamber, and for 4 of 4 isolations from the diving suits. The remaining strains isolated were of type 2b/5c. The phage typing results indicated that all strains of each serotype were indistinguishable. No other strains of *P. aeruginosa* were isolated from any source during the dive. Although initial chamber contamination may not have been detected, the evidence suggests strongly that *Diver H* introduced the infection.

The 46 chamber isolations made during R_1–R_3 were almost equally divided between 3 serotypes (Nos. 3, 11, and 6), but 91% of the 35 ear isolations were of only 2 of these (Nos. 3 and 11). *Pseudomonas aeruginosa* was isolated from the ears of 17 divers and only three were colonized with type 6 strains. Before the start of R_1, *P. aeruginosa* of serotype 11 was isolated from the 2500 chamber, and by *day 15* of this dive serotypes 11, 3, and 6 were widely distributed in the chamber complex. Once established, this pattern of contamination remained consistent throughout the rest of R_1, and throughout R_2 and R_3.

The data from the *R* complex point to the chambers as a possible reservoir of infection during and between the dives. The data from T_1 do not contradict this view and point to a single diver as the probable source of organisms which, in this dive, caused both ear infection and chamber contamination.

Both sets of data suggest that in a saturation environment certain serotypes of *P. aeruginosa* are more likely than others to colonize the ear canal.

DISCUSSION

A characteristic pattern of diver infection (Fig. 2) and chamber contamination (Fig. 3) was consistently observed in all of the seven dives studied. The results from the divers are compatible with the conclusions of previous studies, in particular those of Wright and Alexander (9). Published data on chamber contamination are scanty, but contamination of submarines and submersibles with bowel organisms and *P. aeruginosa* is well documented (18,19).

The very high incidence of ear pain that precipitated this study was greatly reduced by the control measures employed and none of the divers in the survey suffered incapacitating pain. Early detection and treatment of ear colonization with gram-negative bacilli was probably the most important factor in achieving this result.

The rapid appearance of gentamicin resistance during *Dive* T_1 may have resulted from inefficient distribution of the drug when used in a cream base. Antibiotic resistance was not a problem in dives where antibiotic drops were used, but, in the future, may arise during repeated cycles of infection and treatment, particularly if the latter is merely suppressive.

The scattered contamination of the chamber systems with mixed bacteria of human origin was not unexpected. The S.A.S. areas were frequently wet, and bacterial replication was probably a major factor in the gross contamination detected in them. They were probably a major source of infection.

The serotyping and phage typing data suggest that a single diver may be the source of organisms that rapidly spread both to his colleagues and throughout the chamber complex, and that the chambers may act as a reservoir of infection during and between dives. Bacteriological screening of divers before and during dives is thus probably of reduced value in limiting the spread of infection once the chamber complex is overtly contaminated, unless diver:diver contact, directly or via diving suits and equipment, is important in transmission.

The failure of prophylactic ear drops in the R_1–R_3 surveys parallels the experience of Wright and Alexander (9) who used 0.25% acetic acid in 50% ethanol. Effective prophylactic preparations have been described (2,20,21), but these were not assessed in the conditions of a commercial saturation dive.

The results described are relevant not only to the problem of otitis externa in divers, but also to the general microbiology of confined, hyperbaric environments. There appears to have been no comparable microbiological survey of saturation dives under commercial conditions.

Further investigation has been undertaken in two areas: the properties of *P. aeruginosa* grown in vitro under hyperbaric conditions (22), and the possibility that, in a saturation environment, certain serotypes of *P. aeruginosa* are more pathogenic than others.

References

1. Sperati G, Perfumo G. L'ottite esterna die sommazzatori. Arch Ital Otol Rhinol Laryngol 1967;78:443–449.
2. Thalman ED. A prophylactic program for the prevention of otitis externa in saturation divers. Washington, DC: U.S. Navy Experimental Diving Unit, 1974. (Research Report 10–74).
3. Cobet AB, Wright DW, Warrent PI. TEKTITE I—program: bacteriological aspects. Aerosp Med 1970;41:611–616.
4. Summitt JK, Kelley JS, Herron JM, Saltzman HA. 1,000-foot helium saturation exposure. In: Lambertsen CJ, ed. Underwater physiology. Proceedings of the fourth symposium on underwater physiology. New York: Academic Press, 1971: 519–527.
5. Senturia BH, Liebman FM. Evaluation of the factors which may be of importance in the production of external ear infections. J Invest Dermatol 1956;27:291–315.
6. Taplin D, Zaias N, Rebell G. Environmental influence on the microbiology of the skin. Arch Environ Health 1965;11:546–580.
7. Wright DN, Dineem M. A model for the study of infectious otitis externa. Arch Otolaryngol 1972;95:243–247.
8. Hardy AV, Mitchell RB, Schreiber M, Hoffert WR, Yawn E, Young F. Bacteriological studies of otitis externa. Laryngoscope 1954;64:1020–1024.
9. Wright DN, Alexander JM. Effect of water on the bacterial flora of swimmers' ears. Arch Otolaryngol 1974;99:15–18.
10. Jones DM, Davis P. Upper respiratory tract and aural flora of saturation divers. J Clin Pathol 1978;31:721–723.
11. Hojyo-Tomoka MT, Marples RR, Kligman AM. Pseudomonas infection in superhydrated skin. Arch Dermatol 1973;107:723–727.
12. Cowan ST, Steel AJ. Manual for the identification of medical bacteria. Cambridge University Press, 1965.
13. Brown MRW, Scott-Foster JH. A simple diagnostic milk medium for Pseudomonas aeruginosa. J Clin Pathol 1970;23:172–177.
14. Phillips I. Identification of Pseudomonas aeruginosa in the clinical laboratory. J Med Microbiol 1969;2:9–15.
15. Reller LB, Schoenknecht FD, Kenny MA, Sherris JC. Antibiotic susceptibility of Pseudomonas aeruginosa: selection of a control strain and the criteria for magnesium and calcium content in media. J. Infect Dis 1974;130:454–463.
16. Ericsson HM, Sherris JC. Antibiotic sensitivity testing. Report of an international collaborative study. Acta Pathol Microbiol Scand (B) 1971;(Suppl) 227.
17. Habs I. Research on O-antigens Pseudomonas aeruginosa. Z Hyg Infektionskr 1957;144:218–222.
18. Morris JEN, Fallon NJ. Studies on the microbial flora in the air of submarines and the nasopharyngeal flora of the crew. J Hyg (Camb) 1973;71:761–770.
19. Morris JEN. Microbial pollution in submersibles. Ann Occup Hyg 1975;17:245–246.
20. Beckman EL, Smith EM. TEKTITE II: medical supervision of the scientists in the sea. Tex Rep Biol Med 1972;30:175–184.
21. Hutchison JL, Wright DN. Prophylaxis of predisposed otitis externa. Ann Ottol Rhinol Laryngol 1975;84:16–21.
22. Kenward MA, Alcock SR, Brown MRW. Effects of hyperbaric oxygen upon colonial morphology and resistance of Pseudomonas aeruginosa. Proc Soc Gen Microbiol 1978;5(2):55.

AN EPIDEMIOLOGICAL STUDY OF FATAL DIVING ACCIDENTS IN TWO COMMERCIAL DIVING POPULATIONS

M. E. Bradley

In the past decade, fatal diving accidents in the commercial diving community have attracted considerable public attention and have been of concern to government regulatory groups. As a consequence, both the United Kingdom and United States have enacted standards regulating the conduct of commercial diving operations. In this study, the distribution of fatal diving accidents in commercial diver populations in the Gulf of Mexico and in the British sector of the North Sea is examined, and the factors that influence or determine that distribution are discussed. Recommendations for safer diving practices are presented and areas where research is needed are suggested.

Most accidents involve multiple factors that are mutually interacting. To understand the causes of accidents requires identification and analysis of interactions between variables that differ widely. One successful technique for analyzing accidents is an adaptation of epidemiologic methods (1). This approach analyzes accident data in terms of interaction between "host factors," "environmental factors," and "agent factors." *Host factors* are the characteristics of the person suffering injury; *environmental factors* refer to situational variables that predispose or contribute to injury; and *agent factors* are the agencies capable of producing injury. This approach was therefore used in this study.

METHODS

There were several reasons for examining fatalities in the commercial diver populations of the British Sector of the North Sea and the Gulf of Mexico.

Firstly, the numbers of commercial divers working in both areas were approximately the same. Secondly, reasonably accurate and reliable information was available for both groups. Lastly, it was felt that a comparison of two regions where the environmental conditions vary widely might yield information about the extent these factors contribute.

The period from 1968 to 1975 was reviewed for Gulf of Mexico fatalities, while the North Sea study covers the period 1971 to 1978.

The data on the commercial divers working in the British sector of the North Sea were obtained from various reports (4) and from the British Department of Energy. The information on the commercial diving fatalities in the Gulf of Mexico was obtained from investigation reports of the U.S. Coast Guard, from court records, and from commercial diving companies in the Gulf area. As much information as was available regarding host, environmental, and agent factors was gathered and examined. The data obtained generally were fairly complete, but were scanty in some instances; there was ambiguity and uncertainty, which made interpretation difficult.

RESULTS AND DISCUSSION

There are an estimated 905 commercial divers in the United States who work in the Gulf of Mexico (3). From 1968 to 1975, there was an average of 2.25 deaths per year in this group of divers, an average annual fatality rate of 2.49 per thousand per year. About 700 commercial divers work in the British sector of the North Sea (2). From 1971 to 1978, there has been an average of 3.375 deaths per year in this group, which is a fatality rate of 4.82 per thousand per year. The incidence of fatal diving accidents for each year in these two diver populations is presented in Table I. From this data, it is apparent that commercial diving operations in the North Sea are more hazardous than those in the Gulf of Mexico. In the Gulf, the highest fatality rate occurred from 1968 to 1970; in the North Sea, the peak period was from 1974 to 1976. These periods correspond to the introduction of new diving techniques and heightened diving operations. It is noteworthy that in recent years there has been a substantial reduction in mortality in both areas.

It is useful to compare the number of fatalities in commercial diving with other high-risk occupations, for example, coal mining and fire fighting. During

TABLE 1

Frequency of Fatal Diving Accidents in Commercial Diving

Gulf of Mexico								
Year	1968	1969	1970	1971	1972	1973	1974	1975
No. of Deaths	4	3	5	1	1	1	2	1
North Sea								
Year	1971	1972	1973	1974	1975	1976	1977	1978
No. of Deaths	1	1	2	5	6	7	3	2

the period from 1967 to 1976, the average annual fatality rate for underground operations in anthracite coal mining in the United States was 2.08 per thousand per year (5). From 1964 to 1974, firefighters had an annual average fatality rate of 0.89 per thousand per year in the U.S.A.(6).

It is apparent that commercial diving is a hazardous occupation. Nevertheless, the fatality rates for Gulf of Mexico divers are not much greater than other high-risk occupations, such as anthracite mining in the United States.

A critical problem in an analysis of this sort is the assessment of exposures as a factor in accidents. Much work is needed to develop wholly relevant measures. "Exposure" involves both the frequency with which hazardous situations are encountered, and differences in the intensity or quality of hazard. Because a satisfactory way of measuring exposures has not been developed, one cannot say, for example, that commercial diving is more hazardous than fire fighting or anthracite mining.

This analysis is continued using the approach of examining the contribution of host, environmental, and agent factors to fatal diving accidents.

Host Factors

Age and experience. The average age of the divers who died in the Gulf of Mexico was 34.1 years, with a range of 21 to 50 years. The mean age of the diving fatalities in the North Sea was 26.5 years, with a range of 20 to 40 years. The percent distribution of accidents according to age is presented in Table II. Because the data were inadequate, the degree of experience could not be assessed for either group; however, the younger age of the North Sea fatalities, in which 77% of the divers were between 20 and 29 years of age, suggests a lesser level of diving experience.

Health of a diver. The nature of diving requires that divers be in good health. Nevertheless, a small number of diver fatalities occur because of medical conditions that contribute to the accident. In one (6% total) of the accidents in the Gulf, and in two (7%) deaths in the North Sea, medical conditions that contributed to the fatality were present.

Behavioral factors. Behavioral dysfunction in diving is a major contributor to diving accidents in all diving populations. Behavioral dysfunction in divers may take the form of poor judgment. Anxiety and panic have also been

TABLE II

Age Distribution of Diving Fatalities

Age (yr)	Gulf of Mexico (%)	North Sea (%)
20–29	34	77
30–39	33	18
40–50	33	5

recognized as important contributors to fatal diving accidents. In 17% of the Gulf accidents and in 15% of those in the North Sea, poor judgment or panic on the part of the diver was reported as having been present.

Summary of host factors. North Sea divers involved in fatal accidents during the period studied tend to be significantly younger than their counterparts who died in the Gulf of Mexico. It is suspected that this may reflect a lesser level of experience of the divers involved in North Sea diving fatalities. Poor judgment or panic by divers in both groups are significant contributors to the accident.

In all diver populations, the well-trained, experienced diver is less at risk for an accident. In an analysis of 21 deaths associated with recreational scuba diving in the state of Michigan, Denney and Read (7) reported that 15 of the 21 fatalities in their series occurred in inexperienced divers. During the period from 1965 to 1975, inexperience was cited as a contributory factor in about 25% of the U.S. Navy's fatal diving accidents.

Acts of poor judgment and panic have been appreciated as a significant contributory factor in fatal diving accidents. Panic or poor judgment have been implicated as a contributory factor in 20% to 40% of the recreational diving deaths in the United States. About 30% of the investigations of diving fatalities in the U.S. Navy from 1965 to 1975 mention panic as an important factor in the accident. Nor is the commercial diver immune from behavioral dysfunction. Although it is apparent that even the experienced diver may act inappropriately in certain situations, it is generally agreed that he is less likely to do so than the diver with a lesser level of experience.

The host factors most important in fatal diving accidents, level of experience and behavioral dysfunction, are most amenable to change through the requirement for improved and more thorough training.

Environmental Factors

Environmental factors that can contribute to a fatal diving accident are varied. They include, but are not limited to: a) depth of dive, (b) breathing gas, c) weather, d) sea state, e) current, f) equipment failure, g) capability of others, h) narcosis, and i) clarity of water.

TABLE III

Distribution of Fatal Diving Accidents According to Depth

Dive Depths (ft)	Gulf of Mexico (%)	North Sea (%)
Surface	17	16
1–100	25	16
101–200	33	16
201 +	25	52

Depth of dive. In the Gulf, the mean depth of dive in which there was a fatality was 136 ft (range 0–340 ft). The mean depth of North Sea dives was substantially greater (223 ft, range 0–500 ft). The percent distribution of these accidents according to depth is presented in Table III. The majority of fatal diving accidents in the North Sea occurred during dives in excess of 200 ft. In both the Gulf and North Sea, episodes of unexplained diver unconsciousness or unaccountable actions have been contributory to accidents occurring during dives of 300 ft and greater. The three deepest North Sea fatalities during this time period typify this situation. During a 500-ft dive, a diver is thought to have "fainted," and fell into the bell trunk where he drowned. During a 480-ft dive, a diver drowned after possibly switching off his own gas supply. A diver making a 460-ft dive died of "anoxia"; he refused to take the advice of topside to slow down his operations when he was noted to be overworking.

Analysis of the three deepest fatalities reported in the Gulf of Mexico reveals a similar thread of inexplicable diver unconsciousness or behavior. A diver making a 340-ft dive was noted to be "unconscious" and "moaning" after 17 minutes of bottom time. Another diver demanded to be brought to the surface 35 minutes into a 272-ft dive after a nonserious injury to his hand. And, 54 minutes into a 300-ft dive, a diver reported that "I have to get out of here," and began to climb the ascent line. It is noteworthy that these three Gulf of Mexico fatalities were brought directly to the surface without any water decompression, but with a predictable unfortunate outcome. Divers are exuberant spirits, who must be gently decanted.

Breathing gas. Compressed air was the breathing gas in use during the majority (67%) of fatal accidents in the Gulf. Helium-oxygen mixtures were most commonly (63%) in use during fatal North Sea accidents.

Cold. Cold was mentioned as a contributory factor in 11% of the North Sea fatalities. It was not a factor in any of the Gulf accidents.

Sea state. Heavy sea states were considered to be a factor in 15% of the North Sea accidents; all of these accidents occurred on the surface. In none of the Gulf accidents were bad weather conditions considered to be a factor.

Equipment failure. Severed or fouled hoses occurred in 33% of the fatalities in the Gulf and in 11% of the North Sea accidents. In 11% of the North Sea deaths, a diving bell was dropped; in another 19% of the North Sea fatalities there was some form of equipment failure, usually concerned with the underwater breathing gear (see Table IV).

TABLE IV

Types of Equipment Failure Occurring in Fatal Diving Accidents

Equipment Failure	Gulf of Mexico (%)	North Sea (%)
Severed or Fouled Hoses	33	11
Dropped Bells	0	11
Other—Usually Breathing Gear	0	19

Capability of others. In 33% of the Gulf fatalities and in at least 22% of the North Sea accidents there was some form of error by the diving supervisor, tender, or bellman. Difficulty in communication appears to be contributing to the North Sea accidents. This is in part a result of conducting diving operations where the diver, the dive supervisor, and support personnel frequently are of different nationalities.

Summary of environmental factors. There is considerable influence of environmental factors in commercial diver fatalities. Deeper dives appear to carry a greater risk. Cold and sea state contribute heavily in the North Sea. However, the most important environmental factors present in fatal accidents are equipment failure and diving supervisor/tender errors during the conduct of the dive. Improved equipment selection, maintenance, and operation together with adherence to cogent, safe operating and emergency procedures would appear to offer the greatest possibility for reducing accidents.

Agent Factors

Agent factors are those agencies that constitute the direct causes of injury. The distribution of agent factors in these two populations is given in Table V. In both groups, drowning was the most common proximate cause of death. Decompression sickness/air embolism and asphyxia were next in order.

SUMMARY

Commercial diving is a hazardous occupation. Nevertheless, the fatality rates are not appreciably greater than those for other high risk occupations, such as anthracite mining in the United States. In recent years, there has been a significant downward trend in mortality rates in the commercial diver populations in the North Sea and the Gulf of Mexico.

The interactions of host factors, environmental factors, and agent factors in commercial diving fatalities have been examined. The contribution of host

TABLE V

Distribution of Causes of Death in Diving Accidents

Cause	Gulf of Mexico (%)	North Sea (%)
Drowning	44	63
Decompression Sickness/Air Embolism	28	19
Asphyxia	17	7
Trauma	11	0
Other	0	11

and environmental factors to diving fatalities appears to be the greatest problem and the most amenable to change. Research into the cause of diver unconsciousness and inexplicable actions occurring at depths below 300 ft is needed.

Acknowledgments

References

1. McFarland RA. Research-driver capability. In: Proceedings of the national conference on medical aspects of driver safety and driver licensing. Chicago: American Medical Association; 1964.
2. Warner SA. Diving accidents: Loss of consciousness of divers in the water; resuscitation in diving bells. In: Lambertsen CJ, O'Neil SR, Long ML, eds. The human factor in North Sea operational diving. Allentown, PA: Air Products and Chemicals, Inc., 1978;35–37.
3. National Oceanic and Atmospheric Administration. An analysis of the civil diving population of the United States. Manned Undersea Sciences and Technology (MUST) Rpt., Washington, DC: Dept. of Commerce, March 1975.
4. Simpson, G. Panel discussion. In: Lambertsen CJ, O'Neil SR, Long ML. eds. The human factor in north sea operational diving. Allentown, PA: Air Products and Chemicals, Inc, 1978:12–15.
5. Metropolitan Life Insurance Company. Hazards in coal mining. Statistical Bulletin 1978;59(2):2–4.
6. Occupational Health and Safety Letter. 1975;5(24):4–5.
7. Denney MK, Read RC. Scuba-diving deaths in Michigan. JAMA 1965;192(3):120–122.

DECOMPRESSION SICKNESS IN A COMMERCIAL DIVING POPULATION

M. Cross and L. Booth

Considerable uncertainty exists as to the incidence of decompression sickness in the commercial oil-field diving community. While the published incidence of decompression sickness on the U.S. Navy Tables is often quoted as being below 2% for nonsaturation procedures, some workers have expressed the view that the true incidence in the working diving situation offshore might be nearer 10%. The aim of this study was to determine the number of men in a commercial diving population with a history of decompression sickness of various types and to correlate this with the previous exposure, age, experience, and maximum career depth.

METHOD

Questionnaires were distributed to doctors who carried out annual diving medical examinations, and each doctor was asked to distribute the forms to divers on a random basis; 260 replies were received.

RESULTS

Characteristics of the Population

The population was first analyzed with respect to age, years of experience, types of diving performed, and maximal and habitual depth of work. A preliminary analysis of the forms showed that all men had done air diving and 96% of them had used surface decompression. Of those who replied, 61% had performed dives with oxy-helium mixtures, the overwhelming majority having

performed at least one saturation. A number of men gave a history of diving with "other gas mixes," and upon investigation this group consisted of men who had used oxy-nitrogen mixes in relationship to military diving. Table I presents the mean age and years of experience in relationship to types of diving performed for the population.

The air divers are younger than any others, so they tend to have slightly fewer years of experience, although because of the size of the standard deviations, the differences are not significant. It is interesting to note, however, that the oxy-helium divers who have not done saturation diving are both slightly older than those with saturation experience and have also spent a slightly longer time as commercial divers. Perhaps this reflects the relative late arrival of saturation diving as compared with "bounce" diving in the population we have studied. Figure 1 presents the maximum career depth of the divers, in bar plot form. It is interesting to note the bimodal distribution, which generally reflects the depths of diving both worldwide and around the British coast.

The two most common depth ranges are the air range and the range from 126–175 m, which represents the most northly worksites. There is much less mixed gas diving in the shallow ranges just beyond the depth range permitted for the use of air. This trend is equally obvious in the following data, which present the population analyzed according to the most frequent diving depth reported by the men:

Depth Range (m)	Number of Men	% Population
0–50 m	83	40.6
51–100 m	14	6.8
101–150 m	96	47.0
151–200 m	12	5.8

TABLE I

Mean Age and Years of Commercial Experience in the Population Studied

Type of Diving	Mean Age	SD	Mean Years Experience	SD	No. of Men
Men With *Air* Experience Only					
Group A					
Without Surface Decompression Experience	26.15	3.69	3.78	3.53	40
Group B					
With Surface Decompression Experience	30.00	6.84	5.18	6.65	57
Men With *Air* And *Oxy-Helium* Experience					
Group C					
Without Saturation Experience	31.81	9.07	7.18	7.87	27
Group D					
With Saturation Experience	30.91	4.06	6.73	3.91	133
Whole Population	30.07	5.67	5.7	4.9	257
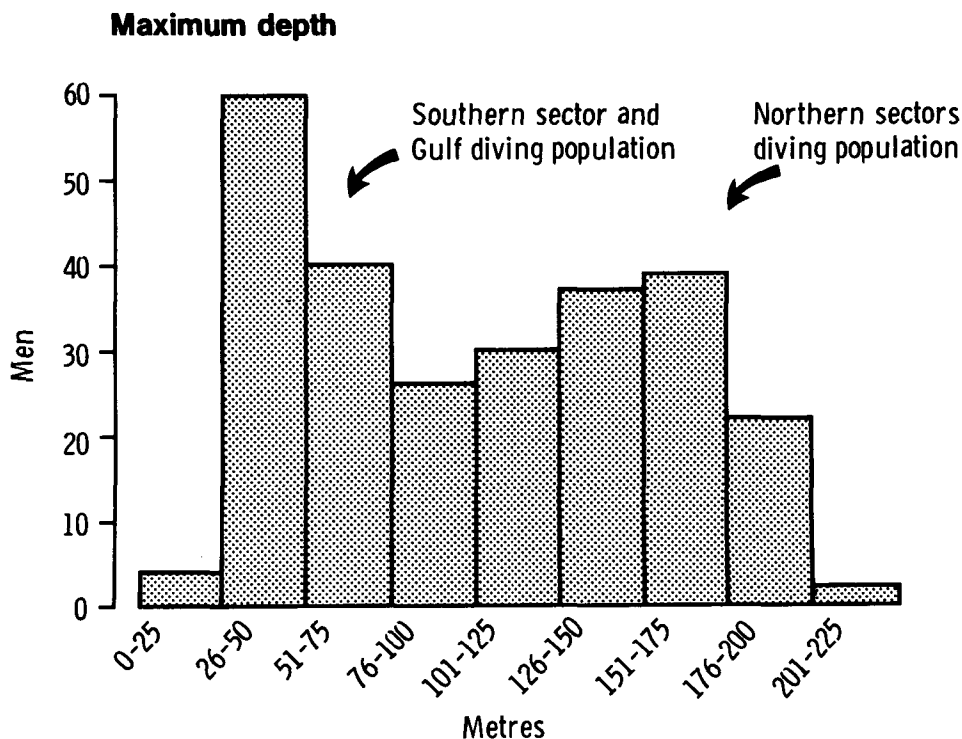
Maximum depth

Fig. 1.   This bar plot presents the maximum career depth of the divers.

It should be noted that a number of men had achieved quite deep dives in their career, but nevertheless reported that their *most frequent* diving depth was 50 m or less.

Incidence of Decompression Sickness

In the questionnaire, enquiry was made into the decompression sickness history of the divers. Table II presents a preliminary analysis of decompression sickness history with air or oxy-helium. This analysis includes a number of men with air experience deeper than 50 m, gained, presumably, in fields other than the British North Sea Sector, where diving deeper than 50 m on air is ordinarily prohibited by regulation.

The "hierarchy of modes of diving," upon which Table II is based, may seem at first arbitrary because the groups of the modes are not necessarily exclusive. Thus, a diver in *Group C* who has done oxy-helium diving without saturation may also have experienced air diving, both with or without surface decompression. A statistical analysis of the data presented in Table II demonstrates that.

TABLE II

Analysis of the History of Decompression Sickness on Air and Oxy-Helium

Type of Diving	Number of Subjects	Numbers of Men with History of DCS				
		Total	Skin	Limb Bends	Niggles	Type 2
Group A						
Air < 25 m	4	0	—	—	—	—
Air 25–50m						
No SD	29	2	2			
Group B						
Air 25–50 m						
With SD	31	12	3	2	6	2
Air 50 m +						
With SD	22	8	2	3	6	1
Group C						
Oxy-Helium:						
No Saturation	28	18	8	9	10	1
Group D						
Oxy-Helium:						
Saturation	134	89	39	58	57	11

DCS is decompression sickness.   SD is surface decompression.   This table is progressive, i.e., men who appear in *Group C*, for instance, may also have experience relevant to *Groups A* and *B*.

1) Divers with surface decompression experience have a higher incidence of decompression sickness than divers who have done only maximum no-decompression dives or dives using in-water decompression stops ($0.005 > P > 0.001$).

2) Divers with oxy-helium diving experience have a significantly higher incidence of decompression sickness than those in the whole air diving group ($P < 0.0005$).

3) It is not possible to demonstrate that more men in the group who have used surface decompression on air deeper than 50 m have a history of type 1 decompression sickness than do men who restricted themselves to 50 m or less.

4) Although there appears to be a significantly larger number of men in the oxy-helium saturation group who have experienced type 2 decompression sickness than in other groups, it is not possible to substantiate this statistically.

Further analysis of the questionnaire data was made to determine the relationship between the most frequent and the maximum career depths of the men and their history of decompression sickness. This information is presented in Tables III and IV.

Men were asked to indicate the sites of the body where the pain and discomfort of both "bends" and "niggles" occurred. Figures 2 and 3 present the analysis of the replies.

TABLE III

Relationship Between *Maximum* Career Diving Depth and History of Type 1 Decompression Sickness in the Population

Maximum Depth of Dive in Career	No. of Men	No. with History of Type 1 DCS*	%
Less than 25 m	4	0	0
25–50 m	60	14	23
51–100 m (air)	22	8	36
51–100 m (mixed gas)	44	25	56
101–150 m (mixed gas)	65	42	64
151–200 m (mixed gas)	61	43	70
200 m +	2	1	—

*Type 1 DCS includes all "niggles", limb bends, and skin bends.

TABLE IV

Number of Men With a History of Type 1 Decompression Sickness in Relation to Stated *Most Frequent* Diving Depth

Most Frequent Diving Depth (m)	No. of Men	No. with History of Type 1 DCS	%
Less than 50 m	64	14	21
More than 50 m (air)	22	8	36
51–100 m (mixed gas)	14	6	42
101–150 m (mixed gas)	97	63	65
151–200 m (mixed gas)	61	43	70

A number of men gave two depth ranges as their most frequent diving depth. For the purposes of this table they have been included in the ranges appropriate to *both* of their answers, hence the total number of men exceeds that of other tables.

14.1 ──────▶   1.2   ◀────── 12.2

10.3 ──────▶   ◀────── 10.9

3.2 ──────▶   ◀────── 3.8

2.5 ──────▶   ── 1.9

1.2 ──────   ── 0.6

0.6 ──────▶   ◀──────   0.6

16.1 ──────▶   ◀──────   14.2

0.6 ──────▶   ◀──────   0.6

0.6 ──────▶   ◀──────   0.6

1.2 ──────   ────── 1.9
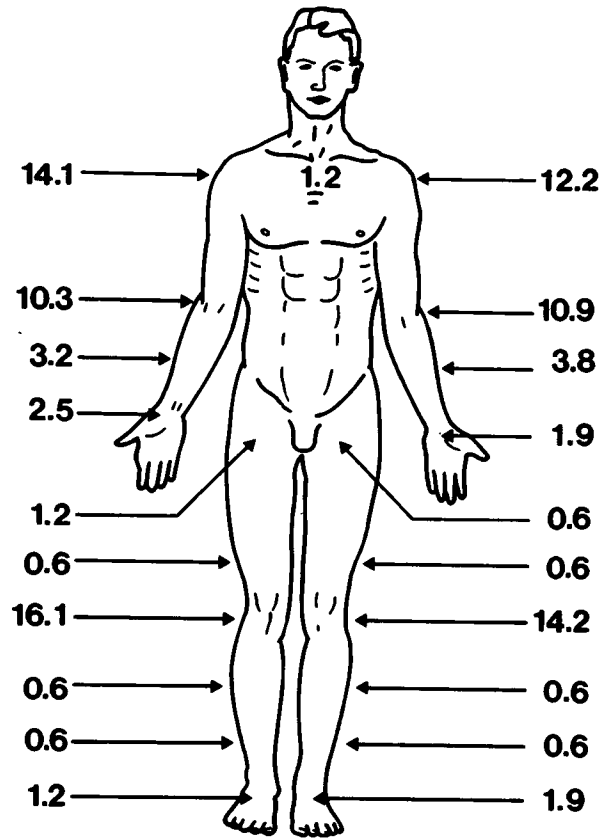
**Sites of pain reported to be type 1
decompression sickness**

(Figures are percentages)

Fig. 2.   This figure shows the frequency, in percentage, with which men who had experienced bends ascribed them to particular body areas. There is a slight preponderance towards the right side.

The figures indicate the percentage frequency with which the particular site was mentioned.

The divers were asked about the regularity with which they experience and report niggles. It was interesting to find that not only was the incidence of niggles higher in the mixed gas group, but also over half of these men who had experienced niggles admitted to not always reporting them.

Range	Total	Admit to Niggles	Admit to Not Always Reporting "Niggles"
All air divers	98	12 (12.2%)	7 (7.1%)
All mixed gas divers	162	67 (41.3%)	30 (18.5%)

Sites of pain reported to be 'niggles'
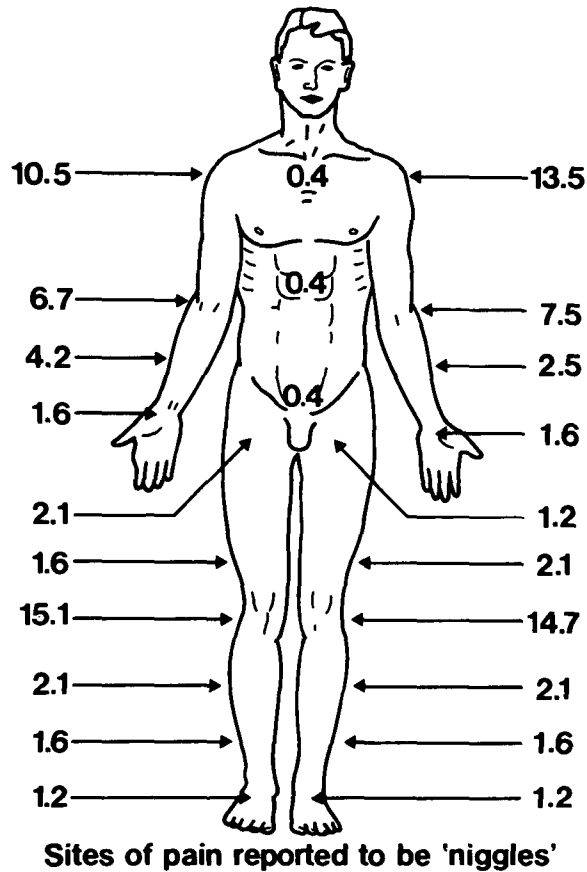
(Figures are percentages)

Fig. 3. This figure presents in percentage terms the frequency with which particular areas of the body were indicated as being the site of discomfort in men with niggles.

Divers were also asked about the feeling of "unusual fatigue" after a dive and, particularly, to indicate the types of diving with which this phenomenon was associated. An analysis of the responses is presented below:

Type of Diving	No. of Men Who Have Used This Mode	No. Reporting Unusual Fatigue
Air range diving	260	37 (14.2%)
Air range with surface decompression	250	40 (16.0%)
Air saturation	18	2 (11.0%)
Oxy-helium bounce	139	27 (19.4%)
Oxy-helium saturation	134	43 (32.0%)
Other mixes	52	8 (15.3%)

DISCUSSION AND CONCLUSIONS

Exposure to decompression sickness is widespread throughout the population studied. The major determinant of incidence seems to be the depth of the dive, from both the point of view of the maximum career depth and the most frequent diving depth.

It would appear that decompression procedures associated with surface decompression modes are significantly more likely to produce manifestations of decompression sickness than either mximum no-decompression dives, or in-water stops in the same depth range. It has not been possible to demonstrate that surface decompression diving from depths greater than 50 m is associated with any higher incidence than the same technique used to 50 m or less. One possible conclusion is that surface decomression diving tables are less safe because the fundamental physiology of this mode of diving is less well understood.

The relationship between the deepest career depth or the most frequent diving depth and the number of men with overt decompression sickness is clear. With increasing depth, the risk of decompression sickness increases considerably. Saturation diving, in particular, seems to be associated with significantly higher incidences of decompression sickness. This may again be because the fundamental physiology of decompression from great depths is poorly understood, and extrapolation from satisfactory models relevant to shallower depths may be less than adequate.

Particularly disappointing is the large number of divers who do not report niggles consistently. Although it is sometimes in vogue to attack diving contractors for competing commercially over diving tables, the figures relating to divers not reporting minor manifestations of decompression sickness must inevitably mean that many contractors may not have the information from the worksite necessary for them to make a proper evaluation of their tables.

An additional problem making the analysis of saturation decompression tables difficult is the interpretation of minor manifestations of decompression sickness. Since during oxy-helium decompression from saturation any minor and early signs of decompression sickness are treated immediately, it is difficult to decide if, in the absence of treatment, the minor manifestation would develop into a bend. Figures 2 and 3, which show the distribution of both limb bend pain and also of niggles, are similar to those reported by other workers (1). The preponderance, however slight, for the pains in the shoulders and knees to occur on the right more than the left has been noted before and is as yet unexplained. The phenomenon is still present in Fig. 3 relating to niggles.

The significance of fatigue or undue tiredness after diving has been the subject of some discussion (2). Its significance remains difficult to elucidate. However, Histogram 1, which relates the percentage of divers reporting either type 1 decompression sickness or fatigue of an unusual degree to types of diving, suggests that there is a correlation which cannot be ignored, even if it is difficult to explain.

Considering the population as a whole, analysis reveals a simple relationship between the number of years of experience the men have as divers and
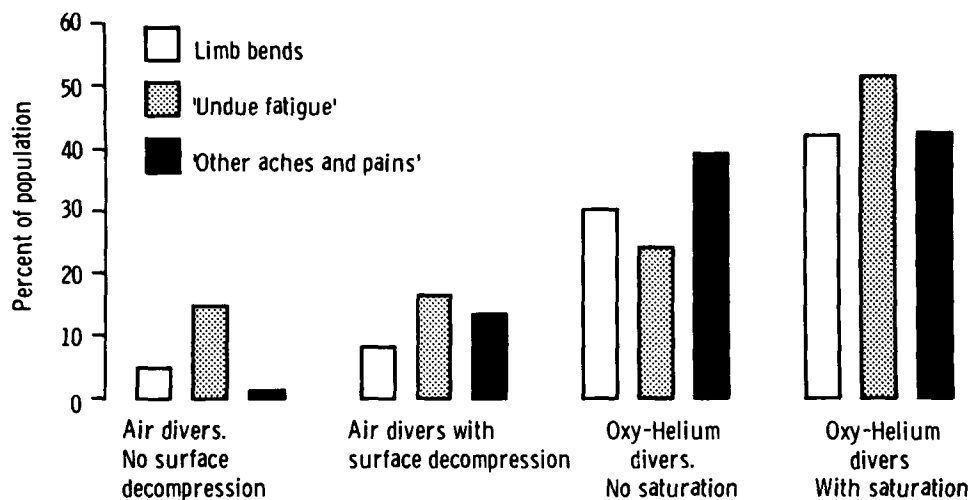
Histogram 1. This histogram indicates the relationship between the various modes of diving and the incidence of all forms of decompression sickness and undue fatigue.

the number of divers with a history of some kind of dysbaric manifestion, however minor. This relationship is presented below:

No. of Years as a Professional	Men With a History of DCS (%)
1–2	35
3–4	50
5–6	55
7–8	52
9–10	64
11+	72

In conclusion, the evidence presented in this paper supports the suggestion that decompression sickness in any of its manifestations is commoner in the commercial diving population than normally suspected. The depth of the dive seems to be the major determinant rather than any other factor demonstrated in this study. This factor may reflect a poor understanding of the fundamental processes of decompression from the greater depths.

References

1. Slark AG. Treatment of 137 cases of decompression sickness. London: Medical Research Council, RN Personnel Research Committee Report 63/1030, 1962.
2. Dewey WA. Decompression sickness—an emerging recreational hazard. N Engl J Med 1962;267:759–820.

AN EVALUATION OF CARDIOPULMONARY RESUSCITATION TECHNIQUES FOR USE IN A DIVING BELL

R. Myers and M. E. Bradley

Divers who lose consciousness while operating out of a diving bell require rescue and resuscitation. The small size of these bells and the configuration of the bell interior, with its skirt and center trunk and hatch, pose special problems in delivering cardiopulmonary resuscitation (CPR). Because of these conditions in the bell, it is impossible to place the unconscious diver in the supine position usually used for CPR.

An operational schema has been devised that is purported to be effective in the resuscitation of a diver who is retrieved into a bell(1). Review of this schema made us seriously doubt its effectiveness. Therefore, we evaluated this method together with other CPR procedures that might be used in the bell.

METHODS AND MATERIALS

The effectiveness of two groups of individuals acting as resuscitators and one mechanical CPR system were evaluated. The first group of resuscitators was comprised of three CPR instructors, who were highly experienced with resuscitation procedures. The second group consisted of five individuals who had received CPR instruction and certification. (Divers having recent CPR training might be considered to have equivalent capability to the second group.) Lastly, we evaluated a gas-driven CPR machine, which delivers both compression and ventilation.

To test the efficacy of CPR methods, we employed two types of subjects. The first was a recording mannequin used for training individuals in CPR (Resussci-Anne: Laedral Medical Corporation). With this device we measured a)

the compression pressure, b) the appropriateness of the location where the compression pressure was applied, c) the tidal volumes achieved during ventilation, and d) the duration of effectively sustained CPR. The second group of subjects employed were fresh human cadavers before autopsy. The adequacy of cardiac compression was assessed by monitoring radial arterial blood pressure, with arm and pressure transducer maintained at the level of the heart. The cadavers were ventilated by machine with constant, appropriate tidal volumes. All procedures on the cadavers were done both with and without medical antishock trousers. The medical antishock trousers simulated to some degree the increased central venous return that would occur during immersion in water.

Six combinations of subject positions and resuscitation techniques were studied:

1) Subject supine on a firm bed with the resuscitator providing compression and ventilation from above (Figs. 1 & 2).
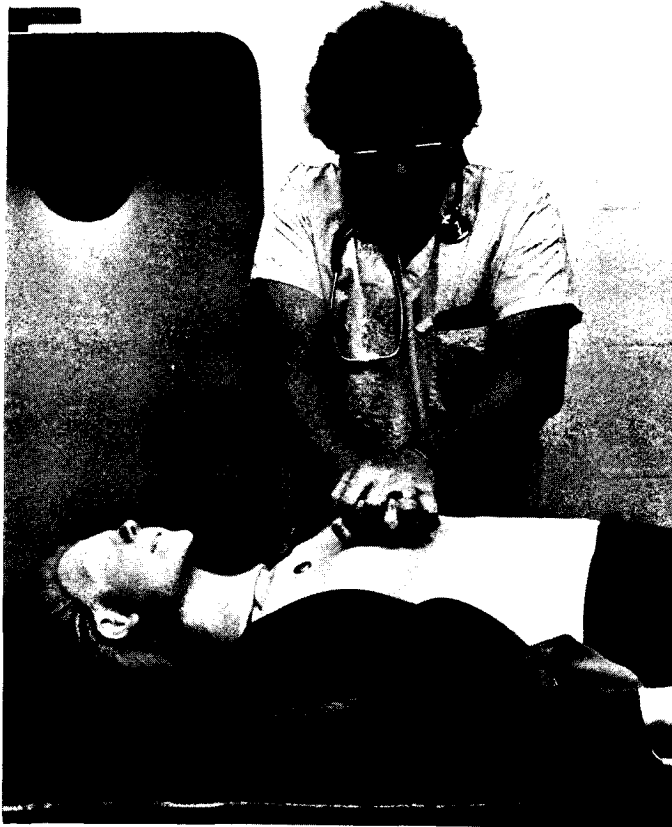
Fig. 1.   A resuscitator providing chest compression from above with the subject supine.

Fig. 2.   Resuscitator providing ventilation from above with the subject supine.

2) Subject upright with the back against a firm surface and compression administered by hand to chest with the resuscitator in front of the subject.

3) Subject upright with compression administered by pulling the subject's chest onto the head of the resuscitator (Fig. 3).

4) Subject upright with compression administered by pulling the subject's chest against the knee of the resuscitator.

5) Subject upright with the back against a firm surface and compression administered by pushing against the subject's chest with the resuscitator's knee (Fig. 4).

6) Subject upright with the resuscitator behind the subject, arms around the subject and fist compressing the subject's chest (a modified Heimlich maneuver) (Fig. 5).

RESULTS AND DISCUSSION

Mannequin Subjects

The efficiency data of the CPR instructors with the resuscitation manne-quin in the supine and upright positions with various resuscitation techniques is

Fig. 3. Subject upright with compression administered by pulling the subject's chest onto the head of the resuscitator.

presented in Table I. The efficiency data for the CPR-certified resuscitators is given in Table II.

With the subject in the supine position, the instructors were more consistent than the CPR-certified resuscitators in providing adequate ventilation and pressure generation and showed less deterioration in performance over time, especially after 10 min had elapsed.

In all of the upright positions, adequate ventilation was very difficult to achieve because we had to hyperextend the subject's head to maintain an open airway. The rigid collar, previously designed, did not provide adequate hyperextension. We have therefore developed a collar of different design, which did provide enough hyperextension to adequately ventilate the subject in the upright position (see Fig. 6).

Most of the resuscitation techniques with the subject in the upright position failed to attain adequate compression pressure or good pressure location and could be sustained for periods of less than 3 min before the resuscitator was exhausted. The least-effective techniques were the hand-to-chest (#2), head-to-chest (#3), and pulling the subject knee-to-chest (#4). The modified Heimlich technique (#6) was least tiring for the resuscitator but was generally

Fig. 4. Subject upright with the back against a firm surface and compression administered by pushing against the subject's chest with the resuscitator's knee.
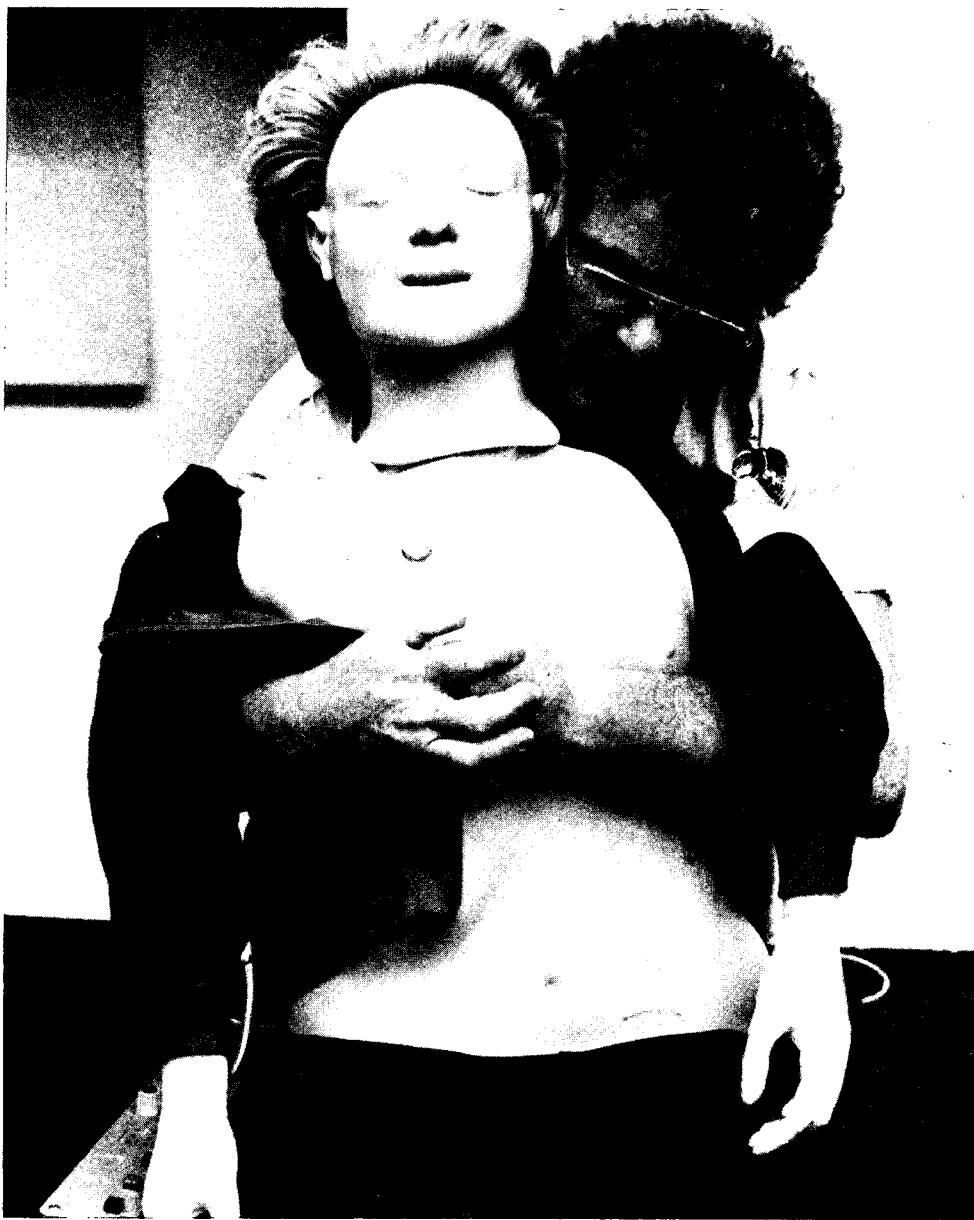
Fig. 5. Subject upright with the resuscitator behind the subject, arms around the subject, and fist compressing the subject's chest.

TABLE I

The Effectiveness of CPR Instructors Using Various Cardiopulmonary Techniques on a Mannequin in the Supine and Upright Position

Subject Position / Resuscitation Techniques	Compression Pressure* (lb)	Compression Pressure Location	Ventilation† (L)	Duration Sustained Effectively (min)
Supine / From Above	110	very good	1.7	>15
Upright / Hand to Chest From Front	100	good	2.0	<3
Upright / Head to Chest	63	poor	1.3	< 1
Upright / Knee to Chest Push	110	very good	1.7	>5, <10
Upright / Modified Heimlich	50	fair	1.9	>10

*The American Heart Association considers a compression pressure of 110 lb to be optimal, 80–100 lb acceptable, and below 80 lb unacceptable (2).   †Ventilation must be 1.0 litre (L) or more.

ineffective in generating adequate compression. Technique #5, with the mannequin seated with its back against a firm surface and chest compression administered by pushing with the resuscitator's knee, was acceptable.

Cadaver Subjects

The results obtained by testing the various chest compression techniques on supine and upright human cadavers generally substantiated the findings from the mannequin phase of the study. Again, the supine position proved to be the best for providing adequate blood pressure of 140/44. With the subject in the upright position, the next most effective technique depended on the relative size of both the victim and the resuscitator. When the resuscitator was larger than the subject, compression of the cadaver's chest from behind (a modified Heimlich maneuver) resulted in adequate arterial blood pressure (120/70) and the least fatigue to the resuscitator. However, when the subject's size

TABLE II

The Effectiveness of CPR-Certified Personnel Using Various Cardiopulmonary
Resuscitation Techniques on a Mannequin in the Supine and Upright Position

Subject Position / Resuscitation Techniques	Compression Pressure* (lb)	Compression Pressure Location	Ventilation† (L)	Duration Sustained Effectively (min)
Supine / From Above	100	good	1.5	>15
Upright / Hand to Chest From Front	70	good	1.7	<3
Upright / Head to Chest	50	fair	1.9	<2
Upright / Knee to Chest Pull	65	poor	1.8	1
Upright / Knee to Chest Push	95	good	1.8	>3, <4
Upright / Modified Heimlich	40	fair	1.7	<3

*The American Heart Association considers a compression pressure of 110 lb to be optimal, 80-100 lb acceptable, and below 80 lb unacceptable (2).   †Ventilation must be 1.0 litre (L) or more.

was equal or larger than that of the resuscitator the knee-chest position was more effective and a blood pressure of 130/0 was produced. With this technique, the resuscitator's knee compresses the subject's chest, while the subject is supported by the resuscitator's hand on the shoulders and the back is against a firm support (Fig. 4). In equal or larger sized subjects the modified Heimlich maneuver produced a blood pressure of 50/0, which is unacceptable. Attempts to perform chest compression on a freely suspended upright cadaver (as in a safety diving harness) by pulling the chest onto the resuscitator's knee or head was rapidly exhausting (1-2 min) and produced an unsatisfactory arterial blood pressure of 40–50/0.

Fig. 6.   Modified Philadelphia collar to provide adequate hyperextension of the head.

The use of medical antishock trousers produced an elevation of systolic blood pressure about 25 mmHg above systolic blood pressure when trousers were not used. Nevertheless, their use did not substantially increase arterial blood pressure to acceptable levels in the suspended upright position.

Finally, a gas-driven CPR machine (Fig. 7), which delivers both compression and ventilation, was evaluated on the mannequin and cadavers in the supine (Fig. 8) and upright positions (Fig. 9). For subjects in the erect
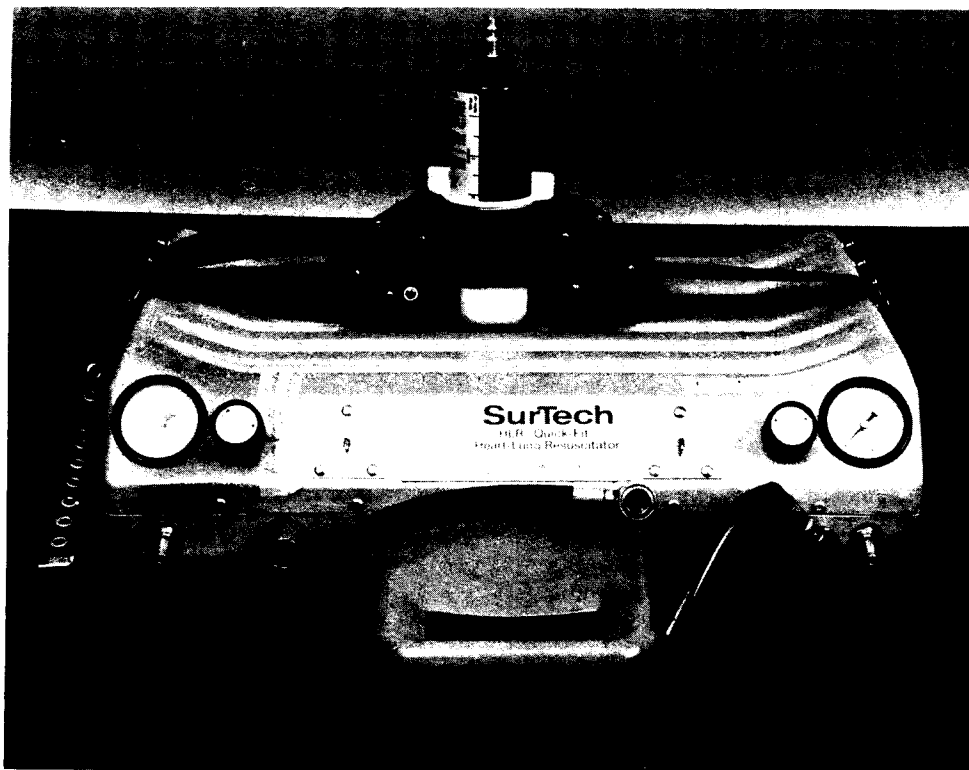
Fig. 7. Pneumatically operated CPR machine. Dimensions are 22 in. × 17 in. × 8 in.

sitting position, the device provided adequate and even compression and venti-
lation and required little energy expenditure from the individual doing the
resuscitation.

CONCLUSIONS AND RECOMMENDATIONS

In summary, we have found that a collar, previously developed for resus-
citation in the upright position, does not adequately hyperextend the head in
the mannequin or human subjects to maintain an open airway. Secondly, we
found that pulling the subject's chest against the resuscitator's head or knee to
provide cardiac compression produces grossly inadequate compression pres-
sures and rapidly exhausts the resuscitator. Thirdly, resuscitation cannot be
performed with the subject suspended by a harness at the back of the neck.
Finally, using either a modified Heimlich maneuver (when the resuscitator is
larger than the subject) or a push-with-the-knee-against-chest technique, we
have shown that marginally satisfactory resuscitation can be performed for
short periods with the subject sitting with the back against a firm surface.
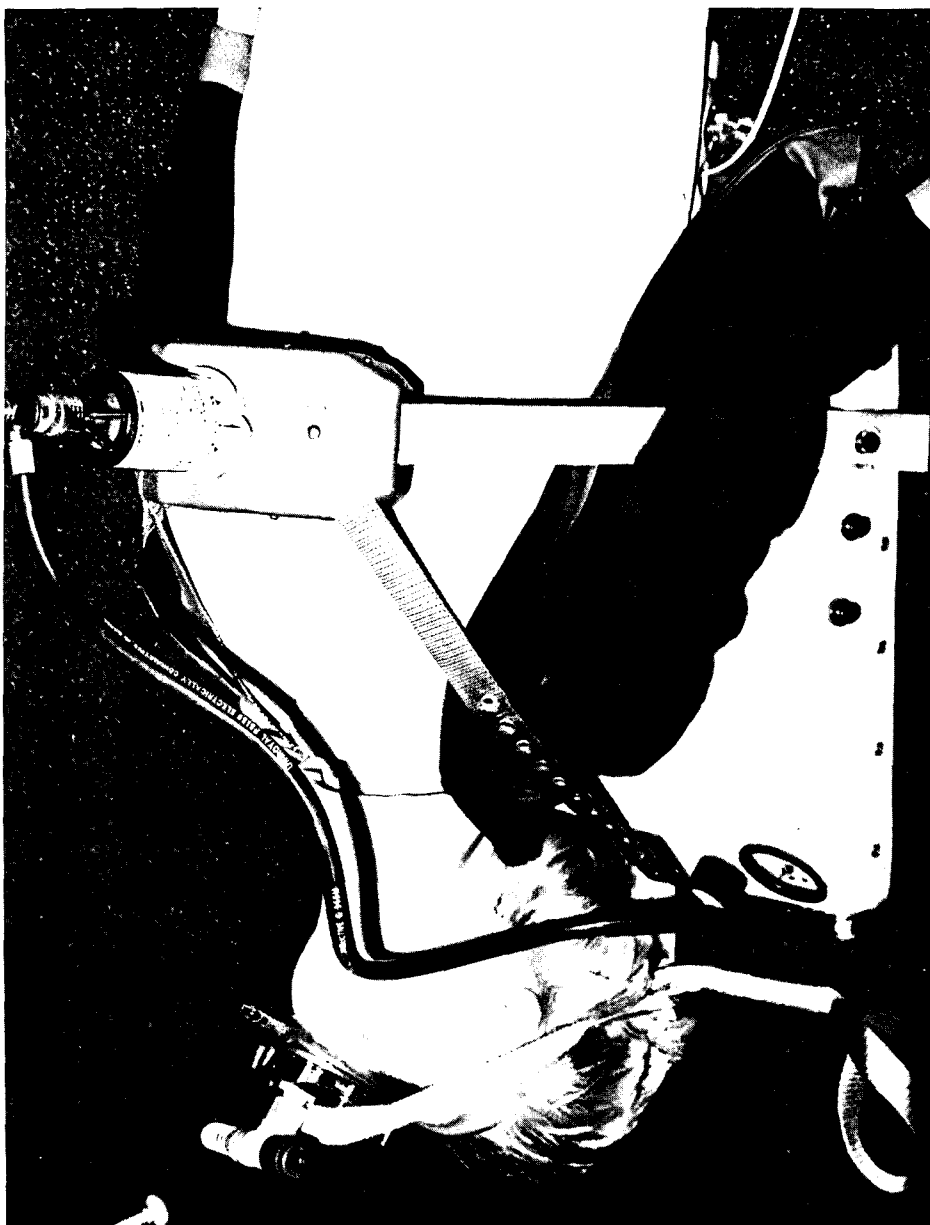
Fig. 8. Compression and ventilation by a CPR machine with the subject in the supine position.

Fig. 9.   Compression and ventilation by a CPR machine with the subject in the upright position. Note collar to adequately hyperextend the head.

These findings lead us to recommend that resuscitation be provided in the manner described for subjects in the sitting position. If normal resuscitation is to be done for longer periods, it must be performed in the supine position, which will require some modifications to bell interiors. As an alternative, bells could be outfitted with a gas-driven mechanical cardiopulmonary resuscitator to be used with the subject in a seated position with a backboard.

Acknowledgments

References

1. COMEX Diving Limited Safety Department. The handling of an unconscious diver in a diving bell. Marseilles: 1978.
2. Standards and guidelines for CPR and emergency cardiac care. JAMA Aug. 1980.

AUTHOR INDEX

SUBJECT INDEX

A

Accidents, fatal, diving, 869–875
Acetylcholine, 629, 631
Action potential
  squid giant axon, 611
Adenosine triphosphate, 55–62
Adrenaline, 37, 39
Air
  diving, 877–878
  embolism, 741–750
    venous system, 741
  pressure, see Pressure
Albumen
  fat cells and, 47, 49
Alcohol
  diving reflex, 241–247
Alkalosis
  anticonvulsant, 123
Alveolae
  filter, 767–773
Amino acids, 39
Ammonia
  metabolism, 37–43
Analysis
  mathematical, 661–665
Anesthesia, 312–313, 317–326, 337–342, 357,
    363, 391, 661–665
  anesthetic effects, 661–665
  pressure and, 312–313, 853–856
Animal behavior, see Behavior, animals
Animals, research
  cat, 274, 457, 700
  dog, 96, 700, 743
  eel, 601
  guinea pig, 103, 318, 731, 811, 853
  monkey, 381
  mouse, 27, 88, 115, 330, 392, 421, 676, 754,
    838
  rabbit, 466–476, 483
  rat, 38, 45, 55, 66, 122, 130, 338, 372, 416,
    700
  snail, 621
  squid, 614
Aortic body, 458
Apparatus, see Equipment research
Arrhythmia, cardiac, 235–240
  temperature effects, 239
Aspirin, 131

Atlantis

Atlantis I, 181–194, 348
Atlantis II, 181–194, 351
ATP, *see* Adenosine triphosphate
ATPase, measurement, 590, 593
Aural, *see* Ear
AUTODEC, computer program, 711, 715
Axon, giant squid, 611–618

B

Bacteria, 483–488, 859–867
Bacterial endotoxin, 65–73
Barotrauma
  inner ear, 805–810
  middle ear, 811–815
Behavior, animal, 415
Bell, diving
  resuscitation in, 887–899
Benzodiazeprine, 87–93
Biochemistry
  of brain damage, 26–35
  of lung damage, 11–12
  of oxygen poisoning, 4–5
  of oxygen utilization, 449
Blood
  ammonia during HBO, 37–43
  analysis, 152, 164–165, 188
  metabolites, 153–154, 166
  plasma, 152, 165, 550
Blood chemistry
  simulated dive to 55 bars, 523
Bone
  divers radiological study, 847–851
  marrow, 45–52
  necrosis, *see* Dysbaric osteonecrosis
  osteomyelitis, 483–488
Bradycardia, *see* Heart rate
Brain, *see also* Central nervous system
  ammonia during HBO, 37–43
  metabolism, 675–683
  oxygen poisoning, 5–8, 25–35, 87–93
Breathhold, 267–271
Breathing, *see* Respiration
Bubbles, 82, 692–694, 699–705, 729–739
  dynamics, model, 775–782
  formation in gelatin, 793–801
  lung filter for, 95–101, 741
  silent, 741